NASA Conference Publication 3119

The 1990 NASA Aerospace Battery Workshop

Proceedings of a workshop held at
Huntsville, Alabama
December 4–6, 1990

NASA

NASA Conference Publication 3119

The 1990 NASA Aerospace Battery Workshop

Compiled by
Lewis M. Kennedy
George C. Marshall Space Flight Center
Marshall Space Flight Center, Alabama

Proceedings of a workshop sponsored by the NASA Aerospace Battery Steering Committee, hosted by the George C. Marshall Space Flight Center, and held at the U.S. Space and Rocket Center
Huntsville, Alabama
December 4–6, 1990

NASA
National Aeronautics and Space Administration
Office of Management
Scientific and Technical Information Program
1991

PREFACE

This document contains the proceedings of the 21st annual NASA Aerospace Battery Workshop, hosted by the Marshall Space Flight Center on December 4-6, 1990. The workshop was attended by scientists and engineers from various agencies of the U.S. Government, aerospace contractors, and battery manufacturers as well as participation in like kind from the European Space Agency member nations.

The subjects covered included nickel-cadmium, nickel-hydrogen, silver-zinc, lithium based chemistries, and advanced technologies as they relate to high reliability operations in aerospace applications. A sampling of the workshop scope ranges over:

- reports on current flight operations including Hubble Space Telescope, COBE, Magellan, CRRES, Solar Max, and Eutelsat II.
- histories of development and performance, and expected performance of current design developments.
- electrode and separator performance.
- problem analysis.
- testing.
- cell and cell test safety.

INTRODUCTION

I want to thank everyone who attended the 1990 NASA Aerospace Battery Workshop, as well as those who delivered presentations, for all were participants.

The tradition of the workshop dates back to 1968, and for many of those years it has been referred to as the Goddard Space Flight Center Battery Workshop. 1990 is the first year that the workshop has been hosted by the Marshall Space Flight Center. The workshop is sponsored by the NASA Battery Steering Committee with funding and management responsibilities supported by NASA Headquarters, Code Q.

The workshop covered three very busy days with NiCd topics being on the first, primary cells on the second, advanced technologies early on the third, and the remainder filled with NiH_2. The preface to these proceedings, and the workshop agenda contained within, further delineate the scope of the workshop.

I will take this opportunity to specifically thank the individuals whose efforts significantly contributed to the success of the workshop.

DR. DAVID F. PICKETT, Hughes Aircraft, commenced the workshop by delivering the keynote address which profiled the history of the Battery Workshop. I personally do not think a better address could have been conceived, considering that this workshop was somewhat of an evolutionary mark upon the history of the workshop itself, and a vantage point from which to reflect.

Thomas Yi,	Goddard Space Flight Center
Chuck Lurie,	TRW
Michell Manzo,	NASA Lewis Research Center
George Methlie,	DOD
Karla Clark,	Jet Propulsion Laboratory
Sal Di Stefano,	Jet Propulsion Laboratory
Larry Thaller,	Aerospace Corp
Tom Miller,	NASA Lewis Research Center
Chip Koehler,	Space Systems/LORAL
Eric Lowery,	Marshall Space Flight Center

Each volunteered and gave of their own time to solicit presentations, collect, organize an agenda, and serve as session chairmen to the Battery Workshop.

Dr. Constance Dees, Alabama A&M University, provided excellent contract management support and coordinated the arrangements for the workshop with the U.S. Space & Rocket Center.

Jim Miller, Marshall Space Flight Center, prompted this Steering Committee member to volunteer the Marshall Center as the host site for this workshop, and remained an advisor throughout many months of preparation, culminating with the workshop.

Frank Manning, NASA Headquarters, Code Q, Chairman of the Battery Steering Committee and manager of the NASA Aerospace Flight Battery Systems Program through which the workshop was funded, provided the money, a good ear, and optimism and moral support.

And finally, I want to publicly thank the U.S. Space & Rocket Center for furnishing a superb setting, excellent facilities support, and the hospitality shown to us.

Lew Kennedy
NASA Battery Steering Committee
Marshall Space Flight Center

TABLE OF CONTENTS

Nickel-Cadmium Technologies

Primary Technologies

Advanced Technologies

Nickel-Hydrogen Technologies

*** Presentations not submitted at the time of publication.

The 1990 NASA Aerospace Battery Workshop

Chairmen

Nickel-Cadmium

Thomas Yi,	Goddard Space Flight Center
Chuck Lurie,	TRW

Primary

Michell Manzo,	NASA Lewis Research Center
George Methlie,	DOD

Advanced

Karla Clark,	Jet Propulsion Laboratory
Sal Di Stefano,	Jet Propulsion Laboratory
Larry Thaller,	Aerospace Corp

Nickel-Hydrogen

Tom Miller,	NASA Lewis Research Center
Chip Koehler,	Space Systems LORAL
Eric Lowery,	Marshall Space Flight Center

ATTENDANCE

1990 NASA AEROSPACE BATTERY WORKSHOP

Brian Alexander
Jon D. Armantrout
John Baker
James A. Barnes
Wilbert L. Barnes
Louis Barraza
Klaus von Benda
Chuck Bennett
Gerard Boyle
B.J. Bragg
Jeffery C. Brewer
Jack Brill
Joe Bytella
Lee Christensen
William D.K. Clark
Richard Congo
Dennis B. Cooper
Timothy Counts
Edward F. Cuddihy
Penni Dalton
Eric Darcy
Stuart Daughtridge
Frank Deligiannis
Dan Dell
Kurt Dobrenz
Rajiv Doreswamy
Loxie L. Doud
G.J. Dudley
Andrew Dunnet
Tim Edgar
Teddy M. Edge
Rex Erisman
David O. Feder
Ed Fitzgerald
Randall Gahn
Wm. O. Gentry
Pete George
Richard M. Gerber
Ann Gibney
Richard D. Glover
Peter Gluck
Dee Gnacek
Ray Goins
Glen Gooch
Jaques Goualard
John G. Gray
James A. Gucinski
David K. Hall

Steve Hall

Charles I. Hall

Mike Harrison

Gary L. Hartjen

Robert Hawkins

Jeff Hayden

Ken Hearn

Robert Hellen

Lorna G. Jackson

Jason E. Jenkins

Ian Jenkins

Wade H. Jordon

John R. Lanier, Jr.

Carlos D. Judkins

Quentin L. Kampf

Glenn Klein

C.W. Koehler

Nick Liberto

John E. Lowery

Chuck Lurie

Michael Mackowski

Tyler X. Mahy

Jenny Mai

Frank L. Manning

Michelle Manzo

Tim Martin

Dean W. Maurer

Mitch Mendrek

George Methlie

John Meyer

Dave Miller

Jim Miller

Lee Miller

Kevin Moscatiello

Dave Nawrocki

Chuong Nguyen

Al Norton

Pat O'Donnell

Phil Olbert

Burton Otzinger

Gene Pearlman

David F. Pickett

Olivier Puig

Michael F. Pyszczek

Gopal Rao

Roger E. Rickey

Paul Ritterman

Frank J. Scalici

Stephen Schiffer

Lee Schmidlin

Dave Schmidt

Darren Scoles

Lenard F. Silvester

Owen Smith

D.G. Soltis

Dan Standlee

Sal Di Stefano

Ken Stephens

James A. Stepro

Joseph Stockel

Ralph M. Sullivan

Larry Swette

Mike Takao

Steve Tesney

Lawrence H. Thaller

Daniel L. Thomas

Anne Van Thuyne

Paul Timmerman

Lawrence Tinker

Mark R. Toft

Hari Vaidyanathan

Scott Verzwyvelt

Micheal Viens

Harry Wajsgras

Richard Walraven

Richard V. Whiteley

Thomas H. Whitt

Robert Wright

W. Wright

Thomas Yi

NASA AEROSPACE BATTERY WORKSHOP

December 4 - 6, 1990
U.S. Space & Rocket Center
Marshall Space Flight Center
Huntsville, Alabama

AGENDA

Tuesday Dec.4
Nickel-Cadmium Technologies

8:00 **Registration**

8:45 **Welcome and Keynote Address**
Keynote Speaker: Dr. David F. Pickett,
Hughes Aircraft Co.

9:15 **COBE Battery Handling and Performance.**
Thomas Yi, Smith Tiller, and David Sullivan,
NASA Goddard Space Flight Center

9:45 **End-of-Life Evaluation of the SMM Batteries.**
Doris Jallice and Thomas Yi,
NASA Goddard Space Flight Center

10:15 **Magellan Battery Operations and Overview.**
Paul Timmerman and Peter Gluck,
Jet Propulsion Laboratory

10:45 **The Effect of Switched Array Battery Charge Control on CRRES Spacecraft: 3+ Month Data Summary.**
Phil Olbert, Ball Aerospace

11:15 **Super NiCd Battery Program History and Performance.**
Jeff Hayden and Tim Edgar, Eagle-Picher Industries

11:45	**LUNCH**
1:00	**Update on Hughes Aircraft Company Advanced NiCd Batteries.** Sam Bogner and Allan Powers, Hughes Aircraft Co.
1:30	**Updated SAFT Nickel-Cadmium Cell Performances for GEO and LEO Applications.** Olivier Puig, SAFT
2:00	**Oxygen Recombination in NiCd Cell.** Al Zimmerman and Tom Barrera, Aerospace Corporation
2:30	**Constant Current Charge Techniques in LEO Life Testing.** Peter Gluck, Jet Propulsion Laboratory
3:00	**Chemical Evaluation of Non-Woven Separator in Ni-Cd Cells.** Ed Cuddihy, Jet Propulsion Laboratory
3:30	**Exploring Possible Relationships Between Plate Pore Size Character and Cell Performance.** Lawrence Thaller, Aerospace Corporation and Lawrence Tinker, Gates Aerospace Batteries.

Wednesday Dec 5
Primary Technologies

8:00 **Overview of the Primary Battery Session.**
Manzo & Methlie

8:30 **JSC Primary Battery Applications.**
Bob Bragg, NASA Johnson Space Center

9:00 **STS Li/CFx Cell Problem Analysis.**
Dee Gnacek, USBI/Huntsville

9:30 **Li/CFx Cell Problem Analysis.**
Dr. R. Congo, NASA Marshall Space Flight Center

10:00 **Li/CFx Cell Problem Analysis.**
Dave Miller, Eagle-Picher Industries

10:30 **Li/CFx Cell Problem Analysis.**
John Baker, Catalyst Research

11:00 **Li/CFx Cell Problem Analysis.**
Joseph Bytella, Catalyst Research

11:30 **Large LiCFx Cells.**
Tim Counts, Eagle-Picher Industries

12:00 **LUNCH**

1:15 **Calorimetric Determination of the Thermoneutral Potential for the Li/BrCl in SOCl2 Chemistry.**
Eric Darcy, NASA Johnson Space Center, E. Kalu and R. White, Texas A&M

1:45 **Li/SVO, BCX, CSC and other Cells.**
Dr. W. Clark, Electrochem Industries, Clarence, NY

2:15 **Large Lithium Cells.**
Dr. Jim Barnes, U.S. Navy

2:45 **250 Ahr Lithium Thionyl Chloride Cell Evaluation Test Results.**
Jacques Goualard, SAFT

3:15 **Performance of 300 Ahr High Rate Li/SOCl2 Cell**
Gerald H. Boyle, Yardney Technical Products, Inc.

3:45 **Lithium Cell Safety.**
Tyler Mahy

4:15 **Lithium Cell Safety Testing.**
Nick Liberto, Catalyst Research

4:45 **Examination of the Discharge Mechanism of Li/CFx Cells, Comparison of the Electrochemical Reduction Mechanisms of PFTE and (CFx)n by Lithium.**
C.C. Baxam & N. Margalit, Tracor Technology Resources

5:15 **Zinc Oxygen Battery Development.**
Deborah Bourland, NASA Johnson Space Center

5:45 **Life Testing of Secondary Silver-Zinc Cells.**
Jeff Brewer and Rajiv Doreswamy, NASA Marshall Space Flight Center

6:30 **Rechargeable Cocktail Hour, U.S. Space & Rocket Center Cafeteria.**

8:00 **"The Blue Planet", Spacedome Theater.**

AGENDA

Thursday Dec 6
8:00 Advanced Technologies
10:00 Nickel-Hydrogen Tecnologies

8:00 **Cycle Life Characteristics of Li-TiS2 Cells.**
F. Deligiannis, Jet Propulsion Laboratory

8:30 **Accelerated Cycle Life Performance of Ovonic Ni-MH2 Cells.**
B. Otzinger, Rockwell International

9:00 **Evaluation of Na-NiCl for Space Applications.**
G.J. Dudley and B Hendel, European Space Research and Technology Center

9:30 **Utilization of Bipolar Pb-Acid Battery for the Advanced Launch System.**
R. Miles, Johnson Controls, and
S. Eckles, General Dynamics

10:00 **Recent Developments in Nickel Electrode Analysis.**
R.V. Whiteley, Pacific University; M.E. Daman and
E.Q. Kaiser, Space Systems Loral

10:30 **Eutelsat II Nickel-Hydrogen Storage Battery System Design and Performance Summary.**
L. Miller, Eagle-Picher Industries

11:00 **Low Cost Battery Design for Small Satellite Applications.**
J. Brill, Eagle-Picher Industries

11:30 **The Evaluation of Layered Separators for NiH2 Cells.**
R.F. Gahn, NASA Lewis Research Center

12:00 **LUNCH**

1:15 **Update of a Nickel-Hydrogen Cycle Life Model.**
Dr. L. Thaller, The Aerospace Corporation

1:45 **The Hubble Space Telescope Nickel-Hydrogen Battery Design.**
D. Standlee, Eagle-Picher Industries

2:15 **Hubble Space Telescope Nickel-Hydrogen Six Battery Test.**
J.R. Lanier and T.H Whitt,
NASA Marshall Space Flight Center

2:45 **Mission Simulation Test of a 22 Cell Nickel-Hydrogen Battery for the Hubble Space Telescope.**
J.C. Brewer and T.H. Whitt,
NASA Marshall Space Flight Center

3:15 **Multiple Cell CPV Nickel-Hydrogen Battery.**
J.P. Zagrodnik, Johnson Controls, Inc.

3:45 **Results of a Technical Analysis of the Hubble Space Telescope Nickel-Cadmium and Nickell-Hydrogen Batteries.**
M.A. Manzo, NASA Lewis Research Center

4:15 **NiH2 LEO Cycling at 20-50% DOD.**
E. Lowery, NASA Marshall Space Flight Center

IN MEMORIAM

Dr. Willard R. Scott passed away in January 1990. He was a good friend and colleague to our community of aerospace battery engineers and scientists for more than twenty years.

Will was known throughout the industry as a quiet and modest man whose integrity and professionalism were unquestioned. He was tireless in his efforts to obtain improved empirical and theoretical knowledge of nickel-cadmium and nickel-hydrogen cell and battery performance. He made significant contributions in the areas of cell failure effects analysis, cell and battery design, cell thermal modeling, and safe and effective in-flight battery reconditioning. Many of these are documented in the records of this continuing workshop. He generously gave time and information to many individuals in the spirit of achieving improved sponsor and user confidence in spacecraft battery products. And he shared the breadth and depth of his experience with a wide audience as principal author of a comprehensive nickel-cadmium battery applications manual

Will Scott's natural reserve belied his humor, strength, and concern for others--particularly to his devoted family. From an early start as a dashing Naval officer, through personal academic achievement, to success first as a corrosion prevention expert and then finally as the contributor we have known and respected, his has been a good and productive life. He will be missed.

20 PLUS YEARS OF THE NASA BATTERY WORKSHOP

Keynote Address for the NASA Marshall Battery Workshop, December 4,5,6, 1990

By

David F. Pickett, Manager
Energy Storage Product Line
Hughes Aircraft Company
Industrial Electronics Group
Electron Dynamics Division

OUTLINE

INTRODUCTION: It is indeed an honor to serve as the Kickoff Speaker for the 1990 Session of the NASA Battery Workshop. This meeting has for the past 20 years, or as long as I have been in the battery field, been the pinnacle for discussion and gathering of information within the aerospace battery industry.

After I had accepted the invitation from Lew Kennedy, I had mixed feelings as to what I should cover in this address. It would be easiest for me to talk about our new Battery Product Line that we have had at Hughes since January, but I felt that this would be more like a commercial. Since this is the first session since the Workshop has moved from Goddard to Marshall, I thought a review of past workshops and the origin of the Battery Workshop would be appropriate. I have thus entitled this presentation 20 Plus Years of the NASA Battery Workshop.

ORIGIN OF THE NASA BATTERY WORKSHOP: The reason I have used "20 plus" instead of just 20 in the title is based on the actual origin of the Workshop. The first government sponsored, industry wide meeting to discuss battery problems in a open forum was held October 30 through November 1, 1968 at NASA Goddard Space Flight Center in Maryland. (It's interesting to note that Halloween falls within these dates. Battery technologists are often accused of being witches or warlocks by systems and electrical engineers who don't always understand their "chemical black magic".) This meeting was called Conference on OAO Battery Trouble Shooting. The conference was precipitated by high charge voltage problems on the Orbiting Astronautical Observatories batteries while they were in thermal-vacuum testing in June and July of 1968. Gulton Industries was the cell supplier. Earlier in March of

'68 similar problems were observed in tests at NASA Goddard on 20 ampere-hour Gulton cells. In Goddard's efforts to notify users that a serious problem existed, it was found that similar problems were being experienced throughout the industry by TRW, Hughes, Martin Marietta, NAD Crane and others. A few small meetings were held with the people that were concerned. At one of these meetings it was proposed that a symposium be held at Goddard with the main users of NiCd batteries. It was also suggested Gulton Industries attend. At that time the main concern was with the Gulton cells. The problem areas that were reviewed in the meeting covered such topics as: plate quality, cell formation, negative to positive ratio, radomization of electrodes, nonwoven separators, traceability of materials and standard electrical tests.

During the meeting it was generally agreed that some type of materials control, process control, and uniform test procedures were required to avoid future problems, and to assure long life, high reliability NiCd cells which would apply to all manufacturers.

As a result of the above discussions a task group of attendees were requested to formulate a specification to spell out the required design requirements, material and process controls and test procedures during the cell fabrication process. It was not the intent of this task group to specify how the cells were to be built or to draft a specification to encompass all NiCd battery processes within the allotted time. The working group members did not have a lot of actual battery experience in terms of actual cell fabrication. Their main experience was primarily as users. The group consisted of:

Bill Billerbeck, COMSAT, Chairman
Jerry Halpert, NASA/GSFC
Bob Steinhauer, Hughes Aircraft Co.
Dr. Will Scott, TRW Inc.
Jim Dunlop, COMSAT
Floyd Ford, NASA/GSFC

Dr. Arthur Fleischer was used as a consultant.

Based on the problem areas as the task group saw them a "Model Specification" evolved. The review of this so-called Model Specification was held at an industry wide meeting on October 29 - 31, 1969 at NASA Goddard entitled Technical/Scientific Meeting on Space Battery Specifications. The intent of this workshop was to move on from the specification and make it more relevant. Eventually it was

desired that the specification would be used more by NASA and COMSAT but also by other users. This was the first step towards standardization and the beginnings of the NASA 74-15000 specification. The meeting was attended by some 80 individuals representing 23 companies, four government agencies and three universities.

In November of 1970 this industry wide gathering was continued with the title of 1970 NASA/GSFC Battery Workshop. The purpose of this meeting was to provide an open forum for the industry to discuss battery problems and issues in sort of an extemporaneous manner without formal preapproved presentation material. In all of these meeting up to this time a court recorder was used to document all conversation and a tape recorder was used for backup. This form of recording was later discontinued.

From the above account one could say that there have been 21 to 22 Battery Workshops to date (a Workshop was not held last year and a Mini-workshop was held in 1988 in addition to the regular Workshop), or if you only consider the 1970 meeting to be the first, it is only 19 to 20. That is why I have chosen "20 Plus" in the title of this presentation.

KEY TOPICS AND TECHNOLOGIES ADDRESSED OVER THE PAST 20 YEARS:

There has been a tremendous amount of battery technology that has been addressed in the NASA Battery Workshops over the past 20 years. Needless to say, this information has been of immeasurable help to the industry. Listed below are some of the topics and technologies which I felt have been especially useful. Depending on your point of view, you may choose others as well.

- Review of OAO Cell Problems and Industry Wide Cell Quality Problems, 1968
- Testing Methods and Flight Experience, 1968 - 1988
- Accelerated Testing Concepts, 1968 - 1983
- Seal Improvements, 1968, 1970, 1971, 1972, 1977
- Introduction of Manufacturing/Performance Specifications for Aerospace Cells, 1969
- Manufacturing of Plates using Electrochemical Impregnation Techniques, 1970, 1971, 1972, 1974, 1976, 1978, 1981
- Techniques for Complete DPA of Aerospace Cells and Electrodes, 1970, 1974, 1975, 1978
- Overview of Cell Testing at Crane, Indiana Facility, 1970, 1985
- Effects of Cadmium Precharge, 1970, 1971
- Separator Characterization and Testing, 1968 - 1988
- Thermal Properties of Cells and Batteries, 1971

- Metal Hydrogen Batteries (Nickel Hydrogen, Silver Hydrogen), 1972 - 1988
- Storage Experience with NiCd Cells, 1973, 1974, 1977, 1986
- Low Cost/Standardization Program, 1974, 1977, 1979
- NASA Accelerated Test Program, 1974, 1977, 1979
- NASA Accelerated Test Program, 1974, 1976, 1978, 1979
- Effects of Reconditioning, 1974, 1976, 1977
- Vibrational Effects on Sealed NiCd Cells, 1976
- 25 kw and 100 kw Space Station, 1977
- U.S. Navy (NTS-2) Flight Experiment with Nickel Hydrogen Batteries, 1977
- U.S. Air Force Flight Experiment with Nickel Hydrogen Batteries, 1977, 1979
- Shuttle Safety, 1977
- Lithium Battery Testing and Technology, 1977 - 1988
- Lightweight Nickel Electrodes, 1978, 1986
- Cell Design and Manufacturing Changes, 1978
- Shuttle Payload Requirements & Implementation Procedure, 1978
- Common Pressure Vessel Nickel Hydrogen Battery, 1978, 1984
- Safety Report of Tri-Service Lithium Safety Committee, 1979
- Galileo Lithium - Sulfur Dioxide Batteries, 1979, 1980, 1981, 1985
- Rechargeable Lithium Cells, 1979 - 1988
- Panel Discussion: Safety - Whose Responsibility, 1980
- Future Needs - High Energy Density Rechargeable Battery for Satellite Applications, 1980. 1987
- U.S. Army & U.S. Navy Positions on Lithium Safety, 1981
- Panel Discussion: Which Method of Charge Control Provides the Most Reliable Operation for Near Earth or Synchronous Missions? - 1982
- Panel Discussion: Reconditioning Has Significant Effect on Battery Life, Fact or Fiction? - 1982
- Panel Discussion: Does Nickel Hydrogen Really Have an Advantage over Nickel Cadmium? - 1982
- Bipolar Nickel Hydrogen Battery, 1982, 1983, 1984, 1985
- Separator Qualification for Aerospace Nickel-Cadmium Cells, 1983, 1984, 1985, 1986, 1987, 1988
- Comparitive Performance Assessment of Intelsat V Nickel Hydrogen and Nickel Cadmium Batteries, 1983
- An Industry and Government Survey: A Nickel Hydrogen Testing Data Base, 1984

- o Energy Storage Systems Comparison for the Space Station, 1985
- o Impact of Shuttle Environment on Prelaunch Handling of Nickel Hydrogen Batteries, 1985
- o Nickel Hydrogen LEO Test Program, 1985, 1986, 1987
- o Nickel Hydrogen Battery Flight Status, 1987, 1988
- o Panel Discussion: Merits of Current KOH Concentration in Use for Nickel Hydrogen and Nickel Cadmium Cells, - 1987
- o Task Group Presentation and Discussion from Nickel-Cadmium Cell Mini-Workshop held in June, 1988 (Deja Vu, 1968)

RECENT MAJOR CONCERNS AT NASA BATTERY WORKSHOPS: Some of the most pressing problems that have been addressed recently in the battery workshops have been qualification of the new nylon separator materials, premature hydrolysis of the stored 2505 ML Pellon separator material, low earth orbit testing of nickel hydrogen cells, and lithium battery quality and safety issues. The separator problems recently have received special attention in a Mini-workshop which was held here at Marshall Space Flight Center in June, 1988. The problem is being addressed both by the Government and private industry. European vendors, such as SAFT, have come to the aid of our space program by supplying qualified cells for some of the programs here in the U.S. We at Hughes Aircraft are contributing by offering a new cell design. A presentation on this technology will be given at this Workshop.

Low earth orbit cycle life test data for nickel hydrogen cells is of extreme importance to NASA missions such as Hubble Space Telescope and Space Station. It is also of importance to U.S. Air Force, who is the major sponsor of this effort. It is expected that this data base will be vastly increased once protoflight hardware for Space Station begins life testing. Hughes and NASA Lewis have given presentations at past Battery Workshops and IECEC meetings on our receipt for long life, low earth orbit cells.

Lithium battery technology first became a topic of discussion at the 1977 Battery Workshop. Since that time the number of presentations have blossemed, and rechargeable systems have been addressed from time to time. The main concern with lithium batteries has always been safety, and quality, storage and handling are, of course, related issues. These topics are covered rather extensively in this Workshop and, most likely, will continue to be addressed in future Workshops.

CONCLUSIONS AND RECOMMENDATIONS FOR THE FUTURE: In his keynote address to the 1970 NASA/GSFC Battery Workshop, Chuck MacKenzie stated, "The battery is the most important component in the power system because it is the least understood." From the nature of the present problems we are experiencing it appears that this is still a valid statement. One would hope that after 20 years and some 500 to 600 technical presentations later at the battery workshops that we should have made considerable progress in understanding batteries in the aerospace industry. I think that we definitely have improved our understanding, but it hasn't been good enough in some cases.

We need to take advantage of our 20/20 hind sight. The reason we are still having problems is: it's just the nature of the beast. 30 years of development on space NiCd and 18 years of development on nickel hydrogen batteries is small compared to the 140 years of development on lead acid batteries where improvements are still being made. I will venture to say that we will continue to have even larger problems with our battery systems if we do not continue our development programs. I am of the opinion that the present separator qualification issue could have been avoided with proper development programs in place.

The best receipt for a successful battery program is eternal vigilance, perpetual testing and continued improvement through technology efforts and commitment of government agencies, industry, universities and individual workers. We also need to keep the following points in mind.

- The operation of the entire cell and battery as a system needs to be understood in addition to the function of each component.
- Total Quality Management should apply to battery design and manufacturing.
- Close working relationship between Government agencies, academics, manufacturers and users has to be established.
- Technology efforts need to address improvements in existing couples as well as "revolutionary" new battery systems.

Given the history over the past 20 years, there is never going to be an easy fix to existing battery problems. Solution to the problems is only going to be found through hard work, communication, and coordination between those at all management and working levels.

20 PLUS YEARS OF THE NASA BATTERY WORKSHOP

BY

DAVID F. PICKETT, MANAGER
ENERGY STORAGE PRODUCT LINE
HUGHES AIRCRAFT COMPANY
INDUSTRIAL ELECTRONICS GROUP
ELECTRON DYNAMICS DIVISION

HUGHES
AIRCRAFT COMPANY

ORIGIN OF NASA BATTERY WORKSHOP

HUGHES

- Conference on OAO Battery Trouble-Shooting (October 1968)
- Technical/Scientific Meeting on Space Battery Specifications (October 1969)
- 1970 NASA/GSFC Battery Workshop (November 1970)

KEY TOPICS AND TECHNOLOGIES ADDRESSED OVER PAST 20 YEARS

HUGHES

- Review of OAO Cell Problems and Industry Wide Cell Quality Problems, 1968
- Testing Methods and Flight Experience, 1968 – 1988
- Accelerated Testing Concepts, 1968 – 1988
- Seal Improvements, 1968, 1970, 1971, 1972, 1977
- Introduction of Manufacturing/Performance Specifications for Aerospace Cells, 1969
- Manufacturing of Plates using Electrochemical Impregnation Techniques, 1970, 1971, 1972, 1974, 1976, 1978, 1981
- Techniques for Complete DPA of Aerospace Cells and Electrodes, 1970, 1974, 1975, 1978
- Overview of Cell Testing at Crane, Indiana Facility, 1970, 1985
- Effects of Cadmium Precharge, 1970, 1971
- Separator Characterization and Testing, 1968 – 1988
- Thermal Properties of Cells and Batteries, 1971
- Metal Hydrogen Batteries (Nickel Hydrogen, Silver Hydrogen), 1972 – 1988

KEY TOPICS AND TECHNOLOGIES ADDRESSED OVER PAST 20 YEARS (Continued)

HUGHES

- Storage Experience with NiCd Cells, 1973, 1974, 1977, 1986
- Low Cost/Standardization Program, 1974, 1977, 1979
- NASA Accelerated Test Program, 1974, 1976, 1978, 1979
- Effects of Reconditioning, 1974, 1976, 1977
- Vibrational Effects on Sealed NiCd Cells, 1976
- 25 kW and 100 kW Space Station, 1977
- U.S. Navy (NTS-2) Flight Experiment with Nickel Hydrogen Batteries, 1977
- U.S. Air Force Flight Experiment with Nickel Hydrogen Batteries, 1977, 1979
- Shuttle Safety, 1977
- Lithium Battery Testing and Technology, 1977 – 1988
- Lightweight Nickel Electrodes, 1978, 1986
- Cell Design and Manufacturing Changes, 1978

KEY TOPICS AND TECHNOLOGIES ADDRESSED OVER PAST 20 YEARS
(Continued)

HUGHES

- Shuttle Payload Requirements and Implementation Procedure, 1978
- Common Pressure Vessel NIckel Hydrogen Battery, 1978, 1984
- Safety Report of Tri-Service Lithium Safety Committee, 1979
- Galileo Lithium – Sulfur Dioxide Batteries, 1979, 1980, 1981, 1985
- Recharageable Lithium Cells, 1979 – 1988
- Panel Discussion: Safety – Whose Responsibility, 1980
- Future Needs – High Energy Density Rechargeable Battery for Satellite Applications, 1980, 1987

KEY TOPICS AND TECHNOLOGIES ADDRESSED OVER PAST 20 YEARS
(Continued)

HUGHES

- U.S. Army & U.S. Navy Positions on Lithium Safety, 1981
- Panel Discussion: Which Method of Charge Control Provides the Most Reliable Operation for Near Earth or Synchronous Missions? – 1982
- Panel Discussion: Reconditioning Has Significant Effect on Battery Life, Fact or Fiction? – 1982
- Panel Discussion: Does Nickel Hydrogen Really have an Advantage over Nickel Cadmium? – 1982
- Bipolar Nickel Hydrogen Battery, 1982, 1983, 1984, 1985
- Separator Qualification for Aerospace Nickel-Cadmium Cells, 1983, 1984, 1985, 1986, 1987, 1988
- Comparitive Performance Assessment of Intelsat V Nickel Hydrogen and Nickel Cadmium Batteries, 1983

KEY TOPICS AND TECHNOLOGIES ADDRESSED OVER PAST 20 YEARS (Continued)

HUGHES

- An Industry and Government Survey: A Nickel Hydrogen Testing Data Base, 1984
- Energy Storage Systems Comparison for the Space Station, 1985
- Impact of Shuttle Environment on Prelaunch Handling of Nickel Hydrogen Batteries, 1985
- Nickel Hydrogen LEO Test Program, 1985, 1986, 1987
- Nickel Hydrogen Battery Flight Status, 1987, 1988
- Panel Discussion: Merits of Current KOH Concentration in Use for Nickel Hydrogen and Nickel Cadmium Cells, – 1987
- Task Group Presentation and Discussion from Nickel-Cadmium Cell Mini-Workshop held in June, 1988 (Deja Vu. 1968)

RECENT MAJOR CONCERNS AT NASA BATTERY WORKSHOPS

HUGHES

- Qualification of New Nylon Separator Material
- Premature Hydrolysis of Stored 2505ML Pellon Separator Material
- Low Earth Orbit Testing of NiH_2 Cells
- Lithium Battery Quality and Safety Issues

CONCLUSIONS AND RECOMMENDATIONS FOR FUTURE

HUGHES

- We Need to Take Advantage of our 20/20 hindsight
- Future Problems can be Alleviated with Proper Development Programs in Place
- Best Recipe for Success:
  - Eternal Vigilance
  - Perpetual Testing
  - Continued Improvement
  - Commitment and Dedication of Everyone Involved

COBE BATTERY OVERVIEW:

HISTORY, HANDLING & PERFORMANCE

1990 NASA BATTERY WORKSHOP

DECEMBER 4 1990

THOMAS YI, SMITH TILLER, & DAVID SULLIVAN
SPACE POWER APPLICATIONS BRANCH
NASA/GODDARD SPACE FLIGHT CENTER

AGENDA

- **BACKGROUND**
  - Launch Configuration Change
- **BATTERY**
  - Cell Build History
  - Battery Build History
- **HANDLING PRACTICES**
  - Battery Lab, I&T, Launch Site Prep
- **ON-ORBIT PERFORMANCE**

COBE MISSION BACKGROUND

- PURPOSE: PERFORM A DEFINITIVE EXPLORATION OF THE DIFFUSE COSMIC BACKGROUND RADIATION AND PROVIDE A FULL SKY MAP OF THE BACKGROUND RADIATION
- LAUNCH BY STS FROM VANDENBERG (VAFB) CY89
- ONE YEAR MISSION LIFE
- EXECUTED IN-HOUSE WITH MAJOR SUBSYSTEM PROCUREMENTS
- AFTER THE 51L ACCIDENT, SPACECRAFT REDESIGN TO DELTA 3920A ELV CONFIG
- ACCELERATED SCHEDULE: S/C LAUNCH READINESS IS 29 MONTHS AFTER HQ REDIRECTION
- BASELINED A SUN SYNCHRONOUS POLAR ORBIT (900KM CIRCULAR, 6AM/6PM NODE CROSSING) FROM VAFB
- COBE SUCCESSFULLY LAUNCHED 11/18/89 (900.5KM X 899.3KM, 99.03° Inclination)

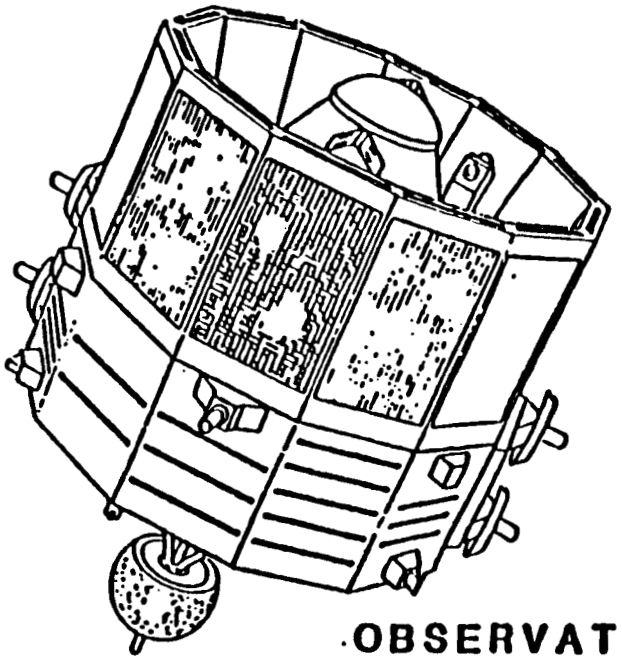

OBSERVATORY

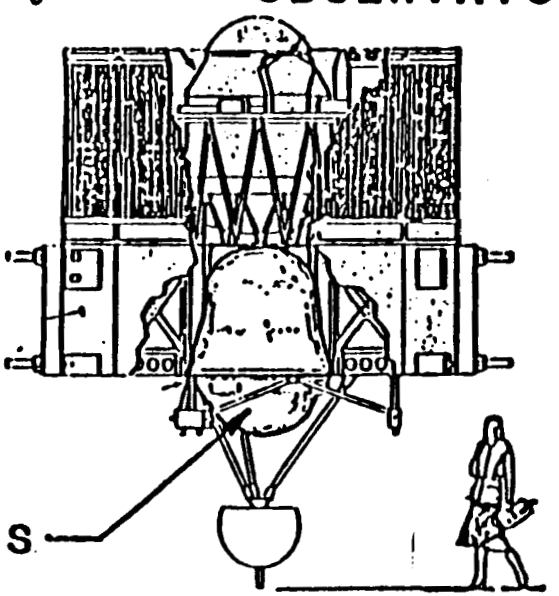

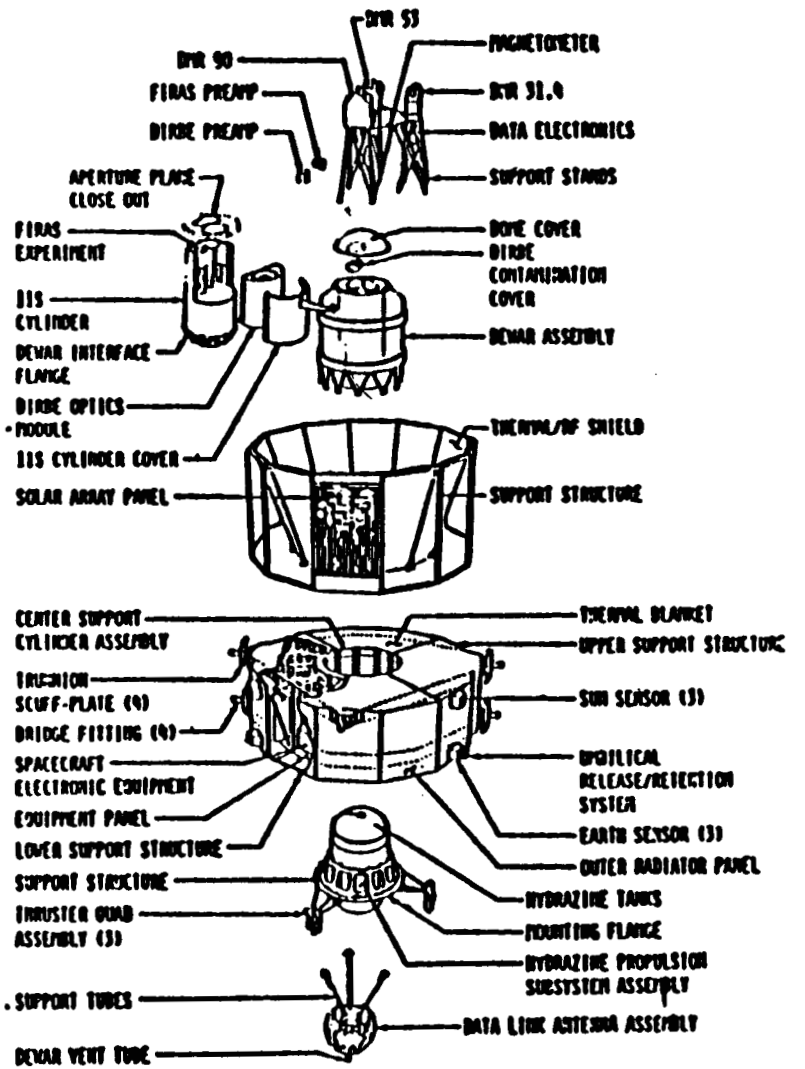

EXPLODED VIEW OF OBSERVATORY

TF-16

BATTERY BACKGROUND

- **BATTERY SPECIFICATION**
  - Temperature Range: -5° to +25° C
  - Output Voltage Range: 18 to 27 V
  - Output CurrenT (Eclipse): 20A/Battery
  - Peak Current Capability: 60A for 5 minutes
  - Mission Life: 1 Year Design Requirement
    (1200 cycles (103 minute orbit) over 2 eclipse seasons per year)
    2 Year Design Goal
  - Max DOD: 25%
  - Solstice Period: Max of 9 Months

- **BATTERY HERITAGE**
  - Originally Baselined NASA Std 50Ah Batteries; Began Std 50Ah Cell Procurement from GE Battery Div, through MDAC
  - Modified Version NASA Standard 20Ah Cells from GAB
  - Modified Version of NASA Standard 20Ah Battery from MDAC

CELL HISTORY

- **GAB CATALOG # 42B024AB31**
  - Originally GAB 42B024AB06 Which Contained Pellon 2505, Lot 30158, Roll 3
  - GAB Proposed Cell Rework with Pellon 2505, Lot 51562; GSFC Informed That This Matl Did Not Pass Sep Degradation Test
  - GSFC Decision to Use Pellon 2536 for COBE
- **MANUFACTURING EVENTS**
  - Double Stamping Noted on Substrate Edges -- Cosmetic Flaw
  - 25 Cells Rejected Due to Exposure to High Temp (115°F) 2/88; Cell Headers and Cases Recovered for Replacement Build
  - Total Cell Rework (quantity 76) with Pellon 2536
  - Cells Successfully Completed ATP 11/88
- **CELL DATA**

- ECT Test Capacity (Ah)	27.17 (+) 52.27 (-)
- Neg/Pos Ratio	1.92
- ATP Capacities (Ah)	26.6 (24°C), 24.2 (30°C), 26.4 (0°C)
- Post Number	33021 (+) 8/13/87 33028 (-) 8/17/87
- Electrolyte	73 - 76cc

BATTERY HISTORY

- **MODIFIED VERSION OF NASA STD 20AH BATTERY**
  - 18 Cells Used Instead of 22 Cells to Reduce Weight for Delta Configuration
- **MANUFACTURING EVENTS**
  - Cracked Thermal Fins During MDAC Vib Test -- Cosmetic Flaw
  - Batteries (2 Flight, 1 Spare) Successfully Completed ATP 2/89
- **BATTERY DATA**
  - Capacity Tests

	0°C	10°C	Room
Capacity (Avg)	24.99Ah	25.91Ah	25.88Ah
EOCV Spread (Max)	11 mV	8 mV	18 mV
EOCV (Max)	1.551V	1.495V	1.483V

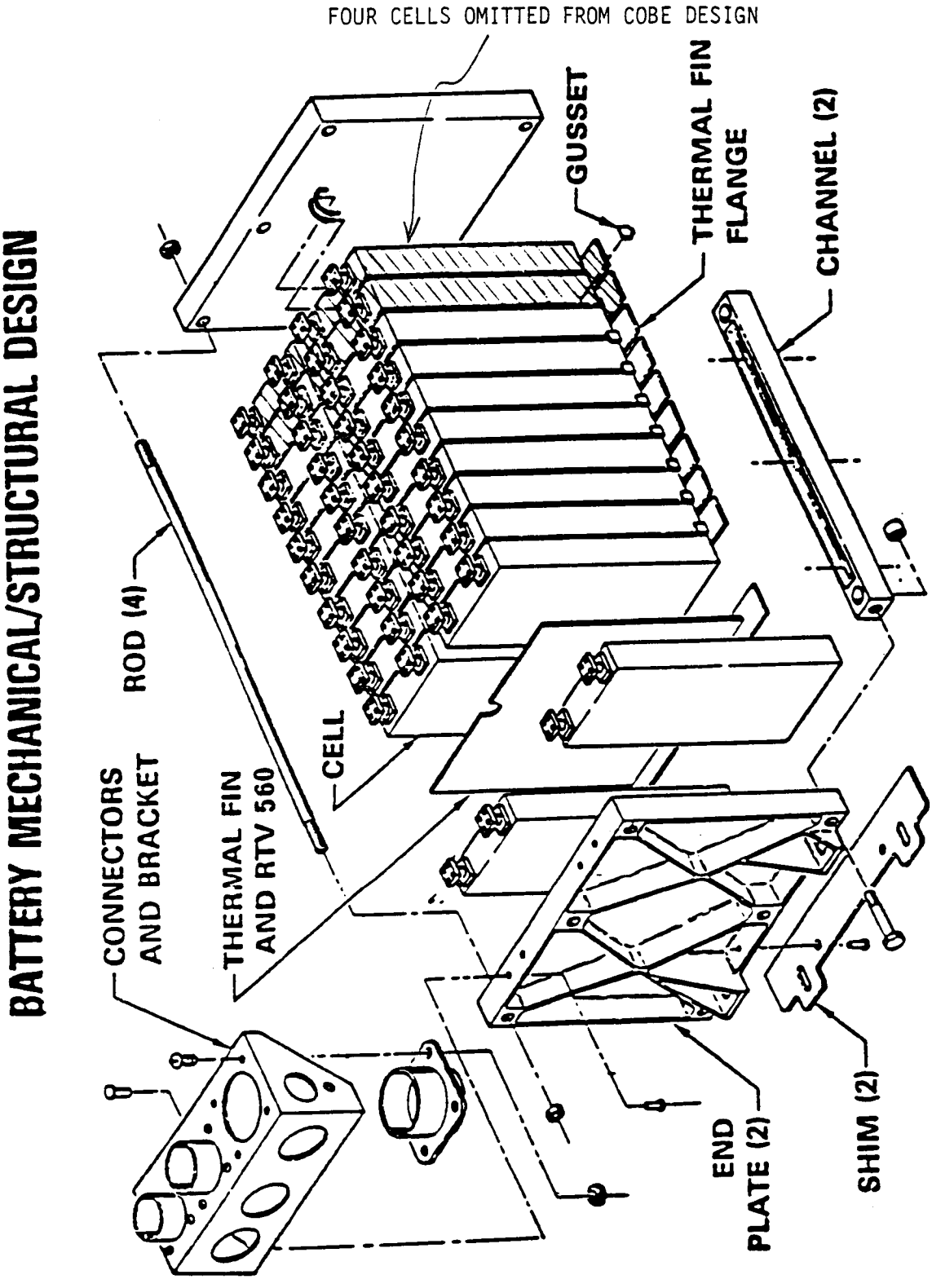
BATTERY MECHANICAL/STRUCTURAL DESIGN
FOUR CELLS OMITTED FROM COBE DESIGN
GUSSET
THERMAL FIN FLANGE
CHANNEL (2)
ROD (4)
CELL
CONNECTORS AND BRACKET
THERMAL FIN AND RTV 560
END PLATE (2)
SHIM (2)

FIGURE 2

BATTERY ACCEPTANCE TEST

mass properties
visual inspection
conditioning charge, C/20
conditioning discharge, C/2
resistive letdown
short
open circuit voltage recovery
capacity charge, C/10
capacity discharge, C/2
leak check
resistive letdown
short
3-step charge
capacity discharge, C/5
resistive letdown
short
visual inspection

BATTERY REVERIFICATION TEST

visual inspection
conditioning charge, C/20
conditioning discharge, C/2
resistive letdown
short
3-step charge
capacity discharge, C/5
resistive letdown
short

BATTERY RECONDITIONING

residual capacity discharge, C/5
resistive letdown
short
3-step charge
capacity discharge, C/5
resistive letdown
3-step charge

BATTERY RECHARGE

residual capacity discharge, C/5
resistive letdown
short
3-step charge

BATTERY POST S/C INTEGRATION CHECK

residual capacity discharge, C/5
resistive letdown
short
3-step charge
capacity discharge, C/5
resistive letdown
short

5.7 OPERATING LIMITS

Table 5-1 shall be referred to for safety limits for the battery tests outlined in this document.

Table 5-1 Operational Limits

MODE	NORMAL	SAFETY LIMIT
DISCHARGE MODE		
Battery Voltage	25.2 to 21.2V	19.0V
Cell Voltage	1.40 to 1.18V	1.0V
Battery Current	0 to20A	30A
Battery Temperature	0 to 25°	-10°C 25°C
Δ Battery Temperature	0 to 5°C	7°C
Δ Half Battery Voltage	0 to 0.2V	0.3V
Cell Voltage Divergence (High to Low Cells)	0 to 0.030V	0.030V
CHARGE MODE		
Battery Voltage	23.4 to 27.4V	0°C 27.4V 10°C 27.2V 20°C 27.0V 25°C 26.6V
Cell Voltage	1.30 to 1.54V	0°C 1.54V 10°C 1.52V 20°C 1.50V 25°C 1.49V
Battery Current	0 to 20A	30A
Battery Temperature	0 to 25°	-10°C 25°C
Δ Battery Temperature	0 to 5°C	7°C
Δ Half Battery Voltage	0 to 0.5V	0.7V
Cell Voltage Divergence (High to Low Cells)	0 to 0.030V	0.030V

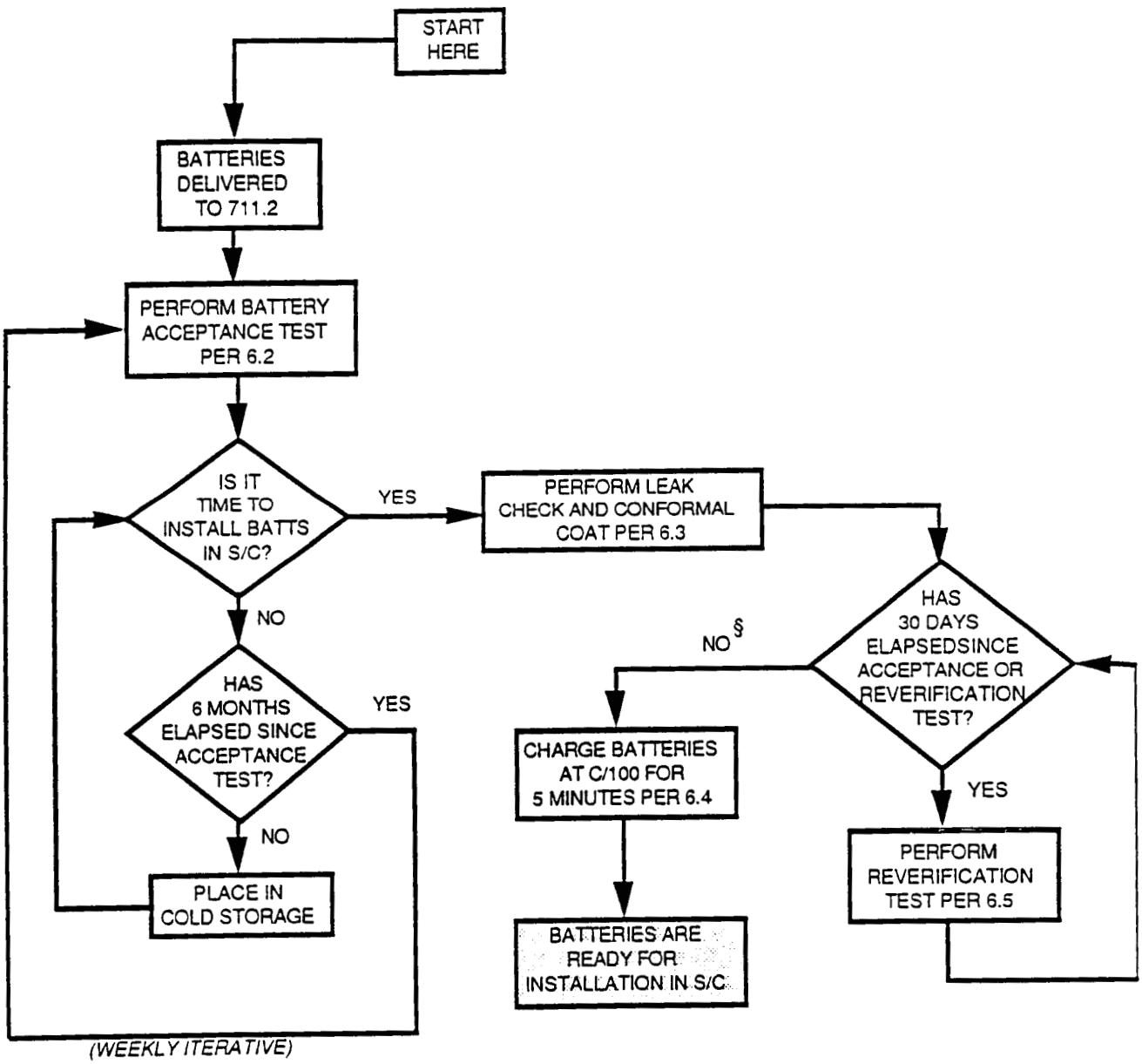

§ IF ANY DELAY IN INTEGRATION OCCURS AT THIS POINT, CONTACT THE BATTERY ENGINEER OR MANAGER FOR FURTHER INSTRUCTIONS.

FIGURE 6-1 BATTERY LABORATORY ACTIVITIES

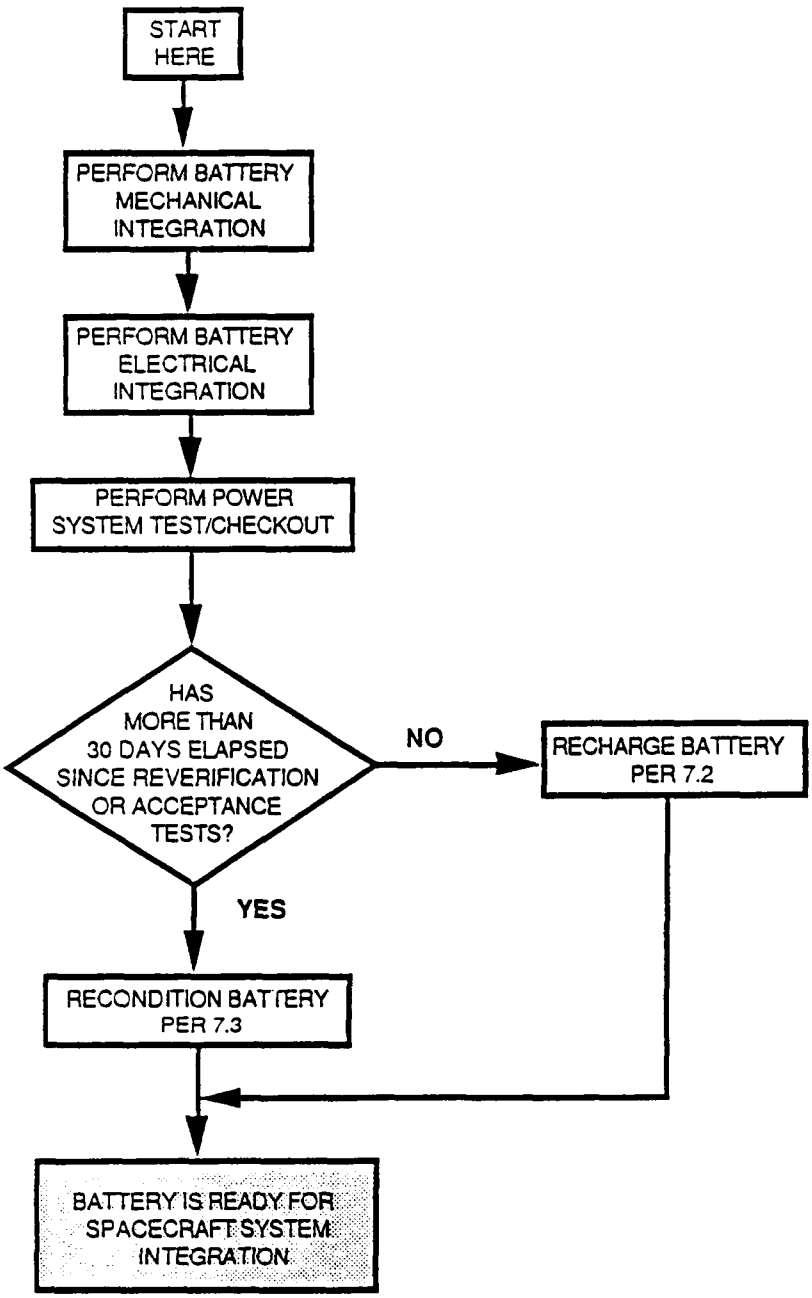

FIGURE 7-1 BATTERY SPACECRAFT INTEGRATION ACTIVITIES

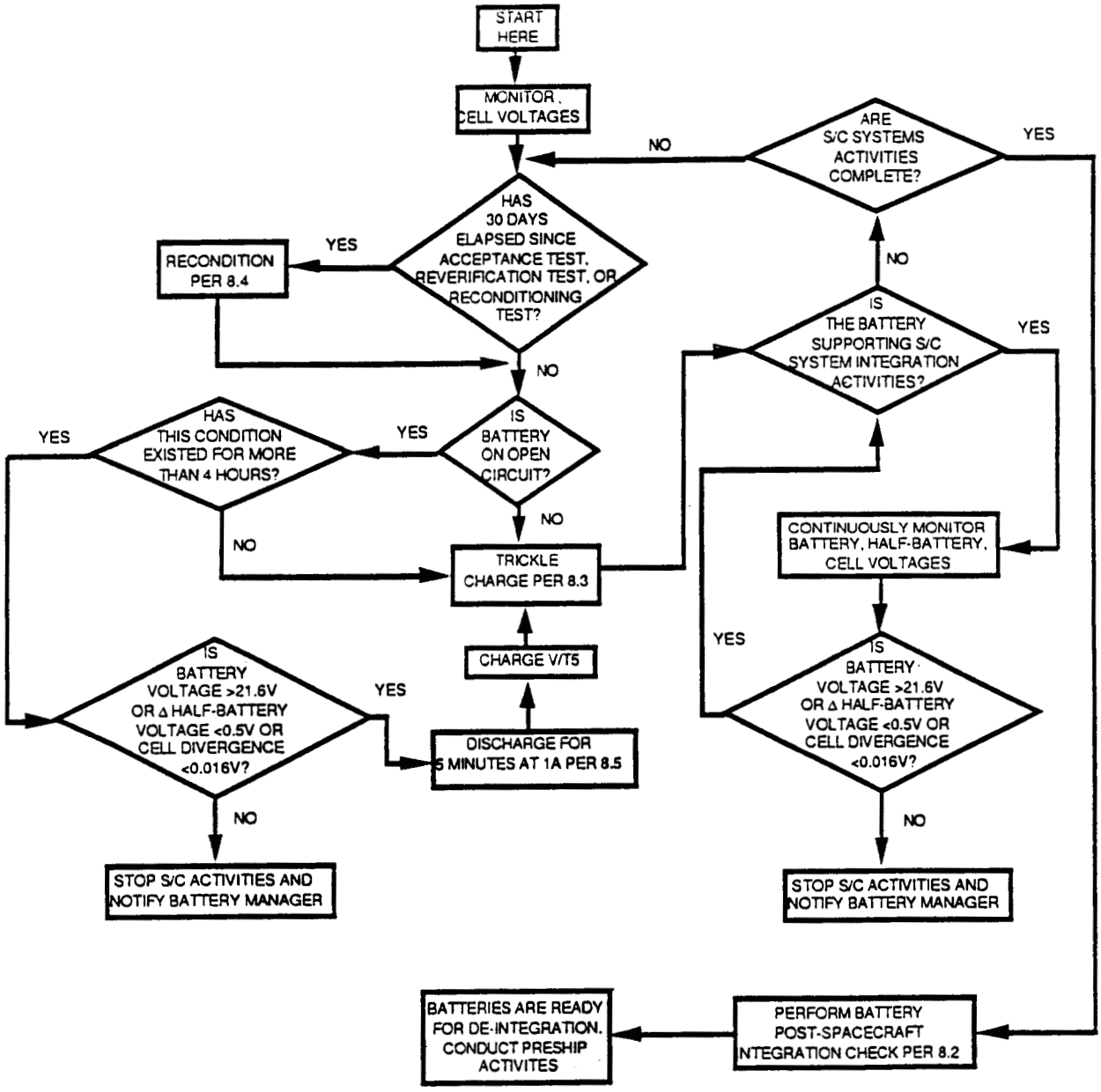

NOTE: SAFETY LIMITS INDICATED ON TABLE 5-1 MUST BE CONTINUOUSLY MONITORED. IN THE EVENT THAT ANY SAFETY LIMIT IS EXCEEDED, DISCONTINUE TEST AND CONTACT THE BATTERY MANAGER OR HIS REPRESENTATIVE.

FIGURE 8-1 SPACECRAFT SYSTEM TEST AND CHECKOUT ACTIVITIES

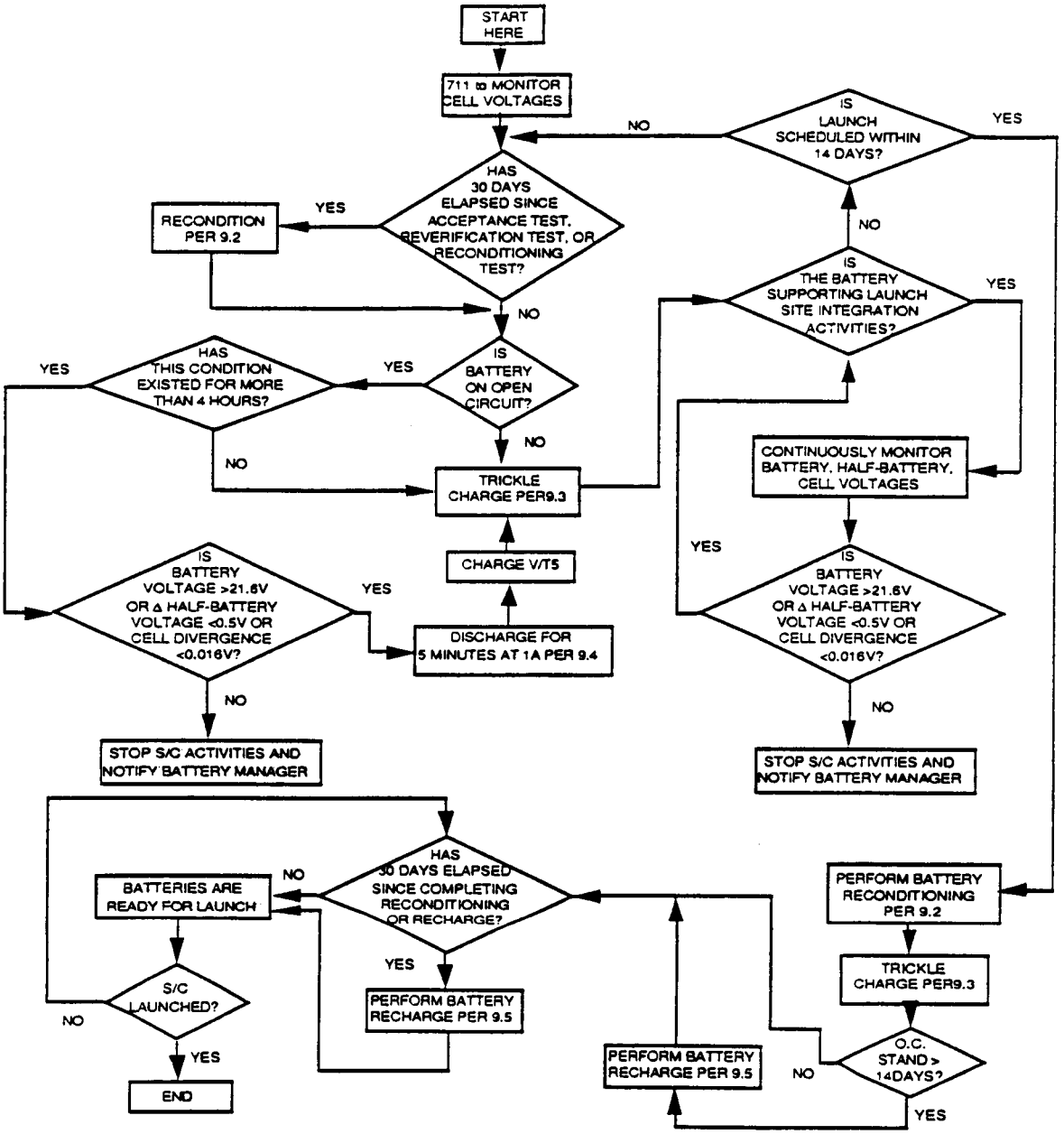

NOTE: SAFETY LIMITS INDICATED ON TABLE 5-1 MUST BE CONTINUOUSLY MONITORED. IN THE EVENT THAT ANY SAFETY LIMIT IS EXCEEDED, DISCONTINUE TEST AND CONTACT THE BATTERY MANAGER OR HIS REPRESENTATIVE.

FIGURE 9-1 SPACECRAFT LAUNCH SITE ACTIVITIES

- SIGNIFICANT PROBLEMS/ANOMALIES DURING I&T

  - GSE Test Connector Connected To Spacecraft Bottom Deck Damaged While Battery Charging During Other I&T Activities in SES Chamber

  - Battery Cells Manufacturered with 2536 Separator Material Have Slightly Higher Terminal Voltages Than Previously Experienced

  - Many WTR Facilitie's AC Power Wired Incorrectly Caused Damage To GSE And Test Delays

- WAIVERS/DEVIATIONS

  - Replaced Suspect 2505 Cell Separator Material In Battery Cells With 2536 Separator Material During Manufacture.

  - Added 3 Wires To Battery Positive and Negative Terminals To Support Termination Points on COBE Power System Electronics

  - Implemented V-Notch To Maintain Battery Vibration Level at ± 3db Flight Specification During Acceptance at Manufacturer's Facilities

  - Accepted Batteries With Cracked (Cosmetic) Thermal Fins Following Manufacturer's Vibration Test

  - Added In-Line Fuse Assemblies Between Battery and Spacecraft Harness To Prevent Possible Spacecraft Damage Due To Harness Shorts.

  - Normal Manufacturing Procedures Had To Be Modified To Avoid To Avoid Contamination Of Spacecraft By Use Of Thermal Grease During Test And Evaluation

- ON-ORBIT PERFORMANCE VS SPECIFIC REQUIREMENTS

  - **Battery Trickle Charge Performance Excellent:**

DATA	ON-ORBIT	SPECIFIC REQUIREMENTS
Cell Voltage	1.43V ±10%	1.43V ±10%
Half Batt. V_Delta	0.000V To 0.007V	-0.5V To 0.5V
Batt. Temp.	12 To 15 Deg. C.	0 To 20 Deg. C.

  - **Battery Life Is Currently Expected To Be 3 Years Or More Due To The excellent Performance Observed Since Launch And Lower Mission Loads Than Initially Predicted**

  - **Spacecraft Thermal-Vac Battery Data Shows Slightly Higher Cell Voltage Than Former Aerospace Batteries**
  - **Anticipate Use Of Slightly HighVoltage/Temperature (VT) Levels During Battery Recharge In Orbit .**

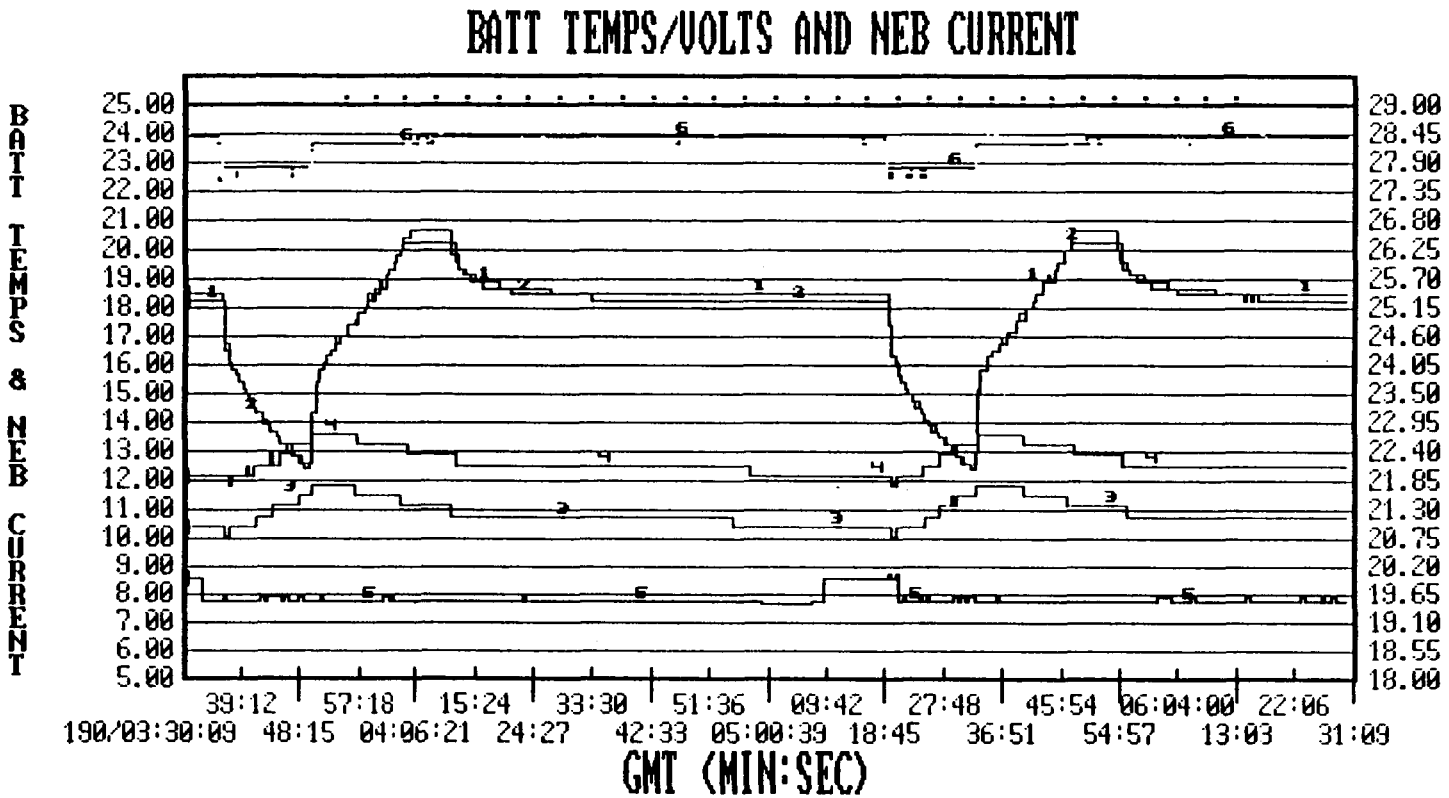

ITEM	MNEMONIC	VALUE	FLAGS	BAD QUALITY	OFF SCALE	SCALE SIDE
1	'B1U	To us	the	0	0	RIGHT
2	PB2U	fo	MTM	0	0	RIGHT
3	'B1T	fo	Rel	0	0	LEFT
4	PB2T			0	0	LEFT
5	PNEBI	To us	a r	0	0	LEFT
6	PEBUC	fo	MTM	0	0	RIGHT

RUN-TIME COMMANDS

CTRL-F6:Activate Page
CTRL-F7:Restart Plot
CTRL-F8:Stop Plot
ALT-F1:ISC Terminal
ALT-F4:Setup Screen

ALT-F10:Quit

Plot started.

PAGE COMPLETE

COBE;ECLIPAGE;G; 155/15/06/01.034;O 02773;S TDE;F 085;FMT B-SCI;SRC R/T;AP 5; P

```
******* BATTERY 1 ********

PB1AH              ON      G
PB1UVDT          ENBL      G
PB1VTLVL         VT-7      G
PB1AHLVL          106      G
PB1V           23.16   V
PB1VTCON         NORM      G
PB1PI            5.83  AM
PB1NI              .0  AM  *
PB1AHSOC      100.00   PC  *
PB1BAL          .007   V
PB1T           12.57   C

*** PWR SYSTEM ELEC ****

PSECMD            LIM     G

** BOOST REGULATORS ****

PBREGS            ABC     G

*** ACE ECLIPSE CONFIG ***

ACELIP
A2AUT             DSBL    G
ASS2XGY
AXGYROSL          G-AX    G
```

```
******* BATTERY 2 ********

PB2AH              ON      G
PB2UVDT          ENBL      G
PB2VTLVL         VT-7      G
PB2AHLVL          106      G
PB2V           23.27   V
PB2VTCON         NORM      G
PB2PI            5.75  AM
PB2NI              .0  AM  *
PB2AHSOC      84.70   PC
PB2BAL          .007   V
PB2T           14.31   C

** INST OT PROTECTION **

PDOTPRLY          BOTH    G

****************** ACS ECLIPSE DATA ******************

AECLPST
ASS1SUNP           SUN     G
ASS2SUNP  NODATA           NOF
ASS1ID              AB     W
ASS2ID    NODATA           NOF
ASUNSPRT          .833
```

```
* SA & SHUNT CURRENT **

PSAI           39.19  AM
PSHI             .0   AM  *

******* BUS STATUS *******

PNEBI            8.64  AM
PNELDA           ENBL      G
PNELDB           DSBL      G
PNEBOCDT         ENBL      G
PBUVDT           ENBL      G
PEBUV              OK      G
PEBI           12.10   AM
PEBUC          28.29    V
PEBUF          28.25    V

* ROLL & PITCH ANGLES **
AROLLANG        -4.88   DG
APTCHANG        -8.91   DG

ASUNAZ           5.57   DG
ASUNEL           4.88   DG
ASUNPAZ          5.57   DG
ASUNPEL          4.88   DG
AXGYROAZ       -40.00   DG
AXGYROID         P-AB       W
```

15:06:06 M:4 ******** THERMAL SUBSYSTEM CHECK COMPLETE ********

COBE-ECLIPSE OPERATIONS

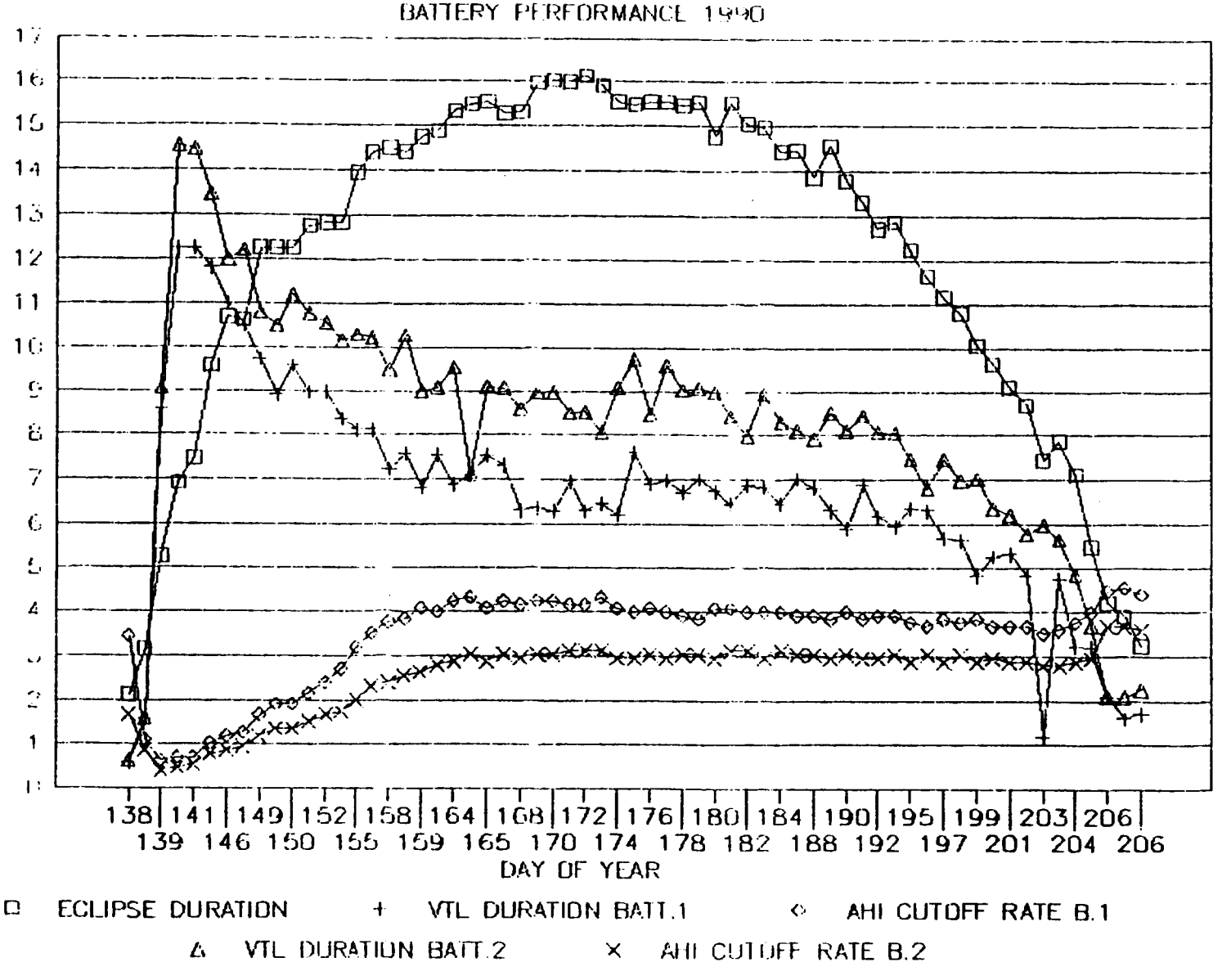

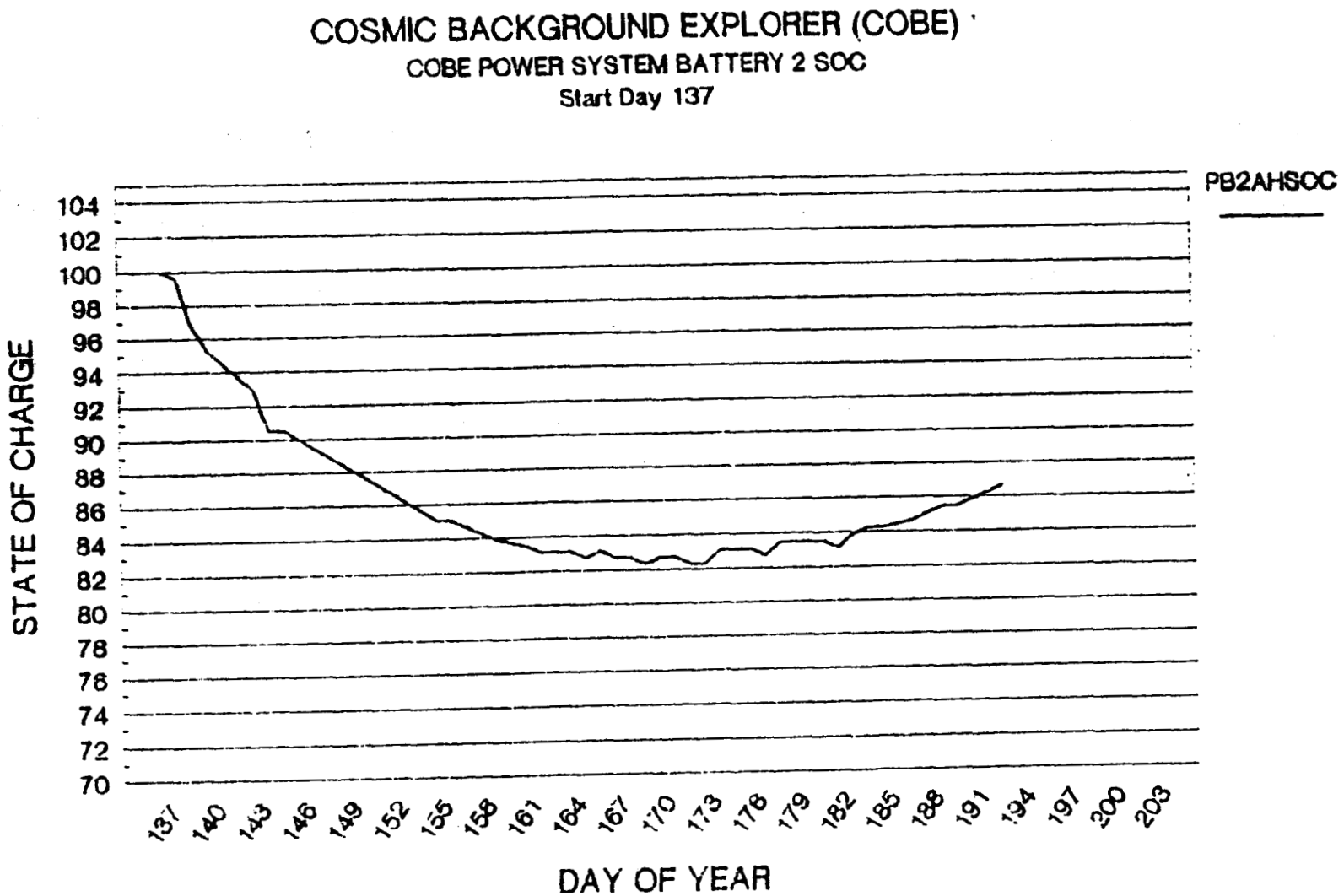
COSMIC BACKGROUND EXPLORER (COBE)
COBE POWER SYSTEM BATTERY 2 SOC
Start Day 137
PB2AHSOC
STATE OF CHARGE
104
102
100
98
96
94
92
90
88
86
84
82
80
78
76
74
72
70
137
140
143
146
149
152
155
158
161
164
167
170
173
176
179
182
185
188
191
194
197
200
203
DAY OF YEAR

COSMIC BACKGROUND EXPLORER (COBE)
COBE POWER SYSTEM BATTERY 1
Start Day 137
PB1V
PB1T
TEMPERATURE
14
12
10
8
6
VOLTAGE
28
26
24
22
20
137
140
143
146
149
152
155
158
161
164
167
170
173
176
179
182
185
188
191
194
197
200
203
206
DAY OF YEAR

- LESSONS LEARNED

  - Newly Designed Battery GSE Failsafe Systems Proven Effective During Several I&T Mishaps

  - Use Of Non-Flight Batteries During Portions Of I&T Provided Experience Necessary For Launch Support Activities

  - Fully Trained Battery Personnel Must Be Present For All Flight Battery Operations

  - Always Coordinate SubSystem Activities With The Spacecraft Structural Engineering Group, Quality Assurance, Contamination Control Etc. To Prevent Operational Impacts

  - Personally Check AC Power In Test Facilities With A Meter For Correct Voltages And Phasing

  - Ascertain That AC Power Provided For GSE Is Independent and Not Shared By Other Users

END-OF-LIFE EVALUATION OF THE SOLAR MAXIMUM MISSION BATTERIES

1990 NASA BATTERY WORKSHOP

DECEMBER 4 1990

DORIS JALLICE & THOMAS YI
SPACE POWER APPLICATIONS BRANCH
NASA/GODDARD SPACE FLIGHT CENTER

AGENDA

- **BACKGROUND**
- **TESTS PERFORMED**
  - V/T Tests
  - Battery Rundown Test
  - Post Solar Array Jettison Battery Rundown Test

SMM BACKGROUND

- PURPOSE: MONITOR & OBTAIN DATA ON SOLAR FLARES DURING THE PART OF THE 11-YEAR SOLAR CYCLE, AKA SOLAR MAXIMUM
- LAUNCHED 2/14/90
- TWO YEAR MISSION LIFE
- SMM REPAIR MISSION OF ACS (4/84) VIA STS 41-C
- STS MISSION UNAVAILABLE TO BOOST SMM TO A HIGHER ALTITUDE
- PROVIDED A UNIQUE OPPORTUNITY TO PERFORM END-OF-LIFE ENGINEERING EVALUATION TESTS
- S/C BURNED-UP 12/2/89

SMM OBSERVATORY ON FSS

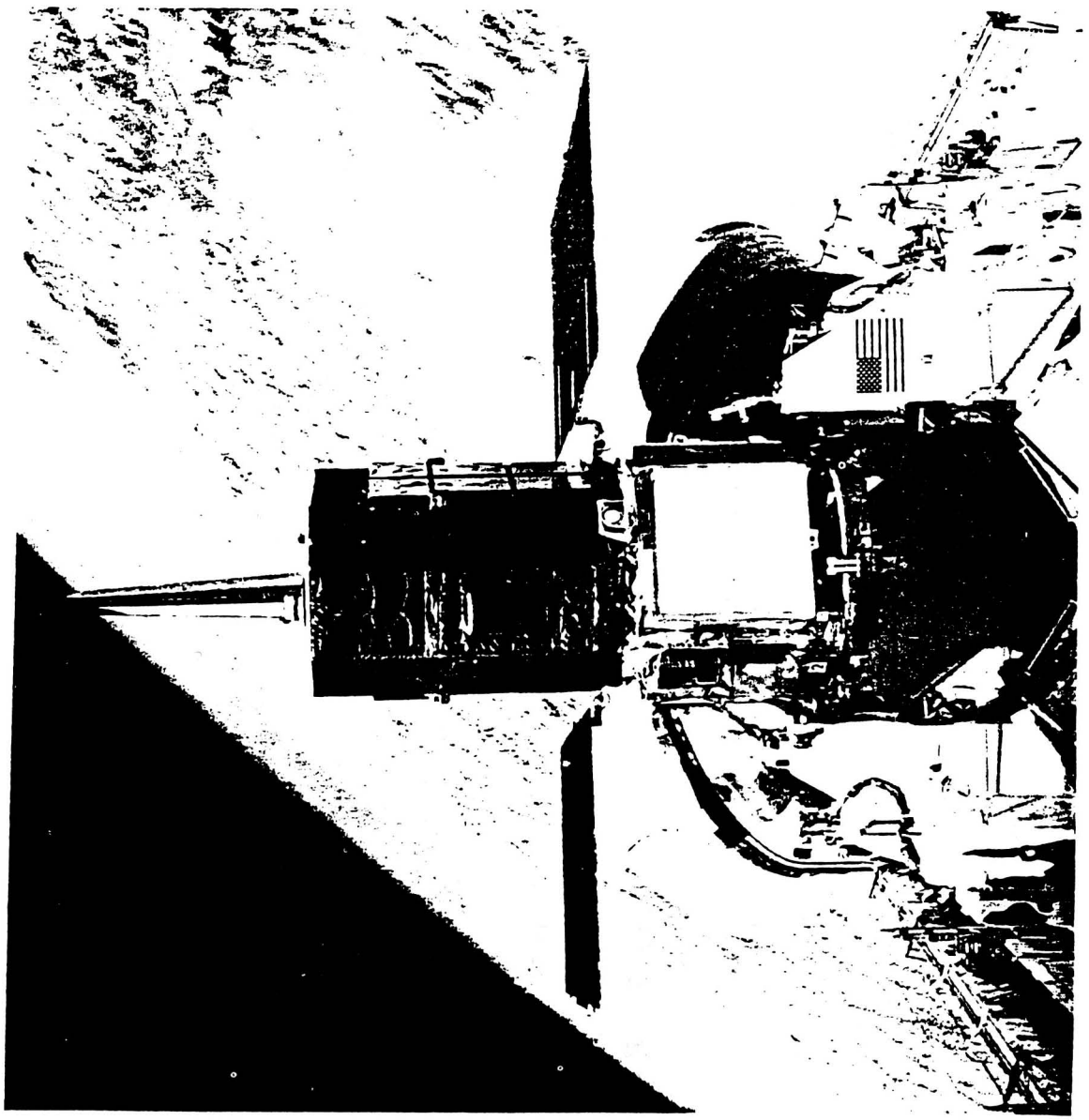

ORIGINAL PAGE IS
OF POOR QUALITY

BATTERY BACKGROUND

- **SMM CONTAINED 3 NASA STANDARD 20AH BATTERIES**
  - Contained within 1 MPS Manufactured by MDAC
  - Each Battery Contained 22 20Ah Cells Manufactured by GE Battery Division
- **BENIGN ENVIRONMENT**
  - 16% DOD
  - 0 - 5°C
  - 92 Min Orbit (36 Min Chg/56 Min Dischg)

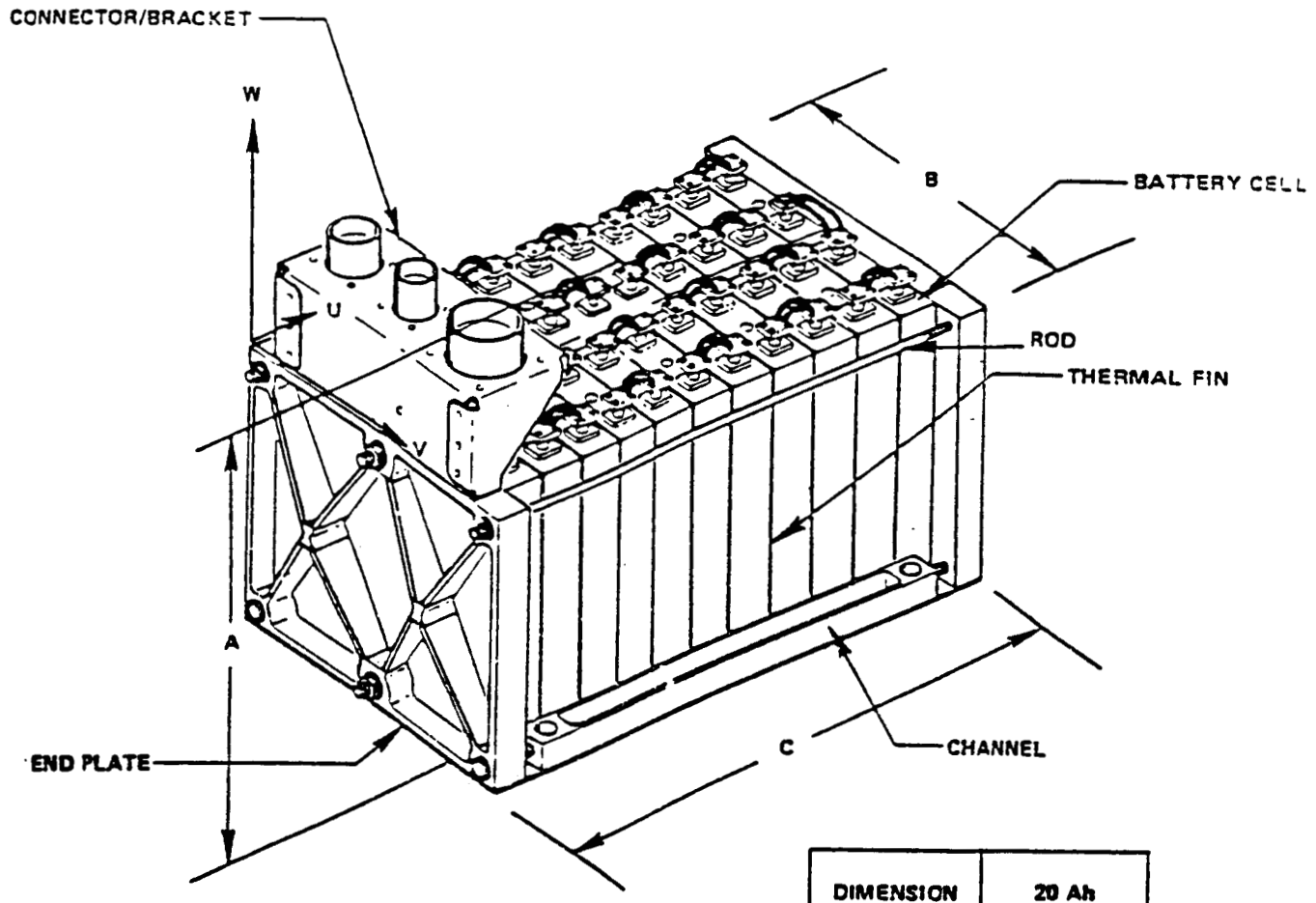

DIMENSION	20 Ah
A	24.96 cm
B	19.88 cm
C	34.87 cm

Figure 2a. Multimission Modular Spacecraft (MMS) Nickel-Cadmium Battery

BATTERY TEST OBJECTIVES

- **TO ESTABLISH PERFORMANCE OF THE BATTERIES AFTER 10 YEARS OF OPERATION, AND TO PROVIDE A REAL-TIME DEGRADATION ANALYSIS**

- **TESTS PERFORMED**
  1) V/T Level Confirmation Test
  2) Battery Rundown Test - "Preliminary"
  3) Battery Rundown Test - Post Solar Array

V/T LEVEL CONFIRMATION TEST

- **TO DETERMINE OPTIMUM V/T LEVEL FOR OPERATION**
  - Began at V/T 4 , Then 5 --> 6 --> 5 --> 4 --> 3 --> 2 --> 4
  - Batteries Allowed to Stabilize at Each V/T for 7 Cycles Min
  - Analyzed Battery Current Sharing, Cell Voltage Uniformity, Temperature Effects, and C/D Ratios

- **OBSERVATIONS**
  - V/T 4 Operation is Acceptable for SMM Operation
  - V/T 5 Also Can Be Used Without Penalty
  - V/T 6 is Not Recommended Because of Elevated Temperatures at Cycling at This Level
  - V/T 2 and 3 Caused Large Deviations in ΔV at EOD

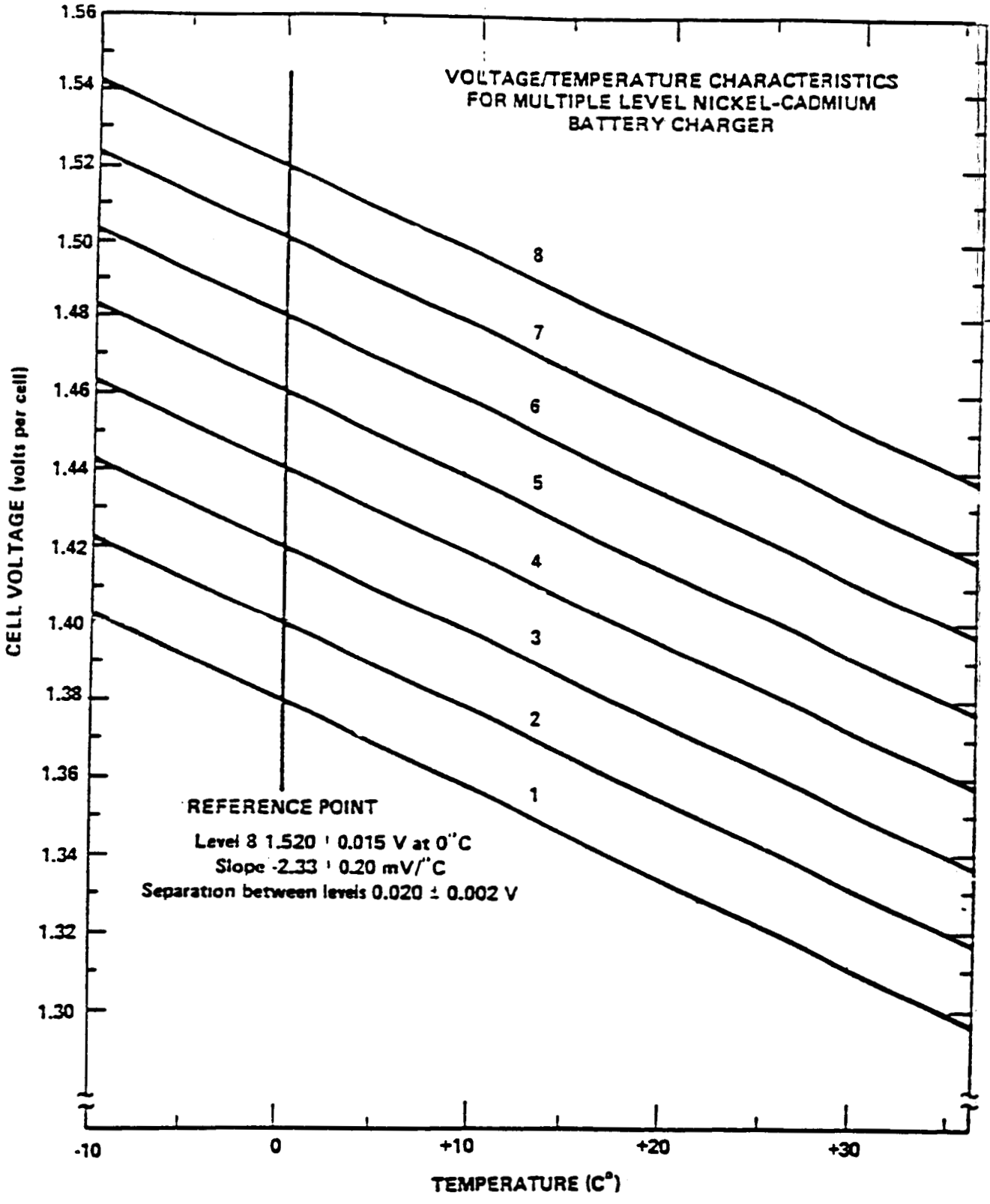

Figure 3. Cell Voltage Limit Versus Temperature

NUMBER OF ORBITS AT EACH V/T LEVEL

Test Condition	V/T Level	# Orbits
1	4	Starting Point
2	5	7
3	6	8
4	5	23
5	4	46
6	3	14
7	2	12

TABLE 4

EOC & EOD CURRENT AND CAPACITY

Charge		V/T LEVEL						
		4	5	6	5	4	3	2
EOC (AMPS)	I_1	0.5	0.6	0.84	0.6	0.56	0.6	0.69
	I_2	0.5	0.6	0.82	0.6	0.57	0.61	0.71
	I_3	0.49	0.6	1.01	0.7	0.54	0.56	0.67
Input	AH_1	3.58	3.71	3.85	3.71	3.70	3.72	3.59
	AH_2	3.66	3.78	3.88	3.75	3.76	3.81	3.70
	AH_3	3.63	3.82	4.01	3.81	3.82	3.93	3.93

Discharge		4	5	6	5	4	3	2
EOD (AMPS)	I_1	-5.2	-5.6	-5.6	---	-6.0	-5.6	-4.4
	I_2	-5.2	-5.6	-5.6	---	-6.0	-5.2	-4.0
	I_3	-5.2	-5.6	-5.6	---	-6.4	-5.6	-4.4
Output	AH_1	3.16	3.28	3.2	---	3.21	3.21	3.27
	AH_2	3.16	3.30	3.19	---	3.22	3.24	3.41
	AH_3	3.16	3.31	3.17	---	3.27	3.41	3.68

TABLE 5

EOC/EOD VOLTAGE

V/T Level	EOC Cell Volts	EOD Cell Volts
4	1.43	1.18
5	1.44	1.19
6	1.45	1.21
5	1.44	1.19
4	1.43	---
3	1.40	1.14
2	1.39	1.11

TABLE 6

BATTERY DIFFERENTIAL VOLTAGE RANGE

V/T Level	ΔV (Millivolts)	
	Maximum During Charge	Maximum During Discharge
4	28	33.6
5	28	33.6
6	28	44.8
5	28	33.6
4	22.4	33.6
3	28	112.0
2	22.4	134.4

TABLE 7

BATTERY AVERAGE TEMPERATURES

V/TLevel	T_1 (°C)	T_2 (°C)	T_3 (°C)	ΔT_{2-3} (°C)
4	3	1.5	5	3.5
5	5	3	7	4
6	8	6.5	11	4.5
5	6	4.5	8	3.5
4	4	3	6	3
3	3	2	5.5	3.5
2	3	2	6	4

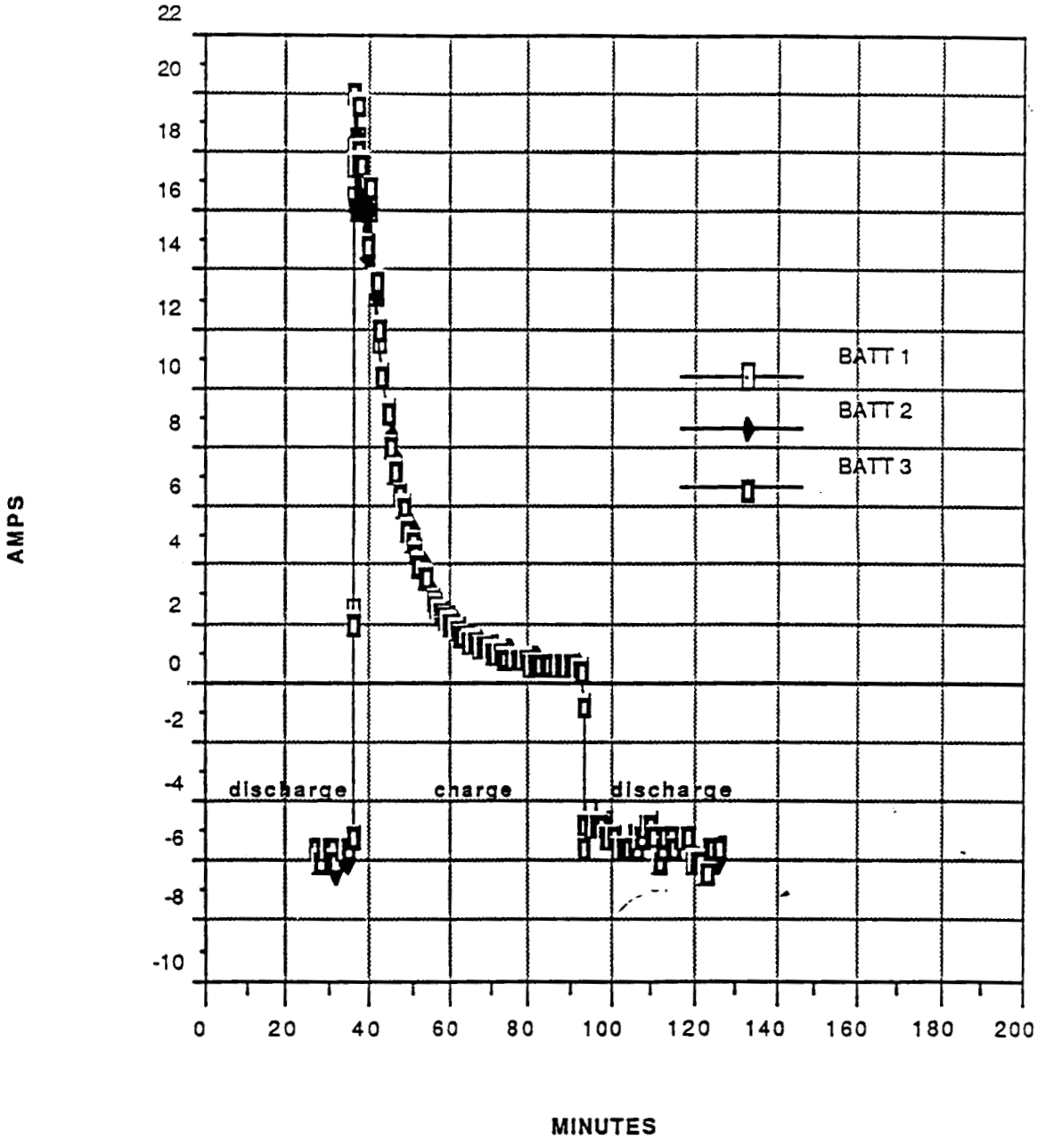

Figure 4. SMM V/T Level 4 Battery Current

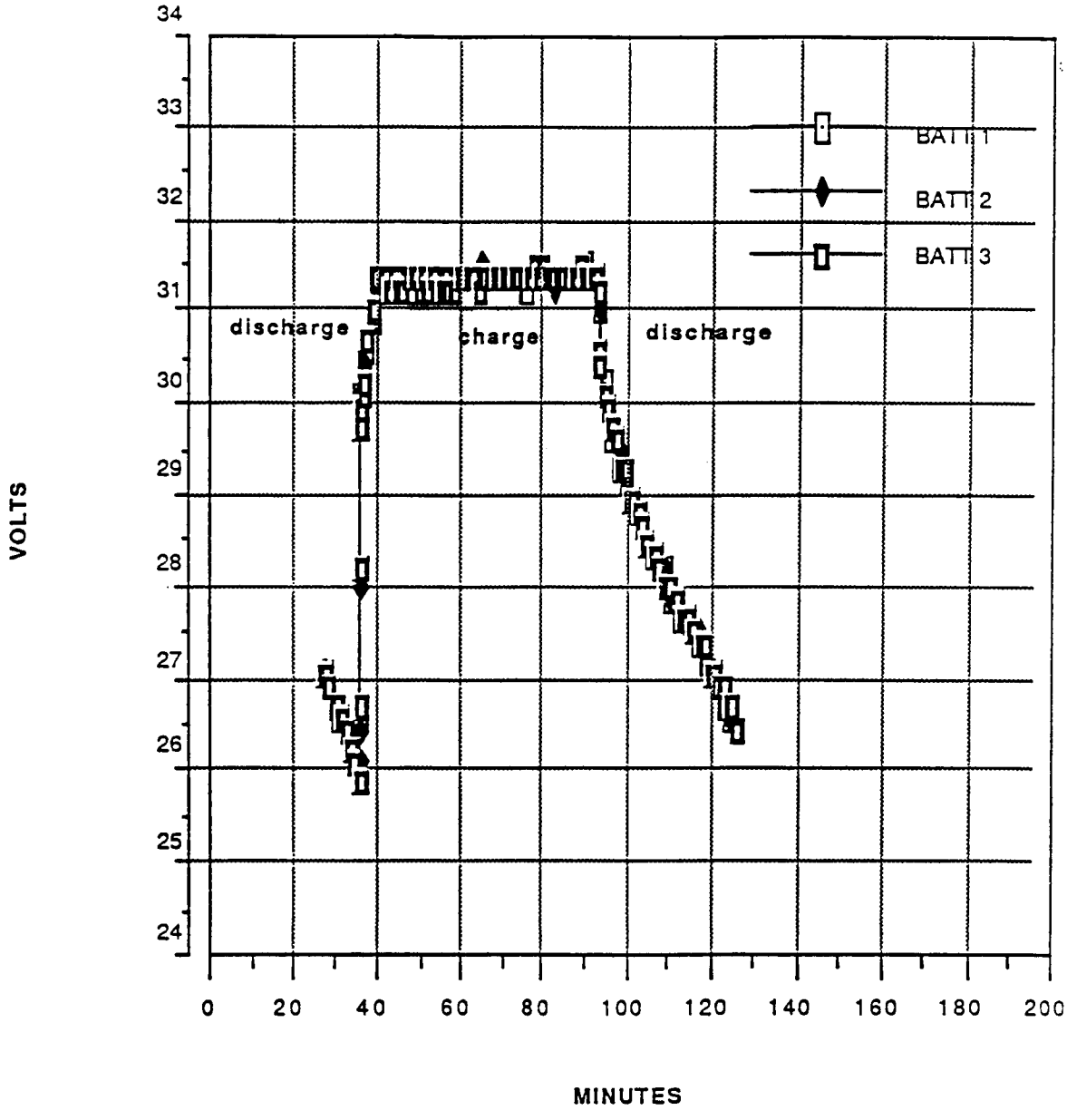

Figure 5. SMM V/T Level 4 Battery Voltages

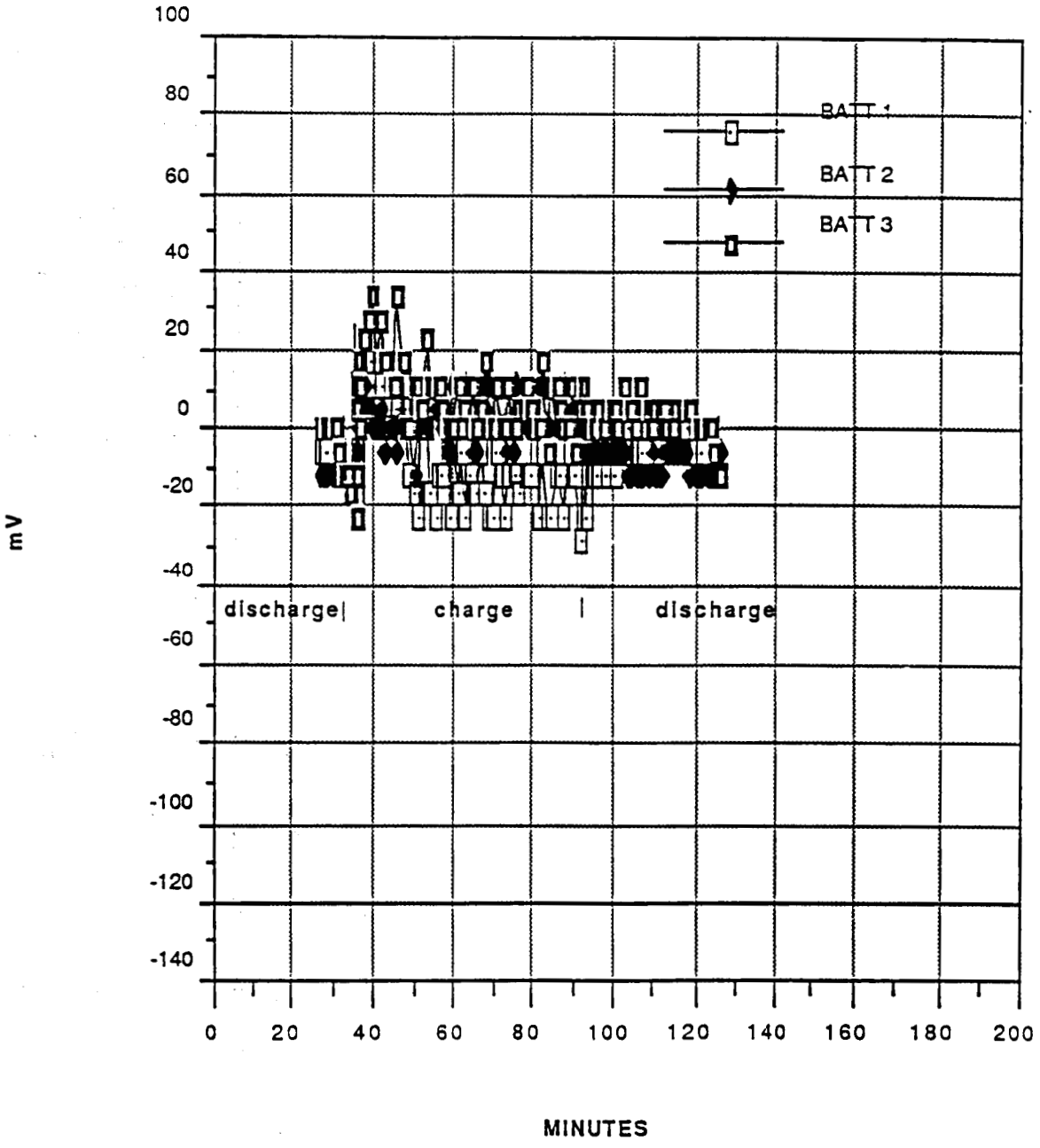

Figure 7a. SMM V/T Level 4 Differential Battery Voltages

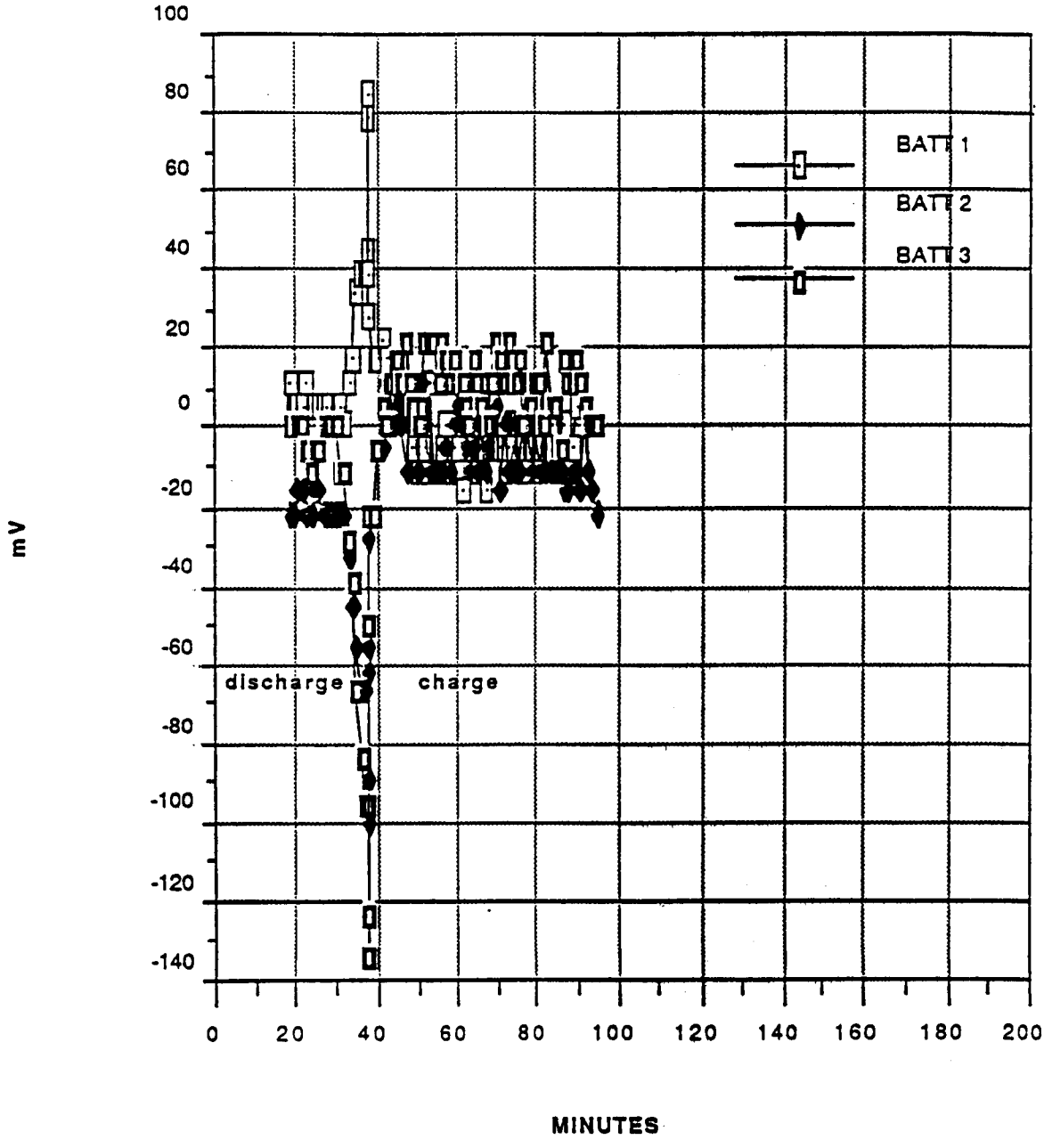

Figure 7c. SMM V/T Level 2 Differential Battery Voltages

BATTERY RUNDOWN TEST - "PRELIMINARY"

- **TO DETERMINE 2ND PLATEAU AND AS A PRECURSOR TO POST SOLAR ARRAY JETTISON TEST**
  - S/C Slewed 90° for 15 Min Upon Entering Day, Then Slew Back 90° (5°/Min)

- **OBSERVATIONS**
  - Additional 2.4Ah Removed During 15 Min 90° Slew for a Total of 5.6Ah
  - Average EODV 23.52V (1.07V/Cell)
  - ΔV in the 20mV Range
  - Inconclusive Result --> Decided Not to Continue with a Longer Slew Period

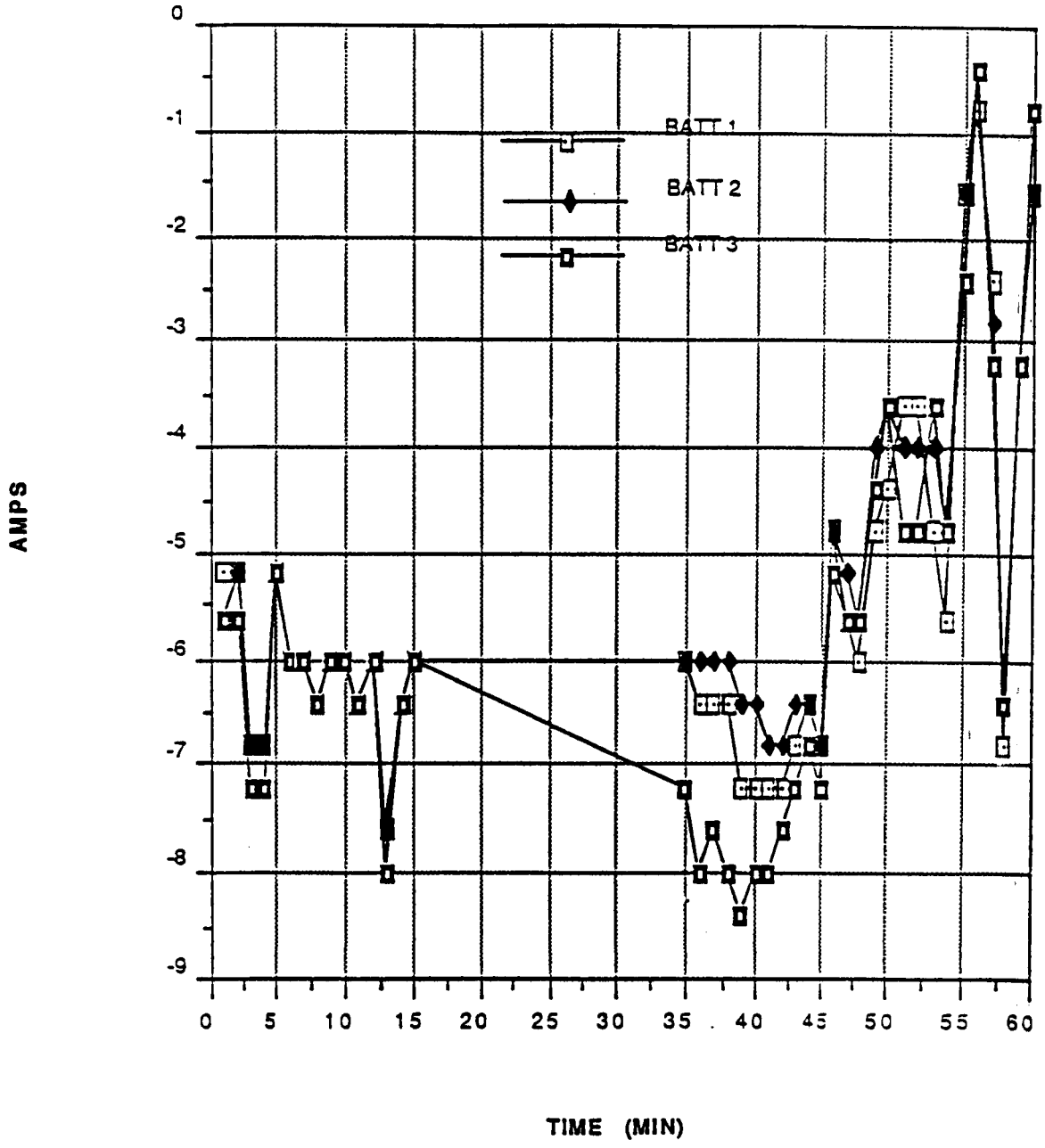

Figure 10. Battery Currents from SMM Rundown

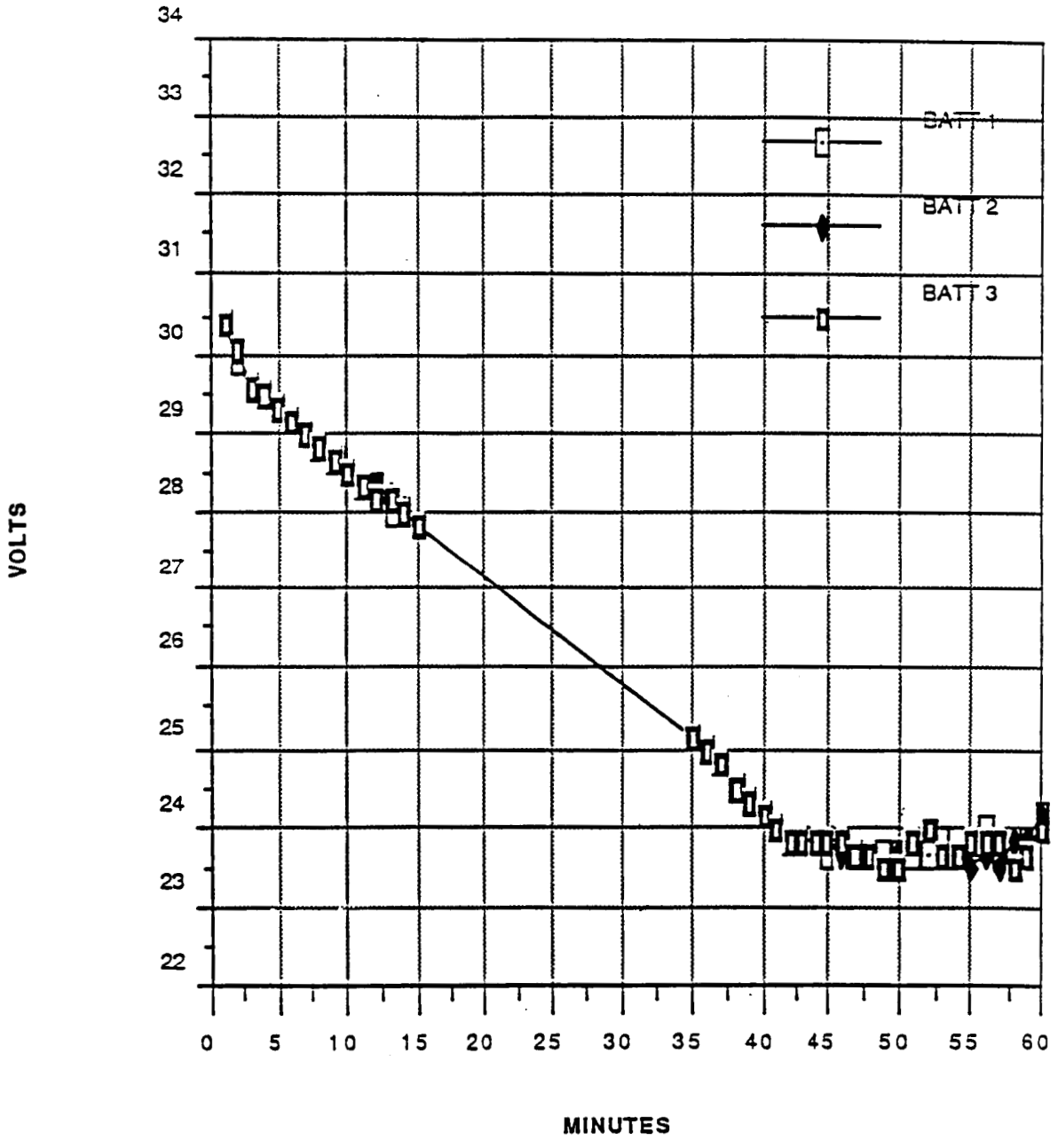

Figure 11. Battery Voltages from SMM Rundown

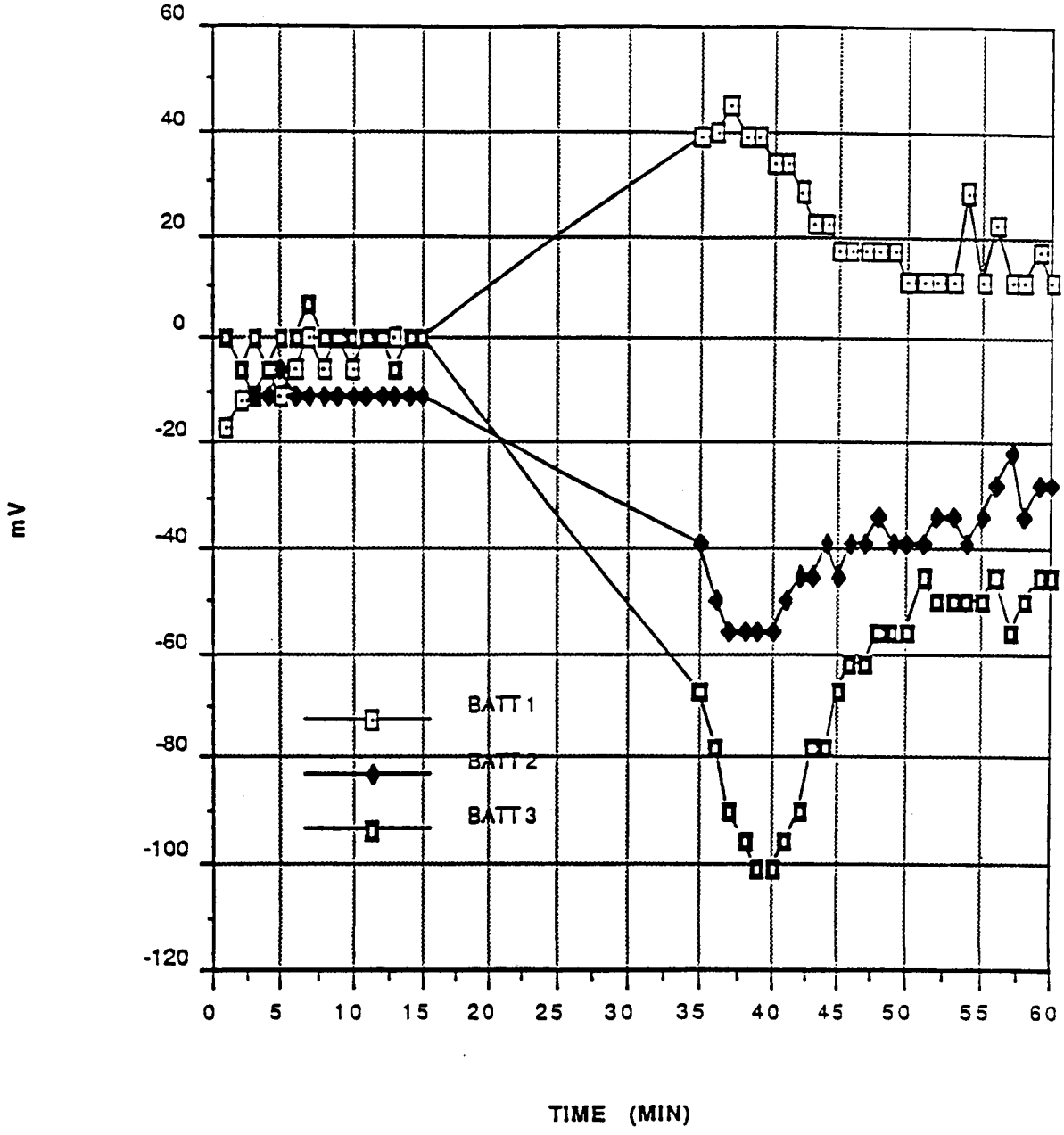

Figure 12. Differential Battery Voltages from SMM Rundown

BATTERY RUNDOWN TEST - POST SA JETTISON

- **TO DETERMINE ACTUAL CAPACITY OF THE SMM BATTERIES**
- **EVENTS**
  - Command Sent to Jettison SA: 16:51:39Z 11/24/89
  - When SMM Came in View of NORAD Site, Only One SA Jettison Confirmed
  - At the Next NORAD Site, Other SA Jettisoned
  - Final Contact With SMM: 20:40:00Z
  - Next NORAD Site, No Telemetry from SMM: 22:07:00Z
- **OBSERVATIONS**
  - 16.5Ah Obtained Until Loss of Telemetry at Last NORAD Site
  - Voltage Plateau around 22.72V/Battery (1.03V/Cell)
  - ΔV around 20mV
  - "Beneficial" Reconditioning Effect of Earlier Rundown Test

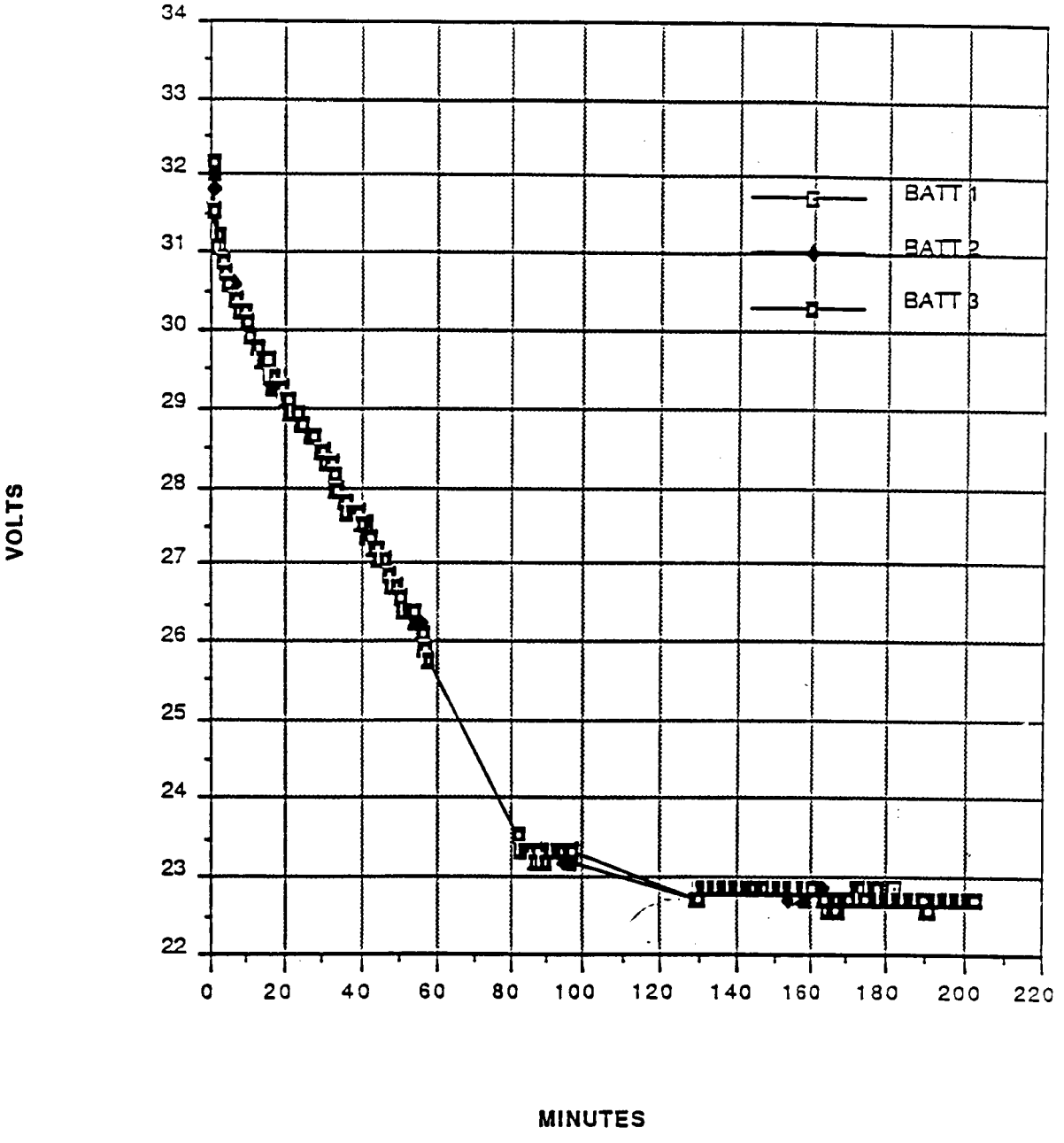

Figure 15. SMM Post Array Jettison Battery Voltages

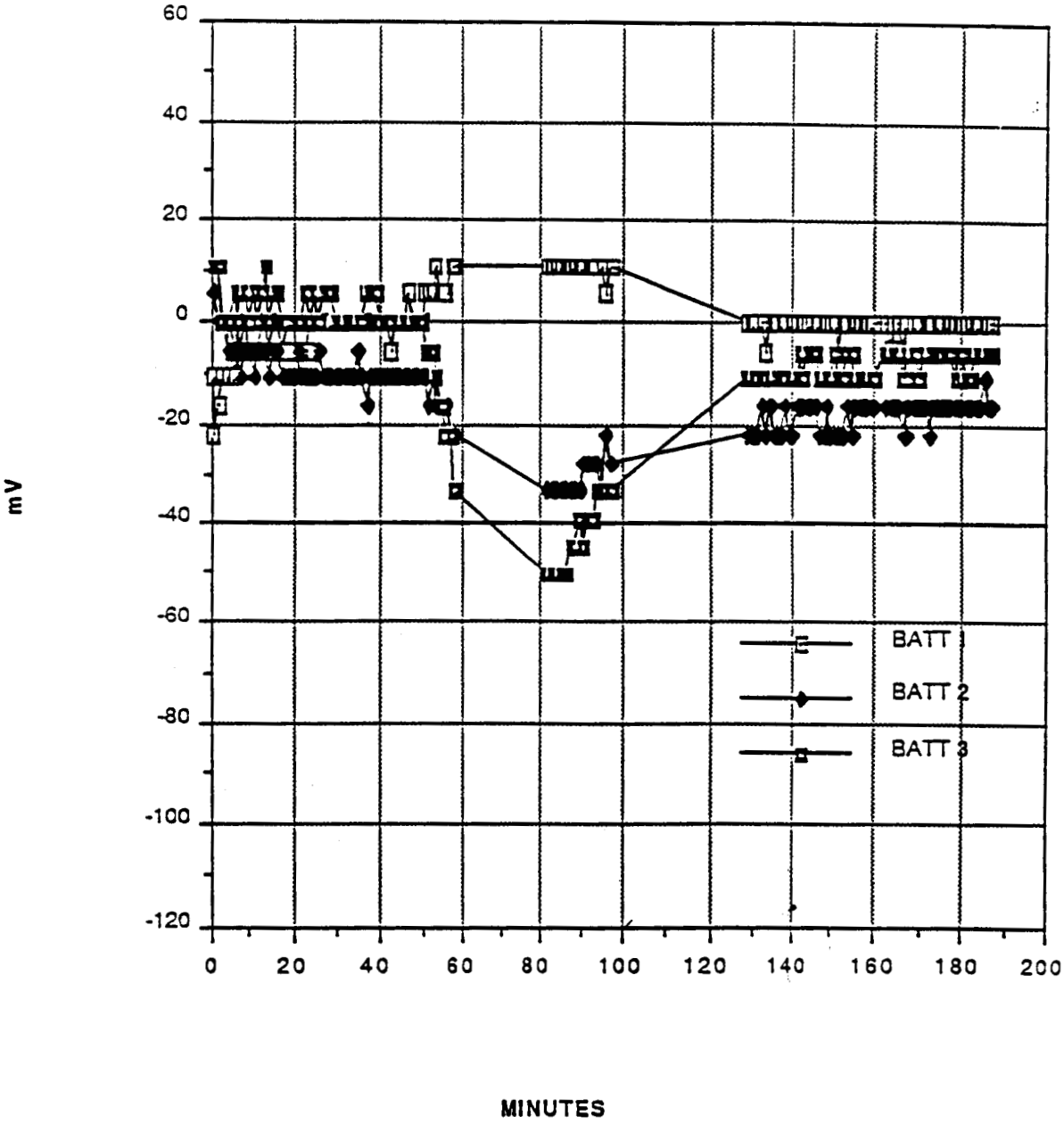

Figure 17. SMM Post Array Jettison Differential Battery Voltages

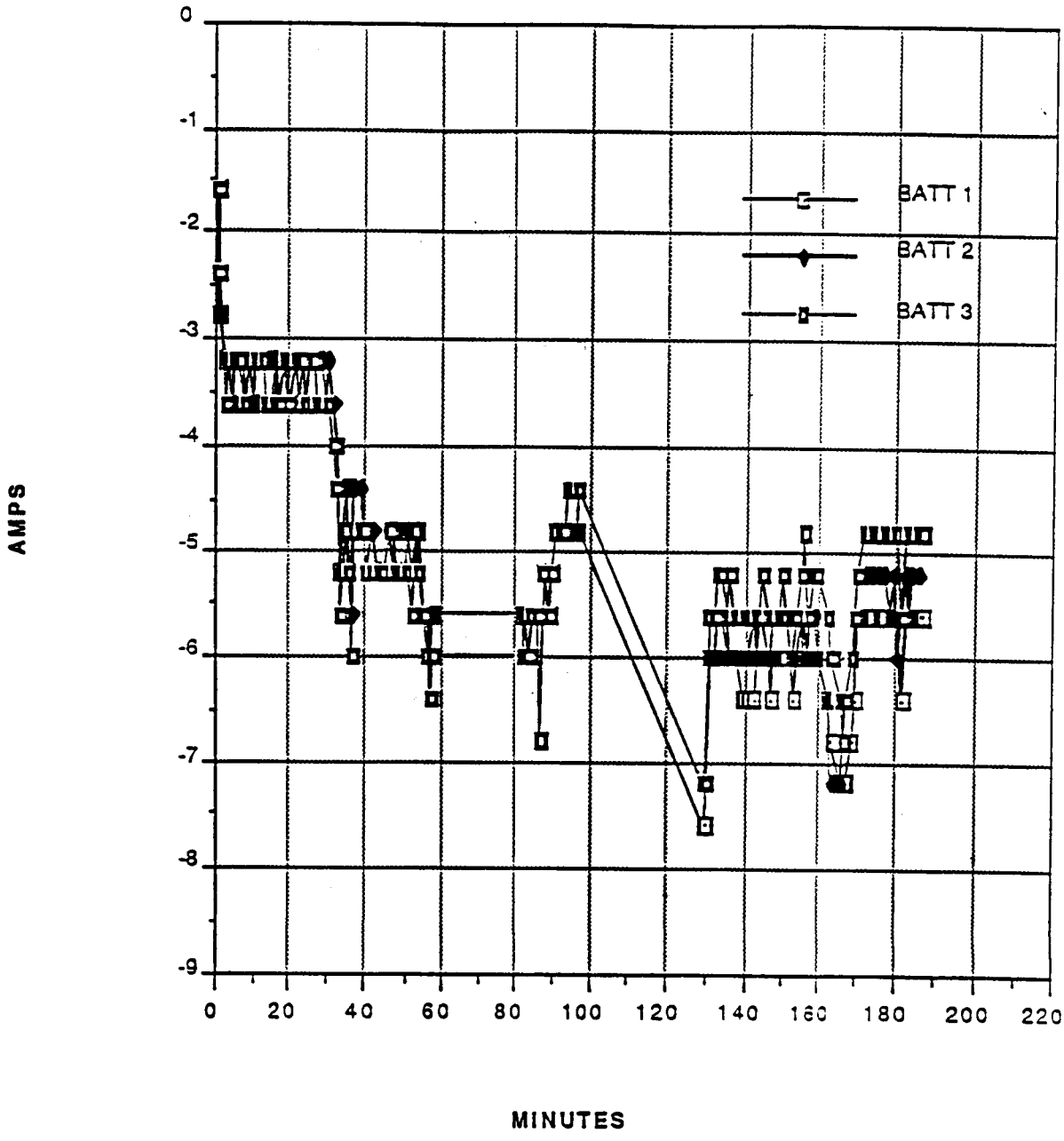

Figure 14. SMM Post Array Jettison Battery Currents

MAGELLAN BATTERY OPERATIONS: AN OVERVIEW

BY PAUL TIMMERMAN AND PETER GLUCK

JET PROPULSION LABORATORY,
CALIFORNIA INSTITUTE OF TECHNOLOGY
PASADENA, CALIFORNIA

1990
NASA AEROSPACE BATTERY WORKSHOP

DECEMBER 4, 1990, HUNTSVILLE, ALABAMA

MAGELLAN BATTERY OPERATION: AN OVERVIEW

Paul J. Timmerman and Peter R. Glück

Jet Propulsion Laboratory
California Institute of Technology
Pasadena, California

ABSTRACT

The Magellan Spacecraft's mission to map Venus's surface provides a unique application for Nickel-Cadmium batteries. An overview of the spacecraft, power subsystem, and battery and the mission unique requirements are presented. The reliability and performance of the batteries were extensively studied with a comprehensive test and analysis programs. Actual data for cruise and a limited number of mapping orbits is also presented.

MISSION DESIGN

Magellan is a NASA sponsored Venus radar mapping mission. The radar is the only instrument onboard the unmanned probe. It can look through the carbon dioxide and sulfuric acid atmosphere to study the Venusian surface. The trip to Venus required delivery to low earth orbit by the space shuttle, and earth orbit ejection via the Inertial Upper Stage (IUS). Magellan (MGN) took a path one and one-half times around the sun, taking 460 days of cruise to reach Venus. Figure 1 is a trajectory diagram. After Venus Orbit Insertion (VOI), the spacecraft enters a highly elliptical polar orbit of 3.1 hour period. Figure 2 describes a typical mapping orbit. The mapping orbit has periods of solar occultation that vary throughout the mission, due to Venus's rotation about the sun. Figure 3 shows the length of solar occultation period during the mapping mission. The solar intensity at Venus is twice as high as it is at earth. During the closest approach to the planet for each orbit, the radar is turned on for 37 minutes. The geographic features will be recorded for approximately 90% of the planet's surface at resolutions around 120 meters. This primary mission will be accomplished in 243 days, which is the length of one Venus day. Extended missions will be used to fill in data gaps and perform gravity experiments.

SPACECRAFT DESIGN

The MGN spacecraft weighs 3550 Kilograms, is three-axis-stabilized, and uses reaction wheels for attitude control. The primary instrument aboard MGN is a Synthetic Aperture Radar (SAR). The 3.7 meter High Gain Antenna is used for both surface mapping and for earth data playback. The SAR, telecommunications, and some power and attitude control equipment are located in the Forward Equipment Module (FEM). The remainder of the electronics are located in the ten-sided bus structure. Figure 4 shows a diagram of the spacecraft configuration

POWER SUBSYSTEM

The Electrical Power Subsystem (EPS) is a photovoltaic / battery system. Two movable solar panels of 12.6 square meters total area provide about 800 watts at earth, and over 1000 watts at Venus. Energy storage is handled by two twenty-two cell, 26.5 ampere-hour (AH) Nickel-Cadmium batteries. Other components of the EPS include a shunt regulator, a shunt radiator, a 28-volt pre-regulator unit, and a 50-volt AC invertor. A set of eight voltage-temperature (VT) curves are used to provide battery charging control. Figure 5 is a block diagram of the electrical power subsystem. Figure 6 is a comparison of MGN and NASA standard VT curves.

BATTERY DESIGN

The battery design is unusual in several ways. The thermal environment imposed by the Venus orbit is a main driver in the novel battery design. The battery has been designed as an integral part of the FEM structure, using a one-piece, aluminum, "ice-cube tray" design with flying buttresses. The cells are potted into the integral baseplate - battery structure using urethane. The design is a derivative of the Viking Orbiter battery. Figure 7 is a mechanical diagram of the battery structure. Mechanically, this packaging approach provides a rigid spacecraft member and, though the battery mass is high (62 kg) in comparison to other comparable batteries, the overall spacecraft structural mass is reduced with this design. The thermal characteristics are excellent because thermal junctions are minimized and conductive paths are short. Additional thermal rejection capability is obtained by optimizing radiative properties of the integral baseplate. The baseplates are covered with 1 cm by 1 cm optical surface reflectors, (OSRs). The OSRs are 2-mil thick glass tiles with a reflective coating on the underside and a textured surface on the top. Resistor and diode isolation are used for pre-launch charging circuits. This insures mishaps cannot occur while charging in the STS cargo bay.

BATTERY CELL DESIGN

The battery cells were built by Gates Energy Products, Aerospace Division, in Gainesville, Florida. The cell catalog number is 42B030AB15, which implies the cell is of 30 AH capacity. However, the cell is derated by NASA to 26.5 AH based upon total plate area considerations. The cell uses 11 positives and 12 negatives. The positives are passivated, and the negatives are teflonated. The cell is rather traditional, in that it is neither low profile nor lightweight in design. The negative to positive ratio exceeds 1.75:1. The beginning of life interelectrode spacing is 7.4 mils. The cells received 83 milliliters of 31% KOH, which calculates out to 3.13 ml/AH. The cells use the Pellon 2536 separator material, which is a blend of Nylon-6/Nylon-66 fibers inert gas bonded into a non-woven cloth. The weight of the cells is approximately 1180 grams each.

BATTERY PERFORMANCE ANALYSIS

LAUNCH AND DEPLOY PHASE

The spacecraft batteries have provided spacecraft power between separation from the Inertial Upper Stage (IUS) launch vehicle and the point of solar array deployment. During the period before deployment out of the STS cargo bay and during IUS operations, MGN batteries were configured to be connected to the spacecraft power bus. This was to prevent loss of spacecraft power in the event of accidental disconnect of IUS battery power. This presented a problem of estimating the load

sharing by the Silver-Zinc IUS batteries and MGN Nickel-Cadmium batteries. It was also desirable to have enough energy reserves to allow extra revolutions around the earth on battery power. The extra revolutions could be required if the MGN/IUS vehicle could not be ejected from the bay after disconnecting the umbilical supplying STS power. Another concern was the possibility of delaying ignition of the IUS for one or more orbits after STS ejection due to STS proximity limitations or other delays. The final concern was the possible impact of a delay in deploying the solar arrays. Figure 8 is a diagram of the IUS-MGN power interface.

CRUISE PHASE

The Cruise phase is the period of transit from earth to Venus. This phase was originally scheduled to be only 140 days. The launch window was changed, however, to accommodate the Galileo spacecraft, resulting in a 460-day cruise period. The cruise period typically consisted of one attitude update maneuver per day. This caused variation in solar array incidence angle and resulted in a battery discharge typically between 0 and 7% depth-of-discharges, (DOD). The batteries were controlled by MGN VT-curve #3 throughout the cruise period, providing a minimum of overcharge.

ORBITAL OPERATIONS

Detailed energy balance analysis of various points along the mission were performed using the VMPWR[1] software. Estimated spacecraft loads were generated from spacecraft sequence generation software. Attitude control prediction software provided solar array incidence angle data. The MIDAS[2] program was used to predict battery and solar array temperatures and heater power. The VMPWR software calculates total load, solar array performance, and battery current as a function of system voltage. The results were charge/discharge rates and times, DOD's, and states-of-charge (SOC) for key points in the mapping mission. Figure 9 shows a plot of predicted DOD's across the mapping mission.

The energy balance analysis facilitated the design of a unique battery mission simulation test. The mission simulation test used variations in occultation times, and solar array incidence angles, and charge-discharge rates. The result is a highly variable DOD, often with several distinct charge discharge periods per orbit.

CELL TESTING

DEVELOPMENTAL TESTING

Extensive battery test programs have been organized at the system integrator, Martin Marietta Astronautics Group, Denver, Colorado, and at JPL, Pasadena, California. Early development tests in Denver were used to help guide the design phase. A prime example is the One-Battery Out Test. A requirement for sustaining performance with one battery lost led to an 80% DOD test on some prototype cells. The cells lasted for about 700 cycles, which was short of the 1800 cycles required. This test demonstrated to project management the need to increase battery capacity from the planned 20 AH to 26.5 AH.

Differences between the Magellan VT curves and the standard NASA curves were a source of some concern. The 3.1 hour orbit was also non-standard. A parametric test was run using various VT curves and temperatures. This test showed the MGN VT curves were acceptable across the range of flight allowable temperatures. In addition, it proved that fairly low VT curves could be used in cruise and in mapping operation due to the time available for recharging.

Concerns over the ability to meet the SAR input voltage requirement during SAR bursts resulted in the Pulse Discharge-Characterization Test. The typical SAR duty cycle results in peaks of up to 13 amperes on the unregulated DC bus. The test was performed with battery cells on a simulated spacecraft bus, with matched inductance, capacitance, and impedance. A dynamic load bank was used to simulate the SAR and spacecraft loads. The test was run in a parametric fashion, with steady-state and peak loads the primary variables. See Figure 10 for sample results. The results showed that the radar input voltage requirement might be a problem, and the effect of cell end-of-discharge voltage degradation must be known to fully access the risk.

LIFE TESTING

A mission simulation test run at Martin Marietta used early spacecraft load and solar array predictions to determine the battery charge/discharge profile. This test consisted of four different regimes, representing four periods of the mapping mission. Each regime included four distinct charge or discharge phases, which best modelled the predicted regime. The test was run for almost three complete 240 day missions, with discharge voltages degrading badly into the second extended mission.

The need to demonstrate reliability before launch prompted the 40% DOD LEO test. The six cells completed 2400 cycles in a traditional NASA regime. The cells showed good discharge voltages, confirming the plate and separator (Pellon 2536) were adequate for at least the primary mission.

The effect of the cruise period on battery performance became more important with the revised trajectory to Venus, which dictated the cruise period be extended from 140 days to 460 days. Thus the JPL Cruise Simulation Test was developed. Six flight quality cells were put onto a cruise simulation test about one year before launch. They were charged to VT# 3 at 3°C and 8.8 amperes for 23 hours and 50 minutes, and discharged for ten minutes at a 10 ampere rate. The end-of-discharge voltages shown in Figure 11 show the trend across the cruise period. The test pack tapered as low as 20 mA at the end of the day long charge, using MGN VT #3. This demonstrated that VT control could very effectively limit overcharge. Figure 12 is a plot of the taper current. But this test did not demonstrate that full charge was being achieved. A reconditioning was performed as per the mission time-line at day 350. The results showed the cells delivered over 35 AH to a 1.1 volt limit at a C/50 rate. Figure 13 shows the reconditioning performed on the cell pack. The effects of cruise on discharge voltage in a orbital cycle had to be evaluated to complete the cruise evaluation.

Upon completion of the cruise test, it was decided to continue with a mapping mission simulation. The JPL Mission Simulation Test featured a number of refinements to accurately simulate the mapping regime. The regimes were based upon the results of a comprehensive energy balance analysis. This analysis took advantage of solar array degradation predictions as a function of mission time. The variations in length of solar occultation were simulated by varying phase times and currents. The test system allowed up to ten distinct charge or discharge phases per orbit. Finally, during the periods of mapping, the SAR pulse current profile was simulated. This required a three-week modification of the test system, during which time the six-cells were placed on a 30 mA trickle-charge. The test computer was upgraded to provide a waveform via a digital-to-analog converter, through an isolation amplifier, to the remote programming terminals of the discharge power supply. After completion of the modifications, seven additional cruise cycles were run, which confirmed that no change in cell performance had occurred during the trickle-charge period. The cells then began the JPL Mission Simulation Test. Results are used to predict whether the minimum voltage requirement of the radar can be met during radar pulses.

SPACECRAFT PERFORMANCE

LAUNCH AND DEPLOY PHASE

Estimating the load sharing during deployment requires knowledge of the voltage of the batteries involved, the total path resistances, and the spacecraft loads. Predicting the voltages of the IUS (Ag-Zn) and MGN (Ni-Cd) batteries is by far the most difficult aspect. During launch, the spacecraft batteries were slightly drained by a memory-keep-alive power supply circuit, maintaining their voltage below the IUS supplied voltage. Hence, there was little drain on the MGN battery until separation. IUS firing, MGN separation and solar panel deployment were all achieved without delays, resulting in a calculated 7% DOD for the MGN battery.

CRUISE PHASE

Analysis of the trends observed in cruise operation show an irregular regime from day to day. This resulted from variations in attitude, proximity to the sun, and amount of off-pointing during navigational maneuvers. The actual cruise DODs are lower than those in the simulation.

Originally, reconditioning of the batteries was scheduled to occur before Venus-orbit insertion. That event, scheduled for mission-day 350, was never performed. It was eliminated due to concerns about the potential for introducing errant commands during reconditioning sequence initiation and loss of redundancy during the reconditioning.

MAPPING OPERATIONS

Actual spacecraft performance is somewhat different than the predicted results. Most of the differences can be attributed to inaccuracies in attitude and thermal predictions. The heater loads for the spacecraft are lower than expected. Figure 14 is a comparison of JPL Mission Simulation Test and actual flight DOD's for a portion of the mapping mission. Variations in the incidence angle have changed the amount of solar array power available. This effect is seen in orbits 450 to 650. Figure 15 shows the simulation and spacecraft voltages associated with the same mapping orbits. The performance is generally worse than the prediction. The projected reason for the lower voltages is the lack of reconditioning onboard the spacecraft. This effect was predicted when the decision to not recondition was made. Data from the cruise simulation test indicated about 0.5 volts lower performance without reconditioning. The voltage has stayed above the radar input threshold so far during the mission, but is about 0.5 volts lower at the lowest point.

During the mapping mission the batteries have been operating at significantly different temperatures, typically about 10°C apart. This exceeds design limits, but is not expected to create a long-term problem, because the temperature gradients will even out throughout the mapping mission as solar orientation changes. The warmer battery is used to set the VT control point. Thus, the colder battery is less fully charged on any given orbit. On discharge the warmer battery takes a larger portion of the load, causing a variation in DOD between the two batteries.

In the remainder of the mission, the need to recondition will be made based upon spacecraft data and the mission simulation data available. The goal is to meet mission objectives with the lowest total spacecraft risk. Decision on battery operation must take into account (1) the likelihood of spacecraft hardware or software errors, (2) the effects of eliminating battery redundancy upon surviving anomalies, and (3) the benefits to the mission of increased voltages after reconditioning. These issues will be continued to be evaluated throughout the mission.

CONCLUSIONS

The Magellan batteries have been able to support all required loads to date at depths-of-discharges up to 22% and with inter-battery temperature differentials of over 10°C. In addition, extensive analysis and testing, both at Martin Marietta and at JPL, has been performed in support of mission-critical events and decisions. In particular, the ongoing JPL Mission Simulation Test has contributed significantly to important operational decisions. For example, the results from the reconditioning performed in the cruise simulation were successfully used to predict that unreconditioned spacecraft voltages would be about 0.5 volts lower. This testing shall continue to play an important role in future Magellan operations.

ACKNOWLEDGEMENT

This work described in this paper was carried out at the Jet Propulsion Laboratory, California Institute of Technology under a contract with the National Aeronautics and Space Administration.

REFERENCES

1. VMPWR Energy Balance Prediction Software, developed for the Magellan Project by Martin Marietta Astronautics Group, Denver, Colorado.

2. MIDAS Thermal Prediction Software, developed for the National Aeronautics and Space Administration by Martin Marietta Astronautics Group, Denver, Colorado.

JPL

HELIOCENTRIC MISSION PROFILE

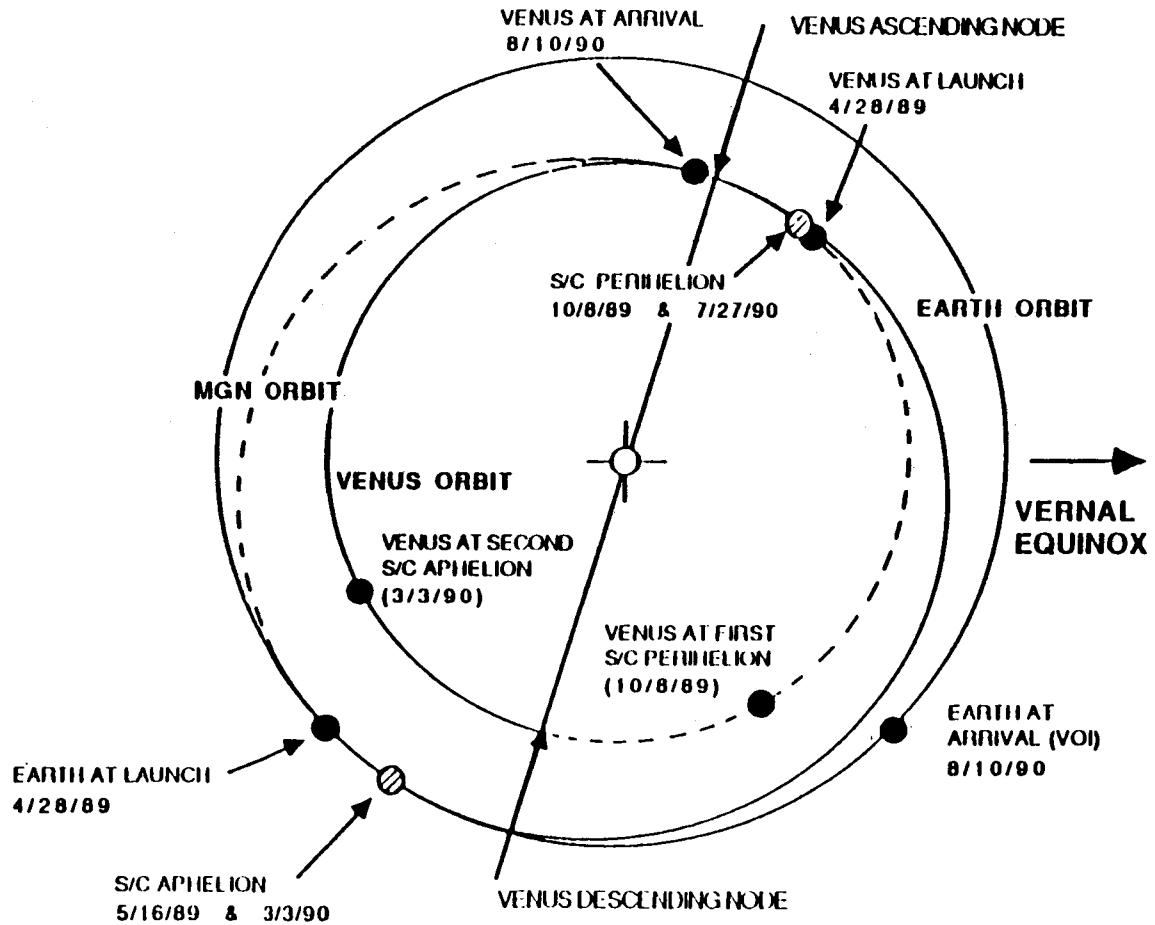

FIGURE 1:

C-2

JPL

VENUS MAPPING ORBIT

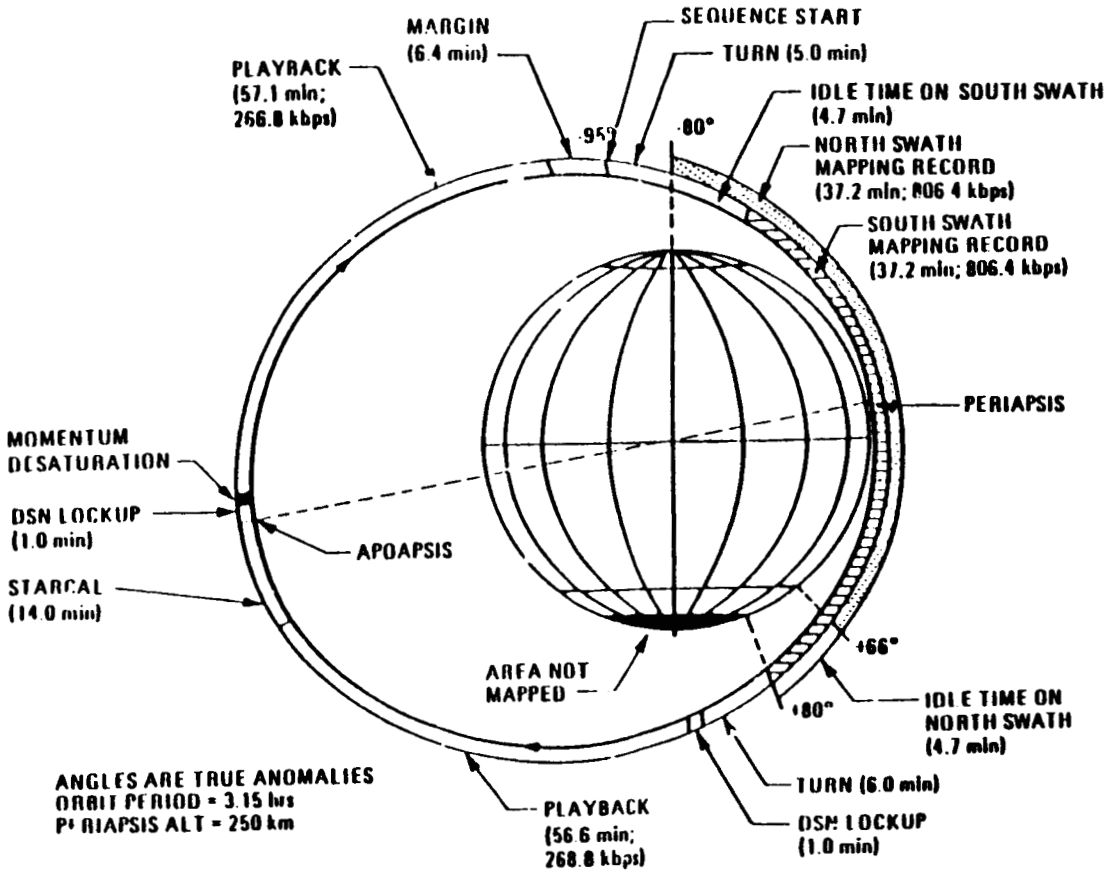

FIGURE 2:

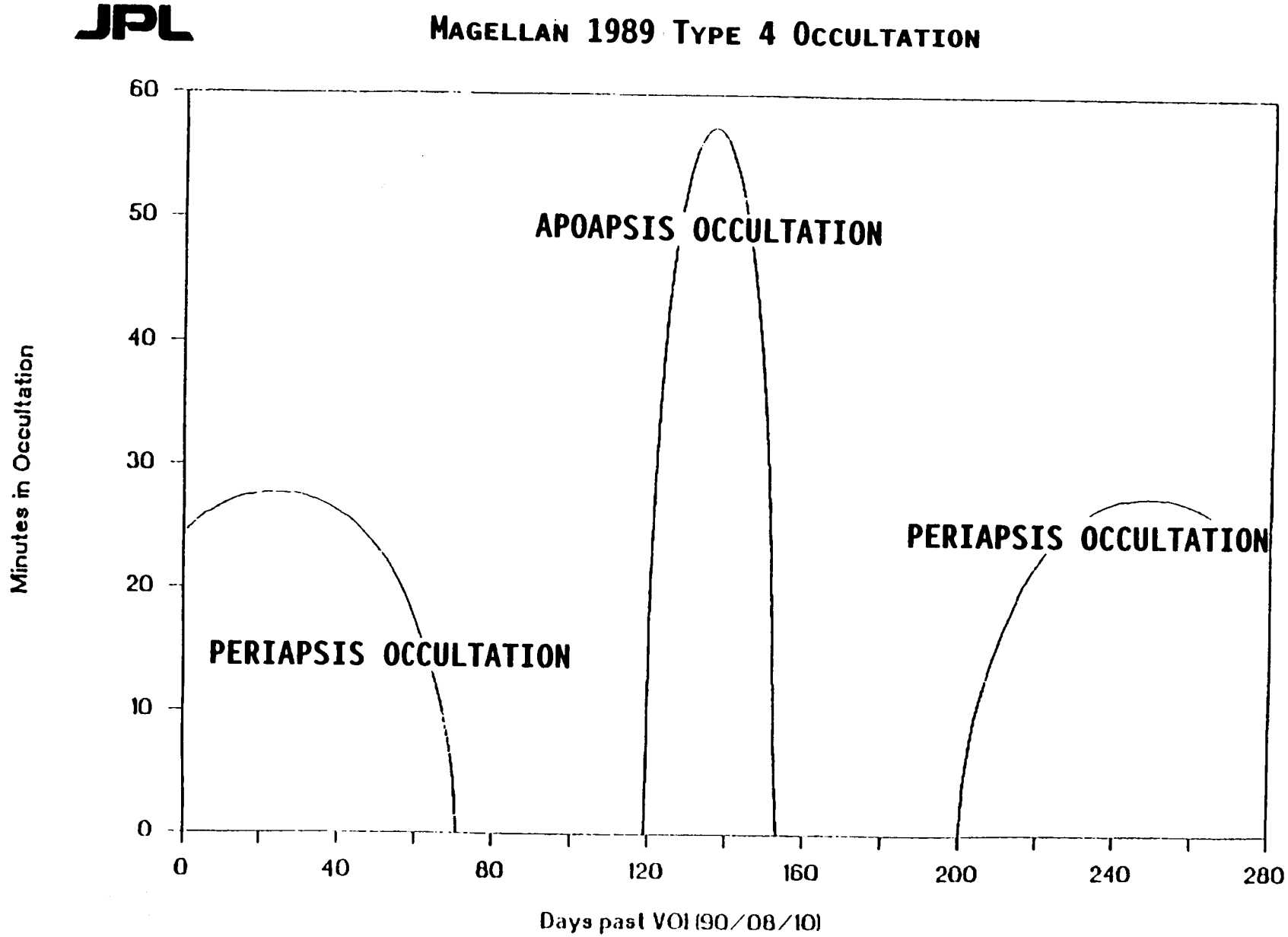
JPL
MAGELLAN 1989 TYPE 4 OCCULTATION
APOAPSIS OCCULTATION
PERIAPSIS OCCULTATION
PERIAPSIS OCCULTATION
Minutes in Occultation
Days past VOI (90/08/10)
0
10
20
30
40
50
60
0
40
80
120
160
200
240
280

FIGURE 3:

JPL

SPACECRAFT DIAGRAM

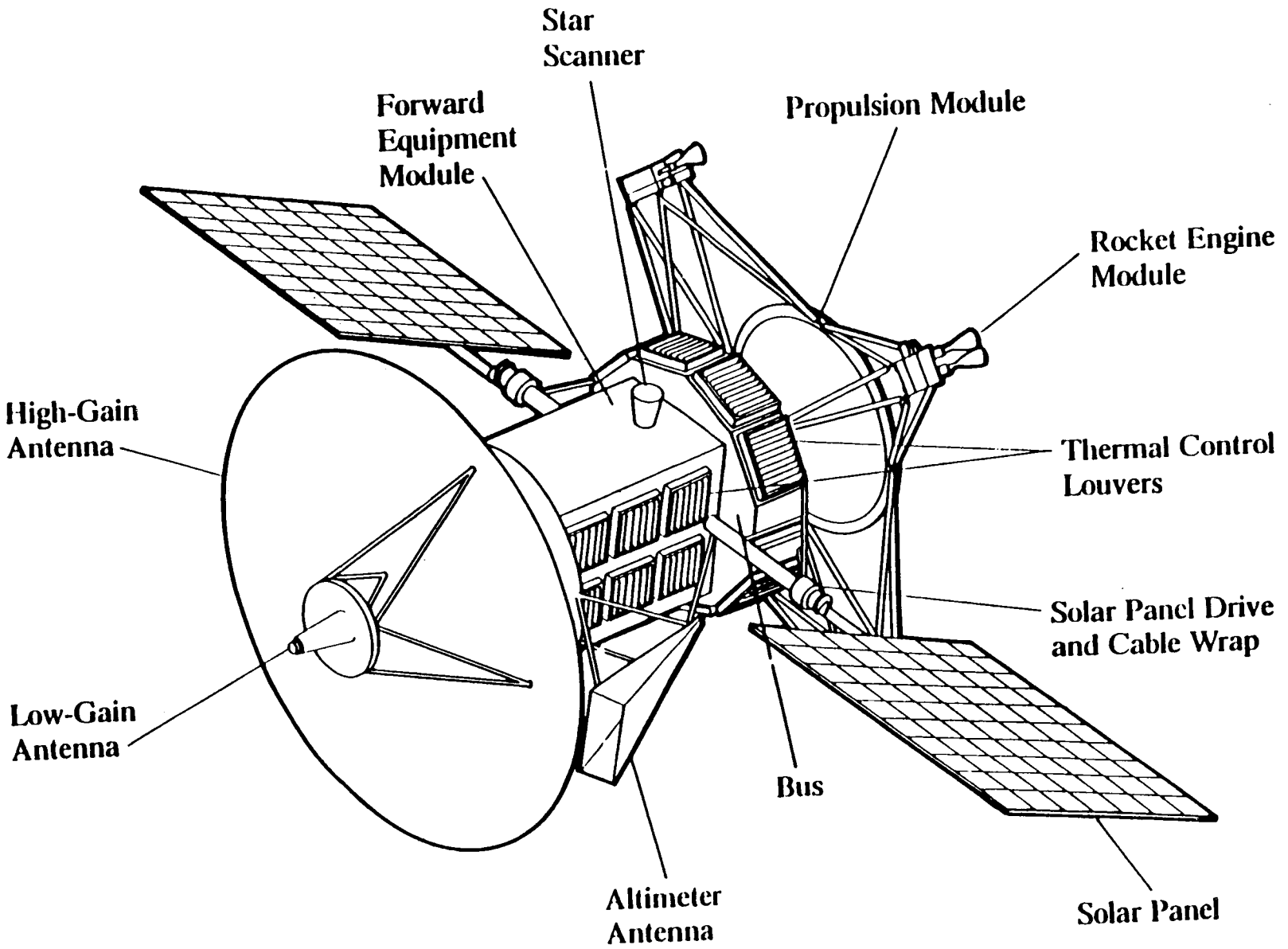

FIGURE 4:

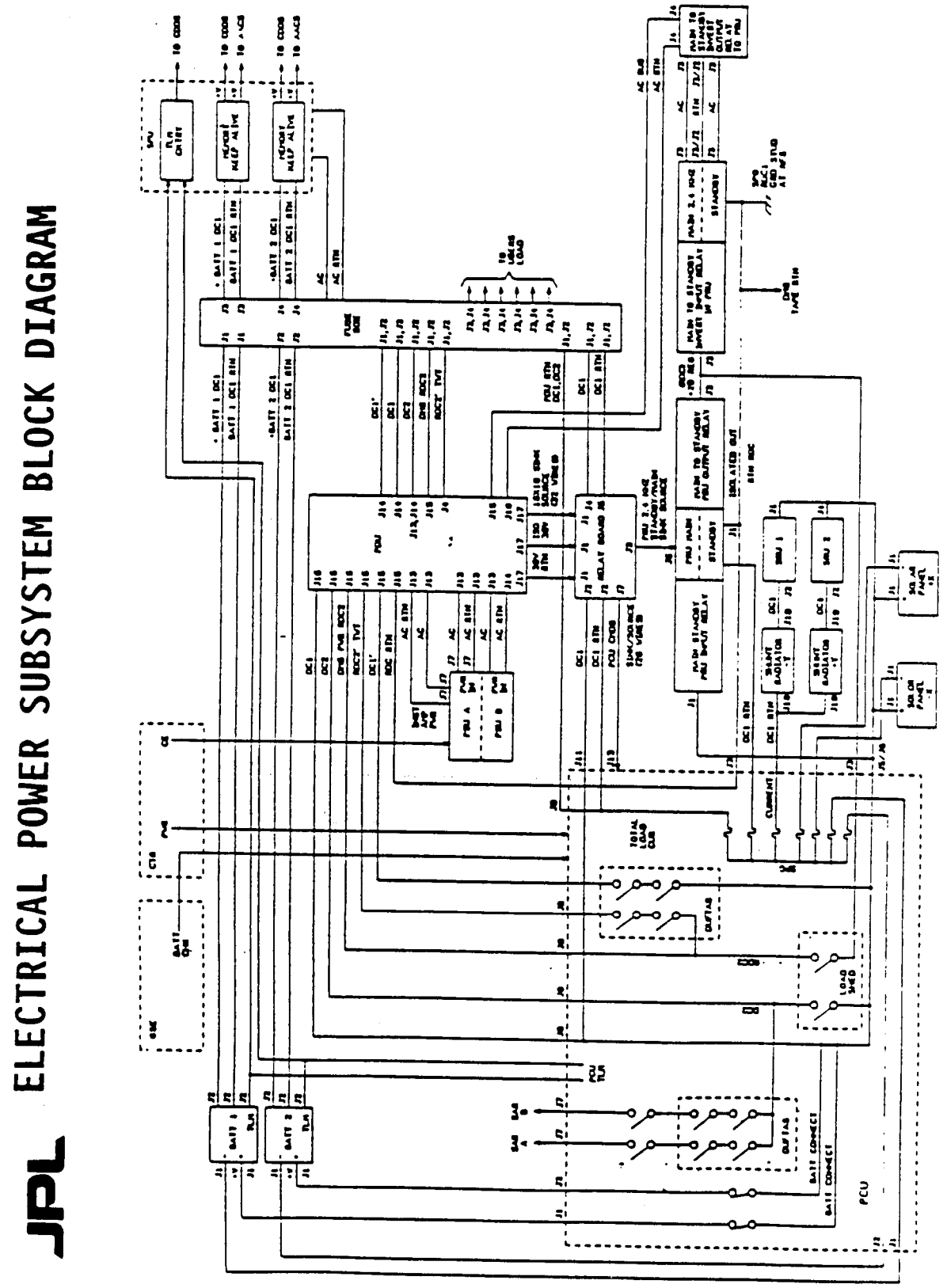

FIGURE 5:

JPL

MGN VT Curve Diagram

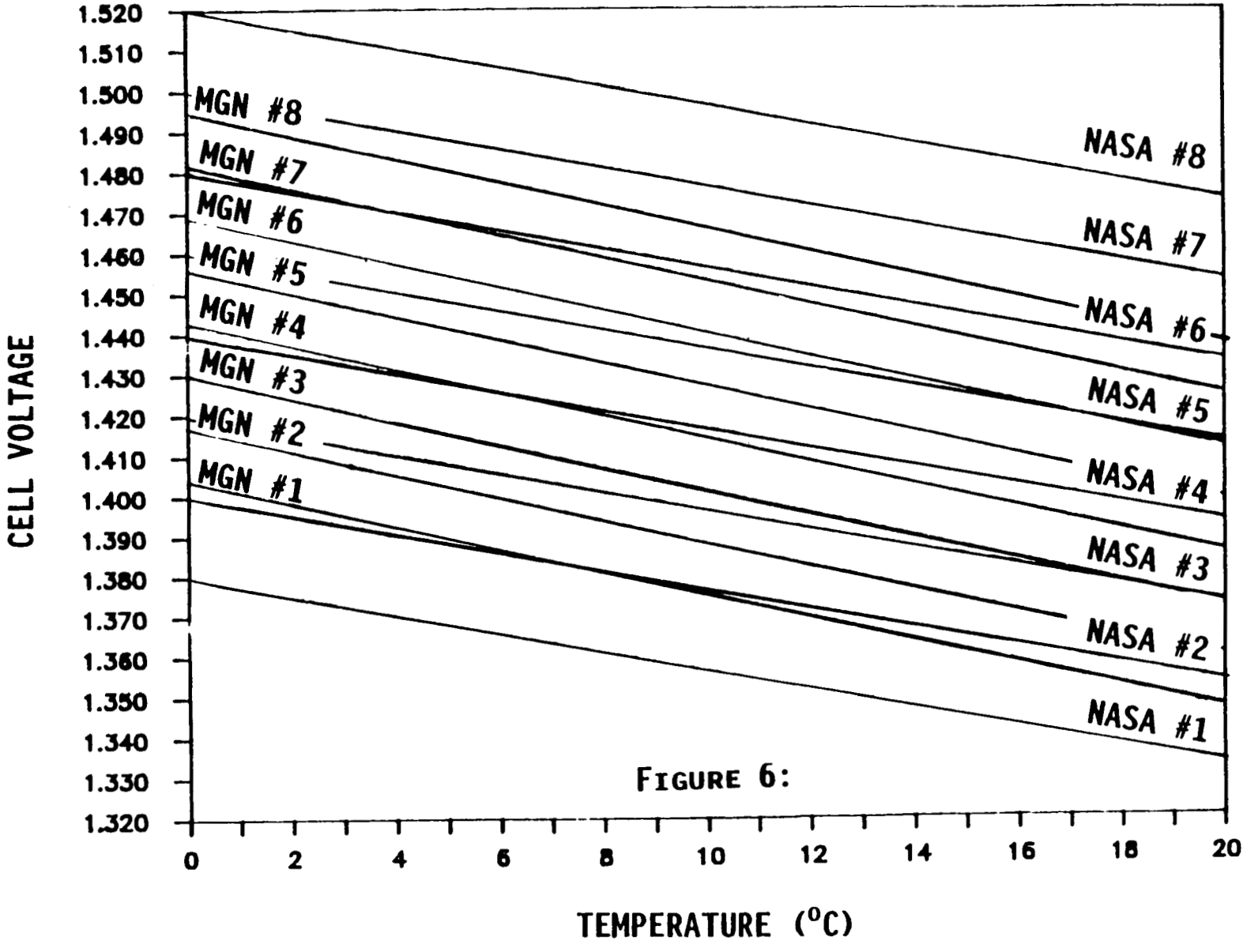

FIGURE 6:

JPL

BATTERY DIAGRAM

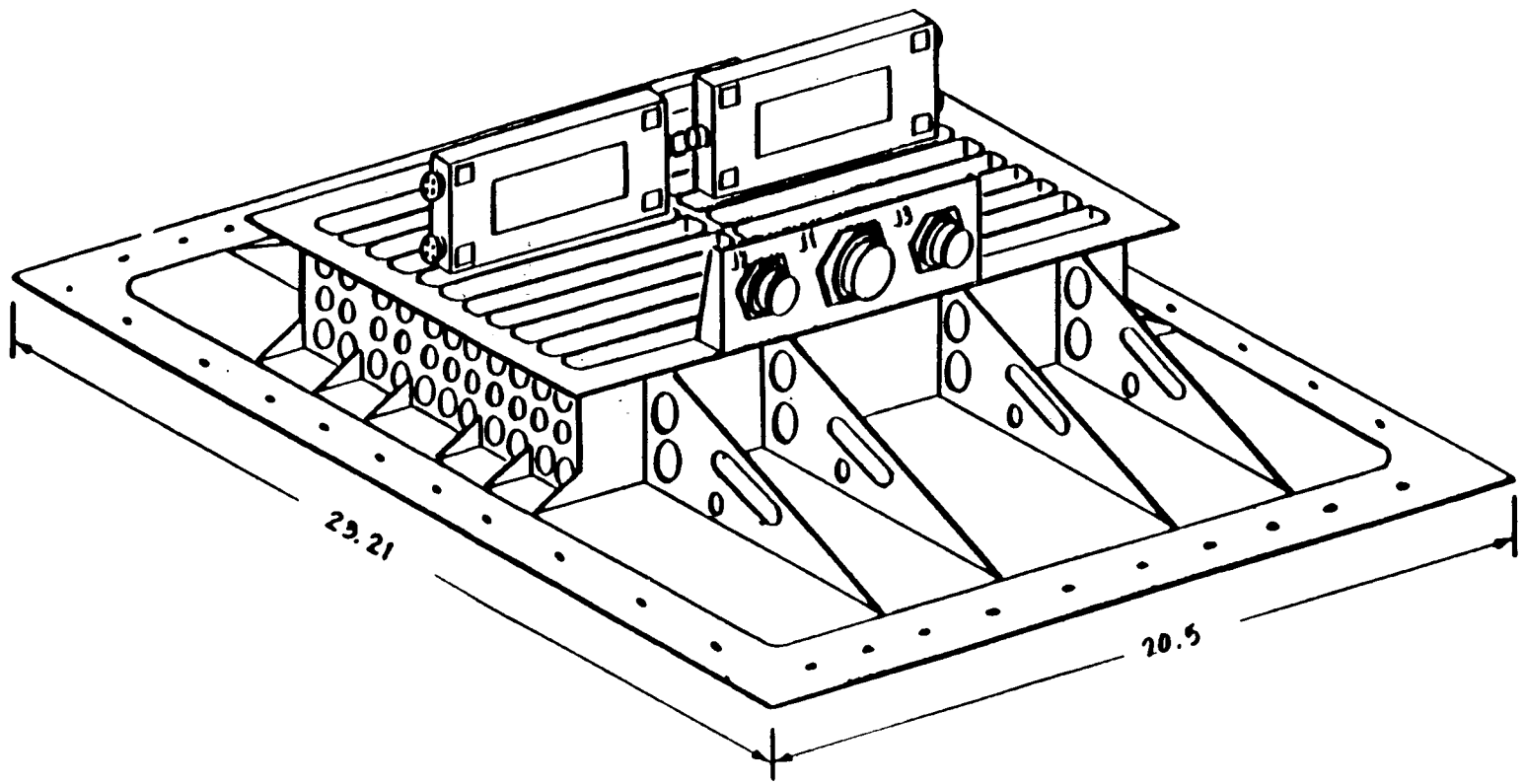

FIGURE 7:

JPL

MGN POWER SOURCES

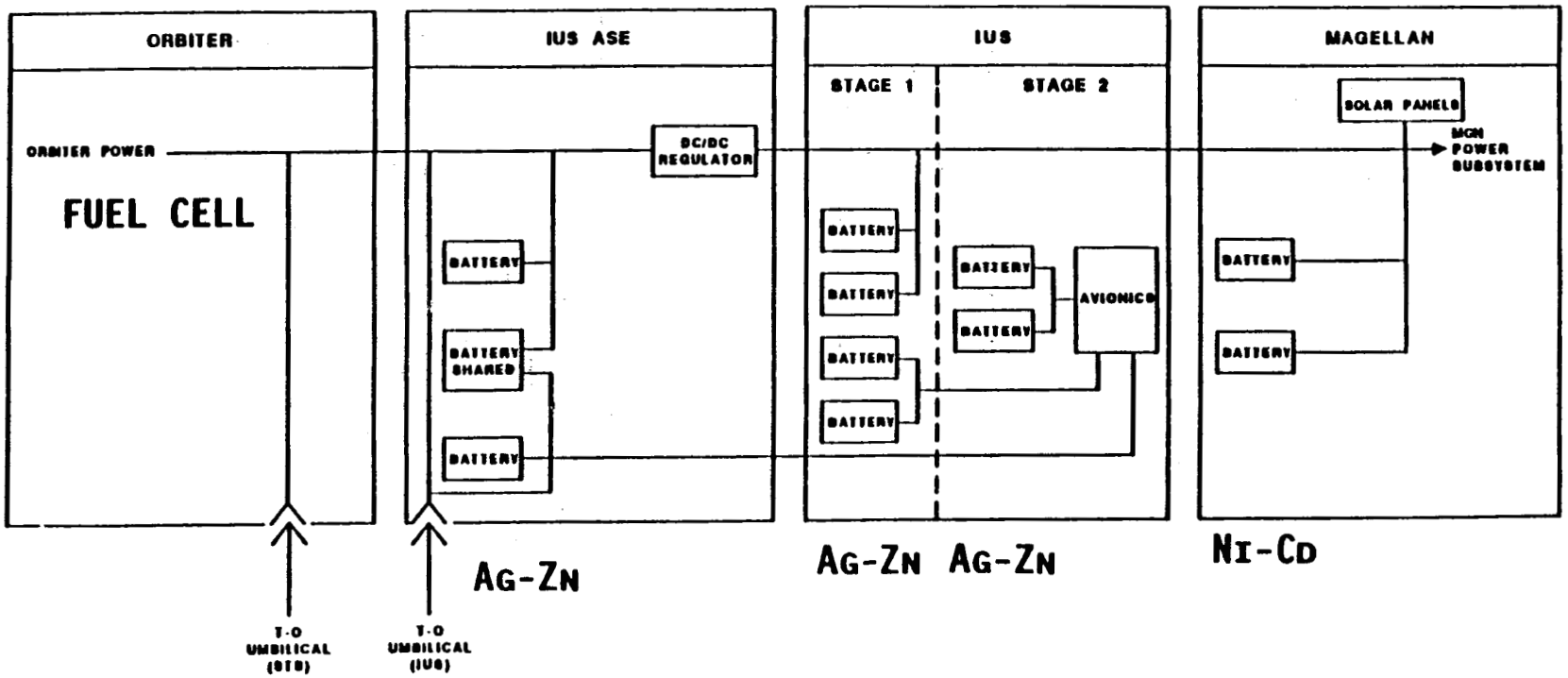

ASE = AIRBORNE SUPPORT EQUIPMENT

FIGURE 8:

JPL

PULSE DISCHARGE VOLTAGE RESULTS

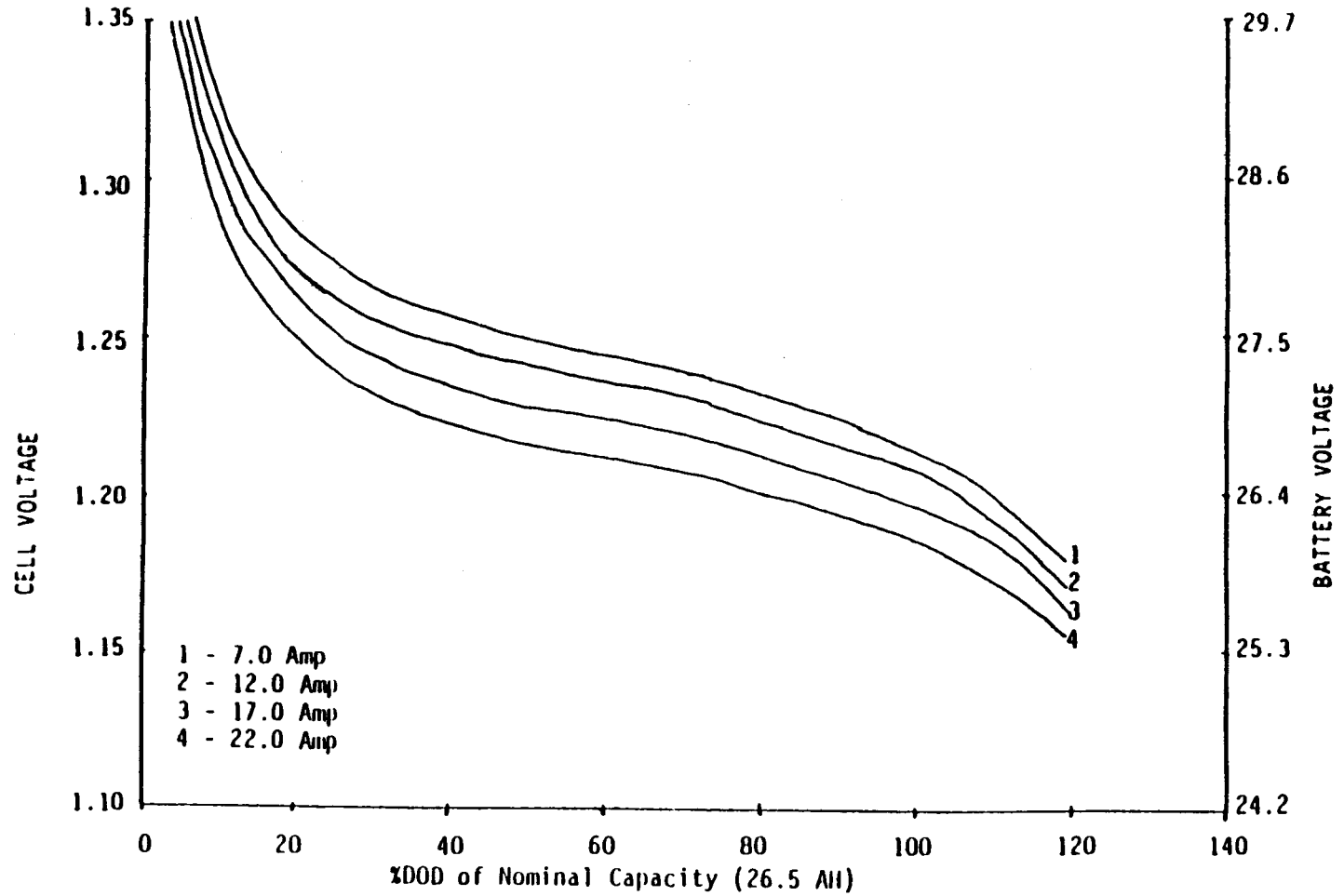

FIGURE 9:

JPL

MAGELLAN CRUISE SIMULATION

EQUIVALENT BATTERY EODV VS. CYCLES

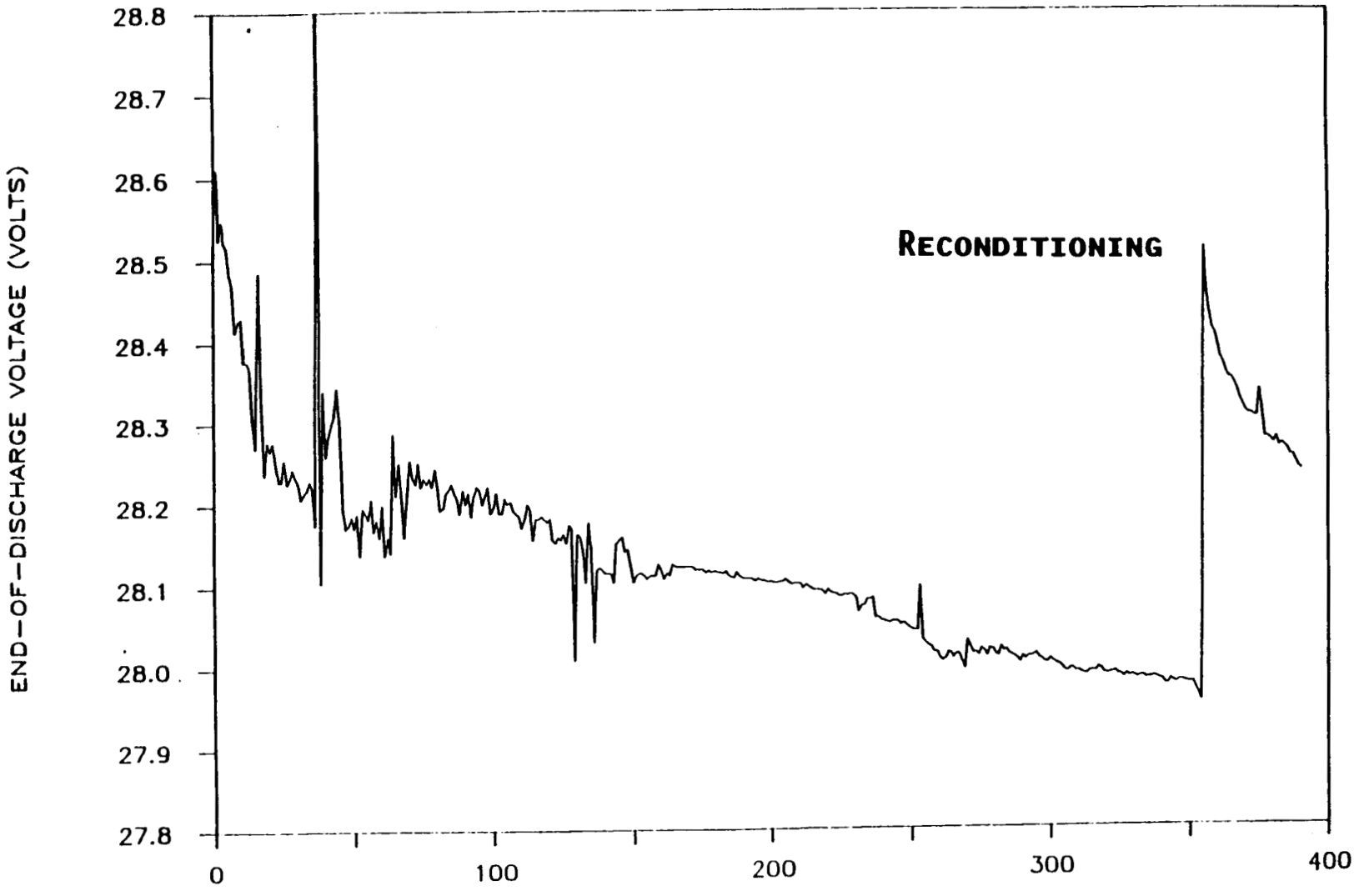

FIGURE 10:

JPL

CRUISE SIMULATION TAPER CURRENT

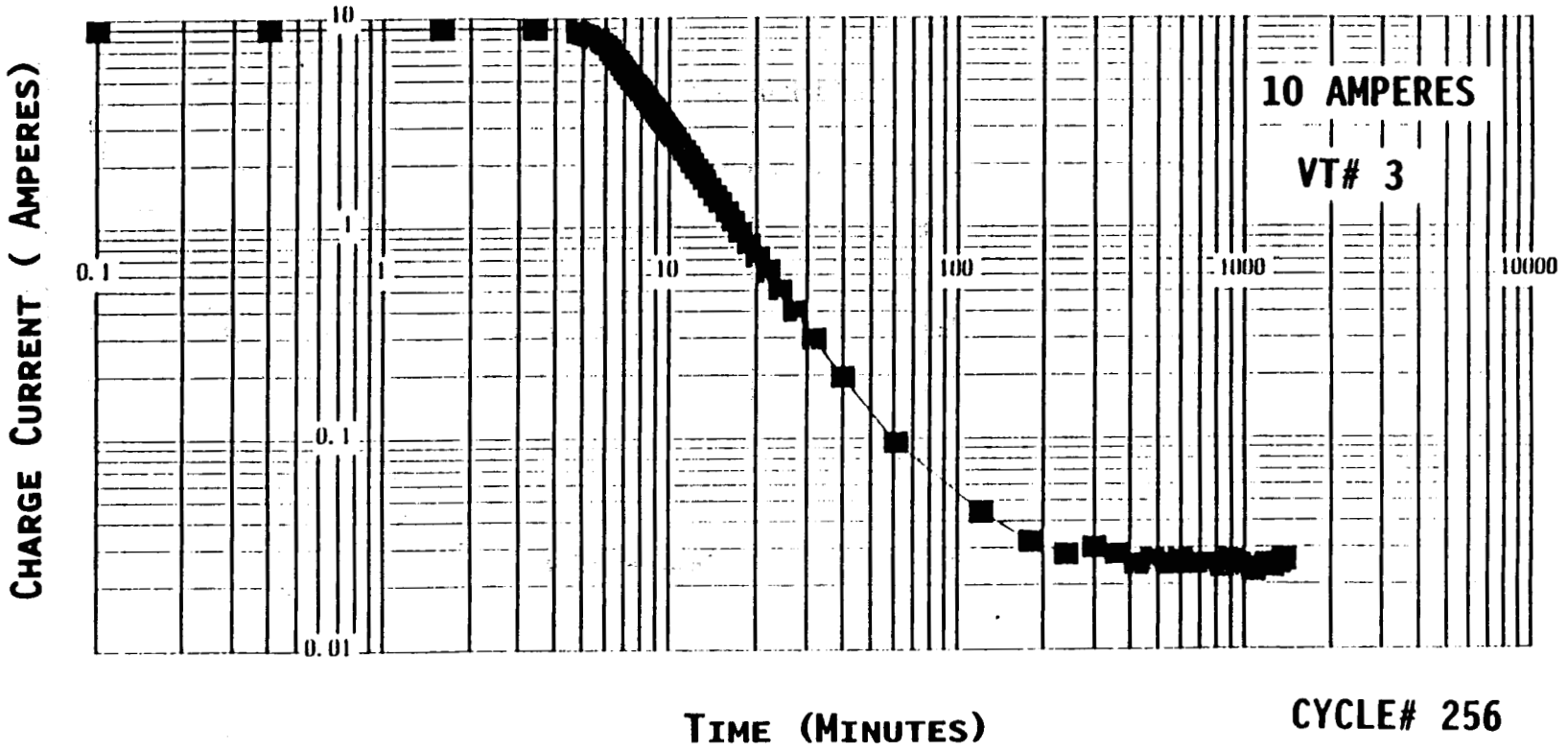

FIGURE 11:

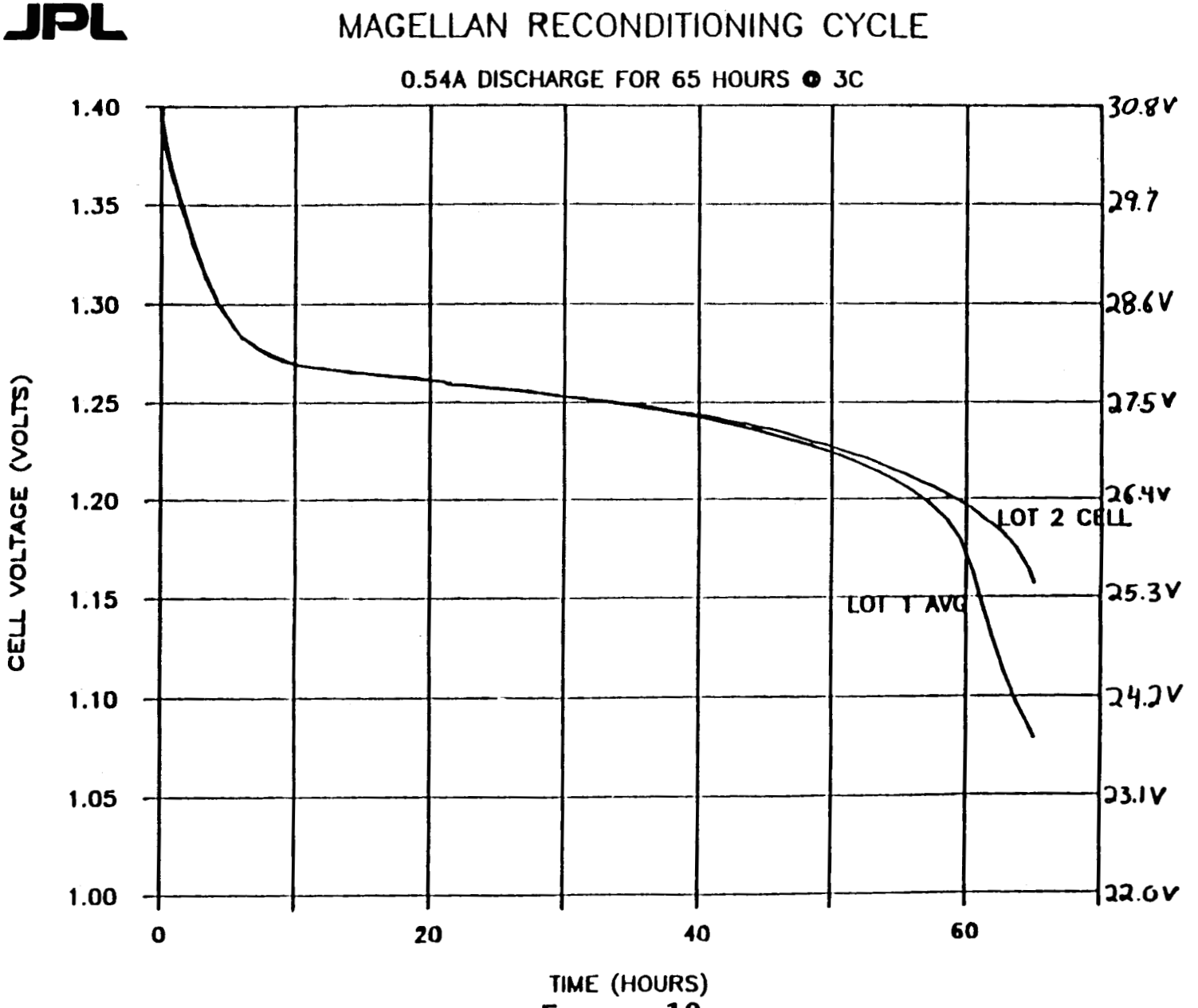
JPL
MAGELLAN RECONDITIONING CYCLE
0.54A DISCHARGE FOR 65 HOURS @ 3C
CELL VOLTAGE (VOLTS)
1.40
1.35
1.30
1.25
1.20
1.15
1.10
1.05
1.00
30.8V
29.7
28.6V
27.5V
26.4V
25.3V
24.2V
23.1V
22.0V
LOT 2 CELL
LOT 1 AVG
0
20
40
60
TIME (HOURS)

FIGURE 12:

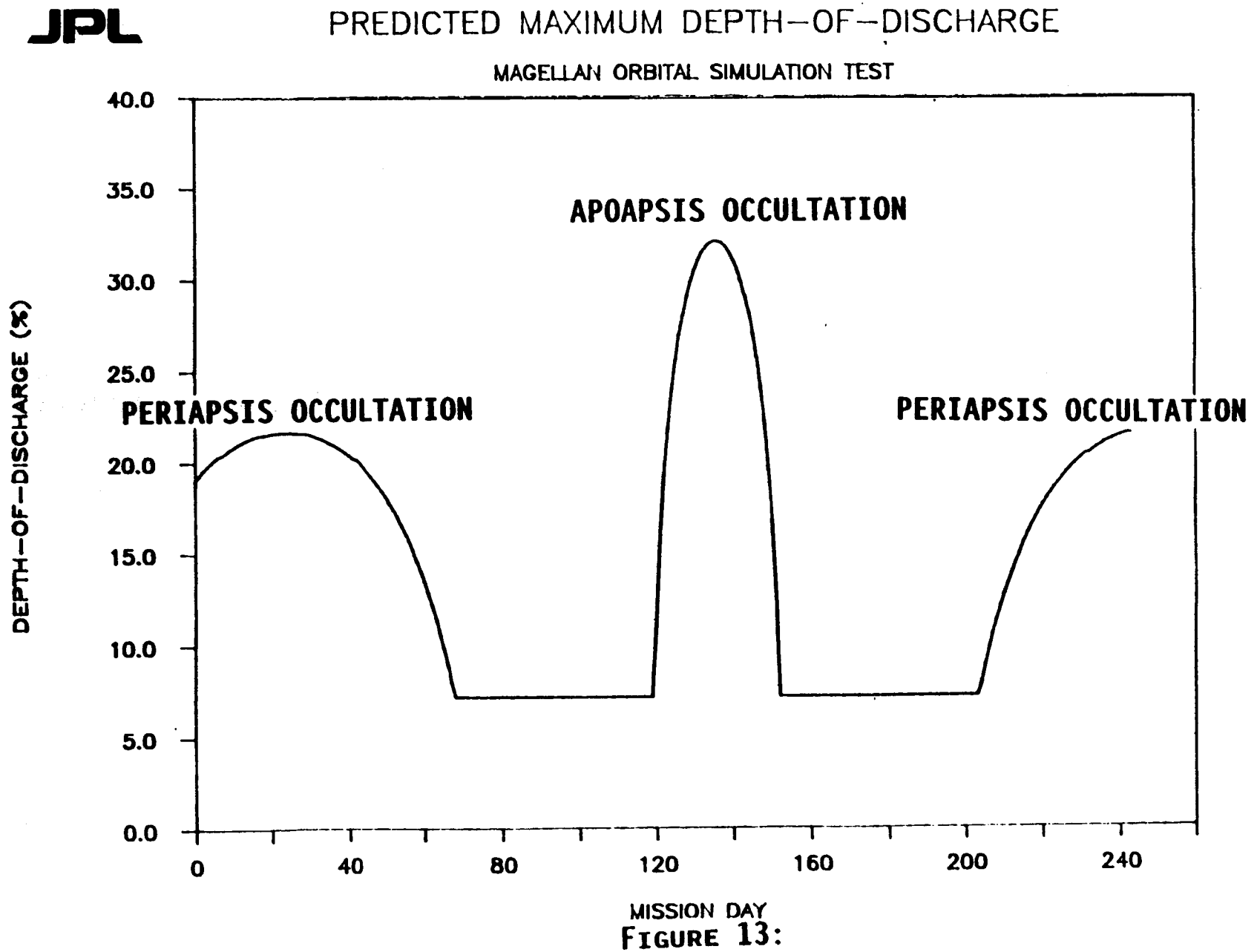
JPL
PREDICTED MAXIMUM DEPTH-OF-DISCHARGE
MAGELLAN ORBITAL SIMULATION TEST
APOAPSIS OCCULTATION
PERIAPSIS OCCULTATION
PERIAPSIS OCCULTATION
DEPTH-OF-DISCHARGE (%)
40.0
35.0
30.0
25.0
20.0
15.0
10.0
5.0
0.0
0
40
80
120
160
200
240
MISSION DAY

FIGURE 13:

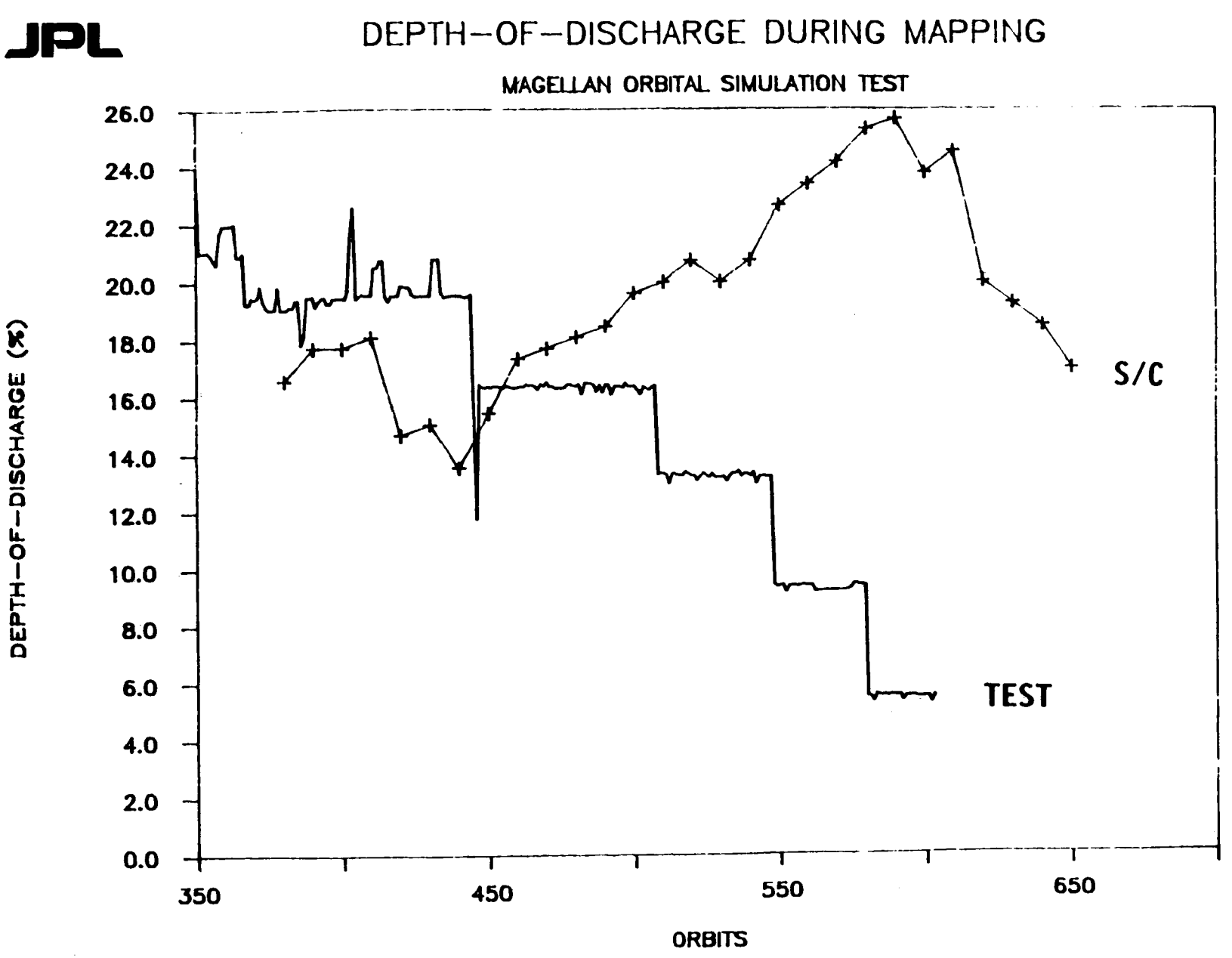
JPL
DEPTH-OF-DISCHARGE DURING MAPPING
MAGELLAN ORBITAL SIMULATION TEST
DEPTH-OF-DISCHARGE (%)
26.0
24.0
22.0
20.0
18.0
16.0
14.0
12.0
10.0
8.0
6.0
4.0
2.0
0.0
350
450
550
650
ORBITS
S/C
TEST

FIGURE 14:

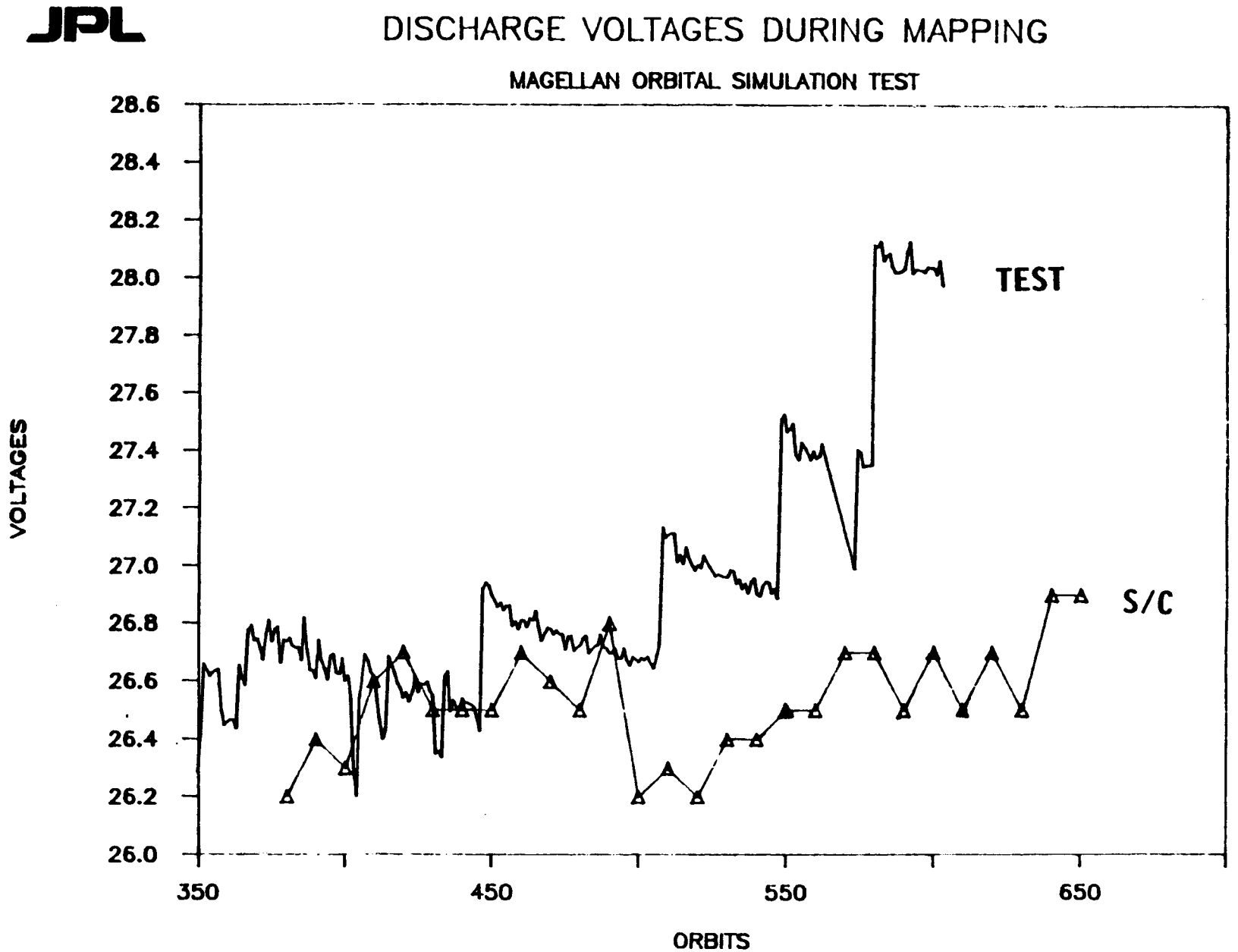
JPL
DISCHARGE VOLTAGES DURING MAPPING
MAGELLAN ORBITAL SIMULATION TEST
28.6
28.4
28.2
28.0
27.8
27.6
27.4
27.2
27.0
26.8
26.6
26.4
26.2
26.0
VOLTAGES
TEST
S/C
350
450
550
650
ORBITS

FIGURE 15:

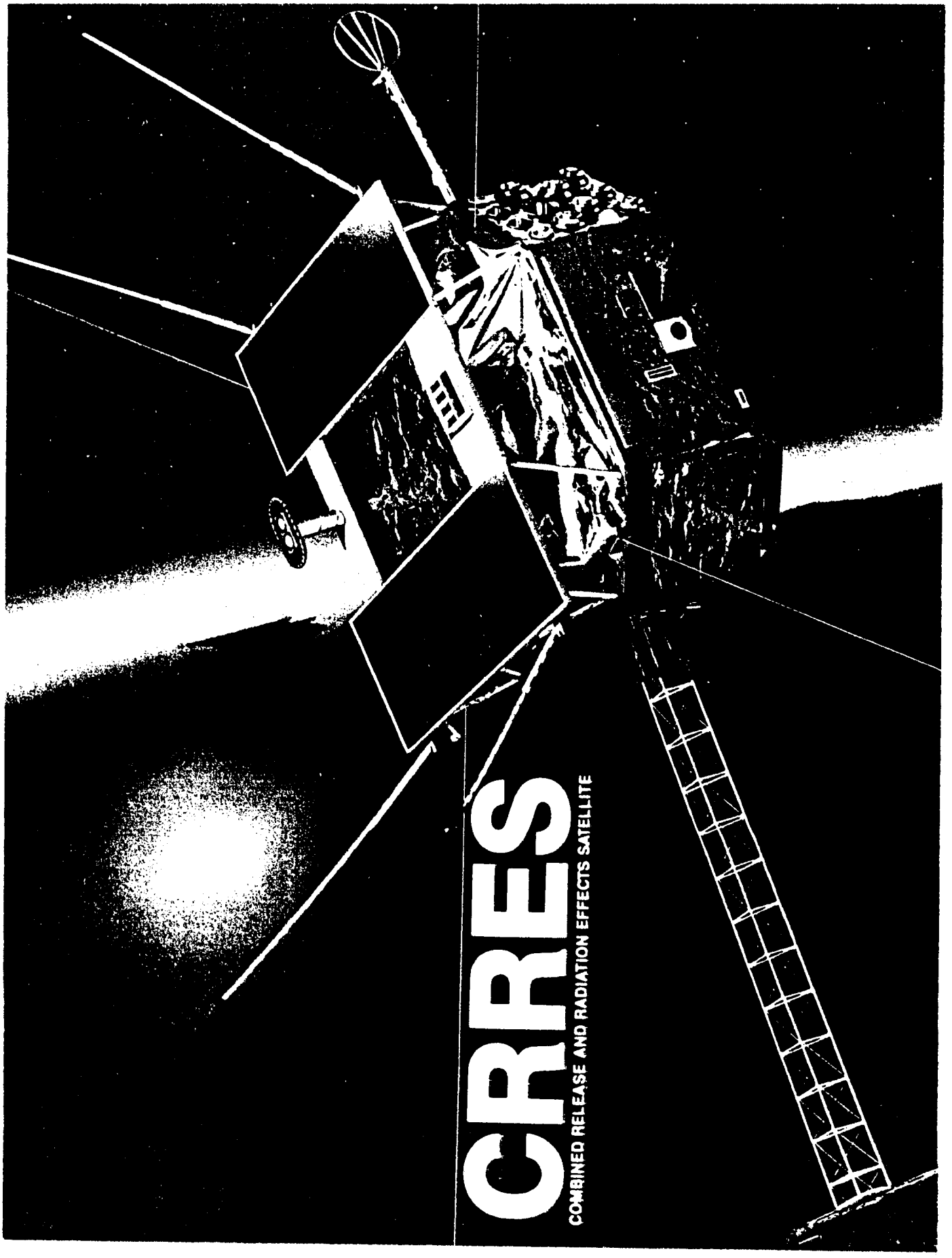

CRRES ORBIT PARAMETERS

* Launched 7/25/90, 12:24 Zulu
* Highly Eliptical Orbit
  32000 km apogee
  375 km perigee
* 18.2 Degrees Inclinition
* 10 Hour Orbit Period

EXPECTED ECLIPSE PERIODS

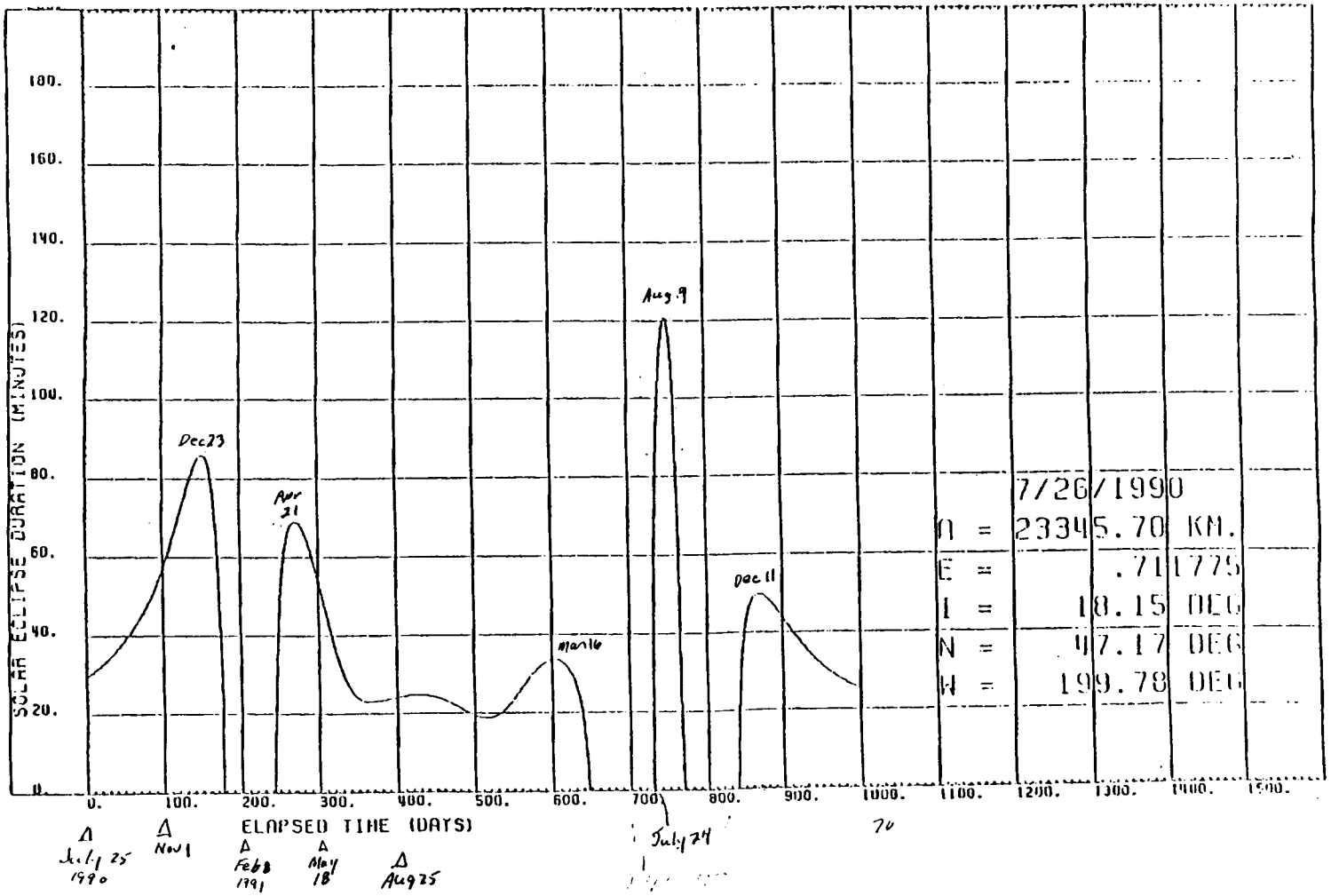

CRRES BATTERY CHARGE CONTROL

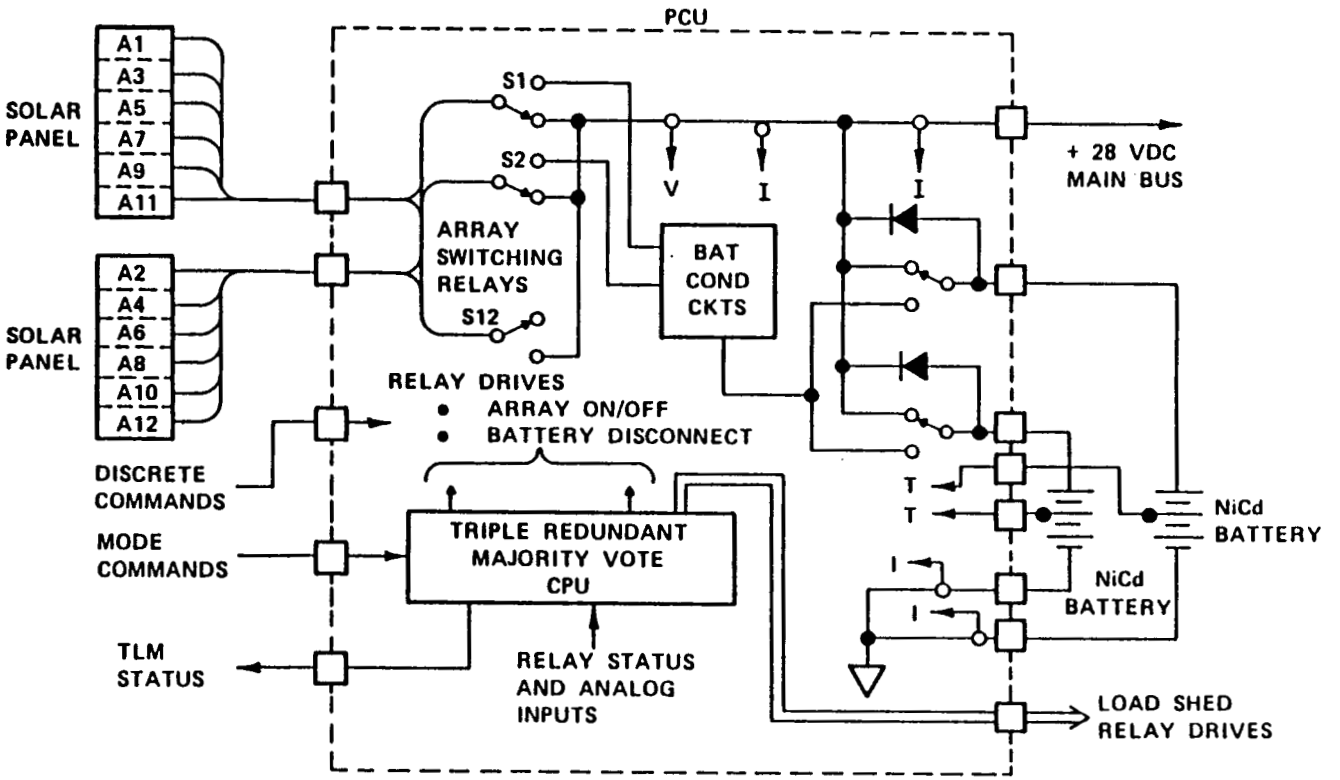

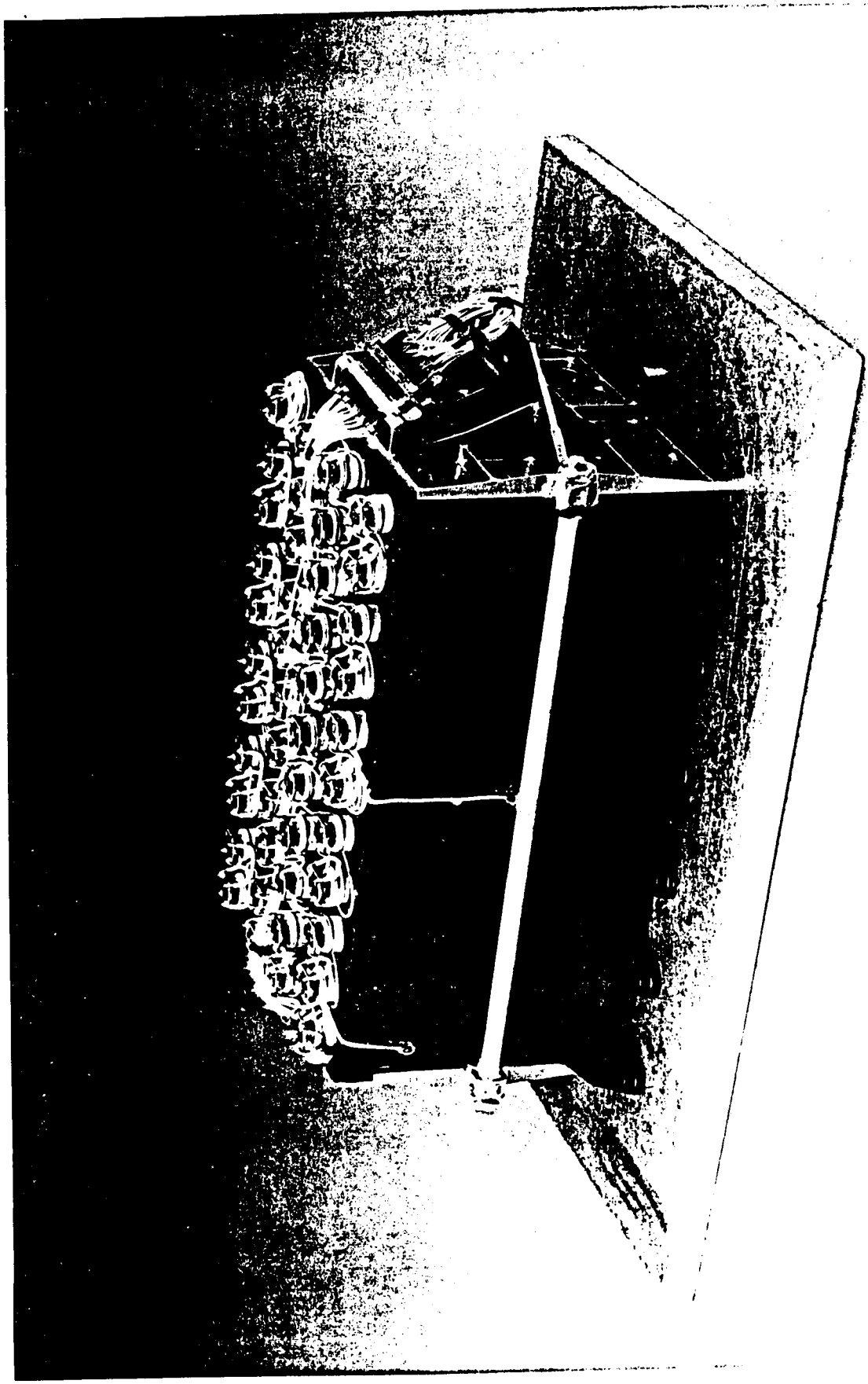

CRRES BATTERY DESCRIPTION

Manufacturer: Ford Aerospace

Basic Cell: Gates 15AB19, Assembled and Tested to Ford Specifications

Battery Compliment: Two batteries, each battery containing 22 cells, 21 wired active.

Battery Heritage: NATO III D

Measured Battery Capacity: > 20.0 Amp-Hours

Final Battery Weight: 15.4 kg

ONE ORBIT BATTERY CURRENT

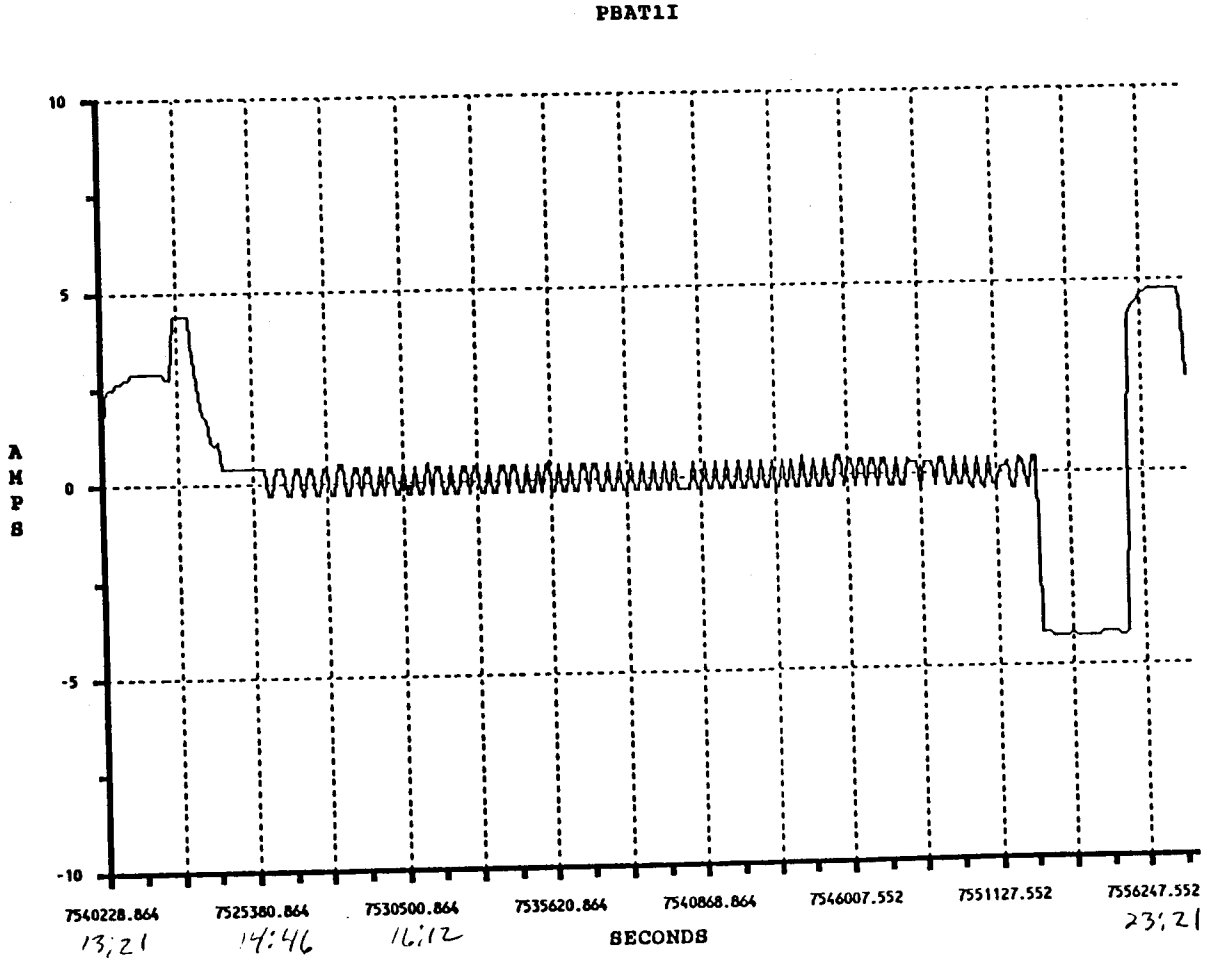

10/20/93

ONE ORBIT BATTERY VOLTAGE

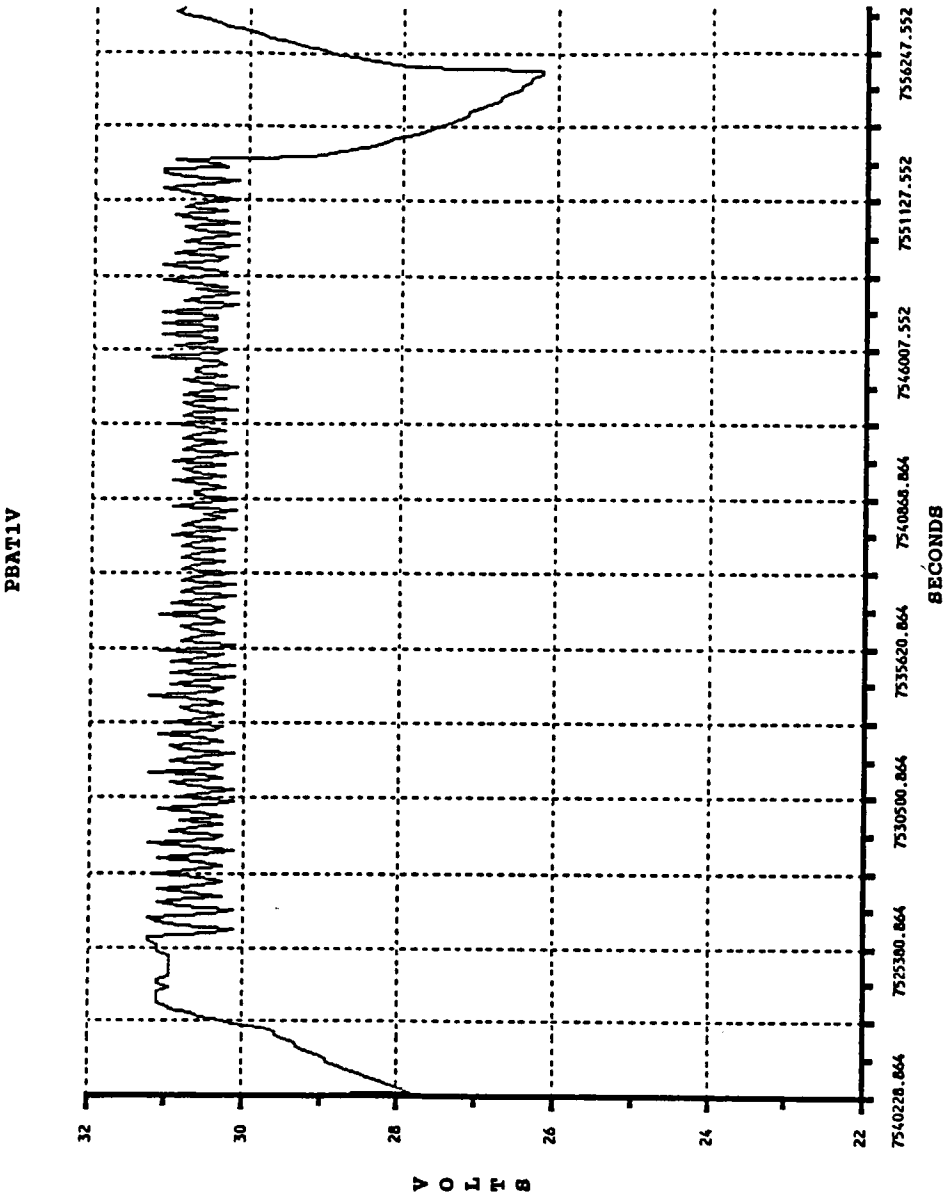

BATTERY RECONDITION CIRCUIT

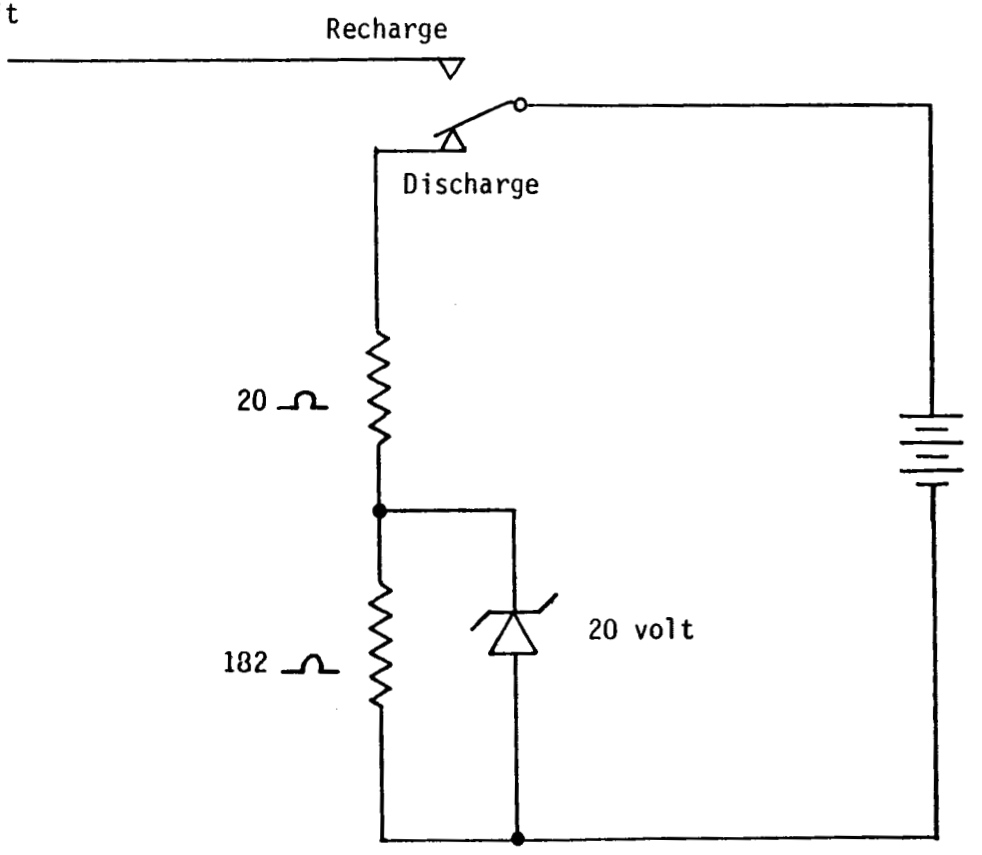

CRRES Battery Reconditioning Discharge Profile

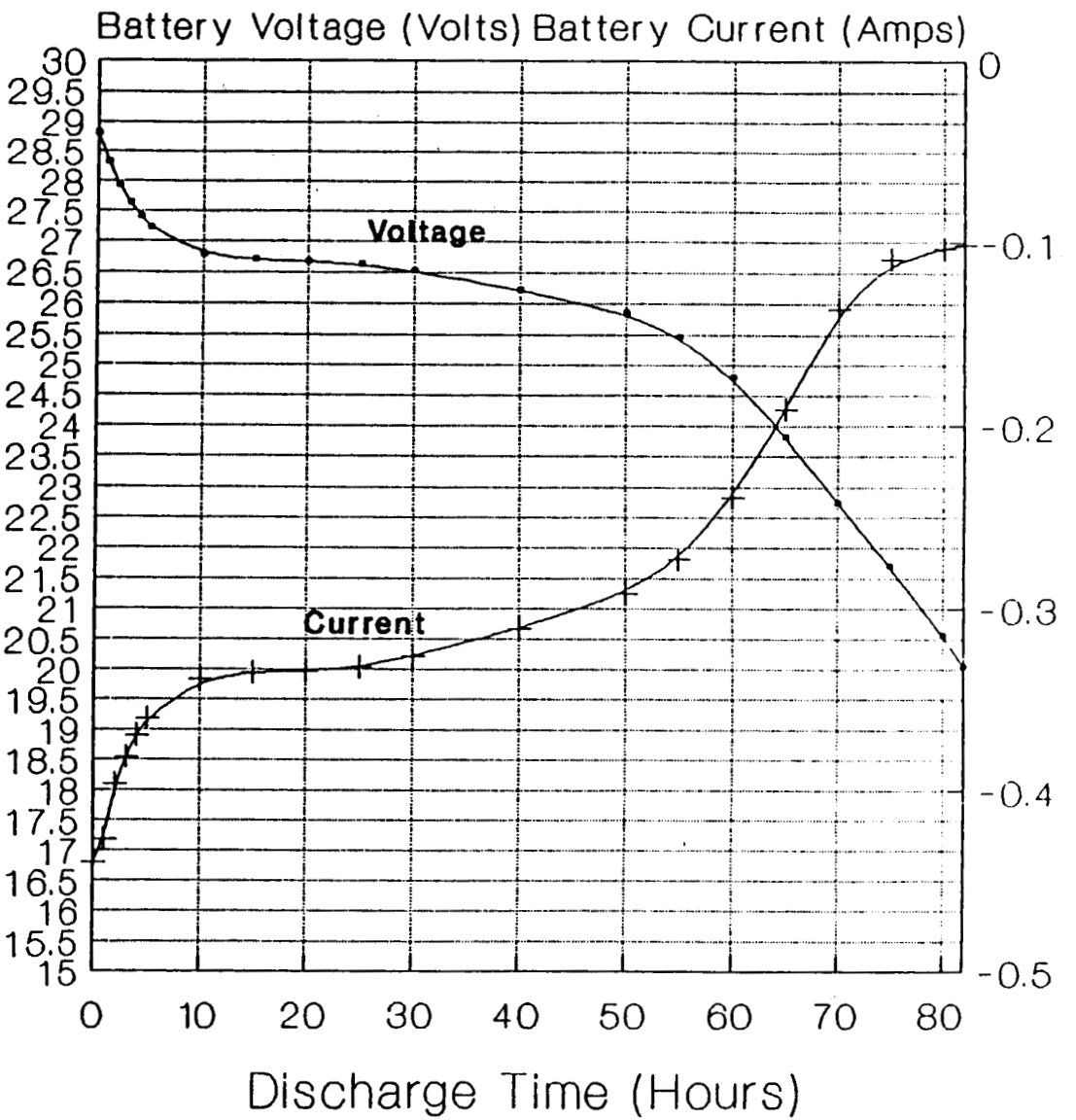

N92-27135

PRIMARY BASIS OF ADVANCED Ni-Cd CELL TECHNOLOGY at EAGLE-PICHER INDUSTRIES, INC COLORADO SPRINGS

ELECTROCHEMICALLY DEPOSITED POSITIVE ELECTRODES
ELECTROCHEMICALLY DEPOSITED CADMIUM ELECTRODES
ELECTRODE DEVELOPMENT ACTIVITIES

EAGLE PICHER
COLORADO SPRINGS

ELECTROCHEMICALLY DEPOSITED POSITIVE ELECTRODES

- Stable, well controlled high porosity sintered nickel substrates.
- USAF Patented electrochemical deposition process, redefined and optimized for space battery requirements.
- Controlled active material loading at levels that prevent electrode expansion over life.
- Multiple cycle formation and characterization testing providing highly stabilized reliable electrodes with extremely low levels of carbonate and nitrate.
- Dedicated electrode processing facilities with high levels of quality control.
- High rate electrochemical stress test to screen and characterize electrodes for swelling, capacity, weight loss, etc.

EAGLE Ep PICHER
COLORADO SPRINGS

ELECTROCHEMICALLY DEPOSITED CADMIUM ELECTRODES

- High porosity sintered nickel substrates with controlled pore size to prevent cadmium migration and increase active material utilization.
- USAF Patented electrochemical deposition process refined for uniform high level active material loading.
- Automated process control ensuring reproducible loading levels and uniform electrodes.
- Dedicated electrode processing facilities equivalent and parallel to positive electrodes.
- Flooded capacity testing to verify electrode performance and cell design N : P ratio.

EAGLE Ep PICHER
COLORADO SPRINGS

ORIGINAL PAGE IS
OF POOR QUALITY

ELECTRODE DEVELOPMENT ACTIVITIES

- Tailored electrodes for varying rate applications LEO, GEO, Pulse Power, etc.
- Improved energy density via higher porosity and/or higher loading.
- Improved energy density via increased electrode thickness.

ORIGINAL PAGE IS
OF POOR QUALITY

SINTERING PROCESS
(Positive Sinter)

- Dry Sinter Process
- Selected density: INCO type 287 powder
- Pure nickel woven wire current conductor
- Thickness: 0.65 to 0.95 +/- 0.05 mm (Thickness dependent on application).
- Sinter Porosity: 84 +/- 2%. Overall Porosity: 80 +/- 2%
- Bond Strength: 550 +/- 50 PSI.
- 100% inspection for thickness, porosity, strength, and physical appearance.
- Entire process MSP controlled with customer approval.
- Proven production process: Millions of electrodes manufactured for Ni-Cd, Ni-H2 flight programs.

EPI/USAF POSITIVE ELECTRODEPOSITION PROCESS

- Basic procedure developed for USAF/WPAFB under contract F33615-76-C-5407, "Manufacturing Methods for Nickel-Cadmium Batteries".
- Further development and optimization for Space Nickel battery applications by EPI (participation by Hughes and NASA).
- Electrodeposition Process Utilizing Aqueous/Ethanol Solvent and Consumable Anodes.
- Automated Process Contols
  - pH, Temperature, Flow, Current Density
- MCD Controlled Process
  - Dedicated solution analyzed prior to each run.
  - Complete traceability for each electrode.
  - Electrical characterization test (capacity and weight at plaque level).
  - 1% lot sampling for stress test (capacity, weight, swelling, and appearance).
  - 100% Inspection: dimensional, appearance, pickup.

EAGLE Ep PICHER
COLORADO SPRINGS

POSITIVE ELECTRODEPOSITION PROCESS PARAMETERS

- 1.6 TO 1.8 M $Ni(NO_3)_2$
- 0.12 to 0.18 M $Co(NO_3)_2$
- 45 +/- 2% Ethanol
- 2.8 to 3.2 pH
- 70 to 80 C
- 0.05 amps/cm^2
- 1.55 to 1.75 gm/cm^3 void volume loading (includes $Co(OH)_2$).
- Batch Process: three separate impregnation tanks and bulk solution tank.
- 120 plaque capacity.
- Run time variable 60 to 180 minutes (plaque type, loading level, etc.).

EAGLE PICHER
COLORADO SPRINGS

POSITIVE FORMATION PROCEDURE

- 5 1/2 Cycles
- 20% KOH
- Initial discharge

Cycle	C/D	Amp/cm^2	Time (minutes)
1	D	0.07	20
	C	0.07	20
2	D	0.07	20
	C	0.07	20
3	D	0.07	20
	C	0.07	20
4	D	0.07	20
	C	0.07	20
5	D	0.02	20
	C	0.02	20
6	D	0.01	20

ELECTROCHEMICAL CHARACTERIZATION TEST

- 20 cycles at C Rate:
  120% Charge Discharge to -0.2V vs Hg/HgO
- 16 Hour Charge at C/10 rate
- Discharge at C/2 rate to -1.0V vs Hg/HgO
  Capacity Calculated
- 20% KOH
- D.I. H_2O Rinse and Scrub
- Final Weight and Thickness

EPI ELECTRODE STRESS TEST

- Hot Formation: 5C Rate, 70 C, 20% KOH, 2 cycles
- Pre-Stress: Weight, Thickness, and Visual Appearance Characterization
- Initial Capacity: Charge 5C for 12 min. C/2 for 1 hour
  Discharge C rate to -1.0V vs Ni sheet
- 200 Cycles: Charge 10C for 12 minutes
  Discharge 10C for 8 min. Diode clamped to -1.0V
- Ending Capacity: 5 cycles same as Initial Capacity
- Visual Appearance
- Scrub, Rinse, and Dry
- Weight Loss and Swelling

EAGLE PICHER
COLORADO SPRINGS

NEGATIVE ELECTRODE PRODUCTION FLOW CHART

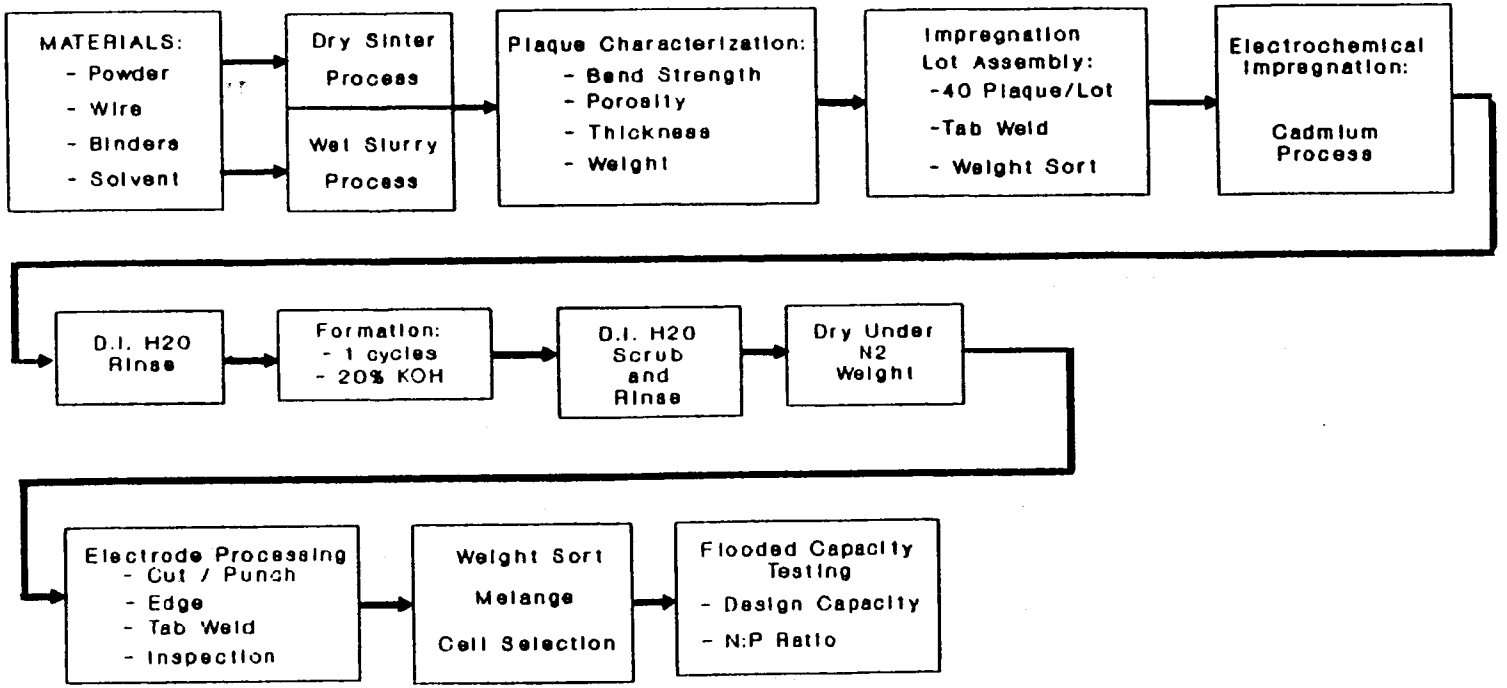

SINTERING PROCESS
(Negative Sinter)

- Dry Sinter Process
- Selected density: INCO type 287 powder
- Pure nickel woven wire current conductor
- Thickness: 0.70 to 1.02 +/- 0.05 mm
- Sinter Porosity: 85 +/-: 2% Overall Porosity: 81 +/- 2%
- Bend Strength: 400 to 700 PSI
- 100% inspection for thickness, porosity, strength, and physical appearance.
- Entire process MCD controlled with customer approval
- Proven production process: Electrodes for advanced Ni-Cd Flight and Test Programs

EPI/USAF NEGATIVE ELECTRODEPOSITION PROCESS

- Basic procedure developed for USAF/WPAFB under contract F33615-76-C-5407, "Manufacturing Methods for Nickel-Cadmium Batteries".
- Further development and optimization for Space Nickel battery applications by EPI (participation by Hughes and NASA).
- Aqueous Electrodeposition Process with Consumable Cadmium Anodes.
- Automated Process Contols
  - pH, Temperature, Flow, Current Density
- MCD Controlled Process
  - Dedicated solution analyzed prior to each run
  - Complete traceability for each electrode
  - 100% Inspection: dimensional, appearance, pickup

NEGATIVE ELECTRODEPOSITION PROCESS PARAMETERS

- 2.0 TO 2.5 M $Cd(NO_3)_2$
- 3.2 +/- 0.1 pH
- 90 to 100 C
- 0.08 Amps/cm^2 Constant Current and Pulsed Current
- 2.0 to 2.3 gm/cm^3 void volume loading
- Batch Process: three separate impregnation tanks and bulk solution tank
- 80 Plaque Capacity
- Run time variable 60 to 200 minutes (Plaque type, Loading level, etc.)

EAGLE PICHER
COLORADO SPRINGS

NEGATIVE FORMATION PROCEDURE

- 1 Cycle
- 20% KOH
- Charge then Partial Discharge

EAGLE PICHER
COLORADO SPRINGS

ELECTRODEPOSITED CADMIUM ELECTRODES

- Uniform Active Material Loading
- Reduced Cadmium Migration
- High Utilization Efficiency without Fading
- Large Surface Area and Improved Recombination Capability
- Automated Process Control Increases Electrode Uniformity
- High Quality Cadmium Electrode to Match Proven Electrodeposited Positive for Long Life even in High D.O.D. Applications

EAGLE PICHER
COLORADO SPRINGS

ELECTRODE PROCESSING FACILITY

- Parallel and Separate Positive and Negative Lines Dedicated to Space Battery Electrodes
- Shearing and Electrode Punching
- Resistance Welding Tab Attachment
- Electrode Edging Application
- 100% Electrode Inspection and Traceability
  - Dimensional
  - Weight
  - Physical Appearance
  - Weld
- Nitrogen Purged Storage at all Process Stages

EAGLE PICHER
COLORADO SPRINGS

ELECTRODE DEVELOPMENT ACTIVITIES
ELECTRODES TAILORED FOR VARIOUS DISCHARGE RATES

- Low Earth Orbit
  - Thinner Electrodes to support rate typically 0.6 to 0.7 mm
  - Active Material Loading to Support 5 year 50 to 60% D.O.D.
- Geosynchronous Orbit
  - Thicker Electrodes to Improve Energy Density 0.7 to 1.2 mm
  - Higher Active Material Loading Consistent with 10 to 15 year life
- Pulsed Power and High Rate Applications
  - Very Thin Electrodes 0.38 to 0.50 mm for extremely high current drains or pulse loads
  - Improved Tab Designs and Geometry to Minimize IR losses
  - Increased Plate Porosity with Low to Medium Active Material Loading Results in Improved Plate-Electrolyte Interface

HIGHER ENERGY DENSITY ELECTRODES

- Higher Porosity Nickel Sinter Substrates
  - Improved lower density carbonyl nickel powders
  - Selected nickel powder particle size distribution
  - Shift in sintered plaque porosity/strength relationship
    - Overall plaque porosity raised to 83 to 84% while maintaining current strength specifications
    - Maintain current plaque porosity while dramatically increasing strength for exceptionally long life, high D.O.D applications
    - Advanced sintering techniques and processes
- Higher Active Material Loading Levels
  - 1.75 to 2.0 gm/cm3 void volume positive electrodes
  - 2.3 to 2.5 gm/cm3 void volume negative electrodes
  - Maintain active material loading uniformity and utilization
  - Meet or exceed current electrode swelling and dimensional specifications

COMPUTERIZED SELECTION OF ELECTRODES FOR CELL ASSEMBLY

- Database is established for positive and negative electrodes
- Electrodes are ranked by active material weight from heaviest to lightest
- Computer program sorts qualified electrodes into cells
- Cell lot theoretical capacities are matched to within +/- 1.0%
- Cell lot electrode pack weight range is +/- 1.0% of the nominal

FLOODED CAPACITY TEST (FCT)

- Cells defined during electrode sort are assembled into temporary cells for test
- Test consists of three charge/discharge cycles at 18 C to establish both positive and negative capacities
- Residual carbonate level is substantially lowered
- Cells are removed from electrolyte and rinsed in DI H_2O
- Cells are dried under nitrogen to a constant weight
- Chemical analysis is performed on one cell from each FCT.
  - Positive - two plates are analyzed for total ionic nickel, trivalent nickel, and insoluble carbonates as potasium carbonate
  - Negative - two plates are analyzed for total cadmium, metallic cadmium, and insoluble carbonates as potasium carbonate

EAGLE PICHER
COLORADO SPRINGS

CELL ASSEMBLY

- Electrode tabs are trimmed to proper length
- Positive and negative electrode tabs are inserted and (GTAW) welded to their respective terminal tabs
- Positive and negative electrode assemblies are interleaved
- Header is (GTAW) welded to terminal tabs
- Plate pack is pressed and thickness measured
- Zircar separator is impregnated with PBI
- Separator is inserted into the plate pack
- Dry pack electrical resistance is checked with pack compressed

EAGLE EP PICHER
COLORADO SPRINGS

CELL ASSEMBLY (cont'd)

- Polypropylene liner and insulators are placed on cell
- Case bottom is (GTAW) welded to case and passivated
- Case is leak-checked with helium mass spectrometer (1 x 10E-8 std. cc/sec)
- Plate pack is inserted into case
- Cell electrical resistance is checked
- Header to case closure (GTAW) weld is performed
- Cell is pressurized with helium to 50 psig and leak-checked with helium mass spectrometer (1 x 10E-8 std. cc/sec)
- Cells are stored under nitrogen atmosphere prior to activation

CELL ACTIVATION

- Electrolyte volume is determined by measuring cell plate/ separator free volume and applying a fill factor
- Cell is evacuated, filled, and test gauge assembly is mounted
- Gauge assembly to cell swagelock fitting is leak-checked
- Cell is evacuated and allowed to stand 24 hours before testing begins

PRE-ACCEPTANCE TESTING PROCEDURES (PRE-ATP)

- Temperatures for all cycles is 18 C

- Five Formation Cycles
  - C/10 charge for 16 hours, C/2 discharge to 0.7 volt
  - C/2 charge for 130 minutes, C/2 discharge to 0.7 volt Short to 0.10 volt maximum
  - C/2 charge for 150 minutes, C/2 discharge to 0.7 volt
  - C/2 charge for 150 minutes, C/2 discharge to 0.7 volt
  - C/10 charge for 18 hours, C/2 discharge to 0.7 volt Short to 0.10 volt maximum

- Negative Precharge Cycle
  - 30% to 40% of the excess negative capacity as determined in FCT is specified
  - The method for setting negative precharge is venting a predetermined volume of oxygen during overcharge
  - C/2 charge for 2.0 hours and current reduced down to approximately C/4 for the remainder of the charge, C/2 discharge to 0.7 volt

EAGLE PICHER
COLORADO SPRINGS

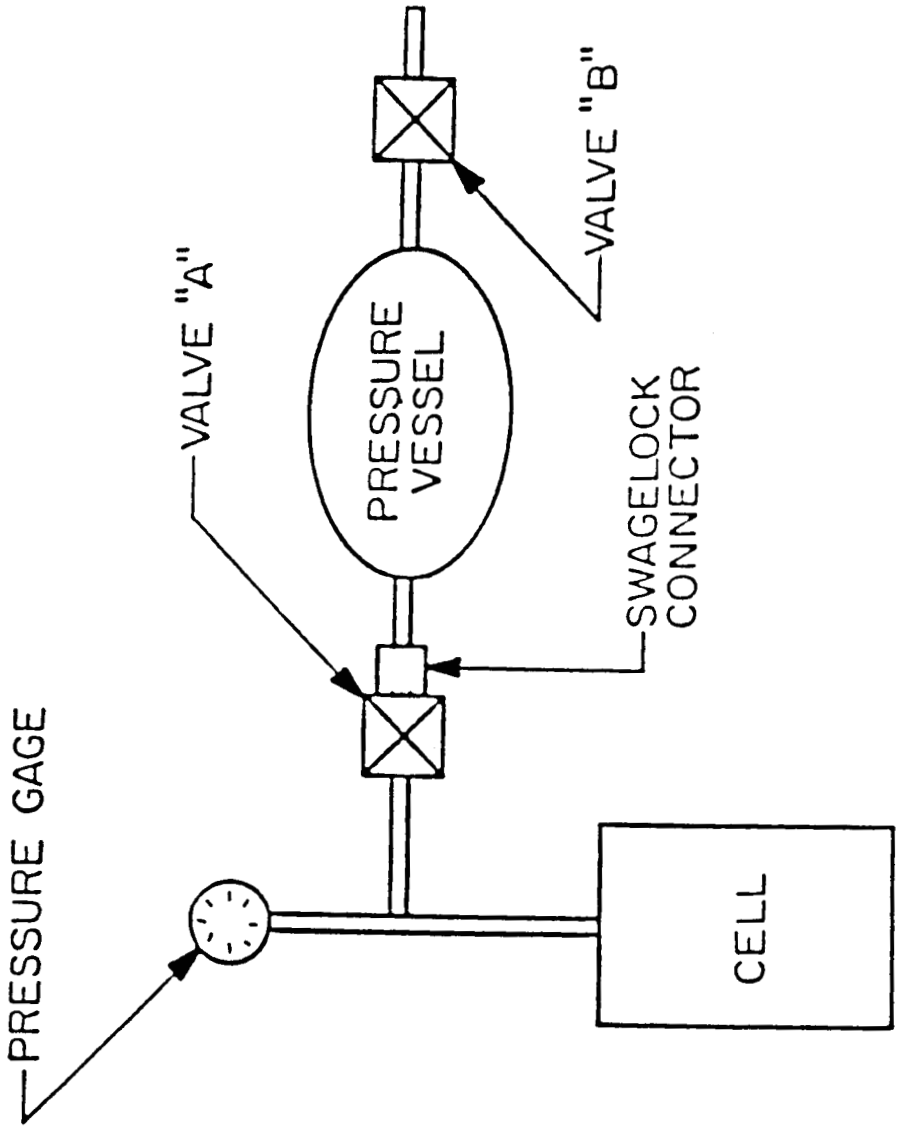
PRESSURE GAGE
VALVE "A"
PRESSURE VESSEL
VALVE "B"
SWAGELOCK CONNECTOR
CELL

PRE-ACCEPTANCE TESTING PROCEDURE (cont'd)

- Three Burn-In Cycles
  - C/4 charge for 4.5 hours, reduce current to C/10 for 4.0 hours, C/2 discharge to 0.7 volt, capacity at 1.0 volt, short down for 13 hours
  - Repeated for a total of three cycles
- Overcharge Cycle
  - C/10 charge for 48 hours, discharge to 0.7 volt, capacity at 1.0 volt

EAGLE EP PICHER
COLORADO SPRINGS

DESTRUCTIVE PHYSICAL ANALYSIS

- One cell per 50 cells on Pre-ATP sample rate
- Precharge Determination
  - Selected cell is charge and deep discharged at room temperature
    - C/10 charge for 20 hours
    - Open circuit stand for .25 hours
    - C/2 discharge to 1.0 volt
    - C/10 discharge to -1.0 volt
  - Cell electrical capacity and Ah equivalent of measured hydrogen volume from the time of reversal to -1.0 volt define the precharge of the cell
- Cell Disassembly and Inspection
  - Cell case is removed and visual inspection is made
  - Plates and separator are removed one by one and visual inspection is made
  - A sample of positive and negative plates is submitted for chemical analysis (Same analysis as FCT sample cell)

DESTRUCTIVE PHYSICAL ANALYSIS (cont'd)

- Two cells are assembled with plates from the sample cell and polypropylene separator
- Positive cell is made-up of positive plates from the sample cell and extra negative plates from the same cell lot (cell is built with excess negative capacity)
- Negative cell is made up of negative plates from the sample cell and extra positive plates from the same cell lot (cell is built with excess positive capacity)

ACCEPTANCE TESTING PROCEDURE (ATP)

- Capacity Test at 10 C
  - Cells are shorted down to 0.010 volt maximum, 16 hour minimum
  - Cells are soaked at 10 C for 4 hours
  - C/10 charge for 20 hours, 1 hour open-circuit stand, C/2 discharge to 1.0 volt
- Overcharge and Capacity Test at 0 C
  - Cells are shorted down to 0.010 volt maximum, 12 hour minimum
  - Cells are soaked at 0 C for 4 hours
  - C/20 charge for 72 hours, 1 hour open-circuit stand, C/2 discharge to 1.0 volt

ACCEPTANCE TESTING PROCEDURE (ATP cont'd)

- High Current Discharge Test at 22 C
  - Cells are shorted down to 0.010 volt maximum, 12 hours minimum
  - Cells are soaked at 22 C for 4 hours
  - C/10 charge for 20 hours, 5C pulse discharge for 10 seconds, C/2 discharge to 1.0 volt
- Charge Retention (Discharged) Test at 22 C
  - Cells are shorted down for 12 hours
  - C/10 charge for 10 minutes, open-circuit for 24 hours, minimum voltage 1.15 volts

NASA ACCEPTANCE TESTING PROCEDURE

- Room Temperature (23 C) Capacity Test
- High Temperature (30 C) Capacity Test
- Low Temperature (0 C) Overcharge Capacity Test
- Low Rate Efficiency Test
- Room Temperature Capacity Test
- High Rate Discharge Test
- Charge Recovery (Discharged) and Impedance Test

EAGLE PICHER
COLORADO SPRINGS

CELL FINAL PREPARATION FOR SHIPMENT OR STORAGE

- Fill tube is crimped, (GTAW) welded, cut, and (GTAW) welded
- Fill tube closure weld is leak-checked with indicating solution (Phenopithalein)
- Cells are cleaned to remove all traces of KOH, leak-checked after minimum 24 hour stand period
- Cells are marked (electoetched) with EPI's part number, customer's part number, lot and serial number, and fill date
- Terminals are tinned
- Cells weight is recorded
- Cells OCV is recorded
- Cells are packaged for shipping or placed in storage

SUPER Ni-Cd CELL DESIGNS

Rated Capacity (Ah at 10 C)	4.8	9.0	12.0(2)	19.0	20.0	21.0	38.0(2)	42.0	50.0
Overall Height (inches)	3.170	4.000	4.000	4.360	4.360	4.670	6.420	6.952	7.250
Case Height (inches)	2.675	3.670	3.670	4.010	4.010	4.302	6.020	6.554	6.488
Case Width (inches)	2.143	2.890	2.890	3.500	3.500	3.740	4.980	4.980	4.941
Case Thickness	0.884	0.905	1.135	1.135	1.135	1.135	1.038	1.038	1.328
Weight (grams)	235	460 (1)	580 (1)	780	820 (1)	880	1570(1)	1728 (1)	2350
Specific Energy (Wh/Kg)	27.6	29.5 (1)	30.4(1)	32.8	32.0(1)	33.5	33.6(1)	31.6 (1)	29.1

(1) Estimated from design
(2) Design and partial tooling completed

For GEO Missions the life expectancy is 10 to 15 years at 80 percent DOD
For LEO Missions the life expectancy is 5 years at 40 percent DOD (approx. 30,000 cycles)
Delivery: Approximately 9 months ARO or 12 months for a new design other than those listed

EAGLE PICHER
COLORADO SPRINGS

MAGNUM Ni-Cd CELL DESIGNS

Rated Capacity (Ah at 10 C)	4.8	10.0	12.0 (2)	20.0	21.0	38.0 (2)	42.0	50.0
Acutal Capacity (Ref. only)	5.4	11.3	14.7	21.9	25.5	43.9	47.5	60.8
Overall Height (inches)	3.170	4.000	4.000	4.360	4.670	6.420	6.952	7.250
Case Height (inches)	2.675	3.670	3.670	4.010	4.302	6.020	6.554	6.488
Case Width (inches)	2.143	2.890	2.890	3.500	3.740	4.980	4.980	4.941
Case Thickness	0.884	0.905	1.135	1.135	1.135	1.038	1.038	1.328
Weight (grams)	209	415 (1)	502 (1)	726 (1)	841	1411 (1)	1570 (1)	1900
Specific Energy (Wh/Kg)	31.0	32.7 (1)	35.13 (1)	36.2 (1)	36.4	37.3 (1)	36.3 (1)	38.4

(1) Estimated from design
(2) Design and partial tooling completed

For Geo Missions the life expectancy is 8 to 12 years at 80 percent DOD
For LEO missions the life expectancy is 4 years at 40 percent DOD (approx. 24,000 cylces)
Delivery: Approximately 9 months ARO or 12 months for a new design other than those listed

EAGLE PICHER
COLORADO SPRINGS

EAGLE-PICHER INDUSTRIES, INC.
COUPLES DEPARTMENT, COLORADO SPRINGS
HISTORY OF "SUPER Ni-Cd" ACTIVITIES

CUSTOMER	PROGRAM	CELL TYPE	QUANTITY	MANUFACTURING PERIOD	SHIP DATE	CURRENT STATUS/COMMENTS
HAC-EDD	LEASAT	21AH "Super Ni-Cd" Lightweight	145	March '88 - March '89	March '89	Launch Date & Site - January '90 Cape Canaveral
HAC-EDD	PALAPA B2R	19AH "Super Ni-Cd" Lightweight	102	August '88 - April '89	April '89	Launch Date & Site - April 13, 1990/ Cape Canaveral
JPL	JPL/CRANE, NWSC Test	21AH "Super Ni-Cd" Lightweight	60	June '88 - June '89	June '89	Test program - Z/PBI, Z/FS and PP/PBI, Separator Types, LEO & GEO
HAC-EDD	ASIASAT 1	19AH "Super Ni-Cd" Lightweight	85	Dec. '88 - July '89	July '89	Launch Date & Site - April 7, 90 Xichang, China
HAC-EDD	GALAXY 6	19AH "Super Ni-Cd" Lightweight	85	Dec. '88 - Oct. '89	Oct. '89	Launch Date & Site - September '90
TRW	TRW Test	19AH "Super Ni-Cd" Lightweight	25	July '89 - Oct. '89	Oct. '89	TRW Test Program
Aerospace Corp.	Aerospace Corp./Crane NWSC test	21AH "Super Ni-Cd" Lightweight	10	Aug. '90 - Feb. '91	Feb. '91	Assembly Completed, Activation & AIP in November '90
Lockheed	Lockheed Test	21AH "Super Ni-Cd" Lightweight	4	Nov. '89 - Dec. '89	Dec. '89	Parametric Testing Completed
MDESC/ NASA	Modular Power Sub-System	50AH "Super Ni-Cd" Standard	118	Jan. '89 - June '90	June '90	MDESC Preparing to assemble batteries
HAC-EDD	GALAXY 5	21AH "Super Ni-Cd" Lightweight	85	Oct. 89 - Sept. '90	Sept. '90	HAC ATP Testing
HAC-EDD	GALAXY 1R	21AH "Super Ni-Cd" Lightweight	85	Oct. '89 - Feb. '91	Feb. '91	Assembly Complete, Dry Storage, Activate Jan. '91
HAC-EDD	GMS-5	5AH "Super Ni-Cd" Lightweight	31 70	Oct. ' 89 - Oct. '90 Oct. '89 - Dec. - 92	Oct. '90 Oct. '92	EPI ATP Complete/Qual. Pack Cells Flight Cells/Dry Storage until Oct. '92
HAC-EDD	PALAPA B4	20AH "Super Ni-Cd" Lightweight	85	Nov. '89 - Feb. '91	Feb. '91	Assembly Complete, Activation - AIP in November '90
HAC-EDD/ Fairchild Indiana	SMEX	9AH "Super Ni-Cd" Lightweight	99	June '90 - April ' 91	July '91	Impregnating Plaque
HAC-EDD/ Aerospace Corp.	Aerospace Corp/Crane NWSC Test	42AH "Super Ni-Cd" Lightweight	10	June '90 - April '91	April '91	Impregnating Plaque

OTHERS NUMEROUS BUDGETARY AND FFP PROPOSALS IN PREPARATION AND EVALUATION

October 1990

CURRENT WORK-IN-PROGRESS

- Expanding Super Ni-Cd and Magnum Product Lines
- Manufacturing Control Document, cell specification data, cell drawing packages and tooling are all being modified as needed for new designs
- Current New Super Ni-Cd Designs under development
  12 Ah and 38 Ah
- Current New Magnum Ni-Cd Designs under development
  5 Ah, 10 Ah, 12 Ah, 20 Ah, 21 Ah, 38 Ah, 42 Ah, and 50 Ah

SEPARATOR QUALIFICATION PROGRAM

- NEAR TERM GOALS
  - Identify Chemical, Physical, and Mechanical Characteristics
  - Identify BOL Cycle Characteristics
- LONG TERM GOALS
  - Perform Accelerated Lifecycle Testing
  - Maximize Cell Electrolyte Volume and Cycle Life
  - Provide Recommendations for Separator Use

EAGLE EP PICHER
COLORADO SPRINGS

SEPARATOR QUALIFICATION PROGRAM
CHEMICAL, PHYSICAL, AND MECHANICAL ANALYSIS

- Wetability
- Absorbency
- Resistivity
- Air Permeability
- Bubble Pressure
- Tensile Strength
- KOH Resistance
- Cost
- Fiber Type and Size
- Surface Area
- Pore Size
- Contaminents
- Thickness
- Basis Weight
- Availibility

Methodology to be developed with NASA

EAGLE EP PICHER
COLORADO SPRINGS

SEPARATOR QUALIFICATION PROGRAM
BOL CYCLE CHARACTERISTICS

- Cell Type
  - Boiler plate construction
  - EPI electrochemically-deposited plates
- Characterization Test Regime
- Information
  - Optimum electrolyte volume
  - Initial capacity data
  - Initial pressure data
  - Cell impedance
  - Cell performance VS Interelectrode spacing and Separator compression

SEPARATOR QUALIFICATION PROGRAM
ACCELERATED LIFECYCLE TESTING

- Simulate GEO Lifecycle
  - DOD 80%
  - Two temperatures (10 C, 25 C)
  - Destructive analysis of all failures
- Simulate LEO Lifecycle
  - DOD 80%
  - Two temperatures (10 C, 25 C)
  - Destructive anlaysis of all failures
- Information
  - Identify failures due to separator
  - Identify mechanism of failure

EAGLE EP PICHER
COLORADO SPRINGS

CYLINDRICAL, FLAT PLATE Ni-Cd CELLS TO MEET LARGE CAPACITY SPACECRAFT REQUIREMENTS

- Projected Performance Advantages Over Prismatic Ni-Cd Cells
- Pressure vessel design would allow cell to operate at pressures as high as 800 psig to 900 psig
- Electrolyte volume could be increased
- Heat dissipation from interior of the cell to the exterior of the cell would be greatly improved over large prismatic type Ni-Cd cell designs
- Specific Energy would be comparable to the prismatic Ni-Cd design
- Inner cell case could be coated with a catalytic platinum coating to facilitate recombination of hydrogen and oxygen in the event of deep discharge and reversal of the cell

EAGLE-PICHER MAGNUM 200

Capacity	200 Ah
Specific Energy (1)	31.7 Wh/Kg
Weight (est.)	16.7 lbs
Diameter	4.7 inches
Length	12.3
Terminal Type	Ziegler Seal
Case Material	304L Stainless Steel

(1) Rated at 10 C and 100% DOD

Specifications Subject to Change Without Notice

EAGLE PICHER
COLORADO SPRINGS

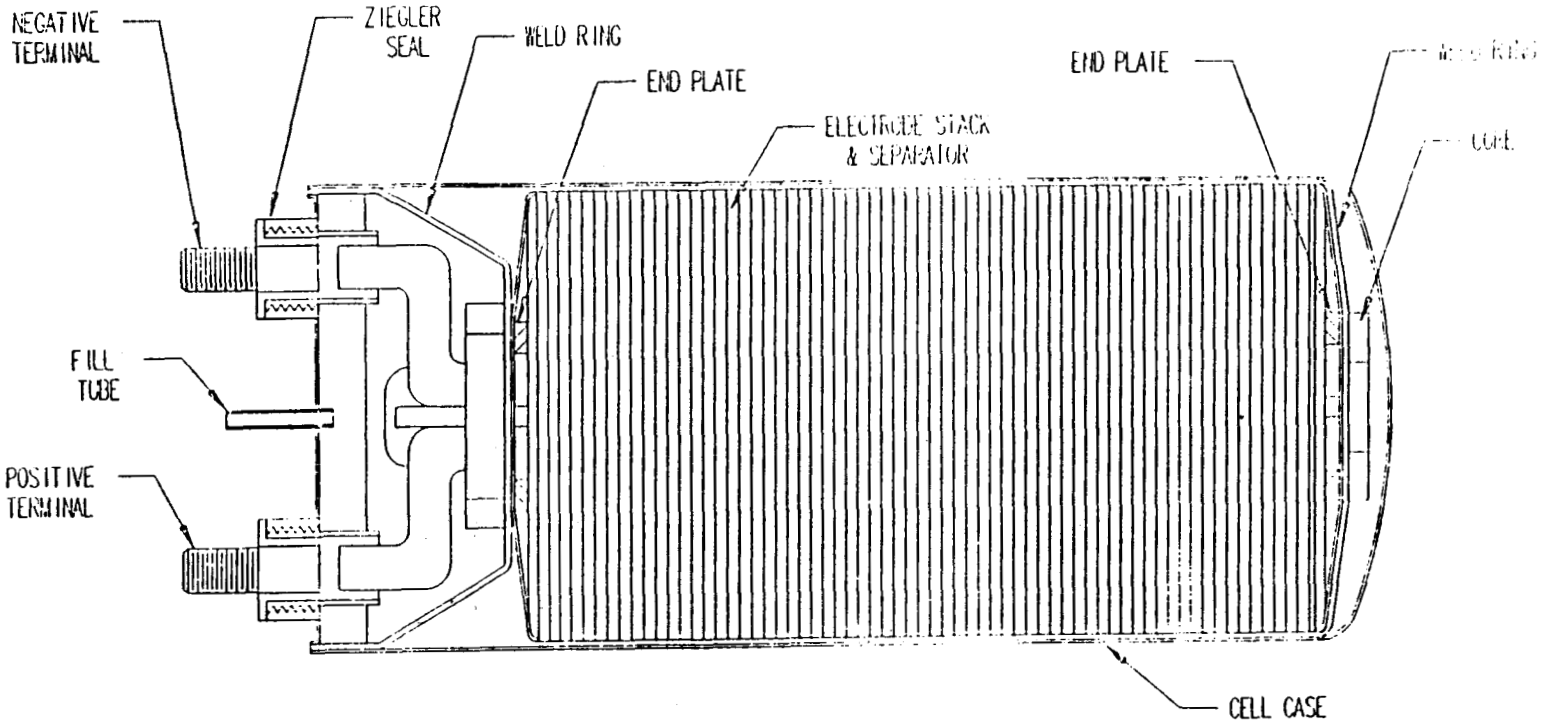

EAGLE-PICHER MAGNUM 200

EAGLE PICHER

COLORADO SPRINGS, CO

HUGHES ADVANCED NICKEL-CADMIUM BATTERIES - AN UPDATE

R. Sam Bogner

Hughes Aircraft Company Industrial Electronics Group
Electron Dynamics Division
Energy Storage Product Line
P.O. Box 2999
Torrance, CA 90509-2999

ABSTRACT

After developing a significant data base on boilerplate and prototype advanced nickel-cadmium (Ni/Cd) battery cells, Hughes Space and Communications Group decided to start using the Advanced Ni/Cd batteries on several of their flight programs. The advanced cell can be operated at 80% depth of discharge (DOD) for more than ten years, and possibly 15 years, in geosynchronous earth orbit (GEO) applications. This cell offers an important weight saving over the standard Ni/Cd cell that is usually only operated at 50 to 60% DOD in GEO applications. The negative and positive electrodes are manufactured using electrochemical deposition methods which reduce the sinter corrosion problems encountered by the chemical deposition process used in standard Ni/Cd cells. The degradable nylon separators used in standard Ni/Cd cells were replaced by polymer-impregnated Zirconia separators. Approximately 1,000 Advanced Ni/Cd cells have been built and several hundred more cells all expected to be built in the next few years. Advanced Ni/Cd batteries currently are employed on six different spacecraft in GEO flight with plans to launch six more spacecraft in the next three years.

INTRODUCTION AND BACKGROUND

Nickel-cadmium batteries have been the workhorse for supplying stored electrical energy for spacecraft since Sputnik and Explorer. The sintered plate technology which is used was developed in Germany and acquired by the United States after World War II. Fleicher described the process in 1948 (1). Basically the process consisted of vacuum impregnating the porous nickel sinter in aqueous cadmium or nickel nitrate solutions for the negative and positive electrodes, respectively. The nitrates were converted by cathodic polarization in hydroxide solutions. The impregnation and cathodization process had to be repeated several times to get the proper quantity of active material in the pores of the sinter. Since the nitrate impregnation solutions are acidic, there is corrosion of the sinter. On cycling the positive electrodes would expand. This expansion of the positive electrodes proved to be a major failure mechanism in Ni/Cd spacecraft cells which is a modification of the process described by Fleicher.

Figure 1 shows plots of positive plate swelling as a function of cycle removed from test (2). This data was developed on the NASA-sponsored "Accelerated Test Program" at Naval Weapons Support Center (NWSC). The test cells were 6-Ah General Electric cells built in 1974 using the SAFT chemical deposition (CD) process*. The plots are for the "Star Point" test packs. From the data, it was postulated that when the positive plates grew from the beginning-of-life nominal thickness of 0.0766 cm to approximately 0.0975 cm, the cells would fail. The point at which the plots cross the 0.0975 cm line is the predicted cycle life. Table I lists the observed and predicted cycle life and the measured thickness of the electrodes at failure (12). In all but two cases, correletation coefficients of predicted cycle life to observed cycle life was greater than 0.9.

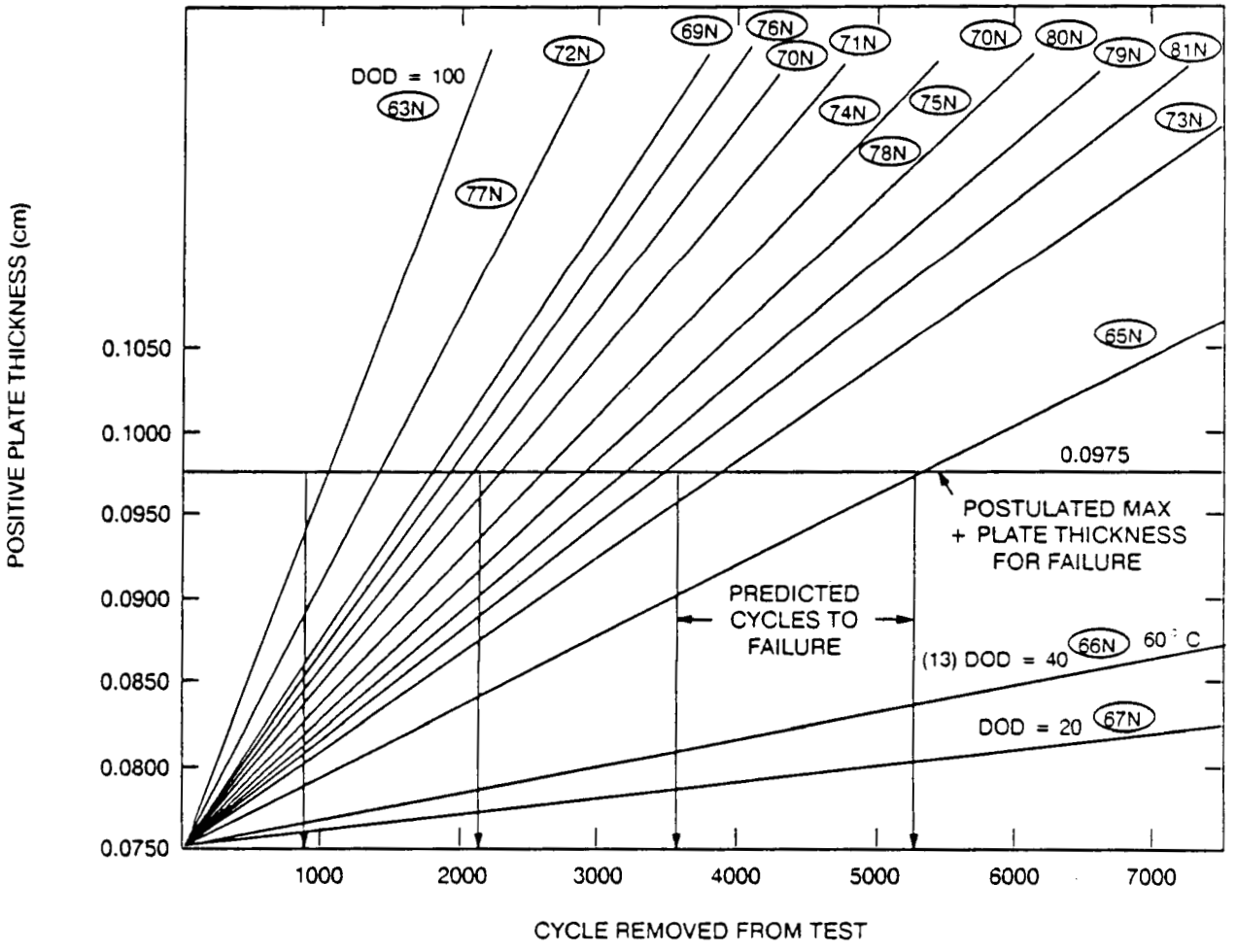

Figure 1 Accelerated test. Plots of positive plate growth for star point-test packs (taken from Reference 2).

*The SAFT process is a high volume production modification of the Fleicher process.

TABLE I

OBSERVED AND PREDICTED CYCLE LIFE (12)
STAR POINT PACKS ON THE NASA ACCELERATED TEST PROGRAM

Pack Number	Observed Cycle Life	Max. Pos. Thickness (cm)	Predicted Cycle Life to 0.0975 (cm)
65N	5660	0.0946	5400
66N	13	—	—
67N	14066	0.0842	38400
68N	955	0.1006	950
69N	591	0.0825	1600
70N	1512	0.0930	1800
71N	1638	0.0925	1900
72N	1717	0.1096	1300
73N	3501	0.0993	3500
74N	1801	0.0954	2150
75N	2557	0.0957	2400
76N	1669	0.0995	1750
77N	1909	0.1106	1450
78N	2368	0.0960	2400
79N	3732	0.1001	3732
80N	3223	0.0989	2600
81N	3055	0.0954	3200

Lim reported on the expansion of CD and electrochemical deposited (ED) electrodes in accelerated cycle tests of boiler plate cells. After 3000 cycles, the CD electrodes expanded by 30%, while the ED electrodes just started to expand. The average expansion of ED electrodes was only about 10% after 5000 cycles.

It is postulated that the expansion of the positive electrodes absorbs additional electrolyte, compresses the separator, and causes a failure mode that has been termed "separator dryout". Another failure mechanism assisted by positive plate expansion is shorting. Shorts are generally produced by cadmium migration into the separator, so as the positive plate expands the distance for a short to accrue becomes smaller and smaller, eventually allowing the cadmium to bridge between the electrodes.

For the past 20 years, aerospace Ni/Cd cells contained a non-woven nylon separator (Pellon 2505) that was originally manufactured for the clothing industry. The Pellon Corporation stopped manufacturing the 2505 material about 1986. Now most aerospace cells contain another

non-woven nylon material designated Pellon 2556. In any event, separator degradation is another critical failure mechanism in the standard Ni/Cd cell and will be discussed later.

The sealed Ni/Cd cell is designed with excess cadmium metal and cadmium hydroxide which allows the cell to be operated and overcharged in the sealed state. Figure 2 shows a schematic of the relative states of the nickel (positive) and the cadmium (negative) electrodes and the cell reaction. The negative electrode contains an excess of cadmium hydroxide in relation to the available capacity of the positive electrode. Therefore, during charge and overcharge, oxygen is generated at the positive electrode. Since there is excess uncharged cadmium hydroxide, hydrogen is not generated at the negative electrode. The oxygen generated at the positive electrode reacts with the cadmium to form more cadmium hydroxide, thus the negative electrode never reaches a full state of charge. If the oxygen generated reacts with other materials in the cell, such as the nickel sinter and the nylon separator, (3) the cadmium electrode will gradually reach a higher state of charge and hydrogen will eventually be generated. Hydrogen does not react rapidly with the

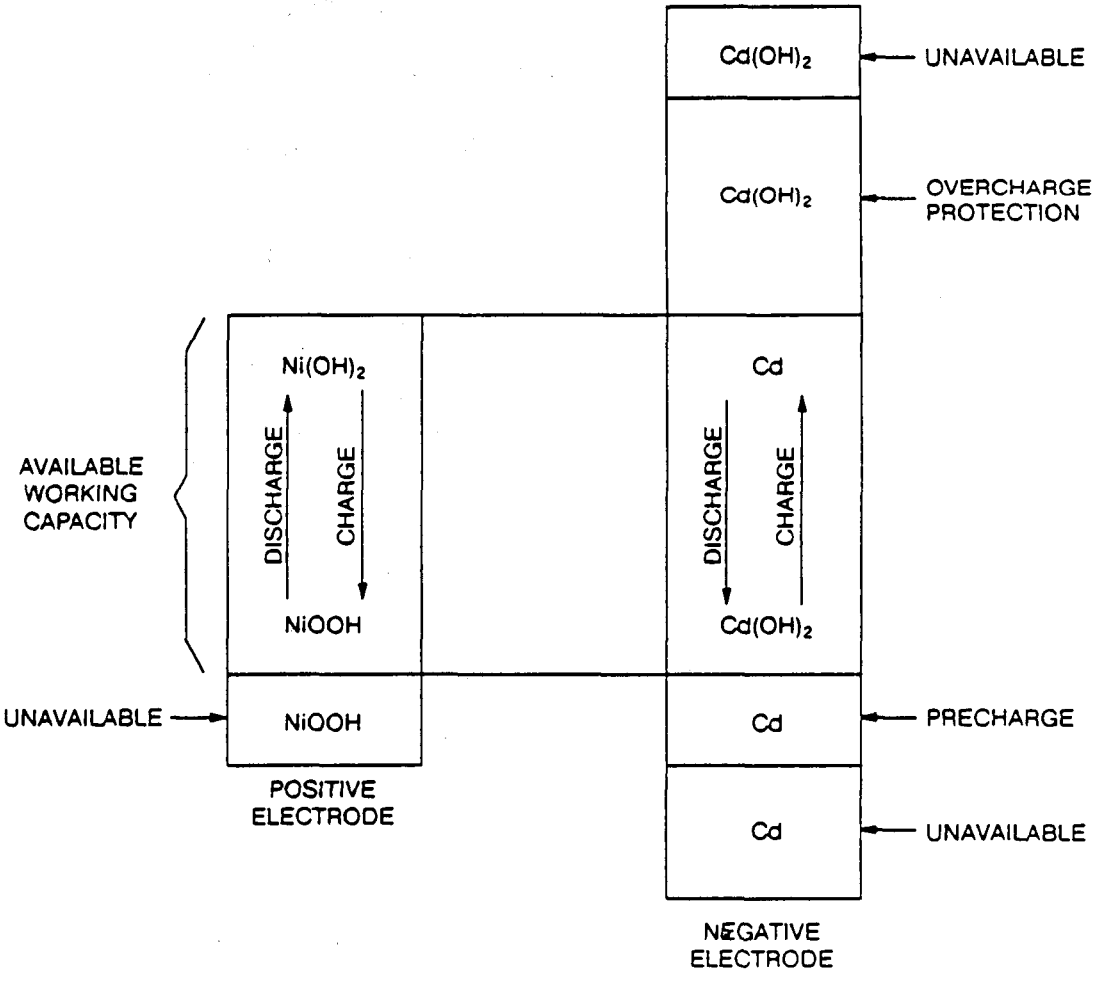

Figure 2 Diagram showing overcharge protection and precharge in a nickel cadmium cell.

positive electrode and the gradual pressure build-up can rupture the cell. The loss of overcharge protection manifests itself by a gradual increase in the charge potential of the cell, so excess pressure build-up can be controlled by stopping the charge based on a voltage, temperature (VT) curve. This, however, reduces the usefulness and capacity of the battery and leads to failure.

ADVANCED CELL DESIGN

Early developments of the Hughes Advanced cell design were presented at the Fourth Annual Battery Conference (4) and in other publications (5)(6)(7)(11). To increase the life capability of the Ni/Cd battery cell it was recognized that new processes and materials were required to ameliorate the failure mechanisms described above. In the early 80's when Hughes embarked on advancing the state of the art in the Ni/Cd system on an IR&D program, development was progressing on the nickel-hydrogen (Ni/H_2) system. Most of the developers of Ni/H_2 were using nickel electrodes that were impregnated using (ED) techniques. A review of electrochemical impregnation for Ni/Cd cell was sponsored by Jet Propulsion Laboratory (8). Pickett (9) presented a review of nickel oxide electrodes and indicated that the time may be near to use ED electrodes in space Ni/Cd cells. In general, the literature indicated the ED positive electrodes can be loaded lighter, swell less, and give higher active material utilizations than CD positive electrodes. It was, therefore, decided to evaluate ED positive electrodes in Ni/Cd cells to determine if ED plates would improve the life of Ni/Cd cells.

As noted above, another major failure mechanism arose from the degradation of the nylon separator. Hughes Research Laboratory (HRL) set out to find an inert separator material. The objective was to develop a separator that is chemically stable for a minimum of 10 years and has better electrolyte retention qualities and better oxygen permeability than the Nylon Pellon 2505 separator. This research produced polybenzimidazole (PBI) and polysulfone (PS) impregnated woven cloth structure zirconium oxide fabrics, Z-PBI and Z-PS, respectively. We have chosen to use the Z-PBI separator in our flight cells. The properties of these separators were reported in a recent paper (10).

In addition to using ED positive electrodes, we are also using ED negative electrodes. By using ED electrodes and the Z-PBI separator material, we can put slightly over 4 ml. of electrolyte per ampere hour of theoretical positive plate capacity into the cell. That is about 1 ml. more electrolyte per ampere hour than is put into a standard Ni/Cd aerospace cell.

The advantages of the Hughes Advanced Ni/Cd cell over the present Ni/Cd cell are as follows:

1. The degradable nylon separator was replaced by an inert zirconia separator similar to those used in Ni/H_2 cells. The advantages are a reduction in loss of negative overcharge protection, better electrolyte retention, and better gas permeability.

2. Replacement of the CD positive electrode with an ED positive electrode. The advantages are less substrate corrosion, less expansion of the electrode with cycling, and reduced loss of overcharge protection because of less oxidation of the nickel sinter.

3. Replacement of CD negatives with ED negatives and the use of an expander. The advantages are reduced substrate corrosion, high active material utilization, and reduced cadmium electrode loss in capacity or fading.

4. The synergism of the design allows a 33% increase in electrolyte quantity in the cell, which, along with the reduced expansion of the positive electrodes, prevents the separator dryout failure mechanism.

SUMMARY OF DEVELOPMENT TESTING

Numerous boilerplate, proto flight, and flight cells have been and are being tested by Hughes on various accelerated cycling regimes and real time GEO cycles. The results of the boilerplate and proto flight cells have been reported in previous papers.(4)(5)(6)(7) Table II summarizes the tests performed and in progress. Below are brief descriptions of the test articles and test regimes listed in Table II.

Accelerated LEO Test

This test was performed on small boilerplate cells assembled in the lab. The cells were rated at 4.36 Ah and yielded from 4.61 to 4.98 Ah at the 0.5 C rate. The cells contained CD positive and negative electrodes and polymer impregnated zirconia cloth. Three cells each were tested at 20°, 40° and 50°C and at 40% DOD. The cycle regime consisted of a 16-minute discharge at 1.5 C rate and 24-minute charge at the 1.5 C rate for a recharge ratio of 1.5. The cycle life of the cells at 50°, 40° and 25°C were 11,500, 16,300 and 43,000 cycles respectively. This was about three times the cycle life of Ni/Cd cells tested at the Naval Weapons Support Center on the NASA sponsored Accelerated Test Program (12).

Two additional cells with ED positive electrodes, CD cadmium electrodes, and polymer-impregnated zirconium cloth separators were cycled at 80% DOD in the termperature range of 27°C ±2°C. The cycle life of these two cells ranged from about 6,200 to 9,300 cycles. From these results, Lim concluded that Ni/Cd cells could be built that would have about the same cycle life as Ni/H_2 cells cycled at 80% DOD.

Accelerated GEO – 16 Cycle Season

This test was performed on boilerplate cells similar to those described previously; however, an additive was added to the electrolyte. The 16-cycle season consisted of cycles varying from 10 to 80% DOD in 10% DOD steps. The test temperature was 10° to 15°C. The discharge rate was 0.5 C and the charge rate was about 0.1 C with a 120% charge return. A nine minute trickle charge at 0.02 C was performed on each cycle. One eclipse period required four days. The cells were reconditioned after three 16 cycle seasons (every 48 cycles similar a normal GEO eclipse season) by discharging at 0.05 C to 1.0 volt and recharging at 0.1 C.

As shown in Table II, these cells cycled for 216 to 313 seasons, which is equivalent to about 3,450 to 5,000 cycles. This is equivalent to 36 to 52 years of cycling in GEO.

A similar test was performed on two groups of 20-Ah proto-flight cells. As listed in Table I, these cells were at 37 and 83 seasons when the test was discontinued. This test regime did not

TABLE II
SUMMARY OF ADVANCED Ni/Cd CELL TESTING

Type Test	Type Cell	No. Cell	Cell A-hr	No. Seasons/ Cycles	DOD %	Status/ Comments
Accelerated LEO	Boiler-plate	12	4.36	6000 to 43,000 Cycles	40 to 80	Complete (45 Min. Cycle)
Accelerated GEO	Boiler-plate	15	6.8	216 to 313 Seasons 3450 to 5000 Cycles	80	Discontinued
Accelerated GEO 46 Day Season	Proto Flight	10	12	24 to 38 Seasons	60 to 80 (2)	Complete (22 Day, 50° Solstice)
Realtime	Proto Flight	8	12	19 Seasons	60 to 80 (3)	Continuing (1)
Accelerated GEO 16 Cycle Season	Proto Flight	11	20	37 to 83 Seasons	80	Discontinued
Accelerated GEO 46 Day Season	Proto Flight	18	20	14 Seasons	80	Continuing (1) 14 Day Solstice
Direct Broadcast or DB Accelerated GEO, 46 Day Season	Flight	5	21	11	80	Continuing 14 Day Solstice
DB Throughput	Flight	6	21	1825 Cycles	80	Continuing 3 Cycles/Day
LEASAT F5 LEO Qual. Pack	Flight	8	21	1300	80	Test at NWSC Crane
LEASAT F5 Accelerate GEO 46 Day Season	Flight	2	21	3 Seasons	80	Continuing 14 Day Solstice
Program A Throughput	Flight	5	19	70 Cycles	80	Continuing
Program B Realtime	Flight	4	19	1 Season	80	Continuing

All Flight and Proto-Flight cell tests run at 10°C.

NOTES: (1) Test put on trickle charge for about 8 months in 1990.
(2) 60 Percent DOD for first 18 seasons.
(3) 60 Percent DOD for first 5 seasons.

appear to be very stressful on the cells since up to 52 years (5,000 cycles) of equivalent cycle life was obtained on the boilerplate cell tests.

Accelerated GEO – 46 Day, Eclipse Season – 22 Day 50°C Solstice

This test consisted of the normal 46 day eclipse season. The cells were discharged at C/2 and recharged at C/10 with 120% charge return, then put on trickle charge at for the remainder of the time to produce a 24-hour cycle period. The maximum DOD was 60% for the first 18 seasons and 80% DOD thereafter. The solstice period was accelerated by raising the temperature of the cells to 50°C for 22 days. The cells were trickle charged at C/36. The cells were given one reconditioning cycle at room temperature between each season by discharging at C/50 to 1.0 V and recharging at C/10 for 16 hours.

The test cells were proto-flight 12-Ah cells using ED electrodes and various combinations of separators (Z-PBI, Z-PS and PP-PBI). Cells containing Pellon 2505 nylon separators were used as controls. The control cells failed after 10 seasons because of high charge voltages. Apparently the 50°C temperature acceleration was too stressful, causing accelerated nylon hydrolysis which resulted in loss of overcharge protection. The Z-PS cells were found to be faulty during initial testing and were not continued. The remaining cells went from 24 to 38 seasons.

Realtime Test

The realtime test simulated the battery operation in GEO, 46-day eclipse periods followed by 136 days of solstice including the time to recondition. Reconditioning was performed as described on the previous test. The test temperature is 10° ±3°C.

This test is being performed on some of the 12-Ah proto-flight as described in the previous test. During the first five eclipse seasons, the cells were cycled to a maximum of 60% DOD. Since then, they have been cycled to 80% DOD. The cells are presently in the 19th eclipse season and is the longest realtime test performed on Super Ni/Cd cells. Figure 3 shows a plot of the end of discharge voltage on the longest eclipse day during each eclipse season.

A group of four 19-Ah flight cells (Program B Realtime) are on a similar realtime test but have only gone through one season.

Accelerated GEO – 46 Day 0.68 C Eclipse Season – 14 Day Solstice

As noted in Table II, there are three different groups of cells on this type of test. The groups are: (a) 20-Ah proto-flight cells; (b) Direct Broadcast or DB 21-Ah flight cells; (c) 21-Ah Leasat flight cells. This test consists of putting the cells through the discharge/charge cycles that would occur during a GEO mission. The longest eclipse day (70 minutes) discharges 80% of rated cell capacity. The cells are discharged at about the 0.68 C (14.4 A for the 21-Ah cells) rate and recharged at the 0.1 C rate for a 115% charge return and switched to a trickle charge rate of approximately 0.023 for the remainder of the 24 hour cycle period. The solstice period is shortened from the usual 136 days to 14 days, during which time the cells are trickle charged at about 0.023 C. After each solstice period, the cells are reconditioned by discharging through a resistor (approximately the 50 hour rate) until the first cell in the group reaches 1.0 V. The cells are recharged at about 0.1 C rate for 120% return. The tests are run in environmental chambers that control the cell temperatures to 10°C ±3°C.

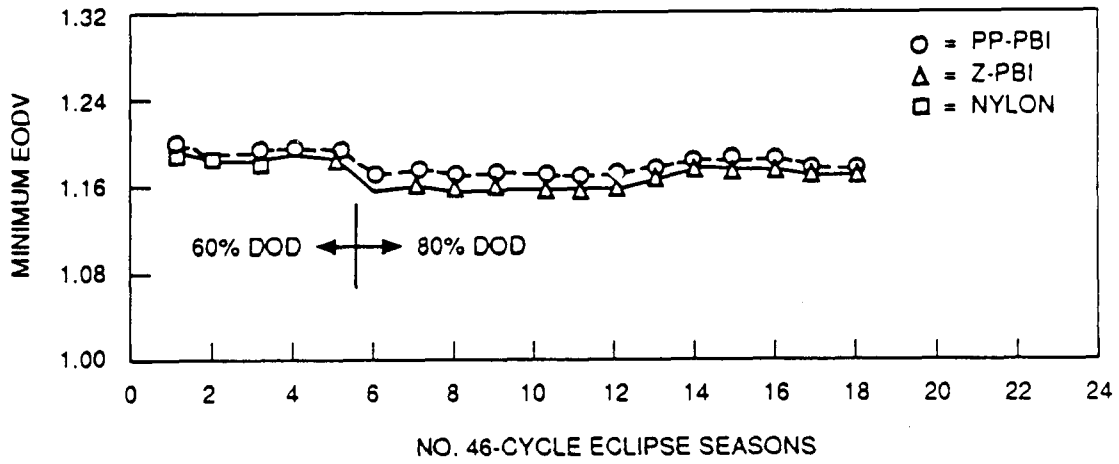

Figure 3 12-Ah protoflight cell realtime GEO test.

The 20-Ah proto-flight cells, 21-Ah DB cells, and 21-Ah Leasat cells have gone through 14, 11, and 3 eclipse seasons. Figure 4 shows the end of discharge voltages and the end of charge voltage during the longest eclipse day for the DB cells. The figure shows that the cell end of discharge voltages level out at about 1.15 V and has remained fairly constant for 11 seasons. There is no indication of any problems with any of the cells and it is anticipated they will last for 20 seasons or more.

Throughput Test

The throughput test consists of three 80% DOD cycles per day. The cells are discharged for one hour and recharged in seven hours with 115% charge return. The test temperature is 10° ±3°C.

Two groups of flight cells, DB and Program A, are on the throughput test. The DB cells have completed over 1825 cycles and the Program A cells are just over 70 cycles. Figure 5 shows plots of the minimum end of discharge voltage (EODV) and the maximum end of charge voltage (EOCV) as a function of cycles. Note that the EODV remained fairly consistent at about 1.13 V out to 1317 cycles where the voltage of one cell dropped to 0.85V. At this time, the cells were reconditioned by discharging each cell through a one ohm resistor for 16 hours. The cell voltages were at about 0.2 V at the end of 16 hours. Two capacity tests were run at 10°C by discharging the pack at 0.5 C until the first cell reached 1.0V. The capacities obtained were 21.6 and 21.9 Ah; however, the cell that dropped out on cycling was not the limiting cell. The cells were put back on their normal cycling regime and are at about 1900 cycles. This represents about 20 years of GEO cycling at 80% DOD.

SUPER NI/CD BATTERIES ON FLIGHT PROGRAMS

Hughes has launched six communication satellites and is planning to launch at least an additional six satellites through 1994 that are using Advanced Ni/Cd batteries. Hughes also has a contract to build 22-cell, 9-Ah batteries for NASA's Small Explorer Satellite Program (SMEX).

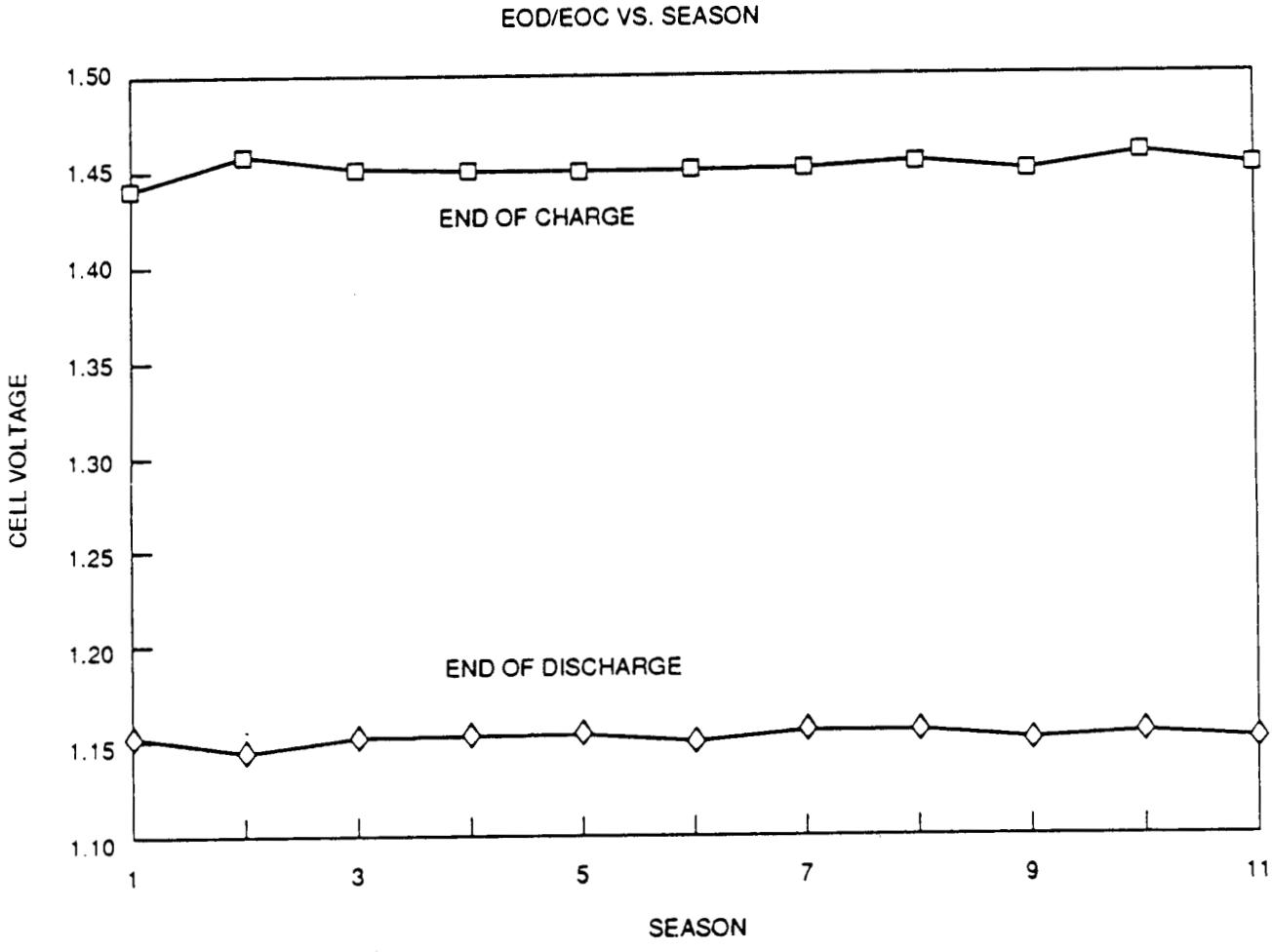

Figure 4 BSB life test realtime eclipse season 14-day solstice test temperature 10° ±3°C.

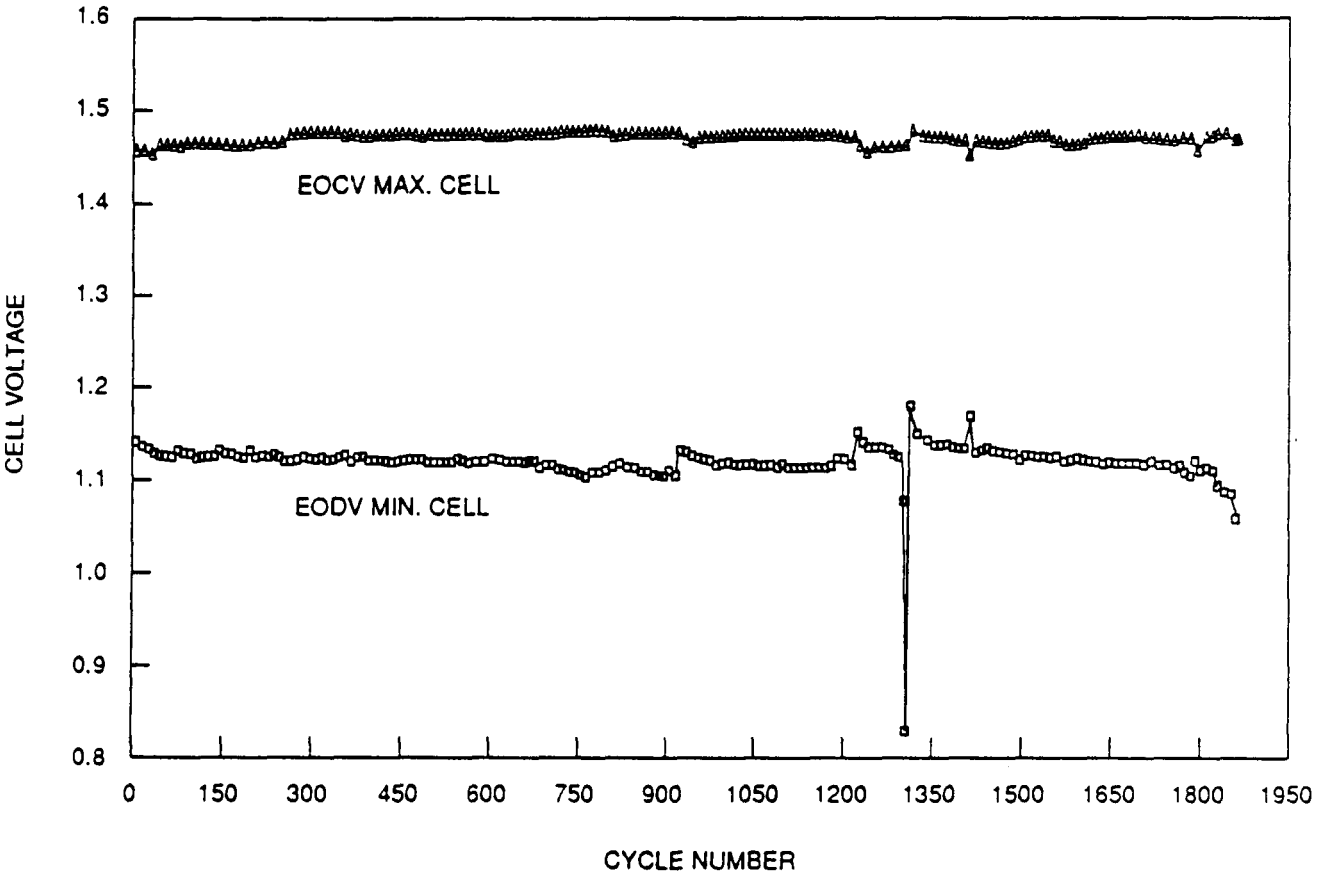

Figure 5 DB throughput test 80% DOD three cycles per day temperature 10° ±3°C.

Table III summarizes the Advanced Ni/Cd battery flight programs. In addition to those listed in the Table, another contractor has procured over 120 50-Ah cells for use in the NASA Standard 50-Ah MMS battery. NASA plans to use the cells on a flight program, provided they pass the battery qualification test which is scheduled for the near future.

ADVANCED NI/CD CELL DESIGNS AVAILABLE

Within about a two-year period, six different sizes of Advanced Ni/Cd have been designed, MCD's prepared, and tooling procured. Table IV lists the dimensions and weights of the present cell designs. Cells of the present designs can be delivered in approximately nine months. If a new cell size or design is required, cells could be delivered in 12 to 14 months.

TABLE III

SUMMARY OF ADVANCED Ni/Cd BATTERY FLIGHT PROGRAMS

Flight Program	Launch(es)	Cell Capacity (Ah)	Cells Per Battery	No. Of Batteries Per SC
DB R1 to R2	3/89 and 9/90	21	32	2
LEASAT - F5	1/90	21	32	3
GALAXY - 6	9/90	19	32	2
PROGRAM A	4/90	19	32	2
PROGRAM B-R2	4/90	19	32	2
GALAXY 5/1R	Mid 91 & Mid 92	21	32	2
PROGRAM - B4	1992	20(1)	32	2
GMS -5 (2)	1992	4.8	27	2
SMEX (3)	1992	9	22	1
PROGRAM - C	1993 & 1994	32	32	2

(1) Upgraded 19-Ah Cell

(2) Japanese Meteorological Satellite

(3) Small Explorer Program

TABLE IV

SUPER Ni/Cd CELL DESIGNS PRODUCED OR PRESENTLY IN PRODUCTION

Rated Capacity, (Ah at 10°C)	4.8	9	19	21	50	42
Height Top Terminals (inches)	3.170	4.000	4.360	4.670	7.250	6.952
Height Case (inches)	2.675	3.670	4.010	4.302	6.488	6.554
Width (inches)	2.143	2.890	3.500	3.740	4.941	4.980
Thickness (inches)	0.834	0.905	1.135	1.350	1.328	1.038
Weight, (grams)	235	460(1)	780	880	2,350	1805(1)

(1) Estimated from design

(2) For GEO Missions the life expectancy is 10 to 15 years at 80 percent DOD.

(3) For LEO Missions, the life expectancy is 5 years at 40 percent ≈ DOD 30,000 Cycles.

(4) Delivery: Approximately 9 months ARO or 12 months for a new design other than those listed.

The useable energy density of a super Ni/Cd battery, assuming a battery packaging factor of 1.1, is estimated to be 9.45 Wh/lb for a GEO Mission at 80% DOD. This represents about a 25% decrease in weight for the battery using standard Ni/Cd cells. A similar weight savings would be accomplished for a LEO mission or the mission life could be extended by using a Super Ni/Cd battery of the same weight as a standard Ni/Cd battery.

CONCLUSIONS

After an extensive 10-year development and test program, Hughes Aircraft Company has developed an advanced Ni/Cd cell (Super Ni/Cd) design that is capable of a 10 to 15-year GEO mission at 80% DOD. By being able to use the battery at 80% DOD, a weight savings of about 25% can be obtained over current Ni/Cd technology.

Boilerplate Ni/Cd cells tested in accelerated LEO regimes (45 minute cycles) at 40% DOD and 20°C have given 40,000 cycles. Flight type cells have not been tested in realtime LEO regimes long enough to develop life data, but it is estimated that they should provide about 30,000 cycles at 40% DOD.

The Super Ni/Cd cell gives a longer life than state-of-the-art Ni/Cd cell because the main failure mechanisms have been reduced or negated:

1. The degradable nylon separator was replaced by a stable polymer-impregnated zirconia cloth, reducing loss of overcharge protection

2. The chemically deposited positive electrode was replaced by a more stable electrochemical deposited electrode which does not swell as much and reduces separator dry out and the tendency to short.

3. The chemically deposited negative electrode was replaced by an electrochemically deposited electrode and an expander was added which reduces cadmium fading.

The life testing will be continued and failure analysis will be performed on failed cells to determine cause of failure.

The Super Ni/Cd battery should be used in small power systems (up to 2 KW) in place of Ni/H_2 batteries because it is less costly, requires less volume, and is not as heavy. It is expected to have about the same cycle life time as the Ni/H_2 cell.

Hughes Aircraft Company was presented an R&D 100 Award by R&D Magazine on September 26, 1990 for the Super Ni/Cd battery cell.

REFERENCES

1. A. Fleischer, *Journal Electrochemical Society*, 94, 289, (1948).

2. S. Bogner, "The 1978 Goodard Space Flight Center Battery Workshop", NASA Conference Publication 2088, Greenbelt, MD November 1978, p. 110-117.

3. H.S. Lim, J.D. Margerum, S.A. Verzwyvelt, A.M. Lockner, and R.C. Knechtli, *Journal Electrochemical Society*, 136, 605, (1989).

4. S. Bogner, "Progress In Advanced Nickel-Cadmium Batteries for Geosynchronous Orbit Application", Fourth Annual Battery Conference, January 1989, Long Beach, CA 895P-5.

5. H.S. Lim, S.A. Verwyvelt, D.F. Pickett, J.D. Margerum, R.C. Knechtli, and H.H. Rogers, Long Life and Low Weight Ni-Cd Cells for Spacecraft, *Proc. of the 19th IECEC*, San Francisco, CA August 1984, p. 609.

6. D.F. Pickett, H.S. Lim, S.J. Krause, and S.A. Verzwvelt, "Advanced Nickel Cadmium Batteries for Geosynchronous Spacecraft", *Journal of Power Sources*, Vol. 22, 1958, pp. 243-259.

7. N.M. Chroneau and R.S. Bogner, "Long Life, High Usable Energy Density Nickel-Cadmium Battery Cell", *Proc. of the IECEC*, Denver, CO, august 1988, p. 341.

8. S. Gross, "Review of Electrochemical Impregnation For Nickel-Cadmium Cells", TPL Cont. No.953984, W.O. 342-46, August, 1977, Reorder No. 77-138.

9. D.F. Pickett, Jr. "Recent Trends in Design and Manufacturing of Nickel Oxide Electrodes for Space Applications". *Porous Electrode Theory and Practice*, ed. Maru, H.D., Katan, T., Klein, M.G., The Electrochemical Society, Princeton, N.J. pp. 12-31, 1984.

10. H.S. Lim, D.F. Pickett, "Separator Evaluation in Nickel-Cadmium Cells", *Proc. of the IECEC*, Reno, NV., August 1990, pp. 61-67.

11. H.S. Lim, S.A. Verzevyvelt, J.D. Margerum and R.C. Knechtly, "Accelerated Cycle Life Tests of Ni/Cd Cells with ED Nickel Electrodes: Comparison of Three Separators", Proc. of the 17th IECEC, Los Angeles, August 1982, p. 707.

12. "Accelerated Test Program for Sealed Nickel-Cadimium Spacecraft Batteries/ Cells", Naval Weapons Support Center, Interim Report WQEC/C pp. 79-145, May 1979.

HUGHES ADVANCED NICKEL-CADMIUM BATTERIES – AN UPDATE

R. SAM BOGNER

HUGHES AIRCRAFT COMPANY
INDUSTRIAL ELECTRONICS GROUP
ELECTRON DYNAMICS DIVISION
ENERGY STORAGE PRODUCT LINE
TORRANCE, CA

ACCELERATED TEST PLOTS

HUGHES

POSITIVE PLATE GROWTH FOR STAR POINT-TEST PACKS

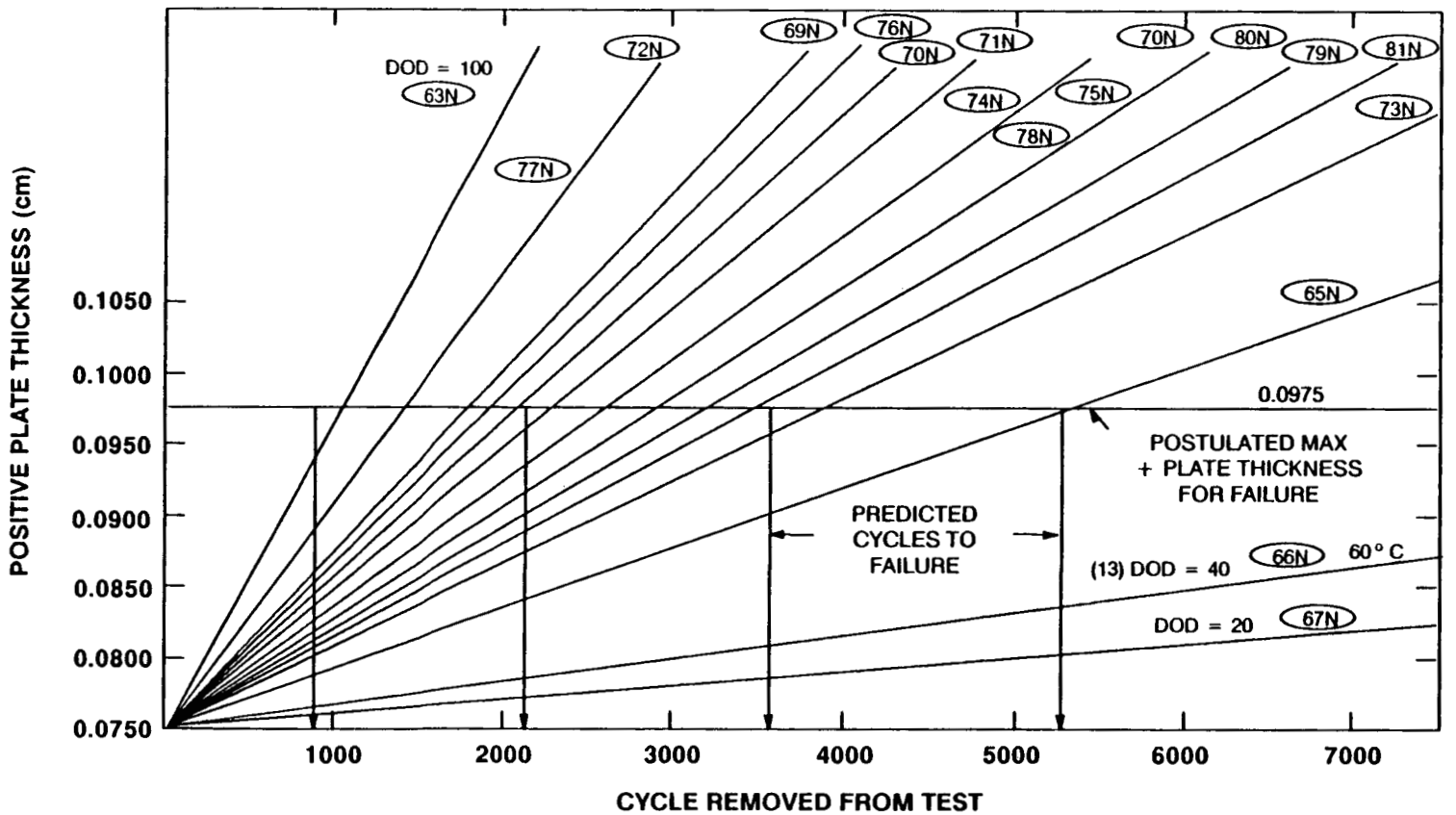

OBSERVED AND PREDICTED CYCLE LIFE (12) STAR POINT PACKS ON THE NASA ACCELERATED TEST PROGRAM

HUGHES

Pack Number	Observed Cycle Life	Max. Pos. Thickness (cm)	Predicted Cycle Life to 0.0975 (cm)
65N	5660	0.0946	5400
66N	13	---	---
67N	14066	0.0842	38400
68N	955	0.1006	950
69N	591	0.0825	1600
70N	1512	0.0930	1800
71N	1638	0.0925	1900
72N	1717	0.1096	1300
73N	3501	0.0993	3500
74N	1801	0.0954	2150
75N	2557	0.0957	2400
76N	1669	0.0995	1750
77N	1909	0.1106	1450
78N	2368	0.0960	2400
79N	3732	0.1001	3732
80N	3223	0.0989	2600
81N	3055	0.0954	3200

DIAGRAM SHOWING OVERCHARGE PROTECTION AND PRECHARGE IN A NICKEL CADMIUM CELL

HUGHES

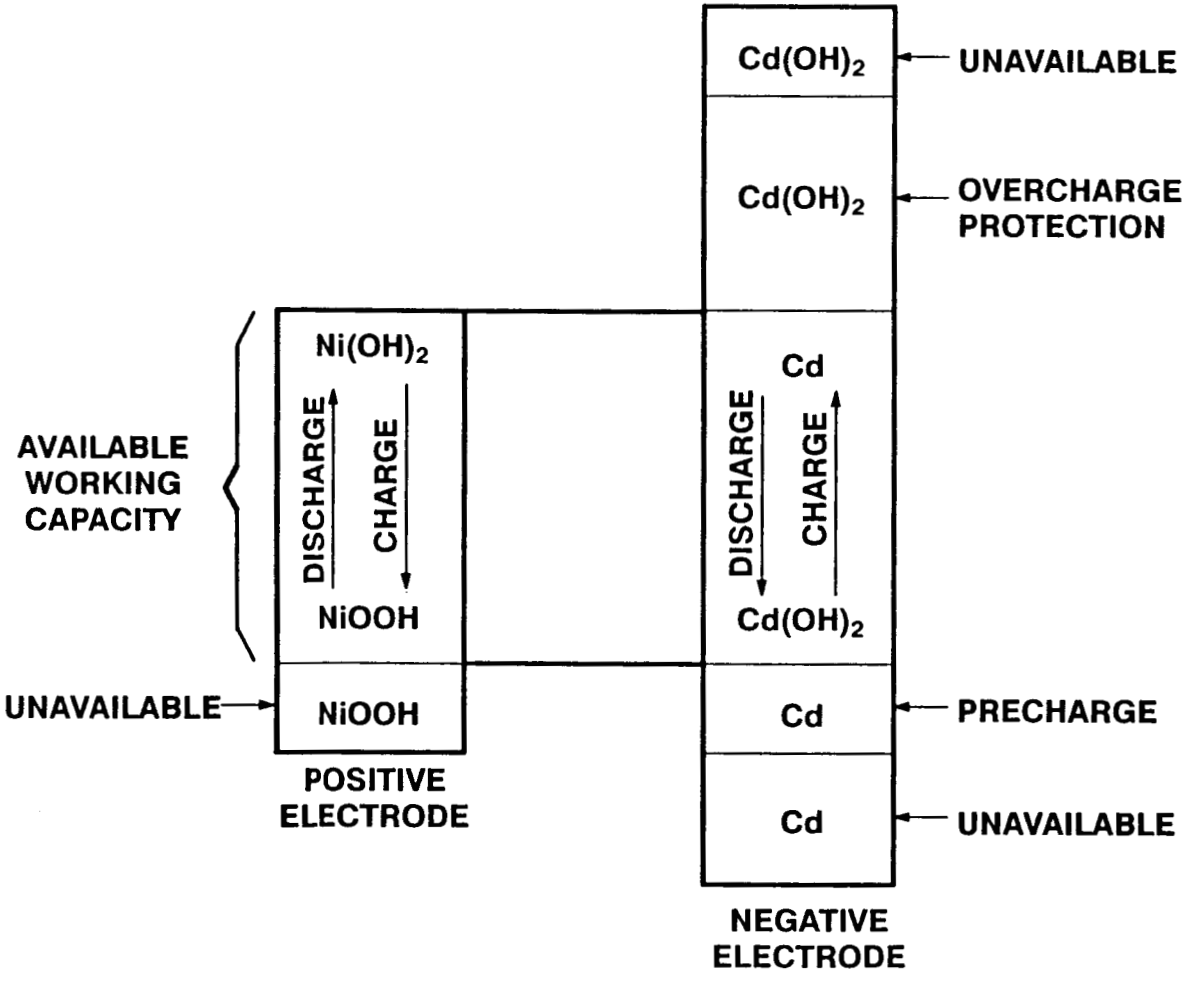

SUMMARY OF ADVANCED Ni/Cd CELL TESTING

HUGHES

Type Test	Type Cell	No. Cell	Cell A-hr	No. Seasons/ Cycles	DOD %	Status/Comments
Accelerated LEO	Boilerplate	12	4.36	6000 to 43,000 Cycles	40 to 80	Complete (45 Min. Cycle)
Accelerated GEO	Boilerplate	15	6.8	216 to 313 Seasons 3450 to 5000 Cycles	80	Discontinued
Accelerated GEO 46 Day Season	Proto Flight	10	12	24 to 38 Seasons	60 to 80 (2)	Complete (22 Day, 50° Solstice)
Realtime	Proto Flight	8	12	19 Seasons	60 to 80 (3)	Continuing (1)
Accelerated GEO 16 Cycle Season	Proto Flight	11	20	37 to 83 Seasons	80	Discontinued
Accelerated GEO 46 Day Season	Proto Flight	18	20	14 Seasons	80	Continuing (1) 14 Day Solstice
Direct Broadcast or DB Accelerated GEO, 46 Day Season	Flight	5	21	11	80	Continuing 14 Day Solstice
DB Throughput	Flight	6	21	1825 Cycles	80	Continuing 3 Cycles/Day
LEASAT F5 LEO Qual. Pack	Flight	8	21	1300	80	Test at NWSC Crane
LEASAT F5 Accelerate GEO 46 Day Season	Flight	2	21	3 Seasons	80	Continuing 14 Day Solstice
Program A Throughput	Flight	5	19	70 Cycles	80	Continuing
Program B Realtime	Flight	4	19	1 Season	80	Continuing

All Flight and Proto-Flight cell tests run at 10°C.

NOTES: (1) Test put on trickle charge for about 8 months in 1990.
(2) 60 Percent DOD for first 18 seasons.
(3) 60 Percent DOD for first 5 seasons.

BSB LIFE TEST REALTIME ECLIPSE SEASON 14-DAY SOLSTICE TEST TEMPERATURE 10° ± 3°C

HUGHES

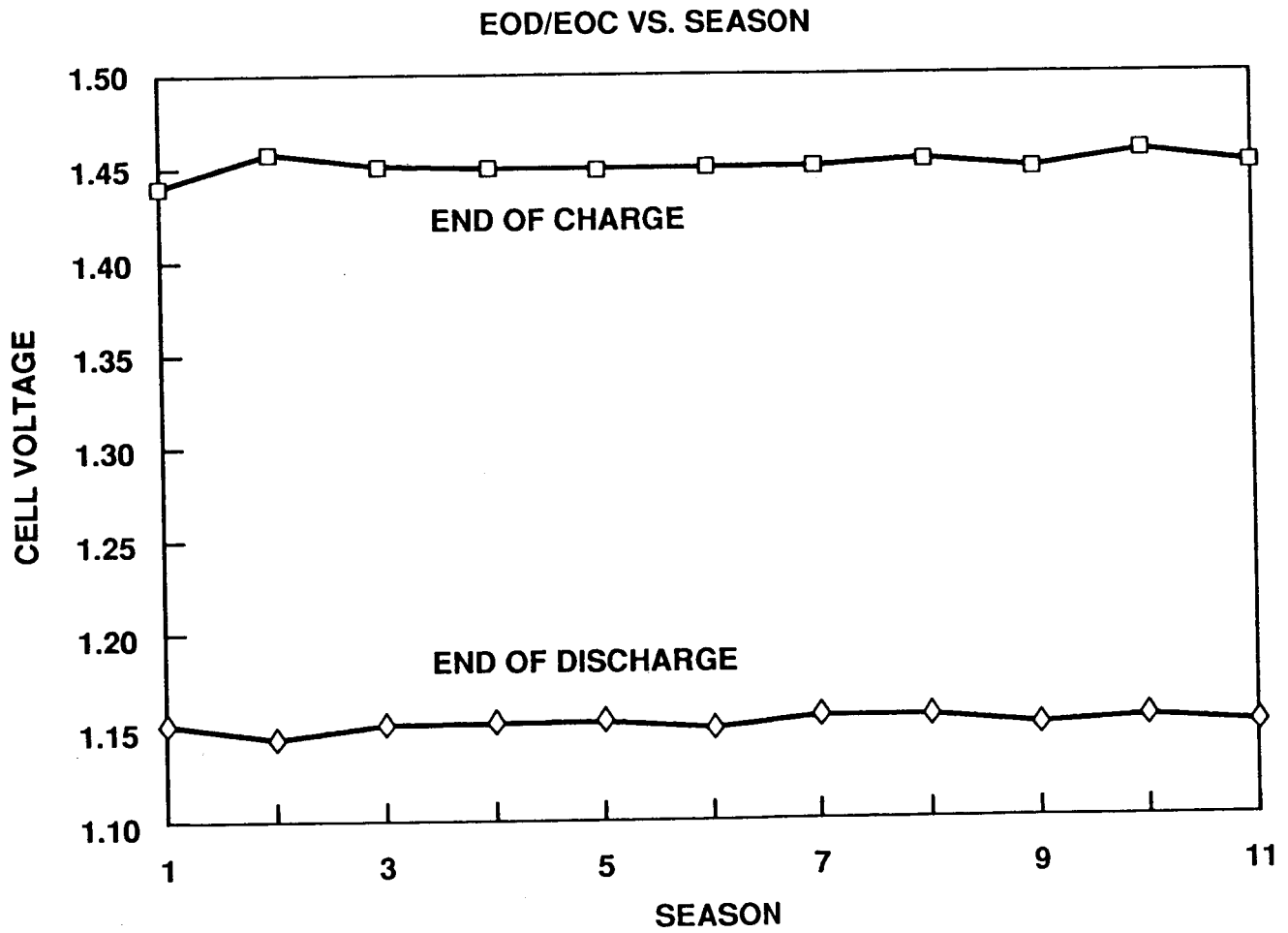

12-Ah PROTOFLIGHT CELL REALTIME GEO TEST

HUGHES

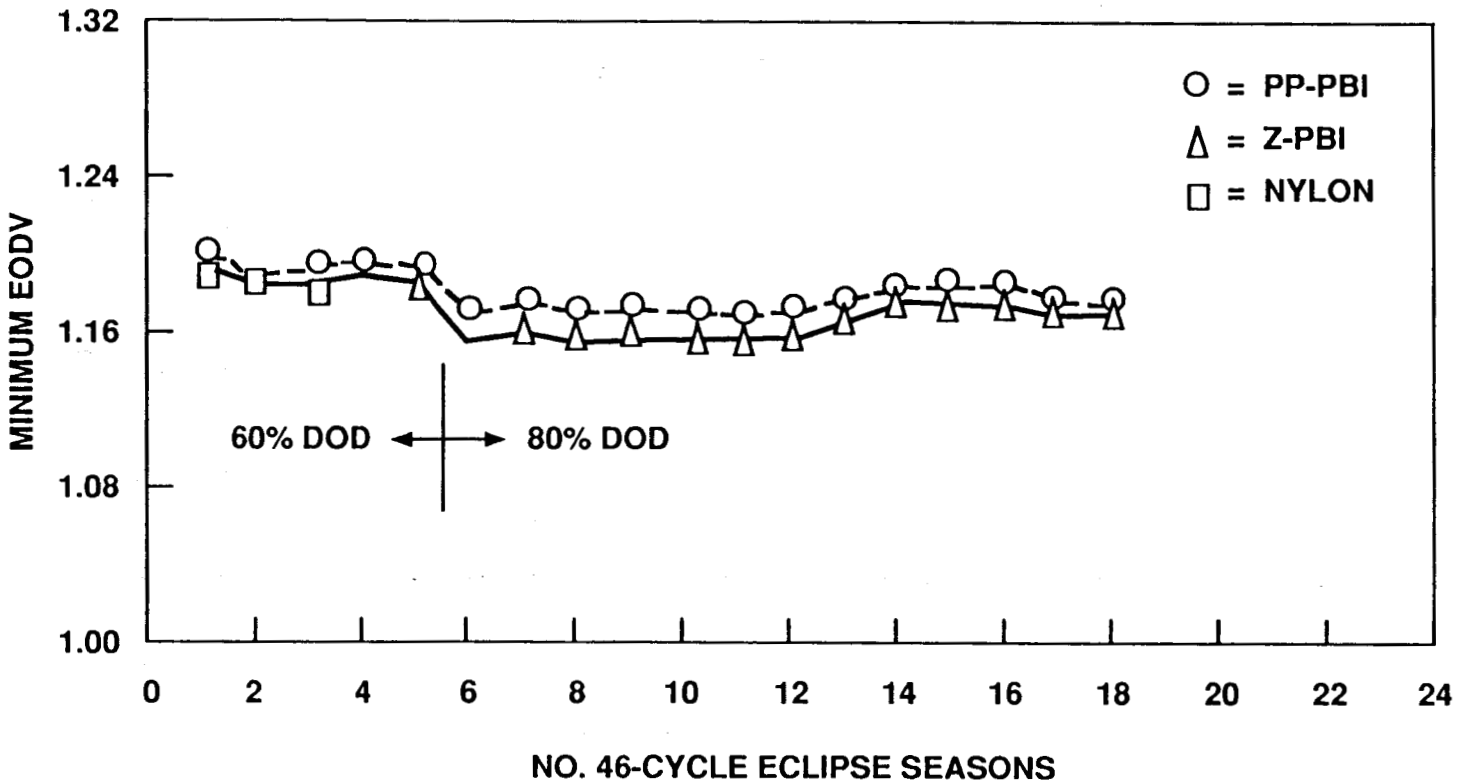

DB THROUGHPUT TEST 80% DOD THREE CYCLES PER DAY TEMPERATURE 10° ±3°C

HUGHES

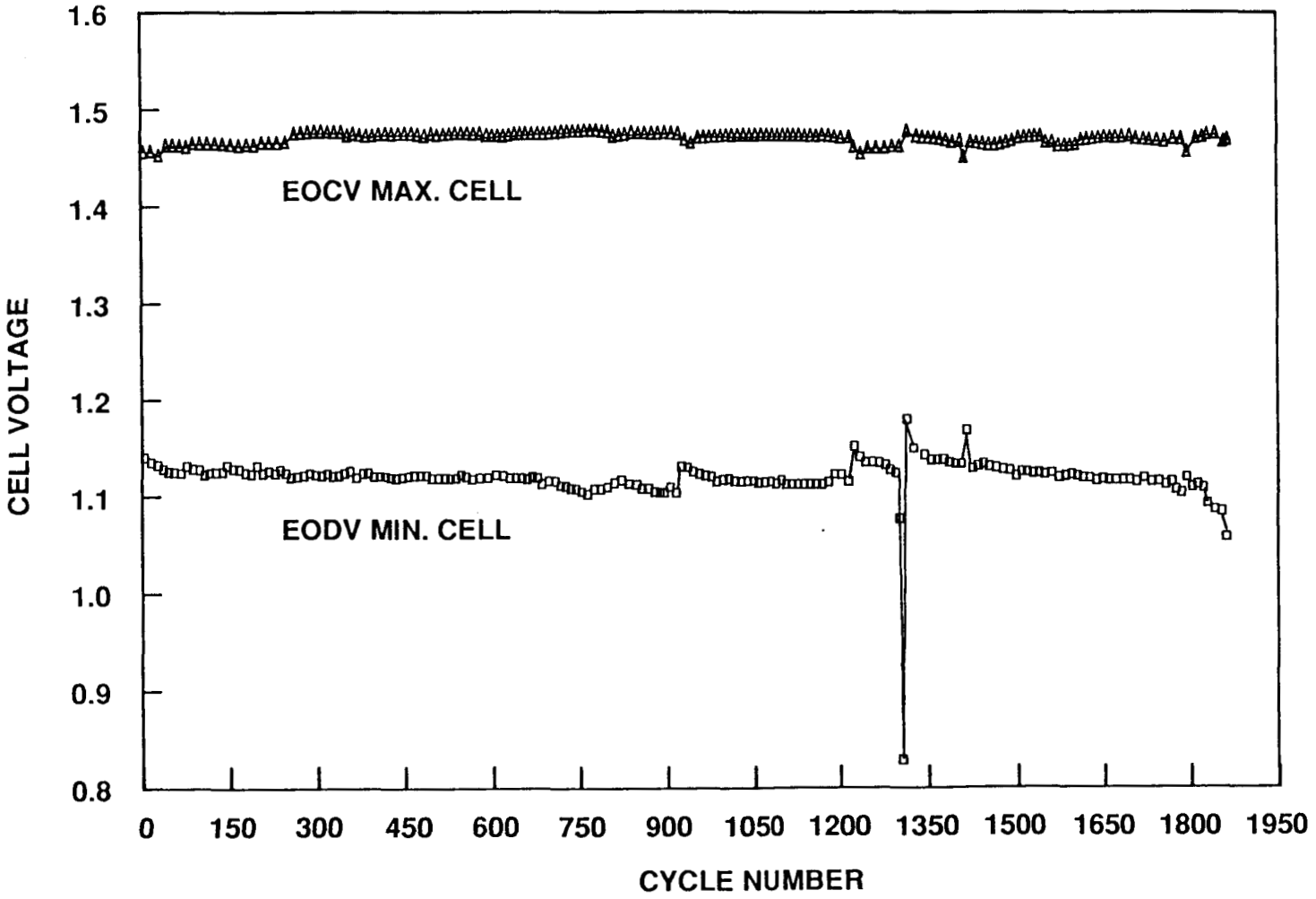

SUMMARY OF ADVANCED Ni/Cd BATTERY FLIGHT PROGRAMS

HUGHES

Flight Program	Launch(es)	Cell Capacity (Ah)	Cell Per Battery	No. of Batteries Per SC
DB R1 to R2	3/89 and 9/90	21	32	2
LEASAT - F5	1/90	21	32	3
GALAXY - 6	9/90	19	32	2
PROGRAM A	4/90	19	32	2
PROGRAM B-R2	4/90	19	32	2
GALAXY 5/1R	Mid 91 & Mid 92	21	32	2
PROGRAM - B4	1992	20(1)	32	2
GMS -5 (2)	1992	4.8	27	2
SMEX (3)	1992	9	22	1
PROGRAM - C	1993 & 1994	32	32	2

(1) Upgraded 19-Ah Cell
(2) Japanese Meteorological Satellite
(3) Small Explorer Program

SUPER Ni/Cd CELL DESIGNS PRODUCED OR PRESENTLY IN PRODUCTION

HUGHES

Rated Capacity, (Ah at 10°C)	4.8	9	19	21	50	42
Height Top Terminals (inches)	3.170	4.000	4.360	4.670	7.250	6.952
Height Case (inches)	2.675	3.670	4.010	4.302	6.488	6.554
Width (inches)	2.143	2.890	3.500	3.740	4.941	4.980
Thickness (inches)	0.834	0.905	1.135	1.350	1.328	1.038
Weight, (grams)	235	460(1)	780	880	2,350	1805(1)

(1) Estimated from design
(2) For GEO Missions the life expectancy is 10 to 15 years at 80 percent DOD.
(3) For LEO Missions, the life expectancy is 5 years at 40 percent ≈ DOD 30,000 Cycles.
(4) Delivery: Approximately 9 months ARO or 12 months for a new design other than those listed.

SAFT NICKEL-CADMIUM CELL PERFORMANCES

FOR

GEO AND LEO

APPLICATIONS

THE 1990 NASA BATTERY WORKSHOP
MARSHALL SPACE FLIGHT CENTER
4 - 6 DECEMBER 1990

C-3

SUMMARY

LEO APPLICATIONS :

. EUROPEAN SPACE AGENCY BATTERY TEST CENTER RESULTS

. ELAN PROGRAM :
- TEST MATRIX AND CYCLING STATUS
- TEST RESULTS AT 30% DOD
- TEST RESULTS AT 40% DOD
- RECONDITIONING EFFECT
- CAPACITY EVOLUTION
- DISSIPATED POWER EVOLUTION

. X 80 TEST

. NWSC TEST RESULTS
. LEO LIFE TIME EXPECTANCY

GEO APPLICATIONS

. FLIGHT EXPERIENCE RESULTS : OTS 2 BATTERY
. HIGH DOD TEST RESULTS : 70-90-100% DOD

SAFT AEROSPACE DEPARTMENT	1990 NASA BATTERY WORKSHOP

LOW EARTH ORBIT CYCLING - ELAN PROGRAM

VOS 24A

TEST NUMBER	53	54	55	56	57	58	59
BATTERY NUMBER	01	02	03	04	05	06	07
DOD %	10	10	10	20	20	20	20
TEMPERATURE (°C)	+6	+16	+25	+7	+17	+26	-2
DISCHARGE (A) STEP 1 (25 min) STEP 2 (10 min)	 3.45 5.77	 3.45 5.77	 3.45 5.77	 3.45 20.0	 3.45 20.0	 3.45 20.0	 3.45 20.0
CHARGE (A)	8	8	8	8	8	8	8
VOLTAGE LIMIT (V)	1.456	1.425	1.412	1.496	1.456	1.450	1.523
RECHARGE RATIO	1.14	1.165	1.17	1.15	1.15	1.17	1.14
CYCLES	28000	28100	28100	28100	28100	28100	26400
END OF DISCHARGE VOLTAGE (V)	1.246	1.246	1.224	1.082	1.132	1.110	1.129
RECONDITIONING	R1	R1	R2 C 8400	R2 C 4130	R1	No	R1

R1 = RECONDITIONING ON A REGULAR BASIS
2500 - 3000 CYCLES
R2 = RECONDITIONING AS MENTIONED

SAFT AEROSPACE DEPARTMENT	1990 NASA BATTERY WORKSHOP

LOW EARTH ORBIT CYCLING - ELAN PROGRAM

VOS 24A

TEST NUMBER	60	61	62	63	64	65	66
BATTERY NUMBER	09	10	08	12	15	13	14
DOD %	20	24	30	30	30	40	40
TEMPERATURE (°C)	+17	+17	+8	-1	+17	+8	+27
DISCHARGE (A) STEP 1 (25 min) STEP 2 (10 min)	 3.45 20.0	 * *	 7.0 26.0	 7.0 26.0	 7.0 26.0	 7.0 40.0	 15.0 20.0
CHARGE (A)	8	*	12	12	12	16	16
VOLTAGE LIMIT (V)	1.468	1.448	1.500	1.534	1.495	1.51	1.464
RECHARGE RATIO	1.16	1.060	1.10	1.12	1.15	1.13	1.14
CYCLES	26500	20700	28150	26300	26500	27900	20385
END OF DISCHARGE VOLTAGE (V)	1.078	1.000	1.033	1.044	1.018	0.940	0.934
RECONDITIONING	No	No	No	R1	No	R2 C 15080	No

* SIMULATION OF THE ERS 1 SPACECRAFT OPERATION

SAFT AEROSPACE DEPARTMENT	1990 NASA BATTERY WORKSHOP

LOW EARTH ORBIT CYCLING
ELAN PROGRAM

	VOS 40A				VOS 20B
TEST NUMBER	67	68	69	70	71
BATTERY NUMBER	11	17	18	19	20
DOD %	30	30	10	20	30
TEMPERATURE (°C)	+27	+17	+5	+5	15
DISCHARGE (A) STEP 1 (25 MIN) STEP 2 (10 MIN)	 20 25	 20 25	 6.80 6.80	 13.70 13.70	 5.80 21.55
CHARGE (A)	20	20	10	10	10
VOLTAGE LIMIT (V)	1.463	1.474	1.457	1.504	1.473
RECHARGE RATIO	1.16	1.16	1.14	1.08	1.16
CYCLES	21264	21300	18200	18000	17600
END OF DISCHARGE VOLTAGE (V)	1.093	1.058	1.268	1.215	1.030
RECONDITIONING	No	No	R1	R1	No

SAFT AEROSPACE DEPARTMENT		1990 NASA BATTERY WORKSHOP
NiCd Cells	ELAN Program	Low Earth Orbit Cycling

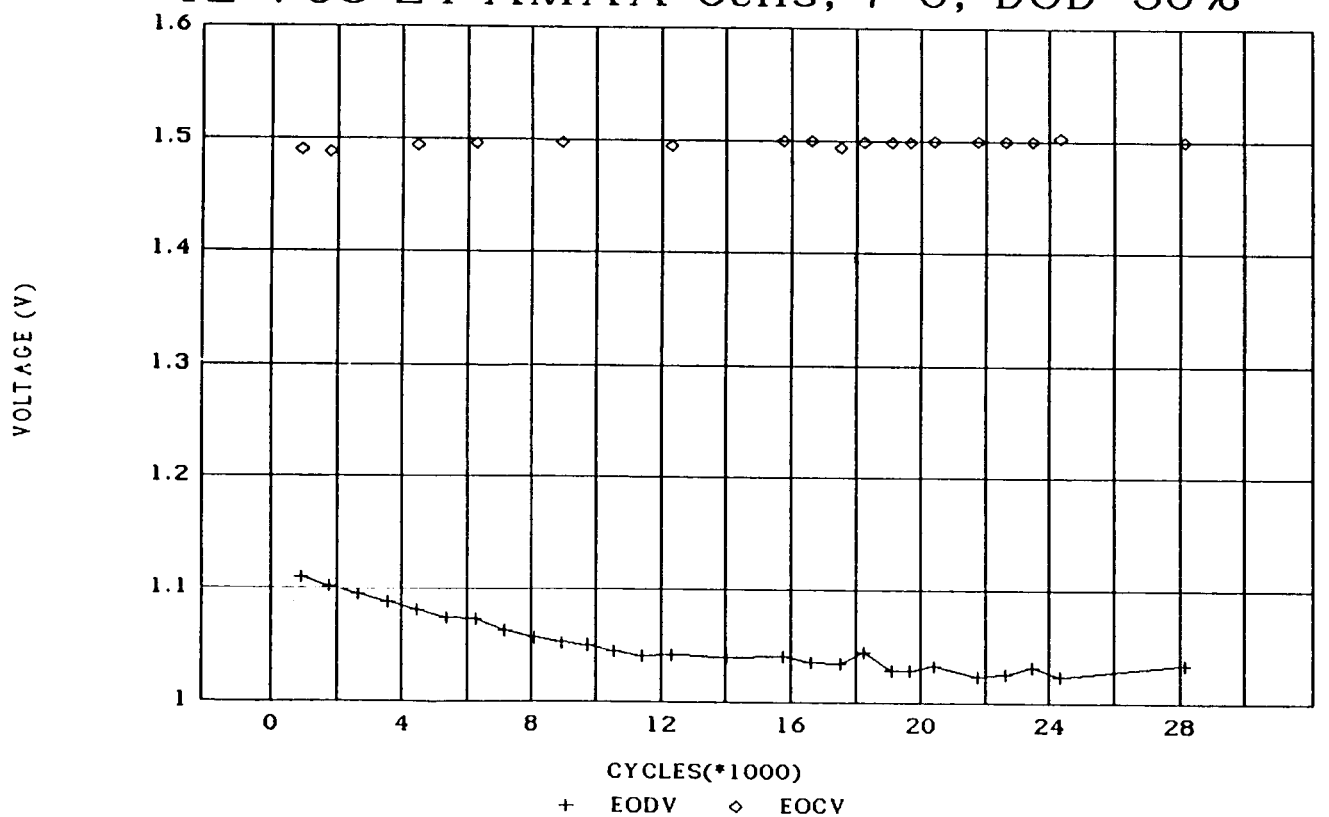

TEST N°62

DISCHARGE: 25 MN AT 7A
10 MN AT 26A

CHARGE: 65 MN AT 12A
MAX CURRENT TAPERING

SAFT AEROSPACE DEPARTMENT		1990 NASA BATTERY WORKSHOP
NiCd Cells	ELAN Program	Low Earth Orbit Cycling

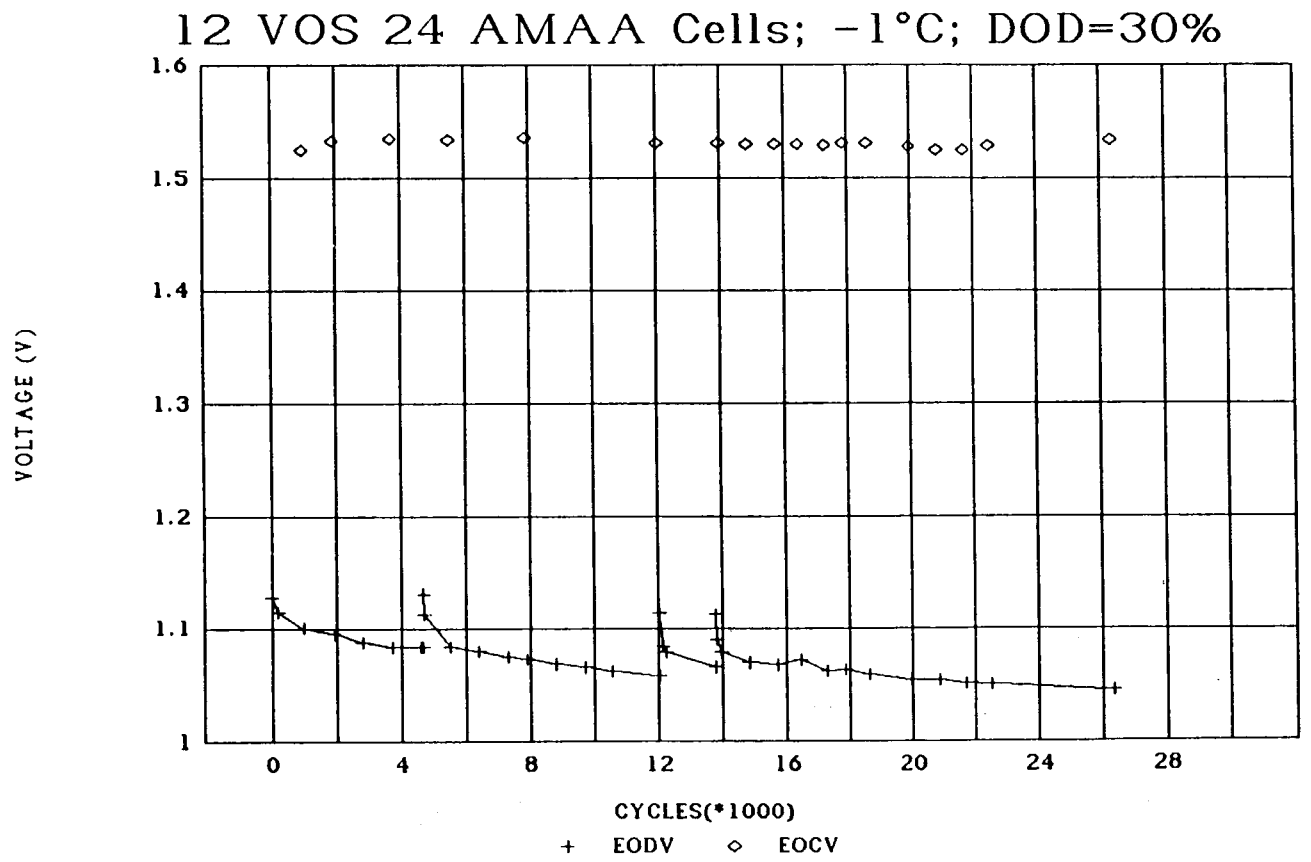

TEST N°63

DISCHARGE: 25 MN AT 7A
10 MN AT 26A

CHARGE: 65 MN AT 12A
MAX CURRENT TAPERING

SAFT AEROSPACE DEPARTMENT		1990 NASA BATTERY WORKSHOP
NiCd Cells	ELAN Program	Low Earth Orbit Cycling

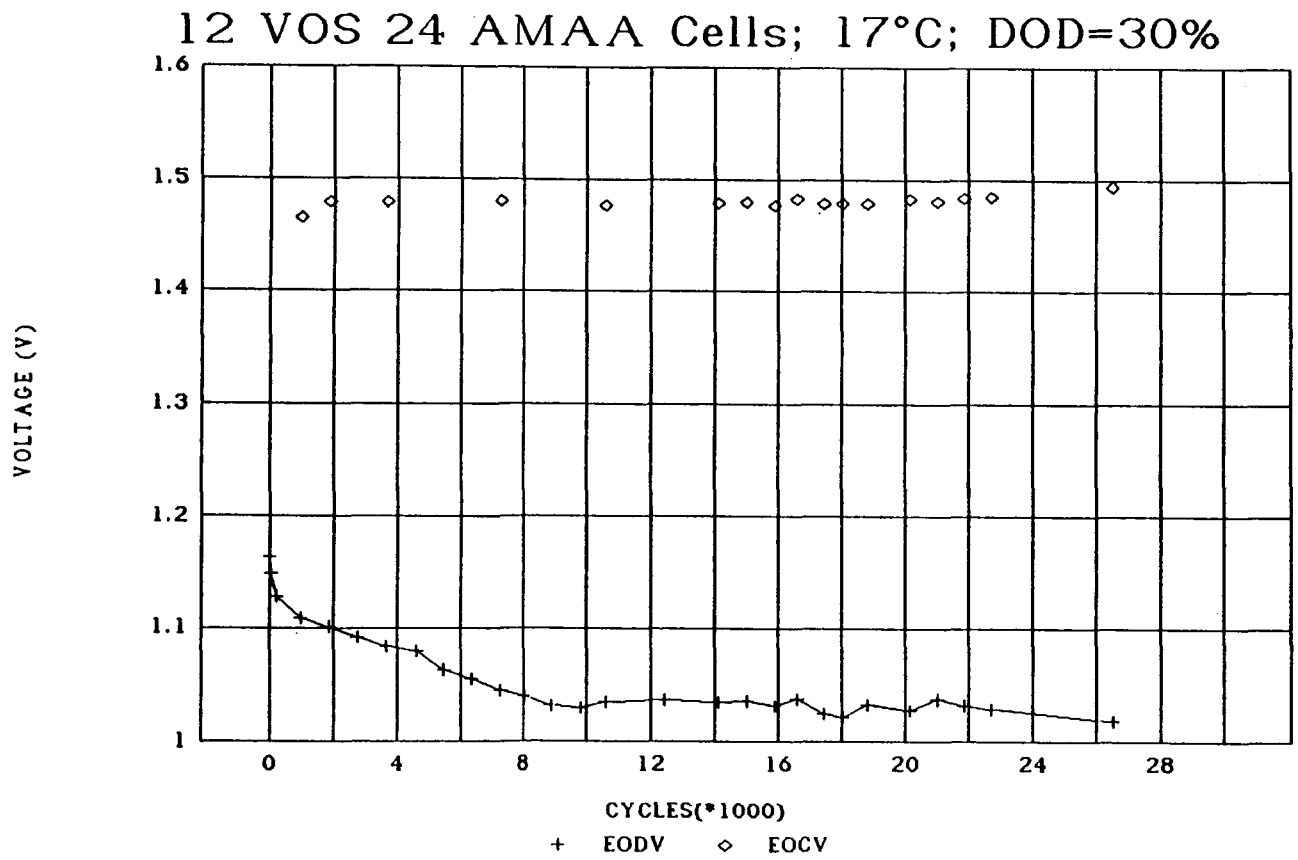

TEST N°64

DISCHARGE: 25 MN AT 7A
10 MN AT 26A

CHARGE: 65 MN AT 12A
MAX CURRENT TAPERING

SAFT AEROSPACE DEPARTMENT		1990 NASA BATTERY WORKSHOP
NiCd Cells	ELAN Program	Low Earth Orbit Cycling

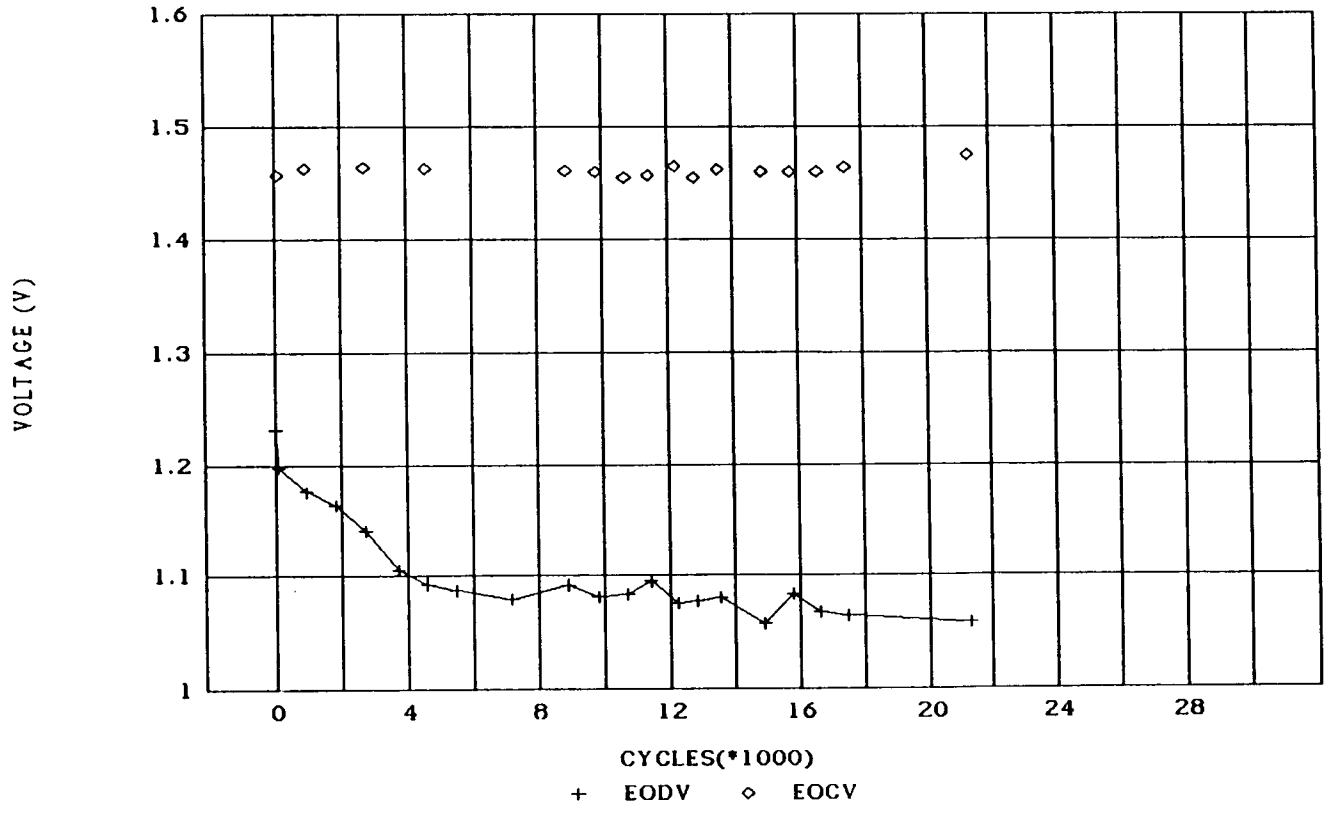

TEST N°68

DISCHARGE: 25MN AT 20A
10 MN AT 25A

CHARGE: 65 MN AT 20A
MAX CURRENT TAPERING

SAFT AEROSPACE DEPARTMENT		1990 NASA BATTERY WORKSHOP
NiCd Cells	ELAN Program	Low Earth Orbit Cycling

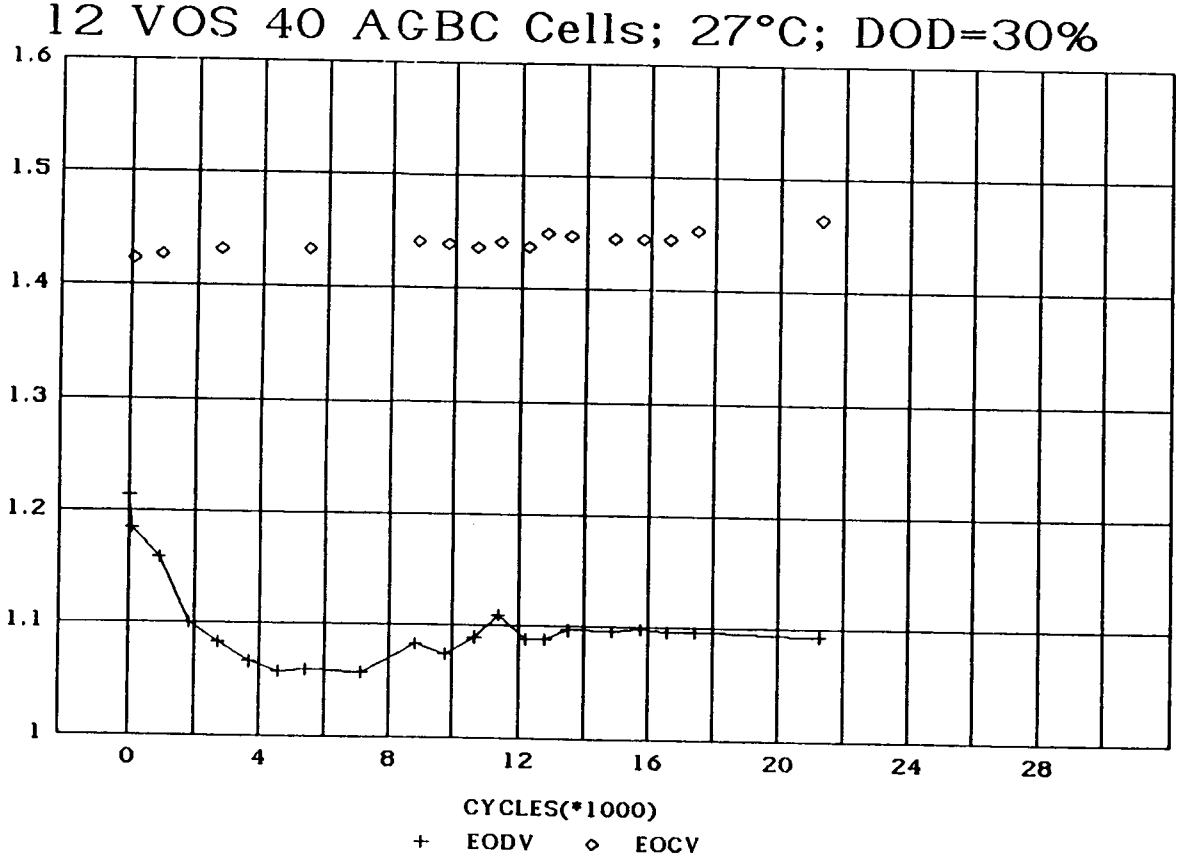

TEST N°67

DISCHARGE: 25MN AT 20A
10 MN AT 25A

CHARGE: 65 MN AT 20A
MAX CURRENT TAPERING

SAFT AEROSPACE DEPARTMENT		1990 NASA BATTERY WORKSHOP
NiCd Cells	ELAN Program	Low Earth Orbit Cycling

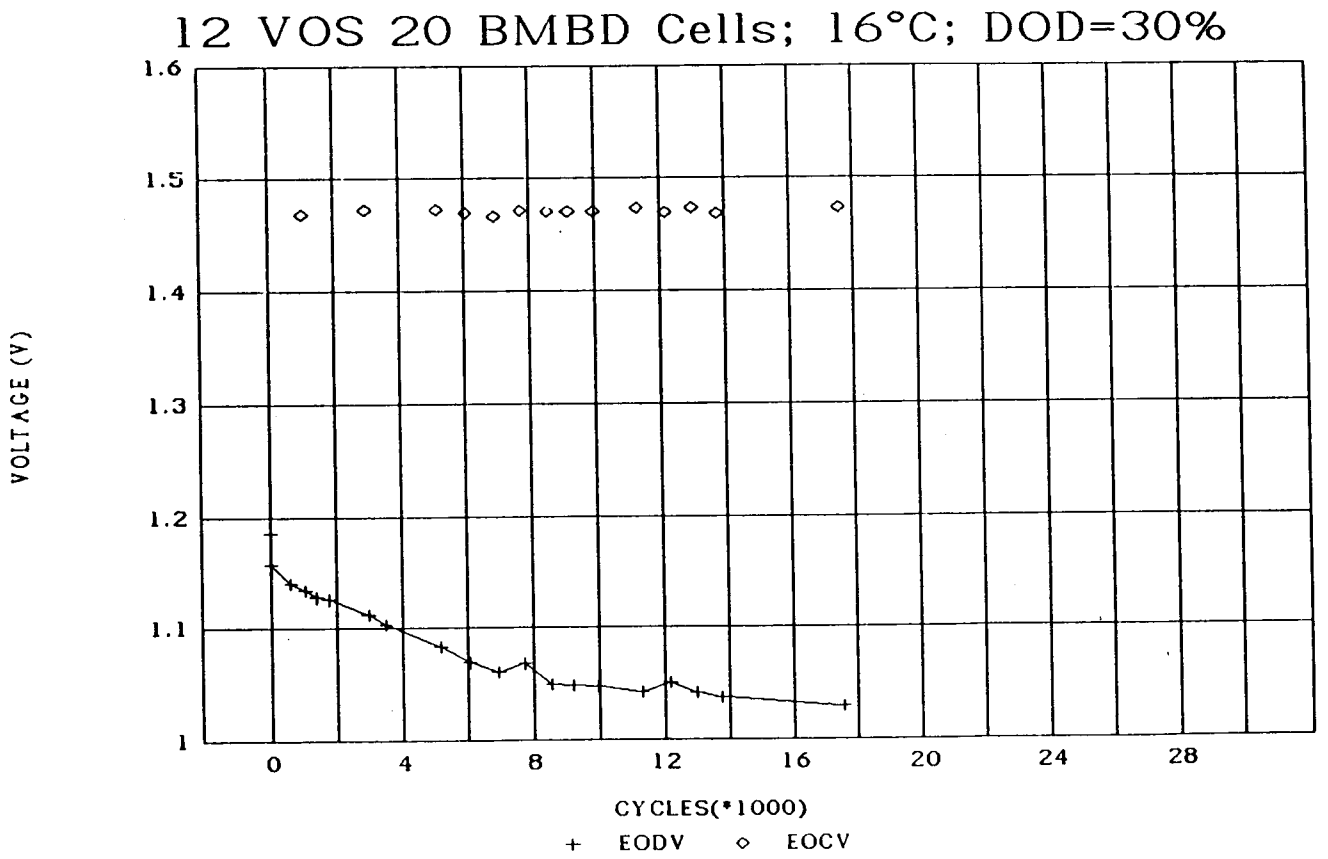

TEST N°71

DISCHARGE: 25MN AT 5.8A
10 MN AT 22A

CHARGE: 65 MN AT 10A
MAX CURRENT TAPERING

SAFT AEROSPACE DEPARTMENT		1990 NASA BATTERY WORKSHOP
NiCd Cells	ELAN Program	Low Earth Orbit Cycling

VOS40AGBC/VOS24AMAA; 17°C; 30%DOD

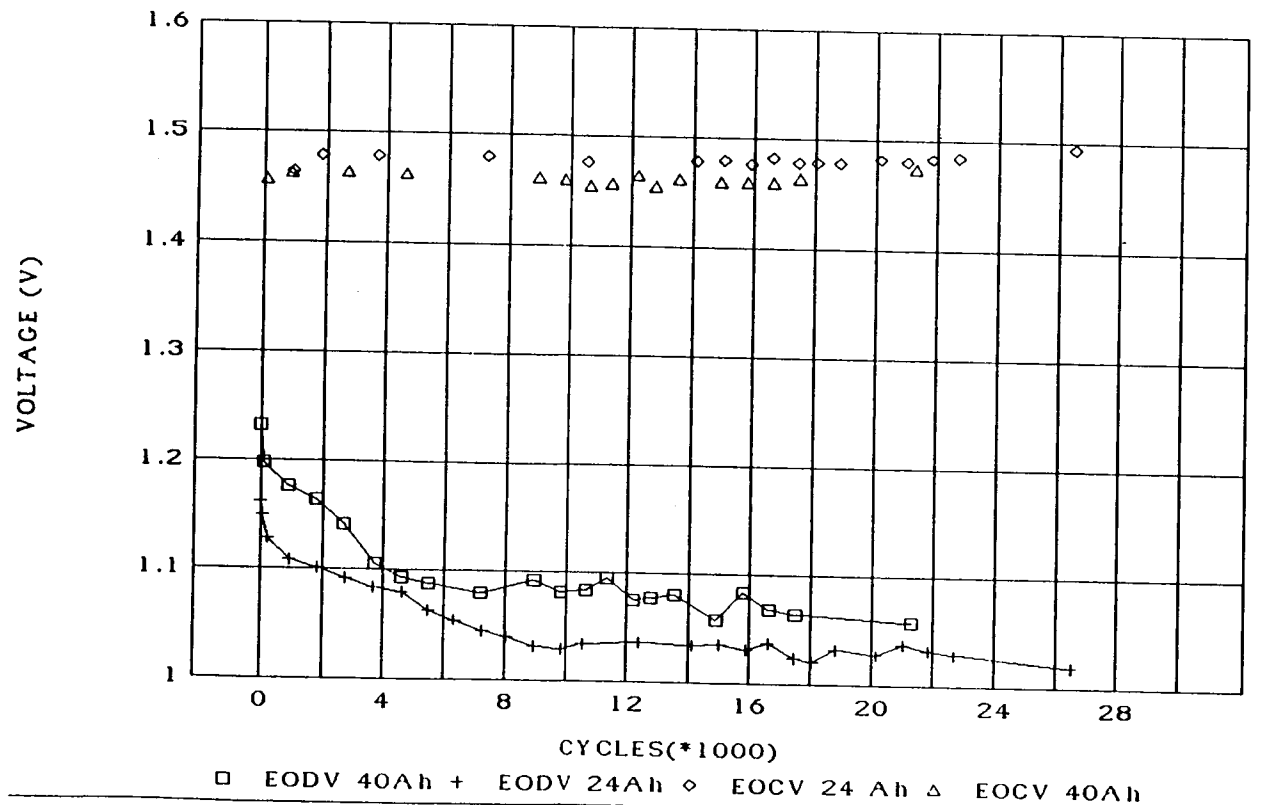

Comparison

VOS40AGBC/VOS24AMAA

SAFT AEROSPACE DEPARTMENT		1990 NASA BATTERY WORKSHOP
NiCd Cells	ELAN Program	Low Earth Orbit Cycling

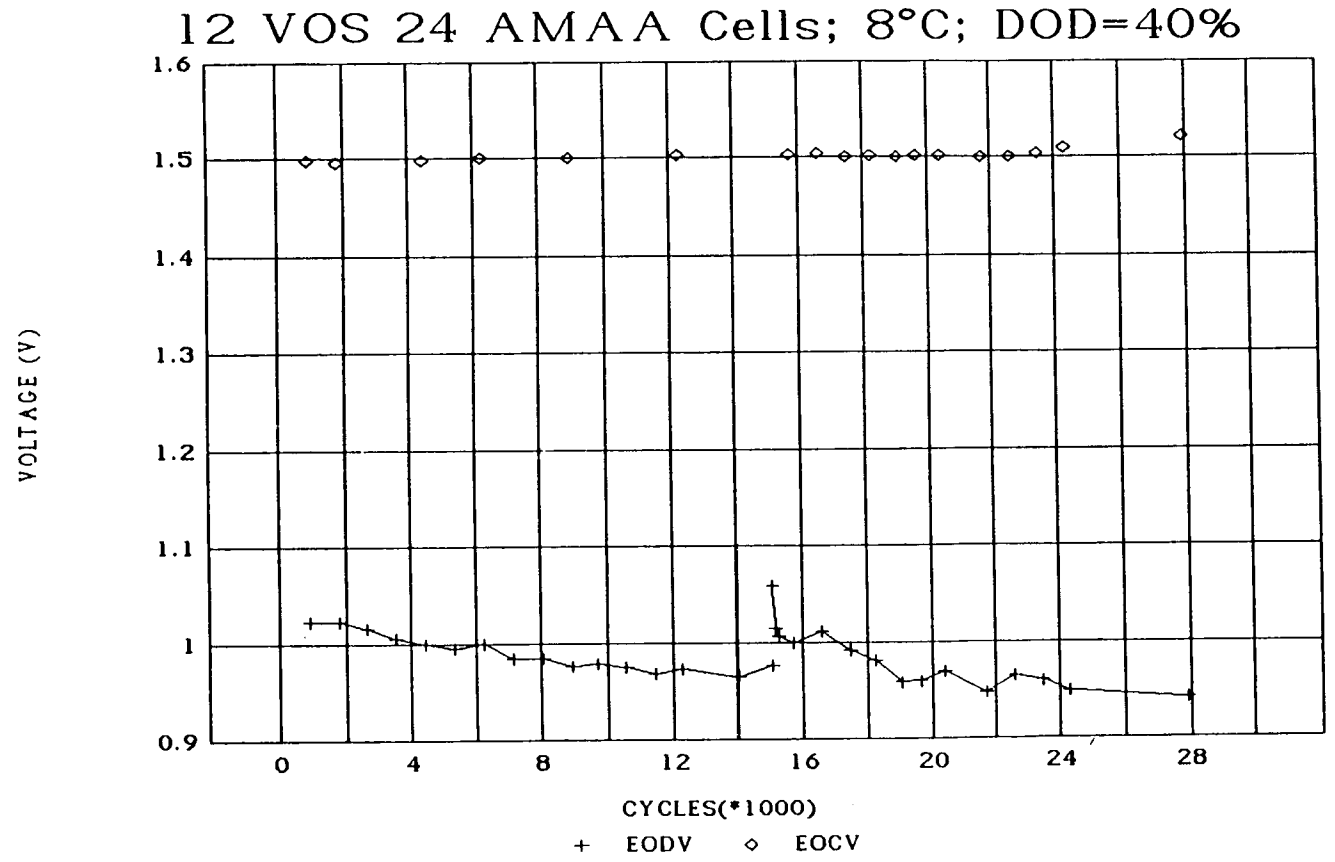

TEST N°65

DISCHARGE: 25 MN AT 7A
10 MN AT 40A

CHARGE: 65 MN AT 16A
MAX CURRENT TAPERING

SAFT AEROSPACE DEPARTMENT

1990 NASA BATTERY WORKSHOP

NiCd Cells

ELAN Program

Low Earth Orbit Cycling

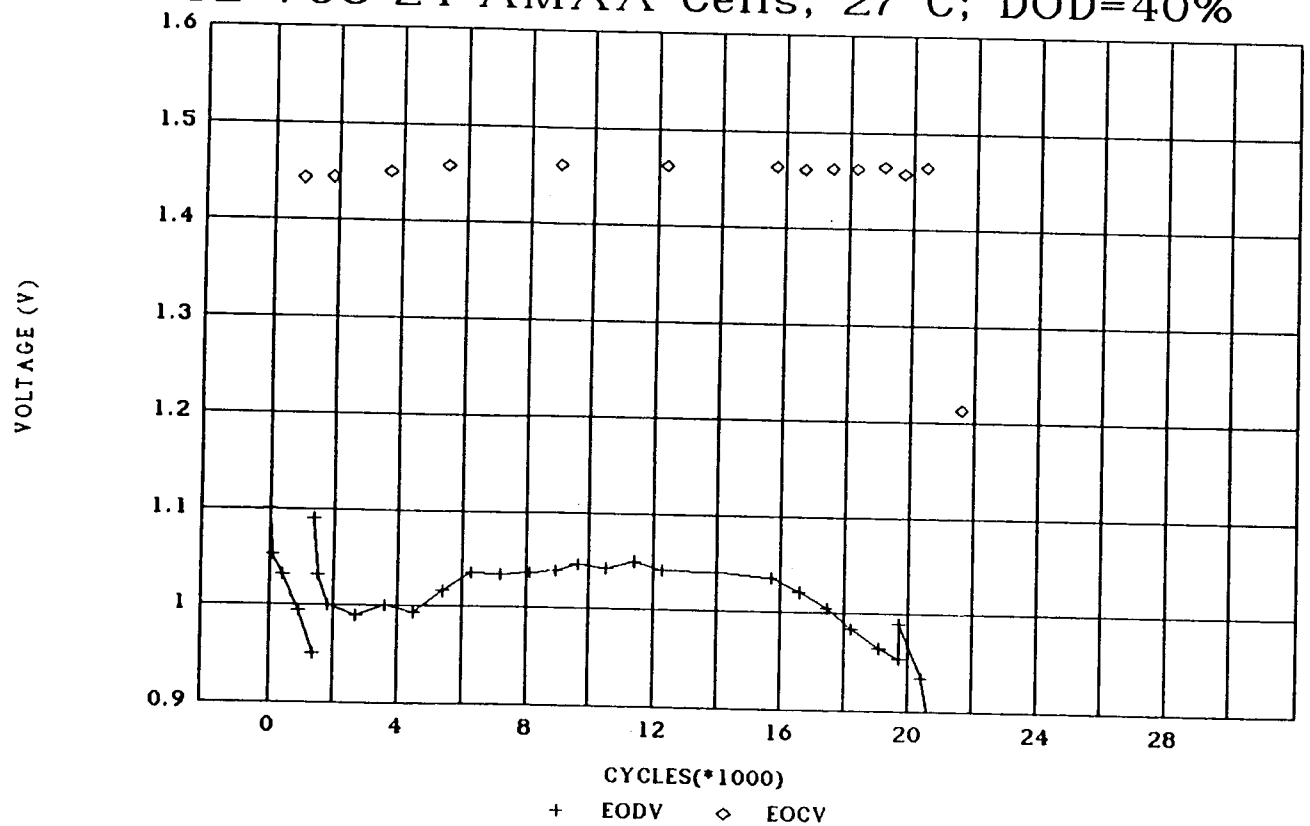

TEST N°66

DISCHARGE: 25MN AT 20A
10 MN AT 20A

CHARGE: 65 MN AT 16A
MAX CURRENT TAPERING

SAFT AEROSPACE DEPARTMENT		1990 NASA BATTERY WORKSHOP
NiCd Cells	ELAN Program	Low Earth Orbit Cycling

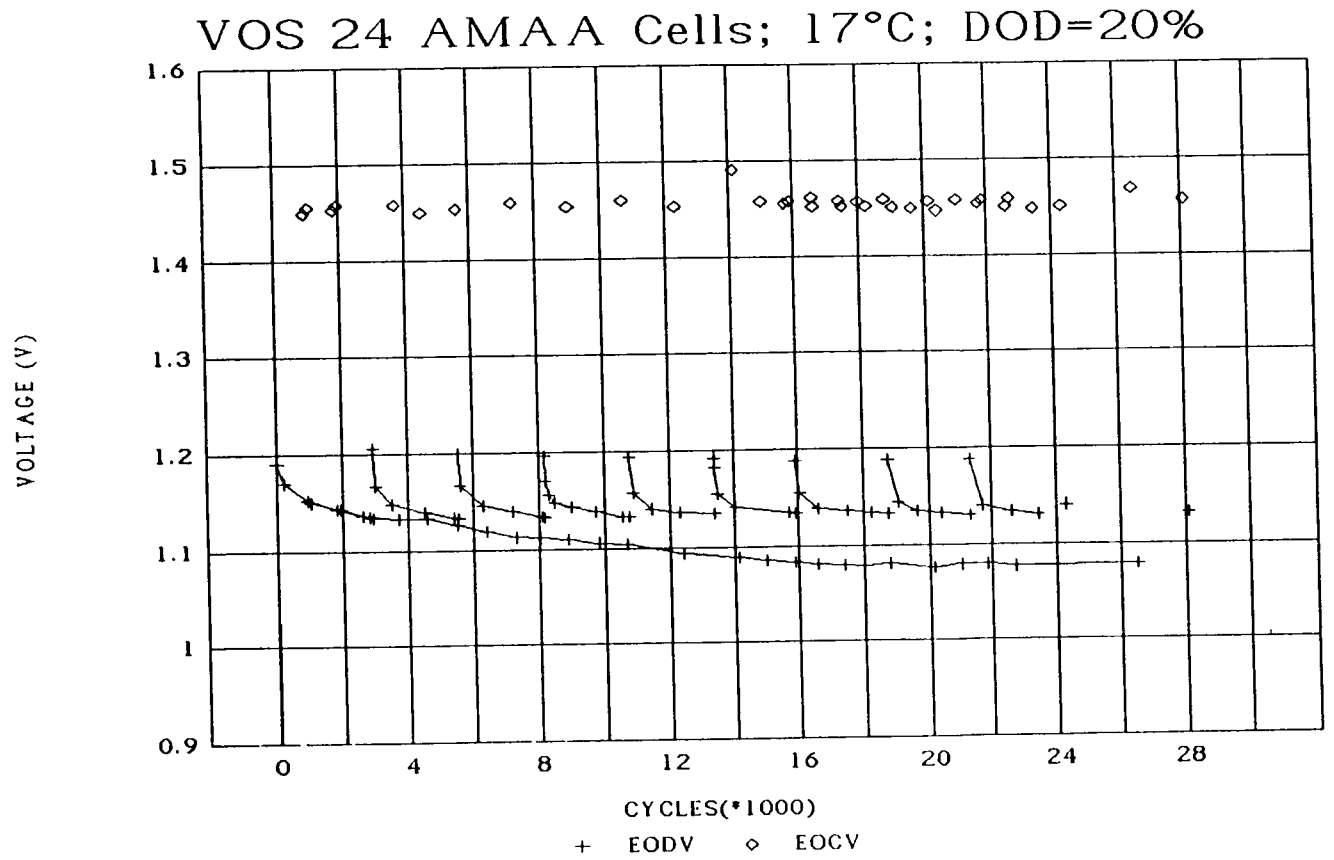

TEST N°57 AND 60

DISCHARGE: 25MN AT 3.5A
10 MN AT 20A

CHARGE: 65 MN AT 8A MAX
CURRENT TAPERING

WITH AND WITHOUT
RECONDITIONING

SAFT AEROSPACE DEPARTMENT		1990 NASA BATTERY WORKSHOP
NiCd Cells	ELAN Program	Low Earth Orbit Cycling

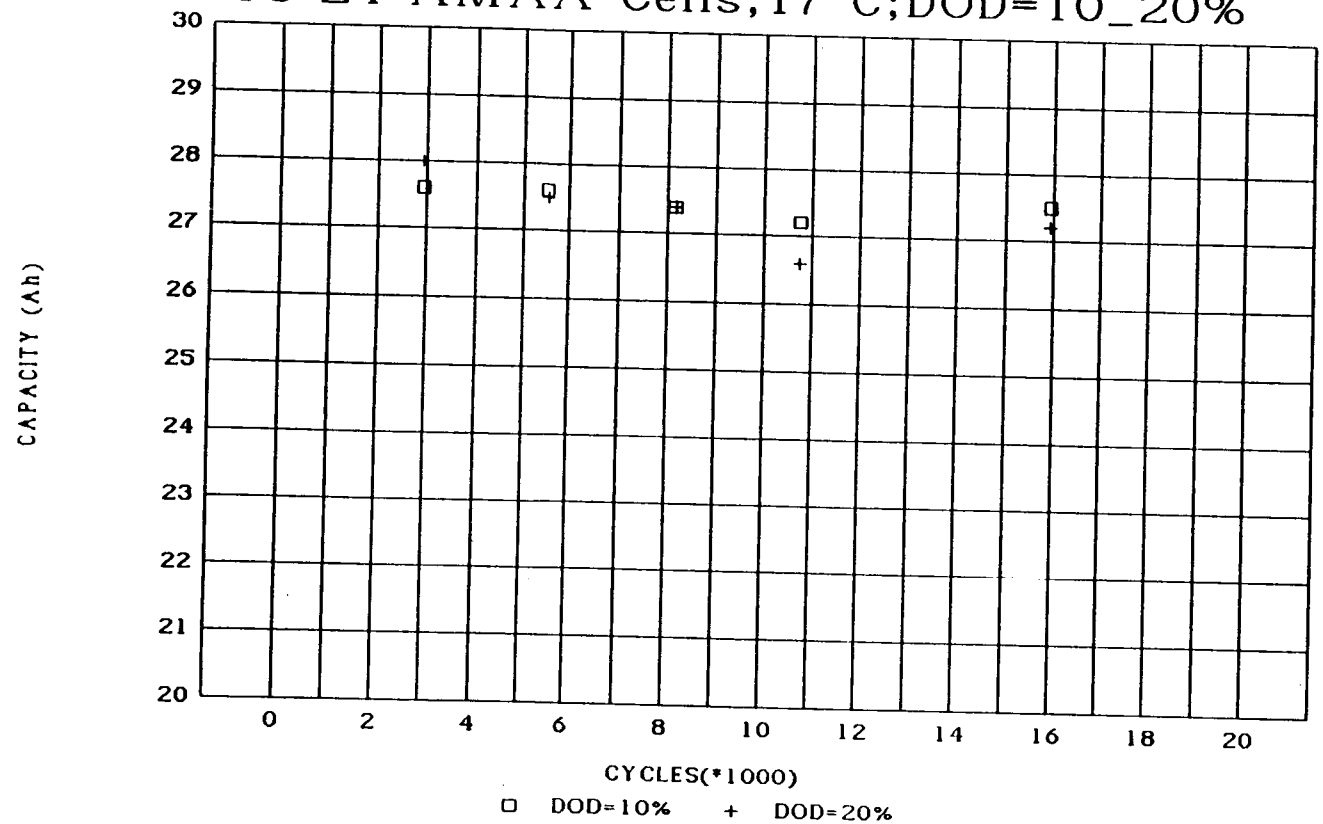

TEST N°54 AND 60
DISCHARGE AT 3.45A
DOWN TO 1V AFTER
CYCLING DISCHARGE

SAFT AEROSPACE DEPARTMENT		1990 NASA BATTERY WORKSHOP
NiCd Cells	ELAN Program	Low Earth Orbit Cycling

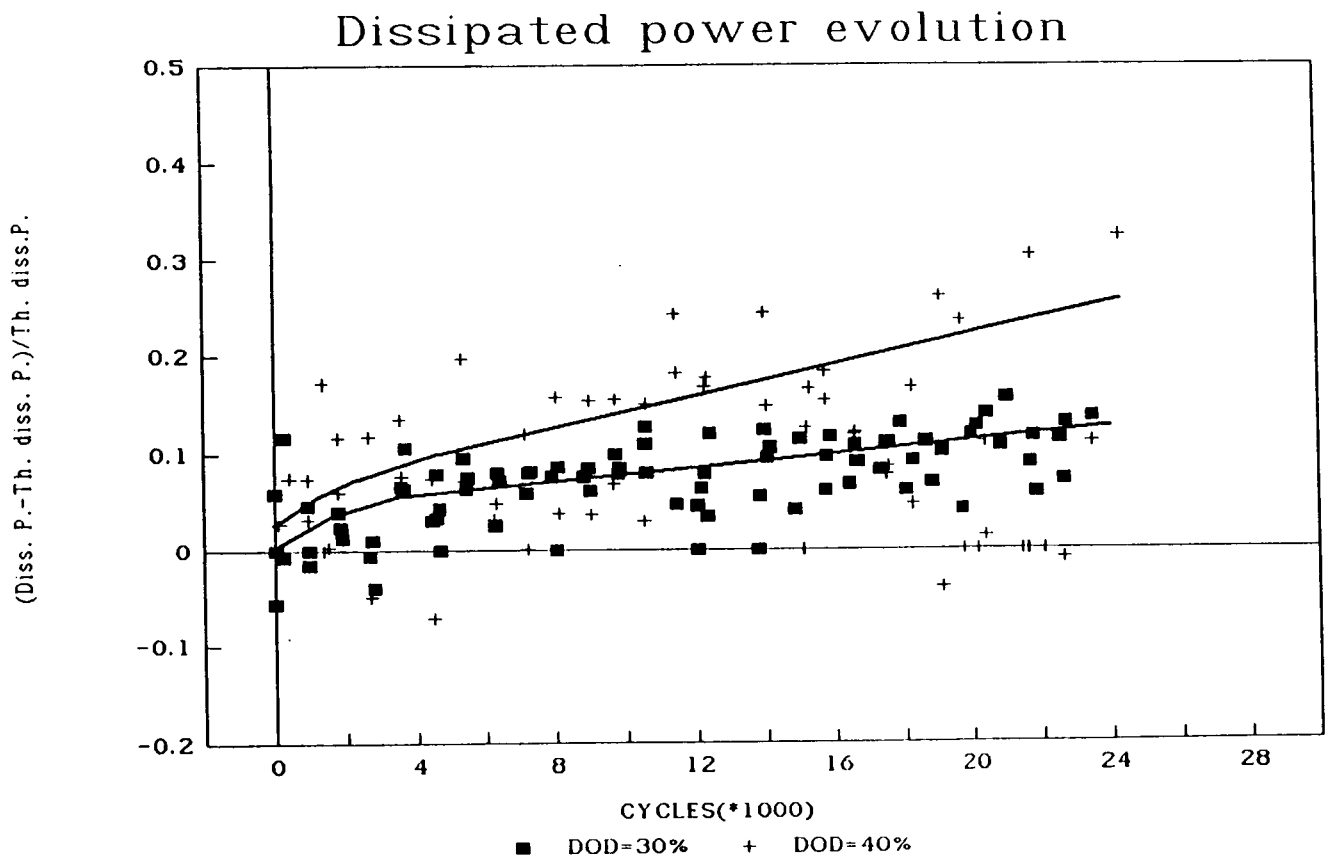

DISSIPATED POWER EVOLUTION COMPARED TO CALCULATED DISSIPATED POWER OF VOS 24 AMAA CELLS (BEGINING OF LIFE) FOR HIGH DOD (30 TO 40%)

SAFT AEROSPACE DEPARTMENT		1990 NASA BATTERY WORKSHOP
NiCd Cells	X80 cycling	Low Earth Orbit Cycling

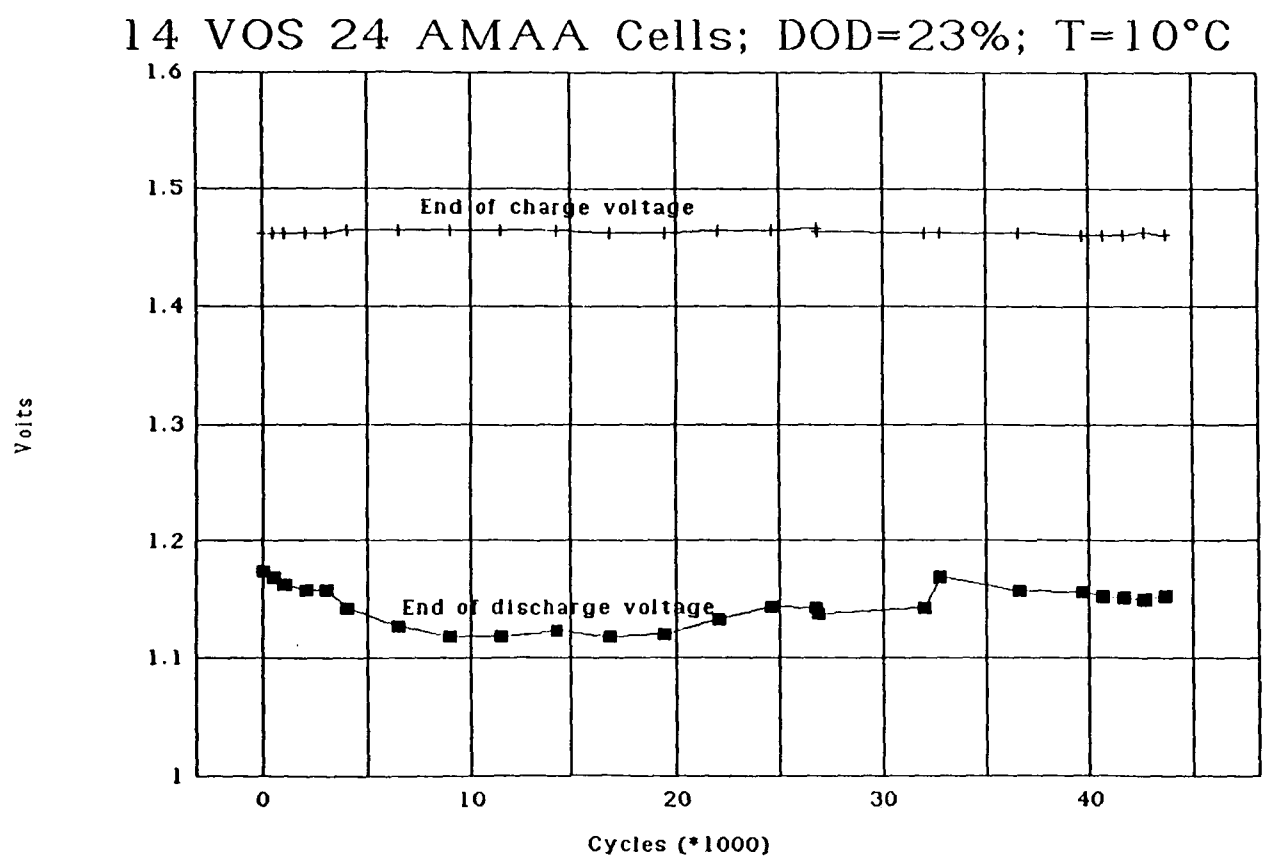

TEST N°50

DISCHARGE: 35MN AT 5.5A

CHARGE: CURRENT TAPERING

SAFT AEROSPACE DEPARTMENT		1990 NASA BATTERY WORKSHOP
NI-CD CELLS	NWSC PROGRAM	LOW EARTH ORBIT CYCLING

	NASA/GSFC		
	VOS 20 B	VOS 24 A	VOS 24 A
TEST NUMBER	93	94	95
BATTERY NUMBER	6120 S	6024 S	6124 S
DOD %	39	39	39
TEMPERATURE (°C)	20	0	20
DISCHARGE (A)	16	19.2	19.2
CHARGE (A)	16	19.2	19.2
VOLTAGE LIMIT	1.453	1.490	1.453
CYCLES	9500	9500	9500
END OF DISCHARGE VOLTAGE (V)	1.10	1.11	1.13

SAFT AEROSPACE DEPARTMENT		1990 NASA BATTERY WORKSHOP
NiCd Cells	NWSC Program	Low Earth Orbit Cycling

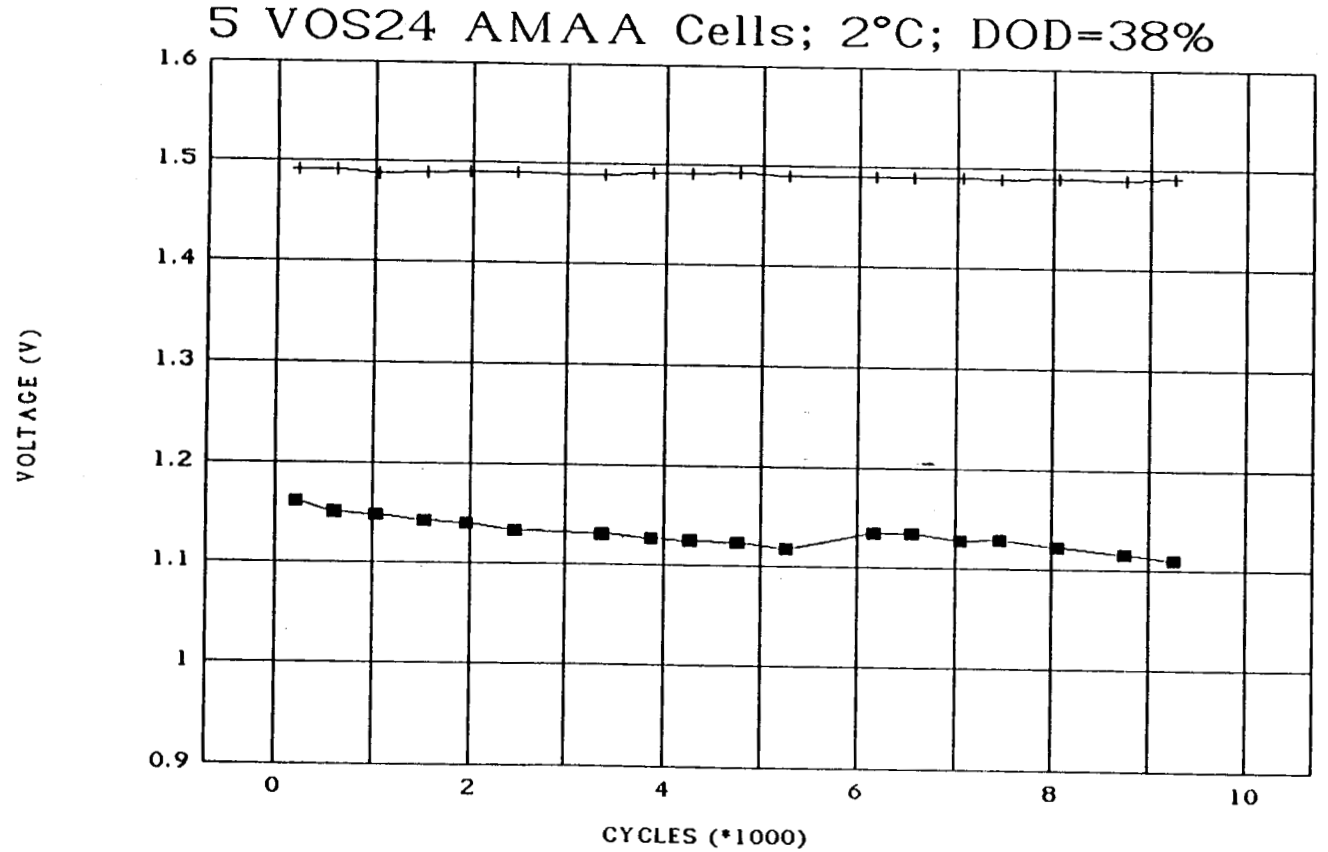

TEST N°94

DISCHARGE: 29MN AT 19A

CHARGE: 60 MN AT 19A
MAX CURRENT TAPERING

SAFT AEROSPACE DEPARTMENT		1990 NASA BATTERY WORKSHOP
NiCd Cells	NWSC Program	Low Earth Orbit Cycling

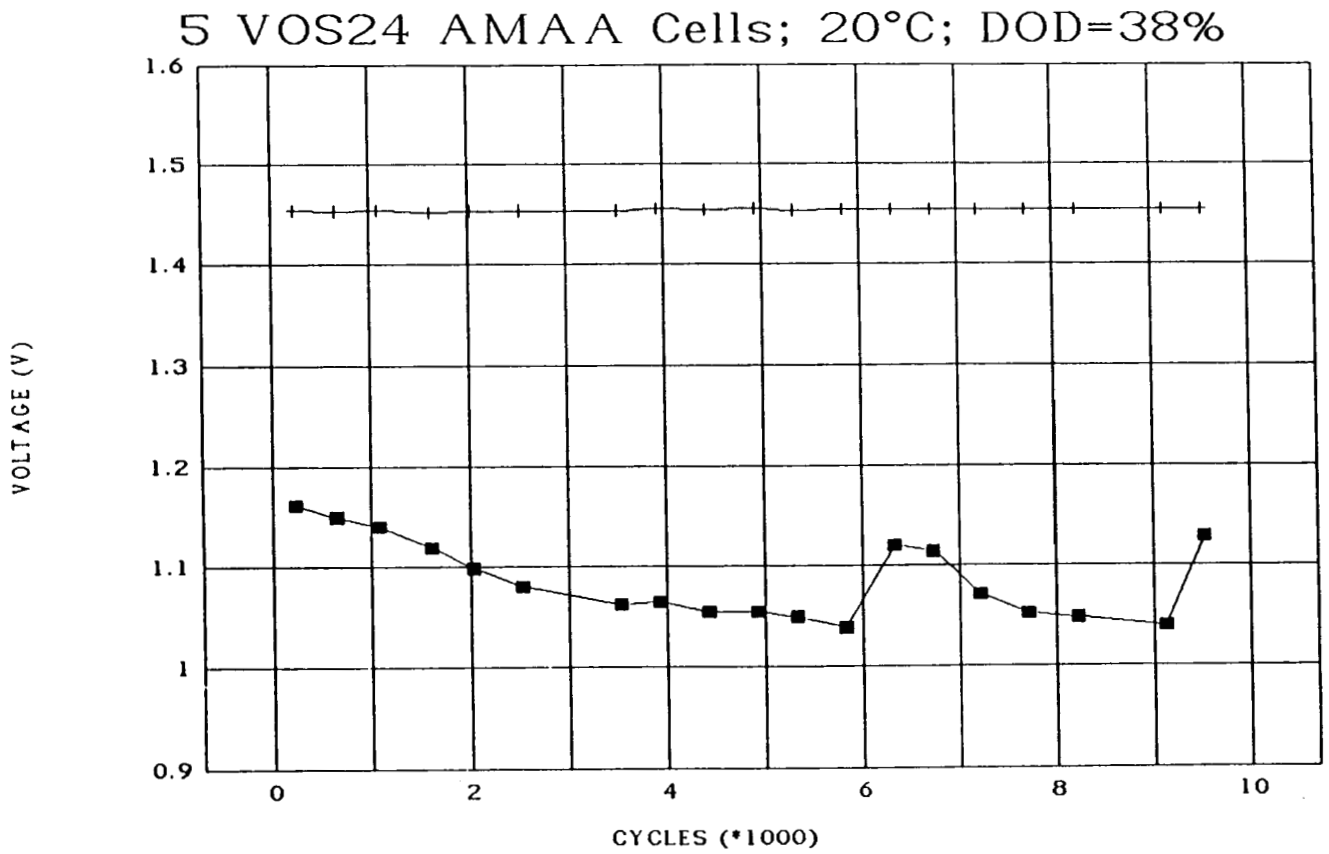

TEST N°95

DISCHARGE: 29MN AT 19A

CHARGE: 60 MN AT 19A
MAX CURRENT TAPERING

SAFT AEROSPACE DEPARTMENT		1990 NASA BATTERY WORKSHOP
NiCd Cells	NWSC Program	Low Earth Orbit Cycling

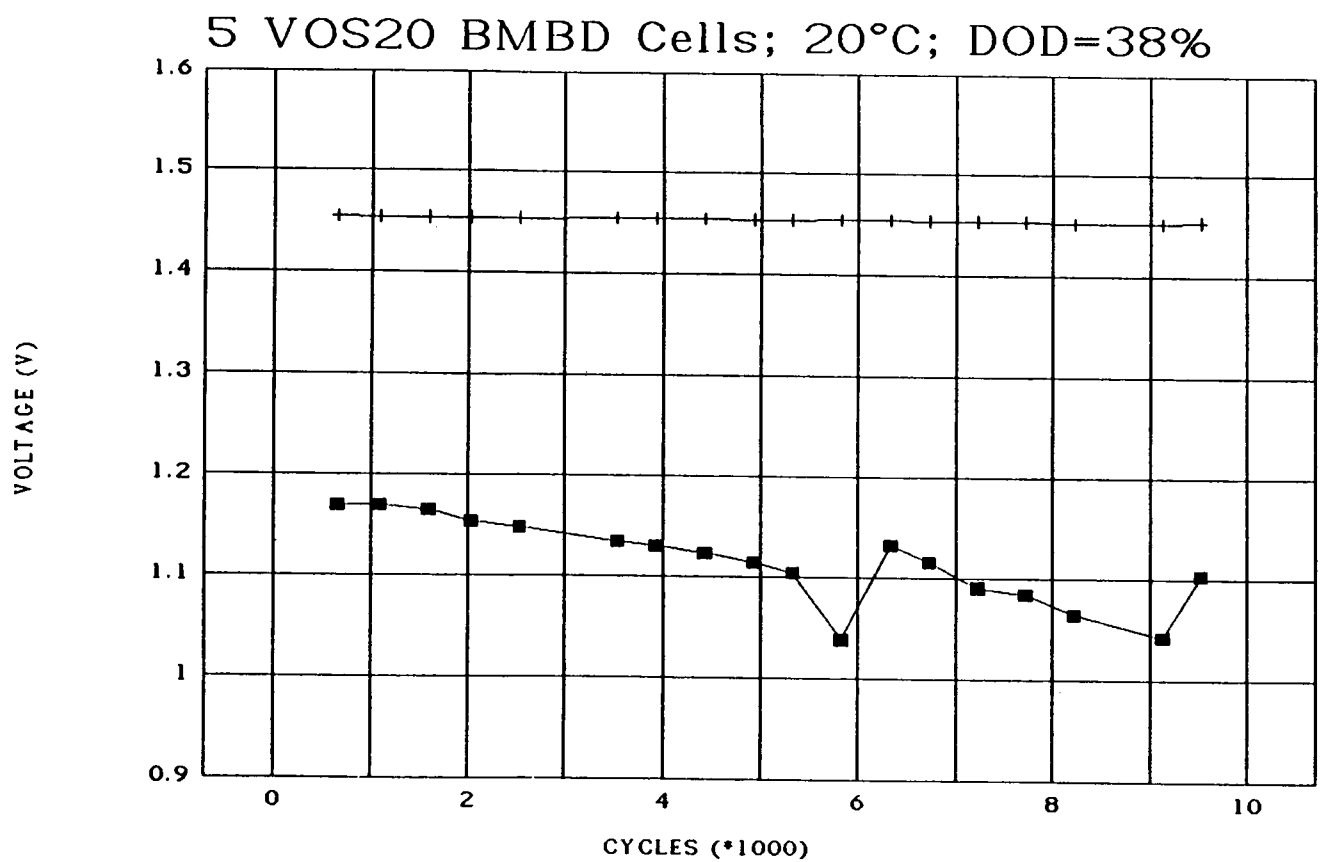

TEST N°93

DISCHARGE: 29MN AT 16A

CHARGE: 60 MN AT 16A
MAX CURRENT TAPERING

SAFT AEROSPACE DEPARTMENT		1990 NASA BATTERY WORKSHOP
NiCd Cells	LIFE TIME	Low Earth Orbit Cycling

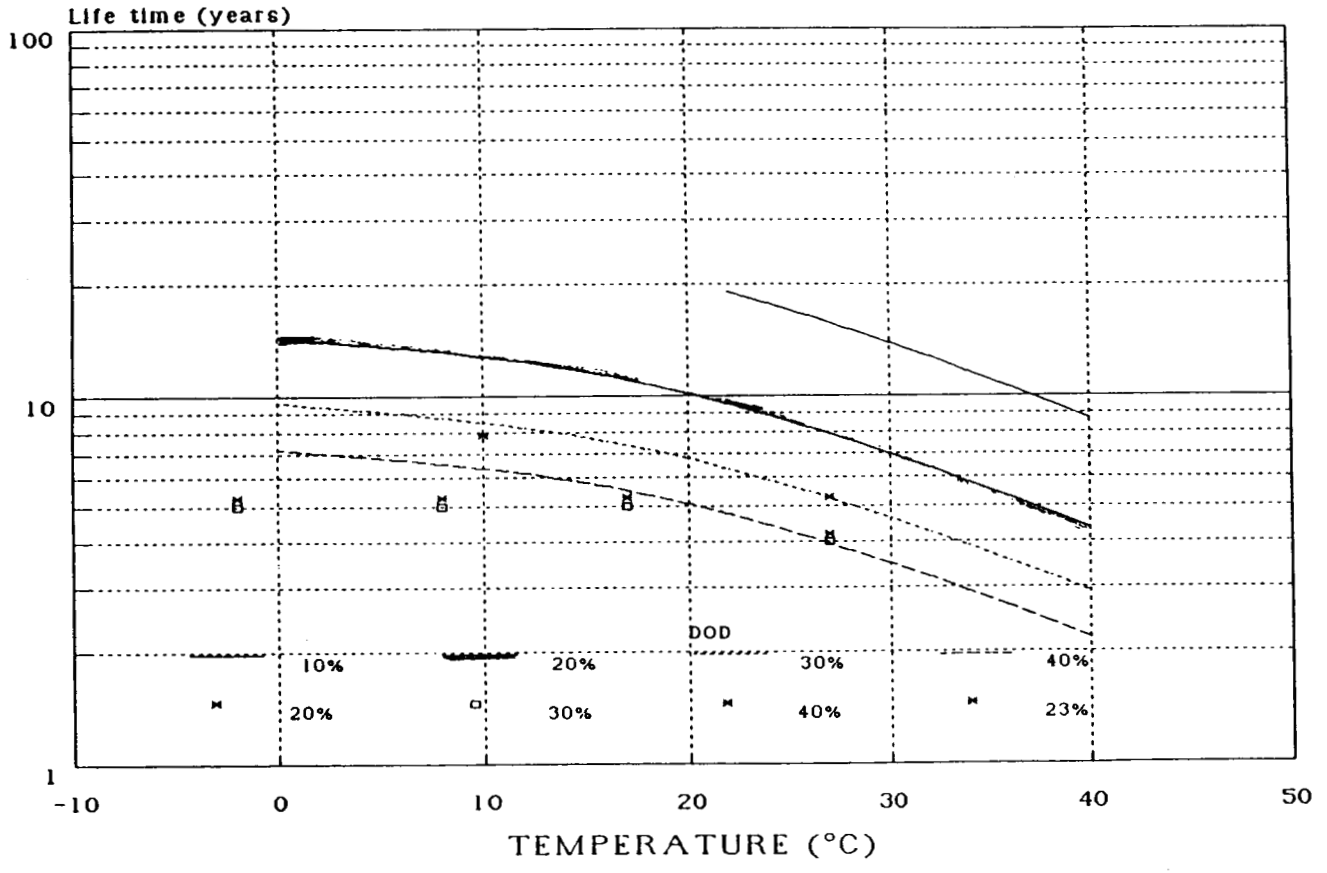

Life Time expectancy
for LEO applications
SAFT Cells

SAFT AEROSPACE DEPARTMENT		1990 NASA BATTERY WORKSHOP
NiCd Cells	LIFE TIME	Low Earth Orbit Cycling

Main parameter toward life time: overcharged capacity
Secondary parameters: Temperature, Overcharge current (constant value was taken for LEO application)

Life time model calculation basis: Weibull distribution for failed cell ratio dependency
Arhenius law for temperature effect

Life time model based on: NWSC cycling results on NiCd cells (Temperature dependency)

$$Cs = e^{\left(\frac{4142}{T} - 6.56 + \frac{\ln(-\ln(1-Q))}{1}\right)}$$

ESA cycling results on NiCd SAFT Cells

$$Cs = e^{\left(\frac{173}{T} - 6.63 + \frac{\ln(-\ln(1-Q))}{21}\right)}$$

Where: Cs= overchargeable capacity in multiple of Cn (nominal capacity)
T= temperature in °K
Q= failed cell ratio

SAFT AEROSPACE DEPARTMENT		1990 NASA BATTERY WORKSHOP
NiCd Cells	OTS2 FLIGHT DATA	Geostationary Orbit Cycling

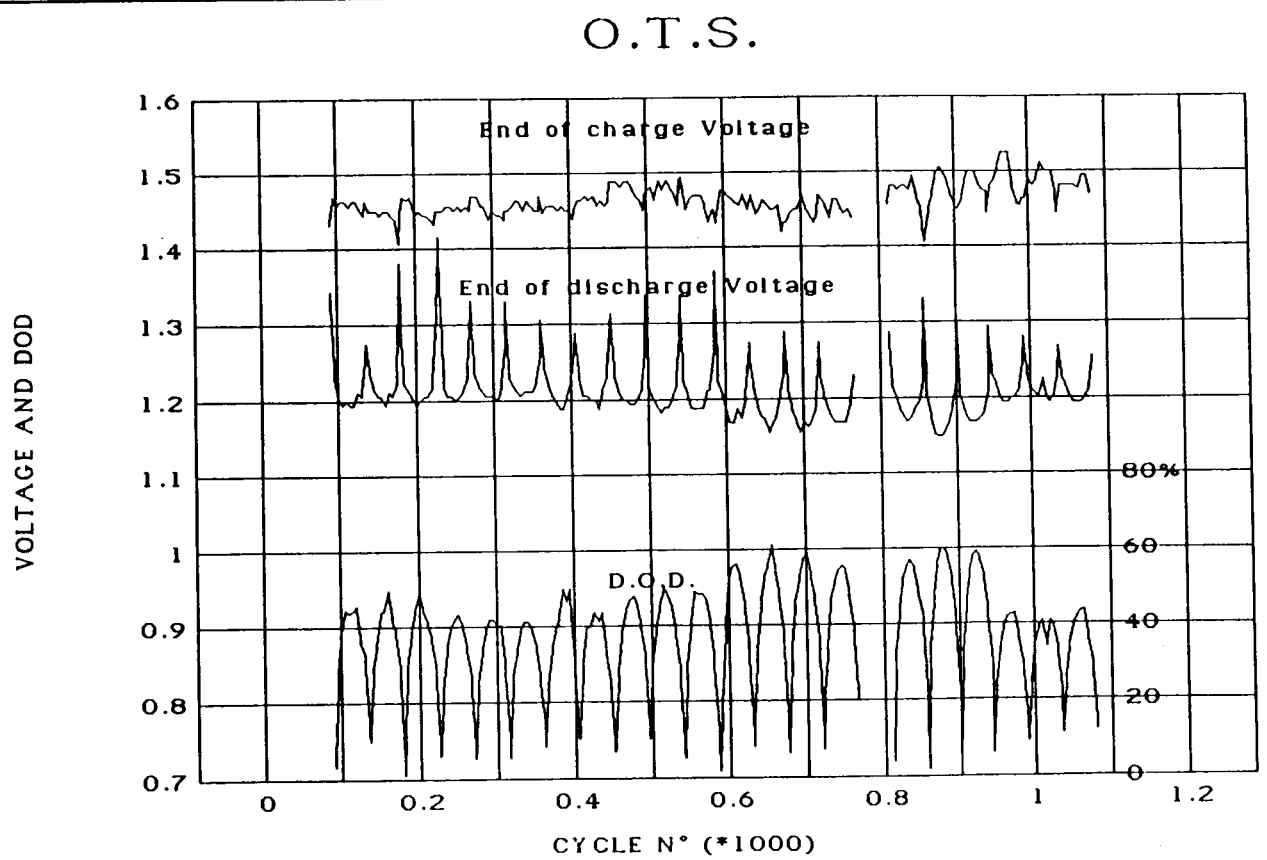

2 packs of 14 VOS18A-MAA cells.

Average temperature: 15°C

12.5 years operational mission

SAFT AEROSPACE DEPARTMENT		1990 NASA BATTERY WORKSHOP
NiCd Cells	ECS SIMULATION	Geostationary Orbit Cycling

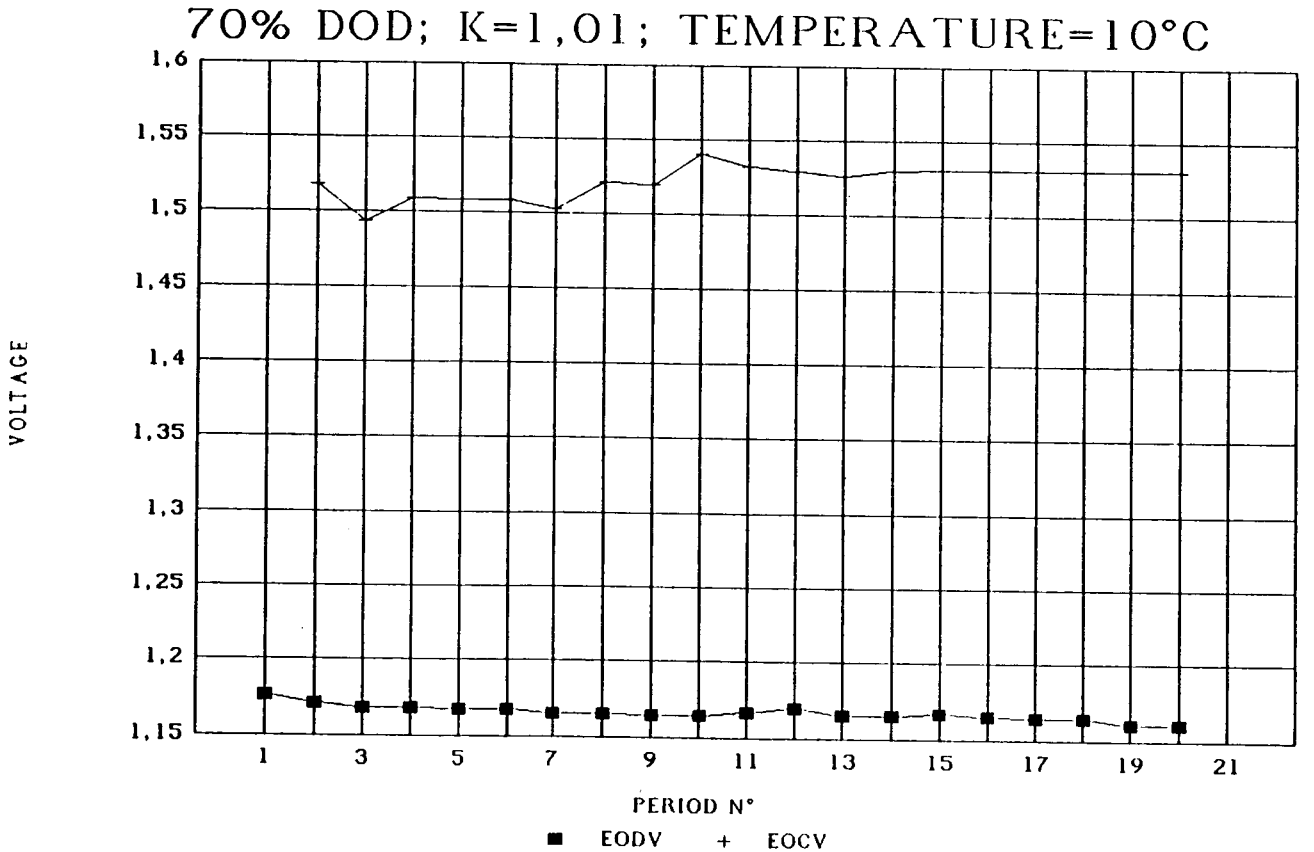

28 VOS18AMBB

45 DAYS SHORTEN SOLSTICES WITH TRICKLE CHARGE

Approximated DOD profile

Temperature: 10°C

11.5 YEARS CYCLING

SAFT AEROSPACE DEPARTMENT		1990 NASA BATTERY WORKSHOP
NiCd Cells	ECS SIMULATION	Geostationary Orbit Cycling

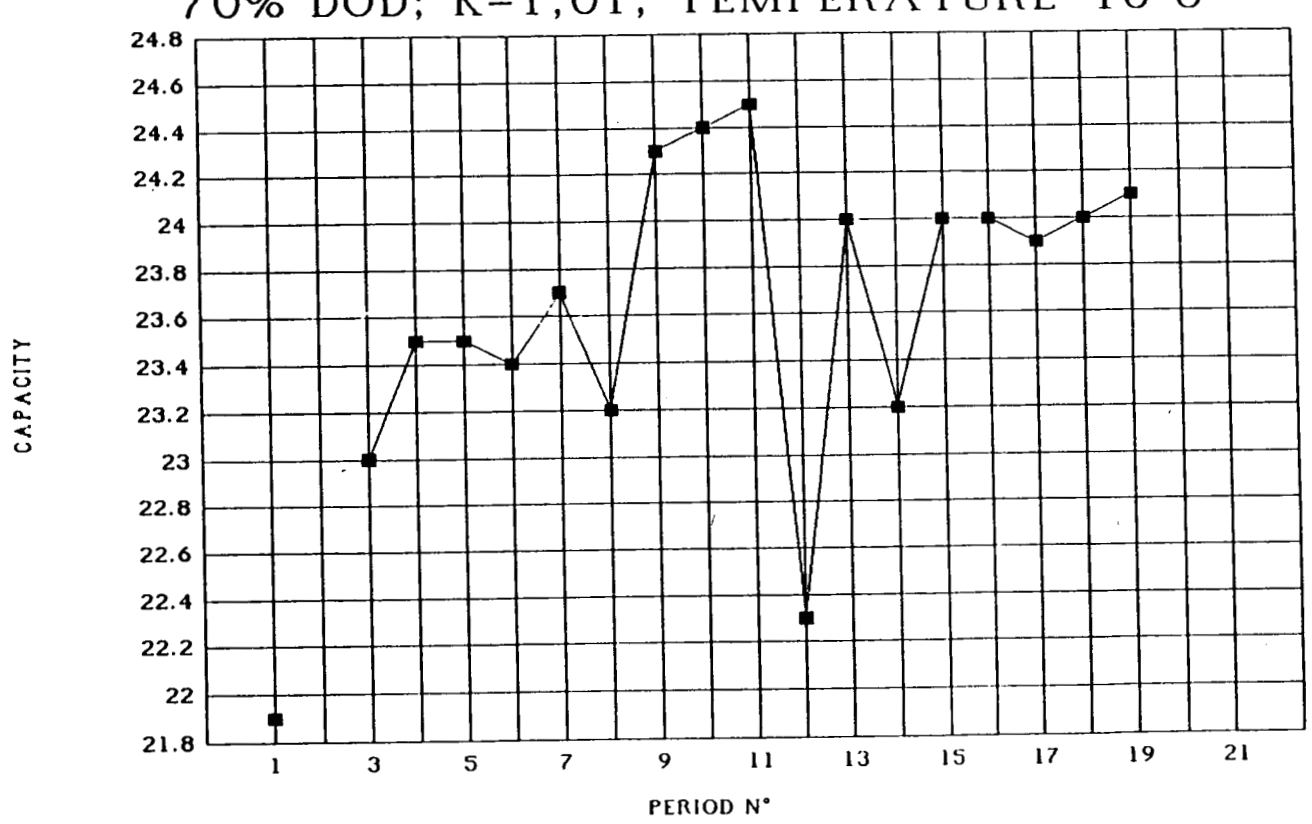

28 VOS18AMBB

45 DAYS SHORTEN SOLSTICES WITH TRICKLE CHARGE

APPROXIMATED DOD PROFILE

TEMPERATURE:10°C

11.5 YEARS CYCLING

SAFT AEROSPACE DEPARTMENT		1990 NASA BATTERY WORKSHOP
NiCd Cells	ECS SIMULATION	Geostationary Orbit Cycling

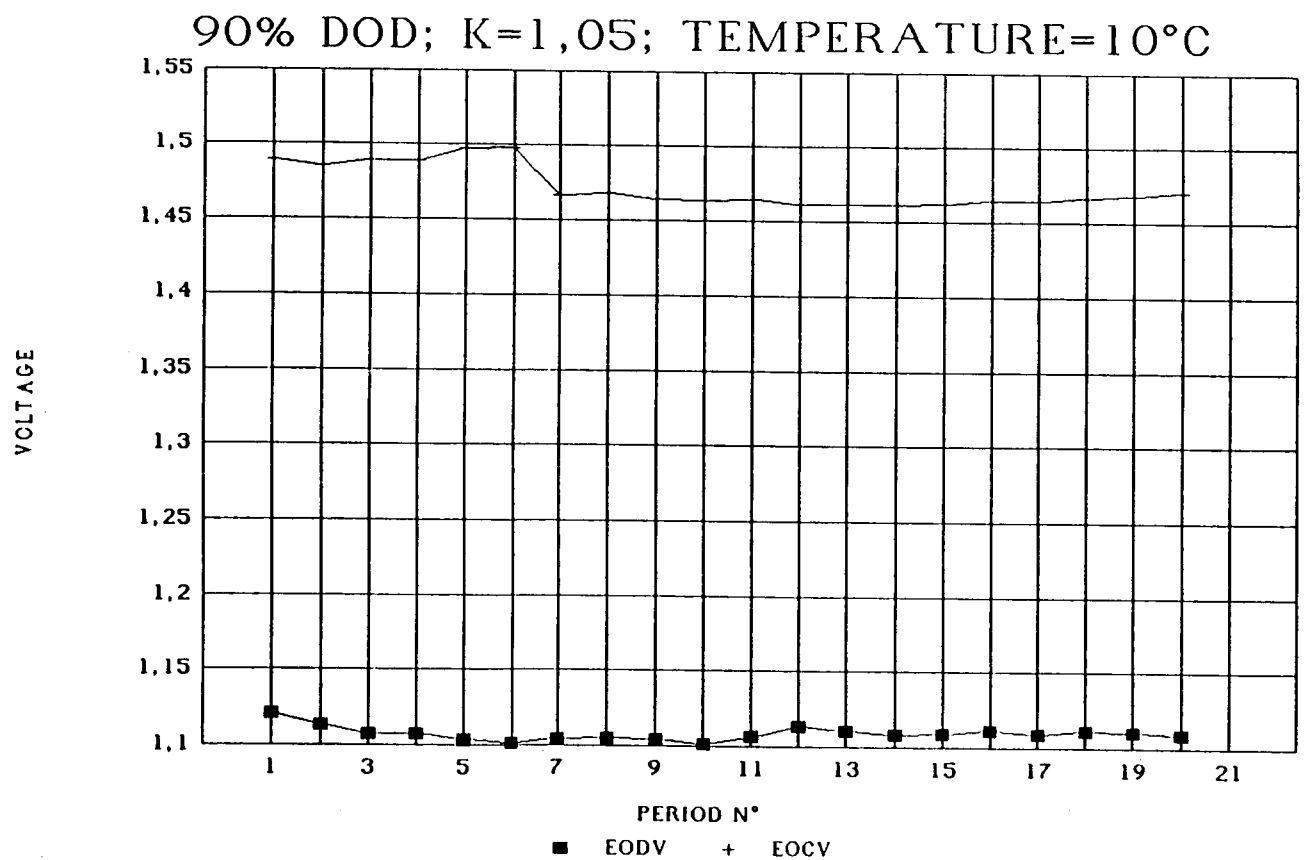

28 VOS18AMBB

45 DAYS SHORTEN SOLSTICES WITH TRICKLE CHARGE

APPROXIMATED DOD PROFILE

TEMPERATURE: 10°C

11.5 YEARS CYCLING

SAFT AEROSPACE DEPARTMENT		1990 NASA BATTERY WORKSHOP
NiCd Cells	ECS SIMULATION	Geostationary Orbit Cycling

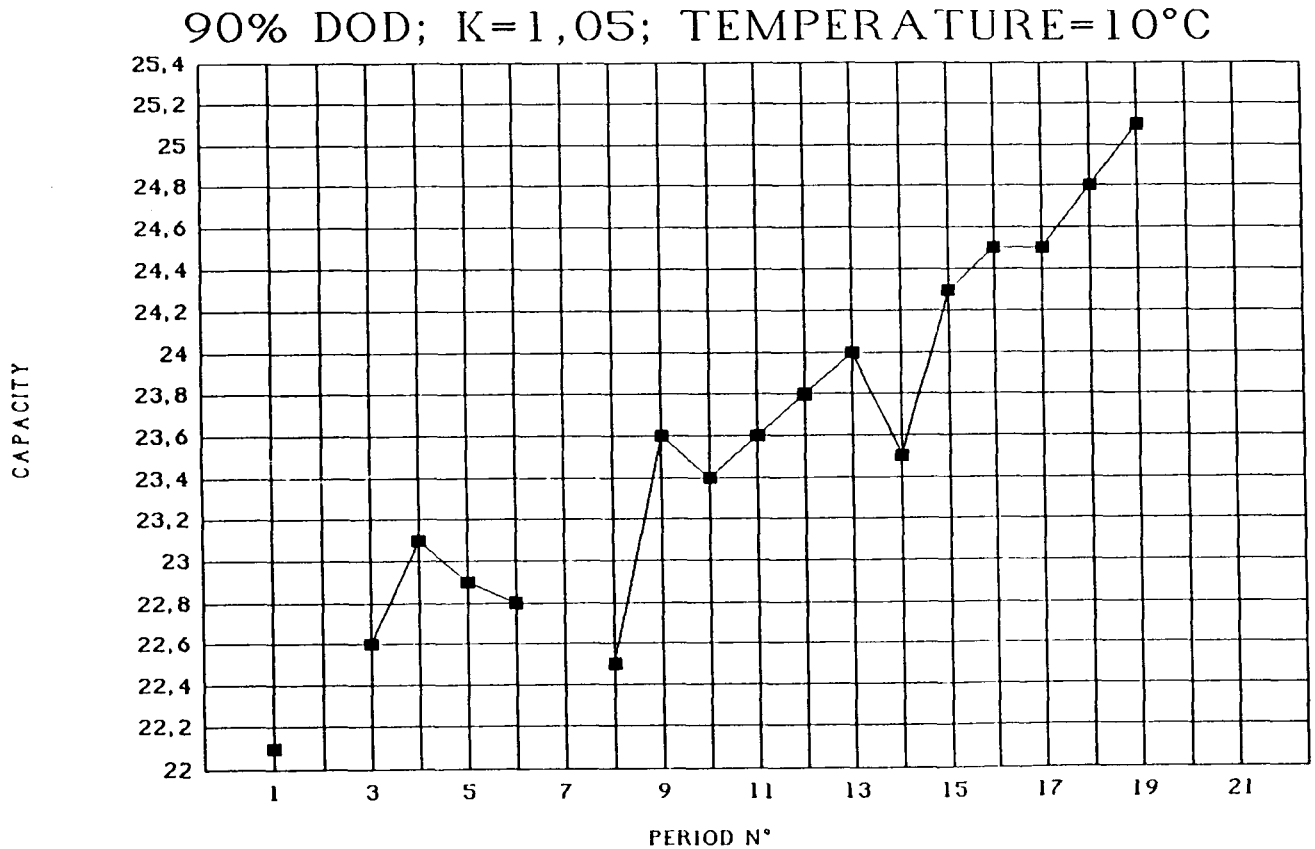

28 VOS18AMBB

45 days shorten solstices with trickle charge

Approximated DOD profile

Temperature: 10°C

11.5 years cycling

SAFT AEROSPACE DEPARTMENT		1990 NASA BATTERY WORKSHOP
NiCd Cells	ECS SIMULATION	Geostationary Orbit Cycling

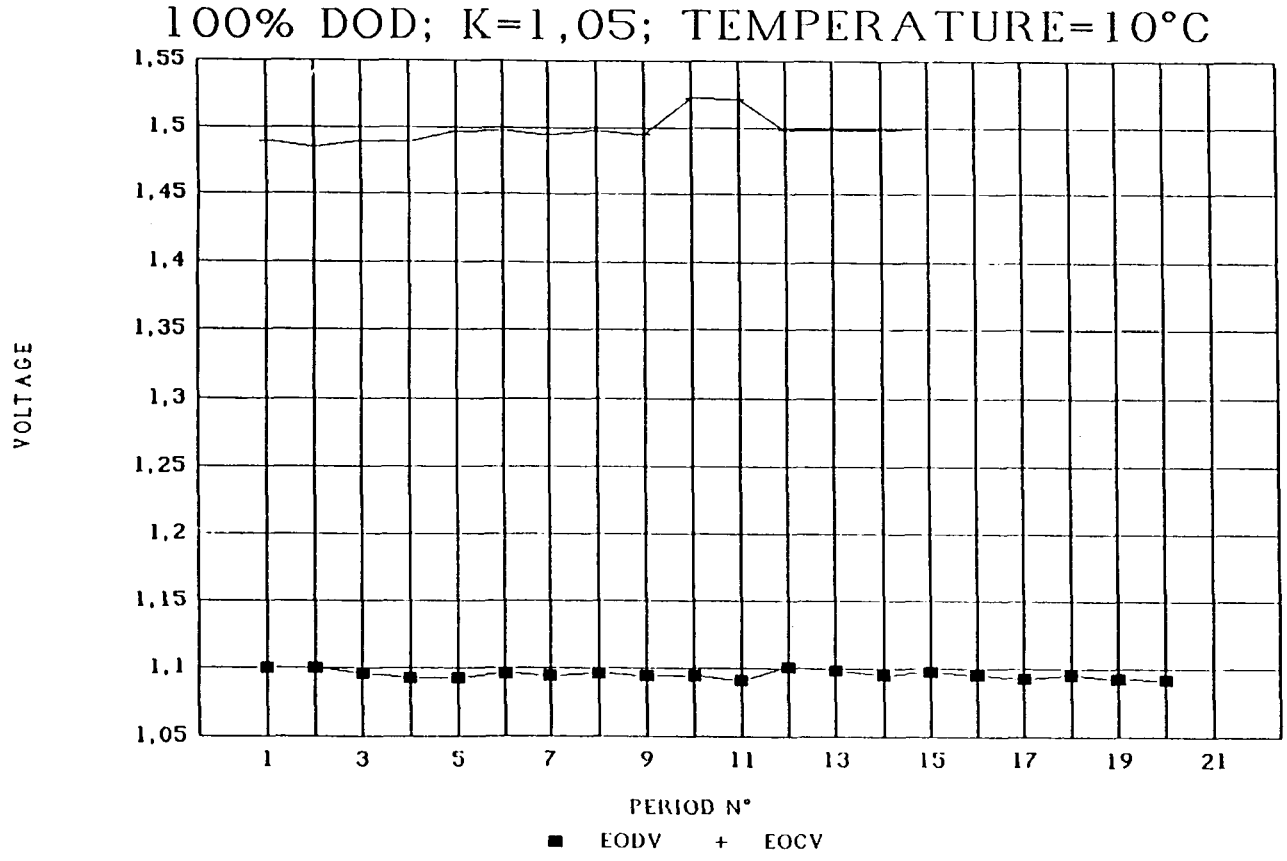

28 VOS18AMBB

45 days shorten solstices with trickle charge

Approximated DOD profile

Temperature: 10°C

11.5 years cycling

SAFT AEROSPACE DEPARTMENT		1990 NASA BATTERY WORKSHOP
NiCd Cells	ECS SIMULATION	Geostationary Orbit Cycling

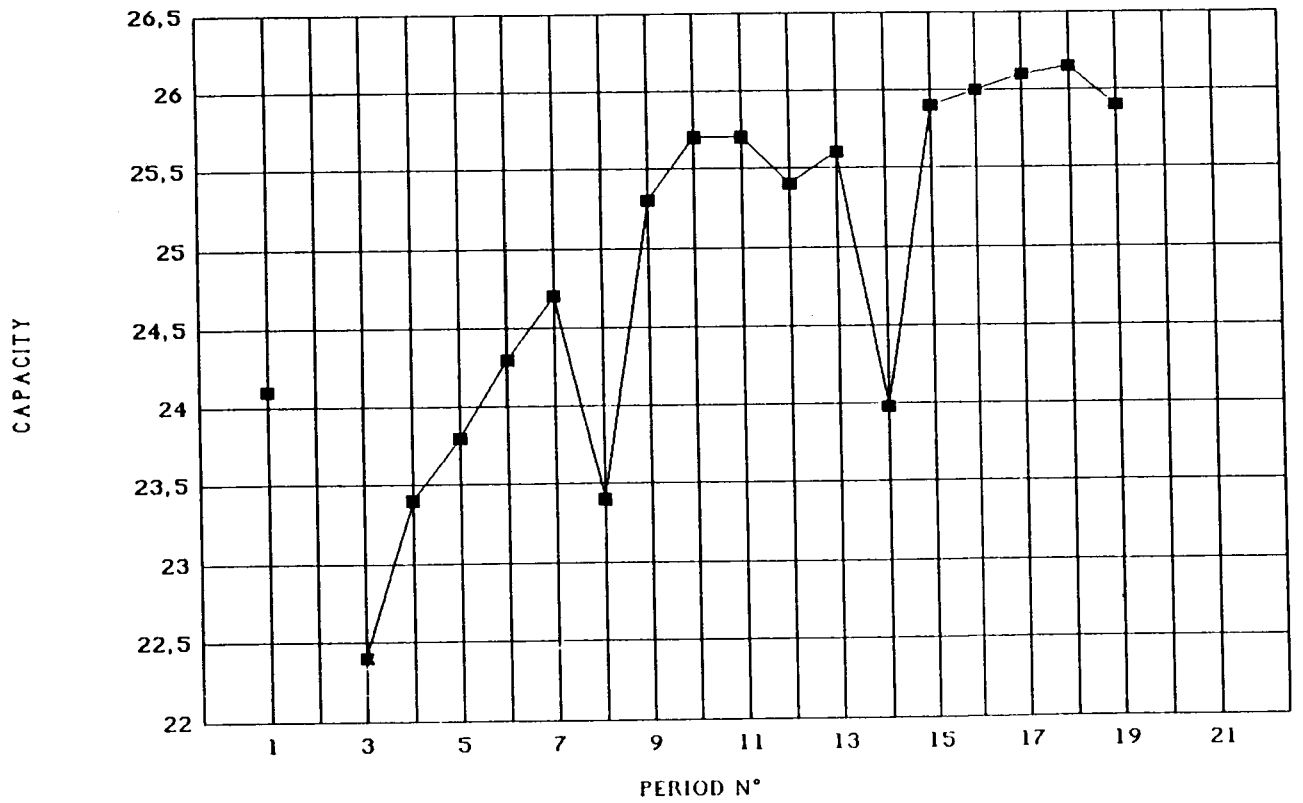

28 VOS18AMBB

45 DAYS SHORTEN SOLSTICES WITH TRICKLE CHARGE

APPROXIMATED DOD PROFILE

TEMPERATURE: 10°C

11.5 YEARS CYCLING

OXYGEN RECOMBINATION IN THE SEALED NICKEL CADMIUM CELL

A. H. ZIMMERMAN AND T. P. BARRERA
CHEMISTRY AND PHYSICS LABORATORY
THE AEROSPACE CORPORATION
EL SEGUNDO, CALIFORNIA

PRESENTED AT THE 1990 BATTERY WORKSHOP
AT MARSHALL SPACE FLIGHT CENTER
4-6 DECEMBER 1990

PURPOSE OF STUDY

To Determine What Parameters Are Most Critical For Controlling Overcharge Pressure In A Sealed NiCd Cell

- o Temperature
- o Overcharge current
- o Cadmium electrode precharge - % Cd in metallic state
- o Electrolyte fill factor -fraction of free pack vol filled
- o Physical structure of the cadmium electrode - pore size distribution

OXYGEN EVOLUTION AND RECOMBINATION IN A SEALED NICD CELL

EVOLUTION AT POSITIVE: $4OH^- \xrightarrow{K_F} 2H_2O + O_2 + 4e^-$

RECOMBINATION AT NEGATIVE: $2Cd + O_2 + 2H_2O \xrightarrow{K_R} 2Cd(OH)_2$

RECOMBINATION RATE = $-d[O_2]/dt = K_R A_{Cd}[O_2] - IRT/4FV$

- o OXYGEN PRESSURE MONITORED ACCURATELY
- o RECOMBINATION RATE MEASURED DIRECTLY FROM PRESSURE CHANGE VS. TIME
- o OVERCHARGE CURRENT AND CELL VOLUME ARE MEASURED
- o UNKNOWN IS $K_R A_{Cd}$ - AN EFFECTIVE OXYGEN RECOMBINATION RATE CONSTANT

Typical Cell Voltage and Pressure Changes During Charge

(12 hr. charge @ C/10 rate , 0 deg. C)

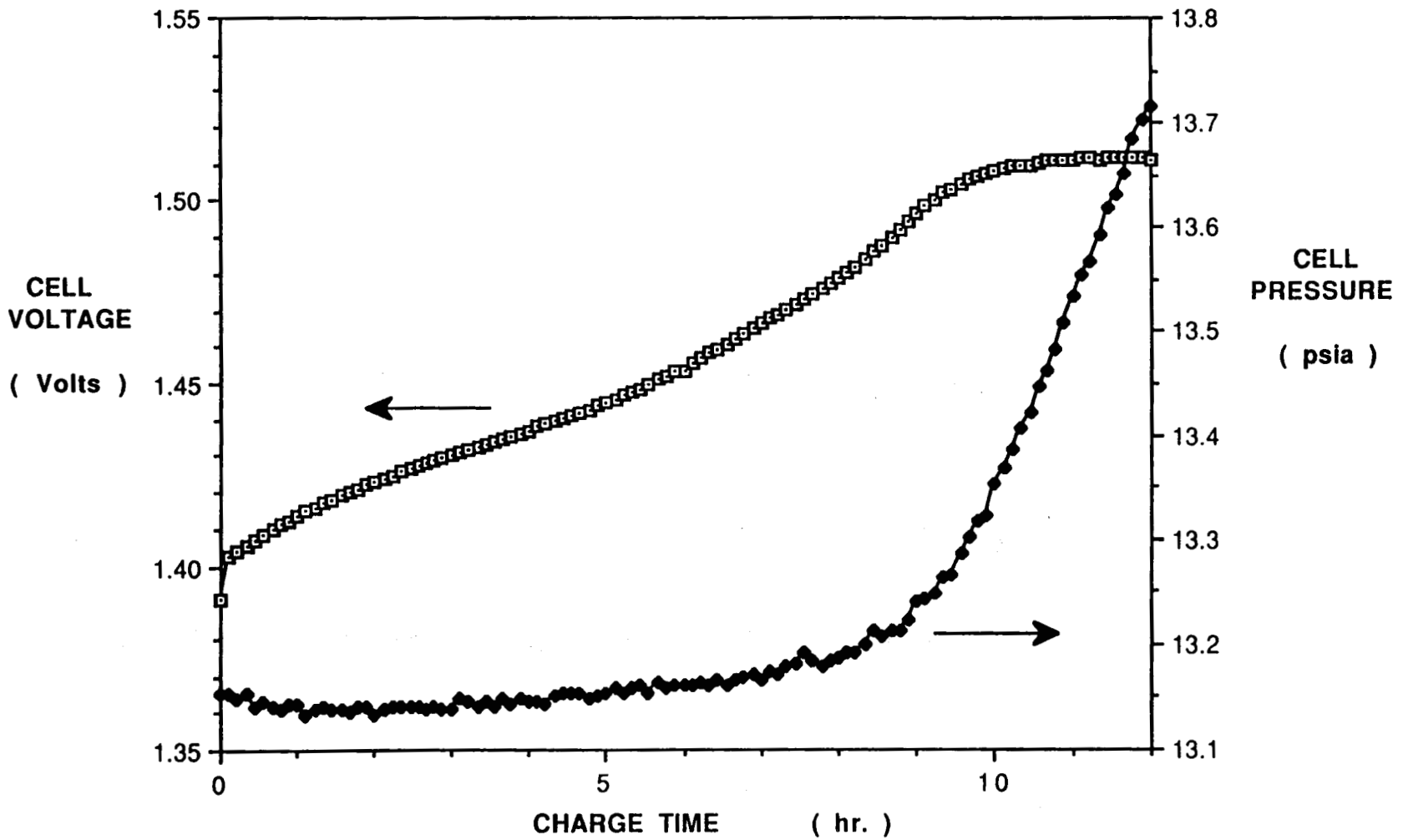

EXPERIMENTAL TEST DESCRIPTION

- o Cell - Starved NiCd cell, 1 positive plate, 2 negatives
  - 14 cm^2 plate area, 280 mAh capacity @ 20 mAh/cm^2
  - Pellon 2505 separator

- o Control Equipment
  - Computer controlled potentiostat in controlled current mode
  - Operation in controlled temperature bath ($\pm$0.01 deg C)

- o Monitoring - Continuous using a computer monitoring and data acquisition system
  - Cell voltage ($\pm$0.0001 volts)
  - Cell pressure ($\pm$0.001 psia)
  - Cell temperature ($\pm$0.001 deg C)

NICD TEST CELL DESIGN

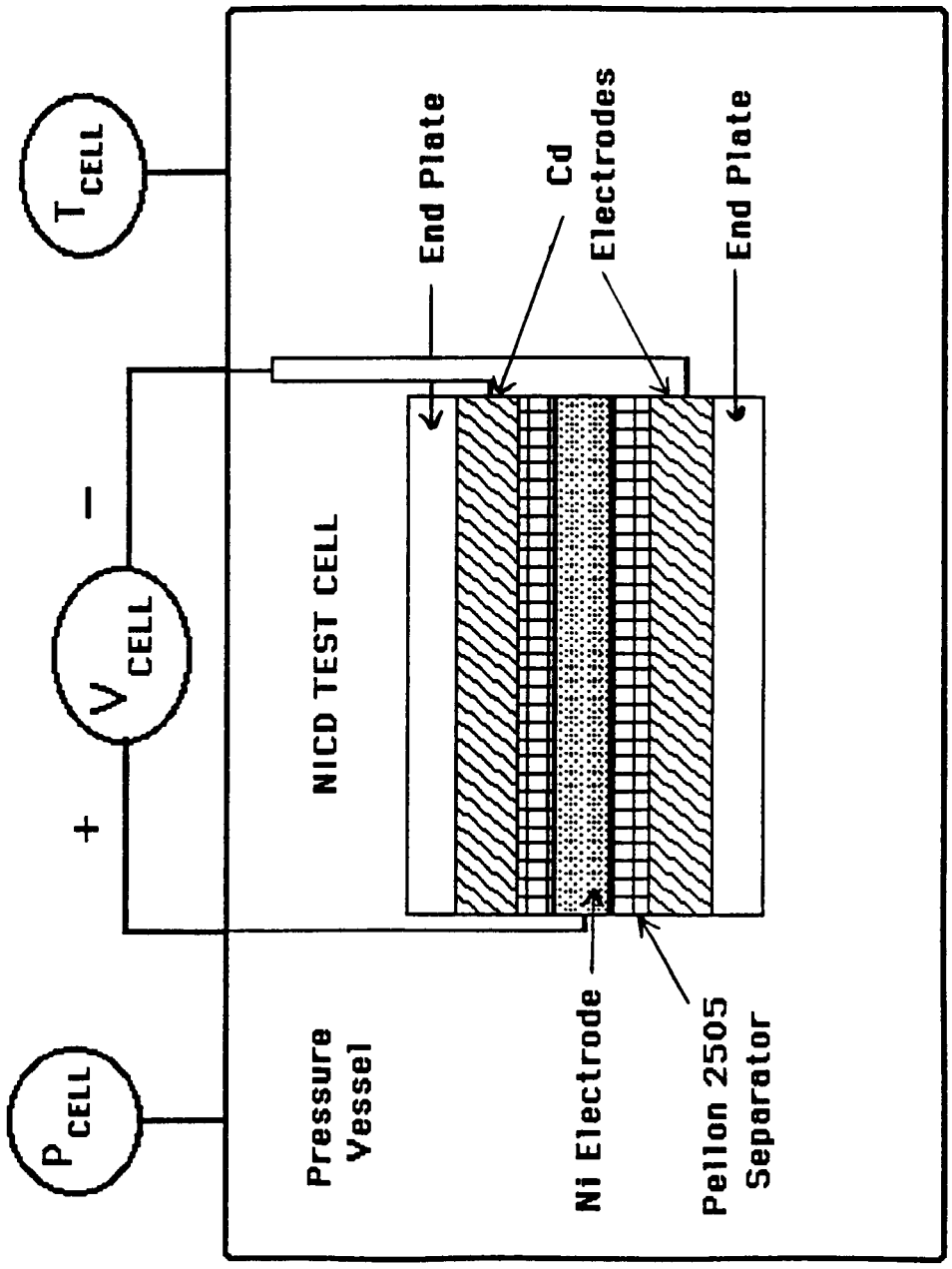

Pore Size Distributions from Mercury Porosimetry for Cd Electrodes Studied

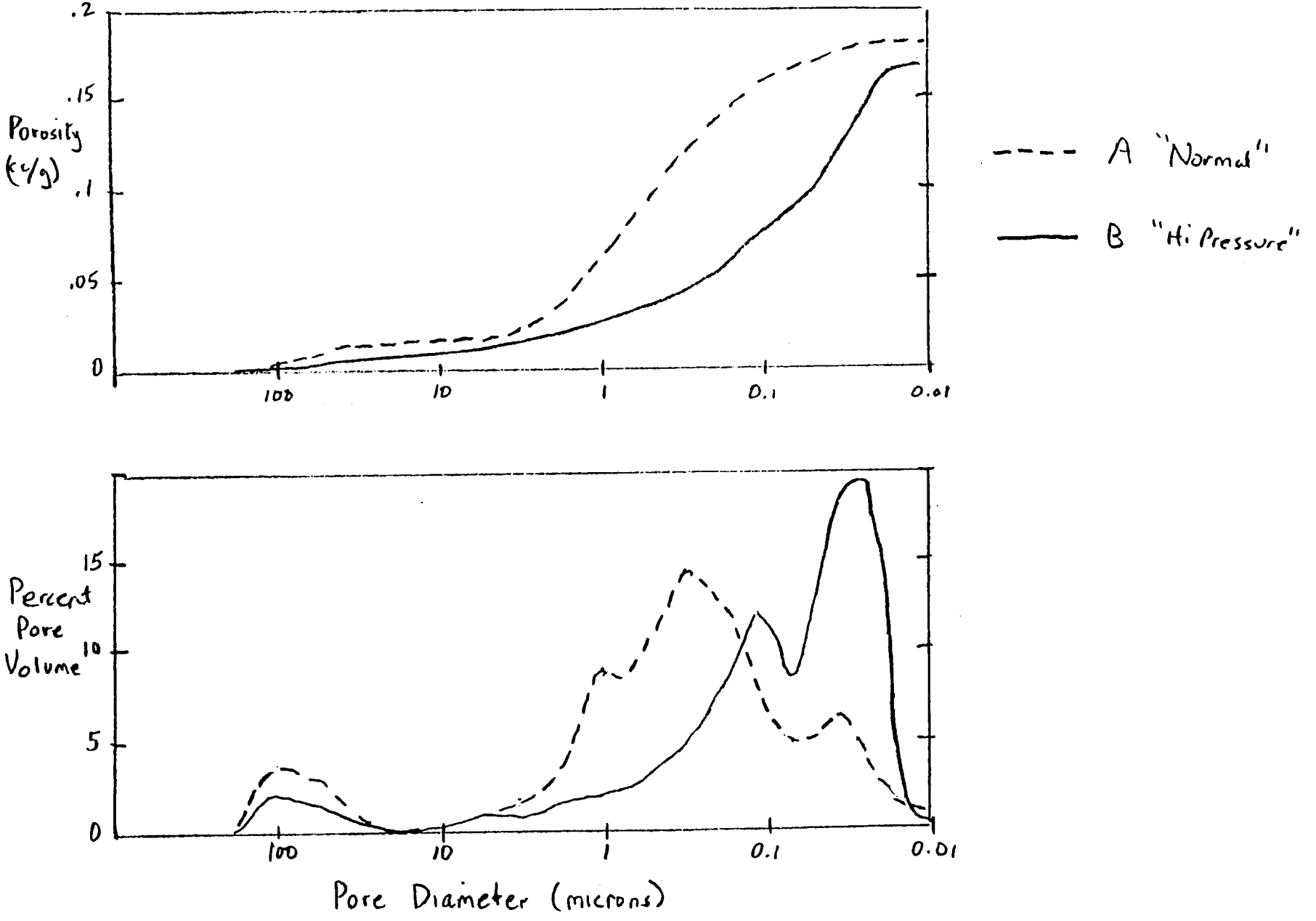

Effective Recombination Rate Constant as a Function of Cell Precharge

(65 % KOH fill , 0 deg. C , C/20 charge rate)

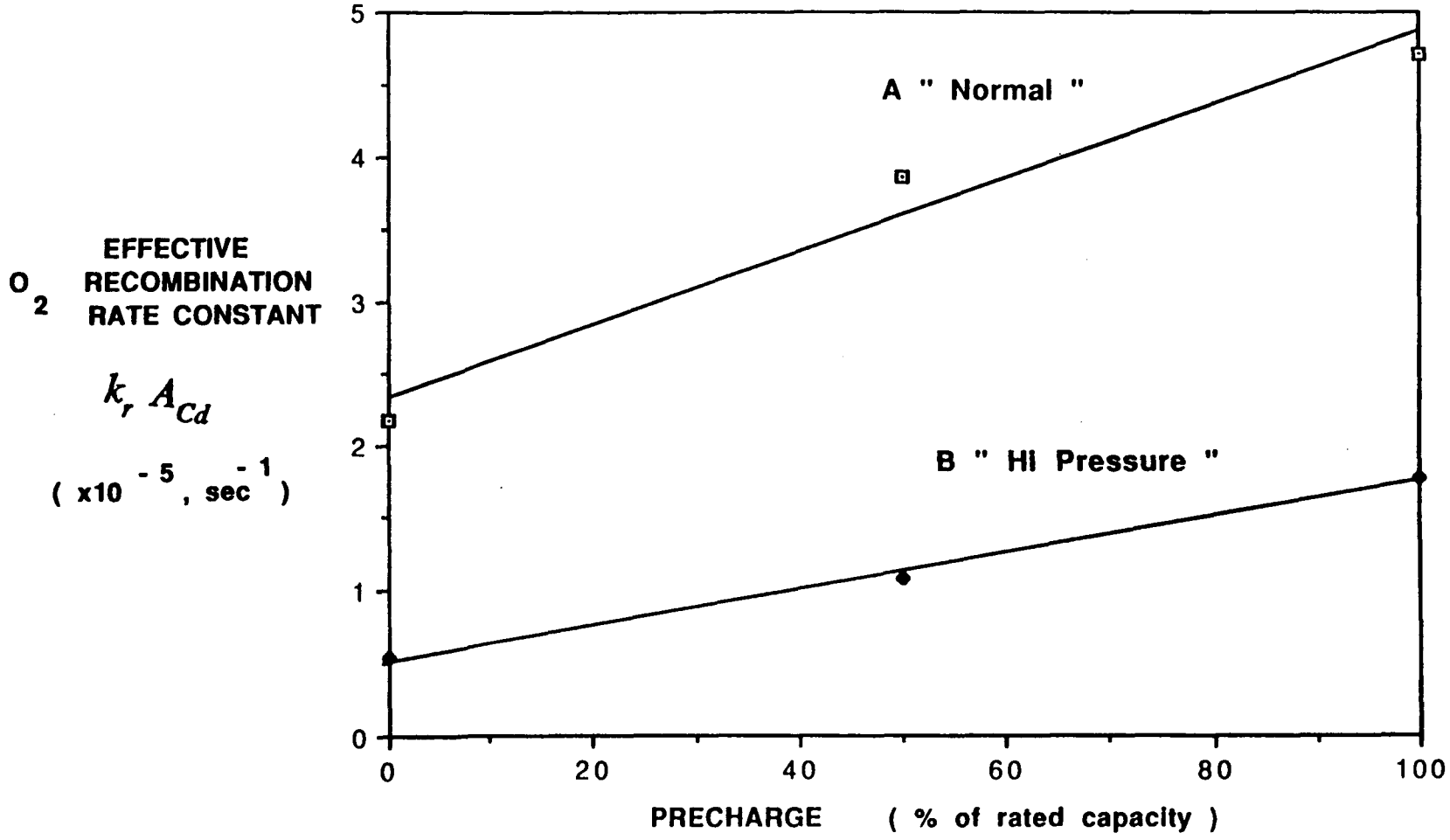

Effects of KOH Fill Factor on O_2 Recombination Rate

(0 deg. C , C/10 charge rate , 0 % precharge)

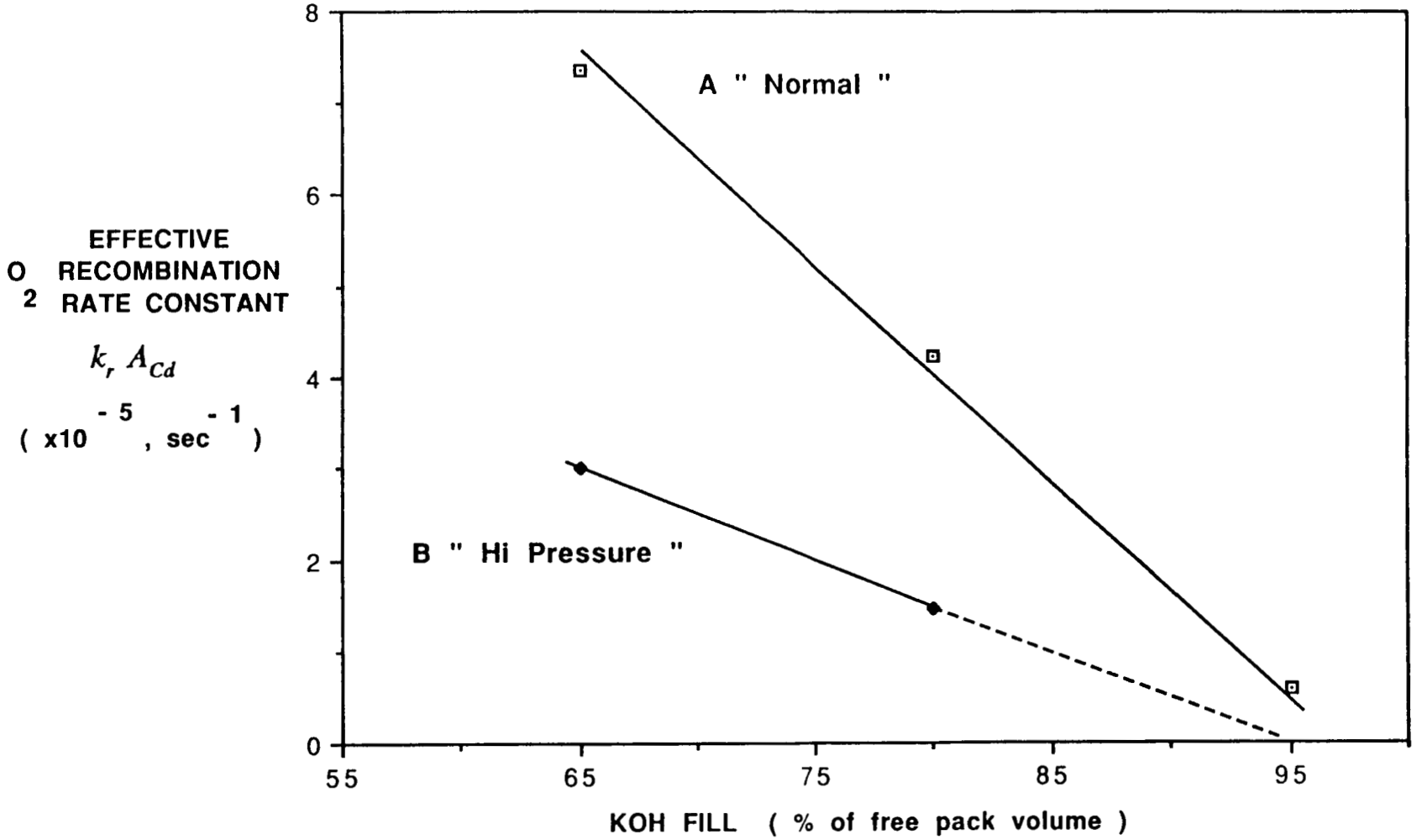

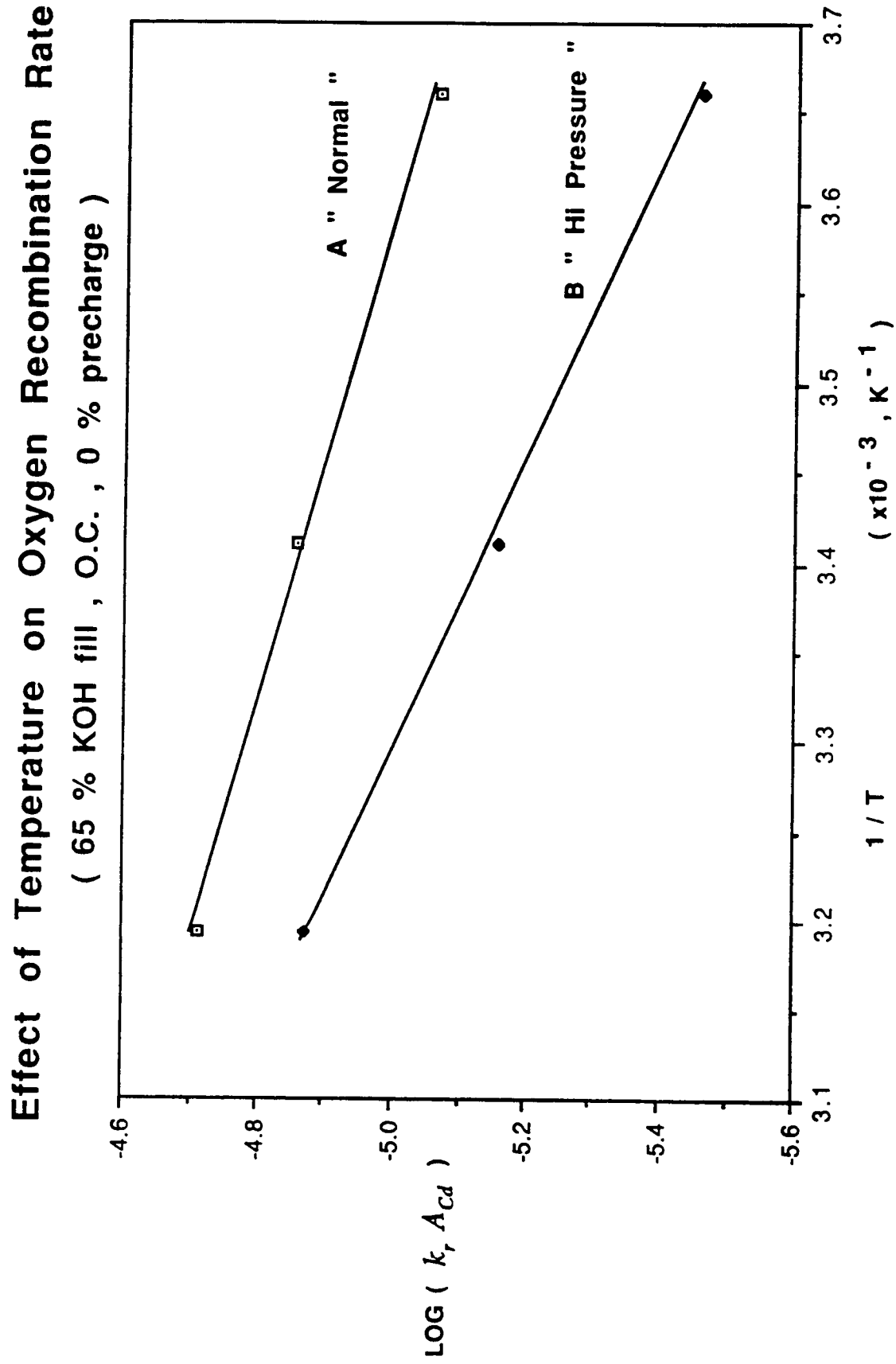
Effect of Temperature on Oxygen Recombination Rate
(65 % KOH fill , O.C. , 0 % precharge)
A " Normal "
B " HI Pressure "
LOG ($k_r A_{Cd}$)
-4.6
-4.8
-5.0
-5.2
-5.4
-5.6
3.1
3.2
3.3
3.4
3.5
3.6
3.7
1 / T
(x10 $^{-3}$, K $^{-1}$)

Effect of Temperature on Oxygen Recombination Rate

(65 % KOH fill , C/10 charge rate , 0 % precharge)

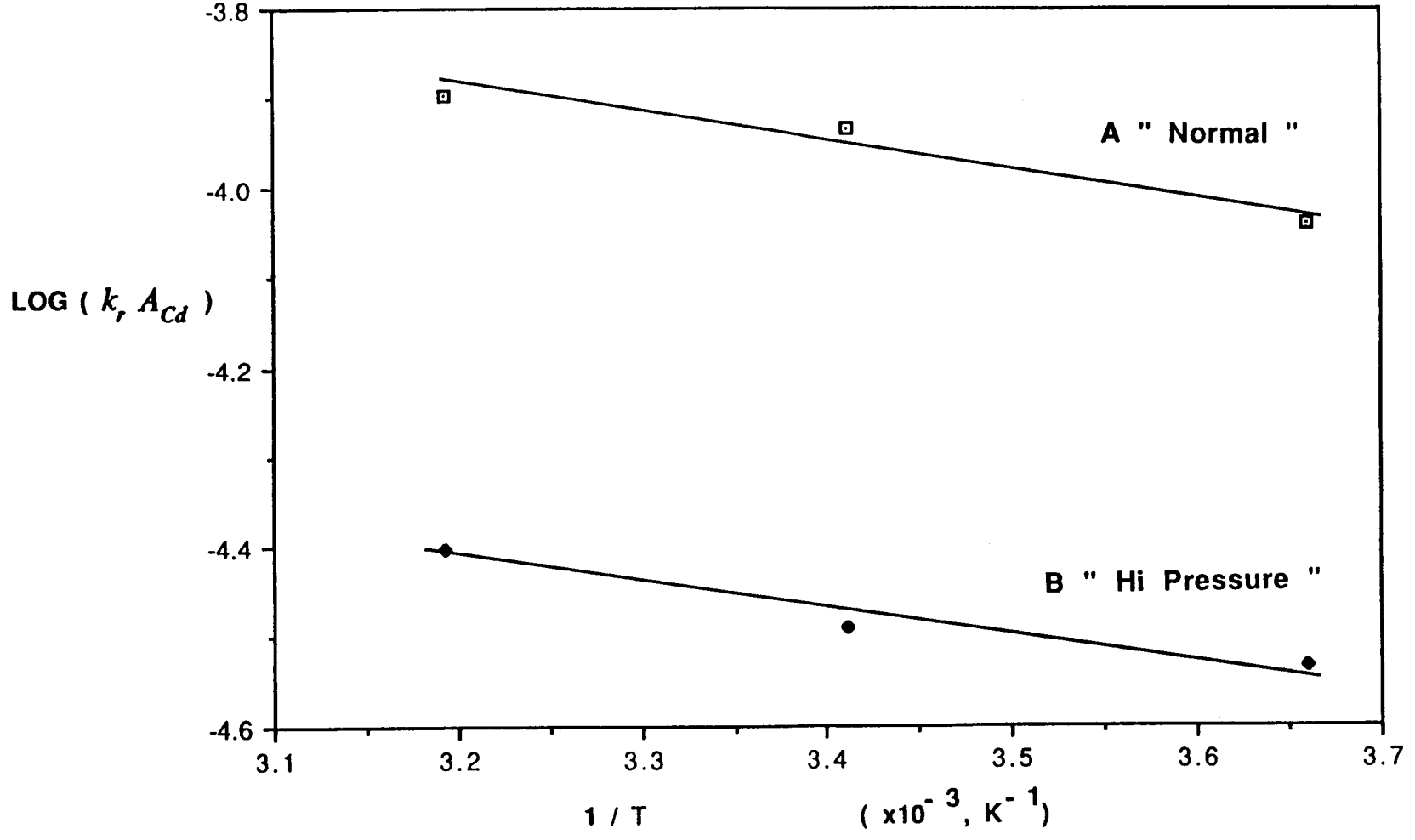

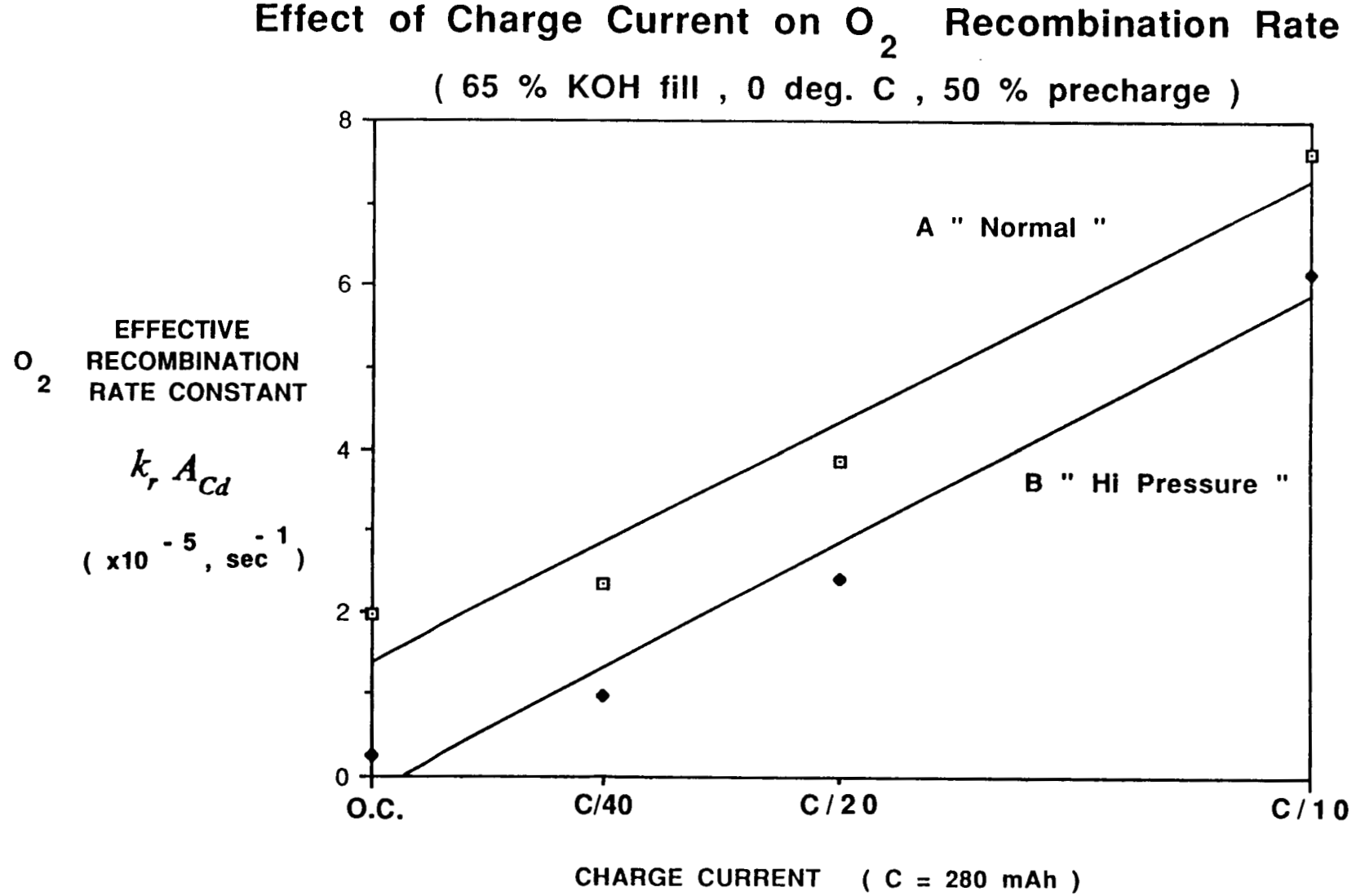
Effect of Charge Current on O_2 Recombination Rate
(65 % KOH fill , 0 deg. C , 50 % precharge)
O_2 EFFECTIVE RECOMBINATION RATE CONSTANT
$k_r A_{Cd}$
(x10 $^{-5}$, sec $^{-1}$)
8
6
4
2
0
A " Normal "
B " Hi Pressure "
O.C.
C/40
C/20
C/10
CHARGE CURRENT (C = 280 mAh)

CONCLUSIONS

- Principal Parameter For Controlling Pressure In A NiCd Cell Is The Area Of Cd Metal Exposed To Oxygen Gas Channels
- The Effective Recombination Rate Constant:
  - Increases linearly with increasing precharge
  - Decreases as Cadmium electrode pores become flooded
  - Decreases at lower electrolyte fill factors if Cadmium electrode has a large number of small pores
  - Increases sharply with increasing overcharge current
- Data Being Correlated Into Model for O_2 Recombination
- To Reproducibly Control Overcharge Pressures, For A Desired KOH Fill Factor A NiCd Cell Design Should Have:
  - Consistent precharge setting
  - Consistent pore size distribution in negatives
    - P vs. fill factor gives signature for anomalous pore size distributions in Cd plates

A CONSTANT CURRENT CHARGE TECHNIQUE FOR LOW EARTH ORBIT LIFE TESTING

BY PETER GLÜCK

JET PROPULSION LABORATORY,
CALIFORNIA INSTITUTE OF TECHNOLOGY
PASADENA, CALIFORNIA

NASA BATTERY WORKSHOP
MARSHALL SPACE FLIGHT CENTER

4-6 DECEMBER 1990, HUNTSVILLE, ALABAMA

A CONSTANT CURRENT CHARGE TECHNIQUE FOR LOW-EARTH ORBIT LIFE TESTING

Peter Glück

Jet Propulsion Laboratory
California Institute Of Technology
Pasadena, California

ABSTRACT

A constant current charge technique for low-earth orbit testing of nickel-cadmium cells is presented. The method mimics the familiar taper-charge of the constant potential technique while maintaining cell independence for statistical analysis. A detailed example application is provided and the advantages and disadvantages of this technique are discussed.

INTRODUCTION

Most charge techniques for nickel-cadmium (NiCd) batteries have two common elements: a high-rate initial charge, typically C/2 to C/5, followed by a low-rate (C/10 to C/100) trickle charge to "top off" the battery. High rates are desired initially because they are more efficient, and, especially for low-earth orbits (LEO), require less time for recharge. As the battery nears full state-of-charge (SOC), however, high rates can cause excessive oxygen generation. Therefore, a lower rate is as the battery approaches full state-of-charge. The two most common methods of recharging nickel-cadmium batteries follow these guidelines. They are the constant potential (V/T) and the constant current (R/F) methods.

The constant potential (V/T) method uses all the available current for charging until a preset voltage limit is reached. At that point the current is tapered (typically following an exponential profile) such that the battery voltage is maintained at the voltage limit. This results in end-of-charge currents around C/20 to C/40 in low-earth orbit cycles, although rates as low as C/1000 have been observed in longer cycles in ground testing [1]. The constant potential limit is generally compensated for temperature, since battery voltage characteristics are dependent on operating temperature. This technique is very common on modern, low-earth orbit spacecraft.

The other common technique is the constant current method. This method recharges at a constant rate until some recharge fraction*, usually around 1.05, is reached. It then switches to a constant rate trickle charge, typically C/50. Since current is essentially independent of temperature, the R/F method does not

---

* Recharge Fraction = Capacity Removed / Capacity Returned

need to be temperature compensated. (There are generally two or three ground-selectable charge rates available to provide operational flexibility.) This method is frequently used on geosynchronous spacecraft, but is rare in low-earth orbit applications. Thus, most life testing for low-earth orbit applications utilizes the V/T method since that is the most common technique used on LEO spacecraft.

Figure 1 demonstrates the differences between the V/T and R/F methods by showing charge rate as a function of time for a typical 90-minute LEO orbit with a 60-minute charge duration. The rates were chosen such that the area under both curves is identical. Thus, both methods provide the same charge return with the same recharge fraction (R/F = 1.052). Note that, while a typical geosynchronous charge rate is C/5 to C/10, rates approaching C/2 must be used in low-earth orbit to sufficiently recharge the battery. This necessity for much higher rates explains why the V/T method is preferred in LEO regimes.

PROBLEM

Over the years, it has become evident that there are difficulties with using both the V/T and the R/F methods for ground life testing. Clearly, it is desirable to simulate the actual flight environment as closely as possible. Hence, the V/T method is most frequently used in ground tests.

But the V/T method controls on total pack voltage. This means that each cell contributes to determining where and how the current taper occurs. Cell voltage characteristics change as they begin to fail. Thus, the failing cell or cells alter the recharge of the entire pack. Cells usually fail "gracefully" rather than "catastrophically." The failing cell may continue to operate in a degraded manner for thousands of cycles before finally dying, providing ample opportunity to influence the overall performance of the remaining cells. This places in jeopardy the assumption of independent events that is so vital to meaningful statistical analysis. In fact, it has been necessary in the past to declare a pack failed when the first cell failed because the cells are not independent [2]. Even though the other cells continued for many more cycles, their lives could not enter into reliability calculations of mean-time-to-failure.

Also, since aerospace NiCd cells are costly, test packs frequently contain only a few cells, compared to the sixteen to twenty-two (or more) cells typical of a spacecraft battery. When the voltage of one cell diverges from the rest in a full spacecraft battery, it accounts for perhaps five percent of the total battery voltage. However, if that same cell is running in a five-cell pack, it contributes twenty percent of the controlling voltage. This is clearly an exaggeration of what would happen in an actual flight application. One suggestion has been to run full-size batteries in ground tests to eliminate this effect. This solution requires enormous additional expense (at least thirty-five thousand dollars per test).

Using the R/F method resolves the concerns about statistical independence and pack size, but also removes the cells from their expected operational profile. Furthermore, R/F techniques can lead to problems like abnormally high charge voltages due to the excessive high-rate charge.

Therefore, the goal of a charge technique for low-earth orbit life testing should be to simulate spacecraft V/T control without allowing individual cells to determine overall pack behavior. The cells should be operated in their expected profile in a way that maintains their statistical independence for later reliability analysis. Note, however, that this goal applies primarily to tests aimed at determining cell quality and reliability. Mission simulations should continue to be run in a manner consistent with expected operation conditions.

SOLUTION

An obvious solution to this dilemma is to simulate the V/T current profile without actually triggering on voltage. Since the taper is very nearly exponential, it is easily modelled mathematically. The entire V/T profile can then be simply modelled by a constant current high-rate charge followed by an exponentially decaying taper. It can be readily implemented on modern, analog or digitally programmable power supplies controlled by inexpensive personal computers. The taper shape and location are primarily a function of depth-of-discharge, temperature, V/T level, and initial charge rate.

Figure 2 shows a general charging profile derived from this technique. The equation for the exponential decay is given as:

$$I = (I_m - I_t)\, e^{B(t - t_o)} + I_t \qquad (1)$$

All that is needed to model this profile are the four parameters: maximum charge rate (I_m), trickle-charge rate (I_t), time-to-taper (t_o), and the exponential time constant (B). The first three are easily obtained from a graph of the V/T profile being modelled. The maximum charge rate, I_m, and the time-to-taper, t_o, can be read directly off of the graph. The trickle-charge rate at end-of-charge, I_t, can be taken off the graph or assumed to be some desired rate. The only real effort is involved in determining the exponential time constant, B.

B is determined by averaging estimates of B for each available point on the taper profile. That is, for every (t_i, I_i) data point, a corresponding time constant, B_i, is generated using the following formula:

$$B_i = \frac{\ln(I_i - I_t) - \ln(I_m - I_t)}{(t_i - t_o)} \qquad (2)$$

B is obtained by averaging the B_i obtained from Equation (2). The more individual B_i that are obtained, the better the final estimate of B will be. The result is substituted into Equation (1) above to complete the profile.

EXAMPLE

An example is provided to demonstrate the use of this technique. The regime chosen is the NASA Standard Stress Life Cycle Test. This is a 90-minute LEO regime cycling to a 40% depth-of-discharge at 20°C and NASA V/T Level 6**. The charge rate is C/1.25.

The data from which this example is derived was obtained from testing at the Naval Weapons Support Center, Crane (NWSCC), Indiana. Four packs representing two manufacturers, three cell designs, and cycle lives of 300 to 6100 cycles were used.

Table 1 lists the three parameters that are obtained graphically. I_m is given as 0.8C (C/1.25). I_t was chosen to be C/20, but other reasonable values (perhaps an average) could also have been used. t_o is an average of the t_o from each of the four tests considered.

Table 2 shows how the B_i are calculated from the (t_i, I_i) pairs, which were read off of the current-versus-time plots provided by NWSCC. Averaging all of the B_i yields a value of -0.09077. Thus, the final equation is

$$I = 0.750e^{-0.09077(t - 17.55)} + 0.050 \qquad (3)$$

Here t is given in minutes and I is normalized charge rate, but any appropriate units will do as long as they are used consistently.

Figure 3 plots the fitted charging profile against the actual data points used to generate the fitted curves. The fit is excellent, especially considering the diversity of the packs used as input. A fit to a single pack would likely be even closer. Table 3 shows the actual recharge ratios of the packs used and the fitted recharge ratio. Note that the fitted recharge ratio is the median of the five values.

SUMMARY AND CONCLUSIONS

There are disadvantages to both charging techniques currently used for low-earth orbit testing of nickel-cadmium cells. The V/T system follows the method most frequently used in actual applications, but does not preserve cell statistical independence for reliability calculations. Conversely, the R/F method does maintain cell independence, but is a poor representation of actual flight conditions.

A technique that satisfies both the requirement for statistical independence and the need to simulate actual flight conditions was presented. It consisted of modelling the V/T charging profile with a constant rate charge

---

** NASA V/T Level 6 at 20°C is 1.434 volts per cell.

to a predetermined time followed by a computer-controlled exponential current taper. The parameters required to model the exponential taper current are easily obtained from analysis of actual V/T charging profiles, and the hardware necessary to implement the technique is readily available and relatively inexpensive.

The proposed method eliminates the difficulties associated with present charging techniques. Because recharge is independent of actual cell voltages, statistical independence of the cells tested is preserved. Hence, each cell is truly a single test article and may be treated as a separate observation in statistical analyses. The data yield is therefore improved by a factor of at least five, improving reliability and quality calculations. Costs are minimized by maximizing output from the current sample size, and the charging profile is highly similar to that used in operational spacecraft.

The main disadvantage of the technique presented is that every regime (and quite likely every cell design) requires a different profile. This can be handled in one of two ways. First, "generic" profiles can be developed as a function of depth-of-discharge, temperature, charge rate, and V/T level. These can then be adapted to the specific cell design being tested. Possibly a better way, however, is to simply characterize each pack tested prior to cycling with a few (say, fifty) V/T cycles. This should be adequate to allow pack behavior to stabilize and provide the desired V/T profile. If aging affects are a concern, the pack could be recharacterized every few thousand cycles and the cycling regime adjusted accordingly. The remaining difficulty may be that some existing test systems may not be capable of implementing this technique with their current equipment. In fact, the government test facility at the Naval Weapons Support Center Crane, Indiana, does have the hardware required to implement this type of testing. Even if more test stations were required, though, the equipment is relatively inexpensive and easy to procure.

ACKNOWLEDGEMENTS

This effort was inspired by the investigations and conclusions of the NASA Battery Task Force Six, "Evaluation of NWSC Data," led by Mr. W. J. Billerbeck of MRJ, Inc. The work described in this paper was carried out at the Jet Propulsion Laboratory, California Institute of Technology, under a contract with the National Aeronautics and Space Administration.

REFERENCES

1. Timmerman, P. J. and Glück, P. R., "Magellan Battery Operation: An Overview," NASA Battery Workshop, U.S. Space and Rocket Center, Huntsville, Alabama, December 1990.

2. Glück, P. R., "NASA Aerospace NiCd Cell Test Database Trend Analysis," Jet Propulsion Laboratory, Pasadena, California, 22 May 1989.

TABLE 1: BASIC PARAMETERS FOR TAPER ESTIMATION

I_m	I_t	t_o
0.800	0.050	17.55

TABLE 2: CURRENT TAPER PROFILE DATA

t_i	PACK A		PACK B		PACK C		PACK D	
	I_i	B_i	I_i	B_i	I_i	B_i	I_i	B_i
19.2	0.640	-0.145	0.640	-0.145	0.750	-0.042	0.686	-0.100
25.2	0.440	-0.085	0.420	-0.092	0.438	-0.086	0.429	-0.089
31.2	0.300	-0.080	0.280	-0.087	0.250	-0.097	0.262	-0.093
37.2	0.210	-0.079	0.170	-0.093	0.175	-0.091	0.152	-0.101
43.2	0.160	-0.075	0.120	-0.092	0.125	-0.090	0.095	-0.109
60.0	0.123	-0.055	0.058	-0.107	0.086	-0.071	0.086	-0.072

TABLE 3: ACTUAL AND FITTED RECHARGE RATIOS

PACK A	PACK B	PACK C	PACK D	FITTED
1.100	1.103	1.051	1.033	1.054

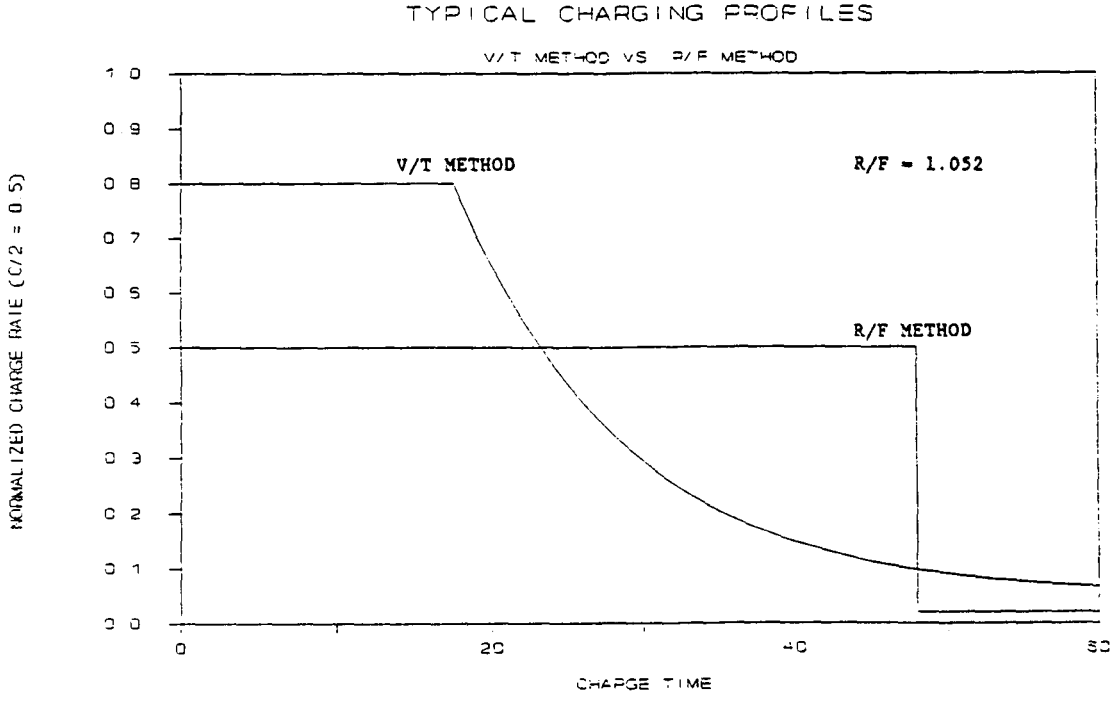

FIGURE 1

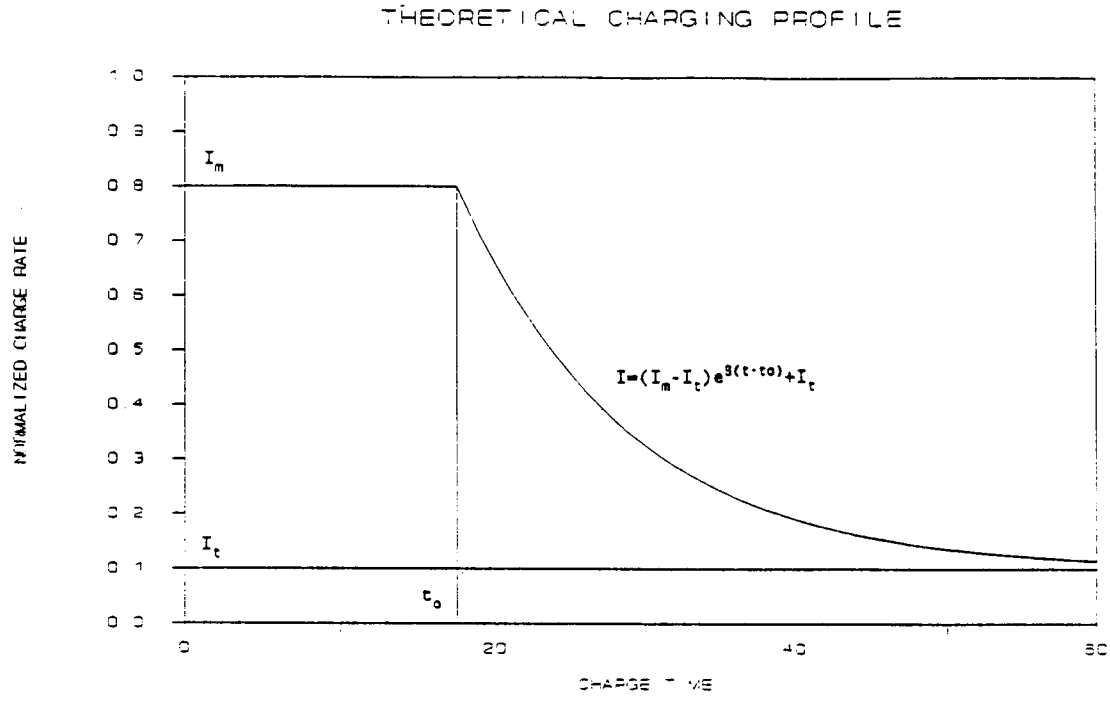

FIGURE 2

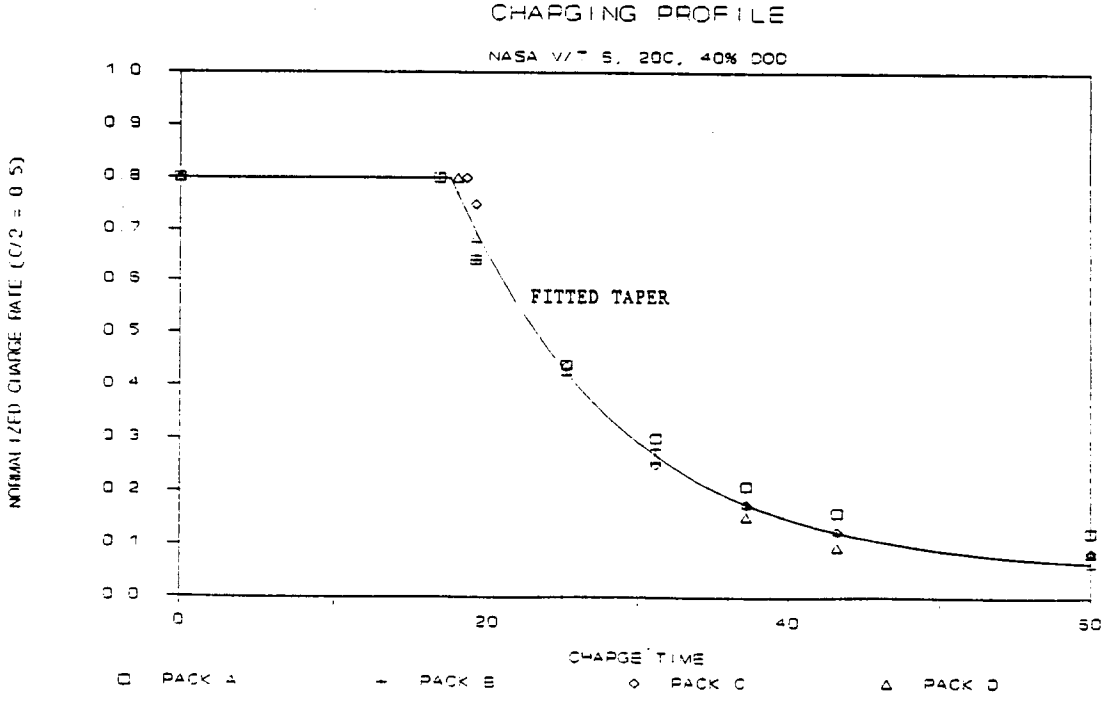

FIGURE 3

JPL

JET PROPULSION LABORATORY

CHEMICAL EVALUATION OF NON-WOVEN NYLON SEPARATORS USED IN Ni/Cd CELLS

PRESENTED AT NASA AEROSPACE BATTERY WORKSHOP

MARSHALL SPACEFLIGHT CENTER

EDWARD F. CUDDIHY

12/04/90

JPL

SEPARATOR HISTORY

- MASTER BATCH OF 2505 PRODUCED BY PELLON IN 1976, USING $ZnCl_2$
- BATCH DISTRIBUTED BETWEEN GATES AND EAGLE-PICHER (EP)
- GATES REQUIRED THAT THEIR SEPARATOR SUPPLY BE TRIPLE WASHED IN WATER TO REDUCE $ZnCl_2$ CONTENT (ACTUAL CONTROL WAS <1% WATER LEACHABLE MATERIALS). EP REQUIREMENTS NOT CLEARLY KNOWN.
- GATES SUPPLY STORED IN GAINESVILLE, FL
- EP SUPPLY STORED IN JOPLIN, MO
- GATES SUPPLY GAVE PROBLEMS STARTING IN CIRCA 1985
- EP SUPPLY HAS NO REPORTED USE OR PROBLEMS

JPL

GOALS OF JPL CHEMICAL STUDIES

- IDENTIFY GATES 2505 DEGRADATION MECHANISM
- DETERMINE IF EP 2505 SUPPLY SUITABLE FOR FLIGHT
- ASSESS THE 2538 AS A CANDIDATE REPLACEMENT, BASED ON CHEMICAL FINDINGS

JPL

NYLON 6 - SELF REACTION OF ϵ- CAPROLACTUM

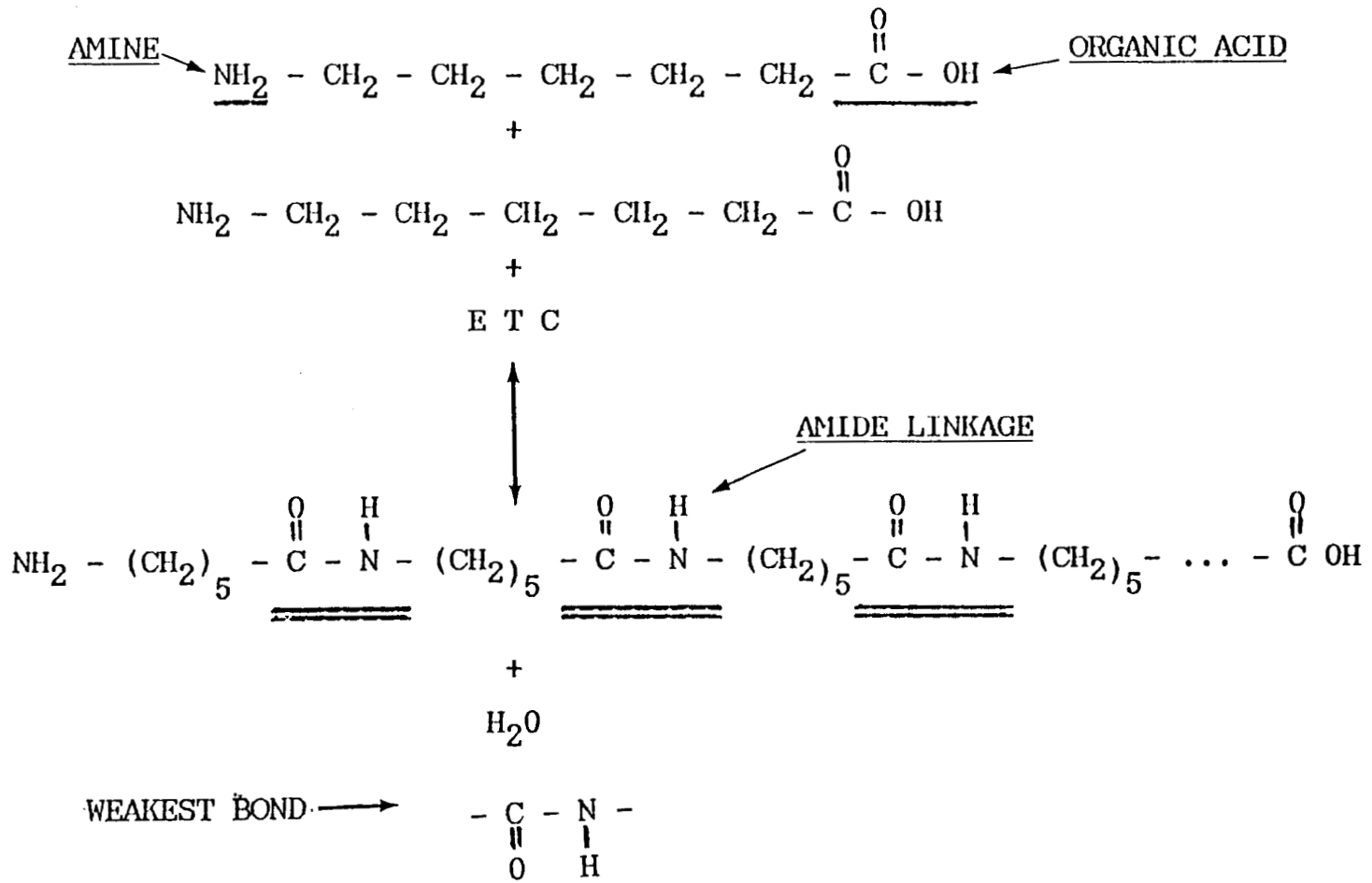

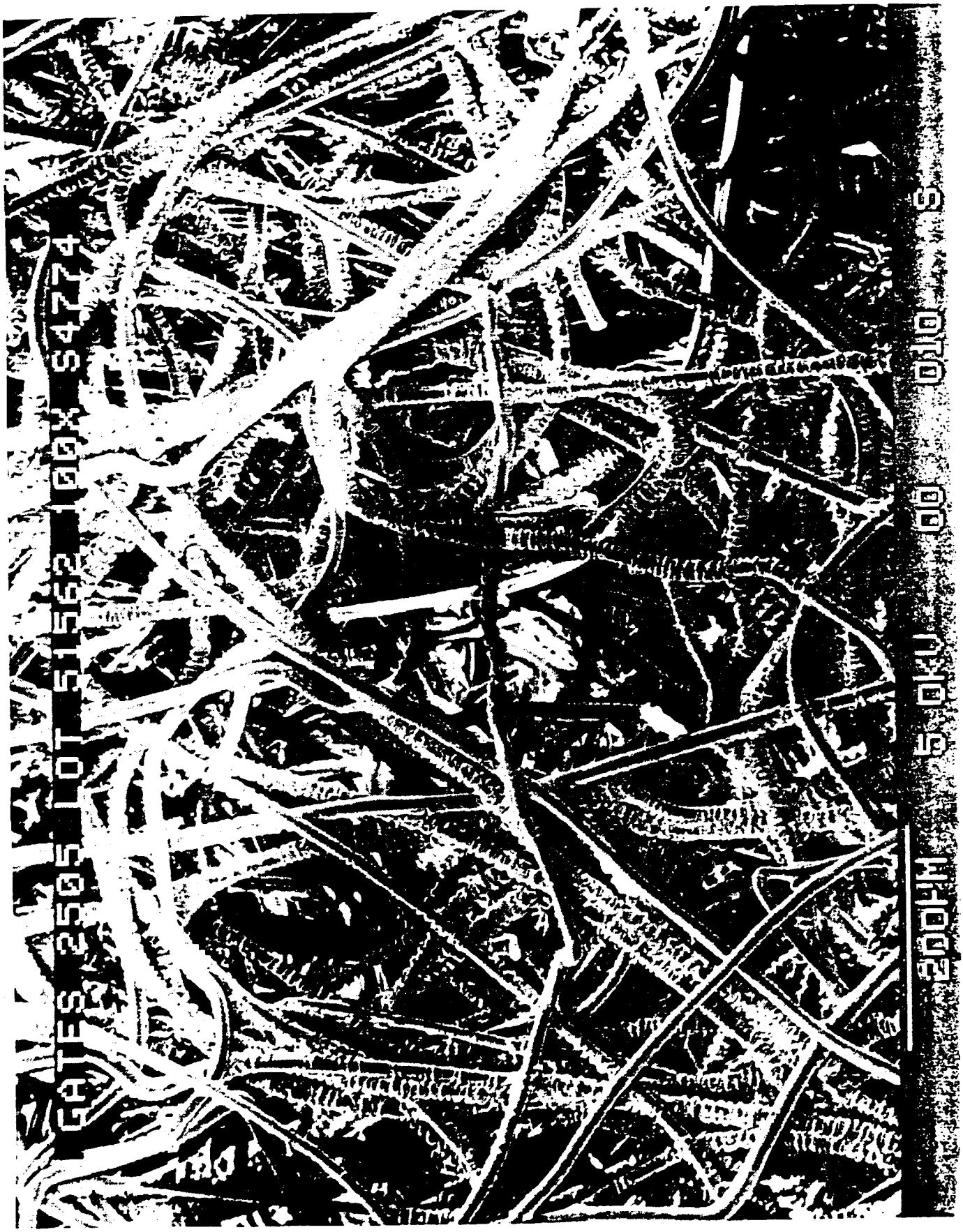
GATES 250 LOT 5162 10X S474
HIGH SPEED 5 DIGIT

GATES 2505 LOT 51562 500X S#74
40µM 5.1KV 00.011 S

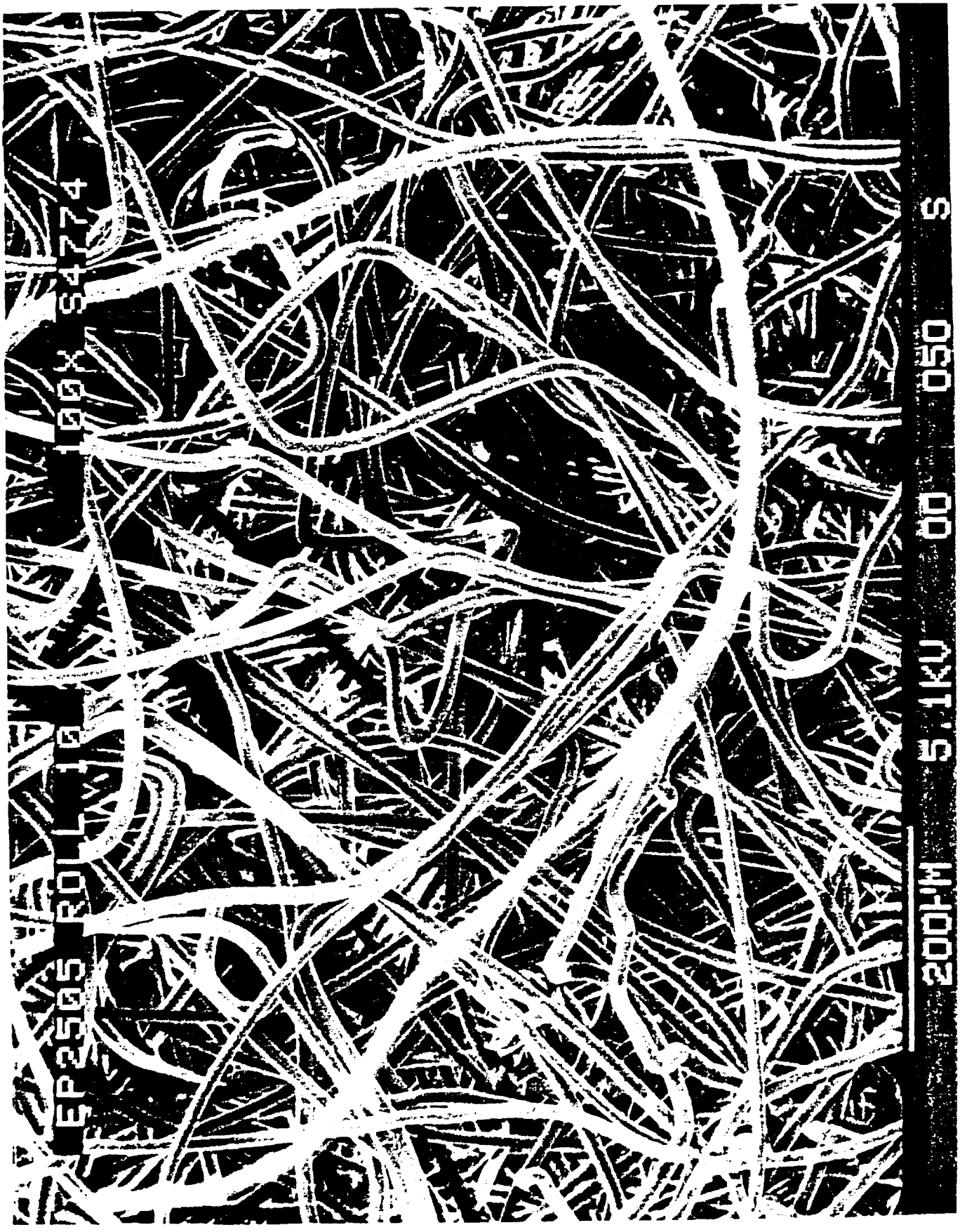
EP2565 ROLL 19
100X S4774
S 050 00 W1.5 200FM


EP2505 ROLL 10
500X S4724
S 040
00
5.0KV
WD04


#2538 ROLL 001
100X S4724
200'M 5.0KV 00 056 S


GATES 2505C
100X S4774
200'M S.OKV 00 070 S

JPL

REPRESENTATIVE INFRA-RED SPECTRA OF A 2505 NYLON 6 SEPARATOR (EP 2505, ROLL 10 OUTSIDE)

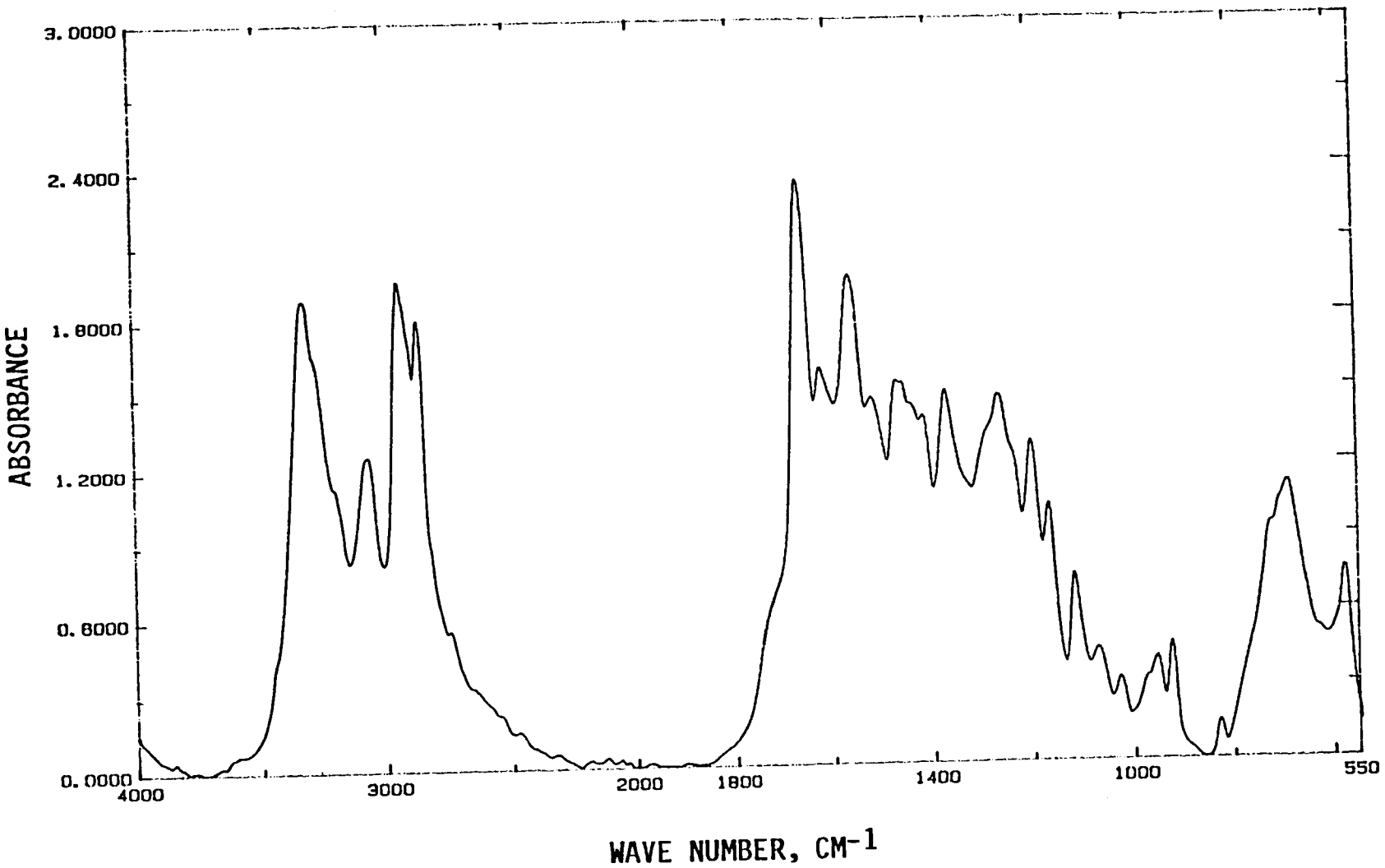

JPL

COMPARATIVE INFRA-RED SPECTRA OF METHYLENE CHLORIDE EXTRACTS FROM GATES 2505 (FLORIDA) AND GATES 2505G (JPL)

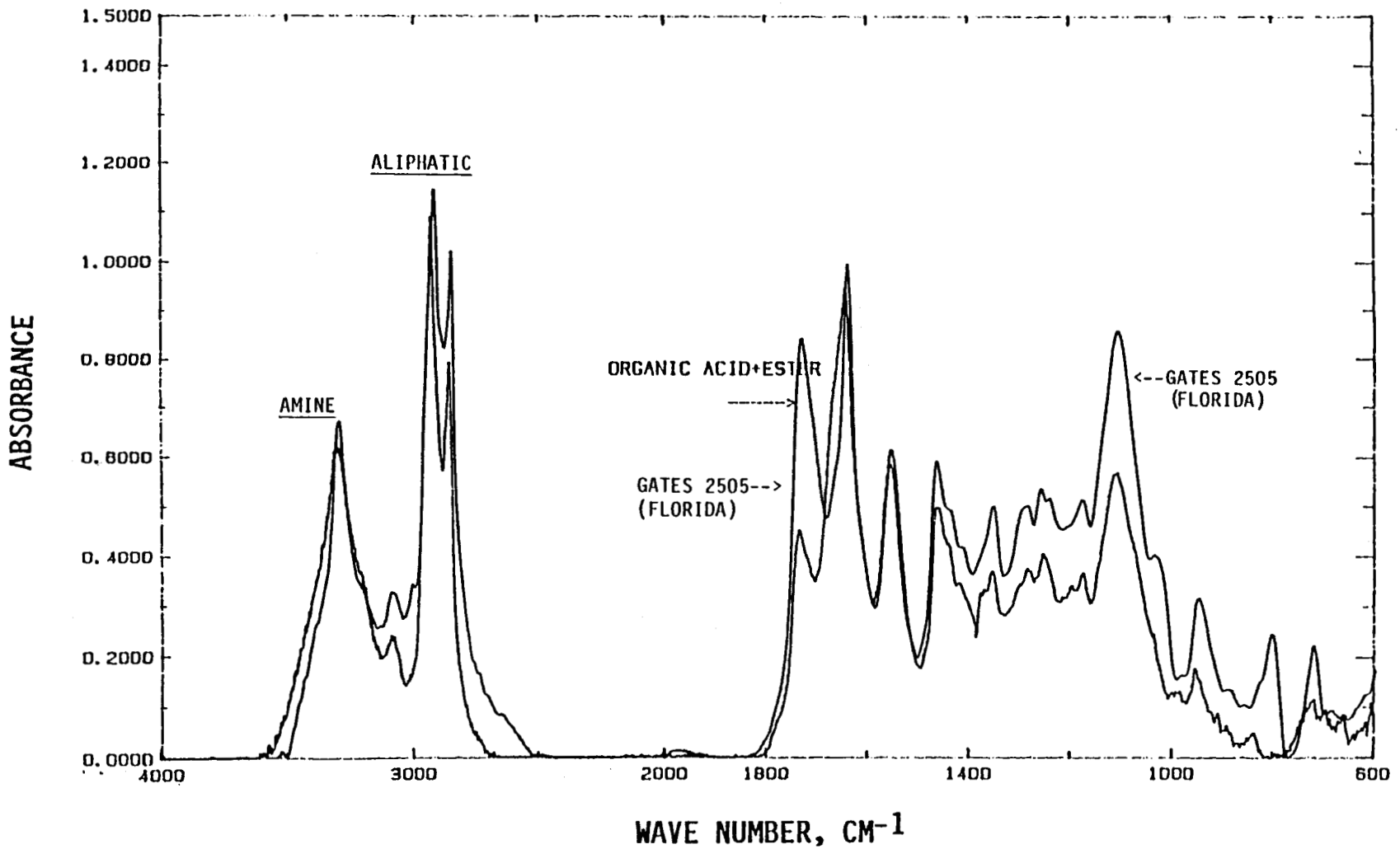

JPL

COMPARATIVE INFRA-RED SPECTRA OF METHYLENE CHLORIDE EXTRACTS

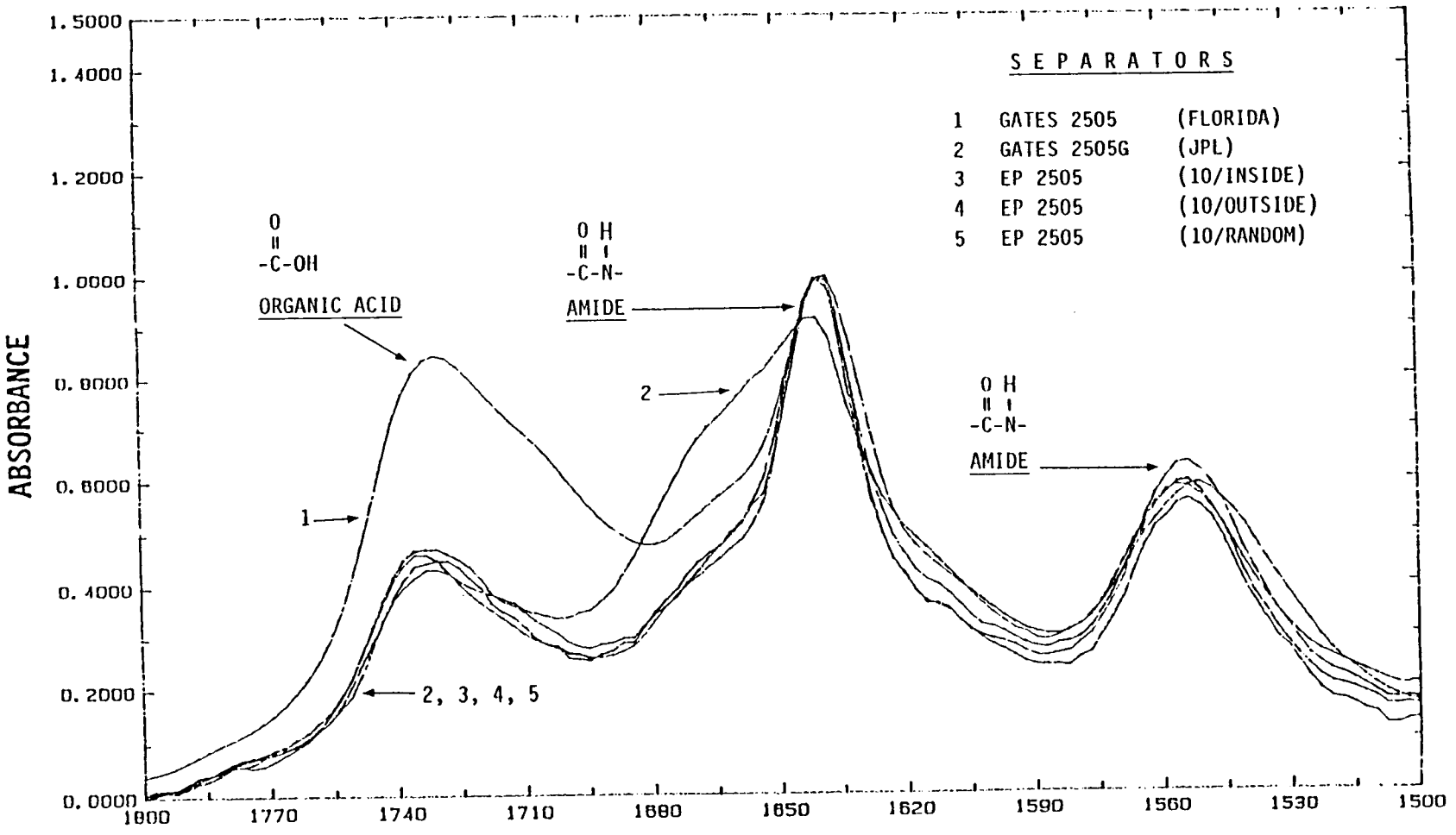

JPL

NUMBER AVERAGE MOLECULAR WEIGHTS (M_N) AND RELATIVE AMOUNTS OF MATERIAL EXTRACTED INTO METHYLENE CHLORIDE

	SAMPLE		QUANTITY*	Mn**
1.	GATES 2505	(FLORIDA)	920 PPM	14,500
2.	GATES 2505G	(JPL)	220 PPM	-
3.	MO EP 2505	(10/OUTSIDE)	121 PPM	-
	MO 2505	(10/RANDOM)	160 PPM	16,000
	MO EP 2505	(10/INSIDE)	336 PPM	-
4.	TOPEX EP 2505	(#6/OUTSIDE)	130 PPM	-
	TOPEX EP 2505	(#2/OUTSIDE)	164 PPM	
	TOPEX EP 2505	(#1/INSIDE)	183 PPM	-
5.	2538	(ROLL 1)	62 PPM	-
	2538	(ROLL 1)	72 PPM	-

*AMOUNT EXTRACTED CALCULATED AS HEXANOIC ACID, FROM FTIR SPECTRA
**COMMERCIAL NYLONS HAVE MOLECULAR WEIGHTS BETWEEN 15,000 AND 30,000

JPL

LITERATURE HYDROLYSIS STUDY (LIM, ET.AL)

INVESTIGATED PELLON 2505 (NYLON 6) IN KOH OVER CONCENTRATION RANGE FROM 4-34%, AND OVER TEMPERATURE RANGE FROM 35°C TO 110°C.

A) VERIFIED CHEMICAL DEGRADATION BY HYDROLYSIS; FOUND NO EVIDENCE FOR OXIDATIVE DEGRADATION.

B) HYDROLYSIS DEGRADATION PRODUCT, 6-AMINOCAPROATE CAN UNDERGO FURTHER ELECTROCHEMICAL OXIDATION TO HARMFUL CARBONATES, AND GENERATION OF AMMONIA AND/OR NITROGEN GAS. THIS REACTION EVENT APPARENTLY CAUSES LOSS OF BATTERY DISCHARGE PROTECTION.

C) HYDROLYSIS REACTION IS THE RATE-DETERMINING STEP, AND IS SLOW.

- THE WEIGHT LOSS OF TWO PELLON 2505 SEPARATORS REMOVED FROM A FAILED AND NEAR-FAILED Ni/Cd CELLS WERE IN THE ORDER OF 6 TO 7 WT.%, CALCULATED FROM MOLECULAR WEIGHT ANALYSIS.

A) THE NUMBER AVERAGE MOLECULAR WEIGHT OF GATES 2505 (FLORIDA) WAS 14,500, COMPARED TO 16,000 FOR EP 2505 ROLL 10. FOR THE GATES 2505, THIS REPRESENTS A WEIGHT LOSS OF NEARLY 9%.

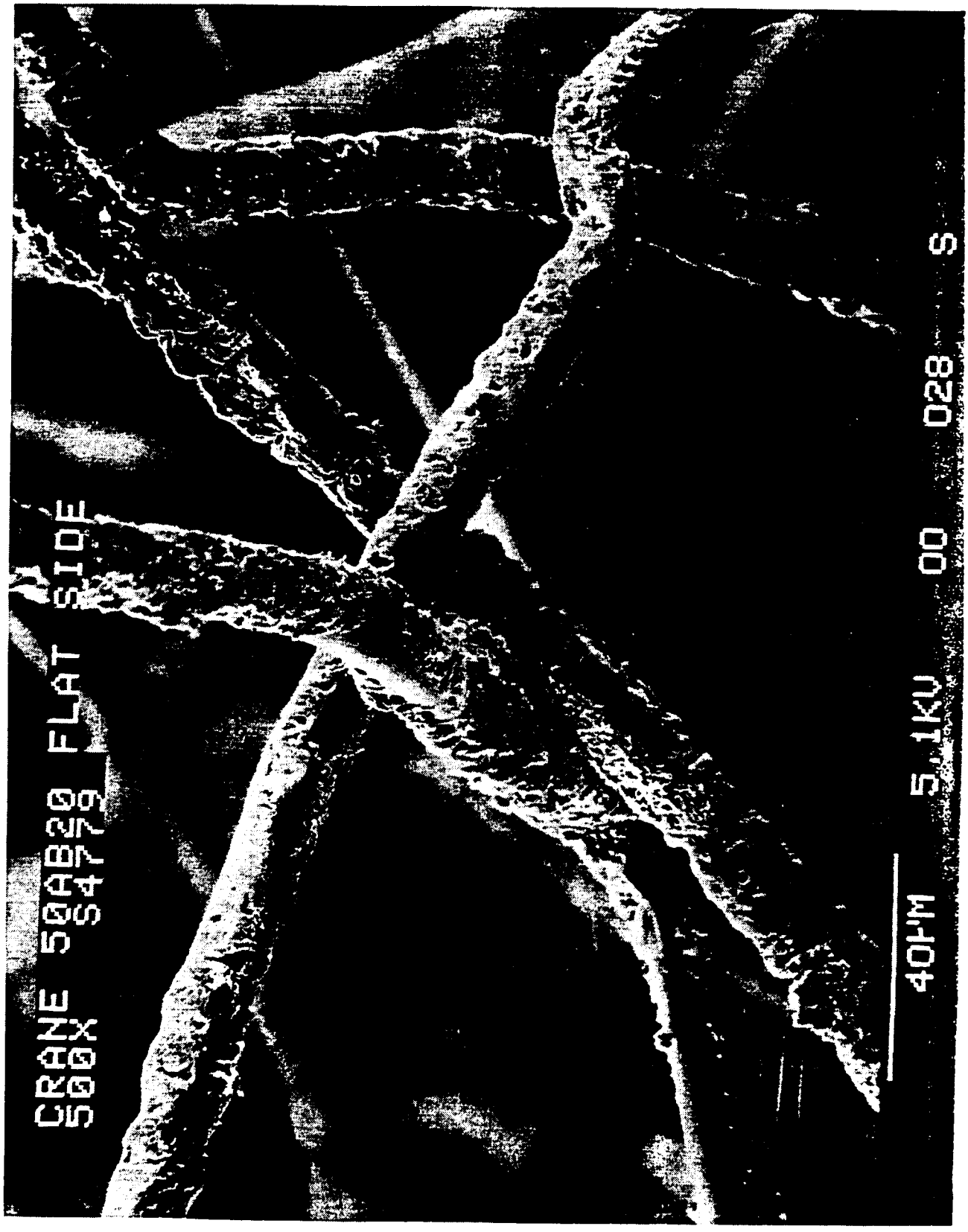
CRANE 50AB20 FLAT SIDE
500X S47Z9
40UM 5.1KU 00 028 S

CRANE 50AB26
500X S4798
5.0KV 00 019 S
40FM

JPL

COMPARISON OF RATES OF HYDROLYSIS OF NYLON 66 AND NYLON 6 IN A 34% KOH SOLUTION AT 100°C

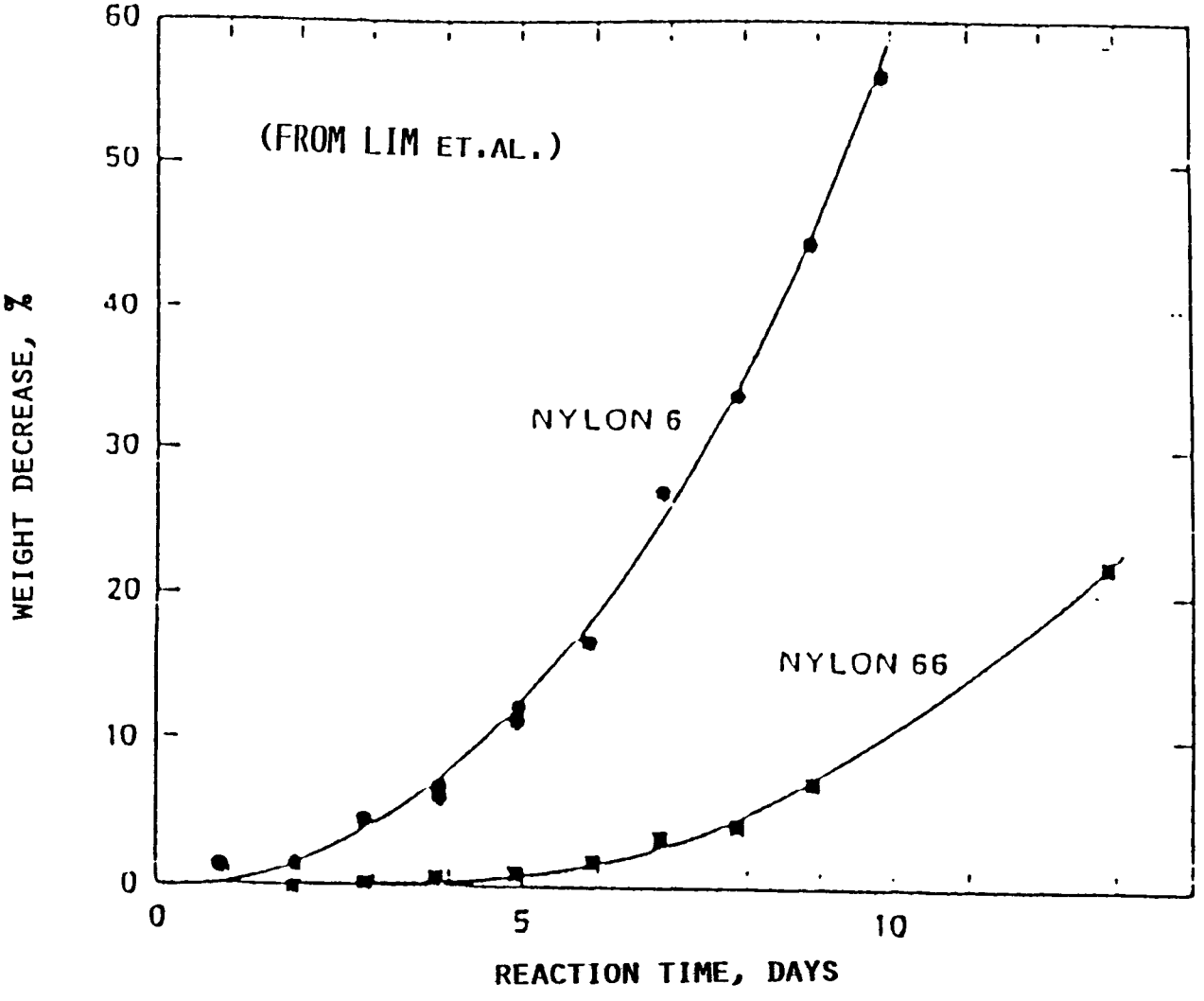

JPL

ELECTRON SPECTROSCOPY FOR CHEMICAL ANALYSIS (ESCA)

AVERAGED DATA

Material	ATOMIC %		
	Carbon	Nitrogen	Oxygen
IDEAL	75.0	12.5	12.5
2536/2538	76.0	5.4	18.6
2505	75.4	9.6	15.0

2536/2538: 67% Nylon 66, 33% Nylon 6

2505: 100% Nylon 6

JPL

ZINC AND CHLORINE CONTENTS BY QUANTITATIVE ANALYSIS[1)]

SEPARATOR	TOTAL ZINC	TOTAL CHLORINE
1) GATES 2505 (FLORIDA)	0.11 WT.% 0.11 WT.%	0.28 WT% 0.30 WT.%
2) EP 2505 (10/INSIDE)	0.42 WT.% 0.44 WT.%	0.61 WT.% 0.67 WT.%
3) EP 2505 (10/OUTSIDE)	0.39 WT.% 0.41 WT.%	0.66 WT.% 0.67 WT.%
4) GATES 2538 (PROTOTYPE)	<15 PPM <15 PPM	388 PPM 397 PPM
5) GATES 2536	<15 PPM <15 PPM	514 PPM 466 PPM

NOTE: 1) TWO TESTS PER SAMPLE
ATOMIC WEIGHT OF ZINC = 63.38
DIATOMIC WEIGHT OF CHLORINE (Cl_2) = 70.91

JPL

QUANTITIES OF ZINC AND CHLORINE EXTRACTED FROM SEPARATORS AFTER TWO HOURS OF WATER IMMERSION AT 25°C

SEPARATOR	<-------WT. %-------> ZINC	CHLORINE
GATES 2505 (FLORIDA)	0.099	0.12
EP 2505 (10/INSIDE)	0.43	0.43
EP 2505 (10/OUTSIDE)	0.47	0.47
EP 2505 (10/RANDOM)	0.41	0.40
GATES 2538 (ROLL 1)	0.0065	<.003

JPL

GENERAL FINDINGS

- NYLON 6 IS THE ONLY POLYMERIC MATERIAL FOUND IN EP 2505 AND GATES 2505 SEPARATORS, CONCLUDING THAT:

  1) "ADHESIVE" SURFACE COATING OBSERVED IN UNUSED EP 2505 IS NYLON 6, OR DERIVED FROM NYLON 6.

  2) "ROUGH" SURFACE COATING OBSERVED IN GATES 2505 (FLORIDA) IS NYLON 6, OR DERIVED FROM NYLON 6.

- $ZnCl_2$ IN UNUSED EP 2505 SEPARATORS FOUND ONLY IN THE "ADHESIVE" SURFACE COATING, BY ELECTRON DISPERSIVE SPECTROSCOPY (EDS).

- CHLORINE FOUND ONLY ON CADMIUM SIDE OF A USED 2505 SEPARATOR AFTER REMOVAL FROM Ni/Cd CELLS; NO Zn DETECTED BY EDS.

- HYDROLYSIS OF USED NYLON SEPARATORS IN THE Ni/Cd CELL APPEARED TO OCCUR PREFERENTIALLY NEAR THE NICKEL ELECTRODE.

JPL

2538 ADVANTAGES

- SLOWER HYDROLYSIS RATE EXPECTED THROUGH USE OF NYLON 66
  - A) LOWER NITROGEN SURFACE CONTENT
- LOW SOLVENT EXTRACTABLES (UNAGED NEW MATERIAL)
- NO $ZnCl_2$

JPL

CONCLUSIONS

- CHEMICAL TESTING STRONGLY INDICATES THAT THE GATES 2505 STORED IN FLORIDA HAD UNDERGONE PARTIAL CHEMICAL DETERIORATION, BELIEVED CAUSED BY EXPOSURE TO HIGH HUMIDITIES AND TEMPERATURE

  → THIS PARTIAL DETERIORATION HAS GENERATED CHEMICAL PRODUCTS REPORTED TO POISON CELL PERFORMANCE - THUS UNCONTROLLED STORAGE AND AGING CAN PREDISPOSE A SEPARATOR TO CAUSE PREMATURE CELL FAILURE

- A SUSPECTED ROLE OF ZINC CHLORIDE ($ZnCl_2$) AS A SEPARATOR CONCERN DURING STORAGE WAS NOT VERIFIED IN THIS STUDY (THE EFFECT OF ZINC CHLORIDE ON CELL/ELECTRODE PERFOMANCE WAS NOT ADDRESSED IN THIS STUDY)

- NO SUBSTANTIVE CHEMICAL ISSUES OR CONCERNS WITH USING EP 2505 AS A Ni/Cd BATTERY SEPARATOR FOR MARS OBSERVER AND TOPEX COULD BE FOUND

  → THIS CONCLUSION IS BASED IN PART ON USING JPL'S SUPPLY OF GATES 2505 AS A DE FACTO CONTROL, AND ASSUMES THAT THIS MATERIAL IS REPRESENTATIVE OF VINTAGE GATES 2505 HAVING SUCCESSFUL FLIGHT HISTORIES

- NO CHEMICAL ISSUES OR CONCERNS WITH USING 2538 AS A Ni/Cd BATTERY SEPARATOR WERE FOUND

  → IN FACT, CHEMICAL EVIDENCE SUGGEST THAT 2538 MAY BE A BETTER MATERIAL, AS COMPARED TO 2505

JPL

RECOMMENDATIONS

- STORE SUPPLY ROLLS IN LOW HUMIDITY, LOW TEMPERATURE CONTROLLED ENVIRONMENTS
- ADOPT METHYLENE CHLORIDE SOLVENT EXTRACTION TECHNIQUE FOR AGING MONITOR TEST
- WASH EP-2505 UNWRAPPED SEPARATORS FOR MINUMUM TWO HOURS IN WATER AT ROOM TEMPERATURE TO REMOVE $ZnCl_2$
- SOLVENT EXTRACT (i.e. METHYLENE CHLORIDE) PRE-EXISTING ENVIRONMENTAL HYDROLYSIS PRODUCTS TO PRODUCE A CHEMICALLY CLEAN SEPARATOR

EXPLORING POSSIBLE RELATIONSHIPS BETWEEN PLATE PORE SIZE CHARACTER AND CELL PERFORMANCE

LAWRENCE H. THALLER AND MELVIN HILL
THE AEROSPACE CORPORATION

AND

LAWRENCE A. TINKER AND R. DAN DELL
GATES AEROSPACE BATTERIES

FOR PRESENTATION AT

THE NASA AEROSPACE BATTERY WORKSHOP

HUNTSVILLE, ALABAMA

DECEMBER 4-6, 1990

OUTLINE

- BACKGROUND IN PORE SIZE ENGINEERING
- DESCRIPTION OF COOPERATIVE EFFORT
- PORE SIZE CHARACTER OF PLATE MATERIAL
  - NEGATIVE PLATE
  - POSITIVE PLATE
- DISTINCTIVE PLATE SIGNATURES
- CELL PERFORMANCE
- SUMMARY STATEMENTS

BACKGROUND

- A 1982 PAPER ON PORE SIZE ENGINEERING CONSIDERED THE EFFECTS OF:
  - PORE SIZE
  - COMPONENT WETABILITY
  - DESIGN FEATURES OF STARVED CELLS
  - VARIABILITY OF COMPONENTS
- ONLY LIMITED DATA AVAILABLE FOR REVIEW

GATES-AEROSPACE COOPERATIVE EFFORT

- AS PART OF THIS EFFORT:
  - SAMPLES OF OLDER PLATE MADE AVAILABLE
  - SOME MANUFACTURING INFORMATION
  - ACCEPTANCE TEST RESULTS WERE REVIEWED
  - CORRELATIONS BETWEEN COMPONENT SIGNATURES AND PERFORMANCE WERE SOUGHT
  - ATTEMPTS WERE MADE TO QUANTIZE PROPERTIES

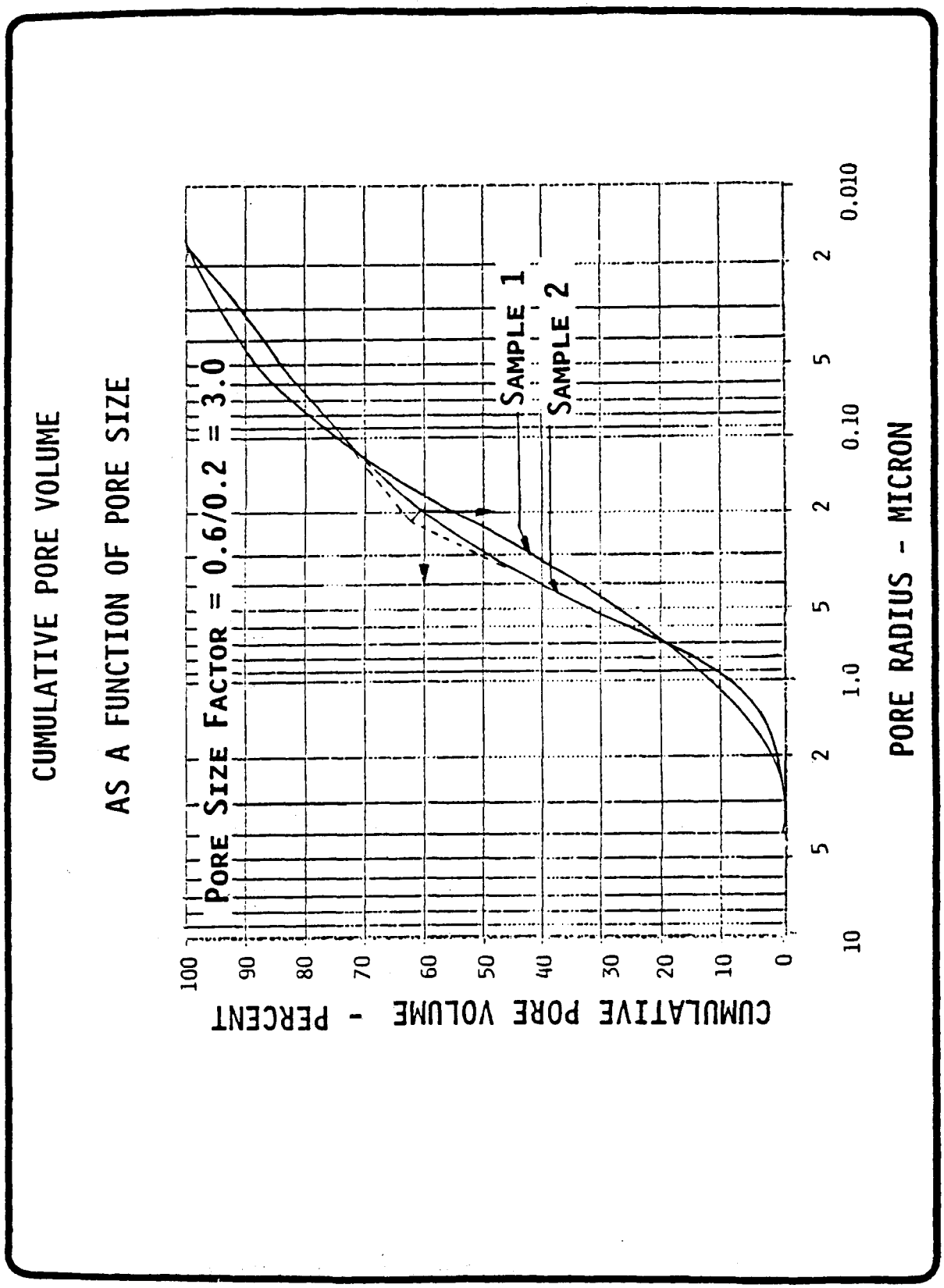
CUMULATIVE PORE VOLUME
AS A FUNCTION OF PORE SIZE
PORE SIZE FACTOR = 0.6/0.2 = 3.0
SAMPLE 1
SAMPLE 2
CUMULATIVE PORE VOLUME - PERCENT
100
90
80
70
60
50
40
30
20
10
0
10
5
2
1.0
5
2
0.10
5
2
0.010
PORE RADIUS - MICRON

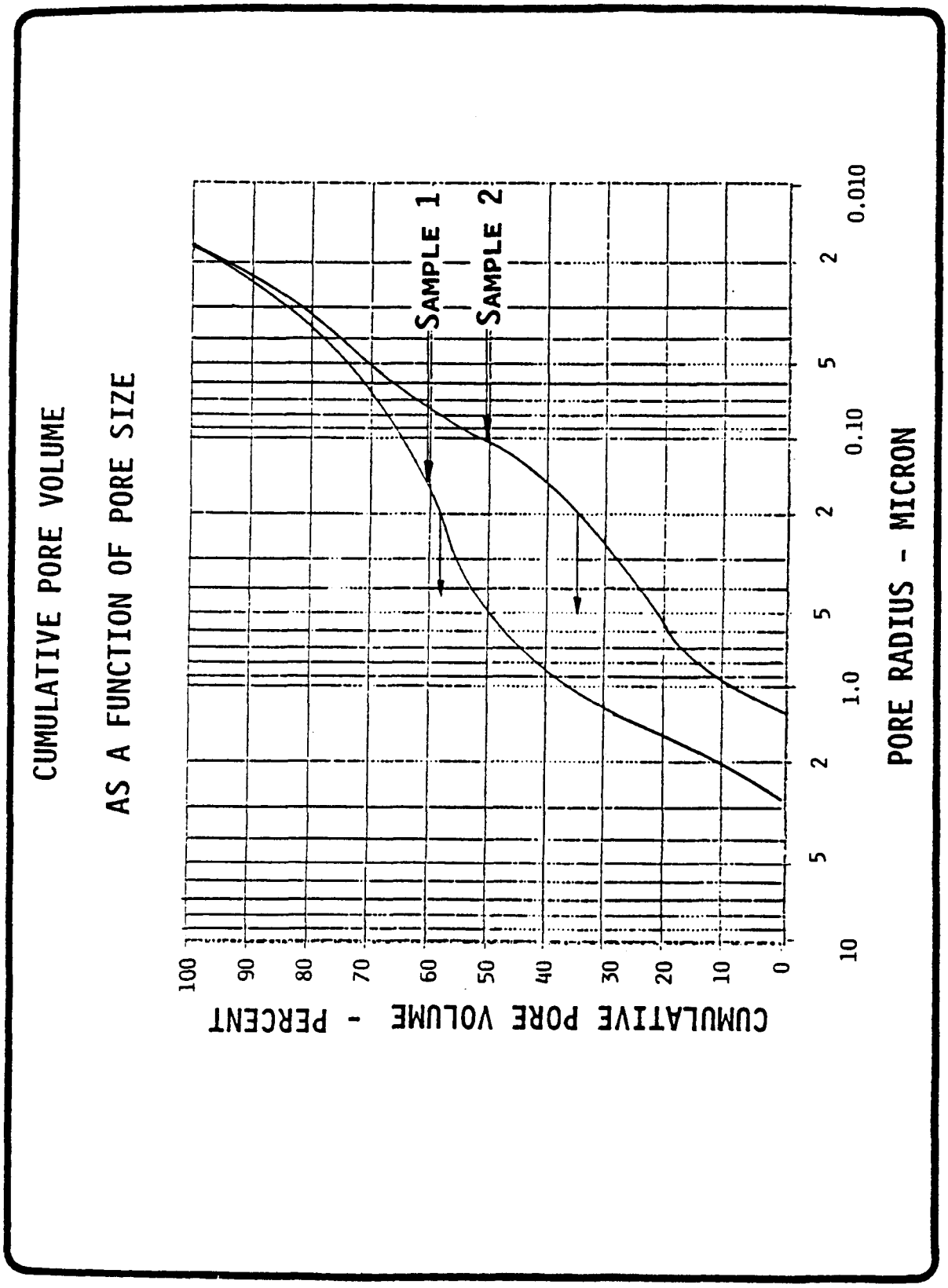
CUMULATIVE PORE VOLUME
AS A FUNCTION OF PORE SIZE
SAMPLE 1
SAMPLE 2
CUMULATIVE PORE VOLUME - PERCENT
100
90
80
70
60
50
40
30
20
10
0
10
5
2
1.0
5
2
0.10
5
2
0.010
PORE RADIUS - MICRON

PERFORMANCE CHARACTERISTICS

- 0 CADMIUM PLATE SAMPLE 1 CELLS
  - 0 HIGH PRESSURE ON OVERCHARGE
  - 0 LOW ELECTROLYTE LEVEL
  - 0 POOR RESPONSE TO ELECTROLYTE ADJUSTMENTS
  - 0 OXYGEN RECOMBINATION RETARDED

PERFORMANCE CHARACTERISTICS

- 0 NICKEL PLATE SAMPLE TWO CELLS
  - 0 LOW CELL CAPACITY
  - 0 LOW UTILIZATION OF ACTIVE MATERIAL
  - 0 NORMAL LOADING IN SMALL PORE SIZES
  - 0 PORE BLOCKING MAY LEAD TO POOR UTILIZATION

PARAMETERS FOUND TO BE USEFUL

- O CADMIUM PLATE MATERIAL
  - PORE SIZE FACTOR USING CUMULATIVE PORE VOLUME
  - LOCATION OF PEAK OF PORE SIZE DISTRIBUTION
- O NICKEL PLATE MATERIAL
  - PERCENT OF PORE VOLUME GREATER THAN 0.2 MICRON IN RADIUS
  - RATIO OF HEIGHT OF LARGE PORE PEAK TO SMALL PORE PEAK

SUMMARY STATEMENTS

- THE PORE SIZE CHARACTER AND PLATE MANUFACTURING INFORMATION FOR SELECTED SAMPLES OF OLDER PLATE MATERIAL WERE REVIEWED
- WHEN COMPARED TO CERTAIN CELL PERFORMANCE PARAMETERS, CERTAIN CORRELATIONS WERE FOUND BETWEEN PLATE PORE CHARACTER AND CELL PERFORMANCE
- THIS TECHNIQUE MAY BE USEFUL FOR SCREENING OUT CERTAIN TYPES OF PLATE MATERIAL PRIOR TO ASSEMBLY INTO CELLS

Memo for: M. Manzo/NASA/LeRC
Subject : Overview of the Primary Session
From : G.J. Methlie
Date : 12/15/90

1. A Wide Range of Primary Cells and Batteries are used in Aerospace Applications from "Button Cells" for Volatile Memory Preservation to Huge Batteries Providing Hundreds of Kilowatt-Hours of Propulsion Power for Systems like ACRV for the Space Station. In Some Cases it is more convenient, simpler, less Expensive, Lighter in Weight or Smaller to use Primaries. In Others, like ACRV, they are Enabling Technology. Primary Cells can be Designed to Give Much Higher Energy Density, Specific Energy, and Power Density than any Rechargeable System that will be Available in the near Future. Of Course, it isn't Possible to Design a Cell to Give Both Optimal Power and Energy. Peaks on the Response Surface tend to be somewhat Mission-Specific. As Bobby Bragg will Explain in his Paper on NASA Applications, Alkaline Manganese Dioxide/Zinc, Silver Oxide/Zinc, Numerous Lithium Electrochemistries as well as Mission Specific Developments such as the Large Lithium/Thionyl Chloride Reserve Batteries Proposed for ACRV, the Lithium/Sulfur Dioxide Batteries used on Galileo, and the Lithium/Carbon Monofluoride Batteries used in the Shuttle Range Safety Devices and Elsewhere are Involved. Thermal Batteries are Also Used where Very High Power Density is Required. Primary Batteries are somewhat like Flashbulbs in that the only way to tell for sure what each unit will do destroys the unit. Statistical Methods, thorough Qualification Testing, Configuration Control and Close Monitoring by the Program usually Combine to give acceptable Probabilities of Success. The Alternative is not to know what to Expect. Unfortunately, the more Data is Collected on a Design and Process, the more is known about its Imperfection, and the more Work is Required before Use. Instability in the Contractor Base and Tightening Environmental Requirements make the Job even more difficult. Extensive Safety Testing often sends Designs "Back to the Drawing Board". Not doing the Performance and Safety Testing is a Prescription for Failure. We have a Variety of Papers Today describing the Results of Some of these Tests on a Variety of Systems and the kinds of Work that has been done to Anticipate and Solve Problems.

2. Everyone here is Familiar With Alkaline Cells, the Type they use in their Flashlights. As long as the Contacts aren't Corroded, they Work Fine. They may not Realize that when these Cells are Submitted to Extensive Lot Acceptance Testing, about Half of Lots Fail. Which Manufacturer makes the Best Cells Depends on when you ask the question. With Environmental Regulations around the World Tightening on Mercury, the Prognosis isn't Bright. Performance, Storage Life, and Leakage will all be Worse in the Near Future than they are now. The Manufacturers are all working hard on this Tough Electrochemical Problem. In the Meantime, Cell Designs are unlikely to Remain Static for Long. Accordingly, Closer Monitoring of Designs (i.e. Contractor Visits and Pre-Mortems) and Frequent Lot Sample Tests are needed to Assure Performance. Very Forgiving System Designs require Large Deratings which means more Size and Weight and Shelf Life and Leakage Considerations still Exist.

3. Most Everyone here has worked with Silver/Zinc Batteries. They are a Mature Technology which can Deliver as much Performance Today as they Ever Will. They have been used in many Missions without problems. They also have been responsible for some Performance and Safety Problems, Particularly After Storage and if Short-Circuited. Like Alkaline Cells, they Generally Contain Mercury and Evolve Some Hydrogen on Stand. Minor Impurities in the Silver Oxide can Greatly Affect Self-Discharge and Gassing, Particularly at High Temperatures. Minor Impurities in the Zinc also Affect Self-Discharge and Gassing. Pulse Performance after Storage can be affected by the amount of Silver (I) Oxide Formed on the Positive Current Collector. Position Sensitivity is also a Consideration, due to the Possibility of Expelling Electrolyte from the Bunsen Vents after Inversion.

4. Most Everyone here has also worked with Mercury/Zinc Cells. Mercury/Zinc Cells Can Deliver Comparable Energy Density to Lithium Cells at about 1/4 the Specific Energy. They (Some Designs) have good Shelf Life if they have never been discharged at all. They all Leak Eventually, mainly on the Negative Side of the Cell. They don't do well at High or Low Temperatures. With Severe Environmental Problems in Manufacture and Disposal, their Availablity will Decrease Quickly.

5. The "Numerous Lithium Electrochemistries" Referred to by Bobby is where the fun starts. In almost every Performance Category, a Lithium Anode Design can do Better than Anything Else. If Something Else has been Demonstrated to do the Job Reliably, it should probably be used. It will be enough Work just Maintaining that Capability in the next few years. If the Higher Performance of Lithium Cells is Required to do the Job, do it Reliably, meet the Weight Budget, or have Engineering Margin, then they should be Used. Lithium Cells have Reliably Supported many Mission Requirements since the Mid-70's that couldn't be done other ways. The Greater the Energy Required, the Greater the Advantage Lithium Systems can Offer, and the Greater the Potential Safety Problems. Relatively Few Large Lithium Cells have been Developed. Because of Liability Concerns, Shipping and Disposal Problems, they will remain Specialty Items for the Foreseeable Future. Each Design must be Considered on its own merit. Packaging Considerations are also very Important in integrating Cells into Batteries. Doing this to meet (i.e.) Shuttle Specifications is not Trivial. Because of the High Reactivity of Lithium, trace Impurities can have a large Impact on Reject Rates, Storage, Performance, and Reliability. For some systems considerable Work has been done in these Areas. In Others, it hasn't, but will be in the future.

6. Most of the Lithium Systems Developed to Date Originated in the Mid-60's to Early 70's, to meet Requirements Arising from the Beginning of the Space Program and the Vietnam War. Relatively little "High Risk-High Payoff" R&D has been done in this area Since. To Borrow from Gabano, for Convenience, Available Couples have the Theoretical Energy Density and Specific Energy Shown in Figure 1 and Figure 2. Practical Performance of some of these Systems is shown in the Ragone plot in Figure 3. The difference is room for Progress.

G.J. Methlie

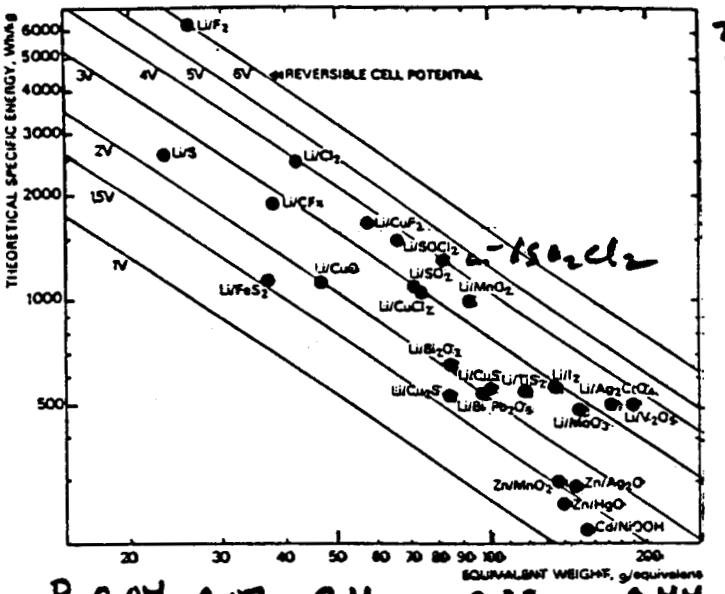

Fig. 1. Effect of the difference of electronegativity between anode and cathode (as reflected by the cell reversible voltage) and of the equivalent weight (of anode plus cathode materials) on the theoretical specific energy on weight basis of various electrochemical systems.

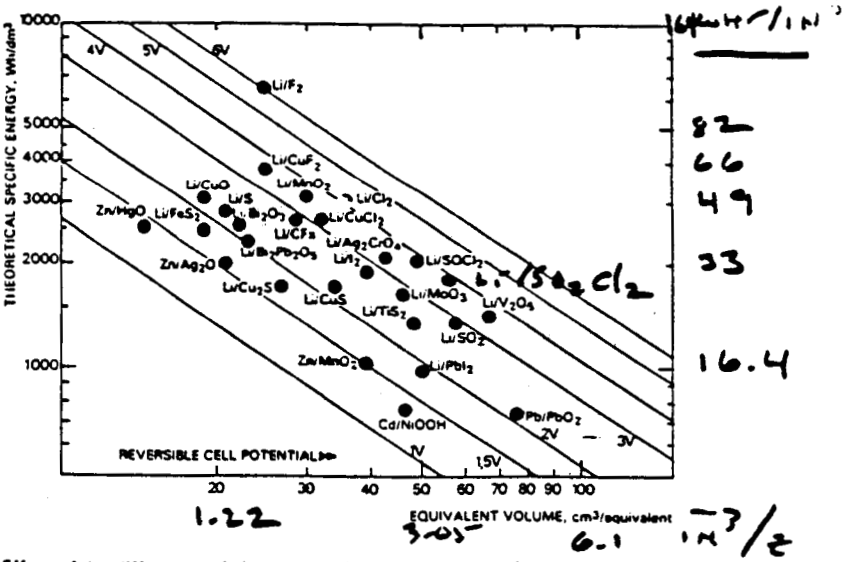

Fig. 2. Effect of the difference of electronegativity between anode and cathode (as reflected by the cell reversible voltage) and of the equivalent volume (of anode plus cathode materials) on the theoretical specific energy on volume basis of various electrochemical systems.

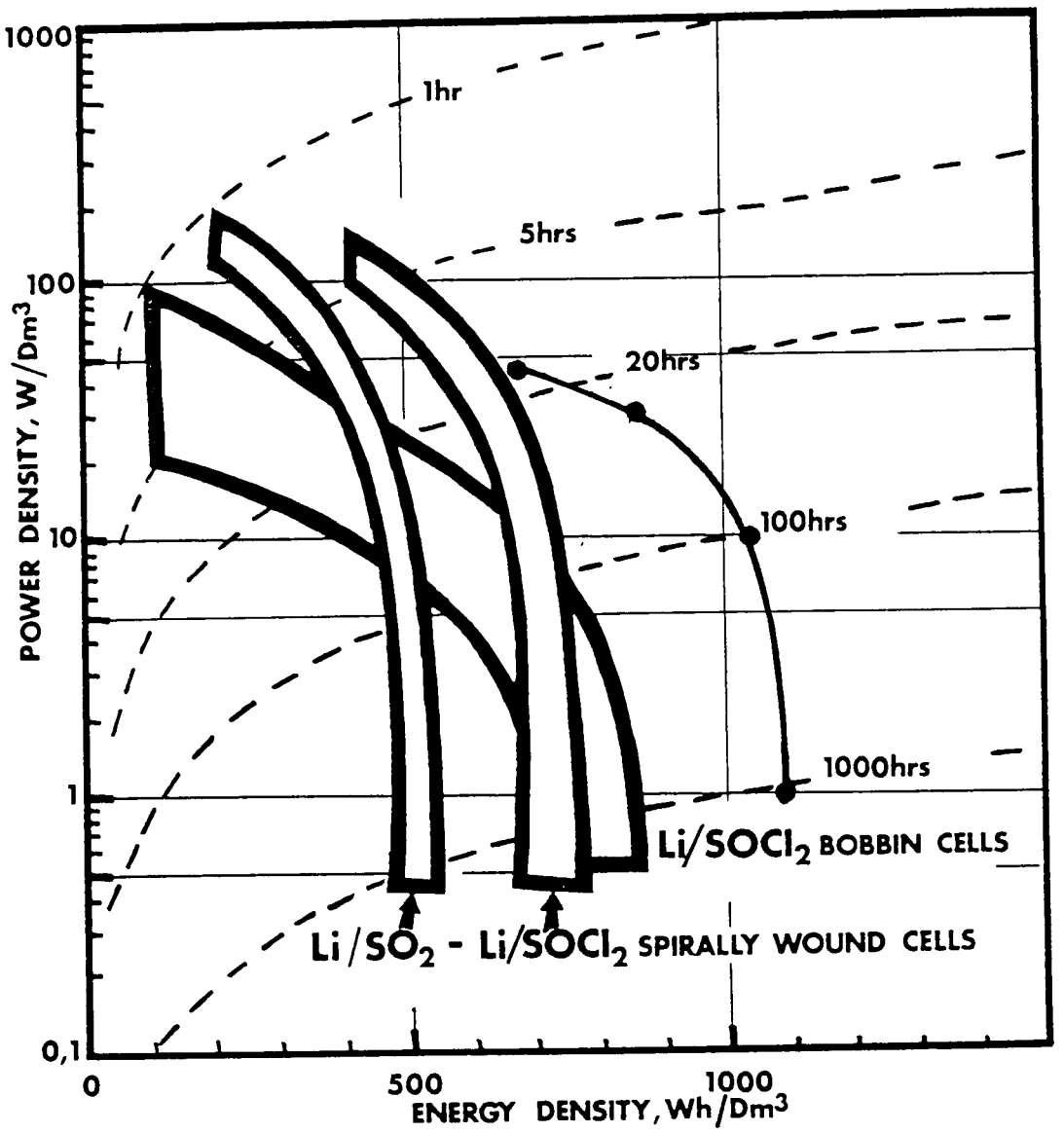
1000
100
10
1
0,1
POWER DENSITY, W/Dm3
1hr
5hrs
20hrs
100hrs
1000hrs
Li/SOCl2 BOBBIN CELLS
Li/SO2 - Li/SOCl2 SPIRALLY WOUND CELLS
0
500
1000
ENERGY DENSITY, Wh/Dm3

Figure 3

N92-27142

Johnson Space Center - Houston, Texas

PROPULSION AND POWER DIVISION	
B. J.BRAGG	12-3-90

JSC PRIMARY BATTERY APPLICATIONS

C-4

JSC PRIMARY BATTERY APPLICATIONS

Johnson Space Center - Houston, Texas

PROPULSION AND POWER DIVISION

B. J.BRAGG

12-3-90

- PAST APPLICATIONS
- CURRENT APPLICATIONS
- SPECIFIC APPLICATION EXAMPLES
- PROJECTED PRIMARY APPLICATIONS
- JSC - POWER BRANCH ROLE IN ORBITER APPLICATIONS

JSC Primary Battery Applications

This presentation addresses JSC Primary Applications. An overview is presented of past primary battery applications, and of current Orbiter applications. Specific application examples are described , as are several projected applications. Finally, the role the Power Branch of JSC plays in the use of primary batteries on the Orbiter is described

JSC PRIMARY BATTERY APPLICATIONS

PROPULSION AND POWER DIVISION

B. J.BRAGG | 12-3-90

PAST APPLICATIONS - EXAMPLES

- APOLLO AND ASTP, SKYLAB
  - VEHICLE POWER - AG-ZN (PRIMARY/LIMITED SECONDARY)
    - APOLLO, ASTP
      - 3 CM E&PL BATTERIES - 30V, 40 AH @28.5 LBS
      - 1 SM EMERGENCY BATTERY - 30V, 415 AH, @140 LBS
      - 2 CSM/ AND 2 LM PYRO BATTERIES - 30V, 0.75 AH, @3.5 LBS
      - 5 LM DESCENT BATTERIES - 30V, 415 AH, @140 LBS
      - 2 LM ASCENT BATTERIES - 30V, 296 AH, @132 LBS
    - SKYLAB
      - 2 CM E&PL BATTS SUBSTITUTED FOR CM PYRO BATTS
      - 3 DESCENT BATTERIES - 30V, 500 AH, @245 LBS
  - CREW EQ/EXPERIMENTS/TOOLS - MULTIPLE CHEMISTRIES
    - EMU - PLSS - AG-ZN BATT, 17V, 20 AH
    - FLASHLIGHTS, RECORDERS, CAMERAS, ETC - ALKALINES - AA, C, D, F
    - EXPERIMENTS - ALKALINES, CYLINDRICAL NI-CD (AS PRIMARIES)
    - WATCHES, CAMERAS - AG-ZN AND HGO-ZN BUTTON CELLS.

Past Applications - Examples

Examples of past primary battery applications are presented for Apollo, ASTP (Apollo-Soyez Test Project), and Skylab. Batteries are described for vehicle power and tools.

Apollo and ASTP vehicle Ag-Zn batteries include CM (Command Module) E&PL (entry and post landing) limited secondary batteries of 40 AH; SM (Service Module) emergency batteries of 415 AH; CSM/LM (Command Service Module/Lunar Module) pyrotechnic batteries of 0.75 AH; LM ascent batteries of 296 AH.

Skylab descent batteries of 500 AH were used in the SM CSM return from orbit at the end of the Skylab mission.

Batteries used in all these missions in the past were Ag-Zn, alkalines of various sizes, Ni-Cd used as primaries, and Ag-Zn and HGO-Zn button cells; all for the numerous pieces of crew equipment, experiments, and tools.

JSC PRIMARY BATTERY APPLICATIONS

PROPULSION AND POWER DIVISION

B. J.BRAGG | 12-3-90

CURRENT APPLICATIONS - SHUTTLE ORBITER

- NO ORBITER VEHICLE BATTERIES - 3, 30V, 7KW FUEL CELLS
- CREW EQUIPMENT, TOOLS, EXPERIMENTS, PAYLOADS
  - AG-ZN
    - EMU-PLSS, MMU, EVA POWER PACK
      - 11 CELLS, 30 AH
  - LI-BCX - C CELL (6 AH, 3.5V), D CELL (13 AH, 3.5V)
    - EMU-LIGHT - 1 D CELL
    - EMU TV - 8 D CELL IN SERIES
    - ARU - 2, 3-C CELL SERIES BATTERIES
    - CDTR - 2 D CELLS IN SERIES
    - MOS - 4 D CELLS IN SERIES
    - ULP - 2 CELLS IN SERIES
    - PRC-112 - 3 C CELLS
  - ALKALINES - (MNO2/KOH/ZN) - ALL SIZES; BUTTON THRU F CELL
    - CAMERA, EXPERIMENTS, FLASHLIGHTS, TOOLS, RECORDERS, ETC.
  - LEAD ACID - "SEALED" CYLINDRICAL AND "GEL-CELL"
    - MACINTOSH LAP-TOP COMPUTERS, PL BAY EXPERIMENTS, PL MEDICAL EXPERIMENTS
  - NI-CD (CYLINDRICAL, BUTTON THRU F CELL) - USED AS PRIMARIES FOR HIGH RATE
    - MEDICAL SUPPORT EQUIPMENT, CAMERAS

Current Applications

Current applications on the Shuttle Orbiter exclude the use of batteries for vehicle power; instead, fuel cell utilizing hydrogen and oxygen at 7 KW each.

Primary batteries are used on crew equipment, tools, experiments, and payloads.

An Ag-Zn battery (11 cells, 17V, 30 AH of 8, 26.6 AH cycles, 135 day wet life) is used for the EMU-PLSS (Extravehicular Mobility Unit - Personal Life Support System); The MMU (Manned Maneuvering Unit); and the EVA (Extravehicular Activity) power pack.

LI-BCX (Lithium-Bromine complex) batteries are used in the following applications:

EMU-LIGHT - EXTRAVEHICULAR MOBILITY UNIT LIGHT
ARU - ACCELEROMETER RECORDING UNIT
CDTR - CASSETTE DATA TAPE RECORDER
MOS - MINIOSCILLOSCOPE
ULP - ULTRASONIC LIMB PLETHYSMOGRAPH
PRC-112 - MILITARY RADIO

Additionally, alkalines of all sizes are used in various pieces of commercial equipment.

Lead-acids are used as primaries in a MACINTOSH LAP-TOP COMPUTER, in payload bay experiments, and in various medical experiments.

JSC PRIMARY BATTERY APPLICATIONS

PROPULSION AND POWER DIVISION

B. J.BRAGG | 12-3-90

- HGO-ZN - BUTTON THRU SMALL CYLINDRICAL CELLS
  - SURVIVAL RADIO (PRC-90), CAMERAS, MEDICAL EQ.
- ZN-AIR (O2) - BUTTON THRU LARGE DISC CELLS
  - WCCU - RADIO - 5 STRINGS OF 12 DURACELL 796 1 AH CELLS
  - WCCS - RADIO - 5 STRINGS OF 6 DURACELL 796 1 AH CELLS
  - MOS - 4 STRINGS OF 13 DURACELL 1200 2.5 AH CELLS
  - PMS - MULTIPLE STRINGS OF VARIOUS 630 .95 AH CELLS
  - WCCS - RADIO, OPERATIONAL VERSION - 2 STRINGS OF 6 DURACELL 1204 6.5 AH CELLS
- LITHIUM - X- MULTIPLE BUTTON, DISC, AND SMALL CYLINDRICAL
  - - SOCL2, -BCX, -SO2, -CFx, -MNO2, -I, -AG2CRO4
  - CAMCORDER/CAMERA/COMPUTER BACK-UP MEMORY/CLOCK POWER
  - PRIMARY POWER FOR LOW POWER EXPERIMENTS, PAYLOADS

Additional Shuttle Orbiter Applications

Additional types of batteries in Orbiter use are Ni-Cd (used as primaries) and HGO-ZN batteries.

Zn-Air applications include the following:

WCCU RADIO - WIRELESS CREW COMMUNICATIONS UNIT
WCCS RADIO - WIRELESS CREW COMMUNICATIONS SYSTEM
MOS - MINIOSCILLOSCOPE
PMS - PHYSIOLOGICAL MONITORING SYSTEM, WCCS RADIO; OPERATIONAL VERSION

Various lithium chemistries of button, disc and small cylindrical cell sized are in use for primarily low rate applications such as memory back-up and for low power experiments and payload.

Johnson Space Center - Houston, Texas

JSC PRIMARY BATTERY APPLICATIONS

PROPULSION AND POWER DIVISION

B. J.BRAGG | 12-3-90

SPECIFIC APPLICATION EXAMPLES

- ADVANCED WIRELESS CREW COMMUNICATION SYSTEM (WCCS) ZINC-AIR
  - WORN ON CREW PERSON'S LEG FOR CREW-TO-CREW AND CREW-TO-GROUND COMMUNICATION
  - CHARACTERISTICS
    - 12 ZN-AIR CELLS, DURACELL MODEL 1204, 6.5 AH
    - 2 PARALLEL STRINGS OF 6 CELLS IN SERIES
    - 6V, 13 AH, RUNNING AT 162 MA
    - 0.79 LBS, 3" X 2.7" X 1.6"
  - ENVIRONMENT: IN-CABIN AIR UTILIZATION, 60% RH, 25°C
  - PACKAGING FLEXIBILITY: 4 STACKS OF 3 CELLS.
    - 6V, 12 AH, 160 MA BATT AS DESIGNED
    - 12V, 6.5 AH, 80 MA BATT - - - - MINIMAL ELECTRICAL
    - 3V, 26 AH, 320 MA BATT - - - - MODIFICATION REQUIRED

APPLICATION SPECIFIC EXAMPLES

One specific example of an application is the Advanced Zn-Air Battery for the Operational WCCS Radio. This battery consists of two strings of 6 Duracell Model 1204 cells of 6.5 AH capacity of approximately 1 volt each. This battery is thus capable of 6 volts, 13 AH, and 162 ma. Each battery provides at least 72 hours of operation for the leg-worn WCCS. Additional batteries are carried on-board to allow each crewperson full utilization of their own radio for the entire duration of the mission.

The unique packaging of the battery as physically arranged in 4 3-cell stacks allows utilization of the battery for other applications with minimal electrical modification. Two additional electrical configurations are possible: 3 volts, 26 AH, 320 ma; and 12 volts, 6.5 AH, 80 ma.

The battery was designed, fabricated, and qualified by in-house elements of JSC and JSC support contractors; and has flown on STS-41 and STS-35.

JSC PRIMARY BATTERY APPLICATIONS

PROPULSION AND POWER DIVISION

B. J.BRAGG | 12-3-90

SPECIFIC APPLICATION EXAMPLES

- EMU HELMET - LIGHT LI-BCX
  - CHARACTERISTICS
    - 2 LIGHTS PER HELMET, 2 BULBS PER LIGHT
    - ONLY ONE BULB/LIGHT UTILIZED AT A TIME @0.7A
    - 12 LIGHT BATTERIES CARRIED PER MISSION
      - 2 EMU, 2 BATTS/EMU X 3 EVA'S MISSION
      - CONTINGENCY EVA'S ARE PRIMARY REQUIREMENT
      - 7 HR EVA X 0.7 A = 4.9 AH REQUIREMENT FOR LI-BCX D CELL
      - 1 LI-BCX D CELL/LIGHT, 3.5V, 8-10 AH @ 0.7A
      - LI-BCX D CELL IS 1.3" DIA, 2.3" LONG, 115 GM.

APPLICATION SPECIFIC EXAMPLES - Continued

An additional application example is the EMU Helmet Light Li-BCX battery. It consists of a single Li-BCX D cell packaged in an aluminum can for insertion into the EMU Light assembly. There are two light assemblies worn on the EMU Helmet for use during EVA. Each light assembly requires one battery; there are two EMU's supporting each mission ; and the potential of supporting three EVA's. This requires carrying 12 batteries per mission. Each light draws 0.7 amps for 7 hours, thus requiring 4.9 AH per battery. Each battery is capable of 8-10 AH at the required 0.7 amp rate. Two 160 degree F thermostats are installed in series with each battery to preclude overtemperature operation, and an extra mass of aluminum is incorporated in each light assembly as a heat sink for battery thermal control.

Johnson Space Center - Houston, Texas

JSC PRIMARY BATTERY APPLICATIONS

PROPULSION AND POWER DIVISION

B. J.BRAGG | 12-3-90

PROJECTED PRIMARY APPLICATIONS AT JSC

- ACRV - ASSURED CREW RETURN VEHICLE
  - 30-170 KWH STORED ENERGY REQUIREMENT
  - LONG LIFE - >5 YEARS QUIESCENT LIFE
  - JSC RECOMMENDED BASELINE - MODULAR LI-BCX DD
  - ALTERNATE SYSTEMS STILL UNDER CONSIDERATION
- LIFESAT - LARGE PAYLOAD
  - 50-100 KWH OF STORED ENERGY
  - APPROXIMATELY 30 DAY+ MISSION
  - INITIALLY NON-SHUTTLE LAUNCHED
- ALTERNATE EMU-PLSS BATT FOR CONTINGENCY EVA'S
  - ONE BATT FOR 3 REDUCED DURATION EVA'S
  - PRELIMINARY ESTIMATES OF 14 HRS EVA TIME
  - 1 - 7 HR, 1 - 3 HR, 1 - 4 HR EVA (53.2 AH TOTAL)
  - LONG LIFE (1-3 YEARS SHELF LIFE)
  - MUCH LOWER BATTERY LOGISTICS COST

POTENTIAL PRIMARY BATTERY APPLICATIONS

Several potential applications for primary batteries are projected at JSC.

The ACRV (Assured Crew Return Vehicle) is a rescue vehicle which is designed to support the Space Station. It requires energy storage of from 30 to 170 KWH, dependent upon specific mission scenarios. Long quiescent life (>/= 5 years) is required The JSC recommended baseline is a modular Li-BCX DD system; however, alternative systems are still under consideration.

A large payload known as LIFESAT is being proposed. This payload is initially to be launched on expendable propulsion systems, and requires 50-100 KWH of stored energy over a 30+ day period.

Finally, an alternative EMU-PLSS battery of 53.2 AH yielding 14 hours total of contingency EVA time is needed with 1-3 years shelf life and reduced logistics costs. This requirement is envisioned to be met within the current volume and weight constraints of the current EMU-PLSS Ag-Zn battery via the use of a lithium system.

Johnson Space Center - Houston, Texas

JSC PRIMARY BATTERY APPLICATIONS

PROPULSION AND POWER DIVISION

B. J.BRAGG | 12-3-90

JSC - POWER BRANCH ROLE IN ORBITER APPLICATIONS

- SUPPORT JSC ORGANIZATIONS WITH APPLICATION RESPONSIBILITY
  - PERFORM TRADE STUDIES
  - MAKE BATTERY SELECTION RECOMMENDATIONS
  - PROVISION BATTERY TO USERS
- PROVIDE SUBSYSTEM MANAGEMENT FOR APPLICATION WITH BATTERY SUBSYSTEM
- PROVIDE BATTERY SELECTION CONSULTATION FOR ANY USER
- SUPPORT JSC PAYLOAD SAFETY PANEL
  - REVIEW PAYLOAD HAZARD REPORTS (PLHR)
  - SUPPORT USERS IN THEIR PREPARATION OF PLHR
    - SUPPORT USERS (JSC ET.AL.) WITH TEST/ANALYSIS CAPABILITY
    - PROVIDE CONSULTATION ON SAFETY ISSUES.
  - DEFINE AND MAINTAIN BATTERY SAFETY REQUIREMENT DOCUMENTATION

JSC POWER BRANCH ROLE IN PRIMARY BATTERY APPLICATIONS

The role of the Power Branch/EP5 of JSC in primary battery applications is to support those JSC organizations having direct application responsibility with trade studies, battery selection recommendations, and with development, qualification, and provisioning of primary batteries.

Battery subsystem management is provided.

Payload hazard report preparation is supported, as is the review and comment of such reports for the JSC Payload Safety Panel, who approves the flight safety for all Orbiter payloads.

JSC battery users are provided with safety analysis and test support to achieve safety approval.

Finally, it is the responsibility of the Power Branch to define and maintain battery safety requirement documentation for JSC.

STS LITHIUM/CFx BATTERY

D. Gnacek
5 December 1990

UNITED TECHNOLOGIES USBI

STS LITHIUM/CFx BATTERY

INTRODUCTION

- LITHIUM/CFx BATTERIES ARE UTILIZED ON SPACE SHUTTLE SOLID ROCKET BOOSTERS AND EXTERNAL TANK

- PROGRAM HAS BEEN EXTREMELY SUCCESSFUL IN TERMS OF MISSION RELIABILITY WITH EXCEPTION OF CELL YIELD VARIANCES

UNITED TECHNOLOGIES USBI

STS LITHIUM/CFx BATTERY

FUNCTION/SYSTEM DESCRIPTION

- LITHIUM BATTERIES PROVIDE POWER TO THE ET/SRB RANGE SAFETY COMMAND/ DESTRUCT SUBSYSTEM
  - SYSTEM OPERATIONAL APPROXIMATELY 1 HOUR PRIOR TO LAUNCH THROUGH SRB/ET SEPARATION
  - SYSTEM VOLTAGE: 28.0 VDC NOMINAL (REGULATED)
  - SYSTEM CURRENT: 0.5 AMPERES NOMINAL
    3.5 AMPERES 100 MS PULSE
  - 4 BATTERIES PER MISSION

UNITED TECHNOLOGIES USBI

STS LITHIUM/CFx BATTERY

BATTERY DESCRIPTION

- o DIMENSION: 8.8" x 6.7" x 5.5"
- o WEIGHT: 9.5 LBS
- o # OF CELLS: 13 (SERIES STRING)
- o CAPACITY: 18 AMPERE-HOURS
- o VOLTAGE: 27.0 VDC MIN @ < 1.0 AMPERES
- o CHEMISTRY: LITHIUM POLYCARBON MONOFLUORIDE
- o SHELF LIFE: 2 YEARS

UNITED TECHNOLOGIES USBI

Range Safety System

RSS Battery

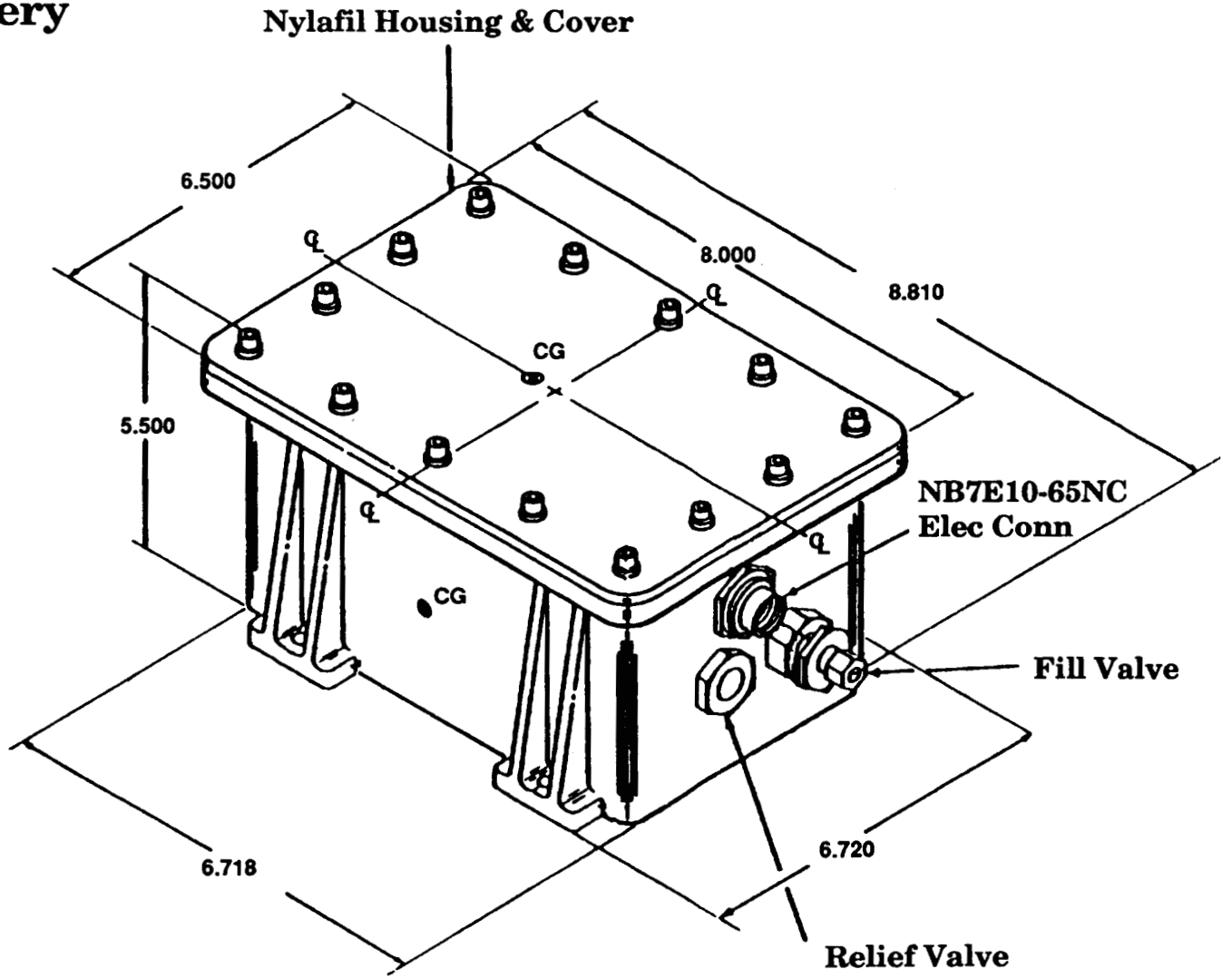

1724-4

UNITED TECHNOLOGIES USBI

Range Safety System

Lithium Battery Components

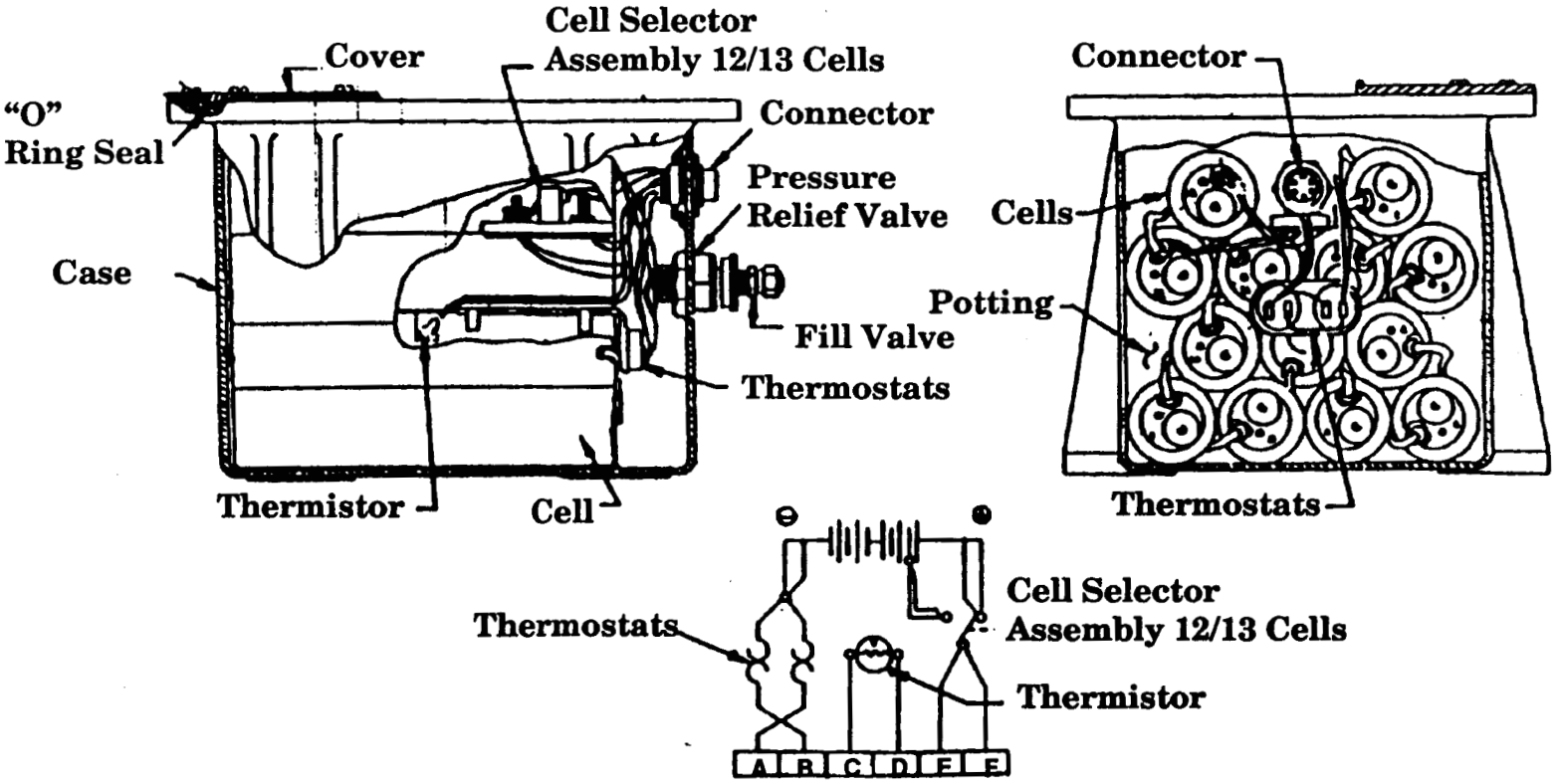

Electrical Schematic

1724-3

UNITED TECHNOLOGIES USBI

STS LITHIUM/CFx BATTERY

HISTORY

- o DEVELOPED IN 1974/1975 FOR SHUTTLE PROGRAM
- o QUALIFICATION TESTED 1977/1978
  - SINGLE MISSION
  - THERMAL QUALIFICATION: 20 DEG F - 140 DEG F
- o 3000+ CELLS BUILT
- o SUCCESSFULLY FLOWN ON 38 SHUTTLE MISSIONS - (148 BATTERIES)
  - NO PRELAUNCH ANOMALIES
  - NO INFLIGHT ANOMALIES

UNITED TECHNOLOGIES USBI

STS LITHIUM/CFx BATTERY

HISTORY (CONTINUED)

- o CELL YIELD PER BUILD VARIES
  - ATTRITION DENOTED BY DECLINE IN OPEN CIRCUIT VOLTAGES
- o PREVIOUS YIELDS ADEQUATE TO SUPPORT PROGRAM WITHOUT HARDWARE SHORTAGE CONCERN
- o TWO RECENT BUILDS WITH OFF NOMINAL CELL YIELD (< 90%)
- o TROUBLESHOOTING REVEALED PROBLEM LOCATED IN CELL HEADER AREA
  - OCV RISES SIGNIFICANTLY WHEN CELL HEADERS REMOVED
- o DPA REVEALED MATERIAL DEPOSIT AROUND POSITIVE TERMINAL PIN/ GLASS INSULATOR
- o MATERIALS INVESTIGATION CONDUCTED ON CELL HEADERS FROM NOMINAL AND OFF NOMINAL BUILDS

CELL YIELD PERCENTAGES PER BUILD
88 BATTERIES / 1496 CELLS

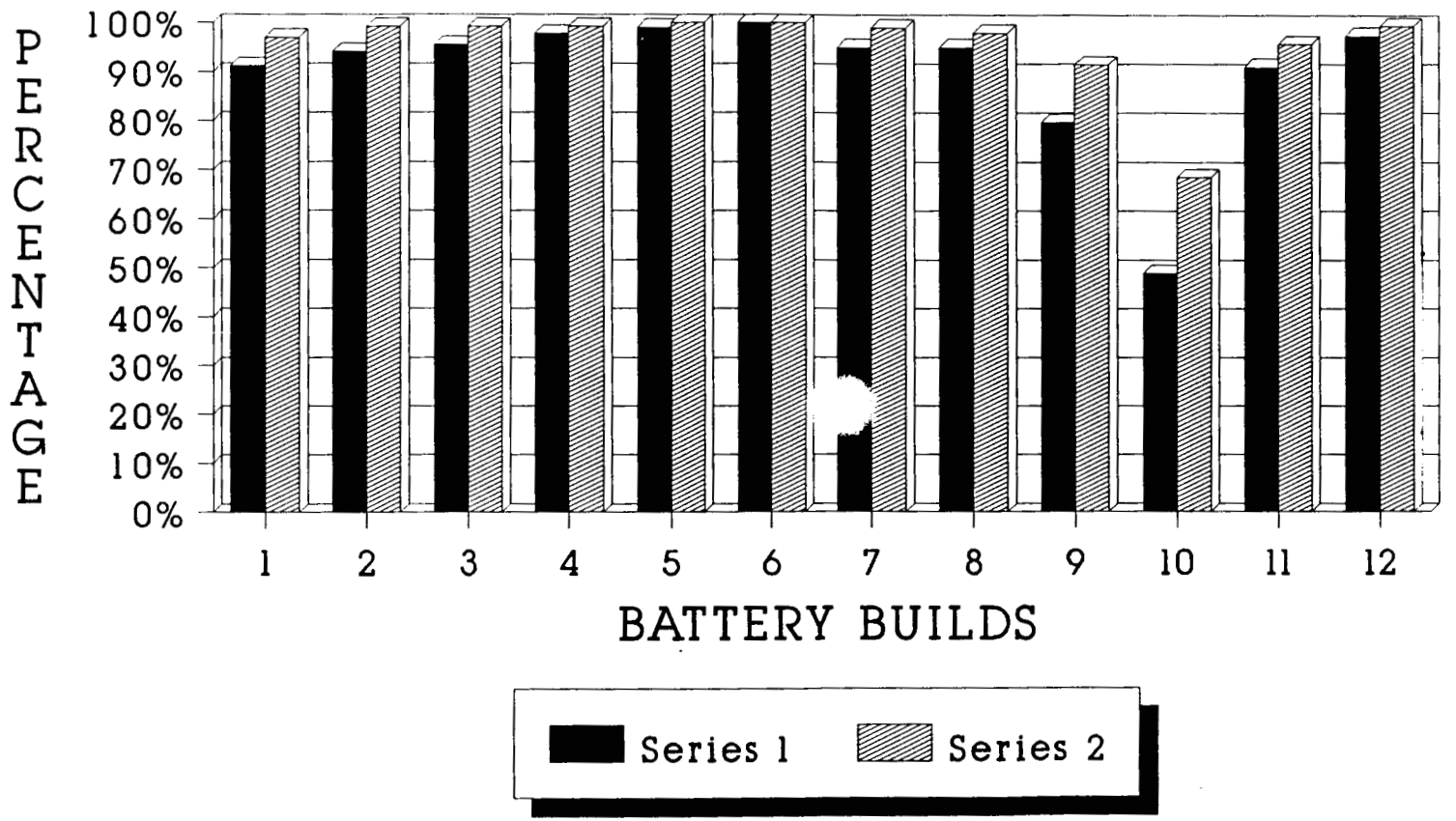

SERIES 1: 2.95 MINIMUM OCV SCREEN
SERIES 2: 2.85 MINIMUM OCV SCREEN

BUILDS 1-8
OCV MEASUREMENTS / 30 DAYS ACTIVATE
BLOCKS 360-384/389-402/410-415

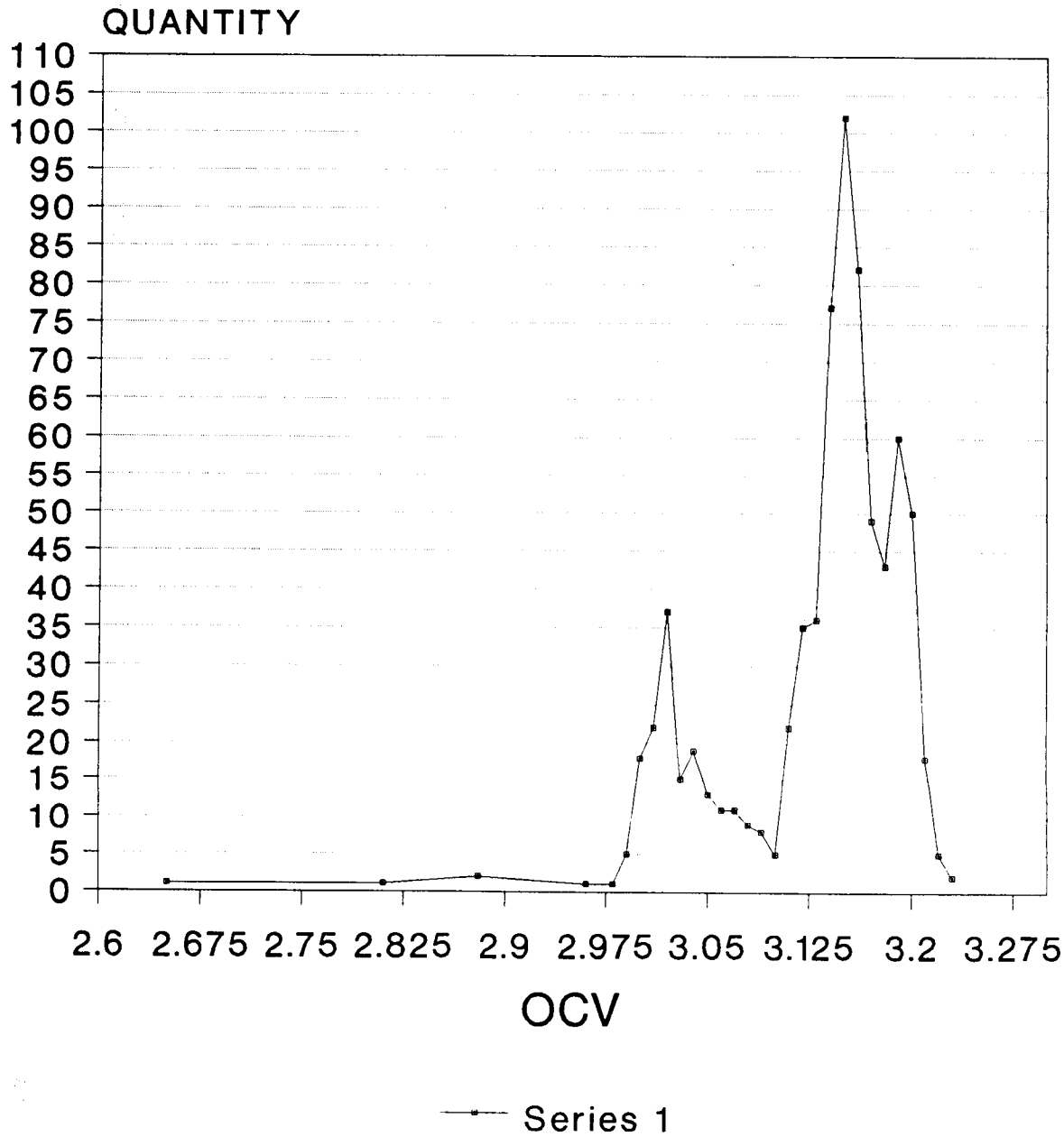

760 CELLS TOTAL

BUILD #'S 1-8 STORAGE CELL OCV MEASUREMENTS (44 CELLS TOTAL) (686/589/561/508/469/436/373/268 days)

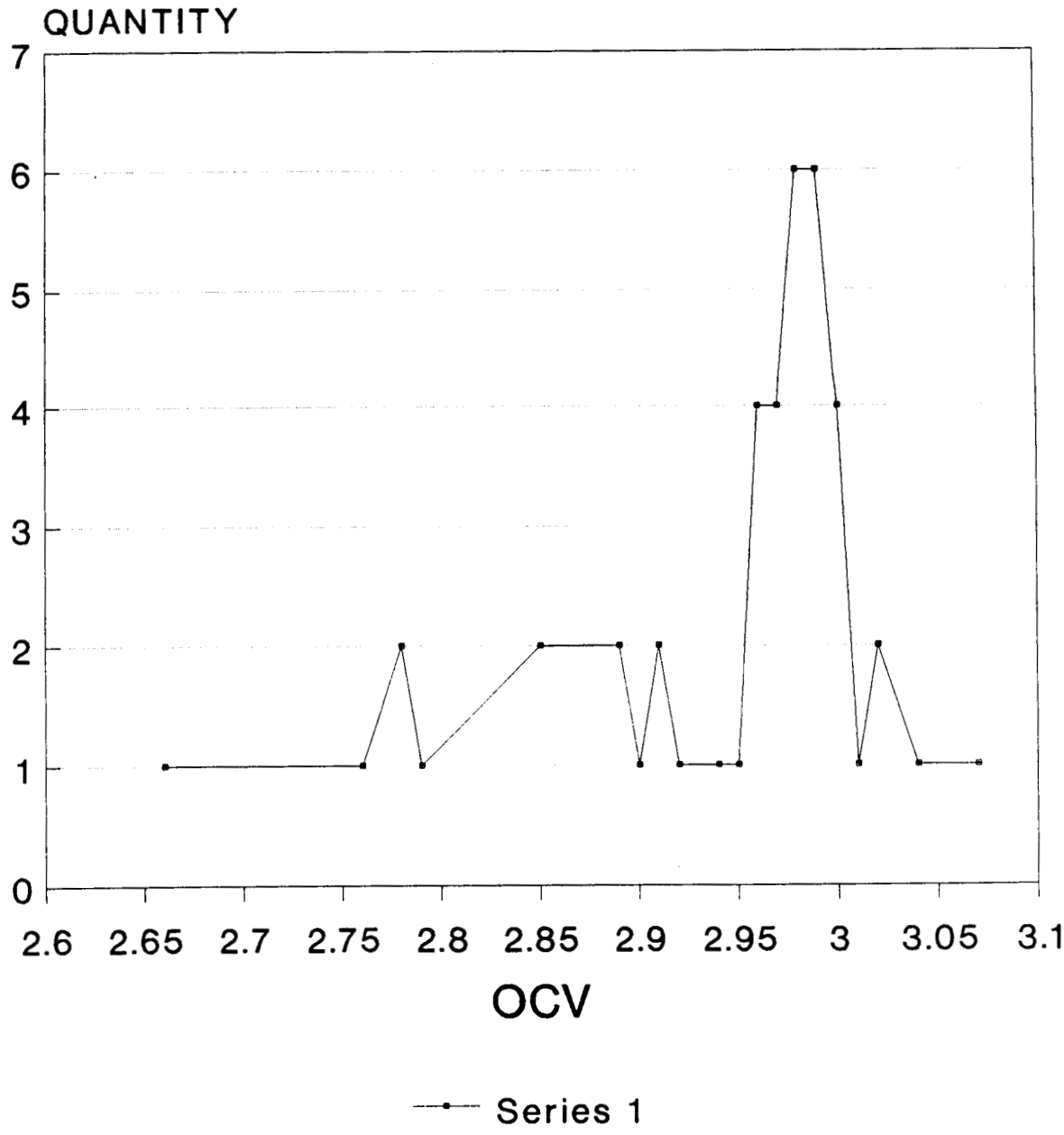

BLOCKS 360-384/389-402/410-415

BUILD #12
OCV MEASUREMENTS /92 DAYS ACTIVATED

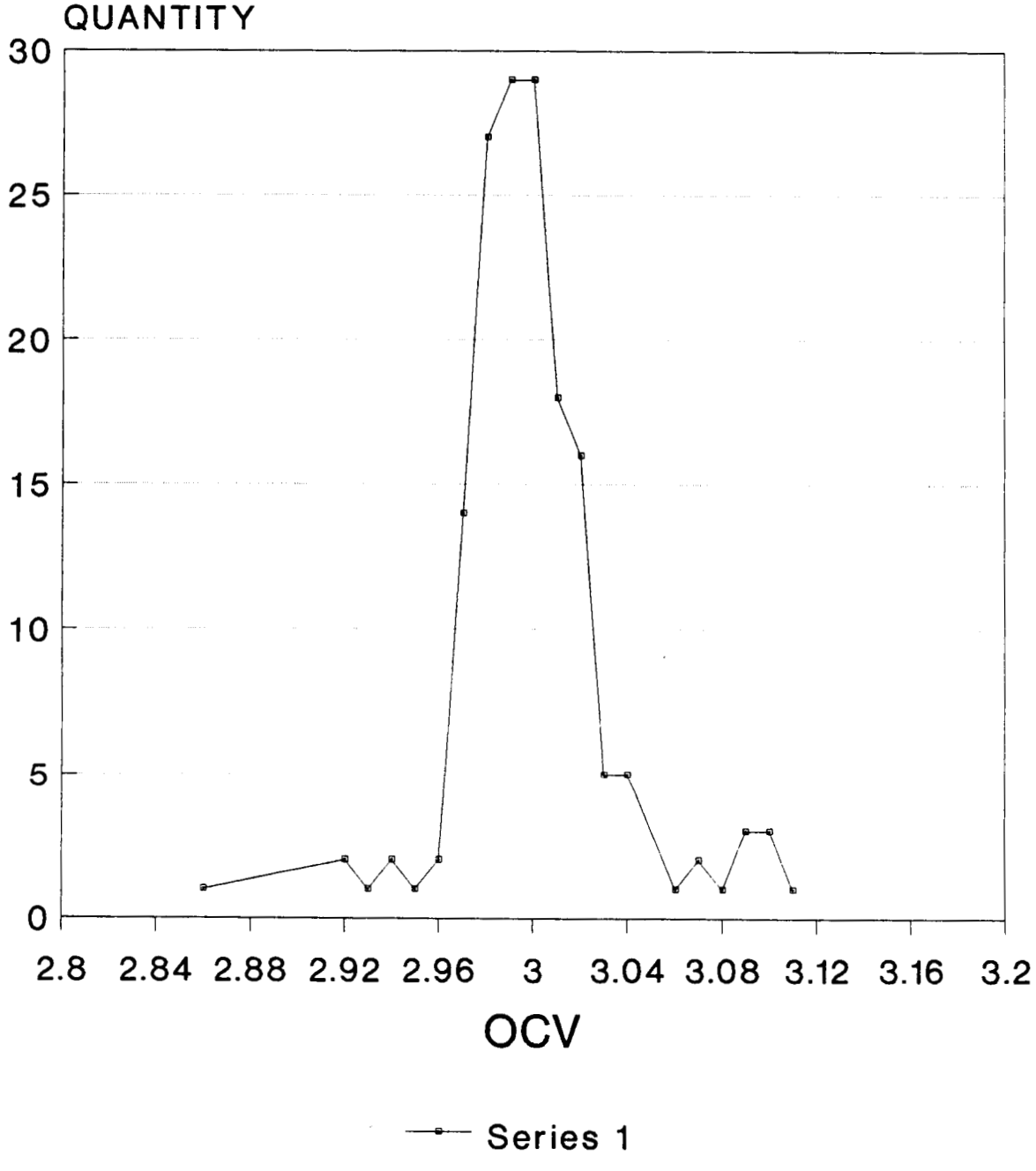

BLOCKS 437-445/447-448 173 CELLS TOTAL

BUILD #10
OCV MEASUREMENTS 230 DAYS ACTIVATED

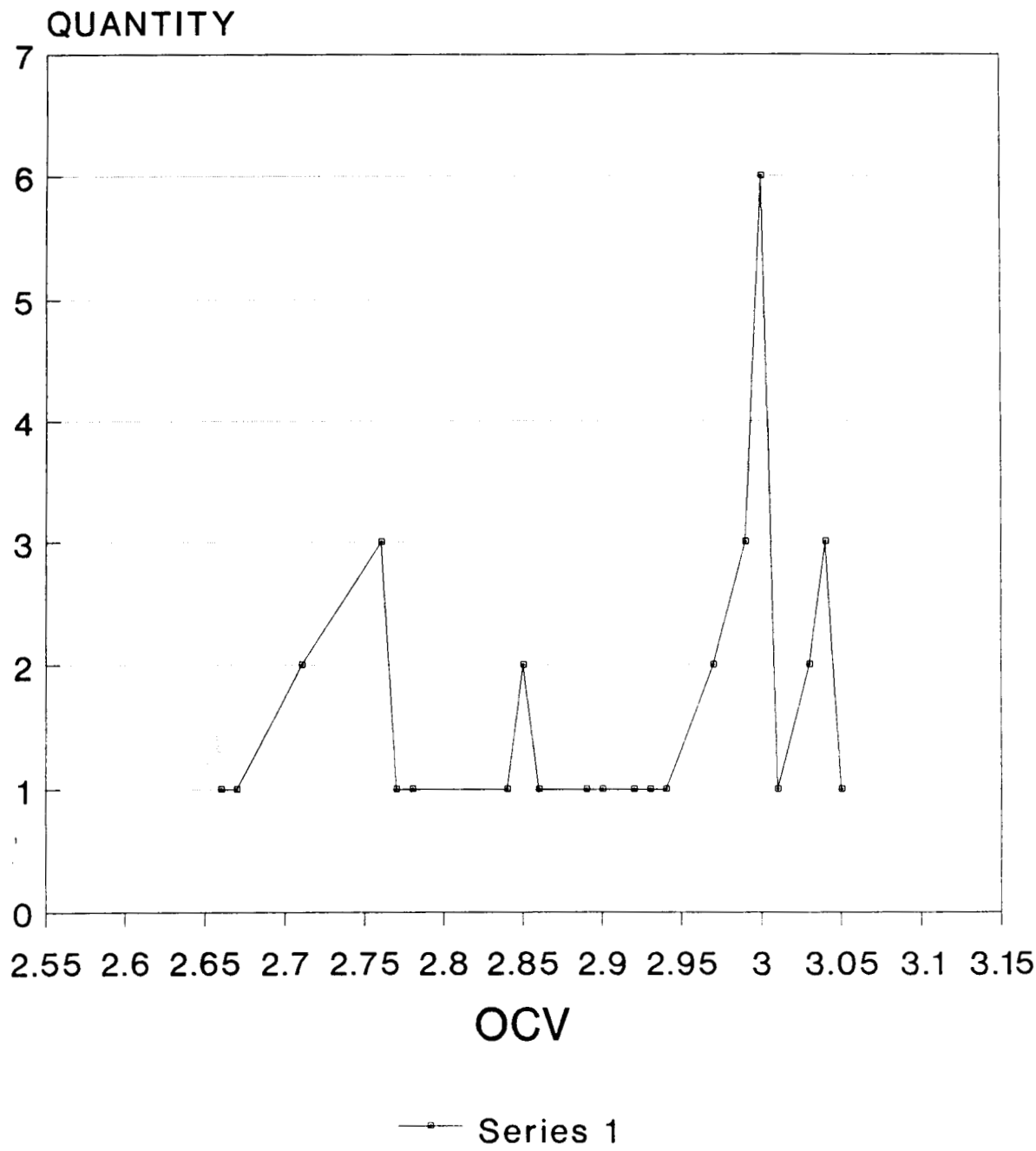

BLOCKS 424-426 / 36 CELLS TOTAL

CELL OCV

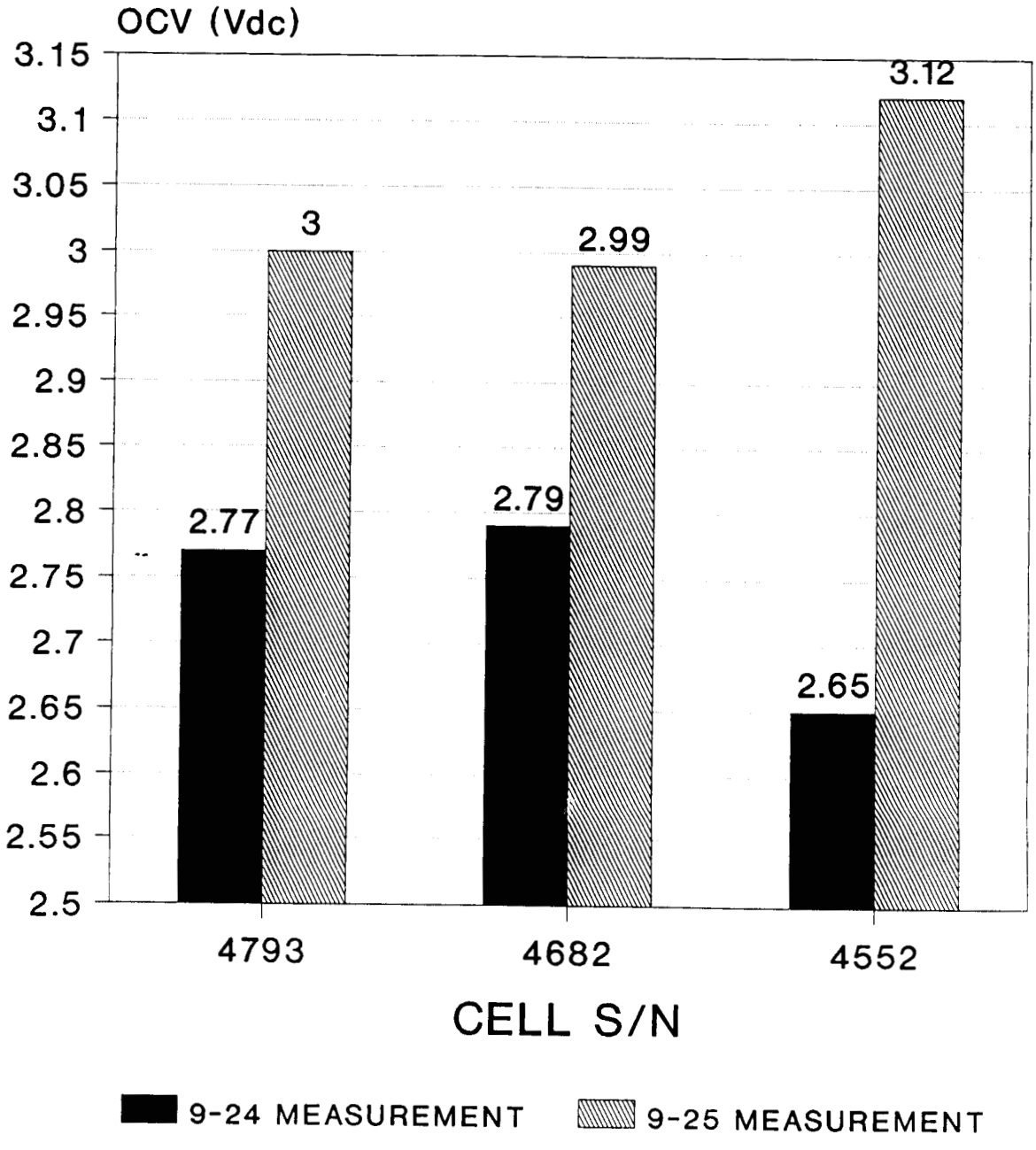

9-25 MEASUREMENTS MADE AFTER CELL HEADER REMOVAL

CELL OCV

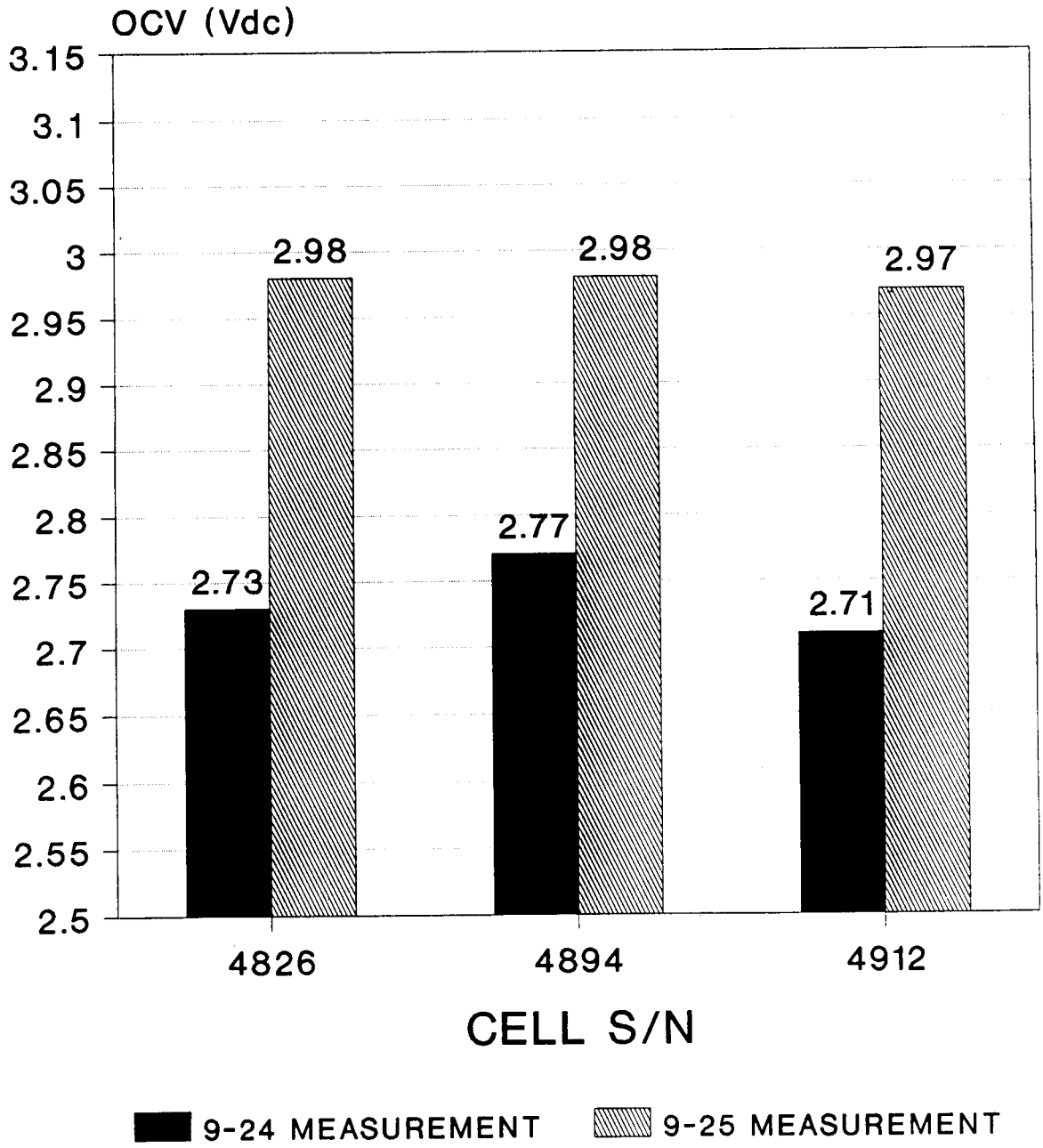

9-25 MEASUREMENTS MADE AFTER CELL HEADER REMOVAL

Range Safety System

Cell Header Assembly

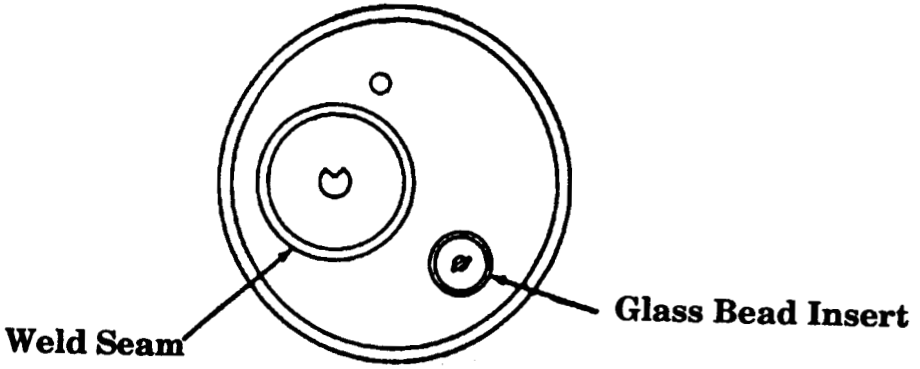

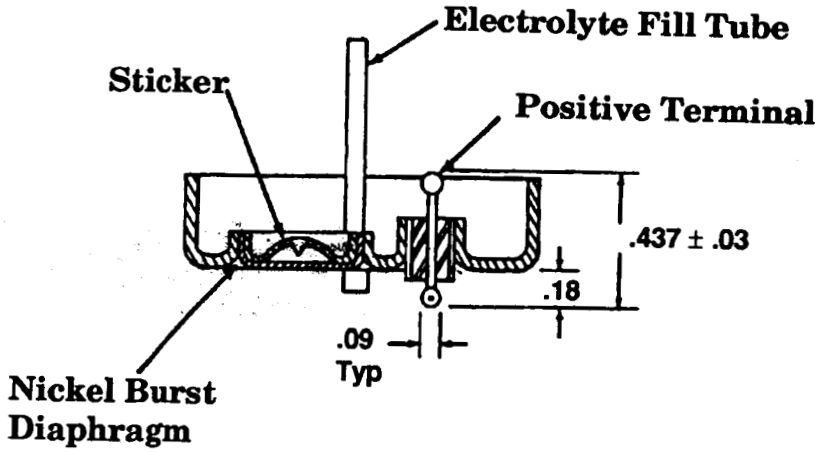

UNITED TECHNOLOGIES USBI

Range Safety System

Lithium Carbonmonofloride Cell Cross Section

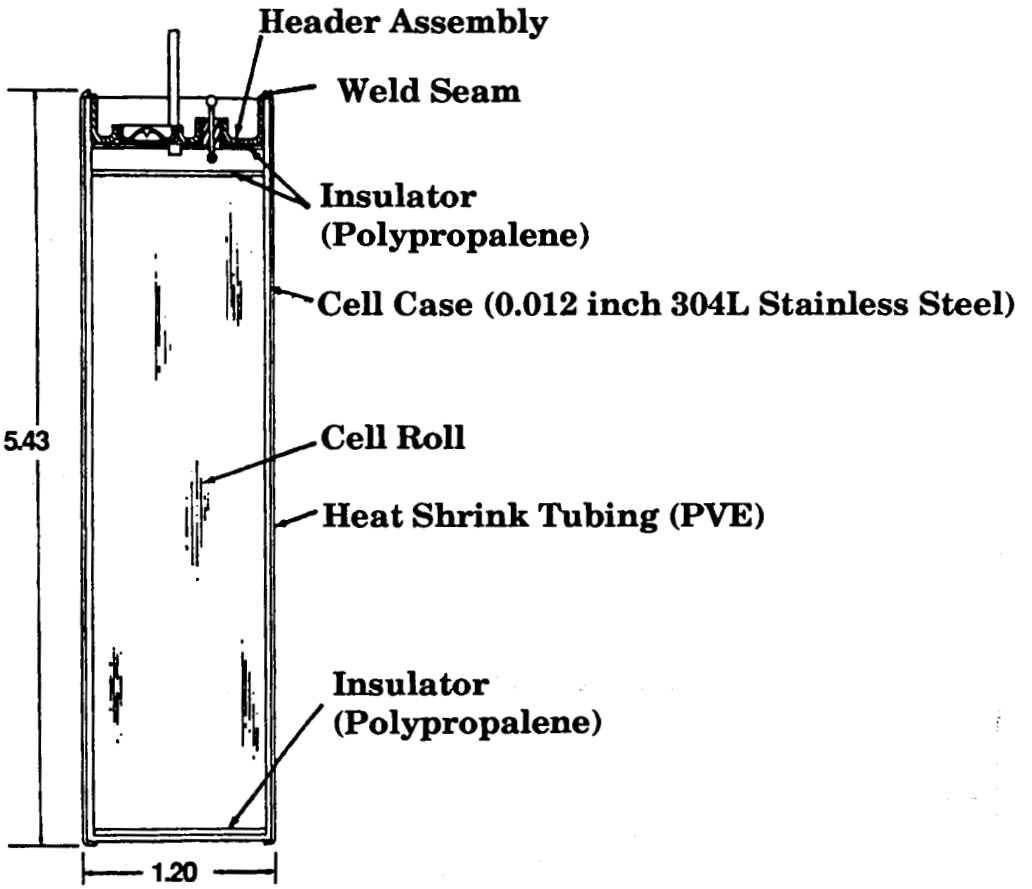

1724-1

UNITED TECHNOLOGIES USBI

ORGANIZATION: NASA/MSFC EH32	MARSHALL SPACE FLIGHT CENTER SOLID ROCKET BOOSTER RANGE SAFETY BATTERY CONTAMINATION ANALYSIS STATUS REPORT	NAME: DR. RICHARD CONGO
CHART NO.:		DATE: DECEMBER 4, 1990

PROBLEM STATEMENT: POTENTIAL THIONYL CHLORIDE CONTAMINATION CAUSED THE HIGH ATTRITION RATE.

- ANALYTICAL METHODOLOGY
  - DESTRUCTIVE PHYSICAL ANALYSIS -- CELL HEADERS
    - SCANNING ELECTRON MICROSCOPY (SEM)
    - ENERGY DISPERSIVE ANALYSIS BY X-RAYS (EDAX)
    - ELECTRON SPECTROSCOPY FOR CHEMICAL ANALYSIS (ESCA)
  - CELL CAN ANALYSIS
    - FOURIER TRANSFORM INFRARED SPECTROSCOPY (FTIR)
    - NON-VOLATILE RESIDUE (NVR)

ORGANIZATION: NASA/MSFC EH32	MARSHALL SPACE FLIGHT CENTER SOLID ROCKET BOOSTER RANGE SAFETY BATTERY CONTAMINATION ANALYSIS	NAME: DR. RICHARD CONGO
CHART NO.:		DATE: DECEMBER 4, 1990

FUTURE RECOMMENDATIONS

- STUDY CONTRACT TO INVESTIGATE SUSCEPTIBILITY OF LITHIUM BATTERIES TO ORGANIC CHLORIDES
- ADDITIONAL ANALYTICAL METHODOLOGIES
  - X-RAY DIFFRACTION
  - ELECTRON DIFFRACTION
- INVESTIGATE MICROCRACKS FOUND IN GLASS SEAL

N92-27144

NASA Li/CFx Cell Problem Analysis

Scanning Electron Microscopy with Energy Dispersive X-ray Spectrometry

4 - 6 December 1990
John Baker

The Specialty Battery Facility was charged with analyzing Li/CF_x cell parts for possible chloride contamination induced by exposure to thionyl chloride ($SOCl_2$); various samples were submitted for analysis. This paper covers only a portion of the analysis which has been conducted, namely analysis by scanning electron microscopy with energy dispersive X-ray spectrometry (SEM/EDS).

Initially, a strip of nickel was exposed to $SOCl_2$ vapors to observe variations in surface concentrations of sulfur and chlorine with time. The concentrations of sulfur and chlorine were monitored periodically using a standardless semi-quantitative EDS analysis routine. Monitoring the nickel test strip indicated that chlorine needs to be in the percent range for quantification, and chlorine and sulfur concentrations are not necessarily related. Therefore, by detecting chlorine one can not infer contamination by $SOCl_2$ only that contamination is present.

Six samples of stainless steel 316L foil were analyzed for chlorine using EDS. The six samples were divided into two sets, those that were degreased prior to contamination and those that were not. Each set contained a background sample, a sample which had been handled (fingerprints), and a handled sample which had been cleaned. Chlorine was not detected on either background sample and was detected on the samples which had been handled, even those which had been cleaned.

Cell covers suspected of being contaminated while in storage and covers which were not exposed to the same storage conditions were analyzed for chlorine. Also, covers from cells with low open circuit voltages were analyzed. Although no chlorine was found on the covers from cells (As, S, O, and F suspected of originating from the electrolyte were found), it was found on all stored covers.

This presentation will detail the results, showing techniques for analysis and identification. Relevent photomicrographs will also be presented.

S B F
Specialty Battery Facility

NASA Li/CFx CELL PROBLEM ANALYSIS

SEM/EDS Analysis

John Baker

NASA Aerospace Battery Workshop
4 - 6 December 1990

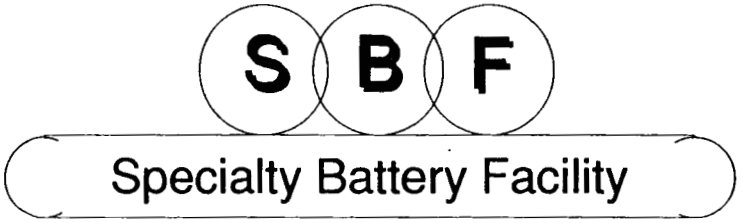

NASA Li/CFx CELL PROBLEM ANALYSIS
Samples

- Nickel Test Strip (1)
- Stainless Steel 316L Foil (6)
- Covers Under Various Storage Conditions (4)
- Covers From Dissected Cells (3)
- Covers For Glass-To-Metal Seal Analysis (3)

Specialty Battery Facility

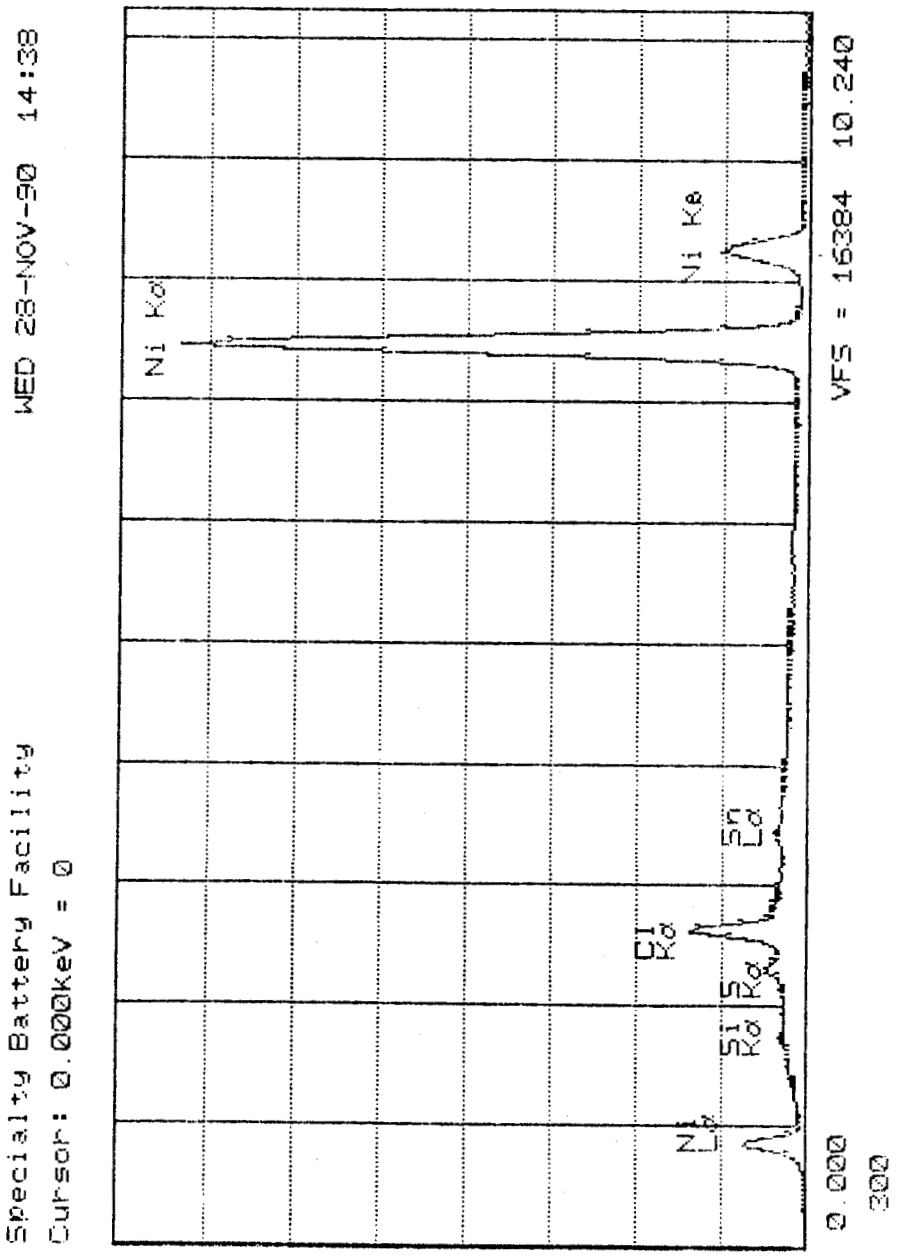
Specialty Battery Facility
Cursor: 0.000keV = 0
WED 28-NOV-90 14:38
Ni Kα
Ni Kβ
Cl Kα
S Kα
Si Kα
Sn Lα
N Kα
0.000
VFS = 16384 10.240
300

NASA Li/CFx CELL PROBLEM ANALYSIS

Ni Exposure to Thionyl Chloride

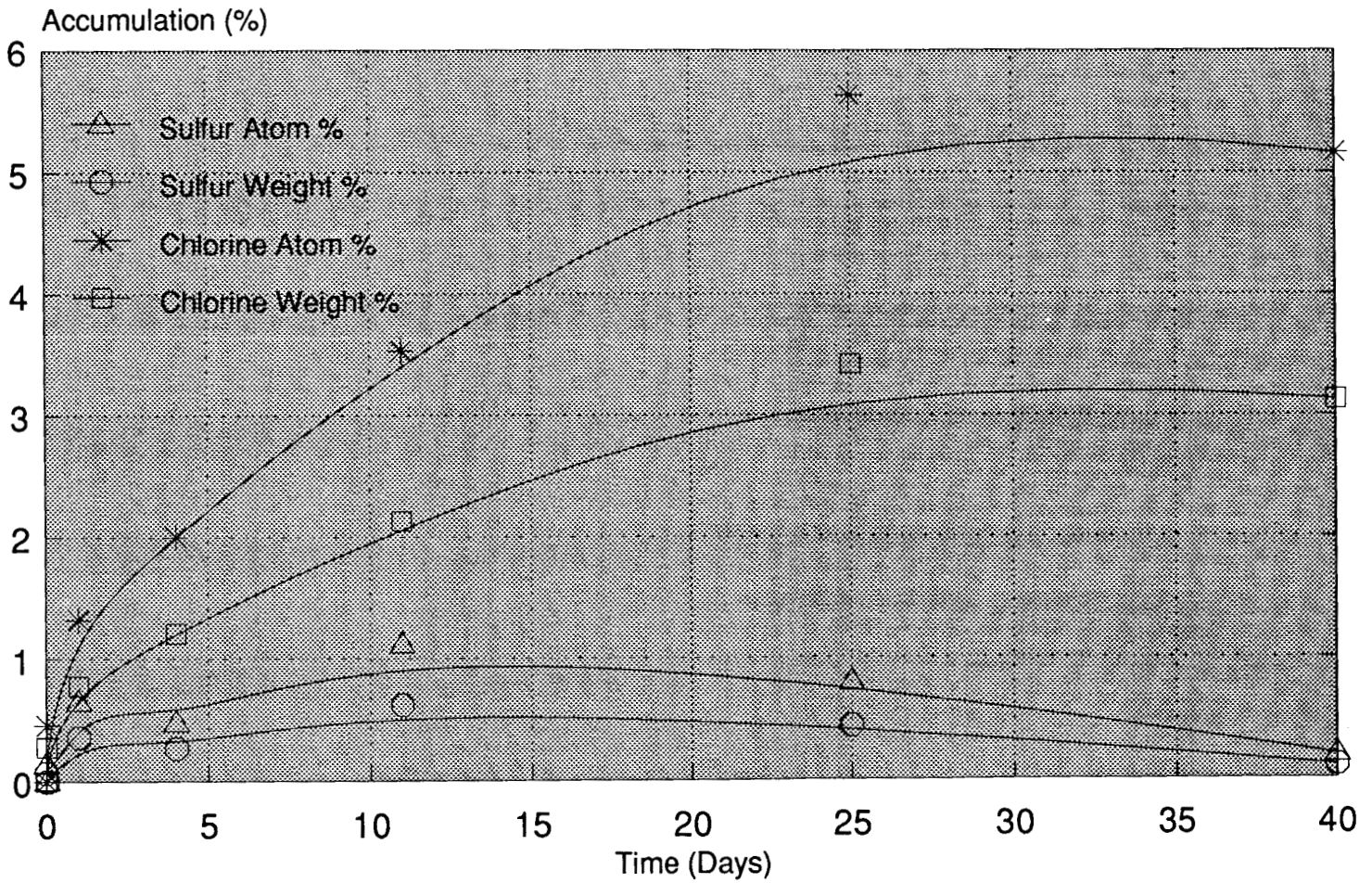

Specialty Battery Facility

NASA Li/CFx CELL PROBLEM ANALYSIS
Foil Samples

- B3 - Background 316L SS foil from inner roll
- C1 - Same as B3 but handled with bare hands
- C2 - Same as C1 but wiped off
- D1 - anode foil trike degreased then cleaned (EP-MP-583)
- D2 - Same as D1 but handled with bare hands
- D3 - Same as D2 but wiped with utility wipe and DI H O

2

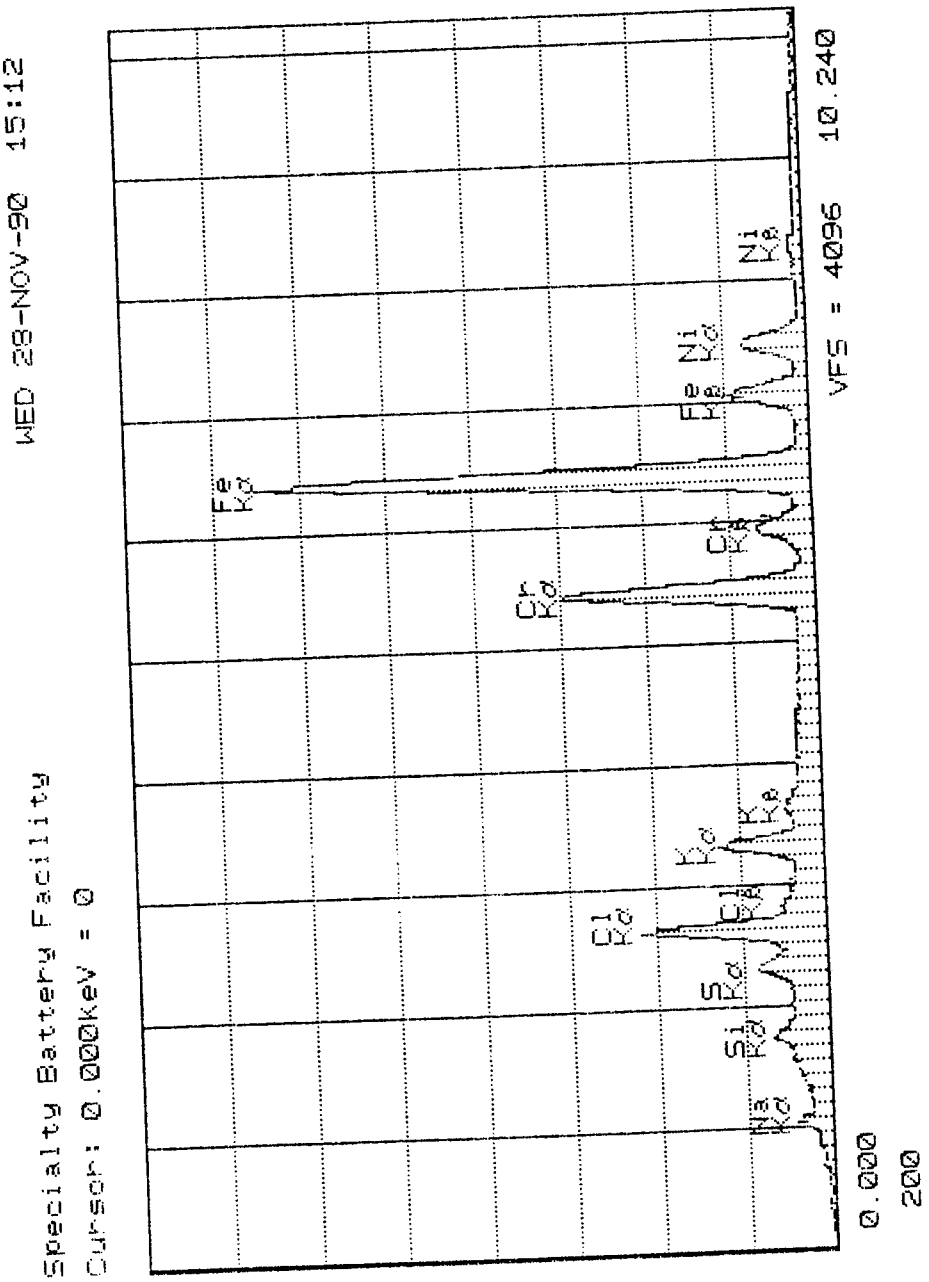
WED 28-NOV-90 15:12
Specialty Battery Facility
Cursor: 0.000keV = 0
VFS = 4096 10.240
0.000
200
Na Kα
Si Kα
Si Kβ
S Kα
Cl Kα
Cl Kβ
K Kα
K Kβ
Cr Kα
Cr Kβ
Fe Kα
Fe Kβ Ni Kα
Ni Kβ

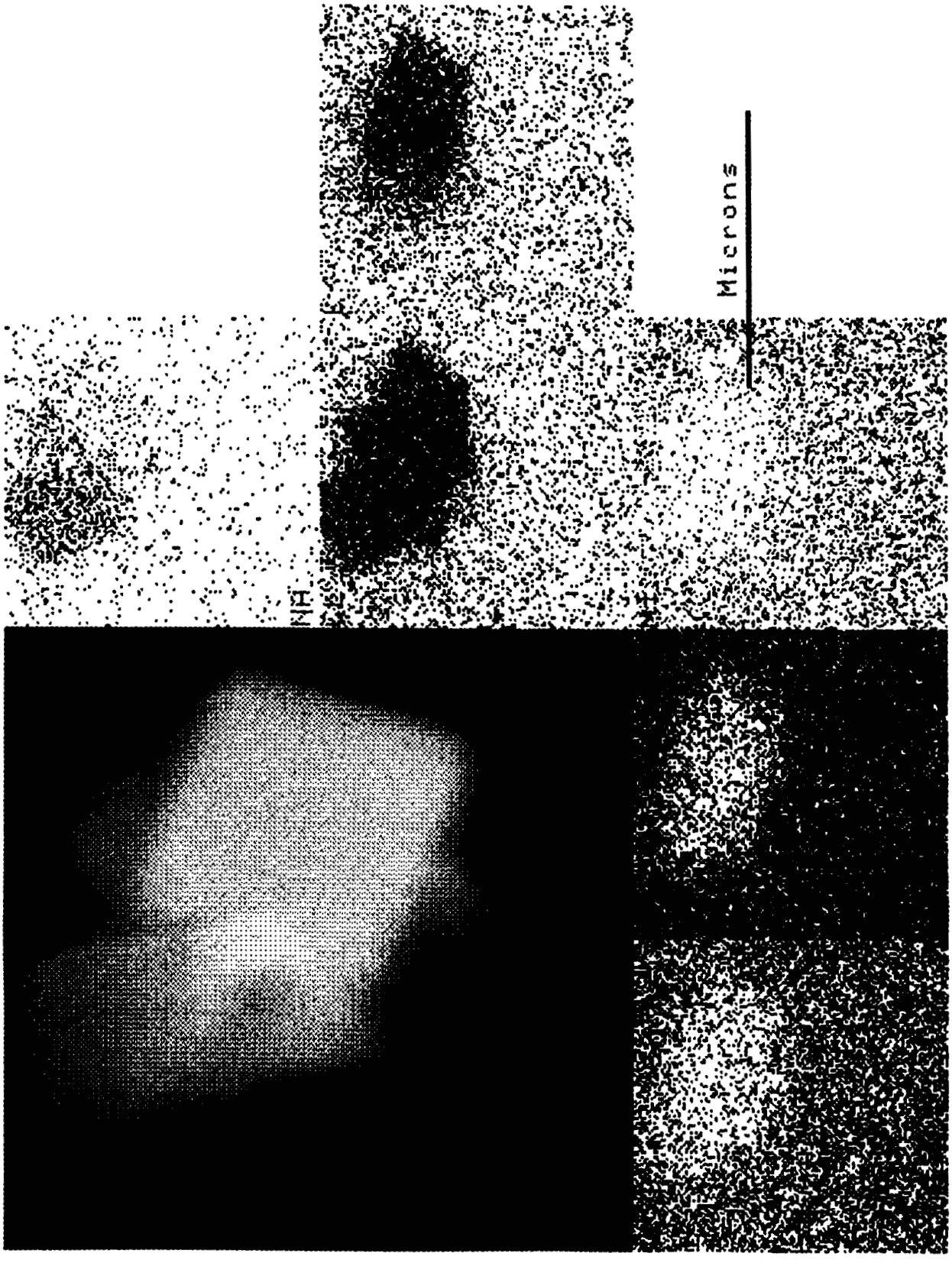
Microns

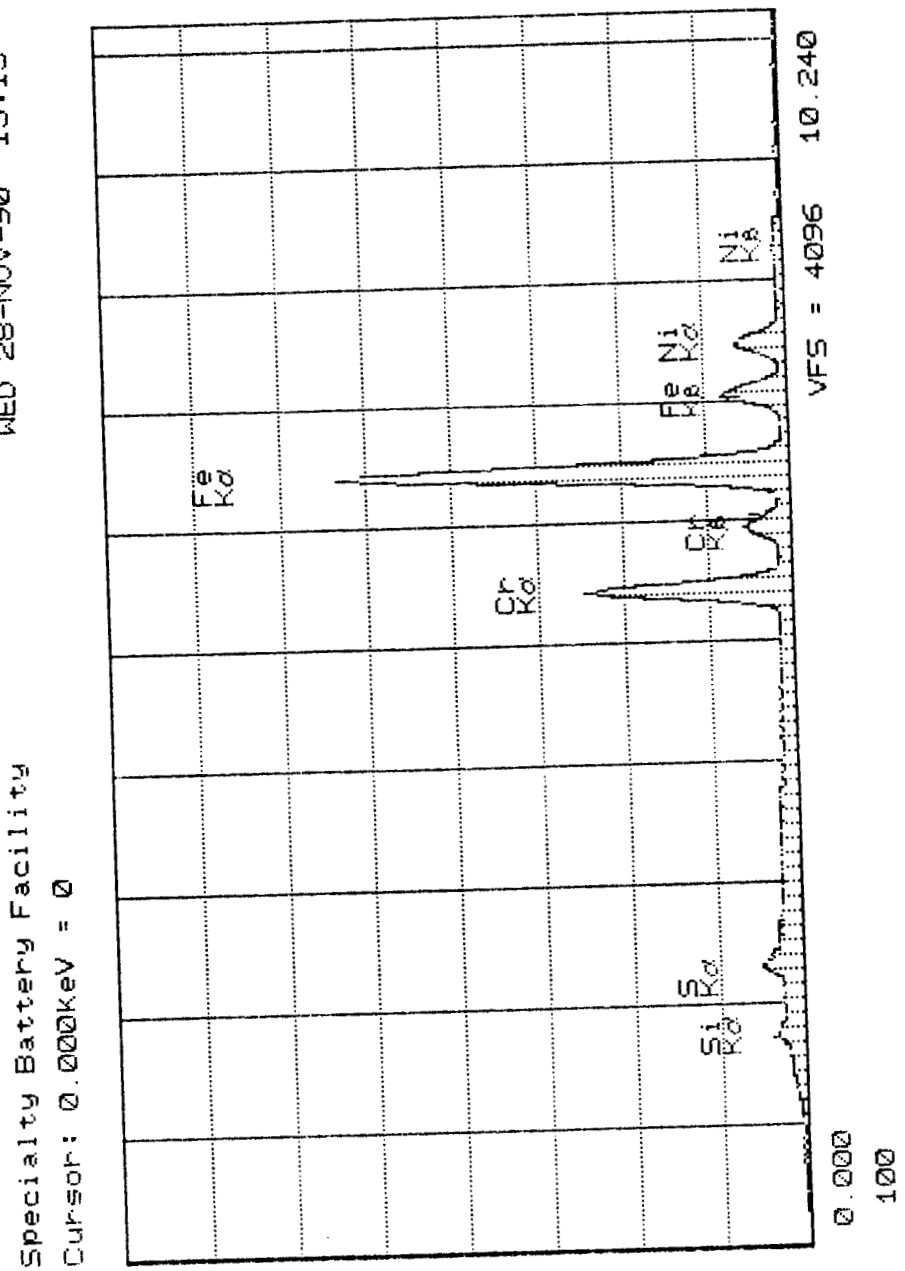
WED 28-NOV-90 15:15
Specialty Battery Facility
Cursor: 0.000keV = 0
Fe Kα
Cr Kα
Cr Kβ
Fe Kβ Ni Kα
Ni Kβ
Si Kα
S Kα
VFS = 4096
10.240
0.000
100

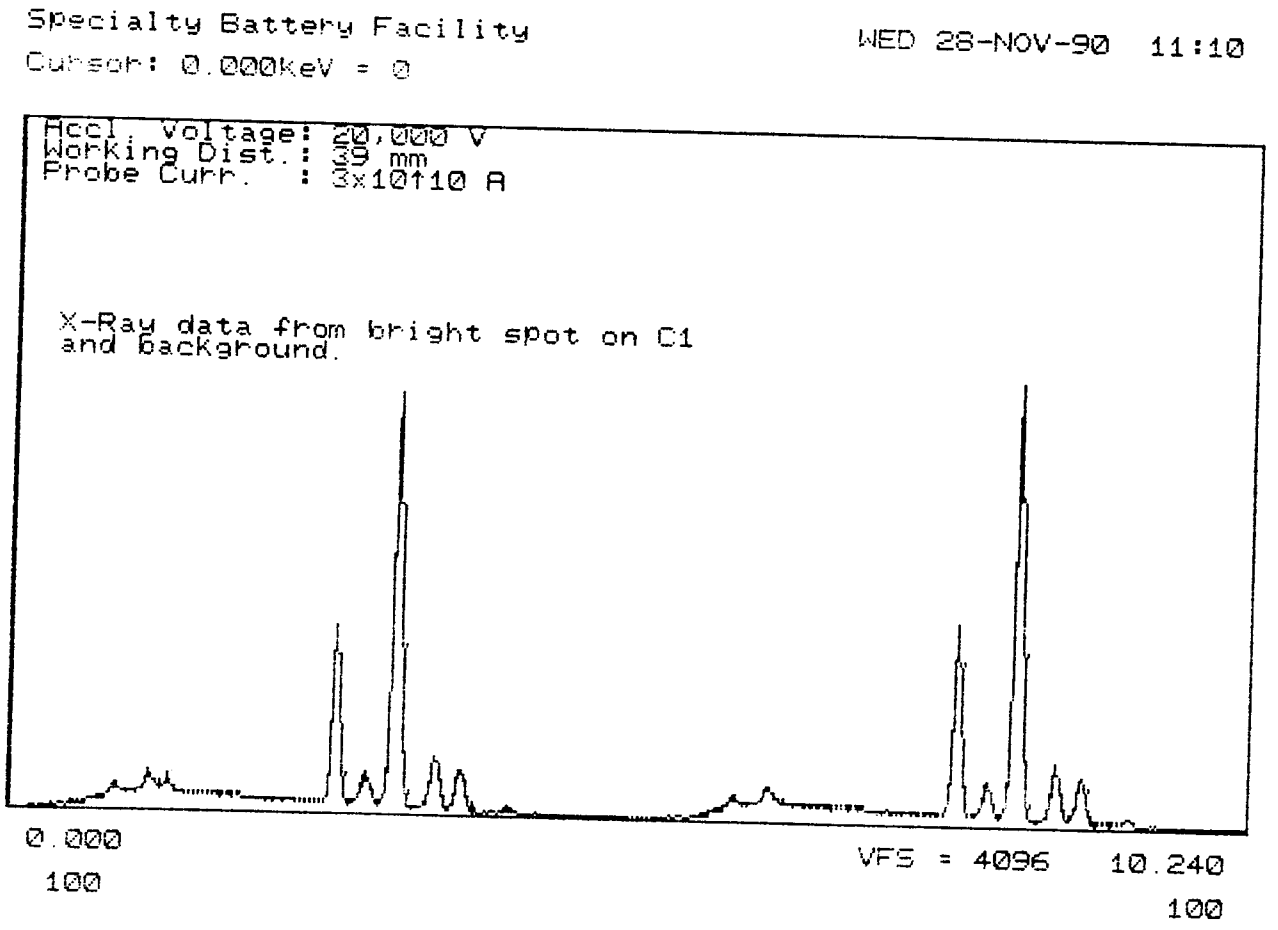
Specialty Battery Facility
Cursor: 0.000keV = 0
WED 28-NOV-90 11:10
Accl. Voltage: 20,000 V
Working Dist.: 39 mm
Probe Curr. : 3x10↑10 A
X-Ray data from bright spot on C1
and background.
0.000
100
VFS = 4096
10.240
100

NASA Li/CFx CELL PROBLEM ANALYSIS
Foil Analysis Findings

- B3 - No Cl found
- C1 - Cl found
- C2 - Paper towel fragments contained Cl
- D1 - No Cl found
- D2 - Cl found
- D3 - Cl on sample and in paper towel fragments

Specialty Battery Facility

NASA Li/CFx CELL PROBLEM ANALYSIS
Cover Samples

- 237 - NASA cover stored in dryroom
- 239 - NASA cover stored in dryroom
- 246 - NASA cover never exposed to dryroom
- 247 - 'Other' cover kept in open storage

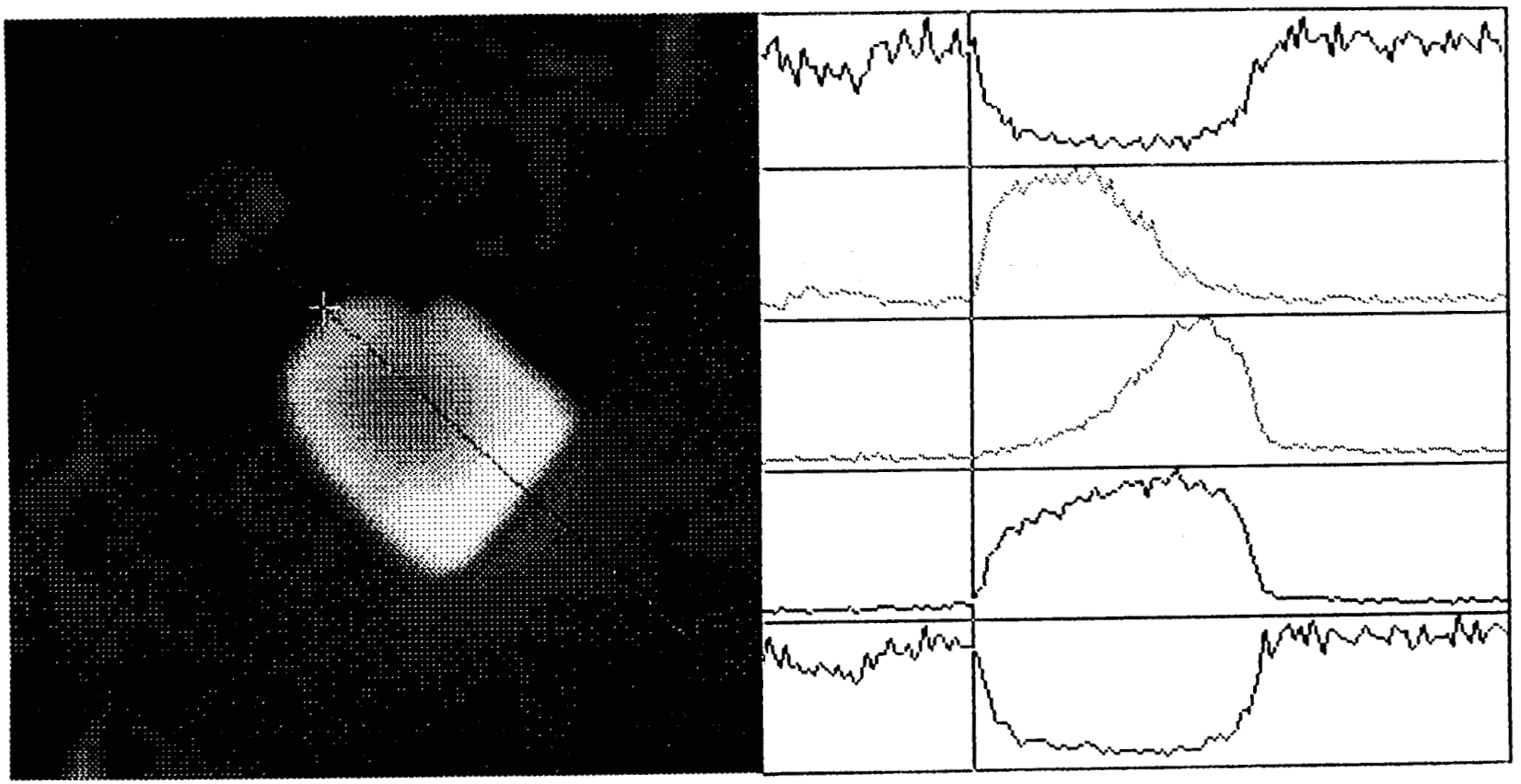

ELEMENT	VFS	INTENSITY
CR	117	89
K	368	25
MN	369	13
CL	453	34
FE	237	192

CURSOR DATA	
POINT: 36	DISTANCE: 28.58 uM

LABEL: CRYSTAL ON 246

NASA Li/CFx CELL PROBLEM ANALYSIS

Cover Analysis Findings

- Cl was found on all samples
- Salt crystals (NaCl and/or KCl) were found on all
- Other elements found: S, Ca, Si, Ni, Fe, Cr, Al, C, F, Mg, Cu, P, O, K, As, Ti, Al (Br), Mg (As), and C (K)

NASA Li/CFx CELL PROBLEM ANALYSIS

Dissected Cell Covers

- S/N 4589 G8 Block 419 - Cell voltage: 2.85 V
  Cell impedance: 0.28 ohms
- S/N 5040 G12 Block 440 - Cell voltage: 2.92 V
  Cell impedance: 0.34 ohms
- S/N 4777 G10 Block 425 - Cell voltage: 0.03 V
  Cell impedance: 12.0 ohms

Specialty Battery Facility

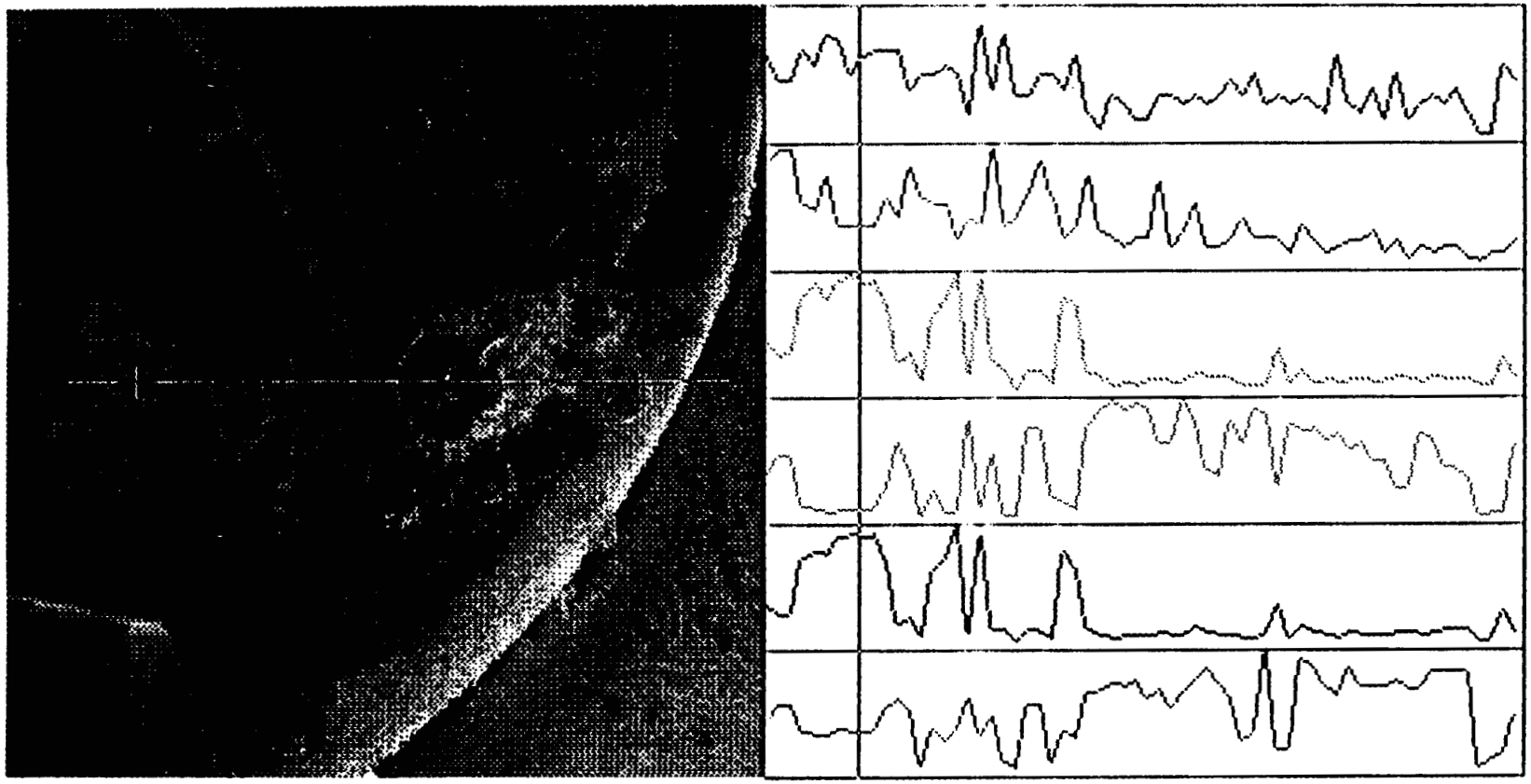

ELEMENT	VFS	INTENSITY
FE	15	8
NI	22	7
[illegible]	[illegible]	[illegible]
[illegible]	[illegible]	54
F	1624	1536
O	916	288

CURSOR DATA	
POINT: 7	DISTANCE: 558.26 uM

LABEL: LSCAN VENT AREA

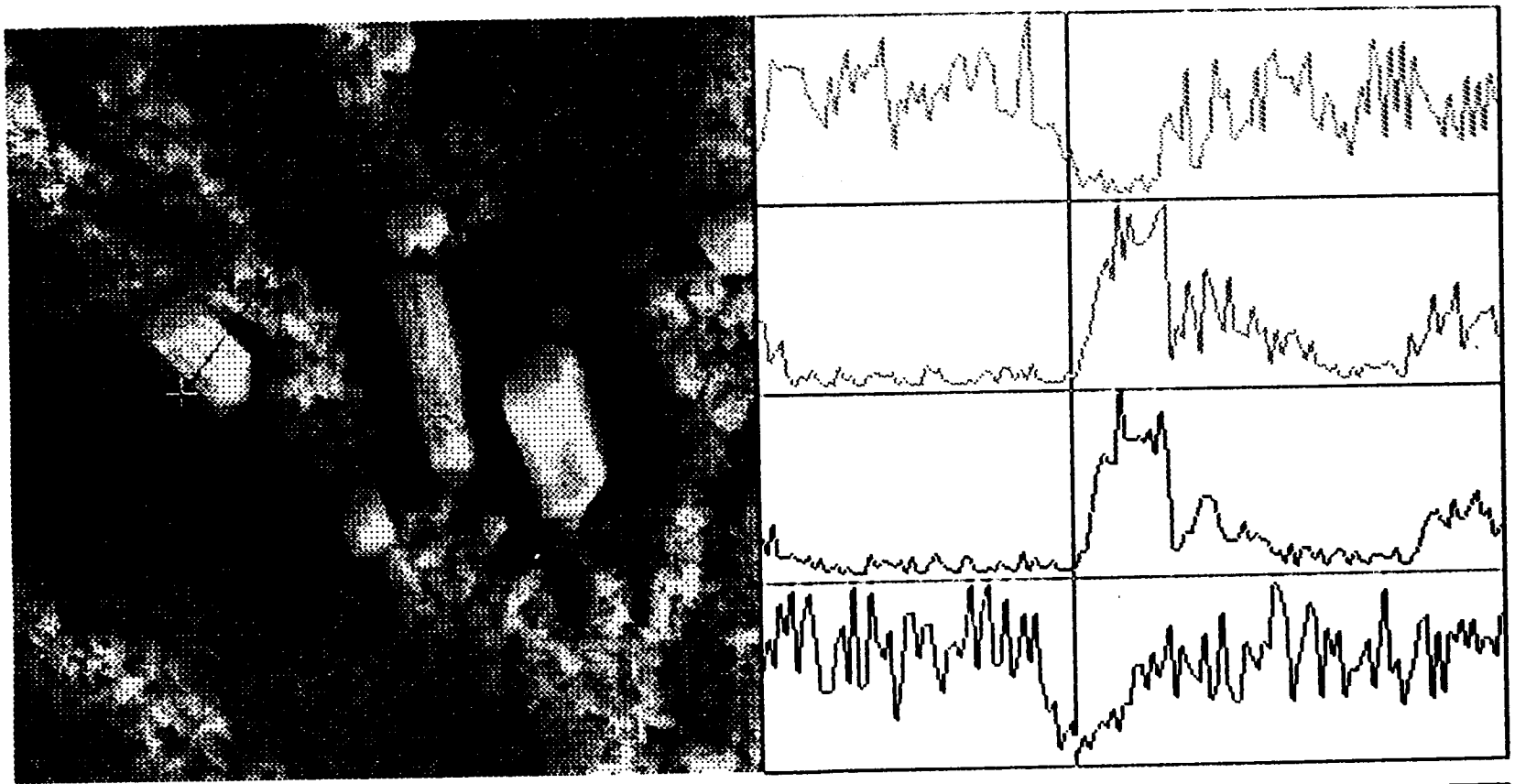

ELEMENT	VFS	INTENSITY
Ti Si	41 55	30
F	81	0
O	47	10

CURSOR DATA	
POINT: 53	DISTANCE: 19.92 uM

LABEL: LSCANTST2

NASA Li/CFx CELL PROBLEM ANALYSIS
Dissected Cell Cover Findings

- Basic components of 316L SS were found on all covers (Fe, Cr, and Ni)
- G8 - Be window detector used
  Found As, Si, and S
- G12 - Ultra thin window detector used
  Found O, F, As, S, Al, Si, and Na
- G10 - Ultra thin window detector used
  Found O, F, As, S, and S

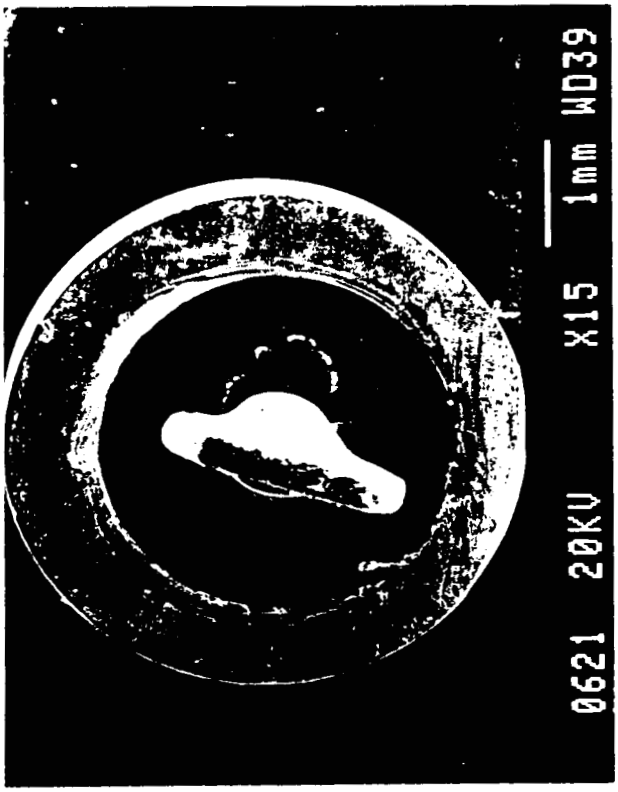
0621 20KV X15 1mm WD39

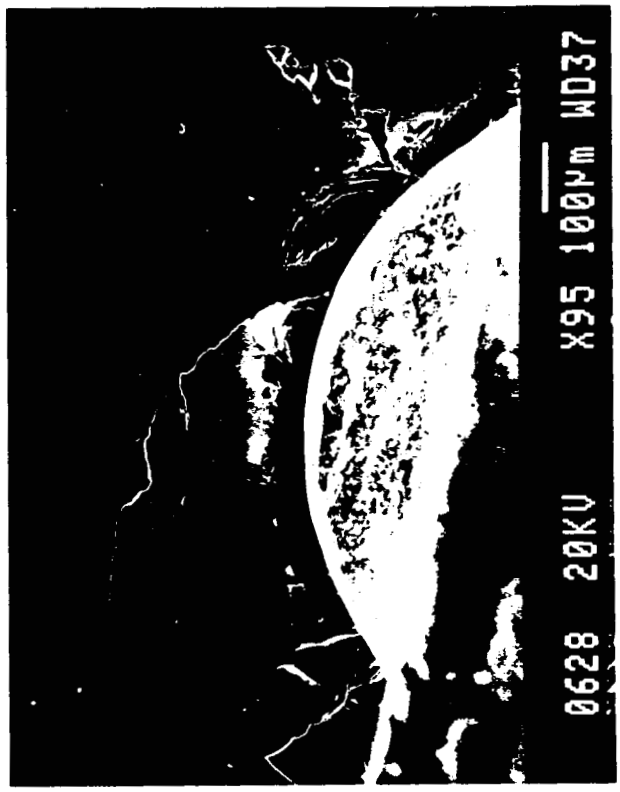
0628 20KV X95 100µm WD37

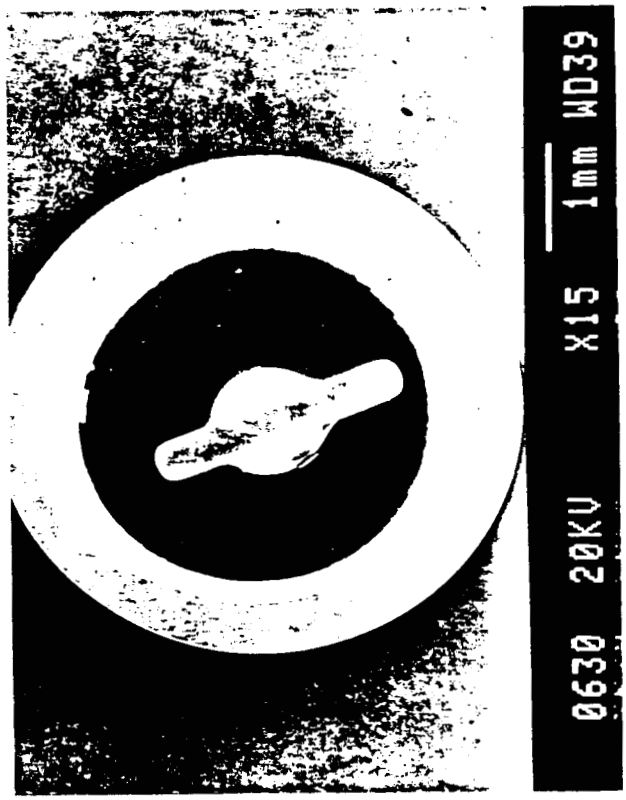
0630 20KV X15 1mm WD39

NASA Li/CFx Cell Problem Analysis
Anion Exchange Chromatography Analysis

December 4 - 6, 1990
Joseph Bytella

The Specialty Battery Facility (SBF) was responsible with the analysis of wiper samples (Scott Utility Wipes) used to wipe down Li/CFx battery components and production equipment. These components and equipment were potentially exposed to thionyl chloride vapors. In the presence of moisture thionyl chloride decomposes to sulfur dioxide and hydrogen chloride. The wipers samples were analyzed for soluble chlorides and fluorides by anion exchange chromatography.

Samples from an identical lot of Scott Utility Wipes (virgin) were cut into the minimum and maximum area sizes (4 and 25 square inches) as the potentiallly exposed samples. These samples were boiled with a minimum of hot deionized water (18 mega ohm) then squeezed and rinsed several times with deionized water into 25ml volumetric flasks. These extracts were tested by an "initial" anion exchange chromatography method for chlorides.

An "optimized" method was developed for optimum accuracy and precision and the virgin samples were retested. The chloride results from this virgin wiper population were statistically analyzed to determine the range of water soluble chlorides. The potentially exposed wiper samples were then analyzed and the results were compared with that of the background population (virgin) to determine if chloride contamination existed.

The virgin and potentially exposed wiper samples were reextracted 4 more times to determine the efficiency of the initial chloride extraction process. The total chlorides (5 extracts) from the both sample groups were reevaluated to determine the extent of chloride contamination on the battery components and equipment.

During the examination of the test chromatographs, fluoride contamination was discovered in wiper samples from the test equipment. An analytical method to determine fluoride was developed. The first 3 extracts from the potentially exposed and virgin wiper samples were tested, and the total fluoride from both groups determined. A comparison of the results from both groups was made to determine the extent of fluoride contamination.

NASA Li/CFx CELL PROBLEM ANALYSIS

Anion Exchange Chromatography Analysis

Joseph Bytella

NASA Aerospace Battery Workshop
4 - 6 December 1990

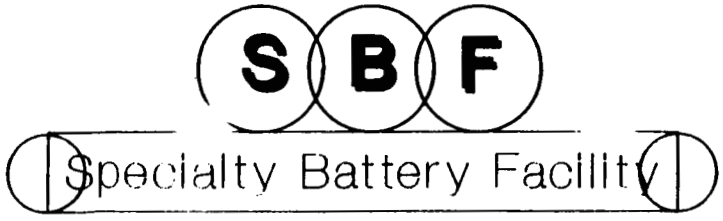

Chloride/Fluoride Contamination

Analysis of Wipers: Sampled Areas

- Analysis of Wipers: Ion Exchange Chromatography
  hot/cold water extraction of SBF wiper blanks
  analyses by initial method
  method optimization and reanalysis
- Accuracy and Precision of Analyses
  accuracy from optimized calibration curve
  precision from multiple injections
- Analysis of Sponsor's Samples/Blanks
  with optimized analytical method
  statistically compared with SBF wiper blanks
- Multiple Extraction Methods
  total fluoride and chloride determinations
  sponsor's sample/blank reanalyses: vs SBF blanks

Analysis Via Ion Exchange Chromatography

Chloride/Fluoride Extraction Methods
Comparison of Methods' Parameters

	Initial Method	Optimized Method
HPLC Column:	anion exchange	anion exchange
Mobile Phase:	borate/gluconate	borate/gluconate
Conductivity Detector Scale:	50 ppm chloride (full scale)	20 ppm chloride (full scale)
Flow Rate:	1.2 ml/min	1.2 ml/min
Injection Size:	50 ul	250 ul
Injection Mode:	syringe	loop (100 ul)
Calibration Range:	0.5 - 50.0ppm Cl	0.10 - 20.0ppm Cl 0.10 - 5.00ppm F
Calibration Curve Standard:	1 point/standard	4 point average/ standard

SAMPLE CHROMATOGRAPHS

Peaks:
"A" - Fluoride
"B" - Bicarbonate
"C" - Chloride

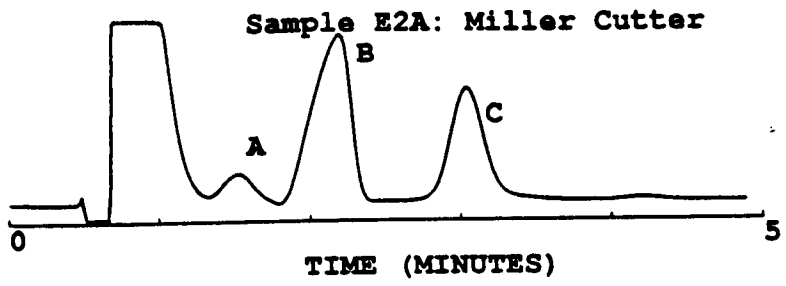

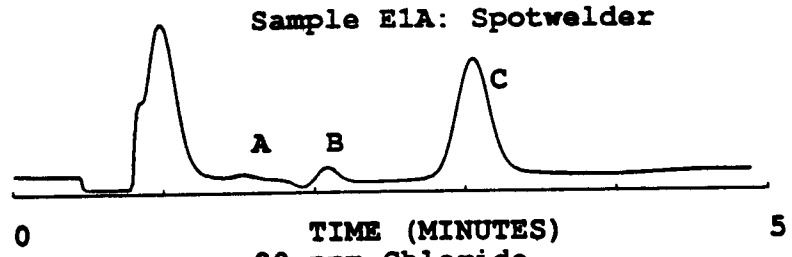

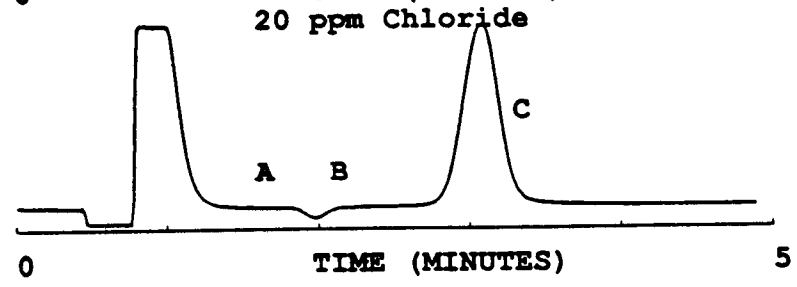

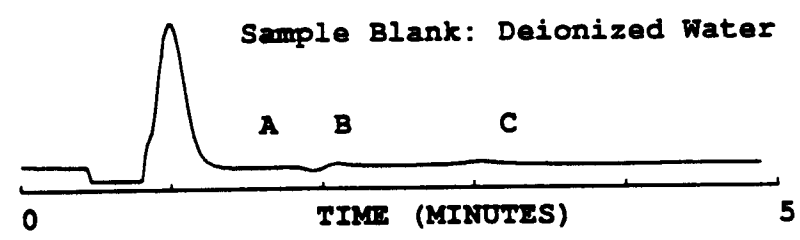

Typical Chloride Calibration Curve
Initial Method: 1 Sam/Cal. Pt.

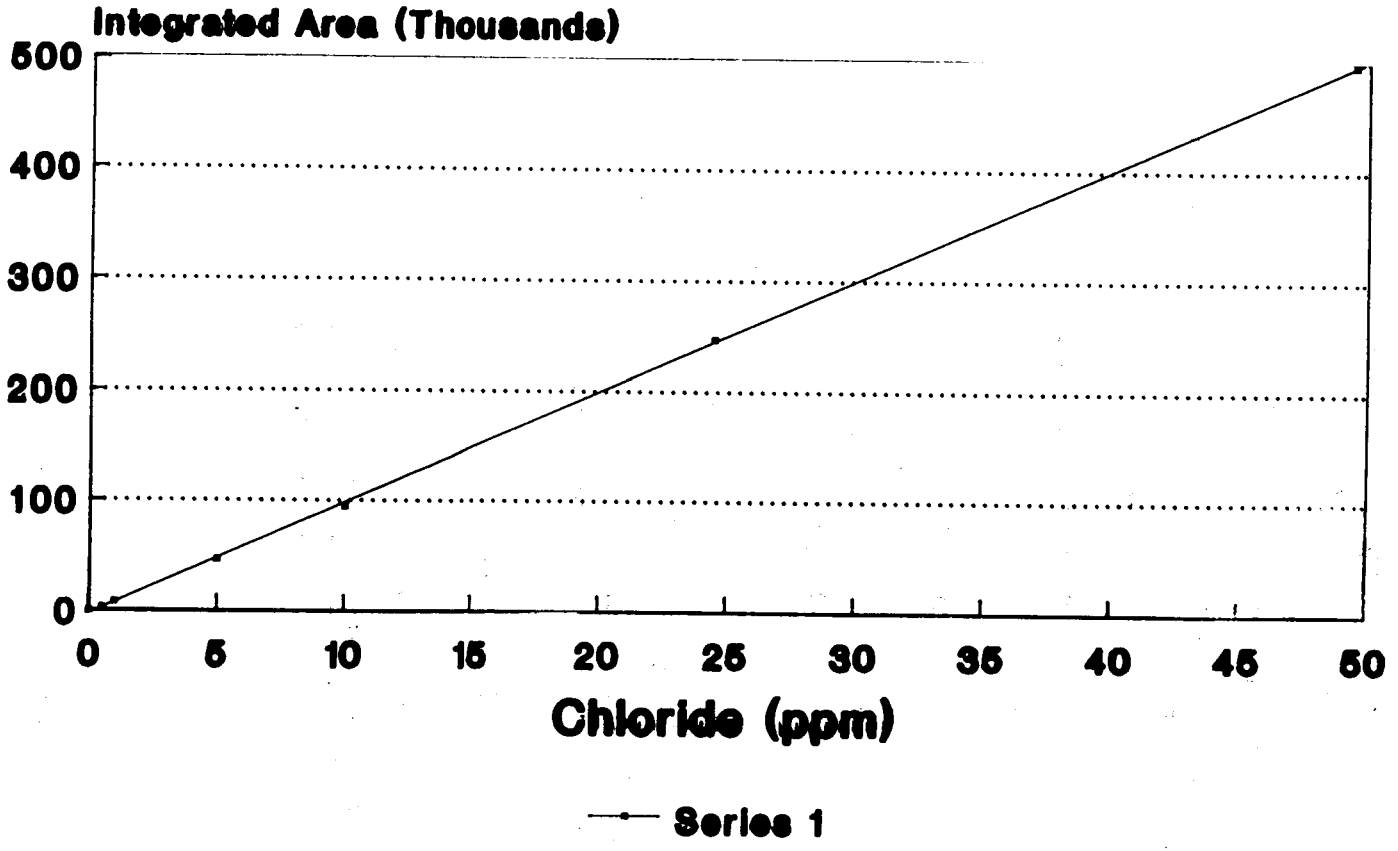

R Squared = 0.9999, 0.50-50ppm Cal.

Chloride in Scott Utility Wipes
Ion Exchange Chromatography

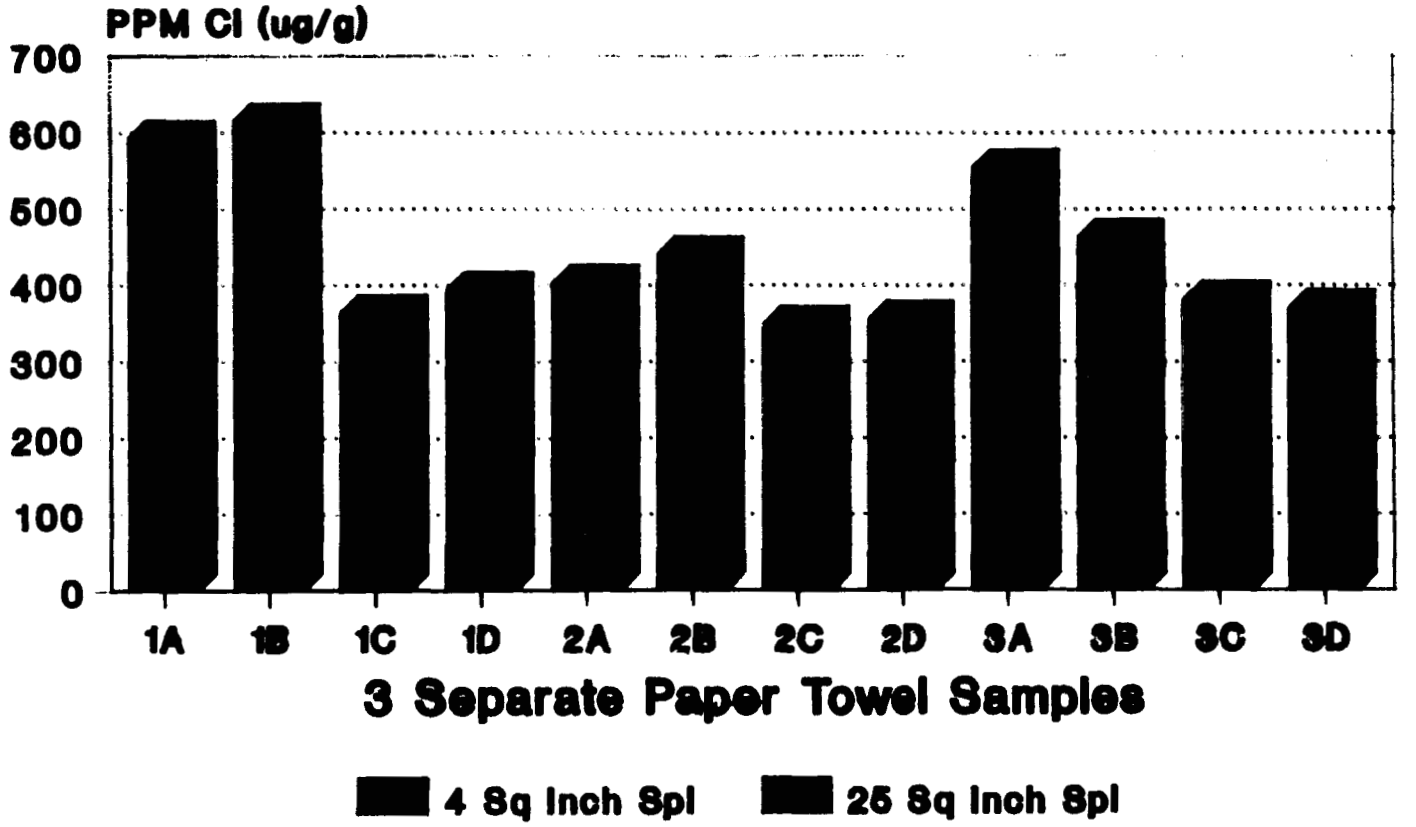

Hot/Cold Water Extracts; 1-50ppm Calibr.

Comparison of Chloride Results(ug/g)
Statistical Analysis of Initial Method

Group	Average	Confidence Limit(99.9%)
2"X 2"	492.2	492.2 +/- 194.1 (39.4%)
5"X 5"	356.0	356.0 +/- 36.6 (10.2%)

Comparison of Two Experimental Means:

If $\bar{X}$(2"X2") - $\bar{X}$(5"X5") < $ts((N1+N2)/N1N2)^{1/2}$ then
No experimental difference between means.

$\bar{X}$(2"X2") - $\bar{X}$(5"X5") = 136.2; $ts((N1+N1)/N1N2)^{1/2}$ = 233.2

Therefore, Both Groups Analyzed As One:

$u = \bar{X} +/- ts/(N)^{1/2}$ = 424.1 +/- 112.8 (26.6%)

12 Sample Group

Precision/Accuracy of Chloride Injections

Initial Cal. Method: 3 Pts/injection

Injections (ppm)	Average Results (ppm)	COV
50.00	50.07 (+0.14%)	2.00 %
25.00	25.03 (+0.12%)	0.73 %
10.00	9.67 (-3.30%)	4.60 %
5.00	4.59 (-8.20%)	9.44 %
1.00	1.20 (+20.00%)	42.55 %
0.50	0.62 (+4.00%)	60.38 %

Group Results Before Dilution Calculations:

2" X 2" Group: 2.00 - 3.00 ppm Chloride

5" X 5" Group: 13.00 - 15.00 ppm Chloride

COV = Coefficient of Variation

Accuracy/Precision of Chloride Injection
5 Injections Vs Calibration Curve

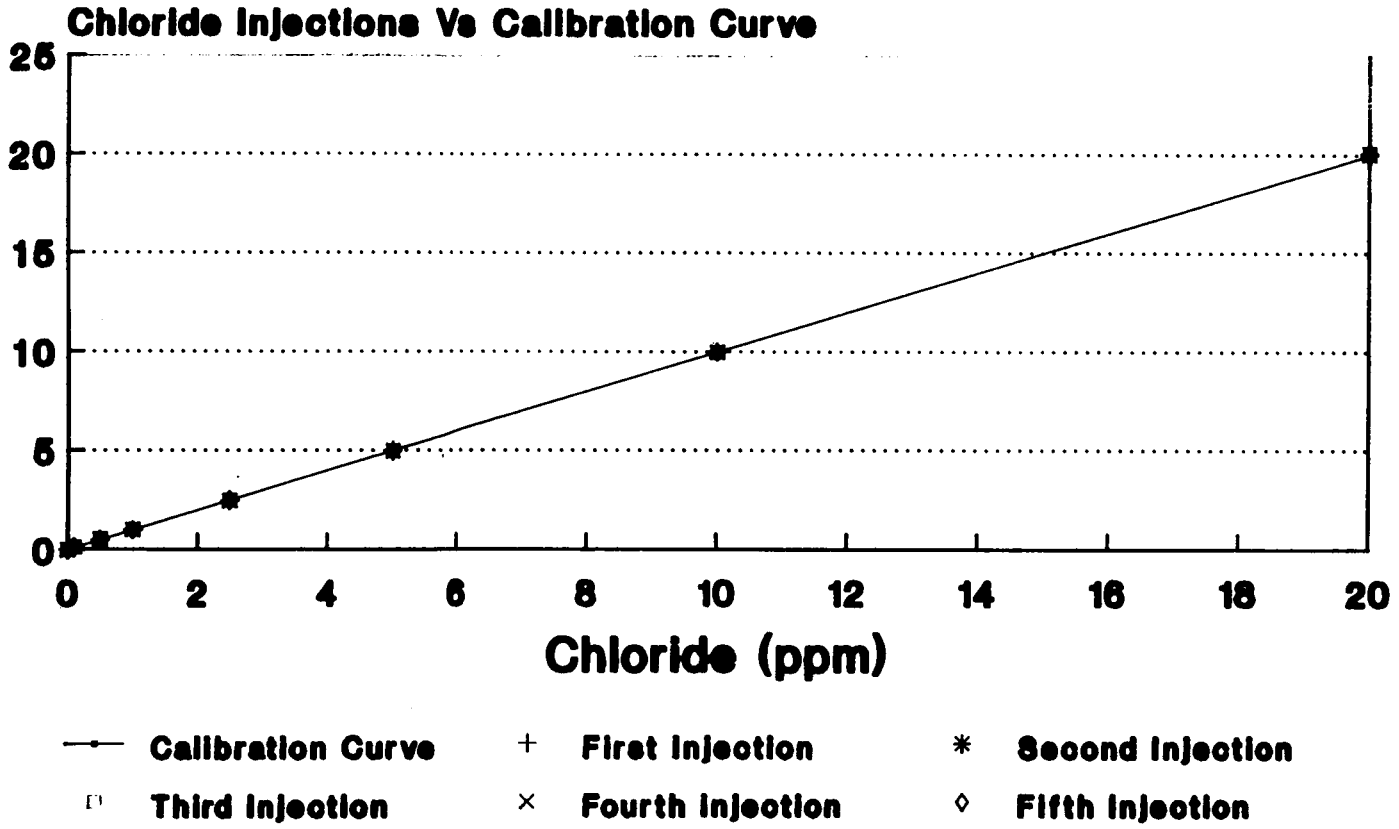

4 Injections/Cal Std, R Squared = 1.0000

Precision/Accuracy of Chloride Injections

5 Separate Injections Vs Cal. Curve

Injections (ppm)	Average Results (ppm)	COV
20.00	20.04 (+0.20%)	0.30 %
10.00	9.98 (-0.20%)	0.20 %
5.00	4.97 (-0.60%)	0.60 %
2.50	2.49 (-0.40%)	1.61 %
1.00	1.01 (+1.00%)	0.99 %
0.50	0.52 (+4.00%)	5.77 %
0.10	0.13 (+30.0%)	7.69 %

COV = Coefficient of Variation

Chloride in Wipes: Optimized Method
Ion Exchange Chromatography

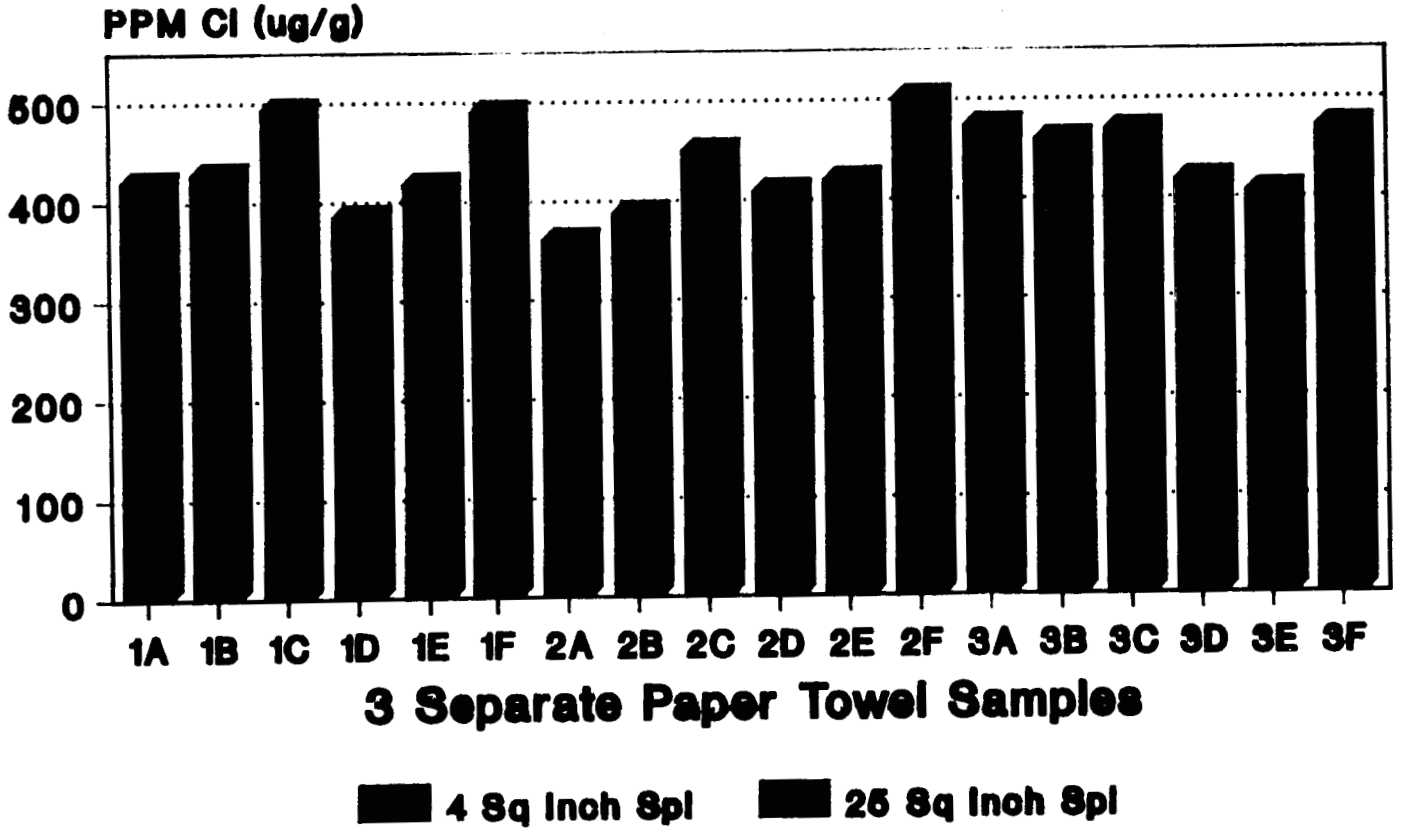

Hot/Cold Water Extracts; 0.05-20 ppm Cal

Comparison of Chloride Results(ug/g)
Analysis of Entire Sample Group: 18

Group	Average	Confidence Limit(99.9%)
2"X 2"	438.4	438.4 +/- 72.2 (16.5%)
5"X 5"	435.9	435.9 +/- 69.6 (16.0%)

Comparison of Two Experimental Means:

If $\bar{X}$ (2"X2")- $\bar{X}$(5"X5") < $ts((N1+N2)/N1N2)^{1/2}$ then
No experimental difference between means.

$\bar{X}$(2"X2")-$\bar{X}$(5"X5")= 2.5; $ts((N1+N1)/N1N2)^{1/2}$ = 53.1

Therefore, Both Groups Analyzed As One:

$u = \bar{X} +/- ts/(N)^{1/2}$ = 437.1 +/- 23.2 (5.3%) ug/g

Optimized Analytical Method

Chloride in Sponsor's Samples
Analysis Via Ion Exchange Chromatography

Spl#	Type	Chloride (ug/g)	Mean Chloride(ug/g)
B2	Back/H2O	465.9/489.9	477.9
B1	Back/Virgin	439.4/523.5	481.5
C3	316L SS	486.2/545.0	515.6
D4	Anode Foil	547.2/580.9	564.1
E1	Spotwelder	839.3	-
E2	Miller Cutter	903.0	-

Statistical Groups (99.9% confidence interval):

Sponsor's Blanks:
476.9 +/- 230.9 ug/g

SBF Blanks:
437.1 +/- 23.2 ug/g

Sponsor's Range:
246.0 - 707.8 ug/g

SBF Range:
413.9 - 460.3 ug/g

Optimized Analytical Method

Total Chloride in Wipes: 5 Extractions
SBF Wiper Blanks: Results (ug/g)

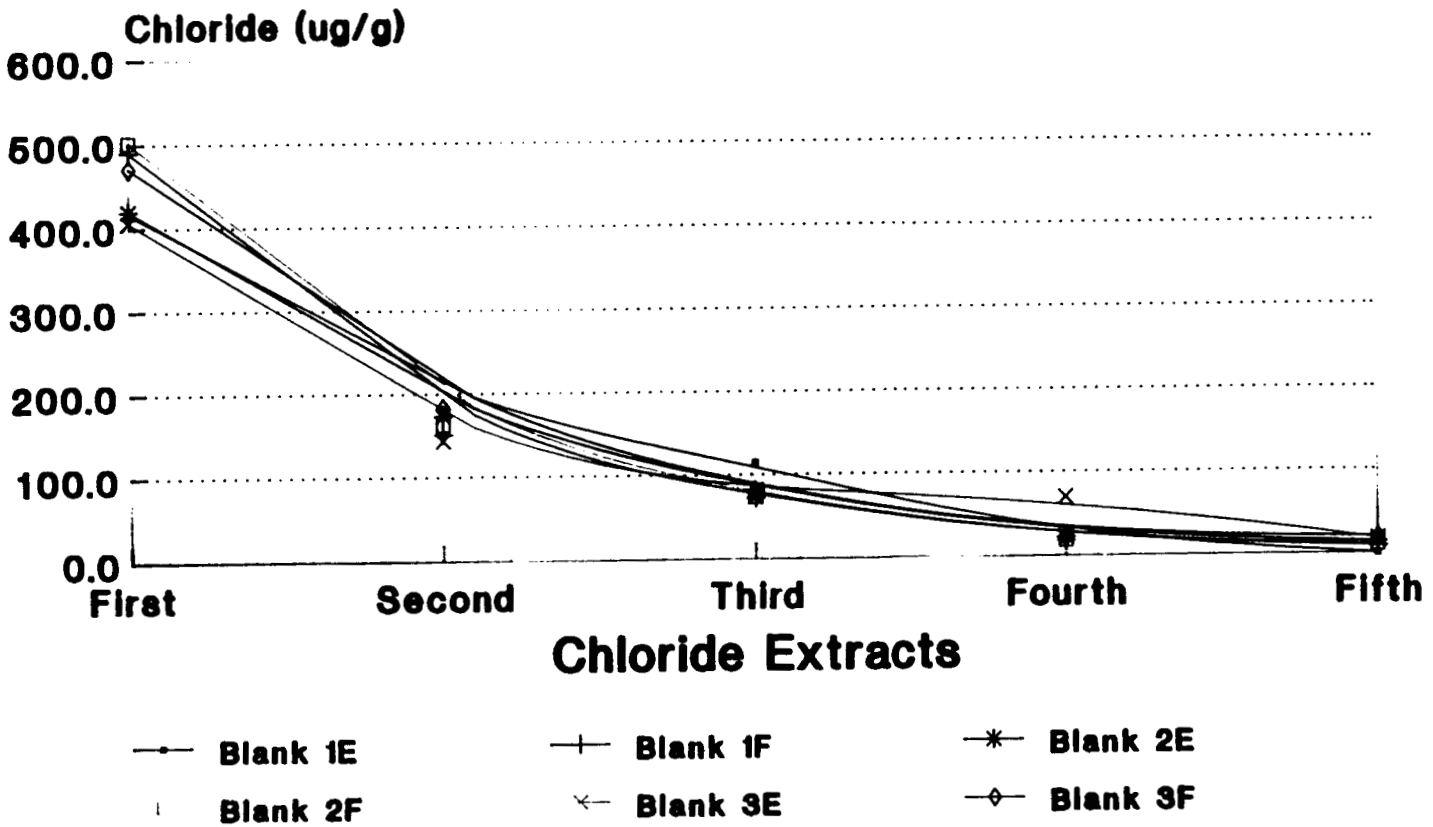

Ion Exchange Chromatography

Total Chloride in Wipes: 5 Extractions
Sponsor's Wipers: Samples/Blanks

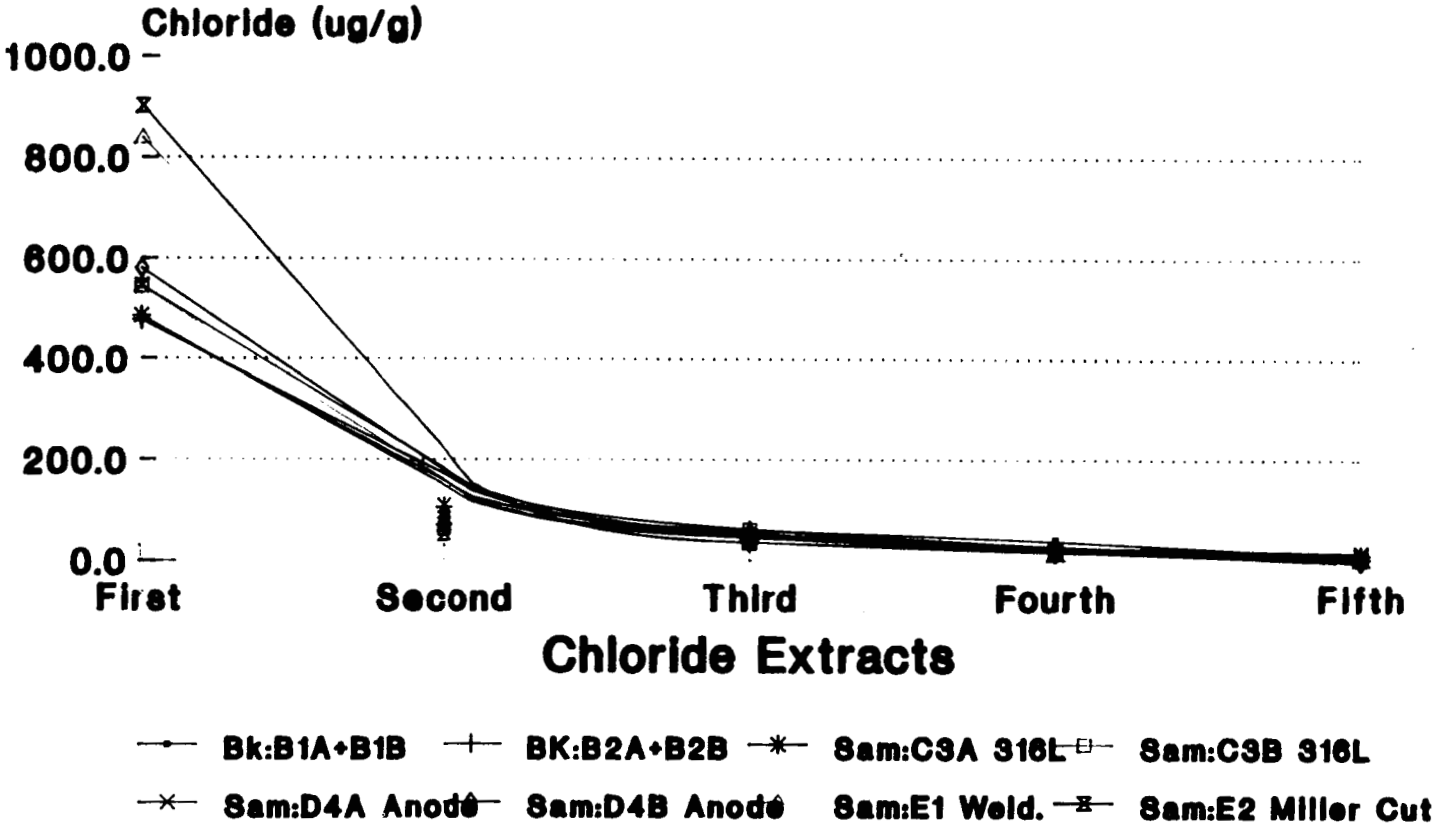

Ion Chromatography, Bks: Aver from 2 Sam

Normalized Graphs: Chloride in Wipes

5 Chloride Extractions: SBF Wiper Blanks

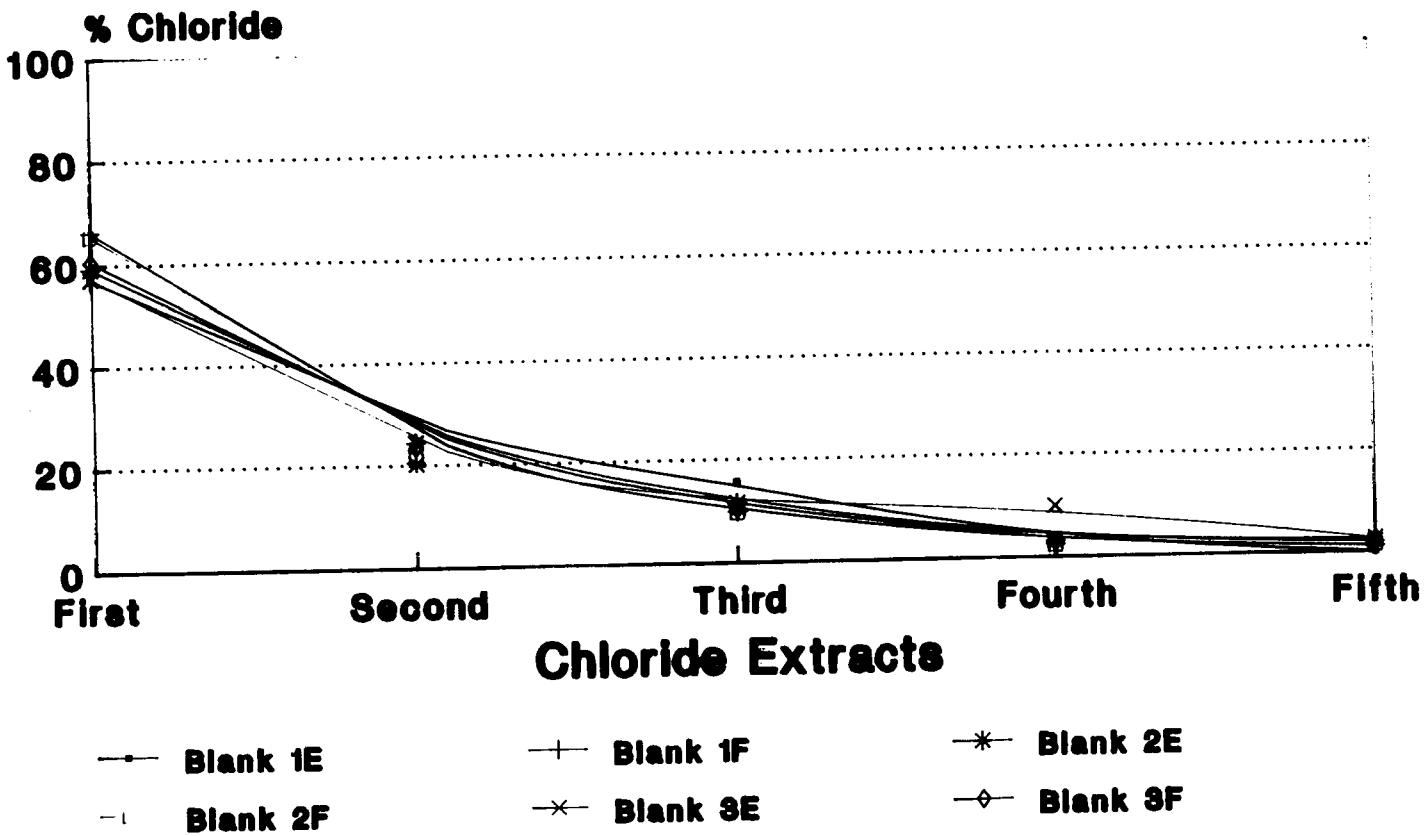

Ion Exchange Chromatography

Normalized Graphs: Chloride in Wipes

5 Chloride Extracts:Sponsor's Blanks/Sam

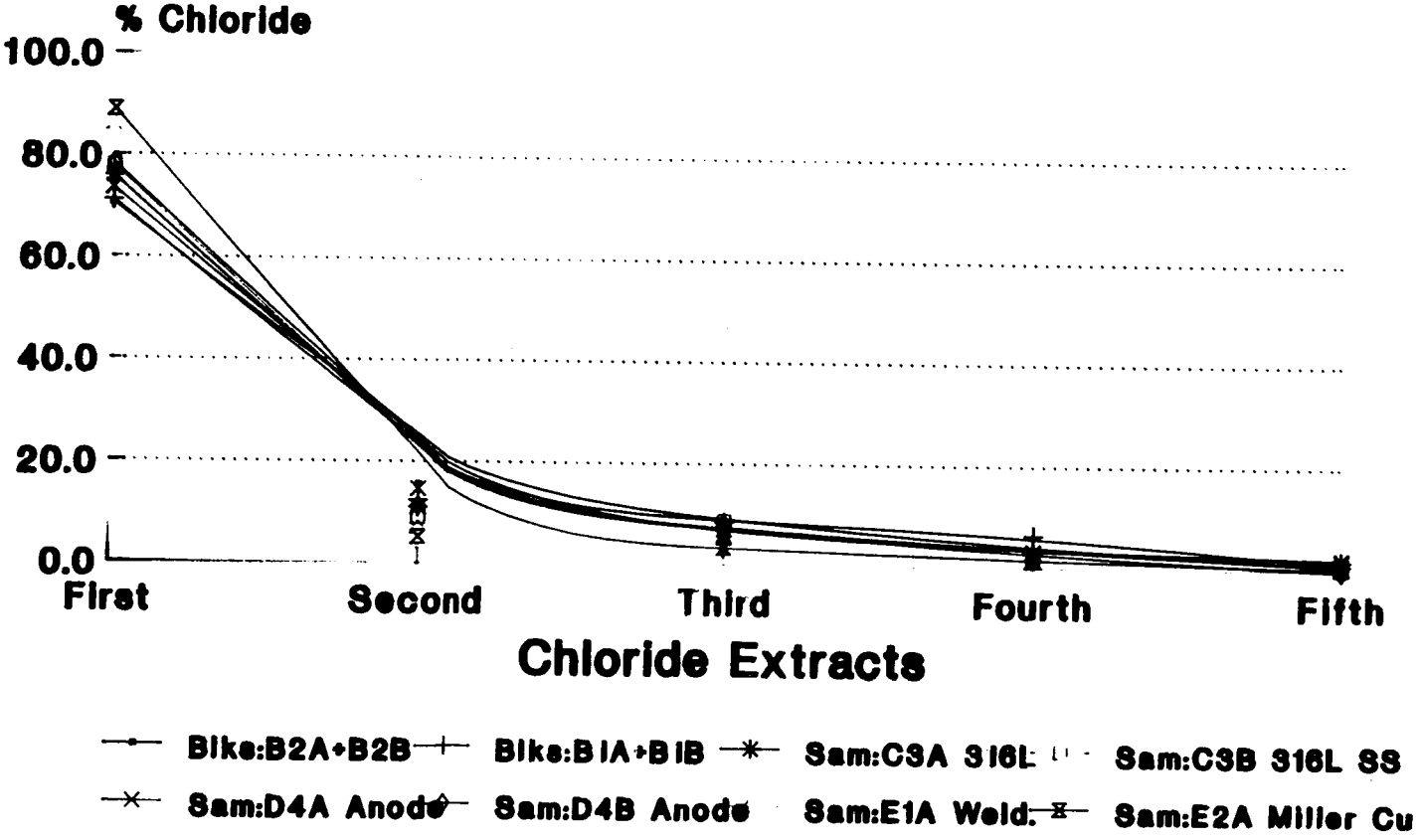

Ion Exchange Chromatography

Total Chloride in Wipes:5 Extractions
Ion Chromatography: Optimized Method

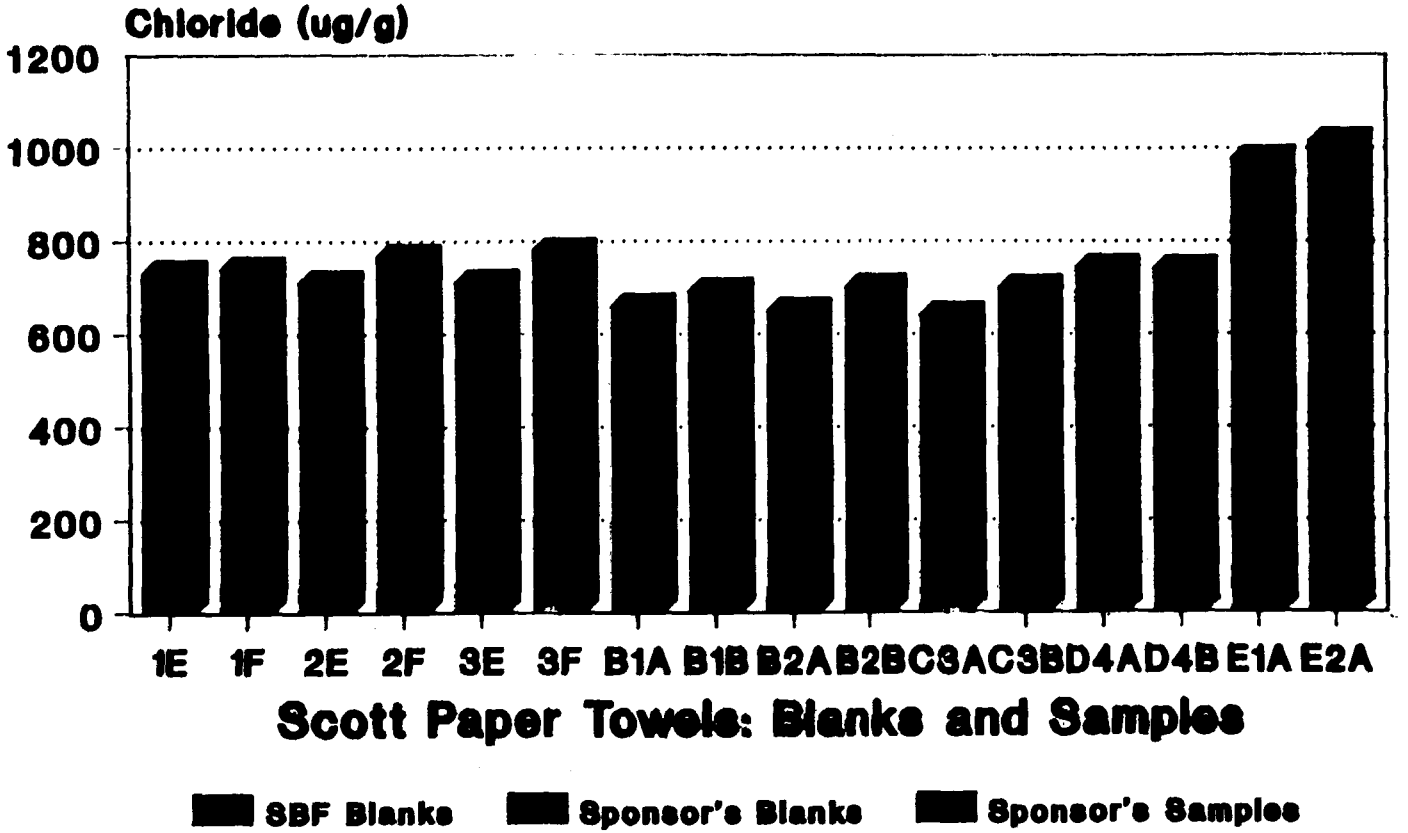

Hot/Cold Water Extracts; 0.10-20 ppm Cal

Chloride in Sponsor's Blanks/Sample

Total Chloride: 5 Extractions

Spl#	Type	Chloride (ug/g)	Mean Chloride(ug/g)
B2	Back/H2O	649.9/700.6	675.3
B1	Back/Virgin	658.7/692.1	675.4
C3	316L SS	639.9/698.9	669.4
D4	Anode Foil	742.7/739.8	741.3
E1	Spotwelder	976.7	-
E2	Miller Cutter	1014.4	-

Statistical Groups (99.9% Confidence Interval):

Sponsor's Blanks:
675.3 +/- 160.0 ug/g

Sponsor's Range:
515.3 - 835.3 ug/g

SBF Blanks:
740.1 +/- 79.3 ug/g

SBF Range:
660.8 - 819.4 ug/g

SAMPLE CHROMATOGRAPHS

Peaks:

"A" - Fluoride
"B" - Bicarbonate
"C" - Chloride

Sample E2A: Miller Cutter

TIME (MINUTES)

Sample E1A: Spot Welder

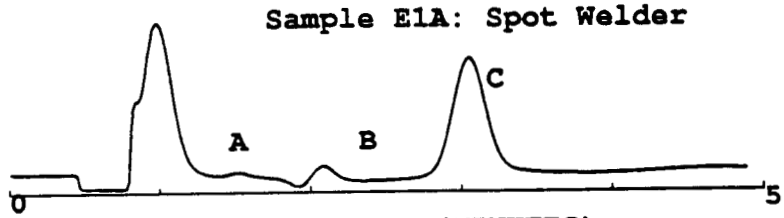

TIME (MINUTES)

150 ppm Bicarbonate

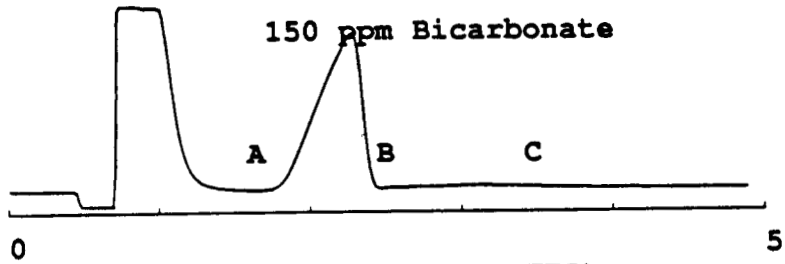

TIME (MINUTES)

5 ppm Fluoride

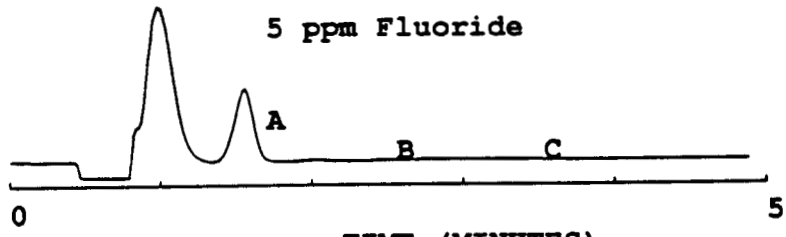

TIME (MINUTES)

Accuracy/Precision of Fluoride Injection
5 Injections Vs Calibration Curve

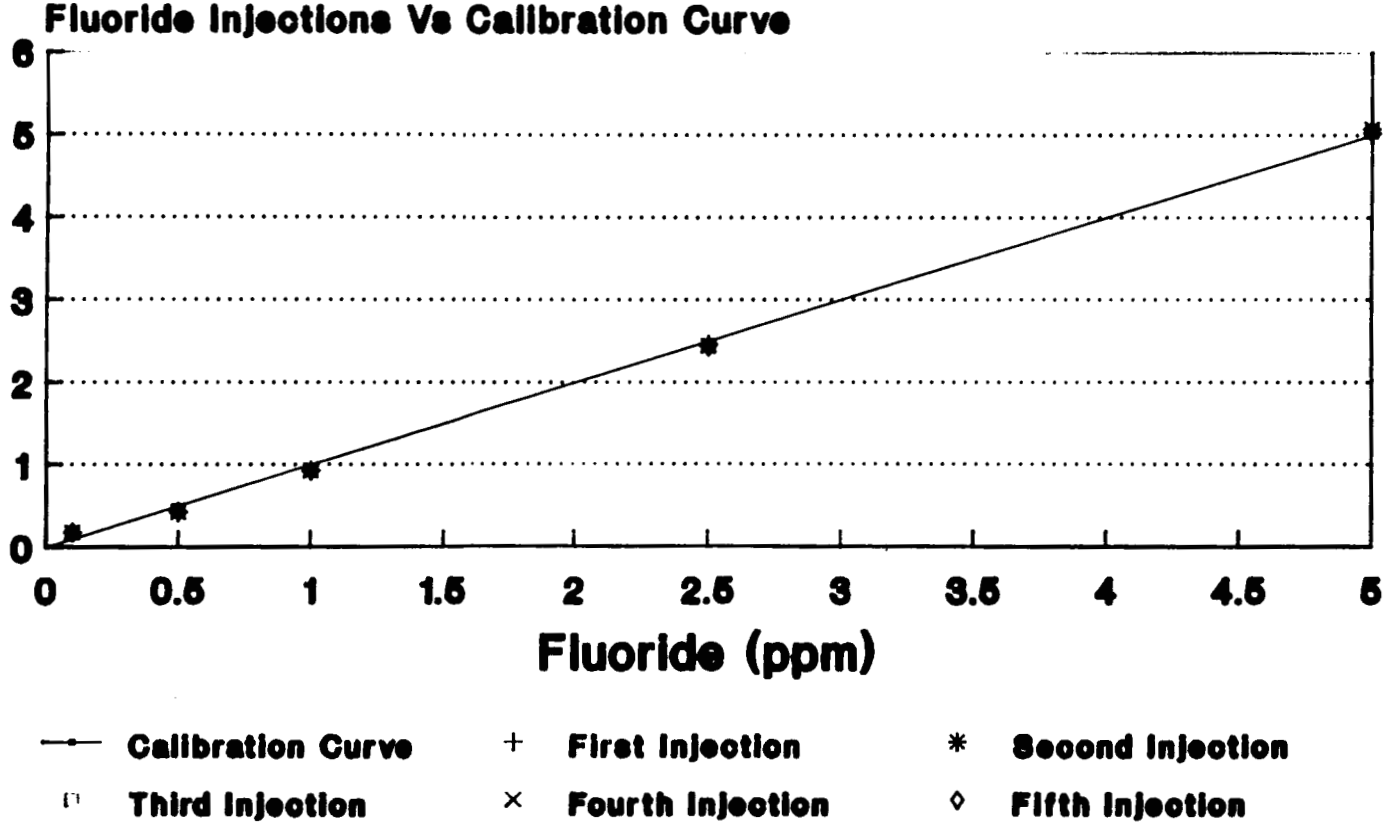

4 Injections/Cal Std, R Squared = 0.9992

Precision/Accuracy of Fluoride Injections

5 Separate Injections Vs Cal. Curve

Injections (ppm)	Average Results (ppm)	COV
5.00	5.06 (+1.20%)	0.43 %
2.50	2.45 (-2.00%)	0.47 %
1.00	0.93 (-7.00%)	0.56 %
0.50	0.43 (-14.00%)	2.54 %
0.10	0.18 (+80.00%)	2.46 %

COV = Coefficient of Variation

Total Fluoride in Wipes: 3 Extractions
SBF Wiper Blanks: Results (ug/g)

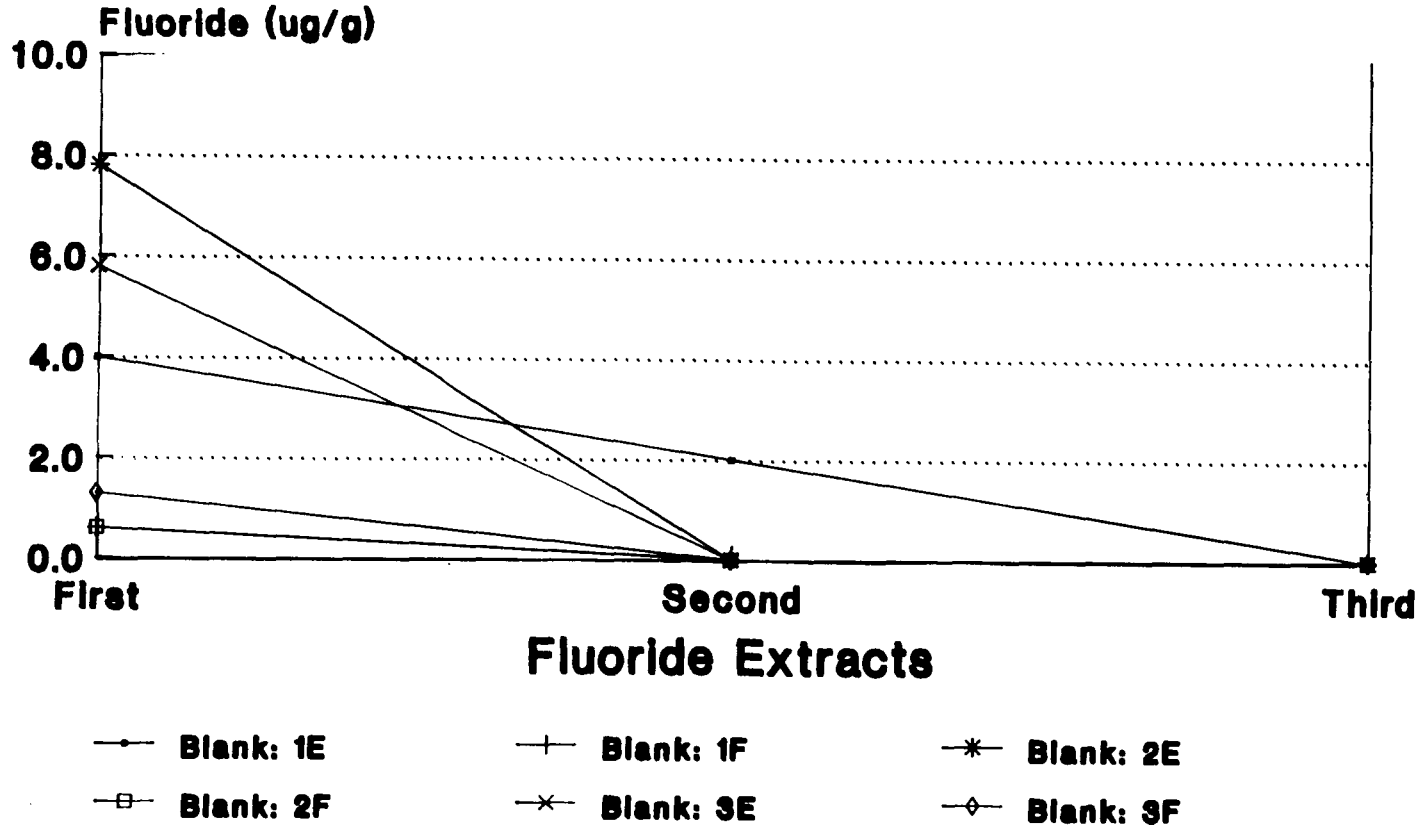

Ion Exchange Chromatography

Total Fluoride in Wipes: 3 Extractions
Sponsor's Wiper Blanks and Samples

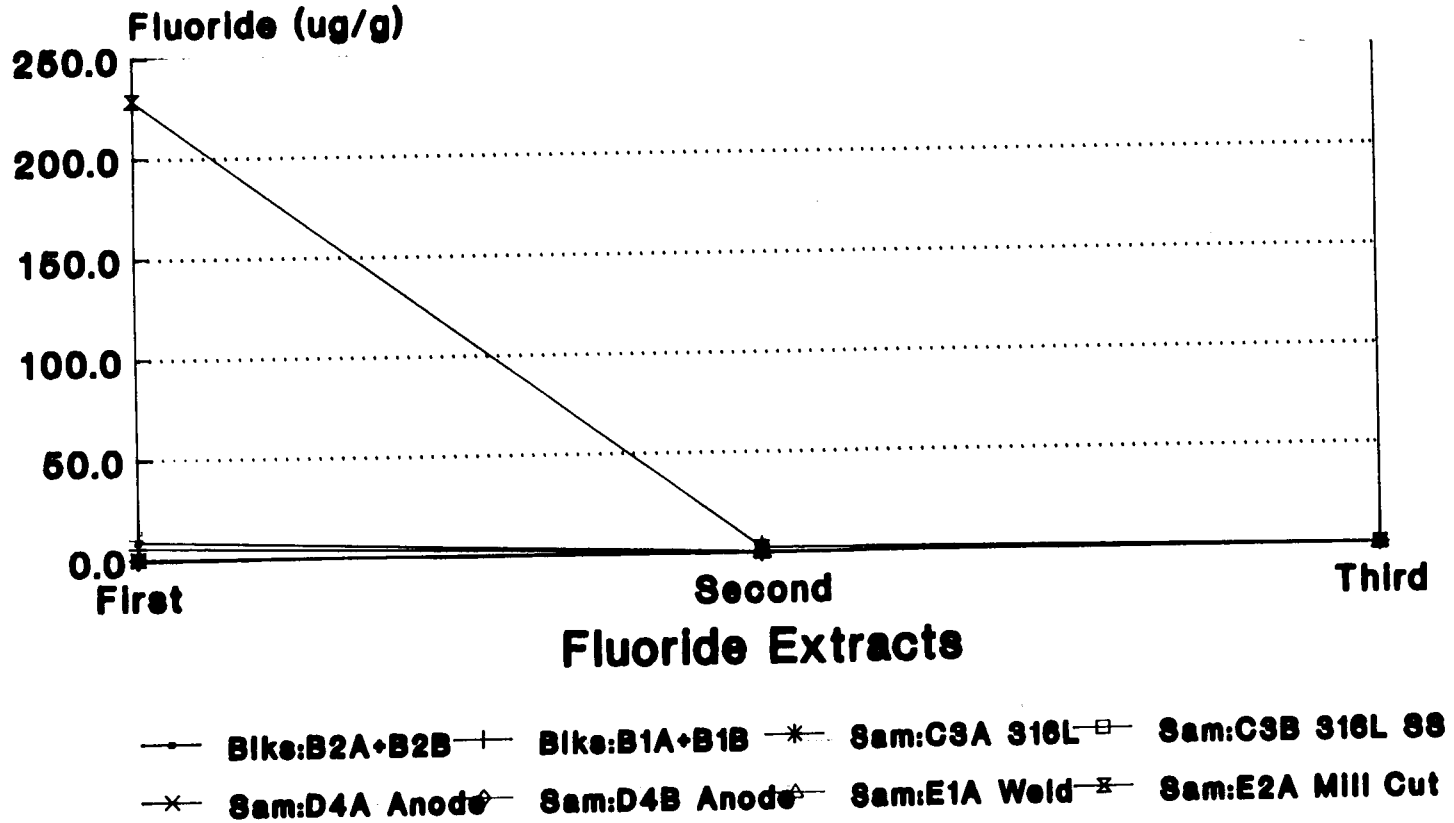

Blanks: Average from 2 Samples

Total Fluoride in Wipes:3 Extractions
Ion Exchange Chromatography

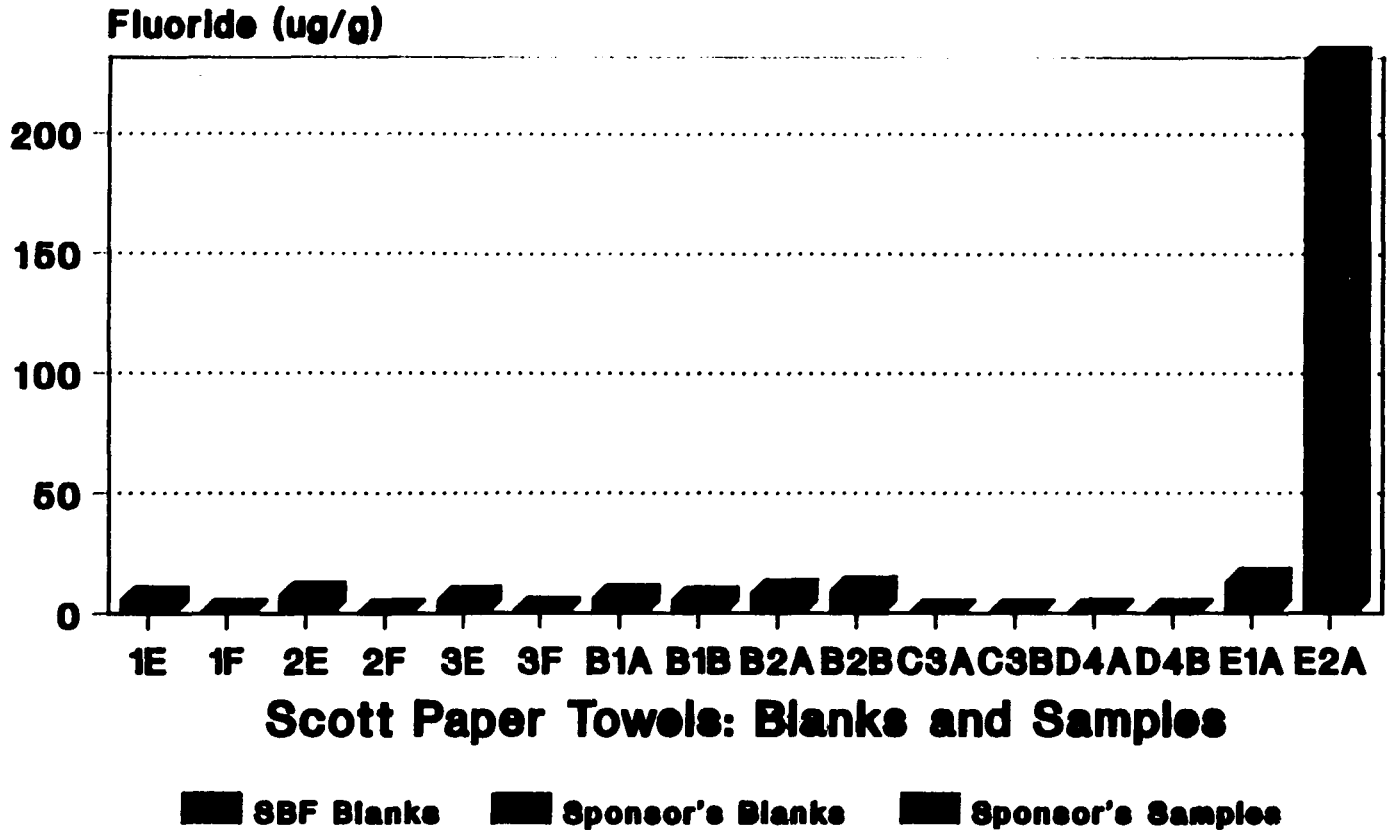

Hot/Cold Water Extracts; 0.1-5.0 ppm Cal

Fluoride in Sponsor's Samples

Total Fluoride: 3 Extractions

Spl#	Type	Fluoride (ug/g)	Mean Fluoride(ug/g)
B2	Back/H2O	8.8/9.9	9.4
B1	Back/Virgin	6.5/5.6	6.1
C3	316L SS	0.3/0.3	0.3
D4	Anode Foil	0.6/0.7	0.7
E1	Spotwelder	13.5	-
E2	Miller Cutter	231.1	-

Statistical Groups (99.9% confidence interval):

Sponsor's Blanks:
7.7 +/- 12.8 ug/g

SBF Blanks:
3.7 +/- 9.0 ug/g

Sponsor's Max:
20.5 ug/g Fluoride

SBF Max:
12.7 ug/g Fluoride

Analysis Via Ion Exchange Chromatography

Conclusions and Results
Extent of Chloride/Fluoride Contamination

- Chloride/Fluoride Extraction Method Optimized
- SBF and Sponsor's Samples/Blanks Analyzed
  total chloride/fluoride: multiple extractions
- Miller Cutter/Spotwelder Contaminated With Chloride
  approximately 150 - 200 ppm above blanks
- Miller Cutter Contaminated With Fluoride
  approximately 200 - 250 ppm above blanks

Calorimetric Determination of the Thermoneutral Potential for Li/BrCl in $SOCl_2$ (BCX) Cells

by

Eric C. Darcy
NASA-Johnson Space Center, Houston, TX

Eric E. Kalu and Ralph E. White
Texas A&M University, College Station, TX

BATTERY WORKSHOP PROCEEDINGS

1990

ABSTRACT

Proliferation of lithium cells into large modular battery packs are projected for future space applications. Assuring battery design safety while maintaining high energy density requires accurate and precise knowledge of the thermal parameters of the battery cell. Specifically, the thermoneutral potential was determined using heat conduction calorimetry on Li/BrCl in $SOCl_2$ (BCX) DD-cells and compared to measurements obtained on Li/$SOCl_2$ D-cells. Over 20 to 60 °C, the Li/BCX cells were found to have a thermoneutral potential significantly higher (near 4.0 volts) than that for the Li/$SOCl_2$ cells tested. The higher heat generation measured during discharge reflects the higher electrochemical polarization observed with the BCX cells.

NASA Johnson Space Center | Engineering Directorate

Agenda	Propulsion and Power Division	
	Eric Darcy	12/6/90

- Theory
- Experimental Method and Equipment
- Cells Tested
- Results
  - Heat Conduction Calorimetry
  - Drop Calorimetry
- Conclusions

Proliferation of the cells into large modular battery designs are projected for future space applications. These designs will require precise determination of cell thermal parameters. This will enable accurate thermal analysis of the battery system to insure design safety while maintaining a maximum energy density. Specifically, the heat capacity and the thermoneutral potential are parameters of key interest.

The method of drop calorimetry involves measuring the energy (Joules) gained or lost from a sample that is transferred from a bath at temperature A to one at temperature B. This energy, E, is related to the heat capacity of the sample, C_p, according to

$$E = \int Q\, dt = \int m\, C_p\, dT \qquad [1]$$

where m = mass of the sample, kg
T = temperature, °K
Q = heat rate, W
t = time, s

By integrating the area under the heat rate curve one can obtain the bulk heat capacity of a cell transferred from one temperature bath to another, $C_p = E/m(T_B - T_A)$.

Heat conduction calorimetry enables measuring the heat generation rate, Q, of the cell during discharge which is related to the cell thermoneutral potential, E_{tn}, according to

$$Q = (E_{tn} - E_{lv})\, I \qquad [2]$$

where E_{lv} = cell load voltage, V
I = cell load current, A

The thermoneutral potential is defined as the cell potential where the cell electrochemical reactions are neither exothermic nor endothermic. Measuring Q allows a calculation of E_{tn} which can be used to predict cell heat generation at various load conditions.

NASA Johnson Space Center

Engineering Directorate

Calorimetry Theory	Propulsion and Power Division	
	Eric Darcy	12/6/90

Drop Calorimetry

- Transfer cell from equilibration bath (T_A) to calorimeter bath (T_B)
- Energy gained or lost by cell is related to its effective heat capacity (Cp)

$$E = \int Q\,dt = \int m\,Cp\,dT$$

- Calculate Cp from measured values of heat (Q), mass (m), time (t) and temperature (T)

Heat Conduction Calorimetry

- Measure cell heat generation (Q) during discharge
- Heat generation is related to the effective thermoneutral potential (E_{tn})

$$Q = (E_{tn} - E_{lv})\,I$$

- Calculate E_{tn} from measured cell voltage (E_{lv}), current (I), and heat (Q)

A Hart Scientific Calorimeter System, Model # S77XX, designed for heat conduction calorimetry and drop calorimetry was used. The system can accommodate samples 5.5" diameter by 11" tall and measure heat sources from 10 mW to 50 W. An aluminum cell holder was designed to conduct heat from the cell to the chamber walls (Fig. 1).

The calorimeter relies on the Seebeck Effect of thermoelectric sensors mounted in the chamber walls to generate a voltage signal proportional to the small temperature gradient between the sample and chamber walls immersed in a water bath. This design permits standard shaped samples to be tested dry without immersing them in liquid. The calorimeter system contains an additional water bath to equilibriate the sample for the drop method. The water baths are continuously stabilized to set temperatures within +/- 0.002 °C.

NASA Johnson Space Center — Engineering Directorate

Experimental Method and Equipment	Propulsion and Power Division	
	Eric Darcy	12/6/90

Calorimeter system (Hart Scientific, Inc.) features

- Thermoelectric sensors in chamber walls to measure temperature gradient as a voltage gradient
- Chamber volume; 5.5"diameter by 12" high
- Cells placed in a conductive holder
  - cell leads are heat sinked by copper segments
  - no oil mess
- Separate equilibration bath for drop calorimetry
- Heat, voltage, current, time, and water bath temperature digitally recorded

Precision and Accuracy

- Heat conduction calorimetry (HCC) calibrated with a resistor
- Drop calorimetry calibrated with a known metal sample
- Baths are maintained at set temperatures from 0 to 100 C within +/- .002 C
- Heat losses through leads and/or air bath are zeroed
- Cell runs are performed under the same conditions as calibration runs
- Previous HCC experiment achieved < 0.4% error for 18 to 40 W sources

The main calorimeter water bath has an air bath above it which can be set at the same temperature to minimize temperature gradients in wire leads from the cell to the exterior of the chamber. The data acquisition system monitored the cell current and voltage, the water bath temperature, and the heat rate from the source or sink. A Kepco bipolar operational power supply, Model BOP36-12M, was used for the constant current cell discharge.

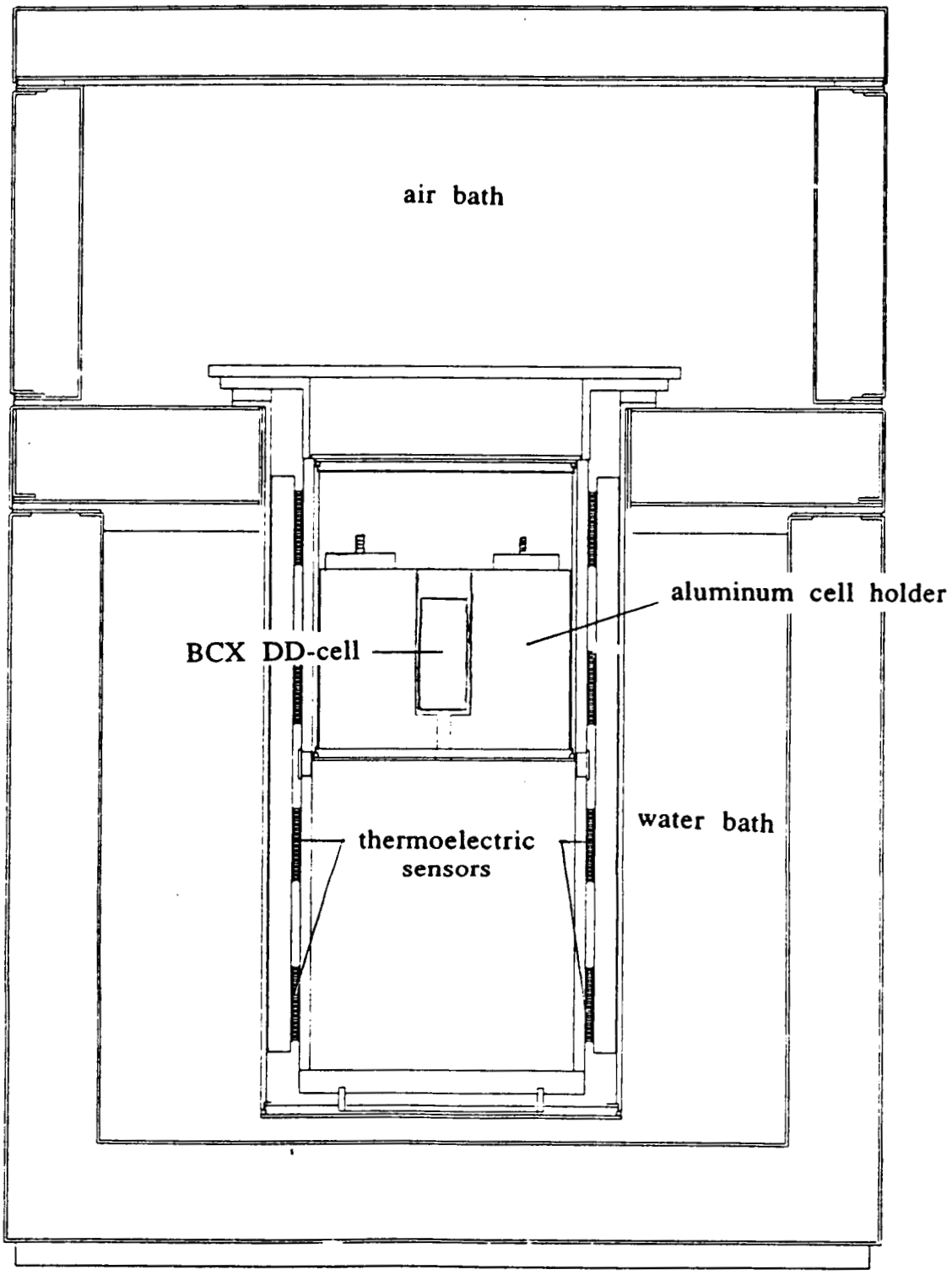

Fig. 1. Schematic of calorimeter with DD-cell and cell holder inside calorimeter chamber.

The cells tested were JSC's Li-BCX DD-cell, P/N 3B2085-XA, and JPL's Li-$SOCl_2$ D-cell, P/N 6P204-ST, both manufactured by Wilson Greatbatch, Ltd. The DD-cell has a capacity of 20 Ah at a maximum load of 1.0 ohm at room temperature with a working electrode surface area of 372 cm^2. The cell has been extensively characterized and will soon be qualified. It is a direct scale-up of JSC's D-cell which has flown on Shuttle since 1982. The high-rate $SOCl_2$ D-cell tested is rated at 10 Ah at 5A at room temperature and has a working electrode area of 530 cm^2. Prototypes of these cells are being evaluated at JSC. Full scale characterization and qualification have not begun yet.

Lithium Cells Tested

- BCX DD-cell (P/N 2085-XA)
  - 20 Ah capacity at 1 ohm @ room temperature
  - working electrode surface area = 372 sq. cm
  - BCX D-cell has flown on Shuttle since 1982

- $SOCl_2$ D-cell (P/N 6P204-ST)
  - 10 Ah capacity at 5A @ room temperature
  - JPL design with working electrode surface area = 530 sq. cm
  - prototypes tested at JSC, not qualified for flight or characterized yet

The heat conduction calorimetry calibration was conducted by powering a resistor inside the cell holder in the calorimeter chamber. The calorimeter and cell holder combination has a response time of slightly less than three hours to reach equilibrium. The D and DD-cells were discharged at a constant current of 1.00 A and 2.00 A, respectively, with all leads and connections identical to the resistor calibration run, which exhibited no more than 0.8% error in measuring heat. The cell voltage, the measured heat generation, and the calculated effective thermoneutral potential are shown for each cell in the following figures. The effective thermoneutral potential appears to depend on temperature, depth-of-discharge, and cell design and chemistry.

At all the temperatures, the BCX cells have a higher effective thermoneutral potential by at least 0.1 volts. Referring to other discharge data on both cells to compare them at the same current density, the $SOCl_2$ cells discharge at very slightly higher average load voltage than the BCX cells Consequently, the BCX cell generates more heat the $SOCl_2$.

Interestingly, boths cells appeared to be more thermal efficient at 40 C than at 20 or 60 C. Two BCX cells were discharged in identical conditions at 20 C and variances obtained between the thermoneutral potentials measured was 0.03 volts or 0.8%.

Results	Propulsion and Power Division	
	Eric Darcy	12/6/90

Heat Conduction Calorimetry Results

Temperature in C	Cell chemistry	Range of effective E_{tn}, volts	Ave Polarization (E_{tn} - E_{tv}), volts
20	$Li/SOCl_2$	3.78 - 3.82	0.63
	Li/BCX	3.87 - 3.92	0.90
40	$Li/SOCl_2$	3.80 - 3.83	0.48
	Li/BCX	3.93 - 3.97	0.83
60	$Li/SOCl_2$	3.80 - 4.00	0.55
	Li/BCX	4.00 - 4.21	0.92

* $Li/SOCl_2$ cells were discharged at 1 A (1.89 mA/cm^2)
** Li/BCX cells were discharged at 2 A (5.37 mA/cm^2)
*** Error on thermoneutral potential is +/- 0.8%
**** Reproducibility on thermoneutral potential is +/- 0.8% at 20 C

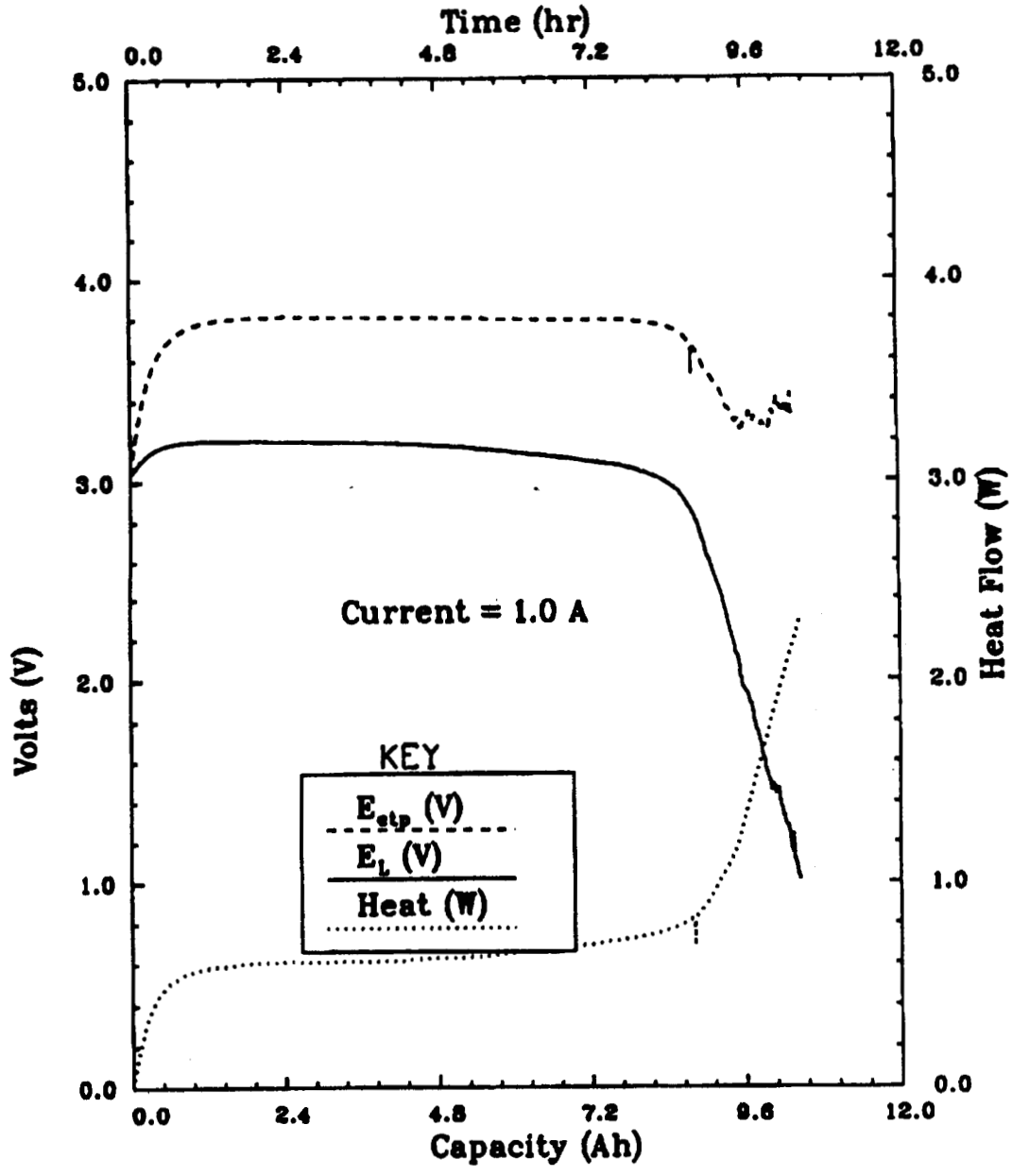

Fig. d10: Effective thermoneutral Potential, load voltage and rate of heat generation for a Li/$SOCl_2$ cell at 20° C.

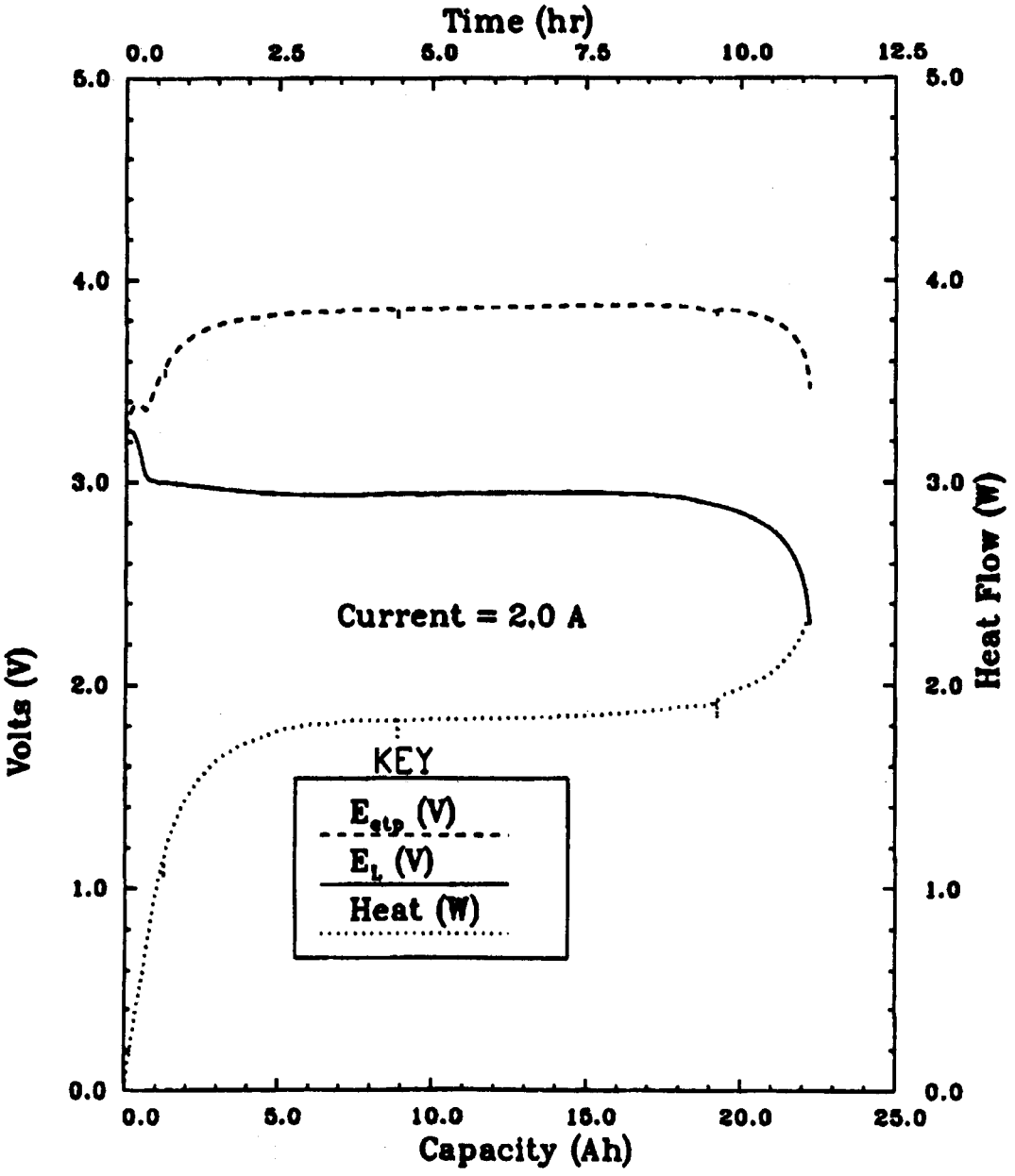

Fig. dd1: Effective thermoneutral Potential, load voltage and rate of heat generation for a Li/BCX cell at 20° C.

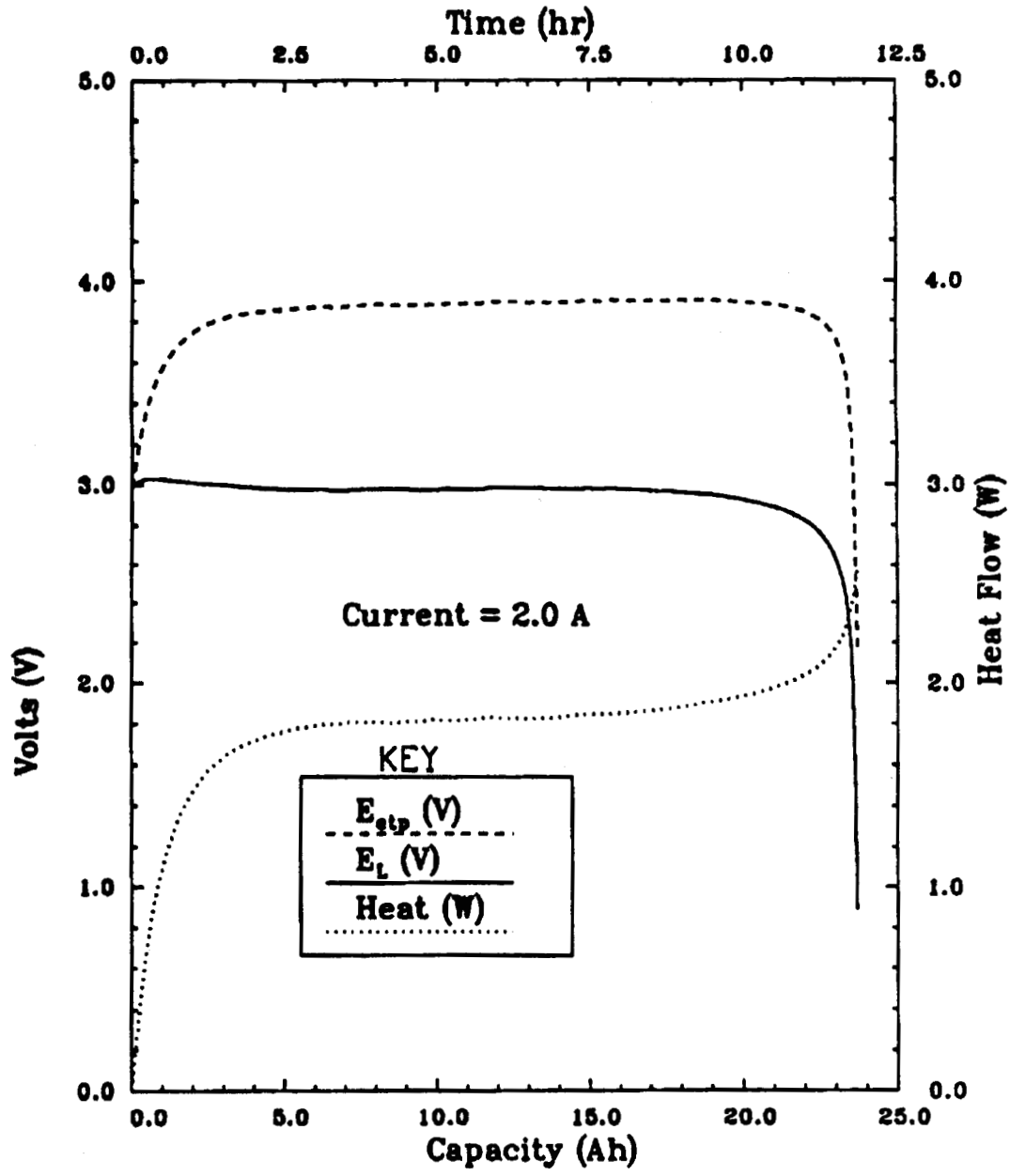

Fig. dd44: Effective thermoneutral Potential, load voltage and rate of heat generation for a Li/BCX cell at 20° C.

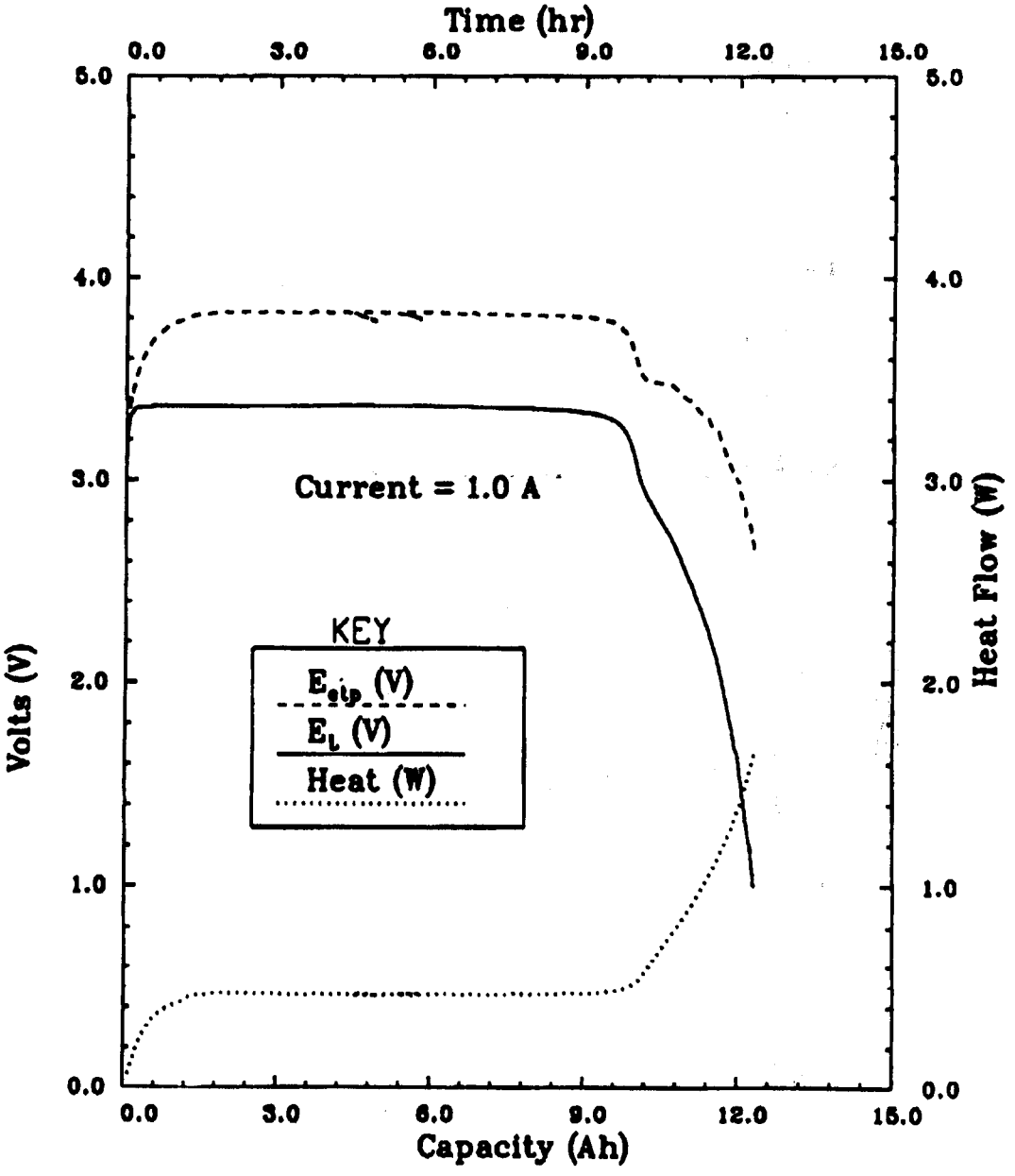

Fig. d6: Effective thermoneutral Potential, load voltage and rate of heat generation for a Li/$SOCl_2$ cell at 40° C.

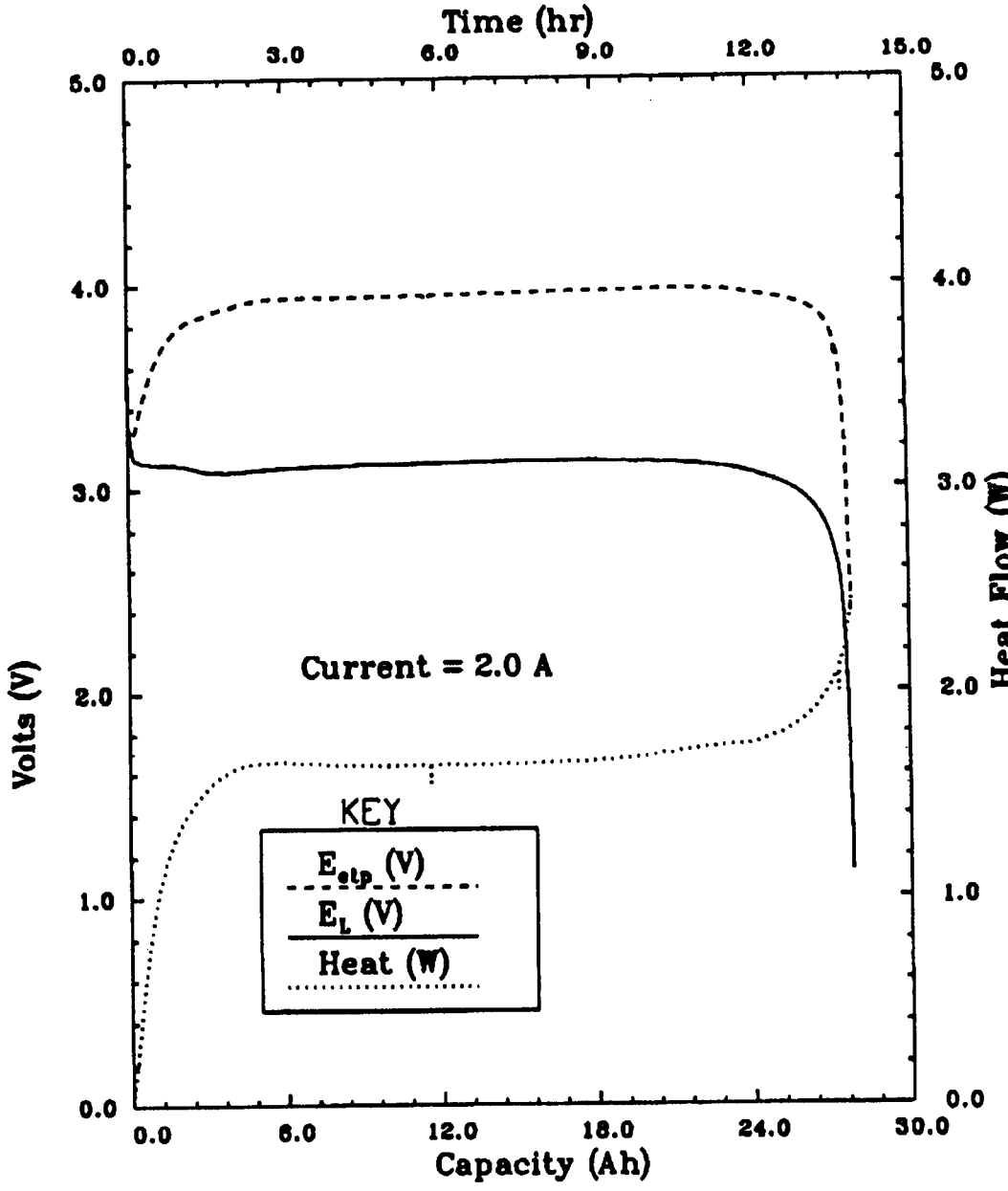

Fig. dd12: Effective thermoneutral Potential, load voltage and rate of heat generation for a Li/BCX cell at 40° C.

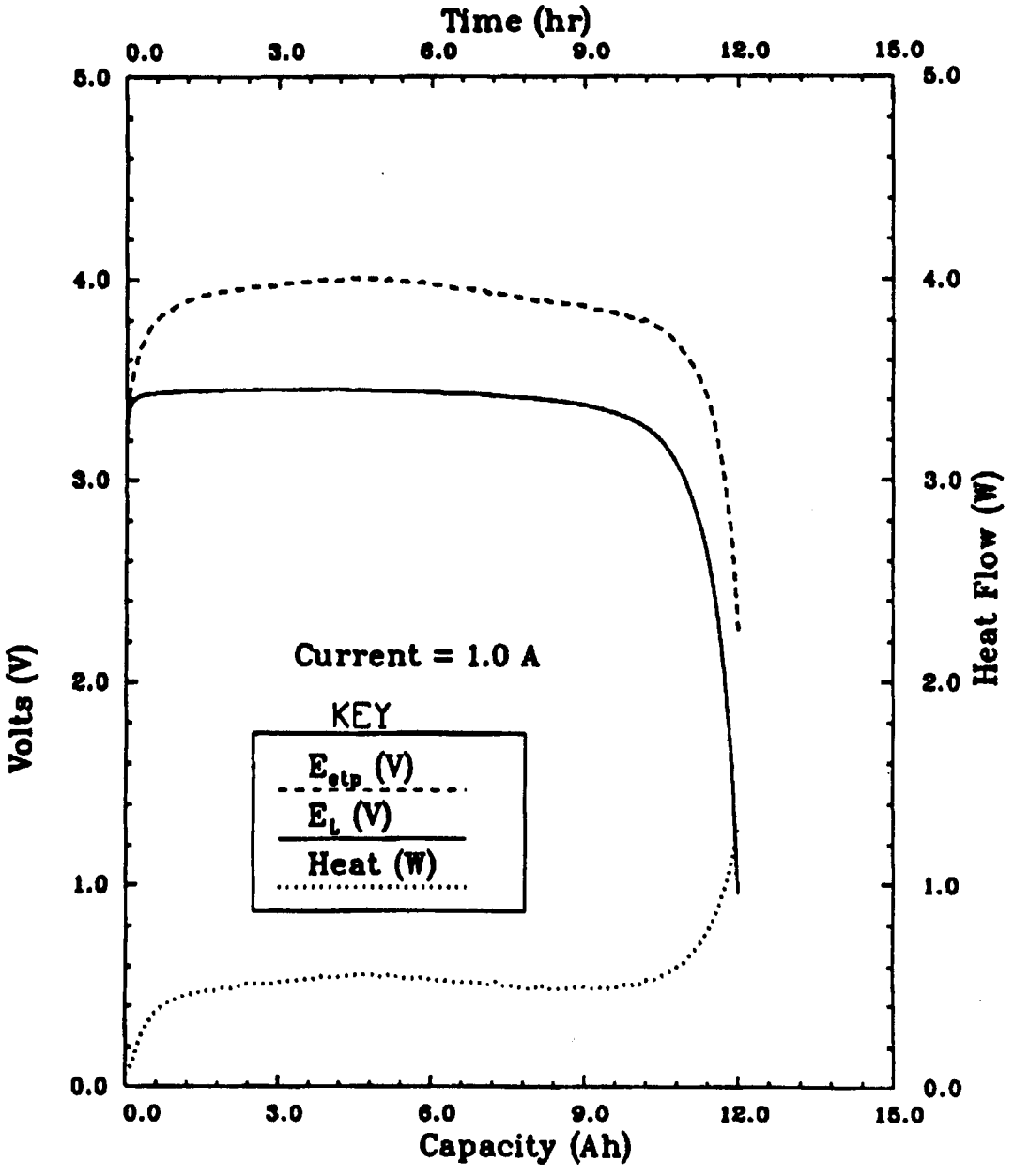

Fig. d7: Effective thermoneutral Potential, load voltage and rate of heat generation for a Li/$SOCl_2$ cell at 60° C.

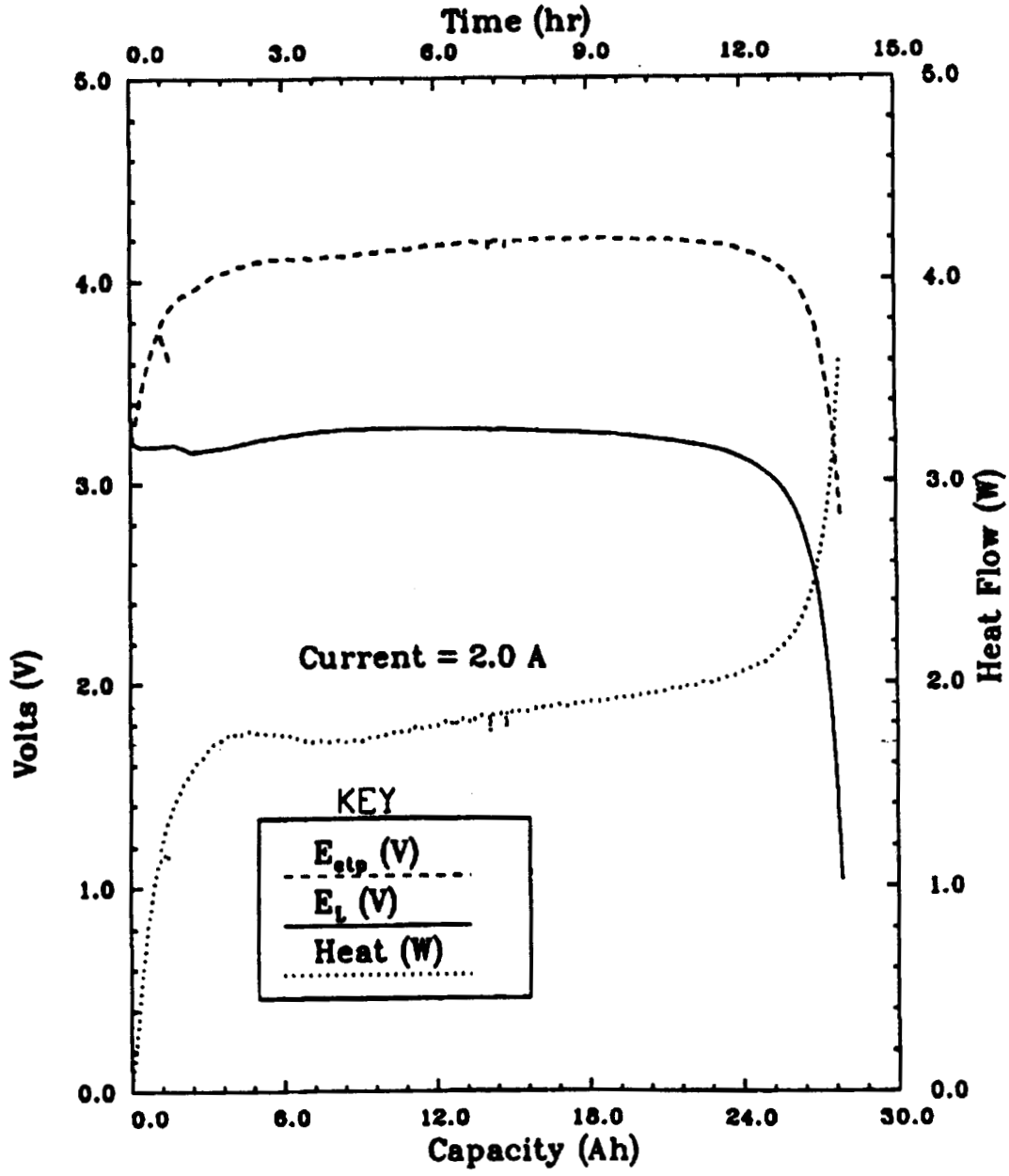

Fig. dd41: Effective thermoneutral Potential, load voltage and rate of heat generation for a Li/BCX cell at 60° C.

The process of drop calorimetry was performed by equilibrating a sample (or cell) at 30 °C for a minimum of 12 hours. The sample (or cell) was manually transferred to the calorimeter chamber set at 20 °C and the resulting heat flux was measured for a minimum of 10 hours. The calibration sample was made of aluminum 6061-T6 and shaped to the same dimensions as a DD-cell. The complete procedure and set-up for droping the sample and the cell were identical. The resulting plot (similar to Fig. 3) shows a rapid rise in heat flux measured in microjoules as the sample is introduced into the chamber. The time constant of the sample was measured as the time difference between the peak and the point where the heat has decayed by 63.2%. The area underneath the heat curve represents the total energy lost by the sample. The integration time boundaries were set at the initiation of transfer to a minimum of five time constants past the time of peak heat flux. The calorimeter system was calibrated to the heat capacity of aluminum 6061-T6 which is 0.214 cal/kg-C (1).Figure 3 shows the heat flux transients of a 210 gram Li-BCX DD-cell at 0% and 100% depth-of-discharge (DOD) when "dropped". The curve integrations yield energies of 1708 J and 1403 J, respectively. The temperature differences were 9.968 °C and 9.970 °C, respectively.

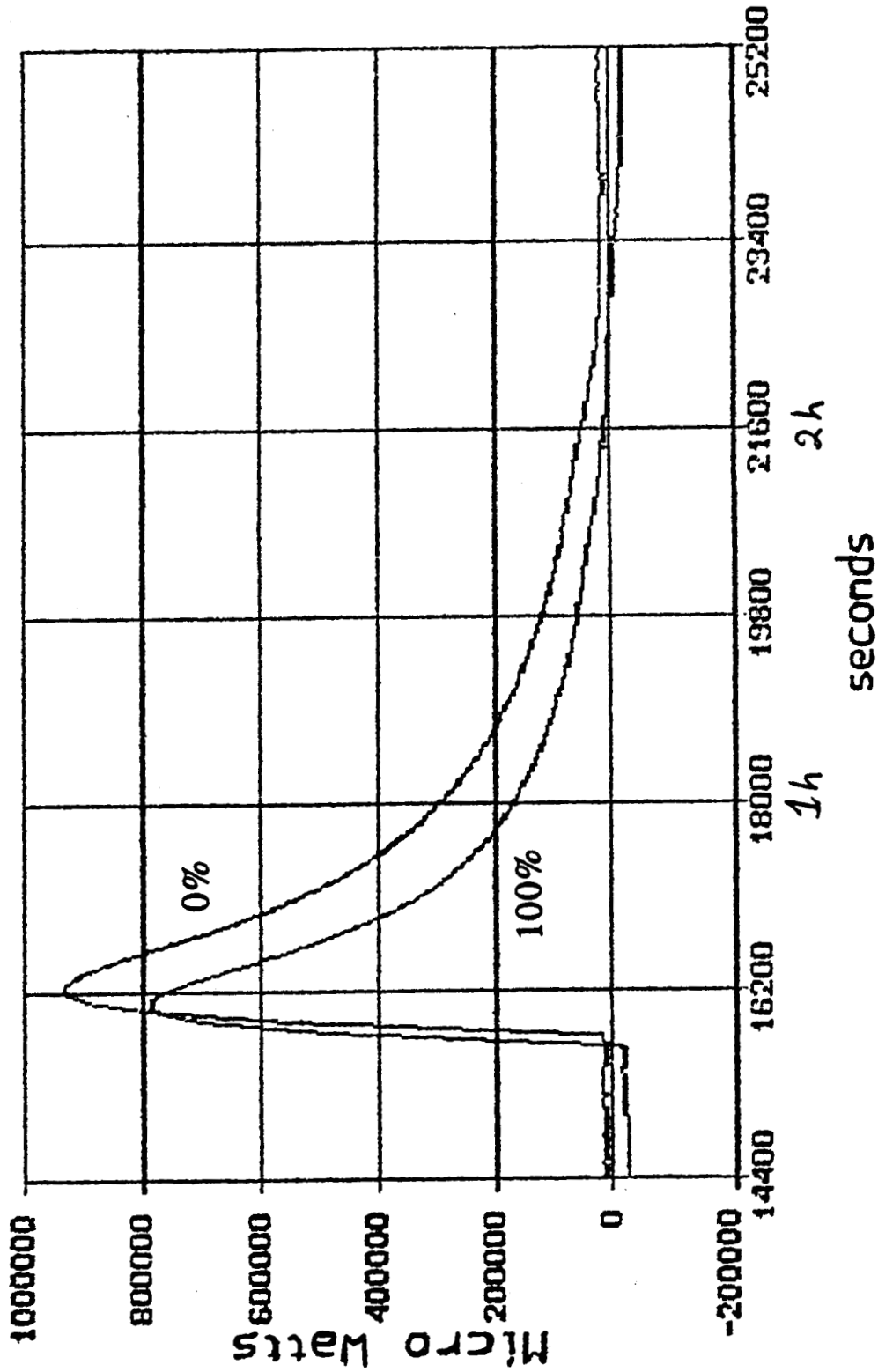

Fig. 3. Heat pulses from Li-BCX DD-cell drops at 0% DOD and 100% DOD at 19 C.

The resulting heat capacities at 0, 20, 40, 60 C are listed and indicate a significant change in C_p with the state of charge for the BCX cells but not for the $SOCl_2$ cells. Repeating the measurements four times for one cell at 40 C yielded a precision of +/- 2.9% with a 90% confidence interval.

Results (cont.)

Drop Calorimetry Results

Temperature in C	Cell number	Cell Heat Capacity, cal/g C Fresh	Discharged
	$Li/SOCl_2$		
0	d8	0.199	0.204
20	d10	0.190	0.192
40	d6	0.237	0.237
60	d7	0.227	0.222
	Li/BCX		
0	dd3	0.210	0.212
20	dd1	0.157	0.206
	dd42	0.197	0.147
	dd44	0.206	0.257
40	dd12	0.186	0.202
60	dd41	0.208	0.194

* precision of each measurement is +/- 2.9% with a 90% confidence interval

In conclusion, the drop calorimetry experiment indicates that the bulk heat capacity of the cells can vary widely with depth-of-discharge (DOD), temperature, and from cell to cell due to manufacturing variations. The BCX cell varied more with DOD than $SOCl_2$ for some unexplained reason. The heat conduction calorimetry experiment indicates that the effective thermoneutral potential (Etn) varies with temperature, DOD, and cell design and chemistry. The Etn of the BCX cells is significantly higher than that for the $SOCl_2$ cells. For the same current density, the load voltage of both cells are nearly identical. Hence, the BCX cells generate more heat per ampere-hour. Interestly, both cells appear to be most thermally efficient at 40 C.

Calorimetry	Propulsion and Power Division	
	Eric Darcy	12/6/90

Conclusions

- Cp = Cp (DOD, Temperature, Manufacturing variances)
- Cp of BCX cells were more dependent on DOD than $SOCl_2$
- $E_{tn} = E_{tn}$(Temperature, DOD, cell design)
- The effective thermoneutral potential of the BCX cells is higher than that for the $SOCl_2$ cells at all temperatures tested
- Both cells were most efficient at 40 C, generating less heat
- Since the average load voltage of both types of cell are similar at the same current density, the BCX cells generate more heat than the $SOCl_2$ cells.

Li/BCX, SVO, and CSC Cells

POWER SOURCES FOR AEROSPACE APPLICATIONS

Dr. William D. K. Clark

Wilson Greatbatch Ltd.
Clarence N.Y.

presented at the
NASA Aerospace Battery Workshop
Marshall Space Flight Center
Huntsville, Alabama
December 4-6, 1990

Chemistries at WGL

Lithium Silver Vanadium Oxide

Lithium BCX (BrCl/thionyl chloride)

Lithium Thionyl Chloride

Lithium CSC (chlorinated sulfuryl chloride)

Lithium Iodine

Lithium Sulphur Dioxide

Lithium Carbon Monofluoride

Lithium Titanium Disulphide (Rechargeable)

Donnington Corporation
Invictus
BDT
Wilson Greatbatch Ltd.
Machining Services
Electrochem Industries
Medical
Technology
G&A

BCX lithium oxyhalide primary cells

3B75-FF

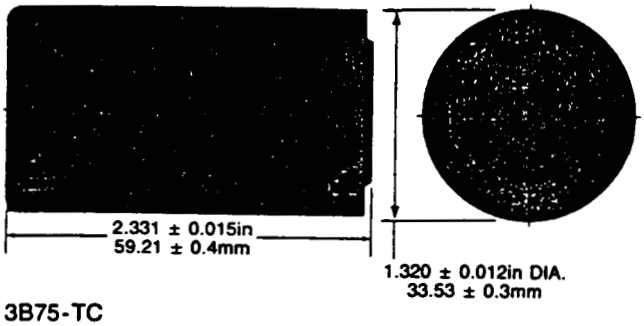

3B75-TC

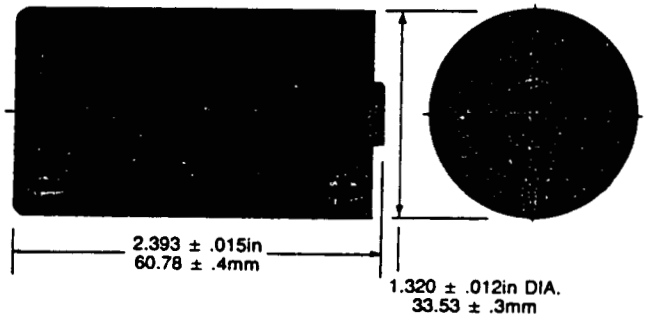

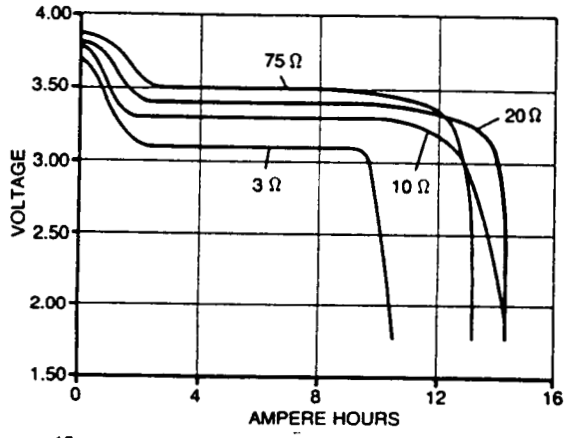

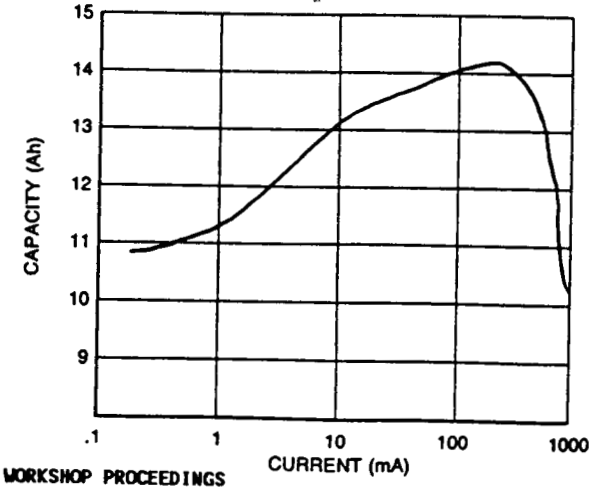

BCX
SERIES BCX72
3B75
D SIZE

SPECIFICATIONS

Open Circuit Voltage (Nominal)	3.9V
At Room Temperature:	
Rated Average Load Voltage	3.4V
Rated Discharge Current	175mA
Rated Capacity	14 Ah
Maximum Continuous Discharge Current	1000mA
Operating Temperature Range	−40°C to 72°C (−40°F to 162°F)
Weight	115g
Safety Fuse	4 Amp
Energy Density	413 Wh/kg

(Also available in Non-Magnetic cell configuration) P/N 3B1320

Sample Discharge Table

Discharge Current (mA)	175	330	1000
Average Load Voltage (Volts)	3.4	3.3	3.1
Capacity (Ampere hours)	14	14	10

TEMPERATURE RANGE

°C	°F
200	392
190	374
180	356
170	338
160	320
150	302
140	284
130	266
120	248
110	230
100	212
90	194
80	176
70	158
60	140
50	122
40	104
30	86
20	68
10	50
0	32
−10	14
−20	−4
−30	−22
−40	−40
−50	−58
−60	−76

List of the Redesigns

- Reduce thickness of anode and cathode
- Increase thickness of header
- Shorten wound cell stack

5 of 18

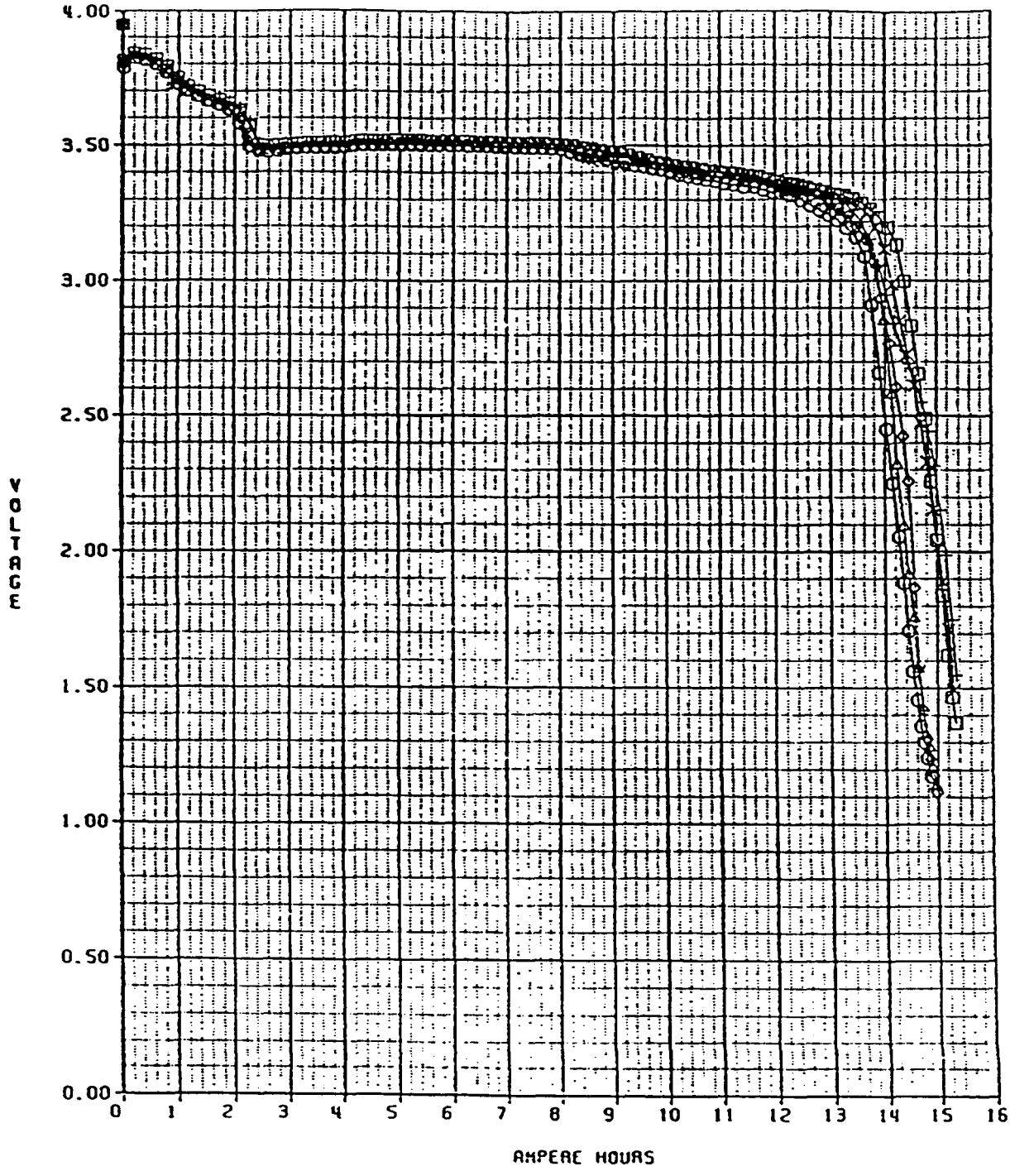

Figure 10. Discharge curves of a group of D cells (redesign III, production build), discharged under a 20 ohm constant load.

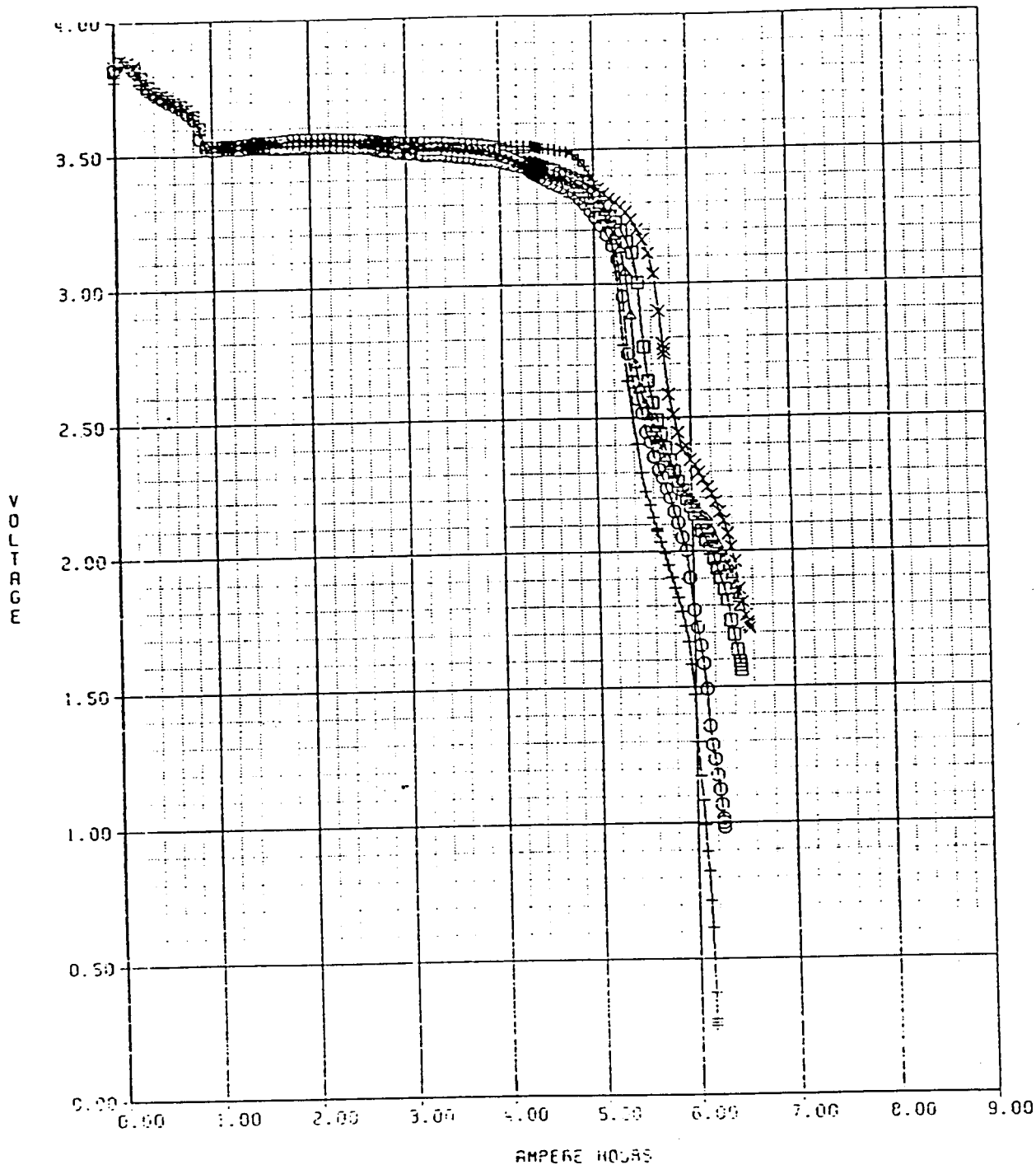

Discharge curves of a group of redesigned C cells discharged under a 56.2 Ω constant load.

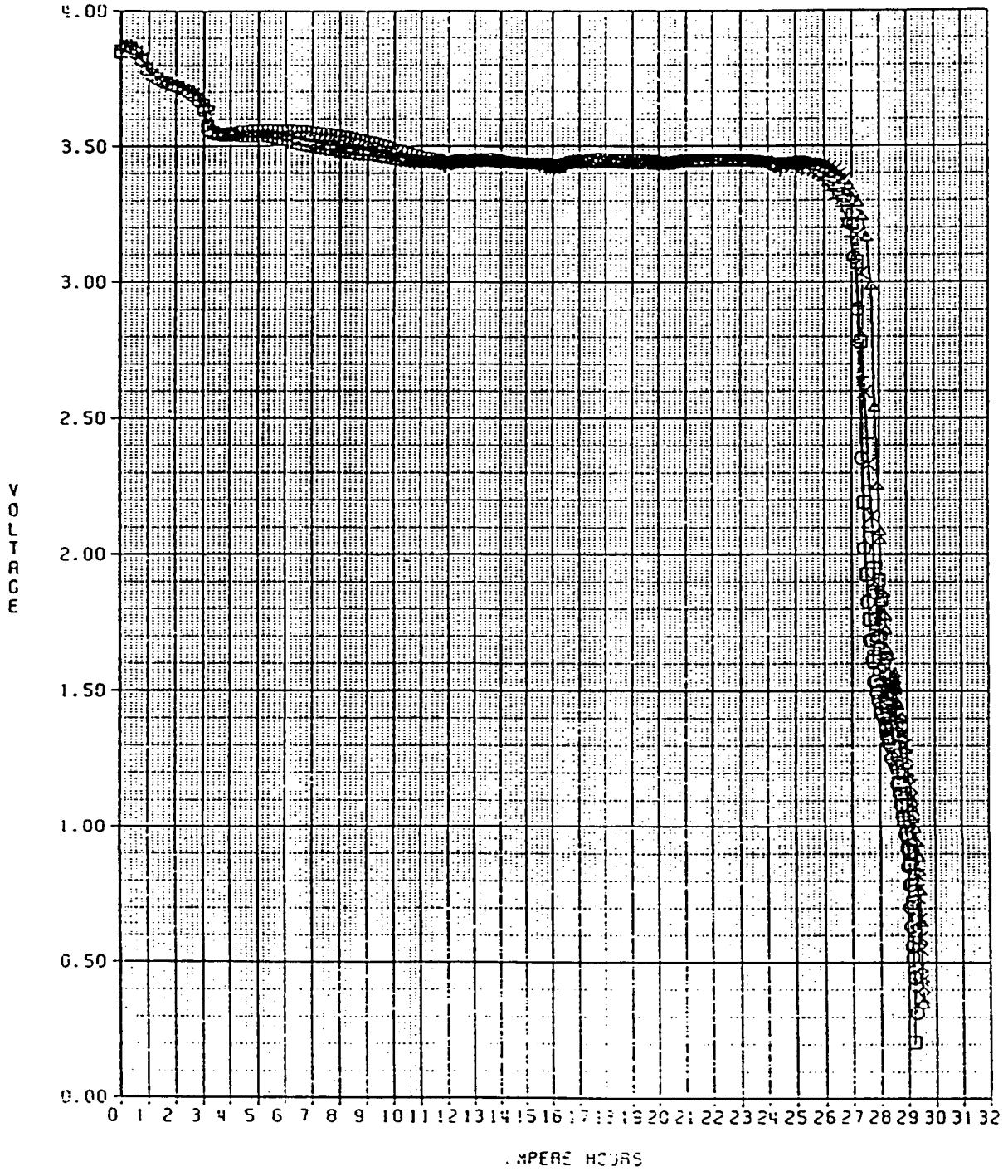

Discharge curves of a group of redesigned DD cells discharged under a 20 Ω constant load.

UNIVERSAL BCXC PROTOTYPE
NASA AN/PRC SURVIVAL RADIO CONTRACT
.062" HEADERS

S/N 2103 □ 59291 S/N 2104 ○ 59277
S/N 2105 △ 58847 S/N 2106 + 58846
S/N 2107 × 58869
DISCHARGED AT 21 DEG.C UNDER A 6 OHM LOAD

DISTRIBUTION:

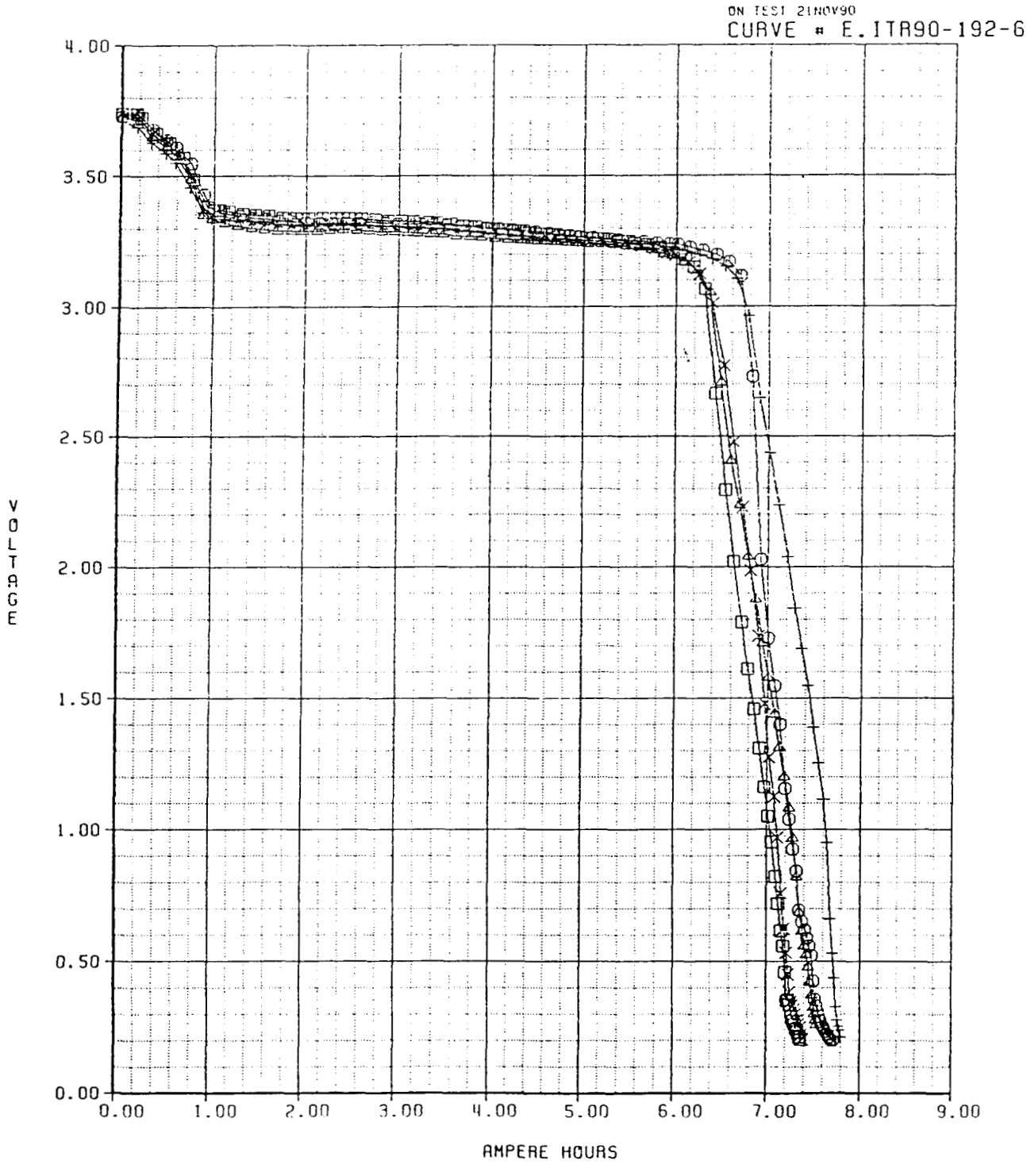

CSC lithium oxyhalide primary cells

3B35-FF

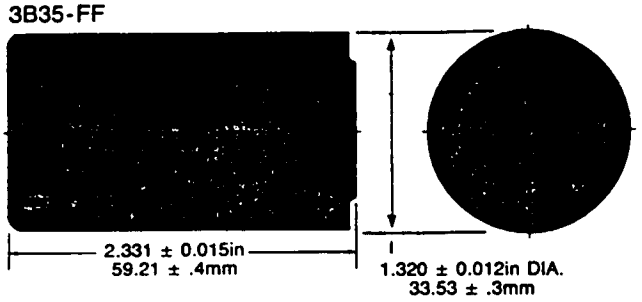

3B35-TC

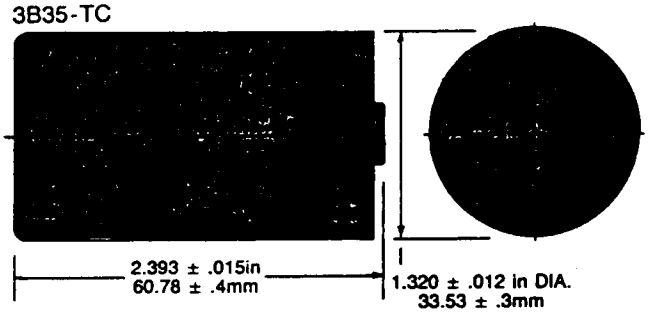

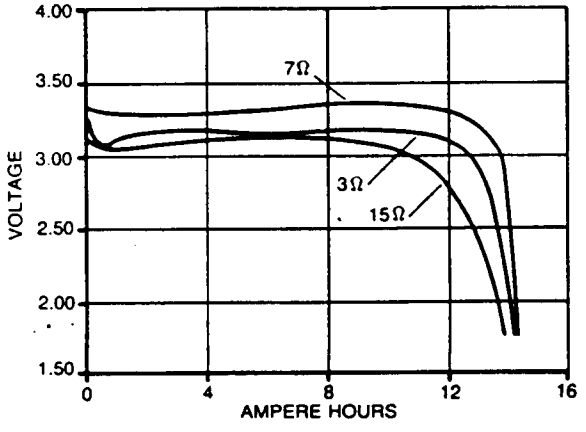

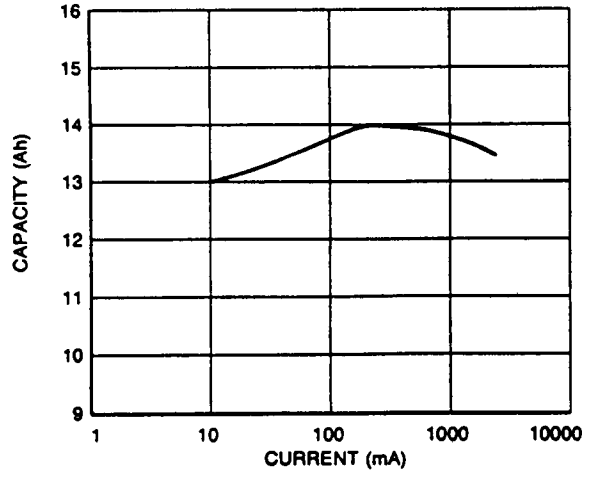

CSC
SERIES CSC93
3B35
D SIZE

SPECIFICATIONS

Open Circuit Voltage (Nominal)	3.95V
At Room Temperature:	
Rated Average Load Voltage	3.4V
Rated Discharge Current	500mA
Rated Capacity	14 Ah
Maximum Continuous Discharge Current	2000mA
Operating Temperature Range	−32°C to 93°C (−26°F to 199°F)
Weight	116g
Safety Fuse	4 Amp
Energy Density	410 Wh/kg

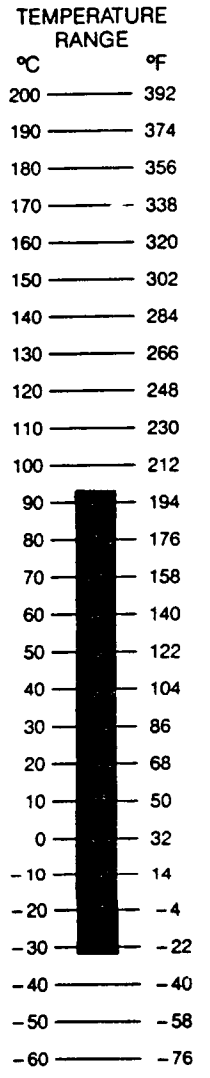

36

EMATT discharge of PWR DD cells after 3 months aging at room temp.

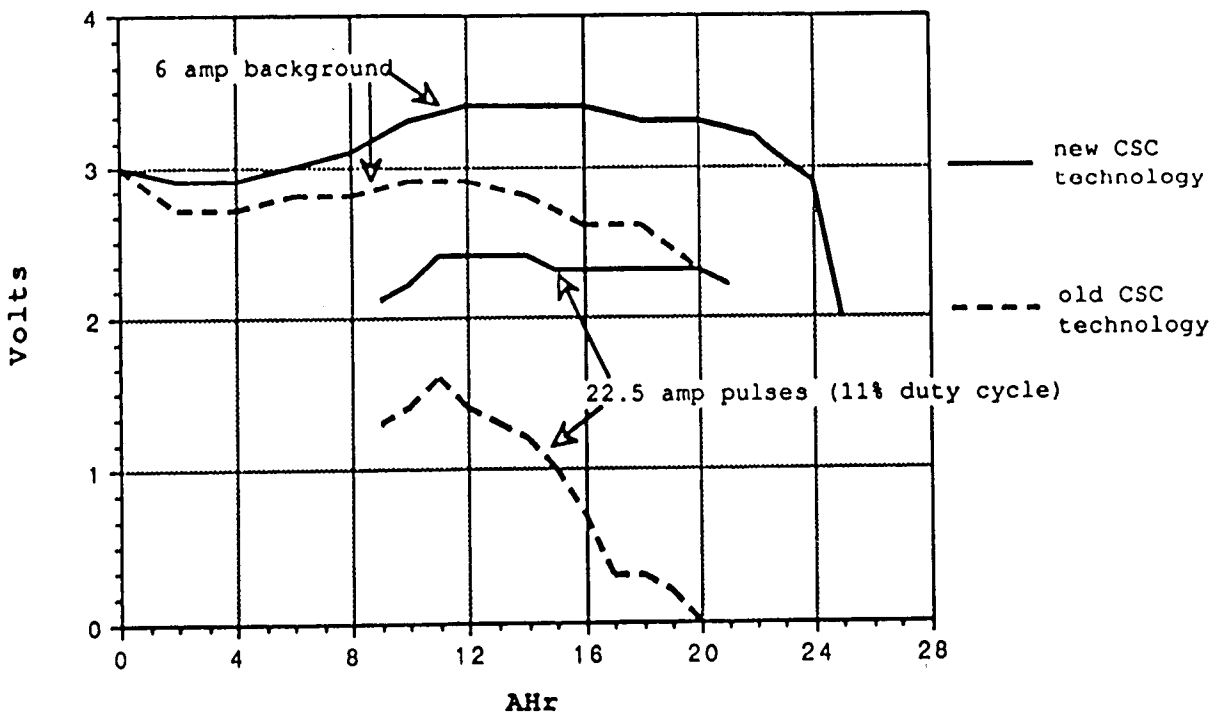

EMATT discharge regimen: -20 to 0°C temperature gradient. 6A constant for 90 min. followed by 22.5A pulses (11% duty) with 6A background for 90 min. 2 volt cutoff.

CAPACITY RETENTION OF CSC D CELLS

Test conditions	Storage Temp.	Storage time	Ahr to 3.0V	Ahr to 2.0V	% 2.0V Capacity Retention
6Ω RT discharge	RT	12 months	12.50 ± 0.87	13.58 ± 0.65	95.6
	57°C		10.75 ± 0.35	12.92 ± 0.40	91
	72°C		9.13 ± 1.30	11.94 ± 1.10	84
	RT	24 months	10.80 ± 1.47	13.57 ± 0.40	95.6
6Ω -20/0°C discharge	RT	12 months	NA	13.90 ± 0.26	95.2
	57°C		10.28 ± 0.32	12.70 ± 0.00	87
	72°C		7.71 ± 0.90	11.84 ± 0.34	81.1
	RT	24 months	NA	13.07 ± 0.75	89.5
1Ω RT discharge	RT	12 months	8.45 ± 1.56	11.47 ± 1.47	83.7
	57°C		9.78 ± 1.30	12.37 ± 0.38	90.3
	72°C		9.10 ± 1.84	9.82 ± 1.93	71.7
1Ω -20/0°C discharge	RT	12 months	NA	12.08 ± 0.28	86.9
	57°C		9.47 ± 0.82	12.41 ± 0.22	89.3
	72°C		NA	10.93 ± 0.70	78.6

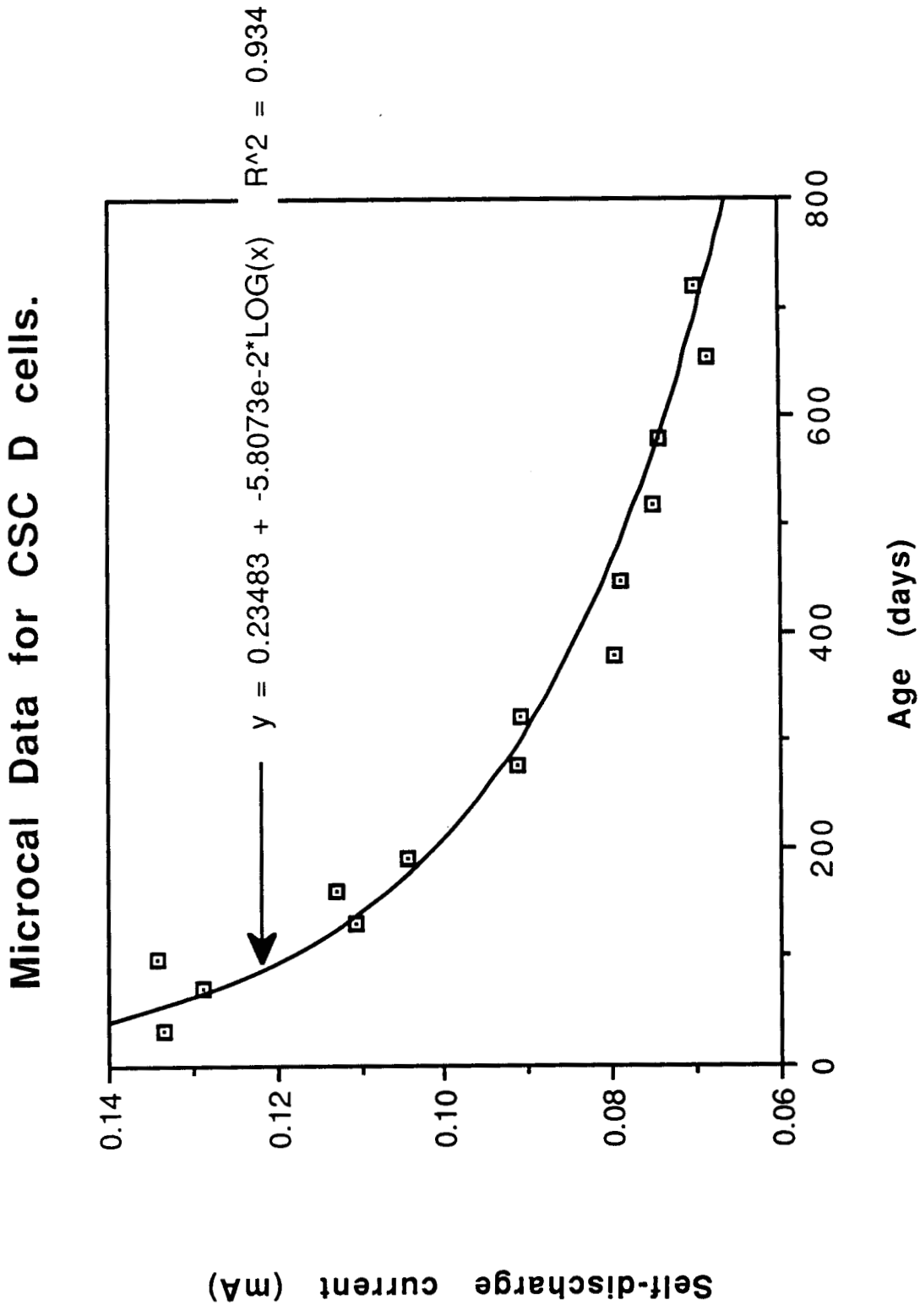
Microcal Data for CSC D cells.
y = 0.23483 + -5.8073e-2*LOG(x)
R^2 = 0.934
Self-discharge current (mA)
0.14
0.12
0.10
0.08
0.06
0
200
400
600
800
Age (days)

Average (±st.dev) 6Ω room temperature start up after 24 months at room temperature.

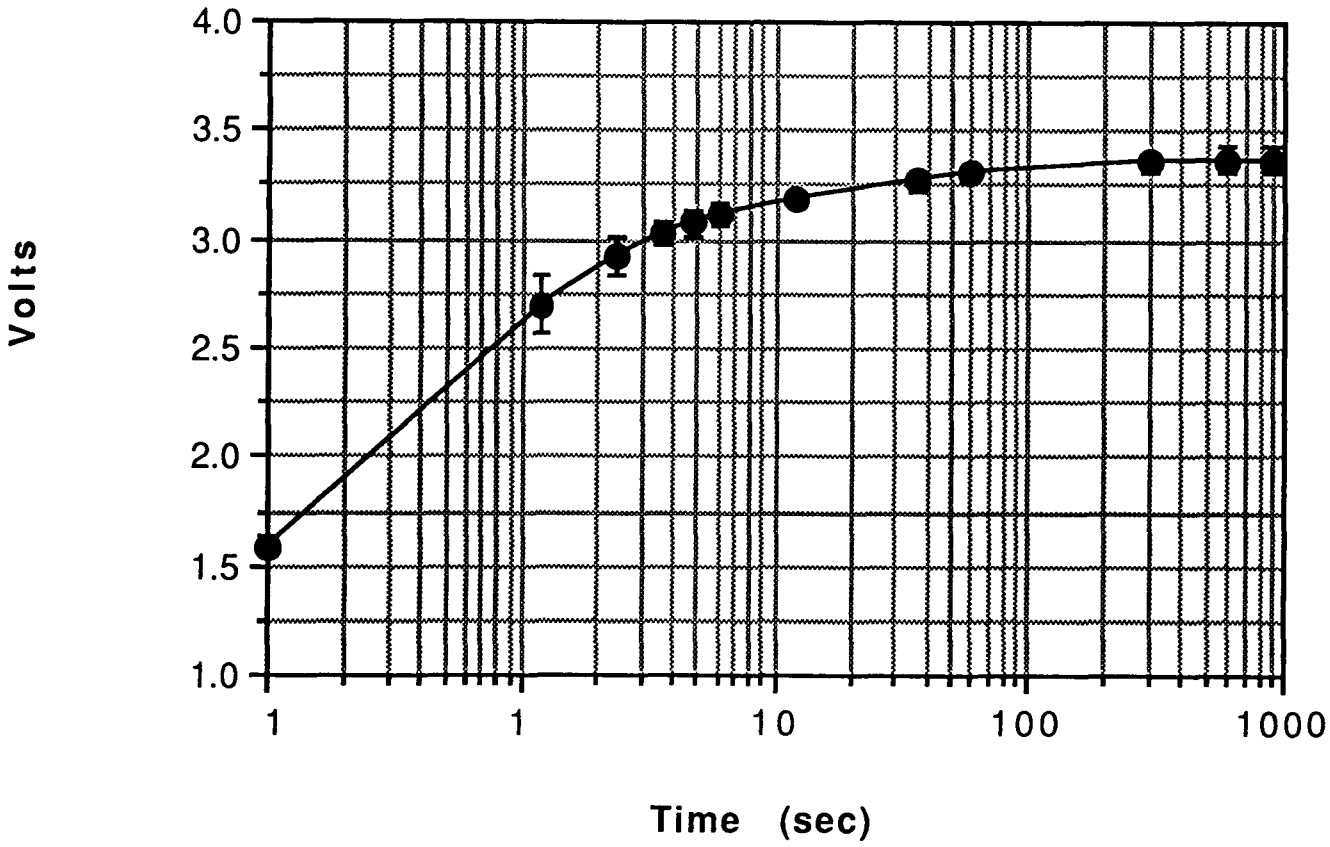

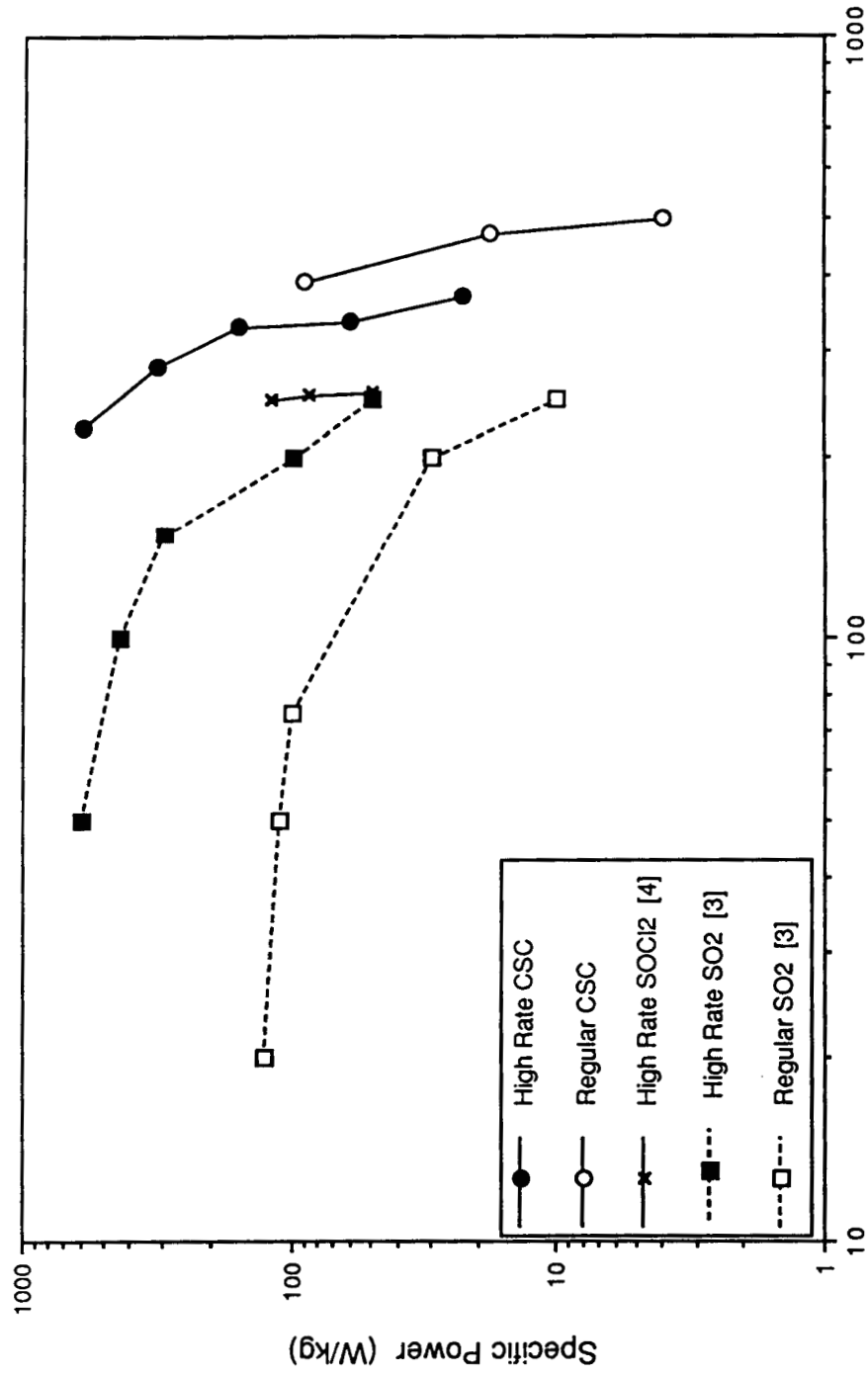

Figure 1. Comparative specific power vs. specific energy plots.

Electrochem

PWR AA-V: Preliminary Specification Sheet
April, 1990

6P1041

Nominal Fused Cell Dimensions	ht. 1.949"*, dia. 0.538"
Finished Cell Weight Minus Solder Tabs	17.2 g
Finished Cell Volume Minus Solder Tabs	0.450 in^3 (or 7.37 cm^3)
Nominal Discharge Current	0.75 A
Maximum Continuous Discharge Current	3 A
Maximum Pulse Current	10 A
Nominal Capacity	1.3 Ahr
Maximum Achievable Capacity	1.5 Ahr (≤20 mA rate)
Operating Temperature Range	-30 to +72°C
Gravimetric Energy Density - Nominal Load	370 Wh/Kg
Volumetric Energy Density - Nominal Load	0.85 Wh/cm^3
Estimated Self-Discharge Rate	25 % per year

3.5V @ 1A
~3.0V @ 2.5-3.0A

* *nominal length does not include bottom spacer and terminal cap as shown below.*

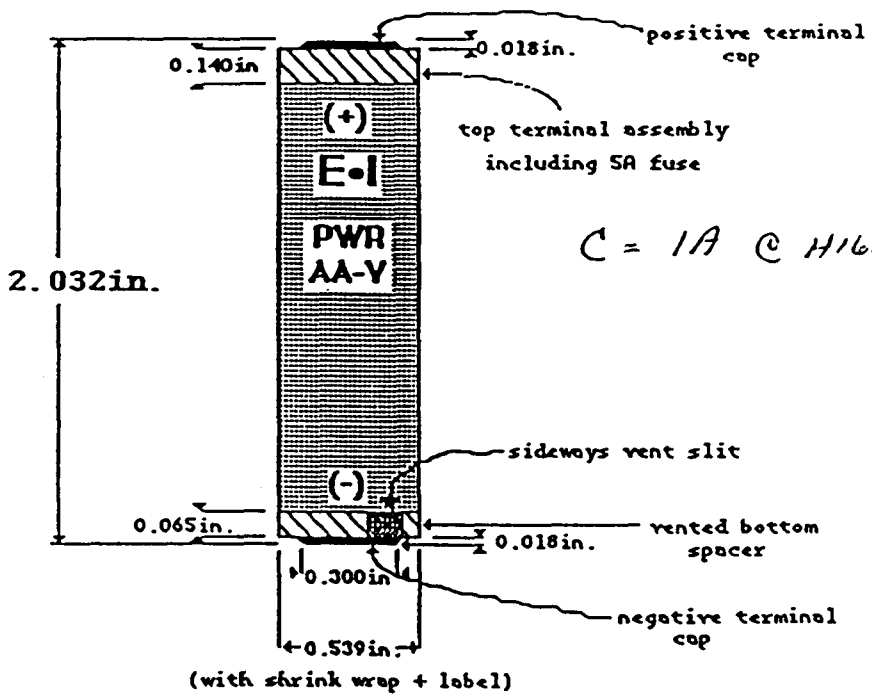

Electrochem Industries

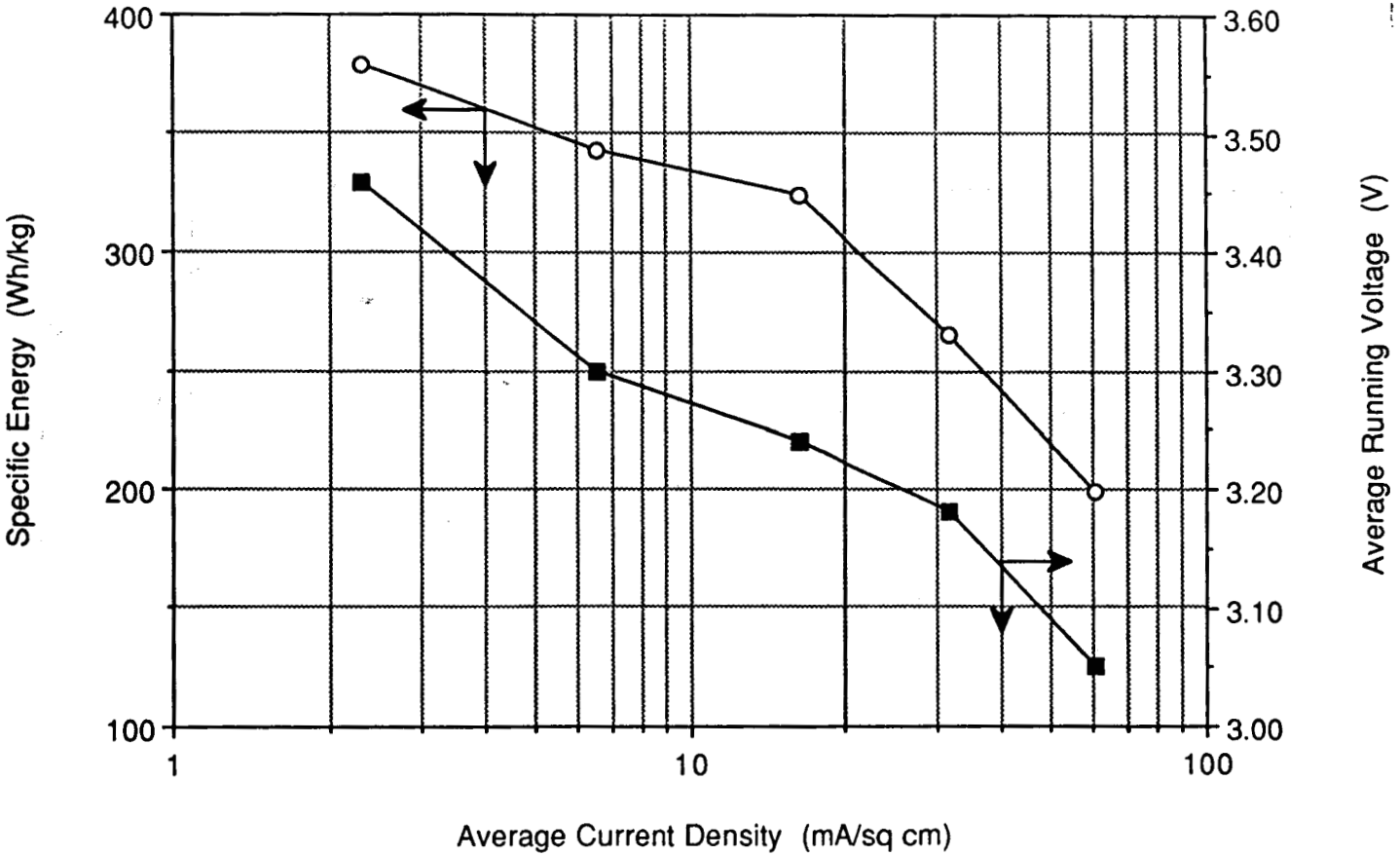

Figure 4. Energy and running voltage characteristics of Li/CSC cells as a function of discharge rate. Continuous discharge.

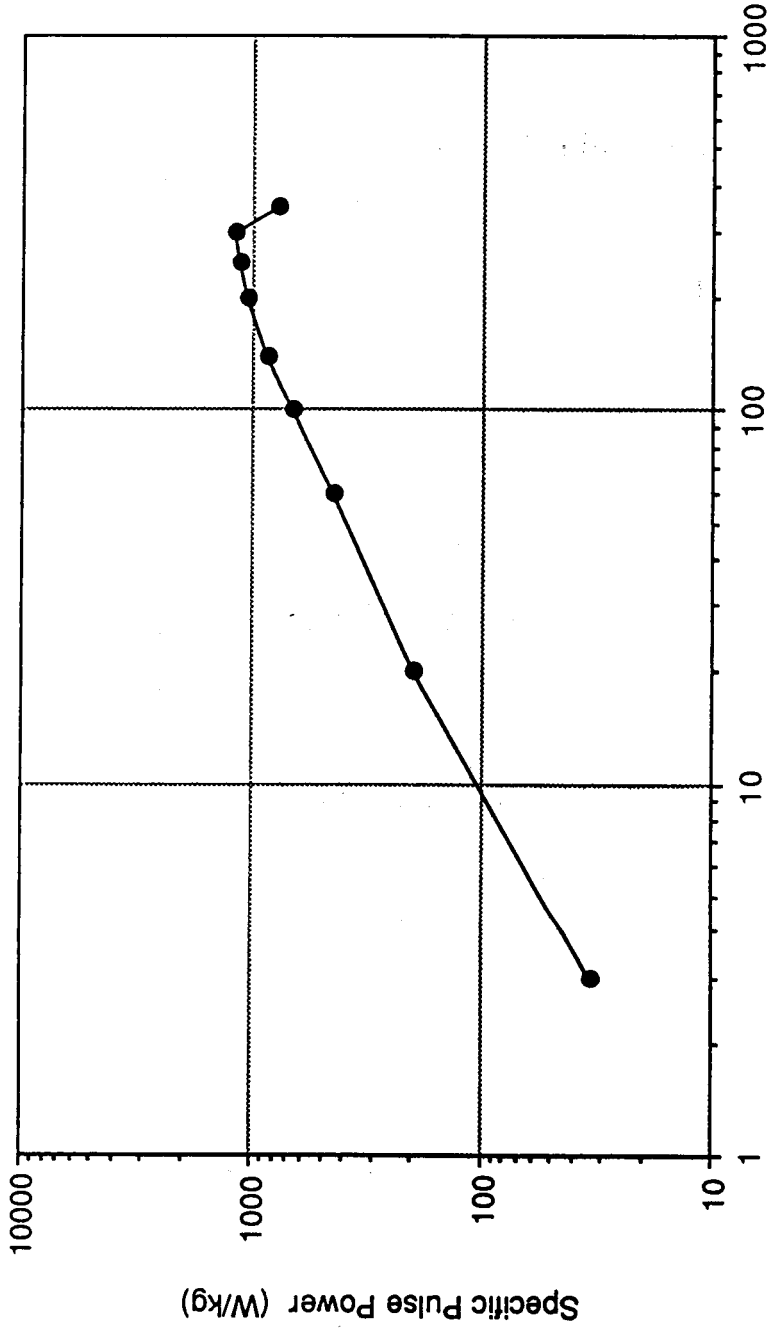

Figure 2. Pulse power output - obtained at 50% depth of discharge.
Pulse regimen was 50% duty cycle, 1 sec. pulse width.

QTC lithium thionyl chloride primary cells

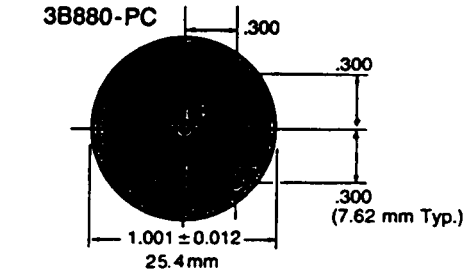

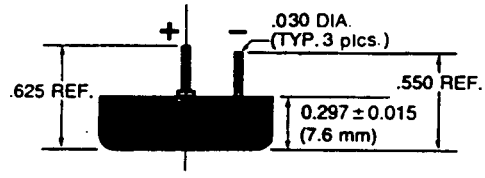

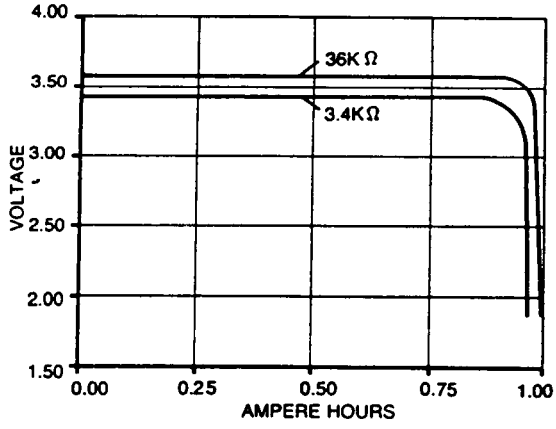

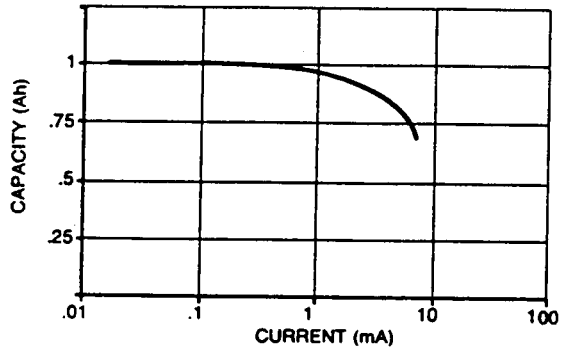

QTC

SERIES QTC85

3B880

PC SIZE

SPECIFICATIONS

Open Circuit Voltage (Nominal)	3.6V
At Room Temperature:	
Rated Average Load Voltage	3.6V
Rated Discharge Current	100 μ A
Rated Capacity	1.0Ah
Maximum Continuous Discharge Current	1mA
Operating Temperature Range	−40°C to 85°C (−40°F to 185°F)
Weight	10g
Energy Density	360 Wh/kg

- This product is manufactured under a quality system designed to meet MIL-I 45208A (Inspection Systems Requirement).

-Recognized Component

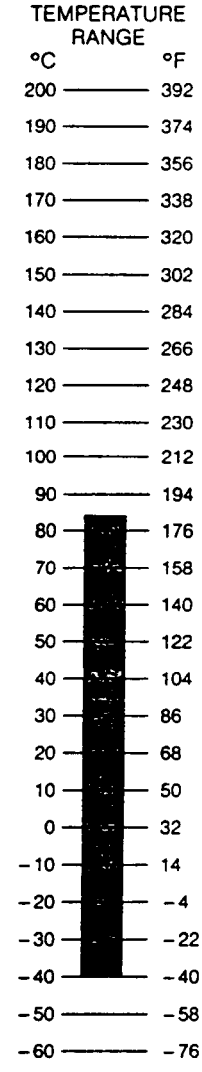

39

WILSON GREATBATCH LTD
HIGH RATE LITHIUM/THIONYL CHLORIDE
ULTRA THIN PRISMATIC CELL

PHYSICAL CHARACTERISTICS

Dimensions: 0.465"L X 1.076"W X 0.195"T
Weight: 5.08 grams
Volume: 1.599 cc
Hermetically sealed/internally fused

PERFORMANCE

Open Circuit Voltage: 3.65V
Rated Capacity to 2.67V (200 mA): 200 mAhrs
Operating Voltage: 3.1V
Gravimetric Energy Density: 122 Whrs/kg
Volumetric Energy Density: 388 Whrs/L
Voltage Delay: Eliminated by 500 mA burn-in for 1 minute

PERFORMANCE SUMMARY

200 mA Constant Current Discharge

Age of Cell	Temperature		
	-10°C	+25°C	+50°C
Fresh	200	200	250
3 Months	N/A	200	250
6 Months	N/A	200	250

cells discharged under 200 mA loads

Cells discharged at +50°C

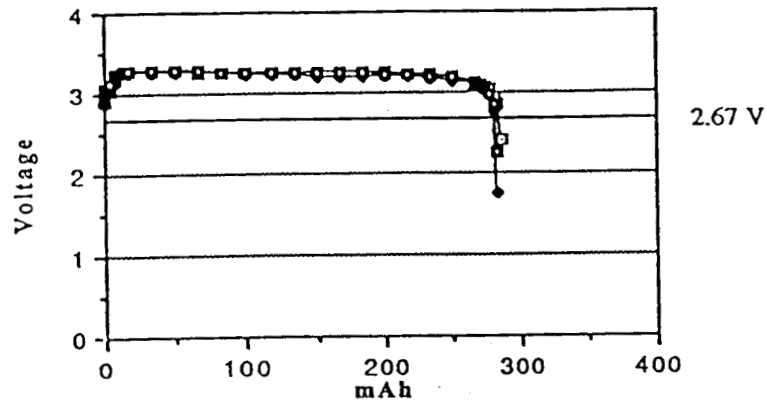

Cells discharged at room temperature

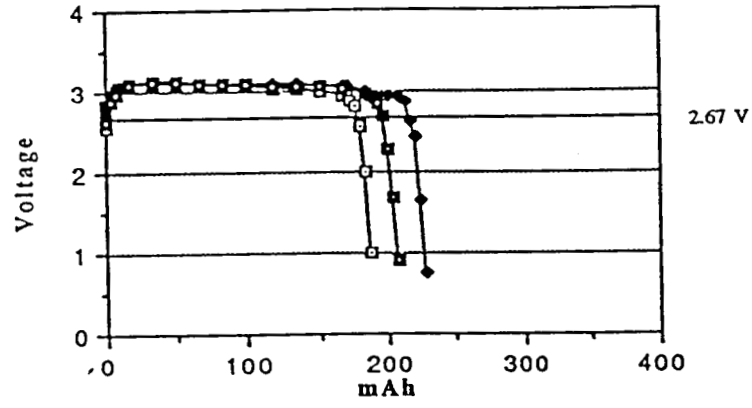

Cells discharged at -10°C

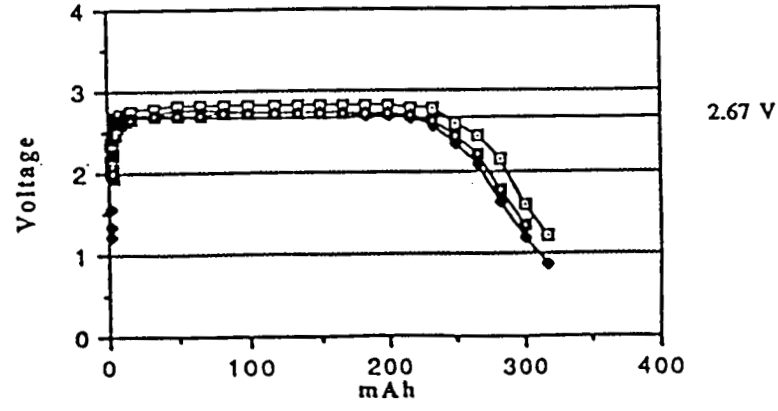

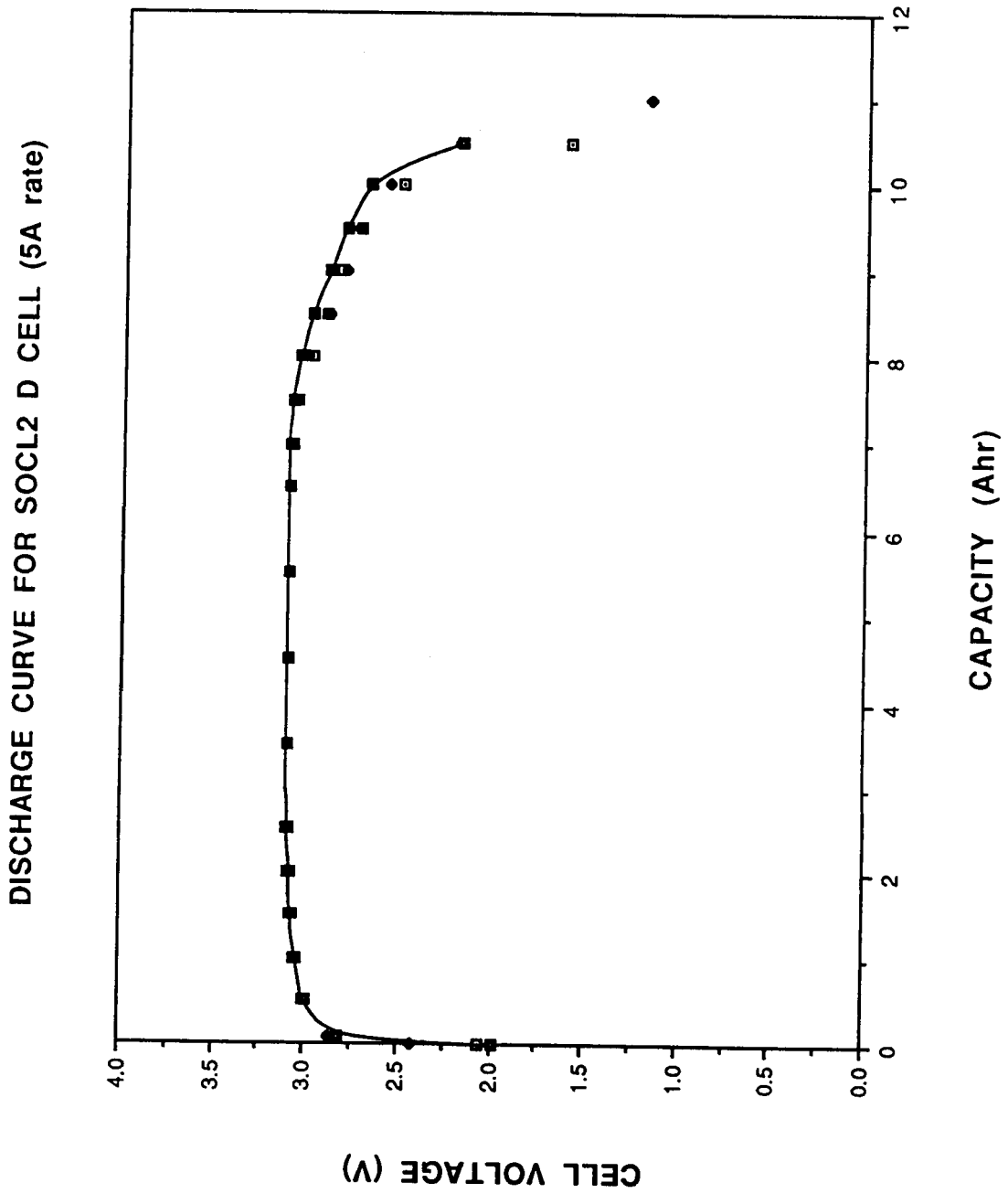
DISCHARGE CURVE FOR SOCL2 D CELL (5A rate)
CELL VOLTAGE (V)
4.0
3.5
3.0
2.5
2.0
1.5
1.0
0.5
0.0
0
2
4
6
8
10
12
CAPACITY (Ahr)

LITHIUM/SULFUR DIOXIDE

HIGH RATE D CELL

DATA SHEET

PHYSICAL CHARACTERISTICS

Dimensions: 1.273"D x 2.40"H
Weight: 97 g
Volume: 50 cc

PERFORMANCE

Open Circuit Voltage: 2.95V
Rated Capacity to 2.0V (4 ohms): 9.0 Ahrs
Operating Voltage: 2.8V

Gravimetric Energy Density: 260 Whrs/kg
Volumetric Energy Density: 503 Whrs/L

Discharge Rate (Amps)	Temperature (°C)	Capacity to 2V (Ahrs)	Operating Voltage
0.7	20	9.0	2.80
0.7	-35	6.85	2.60
6.0	20	6.25	2.55
6.0	-35	6.20	2.25

SAFETY

Cells vent mildly through the designated slit vent structure at 90-130°C
under the following conditions:

.040 ohm short circuit

2A forced charge

2A forced overdischarge

SANDIA S02 D -
CHARACTERIZATION

S/N 3621 □ 48103 S/N 3622 ⊙ 48106
S/N 3623 △ 48107 S/N 3624 + 48109
S/N 3625 × 48113
DISCHARGED AT ROOM TEMPERATURE UNDER A 4 OHM LOAD

DISTRIBUTION:

WG

ON TEST 25 SEPT 89
CURVE # E.ITR89-103-13

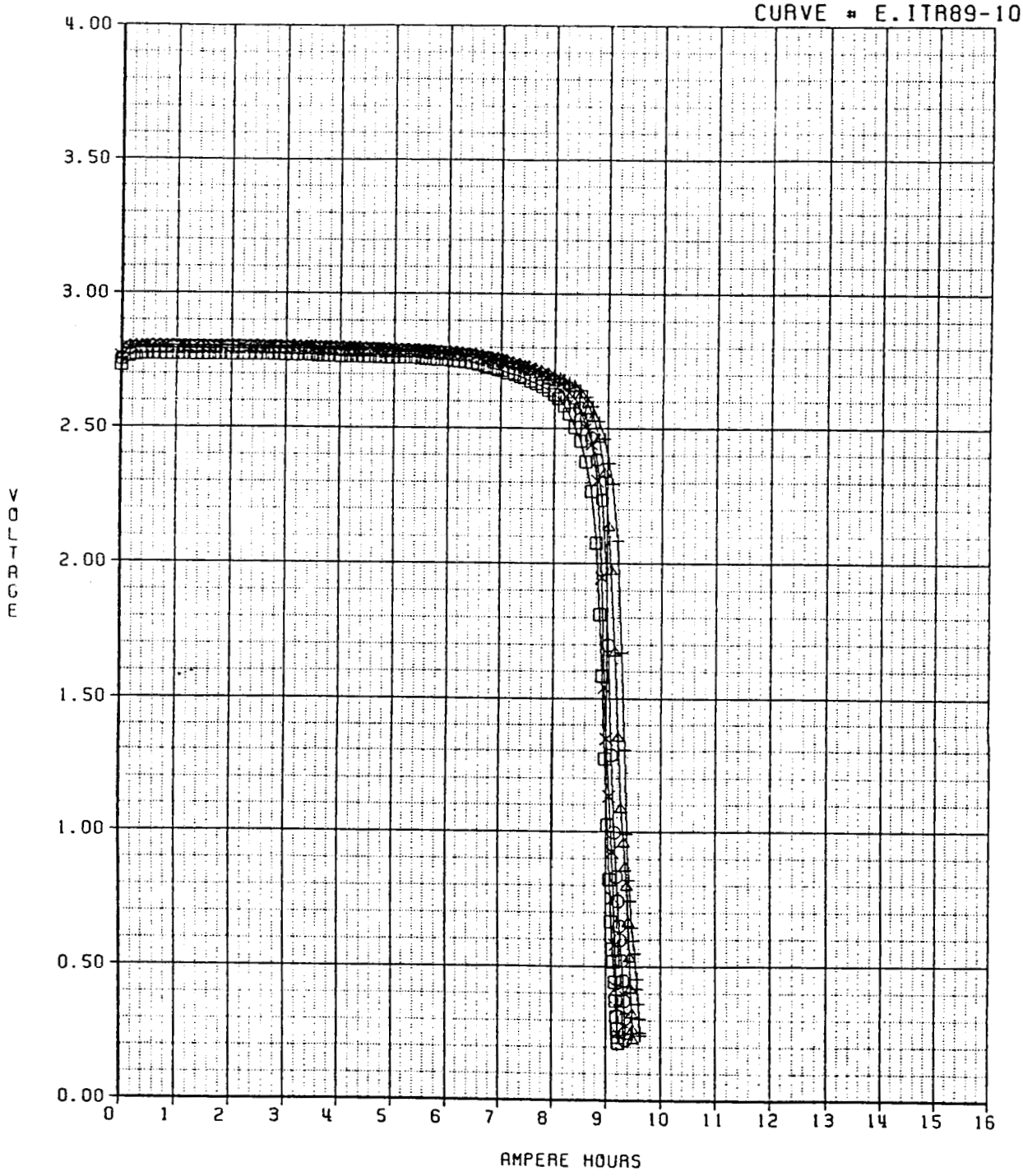

GPLOT (REV. 3.1)

DAY 269 TUE. SEP 26 1989 09:26:55 AM

WILSON GREATBATCH LTD
LITHIUM/SULFUR DIOXIDE
STANDARD RATE D CELL

PHYSICAL CHARACTERISTICS

Dimensions: 1.316" O.D. x 2.40" H
Weight: 97 grams
Volume: 53.5 cc
Bottom Slit Vent Structure

PERFORMANCE

Open Circuit Voltage: 2.95V
Rated Capacity to 2.0V (6.25 ohms): 9.6 Ahrs
Operating Voltage: 2.8V
Gravimetric Energy Density: 277 Whrs/kg
Volumetric Energy Density: 502 Whrs/L
Self Discharge: 1% per year

AMBIENT AND LOW TEMPERATURE PERFORMANCE

Discharge Rate	Temperature (°C)	Capacity to 2V (Ahrs)	Operating Voltage
4 ohms (0.7 A)	-35	6.3	2.30
	+21	9.4	2.75
	+55	9.6	2.80
6.25 ohms (0.45 A)	-35	7.1	2.60
	+21	9.6	2.80
	+55	9.6	2.80
8 Ohms (0.35 A)	-35	7.1	2.60
	+21	9.7	2.80
	+55	9.6	2.80

SANDIA S02 D
PERFORMANCE
CELLS STORED FOR 48 HRS. AT 54 DEG.C

S/N 1289 ☐ 57661 S/N 1290 ⏱ 57645
S/N 1291 △ 57666 S/N 1292 + 57675
S/N 1293 × 57646
DISCHARGED AT ROOM TEMPERATURE UNDER A 6.25 OHM LOAD

WG

ON TEST 31 AUG 90
CURVE # E.ITR90-119-8

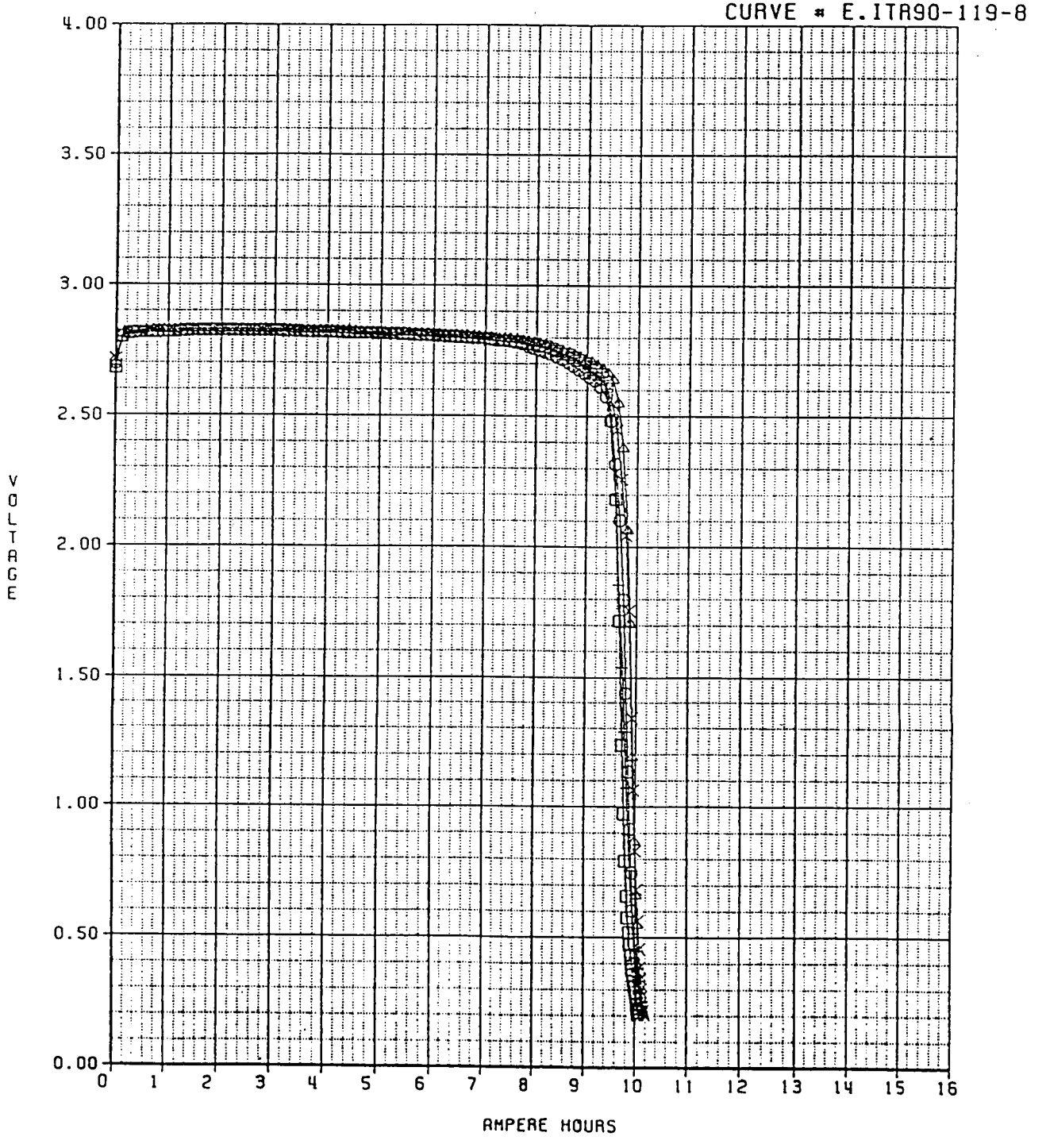

GPLOT (REV. 3.1)

DAY 247 TUE. SEP 04 1990 09:24:26 AM

6 X 6 mm CYLINDRICAL CELL
(nominal specifications)

Ampere hours	0.025
Average Voltage	2.65
Energy Delivered, Wh	0.066
Weight, g	0.52
Dimensions, mm	6 x 6
Volume, cc	0.17
Energy Density, Wh/g	0.13
Energy Density, Wh/cc	0.39

TYPE: APL/CF_x

20KOHM LOAD

SNS: □ 8 ○ 9 △ 10 ✳ 11

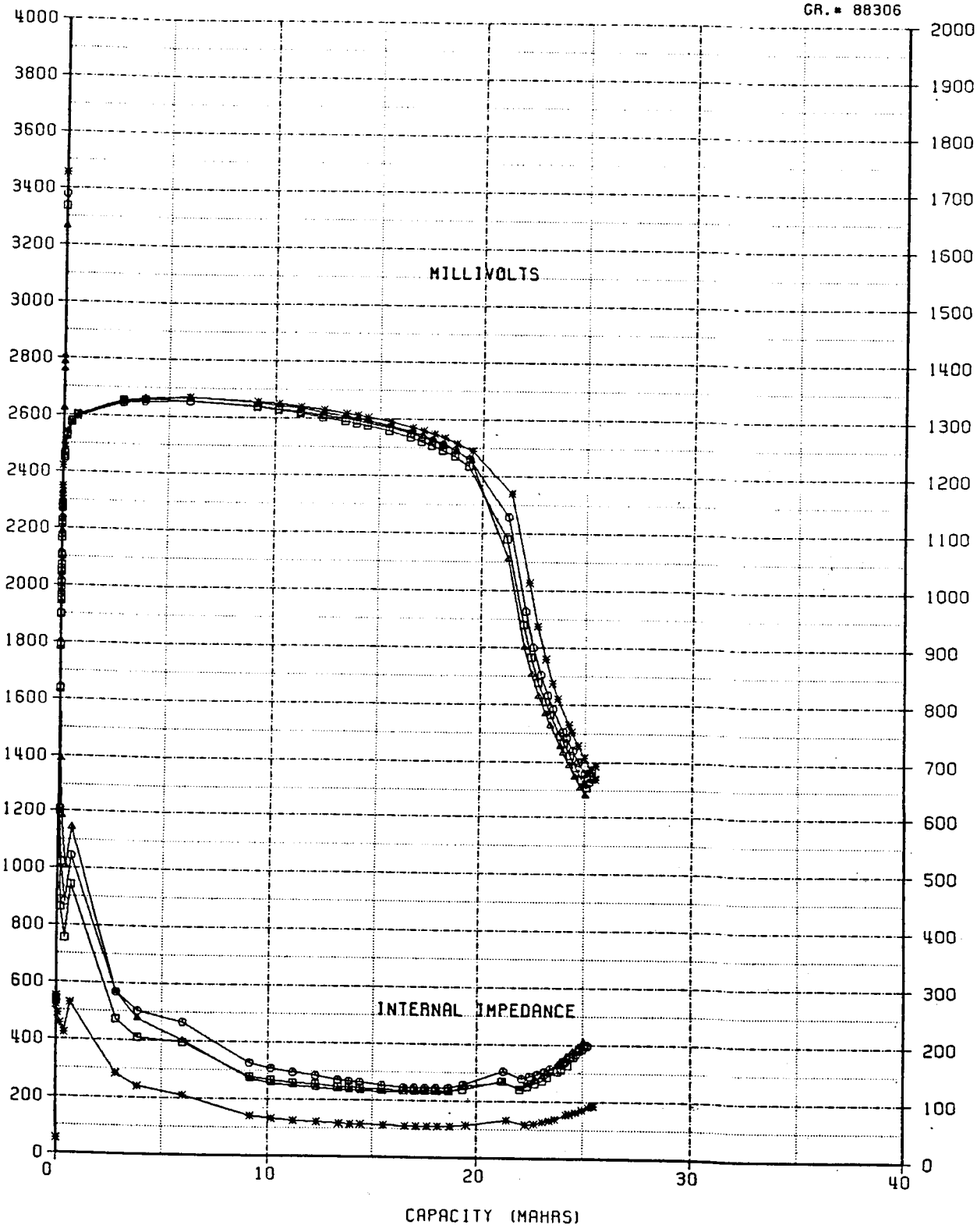

GPLOT (REV. 3.1)

DAT 315 THU. NOV 10 1988 08:42:42 AM

Specifications for CFx Titanium Cells

Capacity (Ah)	2.58
Average Voltage (500Ω load)	2.65
Weight, g	14
Dimensions, cm	2.3 x 4.5 x 0.86
Volume, cc	6.95
Energy Density (Wh/g)	0.49
Energy Density (Wh/cc)	0.98

SN: 36788 - TYPE: 94CFX

499 OHM LOAD - TESTED AT ROOM TEMP. (25°C)

⏲ MVOC ✳ INTERNAL IMPEDANCE

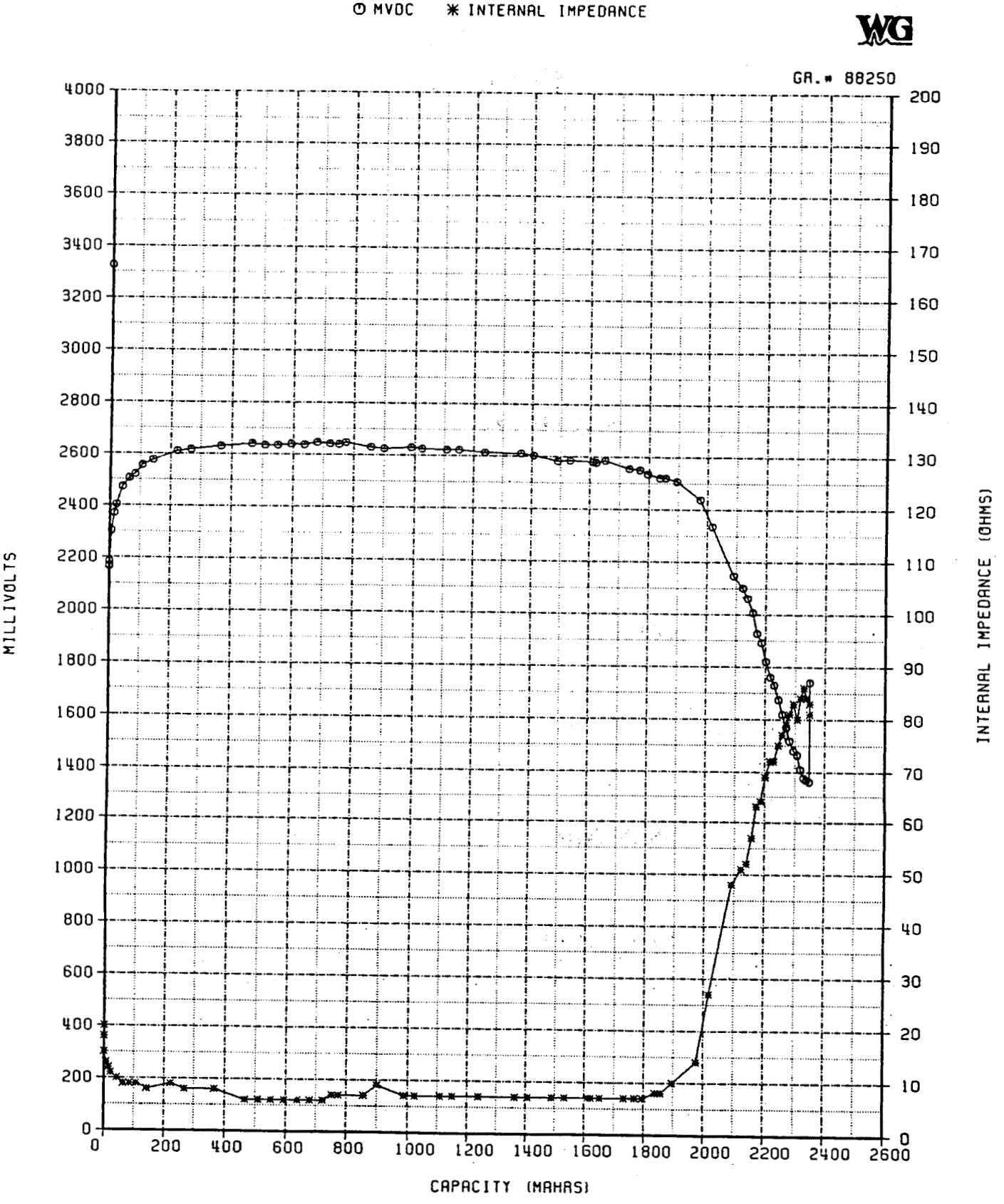

3B1750-FF

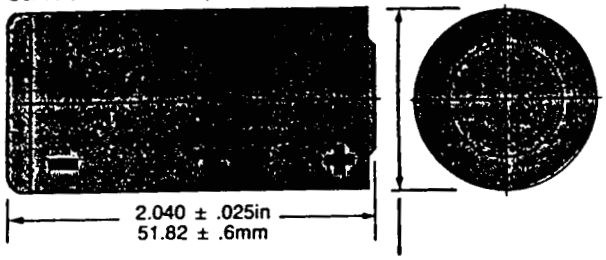

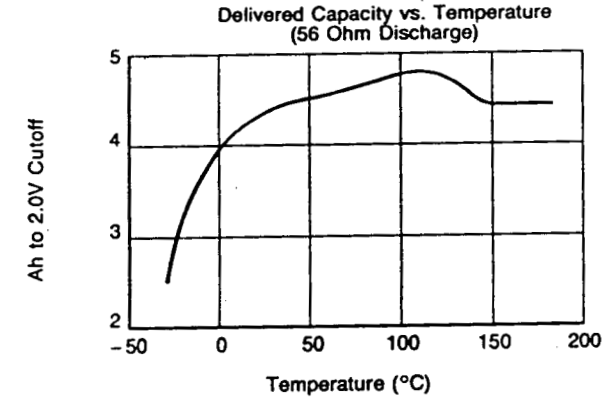

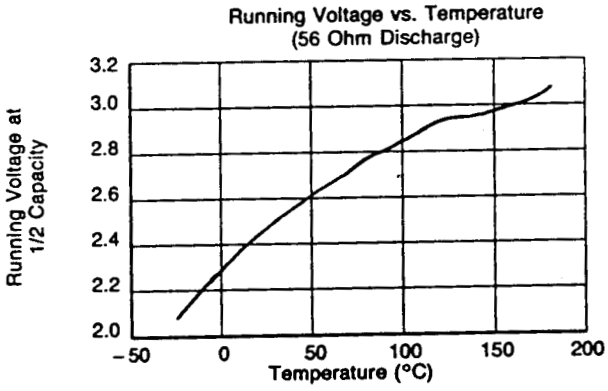

PMX

SERIES PMX-HT

3B1750

C SIZE

SPECIFICATIONS

Operating Temperature Range	-20°C to 180°C
Nominal Discharge Rate	45mA
Maximum Continuous Rate	250mA
Nominal Capacity	4.0Ah
Volume	25.5cm³
Weight	46g
Fuse	1A

PERFORMANCE CHARACTERISTICS

(Under 56 Ohm Load)	at 25°C	at 180°C
Energy	10.0Wh	13.0Wh
Gravimetric Energy Density	220Wh/kg	280Wh/kg
Volumetric Energy Density	0.39Wh/cm³	0.51Wh/cm³

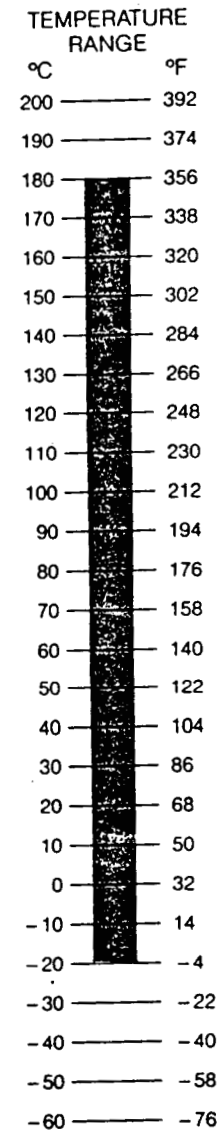

54

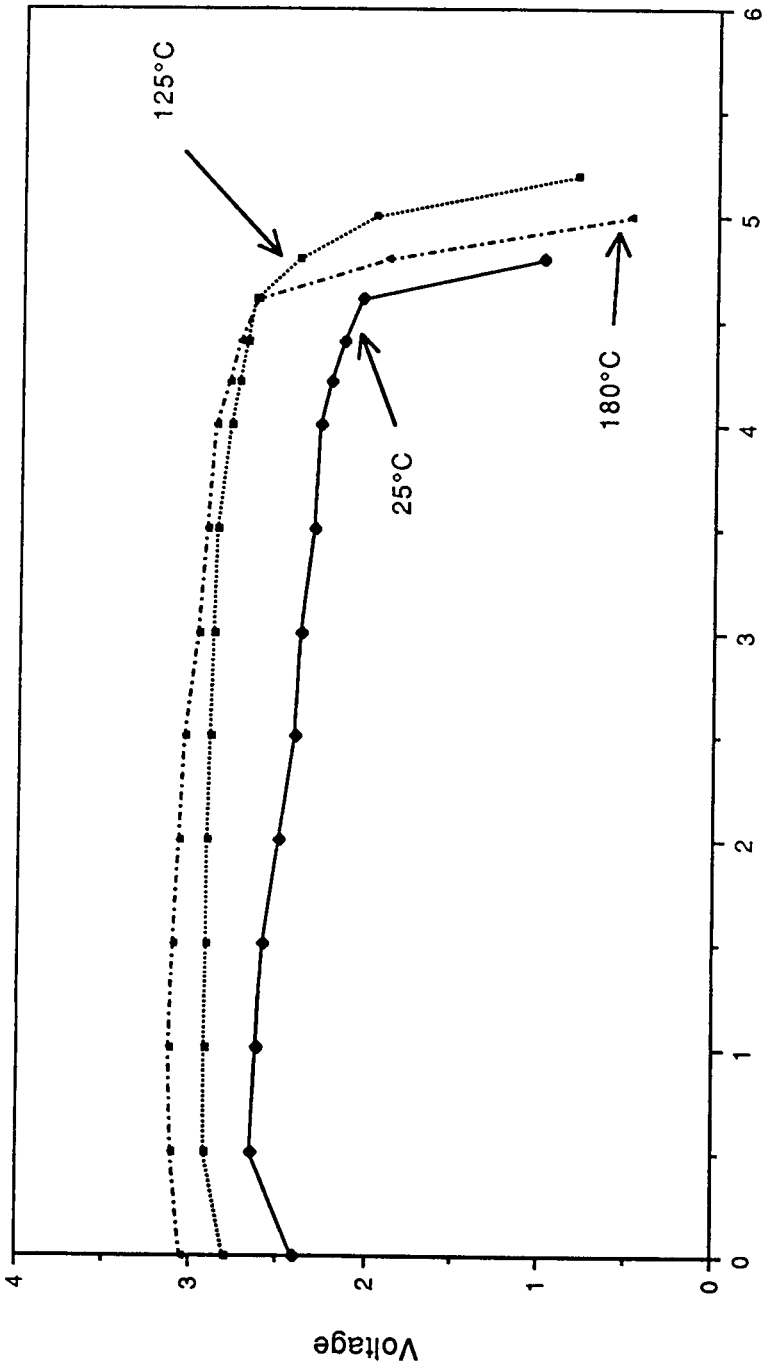

Figure 1. PMX-HT C: Typical 56Ω (≈50 mA) discharge characteristics.

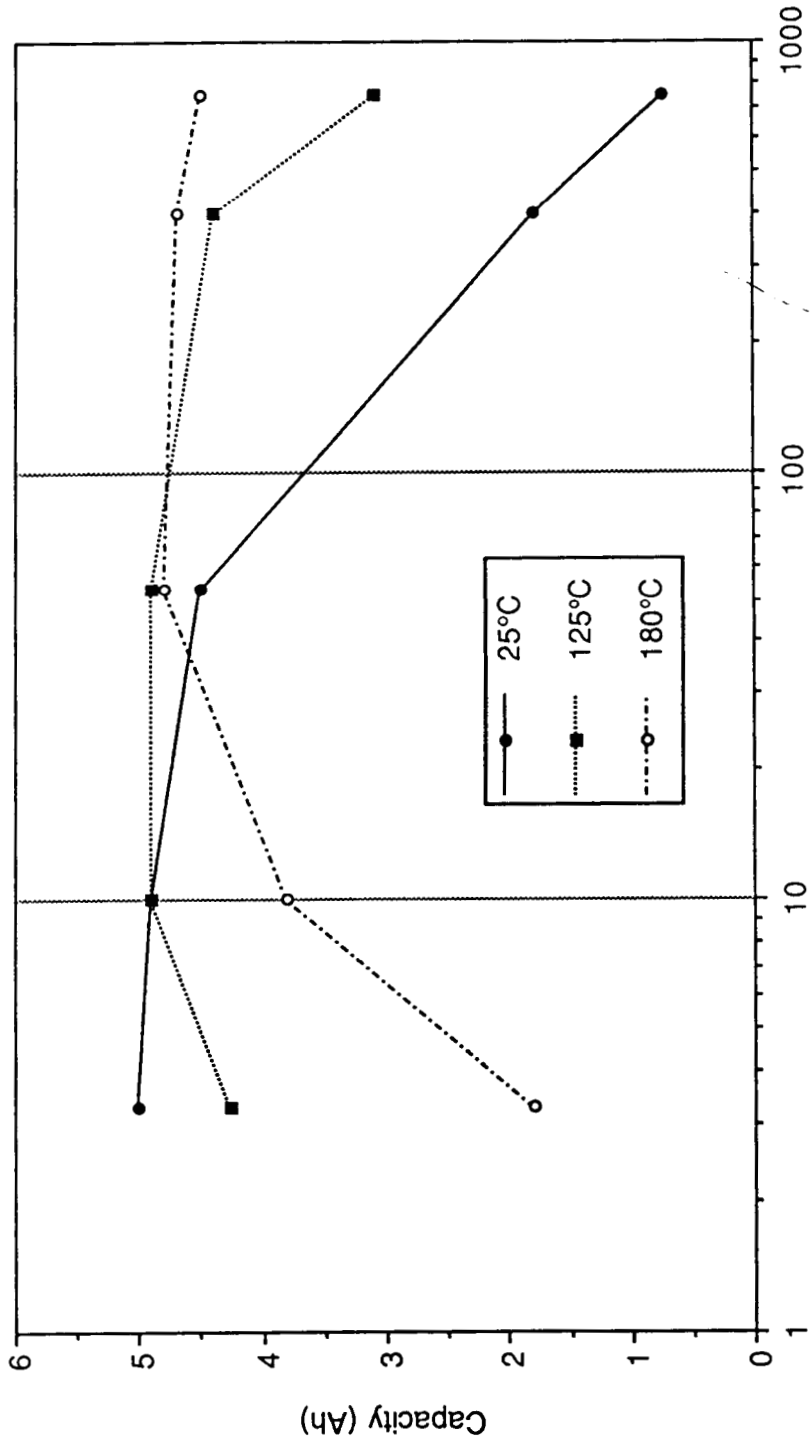

Figure 5. Capacity vs. discharge rate characteristic at three temperatures.

WILSON GREATBATCH LTD. 10,000 WEHRLE DR., CLARENCE, NY 14031 U.S.A TELEX: 91 386 FAX: 716 759 8579
TELEPHONE: 716/759-6901

PMX-HT 1/2AA

Lithium / Fluorinated Carbon

Preliminary Specifications

Capacity	0.6Ah
Operating Temperature Range	-20°C to 180°C
Average Running Voltage	3.0V
Energy	1.7Wh
Weight	8g
Volume	4.2cm^3
Energy Density (gravimetric)	220Wh/Kg
Energy Density (volumetric)	0.43Wh/cm^3
Maximum Continuous Rate	200mA
Nominal Discharge Rate	45mA

LITHIUM/SILVER VANADIUM OXIDE HIGH RATE AA CELL

PRELIMINARY SPECIFICATIONS

THEORETICAL CAPACITY	2.0 AH
OPEN CIRCUIT VOLTAGE	3.2 VOLTS
AVERAGE RUNNING VOLTAGE	2.6 VOLTS
WEIGHT	23 GRAMS
DIMENSIONS	1.43 CM O.D. 4.98 CM HEIGHT
VOLUME	7.97 CC
GRAVIMETRIC ENERGY DENSITY	224 WH/KG
VOLUMETRIC ENERGY DENSITY	652 WH/L

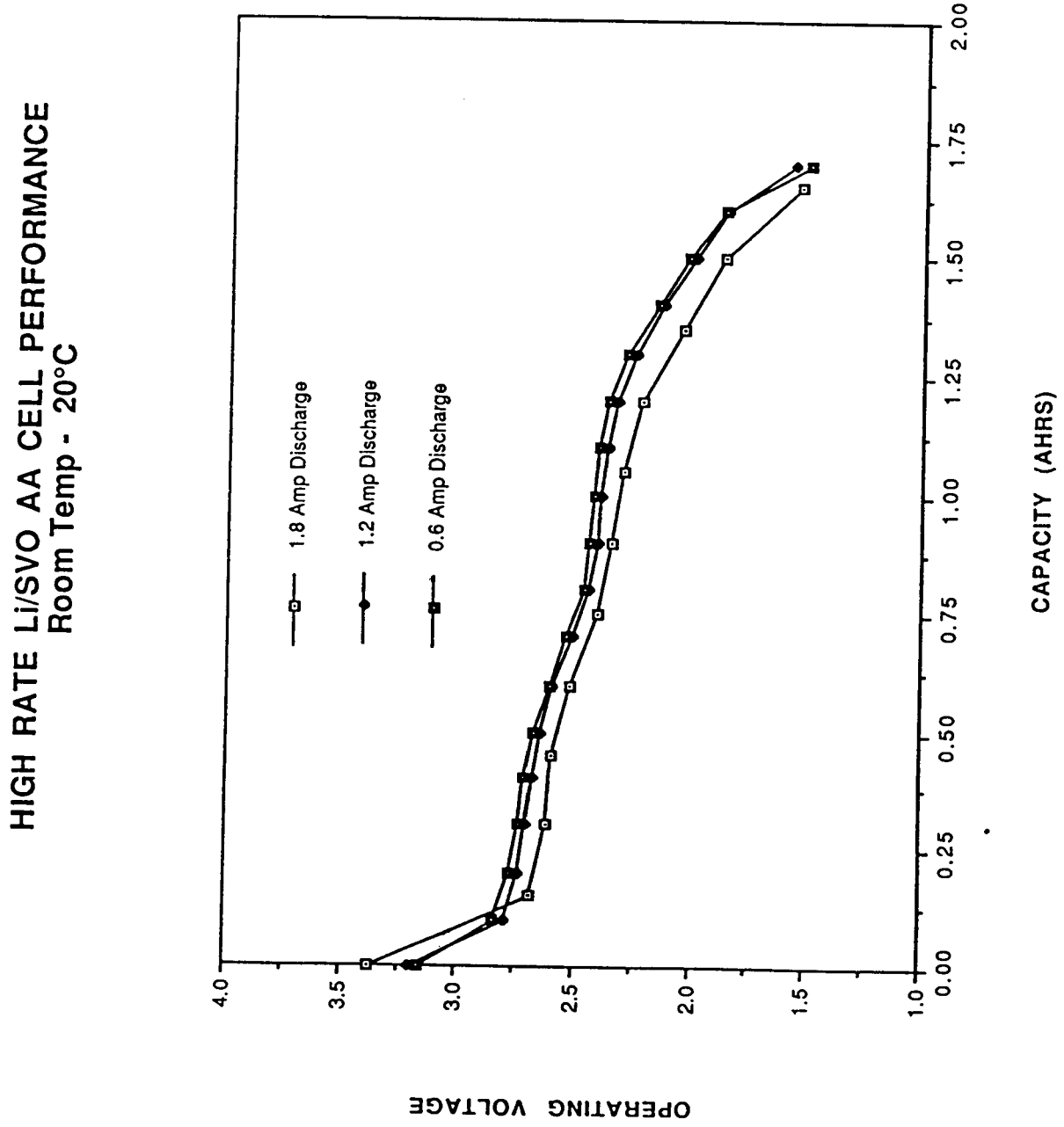
HIGH RATE Li/SVO AA CELL PERFORMANCE
Room Temp - 20°C
1.8 Amp Discharge
1.2 Amp Discharge
0.6 Amp Discharge
OPERATING VOLTAGE
4.0
3.5
3.0
2.5
2.0
1.5
1.0
0.00
0.25
0.50
0.75
1.00
1.25
1.50
1.75
2.00
CAPACITY (AHRS)

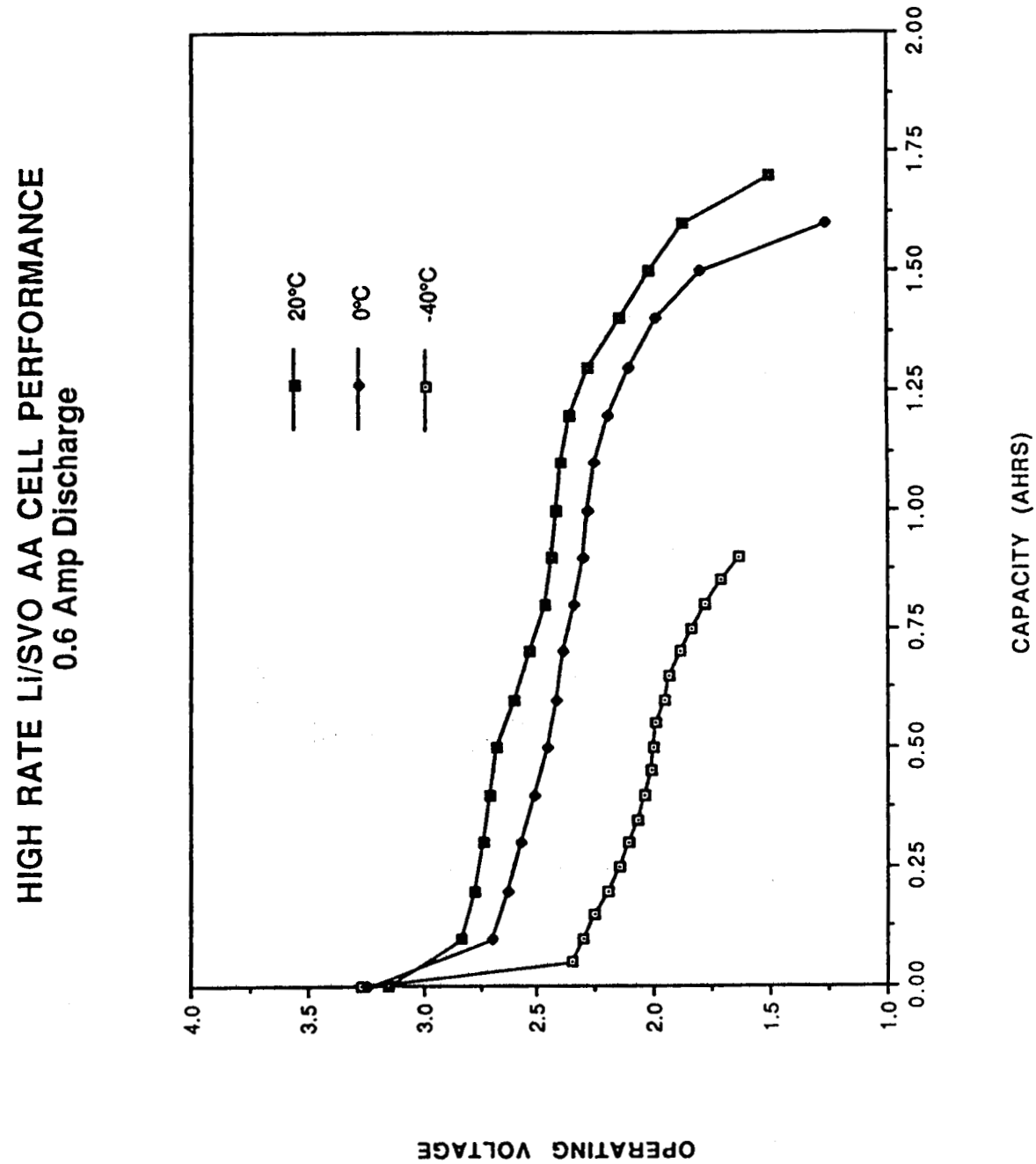
HIGH RATE Li/SVO AA CELL PERFORMANCE
0.6 Amp Discharge
20°C
0°C
-40°C
OPERATING VOLTAGE
4.0
3.5
3.0
2.5
2.0
1.5
1.0
0.00
0.25
0.50
0.75
1.00
1.25
1.50
1.75
2.00
CAPACITY (AHRS)

WILSON GREATBATCH LTD. 10,000 WEHRLE DR., CLARENCE, NY 14031 U.S.A TELEX: 91-386 FAX: 716/759-8579
TELEPHONE: 716/759-6901

LITHIUM/SILVER VANADIUM OXIDE HIGH RATE C CELL

PHYSICAL CHARACTERISTICS

Dimensions: 1.009" O.D. x 1.82" H
Weight: 61.7 grams
Volume: 23.8 cc

PERFORMANCE

Open Circuit Voltage: 3.35V
Theoretical Capacity to 2.0V: 6.48 Ahrs
Average Operating Voltage: 2.6V
Gravimetric Energy Density: 273 Whrs/kg
Volumetric Energy Density: 696 Whrs/L
Self Discharge: less than 1% per year

PROJECTED PERFORMANCE CHARACTERISTICS AMBIENT AND LOW TEMPERATURE

Discharge Rate (Amps)	Temperature (°C)	Capacity to 2V (Ahrs)
3.0	20	4.54
2.0	20	4.86
1.1	20	4.86
1.1	0	4.54
0.5	0	4.21
1.1	-40	1.62
0.5	-40	1.62

WILSON GREATBATCH LTD. 10,000 WEHRLE DR., CLARENCE, NY 14031 U.S.A TELEX: 91-386 FAX 716/759-8579
TELEPHONE: 716/759-6901

LITHIUM/SILVER VANADIUM OXIDE HIGH RATE D CELL

PHYSICAL CHARACTERISTICS

Dimensions: 1.316" O.D. x 2.45" H
Weight: 129.5 grams
Volume: 54.5 cc
Bottom Slit Vent Design

PERFORMANCE

Open Circuit Voltage: 3.35V
Theoretical Capacity to 2.0V: 13.81 Ahrs
Average Operating Voltage: 2.6V
Gravimetric Energy Density: 277 Whrs/kg
Volumetric Energy Density: 659 Whrs/L
Self Discharge: less than 1% per year

PROJECTED PERFORMANCE CHARACTERISTICS AMBIENT AND LOW TEMPERATURE

Discharge Rate (Amps)	Temperature (°C)	Capacity to 2V (Ahrs)
6.0	20	9.67
4.2	20	10.36
2.3	20	10.36
2.3	0	9.67
1.1	0	8.95
2.3	-40	3.45
1.1	-40	3.45

U.K. OFFICE: TRING HOUSE, 9 ST. CUTHBERTS STREET, BEDFORD MK40-3JB TELEPHONE: 0234-215763 FAX: 0234-212912

CELL CHARACTERISTICS

LITHIUM/TITANIUM DISULFIDE AA CELL

CAPACITY	0.75 Ah
AVERAGE VOLTAGE	2.1V
CYCLING VOLTAGE LIMITS	2.6 TO 1.6V
DIMENSIONS	1.4 x 4.0 cm
VOLUME	7.9 cc
WEIGHT	18.0 g
ENERGY DENSITY (GRAVIMETRIC)	87.5 Wh/kg
ENERGY DENSITY (VOLUMETRIC)	200 Wh/L

AA Li/TiS2 CYCLE LIFE PERFORMANCE
100/400 mA Charge/Discharge regime
Cell: 45716

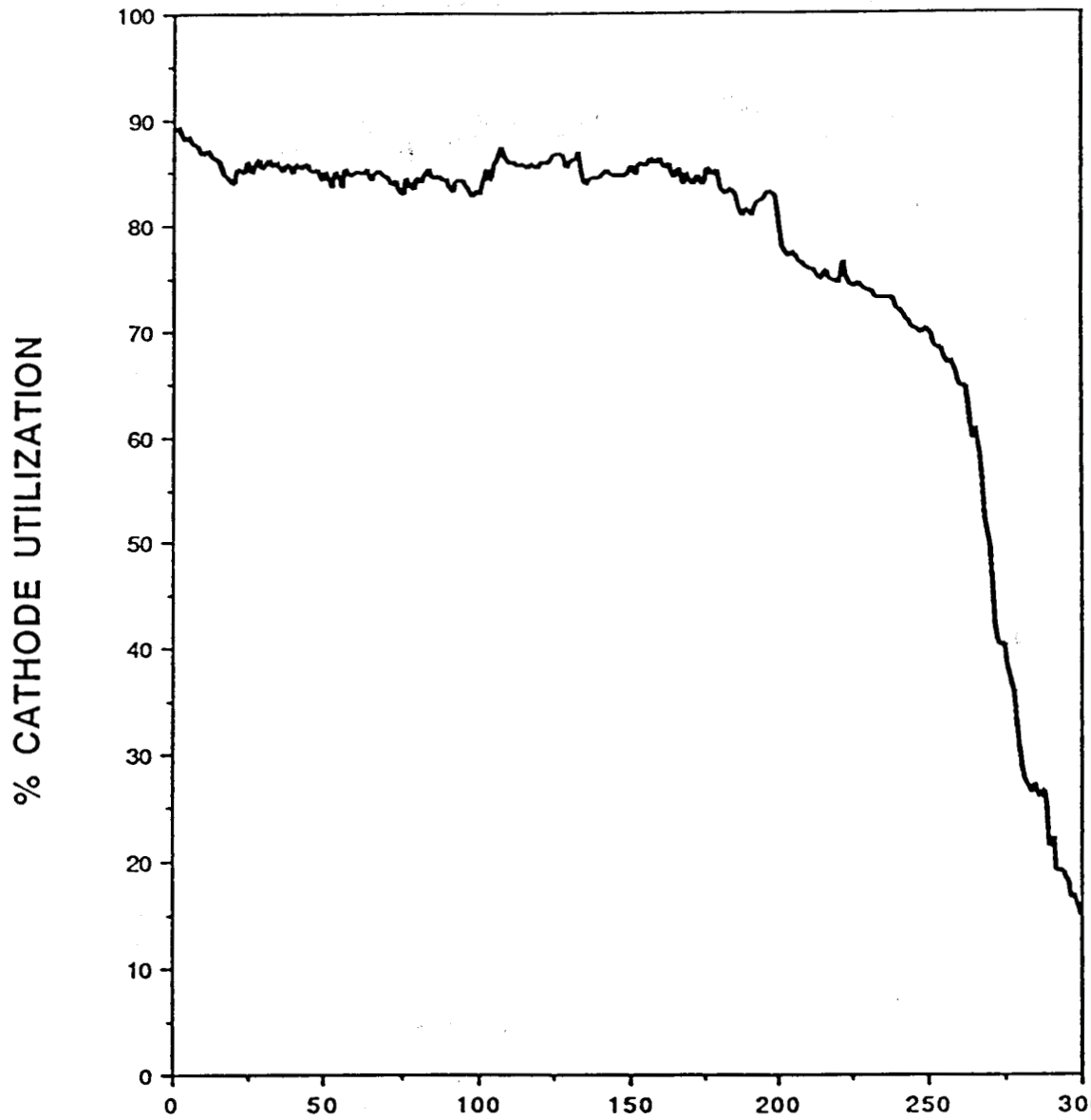

AA Li/TiS2 Cell Performance
1.0A Discharge .250A Charge

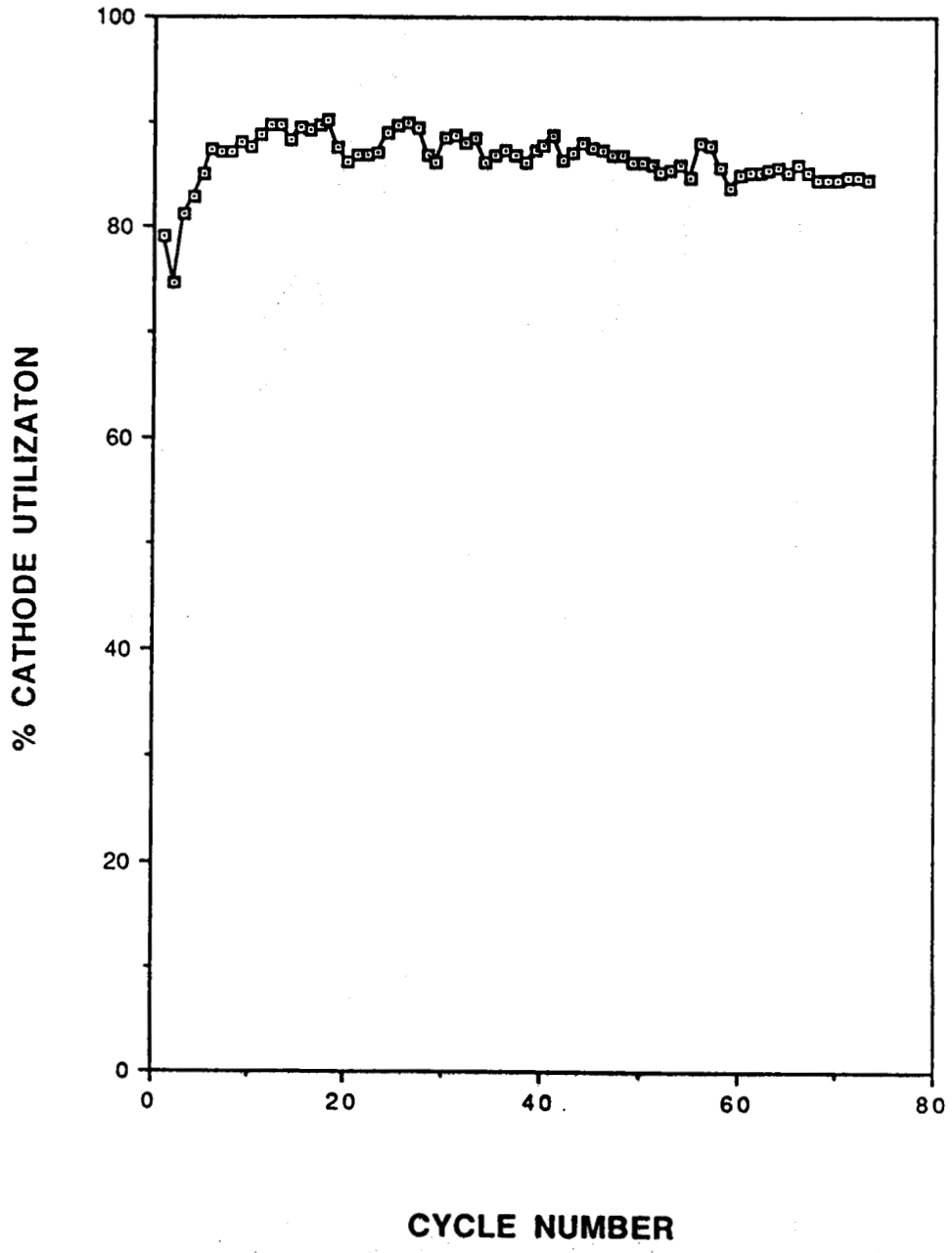

WILSON GREATBATCH LTD.

R&D CONTRACTS

(1) JET PROPULSION LABORATORY/CALIFORNIA INSTITUTE OF TECHNOLOGY
No. 957092
Developing a Flight Quality Lithium Thionyl Chloride Cell
Contract ended July 1985

(2) JET PROPULSION LABORATORY/CALIFORNIA INSTITUTE OF TECHNOLOGY
No. 958449
High Rate D Size Lithium-Thionyl Chloride ($Li-SOCl_2$) Cells
Contract ended 31 October 1989

(3) JOHNS HOPKINS UNIVERSITY/APPLIED PHYSICS LABORATORY
No. 605127-S
Development of a Lithium Battery for the Ingestible Telemetry Device
30 May 1989 - 31 December 1989

(4) NASA/GODDARD SPACE FLIGHT CENTER
No. NAS5-30492 - Phase I
Low Temperature Electrolytes for Emergency Locator Transmitter
27 January 1989 - end of July 1989

(5) NASA/JOHNSON SPACE CENTER
No. NAS9-17701
Li-BCX Cell Design Improvement and Data Generation
17 September 1986 - 31 January 1987

(6) NASA/JOHNSON SPACE CENTER
No. NAS9-17821
Support Testing and Improvement of Lithium/Bromine Complex Cells
25 June 1987 - 1 July 1988

(7) NASA/JOHNSON SPACE CENTER
No. NAS9-18142
Testing and Evaluation of Li-BCX Battery Cells (Size DD)
27 April 1989 - 28 February 1990

(8) SANDIA NATIONAL LABORATORIES
No. 66-7980
Lithium Sulphur Dioxide D Cell
Early February 1990 - 26 September 1990

1

(9) JET PROPULSION LABORATORY - NASA - SBIR - PHASE I
No. NAS7-1081
Rechargeable Li/TiS_2 Cells with Long Cycle Life
Early February 1990 through July 29, 1990

(10) NASA/GODDARD SPACE FLIGHT CENTER - SBIR - PHASE II
No. NAS5-30964
Development of a Battery for the Emergency Locator Transmitter
29 May 1990 - 29 May 1992

(11) NIH - NATIONAL HEART, LUNG, AND BLOOD INSTITUTE - Phase I
No. R43 HL40740-01
Rechargeable Lithium Battery/Ventricular Assist Systems
7 April 1988 - 6 October 1988

(12) NIH - NATIONAL HEART, LUNG, AND BLOOD INSTITUTE - Phase II
No. 2 R44 HL40740-02
Rechargeable Lithium Battery/Ventricular Assist Systems
March 1990 - March 1992

(13) NASA/JOHNSON SPACE CENTER
NAS 9-18395
Lithium/Bromine Complex Cells for Use in AN/PRC-112 Survival Radio
August 1990 - July 1991

(14) SANDIA NATIONAL LABORATORIES
No. 75-0840
Lithium Sulphur Dioxide HR "D" Cells
January 1989 - August 1989

ACKNOWLEDGEMENTS

Development Activities

Dr. Esther Takeuchi, Mr. Steve Ebel, Mr. Cliff Post, Mr. David Spillman, Ms. Christine Frysz, Ms. Denise Tuhovak, Mr. William Thiebolt, Mr. Michael Pyszczek, Mr. Michael Zelinsky

Testing/Analysis/Consultation

Mr. Tom Umphreyville, Mr. Doug Eberhard, and Mr. Paul Krehl

SAFT ADVANCED BATTERY DIVISION

AEROSPACE DEPARTMENT

PERFORMANCES OF 250 AH LITHIUM/THIONYL-CHLORIDE CELLS

THE 1990 NASA BATTERY WORKSHOP
MARSHALL SPACE FLIGHT CENTER
4 - 6 DECEMBER 1990

1 INTRODUCTION.

SAFT is developing a 250 Ah Lithium Thionyl Chloride Battery for an US booster.
In the frame of this development, extensive cell testing is running to evaluate functional and safety performances. We will present to-day some significant results obtained during this evaluation phase.

2 DESIGN.

Cell was designed to provide a 250 Ampere hour capacity with discharge currents from 4 to 60 Amps with voltage requirements at more than 3.3 Volts per cell.
In addition, the battery has to provide 75 Amps pulse current with relaxed voltage.
Cells designed to fulfil these requirements have a cylindrical shape with 133 mm diameter (5.24') and 98 mm height on case (3.86'). Cell weight is 2.8 Kg (6.17 Lb).

3 TEST CONDITIONS.

It has to be well understood that the cells being not the final product to be used alone, but the battery, individual cell testing depends strongly of cell interfaces and test procedures used.
Cell evaluation testing has not the ambition to verify that a full battery in flight conditions will pass a given specification, but to give data to achieve the same goal by analysis.
So, the test conditions used for the various test presented hereafter are the following; as summarized in Figure 1:

3.1 TEST TYPE 1.

Cell stack is tested in boiler plate conditions. Temperature of the boiler plate is controlled by circulation of a fluid into the wall of the boiler plate case.
Cell is filled by a remote system before discharge. So, stand-by time between activation and discharge could vary from minutes to days. All this equipment is very heavy and has a wide thermal capacity. Temperature of the electrochemical system is maintained by the temperature of the wall in contact with electrolyte.

3.2 TEST TYPE 2.

Cell exists physically, with its cell case, cover, bottom, in final configuration.
The cell is electrically insulated from an aluminium sleeve, 3 mm thick, which is clamped in a thermally controlled water jacket, and this provides a thermal resistance to the reference temperature.
Cell is filled and activated before discharge by the same remote system as above.

3.3 TEST TYPE 3.

Cell is installed, electrically insulated, into a 8 mm thick aluminium sleeve. This sleeve is clamped into the water jacket to control its temperature.

3.4 TEST TYPE 4.

Cell is installed, electrically insulated into a 8 mm thick aluminium sleeve, as above, but this sleeve is placed into a thermal chamber or ambient to control its temperature only by convection.

4 TEST RESULTS.

4.1 PRE-TEST CONDITIONS.

Unless otherwise stated, all tests are done after a preliminary discharge having the role to check cell integrity before further testing.
This preliminary discharge consists in discharging one minute at 65 Amps followed

by thirty seconds at 35 Amps. This test is repeated three consecutive days. Typical results are shown in figure 2.
It can be seen that there is no significant voltage delay in these conditions, as the voltage drop when current is switched on is 3.15 Volts the first day, which is higher than the following voltage plateau, which is normal at the test temperature.
It can be seen also that this voltage drop decreases from day one to day three.

4.2 ABUSE TESTS ON FRESH CELLS.

Safety is one of the major concerns when we consider the use of so high energy density systems as Lithium Thionyl Chloride. So we will talk now of cell behaviour in abuse condition.
Cells are fresh cells, having passed only the pre-test above. They are interfaced in test condition type 4.

4.2.1 Short circuit.

Cell is dead shorted by an approximately 6 milliohms system. Figure 3 shows the voltage monitoring during that test. Current measurement was not accurate, but short circuit current was estimated around 600 Amps. After 15 or 17 seconds, positive terminal melts, destroying the glass to metal seal, and cell stack burns through positive terminal and burst disc apertures during approximately 15 minutes. Figure 4 shows the temperature evolution of two different locations, on cover side and on wall side.
This test shows that this type of abuse could be easily prevented by an adequate fuse system if necessary.

4.2.2 Charge.

Cell is treated as a secondary cell and is charged with a constant 40 Amps current.
Figure 5 shows voltage and temperature evolution during that test for a cell tested with forced convection at 15 °C. As cell is not a secondary system, all the electrical energy supplied is turned into heat and final equilibrium temperature and voltage depends of thermal environment.
If heat exchange is not high enough, cell vents.
In fact, charging a cell is a way to heat a cell by the inside and safety issues are the same as for external heating we will see now.

4.2.3 Overtemperature.

Cell is externally heated. Figure 6 shows the voltage and cell housing temperature evolution. Test is continued up to venting.

4.3 DISCHARGES AT DIFFERENT CURRENTS, TEMPERATURES.

4.3.1 Effect of temperature.

Discharges with steady state currents of 60 Amps are presented in Fig 7 for temperatures ranging from 5 to 80°C.
For temperatures of 10 and 40°C, that's fresh cells, without pre-test discharge, with test conditions type 2.
For temperatures 5, 45 and 80°C, that's cells having previously sustained the pre-test discharge at ambient temperature (which represents 4.2 Ampere hours), and tested in type 3 conditions.
Two particularities have to be noted on these curves:
One is for the shape of the curve at 10°C versus the others. That could be explained by the cell self heating, in an area where some degrees increase of internal temperature has a strong effect on performances.
The other is the important voltage delay (2.3 Volts) observed at the beginning

of discharge after stabilisation at 80°C for a cell already discharged by 4.2 Ampere hours at ambient temperature. This confirms the impact on performances presented by storage at high temperature of partially discharged cells.

4.3.2 Effect of discharge current.
Figure 8 presents discharge curves at various currents for a temperature of 40°C.
Performances presented here are on cells having not been submitted to preliminary discharge and tested in condition 2 and 3.
Discharge at 14 Amps including several pulses at various different currents than 14 Amps, these pulses are not presented for more clarity.
Discharge at 60 Amps is one of the above presented.
On the same graph is presented a typical discharge with currents varying from 42 to 60 and 75 Amps. On this curve, we can see, by comparing it to the constant 60 Amps discharge, the effect of cell internal temperature rise up: During the final 60 Amps pulse, voltage is lower on cell continuously discharged at 42 Amps, which is due to the fact that at this time, internal temperature is lower. In the same way, it can be seen that the slope of the decreasing voltage is worst during discharge at 42 Amps than during discharge at 60 Amps; this is due to the fact that as already mentioned about comparisons of several discharges at 60 Amps, voltage decay is less compensated by internal heating for discharges at 42 Amps than for discharges at 60 Amps.

4.3.3 Summary of electrical performances.

4.3.3.1 Capacity.
From the type of tests presented above, we have deduced the following mean performances:
Fig 9 presents the evolution of capacity versus temperature for average discharge currents of 14, 43, and 60 Amps.
Capacity is computed including the eventual preliminary discharge if necessary, and with a cutoff of 2.8 Volts, which is always under the "knee" of the discharge curve whatever the discharge conditions are.
For 60 Amps, discharges are really made at 60 Amps constant current.
For 43 Amps, discharges are made with currents 42, 60, 75 Amps, and the average is 43 Amps for the generally observed returned capacity.
For 14 Amps, discharges are made at 4, 14, 20 and 25 Amps and the average value is close to 14 Amps.
Curves are plotted by using average values for each temperature and currents.
The more accurate one is for 43 Amps, giving the already well known evolution of efficiency versus temperature, with its maximum around 45°C. The main observation to be made is the confirmation of the strong effect of coldest temperatures, with an important loss of capacity.

The evolution observed for constant currents of 60 Amps, shows the highest capacities at temperatures of less than 40°C. This is due to the fact that as already explained, at this current, actual cell internal temperature is higher than test temperature. This phenomenon also exists at 43 Amps, but is less severe.
The value obtained at 60 Amps and 80°C coresponds to the maximum test conditions, as at end of discharge, cells are near the limit of venting.
It is sure that for high temperatures and high currents, capacity will be limited by venting problems. Future test will allow us to go into more details for these limitations.

The evolution for 14 Amps is supposed as we have to-day only one plot! By deduction from the above observations, we think that maximum efficiency will probably be observed at temperatures higher than 40°C. Why?
For 60 Amps, we have the maximum efficiency around 30°C, this corresponds to a given optimum internal temperature, for 43 Amps, it's 45°C, which corresponds to the same internal temperature. As at 14 Amps, current internal thermal gradient will be less than for the others, it will be necessary to have a higher test temperature to obtain the same internal optimum temperature. Further test to be performed in the future will infirm or confirm this assumption.
So, determination of optimum cell capacity versus cell wall temperature is a way to evaluate the efficiency of cell internal design: As high is this maximum, as good is the cell internal thermal conductivity.
The consequence is that a cell having been designed for high currents, high temperature, with small thermal gradients, will have low performances at cold temperature, as self heating will be lower.

4.3.3.2 Voltage.
Figure 10 presents the evolution of voltage versus currents for different temperatures.
Plotting is made by using the average value of all voltages recorded during discharges, including the various pulses, all along the discharges.
Nevertheless, the "knee" of the discharge curves are not taken into account, by limiting the data to:

250 Ampere hours for cells exceeding 275 Ampere hours.
200 Ampere hours for cells which capacity is comprised between 225-275 Ampere hours .
100 Ampere hours for cells which capacity is less than 225 Ampere hours.
In the above limit, we made the average of all plots describing the curve, including the main discharge and the various pulses.
So, the presented curve represents the average voltage versus current and temperature, whatever the time is during during discharge.
A more accurate data treatment has to be made to separate performances at the beginning of discharge, during the "plateau" and during end of discharge.

4.4 POST DISCHARGE SAFETY TESTS.

4.4.1 Reversal
Some discharges have been followed by reversal at a current of 42 Amps.
Two procedures have been experienced for that:
The first procedure consists in an uninterrupted discharge, the current being automatically switched to 42 Amps when the cutoff of 2.8 Volts of the normal discharge is reached, and the discharge being continued in these conditions with no stop, at the same temperature conditions than the main discharge. This is what is shown on Figure 11 after a discharge at 5°C and 60 Amps constant current. This type of test is representative of continuing a discharge of a battery in which, for any reason, a cell has a lower capacity than the other ones.
As presented here, a stable reversal is obtained when the temperature is sufficiently low.
Figure 12 presents what could happen if stable conditions are not achieved: For that test, vent was replaced by a pressure gauge, the cell was first discharged at 45°C and 283 Ampere hours have been drawn. When going to reversal at 42 Amps, voltage and pressure rise and the cell would have vented in normal conditions. As it was not present, reversal continues, but with a negative voltage higher than "normal".

The second procedure consists to stop the discharge at the normal cutoff of 2.8 Volts, then to allow the cell to rest in open circuit voltage for hours or days, and to start a new discharge-reversal at the specified current of 42 Amps after stabilisation at room (or specified) temperature, different from the conditions where main discharge was made.
This type of test is representative of a discharge initiated on preliminary discharged cells.
Test results corresponding to that case are not yet available.

4.4.2 Overtemperature
Some cells have been submitted to the same overtemperature test after discharge than already presented on fresh cells. Figure 13 shows the temperature and voltage evolution up to venting, showing that the cell is still safe in discharge condition, as venting temperature is lower than lithium melting point, which is 182°C.

4.5 DISCHARGES ON AGED CELLS.

Very few results are available to day, but main of the cells are in storage now and we hope to be in a position to present you more results next year.
Figure 14 shows the pre-test characteristics of the same cell before and after a period of four months of storage at a temperature of 5°C. Performances are not significantly affected, ambiant temperature for the test being slightly worst for the post storage test.
For the same cell, Figure 15 shows discharge after 4 months storage at 5°C, the discharge being made at 40°C in test conditions type 4.(i.e cell in thermal chamber). This cell was predischarged of 4.2 Ampere hours before storage, and one additional Ampere hour was drawn in the same condition after the storage period, as presented above.
Capacity returned is slightly higher than the above presented results, this is due to the fact that for the first time we discharged cells into a thermal chamber instead of controlling the cell temperature by a fluid loop. This leads to a higher thermal gradient (cell wall temperature was 53°C at end of discharge) with the consequence of higher performances.

4.6 CONCLUSION.

This brief presentation of some of the typical test results presented to-day leads to the following conclusions:
For the users:
The Lithium/Thionyl-Chloride batteries are elected for their high energy density, which is to say their low weight, compared to others sources.
The temperature of a lower weight item will be more sensitive to variations of internal and external heat fluxes than an heavier one. So, if previously temperature could be considered as a relatively independent parameter, it's no longer true.
The use of high energy density Lithium/Thionyl-Cloride batteries is subjected to stringent thermal requirements to have benefit of energy density and to stay safe in any conditions.
The battery thermal environment and discharge rate have to be adjusted to obtain the right temperature range at cell level, to have the maximum performances.
Due to the strong correlation between performances and environment, users are to be very careful in specifying their need. Especially, what they imagine to be the worst cases could not be the right ones.

For the designers:
Voltage and Capacity of Lithium/Thionyl-Chloride cells are very sensitive to temperature.
This temperature is the cell internal actual temperature during discharge.
This temperature is directed by external thermal environment and by cell internal heat dissipation, i.e cell actual voltage.
Thus, the only way to pass from test results to prediction of operational performances is through a modelization of all this parameters. Direct extrapolation from test results to operational conditions is hazardous and must be avoided.

SAFT AEROSPACE DEPARTMENT	1990 NASA BATTERY WORKSHOP

VHS 250 AM CELL DESIGN

FIGURE 0

CAPACITY : 250 Ah

CURRENT : 4 to 60 Amps

PULSES : 75 Amps 2 minutes

VOLTAGE REQUIREMENT : > 3.3 Volts

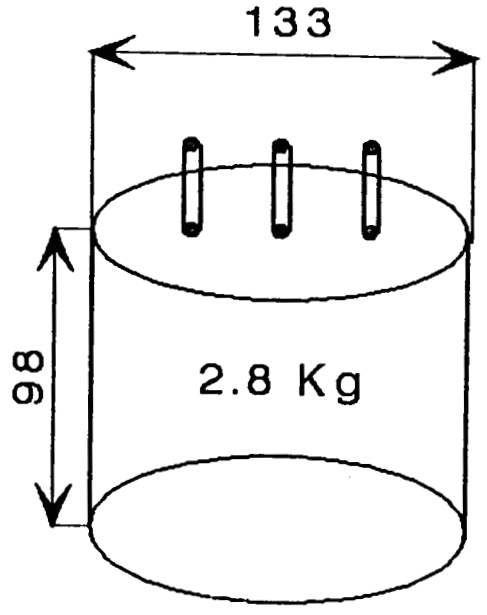

SAFT AEROSPACE DEPARTMENT	1990 NASA BATTERY WORKSHOP

TEST CONDITIONS

FIGURE 1

TYPE 1

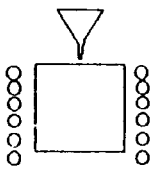

TYPE 2

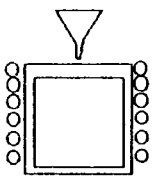

TYPE 3

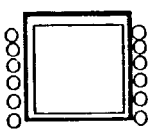

TYPE 4

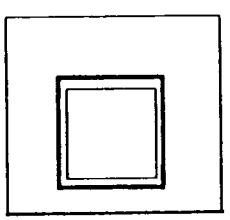

SAFT AEROSPACE DEPARTMENT

1990 NASA BATTERY WORKSHOP

VLS 250 AM - PRELIMINARY DISCHARGE

FIGURE 2

SAFT AEROSPACE DEPARTMENT	1990 NASA BATTERY WORKSHOP

VLS 250 AM - SHORT CIRCUIT

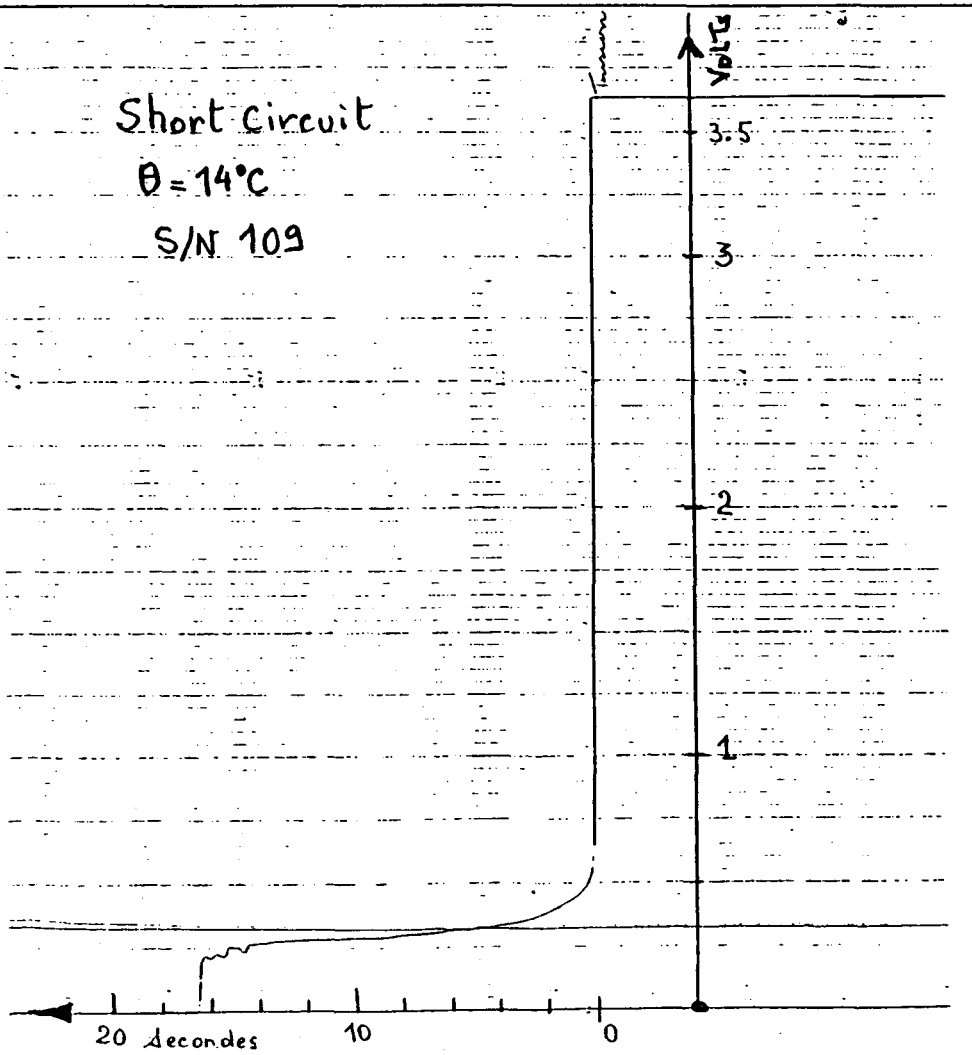

FIGURE 3

SAFT AEROSPACE DEPARTMENT	1990 NASA BATTERY WORKSHOP

VLS 250 AM - SHORT CIRCUIT

FIGURE 4

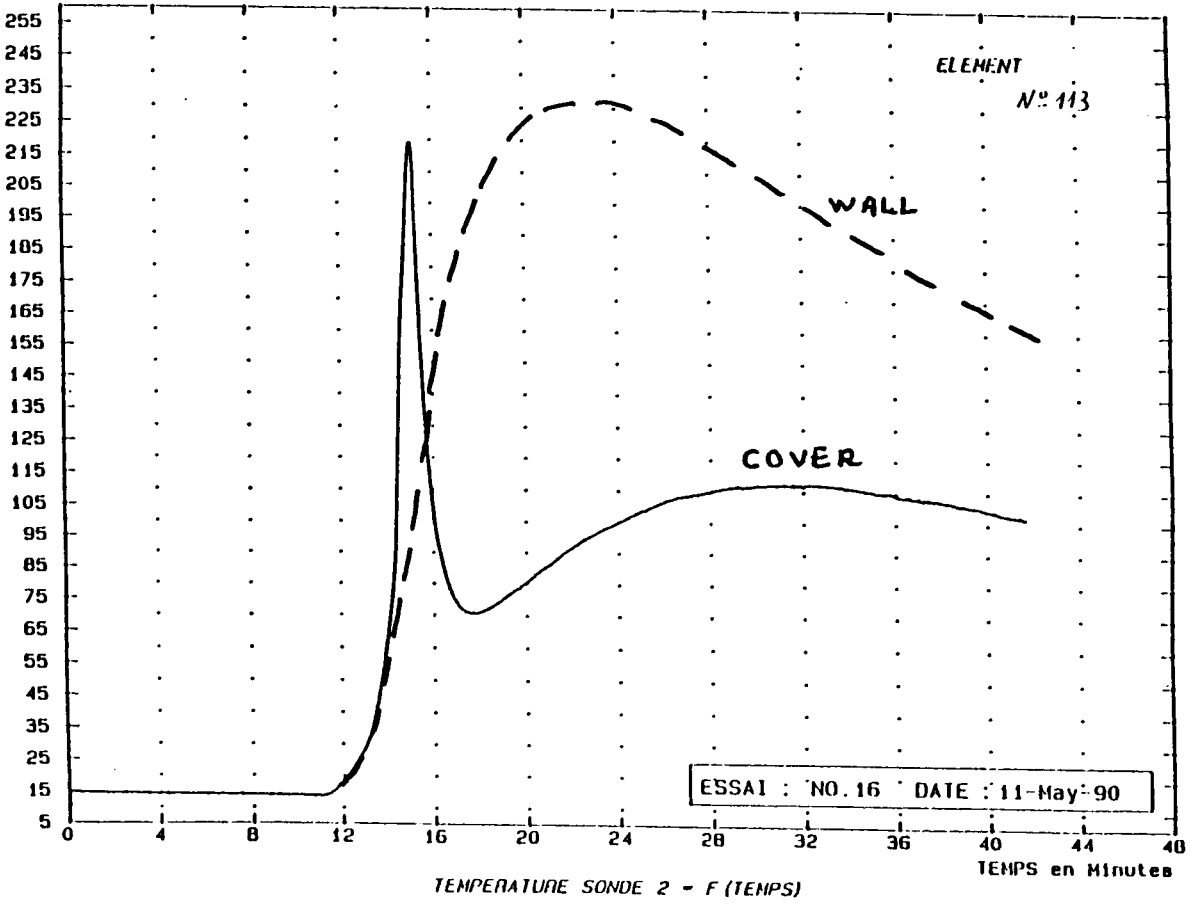

SAFT AEROSPACE DEPARTMENT	1990 NASA BATTERY WORKSHOP

VLS 250 AM - CHARGE

FIGURE 5

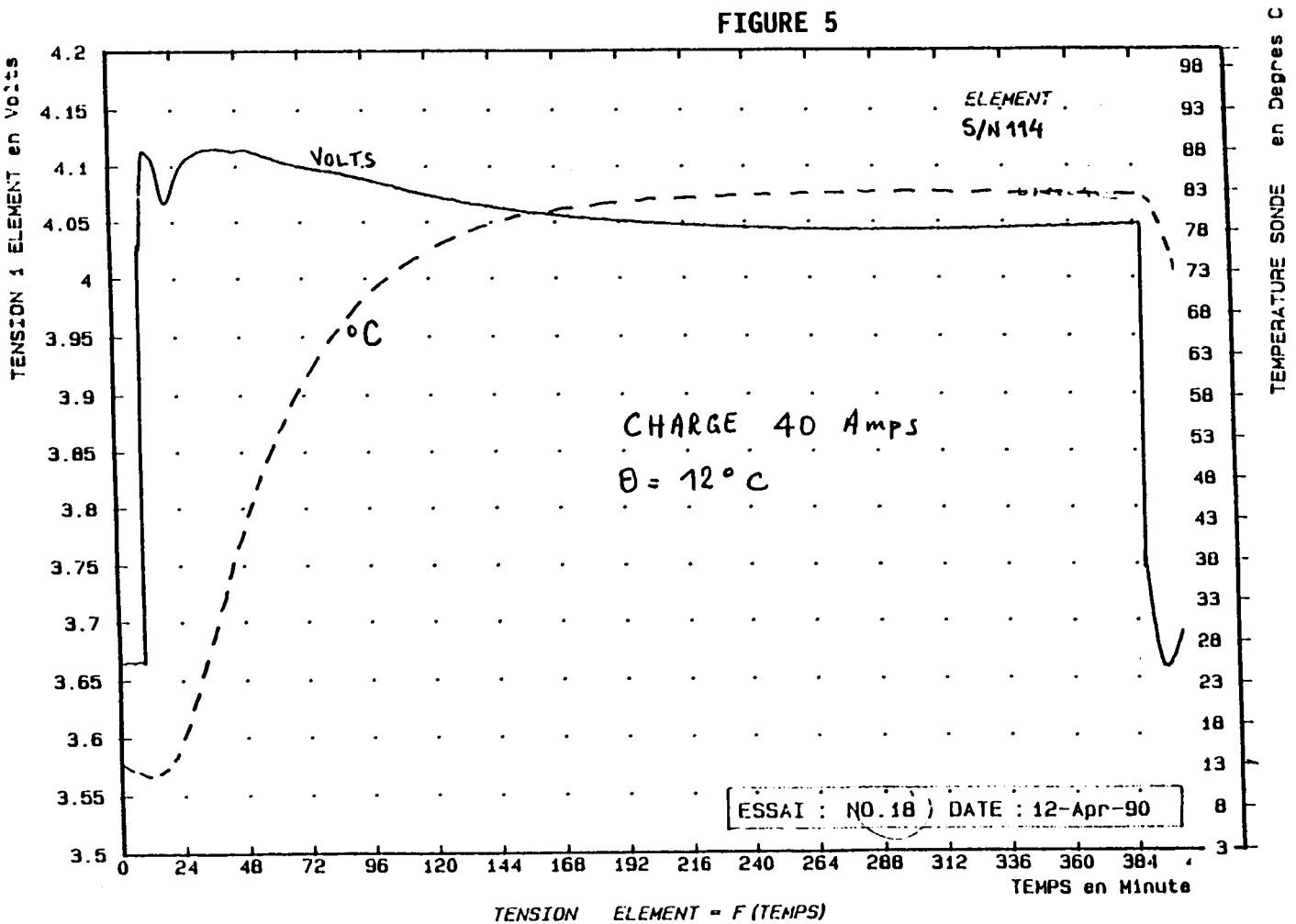

TENSION ELEMENT = F (TEMPS)

SAFT AEROSPACE DEPARTMENT	1990 NASA BATTERY WORKSHOP

VLS 250 AM - OVERTEMPERATURE

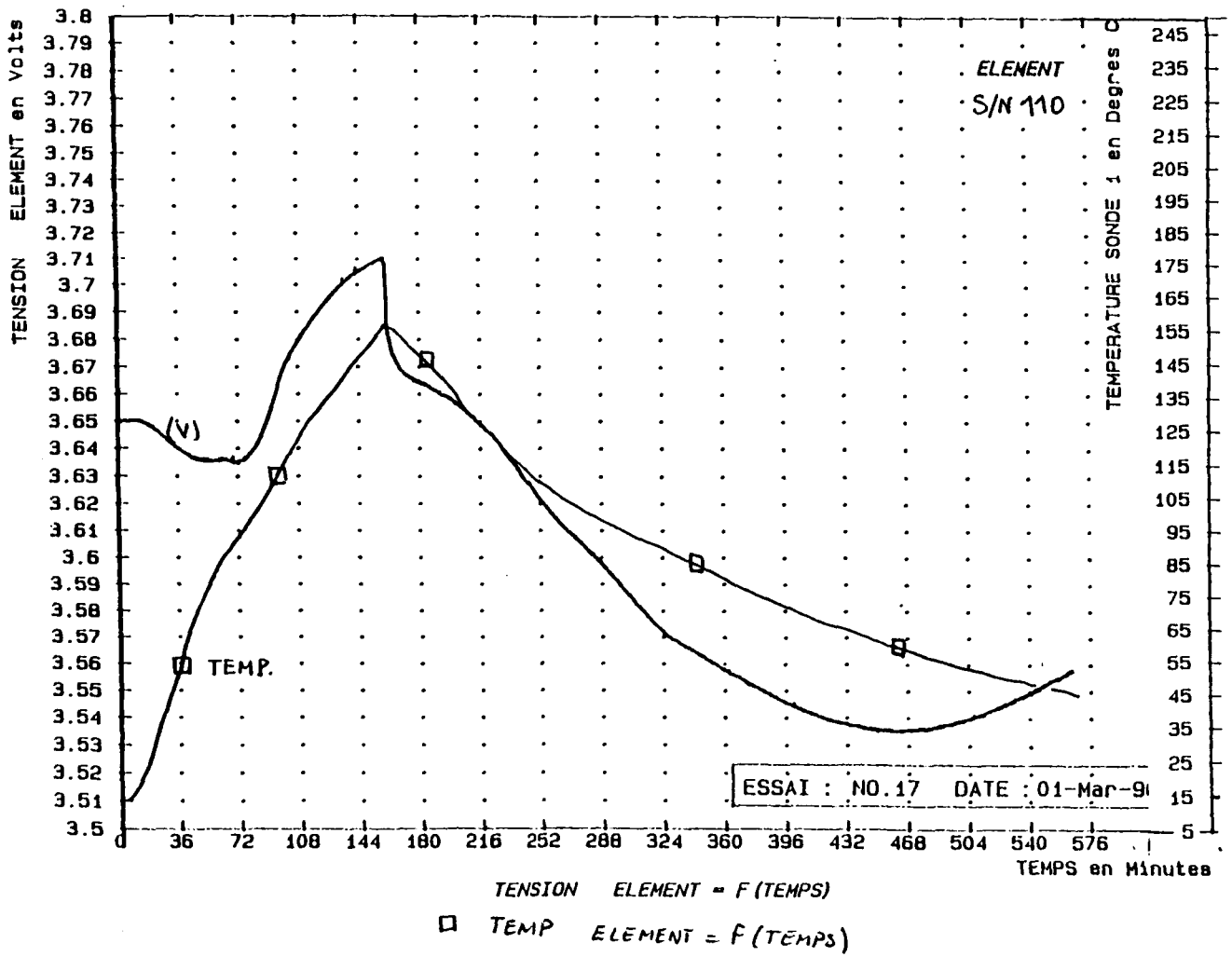

FIGURE 6

SAFT AEROSPACE DEPARTMENT | 1990 NASA BATTERY WORKSHOP

VLS 250 AM - 60 AMPS DISCHARGES

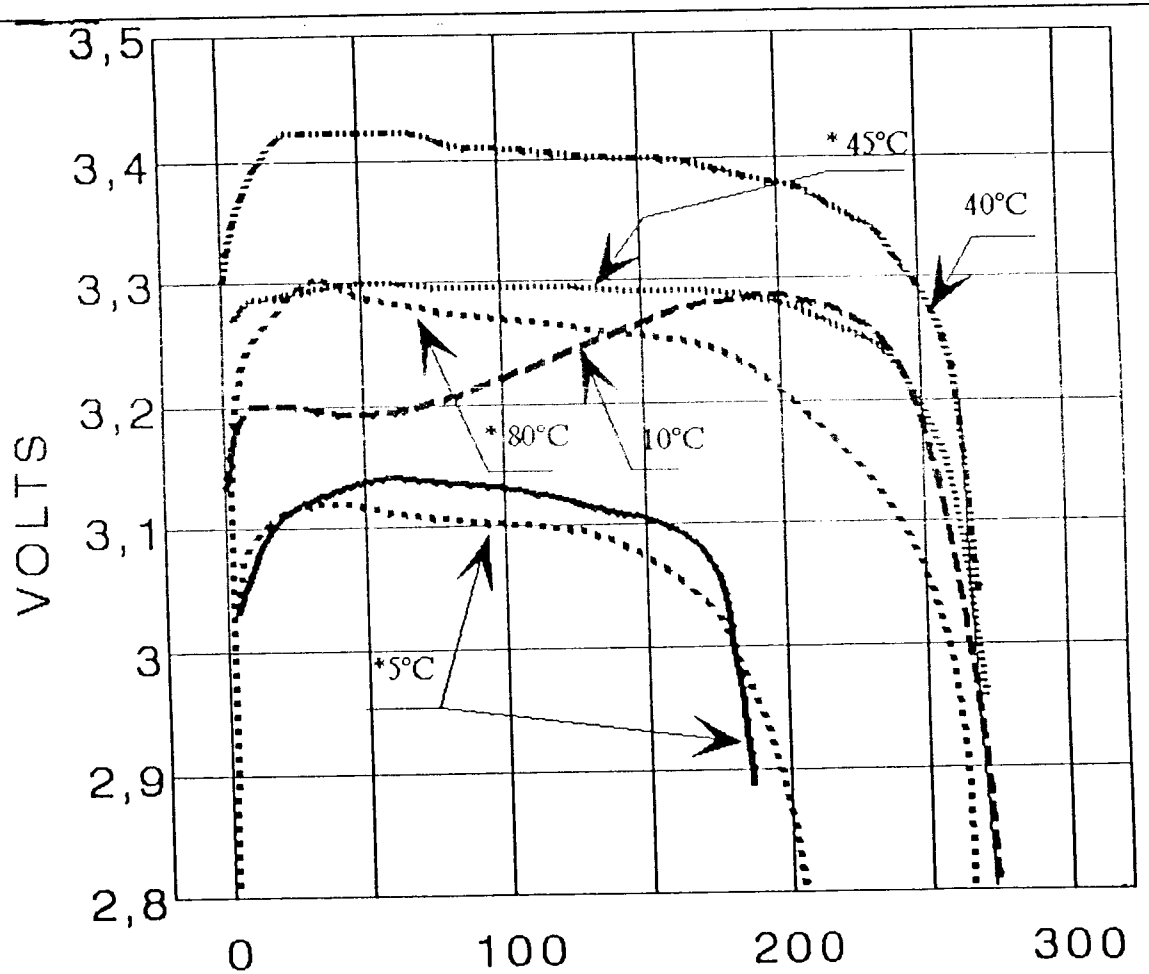

NOTE: (*) 4.2 Ah Already discharged at ambiant temperature

FIGURE 7

SAFT AEROSPACE DEPARTMENT | 1990 NASA BATTERY WORKSHOP

VLS 250 AM - DISCHARGES VS CURRENTS AT 40°C

FIGURE 8

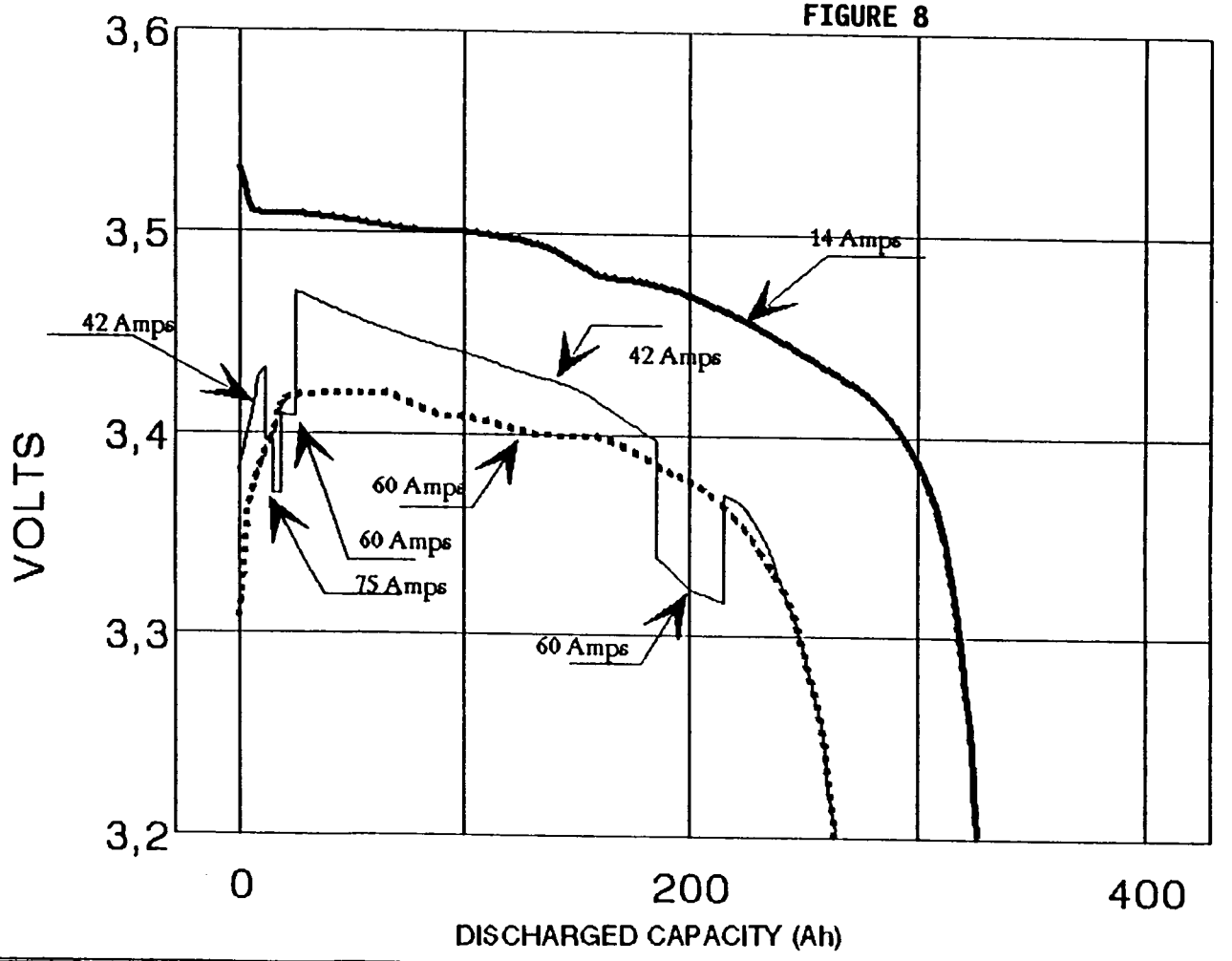

SAFT AEROSPACE DEPARTMENT | 1990 NASA BATTERY WORKSHOP

VLS 250 AM - CAPACITY VS CURRENT/TEMPERATURE

FIGURE 9

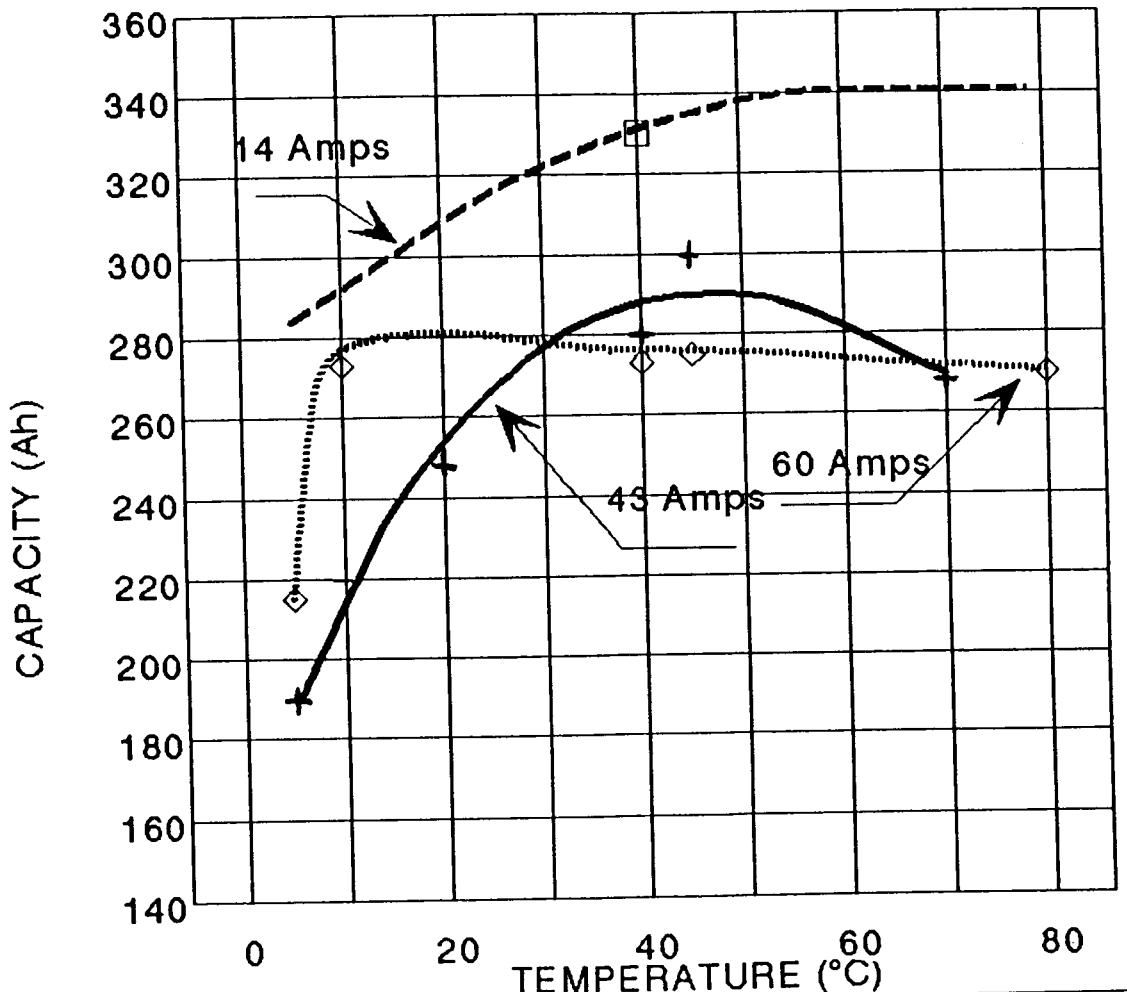

SAFT AEROSPACE DEPARTMENT	1990 NASA BATTERY WORKSHOP

VLS 250 AM - VOLTAGE VS CURRENT

FIGURE 10

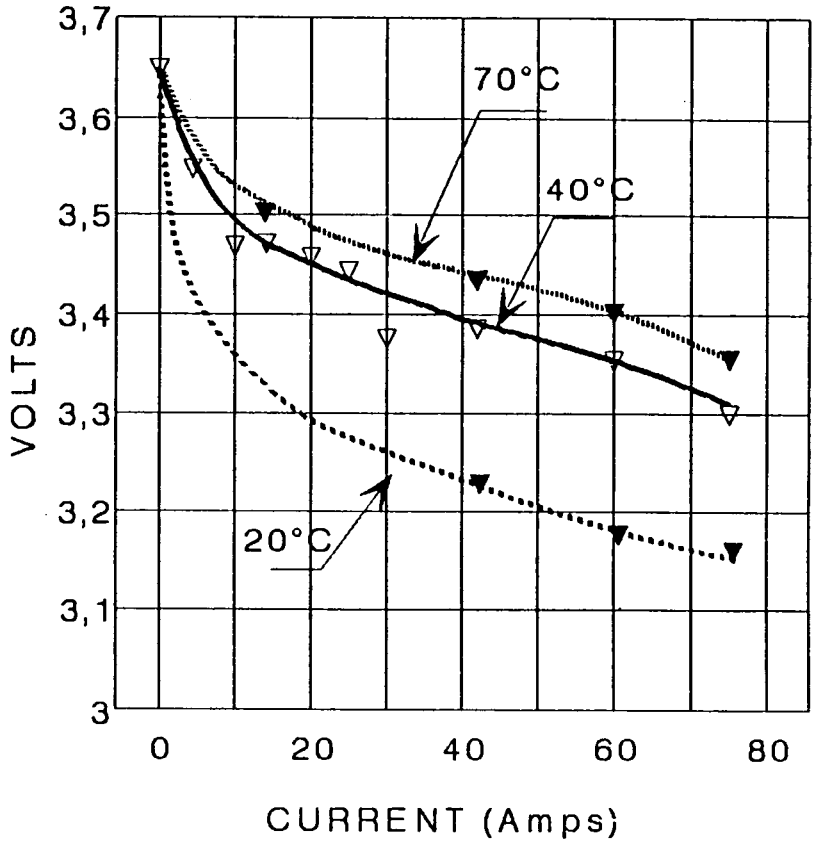

SAFT AEROSPACE DEPARTMENT	1990 NASA BATTERY WORKSHOP

VLS 250 AM - REVERSAL

FIGURE 11

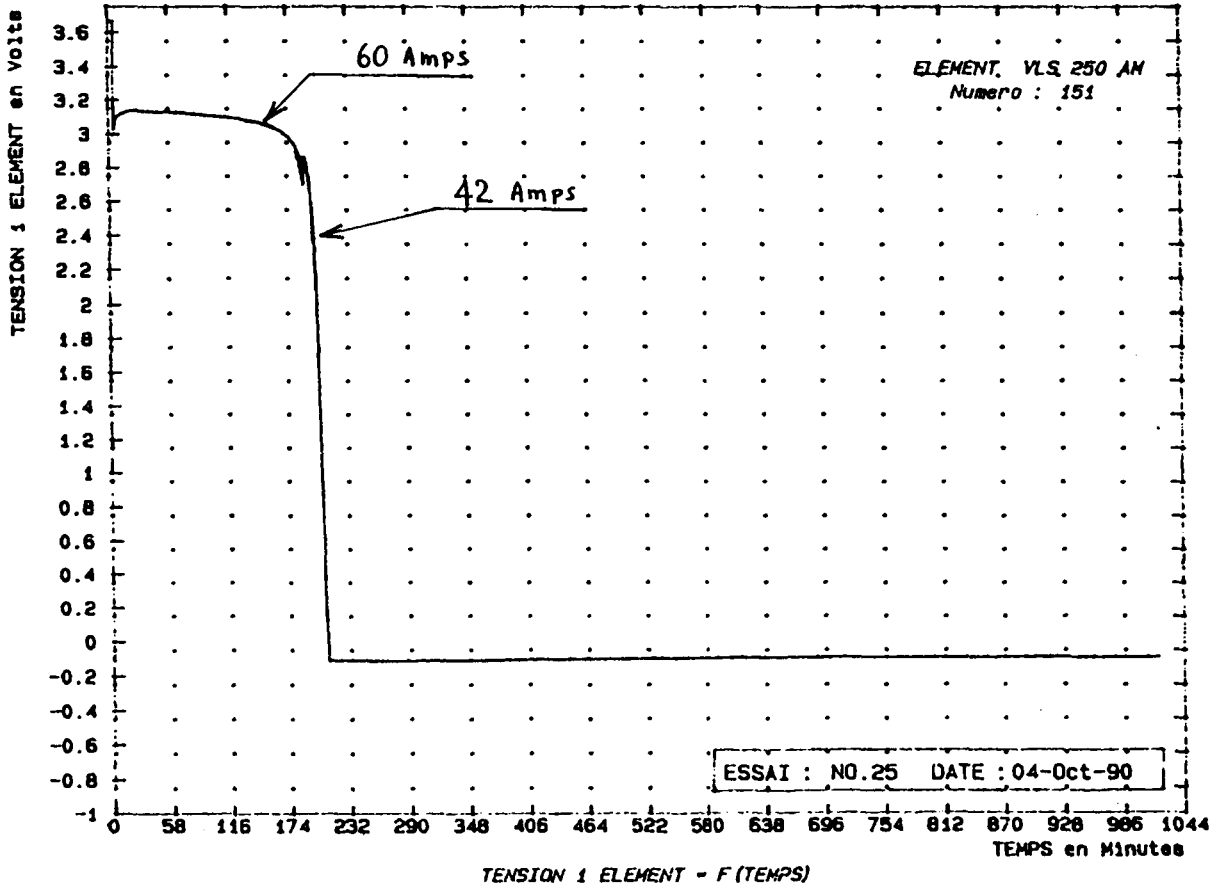

TENSION 1 ELEMENT = F (TEMPS)

SAFT AEROSPACE DEPARTMENT	1990 NASA BATTERY WORKSHOP

VLS 250 AM - REVERSAL

FIGURE 12

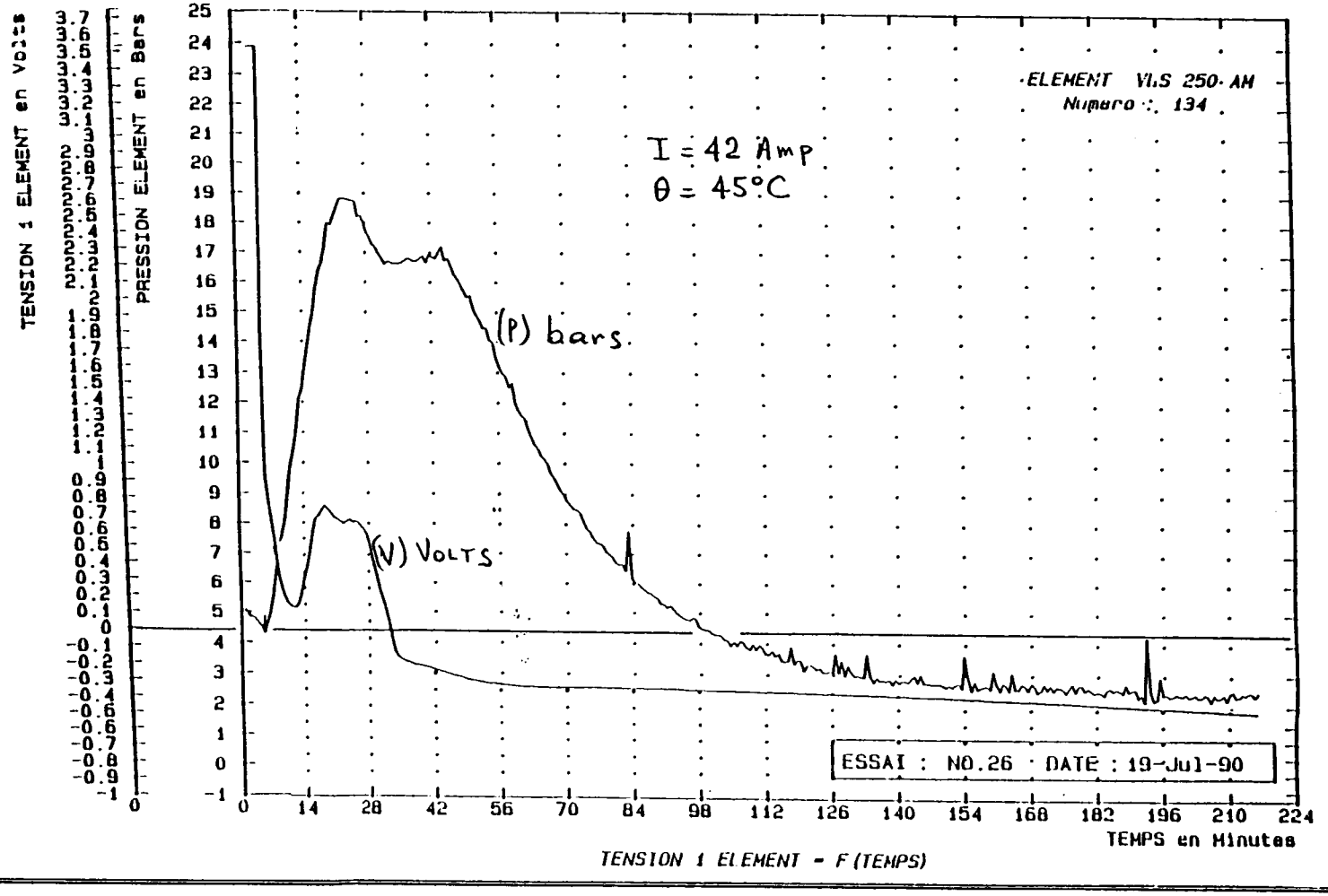

SAFT AEROSPACE DEPARTMENT	1990 NASA BATTERY WORKSHOP

VLS 250 AM - OVERTEMPERATURE AFTER DISCHARGE

FIGURE 13

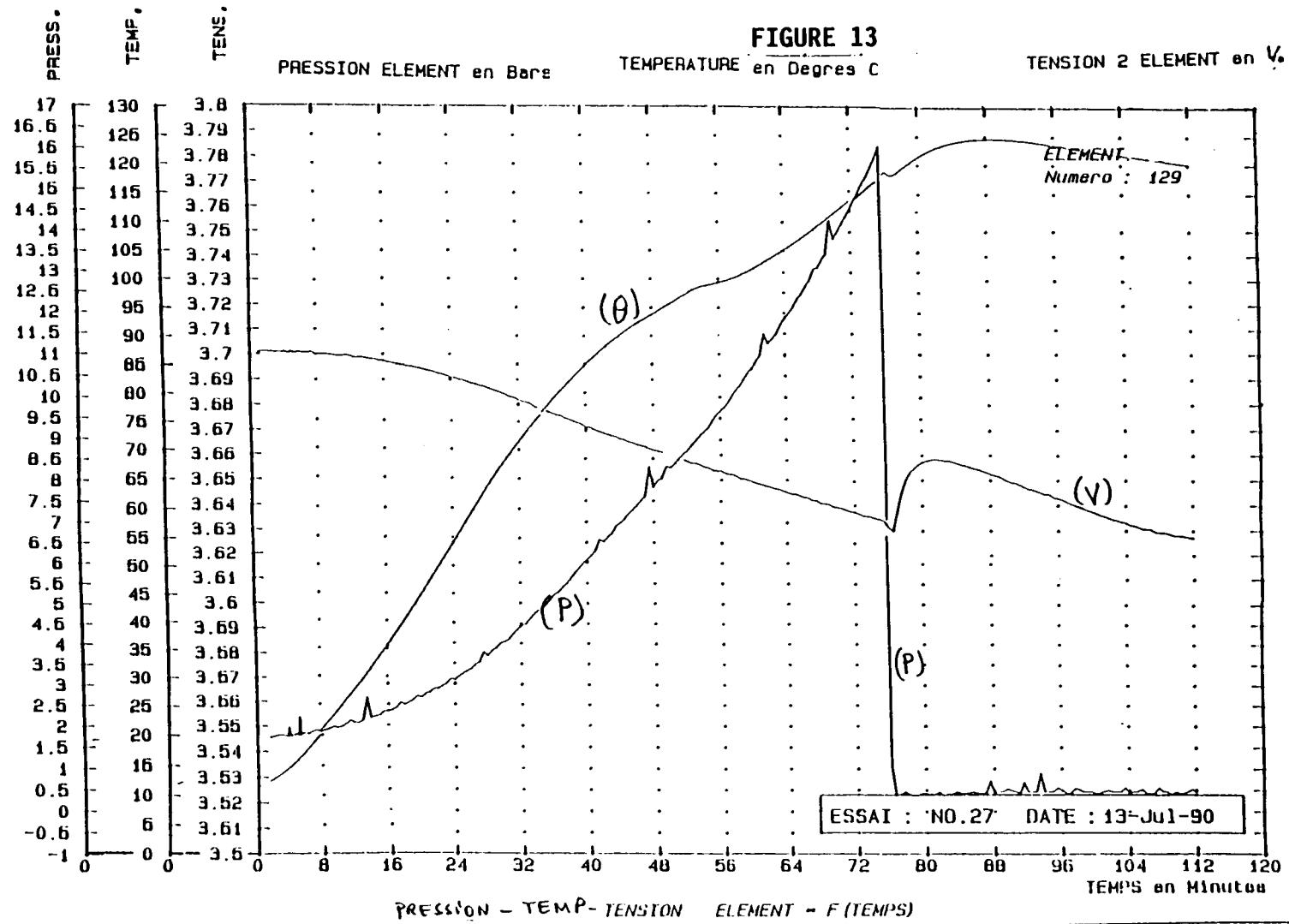

SAFT AEROSPACE DEPARTMENT	1990 NASA BATTERY WORKSHOP

VLS 250 AM - PULSE BEFORE AND AFTER STORAGE

FIGURE 14

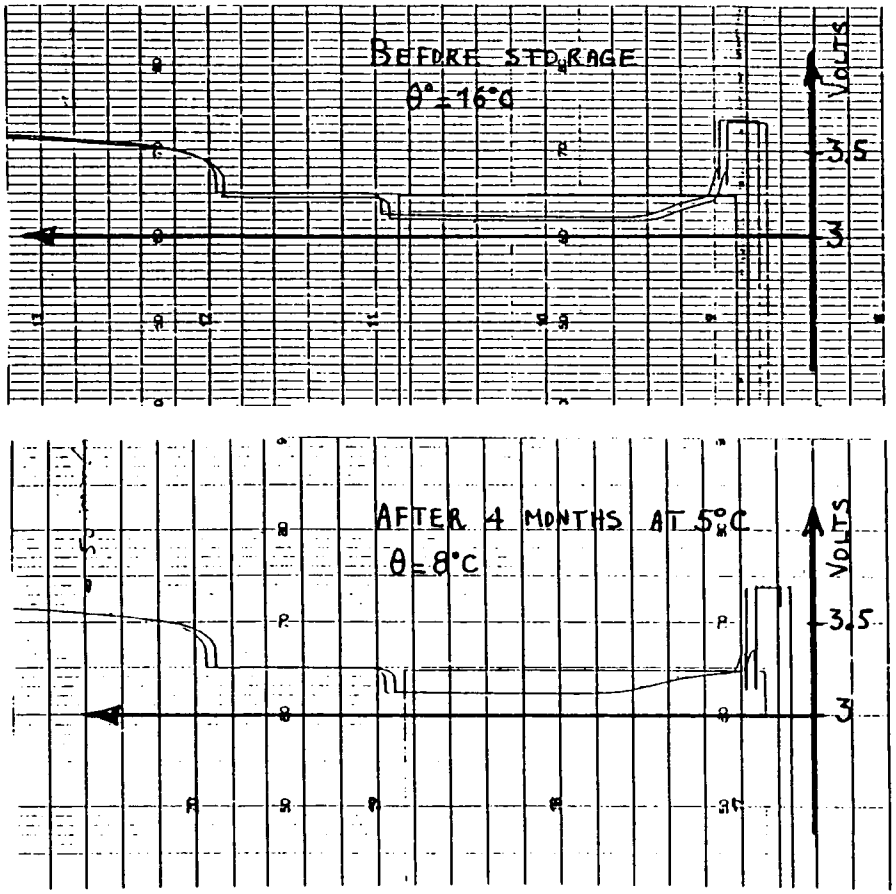

SAFT AEROSPACE DEPARTMENT	1990 NASA BATTERY WORKSHOP

VLS 250 AM - DISCHARGE AT 40°C AFTER 4 MONTHS STORAGE

FIGURE 15

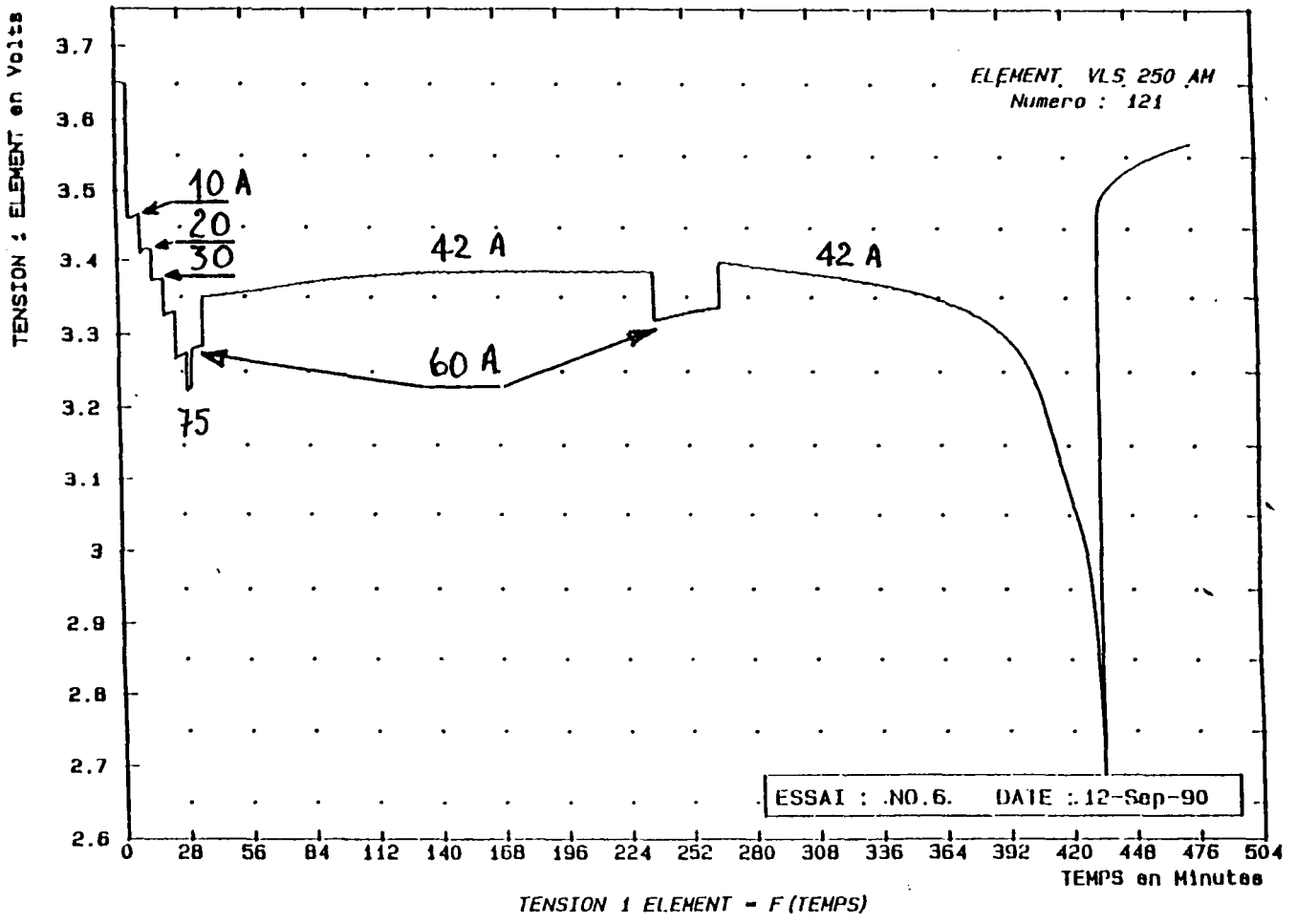

TENSION 1 ELEMENT = F (TEMPS)

Development of a 300 Ampere Hour High Rate Lithium Thionyl Chloride Cell

Gerard H. Boyle
Yardney Technical Products, Inc.

Yardney Technical Products, Inc. has been developing a high rate lithium thionyl chloride cylindrical cell with parallel plate electrodes. The development has been divided into three phases:

Phase I	150 Ampere hour low rate (1 mA/cm^2) design
Phase II	25 Ampere hour high rate (5 mA/cm^2) design
Phase III	300 Ampere hour high rate (5 mA/cm^2) design

The basic design is the same for all three cells. The electrodes are perpendicular to the axis of the cylinder. Multiple electrodes are bussed up the side of the cylinder, 180^o apart allowing excellent anode and cathode utilization. It is a lithium limited design with excess electrolyte. The cathode is Shawinigan or Gulf Acetylene black with no catalyst. The electrolyte is 1.8 Molar lithium tetrachloroaluminate ($LiAlCl_4$) in thionyl chloride. All cell cases are 304L Stainless Steel with a BS&B burst disc.

There are two primary advantages in a cylindrical parallel plate design: 1) Electrical performance--good electrode utilization; and 2) Thermal performance--heat conduction path is one radius for a high surface area cell whereas a wound cell of equivalent surface area would retain heat in the core of the cell.

The 150 Ampere hour cell was chosen to work out the design in a low rate cell and verify electrical performance. A Number 6 cell case was chosen. The design differed from Phase II and III designs in that only one feedthrough electrode was used (anode). The cathode bus bar was welded to the cover making a case positive design. The parameters are as follows.

150 Ampere Hour Cylindrical Cell

Voltage:	3.65 Volts
Capacity:	150 Ampere hours
Active Surface Area:	547 cm^2
Discharge Rate:	0.5 Amperes Continuous
Size:	2.53" Diameter x 6.25" High (No. 6)
Weight:	2.3 Pounds

Cells were tested at +40°F and +90°F with the following results:

150 Ampere Hour Cell Test Data

Storage Condition	Test Temperature	Test Current	Median Voltage	Capacity
Fresh	+40°F	0.5A	3.43V	156 Ahr
Fresh	+90°F	0.5A	3.55V	162 Ahr
100°F (55 Days)	+90°F	0.5A	3.51V	150 Ahr
Fresh	+40°F	1.0A	3.35V	130 Ahr
Fresh	+90°F	1.0A	3.48V	133 Ahr
100°F (38 Days)	+90°F	1.0A	3.45V	109 Ahr

The following safety and abuse tests were conducted successfully on this cell.

Safety and Abuse Tests

DOT-E 8978:	Shock, Vibration, Altitude, Thermal
External Short Circuit:	62 Ampere Peak - Max.Temperature 100°C
Overtemperature:	Venting through Vent 120°C to 130°C
Cell Reversal:	Over 100 Hours
Drop Test:	Repeated 20 Foot Drops

During Phase II a one-tenth size cell of 25 Ampere hour capacity was developed. The cell stack and the electrodes are the same diameter as in the final design.

The individual electrodes use the same substrates and the same thickness of cathode carbon and lithium. The following are the 25 Ampere hour cell parameters.

25 Ampere Hour Cylindrical Cell

Voltage:	3.65 Volts
Capacity:	25 Ampere Hours
Active Surface Area:	1005 cm^2
Discharge Rate:	4.2 Amperes
Size:	3.20" Diameter x 2.10" High
Weight:	1.19 Pounds

The following test data was obtained during performance testing and environmental testing.

25 Ampere Hour Test Data

Test Temperature (^oF)	Cell Case Temperature (^oF)	Capacity to 2.88V (Ah)	Average Load Voltage At 4.2A	At 6.0A
+40	73.6	27.63	3.318	3.254
+55	89.2	30.90	3.304	3.255
+60	91.8	31.00	3.313	3.269

DOT-E-7054
Vibration, Altitude, Thermal

Short Circuit
125 Amperes, 5 Minutes, g/m Seal Cracked

The 25 Ampere hour cell was used to evaluate electrochemical performance and to develop and test assembly procedures and fixturing.

The 300 Ampere hour cell is a direct scale up of the 25 Ampere hour cell. The actual capacity is 328 Ampere hours. The requirement is to deliver 250 Ampere hours after seven years storage. Based on data developed on the MESP program on capacity loss during storage, the internal geometry of this cell made it necessary to design in a capacity of greater than 300 Ampere hours.

The design parameters of the 300 Ampere hour cell are as follows:

300 Ampere Hour Cell

Voltage:	3.65 Volts
Capacity:	300 Ampere Hour
Active Surface Area:	10,203 cm^2
Discharge Rate:	42 Amperes Continuous
Size:	3.20" Diameter x 11.0" High
Weight:	6.5 Pounds

The following is the electrical performance data.

300 Ampere Hour Cell Test Data

Test Temperature (^oF)	Cell Case Temperature (^oF max)	Capacity to 2.88V (Ah)	Average Load Voltage At 42A	At 60A
40	123	325	3.39	3.28
70	151	320	3.42	3.32
90	144	329	3.45	3.33

The following safety and abuse testing was conducted on this cell.

Vibration:	25.4 grms to 73 grms at 42 Ampere Load (Three axes)
Shock:	2000 G's at 60 Ampere Load (Three axes)
Overtemperature:	Vented through the vent.
Reversal:	Discharge at +40°F then reversal. Benign vent through vent after 2.5 Hrs.
Short Circuit:	660 Amperes, 39 seconds internally fuzed

The 300 Ampere hour cell has met most of the design requirements. The current task is to build and test a nine-cell battery.

A summary of the three designs presented are cylindrical cells using the lithium thionyl chloride chemistry. The design is anode limited with an excess of electrolyte. A summary of the three cells is as follows:

Summary

Capacity Ah:	150	25	300
Discharge Rate-Amperes:	0.5	4.2	42
Voltage at Rate:	3.50	3.31	3.42
Diameter Inches:	2.53	3.20	3.20
Height Inches:	6.25	2.10	11.0
Weight Pounds:	2.3	1.19	6.5

This work was funded by the U.S. Air Force through Jet Propulsion Laboratories.

SAFETY TESTING OF LITHIUM CELLS

Nick Liberto
Catalyst Research

INTRODUCTION

Safety testing is intended to simulate, under laboratory conditions and controls, situations that will subject a cell to externally induced stress. These stresses(or abuses) can occur at any time during the useful life of the cell, from the time of manufacture until it is expended during mission deployment. Abuse testing can be divided into three major categories: Electrical, Mechanical, and Thermal. Although electrical abuses are generally found to occur during handling or deployment, Mechanical and Thermal stresses can be induced during transportation and storage. Therefore, it would be prudent to include predicted environmental exposure as part of the test plan. In the selection of a test program, specific test requirements should be tailored to meet the predicted mission requirements.

ELECTRICAL ABUSE TESTING

SHORT CIRCUIT: The short circuit test is probably the most important electrical abuse test because it is the most likely to occur during handling. It is important to conduct the tests at both Room Ambient (75F) and Elevated Temperature (160F) because sometimes the results can surprise you.

FORCED DISCHARGE INTO REVERSAL: This test is generally performed at a 10 hour, 100 hour, and 1000 hour discharge rate. It is especially useful with multi-cell battery packs.

MECHANICAL ABUSE TESTING

DROP TEST: This test consists of dropping a cell from a height of 36 inches onto a concrete surface having a minimum thickness of 3 inches. The cell should be dropped at least once on each of three mutually perpendicular axes. Because this test is intended to simulate real-world mishandling, the abuse may occur at a temperature other than room ambient. Therefore the test sample should be divided into 3 groups; Low Temperature, Room Ambient, and High Temperature.

PROJECTILE IMPACT: There are basically two reasons why this test is conducted. First; in a military scenario, unfriendly fire could penetrate a man-carried equipment and subsequently puncture a cell. We need to know whether this will cause a secondary and more serious problem than the original projectile. Second; The entrance, penetration, and exit of a high velocity projectile imparts a massive shock to the cell accompanied by physical disruption. The observations and data derived from this test allow us to compare the reaction of one cell chemistry and design versus another.

CRUSH: In this test, the cell should be electrically monitored to determine the point at which internal shorting has occurred. The cell under test is crushed in a hydraulic press until the cell has reached a thickness equal to 1/3 to 1/4 of it's original dimension.

DRILL TEST: Maintenance in and around a piece of equipment in which a Lithium cell has been installed could inadvertently be subjected to penetration by a high speed drill. It is important to know how the cell will react.

NAIL PENETRATION: This is the type of abuse which could occur during packaging and shipping if wooden crates are utilized as the outer shipping container.

FUTURE PLANS

In conjunction with physical abuse tests we plan to perform a thermal survey of the cells which exhibit venting with flame in order to characterize the intensity of the flame. This data will enable us to evaluate the degree of hazard associated with this event and it's subsequent effect on adjacent structures. To accomplish this we plan to use an Infrared thermal imaging system.

We also have plans to perform measurements of the peak pressure and the velocity of the pressure wave generated by the occurrence of a Dynamic Event. The data generated by this test will also enable us to determine the degree of hazard associated with this event.

SAFETY TESTING OF LITHIUM CELLS

- ELECTRICAL ABUSE TESTING
  - SHORT CIRCUIT
  - FORCED DISCHARGE INTO REVERSAL
- MECHANICAL ABUSE TESTING
  - DROP TEST
  - PROJECTILE IMPACT
  - CRUSH
  - DRILL TEST
  - NAIL PENETRATION
- FUTURE PLANS

SLIDE SHOW

1) Short Circuit Test at +160 F, Li/SOCl2, 1.5 amp-hr, prismatic cell.
2) Short Circuit Test at 75F, Li/SOCl2, 3-cell battery, 1 amp-hr each, prismatic cell.
3) blank space
4) Projectile Impact, Li/(CF)x, DD cell.
5) Same cell
6) Same cell
7) Projectile Impact, Li/SOCl2, D cell.
8) Projectile Impact, Li/(CF)x, C cell.
9) Same cell.
10) Projectile Impact, Li/SOCl2, D cell.
11) Projectile Impact, Li/SO2.

EXAMINATION OF THE DISCHARGE MECHANISM OF LI/CF_x CELLS, COMPARISON OF THE ELECTROCHEMICAL REDUCTION MECHANISMS OF PTFE AND $(CF_x)_n$ BY LITHIUM

C. C. BAXAM AND N. MARGALIT

Battery Technology Center
Tracor Technology Resources
Rockville, MD 20850

ABSTRACT

Swelling of $(CF_x)_n$ electrodes in commercial Li/$(CF_x)_n$ cells presents a limiting factor in cell design optimization. Examination of cathodes from such cells, after discharge, reveals a relation between cell operating temperatures and cathode swelling. Attempts to explain the swelling using the prevailing model for the cathode reaction have failed.

A more suitable reaction mechanism is proposed based on the observed behavior of $(CF_x)_n$ electrodes on discharge and a comparison of the reaction products of $(CF_x)_n$ and PTFE with lithium amalgams. The proposed mechanism is in agreement with the experimental data found in the literature.

- INTRODUCTION
- TEARDOWNS OF COMMERCIAL CELLS
- LITHIUM AMALGAM REACTIONS
- DISCUSSION
- REACTION MECHANISM
- ONGOING WORK
- CONCLUSIONS

INTRODUCTION

Early developers of lithium-organic electrolyte cells were attracted to $(CF_x)_n$ as a potential cathode material. This attraction was based on calculated theoretical energy values of which the most outstanding was a theoretical specific energy approaching 2000 wh/kg*. Calculations of solid volume changes in the Li/$(CF_x)_n$ cells, based on "crystalographic" densities, indicated a volume reduction caused by active materials transforming into products of about 35%. However, in practice, loading of active materials was limited by an unexplained severe cathode swelling which resulted in cell choking and/or bulging of flat cell walls.

This investigation was aimed at trying to understand the cathode swelling phenomenon and, if possible, find a way to increase the active material loading in Li/$(CF_x)_n$ cells. The assumption that a "cure" might be found was based on the introduction of the solvated lithium ion "intercalation" model by Watanabe and coworkers in Japan**.

This presentation covers some of the results of the first three stages of this investigation: pre and post discharge teardowns of commercial cells, lithium amalgam reaction with $(CF_x)_n$, a discussion of results and postulation of a plausible reaction mechanism. Some comments regarding on-going work will also be made.

---

* This number is based on the assumption that the EMF of the electrochemical reaction is between 2.8 and 2.9 volts. See - J. P. Gabano, "An Overview" in "Lithium Batteries" (J. P. Gabano ed) P. 2, Academic Press, New York, NY, 1983.

** For a full presentation of Watanabe's group work see "Graphite Fluorides and Carbon-Fluorine Compounds", T. Nakajima and N. Watanabe, CRC Press, Boca Raton, FL, 1990.

VOLUME CHANGES OF CATHODES IN BR-2325 CELLS DUE TO DISCHARGE

WET CATHODES VOLUME BEFORE DISCHARGE

	Volume *(Cm^3)
PC/DME	0.261
GBL	0.251

CATHODES FROM DISCHARGED CELLS

32°F and 120°F Discharge Across a 37,500 ohm Load

Δ Volume* (%)

	32°F	120°F
PC/DME	36	1
GBL	36	2

75°F Discharge Across a 15,000 ohm Load

Δ Volume* (%)

PC/DME	27
GBL	28

* ± 1%

TEARDOWN OF COMMERCIAL CELLS

A number of commercial cells were torn down, pre and post discharge. In all cases significant cathode swelling was observed during discharge. For example, the cores of pin cells, which were easily removed from the cell can before discharge, could not be released without cutting the can, after discharge.

The most interesting observations were made in button cells where special provisions were made to accommodate cathode swelling.

Most significant were results obtained from measurements of the dimensions of $(CF_x)_n$ cathodes from button cells before and after discharge at different temperatures, for example, the results obtained from BR2325 cells. Considering that manufacturer I used a propylene-carbonate (PC) - dimethoxyethane (DME) solutions and manufacturer II used a 4-butyrolactone (GBL) solution and that the obtained cell capacities were similar, one is hard pressed to claim a major impact of solution composition on swelling.

However, a clear trend regarding the degree of swelling and its relation to temperature and perhaps rate of discharge is apparent.

MICROSCOPY OF REACTION PRODUCTS

Original $(CF_x)_n$ Powder

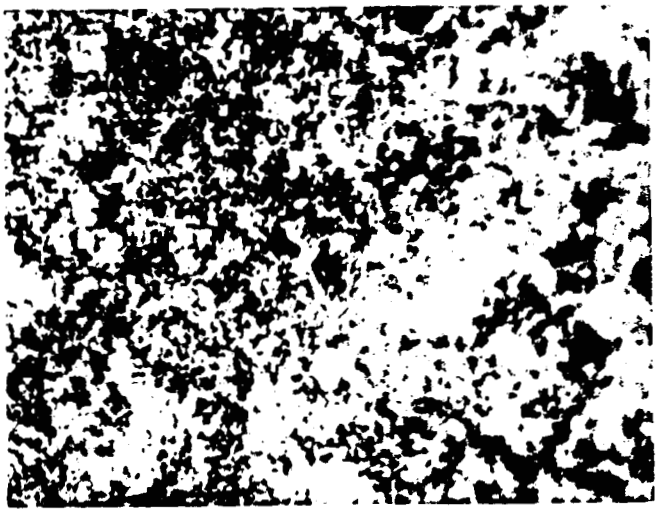

RT Amalgam Reaction Product

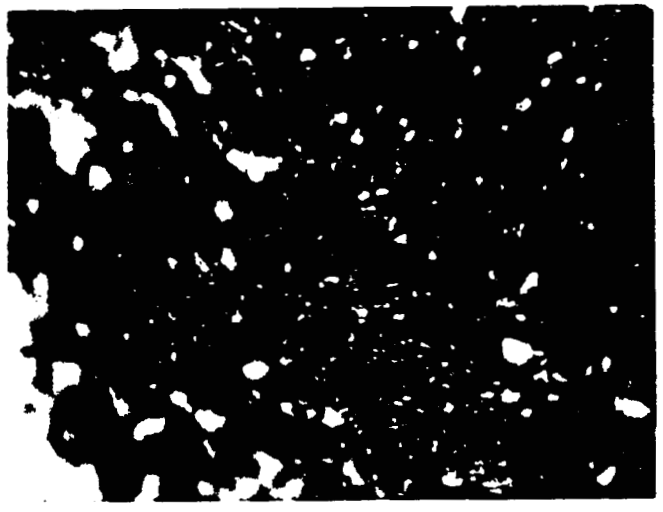

60°C Amalgam Reaction Product

SEM MICROGRAPHS OF DISCHARGE PRODUCTS

Original $(CF_x)_n$ Powder

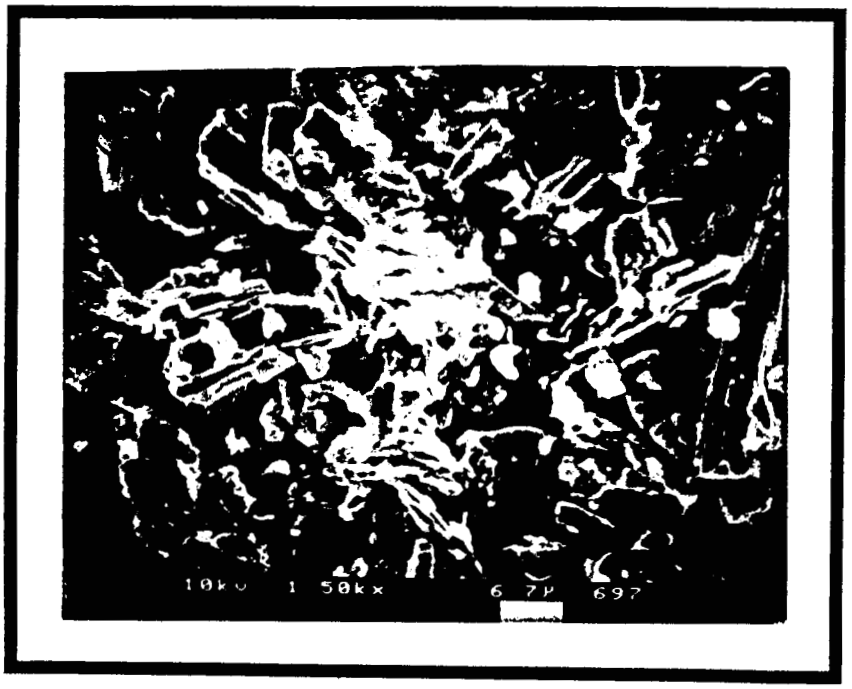

60 C Amalgam Reaction Product

SEM MICROGRAPHS OF DISCHARGE PRODUCTS (Cont.)

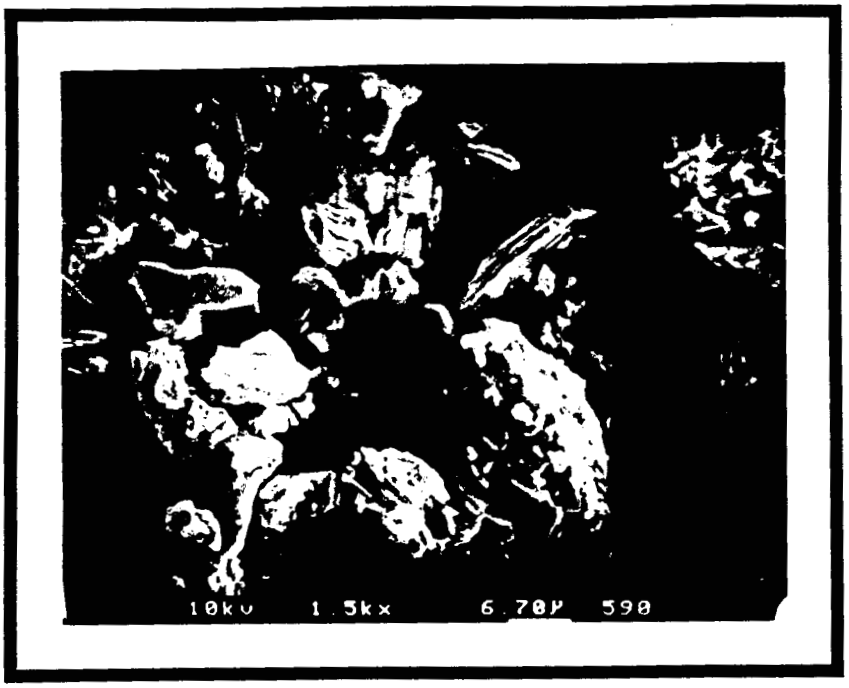

RT Amalgam Reaction Product

RT Reaction Product From Li/1M $LiAsF_6$ in DMSI
$(CF_x)_n$ Hg Cell

LITHIUM AMALGAM REACTIONS WITH $(CF_x)_n$

Dousek and coworkers have investigated the reaction of PTFE, a similar fluorocarbon, with lithium amalgams*. They reported that the reduction proceeded by lithium ions and electrons migration to C-F reaction sites through the polymer without involving the solvent.

Attempts to run a similar experiment by submerging $(CF_x)_n$ in a lithium amalgam failed. However, $(CF_x)_n$ powder spread over the amalgam surface, in a controlled atmosphere box under argon, started reacting and turning first gray and ultimately black at room temperature.

A similar experiment was run by placing $(CF_x)_n$ powder on the amalgam in a sealed vessel and storing it at 60°C.

The reaction products from both reactions were examined under the microscope and by SEM. The room temperature product consisted of a finer powder while the 60°C product appeared more coarse.

SEM micrographs of both reaction products showed opening of the $(CF_x)_n$ layers and small crystallites in the openings. It appears that more and bigger crystallites formed in the high temperature product. Note also the similarity between the SEM micrographs of $(CF_x)_n$ discharged, with Hg as a current collector and a 1M $LiAsF_6$ solution, vs lithium and the SEM micrograph for the room temperature amalgam reaction product.

---

* Dousek and coworkers published a number of papers on this subject. Of particular interest should be:

1. F. P. Dousek and J. Jansta, Electrochemical Acta, 20, 1 (1975).
2. F. P. Dousek and J. Jansta, Carbon, 18, 13 (1980).
3. L. Kavan, F. P. Dousek, D. Micka and J. Weber, Carbon, 26, 235 (1988).

ELECTROCHEMICAL REDUCTION OF PTFE AND $(CF_x)_n$ BY LITHIUM

PROPOSED MECHANISMS

PTFE (Dousek et al)

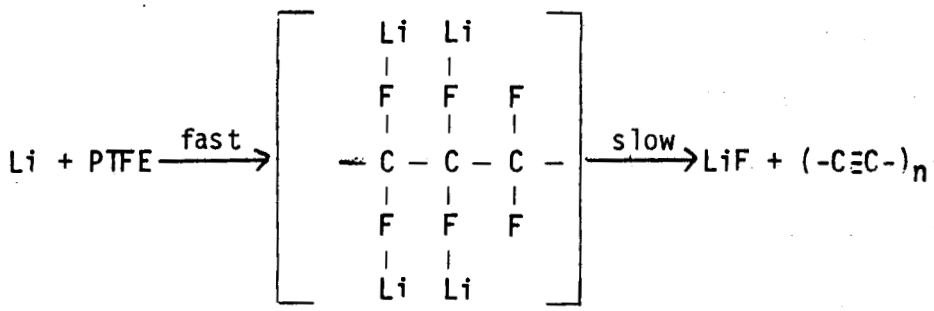

$[-C\equiv C-]_n \longrightarrow$ to more ordered form

LiF $\longrightarrow$ to larger crystals

$(CF_x)_n$ by analogy

$$n\,Li + (CF)_n \longrightarrow [CFLi]_n \longrightarrow nLiF + nC$$

DISCUSSION

These results, the $Li/(CF_x)_n$ literature and Dousek's work on the electrochemical reduction of PTFE by lithium amalgam suggest that both fluorocarbons react similarly with lithium amalgams.

In the case of PTFE, lithium ions migrate through the solid, electrons migrate through the carbon chain, crystallites of LiF are formed and the carbon chains attempt to form carbon rings if not small graphene layers. X-ray diffraction indicates the presence of LiF but "no carbon". Active carbon released by room temperature removal of the LiF is soft and springy. When LiF is released by melting, the remaining carbon is more coarse. Most noteworthy are the observations that:

- Resistivity measurements on PTFE reaction products indicate an exponential decline still measureable about a year after the material was formed.
- The rate of LiF crystal growth and decreasing resistivity are also temperature dependent.

A similar mechanism can be proposed for the cathode reaction in $Li/(CF_x)$ cell assuming that the chemical step following the electrochemical step is also slow.

MARGRAVE

THERMODYNAMIC AND E^o VALUES FOR THE REACTION
$XnLi + (CF_x)_n \longrightarrow XnLiF + xnC$

THERMODYNAMIC AND E^o VALUES FOR EQUATION

X in CF	$-\Delta G^o_{298}$ kJ/mole	$-\Delta S^o_{298}$ J/mole K	E^o Volts
0.8	378.2	7.57	4.90
0.9	413.8	8.51	4.76
1.0	499.4	9.46	4.66

EBEL AND KIESTER

HEAT RELEASED BY NON-ELECTROCHEMICAL PROCESS

Current	KJ/mol*
50 μA	120
150 μA	110
300 μA	100
0 μA**	135

* Estimated from graph
** Extrapolated

Such a mechanism could explain the apparent "anomaly" reported by Ebel and Keister regarding the heat released by a Li/$(CF_x)_n$ cell due to non electrochemical process(es) during discharge*. They reported that the heat per mole evolved by such process(es) increased as the current decreased approaching a value predicted on the basis of Margrave's thermodynamic calculations**. As their currents went down to values below 50 A one could assume that they were discharging their cell slow enough so that a significant amount of the forming intermediate decomposed during discharge. As the rate of discharge increased, less heat per mole was generated by these processes during discharge.

The slow decomposing intermediate model also helps in understanding how cells survive relatively high rate discharges and are not destroyed by the amount of heat which must be released by the non electrochemcial processes.

The implication of this proposed reaction mechanism in terms of heat management and preferred discharge regimes are interesting but go beyond the scope of this presentation.

Still X-ray diffraction does not show the presence of a [CFLi] entity on the surface of the discharge product composite neither in the case of $(CF_x)_n$ nor in the case of PTFE. The question remains, how does the lithium ion reach C-F reaction sites in both cases after the intermediate on surface layer has decomposed.

---

* S. J. Ebel and P. Keister in "Proceeding of the Electrochemical Society Meeting" Las Vegas, October 1985, Abstract 91.

** For a detailed account of Margrave's work see - J. L. Wood, A. J. Valerga, R. B. BaLachhope, and J. L. Margrave. ECOM-0105F (AD 755934), Final Report, December 1972.

PROPOSED MECHANISM

STEP 1: Lithium ion enters through carbon.

STEP 2: Lithium ion reaches C-F reaction site.

STEP 3: Intermediate formation.

STEP 4: Intermediate decomposition.

STEP 5: Growth of LiF crystallites and ordering of carbon.

PROPOSED MECHANISM

We propose that after the surface of the fluorocarbon is covered with carbon and LiF, lithium ions proceed to enter the composite solid reaction product through the carbon. Indeed the more ordered the product carbon is the faster lithium ions should migrate through it, hence, the preference for relatively ordered carbons for the production of $(CF_x)_n$.

Electrons entering through the carbon skeleton and lithium ions migrating through the carbon can reach reaction sites and form the intermediate.

The intermediate will decompose into carbon and LiF at a rate depending on temperature. The nature of the resultant composite, i.e. size of LiF crystallites and the degree of order of the carbon, will depend on the temperature history of the reaction and the stored reaction product.

ONGOING WORK

1. Testing the "lithium moving through carbon" hypothesis.
2. Examining $(CF_x)_n$ powder discharged at different temperatures.
3. Starting to look for "post discharge" heat generation.

CONCLUSION

- It appears that cathode swelling in Li/$(CF_x)_n$ cells is a result of changes in particles morphology during discharge.
- Electrodes swelling, at least in commercial button cells, appears to be temperature dependent.
- The postulated mechanism seems to explain available data.
- The challenge remains - can the swelling of $(CF_x)_n$ cathodes during discharge be reduced so as to allow significally better performance of Li/$(CF_x)_n$ cells.

ZINC-OXYGEN BATTERY DEVELOPMENT PROGRAM

Deborah S. Bourland

National Aeronautics and Space Administration

Johnson Space Center

Houston, Texas

December 5, 1990

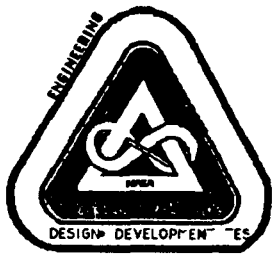

PURPOSE

Johnson Space Center - Houston, Texas

PROPULSION AND POWER DIVISION

D.S.BOURLAND

12/5/90

- INCORPORATE IMPROVED AIR/OXYGEN CATHODE AND ZINC ANODE TECHNOLOGY

- DEVELOPMENT OF RELATIVELY LARGE CELLS
  - 150 - 200 AH
  - 25 - 100 HOUR RATE

- DEVELOPMENT OF HIGH RATE CELLS
  - 9 - 12 AH
  - 3 - 12 HOUR RATE

Zinc-Oxygen Battery Development Program

Deborah S. Bourland
12/4/90

PURPOSE

The purpose of this Zinc-Oxygen development program is to incorporate the improved air/oxygen cathode and zinc anode technology developed in recent years into relatively large cells (150-200 AH, 25-100 hour rate) and smaller high rate cells (9-12 AH, 3-12 hour rate). Existing commercial cells manufactured by Duracell and Rayovac are currently being utilized on the Space Shuttle Orbiter in a mini-oscilloscope, crew radio and other crew equipment. These applications provide a basis for other Orbiter systems that require portable, storable, electrical power as well as emergency power for the Space Station major payload systems power and for Space Station equipment applications.

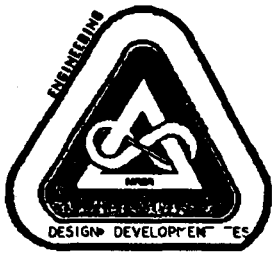

OBJECTIVE

Johnson Space Center - Houston, Texas

PROPULSION AND POWER DIVISION

D.S.BOURLAND

12/5/90

- DEVELOPMENT OF LARGE CAPACITY AND HIGH RATE CELLS
  - DESIGNED, FABRICATED, AND TESTED WITH 120 DELIVERED TO THE NASA-JSC FOR VERIFICATION/ACCEPTANCE TESTING
- DEVELOPMENT OF MATHEMATICAL MODELS
  - OPTIMIZE ELECTRICAL DESIGNS OF CELLS
  - OPTIMIZE THERMAL DESIGNS OF CELLS
  - PREDICTION OF CELL PERFORMANCE
- EXPANDED FAMILY OF ZINC-AIR CELLS FOR SPACE APPLICATIONS

Zinc-Oxygen Battery Development Program

Deborah S. Bourland
12/4/90

OBJECTIVE

The objective of this effort is to develop both a large capacity stackable cell, and a high rate stackable cell. These cells will be designed, fabricated and tested, with 120 cells of each type delivered to the NASA JSC for verification/acceptance testing. In addition to the development of cells, a mathematical model will be developed to optimize the electrical and thermal design of the cells prior to fabrication of the final cell hardware. These efforts should result in an expanded family of zinc-air cell sizes available to the NASA JSC for potential flight applications.

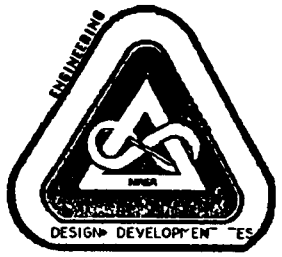

REQUIREMENTS

Johnson Space Center - Houston, Texas

PROPULSION AND POWER DIVISION

D.S.BOURLAND

12/5/90

- LARGE CAPACITY CELLS
  - 150 AH AT A 6 AMP RATE
  - 200 AH AT A 2 AMP RATE
  - END VOLTAGE OF 0.9 V AT 21° C, 14.7 psia
  - MINIMUM OF 10 ma/cm2
  - MINIMUM ENERGY DENSITY $\geq$ 200 WH/#

- HIGH RATE CELLS
  - 9 AH AT A 3 AMP RATE
  - 12 AH AT A 1 AMP RATE
  - END VOLTAGE OF 0.9 V AT 21° C, 14.7 psia
  - 30 ma/cm2 MINIMUM
  - MINIMUM ENERGY DENSITY $\geq$ 160 WH/#

Zinc-Oxygen Battery Development Program

Deborah S. Bourland
12/4/90

REQUIREMENTS

Requirements for the large capacity development cells are 150 AH at a rate of 6 amps to an end voltage of 0.9 volts at room temperature and pressure, with a minimum of 10 ma/cm2. Also, these cells should be capable of providing 200 AH at 2 amps at room temperature and pressure (21°C, 14.7 psia). The minimum energy density should be > 200 WH/lb. The high rate cell requires 30 ma/cm2 to an end voltage of 1.0 volts. The cell should provide 9 AH at a 3 amp rate to a 0.9 v end voltage, 12 AH at a 1 amp rate with a 0.9 v end voltage. The minimum energy density for these high rate cells is > 160 WH/lb.

APPLICATIONS

Johnson Space Center - Houston, Texas

PROPULSION AND POWER DIVISION

D.S.BOURLAND

12/5/90

- SPACE SHUTTLE ORBITER
  - MINI-OSCILLISCOPE
  - CREW RADIO
  - CREW EQUIPMENT

- SPACE STATION FREEDOM
  - EMERGENCY BACKUP POWER
    - LIFE SUPPORT EQUIPMENT
    - MEDICAL EQUIPMENT
    - LIGHTING
  - SAFE HAVEN POWER

- ASSURED CREW RETURN VEHICLE
  - EMERGENCY BACKUP POWER

- LUNAR/ MARS OUTPOST
  - EMERGENCY BACKUP POWER

Zinc-Oxygen Battery Development Program

Deborah S. Bourland
12/4/90

APPLICATIONS

Presently there are zinc-air cells on the Space Shuttle Orbiter in a mini-oscilliscope, crew radio and other crew equipment. With the improvements made in during this development program, the applications for this cell chemistry can be expanded to include other portable equipment in the Orbiter. Additionally, these types of cells can be used on the Space Station Freedom as emergency power supplies or as temporary backup for rechargeable cells. The applications could include emergency power for life support and medical equipment as well as for light sources. An ideal application for these cells would be for power in a safe haven in which safe, reliable power is needed. These cells could be used in similar situations on the Assured Crew Return Vehicle (ACRV), the Lunar Outpost and the Mars Outpost. In addition to space applications, these cells could be used on earth as emergency lighting in mines.

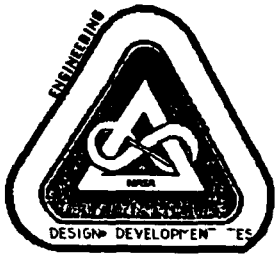

PROGRESS TO DATE

Johnson Space Center - Houston, Texas

PROPULSION AND POWER DIVISION

D.S.BOURLAND | 12/5/90

- MATERIALS SELECTION
  - SEPARATOR -- CHICOPEE ® 7600 PAPER
  - BONDING AGENT -- ASPHALT SEALANT
  - CURRENT COLLECTOR -- EXPANDED COPPER MESH
  - FOAM LAYER FOR EXPANSION DURING DISCHARGE -- CLOSED-PORE, POLYPROPELENE COMPRESSIBLE
- RESULTS
  - HIGH RATE CELL
    - CURRENT DENSITY -- 50 ma/cm2
    - 3 A FOR 3 HOURS
    - SPECIFIC ENERGY DENSITY -- 160 WH/#

Zinc-Oxygen Battery Development Program

Deborah S. Bourland
12/4/90

PROGRESS TO DATE

Current efforts focused on the electrochemical characterization of the Zn-O2 cell, to provide data for the mathematical model. Chicopee ® 7600 paper has been selected as the separator due to its seal performance. An asphalt sealant has been selected as the bonding agent. Expanded copper mesh is the final selection for the current collector. The cells will use a closed pore, polypropylene compressible foam layer beneath the current collector to allow for expansion of the anode during discharge. This design configuration for the high rate cell has a current density of 50 ma/cm2, and can deliver the required 3 A for 3 hours while meeting the specific energy specification of the 160 Wh/lb at the 1 A rate.

Life Testing of Secondary Ag-Zn Cells

by

Jeffrey C. Brewer and
Rajiv Doreswamy
NASA
Marshall Space Flight Center

Abstract

In the past, the silver-zinc (Ag-Zn) cell has been considered strictly a high energy-density primary cell. Because of its relatively short "wet" life, the Ag-Zn cell was overlooked for any application which required any substantial cycle life. Unique applications, however, that would demand a high energy-density power system along with an intermediate "wet" life would match up rather well with the Ag-Zn cell's capabilities.

Testing on a variety of secondary Ag-Zn cells has been going on at the Marshall Space Flight Center for nearly six years. The latest test involves a 350 ampere-hour cell design that has been cycled now for 12 months and has achieved approximately 5400 low-earth-orbit cycles as well as 12 deep discharges. This test not only is a life test on these cells but also addresses different methods of storing these cells between the deep discharges. Also, impedance measurements are made on one of the packs during periodic deep discharges. It is hoped that this will give a good correlation between the health of a cell and its impedance.

This test began in mid-November, 1989, and will be completed in the spring of 1991.

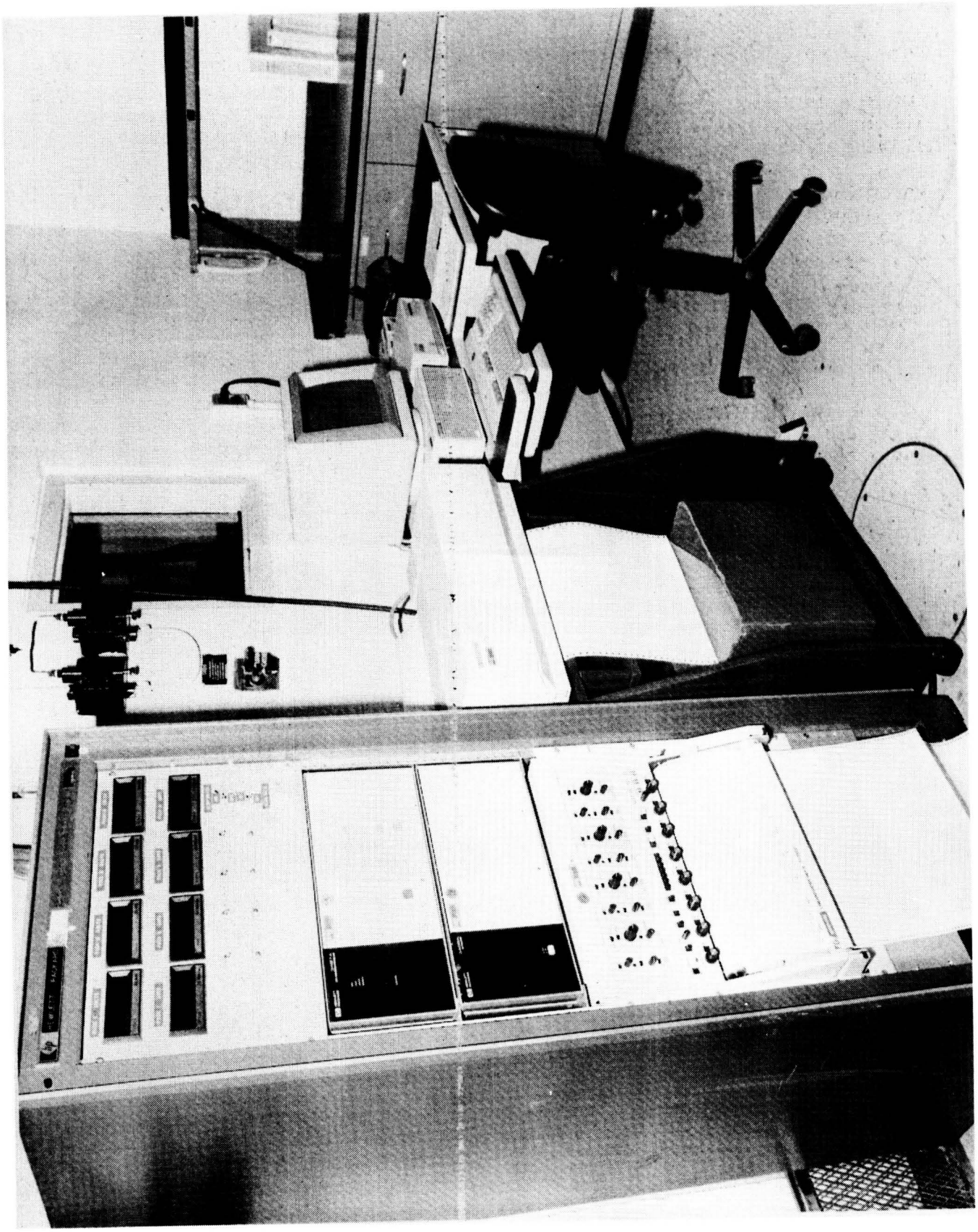

FIGURE 1

Instrumentation and Data Acquisition System

The overall test control is performed by an HP9000/300 workstation running HP Basic. This system controls all major data acquisition functions as well as regulation of day/night times and charge and discharge control. The actual data acquisition is performed by an HP3497 system equipped with an extender chassis.

In addition to computer based data acquisition and storage, visual displays are provided. These include voltage and current panel meter readings for all packs. This data is also tracked in real time on strip chart recorders. This provides a quick visual overview of test activity and aids in tracking system anomalies and disturbances.

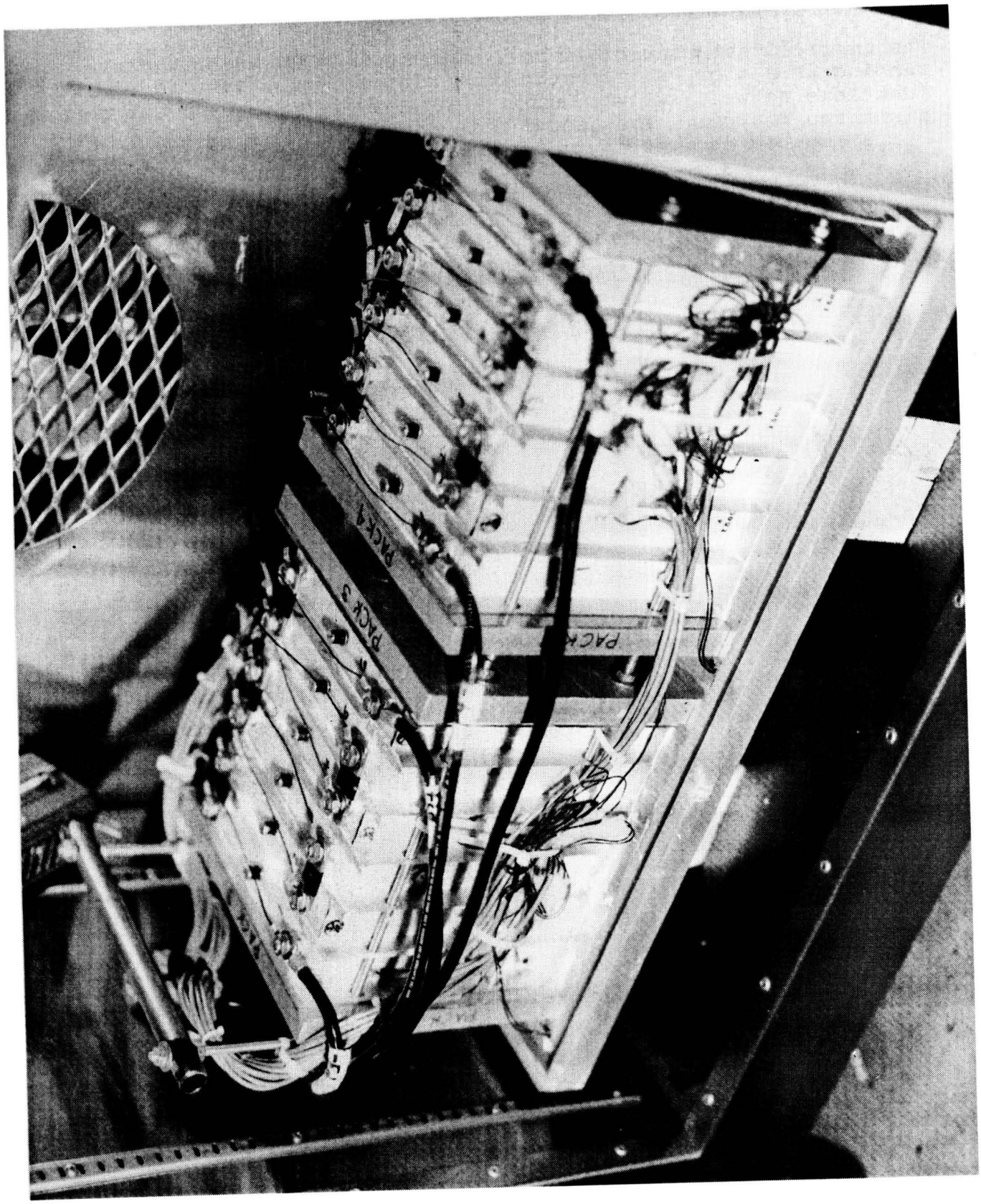

FIGURE 2

Pack Assembly

The four, six-cell packs are tested in two environmental chambers for accurate thermal control. The solar arrays are simulated by four Hewlett-Packard power supplies, one for each pack. Electrical loads are simulated by individual PS²L programmable load banks, operating in constant current mode.

The 24 cells were grouped in four packs of six cells each. Two of the four packs are pictured here. They were assembled on a common aluminum baseplate and were placed in one of two environmental chambers used in this test. An identical set-up was done for the other two packs.

Table I -- Initial and Current LEO Cycle Profiles for All Packs

Ag-Zn 4-Pack Test
Initial LEO Cycle Profiles

Pack #	Orbit # (since last discharge)	Description of Cycle Profile
1 & 2	1 - 112	Pack voltage cut-off at 11.16 V Cell voltage cut-off at 2.05 V
"	113 - 288	Pack voltage cut-off at 11.94 V Cell voltage cut-off at 2.05 V
"	289 - 416	Same voltage cut-offs; but will go off-line for 256 min. each time this limit is reached
"	417 - 448	Pack voltage cut-off at 11.94 V Cell voltage cut-off at 2.05 V
2	449 - 468	Pack voltage cut-off at 11.94 V Cell voltage cut-off at 2.05 V
3	1 - 468	Pack voltage cut-off at 11.94 V Cell voltage cut-off at 2.05 V
4	1 - 112	Pack voltage cut-off at 11.16 V Cell voltage cut-off at 2.05 V
"	113 - 400	Pack voltage cut-off at 11.79 V Cell voltage cut-off at 2.05 V
"	401 - 468	Pack voltage cut-off at 11.94 V Cell voltage cut-off at 2.05 V

Ag-Zn 4-Pack Test
Current LEO Cycle Profiles

Pack #	Orbit # (since last discharge)	Description of Cycle Profile
1	1 - 112	Pack voltage cut-off at 11.16 V Cell voltage cut-off at 2.05 V
"	113 - 288	Pack voltage cut-off at 11.94 V Cell voltage cut-off at 2.05 V
"	289 - 416	Same voltage cut-offs; but will go off-line for 256 min. each time this limit is reached
"	417 - 448	Pack voltage cut-off at 11.94 V Cell voltage cut-off at 2.05 V
2	———	Open circuit for 6 to 10 weeks; then recharge
3	1 - 448	Pack voltage cut-off at 11.94 V Cell voltage cut-off at 2.05 V
4	1 - 112	Pack voltage cut-off at 11.16 V Cell voltage cut-off at 2.05 V
"	113 - 400	Pack voltage cut-off at 11.79 V Cell voltage cut-off at 2.05 V
"	401 - 448	Pack voltage cut-off at 11.94 V Cell voltage cut-off at 2.05 V

Initial LEO Cycle Profiles

The facing table (table I) shows the initial LEO cycle profiles for all four packs. A total of 468 orbits are shown between each deep discharge. Pack 1 shows only 448 cycles because of a longer deep discharge (30 hours longer) than the other three packs. The different cycling profiles are being used in order to investigate an optimum method of storing these secondary Ag-Zn cells while not in use. The cells are not designed for LEO application; this is simply a possible storage method.

Current LEO Cycle Profiles

The table also shows the current LEO cycle profiles being used. Changes were made in the test plan that altered the LEO cycle profiles following the third "month" of LEO cycling. All packs are currently running a 35-hour deep discharge; thus, each pack now only cycles for a total of 448 orbits before beginning the next deep discharge. Also, pack 2 is no longer cycling but remains open circuit in the discharged condition for six weeks before being recharged for another deep discharge. This is another potential storage method being investigated.

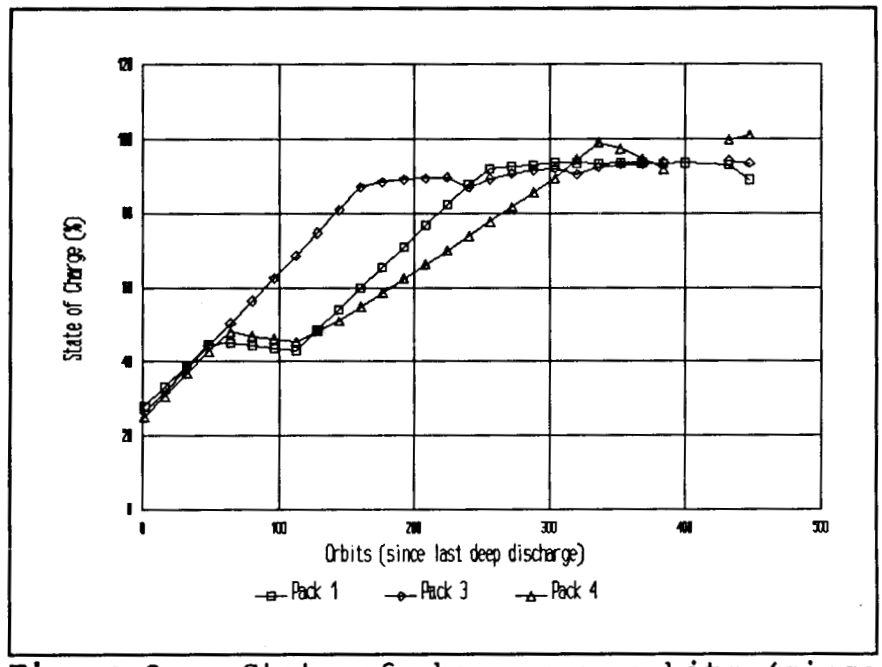

Figure 3 -- State of charge vs. orbits (since last deep discharge) during 4th month of LEO cycling for packs 1, 3, and 4.

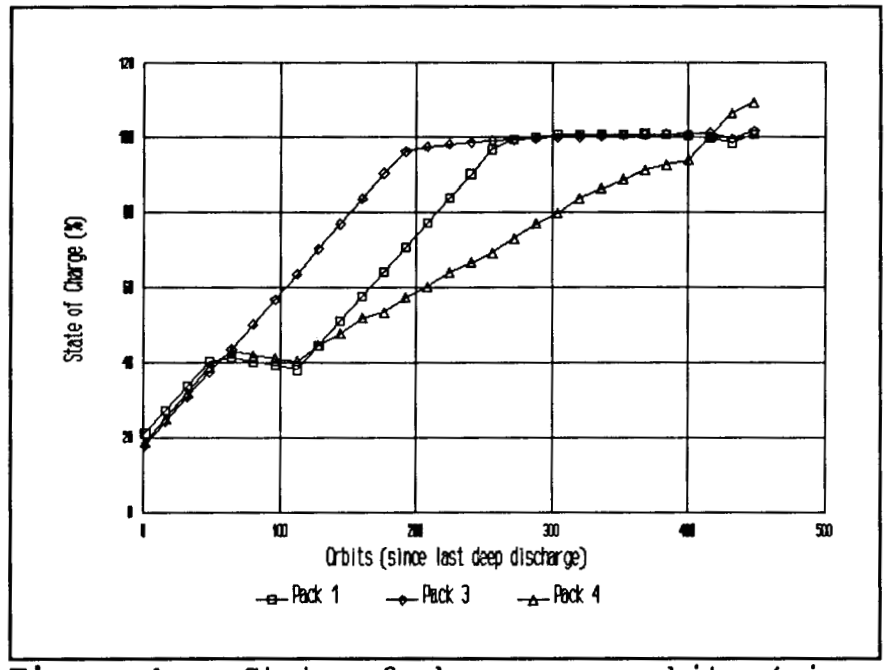

Figure 4 -- State of charge vs. orbits (since last deep discharge) during 11th month of LEO cycling for packs 1, 3, and 4.

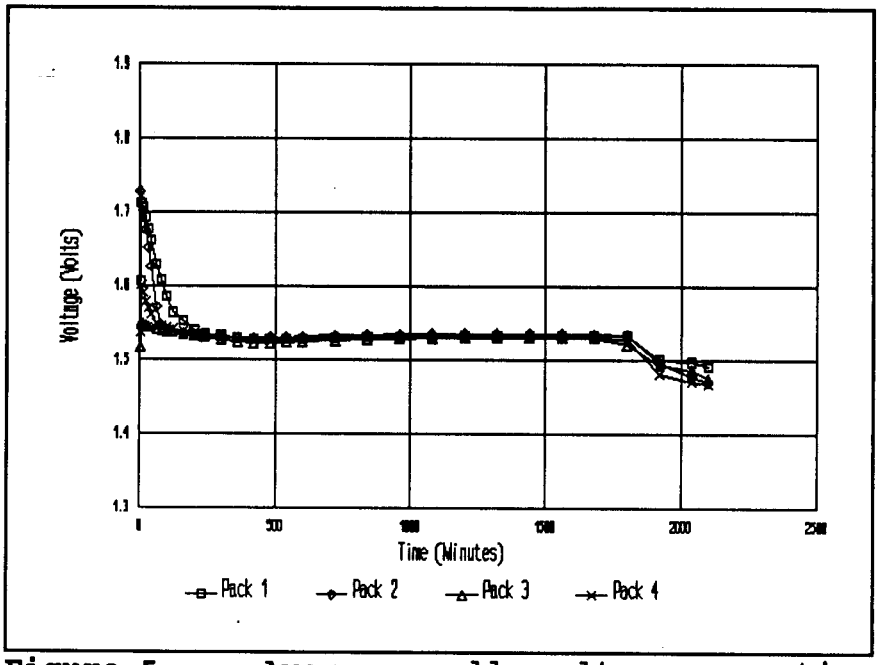

Figure 5 -- Average cell voltage vs. time during 6th deep discharge for all four packs.

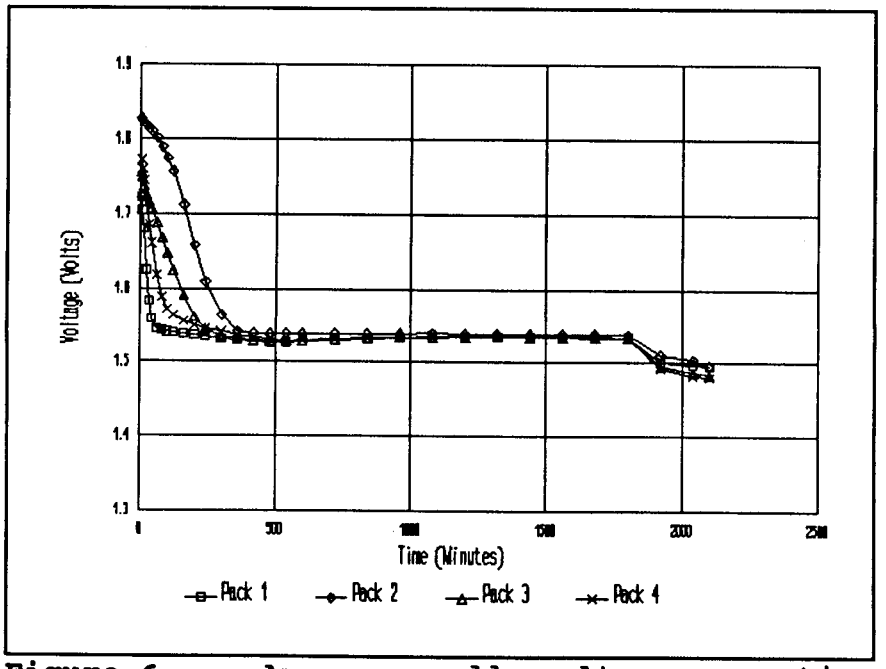

Figure 6 -- Average cell voltage vs. time during 12th deep discharge for all four packs.

Ag-Zn 4-Pack Test

Capacity Test Summary

Pack #	Baseline Capacity	Ten-Month Capacity	Percent Loss
1	431 (7.5 A)	369 (6.9/17.5 A)	14.4
2	389 (45 A)	343 (6.9/17.5 A)	11.8
3	395 (45 A)	354 (6.9/17.5 A)	10.4
4	392 (45 A)	359 (6.9/17.5 A)	8.4

Table II -- Baseline and Ten-Month Capacity Test Results for All Four Packs.

Test Results and Discussion

All packs continue to operate nominally following the 12th deep discharge. There are few signs of degradation in any of the four packs. There do appear to be some trends developing that will be discussed momentarily. The SOC levels at the end of the month of LEO cycling for each pack has remained relatively constant over the course of the test (figures 3 and 4). Likewise, no degradation has been seen during the deep discharges (figures 5 and 6). As expected, the capacity test during the 10th deep discharge yielded reduced capacity values compared to the baseline capacity test (table II). Although a decline was expected, some of the capacity loss shown could be artificial. Early in the month of LEO cycling prior to the capacity test, an inadvertent capacity test was run on packs 1, 3, and 4. Because there was thought to be sufficient time remaining in the month for the packs to be fully recharged, no adjustment was made to allow for extra charging. The SOC for each of the three packs, however, was increasing at the time of the capacity test and would have undoubtedly increased further had there been a normal amount of cycling throughout the month (an extra 150 orbits). Thus, a comparison of these capacities to the baseline capacities for these three packs would not be valid, although a comparison between packs is valid to some degree. These comparisons, however, are hindered further by the fact that the baseline capacity test for packs 2, 3, and 4 were made at 45 amps (A) while the rate for pack 1 was 7.5 A. Also, the capacity for pack 2 was unaffected by the LEO cycling and is therefore an accurate capacity measurement. With all of this in mind, it may be difficult to come to many conclusions about the capacities shown. One clear observation is the 11.8% loss seen in pack 2. Since it was unaffected by any LEO cycling anomalies, it should have shown a smaller loss than the packs that were not able to be fully recharged. However, packs 3 and 4 both showed a lower calculated loss (10.4 and 8.4, respectively), and would have lost even less under normal cycling conditions. (Pack 1 is not a valid comparison here because of the rate used in its baseline capacity measurement). This could be an indication that, by leaving Ag-Zn cells open circuit between deep discharges a faster cell degradation may result. This may be true even if left open circuit at low SOC levels. The only other valid comparison is between packs 3 and 4, which have seen identical test conditions with the exception of the method of storage between deep discharges. A difference in capacity loss can be seen between these two packs. This can be attributed to the different LEO cycling methods used for these two packs. The greater capacity loss observed in pack 3 supports theories stating that continually cycling to a full SOC will result in an accelerated degradation of the cell. This is due to increased separator oxidation and zinc dendrite growth resulting from the inevitable overcharge that will occur as a cell approaches a fully charged state.

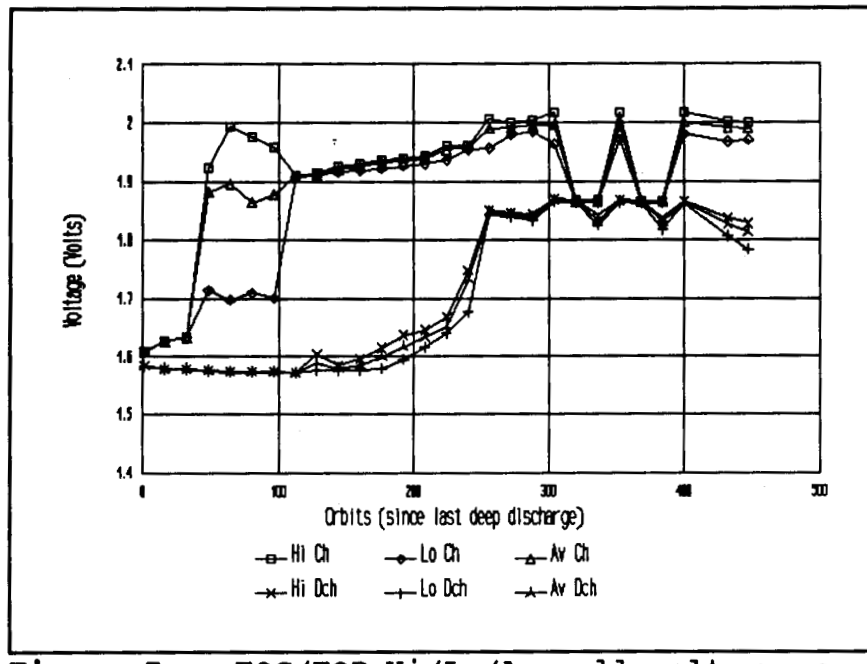

Figure 7 -- EOC/EOD Hi/Lo/Av cell voltages vs. orbits (since last deep discharge) during the 4th month of LEO cycling for pack 1.

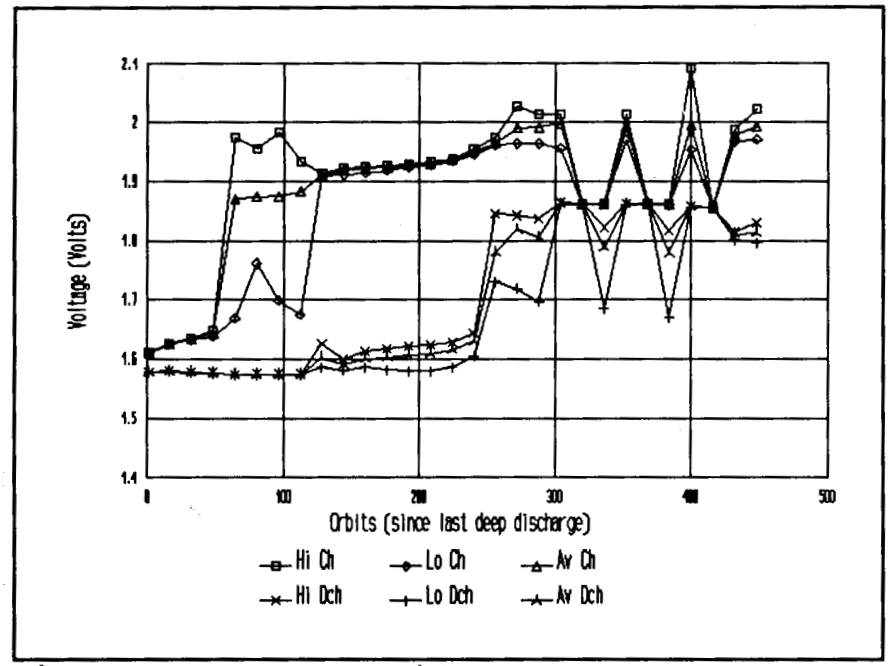

Figure 8 -- EOC/EOD Hi/Lo/Av cell voltages vs. orbits (since last deep discharge) during 11th month of LEO cycling for pack 1.

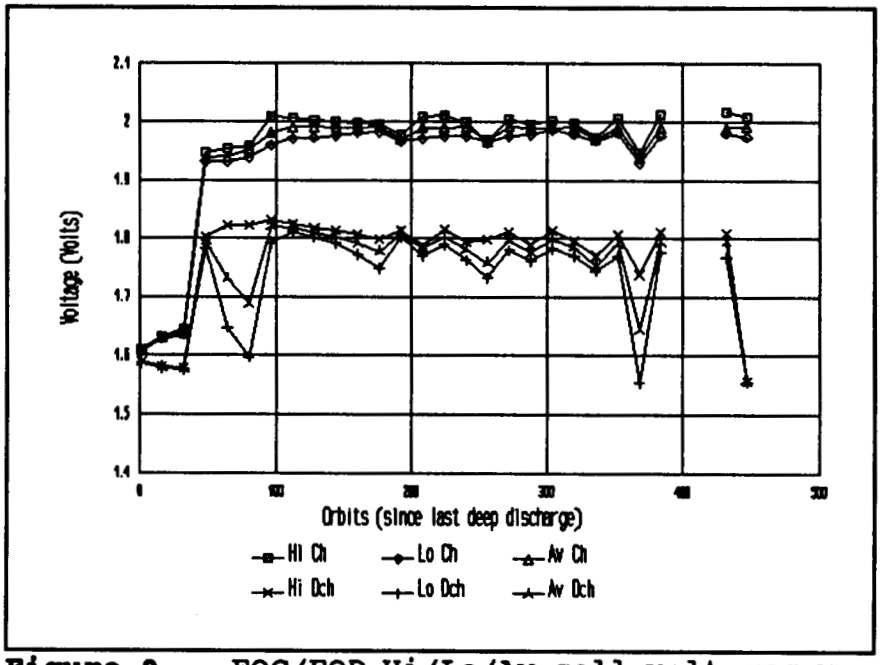

Figure 9 -- EOC/EOD Hi/Lo/Av cell voltages vs. orbits (since last deep discharge) during the 4th month of LEO cycling for pack 3.

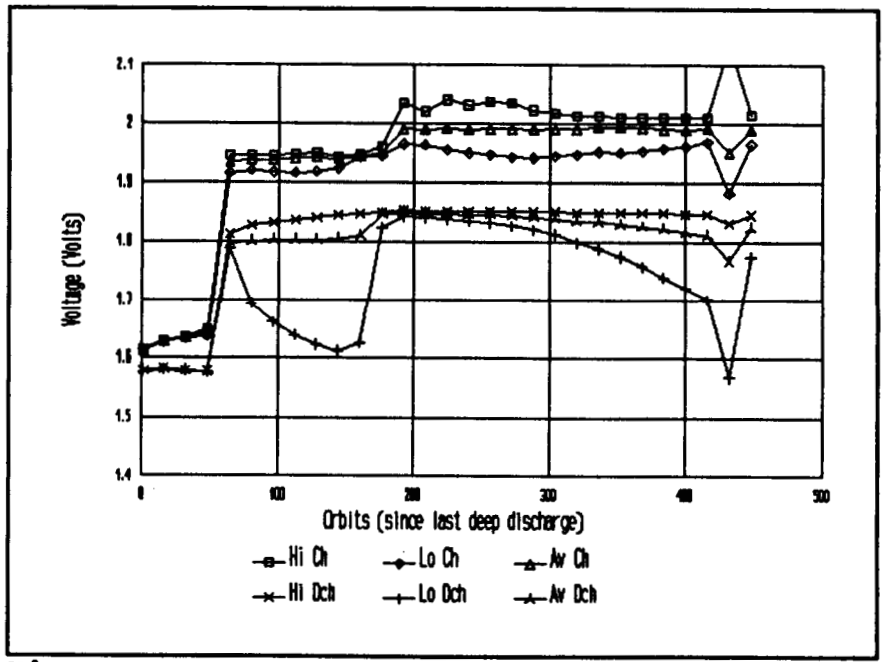

Figure 10 -- EOC/EOD Hi/Lo/Av cell voltages vs. orbits (since last deep discharge) during the 11th month of LEO cycling for pack 3.

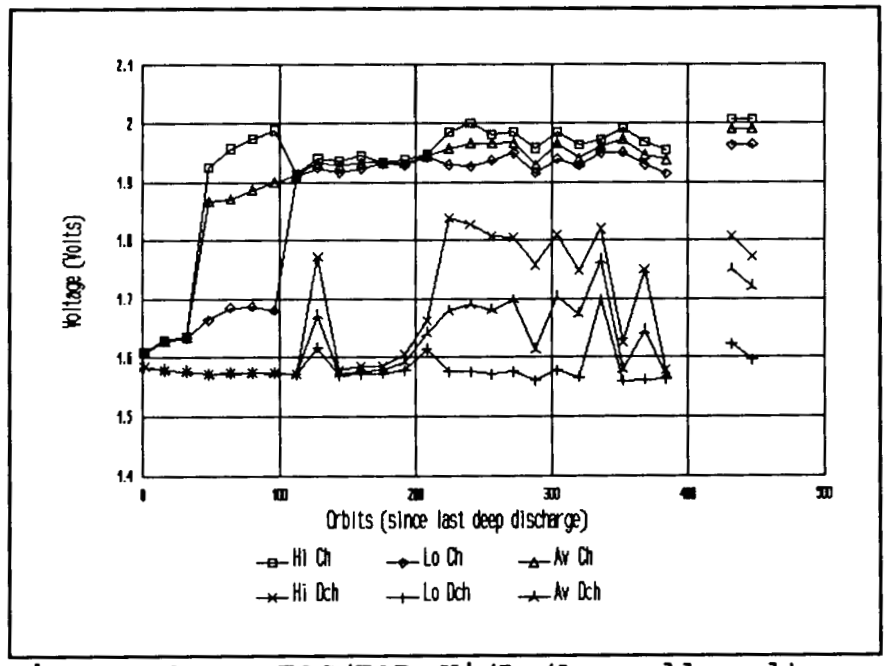

Figure 11 -- EOC/EOD Hi/Lo/Av cell voltages vs. orbits (since last deep discharge) during the 4th month of LEO cycling for pack 4.

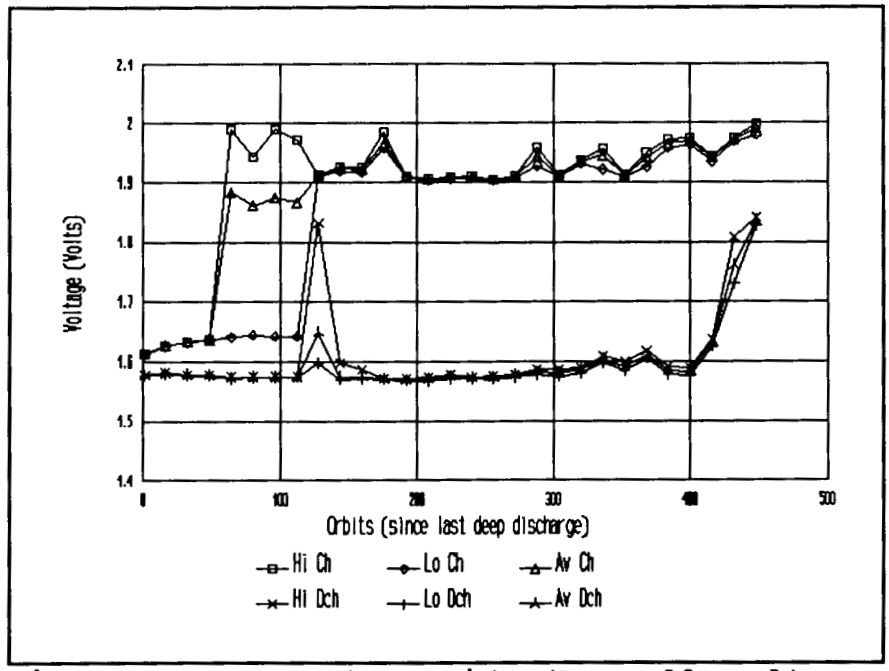

Figure 12 -- EOC/EOD Hi/Lo/Av cell voltages vs. orbits (since last deep discharge) during the 11th month of LEO cycling for pack 4.

Test Results and Discussion (continued)

Figures 7 and 8, 9 and 10, and 11 and 12 show the high, low, and average cell voltages at the end of charge (EOC) and discharge (EOD) during the 4th and 11th months of LEO cycling for packs 1, 3, and 4, respectively. There seems to be little difference between the 4th and 11th months for pack 1. Pack 4 seems to have improved in that there is a reduced amount of cell-to-cell variation as well as slightly lower EOC voltages. Pack 3, however, shows an increase in cell-to-cell variation (both on charge and discharge) as well as an accompanying fall-off in low cell EOD voltage as the pack approaches the end of the month of LEO cycling. This divergence can be attributed to the increased stress on the cells that occurs as they see more and more cycling time at a full SOC.

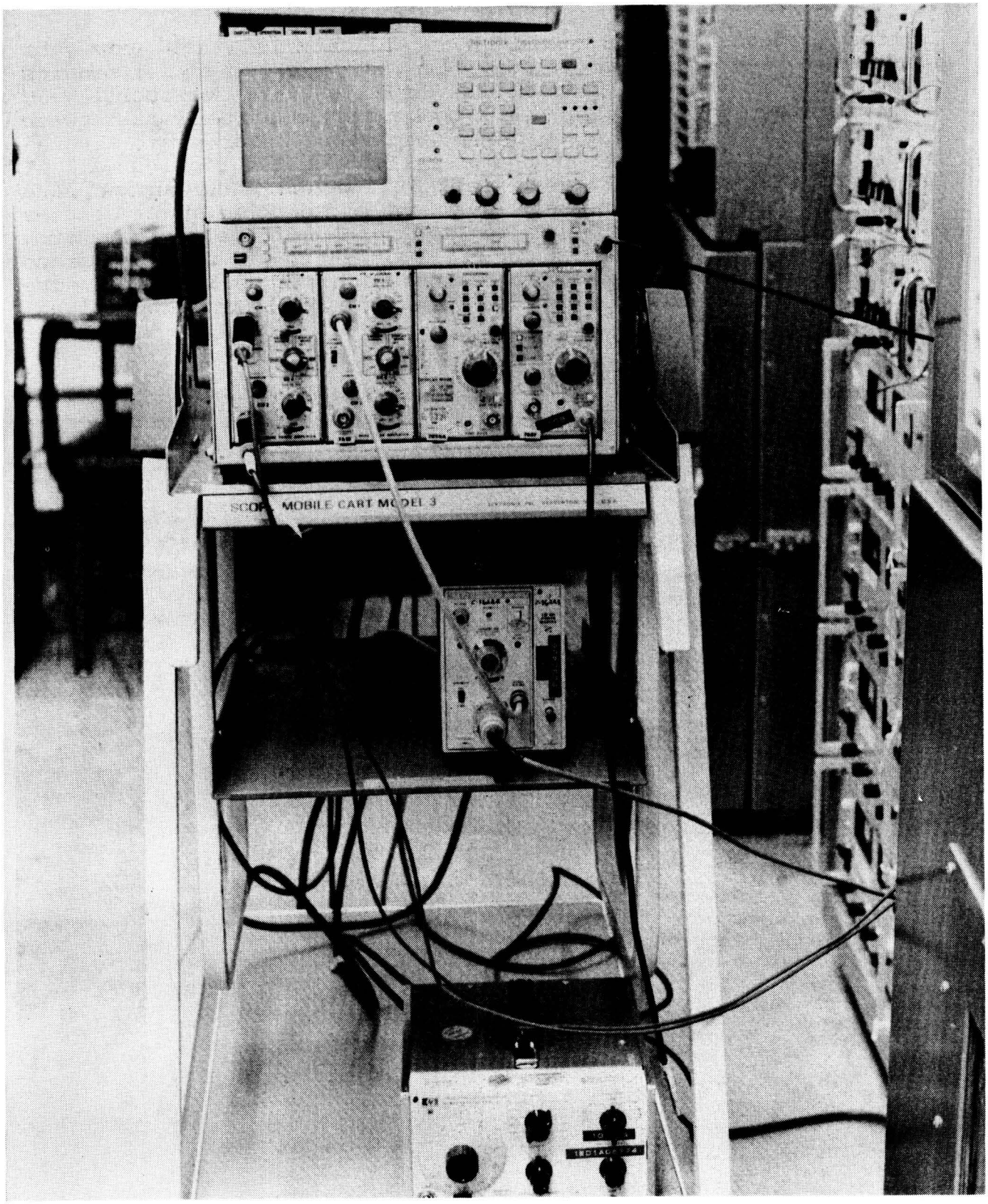

FIGURE 13

Impedance Test Procedure / Setup

Impedance tests have been performed on the Ag-Zn six-cell pack four times since the commencement of testing. These tests will be used to characterize the impedance of the Ag-Zn cells at various levels of discharge. To insure consistent test conditions all tests were performed during deep discharges or capacity tests.

The test was performed by injecting a sinusoidal current and measuring the magnitude and phase angle of the resultant voltage. Frequency was swept from 10 Hz to 1 MHz and DOD levels varied from 0% to 70%. The actual calculations and measurements were performed by using a Textronix 7854 programmable digital oscilloscope. The input signal was provided by an HP 3310A variable frequency signal generator (figure 13).

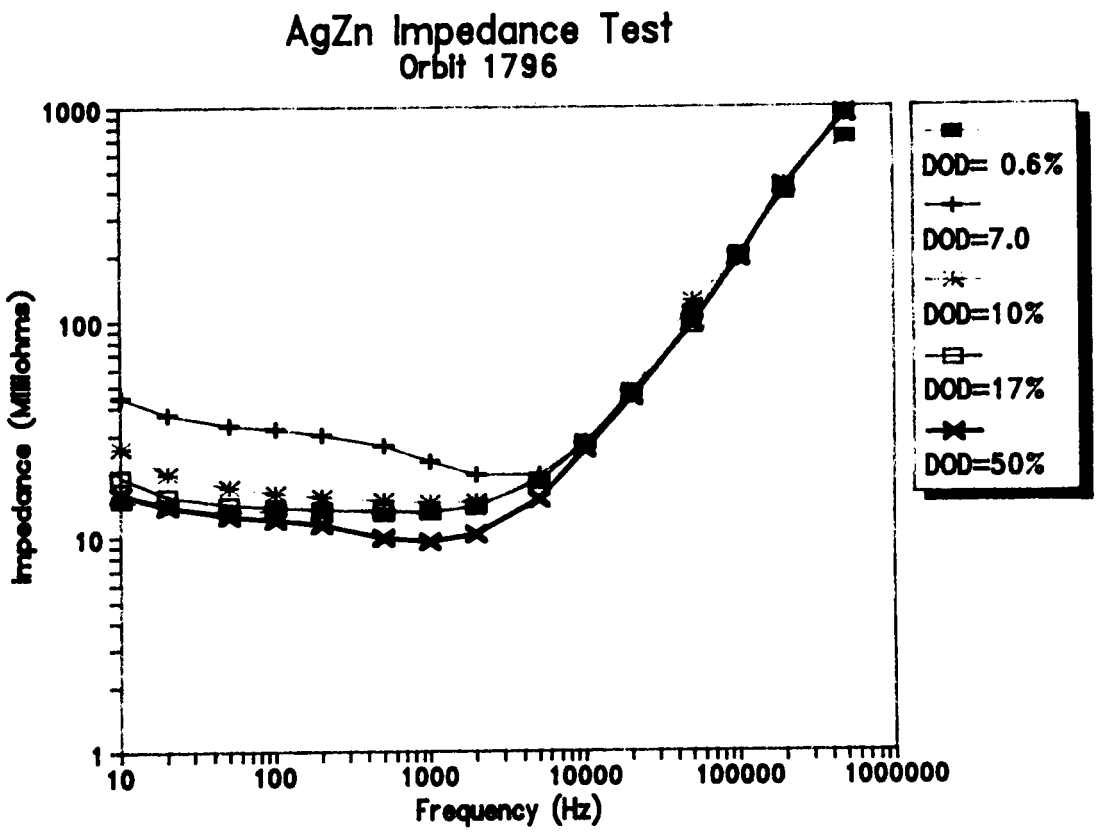
AgZn Impedance Test
Orbit 1796
Impedance (Milliohms)
1000
100
10
1
10
100
1000
10000
100000
1000000
Frequency (Hz)
DOD= 0.6%
DOD=7.0
DOD=10%
DOD=17%
DOD=50%

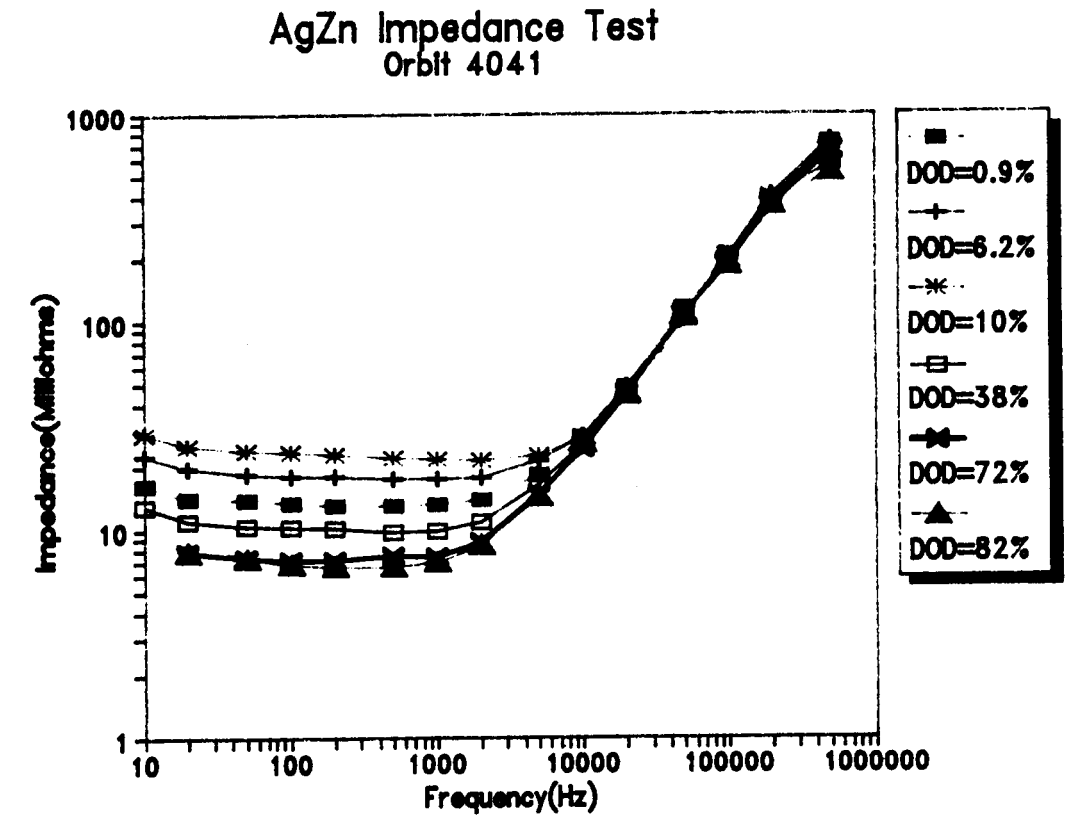
AgZn Impedance Test
Orbit 4041
Impedance(Milliohms)
1000
100
10
1
10
100
1000
10000
100000
1000000
Frequency(Hz)
DOD=0.9%
DOD=6.2%
DOD=10%
DOD=38%
DOD=72%
DOD=82%

FIGURE 14

Impedance Test Results: Magnitude

The basic results of this test have yielded an impedance "envelope" for various frequencies and DOD levels. The low frequency impedance magnitude varied between 10 and 100 milliohms. The magnitude is relatively constant to approximately 5000 Hz, at which point it begins to climb at 20 dB/decade. The low-frequency impedance is generally lower as DOD levels increase (figure 14).

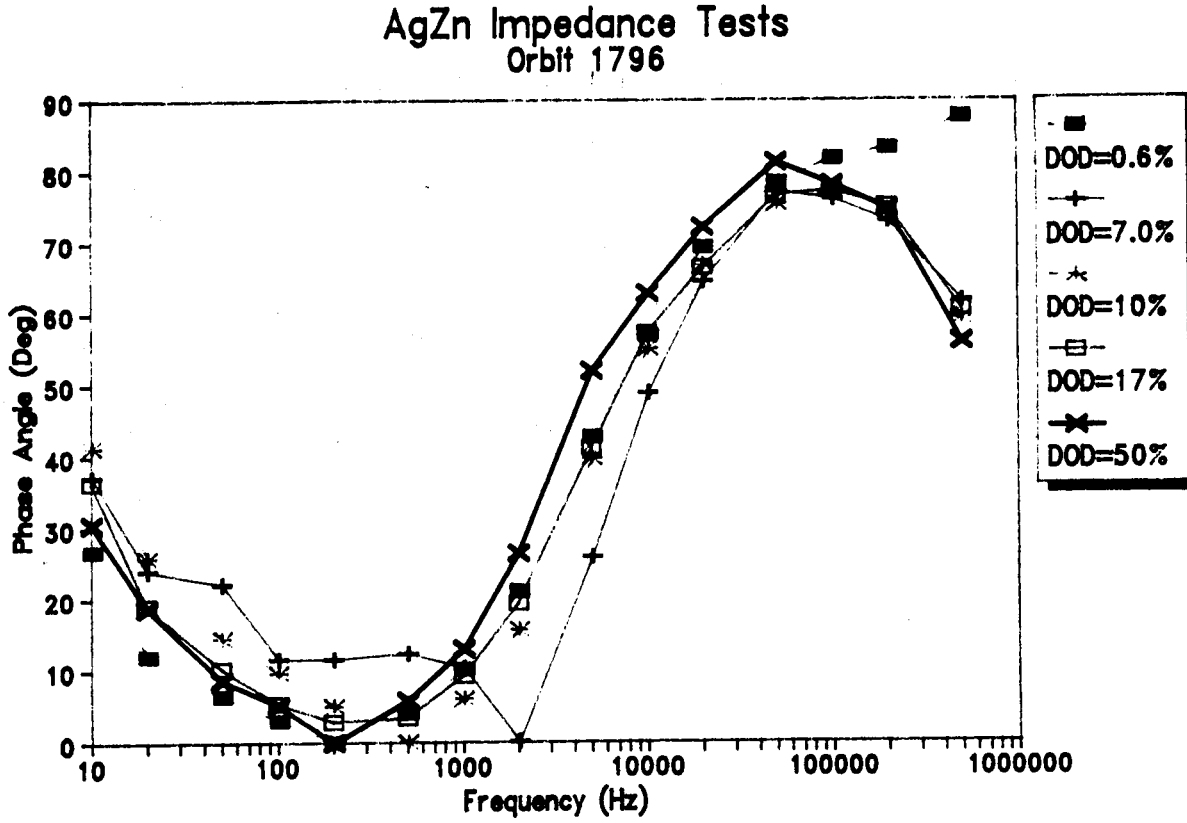
AgZn Impedance Tests
Orbit 1796
Phase Angle (Deg)
Frequency (Hz)
DOD=0.6%
DOD=7.0%
DOD=10%
DOD=17%
DOD=50%

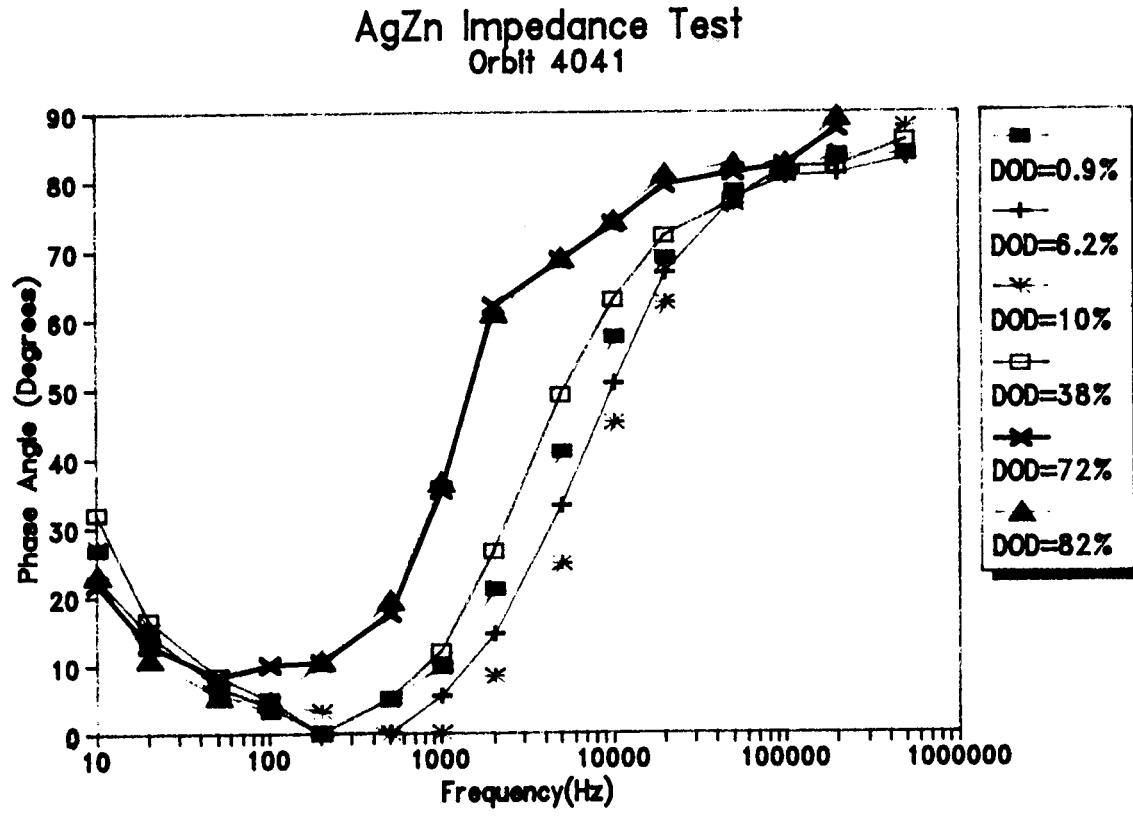
AgZn Impedance Test
Orbit 4041
Phase Angle (Degrees)
Frequency(Hz)
DOD=0.9%
DOD=6.2%
DOD=10%
DOD=38%
DOD=72%
DOD=82%

FIGURE 15

Impedance Test Results: Phase Angle

The phase angle characteristics are not as consistent as the magnitude results. Low frequency phase angle varies from 45 degrees to 20 degrees. The phase angle approaches zero degrees (resistive impedance) in a frequency range of 100 Hz to 1500 Hz. The phase angle then began a climb to 90 degrees (inductive load) as the frequency increased (figure 15). This climb may be due to the transformer used in the test apparatus. In some cases, however, the phase angle proceeded to start a descent at higher frequencies (see plot). This behavior is unusual but may be explained in part by the limitations of the ac voltage source.

CYCLE LIFE CHARACTERISTICS OF Li-TiS_2 CELLS

JPL

F. DELIGIANNIS, D. SHEN, C-K. HUANG AND S. SURAMPUDI

JET PROPULSION LABORATORY,
CALIFORNIA INSTITUTE OF TECHNOLOGY
PASADENA, CALIFORNIA

NASA AEROSPACE BATTERY WORKSHOP
DECEMBER 4-6, 1990
MARSHALL SPACE FLIGHT CENTER
HUNTSVILLE, ALABAMA

PROGRAM OBJECTIVES

* DEVELOP LITHIUM AMBIENT TEMPERATURE RECHARGEABLE CELLS.
  - DEVELOP AN UNDERSTANDING OF THE MATERIALS, PROPERTIES AND DESIGN OF A Li-TiS_2 CELL AND IT'S COMPONENTS.
  - DEMONSTRATE 100 Wh/Kg, 1000 CYCLES AT 50% DEPTH OF DISCHARGE BY 1995.

BATTERY WORKSHOP PROCEEDINGS 1990

RECHARGEABLE AMBIENT-TEMPERATURE LITHIUM BATTERIES

JPL

SCHEMATIC DIAGRAM OF A Li-TiS_2 CELL

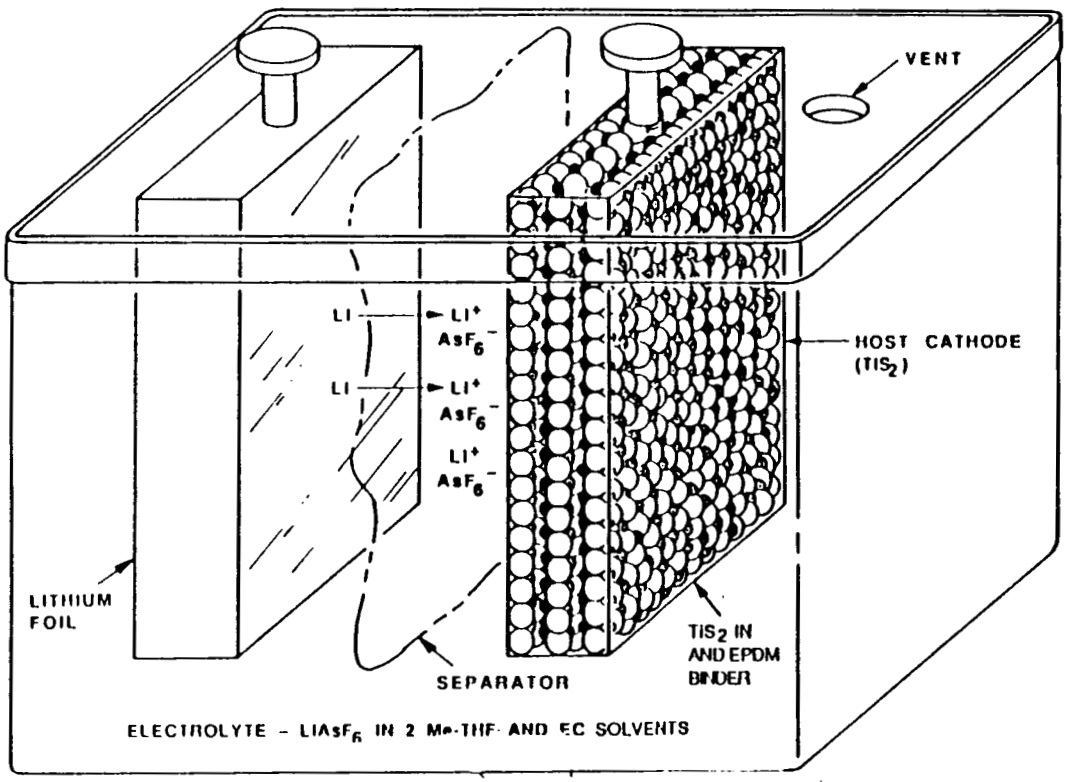

CELL REACTIONS

DISCHARGE . . LI INTERCALATION (INSERTION)

CHARGE. . . . . LI DE-INTERCALATION (REMOVAL)

$$LI + TiS_2 \underset{C}{\overset{D}{\rightleftharpoons}} LI\text{-}TiS_2$$

ELECTROLYTE

LITHIUM ARSENIC HEXAFLUORIDE ($LiAsF_6$) – SALT

2-METHYL TETRA HYDROFURAN (2-MeTHF) WITH

ETHYLENE CARBONATE (EC) – MIXED SOLVENT

JPL

PROGRAM APPROACH

- IDENTIFY SUITABLE ALLOY AND ALTERNATIVE ANODE MATERIALS.
- DEVELOP THIN HIGH POROSITY CATHODES.
- PERFORM DESIGN OPTIMIZATION STUDIES.
- CONTINUE TO UPDATE PERFORMANCE DATABASE OF STATE OF ART LITHIUM SECONDARY CELLS.
- ASSESS REDOX ADDITIVE FOR OVERCHARGE TOLERANCE.
- ASSESS USE OF POLYMER ELECTROLYTES IN A CELL.

JPL

EXPERIMENTAL CELL DESIGN

CONFIGURATION	CYLINDRICAL
NOMINAL CAPACITY (mAh)	875
ELECTRODE DESIGN	SPIRAL WOUND
ELECTROLYTE	$LiAsF_6$/2MeTHF+EC
SEPARATOR	POLYPROPYLENE
ELECTROLYTE QUANTITY (cc)	4, 7, 10
Li/TiS_2 CAPACITY RATIO	3/1, 6/1, 9/1

TESTING CONDITIONS

- PRECONDITIONING
  - 10 CYCLES AT C/5 DISCHARGE, C/10 CHARGE
    100% DOD BETWEEN 2.6 V AND 1.7 V

- LIFE CYCLING
  - CONSTANT CURRENT DISCHARGE FOR 500 mAh
    C/5 (1 mA/cm^2) 57% DOD
  - CONSTANT CURRENT CHARGE TO 2.6 V
    C/10 (0.5 mA/cm^2)
    MAX RECHARGE FRACTION 1.05
  - 30 MINUTE OPEN CIRCUIT BETWEEN OPERATIONS

- CYCLING TEMPERATURE: AMBIENT

JPL

CYCLE LIFE PERFORMANCE OF Li-TiS2 CELLS

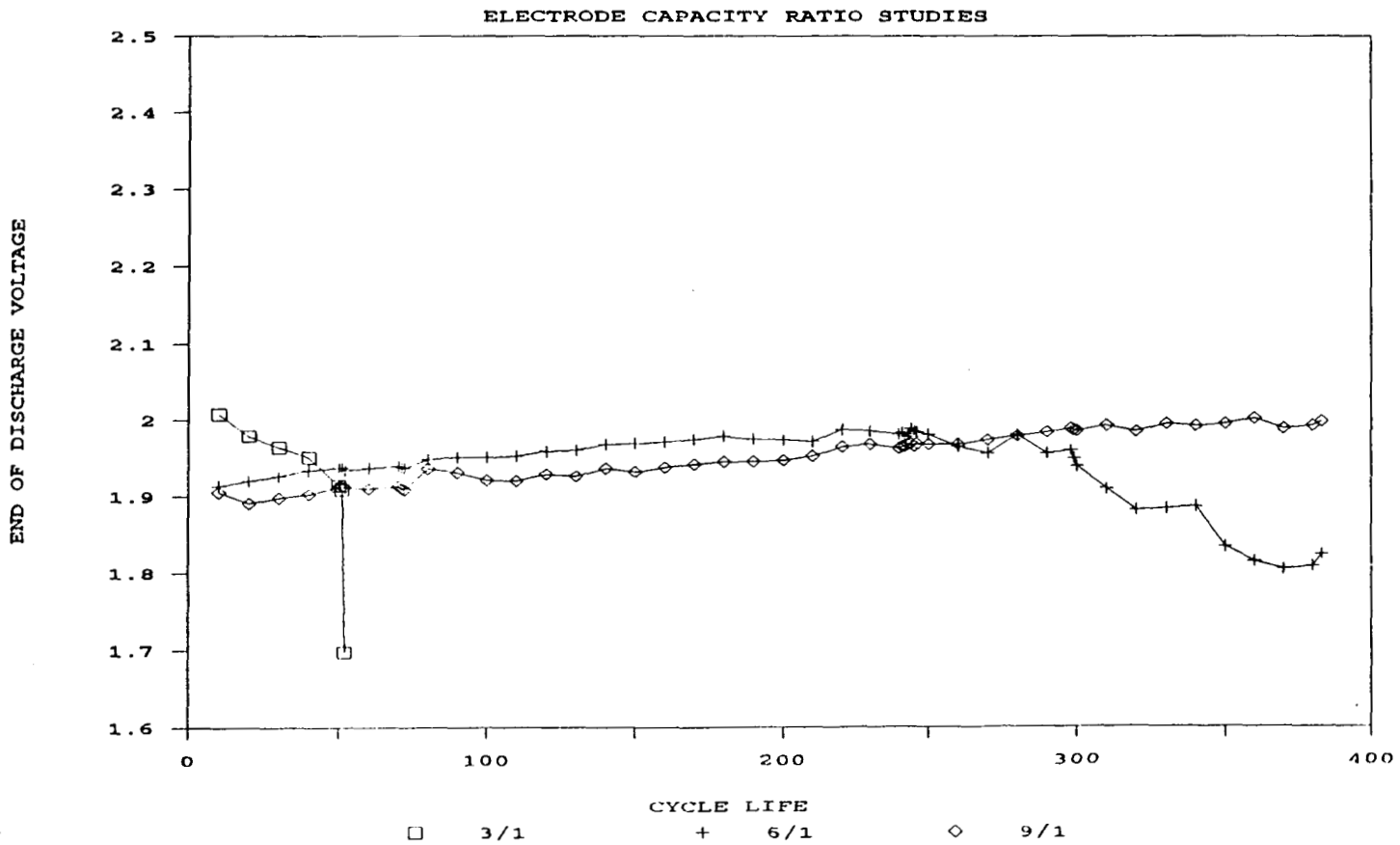

JPL

DISCHARGE - CHARGE CHARACTERISTICS OF Li-TiS_2 CELLS (ELECTRODE RATIO)

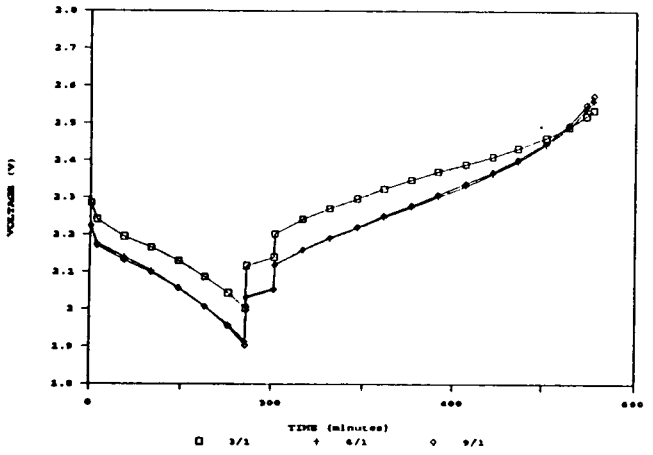

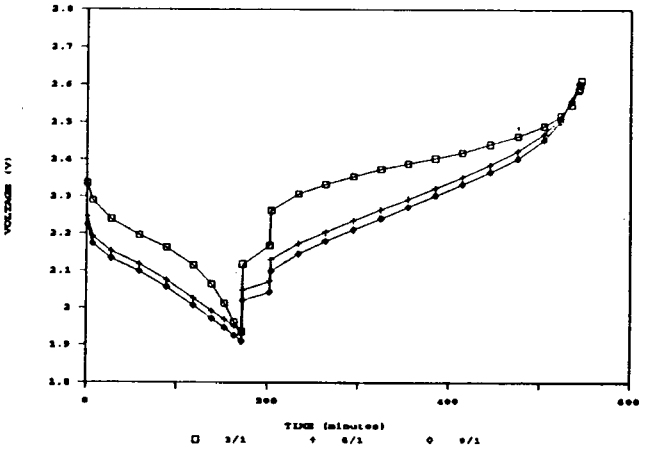

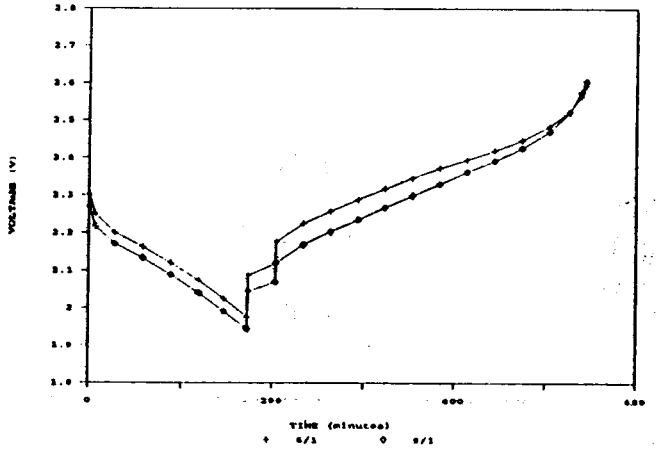

CYCLE LIFE PERFORMANCE OF Li-TiS2 CELLS

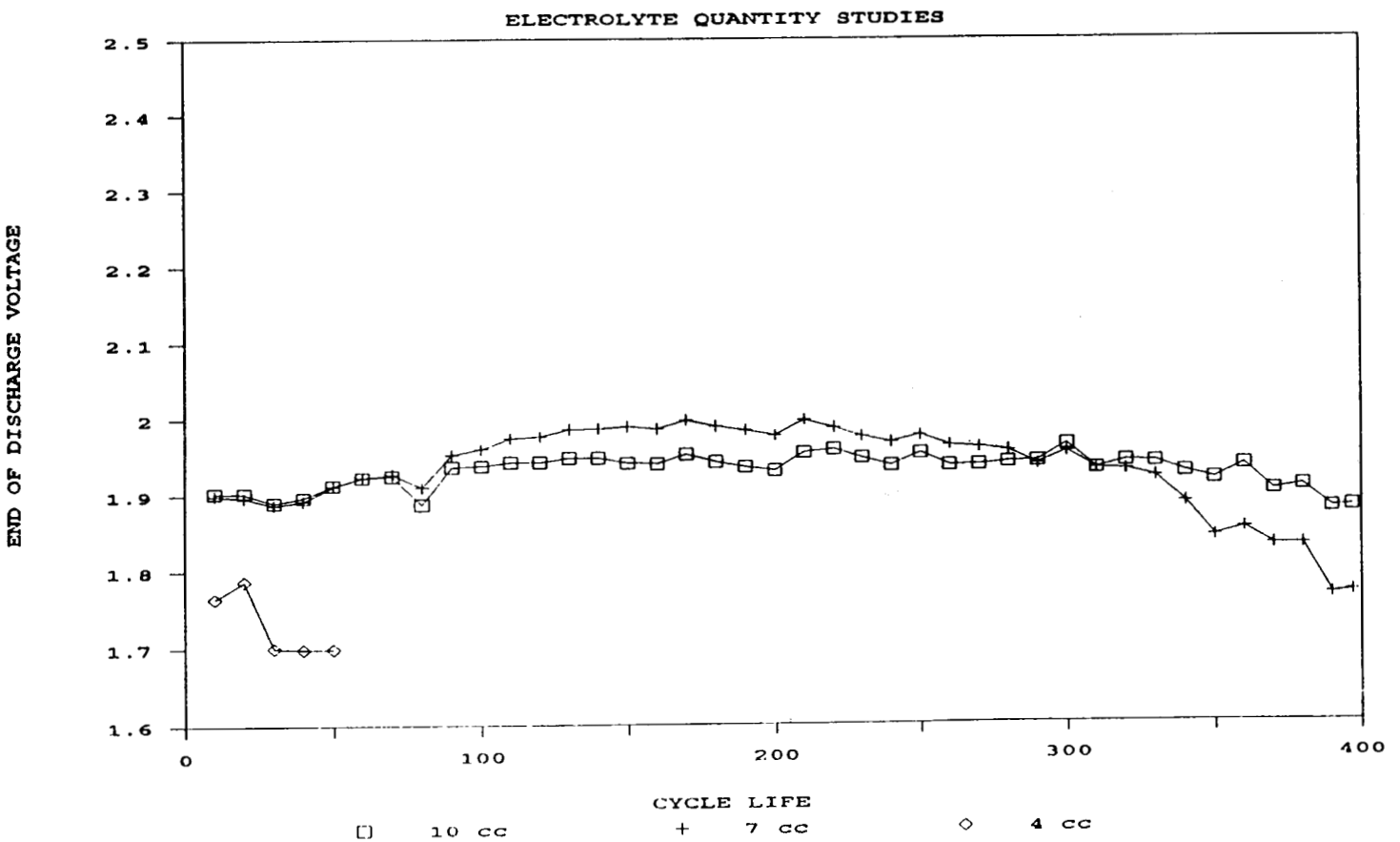

JPL

DISCHARGE - CHARGE CHARACTERISTICS OF Li-TiS_2 CELLS (ECTRLTE QUANT)

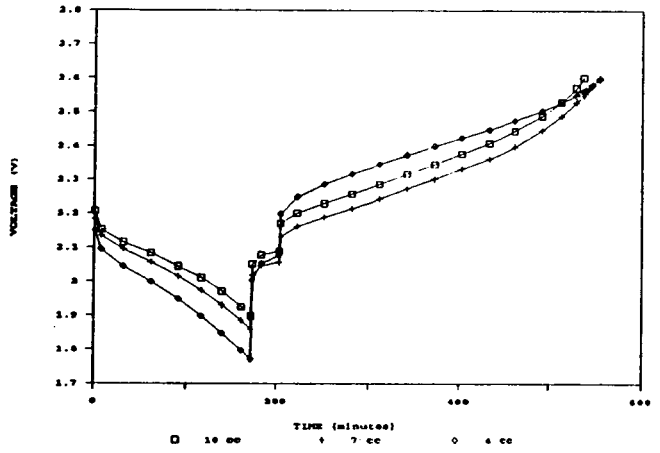

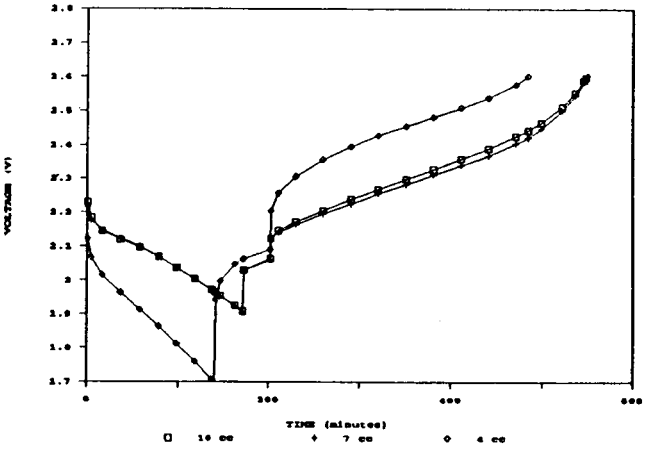

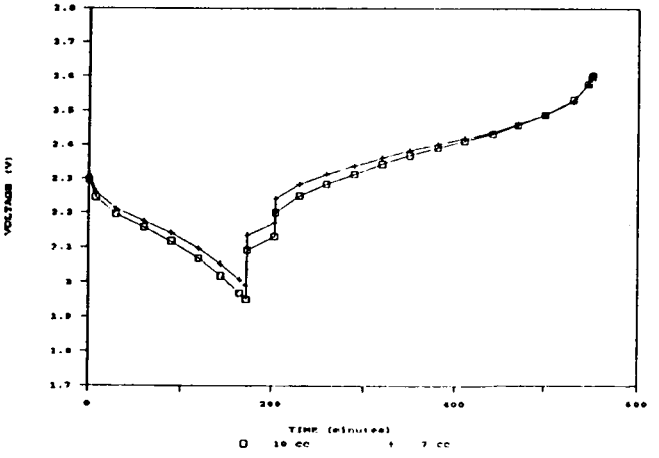

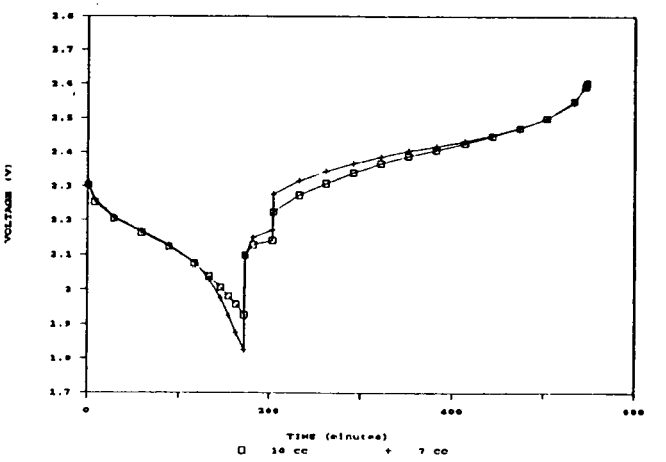

SUMMARY OF TEST RESULTS

QUANTITY OF ELECTROLYTE (cc)	ELECTRODE RATIO	NO. OF CYCLES
10	3/1	50
10	6/1	383 *
10	9/1	383 *
4	6/1	55
7	6/1	400 *
10	6/1	400 *

* CYCLING OF CELLS IS CONTINUING AS OF DATE

SUMMARY OF PERFORMANCE CHARACTERISTICS

CAPACITY (mAh)	875
VOLTAGE (T/2) (V)	2.1
DISCHARGE RATE	C/5 (1 mA/cm^2)
CHARGE RATE	C/10 (0.5 mA/cm^2)
CYCLE LIFE	IN EXCESS OF 400 AT 57% DOD

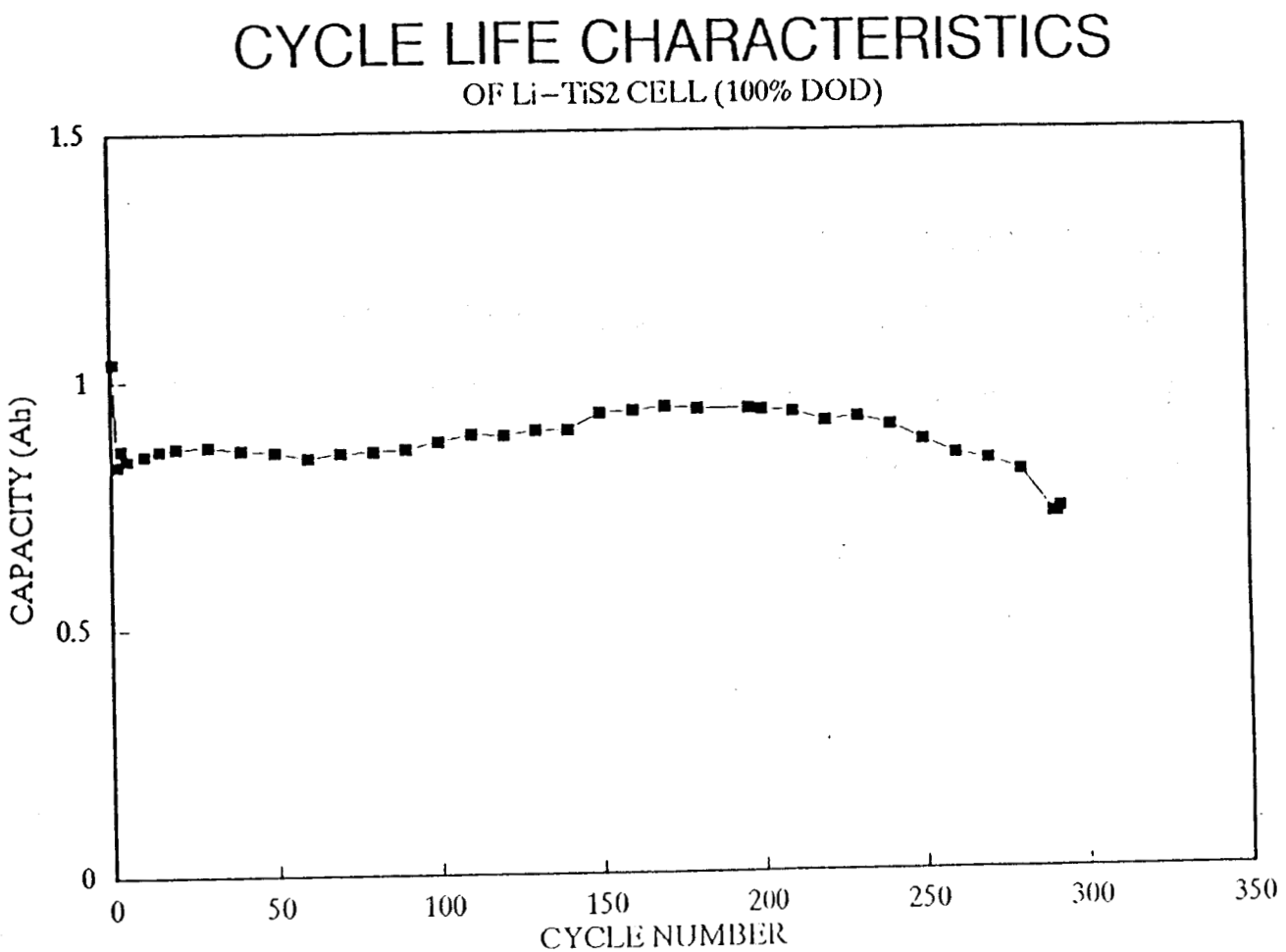

Figure 3. Cycle life of JPL 1 Ah Li-TiS_2 Cell

CYCLE LIFE PERFORMANCE OF Li-TiS2 CELL

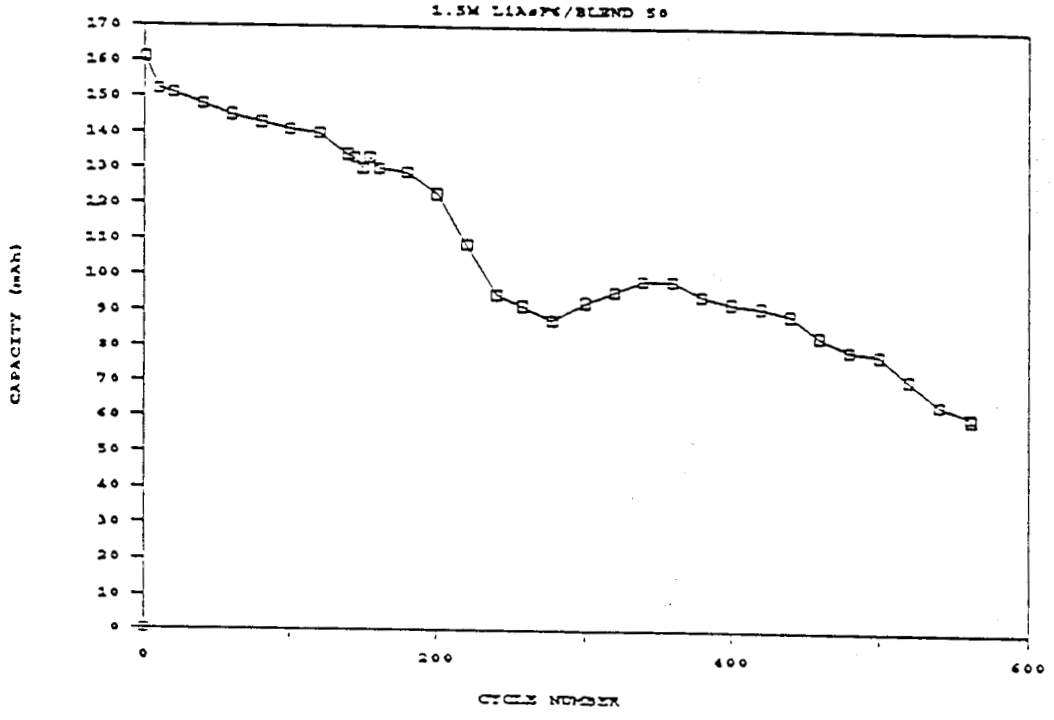

CONCLUSIONS

- GREATER THAN 3/1 ELECTRODE CAPACITY RATIO IS NECESSARY TO OBTAIN LONG CYCLE LIFE.
- 6/1 AND 9/1 RATIO DID NOT EXHIBIT ANY EFFECTS ON THE CYCLE LIFE OF THE CELLS AS OF DATE (CYCLING OF CELLS CONTINUING).
- GREATER THAN 4 cc OF ELECTROLYTE IS NECESSARY TO OBTAIN LONG CYCLE LIFE
- CELLS WITH 7 cc OF ELECTROLYTE HAVE EXHIBITED SMALL DEGRADATION AFTER 400 CYCLES.

ACCELERATED CYCLE LIFE PERFORMANCE FOR OVONIC NICKEL-METAL HYDRIDE CELLS

By Burton M. Otzinger
Rockwell International

Rockwell International
Satellite & Space Electronics Division

MGS-901102-8508

Introduction

NICKEL-METAL HYDRIDE RECHARGEABLE BATTERIES HAVE RECENTLY EMERGED AS THE LEADING CANDIDATE FOR COMMERCIAL REPLACEMENT OF NICKEL-CADMIUM BATTERIES. AN IMPORTANT INCENTIVE IS THAT THE Ni-MH CELL PROVIDES APPROXIMATELY TWICE THE CAPACITY OF A Ni-CD CELL FOR A GIVEN SIZE. A QUANTITY OF "C" SIZE CELLS WERE PURCHASED FROM OVONIC BATTERY CO.; SOME WITH AEROSPACE QUALITY SEPARATION & THE REMAINDER WITH COMMERCIAL SEPARATION. A SIX-CELL BATTERY WAS COMMITTED TO AN ACCELERATED CYCLE LIFE TEST TO DETERMINE THE EFFECT OF SEPARATION TYPE ON PERFORMANCE. RESULTS OF THE TEST MAY ALSO SHOW THE Ni-MH BATTERY TO BE A REPLACEMENT CANDIDATE FOR THE AEROSPACE Ni-CD BATTERY.

Test Cell Description

PART NUMBER	OVONIC BATTERY CO., "C" SIZE NO. 00676
CONFIGURATION	CYLINDRICAL, SPIRAL WOUND
CAPACITY	3.5 AMPERE-HOURS
DISCHARGE VOLTAGE	1.23 AVERAGE
INTERNAL IMPEDANCE	15 MILLI-OHMS AT 1,000 Hz
VENT VALVE	350 PSIG
POSITIVE PLATE AREA	182 CM^2
POSITIVE PLATE LOADING	2.1 GM/CC
SEPARATION	COMMERCIAL OR AEROSPACE
ELECTROLYTE	30% KOH
SIZE	DIAMETER: 2.54 CM LENGTH: 4.8 CM WEIGHT: 80 GRAMS

Accelerated Cycle Life Test Method

- SEPARATION DRY-OUT IS ANTICIPATED FAILURE MODE
- SIX-CELL TEST BATTERY CONSISTS OF FOUR CELLS WITH AEROSPACE SEPARATION & TWO CELLS WITH COMMERCIAL TO EVALUATE SEPARATION TYPE ON CYCLE LIFE. ELECTROLYTE RETENTION OF AEROSPACE SEPARATION IS BETTER
- ACCELERATION FACTORS ARE TEMPERATURE & DEPTH OF DISCHARGE
- TEST PARAMETERS

— TEMPERATURE	25°C to 30°C
— DOD	30%
— RATED CAPACITY	2.8 A-h (F = 0.2)
— DISCHARGE RATE	C/2 (1.4 AMPERES)
— CHARGE RATES	C (2.8 AMPERES) TO 85% SOC PLUS C/2 (1.4 AMPERES) TO CUT-OFF AT 114% CHARGE/DISCHARGE RATIO
— TEST RATE	21 CYCLES PER DAY

Aerospace Ni-Cd Cell Cycle Life vs. Depth-of-Discharge

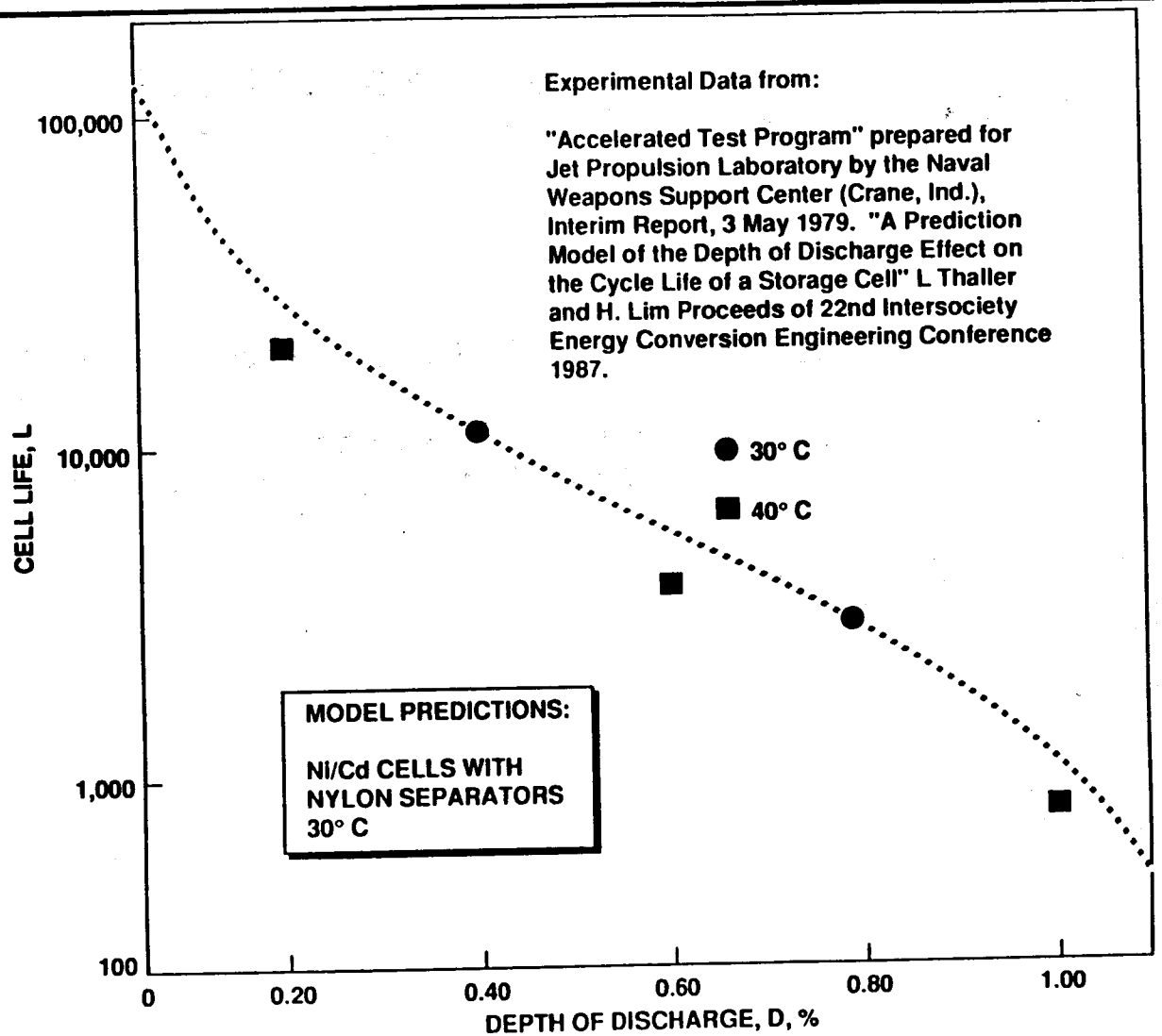

Rockwell International
Satellite & Space Electronics Division

MGS-901106-8523

Predicted Cycle Life For Ni-Cd Cells at 30% DOD

$$L = \frac{1 + F - D}{RD}$$

F = EXCESS CAPACITY OVER THE RATED VALUE

D = DEPTH OF DISCHARGE

R = CONSTANT ASSOCIATED WITH RATE OF CAPACITY LOSS

$R = 1.9 \times 10^{-4}$ FOR Ni-Cd CELLS WITH NYLON SEPARATION AT 30°C

F = 0.2 FOR TEST SAMPLE PLOTTED

THEN,

$$L = \frac{1 + 0.2 - 0.3}{1.9 \times 10^{-4} \times 0.3} = \frac{0.9}{0.57} \times 10^{-4} = 15{,}790 \text{ CYCLES}$$

Ni-MH 6 Cell Battery
Date: 10/26/90
Cycle No. 2700

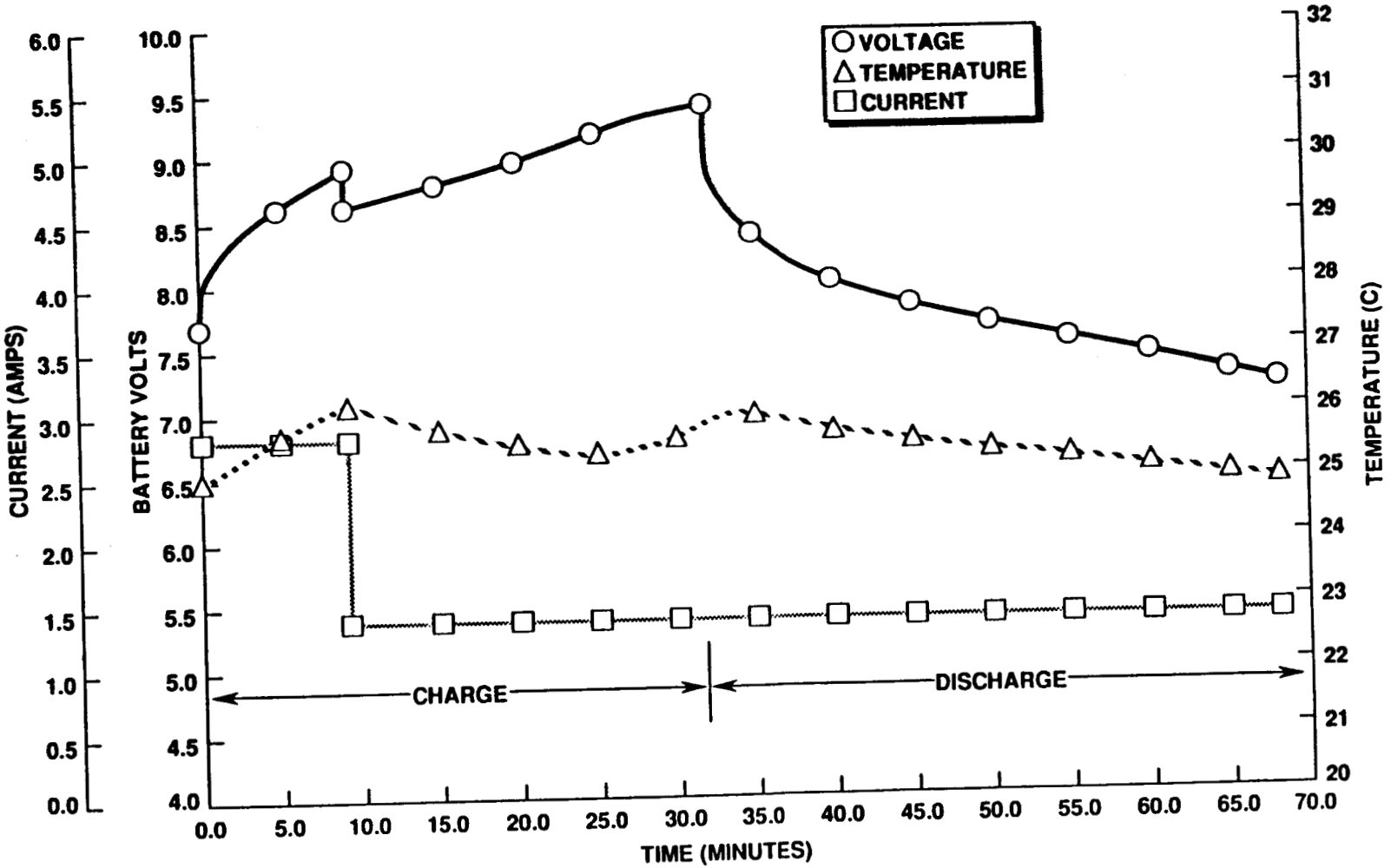

NiMH 30% DOD CHARGE & DISCHARGE VS. CYCLE NUMBER

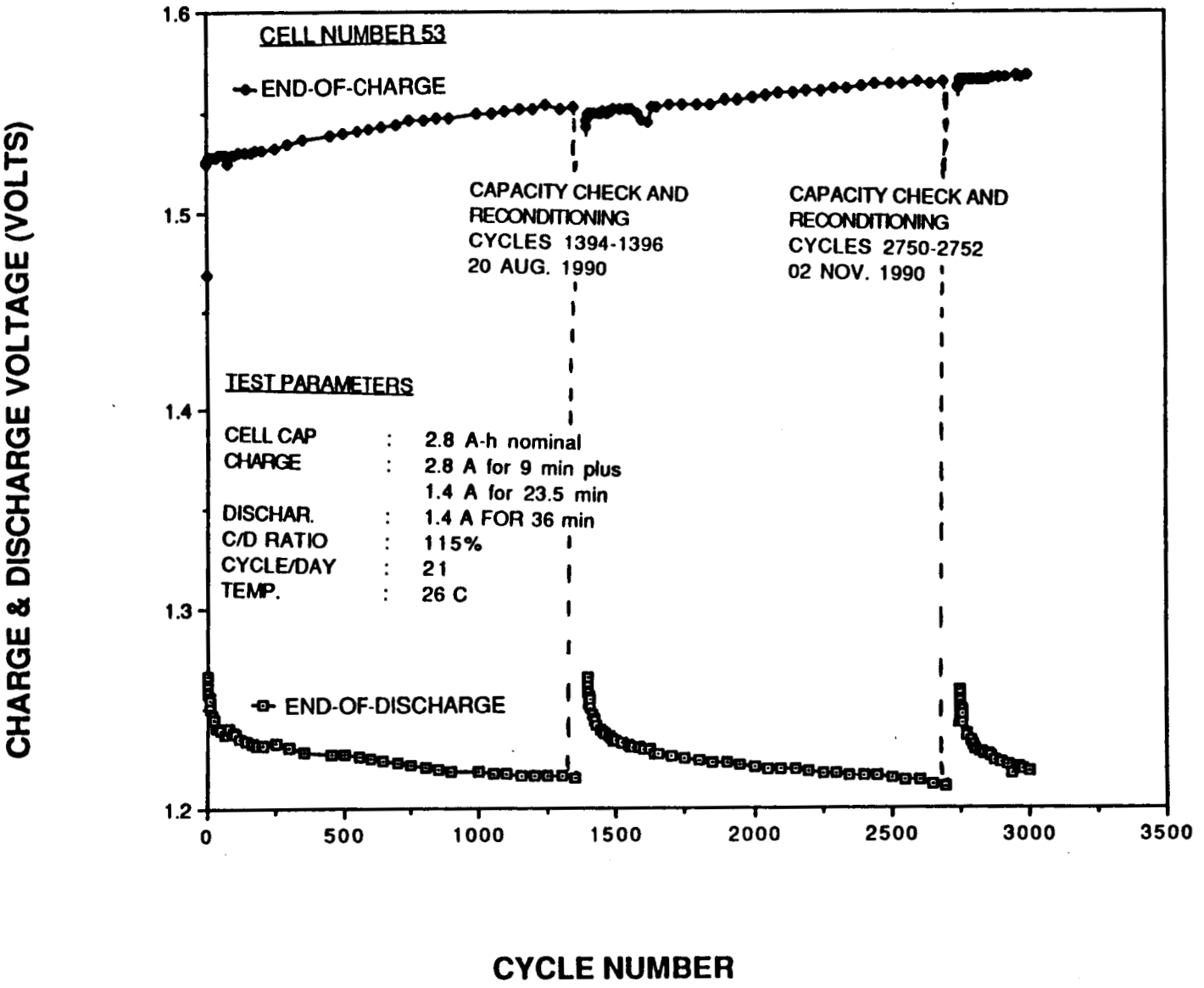

Test Results

CELL SERIAL NO.	IMPEDANCE (MOHM)		CHARGE RETENTION (%)	CAPACITY (A-h)		
	BOL (MΩ)	CYCLE 2,750 (MΩ)		BOL	CYCLE NO. 1,395	CYCLE NO. 2,752
41	13.0	11.0	85	3.678	3.649	3.588
50	13.5	12.0	79	3.648	3.606	3.480
51	13.0	11.3	77	3.720	3.643	3.606
53	14.8	11.3	78	3.728	3.668	3.608
16	12.3	11.0	79	3.264	3.463	3.355
14	12.9	10.6	79	3.270	3.295	3.290

Conclusions

- CAPACITY LOSS SMALL OVER 2,750 CYCLES
- RECONDITIONING SHOWN TO ELIMINATE DISCHARGE VOLTAGE FADING
- END-OF-CHARGE VOLTAGE VALUES INCREASING WITH CYCLING SIMILAR TO NICKEL-HYDROGEN PERFORMANCE
- FAILURE AT 1 VOLT PER CELL ESTIMATED TO OCCUR IN EXCESS OF 16,000 CYCLES WHICH IS COMPARABLE TO AEROSPACE NICKEL-CADMIUM PERFORMANCE

esa estec

european space research and technology centre

NASA AEROSPACE BATTERY WORKSHOP
December 4 - 6 1990

EVALUATION OF SODIUM-NICKEL CHLORIDE CELLS FOR SPACE APPLICATIONS

B. Hendel & G. Dudley
European Space Research & Technology Centre
PO Box 299, 2200AG Noordwijk
The Netherlands

EVALUATION OF SODIUM NICKEL CHLORIDE CELLS FOR SPACE APPLICATIONS

B. Hendel & G. Dudley
European Space Research & Technology Centre
PO Box 299, 2200AG Noordwijk
The Netherlands

ABSTRACT

This paper outlines the status of the European Space Agency programme on sodium nickel chloride batteries and reports the results of initial tests of two prototype space cells. After 2800 cycles typical of a low-earth orbit (LEO) application without failure, the recharge ratio remained at unity, the round trip energy efficiency remained high (87%) and the increase in internal cell resistance was modest. Initial tear-down analysis data show no degradation whatsoever of the beta-alumina electrolyte tubes. The low-rate capacity did, however drop by some 40%, which needs further investigation, but overall results are encouraging for future use of this couple in geosynchronous (GEO) and LEO spacecraft.

INTRODUCTION

Within its technology research programme, the European Space Agency is investigating battery couples which show promise of offering higher performance than those currently used aboard spacecraft. Fig.1 shows the principal needs for future earth - orbital applications and fig. 2, the main candidate systems. The sodium - sulphur couple is a strong contender and has attracted much interest in recent years. However, a relatively recent series of couples in which sulphur is replaced by a partially chlorinated solid transition metal appear to offer a number of advantages over sodium sulphur at the expense of some reduction in gravimetric energy density. These systems are currently under vigorous development in Europe and elsewhere mainly for electric vehicle applications.

The cycling regime and cycle life required for GEO applications are rather comparable with those required for electric vehicles. The main differences are the longer calendar life required (10-15 years rather than 3-5 years), the need to operate under zero gravity (vehicle cells rely on gravity for maintaining the liquid components of the cells in the desired locations) and to a lesser extent the higher mechanical vibration which must be withstood. On the other hand the 20 000 to 30 000 charge-discharge cycles required of typical LEO applications are an order of magnitude above the cycle life demonstrated in terrestrial tests and the rate capability requirement, especially for charge, is much more severe. It is nevertheless felt that the need for a lighter battery system is more pressing for LEO applications than for GEO. Consequently, a major aim of the ESA programme is to determine the cycle life obtainable with this system.

The thermal management of such a battery during launch and in space clearly demands a lot of consideration. The vehicle battery development programme has nevertheless already demonstrated lightweight thermal containment in which heat leaks are reduced to an energy flow comparable or less than the self-discharge rates of a nickel hydrogen battery. Since the self-discharge rate of this couple is nil, the battery itself could easily be called upon to supply the necessary heater power during periods when it is not in use. Provided thermal control of the cells within the battery can be properly managed, the high temperature of operation would require a much smaller radiator for heat rejection and make the battery rather insensitive to the spacecraft ambient temperature.

Fig. 3 outlines the ESA development programme on the Na-NiCl2 system, which is taking advantage of the much larger vehicle battery programme. The Harwell laboratory in the United Kingdom began work on this system in 1980 and Beta Technology, formed from the previous British Rail group, started industrialisation of the technology in 1982. Further milestones were the successful demonstration of electric vehicles in 1984 and in 1987, the introduction of sulphur additions to the nickel cell which cured earlier problems of capacity retention. The first phase of the ESA-funded programme consisted of a feasibility study with the aim of predicting the likely performance and problem areas using experience gained in the electric vehicle programme. Battery reliability was addressed at this early stage since cell lifetime was expected to be limited by electrolyte tube or seal failures and it was anticipated that space batteries would have to be designed to accommodate a significant number of cell failures in order to meet the long no - maintenance lifetimes required. Phase 2 resulted in the delivery to ESTEC of 20 prototype space cells, 10 optimised for GEO and 10 for LEO cycling. Phase 3 is in two parts, running concurrently. The first covers testing of the prototype cells (in the ESTEC Battery Test Centre). The second is a further LEO design iteration aimed at evaluating the performance that could be expected from optimised cell geometries.

CELL CHEMISTRY

Fig. 4 shows the cell reaction. Unlike alkaline nickel (and silver) electrodes the metal/metal dichloride electrode reaction is rather simple, leading to a well-defined open circuit potential. Values for nickel and iron are shown. In addition to the beta-alumina solid electrolyte, a second electrolyte consisting of molten sodium tetrachloroaluminate is used to provide an ionic path between the beta alumina and cathode materials, (both of which it wets readily). This has a wide electrochemical stability 'window' of about 1.6 to 3.5 volts with respect to sodium metal. Its presence also guarantees that the beta alumina electrolyte experiences a rather uniform current density across its whole area, unlike in the case of the sulphur electrode where two liquid phases are present for large part of the charge-discharge cycle, one of which (sulphur) is non-conducting. This feature would lead one to expect an increased beta alumina life, but has yet to be proven.

The temperature of operation is limited at the lower end by the melting point of the sodium tetrachloroaluminate (155 deg.C) and at the upper end by solubility of the metal dichloride in the melt. The wider temperature range, slightly higher energy density and less risk of transition metal contamination of the beta alumina lead to a selection of the nickel system for the prototype space cells.

The design of the prototype space cells in shown in fig. 5. The cell geometry resembles closely that of a sodium sulphur cell and the choice of an internal cathode configuration allows the use of a steel outer container. Safety is considered to be greater with this system than with sodium-sulphur since it has been demonstrated that breakage of the beta alumina tube does not lead to cell rupture. The reaction between sodium and the sodium tetrachloroaluminate melt leads to the rapid formation of aluminium which serves as a barrier to further direct reaction. This also ensures that failure is short-circuit, a distinct advantage to battery reliability, though it remains to be demonstrated that the short will be maintained for the entire remaining life of the battery.

The cells employ standard vehicle-cell size beta alumina tubes but incorporate wicking arrangements for both sodium and chloroaluminate melt and thus do not rely on gravity for correct operation. The seal is of the mechanical type used for early vehicle cells but which has now been superseded by one relying on diffusion-bonding. This will be directly applicable to future space cells and will result in a significant reduction in mass. A comparison between the main features of sodium-sulphur and sodium nickel chloride cells is given in fig. 6. Much

attention was paid to optimising the cathode composition and microstructure to fit the cycle regimes required for the two space applications. Some details are shown in fig. 7.

CELL TESTING

Two of the LEO cells were selected for initial testing at ESTEC. They were heated slowly to the working temperature of 300 deg. C in a fan-oven. Cycling of the two cells in series connection was carried out stopping charge when the first cell reached 2.8 V and stopping discharge when the first cell reached 2.0 V. The current was increased from 1 to 5 amps over successive cycles. Obtained capacities are compared with the theoretical value in fig. 7 and the cycle curves at 1A in fig. 8. The rapid fall in voltage on discharge below 2.5 V corresponds to completion of the reduction of nickel chloride to nickel and the onset of the reduction of the sulphur dopant. The two cells did not reach this point at the same time, showing that cell LE15 was approximately 1.3 Ah more charged than cell LE21. The cells were then cycled under LEO conditions, starting with a depth of discharge of 50% of the 1A capacity. After a few cycles the voltage limits were reached and the DoD had to be decreased. From 400 cycles to 2800 cycles, a DoD of 30% was the highest that could be maintained (although this could have been increased somewhat if the cells had not been 'out of step'). The cycling parameters and results are summarised in figures 9 to 11. The cell voltage curves show an increase in polarisation with cycling (fig. 9), although the round trip energy efficiency remained very high (fig. 11). Cell resistance measurements, made at 5-minute intervals by imposing automatically 100 millisecond reduction to 50% of the current, show that the resistance increases both during charge and discharge which is consistent with the reaction mechanism observed for iron chloride cells (ref. 2). Both on charge and discharge the cathode reaction is believed to start close to the beta-alumina tube and move outwards in a fairly well defined reaction front. As this proceeds, the sodium ion path (in the electrolyte melt contained within the pores of the cathode) increases and hence so does the resistance.

After 2810 cycles the cells were subjected to further capacity checks at the 1 A rate, then cooled and shipped to Harwell for destructive analysis. This analysis is not complete at the time of writing but it has been established that the beta alumina tubes showed absolutely no signs of deterioration. The recharge ratio had remained at unity within experimental uncertainty. Comparisons of the positions of the sulphur-reduction "shoulders" for the two cells in the 1A capacity cycle measurements (fig. 8) before and after cycling suggests that the difference of 1.3 Ah in state of charge between the two cells had not substantially changed. This is consistent with both cells having identical (zero) self-discharge rates. However, the capacity had reduced by some 40 % compared to that before the start of cycling. At present it is an open question what has happened to the lost capacity. Capacity results are in any case under-estimated since charge was limited by one cell and discharge by the other. The shapes of the sulphur-reduction shoulders at the end of the final deep discharge (fig. 12) are rather different, indicating that there is a difference in the state of the cathodes of the two cells after cycling. An open question at the outset of testing was whether or not it is necessary or beneficial to regularly cycle cells into the sulphur-reduction region. It is interesting to note, (though certainly not statistically significant) that cell LE15, which had been cycled in the voltage window 2.85 to 2.1, ie above the S-reduction region, showed a modest increase in internal resistance whilst cell LE21, which had been cycled in the window 2.7 to 2.0, did not.

CONCLUSIONS OF TESTING

Conclusions must be tentative until more tests are completed and tear-down results are available. It is clear that the useful gravimetric energy density of 16 Wh/kg obtained with the prototype cells cycled at 30% DoD needs to be improved considerably. The useable DoD in LEO cycling appears to be limited rather more by diffusion overpotential than was predicted during the

feasibility study. It is concluded that future LEO cell cathodes should be limited to a maximum thickness of 4 mm. The increase in cell internal resistance and round trip efficiency during cycling was modest, although the 1 A rate capacity decrease was considerable. The cause of this capacity reduction will have to looked at carefully in future tests. The lack of any signs of deterioration in the beta-alumina electrolyte tubes after 2810 cycles suggests that this is nowhere near the cycle life limit and leads to optimism that LEO application will be possible.

FURTHER TESTING

Tests are ready to start on a further 16 of the 20 prototype cells. All cells will be individually charged before start of cycling to avoid the mismatch in state of charge experienced in test reported above. (This occurs because all cells were subjected individually to limited cycling before delivery to ESA). Cells are arranged as two batteries each of 4 GEO cells and two batteries of 4 LEO cells. All will be cycled at 300 deg.C in the same oven ~~as shown in fig.15~~. The GEO batteries will be subjected to realistic eclipse season profiles interleaved with a low-rate capacity check. The LEO battery cycling details are in the course of definition, but are expected to include occasional low-rate capacity checks, cycling within different voltage "windows", and investigation of taper-charging. Most will be will be continued until failure (inability to remain within 2.0 and 2.8 V during cycling) and tear-down analyses will be carried out on all failed and selected aged cells.

LEO CELL OPTIMISATION STUDY

The initial feasibility study indicated that a gravimetric energy density above 100 Wh/kg at cell level based upon 100% DoD should be possible in LEO and a value near 120 Wh/kg should be achievable in GEO using simple cylindrical cells. The lower values exhibited by the prototype cells could be moved nearer to the above targets by the incorporation of a number of relatively low-development-risk modifications such as the replacement of heavy mechanical seals by much lighter diffusion bonded seals (which were already foreseen in the feasibility study). Nevertheless, some of the initial design assumptions had proved slightly over-optimistic and taken together with the greater than expected diffusion overpotential, it became clear that a re-evaluation of the LEO cell design was necessary to take account of the lessons learnt during development testing of the prototypes. Phase 3b was therefore dedicated to a more detailed evaluation of alternative LEO cell geometries, imposing an upper limit of 4 mm on the thickness of the cathode.

The initial feasibility study had indicated a theoretical advantage in gravimetric energy density of cells with internal sodium electrodes and external cathodes. However this configuration requires the cell container to be resistant to the cathode and it was not feasible to carry out the necessary development work before delivery of prototype cells. The restriction on cathode thickness has severe consequences for cell design since it limits the optimum diameter of simple cylindrical cells to values which when coupled with the maximum length considered feasible on strength grounds, results in capacities of no more than 6 Ah. The target capacity of the optimisation was 20 Ah. Fig. 13 shows the results of the optimisation study for these simple cell geometries and fig. 14 a proposed "small cell design".

To obtain a 20 Ah capacity from a single cell at an energy density equal to or better than the "small cell" requires the use of multiple or "W" shaped electrolyte tubes. Although feasible, the production of such tubes entails considerable development cost and in addition the required seals become much more complicated. A small increase in gravimetric energy density appears possible compared to the "small" cell, as can be seen from Fig. 15. The highest energy densities appear to require the use of bipolar flat plate geometries. ~~over simple tube cells~~. However in

designs with more complicated electrolyte geometries such as the rectangular channel flat plate proposed by Nelson (ref. 2), our study indicates that energy densities of 120 - 130 Wh/kg would be possible (a rather more conservative figure than that given in the referenced paper). In any case a very considerable development program would be required to master the fabrication and sealing of the electrolyte components.

FUTURE PROGRAMME

The outcome of the cell optimisation study suggests that the best compromise between performance and development cost would be either the simple "small cell" (if low capacity is acceptable) or the "W" or concentric tube designs (if a larger capacity is mandatory). In view of the importance of the assumption about maximum cathode thickness, it is considered essential to validate it before significant development effort is started, so some tests will be necessary using cells with thinner cathodes but which do not need to be optimised in other respects. If adequate lifetime is also demonstrated (using the prototype cells) and the capacity reduction with life does not turn out to be life-limiting, a sufficient level of confidence in the technology and performance obtainable will have been built up to justify embarking upon the development of space-qualifiable batteries. The GEO cells have not yet been tested, but it is expected that the scope for further optimisation of these will be less than for the LEO cells.

ACKNOWLEDGEMENTS

Other than the LEO cycling, the work described here was carried out by R. Bones, D. Smith and D. Teagle at the Harwell Laboratory. The authors would also like to acknowledge the support given by Beta Research & Development Ltd in the form of know-how and components made available from the electric vehicle development programme.

REFERENCES

1. "Characterisation of the Positive Electrode in Sodium-Metal Chloride (Zebra) Cells", N. D. Nicholson, D.S. Demott & R. Hutchings, Proceedings of the 16th International Power Sources Symposium, Brighton 1988,

2. "Modelling of Sodium/Metal Chloride Batteries", P.A. Nelson, 24th IECEC Conference, August 6-11 1989, Washington D.C., p 1363

Fig.1 FUTURE EARTH-ORBITAL SPACECRAFT ENERGY STORAGE NEEDS

PRESENT STATE OF THE ART:

	GEO APPLICATIONS	LEO APPLICATIONS
# cycles	1000 - 2000	10000 - 30000
Current best USEFUL energy density at battery level	40 Wh/kg 50Wh/l (Ni-H2 @ 80% DoD)	20 Wh/kg 25Wh/l (Ni-H2 @ 40% DoD)
Current environmental temp. limits	-10 deg.C + 25 deg.C	-5 deg.C + 20 deg.C

NEEDS:

* Improvements in cycle life (especially in LEO)

* Substantial increase in useable energy density

* Widening of environmental temperature limits, especially upper limit, (to match more closely limits for electronic equipment).

Fig 2. CANDIDATE CHEMICAL COUPLES

Ni-Cd, Ni-H2, Ni-H2 advanced, Na-S, Li-X, H2-O2

Na-NiCl2: variant of the Na-S system, under development for electric vehicles

ASSUMPTION: Same DoDs and battery packaging factors as Ni-H2

TARGET: Useful energy: 100 Wh/kg GEO 50 Wh/kg LEO

Energy densities based on 100% DoD: 120 Wh/Kg for GEO and 100 Wh/kg for LEO

Fig. 3 ESA Na-NiCl2 DEVELOPMENT PROGRAMME:

1987 RFQ for Na battery. Harwell "Zebra" selected

Phase 1. Feasibility Study

* Battery reliability study
* Cell design study
* Cell development plan

Phase 2. Prototype Space Cell Development (Based upon available vehicle cell components)

* Optimisation of cathode (porosity)
* Evaluation of anode sodium wicks
* Molybdenum cathode current collector
* Freeze-thaw resistance
* Seals

* Delivery of 10 GEO + 10 LEO cells

Phase 3a. Testing of Cells delivered from phase 2

* Cycling at ESTEC
* Harwell support to testing
* Teardown analysis

Phase 3b. Alternative LEO Cell Design Study. Completed Nov 1990.

Phase 4. Under consideration

Fig.4 SODIUM METAL-CHLORIDE CELL CHEMISTRY

$$2\,NaCl + M \underset{\text{discharge}}{\overset{\text{charge}}{\rightleftharpoons}} MCl2 + 2\,Na$$

M = Fe 2.35 V @ 250 deg.C. operation range: 200 - 300 deg.C.

M = Ni 2.59 V @ 250 deg.C. operation range: 200 - 400 deg.C.

$$2\,NaAlCl4 \xrightarrow{\text{overcharge}} 2\,Na + 2\,AlCl3 + Cl2 \quad \text{(approx 3.5 V)}$$

$$4\,NaCl + Al \xleftarrow{\text{overdischarge}} NaAlCl4 + 3\,Na \quad \text{(approx 1.6 V)}$$

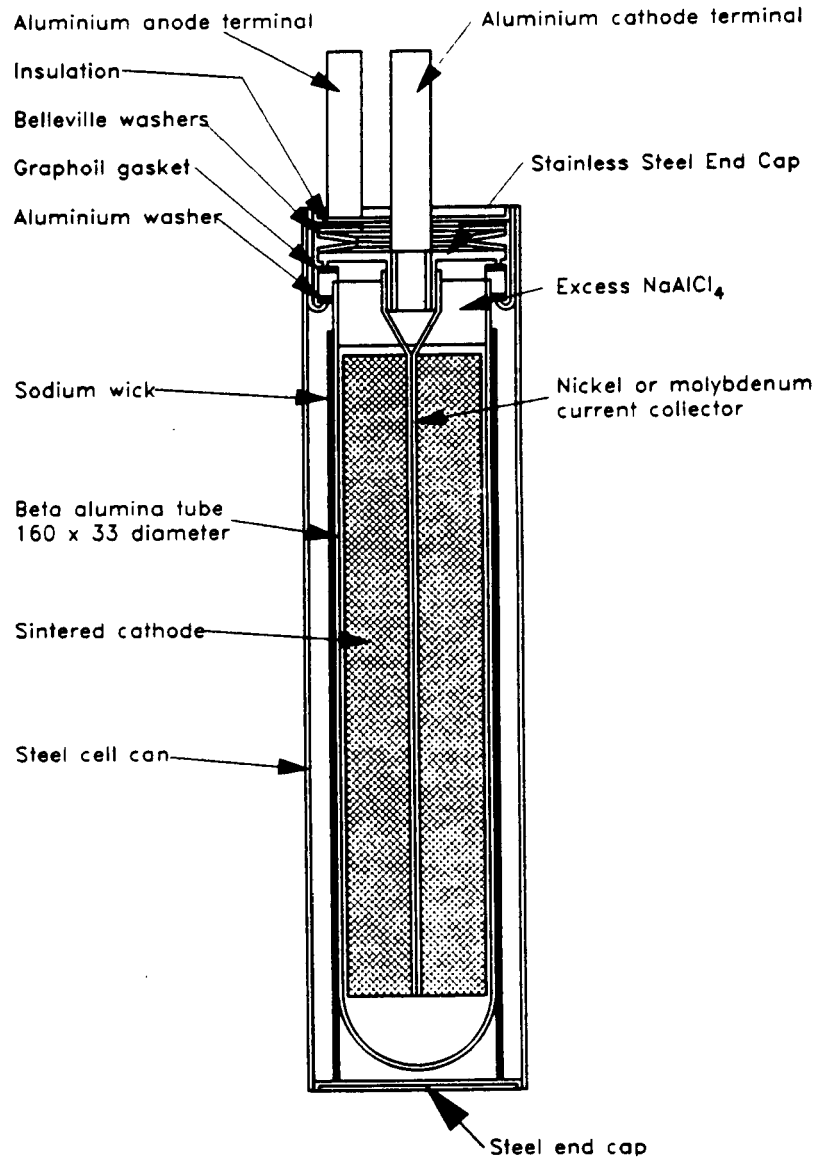

Fig. 5 PROTOTYPE SPACE SODIUM NICKEL CLORIDE CELL

Fig. 6 COMPARISON OF Na-NiCl2 WITH Na-S

Na-S	Na-NiCl2
+ + High energy density	+ Almost as high energy density
-- Limited cycle life	- Possibly better cycle life (more even current density over beta-alumina)
+ Liquid cathode active material	- Solid cathode active mat'l, possibility of morphological changes with cycling.
-- Electrolyte breakage can lead to violent reaction & failure of container	- Non-violent reaction, remains sealed
-- Fails open circuit (battery cell cross-linking or cell bypass required)	+ Fails short-circuit (large capacity cells can be used and cell bypass unnecessary)
-- Sensitive to thermal cycling	- Less sensitive to thermal cycling
-- Manufacture in dry conditions (sodium handling)	+ Can be manufactured overdischarged (sodium generated after sealing)

Fig. 7 SOME DETAILS OF THE PROTOTYPE SPACE CELLS

	GEO Cell	LEO Cell
Theoretical capacity (NaCl), Ah	22	15.3
Measured capacity at 1A rate, Ah	23.5 *	15.3
Cell Mass, g	655	660
Cell Volume, cm3	277	277
Mean discharge voltage	2.1	2.2
Wh/kg (100% DoD)	70.5 (79 with db seal)	52.7 (59 with db seal)
Wh/l (100% DoD)	166	124
Excess sodium	100	100
% Active nickel	33	33
% Cathode porosity (discharged)	89.9%	92.3
Cathode radius	14.9	14.9

* excess due to S reduction

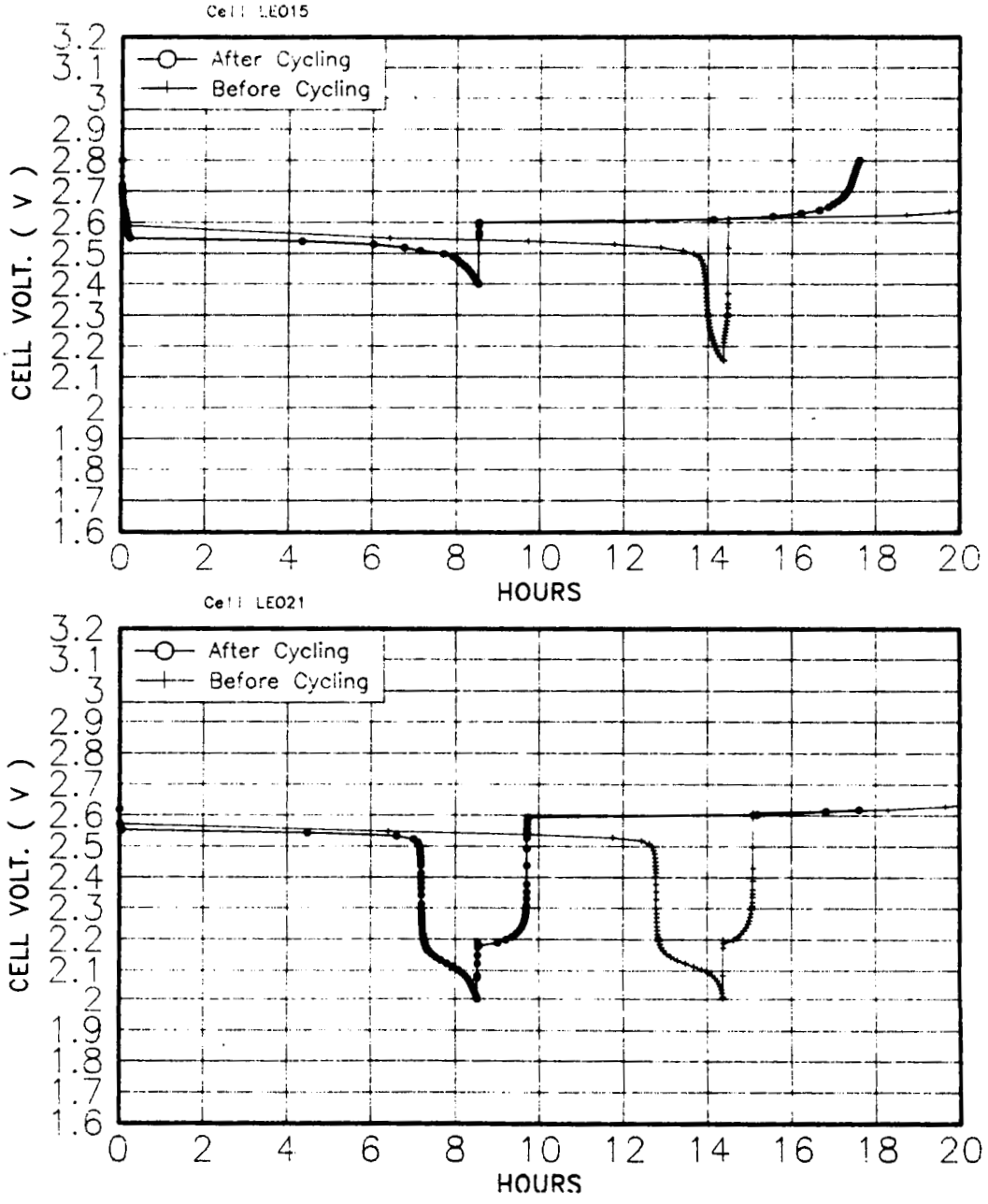

Fig. 8 CELL CAPACITY AT 1 A RATE BEFORE & AFTER 2810 CYCLES

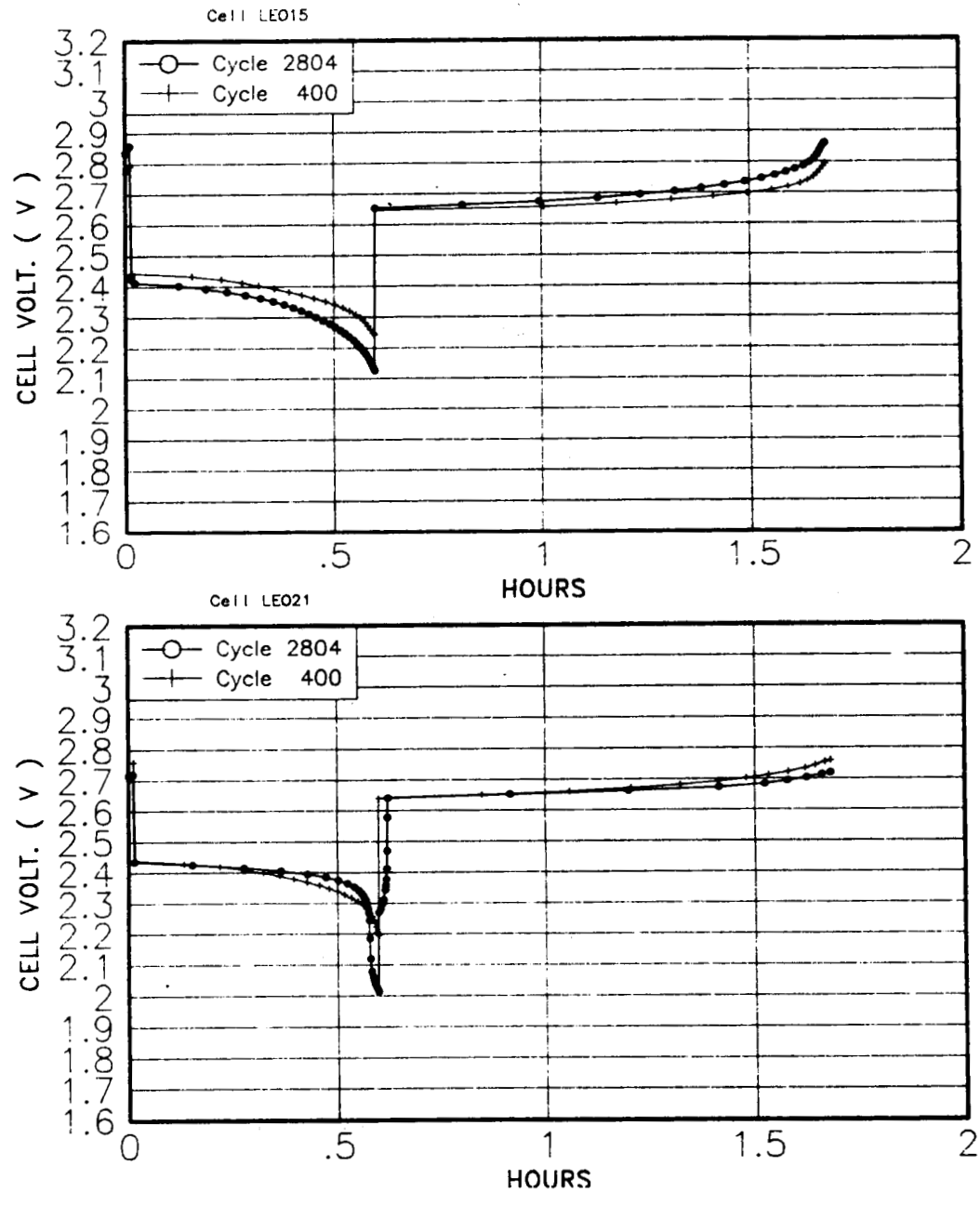

Fig. 9 CELL VOLTAGE DURING LEO CYCLES 400 & 2804

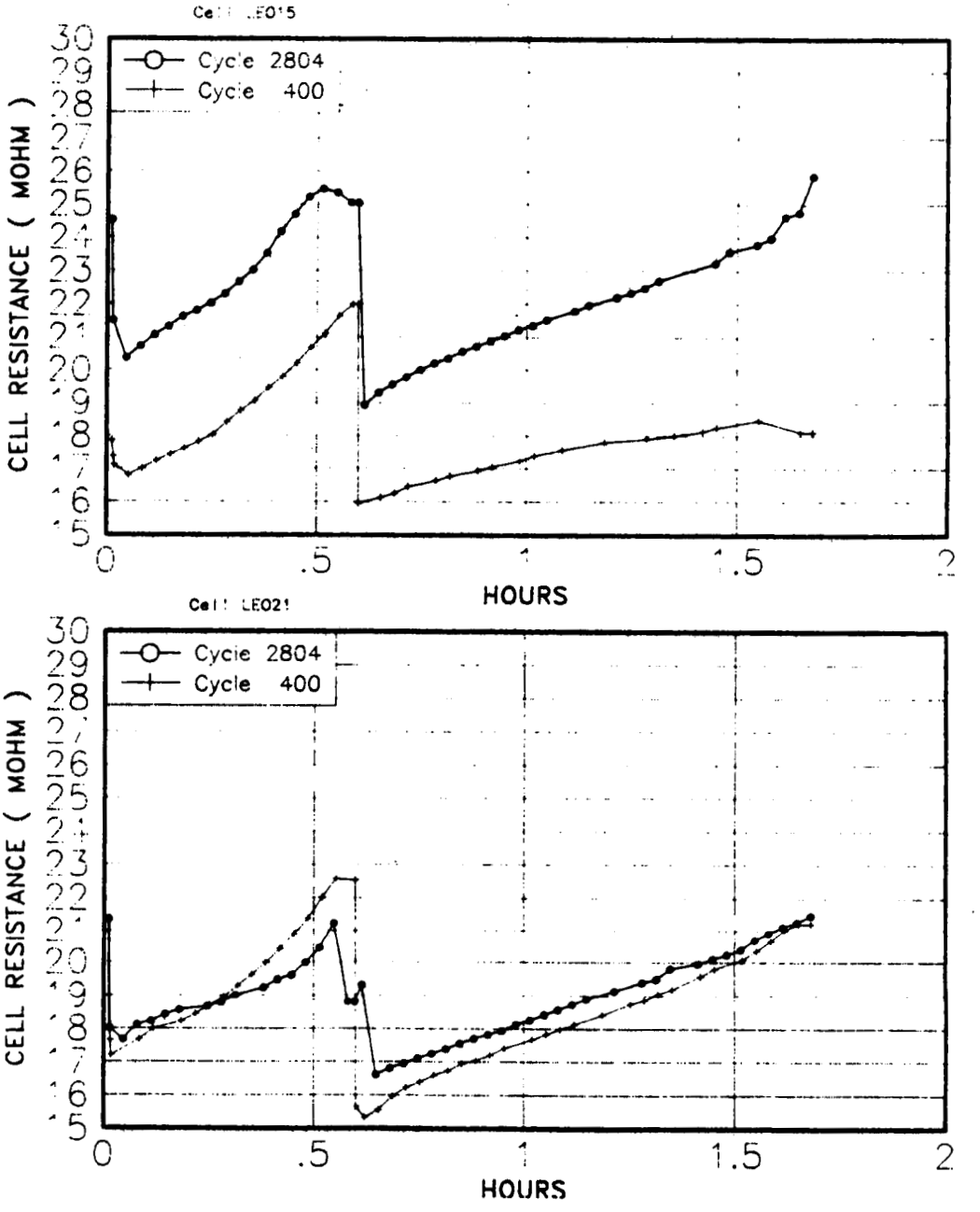

Fig. 10 CELL INTERNAL RESISTANCE DURING LEO CYCLES

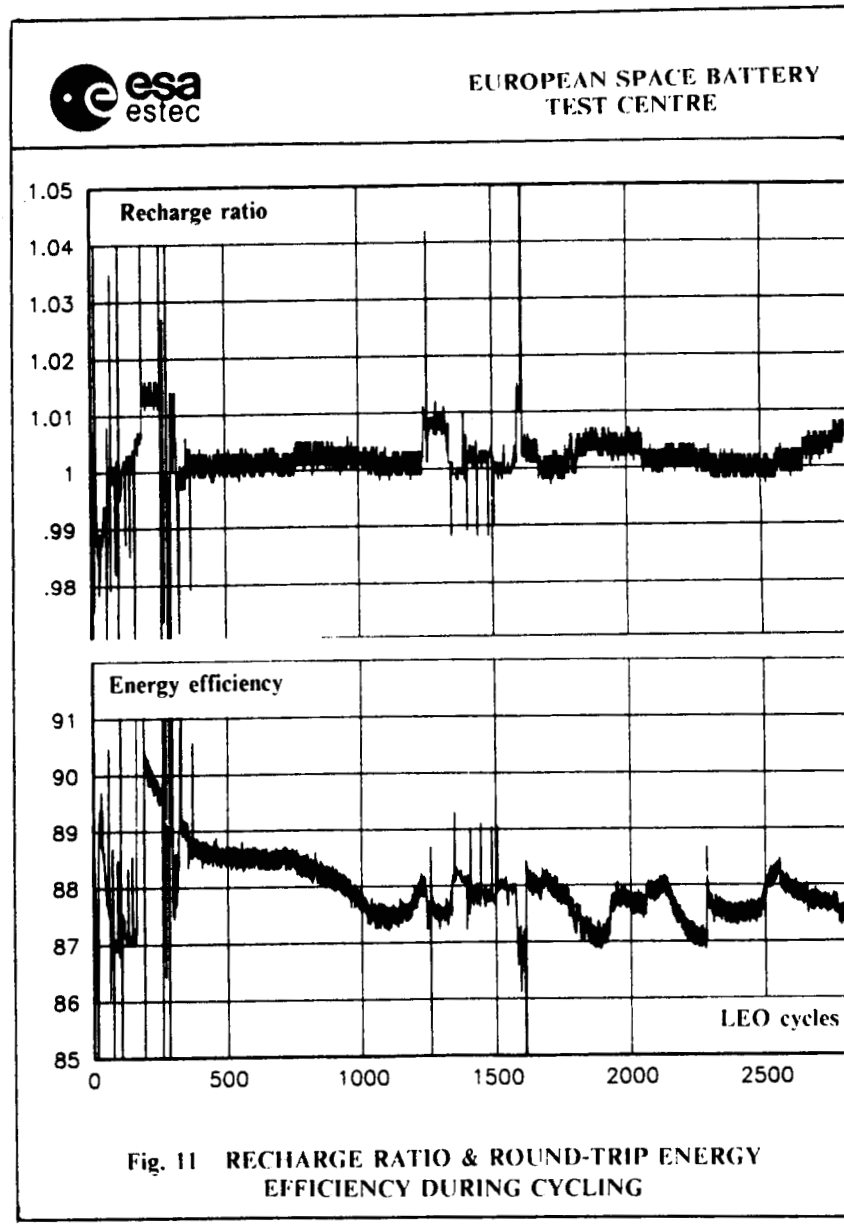

Fig. 11 RECHARGE RATIO & ROUND-TRIP ENERGY EFFICIENCY DURING CYCLING

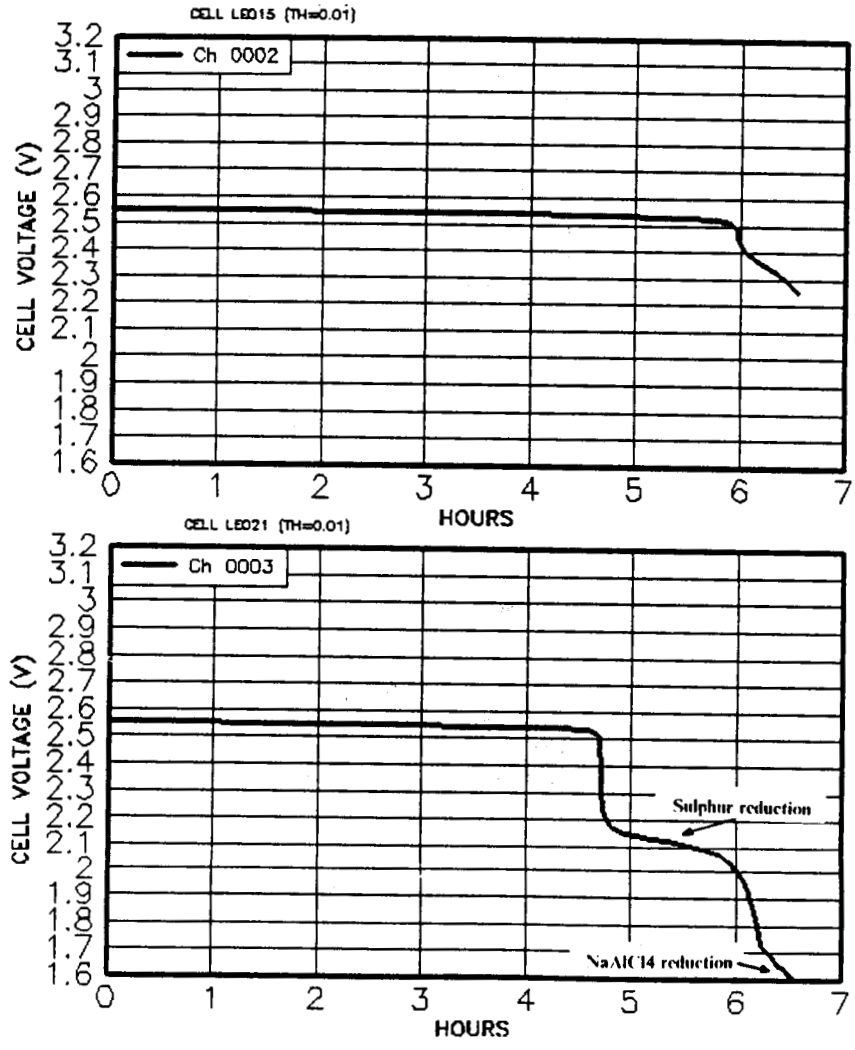

Fig. 12 FINAL DEEP DISCHARGE

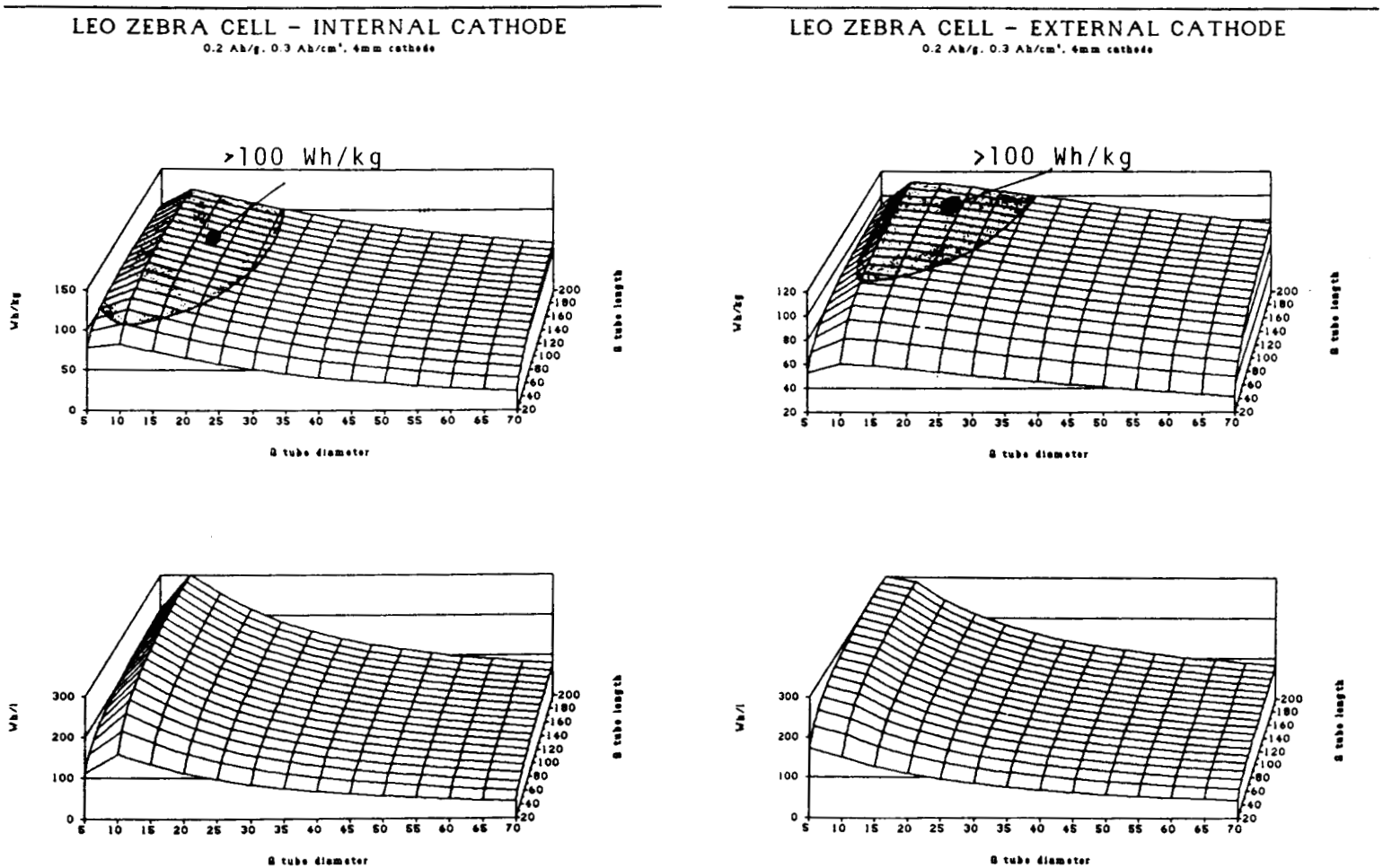

Fig. 13 ENERGY DENSITY OF SIMPLE LEO CELL DESIGNS

Fig.14 DESIGN OF A "SMALL CELL"

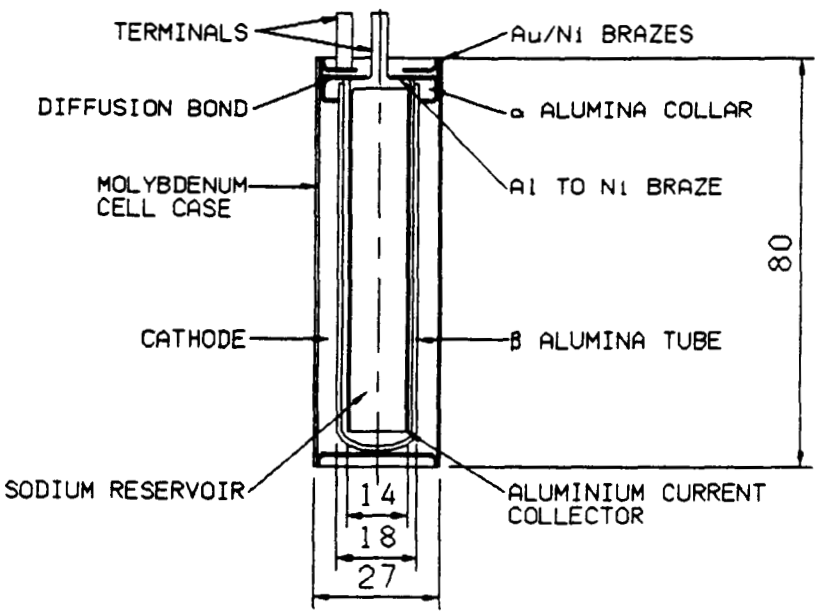

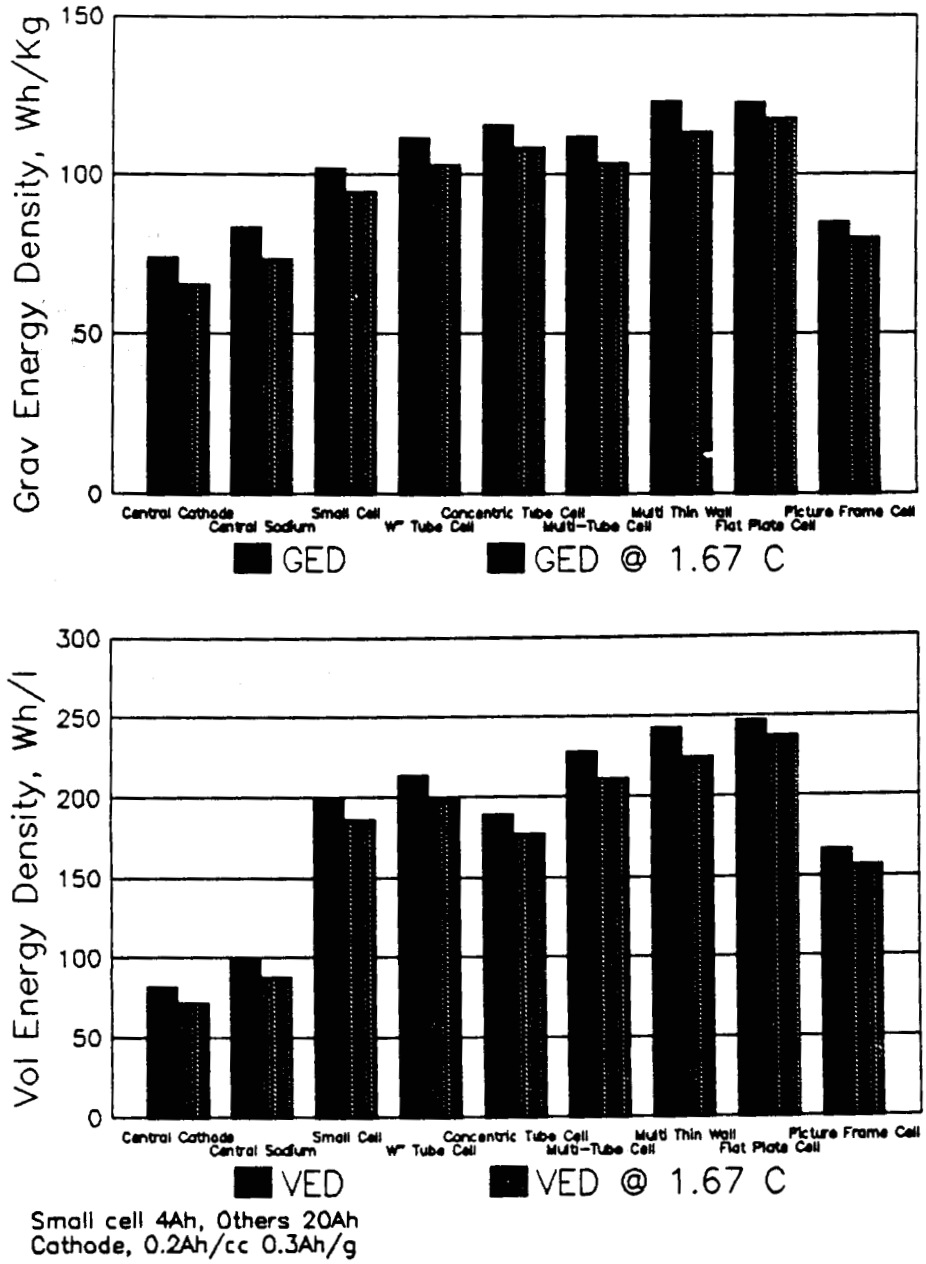

Fig. 15 ENERGY DENSITY OF ALTERNATIVE LEO CELL DESIGNS

UTILIZATION OF A BIPOLAR LEAD ACID BATTERY FOR THE ADVANCED LAUNCH SYSTEM

William Gentry, Robin Vidas, and Ronald Miles

JOHNSON CONTROLS, INC.

Steven Eckles

GENERAL DYNAMICS CORP.

JOHNSON CONTROLS

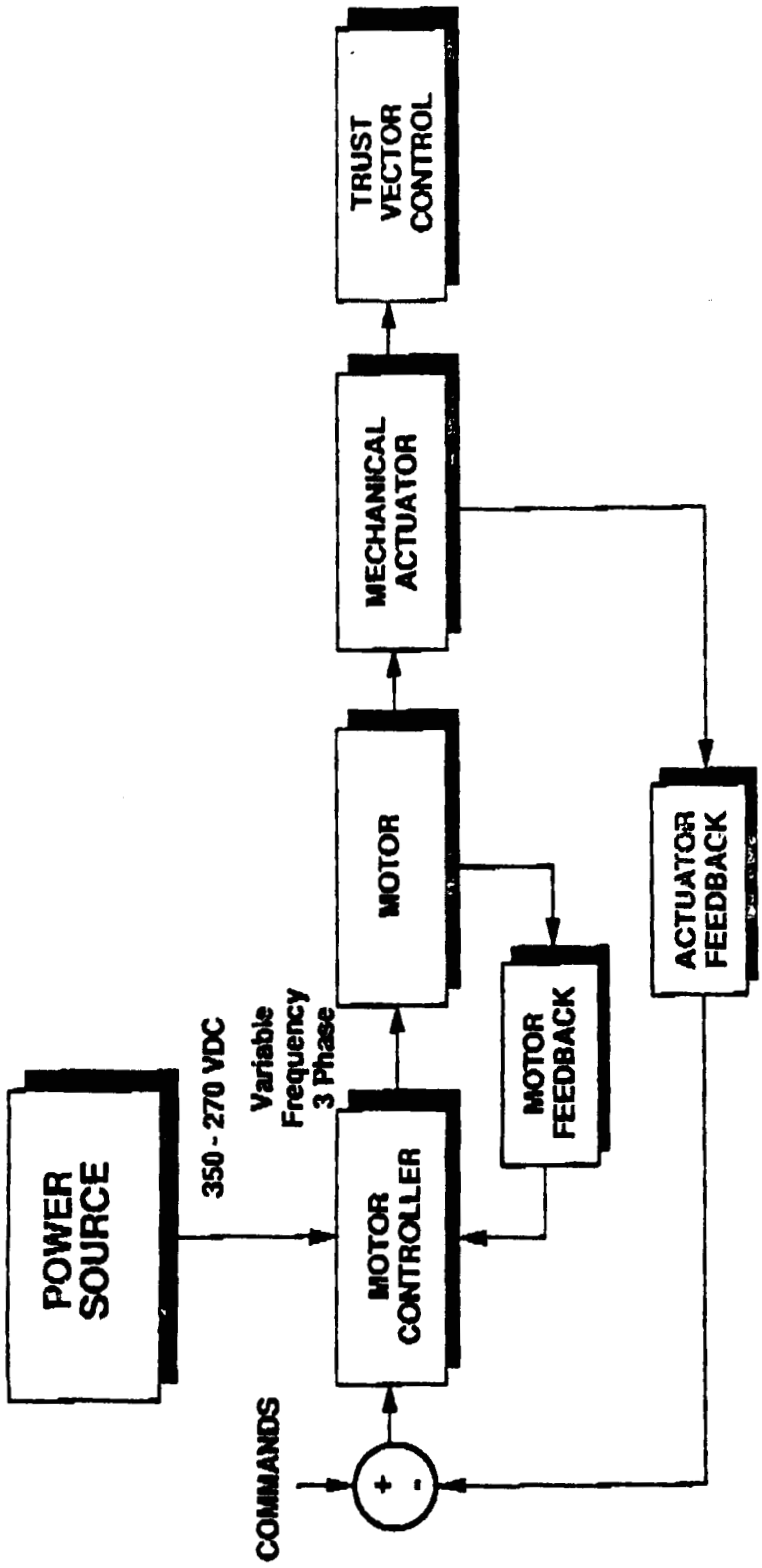

PRECEDING PAGE BLANK NOT FILMED

ALS POWER DEMAND

5.7 kW base discharge for 570 s
Five 0.5 s pulses of 115 kW
120.7 kW maximum
At least 10 seconds between pulses
Battery voltage must stay between 350 and 270 V
Total energy expended = 0.982 kWh
Unattended stand for 60 days during pre-launch period

JOHNSON CONTROLS

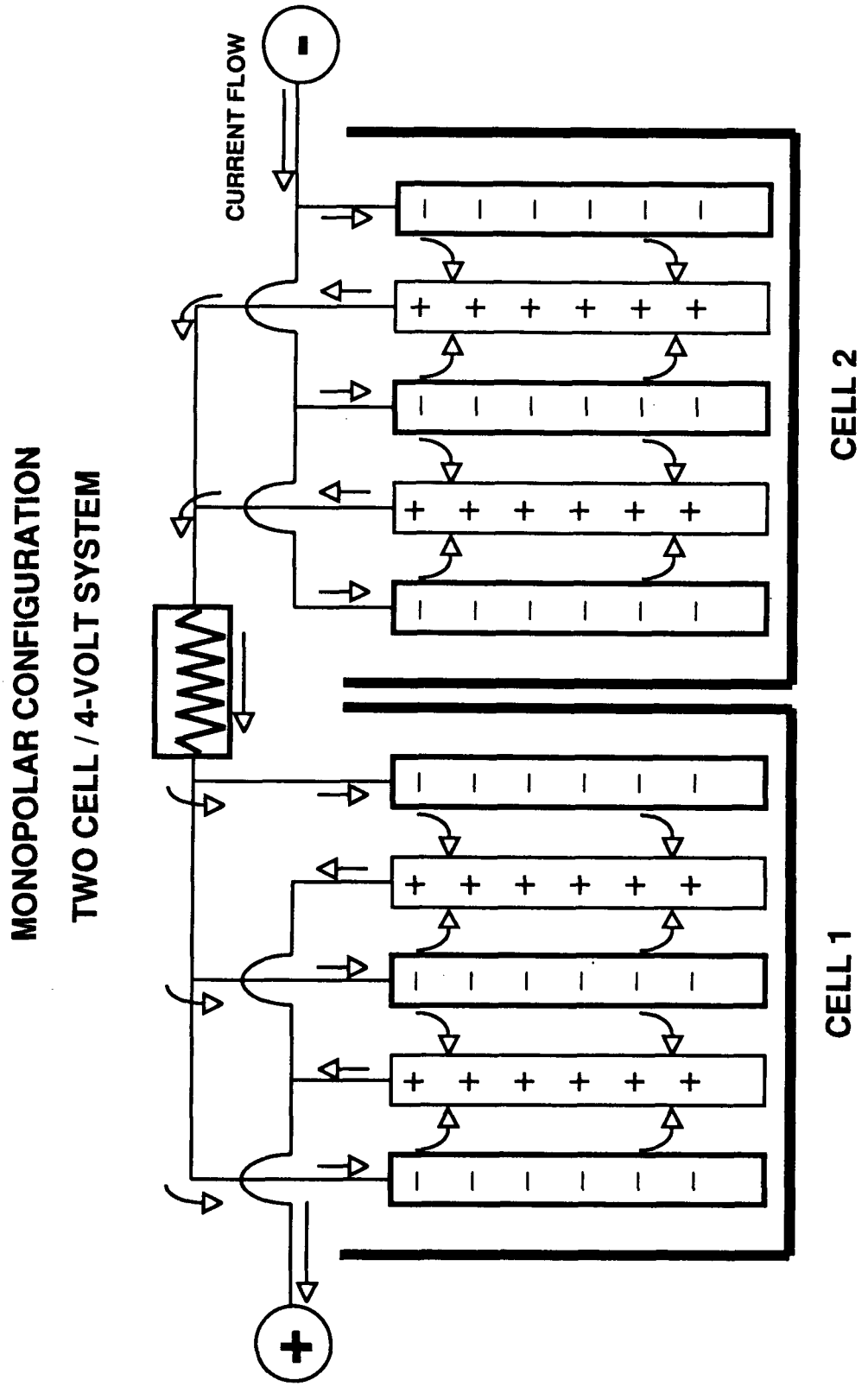
MONOPOLAR CONFIGURATION
TWO CELL / 4-VOLT SYSTEM
CURRENT FLOW
CELL 2
CELL 1

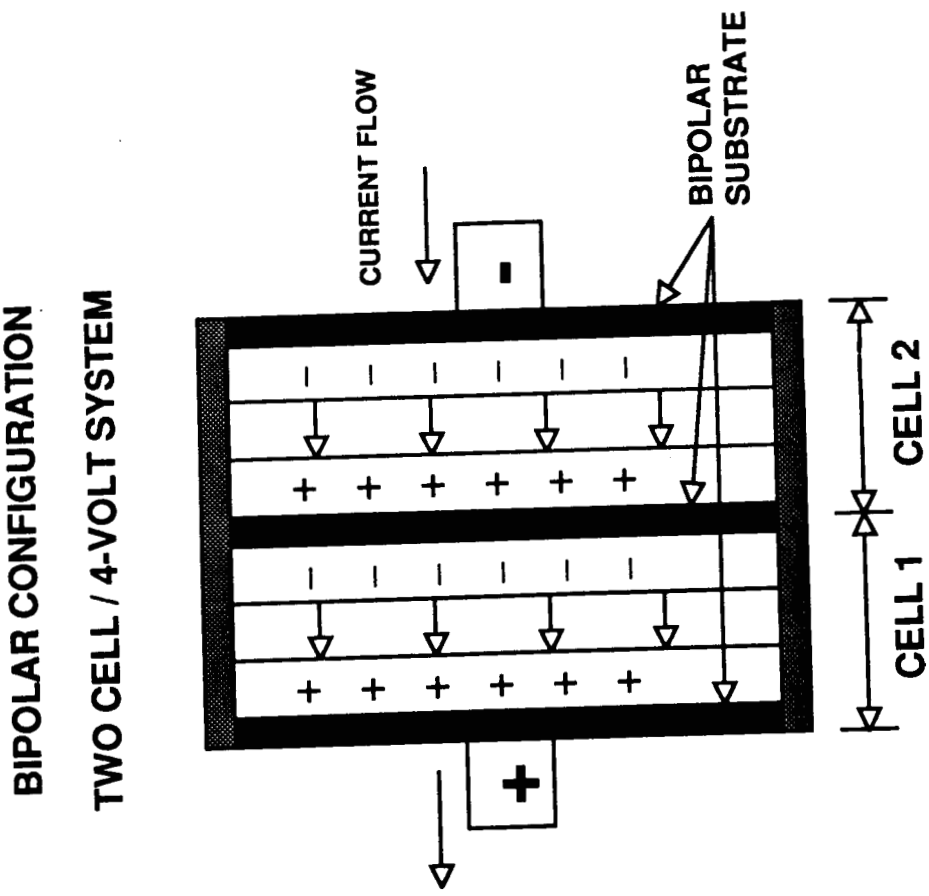
BIPOLAR CONFIGURATION
TWO CELL / 4-VOLT SYSTEM
CURRENT FLOW
BIPOLAR SUBSTRATE
CELL 2
CELL 1

BIPOLAR LEAD ACID

ADVANTAGES:

- High Power
- Low Weight/Volume
- Low Cost
- Reliability
- Any Orientation
- Good Thermal Characteristics
- Low Maintenance

DISADVANTAGES:

- Shelf Life (needs trickle charge)
- High Weight/Volume

JOHNSON CONTROLS

THE BIPOLAR LEAD ACID BATTERY

Features:

Conventional Lead Acid Chemistry
Thin electrodes/active materials
Thin separator
Sealed (gas recombinant)
Welded plastic frames for external seal

History:

Original development was done for NASA, sponsored by the SDIO through the Wright Research and Development Center.

JOHNSON CONTROLS

50 KW STACK ASSEMBLY

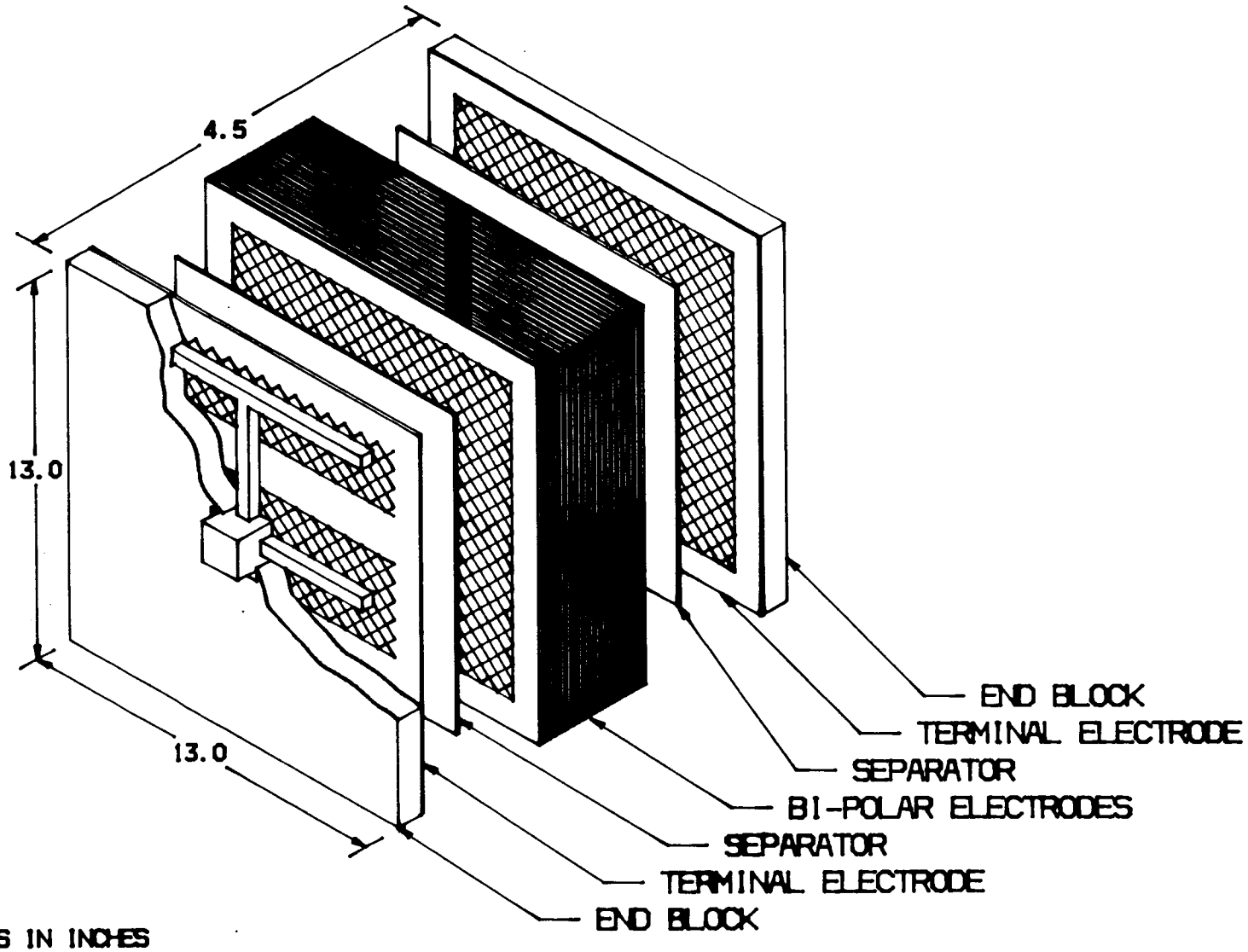

NOTE: ALL DIMENSIONS IN INCHES

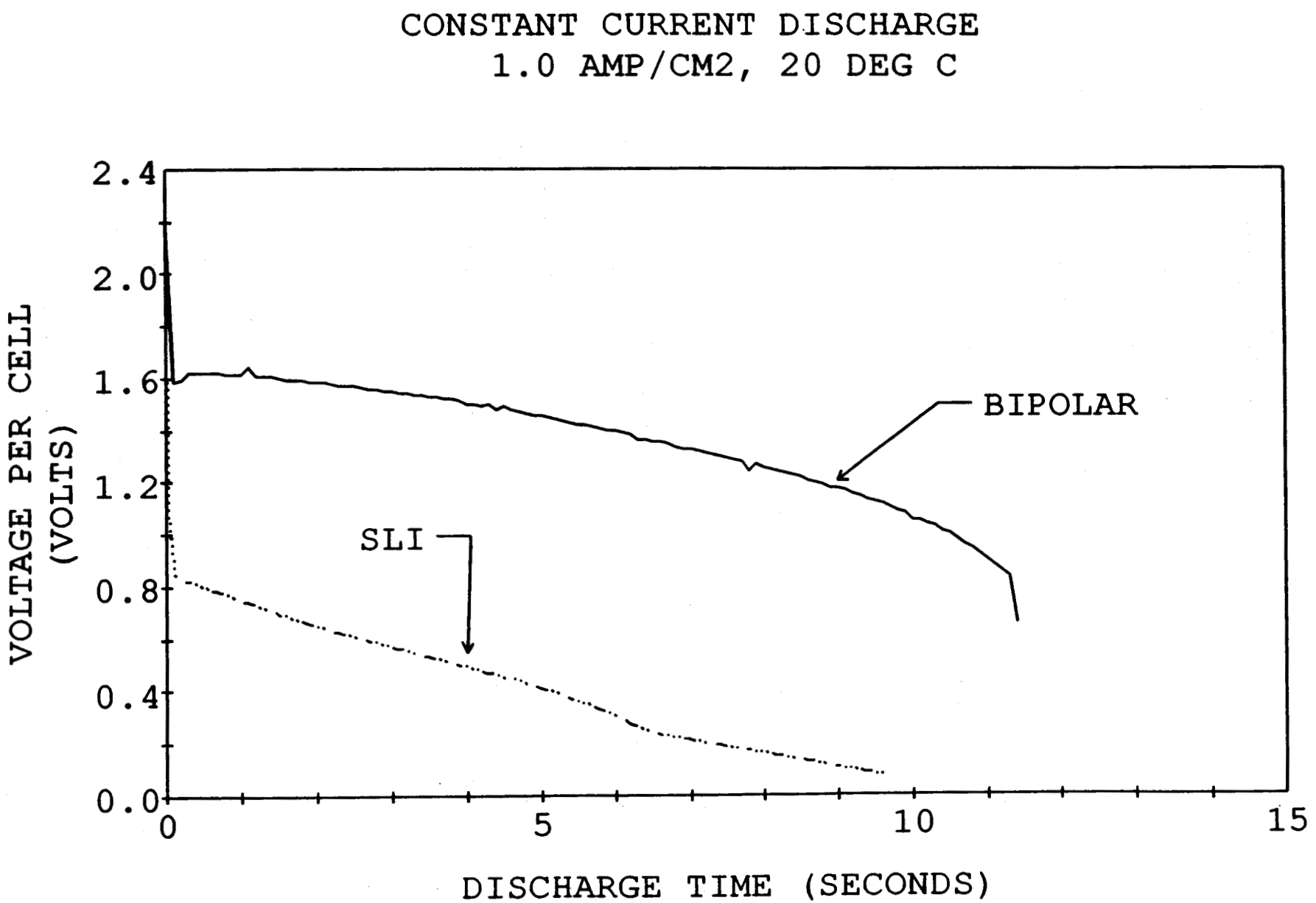
CONSTANT CURRENT DISCHARGE
1.0 AMP/CM2, 20 DEG C
VOLTAGE PER CELL (VOLTS)
2.4
2.0
1.6
1.2
0.8
0.4
0.0
0
5
10
15
DISCHARGE TIME (SECONDS)
BIPOLAR
SLI

MODEL SIMULATION AND
SL #5 BIPOLAR BATTERY
240 AMPS, 20 DEG C

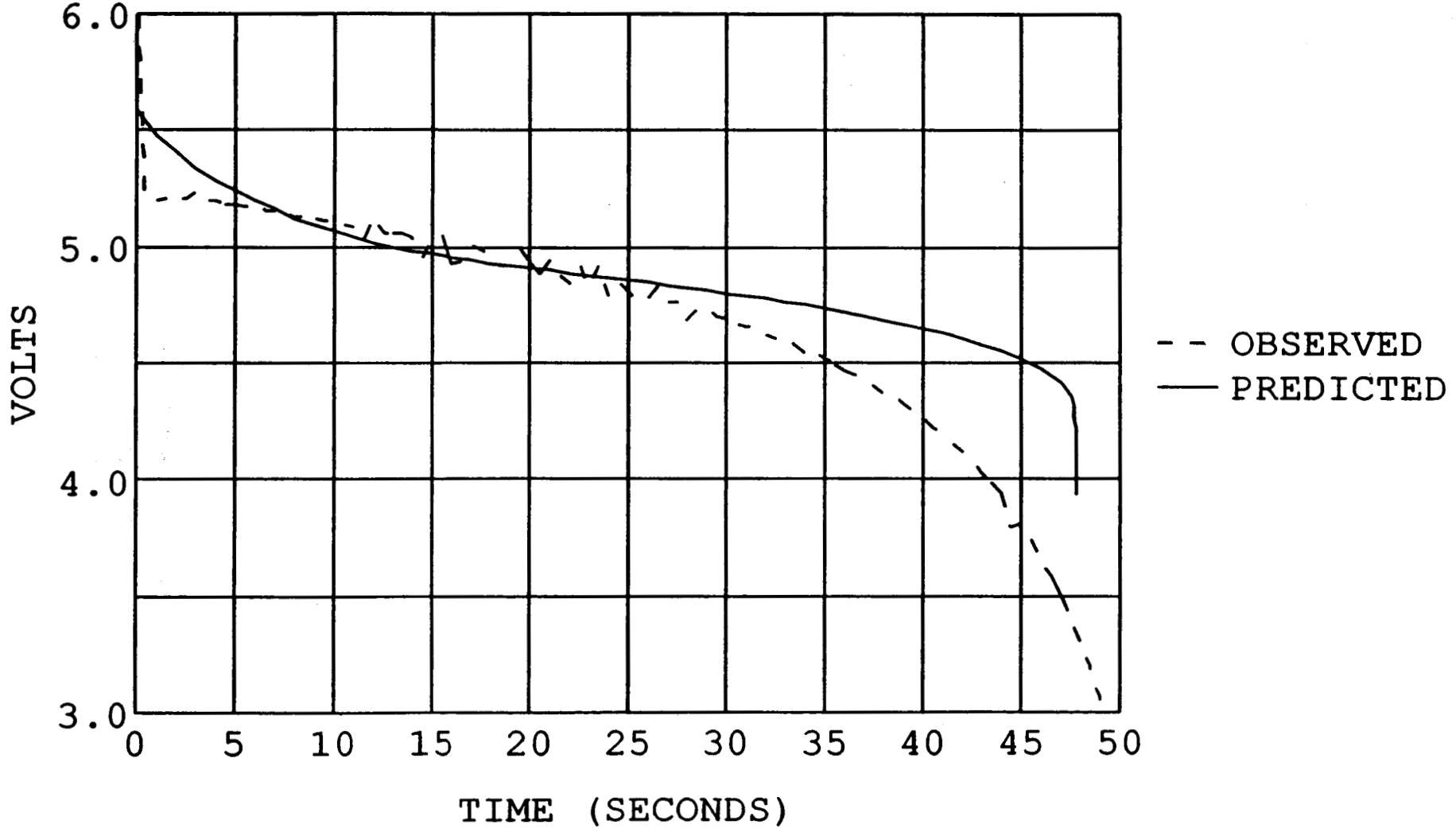

LABMM SIMULATION - CONSTANT CURRENT
BIPOLAR & FLOW-BY LEAD ACID BATTERIES AT 20 DEG C
POWER TAKEN AT 2/3 TOTAL DISCHARGE TIME

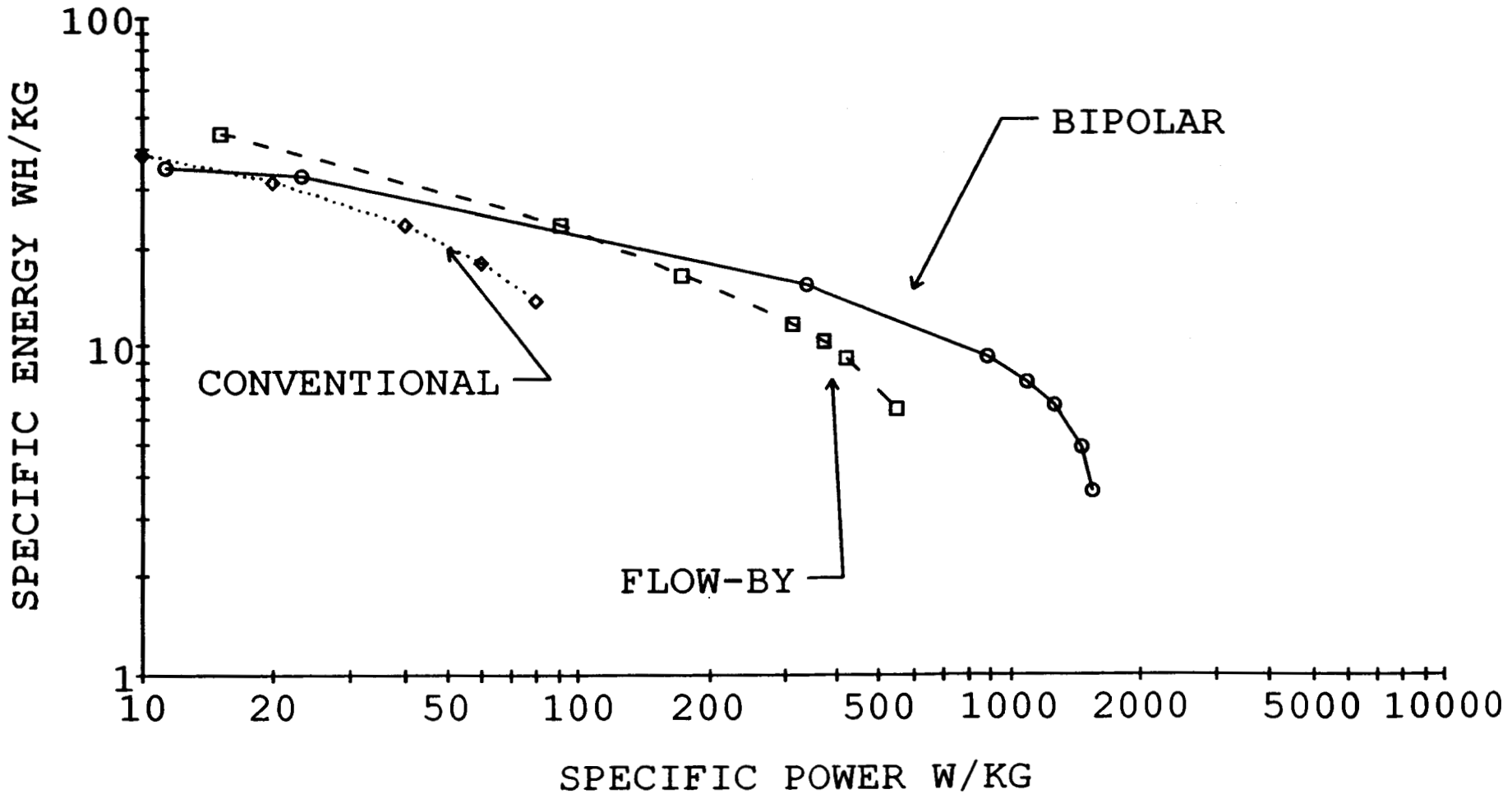

GENERAL DYNAMICS
BIPOLAR BATTERY BUILD OPTIONS

OPTIONS	1	2	3	4
Description	Standard	Standard	Special	Ideal
Active Area, cm^2	521	850	850	850
Stack Weight, kg	197.1	169.7	100.7	83.0
Stack Volume, l	71.4	67.2	38.2	36.8
Paste	Type A	Type A	Type B	Type A
# Cells/Module	40	40	40	40
# Modules	8	8	4	4
# Strings	2	2	1	1
Risk Factor	Low	Medium	Medium	High
Meets 350 V High	Yes	Yes	Yes	Yes
Meets 270 V Low	Yes	Yes	No	No
Meets 250 V Low			Yes	Yes

JOHNSON CONTROLS

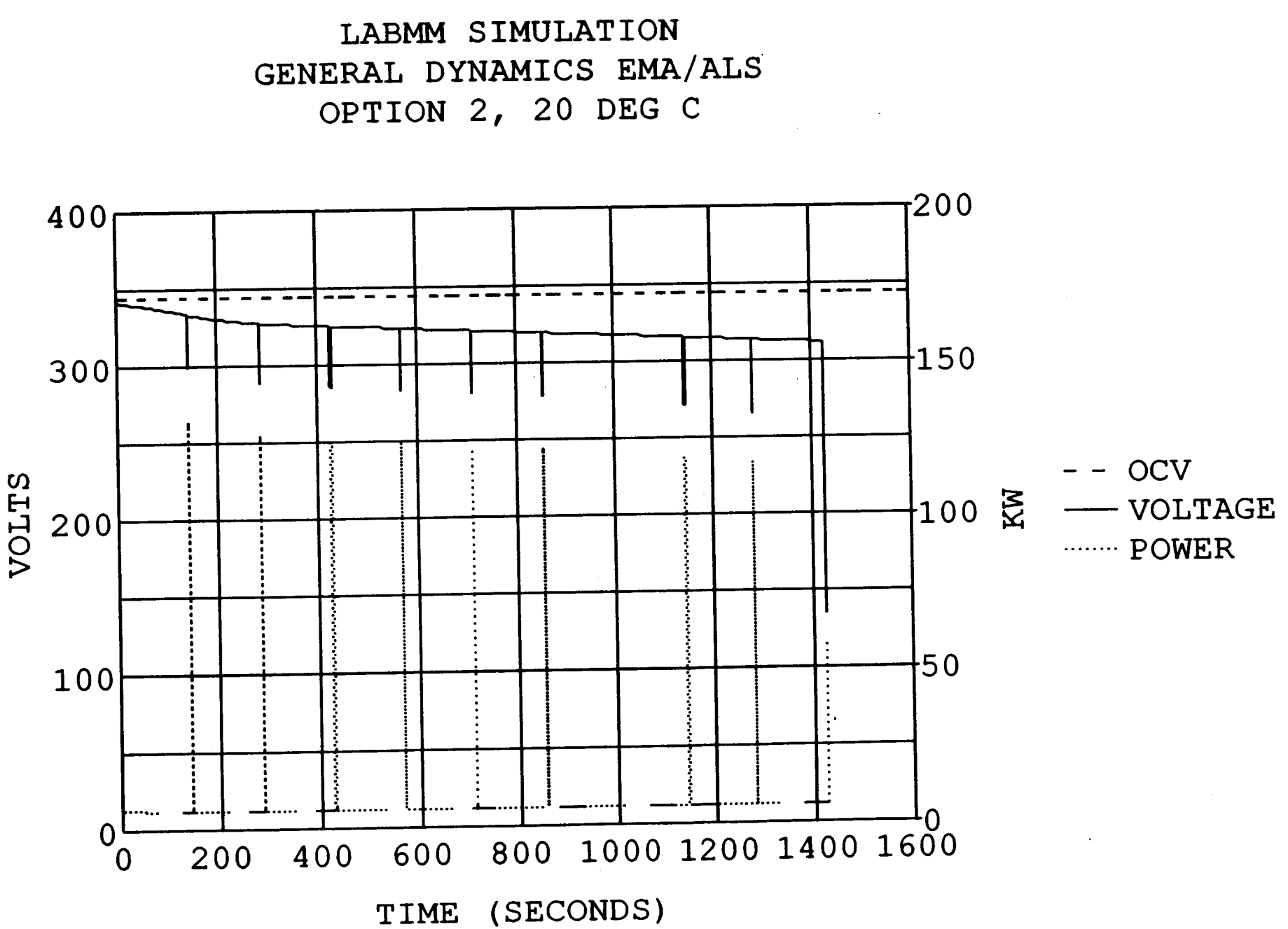
LABMM SIMULATION
GENERAL DYNAMICS EMA/ALS
OPTION 2, 20 DEG C
VOLTS
KW
TIME (SECONDS)
400
300
200
100
0
200
150
100
50
0
0 200 400 600 800 1000 1200 1400 1600
OCV
VOLTAGE
POWER

LABMM SIMULATION
GENERAL DYNAMICS EMA/ALS
OPTION 3, 20 DEG C

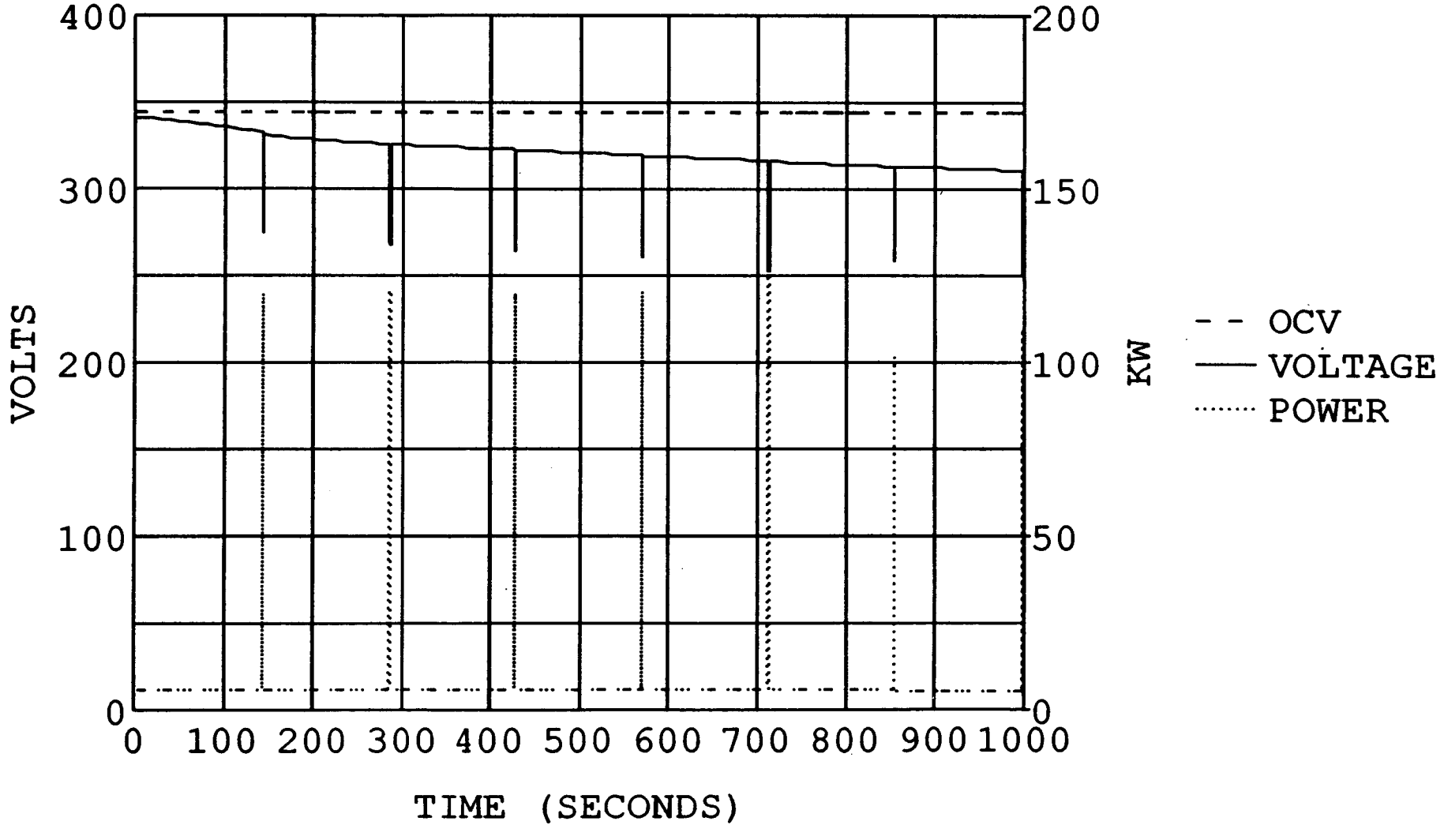

PROPOSED BATTERY

Standard Active Materials
850 cm^2 active area
Eight 40-Cell Modules
4 series / 2 parallel

Meets voltage/power requirements
Parallel strings add to reliability

JOHNSON CONTROLS

CONCLUSION:

Projections based on model and existing batteries indicate a battery made of bipolar lead acid modules would satisfy the ALS requirements.

JOHNSON CONTROLS

RECENT DEVELOPMENTS in NICKEL ELECTRODE ANALYSIS

R.V. Whiteley, ***Chemistry Department, Pacific University, Forest Grove, Oregon.***
M.E. Daman and E.Q. Kaiser, ***Space Systems / Loral, Palo Alto, California***

Abstract

Three aspects of nickel electrode analysis for Nickel-Hydrogen and Nickel-Cadmium battery cell applications are addressed: the determination of active material, charged state nickel (as NiOOH + CoOOH), and potassium ion content in the electrode. Four deloading procedures are compared for completeness of active material removal, and deloading conditions for efficient active material analyses are established. Two methods for charged state nickel analysis are compared: the current NASA procedure and a new procedure based on the oxidation of sodium oxalate by the charged material. Finally, a method for determining potassium content in an electrode sample by flame photometry is presented along with analytical results illustrating differences in potassium levels from vendor to vendor and the effects of stress testing on potassium content in the electrode. The relevance of these analytical procedures to electrode performance is reviewed.

Introduction

The nickel electrode finds extensive use in the Nickel-Hydrogen and Nickel-Cadmium battery cell. The analysis of this (positive) electrode is of particular difficulty because it incorporates nickel in at least three, incompatible oxidation states: Ni^{o} as the nickel screen and sinter, Ni^{2+} as the discharged nickel hydroxide, $Ni(OH)_2$, and finally, the charged form of nickel, the oxyhydroxide, NiOOH which is Ni^{3+} and might exist, in part, as Ni^{4+}, NiO_2.[1] Even the "fully discharged" electrode will be found to contain measurable quantities of all three forms of nickel. The challenge is to isolate these incompatible forms of nickel for analysis without promoting interactions between the oxidation states, such as

1. $Ni^{o} + 2\,NiOOH + 2\,H_2O \longrightarrow 3\,Ni(OH)_2.$

A reaction, such as this, during sample preparation, creates a higher apparent active material composition and a lower apparent charged nickel content in the sample. Moreover, because the amount of active material is increased by effectively adding pure nickel, the Co:Ni ratio in the active material will be suppressed. The Co:Ni ratio has been found to be critical to nickel electrode performance.[2,3]

The analysis of the active material typically entails a determination of nickel and cobalt content, and sometimes includes an analysis for charged nickel as NiOOH. The determination of charged state nickel is complicated by the presence of cobalt which certainly exists in its +3 oxidation state, probably as CoOOH or $Co(OH)_3$, and by the fact that Co^{3+} and Ni^{3+} are powerful oxidizing agents, easily capable of oxidizing either the nickel sinter or the aqueous solvent in which the analysis is performed. This is particularly true in an acidic medium. Consider:

2.	$Co^{3+} + 1\,e^-$	⟶	Co^{2+}	$E^o = +1.81$ V
3.	$Co(OH)_3 + 1\,e^-$	⟶	$Co(OH)_2 + OH^-$	$E^o = +0.17$ V
4.	$NiO_2 + 4\,H^+ + 2\,e^-$	⟶	$Ni^{2+} + 2\,H_2O$	$E^o = +1.68$ V
5.	$NiOOH + 3\,H^+ + 1\,e^-$	⟶	$Ni^{2+} + 3\,H_2O$	$E^o = +2.08$ V
6.	$Ni^{2+} + 2\,e^-$	⟶	Ni^o	$E^o = -0.23$ V
7.	$NiO_2 + 2\,H_2O + 2\,e^-$	⟶	$Ni(OH)_2 + 2\,OH^-$	$E^o = +0.49$ V
8.	$NiOOH + H_2O\ 1\,e^-$	⟶	$Ni(OH)_2 + OH^-$	$E^o = +0.48$ V
9.	$Ni(OH)_2 + 2\,e^-$	⟶	$Ni^o + 2\,OH^-$	$E^o = -0.72$ V

The effectiveness of Co^{3+} and Ni^{3+} (and Ni^{4+}) as oxidizing agents in acidic solutions is immediately evident from the large standard reduction potentials (reactions 2, 4 and 5). Their oxidizing abilities are substantially mitigated in alkaline solutions (reactions 3,7 and 8). When an electrode sample is digested in an acidic solution, the possibility of extraneous oxidation/ reduction reactions must be considered. Furthermore, when charged state nickel is determined by way of a reaction which occurs in an acidic medium, it must be recognized that charged material which is <u>not</u> thermodynamically available in an alkaline medium (as in the battery cell) *might* be included with material which <u>is</u> thermodynamically available.

An aspect of active material analysis often ignored is that of potassium content. The presence of potassium in the $Ni(OH)_2$/ NiOOH matrix is commonly associated with the existence of γ-NiOOH,[4] and γ-NiOOH has been shown to discharge at a lower voltage than β-NiOOH,[5] and lead to enhanced plate growth.[6] Therefore, it would seem prudent to analyze electrode samples for potassium content, and use these data as, at least, an approximation to γ-NiOOH build up in the electrode.

The prediction or explanation of nickel electrode performance through bulk electrode chemical analysis has not been entirely satisfactory. This is due, in part, to some small errors in the plate analysis and to omissions of some analyses, altogether.

Discussion

Electrode deloading

Probably the most important aspect of the electrode make up is the amount of active material contained within its pores. By subjecting an electrode sample to an appropriate solvent, active material can be selectively dissolved from the surface and pores of the sinter, and by noting the sample weight before and after the operation, the percentage of active material is readily calculated. The issues are: what is an appropriate solvent and what is a sufficient period for effective deloading of the electrode sample.

Four deloading solutions were evaluated:

A. An ammoniacal solution of the disodium salt of ethylenediaminetetraacetic acid (EDTA). 34 mL of concentrated ammonium hydroxide + 64 mL of deionized water + 2 mL of aqueous (64%) hydrazine + 10 g of $Na_2H_2C_{10}N_2H_{12}O_8 \cdot 2H_2O$. With the exception of the 2 mL of aqueous hydrazine, this is more or less the industry standard deloading solution. The hydrazine is added as a powerful reducing agent to protect the Ni^o sinter from attack by the NiOOH, Reaction #1, by reducing the Co^{3+} and Ni^{3+} charged material to their innocuous +2 state.

10. $N_2 + 4\,H_2O + 4\,e^- \longrightarrow N_2H_4 + 4\,OH^-$ $\quad E^o = -1.16$ V

Also, by reducing the Ni^{3+} to Ni^{2+} it becomes more accessible for complexation by the EDTA.

B. An ammoniacal solution of ethylenediamine, $H_2NCH_2CH_2NH_2$. 3.2g of ethylenediamine + 34 mL of concentrated ammonium hydroxide + 64 mL of deionized water + 2 mL of aqueous (64%) hydrazine Ethylenediamine is a complexing agent comparable to EDTA, but it is an attractive replacement for

EDTA, because, unlike EDTA, it is freely soluble in acidic solutions. When the deloading solution is made acidic for subsequent analysis, the free ethylenediaminetetraacetic acid precipitates out of solution. Although this free acid will not retain any of the Co or Ni it extracted from the electrode, the acid must be filtered off before proceeding to the next step in the analysis.

C. A mixture of acetic acid and hydrogen peroxide. 66 mL of glacial acetic acid + 34 mL of 30% hydrogen peroxide. In the presence of Co^{3+} or Ni^{3+} the hydrogen peroxide will act as a reducing agent.

11. $O_2 + 2\,H^+ + 2\,e^- \longrightarrow H_2O_2$ $\quad E^o = +0.68$ V

The use of this solution is frequently reported in the literature and it is used in some electrode production laboratories.

D. A 1.1 **M** potassium cyanide solution. 7.1g of KCN diluted to 100 mL with deionized water. Although this solution is not recommended for general laboratory use, it serves as an excellent bench mark. Cyanide ion is one of the most effective complexing agents available. The formation constant for the Ni^{2+} cyanide complex, $Ni(CN)_4^{2-}$ is 10^{31}; for the Co^{3+} cyanide complex $Co(CN)_6^{3-}$, it is 10^{64}. Compare these to Ni^{2+}, Co^{2+}, and Co^{3+} formation constants with EDTA of $10^{18.6}$, $10^{16.2}$, and 10^{36}, respectively.

Coupons of 0.4 to 0.8 g were cut from two types of electrodes: a Ni/H_2 electrode made from plaque which had been sintered using the wet slurry technique and electrochemically impregnated, and a Ni/Cd electrode which had been dry sintered and chemically impregnated. Each coupon was desiccated over concentrated sulfurc acid to bring it to constant weight (*ca.* 5 days). Three, carefully weighed Ni/H_2 coupons and one Ni/Cd coupon were placed in a flask containing 40 mL of the deloading solution of interest. The flask was sealed and held at 50 to 60° C for 24 hours. The solution was replaced with 40mL of fresh solution and deloading was continued at 50 to 60°C for another 24 hours. After decanting the second deloading solution, the electrodes were allowed to soak in 50 mL of deionized water at 50 to 60°C for 10 hours. Each coupon was rinsed in deionized water and desiccated to constant weight over concentrated sulfuric acid before taking a final coupon weight.

The results of deloading with each of the four deloading solutions are illustrated in Figure 1. The acetic acid deloading solution clearly removes the most material from the electrode, but this is considerably more than can be attributed to active material. Evidently, sinter corrosion on this time scale is considerable. Conversely, the ethylenediamine solution is unable to effect a thourogh deloading of either the Ni/H_2 or Ni/Cd electrode type. The agreement between KCN and EDTA deloading is indicative of complete deloading without concomitant sinter attack.

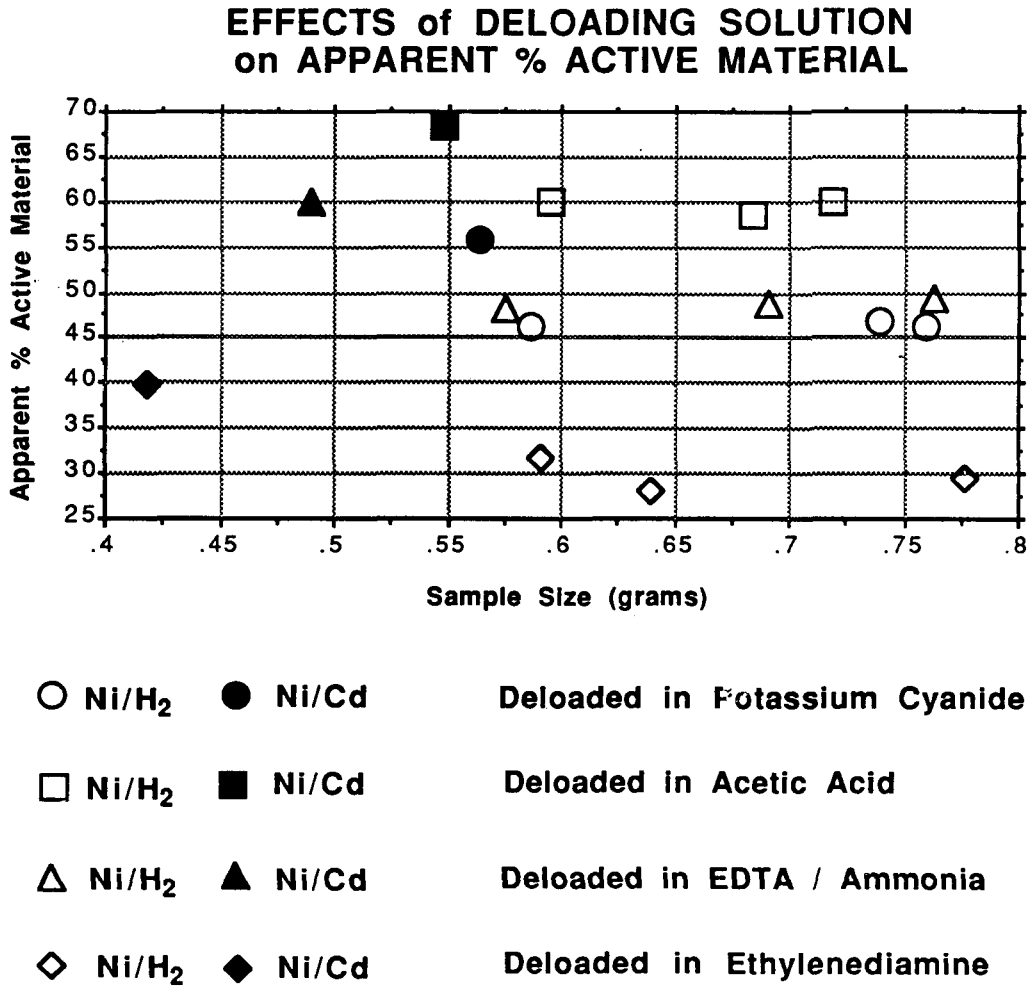

Figure 1. Deloading results for four types of deloading solution and two electrode types. Approximately 2 grams of electrode sample (as four coupons) were deloaded with two, 40 mL portions of deloading solution. Each rinse was at 50 to 60°C for twenty-four hours, followed by a rinse in deionized water and drying to constant weight.

The appropriate deloading procedure was ascertained by monitoring relative weight loss of electrode coupons as a function of time at low temperature (0 to 5°C) room temperature (19 to 23°C) and at elevated temperature (55 to 60°C). Only the EDTA deloading solution was used. Again a dry-sintered, chemically impregnated, Ni/Cd electrode and slurry-sintered, electrochemically impregnated, Ni/H_2 electrode were compared. All coupons were desiccated to constant weight (0.09 to 0.16g) and deloaded in 5.5 mL of deloading solution. After the prescribed deloading period, the coupon was held in 5.5 mL of deionized water for ≥8 hours at the same temperature at which it was deloaded. Finally it was held ≥4 hours in 5.5 mL of deionized water at room temperature, before it was dried at 80°C in a forced air over and desiccated over concentrated sulfuric acid to constant weight.

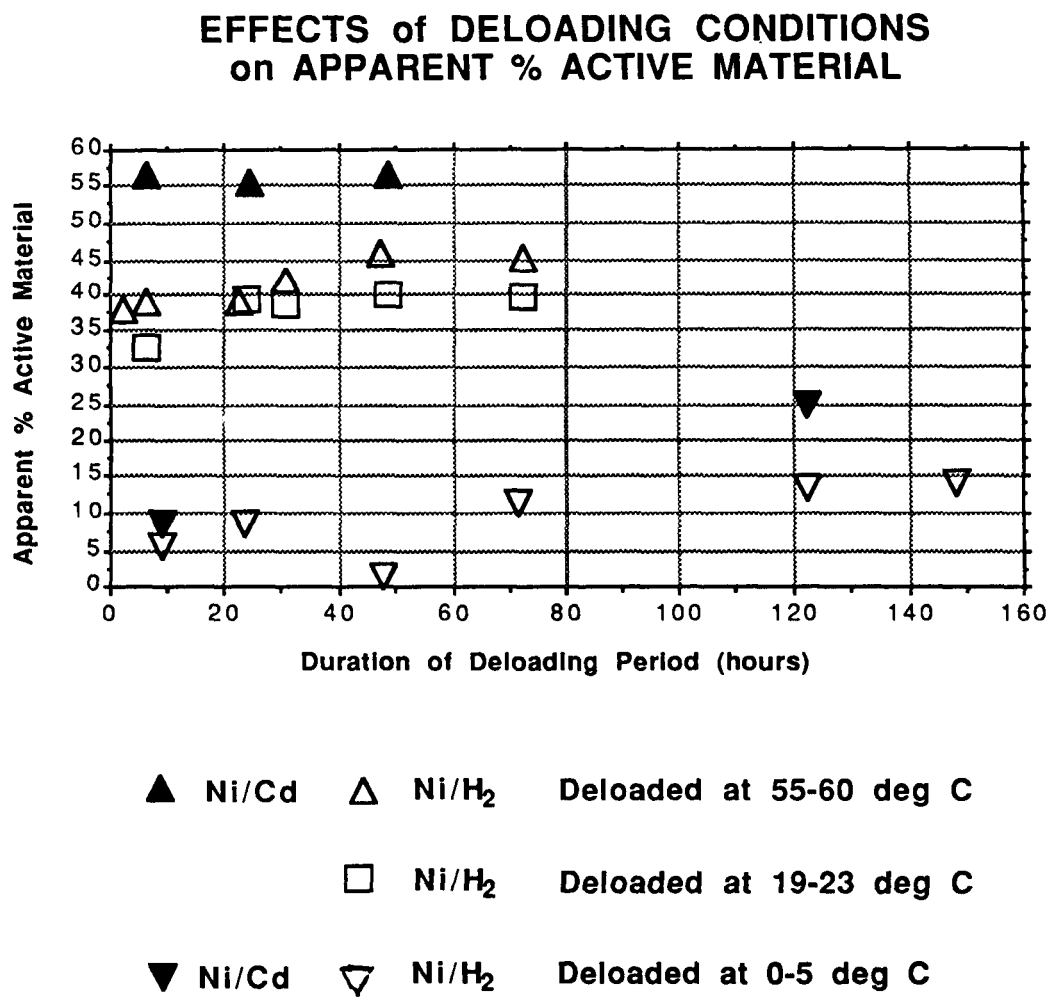

Figure 2. The effects of temperature and deloading duration on the efficiency of the deloading procedure. Deloading is performed with approximately 120 mg coupons using 5.5 mL of the ammoniacal EDTA deloading solution.

It is immediately clear (Figure 2) that low temperature deloading is ineffective, and that room temperature deloading also yields low results, even after three days of soaking. The industry standard of deloading at about 55°C for approximately twenty hours is based on Ni/Cd plate analysis. And from Figure 2, it is apparent that these guide lines are appropriate for Ni/Cd electrodes. However, it appears to require at least 48 hours to achieve a constant relative weight loss (% Active material) when deloading the Ni/H_2 electrode coupons.

Thorough active material removal without associated nickel sinter or nickel grid dissolution is essential to an accurate determination of nickel and cobalt levels in the active material. The effects of Co:Ni ratio on electrode performance have received considerable attention, but without accurate determinations of both Co and Ni, it is not possible to correlate electrode performance to this ratio. Also, it is not possible o estimate this ratio from impregnation bath data: the Co:Ni ratio in either a chemical or electrochemical impregnation bath can differ markedly from the ratio achieved in the finished electrode. This is due largely to the differing solubilities of Co^{2+} and Ni^{2+} hydroxides in strongly alkaline media.

It has frequently presumed that the Ni:Co ratio in an impregnation bath should approximate the Ni:Co ratio found in the active material. This is because the solubility of $Ni(OH)_2$ is taken to be equal to that of $Co(OH)_2$. In fact, however, the solubilities are not only unequal, they change significantly with pH. If C_M is taken as the allowable concentration of metal M in solution, where M can be either Ni or Co, an equation can be written to describe this solubility. (Thermodynamic values are from Reference 7.)

$$C_M = \{1+(K_1[OH^-])+(K_2[OH^-]^2)+(K_3[OH^-]^3)\}K_{sp}/[OH^-]^2$$

Where $K_1 = [MOH^+]/[M^{2+}][OH^-]$

$K_2 = [M(OH)_2^0]/[M^{2+}][OH^-]^2$

$K_3 = [M(OH)_3^-]/[M^{2+}][OH^-]^3$

and $K_{sp} = [M^{2+}][OH^-]^2$

For Ni, $K_1=10^{4.97}$ $K_2=10^{8.55}$ $K_3=10^{11.33}$ and $K_{sp}= 10^{-14.70}$
and for Co, $K_1=10^{4.4}$ $K_2=10^{4.6}$ $K_3=10^{10.5}$ and $K_{sp}= 10^{-14.80}$

These solubility differences are illustrated in Figure 3. While the solubility of either ion, above pH 7 is quite small, when the local pH (*i.e.* in the sinter pores) exceeds 9, the Ni becomes decidedly more soluble than the Co, and consequently, it is less prone to precipitation within the pores. At pH 11, nickel is approximately 10 times as soluble as cobalt.

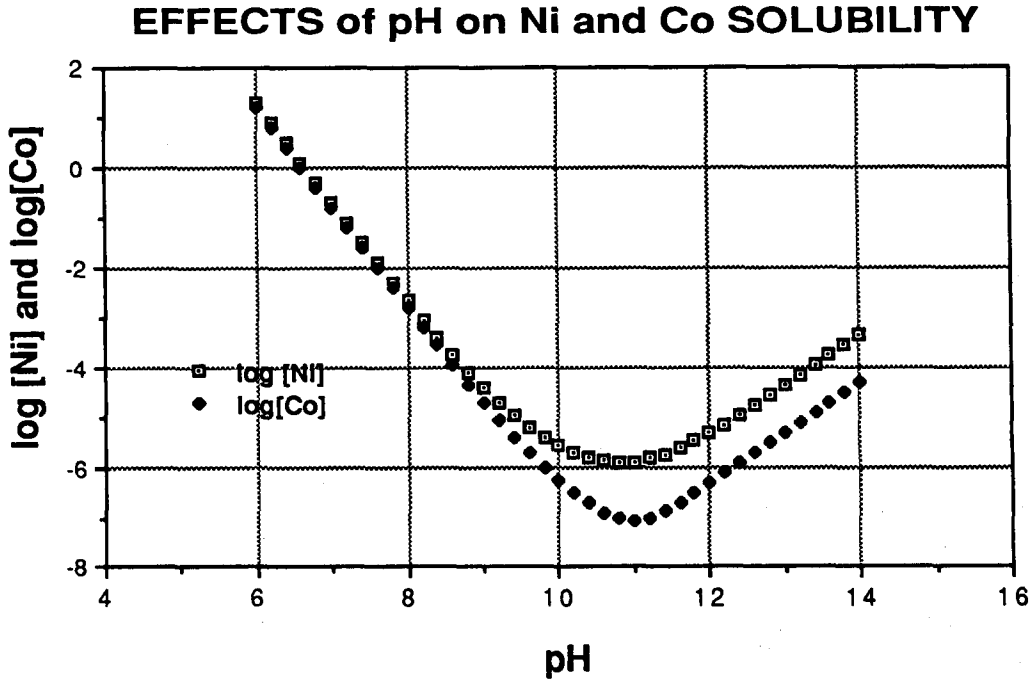

Figure 3 Solubility of cobalt and nickel (expressed logarithmically) as a function of local pH. The soluble forms are M^{2+}, MOH^{+}, $M(OH)_2^{o}$, and $M(OH)_3^{-}$ where M represents Co or Ni.

The application of deloading information to electrode performance is summarized in Table 1. The deloading data are useful at the electrode manufacture stage as well as for electrode evaluation as part of a cell's Destructive Physical Analysis (DPA). But use in the DPA requires access to cell build paper so that comparisons to initial Co and Ni levels can be made. The individual Co and Ni determinations are typically done by atomic absorption spectrophotometry with satisfactory accuracy. Non-instrumental techniques have been developed which provide very accurate results.[8]

Table 1 Some applications of accurate deloading data to electrode performance.

CHARACTERISTIC	INFORMATION
Total Active Material	***electrode manufacture***
	Load level
(with Co or Ni analysis)	**Theoretical capacity**
	electrode manufacture
Cobalt to Nickel Ratio	**Bath cobalt or nickel concentration correctness**
	Bath pH correctness
	Abnormal sinter corrosion (chem. impreg.)
	destructive physical analysis
	Abnormal sinter corrosion
	Selective leaching of Co or Ni
Thickness change on deloading	***electrode manufacture***
	A large Δt is indicative of surface loading
	destructive physical analysis
	A large Δt is indicative of active material extrusion

Charged nickel analysis

Most of the charged material in a discharged electrode can be attributed to cobalt. Given its relatively low standard reduction potential (only +0.17 V, Equation 3, page 2), the cobalt cannot be expected to be driven to the +2 oxidation state by normal discharge procedures. However, in theory, all of the NiOOH should be reduced to $Ni(OH)_2$ as the electrode is discharged. This is never the case. All nickel electrodes, regardless of state of charge, show some higher (<2) oxidation state nickel, implying that all nickel is not fully discharged. A significant quantity of charged material in a supposedly discharged electrode is indicative of a diminished discharge efficiency.

The amount of NiOOH is usually determined by adding a measured excess of Ferrous Ammonium Sulfate (Mohr's Salt) to a moderately acidic solution containing a finely powdered sample of a nickel electrode.[8] Under these conditions, the Ni^{3+} (and Co^{3+}) destroy part of the Fe^{2+} from the ferrous ammonium sulfate. The solution is subsequently titrated with a potassium permanganate solution to determine how much of the Fe^{2+} remains. By subtraction, the quantity of Fe^{2+} destroyed by NiOOH is found.

12. $Fe^{2+} + NiOOH + 3\,H^{+} \longrightarrow Ni^{2+} + Fe^{3+} + 2\,H_2O$

13. $5\,Fe^{2+} + MnO_4^{-} + 8\,H^{+} \longrightarrow 5\,Fe^{3+} + Mn^{2+} + 4\,H_2O$

The procedure is rather simple and yields a good approximation of the amount of charged material remaining in an electrode. But the procedure does show some dependence on sample size, and contrary to established procedure, the total amount of charged material is not measured within the one hour recommended reaction time (Figure 4).

For comparison, a procedure was developed in which the reduction of charged material is effected in an alkaline solution (0.02 **M** potassium hydroxide). The Fe^{2+} reducing agent is replaced with sodium oxalate, $Na_2C_2O_4$. A measured excess of alkaline sodium oxalate solution is added to a sample of pulverized nickel electrode. The oxalate is readily oxidized *via.*

14. $C_2O_4^{2-} + 2\,NiOOH + 2\,OH^{-} \longrightarrow 2\,CO_3^{2-} + 2\,Ni(OH)_2$

After the prescribed digestion period, the solution is made strongly acidic by adding an excess of 6 **M** H_2SO_4, the unreacted nickel powder is removed, and the remaining oxalate is titrated with a potassium permanganate solution.

15. $5\,C_2O_4^{2-} + MnO_4^{-} + 8\,H^{+} \longrightarrow 2\,CO_{2(g)} + Mn^{2+} + 4\,H_2O$

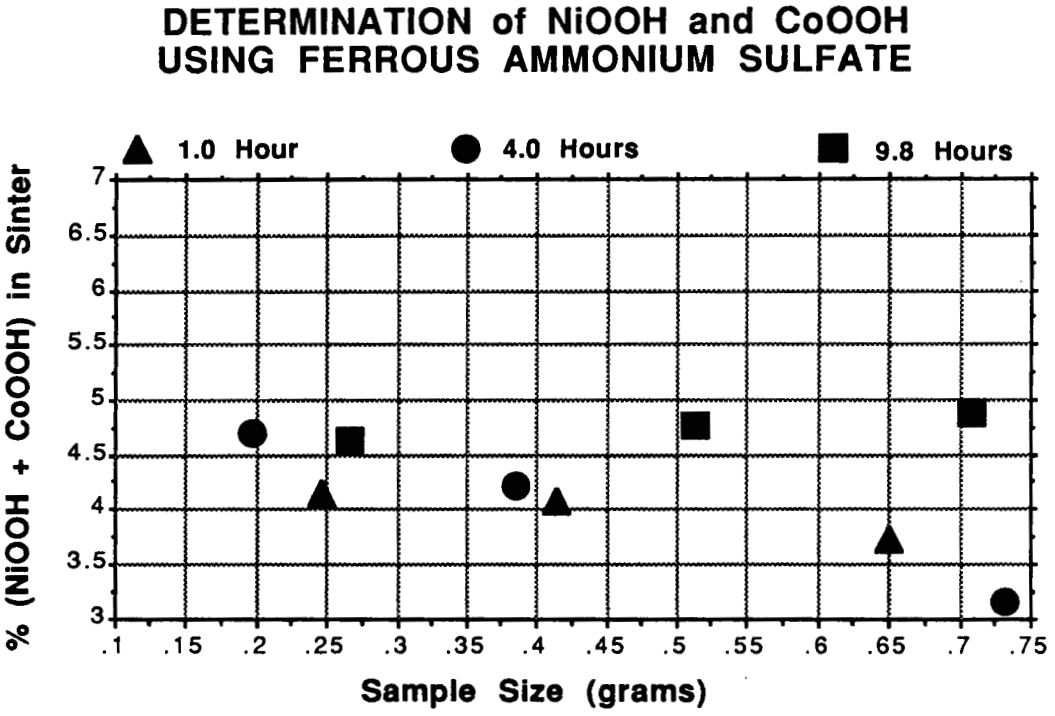

Figure 4 The percentage of charged material (NiOOH *plus* CoOOH) in pulverized nickel electrode (with screen removed). The durations (1.0 hr, 4.0 hrs., and 9.8 hrs.) refer to the period over which the pulverized sample and acidic ferrous ammonium sulfate solution were allowed to stand in contact before proceeding with the titration.

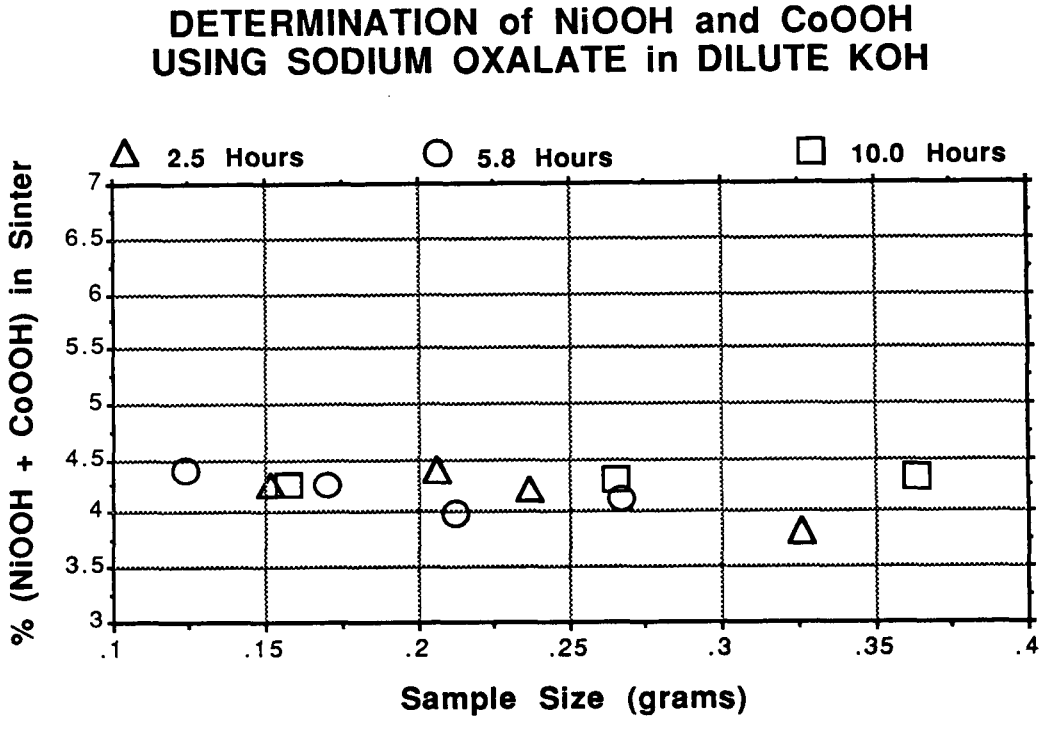

Figure 5 The percentage of charged material (NiOOH *plus* CoOOH) in pulverized nickel electrode (with screen removed). The durations (1.0 hr, 4.0 hrs., and 9.8 hrs.) refer to the period over which the pulverized sample and alkaline sodium oxalate solution were allowed to stand in contact before proceeding with the titration.

The two procedures are identical in that each entails the addition of an excess of a reducing agent and subsequent titration with potassium permanganate to ascertain the amount of reducing agent remaining after the reaction. But some important differences exist.

Ferrrous ammonium sulfate solutions are not extremely stable and so, the reagent should be weighed into each sample.

Sodium oxalate solutions are stable, and so, a stock solution can be prepared and pipetted into each sample.

Ferrrous ammonium sulfate is not available in high purity, and reducing power can vary slightly from bottle to bottle.

Sodium oxalate is available as a primary standard.

The ferrrous ammonium sulfate titration can be done at room temperature.

The titration of excess oxalate with potassium permanganate must be done at ≥60°C.

The unreacted nickel sinter must be promptly removed from the flask prior to titrating for the excess ferrrous ammonium sulfate because the oxidation product from the reaction is Fe^{3+}, and this can react with the nickel metal *via*

16. $2\,Fe^{3+} + Ni^{o} \longrightarrow 2\,Fe^{2+} + Ni^{2+}$

For the oxalate titration, however, the reaction product is CO_2 which escapes the reaction mixture. Therefore, it is possible to allow the acidified solution to react thoroughly with the mixed oxides and hydroxides before removing the unreacted Ni^{o}. This leaves a very clear solution for the permanganate titration which is conducive to accurate end point determinations.

A comparison of the results in Figure 4 to those in Figure 5 shows that larger samples require decidedly more time to react. Note that for the NASA procedure, even four hours does not seem quite adequate. At extended digestion periods, even relatively large samples are thoroughly reacted. The ferrous ammounium sulfate procedure routinely gives higher values than the oxalate procedure. (Both data sets are collected using the same sample throughout.) This could be due to air oxidation of the Fe^{2+}, although the samples were sealed under N_2 for the duration of the digestion step. The difference in apparent charged material between the two procedures might also be indicative of differences in the thermodynamic availability of charges material in acidic *vs.* alkaline media.

Regardless of the method which is used to determine the amount of charged material, the raw data, as illustrated in Figures 4 and 5, require considerable manipulation to produce meaningful values. If the unreacted nickel sinter is carefully isolated, dried, and weighed, then the fraction of sample which is active material can be calculated, and it would be possible to express the results as percent of active material. From the atomic absorption or chemical analyses of the deloading solution, the percent cobalt in the active material should be determined. This can be converted to percent cobalt as CoOOH, and this can be subtracted from the percent charged material which is NiOOH *plus* CoOOH. This will yield the percent NiOOH in the active material. This value is highly indicative of the electrode's discharge efficiency.

Potassium content

The amount of potassium in an electrode is directly determined by flame emission photometry. By using flame emission, in lieu of arc, spark, or plasma excitation modes, cobalt and nickel interferences become imperceptible. It is possible to perform the analysis simply by dissolving the entire electrode sample (in nitric or hydrochloric acid). However, this creates an unnecessary overburden of Ni^{2+} ions. Consequently, an aggressive deloading is used, one part glacial acetic acid to three parts 30% hydrogen peroxide. While this certainly dissolves some of the underlying sinter, it does not cause an error in the analysis because the sinter contains no potassium.

Flame emission determination for potassium is sufficiently sensitive that electrode sample sizes of 40 to 50 mg are adequate for detecting potassium levels as low as 0.02% in the electrode (about 0.04% in active material). A sample this size is digested for one hour in 10 mL of deloading solution. The solution and subesequnt aqueous rinsings of the sample are combined in a 100 mL volumetric flask and diluted to volume with deionized water. Potassium standards are prepared with KCl in the acetic acid/ hydrogen peroxide deloading solution and also contain Ni^{2+} and Co^{2+} in approximately the same concentrations as found in the deloading solutions from sample extractions. Potassium detection is at 766.5 nm with a 0.7 mm slit width.

Several electrode samples from two nickel electrode manufacturers were analyzed for potassium content. These results are illustrated in Figure 6. Clearly, potassium levels are considerably higher in the electrodes of one vendor than in those of the other vendor. The effects of stress testing were evaluated by comparing two electrodes from each vendor, one of each pair was stress tested for 200, 10C cycles in 31% KOH, thoroughly rinsed in deionized water, dried, weighed and digested for potassium analysis. The second electrode of each pair was analyzed without stress testing.

This database is too limited to show any trends, but variations from vendor to vendor and stress test effects are apparent. A potassium analysis on an electrode from a destructive physical analysis of a battery cell might give evidence for the extensive formation of γ-NiOOH, explaining poor performance of the cell.

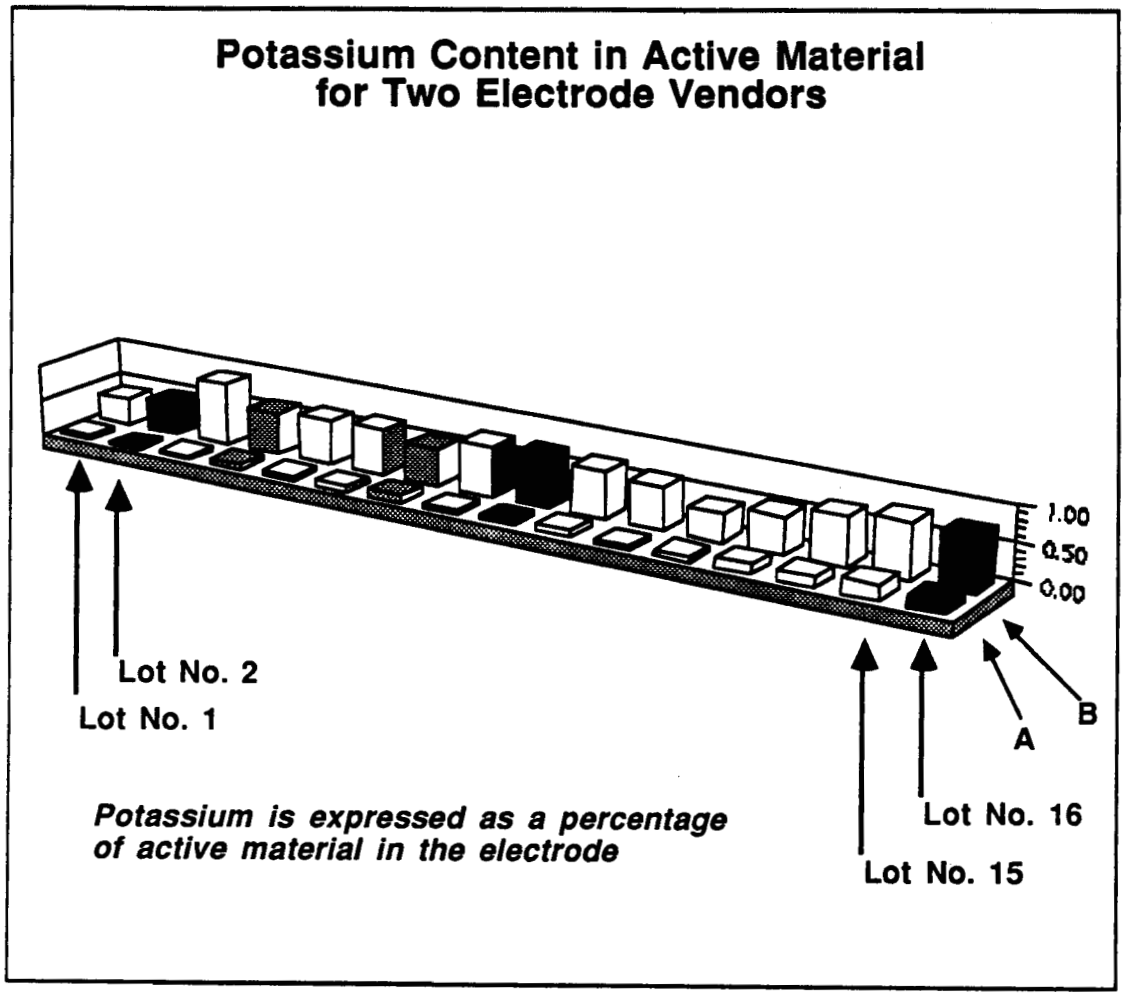

Figure 6 Comparison of Vendor A and Vendor B positive electrodes for potassium content (as a percent of active material).

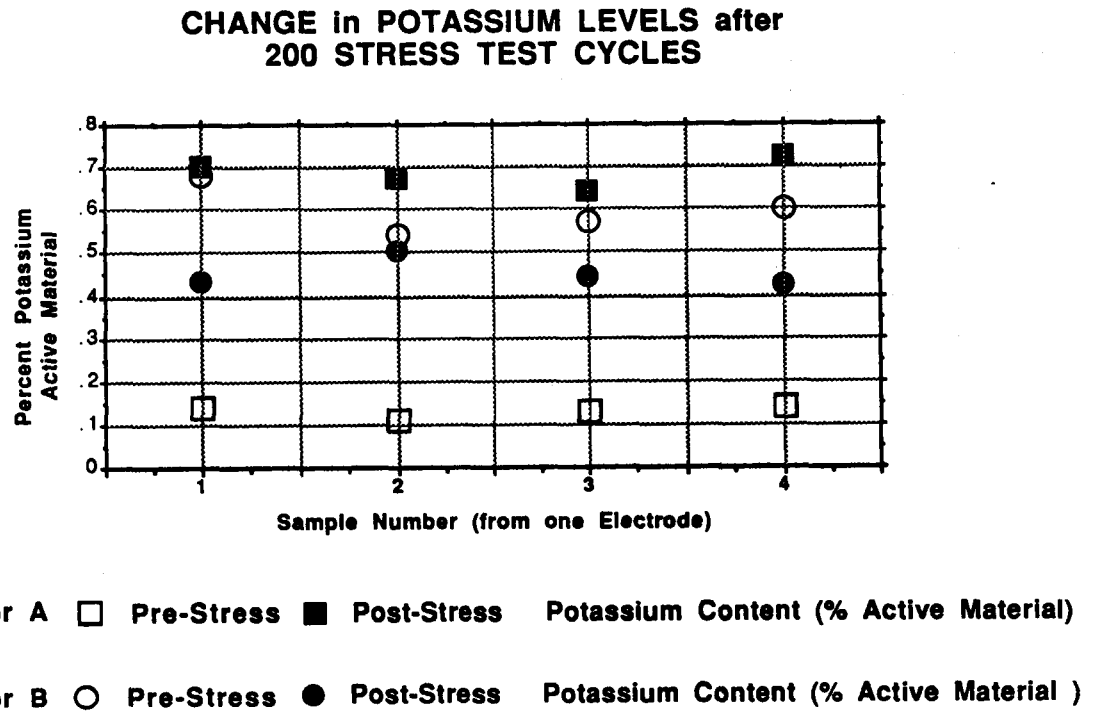

Figure 7. The effects of stress testing on potassium content in active material. Stress testing is at 10C in 31% KOH for 200 cycles. Four samples are taken from each of the four electrodes.

Conclusions

While current analytical procedures for determining the bulk chemical composition of nickel electrodes are adequate, some analytical data are overlooked and some data are slightly in error. Electrode deloading is most effective accomplished with an ammoniacal solution of EDTA, but the operation should be carried out for at least 48 hours to assure total active material removal. Charge nickel can be determined by the standard NASA procedure with reasonable accuracy. but an alkaline solution of sodium oxalate might be better suited for the analysis. For either procedure, a six hour digestion period is recommended. Potassium analysis is easily effected by flame emission photometry. Variations in electrode manufacture, probably the formation process, are readily observed, and the effects of stress testing are apparent.

References

1. P.C. Milner and U.B. Thomas, Advances in Electrochemistry and Electrochemical Engineering, Vol. **5**, 1-86, Interscience Publishers (1967), New York, C.W. Tobias (ed.)

2. D.H. Fritts, *J. Electrochem.Society,* **129** (1982), 118-122.

3. R.D. Armstrong and E.A. Charles, *J. Power Sources,* **25** (1989), 89-97.

4. R.S. McEwen, *J. Physical Chemistry,* **75** (1971), 1782-1789.

5. R. Barnard, G.T. Crickmore, J.A. Lee, and F.L. Tye, *J. of Applied Electrochem.,* **10** (1980), 61-70.

6. M. Oshitani, T. Takayama, K. Takashima, and S. Tsuji, *J. Applied Electrochem.,* **16** (1986), 403-412.

7. Handbook of Analytical Chemistry, pg 285, Mir Publishers (1975), Moscow, Ju. Lurie (ed)

8. Procedures for the Destructive Physical Analysis of Aerospace Nickel Cadmium Cells, MSFC-PROC-1768, October 1989

Acknowledgements

The authors gratefully acknowledge the technical contributions from: Randy Heu, *Lockheed Missiles and Space Co.,* Sunnyvale CA. and Steve Wright, *Pacific University,* Forest Grove, OR.

EAGLE-PICHER INDUSTRIES, Inc.
ELECTRONICS DIVISION
Joplin, MO

ADVANCED SYSTEMS DEPARTMENT
Nickel-Hydrogen Group
1990 NASA Aerospace Battery Workshop

SAR-10009 Nickel - Hydrogen Battery

27 Series Battery Cells

58 AH Rated Capacity

- **Application:** Eutelsat-2 Geosynchronous Communication Satellite
  2 Batteries / Spacecraft
- **Customer:** Eutelsat, Paris, France
- **Prime Contractor:** Aerospatiale, Cannes, France

BATTERY WORKSHOP PROCEEDINGS -619- 1990

SAR-10009
27 Cell/58 AH
Ni-H_2 BATTERY

ORIGINAL PAGE
BLACK AND WHITE PHOTOGRAPH

Unique SAR-10009 Design Features

- Highest Specific-Energy Secondary Space Battery Launched.
- Manufacturing Level Analysis And Testing Sufficient To Allow Direct Launch Site Delivery Option.
- Fully Redundant Battery Structure Electrical Insulation.
- Self-Powered Electronic Support Modules.
- Terrestrial Corrosion Protection Provisions.

SAR-10009 Specific-Energy

- Typical Capacity Measurements

Temperature	Capacity
-6°C	68 AH
25°C	70 AH
36°C	53 AH

- Average Battery Mass: 47.9 Kgrams

- Battery Level Specific-Energy: 48 Whr/Kg

SAR-10009 Analyses and Testing

- Battery Level Thermal Analysis.
- Battery Level Mechanical Analysis.
- Cell & Sleeve Level Fracture Analysis.

Analyses Validated Via Qualification Testing.

- Extreme Temperature Electrical Functional Tests.
- Resistance, Leak And Impedance Tests.
- Charge Retention Tests.
- Thermal Vacuum And Corona Tests.
- Vibration: Random: 14 GRMS Axial
  Sine: 20 G's 0 - Peak

SAR-10009 Redundant Structural Insulation

- Slight Battery Cell Expansion "Breathing" During Cyclic Pressure Operation Creates Potential Cell-To-Sleeve Short Mode.
- Introduction Of Insulated, Captive Mounting Provisions Achieved Reliable Battery-To-Spacecraft Bonding While Maintaining Electrical Isolation.
- Adequate Electrical Bonding Was Achieved Via High Resistance Circuit.

SAR-10009 Electronics

- Self Powered Pressure Sensors (Voltage Regulators) Are Provided With Signal Amplification For Direct Telemetry Interface (0 - 5V).
- Charge / Discharge By-Pass Protection Diodes Are Provided Allowing Mission Compliance With Loss Of One (1) Cell.
- Individual Cell Redundant Heaters Are Provided.
- Fuse Protected, Center Tap Is Provided For Pyrotechnic Activation.
- Multiple Location Temperature Sensors Are Provided.
- Individual Cell Monitoring Protection Resistors Are Provided.

SAR-10009 Corrosion Protection

- During Terrestrial Testing And Handling Of Batteries, Significant Temperatures Changes Can Result In Moisture Condensation.
- Corrosion Potentials Can Be Established Between Cell Case And Battery Structure And Other Points In Battery.
- SAR-10009 Features A Corrosion Protection Sealant Application At All Critical Junctions Within The Battery.

SAR-10009 Battery Cell Life Cycle Test

- Life Cycle Test Regime Features "Real-Time" Eclipse Seasons Divided By Accelerated Solstice Periods (Two Weeks).

- Discharge: C/1.6 Rate

  Depth-Of-Discharge (DOD):
  Versus Nameplate: 83%
  Versus Actual: 69%

- Have Successfully Completed 12 Seasons Or Equivalent Six (6) Years In Orbit.

SAR-10009 Spacecraft Launches

- First Launch August 1990
- Next Launch January 1991
- Four (4) More Launches Are Scheduled At Approximately Six (6) Month Intervals.

Acknowledgements

We Wish To Conclude By Acknowledging The Envaluable Contributions To The Success Of This Program Made By Personnel From The Following Organizations.

Aerospatiale

Eutelsat

Comsat

EAGLE-PICHER INDUSTRIES, INC.
JOPLIN, MO

Advanced Systems Department

NICKEL-HYDROGEN GROUP

LOW COST BATTERY DESIGNS FOR SMALL SATELLITE APPLICATIONS

EAGLE-PICHER INDUSTRIES, INC.
JOPLIN, MO

Advanced Systems Department

NICKEL-HYDROGEN GROUP

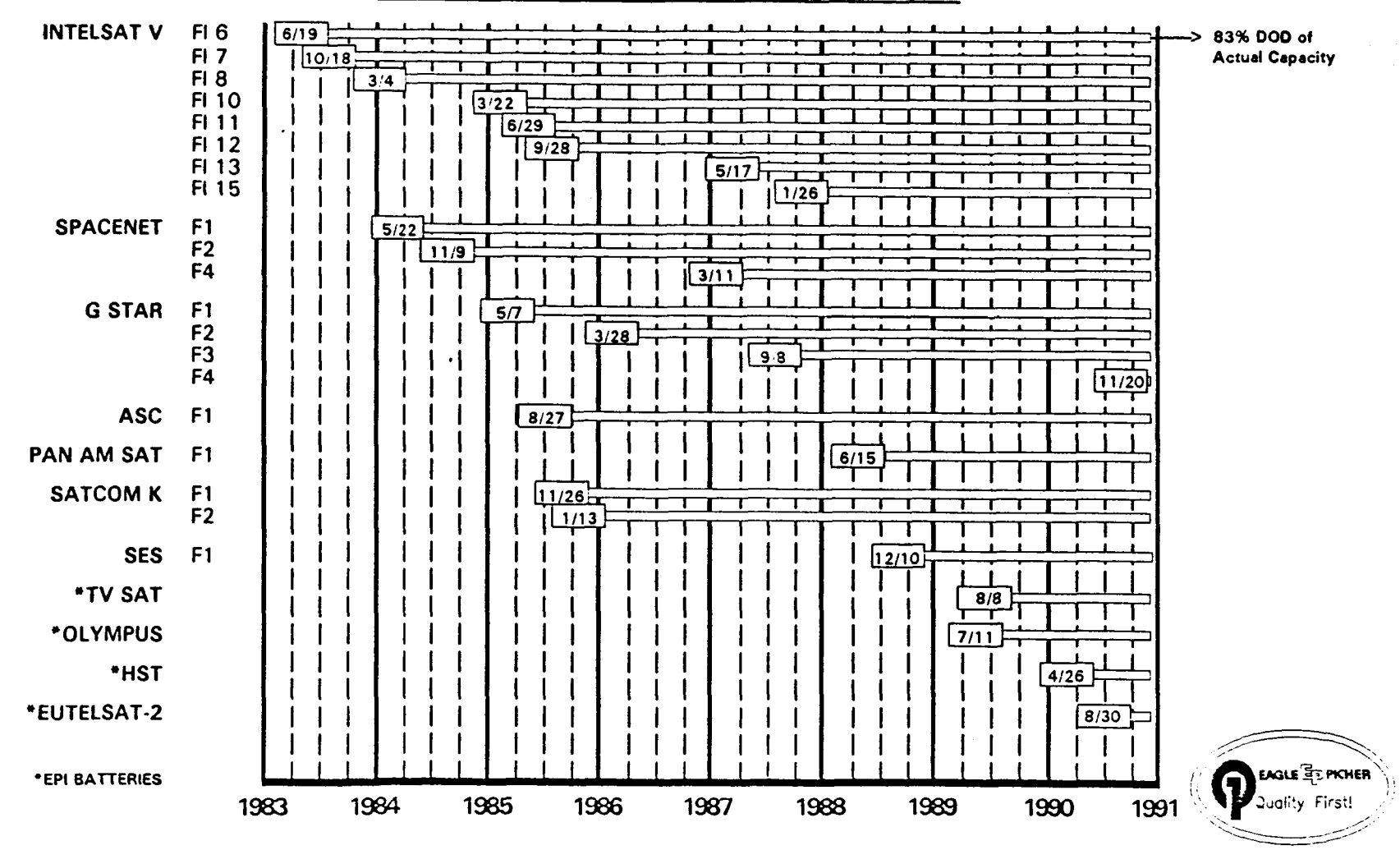

DESIGNS DEVELOPED AND TESTED

- 3.5 INCH DIAMETER CPV

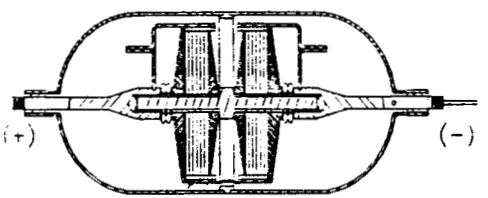

- 2.5 INCH DIAMETER IPV AND CPV

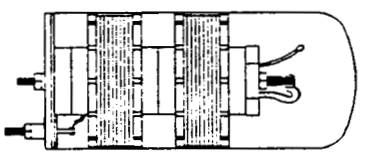

- PRISMATIC NICKEL METAL HYDRIDE

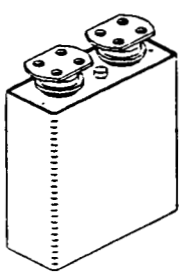

EAGLE PICHER
Quality First!

3.5 INCH DIAMETER COMMON PRESSURE VESSEL

● Rated Capacity (10 Deg C)	12 AH
● Mission Life	3 Years, 30% DOD, LEO
● Thermal / Mechanical	Center Flange Mounting Sleeve
● Pressure Monitor	Strain Gage
● Burst Factor	5 : 1
● Burst Pressure	>2500 psig
● Random Vibration Qualification	18.5 grms

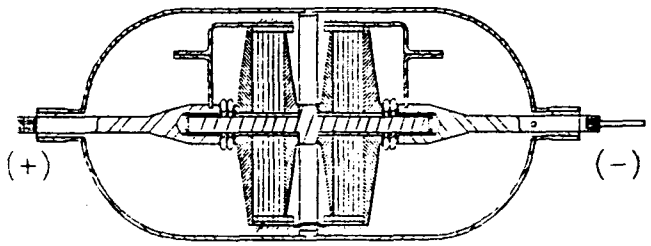

EAGLE PICHER
Quality First!

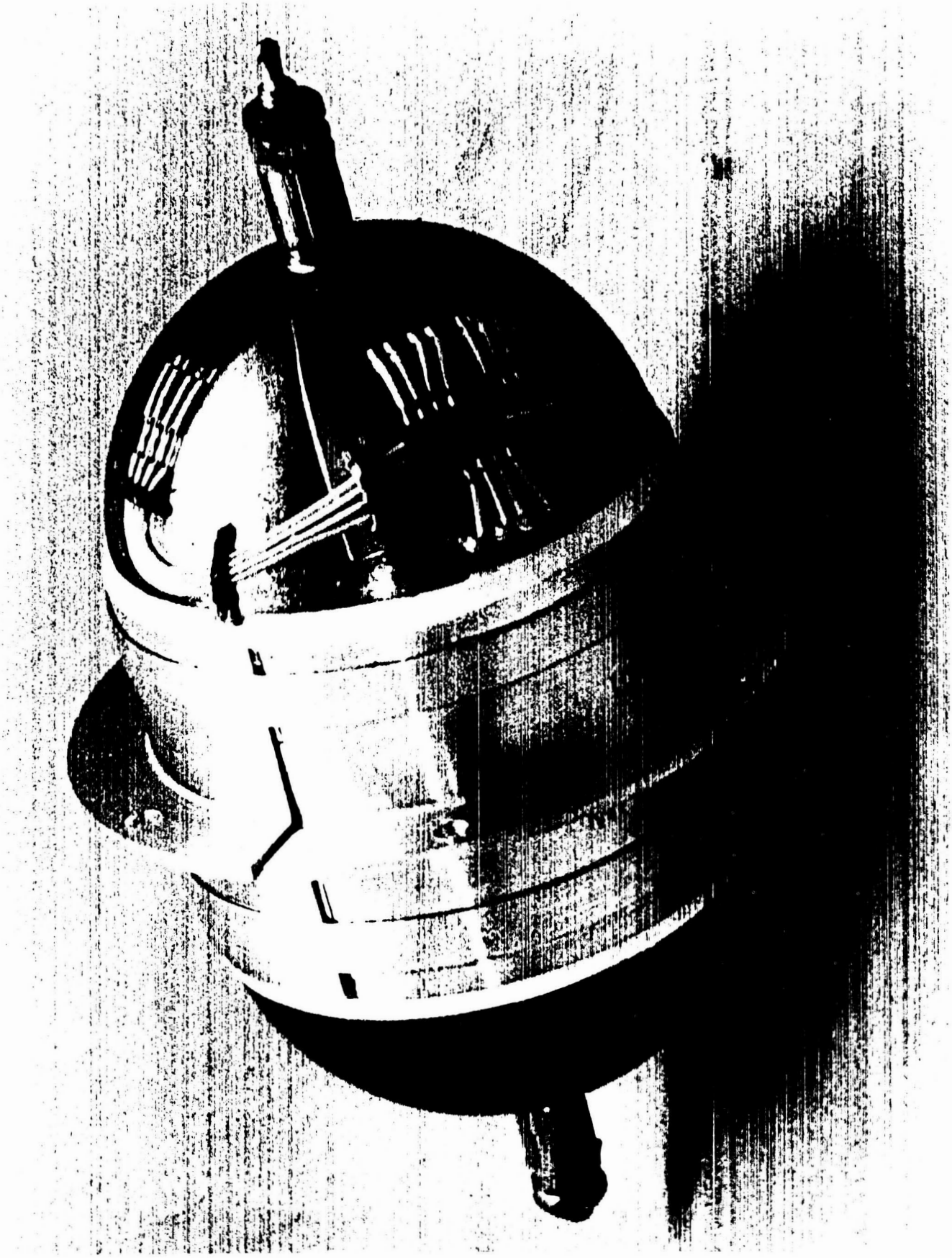

NICKEL-HYDROGEN SYSTEM ADVANTAGES

- Ease of manufacturing
- Significant Cost Savings
- Superior to present Ni-Cd and Sealed Lead Acid batteries in energy density, cycle life, and better tolerance to overcharge
- Longer service-free life
- No toxic components, as those found in Ni-Cd designs
- CPV Design available offering weight savings and cost savings at battery level

RNH-12-1 CPV CELL
Typical C/10 Charge at 10 deg C

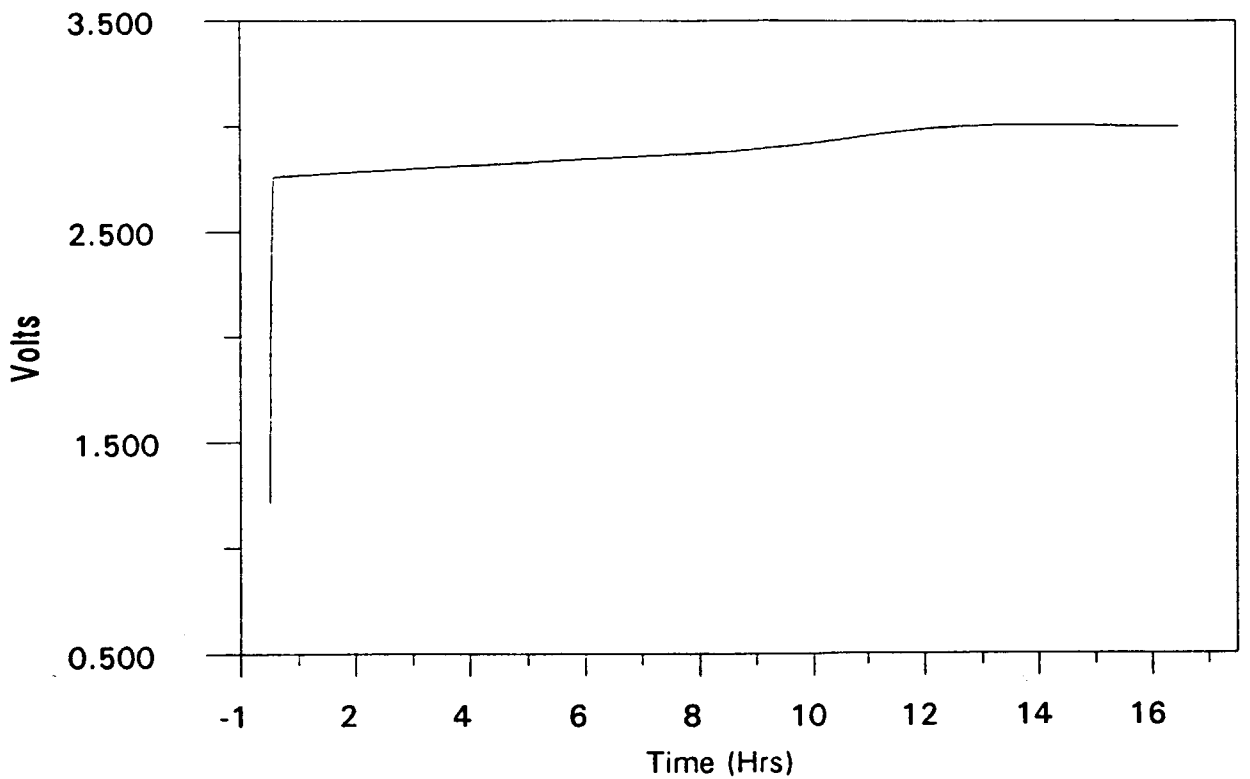

EAGLE PICHER
Quality First!

RNH-12-1 CPV CELL
Typical C/2 Discharge at 10 deg C

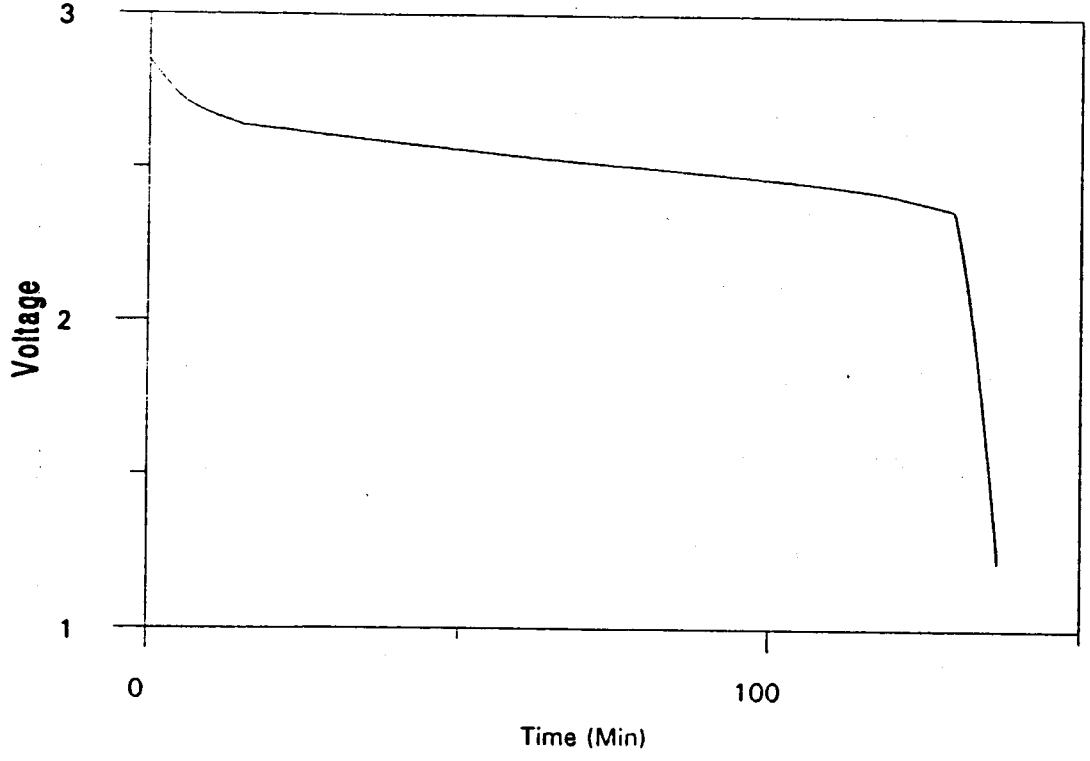

2.5 INCH DIAMETER IPV AND CPV

- 5 to 20 AH Design Capability
- All Components Assembled to Base Plate
- Two Cells Mounted in Tandem for CPV
- Reduced Platinum Loading in Hydrogen Electrode
- Burst Pressure >3000 psig
- 5 AH CPV Cells Under Test

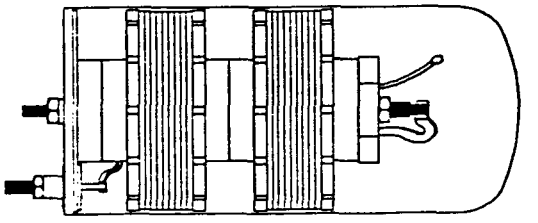

EAGLE PICHER
Quality First!

5 AH CPV CHARGE VOLTAGE / PRESSURE
C/10 Charge at 0 deg C

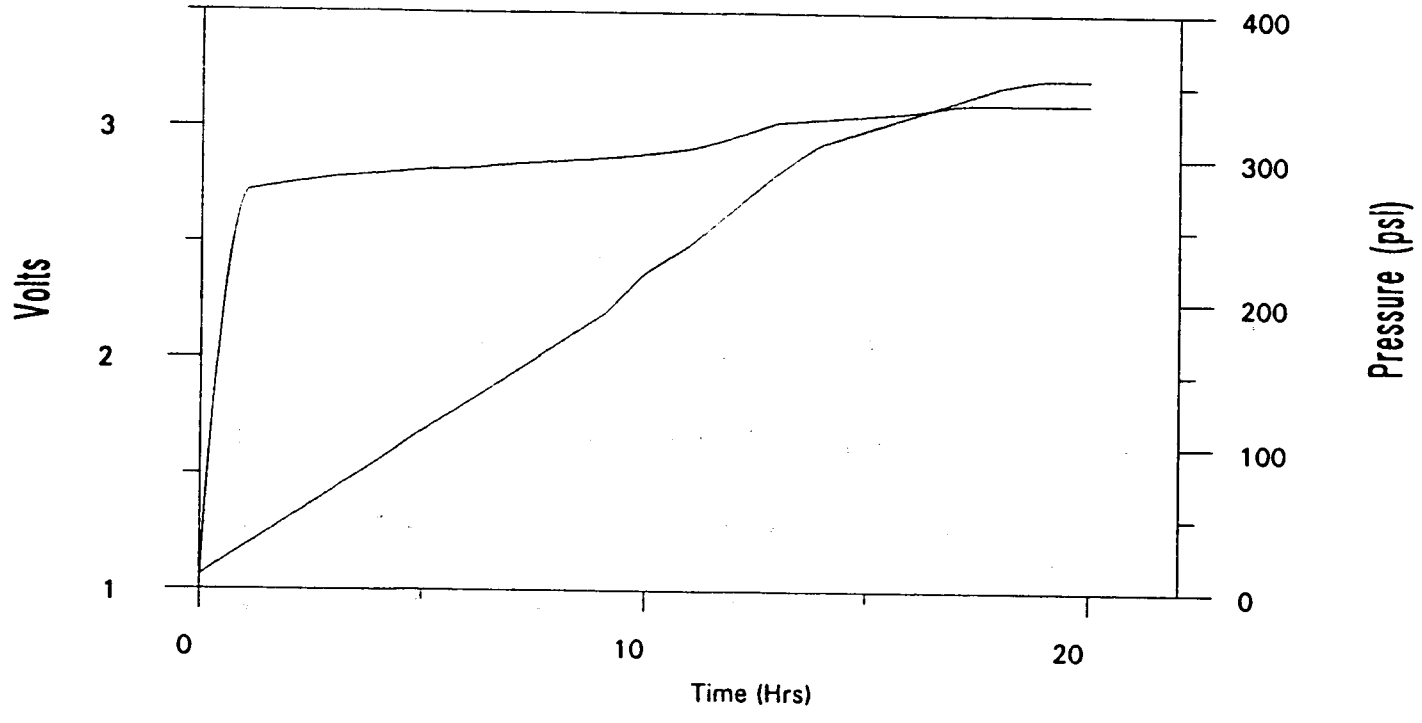

EAGLE PICHER
Quality First!

EAGLE-PICHER INDUSTRIES, INC.
JOPLIN, MO

5 AH CPV CELL DESIGN
Discharge at 1.1 Amps

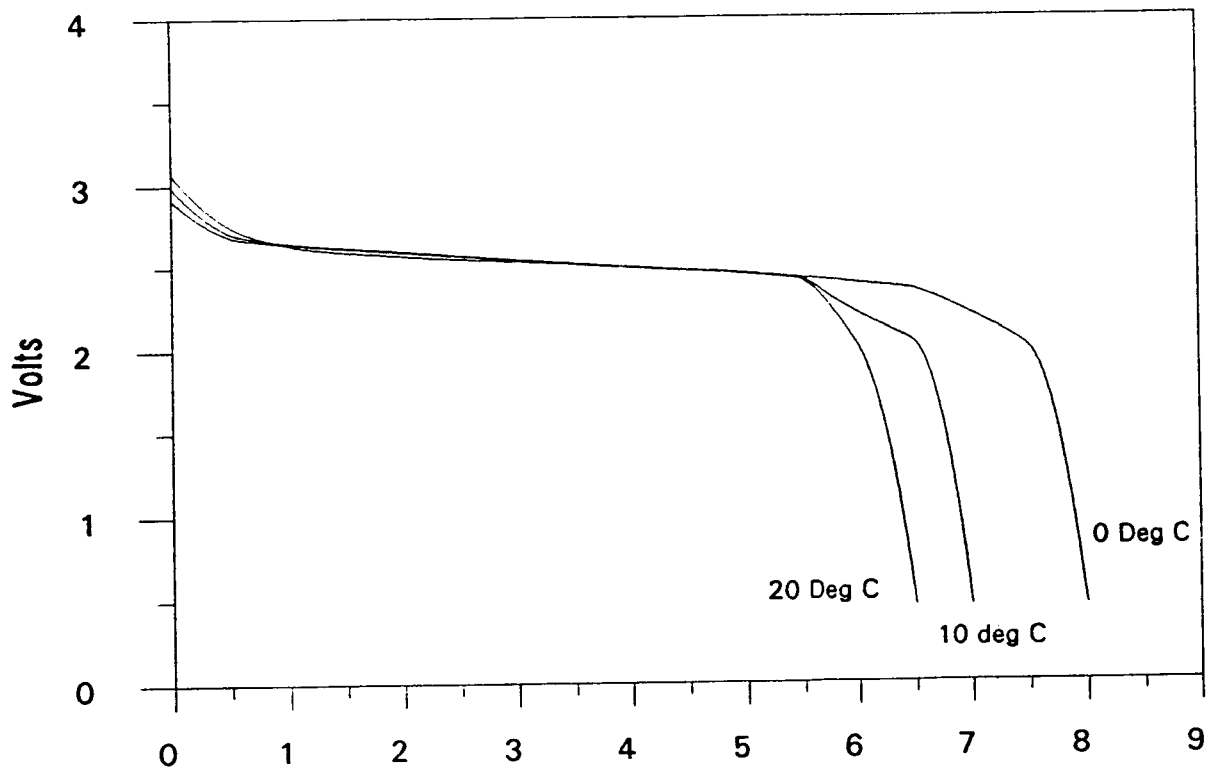

EAGLE PICHER
Quality First!

5 AH CPV CELL DESIGN
Discharge at 2.75 Amps

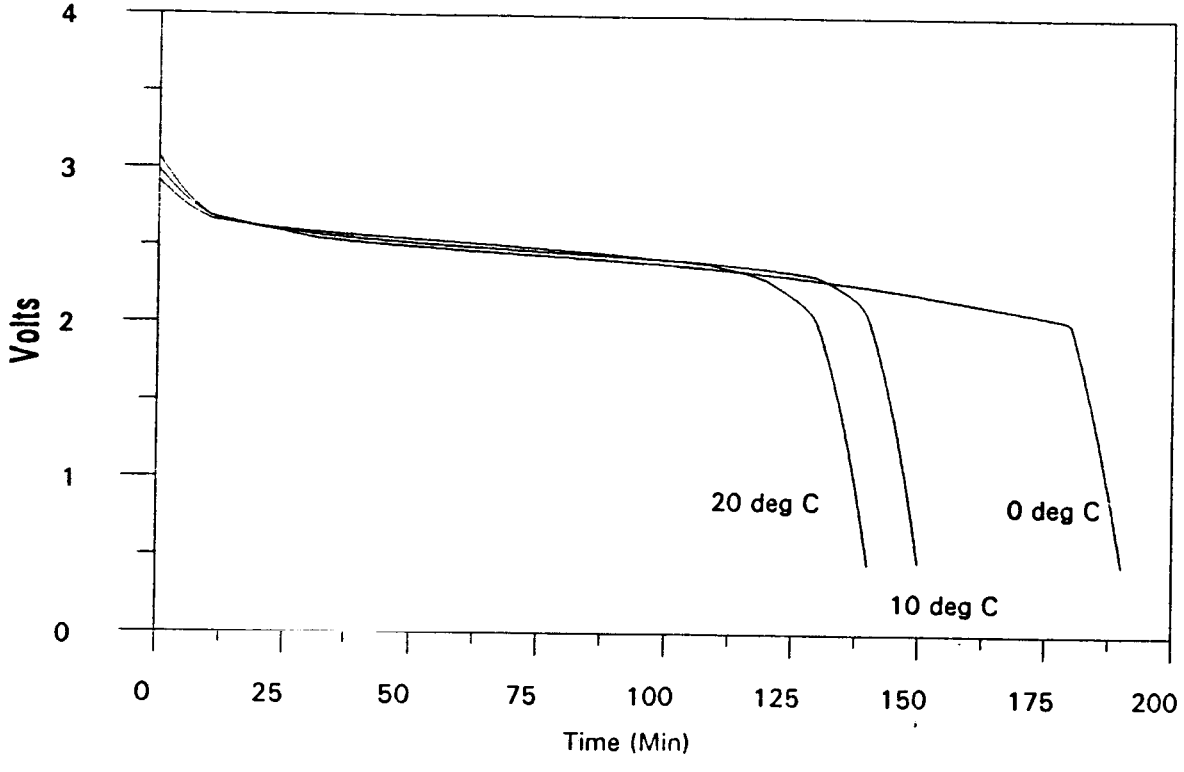

EAGLE PICHER
Quality First!

5 AH CPV CELL DESIGN
Discharge at 5.5 Amps

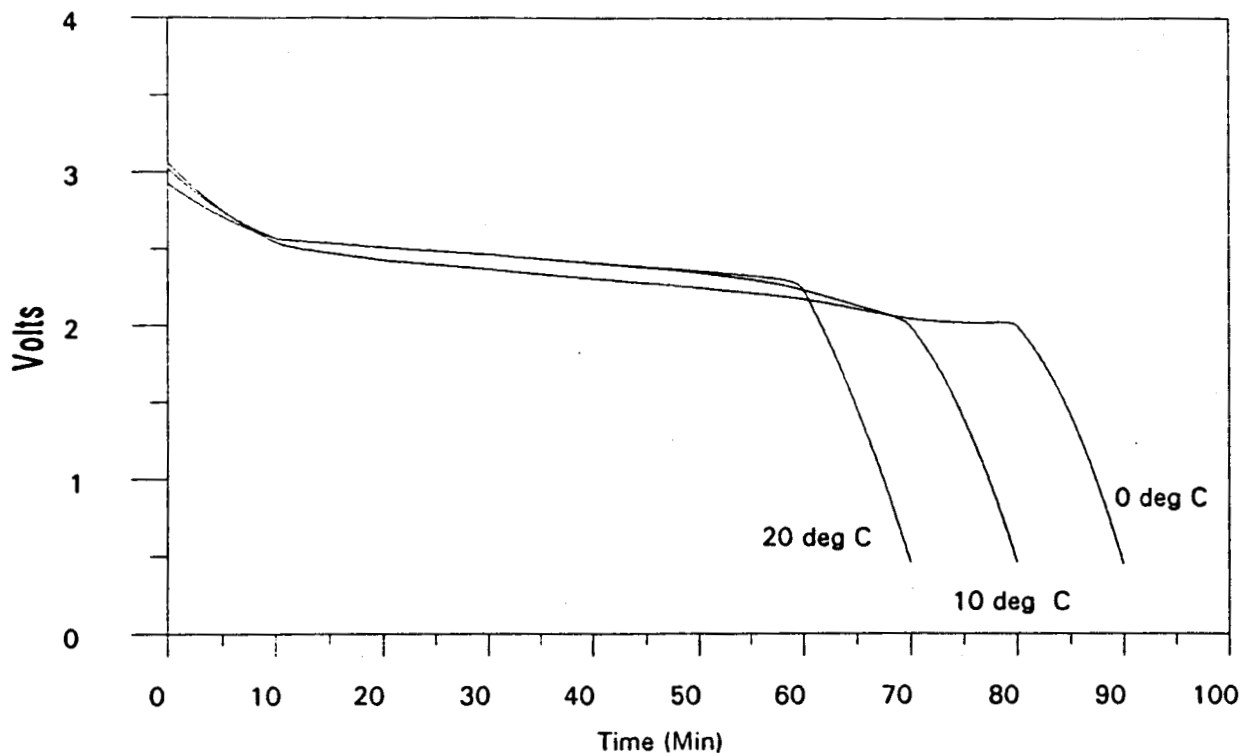

EAGLE PICHER
Quality First!

RNH-5-1 CHARGE RETENTION TEST
10 Degrees C

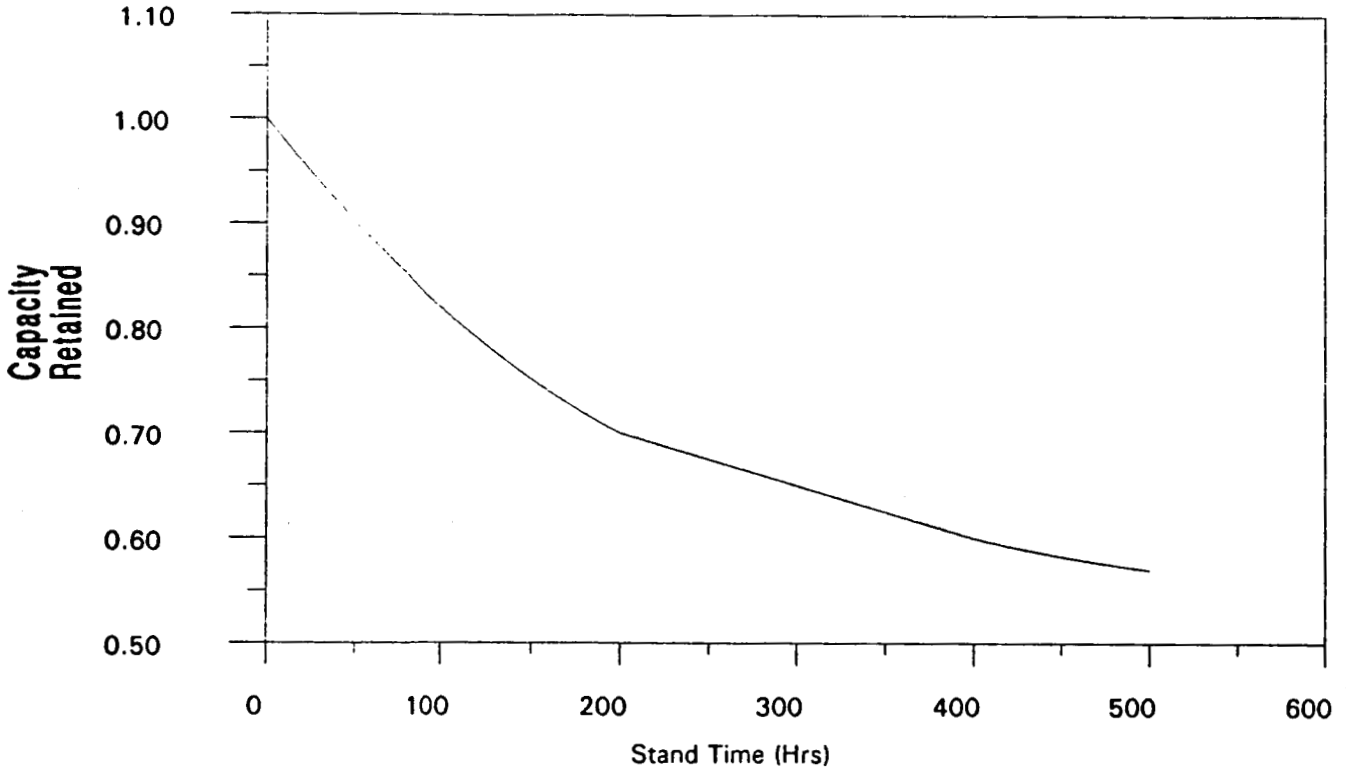

NICKEL-HYDROGEN CELL SPECIFICATIONS

	3.5 Inch Diameter CPV	2.5 Inch Diameter CPV
Rated Capacity (AH)	12	5
Cell Mass (grams)	1020	500
Capacity (AH)*	15	5
Specific Energy (WHr/Kg)	37	24.9
Energy Density (WHr/L)	49	34
Max. Operating Pressure (psig)	480	350

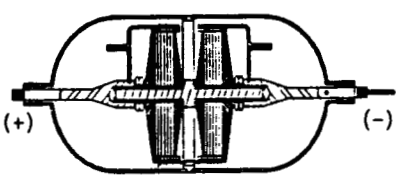

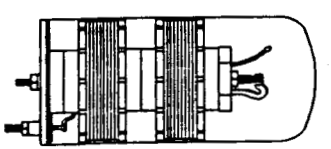

* C/2 Rate to 1.0 Volt at 10 deg. C

EAGLE PICHER
Quality First!

SEALED PRISMATIC NICKEL METAL HYDRIDE

- 4 to 180 AH Cells Assembled
- 4 and 5 AH Cells on Life Test

  800 Cycles Achieved at 30% and 40% DOD

  Cycle: 35 Minute Discharge, 55 Minute Charge
- Operating Pressure Typically 30 to 70 psig

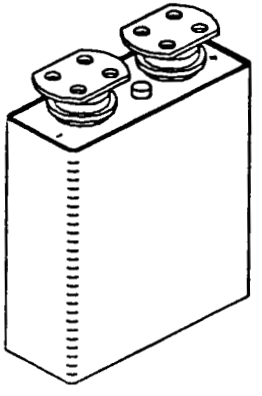

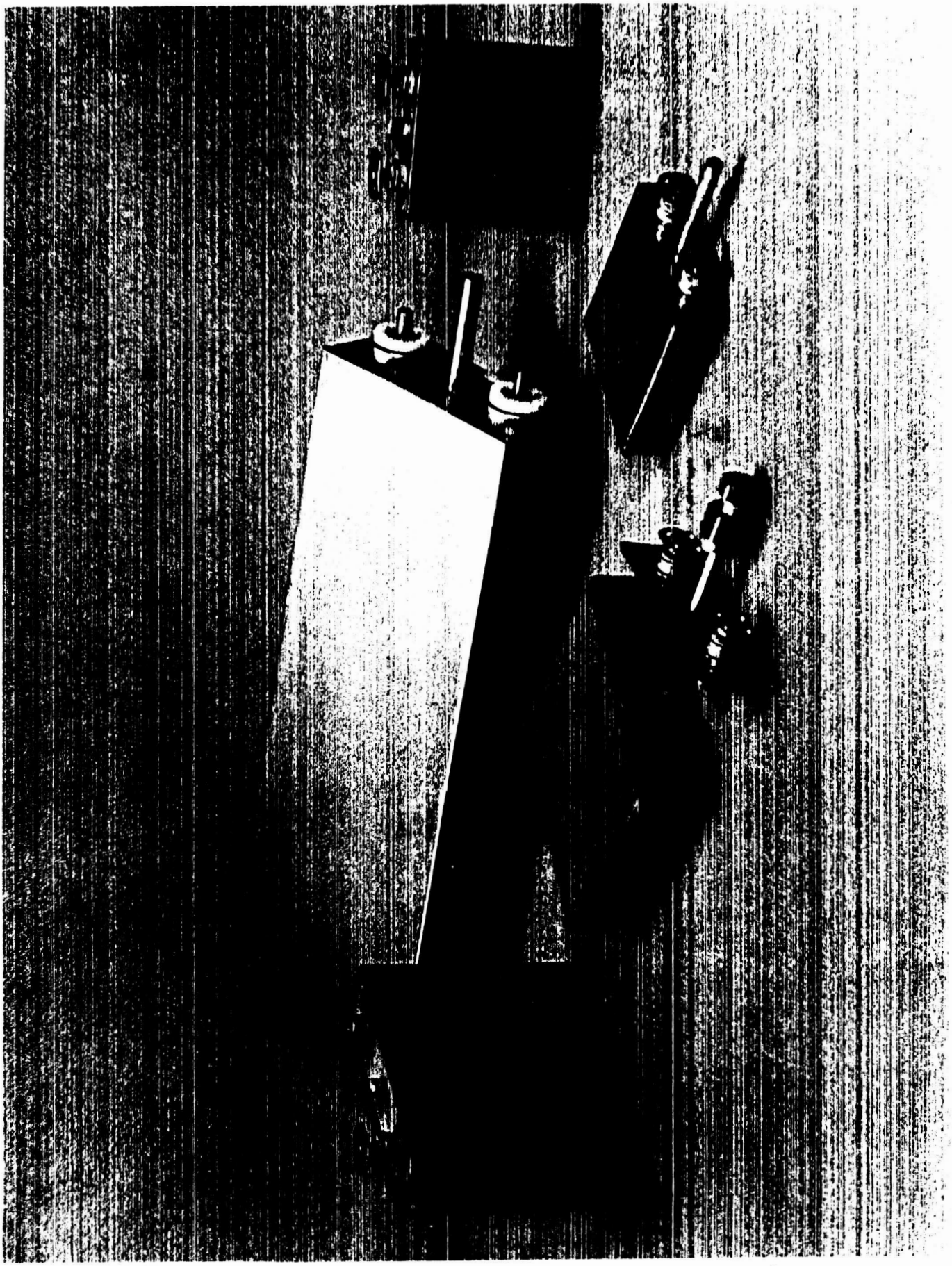

EAGLE-PICHER INDUSTRIES, INC.
JOPLIN, MO

Advanced Systems Department

NICKEL-HYDROGEN GROUP

NICKEL METAL HYDRIDE LIFE TEST

S/N 001 - 55/35 REGIME

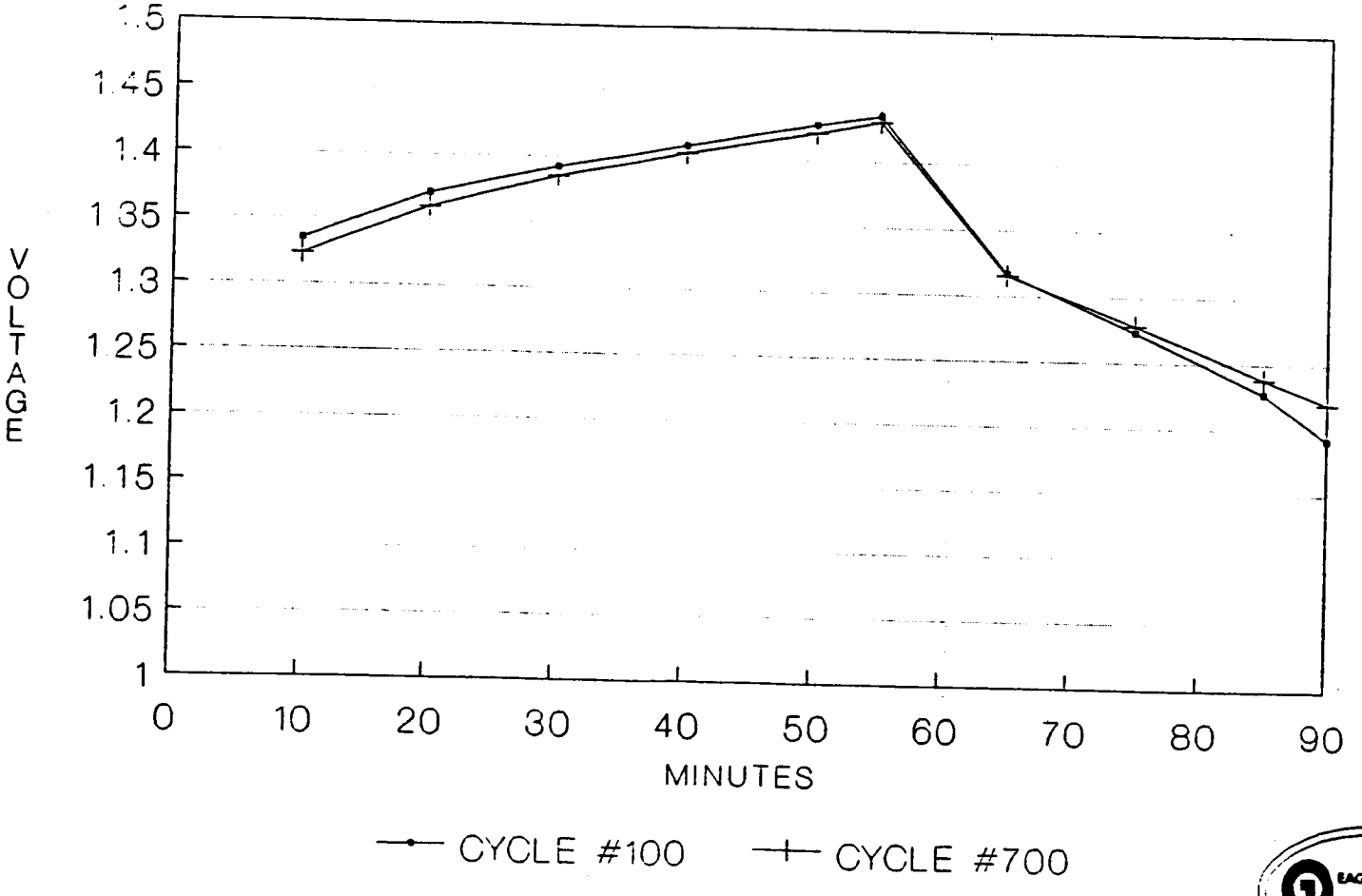

EAGLE PICHER
Quality First!

EAGLE-PICHER INDUSTRIES, INC.
JOPLIN, MO

NICKEL-HYDRIDE CELL SPECIFICATIONS

	Aerospace Ni-Cd	Aerospace Ni-MH	Commercial Ni-MH	OBC Commercial "C" Cell
Rated Capacity (AH)	2.5	4.0	5.0	3.5
Cell Mass (grams)	140	140	140	140
Capacity (AH)*	2.7	4.2	5.3	3.6
Specific Energy (WHr/Kg)	24	38	47	56
Energy Density (WHr/L)	84	130	165	180
Max. Operating Pressure (psig)	100	100	100	100

Prismatic Cell Design Dimensions (cm): 5.5 x 5.2 x 1.4

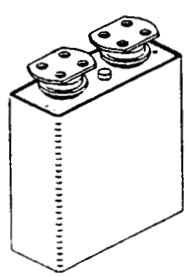

* C/2 Rate to 1.0 Volt at 22 deg. C

EAGLE PICHER Quality First!

NICKEL METAL HYDRIDE SYSTEM ADVANTAGES

- Improved weight energy density over Ni-Cd
- Improved volumetric energy density over Ni-H2
- No cadmium, lead, mercury, or asbestos
- Lower cost on a dollar/AH basis
- Improved packaging efficiency in prismatic cells
- Direct Ni-Cd / Ni-H2 replacement
- No memory effect

EAGLE PICHER
Quality First!

CONCLUSION

- Successfully developed two different models of small AH lower cost Ni-H2 cells for small satellite applications

RNH-5-1	2.5 Inch Diameter Design
RNH-12-1	3.5 Inch Diameter Design

- Proven CPV design thus reducing battery mass and footprint

- Nickel Metal Hydride Prismatic Cells

  Proven Commercial Performance
  Proven Aerospace Cell Designs
  Extensive Testing Underway
  Improved Designs Under Development
  High Energy Density
  Aerospace Quality
  Competitive Cost

EAGLE PICHER Quality First!

THE EVALUATION OF LAYERED SEPARATORS FOR NICKEL-HYDROGEN CELLS

BY

RANDALL F. GAHN

NASA LEWIS RESEARCH CENTER

1990 NASA AEROSPACE BATTERY WORKSHOP

MARSHALL SPACE FLIGHT CENTER

HUNTSVILLE, ALABAMA

DECEMBER 4-6, 1990

For Presentation at
NASA Aerospace Workshop
December 4-6, 1990
Marshall Flight Center
Huntsville, Alabama

THE EVALUATION OF LAYERED SEPARATORS FOR NICKEL-HYDROGEN CELLS

Randall F. Gahn
National Aeronautics Space Administration
Lewis Research Center
Cleveland, Ohio 44135

ABSTRACT

The concept of using layered separators to achieve the required electrolyte retention and bubble pressure for nickel-hydrogen cells was evaluated in a boilerplate cell test. Zircar cloth, polyethylene paper and polypropylene felt were combined with a layer of radiation-grafted polyethylene film to achieve the required properties. Three cells of each layered separator were built and tested by characterization cycling and by LEO cycling for 5000 cycles at 80% DOD. Three cells containing asbestos separators were used as the reference.

PRESENTATION OUTLINE

BACKGROUND

- SEPARATOR REQUIREMENTS
- PREVIOUS WORK
- PRESENT APPROACH

BOILERPLATE CELL TESTS

- MATERIALS EVALUATED
- CELL HARDWARE

RESULTS

- PERFORMANCE
- POST-TEST OBSERVATIONS
- ELECTROLYTE DISTRIBUTION

SUMMARY AND CONCLUSIONS

SEPARATOR REQUIREMENTS

- RESISTANCE TO THE PENETRATION OF OXYGEN AND LOOSE MATERIAL FROM NICKEL ELECTRODE
- HIGH ELECTROLYTE RETENTION
- CHEMICAL AND THERMAL STABILITY
- GOOD IONIC CONDUCTIVITY
- DISTRIBUTION OF PORE SIZES
- COMMERCIAL PRODUCTION QUALITIES
- ENVIRONMENTAL ACCEPTANCE

PREVIOUS WORK

- GOAL WAS TO REPLACE ASBESTOS AS THE STANDARD SEPARATOR
- GAINED AN UNDERSTANDING OF THE ELECTROLYTE DISTRIBUTION AMONG COMPONENTS
- EVALUATED CUSTOM DESIGN AND COMMERCIALLY AVAILABLE MATERIALS FOR REQUIRED PROPERTIES
- COMMERCIAL PRODUCTION USING PAPER MAKING EQUIPMENT FOUND APPLICABLE
- INITIAL EVALUATION OF A LAYERED SEPARATOR USING RADIATION-GRAFTED POLYETHYLENE FILM AND ZIRCAR CLOTH IN BOILERPLATE CELLS GAVE PROMISING RESULTS

OBJECTIVES

- COMPARE PERFORMANCES OF CELLS BUILT WITH ZIRCAR CLOTH, POLYETHYLENE PAPER AND POLYPROPYLENE FELT LAYERED WITH RADIATION-GRAFTED POLYETHYLENE FILM TO CELLS BUILT WITH ASBESTOS SEPARATORS

- EVALUATE SEPARATOR INTEGRITY FOLLOWING CYCLING

APPROACH

- BUILD THREE, FOUR AMPERE HOUR IPV CELLS FROM EACH OF THE FOUR SEPARATOR TYPES
- CHARACTERIZATION CYCLE UP TO THE 2C RATE INITIALLY AND EVERY 1000 LEO CYCLES
- LEO CYCLE CELLS FOR 5,000 CYCLES AT 80% DOD
- DISASSEMBLE CELLS AND EVALUATE THE SEPARATORS AND OTHER COMPONENTS

SEPARATOR PROPERTIES

MATERIAL	THICKNESS mils	THICKNESS cm	AREA RESISTIVITY Ω cm^2	BUBBLE PRESSURE psi	ELECTROLYTE RETENTION, %
ASBESTOS (BTA)	7	.018	.1	>20	134
ZIRCAR	14	.036	.05	4	150
PE PAPER	14	.036	.3	1	240
PP FELT	11	.028	.3	1	85
PE FILM	1	.0025	.05	>20	38

NICKEL-HYDROGEN BOILERPLATE CELL STUDIES

HARDWARE

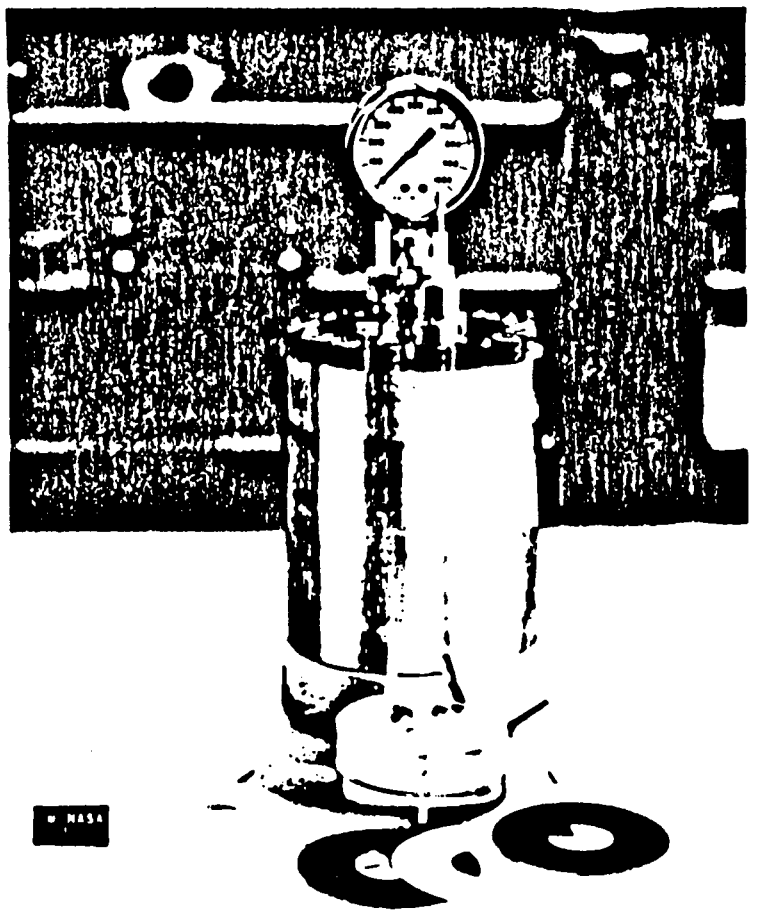

PURPOSE

DESIGN VERIFICATION
COMPONENT EVALUATION
SIMULATE CYCLING MODES

FEATURES

IN-HOUSE CAPABILITY
EASE OF ASSEMBLY
REUSABLE HARDWARE
COST EFFECTIVE

CD-88-37692

Comparison of Initial Discharge Performances

Discharge voltages at the C rate for a cell from each of the separator types are compared. This figure shows the performance prior to any LEO cycling. The Zircar cloth/PE film cell voltages is similar to the asbestos cell. The PE paper/PE film separator cell and the PP felt/PE film cell performance are also equivalent, but about 20 mv lower than the asbestos and zircar cloth PE film cell.

Comparison of Initial Discharge Performances

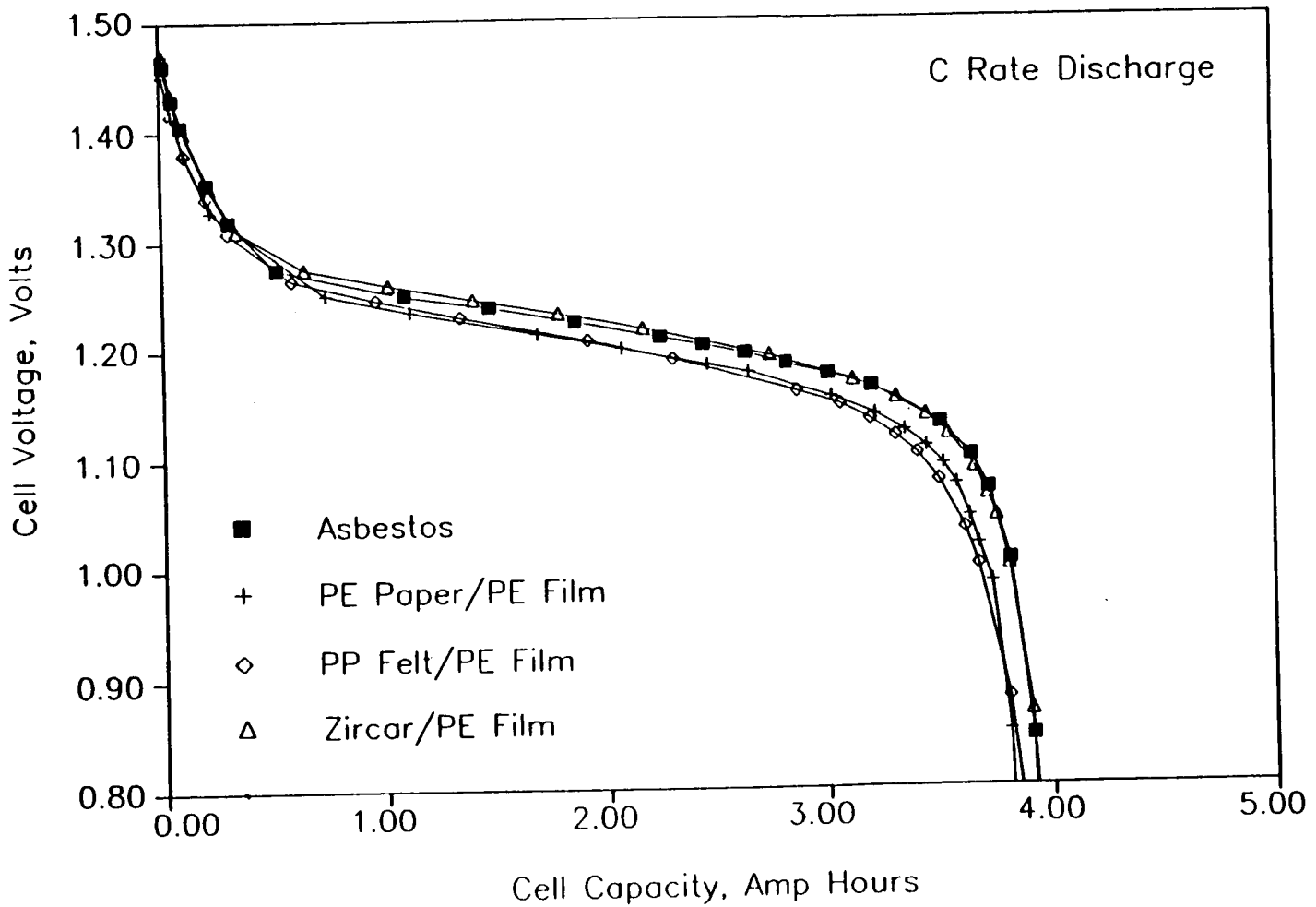

Comparison of Discharge Performances Following 5000 LEO Cycles

Performances of the same cells as the previous figure are shown following 5000 LEO cycles at 80% DOD. Discharge voltages for the Zircar cloth/PE film cell is equivalent to the asbestos cell. The PE paper/PE film cell and the PP felt/PE film cell are both lower in voltage than the asbestos reference. All four cells lost capacity (about 0.5 amp hours) during the cycling period. Discharge voltages for all cells are slightly higher (10mv to 20 mv) for each cell after the 5000 cycles than before any LEO cycling. There appears to be no greater change in the performance of any of the layered separator cells than occurred in the asbestos cell.

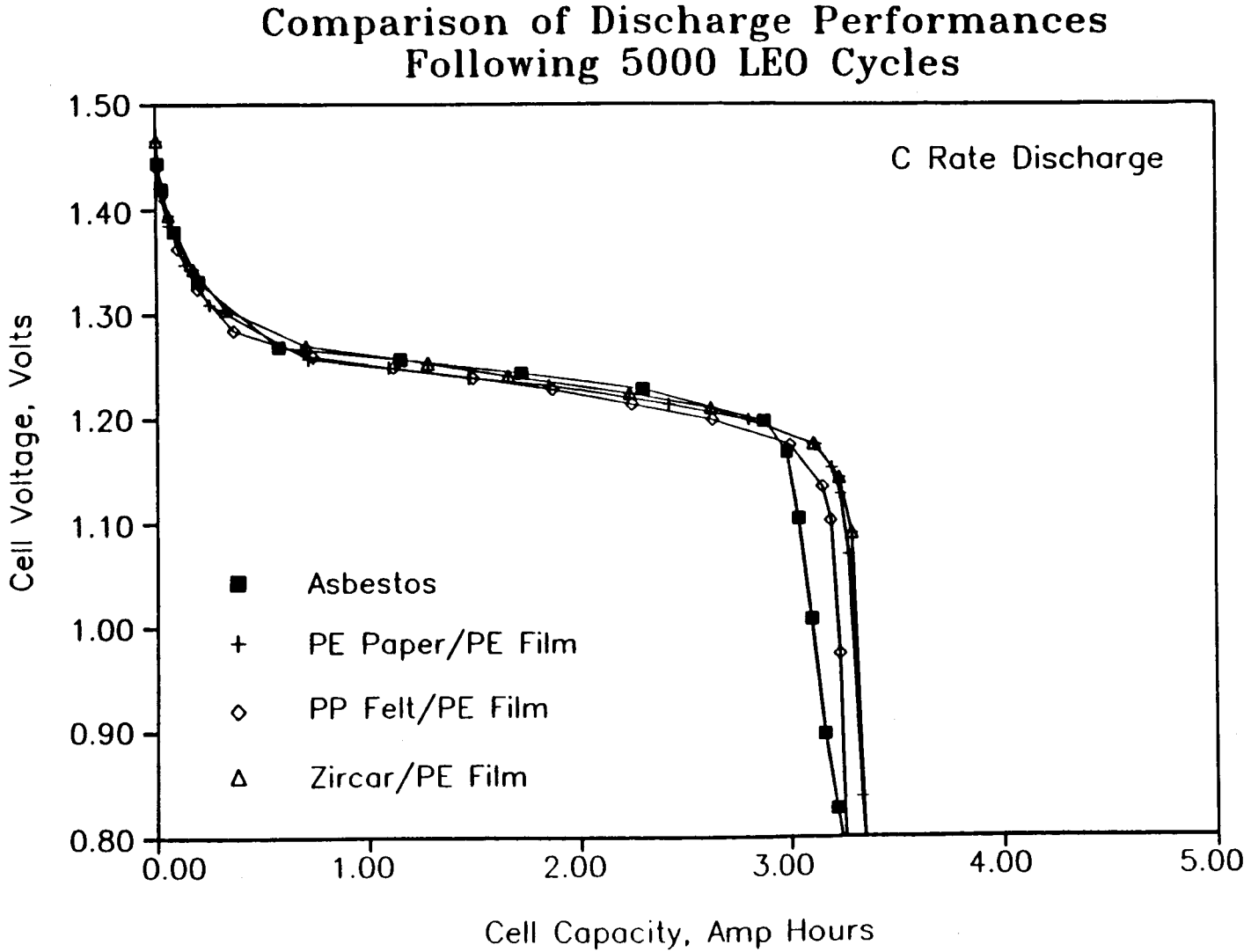
Comparison of Discharge Performances
Following 5000 LEO Cycles
C Rate Discharge
Cell Voltage, Volts
1.50
1.40
1.30
1.20
1.10
1.00
0.90
0.80
0.00
1.00
2.00
3.00
4.00
5.00
Cell Capacity, Amp Hours
Asbestos
PE Paper/PE Film
PP Felt/PE Film
Zircar/PE Film

Mid-Discharge Voltages During LEO Cycling

1000 Cycles

The cell voltages at the mid-point of LEO cycle 1000 are used to compare the performances of all the cells. Cells of the same separator are quite similar in performance. The voltages of the Zircar cloth/PE film cells are higher than the other two experimental separators and the asbestos reference.

Mid-Discharge Voltages During LEO Cycling

4300 Cycles

This figure compares the mid-discharge voltages for all the cells during LEO cycle 4300. There is no change in the order of the performance as a result of the cycling, although there is more variability in voltages for a particular separator. The Zircar cloth/PE film cells continued to have the best voltages.

MID-DISCHARGE VOLTAGES DURING LEO CYCLING

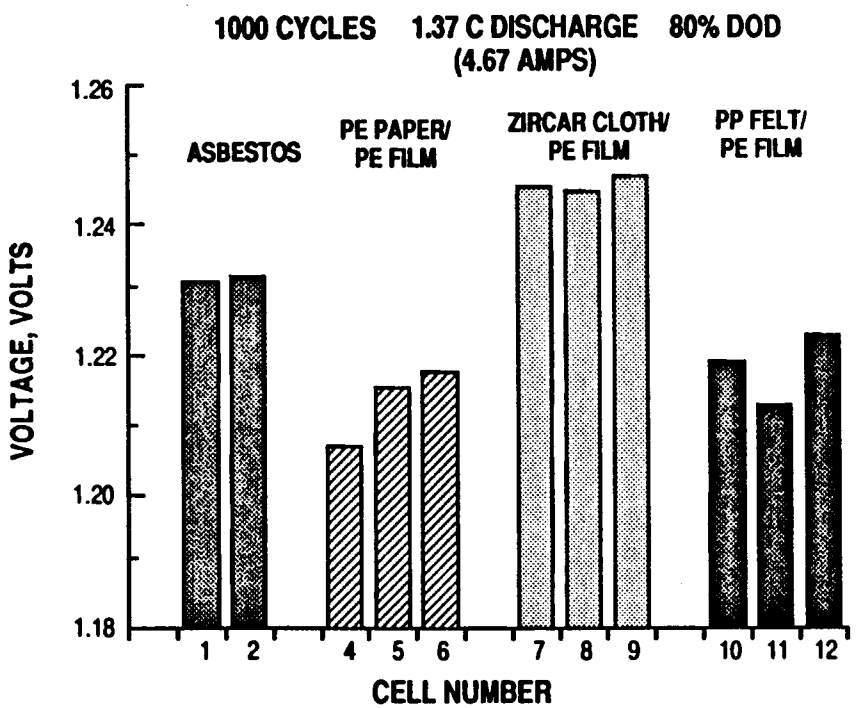

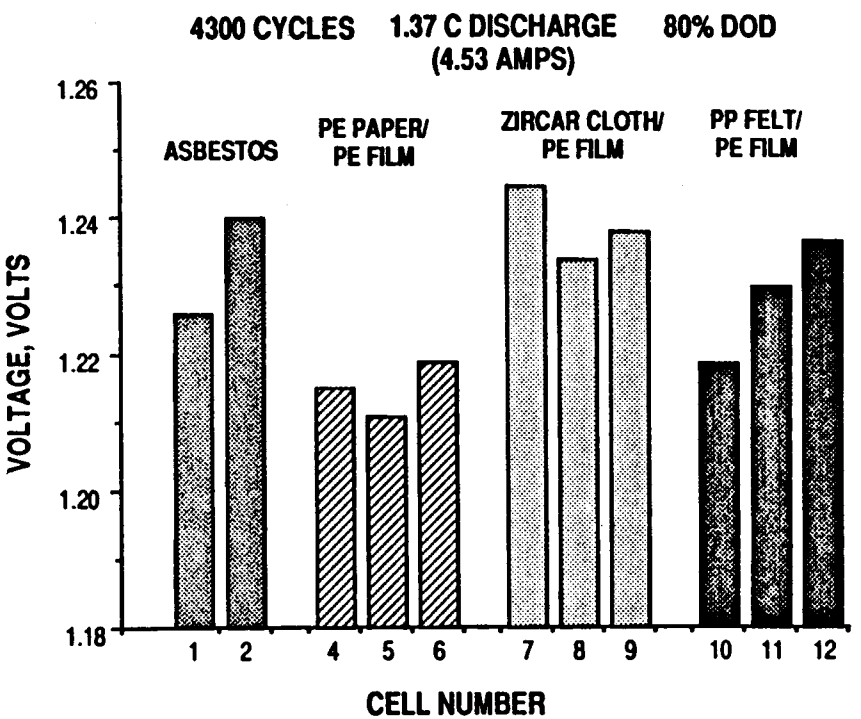

RFG90-001.12

POST-TEST OBSERVATIONS

CELL	SEPARATOR	APPEARANCE
1	ASBESTOS	NORMAL
2	ASBESTOS	NORMAL
3	ASBESTOS	(CELL LEAD BROKEN, CYCLING STOPPED)
4	PE PAPER/PE FILM *	INTACT, MOIST, SLIGHT ADHESION TO PE FILM & H ELECTRODE
5	PE PAPER/PE FILM *	INTACT, DRIER, MORE ADHESION TO PE FILM & H ELECTRODE
6	PE PAPER/PE FILM *	INTACT, MOIST, SLIGHT ADHESION TO ONE H ELECTRODE
7	ZIRCAR CLOTH/PE FILM *	NORMAL, SOME STAINING, GENERALLY MOIST
8	ZIRCAR CLOTH/PE FILM *	NORMAL, SOME STAINING, GENERALLY MOIST
9	ZIRCAR CLOTH/PE FILM *	NORMAL, SOME STAINING, GENERALLY MOIST
10	PP FELT/PE FILM *	INTACT, MOIST, STAIN AROUND PERIMETER
11	PP FELT/PE FILM *	INTACT, MOIST, STAIN AROUND PERIMETER
12	PP FELT/PE FILM *	INTACT, MOIST, STAIN AROUND PERIMETER

* PE FILM FROM ALL CELLS SHOWED NO VISIBLE DETERIORATION

NOTES:

ALL NICKEL ELECTRODE HAD INCREASED IN THICKNESS, WERE SLIGHTLY CRATERED AND HAD VARYING AMOUNT OF BLACK RESIDUE. RESIDUE MIGRATED WITHIN CELL CORE

ALL HYDROGEN ELECTRODES WERE IN GOOD CONDITION.

Separator Electrolyte Content Following LEO Cycling

The weight of KOH electrolyte remaining in the separators of each cell following 5000 LEO cycles is shown in this figure. Results are consistent for each separator type. The Zircar cloth and PE paper separators retained more electrolyte than the asbestos, whereas the PP felt separators retained slightly less. Adequate electrolyte was available in all the separators to maintain good ionic conductivity for the cycling period. There appeared to be no significant loss of wettability of either the PE paper or the PP felt.

SEPARATOR ELECTROLYTE CONTENT FOLLOWING LEO CYCLING

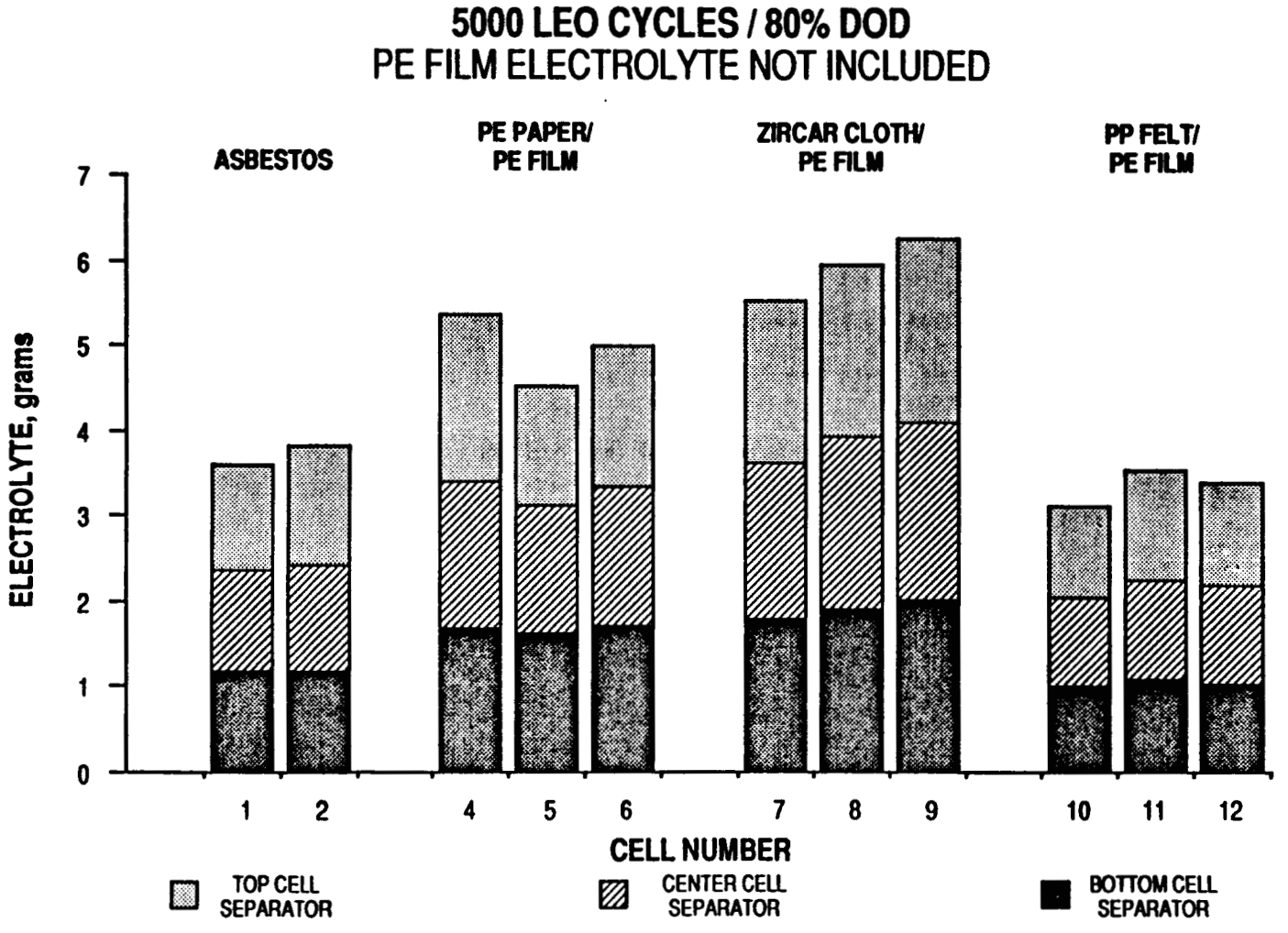

SEI Micrographs of Separator Materials

Photographs of the polyethylene paper, polypropylene felt and polyethylene film in the as-received condition and after 5000 LEO cycles are shown on the next three pages. There is no visible deterioration of the materials as a result of exposure to oxygen generated at the nickel electrode or from the recombination of oxygen with hydrogen.

AERO SPACE TECHNOLOGY DIRECTORATE

POWER TECHNOLOGY DIVISION

NASA Lewis Research Center

SEI MICROGRAPHS OF SEPARATOR MATERIAL

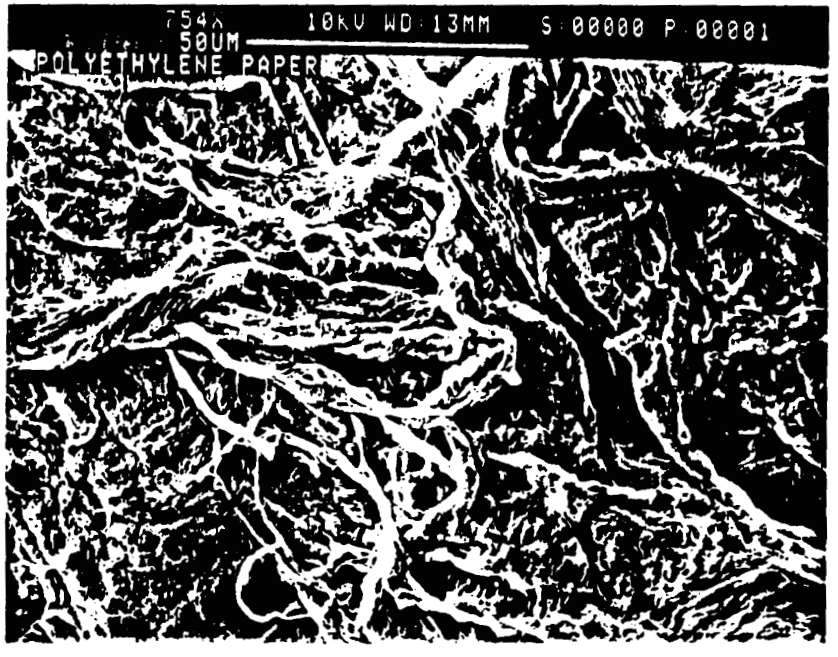

POLYETHYLENE PAPER - AS RECEIVED - 754X

POLYETHYLENE PAPER - 5000 LEO CYCLES - 750X

AEROSPACE TECHNOLOGY DIRECTORATE

POWER TECHNOLOGY DIVISION

Lewis Research Center

SEI MICROGRAPHS OF SEPARATOR MATERIAL

POLYPROPYLENE FELT - AS RECEIVED - 737X

POLYPROPYLENE FELT - 5000 LEO CYCLES - 750X

AEROSPACE TECHNOLOGY DIRECTORATE

POWER TECHNOLOGY DIVISION

Lewis Research Center

SEI MICROGRAPHS OF SEPARATOR MATERIAL

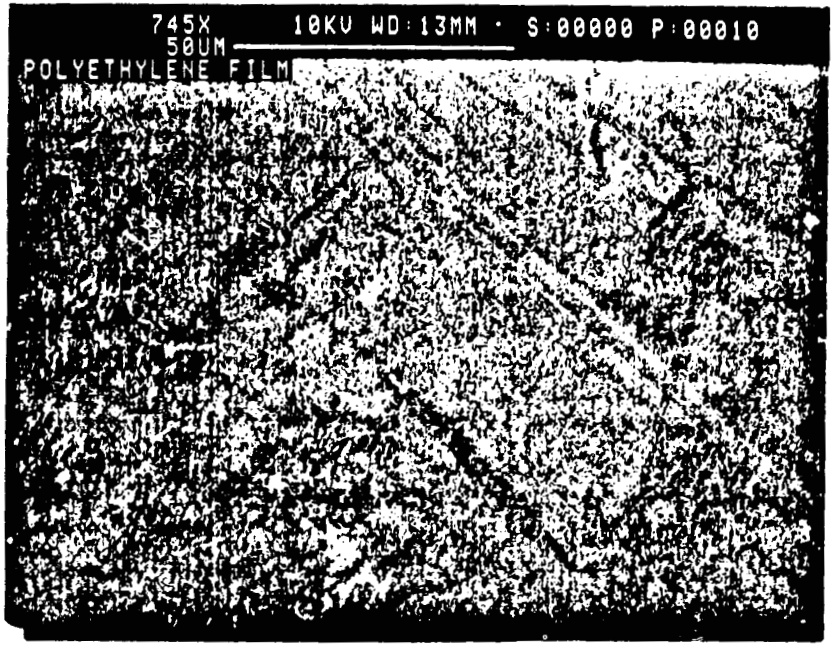

POLYETHYLENE FILM - AS RECEIVED - 745X

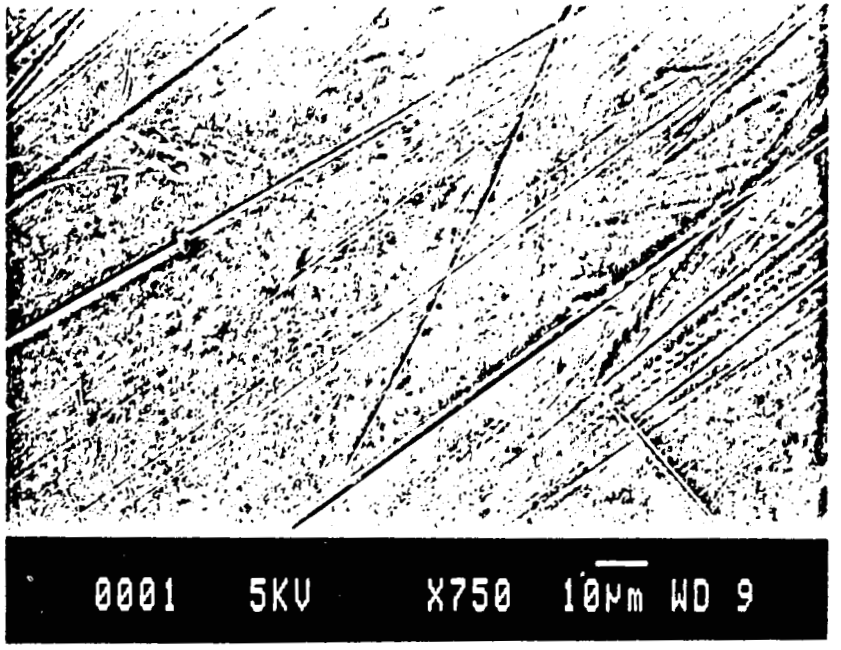

POLYETHYLENE FILM - 5000 LEO CYCLES - 750X

SUMMARY AND CONCLUSIONS

- THREE SEPARATOR MATERIALS WERE LAYERED WITH A RADIATION-GRAFTED POLYETHYLENE FILM AND TESTED IN BOILERPLATE CELLS BY CHARACTERIZATION CYCLING TO 2C AND LEO CYCLING FOR 5000 CYCLES AT 80% DOD

- PERFORMANCE OF THE LAYERED ZIRCAR CLOTH/POLYETHYLENE FILM CELLS WAS COMPARABLE TO THE CELLS CONTAINING ASBESTOS SEPARATORS

- RESULTS OBTAINED WITH THE LAYERED POLYETHYLENE PAPER/ POLYETHYLENE FILM SEPARATOR AND THE LAYERED POLYPROPYLENE FELT/POLYETHYLENE FILM SEPARATOR CELLS WARRANTS FURTHER DEVELOPMENT WORK WITH THESE TYPES OF MATERIALS

- FLIGHTWEIGHT CELLS WILL BE FABRICATED USING THESE SEPARATOR MATERIALS

UPDATE OF A NICKEL HYDROGEN CYCLE LIFE MODEL

PRESENTED BY

LAWRENCE H. THALLER

THE AEROSPACE CORPORATION

FOR PRESENTATION AT

THE NASA AEROSPACE BATTERY WORKSHOP

HUNTSVILLE, ALABAMA

DECEMBER 4-6, 1990

CELL CAPACITY DIAGRAM

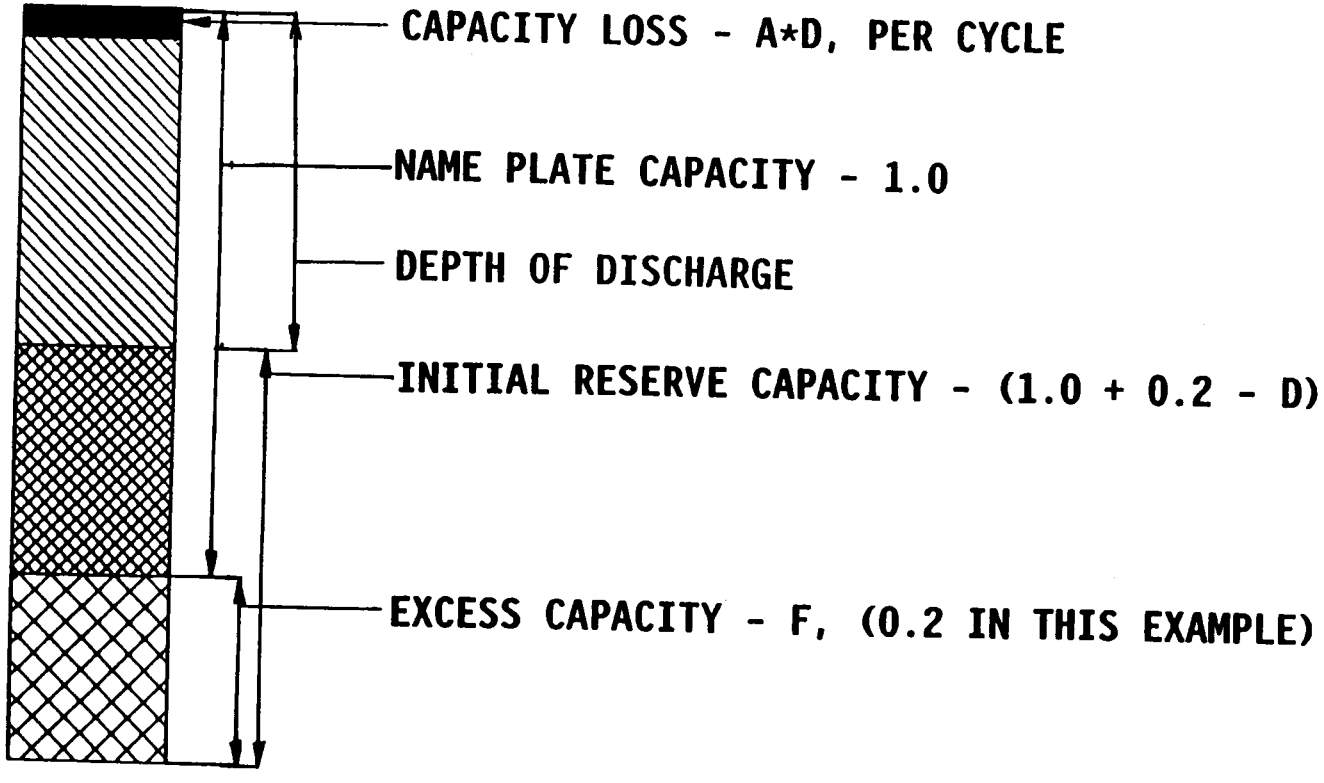

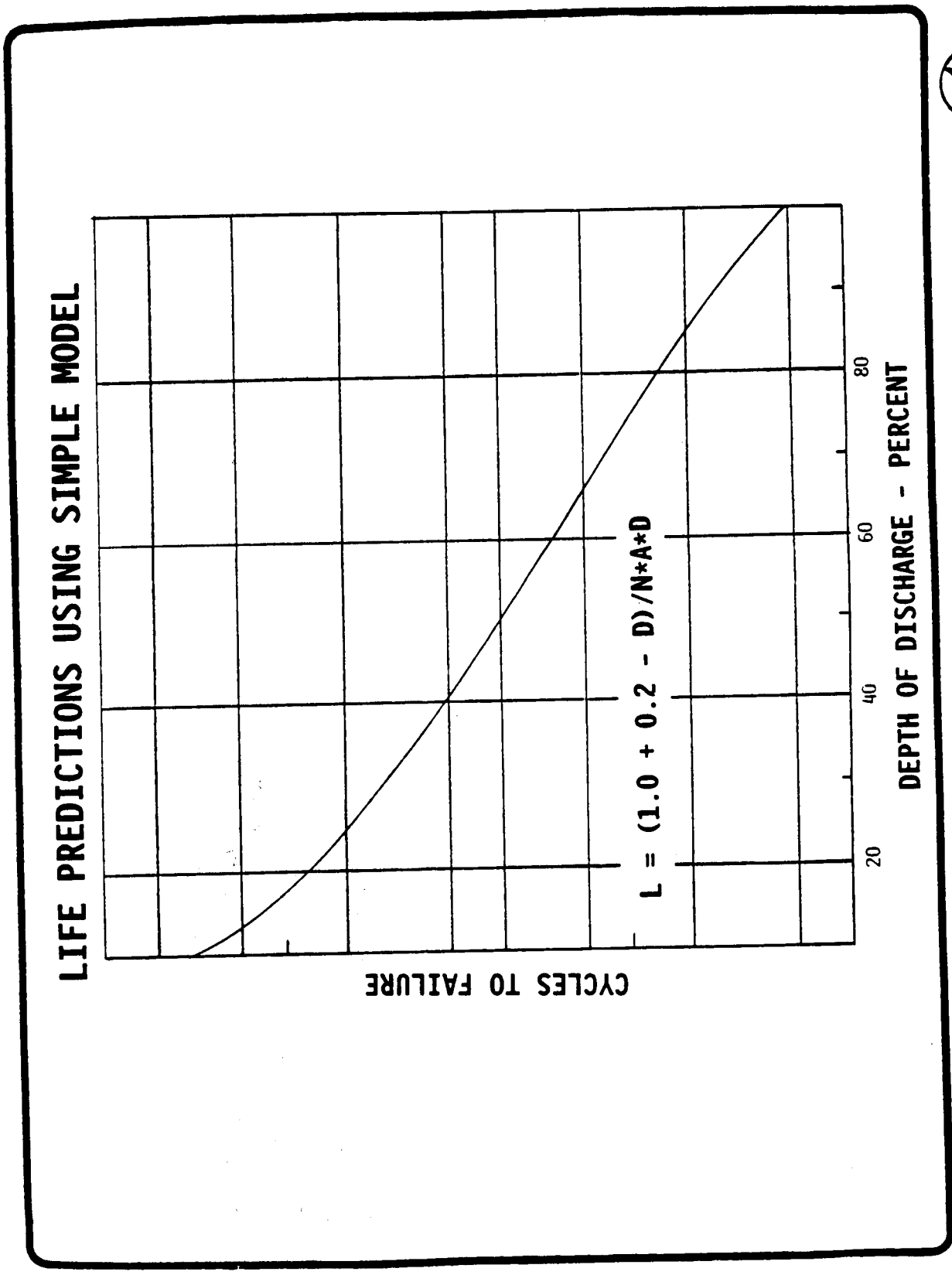
LIFE PREDICTIONS USING SIMPLE MODEL
CYCLES TO FAILURE
L = (1.0 + 0.2 - D)/N*A*D
20
40
60
80
DEPTH OF DISCHARGE - PERCENT

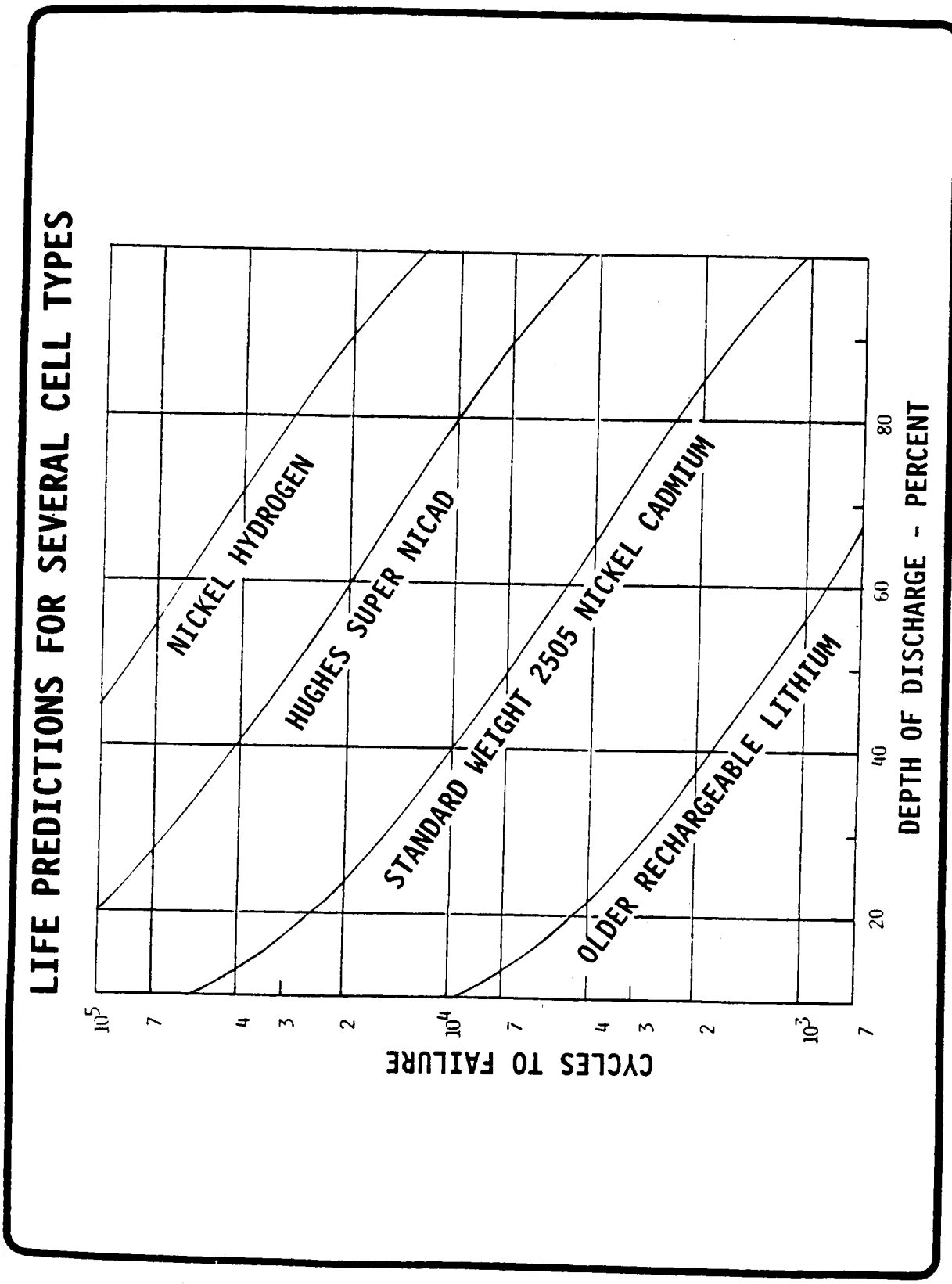
LIFE PREDICTIONS FOR SEVERAL CELL TYPES
NICKEL HYDROGEN
HUGHES SUPER NICAD
STANDARD WEIGHT 2505 NICKEL CADMIUM
OLDER RECHARGEABLE LITHIUM
CYCLES TO FAILURE
10^5
7
4
3
2
10^4
7
4
3
2
10^3
7
20
40
60
80
DEPTH OF DISCHARGE - PERCENT

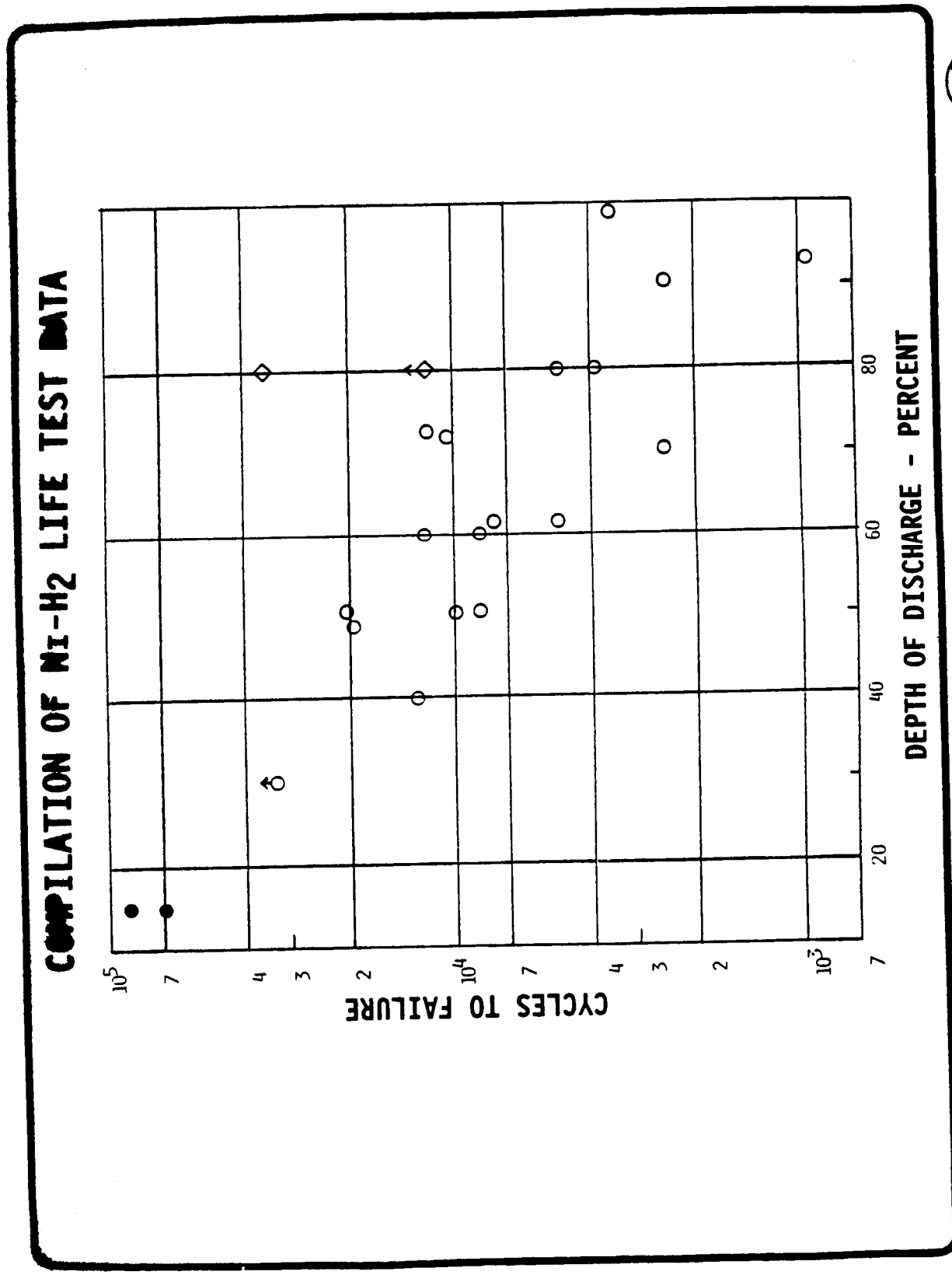
COMPILATION OF Ni-H2 LIFE TEST DATA
CYCLES TO FAILURE
DEPTH OF DISCHARGE - PERCENT
10^5
7
4
3
2
10^4
7
4
3
2
10^3
7
20
40
60
80

FRITTS' ELECTRODE STRAIN

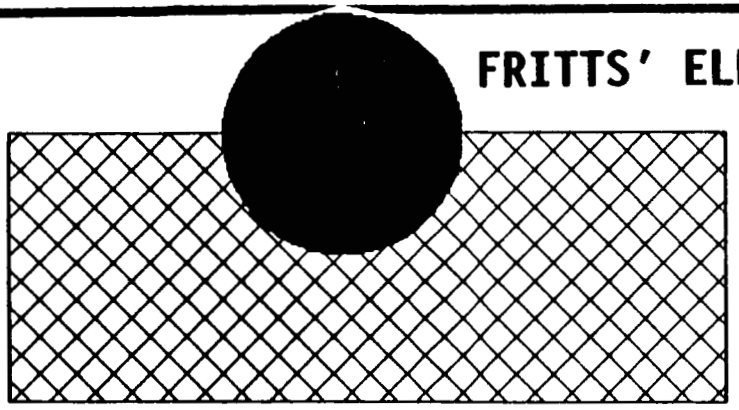

MEASURE PLAQUE HARDNESS

MEASURE PLATE EXPANSION

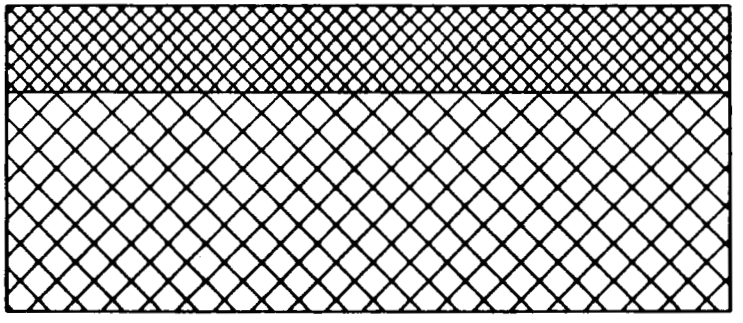

VOLUME OF CHARGED AND UNCHARGED MATERIAL SIMILAR

EXPANSION CHARACTERISTICS RELATED TO % COBALT

ELECTRODE STRAIN RELATED TO LOADING LEVEL OF ACTIVE MATERIAL AND PLAQUE HARDNESS

LIM'S ELECTRODE BENDING

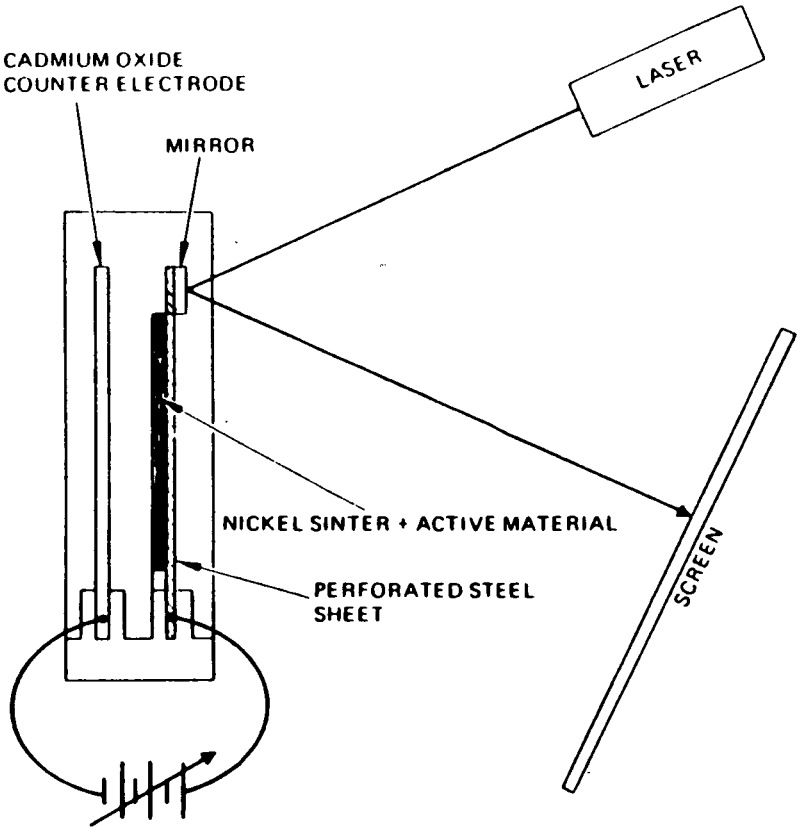

THE BENDING IS DIVIDED INTO A REVERSIBLE COMPONENT AND A CUMULATIVE IRREVERSIBLE COMPONENT

BENDING A FUNCTION OF ADDITIVES, DOD, KOH CONCENTRATION, ETC.

DAVOLIO'S FLEXURAL YOUNG'S MODULUS

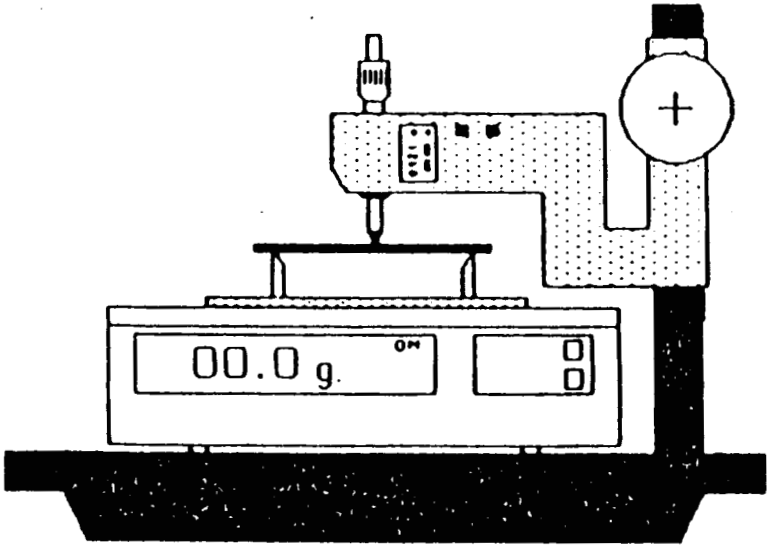

AT A CERTAIN DOD, THE ELECTRODE BECOMES STIFF

FUNCTION OF ADDITIVES, LOADING LEVEL, ELECTRODE TYPE, KOH CONCENTRATION

BEHAVIOR OF SINTERED NICKEL ELECTRODE

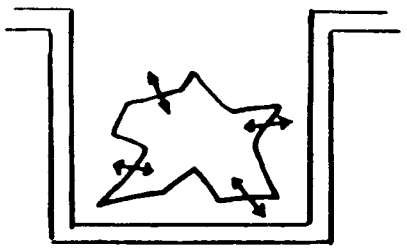

CONSIDERATIONS

1. MAGNITUDE OF THE CONTRACTION/EXPANSION
   - KOH CONCENTRATION
   - DEPTH OF DISCHARGE
   - ADDITIVES
   - OTHER

2. IMPACT OF CONTRACTION/EXPANSION
   - STRENGTH OF SINTER
   - LOADING LEVEL
   - TEXTURE OF ACTIVE MATERIAL
   - OTHER

VISUALIZATION OF MODIFIED MODEL

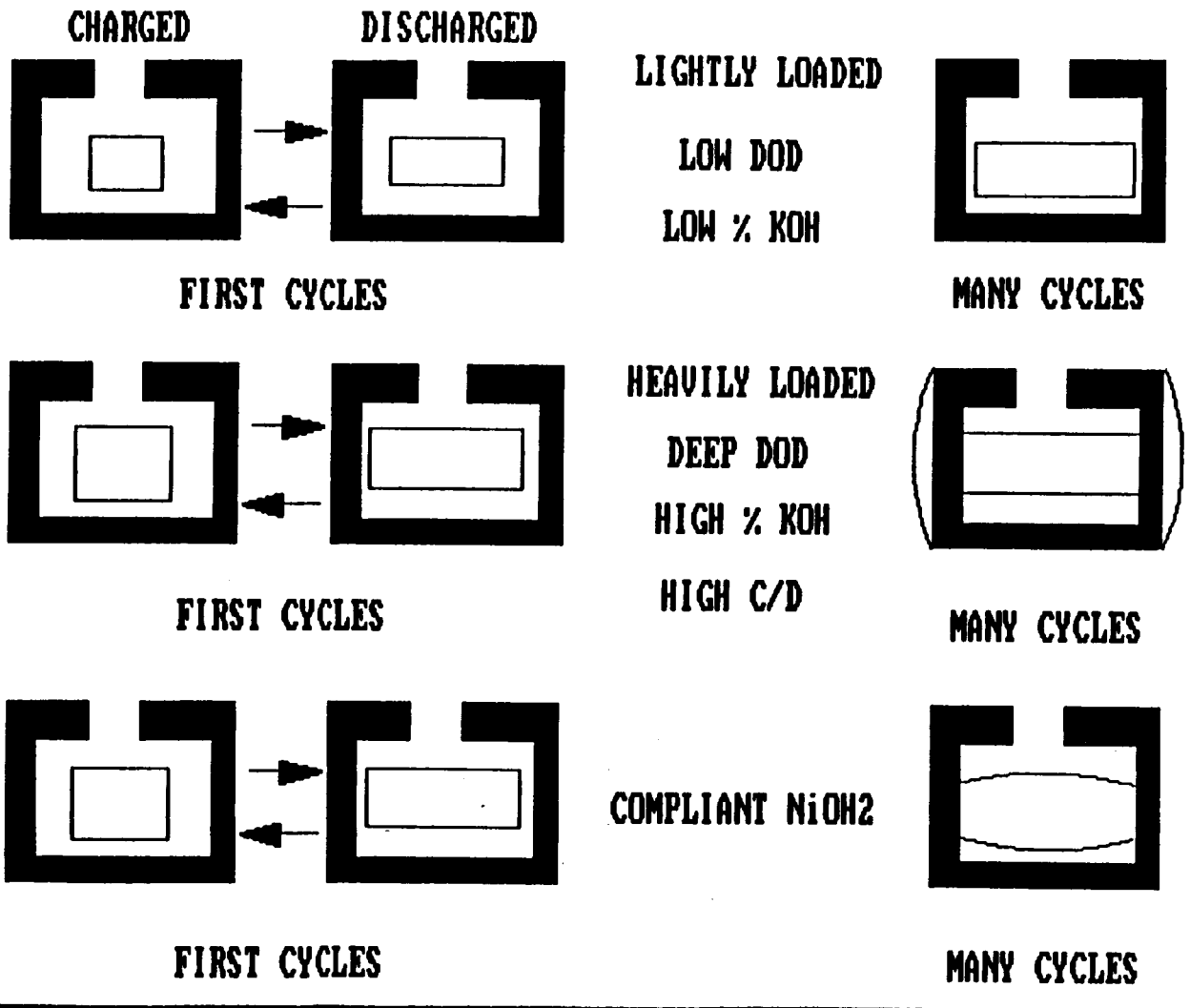

NICKEL HYDROGEN TECHNOLOGY STATUS

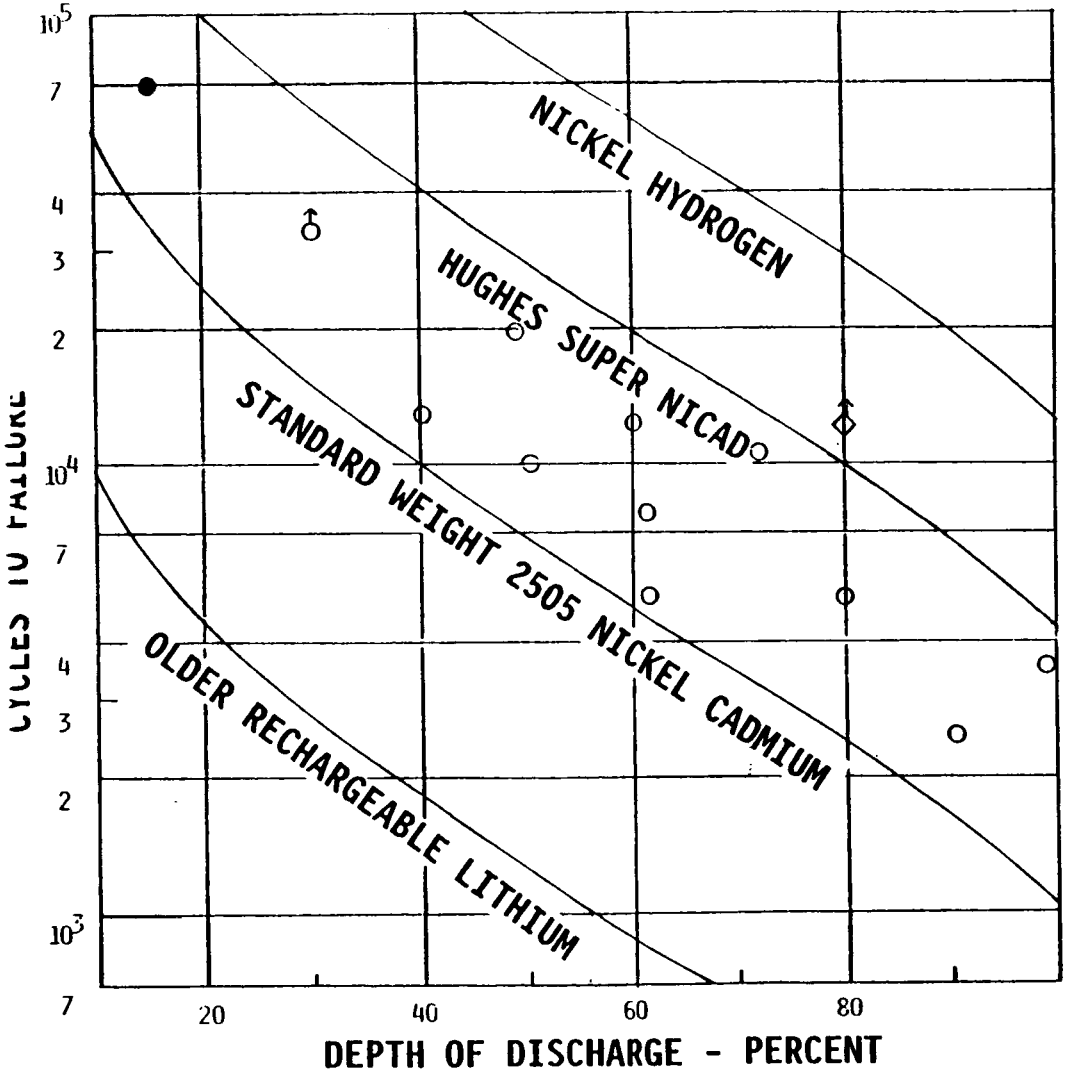

CONCLUSIONS

- SIMPLE WEAR OUT MODEL LIMITED IN APPLICATION
- TWO STEP MODEL MAY BE MORE ACCURATE
- MANY VARIABLES WILL AFFECT THE TWO STEP MODEL
- DOD AND KOH CONCENTRATION SIGNIFICANT FACTORS
- LEO CYCLE LIVES HAVE SHOWN PROGRESS - ROOM FOR GROWTH

N92-27163

HUBBLE SPACE TELESCOPE

BATTERY BACKGROUND

NASA/MSFC HST NICKEL-HYDROGEN BATTERY CONTRACT

- CONTRACT MOD 593 DATED 2 JUNE 1987 DIRECTED LMSC TO DESIGN, DEVELOP, AND DELIVER A NICKEL-HYDROGEN (NiH_2) BATTERY MODULE FOR THE HUBBLE SPACE TELESCOPE (HST) LOW EARTH ORBIT (LEO) MISSION PER NAS8-32697

- END ITEM HARDWARE DELIVERED WITHIN 30 MONTHS OF NASA CONTRACT AWARD BY EAGLE PICHER INDUSTRIES (EPI) LOCATED IN JOPLIN, MISSOURI

- TWO MODULES (FSM AND FM2) HAVE OPERATED SUCCESSFULLY ON-ORBIT WITH NO PROBLEMS SINCE THE HST LAUNCH ON 24 APRIL 1990

HST BATTERY DESIGN REQUIREMENTS

- COMMON (NICKEL-CADMIUM AND NICKEL-HYDROGEN)
  - PROVIDE CONTINUOUS ORBITAL POWER AT 26.4 TO 34.5 VDC
  - PROVIDE 259 Ah FOR CONTINGENCY S/A DEPLOYMENT
  - 30 MONTH CONTRACTUAL LIFE REQUIREMENT
- NICKEL-CADMIUM (330 Ah RATING FOR 6 BATTERIES AT BOL)
  - 30 MONTH OPERATIONAL LIFE
  - 60 MONTH STORAGE LIFE (AS A RESULT OF LAUNCH DELAYS)
- NICKEL-HYDROGEN (528 Ah RATING FOR 6 BATTERIES AT BOL)
  - 60 MONTH OPERATIONAL LIFE
  - 48 MONTH STORAGE LIFE

HST NICKEL-HYDROGEN BATTERY DEVELOPMENT

- A NiH_2 MODULE WITH THREE ELECTRICALLY DISTINCT BATTERIES SHARING A COMMON MECHANICAL STRUCTURE WAS DESIGNED AS AN ORBITAL REPLACEMENT UNIT (ORU) TO BE INSTALLED ON EITHER BAY DOOR 2 OR 3 OF THE HST SUPPORT SYSTEM MODULE (SSM) TO REPLACE SIX TYPE 44 FLIGHT NiCd BATTERIES

- TWO MODULES MAKE UP THE FULL NiH_2 BATTERY COMPLEMENT OF SIX BATTERIES, EACH RATED AT 88 Ah TO 1.2 Vdc PER CELL AT 15 Amp AT 0°C AND HAVING A MINIMUM ORBITAL LIFE OF 5 YEARS AT 12 PERCENT DEPTH OF DISCHARGE (DOD)

- ONE STRUCTURAL ENGINEERING BATTERY AND FIVE MODULES WERE DELIVERED IN 1989 BY EAGLE PICHER INDUSTRIES (EPI) LOCATED IN JOPLIN, MISSOURI

HST NICKEL-HYDROGEN BATTERY MODULE

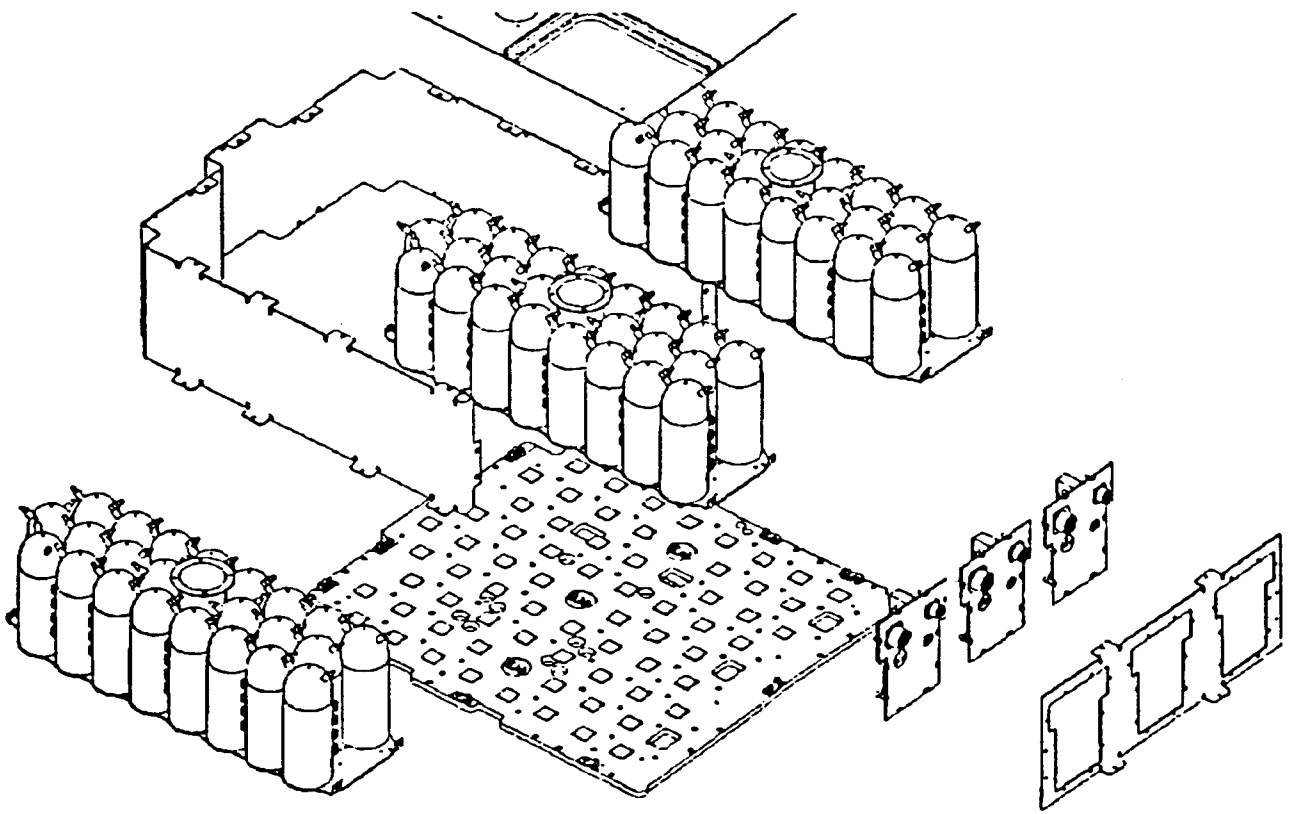

HST NiH_2 BATTERY MODULE HARDWARE

FIVE FULL-UP MODULES (THREE BATTERIES PER MODULE, EACH WITH ELECTRONICS)

- TEST MODULE 1 (DELIVERED APRIL 1989)
  - THERMAL VACUUM TEST COMPLETED AT MSFC
  - LIFE TEST UNDER WAY AT MSFC (1-YEAR COMPLETED AT LAUNCH)

- TEST MODULE 2 (DELIVERED APRIL 1989)
  - SPECIAL RANDOM VIBRATION TESTS COMPLETED AT VENDOR
  - VEHICLE ELECTRICAL CHECK-OUT COMPLETED AT LMSC
  - LIFE TEST UNDER WAY AT MSFC (1-YEAR COMPLETED AT LAUNCH)

- QUALIFICATION MODULE (ORIGINAL FLIGHT SPARE DELIVERED AUGUST 1989)
  - QUALIFICATION COMPLETED AT CELL, BATTERY, AND MODULE LEVELS
  - EMI/EMC TEST AND SPECIAL DYNAMIC IMPEDANCE TEST COMPLETED
  - NEW CELL ACTIVATION PROCEDURE VALIDATED BY VENDOR
  - THERMAL VACUUM TEST AND PAD CHARGING TEST COMPETED AT MSFC
  - ACCEPTANCE DATA REVIEW COMPLETED (LAUNCHED 24 APRIL 1990)

- FLIGHT MODULE 1 (FINAL FLIGHT SPARE DELIVERED NOVEMBER 1989)
  - ACCEPTANCE DATA REVIEW COMPLETED (IN COLD STORAGE AT EPI)

- FLIGHT MODULE 2 (DELIVERED OCTOBER 1989)
  - ACCEPTANCE DATA REVIEW COMPLETED (LAUNCHED 24 APRIL 1990)

PRESSURE VESSEL DESIGN

- PRESSURE VESSEL WALL UTILIZES 0.040 INCH HYDROFORMED INCONEL 718 SHEET
- ELECTRON BEAM WELDING (EBW) TECHNIQUE OPTIMIZED FOR PRESSURE VESSEL WELDS SUCH THAT NO CRITICAL FLAWS HAVE BEEN FOUND IN SPECIFIED SAMPLES
- PRESSURE VESSEL LOT QUALIFICATION INCLUDES TWO RANDOMLY SELECTED VESSELS SUBJECTED TO 120,000 PRESSURE CYCLES PRIOR TO INDUCING FAILURE
- ALL TEST CELLS OF FLIGHT CONFIGURATION BURST AT 4800 PSI OR GREATER (4 TO 1 SAFETY FACTOR FOR MEOP OF 1200 PSI)
- CELL DESIGN MEETS ALL NASA FRACTURE CONTROL REQUIREMENTS FOR MANNED MISSIONS (NO EVIDENCE OF HYDROGEN EMBRITTLEMENT FOUND)

HST NiH_2 CELL DESIGN

- PINEAPPLE SLICE BACK-TO-BACK 3.5 INCH DIAMETER ELECTRODE STACK DESIGN
- 48 DRY-SINTERED ELECTRODES WITH ZIRCONIUM OXIDE WALL WICK FOR IMPROVED ELECTROLYTE MANAGEMENT
- RABBIT EAR TERMINAL CONFIGURATION TO MINIMIZE OVERALL CELL HEIGHT
- DESIGN SERVICE LIFE OF 30,000 CYCLES AT 14% AVERAGE DEPTH-OF-DISCHARGE
- 93 Ah CELL NAMEPLATE RATING AT 0°C

OFFSET NON-OPPOSING VS RABBIT EAR CELL

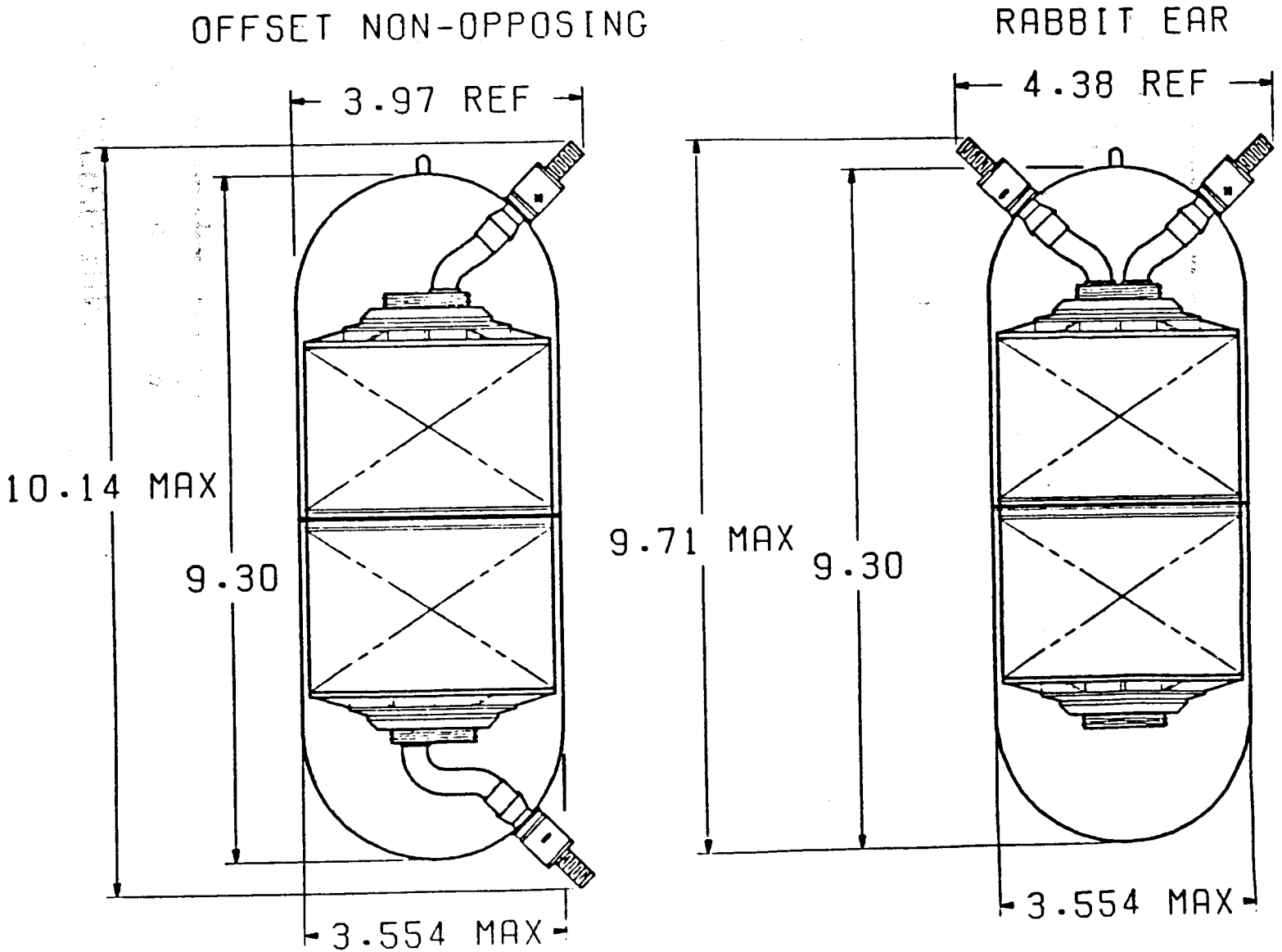

HST NiH_2 SPECIFIED CAPACITY

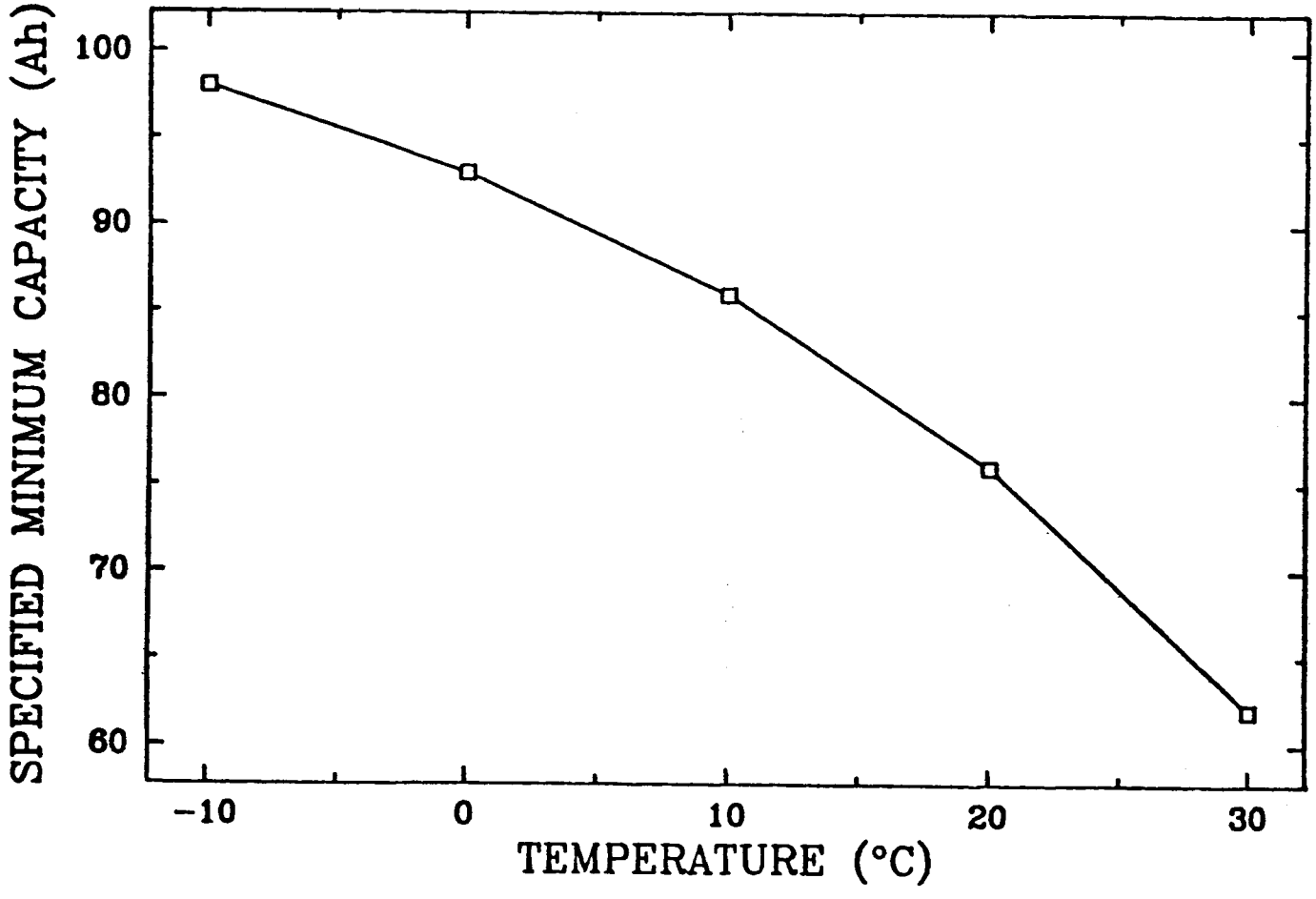

HST NiH_2 BATTERY DESIGN

- CELLS WRAPPED IN SILICONE-COATED FIBERGLASS CLOTH AND CLAMPED IN CAST ALUMINUM SLEEVES WHICH ARE FASTENED TO 0.125 INCH ALUMINUM BASEPLATE
- TWO CONNECTORS FOR POWER AND TELEMETRY/HEATER CIRCUITS (INCLUDES TWO CELL STRAIN GAGE MONITORS FOR PRESSURE AND CAPACITY MEASUREMENTS)
- BATTERY DIMENSIONS AND WEIGHT
  - 33.5 x 10.1 x 10.1 INCHES
  - 130 POUNDS
- BATTERY NAMEPLATE RATING OF 88 Ah AT 0°C

HST NiH_2 MODULE DESIGN

- THREE BATTERIES HOUSED IN AN ALUMINUM ENCLOSURE MOUNTED TO A 0.5 INCH ALUMINUM BASEPLATE WHICH HAS 14 ORBITAL REPLACEMENT UNIT LATCHES
- INSIDE SURFACES OF ALUMINUM ENCLOSURE AND COVER LINED WITH POLYIMIDE FOAM FOR ELECTRICAL SHORT PROTECTION
- TWO BRIGHT YELLOW HANDLES FASTENED TO COVER FOR ON-ORBIT HANDLING
- MODULE DIMENSIONS AND WEIGHT
  - 36.0 x 31.8 x 11.2 INCHES (ADD 3.0 INCHES FOR HANDLE HEIGHT)
  - 470 POUNDS

SYSTEM DESIGN

- TWO MODULES CONNECTED TO A SYSTEM OF THREE DIODE AND MAIN BUSSES
- INDIVIDUAL BATTERIES CAN BE SWITCHED OFF-LINE FOR DEEP DISCHARGE BY A 5 OR 50 OHM RESISTOR TO DETERMINE BATTERY RESERVE CAPACITY
- EACH BATTERY HAS A CHARGE CURRENT CONTROLLER (CCC) FOR TERMINATING FULL-RATE CHARGE BASED ON TEMPERATURE COMPENSATED BATTERY VOLTAGE
- EACH MODULE FASTENED TO AN EXTERIOR DOOR OF THE HST EQUIPMENT SECTION
- MULTI-LAYER INSULATION (MLI) AND PANEL OF THERMALLY CONTROLLED LOUVERS LOCATED ON OUTSIDE OF EXTERIOR DOORS TO MAINTAIN SPECIFIED TEMPERATURES

HUBBLE SPACE TELESCOPE

BATTERY SYNOPSIS

HST NICKEL-HYDROGEN OVERVIEW

- TEST DATA BASE AVAILABLE FOR HST MISSION AT LAUNCH
  - MSFC SIX-BATTERY TEST (COMPLETED 12 MONTHS)
  - EAGLE PICHER CELL TEST (COMPLETED 36 MONTHS)
- CAN TOLERATE LIMITED CELL REVERSALS AND OVERCHARGE
- BETTER CELL MANUFACTURING PROCESS CONTROLS THAN NiCd
- V/T CHARGE CONTROL SYSTEM DEVELOPED FOR NiCd WORKS WELL WITH NiH_2
- HIGHER SELF-DISCHARGE RATE REQUIRES SPECIAL HANDLING OPERATIONS FOR LAUNCH (DOES NOT AFFECT ORBITAL OPERATIONS OR LIFE PERFORMANCE)
- 60+ MONTH PROBABLE LIFE WITH 48 MONTH STORAGE LIFE

HST NiH_2 SELF-DISCHARGE

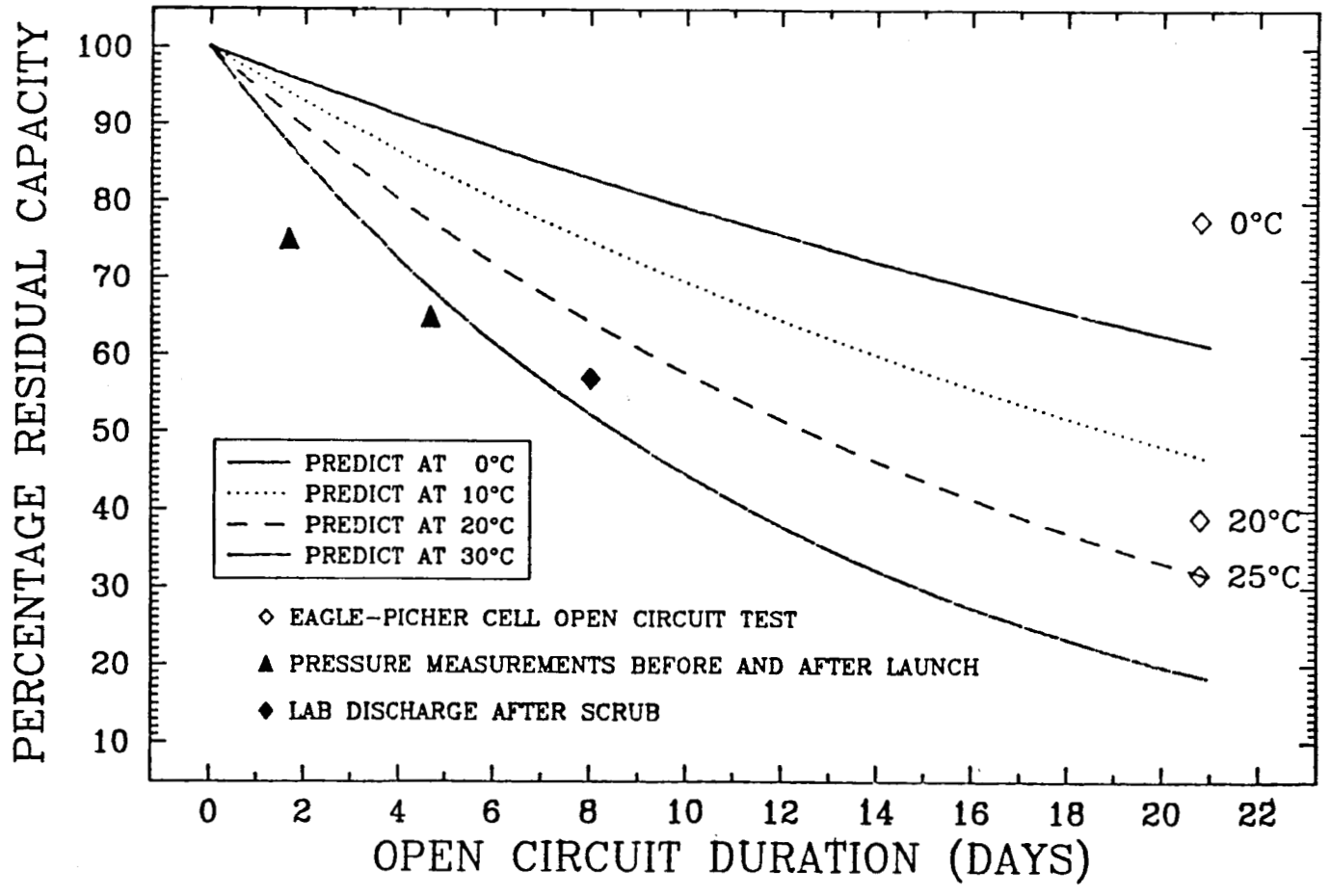

KSC BATTERY CHARGING ON THE PAD

- NOMINAL BATTERY STATE OF CHARGE MAINTAINED ON THE PAD BY STEP CHARGING FOLLOWING STANDARD CYCLING AND RECHARGE AT 28°F IN THE BATTERY LAB
  - 8.0 Amp CHARGE FOR 2.0 MINUTES WITH 68°F MAXIMUM BATTERY TEMPERATURE LIMIT CONTROLLED BY OPEN CIRCUIT PERIODS
  - OPEN CIRCUIT FOR 4.0, 5.5, 8.0, 10.0, OR 13.0 MINUTES DEPENDING ON THERMAL CONDITIONS AND BATTERY CHARGE EFFICIENCY
  - MAXIMUM BATTERY CHARGE ACHIEVED ON THE PAD WITH 50°F AIR BLOWING ON THE MODULE WAS 65 Ah USING AN 8.0 MINUTE OPEN CIRCUIT PERIOD
  - DEW POINT CONTROLS LOWER TEMPERATURE LIMIT OF COOLING AIR WHICH AFFECTS MAXIMUM ACHIEVABLE BATTERY STATE OF CHARGE
- LAST MINUTE BATTERY INSTALLATION ON THE PAD RESULTS IN HIGHEST STATE OF CHARGE FOR LAUNCH
  - REQUIRES EXTRA HANDLING AND ELECTRICAL CHECK-OUT PROCEDURES
- EITHER ON-THE-PAD INSTALLATION OR VPF PROCESSING REQUIRES PERIODIC MONITORING OF STRAIN GAGES (CELL PRESSURES) TO VERIFY NiH_2 BATTERY STATE OF CHARGE

HST 6 BATTERY CHARGE RETENTION

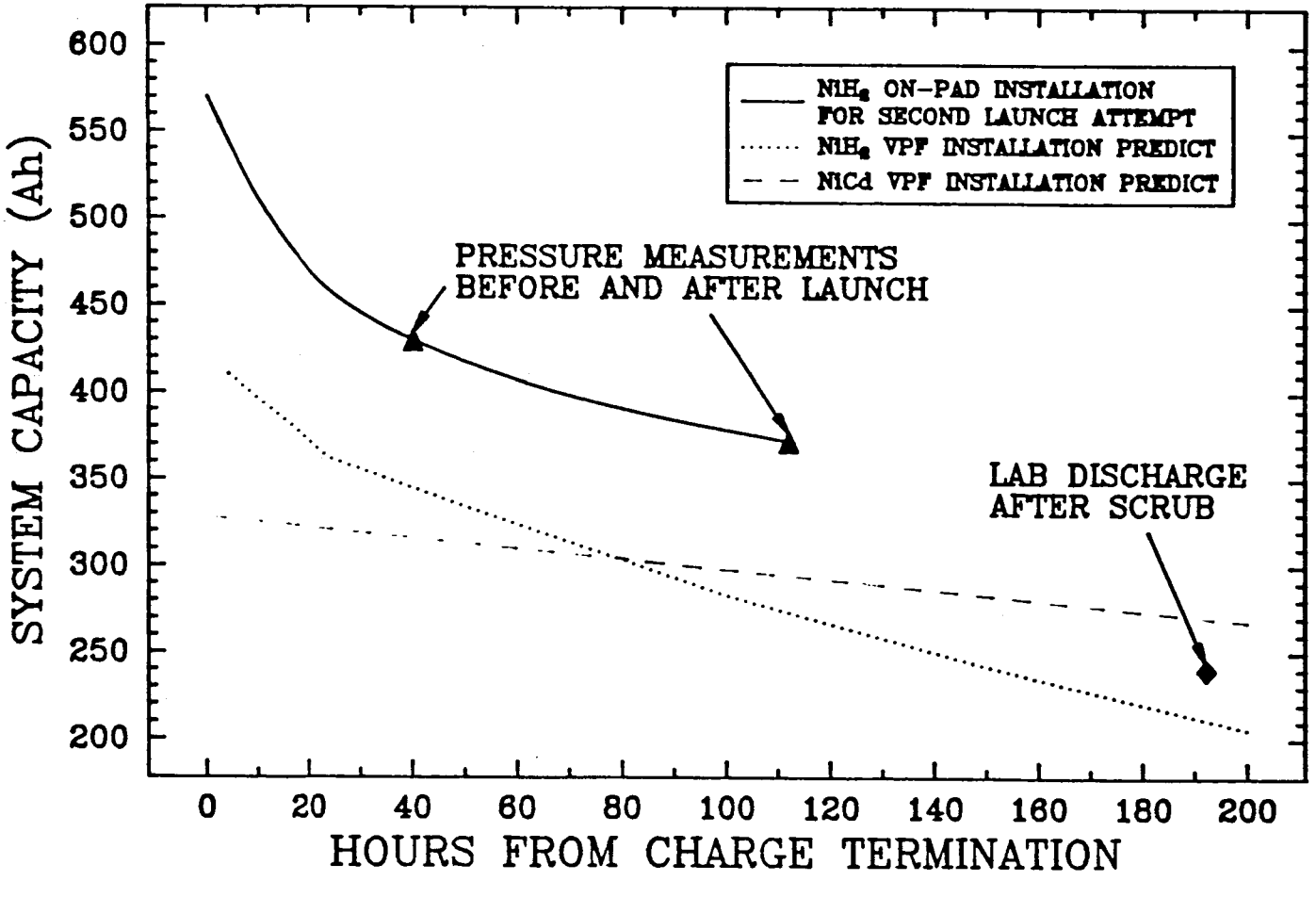

KSC BATTERY LAB CHARGING / DISCHARGING PROCEDURES

- HIGHEST BATTERY CAPACITY OBTAINED BY CHARGING IN THERMALLY STABLE ENVIRONMENT WITH TEST CONDITIONS SIMILAR TO BATTERY/MODULE ATP
  - MODULE MOUNTED TO FLAT COLD PLATE COOLED BY AUXILIARY COOLING SYSTEM DESIGNED BY EPI
  - COLD PLATE ATTACHED TO HANDLING DOLLY LOCATED IN WALK-IN FREEZER
- CHARGE/DISCHARGE CONDITIONS:

	COLD PLATE TEMP (°F)	FREEZER TEMP (°F)
9.3 Amp CHARGE FOR 10 HOURS	28 ± 4	28 ± 4
4.0 Amp CHARGE FOR 14 HOURS	16 ± 4	28 ± 4
15.0 Amp DISCHARGE TO 22.0 Vdc	16 ± 4	28 ± 4
FIVE OHM RESISTIVE LOAD TO 1.0 Vdc OR 17 HOURS, WHICHEVER COMES FIRST	28 ± 4	28 ± 4

HST MODULE FSM
32F CAPACITY CYCLES

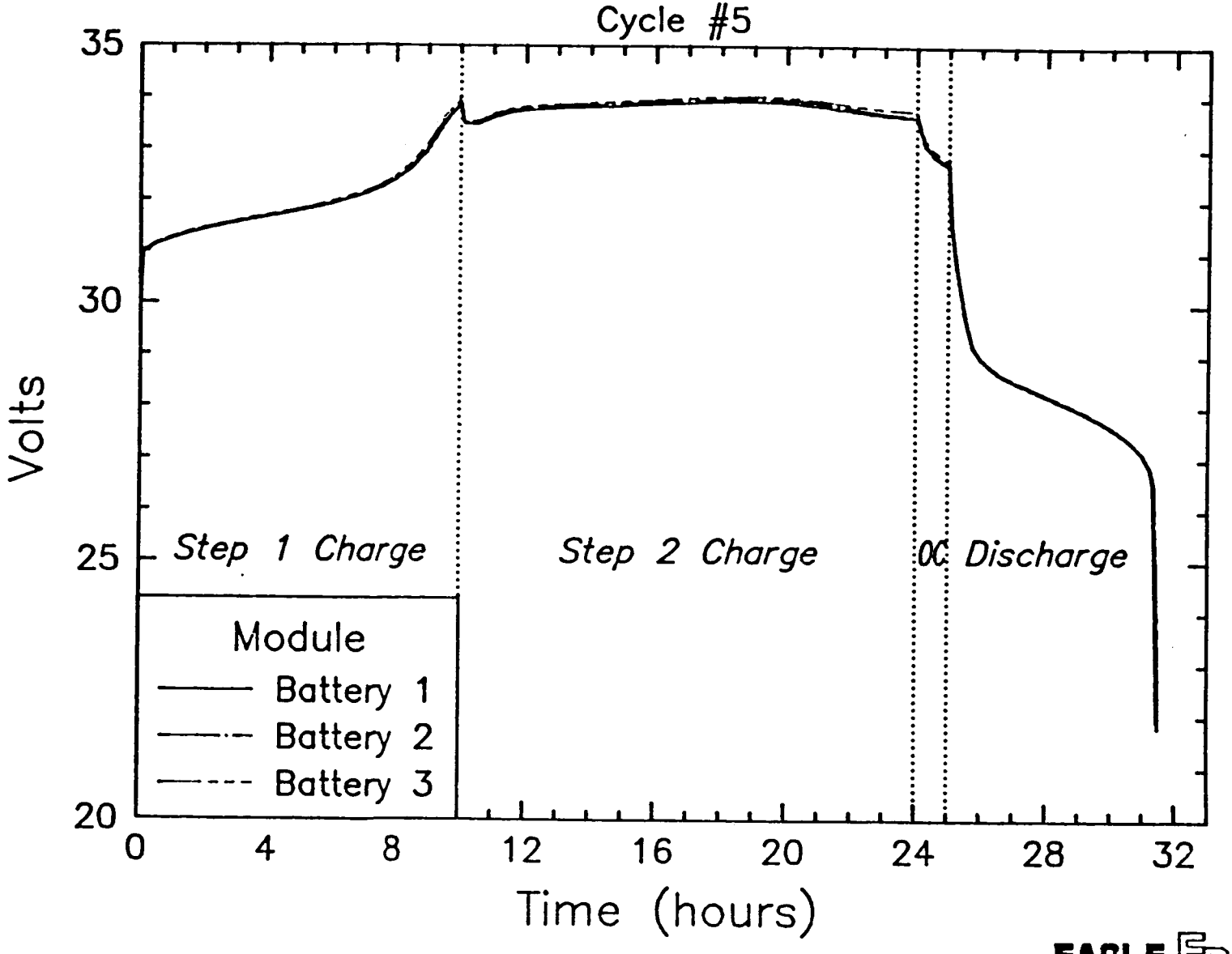

EAGLE PICHER

HST MODULE FSM
32F CAPACITY CYCLES

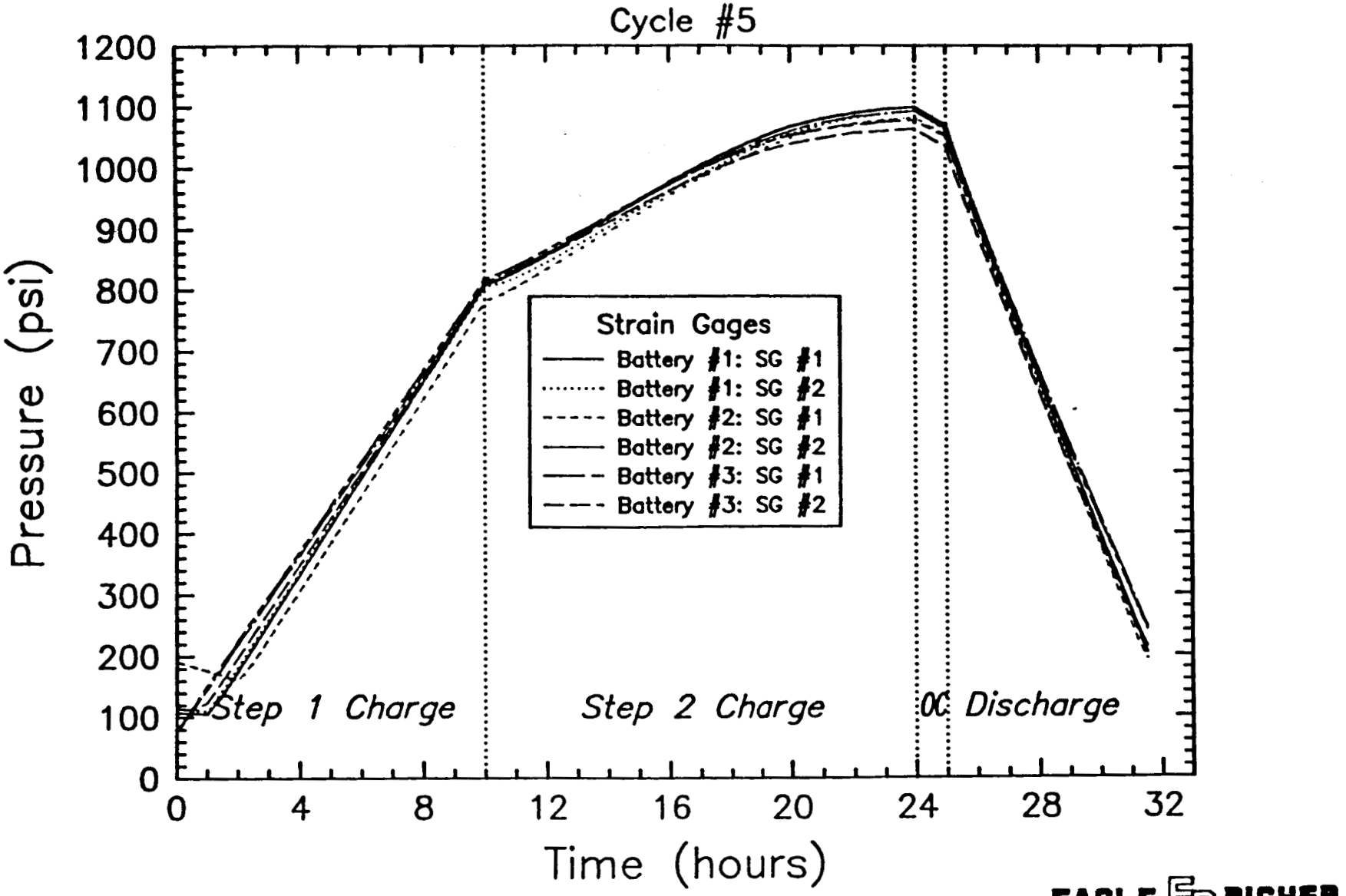

EAGLE PICHER

SUMMARY

- HST NICKEL-HYDROGEN BATTERIES MANUFACTURED BY EAGLE-PICHER ARE PERFORMING TO SPECIFICATION WITH HIGHER THAN PREDICTED CAPACITIES AFTER SEVEN MONTHS ORBITAL OPERATIONS
- BATTERIES HAVE EXPERIENCED OVER 3200 ECLIPSE PERIODS WITH DEPTHS-OF-DISCHARGE RANGING FROM 5 TO 9 PERCENT WHILE OPERATING AT 0±3°C
- BATTERY CELL STRAIN GAGE MONITORS INDICATE NOMINAL END OF CHARGE CAPACITIES RANGING FROM 85 TO 90 Ah AT 0°C
- NASA/MSFC BATTERY LIFE TEST SHOWS NO SIGNIFICANT VOLTAGE PERFORMANCE DEGRADATION AFTER 1 1/2 YEARS OF ORBITAL OPERATION SIMULATION
- EAGLE-PICHER DEVELOPMENT CELL OPERATED AT 15 PERCENT DEPTH-OF-DISCHARGE FOR OVER 36,700 CYCLES AT 0°C SHOWS NO CAPACITY OR VOLTAGE DEGRADATION

NASA

HUBBLE SPACE TELESCOPE
NiH2
SIX BATTERY TEST

Thomas H. Whitt & J. Roy Lanier
NASA/Marshall Space Flight Center
Huntsville, Alabama 35812

HST NiH2 SIX BATTERY TEST

A HST EPS breadboard with six HST NiH2 batteries began operation at MSFC in May of 1989. The primary objectives of the test are:

1. Get a better understanding of the operating characteristics of the NiH2 Batteries in the HST EPS by simulating every aspect of the expected operating environment.
2. Determine the optimum charge level and charge scheme for the NiH2 batteries in the HST EPS.
3. Predict the performance of the actual HST EPS.
4. Observe the aging characteristics of the batteries.
5. Test different EPS anomalies before experiencing the anomalies on the actual HST.

NASA

HST NiH2 BATTERIES

- Manufactured by Eagle Picher in Jolpin, Missouri
- The first reported nonexperimental LEO application of NiH2 Batteries
- Each of the 6 batteries consist of 23 cells with only 22 cells electrically connected
- Battery nameplate capacity of 88 Ah
- The batteries cycle to a 6–10% depth of discharge (DOD)
- Each battery weighs 71 kg
- Internal cell design is a dual stack, back–to–back electrode configuration consisting of alternating positive and negative electrodes with the separator comprised of a double layer zircar cloth
- The electrolyte is a 27% potassium hydroxide solution
- The pressure vessel is 3.5 inches in diameter and has a wall thickness of .04 inches

HST NiH2 BATTERIES

The HST NiH2 batteries are made up of 23 individual pressure vessels with a nameplate capacity of 93 Ah. The battery was designed to be either 22 or 23 cells. Each battery has 23 cells in its footprint with one cell not electrically connected. The use of only 22 cells/battery in the HST EPS allows for more complete charge of the batteries (i.e. charging the cells to a higher voltage and capacity). The benefit of 23 cells/battery would have been a slightly higher operating voltage of the battery and would have resulted in a more effective utilization of the solar array.

The internal cell design is a dual stack, back-to-back electrode configuration. The back-to-back design consists of alternating positive and negative electrode assemblies with separator consisting of a double layer of zircar cloth between each assembly. The positive electrode assembly consists simply of two "back-to-back" positive electrodes while the negative electrode assembly consists of a polypropylene gas screen between two negative electrodes. The electrolyte used in the cell is a 27% (before activation) potassium hydroxide solution.

The pressure vessel is made of hydroformed Inconel 718 material. The vessel is 3 1/2 inches in diameter and has a wall thickness of .040 inches. A flame sprayed zirconium oxide coating is on the interior surface of the vessel. Another notable design feature used on this vessel is the placement of both the positive and negative terminals on the same end of the vessel in a "rabbit-ear" configuration.

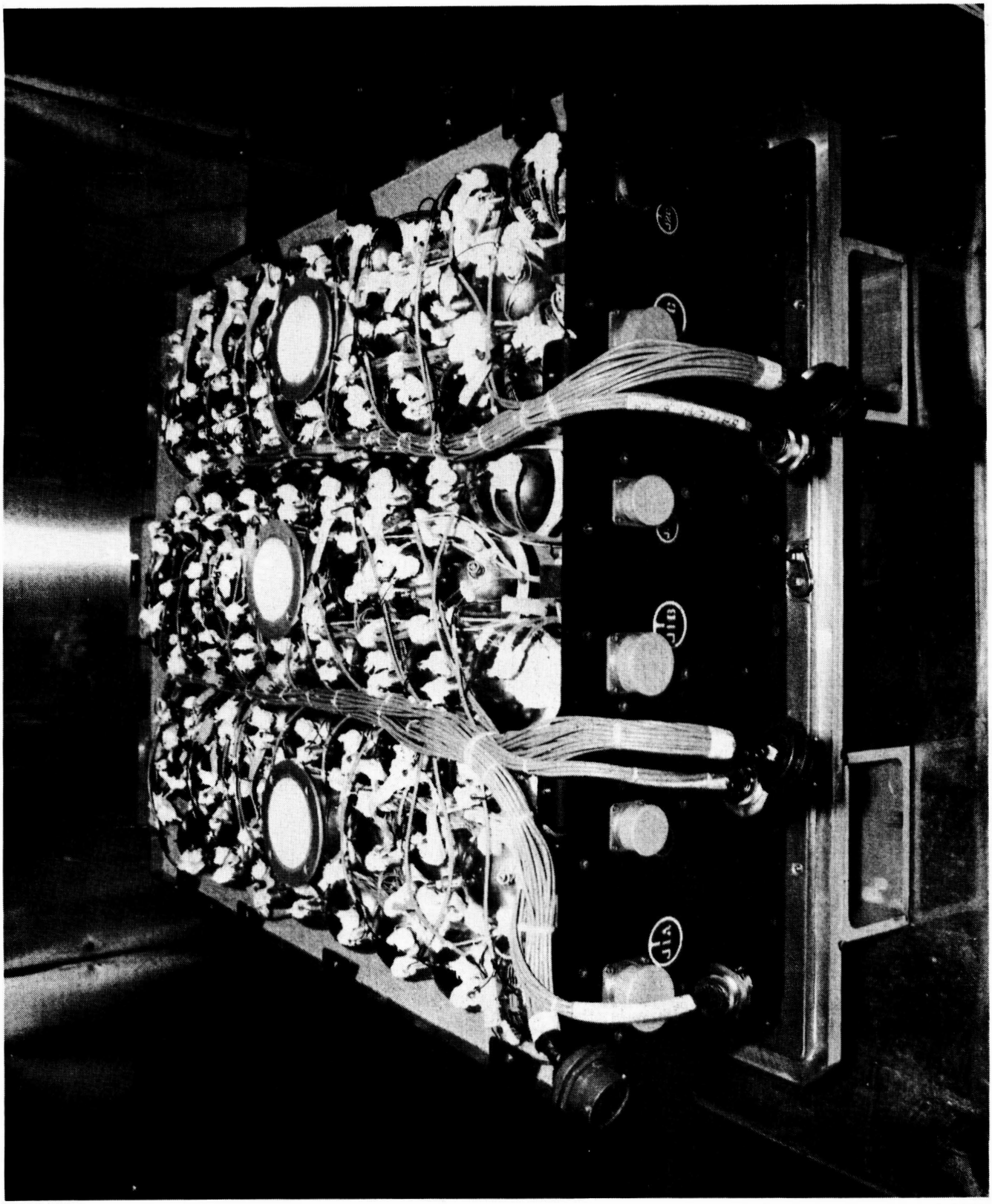

TEST MODULE 1 (TM--1) with cover removed

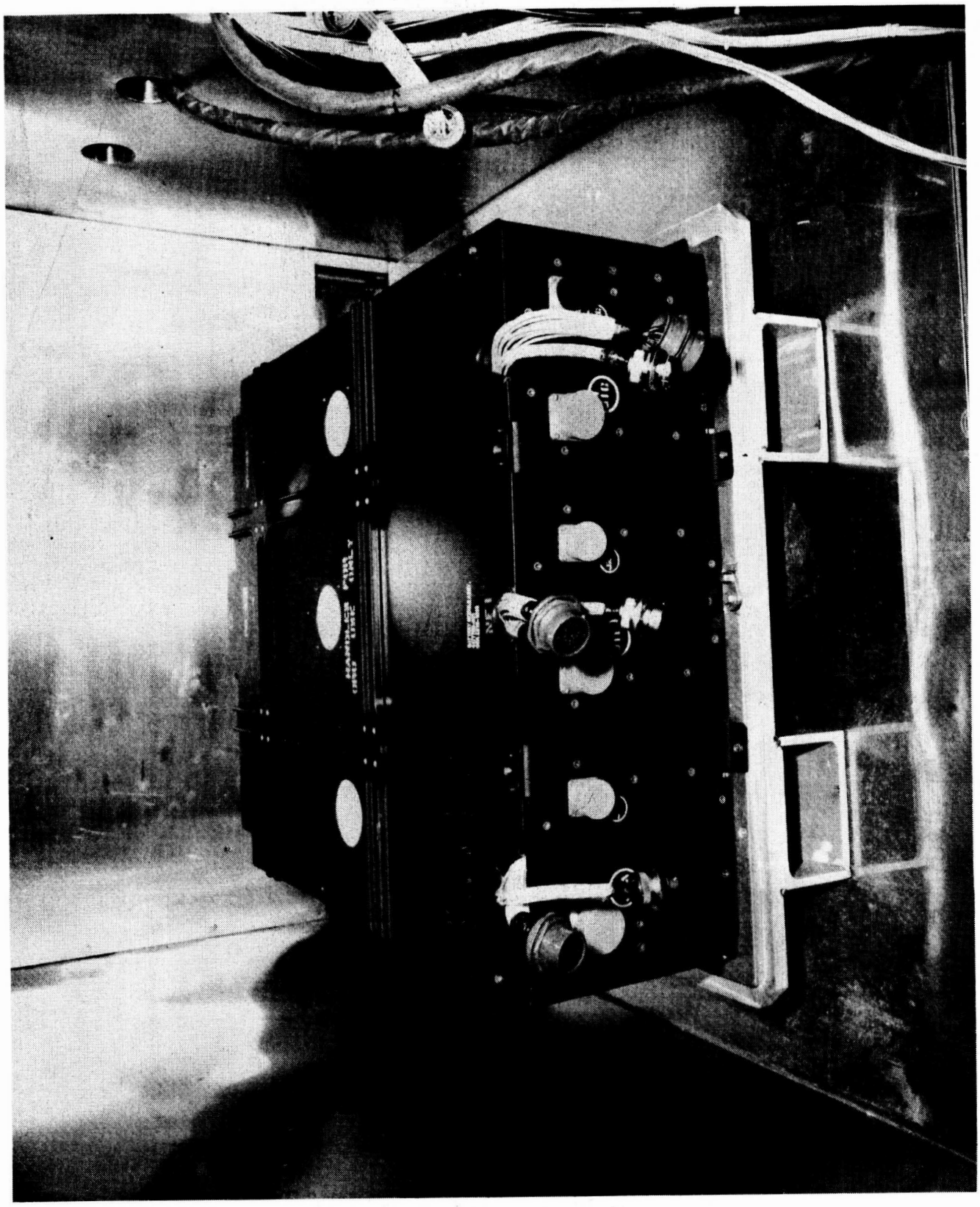

TEST MODULE 1 (TM–1)

BLOCK DIAGRAM OF THE HST EPS

This is a simplified diagram of the HST EPS breadboard. This breadboard contains every pertinent element of the actual HST EPS that is necessary for testing the NiH2 batteries. In each battery channel one power supply simulates the two SPAs on the K1 relay and one power supply simulates the one SPA on the K2 relay. The 13th power supply simulates the two SPAs that are wired directly to the diode bus. The TRIM and CCC relay operations are simulated by a control computer. Battery test modules 1 and 2 (TM-1 and TM-2) contain the 6 test batteries used in the breadboard. The loads are simulated by three programmable load banks.

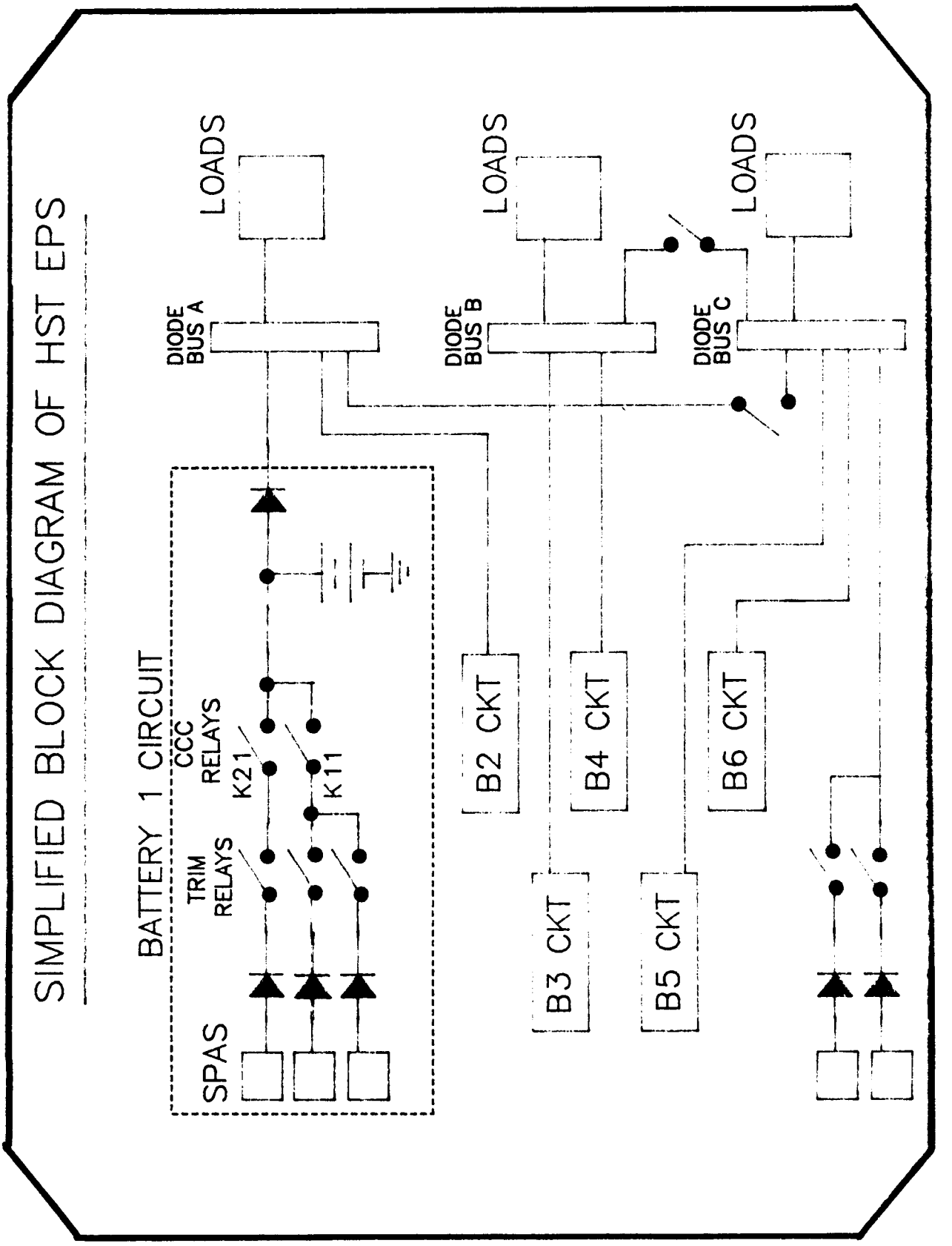
SIMPLIFIED BLOCK DIAGRAM OF HST EPS
LOADS
LOADS
LOADS
DIODE BUS A
DIODE BUS B
DIODE BUS C
BATTERY 1 CIRCUIT
CCC RELAYS
K21
K11
TRIM RELAYS
SPAS
B2 CKT
B4 CKT
B6 CKT
B3 CKT
B5 CKT

BATTERY CHARGE CONTROL

The battery charge control hardware consists of six Charge Current Controllers (CCC) . The CCC for B1 controls K21 and K11, and the CCC for B2 controls K22 and K12, etc. Each CCC provides four selectable levels of temperature compensated charge cutoff voltages for both K2 and K1, resulting in eight charge cutoff voltage levels shown . The CCC opens up the K1 and K2 relays when the battery voltage reaches the selected level during charge. When a K1 relay opens the 2 SPAs supplying current through that relay are removed from the system. When a K2 relay opens only one SPA is removed from the system. The trim relays are controlled by the Flight Computer. The two charge schemes used for battery charging are known as the two step-to-trickle charge scheme and the step-taper charge scheme.

The step-taper is the hardware control charge scheme where the total solar array current is decreased each time one of the batteries reaches the K1 or K2 voltage levels. This decreases the charge current to the batteries in a taper-like fashion. In the two step-to-trickle charge scheme when the first battery reaches the CCC cutback level, 1 or 2 SPAs (1 for a K2 cutback or 2 for a K1 cutback) are disconnected from the battery channel that reaches the cutback level. When the second battery reaches the cutback level, SPAs are disconnected one at a time until the total battery charge current drops below the maximum trickle charge current setting (1 to 2 amps per battery).

During the sun period of an orbit, the solar arrays supply the electrical loads for the telecsope and recharge the batteries. The electrical loads to the telescope are not affected when portions of the solar array are switched out of the system with the battery charge control schemes. The decrease in solar array current only decreases battery charge current. The electrical loads draw the current they need and the batteries get the excess. During the eclipse portion of the orbit, the batteries supply the electrical load.

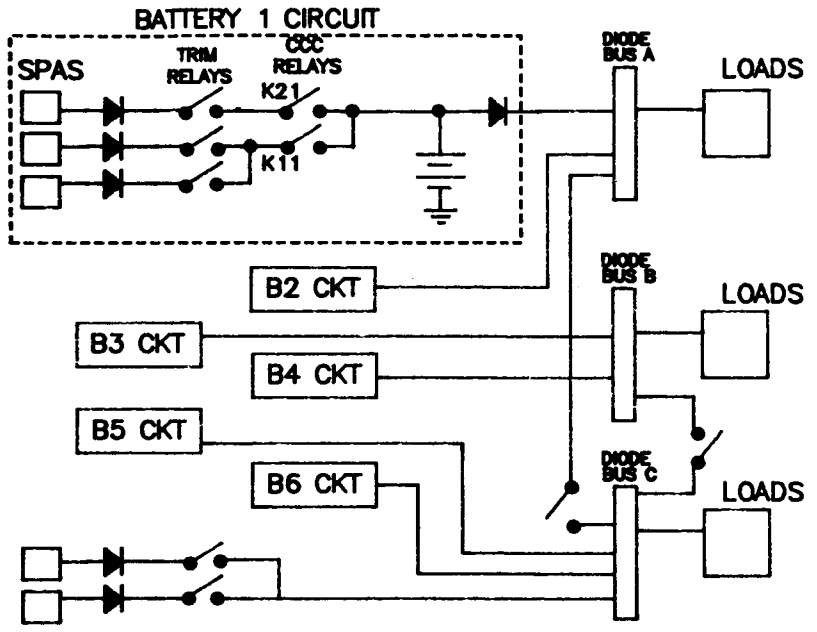
BATTERY 1 CIRCUIT
SPAS
TRIM RELAYS
CCC RELAYS
K21
K11
DIODE BUS A
LOADS
B2 CKT
DIODE BUS B
LOADS
B3 CKT
B4 CKT
B5 CKT
B6 CKT
DIODE BUS C
LOADS

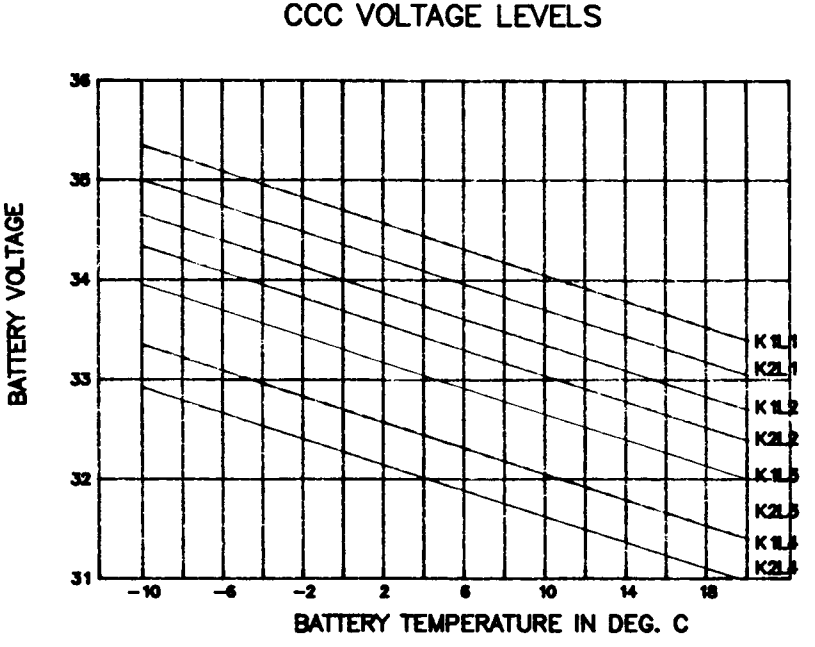
CCC VOLTAGE LEVELS
BATTERY VOLTAGE
36
35
34
33
32
31
-10
-6
-2
2
6
10
14
18
BATTERY TEMPERATURE IN DEG. C

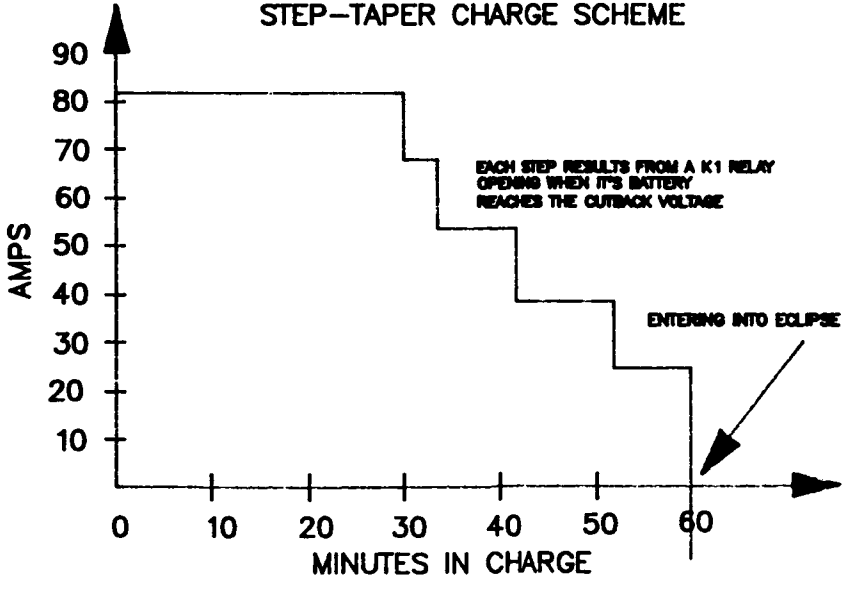
STEP-TAPER CHARGE SCHEME
AMPS
90
80
70
60
50
40
30
20
10
EACH STEP RESULTS FROM A K1 RELAY OPENING WHEN IT'S BATTERY REACHES THE CUTBACK VOLTAGE
ENTERING INTO ECLIPSE
0
10
20
30
40
50
60
MINUTES IN CHARGE

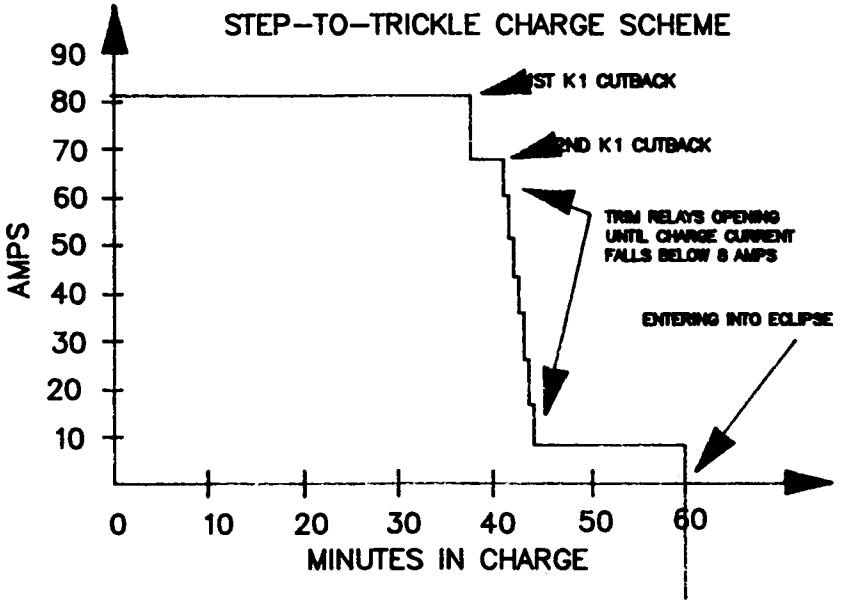
STEP-TO-TRICKLE CHARGE SCHEME
AMPS
90
80
70
60
50
40
30
20
10
ST K1 CUTBACK
ND K1 CUTBACK
TRIM RELAYS OPENING UNTIL CHARGE CURRENT FALLS BELOW 8 AMPS
ENTERING INTO ECLIPSE
0
10
20
30
40
50
60
MINUTES IN CHARGE

HST NiH2 SIX BATTERY TEST

TEST TIMELINE

As of November 1990 the HST NiH_2 Six Battery Test has been operating for 18 months (approximately 8100 orbital cycles). At the beginning of the test the batteries underwent some parametric testing to determine the optimum charge level and charge scheme for the batteries in the HST EPS and to observe how the battery operating characteristics and capacities varied under the different conditions. The goal of the testing was to determine the highest charge level the batteries could operated at efficiently. The testing showed that charging the batteries to an average cell voltages of 1.500 (K2L3) to 1.513 (K1L3) would yield a capacity of about 73 ampere hours per battery and an efficiency of 80 to 85 %. Charging the batteries to a higher charge level could decrease the efficiency to the point that the heat generated by the batteries could not be tolerated by the thermal constraints. At the different charge levels the step-to-trickle charge scheme was more efficient than the step-taper scheme with both charge schemes yielding approximately equal capacities. After parametric testing, the batteries began life cycling at the K1L3 charge level with the 2 step-to-trickle charge scheme. At this charge level and the K2L3 level the battery performance was nominal. A couple of weeks prior to the capacity tests at orbit 6100 the battery test was shutdown for approximately 24 hours due to a facility power outage. During the outage the batteries sat open circuit at room temperature. This open circuit period was probably the reason for the lower than expected capacity. The next capacity test is scheduled for for January 1991. Based on the pressures as of November 28, 1990 the system capacity will be approximately 460 Ah. This capacity compared to 439 Ah capacity at orbit 4400 (the other capacity test after operating on K2L3) indicates that there is no capacity degradation to date.

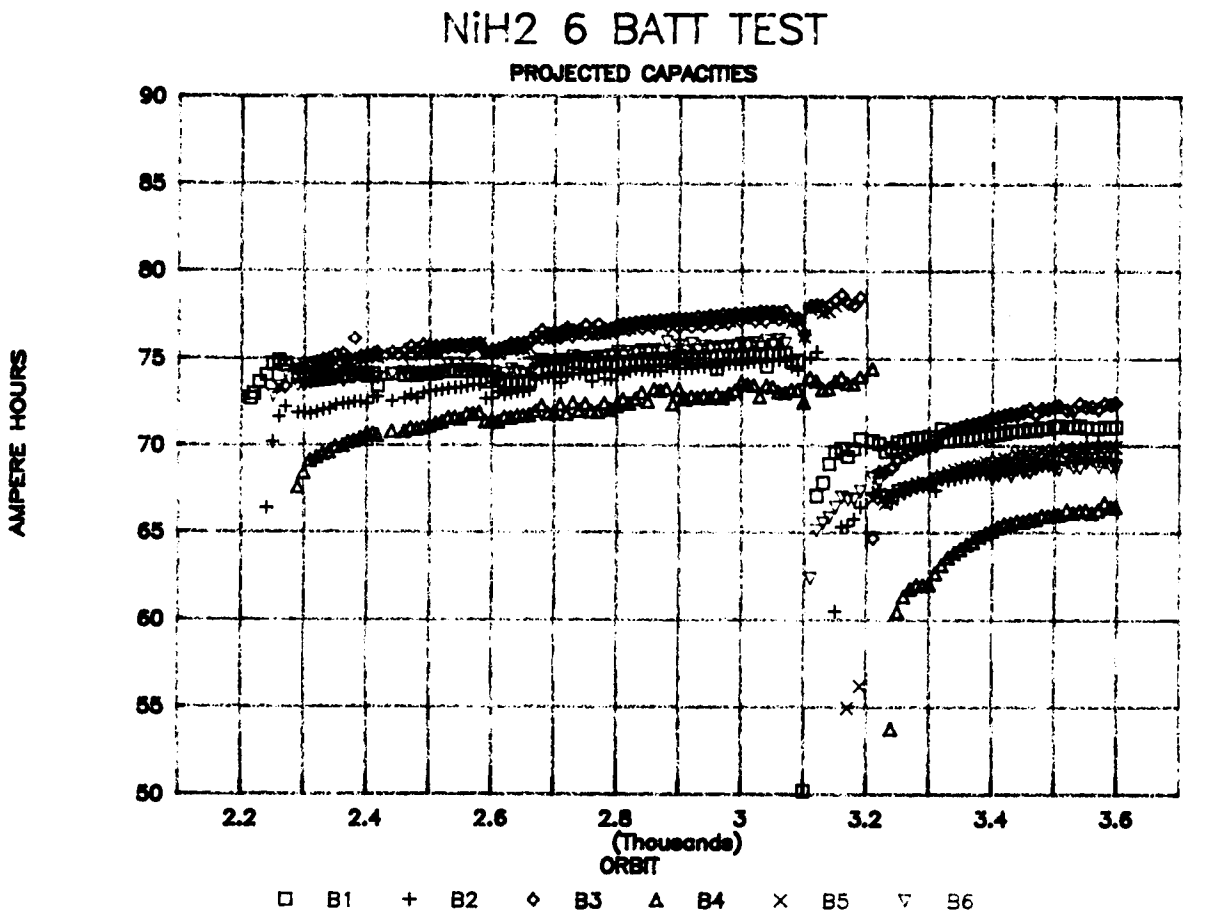
NiH2 6 BATT TEST
PROJECTED CAPACITIES
AMPERE HOURS
90
85
80
75
70
65
60
55
50
2.2
2.4
2.6
2.8
3
3.2
3.4
3.6
(Thousands)
ORBIT
B1
B2
B3
B4
B5
B6

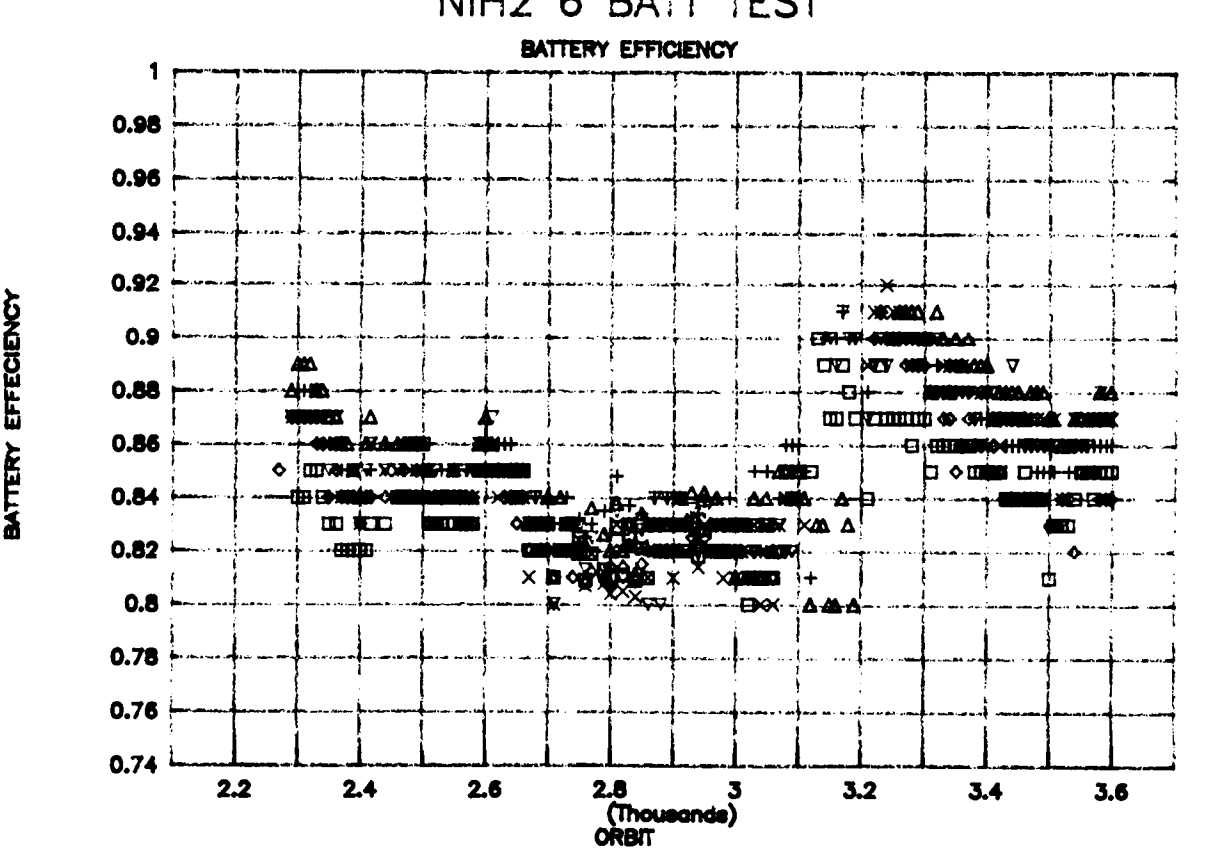
NiH2 6 BATT TEST
BATTERY EFFICIENCY
BATTERY EFFECIENCY
1
0.98
0.96
0.94
0.92
0.9
0.88
0.86
0.84
0.82
0.8
0.78
0.76
0.74
2.2
2.4
2.6
2.8
3
3.2
3.4
3.6
(Thousands)
ORBIT

CAPACITY AND EFFICIENCY TRENDS

(following a capacity test)

As the HST NiH2 batteries cycle to constant charge voltage the battery capacity tends to slowly increase and the battery watt-hour efficiency tends to decrease for the first approximately 1000 orbits. The graphs on the opposite page show the predicted battery capacities and the calculated efficiencies over a 3 month period. At the start of the period the batteries had just resumed normal cycling after a capacity test and reconditioning. The batteries were were cycling on the K1L3 (1.513 v/cell @ 0 deg. C) charge level. As the batteries cycled at this charge level through orbit 3100 the capacitites increased 3 to 4 ampere hours per battery and the average efficiency dropped from 86% to 82%. The slopes of these two curves would have flattened out if the capacity tests would not have been run at orbit 3100. The capacity tests have the effect of reseting the capacities and efficiencies. When the batteries resumed cycling after these capacity tests the charge level was lowered to K2L3 (1.500 v/cell @ 0 deg. C).

HST NiH2 6 BATTERY TEST

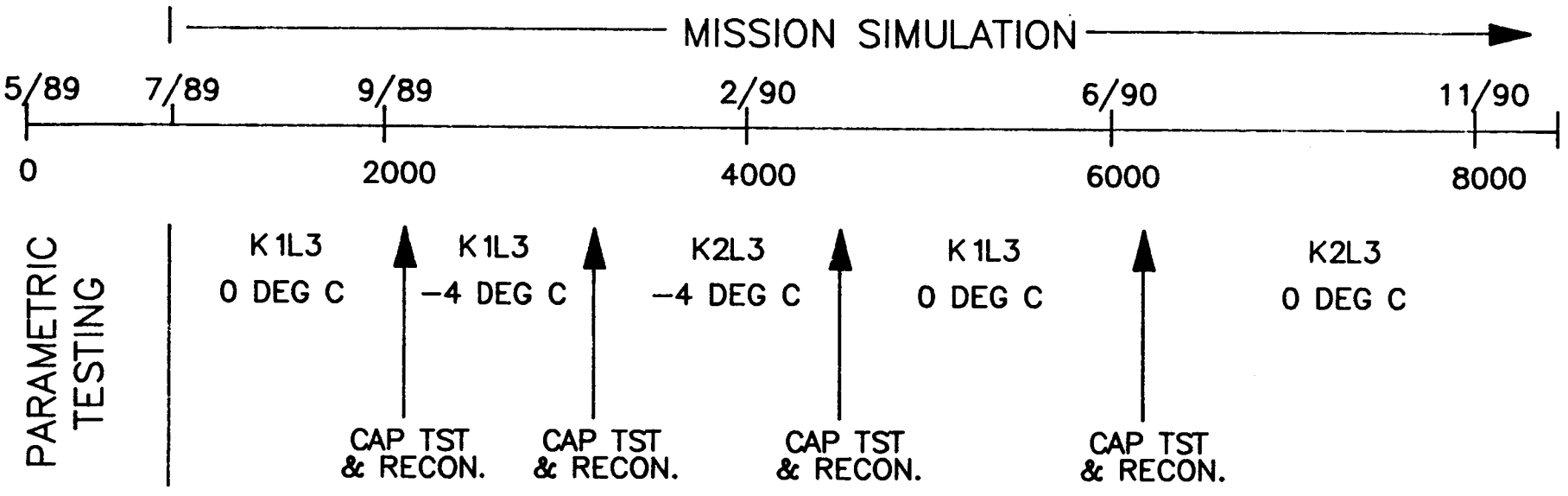

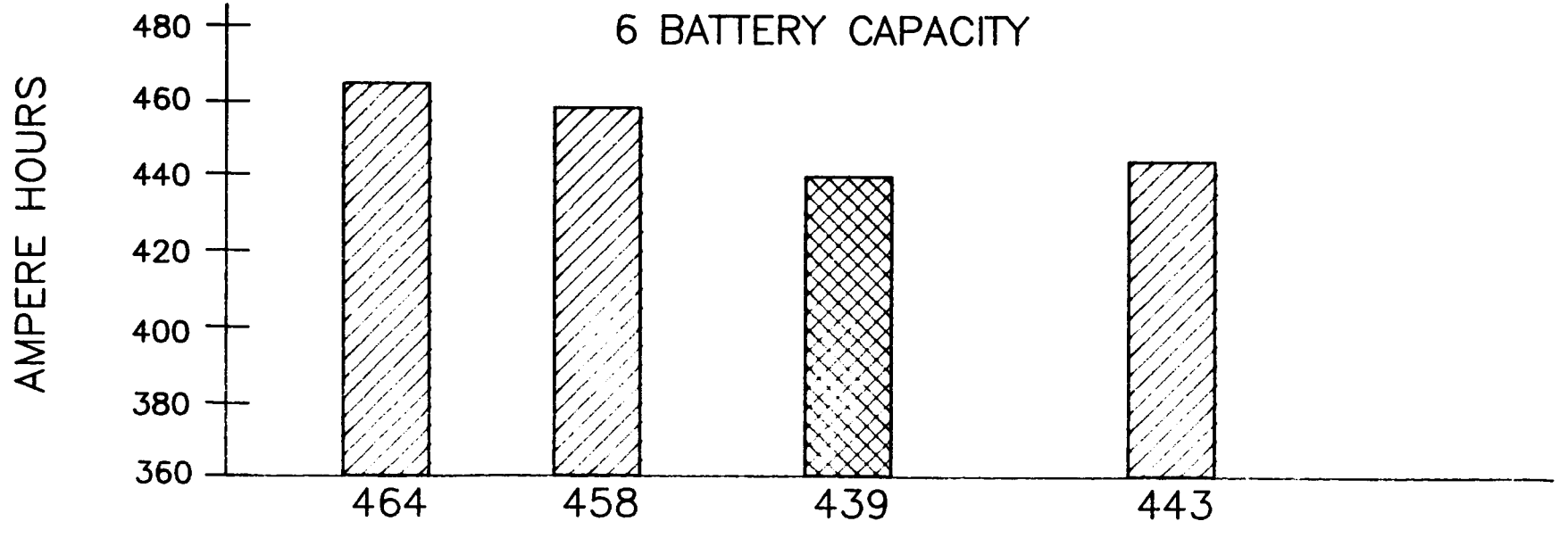

HST BATTERY CAPACITY (PRESSURE)

There is a known relationship between the capacity and the pressure in the NiH2 batteries based on a calibration curve established during ground charge/discharge operations. However, based on these calibration curves, the capacity of the batteries on orbit is approximately 10 ampere hours (AH) higher than similar batteries undergoing mission simulation testing on the ground. This has not been verified to date, but a flight capacity test on two batteries is scheduled for later this month. The gentle rise in pressure with time has been observed in ground testing, and appears to be a gradual increase in state of charge with time with the charge control method used here. Ground capacity tests have resulted in a "resetting" of the pressure to a lower level from which it gradually climbs until the next capacity test. The increased state of charge (the batteries are not operated at 100% state of charge) is accompanied by a decrease in energy efficiency which is predictable based on ground parametric tests. The difference in the ground and flight capacity (if it is shown to really exist) is open to discussion--are the batteries more efficient in space as a result of better gas management of electrolyte distribution?

TOTAL CALCULATED BATTERY CAPACITY
(based on cell pressures @ 0 deg C)

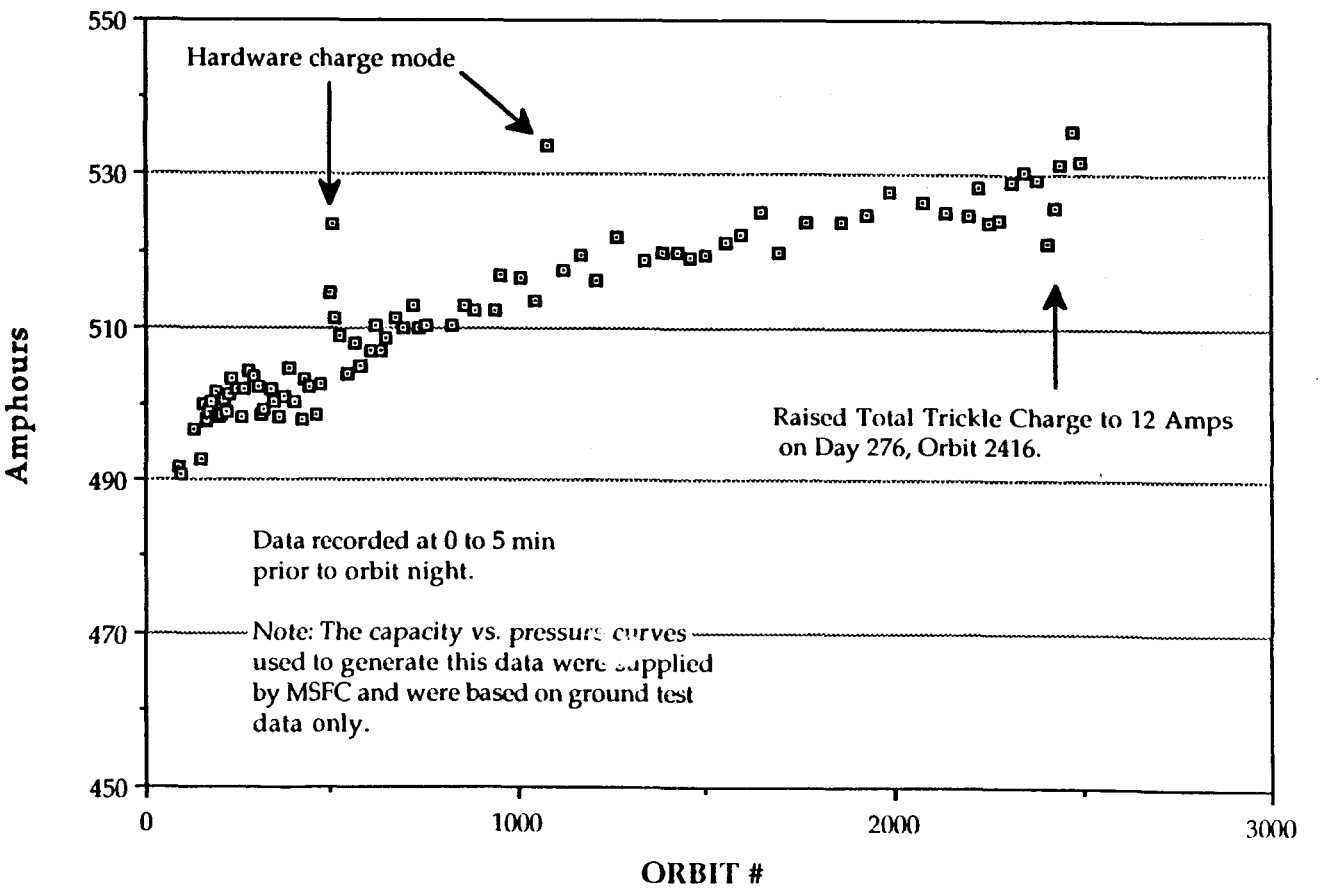

HST BATTERY LOADSHARE HISTORY

The NiH2 batteries on the HST share the load within one percentage point of the total. This sharing is primarily a function of the line impedances which were matched for each battery. However, as the batteries age any significant variation in the sharing could be an indication of variations between batteries.

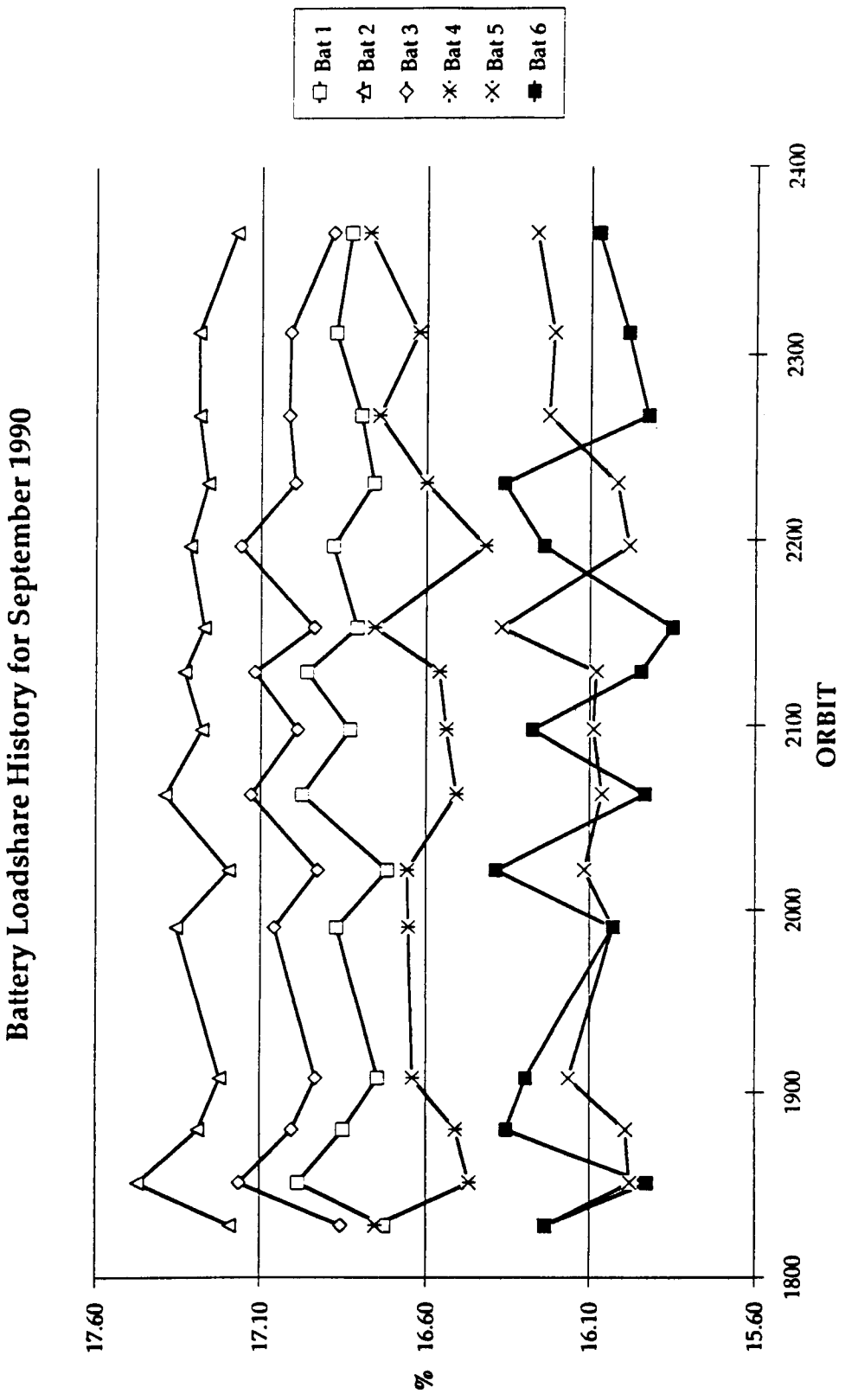
Battery Loadshare History for September 1990
Bat 1
Bat 2
Bat 3
Bat 4
Bat 5
Bat 6
17.60
17.10
16.60
16.10
15.60
%
1800
1900
2000
2100
2200
2300
2400
ORBIT

HST BATTERY END OF DISCHARGE VOLTAGE

The battery average end of discharge voltage (EODV) over the first 2500 orbits (~5.5 months) is very constant after the first 1200 orbits. The major perturbations during the first 1200 orbits resulted from changes in discharge time associated with orbital beta angle changes and the resultant depth of discharge variations. It is too early in the mission to draw conclusions from these results.

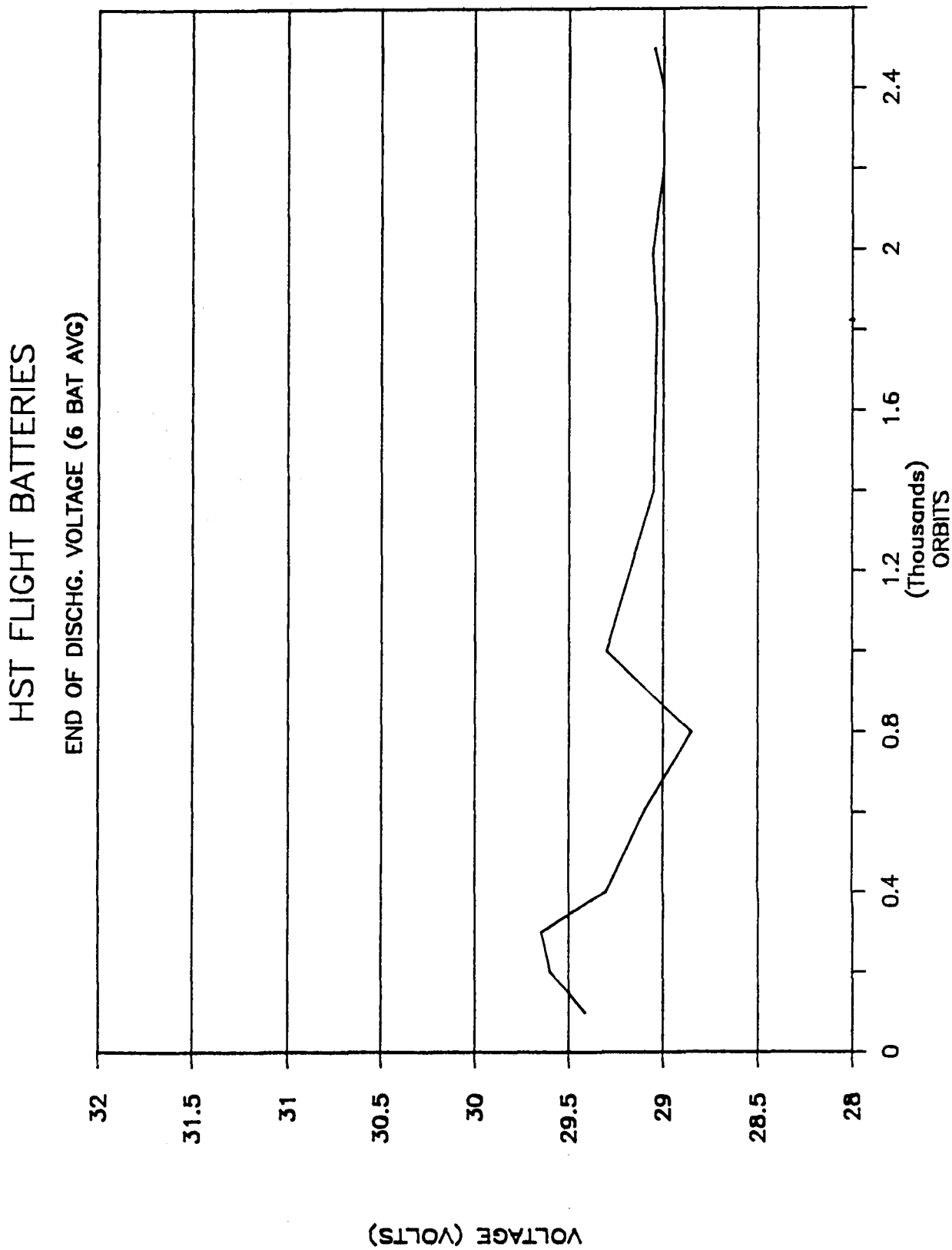
HST FLIGHT BATTERIES
END OF DISCHG. VOLTAGE (6 BAT AVG)
VOLTAGE (VOLTS)
32
31.5
31
30.5
30
29.5
29
28.5
28
0
0.4
0.8
1.2
1.6
2
2.4
(Thousands)
ORBITS

HST BATTERY DEPTH OF DISCHARGE HISTORY

The average depth of discharge (DOD) of the six batteries for the first 2500 orbits is indicative of the benign loads that the batteries are supporting. These very low DOD's resulted from the change from 55 AH NiCd to 88 AH NiH2 batteries late in the program coupled with the rather large "safe mode" requirements. The loads have also been approximately 10% lower than predicted. The variation from a low of 5% to a high of 8% results from the orbital beta angle changes. This effect can also be seen in the end of discharge voltages of the batteries.

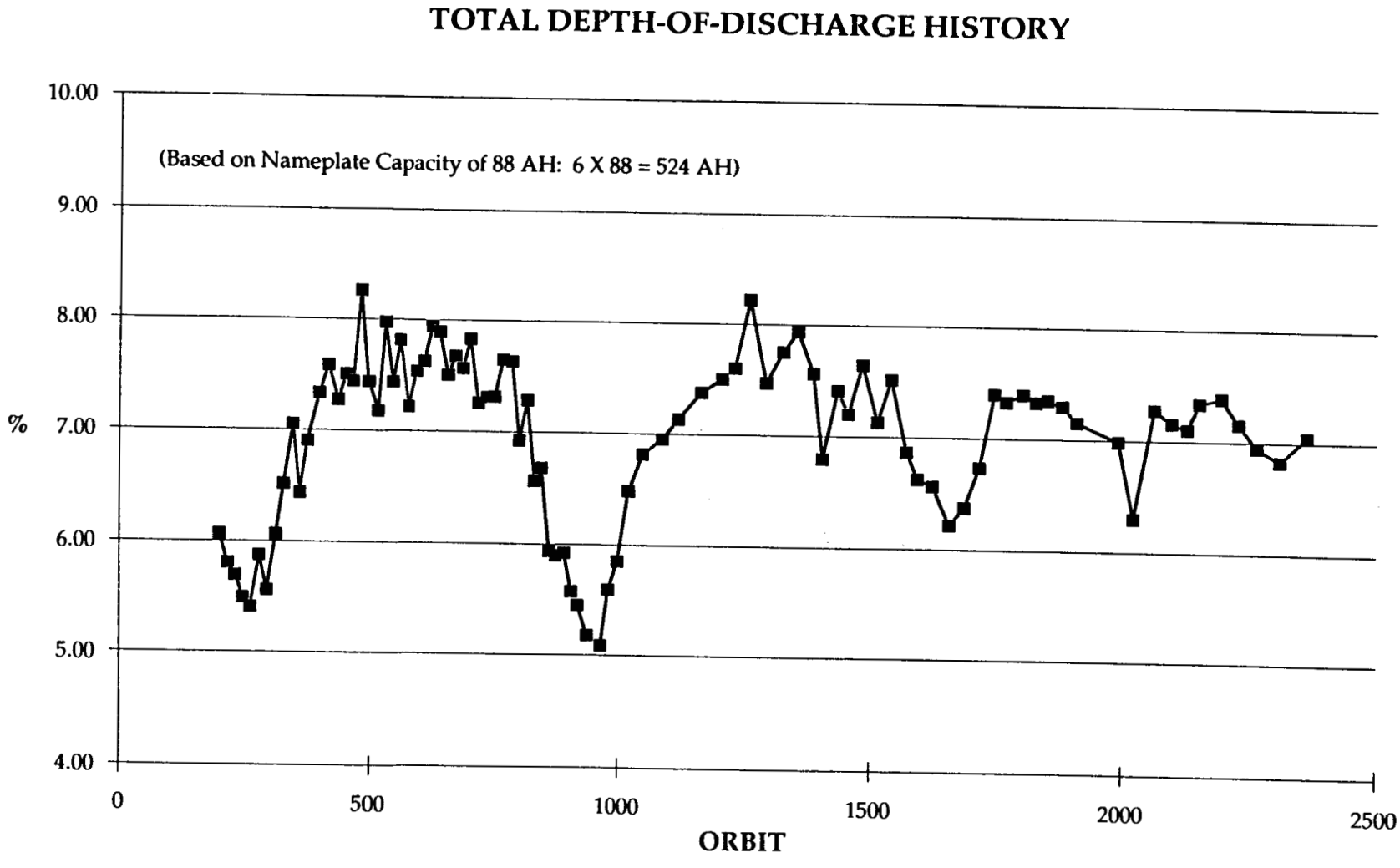
TOTAL DEPTH-OF-DISCHARGE HISTORY
(Based on Nameplate Capacity of 88 AH: 6 X 88 = 524 AH)
10.00
9.00
8.00
7.00
6.00
5.00
4.00
%
0
500
1000
1500
2000
2500
ORBIT

HST BATTERY END OF DISCHARGE VOLTAGE

The battery average end of discharge voltage (EODV) and end of high rate charge voltage (EOCV) plots for orbits 1800 to 2500 are shown. The EODV is very constant after the first 1200 orbits. The EOCV is controlled at a constant voltage-temperature level by charge current controllers. The constant EOCV here reflects the very stable temperature at the end of high rate charge that the batteries are experiencing.

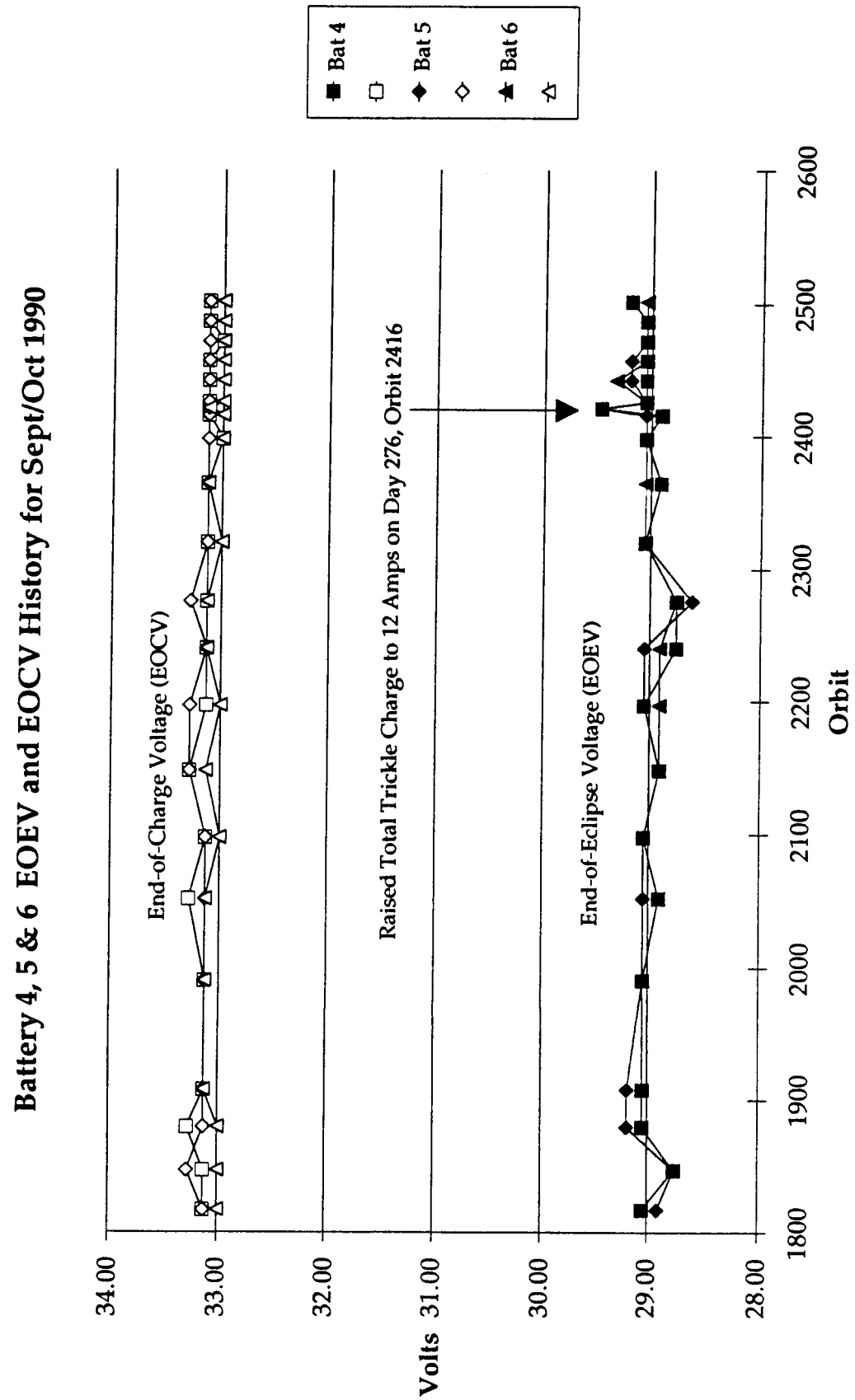
Battery 4, 5 & 6 EOEV and EOCV History for Sept/Oct 1990
Bat 4
Bat 5
Bat 6
End-of-Charge Voltage (EOCV)
Raised Total Trickle Charge to 12 Amps on Day 276, Orbit 2416
End-of-Eclipse Voltage (EOEV)
Volts
34.00
33.00
32.00
31.00
30.00
29.00
28.00
1800
1900
2000
2100
2200
2300
2400
2500
2600
Orbit

NiH2 BATTERY PERFORMANCE

FLIGHT VS. SIX BATTERY TEST

The HST flight batteries are operating more efficiently than the test batteries. This was not totally unexpected since the FSM test cells are operating more efficiently than the TM test cells. However there appears to be a greater difference between the flight FM batteries and the ground TM batteries. At the K2L3 charge level the flight batteries are operating with recharge ratios between 1.01 and 1.10 based on the time based 15 orbit average, while in the Six Battery Test the recharge ratios ranged from 1.08 to 1.14. This could be a result of the flight batteries performing better in the zero-g environment. The cell pressures in the flight batteries indicate the capacities to be at approximately 83 Ah, while the Six TM batteries capacities averaged 73.2 Ah at the K2L3 charge level. The predicted 83 Ah capacity of the flight batteries is based on the capacity vs. pressure curves that were generated during the flight conditioning cycles on the flight batteries. These pressures may not relate to capacity in zero-g as they did in one-g. The flight capacity tests requested by the HST Electrical Panel for December 1990 will indicate how the zero-g pressure relates to capacity. If the capacities are as high as the pressures indicate, this, along with the lower recharge ratios, could be a result of the better electrolyte distribution or gas flow paths in the cells at zero-g. This will continue to be investigated.

NASA

NiH2 BATTERY PERFORMANCE

FLIGHT VS. GROUND TESTING

- The HST Flight Batteries are operating with greater efficiency than the test batteries.

  At the K2L3 charge level the ground test batteries were operating with RR's between 1.08 and 1.14. The flight batteries RR's at this charge level are between 1.01 and 1.10.

- The cell pressures in the flight batteries indicate the capacities to be approximately 83 Ah/battery, while the test batteries capacities averaged 73 Ah at the K2L3 charge level.

- The improved efficiency and capacities in the flight batteries is probably a result of better electrolyte distribution inside the cells in the zero-g environment.

- The flight capacity tests are planned for Dec. 1990 & Jan. 1991.

Hubble Space Telescope Nickel-Hydrogen "Flight Spare" Battery Test

by

Jeffrey C. Brewer and Thomas H. Whitt
NASA Marshall Space Flight Center
Huntsville, Alabama

Abstract

For several years, the Marshall Space Flight Center (MSFC) has been engaged in a series of battery tests in support of the Hubble Space Telescope (HST) program. Now that the HST is in orbit, many of these tests will continue in order to give those responsible for the HST a reasonable prediction on the performance of the flight batteries. These tests will also be a source of needed low-earth-orbit (LEO) data for nickel-hydrogen ($Ni-H_2$) batteries and cells.

One of the tests currently in progress at MSFC is a mission simulation test on a 22-cell $Ni-H_2$ battery. This battery is composed of spare cells taken from the lot of cells out of which the Flight Spare Module was assembled. This module is one of two modules launched on the HST. This battery has been on test since June, 1989, and has completed nearly 8000 LEO cycles. A series of characterization tests were run prior to the start of the mission simulation and a launch scenario test was run in February and March, 1990, to test the behavior of the cells through a simulated launch. The results from these tests as well as the overall performance of the battery as it continues to cycle will be reported on in this presentation.

Cell Description

The 22 Ni-H_2 cells used in this battery were chosen from the Flight Spare Module lot of cells. The manufacturing process for these cells was identical to that used for the Flight Module cells. The process differed, however, from the one used for the Test Module cells in that a slight change was made in the activation procedure. The cells in the Ni-H_2 Six-Battery System Test are Test Module cells.

The internal cell design is a dual stack, back-to-back electrode configuration. The back-to-back design consists of alternating positive and negative electrode assemblies with a separator consisting of a double layer of zircar cloth between each assembly. The positive electrode assembly consists simply of two "back-to-back" positive electrodes while the negative electrode assembly consists of a polypropylene gas screen between two negative electrodes. The electrolyte used in the cell is a 27% (before activation) potassium hydroxide solution.

The pressure vessel is made of hydroformed Inconel 718 material. The vessel is 3.5 inches in diameter and has a wall thickness of .040 inches. A thin zirconium oxide coating is on the interior surface of the vessel. One other notable design feature used on this vessel is the placement of both the positive and negative terminals on the same end of the vessel in a "rabbit-ear" configuration.

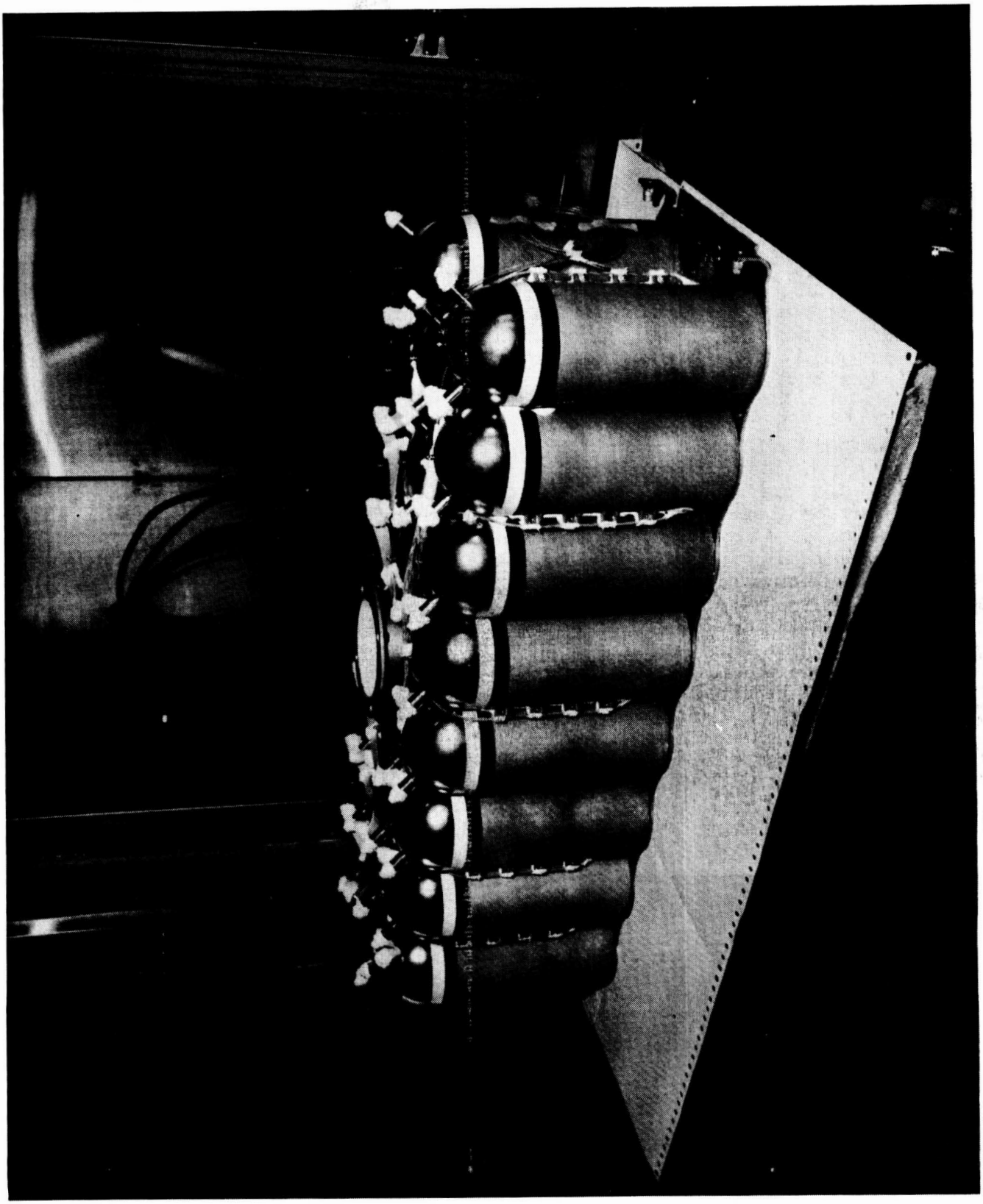

Figure 1

Test Timeline

As of December, 1990, the HST Ni-H_2 "Flight Spare" Battery (FSB) has been operating for 17 months (nearly 8000 LEO cycles). At the beginning of the test the battery underwent some parametric testing to determine how the battery would respond to operating temperatures as high as 15°C. This was done to simulate possible temperature excursions such as might be experienced during a hot thermal condition or a safemode.

After parametric testing, the battery began mission simulation at the K1L3 charge level with the 2 step-to-trickle charge scheme. Prior testing on the HST Ni-H_2 Six-Battery Test concluded that the HST Batteries would be operating on the K1L3 (1.513 v/cell @ 0°C) or K2L3 (1.5 V/cell) charge level at the beginning of the HST mission.

The HST batteries have primary and redundant heaters. The primary heaters maintain battery temperature in the range of -1 to 3°C and the redundant heaters maintain battery temperatures between -6 and -2°C. The FSB is located within a thermal chamber that is used to control temperature. During the mission simulation testing the battery temperature was varied to investigate the effect of operating on the redundant heaters. There was no noticeable improvement in battery performance at this lower temperature.

The capacity of 67.7 ampere-hours (Ahr) at orbit 5700 is 2.6 Ah less than the first capacity shown of 70.3 Ahr. Two weeks before the capacity test at orbit 5700 there was a facility power outage which resulted in the battery being open circuit at room temperature for 24 hours. This open circuit period was probably the reason for the lower than expected capacity. The next capacity test is scheduled for January, 1991. Based on the pressure as of December 2, 1990, the battery capacity will be approximately 70.2 Ah. This capacity compared to 68.5 Ah at orbit 3800 (the other capacity test after operating on K2L3) indicates that there is no capacity degradation to date.

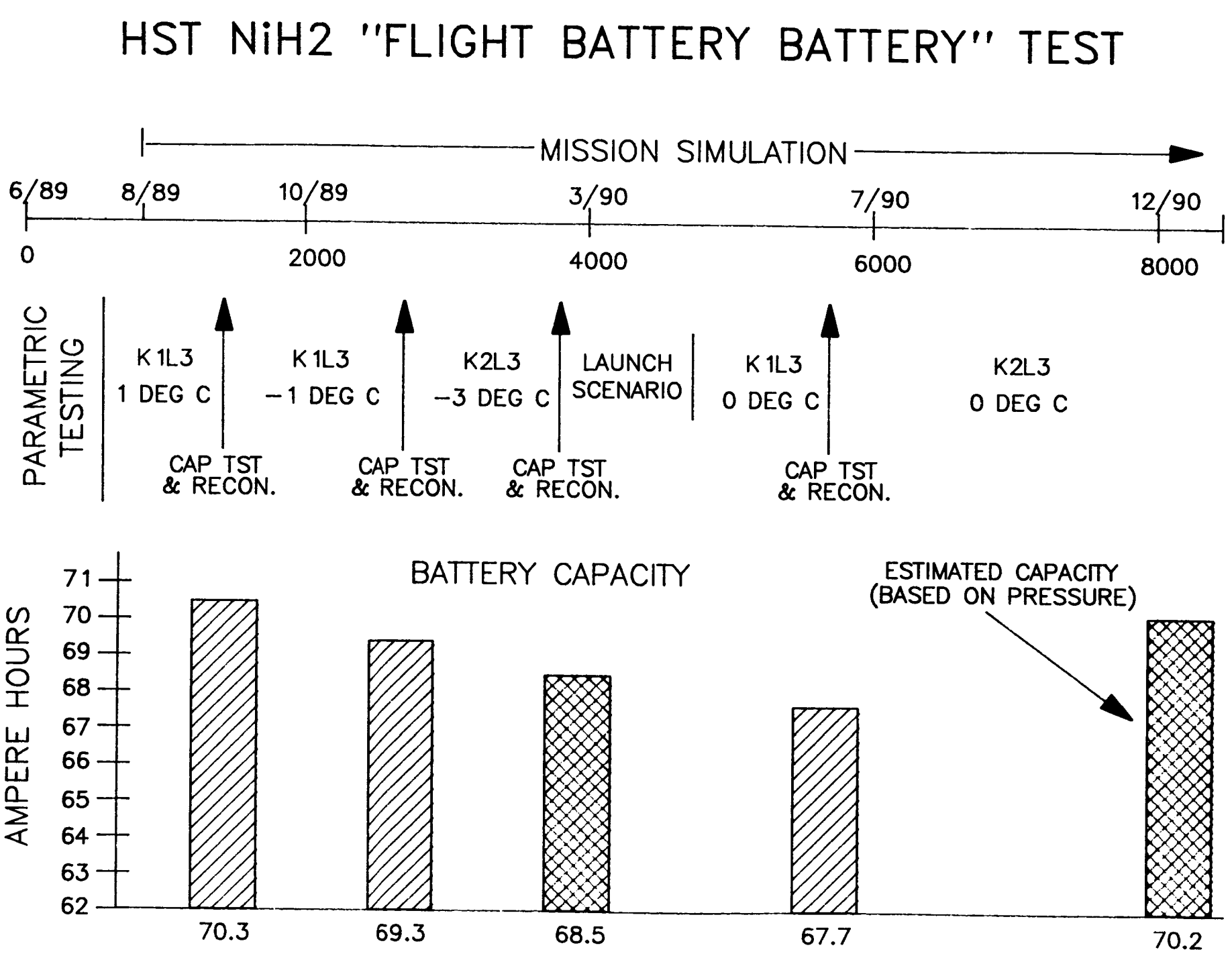

Figure 2 -- Flight Spare Battery test timeline.

Parametric Test Results

Between orbits 200 and 580, the battery was cycled for 1 week periods at 15, 10, 5, and 0°C with a step-taper charge scheme. A capacity test and reconditioning was run at the end of each period. Table I shows the battery recharge ratio, power dissipation, and capacity at the different temperatures. There is relatively no change in the capacities at the different temperatures. Typically, capacity will decrease as temperature is increased. The reason this is not happening here is that the battery is being charged to a V/T curve designed for a nickel-cadmium battery. This is resulting in the battery being charged to a higher state of charge at the higher temperatures and a lower state of charge at the lower temperatures. While the curve that is currently being used will yield basically constant capacities over a range of temperatures, a more constant recharge ratio (efficiency) can be achieved by increasing the slope of the V/T curves currently being used. This would allow higher charge levels at the lower temperatures while reducing the charge levels at the higher temperatures.

HST Ni-H_2 Flight Spare Battery Test

Temperature (°C)	Recharge Ratio	Power Dissipation (Watts)	Capacity (Ahr)
15	1.288	45.61	67.23
10	1.180	31.22	67.10
5	1.142	25.32	67.71
0	1.063	14.82	67.20

Table I -- Parametric Test Results.

Launch Scenario Test Results

The main objective of the launch scenario test was to assure that a minimum capacity would remain in the cells through a 4-day launch window. Meeting this requirement was verified by a pressure-based capacity estimate of approximately 33 Ah at the end of the window. Following the recycle portion of the test, the capacity was estimated (by pressure) to be approximately 25 Ah; however, a capacity test run on the battery indicated approximately 34 Ah. This large capacity delta was completely unexpected and cannot, as yet, be explained.

During this launch scenario test, another issue developed that became a concern. This involved the effect that a long, high-temperature (75 to 85°F) self-discharge would have on the ensuing charge acceptance of the Ni-H_2 cell. All launch scenario testing to date, except for one inconclusive thermal vacuum test, had been performed by "forcing" the cells down, through a discharge, to a capacity level equivalent to one following a 10-day self-discharge. This was done to bypass the 10 days necessary to run the real-time self-discharge. It was thought that this "short-cut" would have no effect on the results and would save considerable amounts of the available testing time prior to the actual launch. It was discovered, however, that there was a possibility that this extended self-discharge at these temperatures could lead to a temporary loss in usable capacity. In order to test this theory, and to determine an estimated minimum "recycle" capacity, the battery was allowed to self-discharge a total of 194 hours before beginning the "recycle" recharge. A distinct difference exists in the performance of the battery before and after the 194 hours of self-discharge. The estimated capacity following the self-discharge was 10 to 12 Ah less than that achieved prior to the self-discharge. It is uncertain what caused this loss in capacity. What is certain is that the capacity can be recovered through a series of baseline charge/discharge cycles, as was done on the HST flight batteries when they had to be recycled in a similar manner. The flight batteries showed no signs of capacity loss (as did this "flight spare" battery) when they were first cycled after being placed in orbit.

One lesson that was learned with this launch scenario test is that while pressure is a good estimate of capacity it is certainly not highly consistent or accurate even over a short period of time. The estimates must always be tempered by the events that are occurring with the cells themselves.

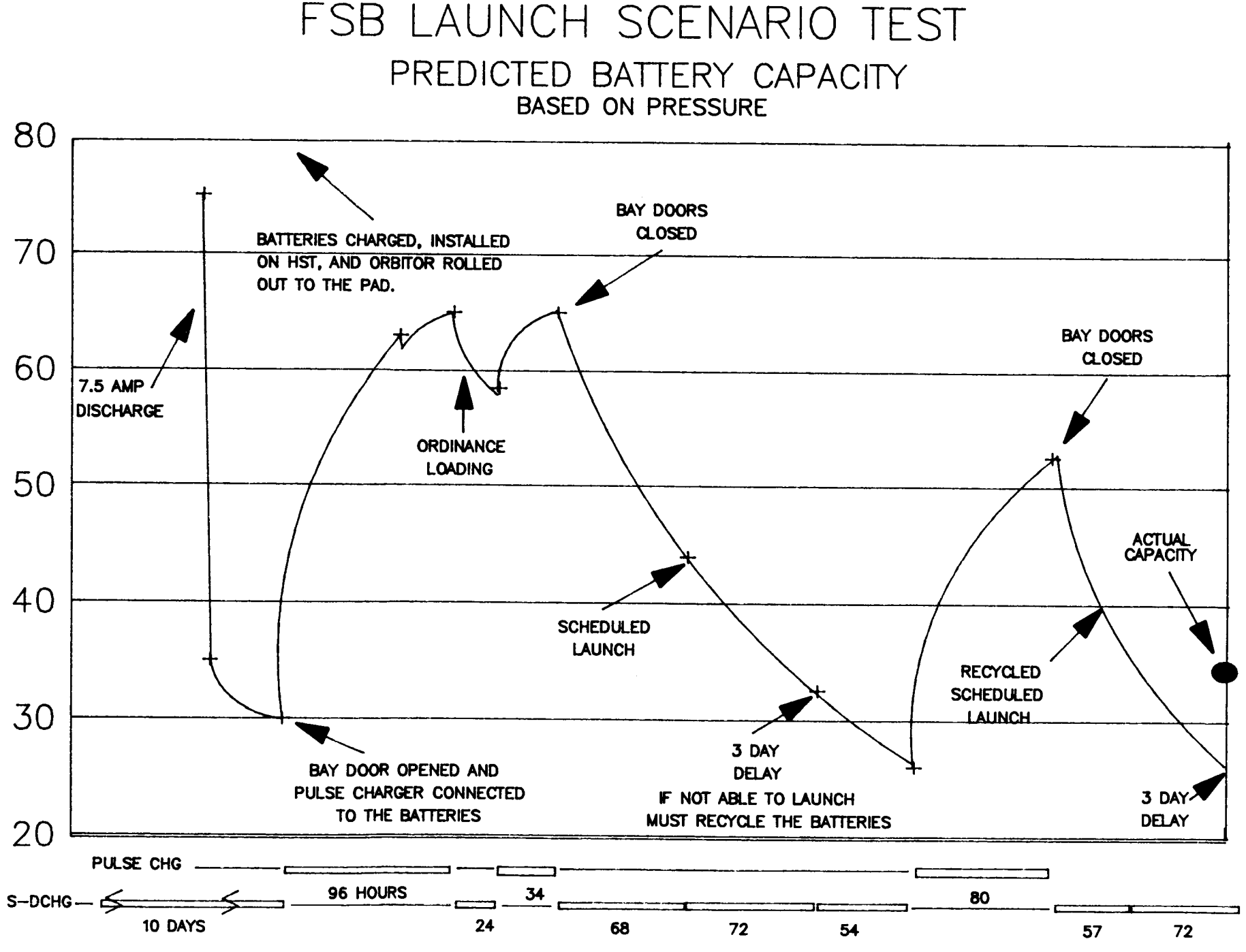

Figure 3 -- Launch Scenario Simulation Test.

Orbital Summary Data

Through the first 18 months of cycling, the FSB has completed over 8000 cycles. Figures 4 and 5 show the last six months of EOC and EOD Hi/Av/Lo cell voltages. Figures 6 and 7 show the estimated capacity and watt-hour efficiency over the last six months. Figure 8, 9, and 10 show the recharge ratio, sun/eclipse times, and battery temperature over the last six months. All of the data basically shows expected results. The "disturbances" in the data can be attributed usually to one of three events: a system shutdown due to power outage, a capacity test (or other planned parametric test), or variations in the sun/eclipse times. For the last 700 orbits shown, a change was implemented in the test software that allowed the loads to change every 8 minutes, compared to a constant load that was used prior to that. This load change is small but over time has caused the data to scatter slightly. This change was made in the test in order to better simulate the actual flight conditions.

The FSB is operating slightly more efficient than the Six-Battery test. The calculated recharge ratios are lower (1.05 to 1.12 vs. 1.08 to 1.14) for the FSB. Also, the EOD voltages are slightly higher (1.32 to 1.35 vs. 1.30 to 1.33) for the FSB. The estimated capacity, however, is 3 Ahr less (70 vs. 73) for the FSB. This is rather puzzling but could be the result of the two different types of cells being used in the two tests. The more efficient performance, however, is likely a result of a better heat dissipation capability inherent in a single battery design versus a three battery module design.

The FSB is operating slightly less efficiently than the flight batteries. Although some of the measurements used to calculate the recharge ratios on flight are suspect, it is still believed that they are operating at a lower recharge ratio than the FSB (1.05 to 1.12 vs. 1.01 to 1.10). The FSB also has a significantly less capacity estimate than the flight batteries (70 vs. 88). This estimate of the flight batteries' capacities will be verified by a capacity test that is scheduled to be run early in 1991. While there are doubts that the capacity will be as high as estimated, there certainly are good reasons why the flight batteries should be operating more efficiently than the FSB. Since the flight batteries are in a zero-G environment, a better electrolyte distribution should be achieved which will create a more efficient operating condition. The ground-based FSB obviously cannot achieve such a condition and should thus be slightly less efficient.

A capacity test is planned on the FSB in early 1991 with subsequent capacity measurements being made every six months thereafter.

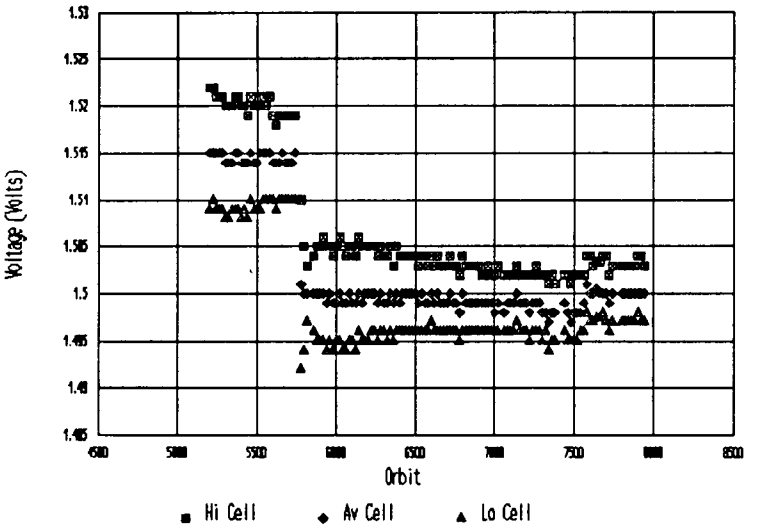

Figure 4 -- EOC Hi/Av/Lo cell voltages vs. orbit number for the previous six months.

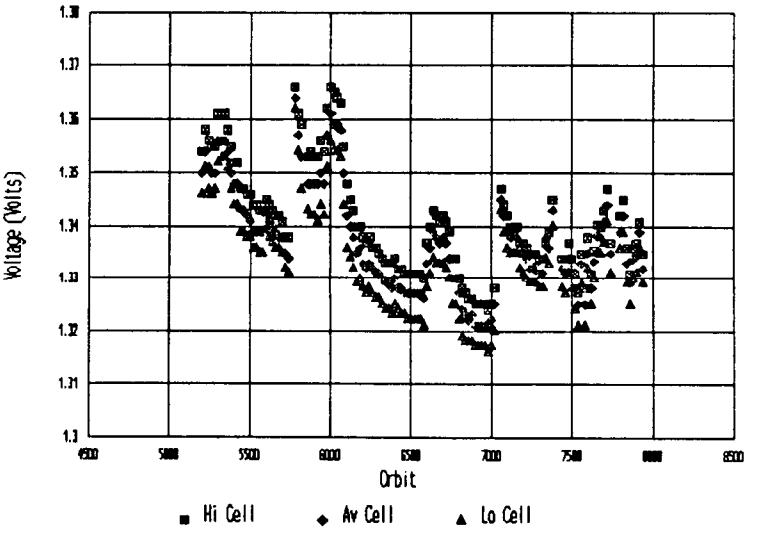

Figure 5 -- EOD Hi/Av/Lo cell voltages vs. orbit number for the previous six months.

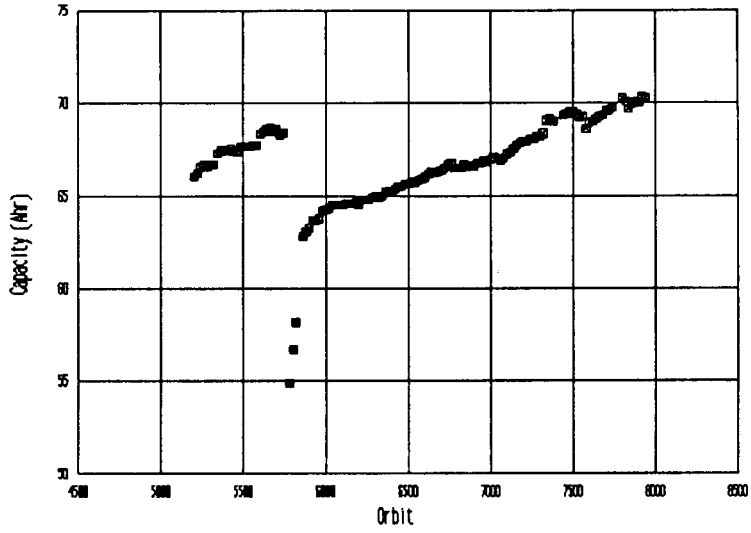

Figure 6 -- Estimated capacity vs. orbit number for the previous six months.

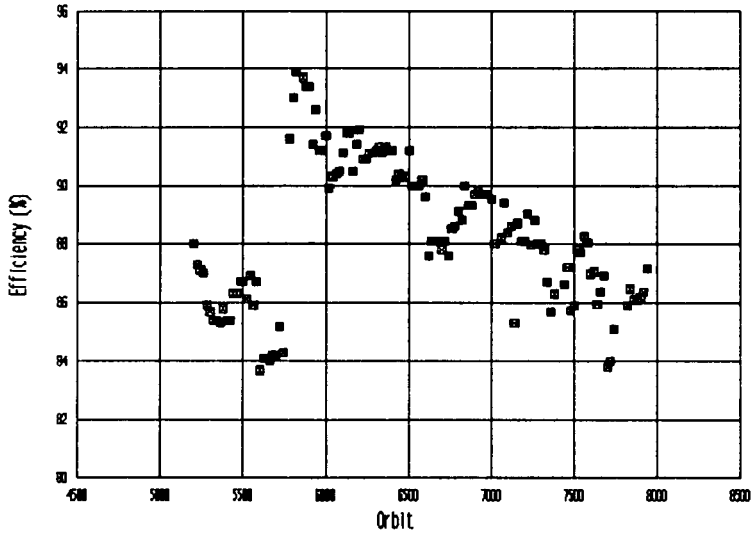

Figure 7 -- Watt-hour efficiency vs. orbit number for the previous six months.

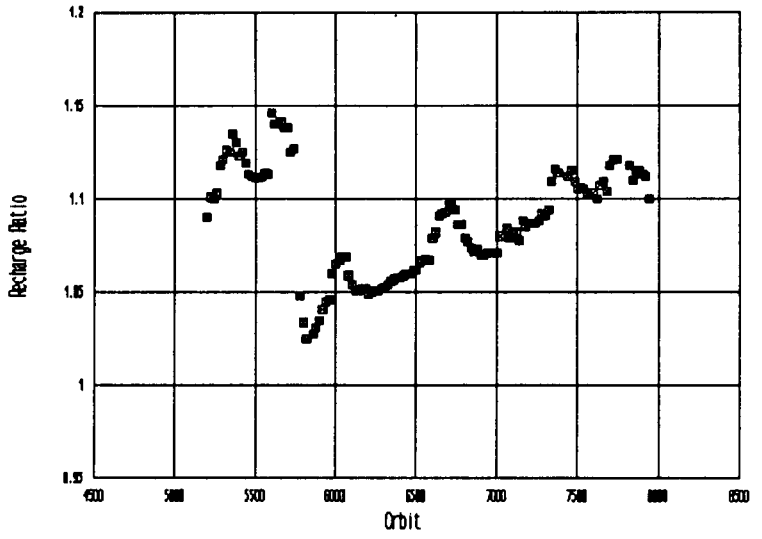

Figure 8 -- Recharge ratio vs. orbit number for the previous six months.

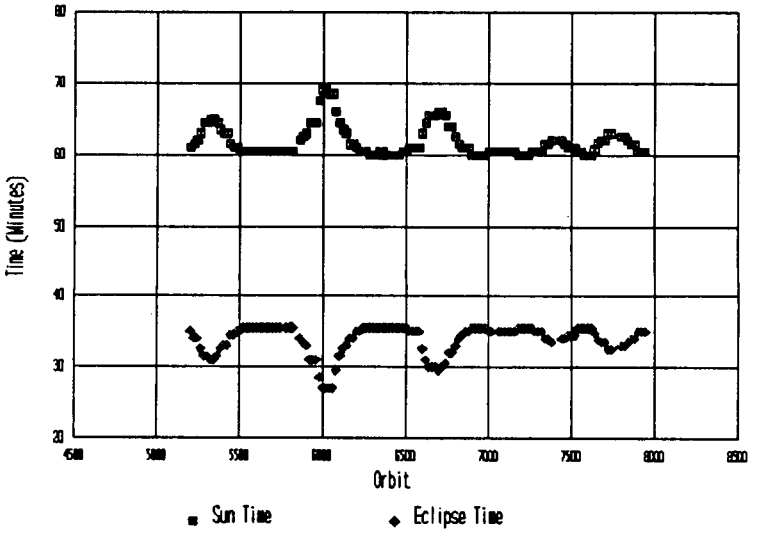

Figure 9 -- Sun/eclipse times vs. orbit number for the previous six months.

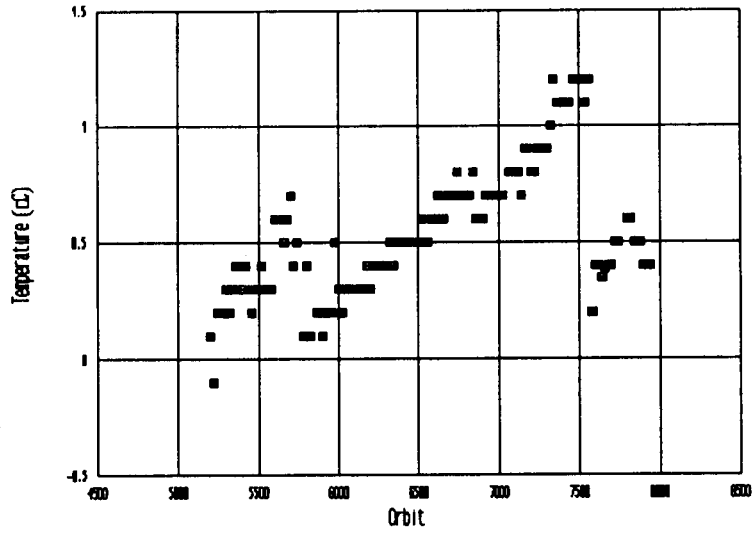

Figure 10 -- Battery temperature vs. orbit number for the previous six months.

MULTIPLE CELL CPV NICKEL HYDROGEN BATTERY

Ken R. Jones, Program Manager
Jeffrey P. Zagrodnik, Technology Manager
Johnson Controls, Inc.

ABSTRACT

Johnson Controls, Inc. has developed a multiple cell CPV Nickel Hydrogen battery that offers significant weight, volume and cost advantages for aerospace applications. The baseline design was successfully demonstrated through the testing of a 26-cell prototype, which completed over 7,000 44% depth-of-discharge LEO cycles. Prototype designs using both nominal 5" and 10" diameter vessels are currently being developed for a variety of customers and applications.

LIST OF TRANSPARENCIES

1. JCI CPV Battery Development
2. Applications of CPV
3. Advantages of CPV over IPV
4. Features of Patented JCI CPV Design
5. Photo of CPV Battery and IPV Cells
6. Photo of 13-cell Prototype #1 Half-Stack
7. Photo of Prototype #1 Fixed Heat Fin Cavity
8. Photo of Prototype #1 Half Stacks in Cylinder
9. Life Cycle Plot for LEO Test of Prototype #1
10. Life Cycle Plot for LEO Test of 2-cell Boilerplate CPV
11. Life Cycle Plot for 2-Cell on Accelerated LEO
12. Photo of 5" Diameter Cell and Loose Heat Fin
13. Photo of 5" 10-cell Stack
14. Photo of 5" 10-cell Stack in Cylinder
15. Photo of 5" 22-cell Battery
16. Photo of 5" Vessel Components
17. Sketch of Weld Ring - Dome - Cylinder Weld Interface
18. Photomicrograph of Weld
19. Photo of MSOE Pressure Test Apparatus
20. Photo of Burst 5" Vessel
21. Photo of Burst 10" Vessel
22. Photo of 2 kWh Fiber-Wound Battery
23. Photo of Carbon-Fiber-Wound Aircraft Starting Battery
24. Family of JCI CPV Batteries

DESCRIPTION OF TRANSPARENCIES

1. JCI CPV Battery Development:Johnson Controls, Inc. (JCI) has developed a family of multicell Common Pressure Vessel (CPV) batteries for a variety of applications. Designs considered to date include voltages between 12 and 100 volts, and capacities ranging from as low as 7 ampere-hour to as high as 250 ampere-hours.

2. Applications of CPV

JCI is seriously pursuing a much broader market than that presently covered by IPV Nickel Hydrogen. The combined volume offered by the aerospace, aircraft starting and terrestrial markets will allow us to incorporate statistical process control (SPC) into the component fabrication processes, providing a significantly higher quality, improved consistency, and ultimately lower cost than is presently achieved in the industry.

3. Advantages of CPV over IPV

The advantages of the CPV design configuration are widely recognized. However, historical concerns related to electrolyte and thermal management had previously prevented the introduction of a working design.

4. Features of Patented JCI CPV Design

The patented JCI design overcomes the electrolyte management concern through the use of a vented electrolyte-containment-system (ECS) and actually provides a thermal advantage over the conventional IPV design. However, the same basic cell components and electrochemistry is used, so that the advantages of the IPV nickel hydrogen battery are retained.

5. Photo of CPV Battery and IPV Cells

The relative advantages of the CPV design are readily apparent based on a visual examination of a CPV battery next to its IPV counterpart.

6. Photo of 13-cell Prototype #1 Half-Stack

To demonstrate the capabilities of the CPV design, a 26-cell prototype was fabricated in a joint effort with COMSAT in 1988. This battery is composed of two 13-cell half-stacks which are connected in parallel within the single common vessel to provide a nominal 32 volts.

7. Photo of Prototype #1 Fixed Heat Fin Cavity

The half-stacks are inserted into fixed heat fin cavities which conduct heat radially from the cell, directly to the vessel wall. It is this direct thermal contact that provides a thermal advantage over the IPV design, which provides no radial pathway for heat conduction to the vessel. It is believed that this thermal advantage will translate to extended life in LEO applications. In GEO applications, where long life is not required, additional improvements in specific energy can be achieved due to the improved thermal pathway.

8. Photo of Prototype #1 Half Stacks in Cylinder

The two half-stacks for the prototype battery are inserted into a drawn Inconel 718 vessel/dome section. Springs push the half-stacks outward against the vessel wall, ensuring intimate contact between the heat fin cavity and the vessel wall. After insertion of the half-stacks a second

dome is welded in place using the same weld ring design approach that is applied in the IPV vessels.

9. Life Cycle Plot for LEO Test of Prototype #1

The Prototype battery was put on a real time LEO life test at COMSAT Laboratories. Over 7,000 44% depth-of-discharge (DOD) cycles were completed at 10°C before the battery.

Voltage performance was relatively stable over the first 6,400 cycles, prior to the rapid voltage degradation which ultimately caused the battery to reach the 1.0 volt/cell battery failure criteria.

Subsequent destructive physical analyses (DPA) showed that some of the ECS's had been damaged at the time of insertion into the heat fin cavity, leading to electrolyte leakage from the cells. The resulting drying out of the positives and separators is believed to have caused the voltage decline and failure of the battery. All cell components, including the negative electrodes were in excellent physical condition. No pinholes or other signs of popping were observed on the negative electrodes. No signs of blistering or other physical degradation were observed on the positives.

10. Life Cycle Plot for LEO Test of 2-cell Boilerplate CPV

Two 2-cell laboratory test batteries of the same baseline design are still on LEO test, one each at JCI and COMSAT. They have now exceeded 7,000 and 9,000 cycles, respectively with no significant performance degradation.

11.Life Cycle Plot for 2-Cell Accelerated LEO

A second JCI 2-cell has now completed 3,600 standard LEO cycles followed by over 6,000 cycles on an accelerated LEO cycle (double the charge and discharge rates and 23°C operating temperature).

12. Photo of 5" Diameter Cell and Loose Heat Fin

A new loose heat fin design was developed to overcome the problems encountered with insertion of the cells into the fixed heat fin cavity. This approach was introduced in a 5" diameter vessel, circular cell component design.

13. Photo of 5" 10-cell Stack

The cells and heat fins are assembled into a stack using a special alignment fixture. The ten cell design shown here has a 9.6 Ah capacity, is 9.7" long and weighs 3 kg. A 22-cell version offers a 13.4 Ah capacity is 20.6" long, and weighs 7.9 kg. In general, the higher the capacity and/or voltage, the better the specific energy. For example a 3.9 kWh design provides 55 Wh/kg.

14. Photo of 5" 10-cell Stack in Cylinder

The 5" cell stack is also inserted into a cylinder, but in this case two separate end domes and weld rings are welded in place. This approach allows an unlimited vessel length for design flexibility.

15. Photo of 5" 22-cell Battery

Although the cell stack for this 22-cell battery is only 9.7" long, the vessel length is 20.6" to provide the required void volume to maintain a 900 psi maximum operating pressure.

16. Photo of 5" Vessel Components

The vessel components for the 5" design include the cylinder, two end domes and two weld rings.

17. Sketch of Weld Ring - Dome - Cylinder Weld Interface

A close pre-weld fit of the components is required to obtain a high quality weld.

18. Photomicrograph of Weld

A photomicrograph of the weld area shows the weld penetration into the weld ring, and the heat effected zone.

19. Photo of MSOE Pressure Test Apparatus

After assembly test vessels are hydraulically burst to qualify their pressure capability. A 2.5-to-1 safety factor is used for the aerospace designs. Other test vessels are pressure cycled to demonstrate four times the number of required operating cycles prior to burst testing.

20. Photo of Burst 5" Vessel

The burst failures occur along the weld seam of the vessel cylinder. this is a favorable failure mechanism in that the vessel remains in one piece.

21. Photo of Burst 10" Vessel

The failure mechanism is the same for the 10" diameter vessel.

22. Photo of 2 kWh Fiber-Wound Battery

Designs for other applications include a 2 kWh terrestrial design intended for photovoltaic applications. This battery employs a fiber-wound vessel design.

23. Photo of Carbon-Fiber-Wound Aircraft Starting Battery

Aircraft starting battery designs also use the fiber-wound vessel approach, but include a carbon filament to enhance heat transfer and minimize weight.

24. Family of JCI CPV Batteries

In summary, a family of CPV battery designs have been developed for a wide variety of applications. Tests indicate that the significant advantages of the CPV design can be realized in a reliable package. At present the test database is limited but growing.

COMMON PRESSURE VESSEL (CPV) NICKEL HYDROGEN BATTERY

JOHNSON CONTROLS

APPLICATIONS

AEROSPACE

AIRCRAFT STARTING

TERRESTRIAL

- PHOTOVOLTAIC
- LOAD MANAGEMENT

ADVANTAGES OF CPV VERSUS IPV

HIGHER SPECIFIC ENERGY

HIGHER ENERGY DENSITY

SIMPLIFIED INTERFACE

POTENTIAL FOR LOWER COST

FEATURES OF PATENTED

JCI CPV DESIGN

MULTIPLE CELLS IN A SINGLE VESSEL

STANDARD NICKEL HYDROGEN CELL COMPONENTS

BACK-TO-BACK POSITIVE CONFIGURATION

ABSORBER BETWEEN POSITIVE ELECTRODES

CELL ENCLOSED IN ECS

VENTED ECS ALLOWS HYDROGEN ACCESS

VENT LOCATION ENSURES IN-CELL RECOMBINATION

DOUBLE ECS ENHANCES RELIABILITY

RADIAL HEAT FIN IMPROVES THERMAL TRANSFER

WELDED INCONEL 718 VESSEL

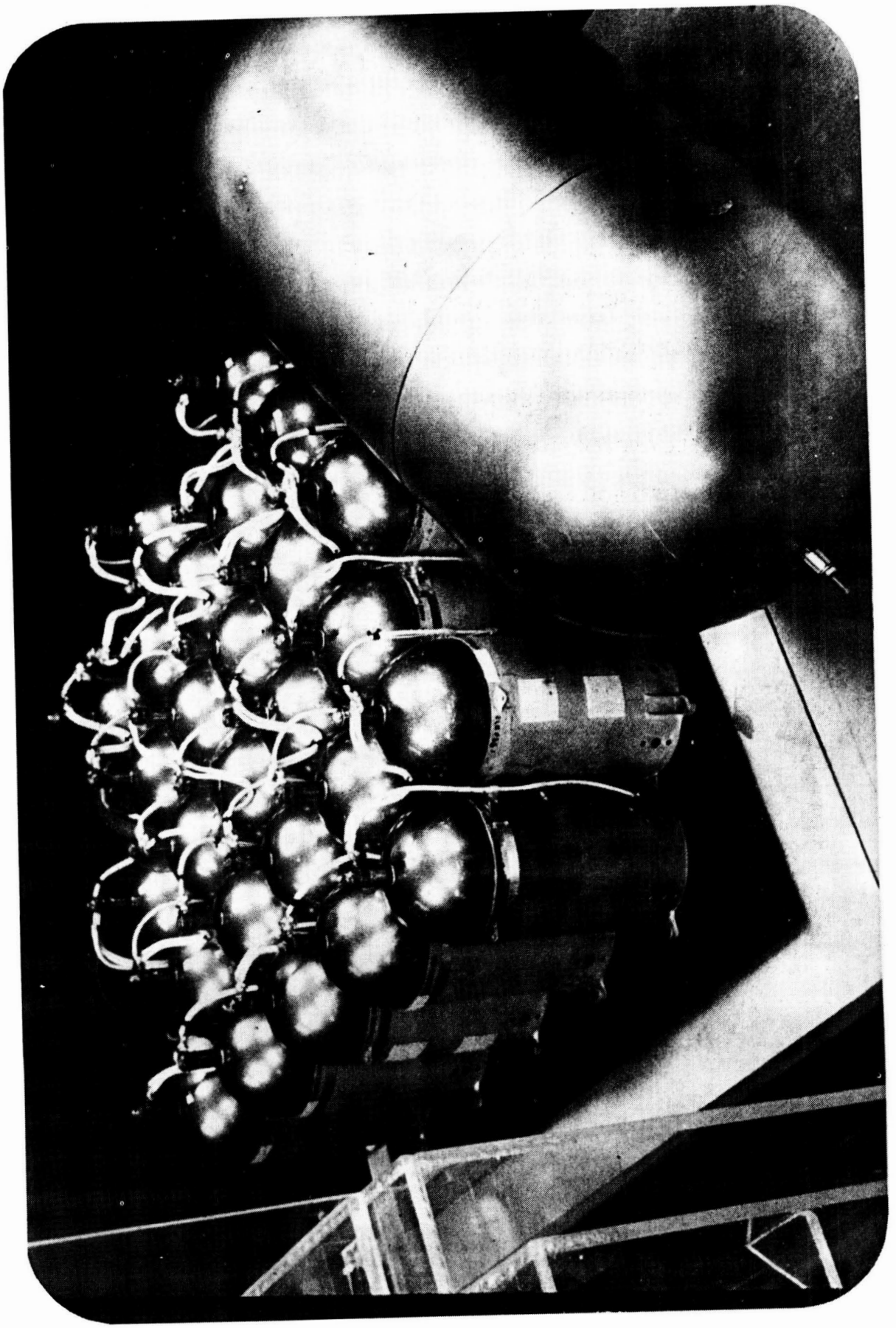

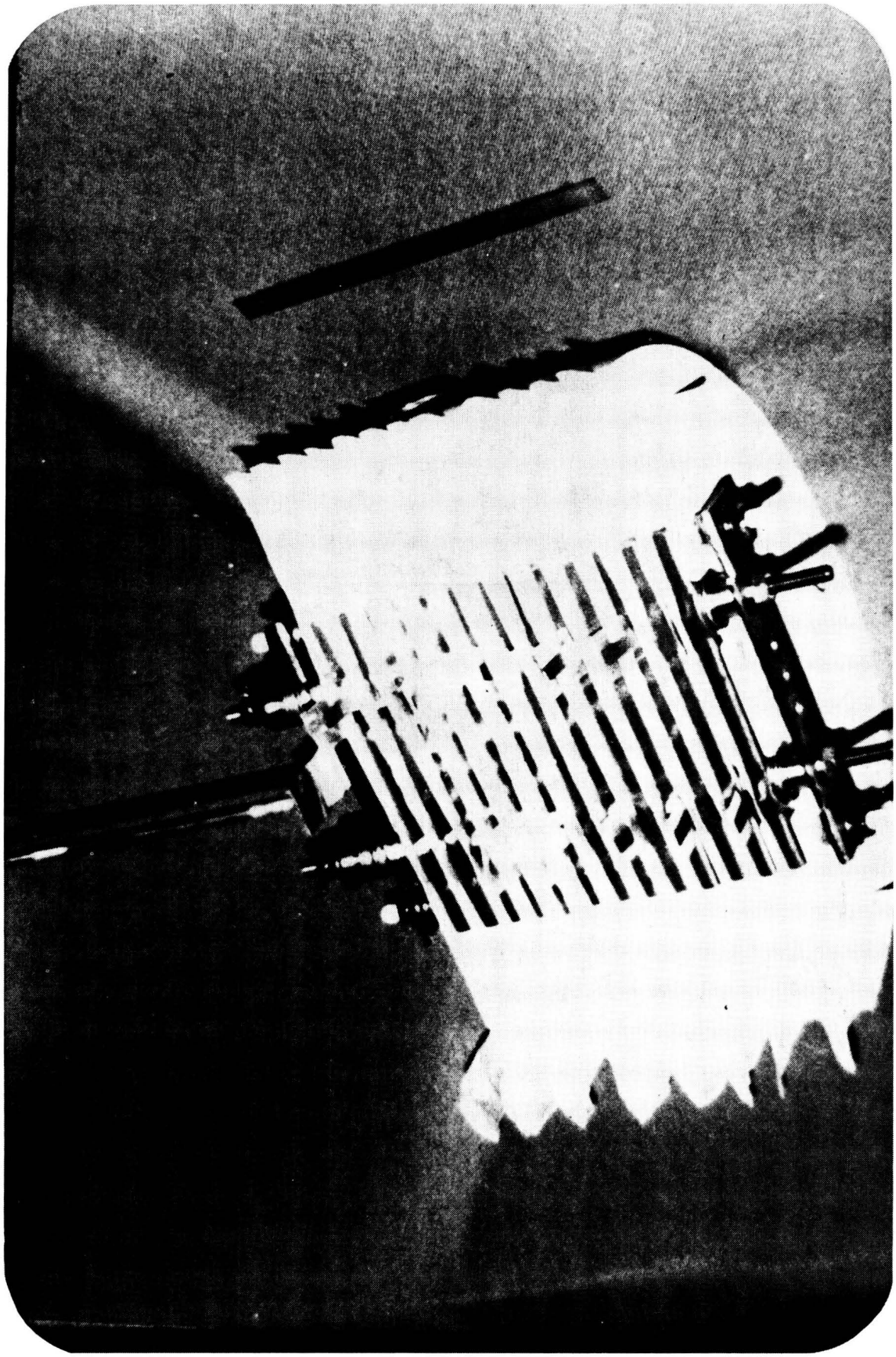

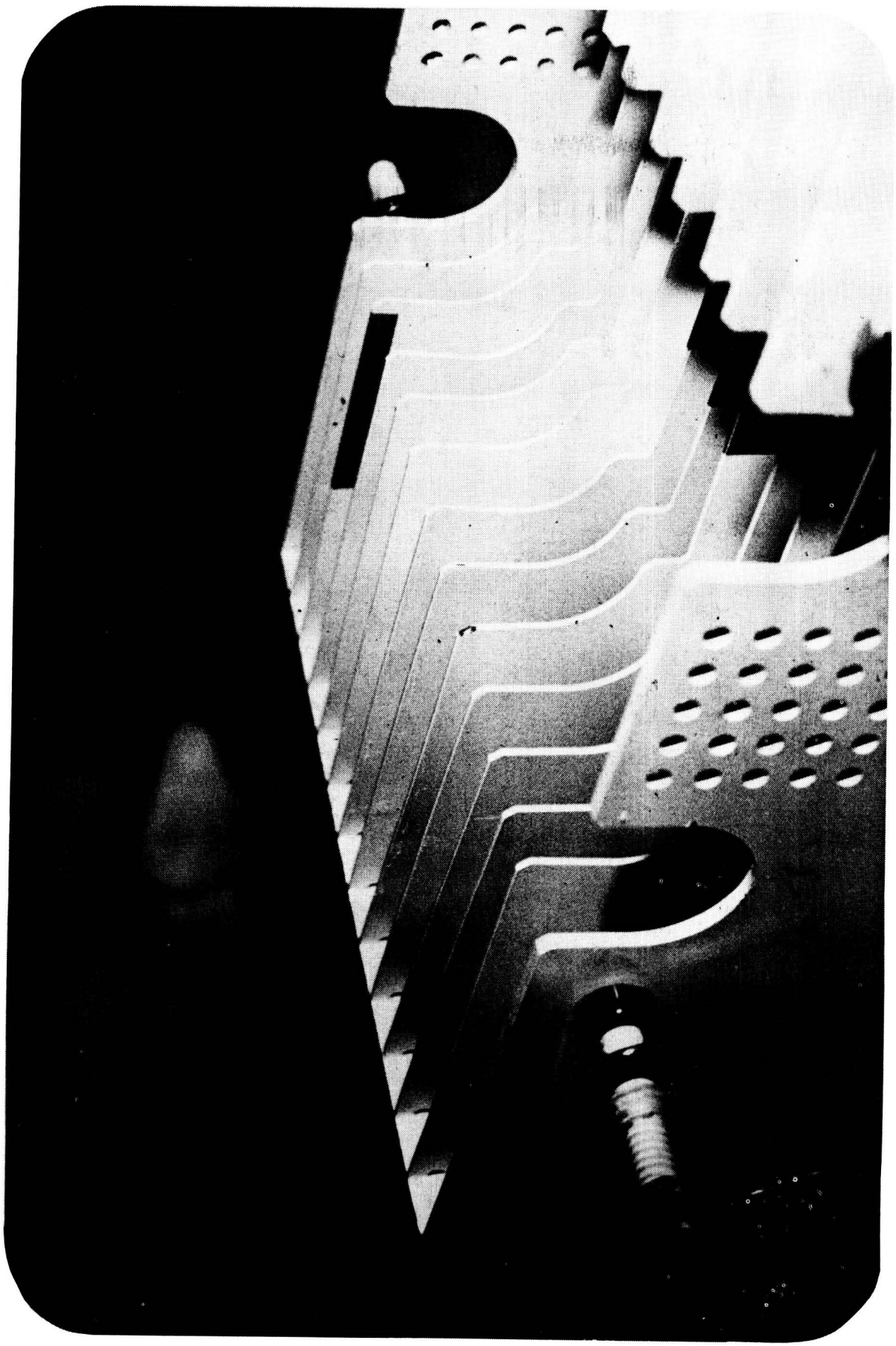

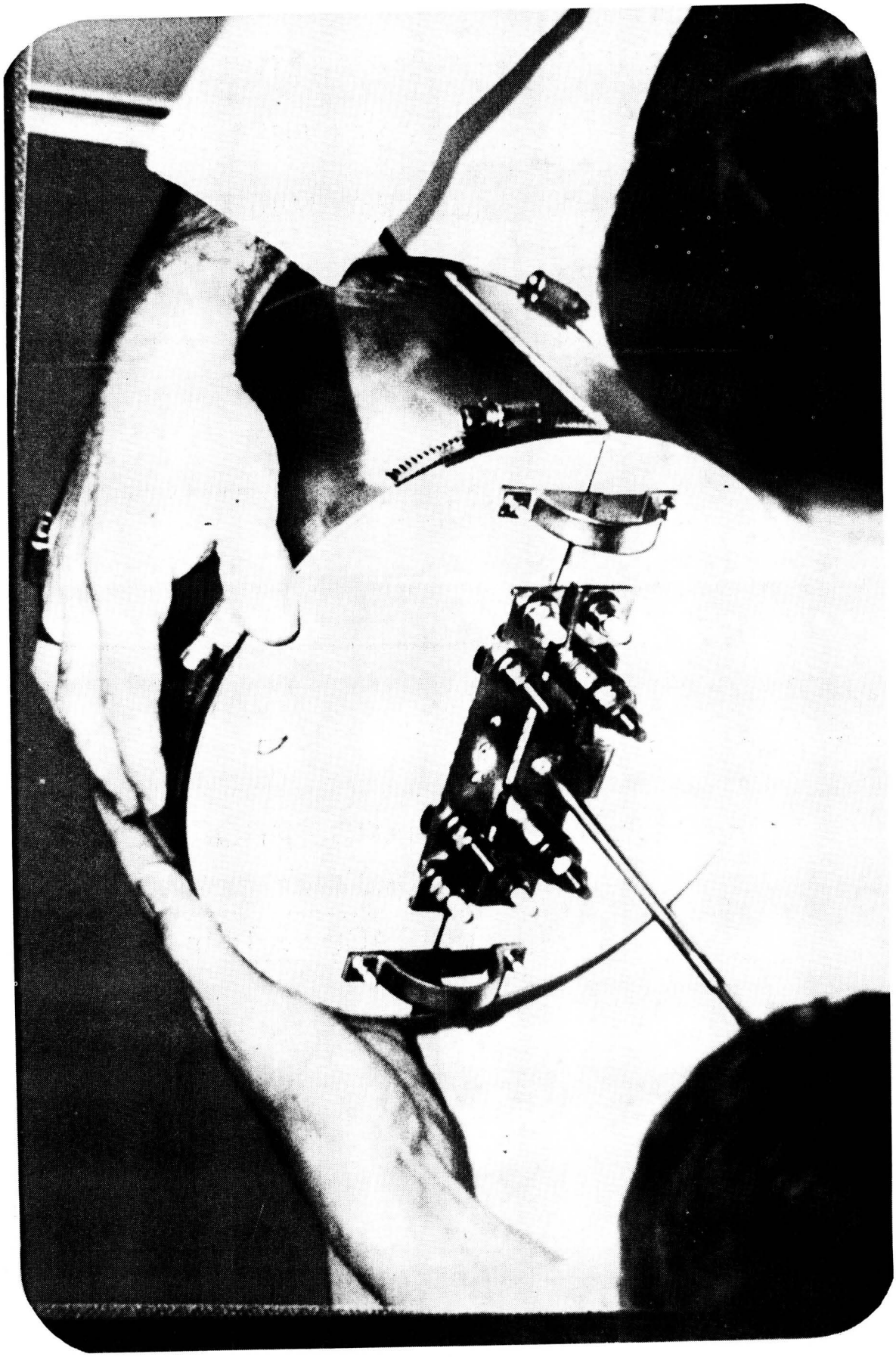

CPV PROTOTYPE BATTERY #1

44% DOD LEO CYCLING TEST

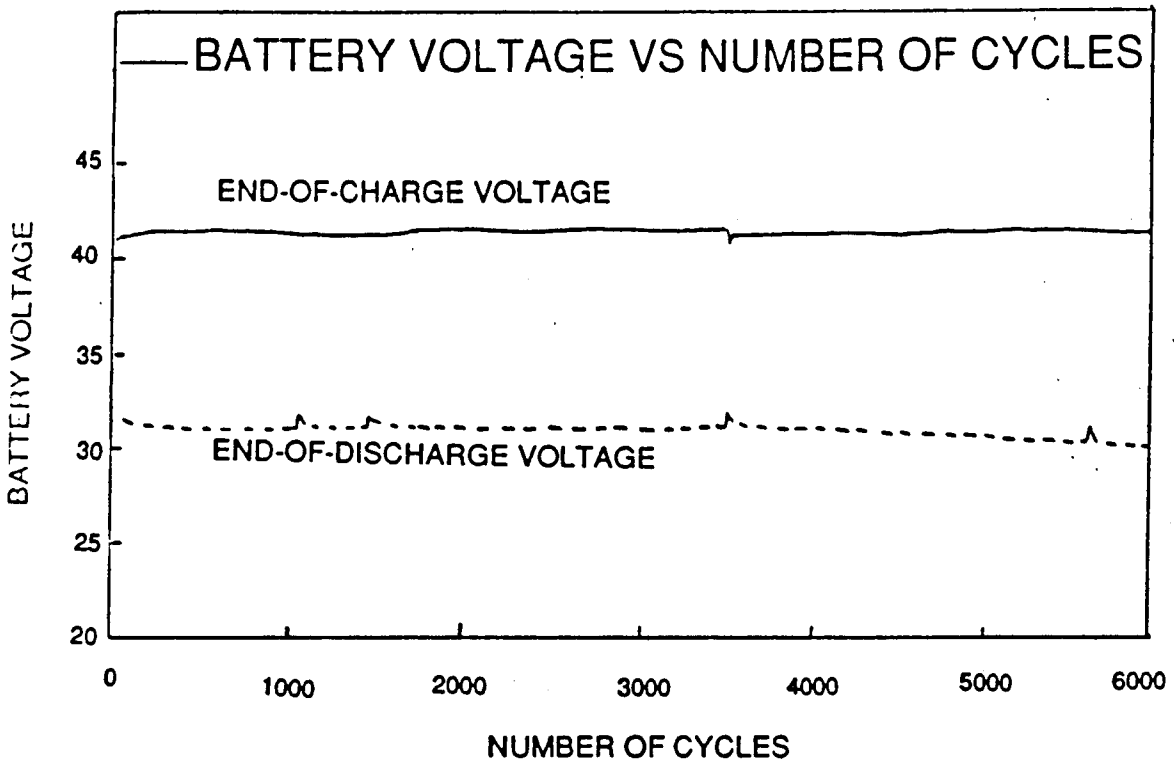

CHARGE DISCHARGE PROFILE

TEMPERATURE = 10°C

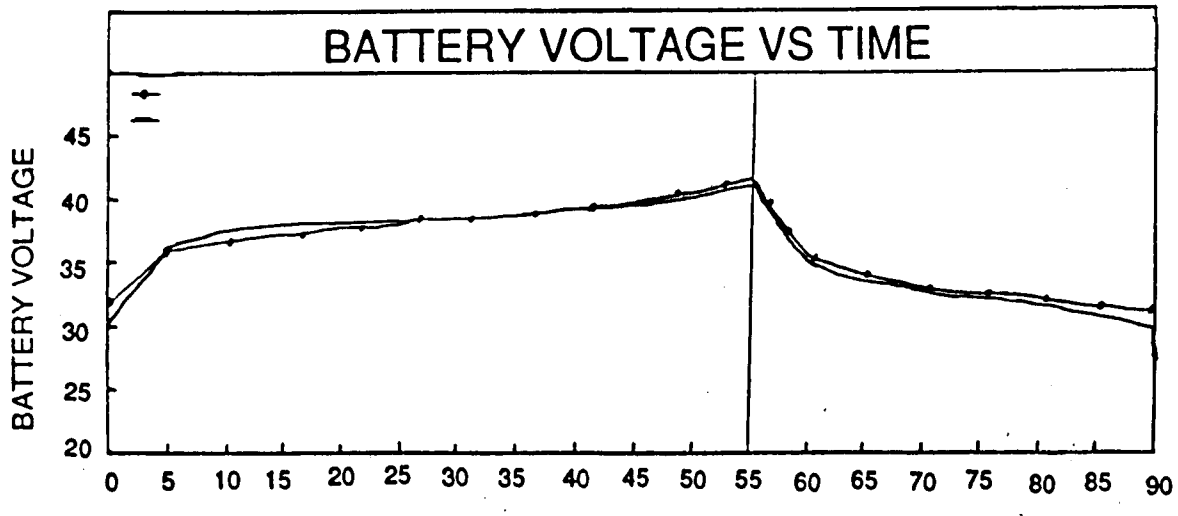

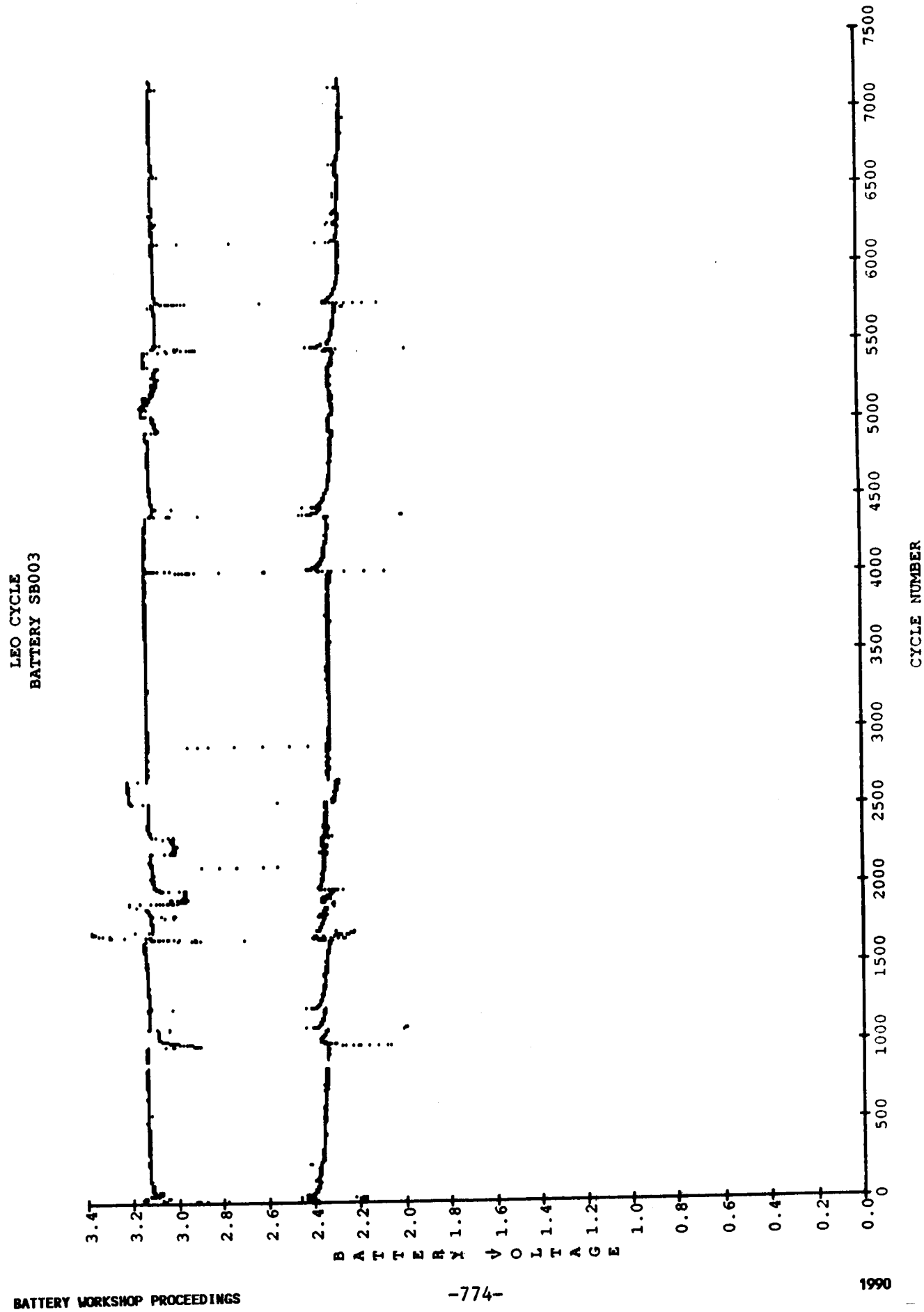
LEO CYCLE
BATTERY SB003
BATTERY VOLTAGE
3.4
3.2
3.0
2.8
2.6
2.4
2.2
2.0
1.8
1.6
1.4
1.2
1.0
0.8
0.6
0.4
0.2
0.0
0
500
1000
1500
2000
2500
3000
3500
4000
4500
5000
5500
6000
6500
7000
7500
CYCLE NUMBER

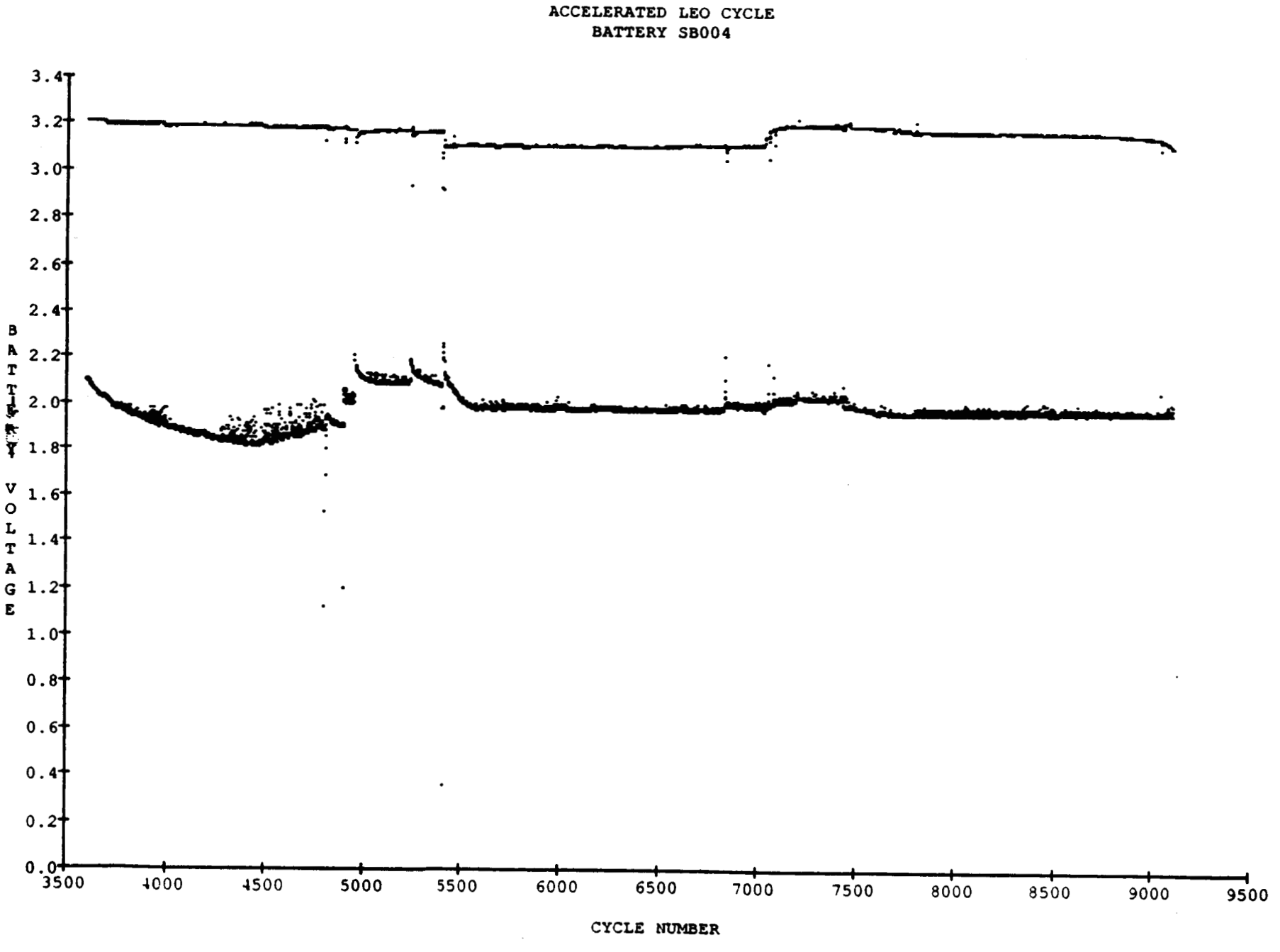
ACCELERATED LEO CYCLE
BATTERY SB004
BATTERY VOLTAGE
3.4
3.2
3.0
2.8
2.6
2.4
2.2
2.0
1.8
1.6
1.4
1.2
1.0
0.8
0.6
0.4
0.2
0.0
3500
4000
4500
5000
5500
6000
6500
7000
7500
8000
8500
9000
9500
CYCLE NUMBER

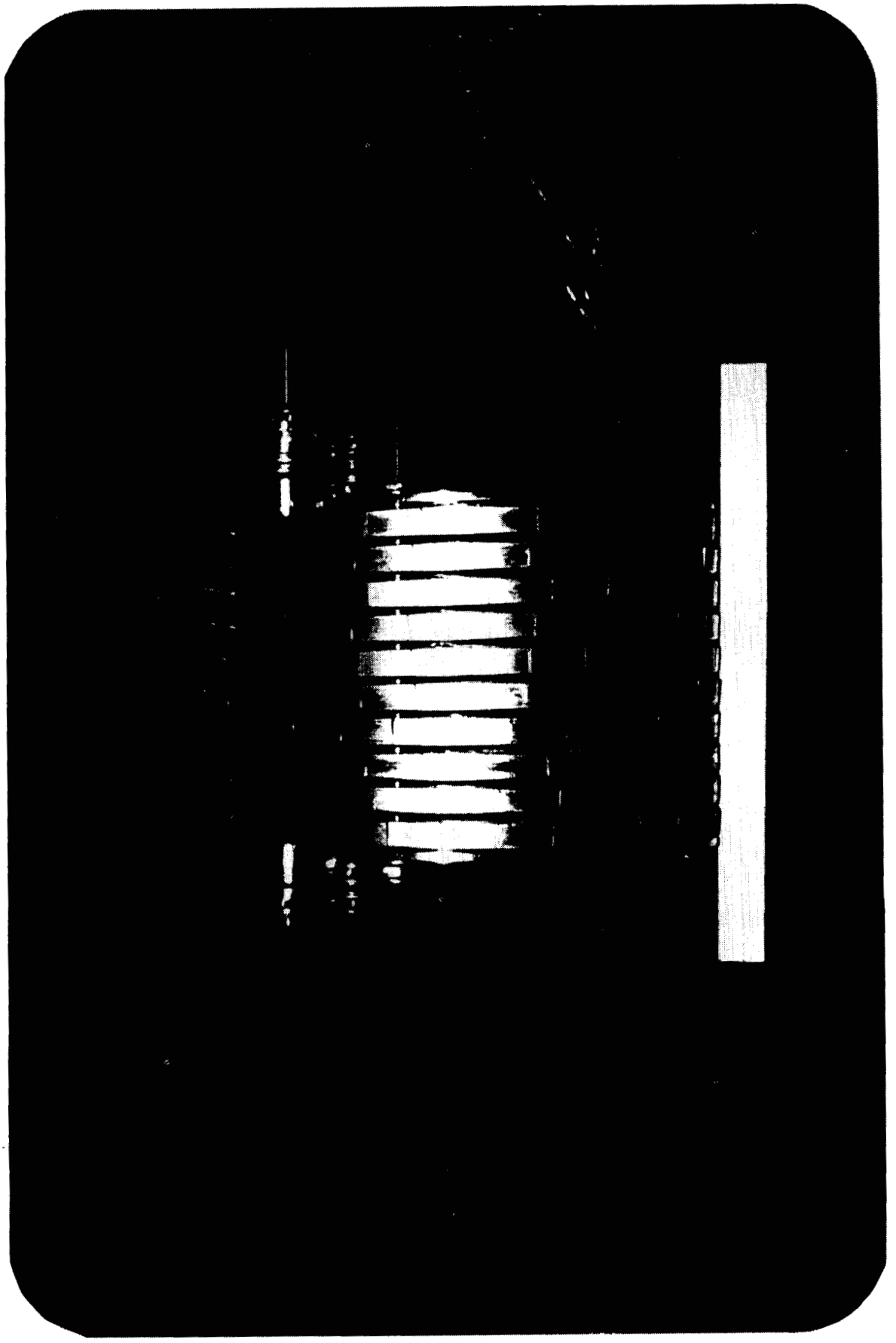

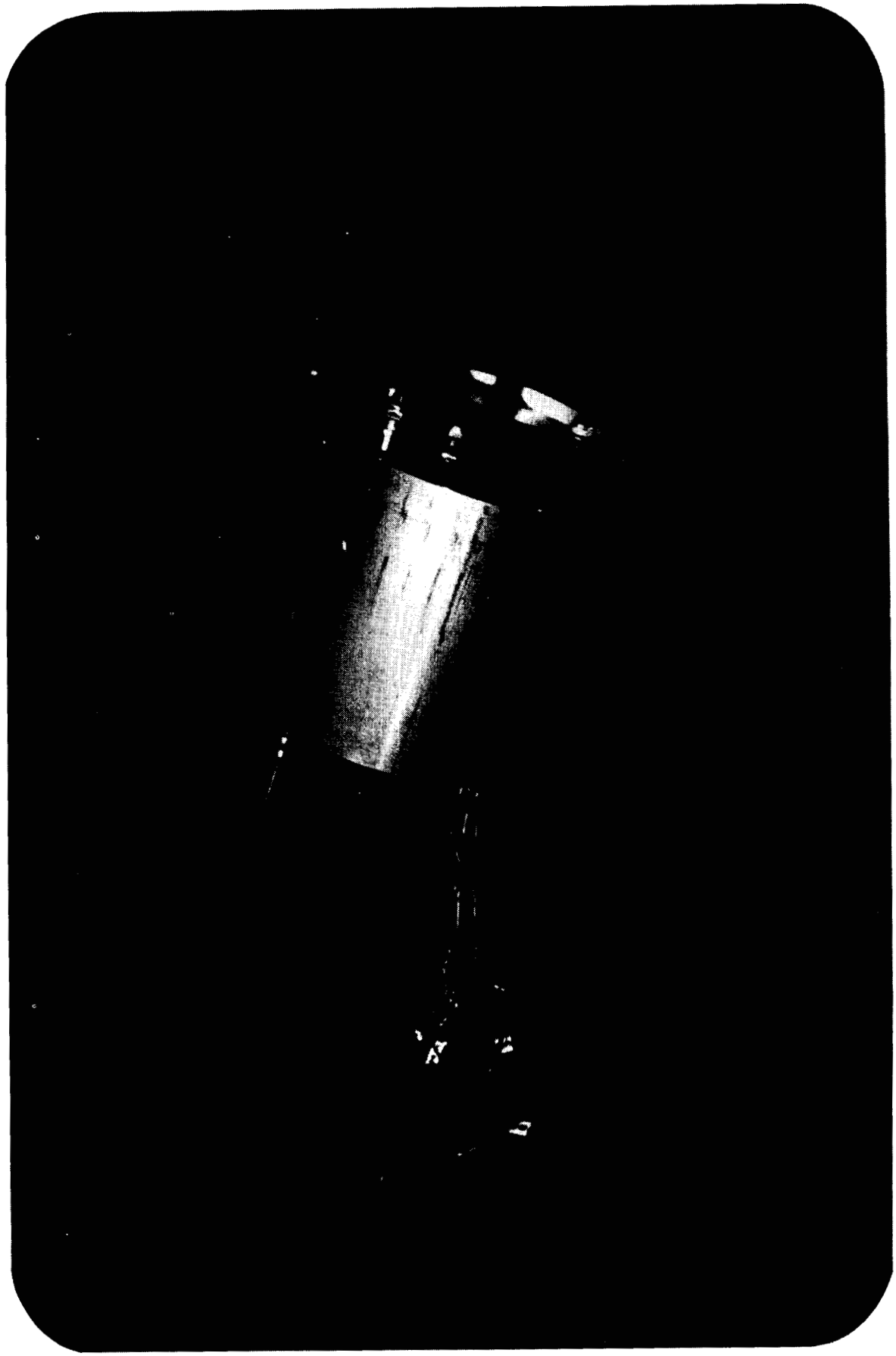

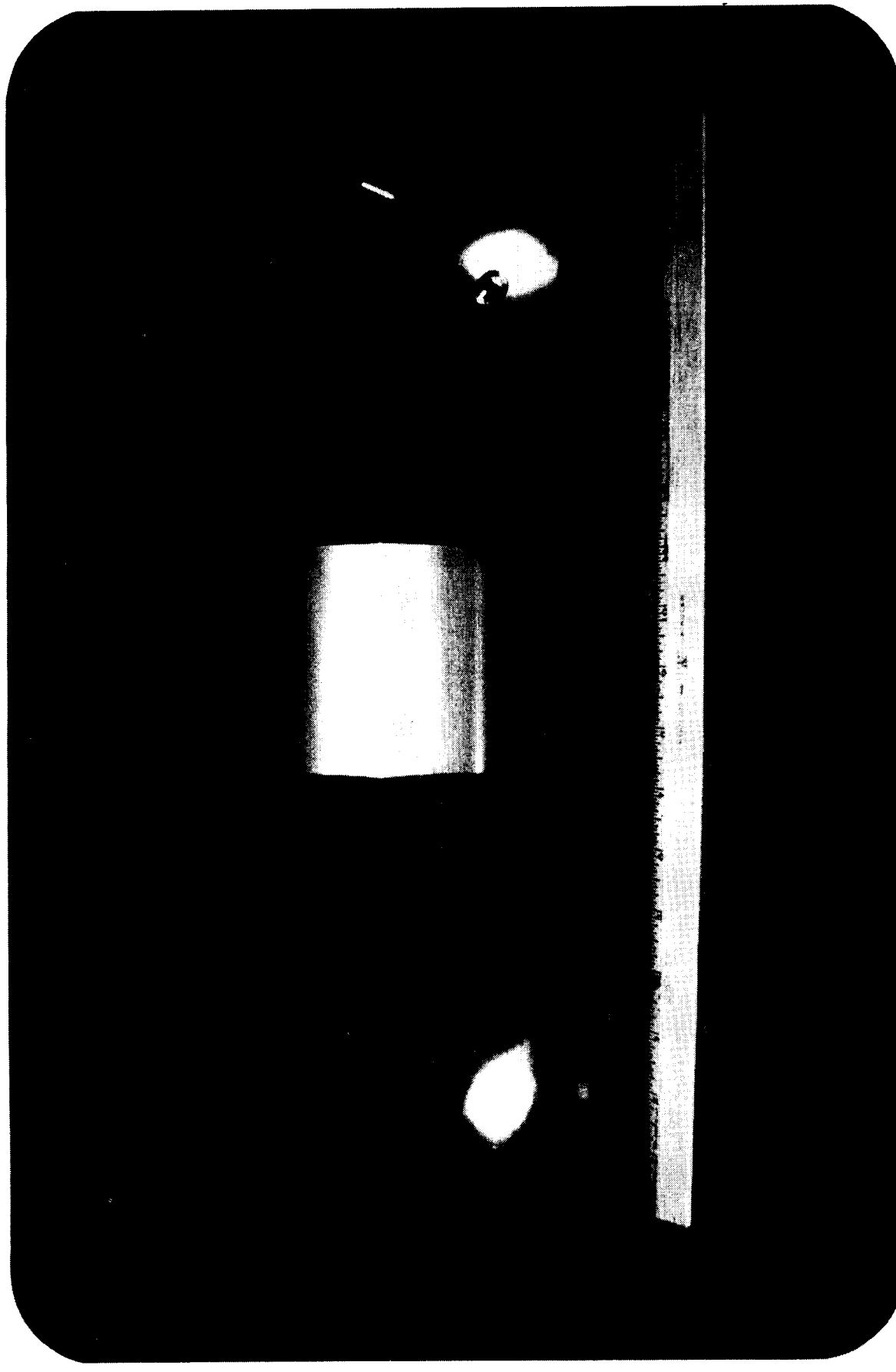

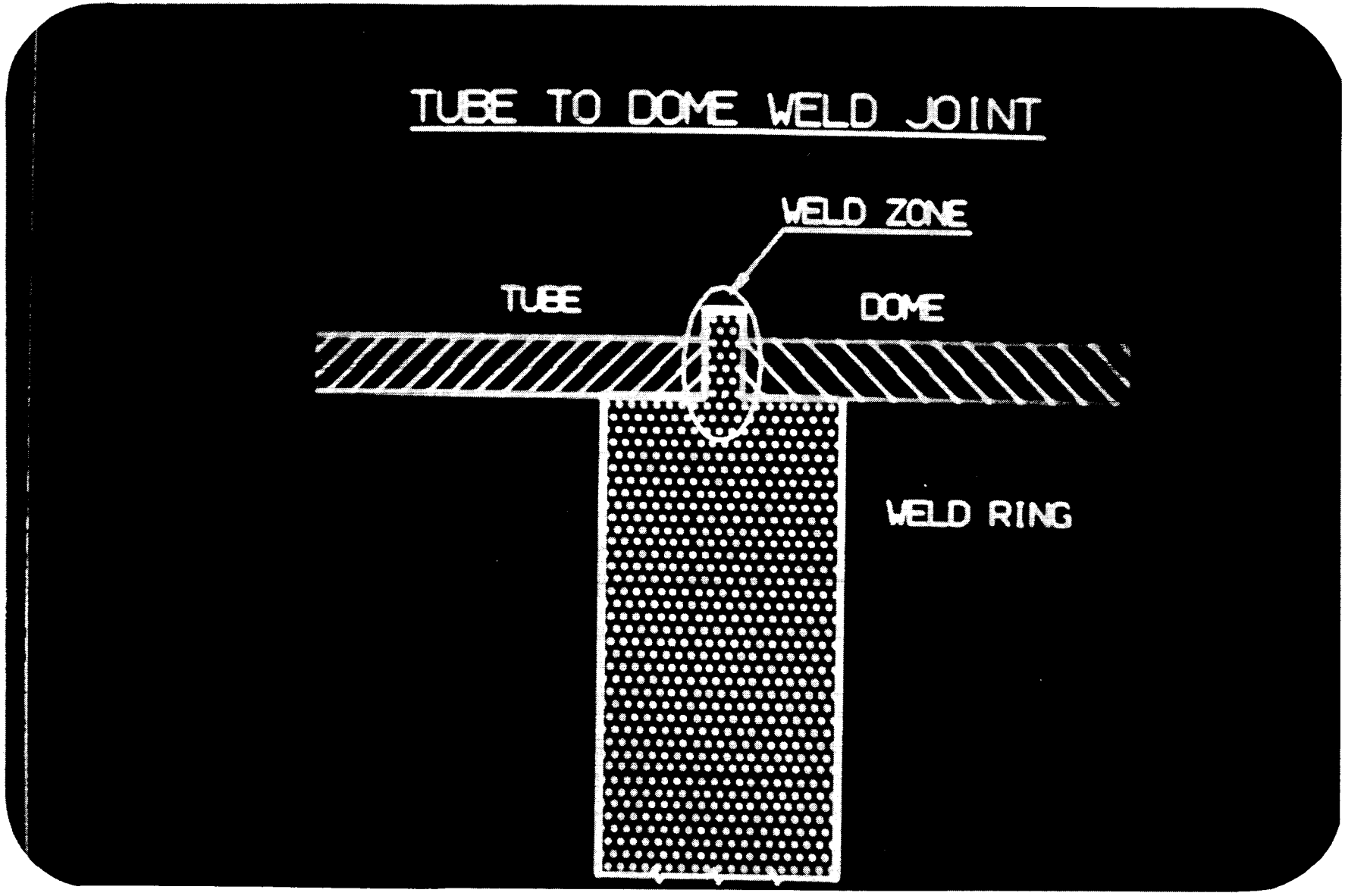
TUBE TO DOME WELD JOINT
WELD ZONE
TUBE
DOME
WELD RING

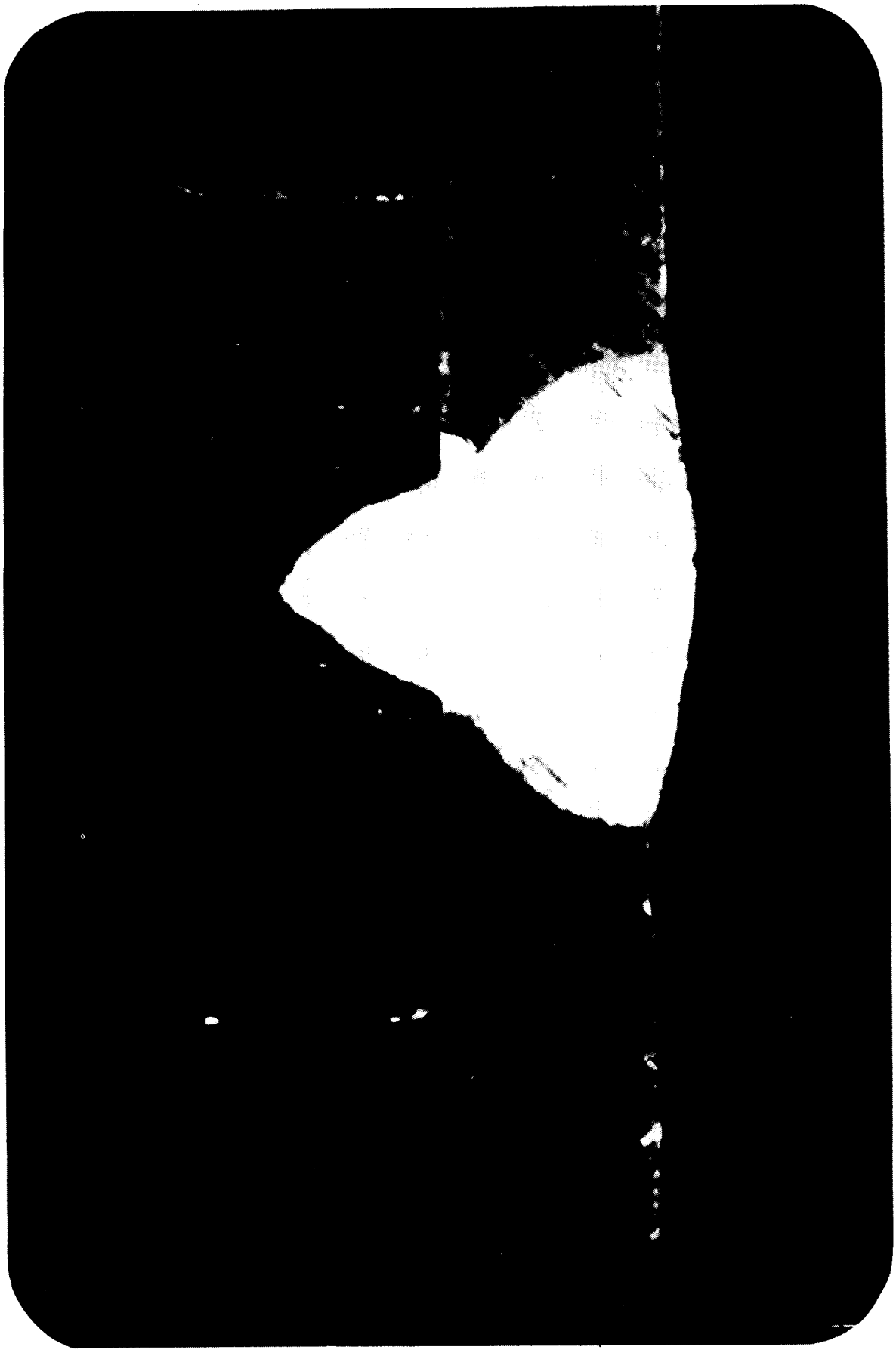

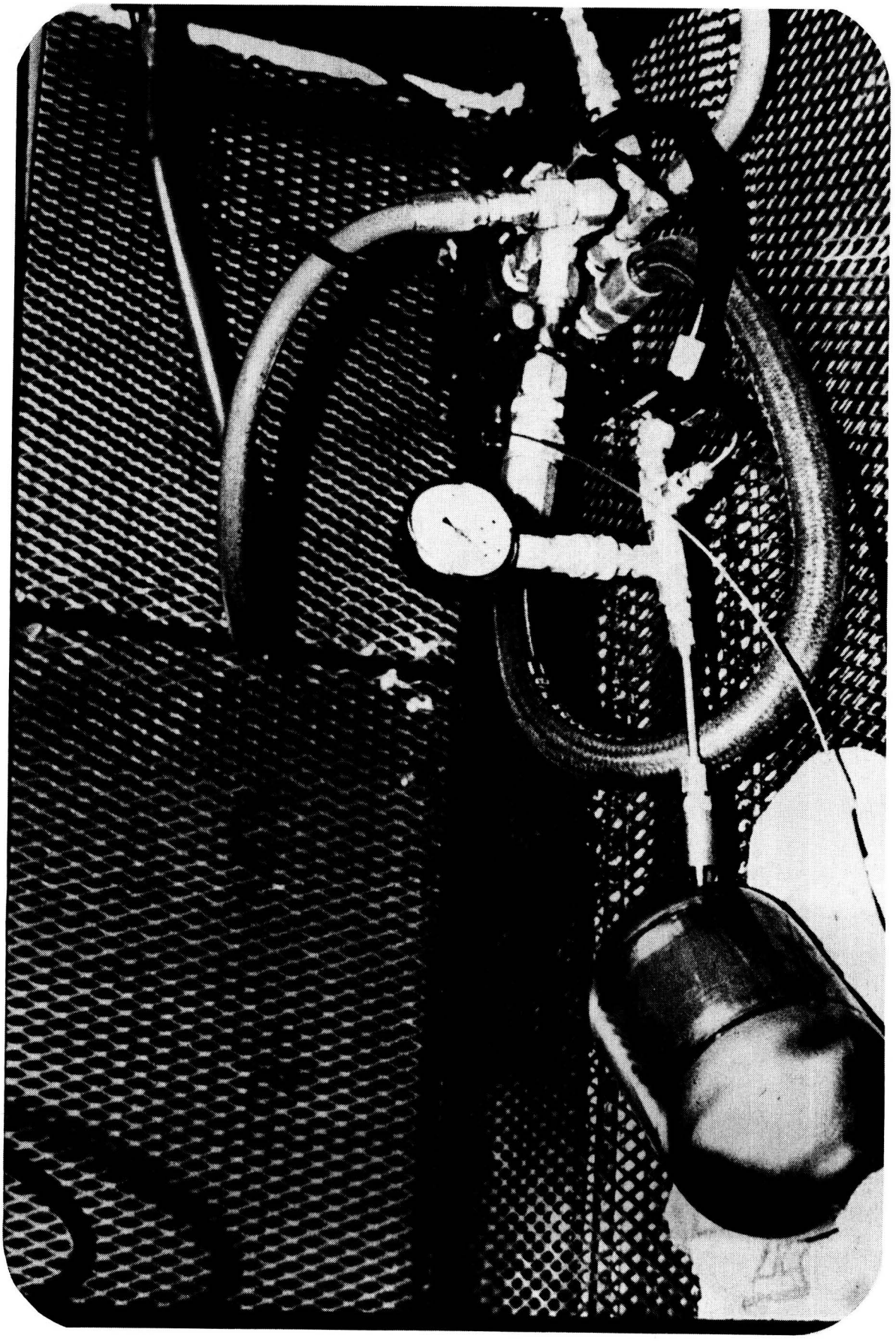

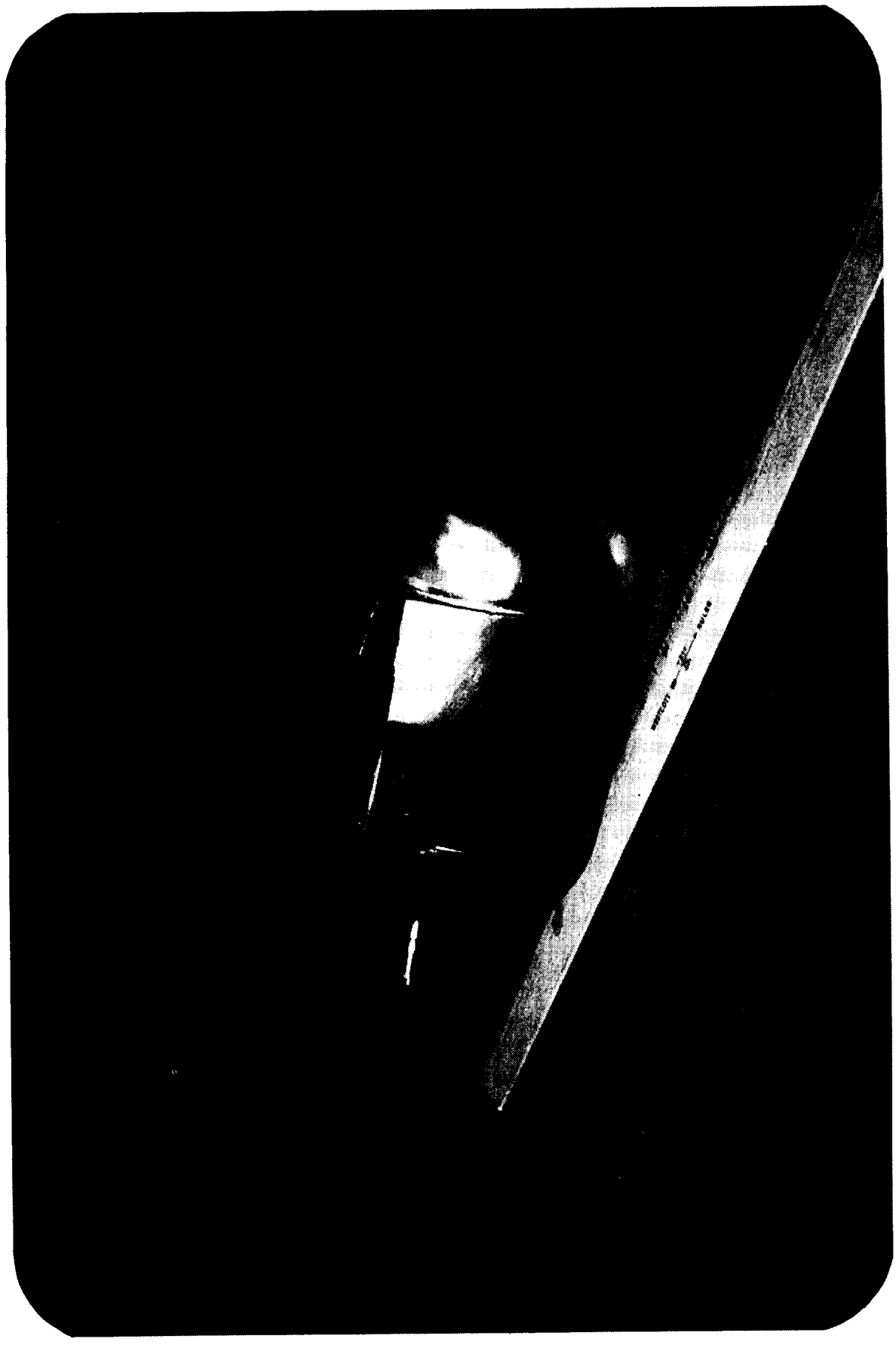

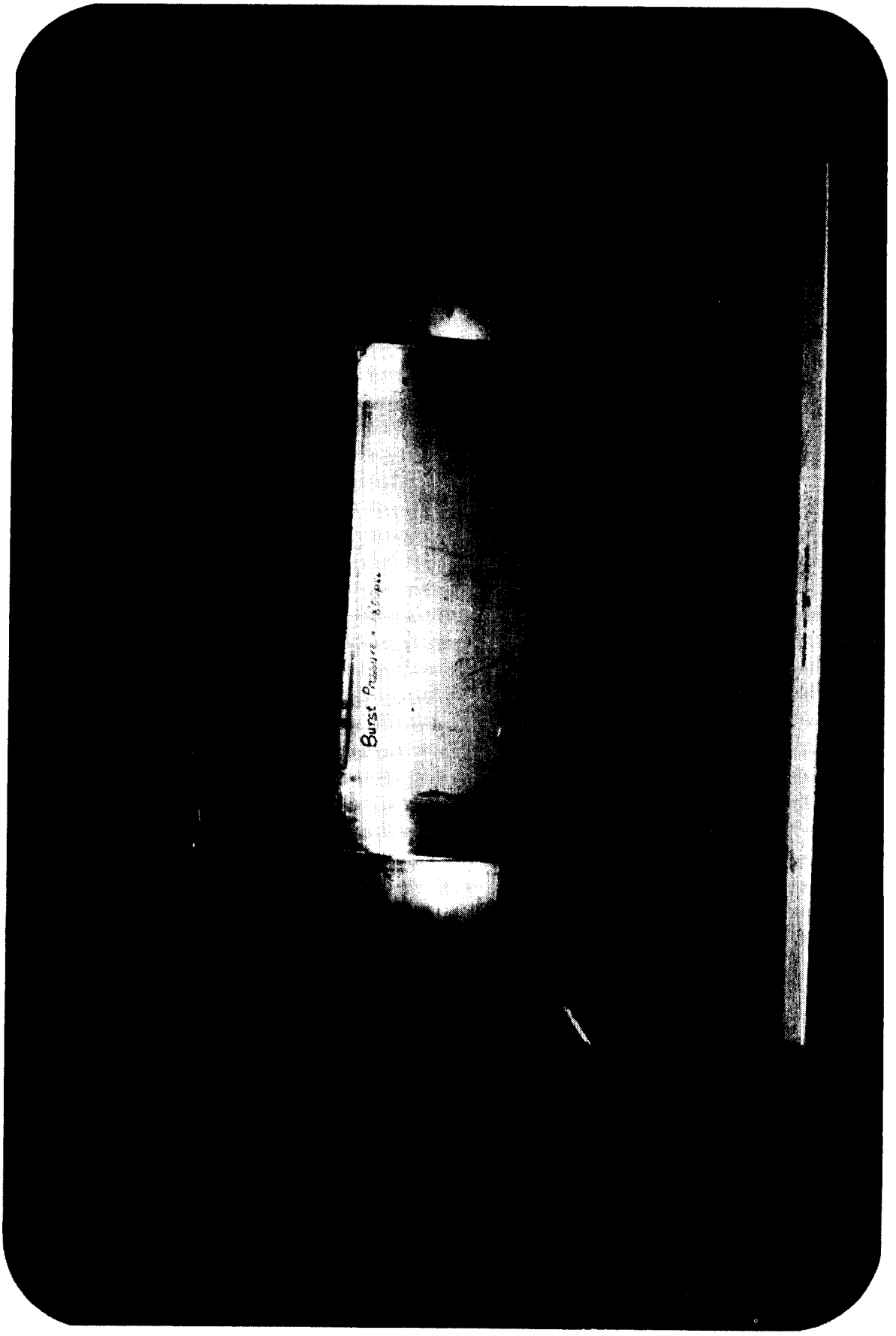

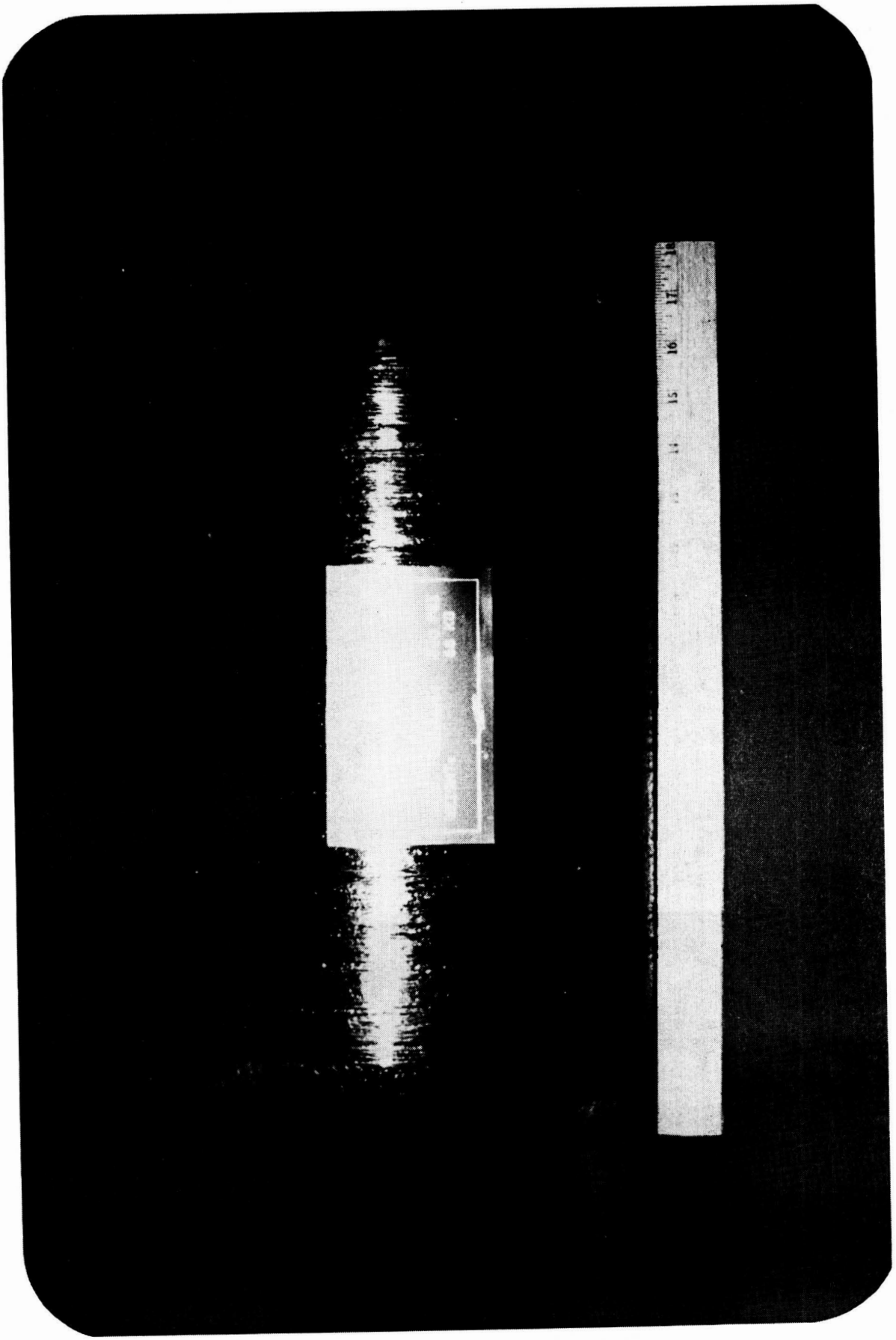

DieHard

RESULTS OF A TECHNICAL ANALYSIS OF THE HUBBLE SPACE TELESCOPE NICKEL-CADMIUM AND NICKEL-HYDROGEN BATTERIES

BY
HST BATTERY REVIEW SUBCOMMITTEE
NASA AEROSPACE FLIGHT BATTERY SYSTEMS STEERING COMMITTEE

NASA BATTERY WORKSHOP
HUNTSVILLE, AL

DECEMBER 6, 1990

HST BATTERY SUBCOMMITTEE REVIEW

INTRODUCTION

The Hubble Space Telescope Program Office requested the expertise of the NASA Aerospace Flight Battery Systems Steering Committee in the conduct of an independent assessment of the Hubble Space Telescope's battery system to assist in their decision whether to fly nickel-cadmium or nickel-hydrogen batteries on the telescope. In response, a Subcommittee to the NASA Aerospace Flight Battery Systems Steering Committee was organized with membership comprised of experts with background in the nickel-cadmium/nickel-hydrogen secondary battery/power systems areas. This presentation summarizes the work and recommendations of that Subcommittee.

It is important to recognize that the recommendations made by the Subcommittee are not intended as an endorsement of one chemistry over the other but rather are specific to the cell, battery, and power system designs for the Hubble Space Telescope. It should also be noted that this presentation reflects the opinion of the subcommittee members. The findings are based upon data and information provided by MSFC, LMSC, and EPI and the subcommittee members' experience. The findings presented in this report do not necessarily reflect the position of the subcommittee members' respective organizations. This information has been reviewed with the MSFC, HST, GSFC, and HQS program offices. It does not necessarily reflect the position of the HST program office.

HST BATTERY SUBCOMMITTEE REVIEW PRESENTATION OVERVIEW

PURPOSE AND OBJECTIVES

SUBCOMMITTEE REVIEW PROCESS

FINDINGS:

- Ni-Cd
- Ni-H_2

HST CONSIDERATIONS

RELATIVE RISKS

SUMMARY

HST BATTERY SUBCOMMITTEE REVIEW

PURPOSE AND OBJECTIVES

HST BATTERY SUBCOMMITTEE REVIEW PURPOSE

ASSIST NASA IN ARRIVING AT THE PROPER BATTERY SELECTION FOR THE HUBBLE SPACE TELESCOPE SPACE OBSERVATORY:

CONDUCT AN INDEPENDENT TECHNICAL ANALYSIS OF THE RELATIVE MERITS OF THE TWO BATTERY CHEMISTRY OPTIONS -- NICKEL-CADMIUM AND NICKEL-HYDROGEN -- AS DESIGNED FOR AND MADE APPLICABLE TO THE HST MISSION.

HST BATTERY SUBCOMMITTEE REVIEW OBJECTIVE

ASSIST CODE E IN ITS DECISION PROCESS FOR THE SELECTION OF EITHER NICKEL-CADMIUM OR NICKEL-HYDROGEN BATTERIES FOR THE HST LAUNCH BY PROVIDING FINDINGS FROM THE SUBCOMMITTEE'S ANALYSIS.

PROVIDE CODE Q WITH AN INDEPENDENT ANALYSIS OF THE HUBBLE SPACE TELESCOPE BATTERY OPTIONS FOR FIRST FLIGHT.

HST BATTERY SUBCOMMITTEE REVIEW

SUBCOMMITTEE REVIEW PROCESS

HST BATTERY SUBCOMMITTEE REVIEW

SUBCOMMITTEE MEMBERSHIP AND AFFILIATION

The HST Program Office requested of the NASA Aerospace Flight Battery Systems Steering Committee an independent review of the nickel-cadmium and nickel-hydrogen battery systems designed to provide energy storage on the HST. Norman Schulze, as chairman of the NASA Aerospace Flight Battery Systems Committee, organized and chaired the subcommittee of experts with extensive experience in the areas of electrochemistry, systems, manufacturing, ground operations, flight, and testing as they relate to nickel-cadmium and nickel-hydrogen cells batteries and power systems. The Subcommittee membership was drawn from government and industry.

HST BATTERY SUBCOMMITTEE REVIEW
SUBCOMMITTEE MEMBERSHIP AND AFFILIATION

NORMAN SCHULZE, CHAIRMAN	NASA HEADQUARTERS
KARLA CLARK	JET PROPULSION LABORATORY
STEPHEN GASTON	GE, ASTRO DIVISION
CAROLE HILL (ALTERNATE TO DR. HWANG)	AEROSPACE
WARREN HWANG	AEROSPACE
MICHELLE MANZO	LEWIS RESEARCH CENTER
DEAN MAURER	AT&T BELL LABORATORIES
GEORGE METHLIE	
DAVID PICKETT	HUGHES
EX OFFICIO:	
WANNEMAKER, HARRY	MDAC (GSFC CONTRACTOR)

HST BATTERY SUBCOMMITTEE REVIEW

SUBCOMMITTEE ACTIVITIES

The Subcommittee was organized in June of 1989, the decision meeting concerning the batteries was held on November 3, 1989. A number of meetings, including visits to the Marshall Space Flight Center and Eagle Picher Industries, were held. MSFC is the NASA center responsible for the construction, and launch of the HST; Eagle Picher is the subcontractor responsible for the construction of both sets of batteries. MSFC, EPI, and Lockheed personnel were available at these reviews to provide the requested information to the Subcommittee members.

HST BATTERY SUBCOMMITTEE REVIEW
SUBCOMMITTEE ACTIVITIES

DATE	EVENT	OBJECTIVE
JUNE 14	NAFBSSC MEETING	ESTABLISH COMMITTEE
JUNE 27	PARTICIPATION LETTERS	ORGANIZE SUBCOMMITTEE
JULY 6	DATA REQUEST TO MSFC	OBTAIN PREVIEW DATA PRIOR TO SITE VISIT
JULY 14	MSFC RESPONSE	DATA TRANSMITTAL SENT TO MEMBERS
JULY 20	SUBCOMMITTEE TELECON	ORGANIZATIONAL MEETING
JULY 25-27	MSFC SITE VISIT	DATA GATHERING
AUGUST 7	SUBCOMMITTEE MEETING AT IECEC	ESTABLISH REPORT OUTLINE, ASSIGNMENTS, AND SCHEDULE
AUGUST 8	NOTIFY MSFC ON EPI VISIT	PREPARATION FOR ESTABLISHING EPI REVIEW TOPICS
AUGUST 16	FLIGHT EXPERIENCE REVIEW	CONSIDER DATA BASE BEYOND NASA'S
AUGUST 22-24	EPI SITE VISIT	REVIEW OF CELL DATA
SEPTEMBER 14-15	SUBCOMMITTEE MEETING AT GE	REVIEW, ANALYZE DATA, DEVELOP POSITIONS
SEPTEMBER 18	DPA TELECON, MSFC	ESTABLISH DPA PROCEDURE
SEPTEMBER 19-22	EPI SITE VISIT	FURTHER DATA REVIEW- ONE MEMBER
SEPTEMBER 27	DPA TELECON, MSFC	OPTIONS, ELABORATIONS ON DPA
SEPTEMBER 27	BRIEF G. RODNEY	TUTORIAL AND STATUS UPDATE
OCTOBER 2	BRIEF MSFC ON FINDINGS	REVIEW FINDINGS WITH PROJECT STAFF
OCTOBER 5	SUBCOMMITTEE TELECON	REVIEW DRAFT PRESENTATION MATERIAL
OCTOBER 10-13	NAFBSSC MEETING	REVIEW SUBCOMMITTEE FINDINGS
OCTOBER 23	BRIEF PROGRAM STAFF	COORDINATE RESULTS WITH HQS. CODE EZ, MSFC, AND GSFC HST PROGRAM OFFICES
OCTOBER 30	SUBCOMMITTEE UPDATE	MSFC UPDATE GIVEN ON DPA, TV, LAUNCH STAND, CELL FAILURE, SHORT REVIEWS
NOVEMBER 3	HQS DECISION MEETING	PRESENT FINDINGS TO CODES E & Q

HST BATTERY SUBCOMMITTEE REVIEW

SUBCOMMITTEE APPROACH TO THE INVESTIGATION

EVALUATE HST'S EXISTING DESIGN FEATURES IN THE "ABSOLUTE" SENSE WITHOUT REGARD TO IMPACT - The Subcommittee approach to the investigation involved a review of the power system design for the HST in the absolute sense. The investigation involved comparing the nickel-cadmium and nickel-hydrogen battery systems and evaluating which battery would best serve the mission requirements.

IDENTIFY PROBLEMS AND CONCERNS REAL TIME TO THE HST STAFF - Problems and areas of concern requiring possible consideration were presented to the HST staff as they were identified. This allowed for greater interaction between the subcommittee and HST staff and resulted in the resolution of issues that otherwise might not have been possible.

EXPEDITE THE REVIEW PROCESS - MINIMIZE FORMALITIES - Due to the short time available for the review, as far as it was practical, the subcommittee members were free to interact directly with the contractor and subcontractor responsible for the power system and battery storage system.

COMMITTEE ROLE TO REVIEW INFORMATION ONLY - It was understood that the subcommittee role was to review information only. The subcommittee members were not in a position to give direction to the program office or the contractors involved or to make any binding recommendations or requests.

HST BATTERY SUBCOMMITTEE REVIEW
SUBCOMMITTEE APPROACH TO THE INVESTIGATION

EVALUATE HST'S EXISTING DESIGN FEATURES IN THE "ABSOLUTE" SENSE WITHOUT REGARD TO IMPACT

IDENTIFY PROBLEMS AND CONCERNS REAL TIME TO THE HST STAFF

EXPEDITE THE REVIEW PROCESS - MINIMIZE FORMALITIES

COMMITTEE ROLE TO REVIEW INFORMATION ONLY

HST BATTERY SUBCOMMITTEE REVIEW
SCOPE OF THE ANALYSIS

THE FOLLOWING AREAS WERE CONSIDERED ON BOTH THE CELL AND BATTERY LEVEL:

- REQUIREMENTS
- DESIGN
- QUALITY
- SAFETY
- RELIABILITY
- TESTING: REQUIREMENTS AND RESULTS TO DATE
  - QUALIFICATION TESTING
  - ACCEPTANCE TESTING
  - OTHER (DEVELOPMENTAL)
- DATA BASE (CELL HISTORY)
- SYSTEM INTEGRATION
- GROUND HANDLING
- FLIGHT OPERATION

HST BATTERY SUBCOMMITTEE REVIEW
HST MISSION DURATION OPTIONS

THE FOLLOWING MISSION DURATIONS WERE CONSIDERED FOR BOTH CHEMISTRIES:

30 MONTHS -- CONTRACTUAL REQUIREMENT

60 MONTHS -- DESIRED

GREATER THAN 60 MONTHS -- FOR CONSIDERATION

HST BATTERY SUBCOMMITTEE REVIEW

ASSUMPTIONS

In general the system was assessed "as is". The design and operation of the overall power system or specific subsystems, beyond the battery storage system, were not addressed. It was assumed that the power system was adequately designed to meet the specific requirements. The Subcommittee assessment rested solely on the evaluation of the specific nickel-cadmium and nickel-hydrogen batteries available for the HST launch scheduled for the Spring of 1990.

Specifically, the solar array power output, the electrical load requirements and the temperature balance requirements, heat load estimates and thermal maintenance were not examined in detail by the subcommittee, but were accepted as reference inputs. It should be noted that any of these parameters can have a significant impact on the decision process with respect to the power system.

HST BATTERY SUBCOMMITTEE REVIEW ASSUMPTIONS

SOLAR ARRAY POWER OUTPUT WOULD BE SUFFICIENT TO PROVIDE REQUIRED POWER OVER THE ENTIRE MISSION

ELECTRICAL LOAD REQUIREMENTS AS PRESENTED ACCURATELY REPRESENT THE BATTERY LOADS - SUBCOMMITTEE DID NOT LOOK FOR TRANSIENT OR PEAK LOADS

TEMPERATURE BALANCE REQUIREMENTS, HEAT LOAD ESTIMATES, AND THERMAL MAINTENANCE ARE ALL ADEQUATELY DESIGNED FOR THIS APPLICATION - NO INDEPENDENT ANALYSIS DONE

HST BATTERY SUBCOMMITTEE REVIEW
BATTERY OPTIONS

NICKEL-CADMIUM BATTERY

MANUFACTURED BY EAGLE PICHER INDUSTRIES
RSN55-15 CELLS - 55 AMPERE HOUR CAPACITY
23 CELLS PER BATTERY - SIX BATTERIES

NICKEL-HYDROGEN BATTERY

MANUFACTURED BY EAGLE PICHER
RNH90-3 - 87 AMPERE HOUR CAPACITY
23 CELLS PER BATTERY - SIX BATTERIES

HST BATTERY SUBCOMMITTEE REVIEW
FINDINGS - ANALYSIS RESULTS

HST BATTERY REVIEW SUBCOMMITTEE NICKEL-CADMIUM FINDINGS

HST BATTERY SUBCOMMITTEE REVIEW

FINDINGS: NI-CD STRONG POINTS

EXTENSIVE TEST PROGRAM - MSFC has conducted an extensive test program with the Ni-Cd cells designed for the HST storage system. A full scale Six Battery Test and a flight lot test of six four cell packs were tested under the HST cycle regime. While there was some question concerning the full integrity of the tests, both tests indicate that the batteries are capable of providing minimum safe mode requirements of 162 Ampere-hours after forty-two months of testing (>18,000 cycles).

POWER SYSTEM BATTERY PROTECTION AND RECONDITIONING CAPABILITY - The battery design incorporates the use of a "Battery Protection and Reconditioning Circuit" (BPRC) which prevents cell reversal during reconditioning. In addition the BPRC will allow the battery to function with a cell shorted by maintaining the voltage seen by the spacecraft bus.

APPROPRIATE CHARGING SYSTEM - The power system on the HST was designed to operate with Ni-Cd batteries and the power system and charging scheme were tailored to the Ni-Cd batteries as designed.

PROPER GROUND HANDLING - During the five year storage time the nickel-cadmium were stored at low temperatures discharged and shorted. This is the recommended storage mode for Ni-Cd cells.

EXTENSIVE OPERATIONAL HISTORY & EXPERIENCE - Ni-Cd batteries have flown on NASA satellites for many years. As a result NASA personnel have extensive experience operating nickel-cadmium batteries.

HST BATTERY SUBCOMMITTEE REVIEW FINDINGS: Ni-Cd STRONG POINTS

EXTENSIVE TEST PROGRAM
- 42 MONTH, 6 BATTERY TEST
- 6 FOUR CELL PACK LIFE CYCLE TEST OF FLIGHT LOT CELLS

POWER SYSTEM BATTERY PROTECTION AND RECONDITIONING CAPABILITY

APPROPRIATE CHARGING SYSTEM

PROPER GROUND HANDLING: CELLS STORED COLD, SHORTED

EXTENSIVE FLIGHT OPERATIONAL HISTORY & EXPERIENCE

HST BATTERY SUBCOMMITTEE REVIEW

FINDINGS: NI-CD WEAK POINTS SUMMARY

This is a summary listing of the Ni-Cd weak points. Because weaknesses exhibit the areas where there is cause for concern, each weak point will be discussed in detail in the following charts.

HST BATTERY SUBCOMMITTEE REVIEW FINDINGS: Ni-Cd WEAK POINTS - SUMMARY

PERFORMANCE OF CELLS SUBSEQUENT TO A FIVE YEAR SHELF LIFE - UNKNOWN

CELL DESIGN - NOT OPTIMUM

CELL QUALITY - QUESTIONABLE

QUALIFICATION PROGRAM NOT CONDUCTED ON FLIGHT CELL OR BATTERY

POSSIBLE LEAKAGE THRU VENT VALVE (A FAILURE MODE CONCERN)

RELATIVELY LITTLE NASA FLIGHT EXPERIENCE WITH THIS MANUFACTURER'S CELL

HST BATTERY SUBCOMMITTEE REVIEW

FINDINGS: Ni-Cd WEAK POINTS

PERFORMANCE OF CELLS SUBSEQUENT TO FIVE YEAR SHELF LIFE - UNKNOWN - The Six Battery Test Program completed 42 months of testing in of October 1989. This demonstrates that the test battery exceeded the minimum capacity requirement of 162 ampere hours following 30 months of cycling with newly built cells. However, the six battery test also exhibited a 40% capacity degradation during the test period and the cells in the six four cell packs, cells from the flight lot, degraded more than 12% during a similar test period. In addition, Ni-Cd cells are known to degrade with time, following activation. The flight cells would have been activated for five years by the time of the HST launch. The effects of separator degradation and positive plate swelling on battery performance and life were areas of concern for the flight batteries with long term storage. This degradation, along with the capacity loss with cycling, contribute to the uncertainty associated with the nickel-cadmium batteries.

Quantitatively, the effects of degradation on the cell performance and life are unknown. In an effort to evaluate the extent of the degradation, destructive physical analyses (DPA's) have been performed on a number of cells both cycled and uncycled HST type cells. Two cycled cells (Type 41) with non-flight separator were DPA'd. The cells were stored for a short time before cycling and had experienced 28000 cycles. The cells had acceptable overcharge protection at the time of the DPA's but the separator had deteriorated significantly. Three uncycled cells with flight lot separator were DPA'd following 3.5 years of storage. The separator showed no signs of degradation. Following a request for further DPA information, MSFC conducted a controlled test of flight lot cells which were then DPA'd to aid in evaluating separator stability and cell acceptability for flight. Plate swelling, separator quality, and carbonate levels were all within reasonable limits.

The long term storage has the potential to reduce cycle life for the flight cells. DPA's indicate that the storage has resulted in minimum degradation to date. In the six battery test, new cells, cycled for 42 months lost 45% of their original capacity. The cycle life margin available in stored cells is questionable. The first cell failure in the six battery test occurred at 18,308 orbits. Given this information, the flight batteries are not expected to exceed three years life.

HST BATTERY SUBCOMMITTEE REVIEW FINDINGS: Ni-Cd WEAK POINTS

PERFORMANCE OF CELLS SUBSEQUENT TO FIVE YEAR STORAGE UNKNOWN

QUALIFICATION TESTING WAS PERFORMED ON NEW CELLS
FLIGHT CELLS HAVE NOT BEEN PROVEN

DISCUSSION:

Ni-Cd CELLS DEGRADE FROM TIME OF ACTIVATION
CAPACITY DEGRADATION ON CYCLE TESTS
FLIGHT CELLS WOULD BE 5 YEARS OLD AT TIME OF LAUNCH
DPA'S PERFORMED TO EVALUATE EXTENT OF DEGRADATION
    MIXED RESULTS
CELL FAILURE IN SIX BATTERY TEST OCCURRED AT 18,308 CYCLES

HST BATTERY SUBCOMMITTEE REVIEW FINDINGS: Ni-Cd WEAK POINTS

PERFORMANCE OF CELLS SUBSEQUENT TO FIVE YEAR STORAGE UNKNOWN (CON'T)

IMPACT:

WITH LONG TERM STORAGE, BATTERY LIFE IS NOT EXPECTED TO EXCEED 3 YEARS

HST BATTERY SUBCOMMITTEE REVIEW

FINDINGS: Ni-Cd WEAK POINTS

THE CELL DESIGN IS NOT OPTIMIZED FOR LONG LEO CYCLE LIFE - The Eagle Picher RSN-55-15 has a number of design features that members of the subcommittee felt were not optimum. There was concern that the negative to positive ratio (1.53:1) should be higher for design life considerations. The high level of precharge and corresponding low amount of overcharge protection in the cells leads to variability in the measurements of the state of charge of the cells as well as large voltage dispersions. Overcharging cells with no overcharge protection would result in hydrogen accumulation, venting and dryout. The plate data showed high levels of carbonate and there appears to be no processing step in the MCD to reduce carbonate levels. The vented cell design was also cause for concern.

The shortcomings of the Eagle Picher cell design could result in performance and cycle life below the potential of the nickel-cadmium system.

HST BATTERY SUBCOMMITTEE REVIEW FINDINGS: Ni-Cd WEAK POINTS

THE CELL DESIGN IS NOT OPTIMIZED FOR LONG LEO CYCLE LIFE.

DISCUSSION:

LOW AMOUNT OF OVERCHARGE PROTECTION
HIGH LEVEL OF PRECHARGE
VENTED CELL DESIGN
PLATE SWELLING NOT MINIMIZED
HIGH PLATE CARBONATE LEVEL

IMPACT:

SHORTER CELL CYCLE LIFE RESULTS FROM THE PERFORMANCE POTENTIAL THAT IS POSSIBLE FROM Ni-CD TECHNOLOGY

HST BATTERY SUBCOMMITTEE REVIEW

FINDINGS: Ni-Cd WEAK POINTS

QUALITY CONTROL/PROCESS CONTROL - The quality control and process control at the cell manufacturer's plant for the nickel-cadmium cell are considered inadequate. The cell components lack the traceability desired for an aerospace product. The variations in component properties indicate a lack of reproducibility and consistency among the components. Significant dispersions in cell performance have been noted. The BPRC compensates for the non-uniformity of the cells and batteries.

These are issues that can result in potentially greater variability of cell performance and cycle life.

HST BATTERY SUBCOMMITTEE REVIEW FINDINGS: Ni-Cd WEAK POINTS

QUALITY CONTROL/PROCESS CONTROL

QUALITY DOCUMENTATION AND PROCESS CONTROLS ARE WEAK
PROCESS NOT UNDER ADEQUATE CONTROL TO BE REPRODUCIBLE

DISCUSSION:

PROCESS LACKS TRACEABILITY
PLATE POROSITY DISTRIBUTION DATA
PLAQUE BENDING DATA
MCD LACKS DETAIL

HST BATTERY SUBCOMMITTEE REVIEW FINDINGS: Ni-Cd WEAK POINTS

QUALITY CONTROL/PROCESS CONTROL (CON'T)

DISCUSSION: (CON'T)

LARGE DISPERSION IN PLATE THICKNESS AND CAPACITY
CELL TO CELL DISPERSIONS
- STATE OF CHARGE
- END OF CHARGE VOLTAGE

IMPACT:

RESULTS IN POTENTIALLY GREATER VARIABILITY OF CELL PERFORMANCE
POSSIBLE REDUCED CYCLE LIFE AND LOSS OF CAPACITY

HST BATTERY SUBCOMMITTEE REVIEW

FINDINGS: Ni-Cd WEAK POINTS

QUALIFICATION TESTING - Neither the Type 44 battery nor its RSN55-15 cell received a formal qualification test program. A protoflight (flight level/short duration) vibration test was performed on the Type 44 battery in lieu of qualification testing. Full qualification testing was performed on the Type 40 cell. However, the cell designs are different. The type 41 cells incorporates seventeen changes over the type 40 cell. Some of these changes could affect the cell susceptibility to damage. Load margins and flight duration time were not demonstrated.
As a result, the nickel-cadmium cells would be flown unqualified and there exists a potential for premature cell failure resulting from unknown performance with respect to the dynamic loads.

HST BATTERY SUBCOMMITTEE REVIEW FINDINGS: Ni-Cd WEAK POINTS

QUALIFICATION TESTING

NEITHER THE TYPE 44 BATTERY NOR ITS RSN 55-15 CELL RECEIVED A FORMAL QUALIFICATION TEST PROGRAM

DISCUSSION:

FULL QUAL PERFORMED ON TYPE 40 CELL
- FLIGHT BATTERY CONTAINS TYPE 44 CELLS
- THE DESIGNS ARE DIFFERENT

PROTOFLIGHT (FLIGHT LEVEL/SHORT DURATION) VIBRATION TEST PERFORMED ON TYPE 44 BATTERY IN LIEU OF QUAL

LOAD MARGINS AND FLIGHT DURATION TIME WERE NOT DEMONSTRATED.

HST BATTERY SUBCOMMITTEE REVIEW FINDINGS: Ni-Cd WEAK POINTS

QUALIFICATION TESTING (CON'T)

DISCUSSION (CON'T)

TYPE 40 CELL WENT THROUGH CELL VIBRATION TESTING
17 CHANGES MADE TO THE TYPE 41 CELL.
CHANGES COULD AFFECT CELL SUSCEPTIBILITY TO DAMAGE

IMPACT:

CELLS WILL BE FLOWN UNQUALIFIED
POTENTIAL FOR PREMATURE CELL FAILURE DUE TO DYNAMIC LOADS

HST BATTERY SUBCOMMITTEE REVIEW

FINDINGS: Ni-Cd WEAK POINTS

CELL DESIGN INCORPORATES A RELIEF VALVE - Aerospace flight cells are traditionally sealed. The Eagle Picher RSN55-15 incorporates the use of a Bunsen pressure relief valve. The valve is set to relieve at 120 psi and cell pressures typically run at approximately 20 psi. The main concern associated with the vent is the loss of the seal integrity. Overcharging may result in the venting of O_2 and H_2 and possibly a permanent leak resulting in the loss of electrolyte and gas and ultimately leading to cell failure. MSFC believes that the system is carefully designed to avoid overcharging and does not expect the valve to present any problems. However, the possibility of cell to cell dispersions could result in some cells being overcharged. Based on limited past Skylab experience, there is no known generic problem with the use of these vents in space but similarly designed relief valves have been known to cause problems in commercial cells. Loss of the seal integrity could result in the premature loss of cells and/or batteries, and corrosion of the battery module. The battery module is also housed in a vented casing and this too would have to leak before the HST science might be affected by contamination.

HST BATTERY SUBCOMMITTEE REVIEW FINDINGS: Ni-Cd WEAK POINTS

CELL DESIGN INCORPORATES A RELIEF VALVE

USE OF BUNSEN CELL PRESSURE RELIEF VALVE PROVIDES POTENTIAL LEAK PATH FOR ELECTROLYTE AND GAS.

DISCUSSION:

VENT MAY RESULT IN LOSS OF SEAL INTEGRITY

SYSTEM DESIGNED CAREFULLY TO AVOID OVERCHARGING

CELL PERFORMANCE DISPERSIONS AT END OF CHARGE COULD RESULT IN SOME OVERCHARGING

OVERCHARGING MAY RESULT IN VENTING OF O_2 & H_2

HST BATTERY SUBCOMMITTEE REVIEW FINDINGS: Ni-Cd WEAK POINTS

CELL DESIGN INCORPORATES A RELIEF VALVE (CON'T)

DISCUSSION:

LEAKAGE STATUS OF FLIGHT CELLS - CURRENTLY UNKNOWN

NO KNOWN GENERIC PROBLEM IN SPACE

IMPACT:

PREMATURE LOSS OF CELLS

CORROSION OF BATTERY MODULE DUE TO KOH ON AL

GAS CONTAMINATION OF ENVIRONMENT

HST BATTERY SUBCOMMITTEE REVIEW

FINDINGS: Ni-Cd WEAK POINTS

SEPARATOR QUALITY - Recent problems experienced at Gates with cells containing Pellon 2505 separator material have raised questions concerning the quality of that material. The nature of the problem is not fully understood and as a result all 2505 material should be reevaluated. Some specific rolls of material have been identified as suspect at Gates, however, not all cells built using that material exhibit the problem. Conversely, some cells built from rolls of material that have been identified as effected have also exhibited anomalous performance. The EP RSN55-15 cells contain Pellon 2505. 162 HST nickel-cadmium cells have been cycled and 7 cells have been DPA'd. To date the HST cells have not exhibited any of the anomalous behavior associated with this problem.

HST BATTERY SUBCOMMITTEE REVIEW FINDINGS: Ni-Cd WEAK POINTS

SEPARATOR QUALITY

QUALITY OF PELLON 2505 IS QUESTIONABLE

DISCUSSION:

IDENTIFICATION OF PROBLEM MATERIAL IS DIFFICULT

EXTENT AND SEVERITY OF 2505 PROBLEM ARE UNKNOWN
COULD EFFECT HST CELLS

162 HST CELLS HAVE BEEN TESTED, 7 OF WHICH WERE DPA'D
TESTED WITHOUT EXPERIENCING THE PROBLEM

ADDITIONAL TESTING DESIGNED TO EVALUATE SEPARATOR
QUALITY SHOWED NO PROBLEM

HST BATTERY SUBCOMMITTEE REVIEW FINDINGS: Ni-Cd WEAK POINTS

SEPARATOR QUALITY (CON'T)

IMPACT:

PREMATURE LOSS OF CYCLE LIFE CAPABILITY HAS BEEN EXPERIENCED WITH GATES CELLS AND COULD OCCUR ON HST

HST BATTERY REVIEW SUBCOMMITTEE
NICKEL-HYDROGEN FINDINGS

HST BATTERY SUBCOMMITTEE REVIEW

FINDINGS: Ni-H2 STRONG POINTS

CELL DESIGN - The basic cell design for the nickel-hydrogen is the MILSTAR design with some modifications. The MILSTAR design has been tested extensively and is sound. The specific design modifications for the HST cells involve the terminal configuration and are expected to have minor impact on cell performance.

MANUFACTURING CONTROL DOCUMENT (MCD) - The manufacturing control document for the nickel-hydrogen cells is very thorough and well written. There is a much greater degree of control associated with the nickel-hydrogen cell manufacturing than with the nickel-cadmium cell manufacturing.

CELL QUALITY - The tighter controls imposed by a more thorough MCD result in better cell quality. The uniformity of components and the final cell quality is much better for nickel-hydrogen than for nickel-cadmium.

PLATE QUALITY - The plates for the nickel-hydrogen system have improved sinter processing. and are electrochemically impregnated. This is a more controlled process than chemical impregnation and it yields a superior product. A higher percentage of the plates pass stress testing, again indicating higher quality plates.

CAPACITY - The nickel-hydrogen, RNH90-3 cells have 87 ampere hours capacity vs 55 ampere hours for the RSN55-15 nickel-cadmium cells. This allows for a greater capacity margin for contingency operations aboard the HST. With the higher capacity, the batteries will operate at a lower DOD which should result in a longer life.

REDUNDANT BATTERIES - The increased capacity also results in a greater system redundancy. Two batteries can be lost before the HST would be in danger of not meeting its minimum capacity requirement.

RECONDITIONING CAPABILITY - The HST nickel-hydrogen battery system has the capability for reconditioning the batteries. It is not clear whether or not reconditioning would be required but if it is the capability is there.

EAGLE PICHER FLIGHT EXPERIENCE -To date, Eagle Picher has more flight experience with nickel-hydrogen batteries than any other manufacturer.

HST BATTERY SUBCOMMITTEE REVIEW FINDINGS: Ni-H_2 STRONG POINTS

CELL DESIGN

MANUFACTURING CONTROL DOCUMENT (MCD)

CELL QUALITY

PLATE QUALITY

CAPACITY

REDUNDANT BATTERIES

RECONDITIONING CAPABILITY

EAGLE PICHER FLIGHT EXPERIENCE

HST BATTERY SUBCOMMITTEE REVIEW

FINDINGS: NI-H_2 WEAK POINTS SUMMARY

This is a summary listing of the Ni-H_2 weak points. Because weaknesses exhibit the areas where there is cause for concern, each weak point will be discussed in detail in the following charts.

HST BATTERY SUBCOMMITTEE REVIEW FINDINGS: NiH_2 WEAK POINTS

LIMITED CELL/BATTERY DATA BASE

HIGH SELF DISCHARGE RATE

NO DIODE PROTECTION

PRESSURE VESSEL INTEGRITY - SEALS

BATTERY DESIGN - SHORTING POTENTIAL

Ni-H_2 CAPACITY MORE SENSITIVE TO TEMPERATURE

LACK OF GSFC OPERATIONAL EXPERIENCE IN FLIGHT

HST BATTERY SUBCOMMITTEE REVIEW

FINDINGS: NiH_2 WEAK POINTS

LIMITED CELL/BATTERY DATA BASE - There is a limited cell/battery flight history with nickel-hydrogen cells. HST would be the first use of nickel-hydrogen batteries by NASA. Nickel-hydrogen batteries have flown in GEO but not yet on a LEO mission. There is a limited data base and as such use of the nickel-hydrogen batteries cannot be justified based on a qualification by similarity. In addition, there was not enough time to complete a mission simulation test prior to launch. Cycle life qualification is not a requirement of the program. This is considered a major weakness in the use of the nickel-hydrogen system.

There is some uncertainty associated with the cycle regime planned for the nickel-hydrogen batteries. They will operate in a LEO regime at a very low depth of discharge, ~8%. They are also expected to operate at less than a full state of charge. Neither of these factors is expected to severely impact operation in a negative way, however, the fact remains that they are untested and thus the full effects are unknown. At the time of launch the ground testing will have accumulated between 5000 and 7000 cycles. The minimum mission requirement is for 2.5 years or 13,500 cycles. Flying the nickel-hydrogen batteries without full qualification increases the risks involved with mission success.

HST BATTERY SUBCOMMITTEE REVIEW FINDINGS: NiH_2 WEAK POINTS

LIMITED CELL/BATTERY DATA BASE

LIMITED DATA BASE/CANNOT QUALIFY BY SIMILARITY
MISSION SIMULATION TEST NOT COMPLETED BEFORE LAUNCH

DISCUSSION

UNCERTAINTY ASSOCIATED WITH TEST REGIME
- LOW DEPTH OF DISCHARGE
- OPERATION AT LESS THAT 100% STATE OF CHARGE

AT TIME OF LAUNCH - GROUND TESTING 5000-7000 CYCLES
- 2.5 YR LIFE ==> 13,500 CYCLES

IMPACT:

INCREASED RISK

HST BATTERY SUBCOMMITTEE REVIEW

$Ni-H_2$ WEAK POINTS

HIGH SELF DISCHARGE RATE - Nickel-hydrogen cells experience a high rate of self discharge on open circuit stand. This is a cause for concern because of any launch delays that may be experienced. The assumed cell capacity requirement at launch is 43 AH, including a 15% contingency requirement. The projected available capacity, based on self discharge rates for the HST cells, cells is approximately that quantity or slightly less if the battery is installed at the VPF based upon trickle charge capability. If the batteries are installed on the pad the available capacity is projected to be 52 to 54 ampere hours. Contingency plans must be formulated to accommodate this feature of the nickel-hydrogen system. Worse case impact results in loss of the satellite. Return to earth is a potential salvage option.

HST BATTERY SUBCOMMITTEE REVIEW FINDINGS: $Ni\text{-}H_2$ WEAK POINTS

HIGH SELF DISCHARGE RATE

CHARGED STAND CAPACITY -- CELL CAPACITY LOSS DURING SHUTTLE LAUNCH TO HST DEPLOYMENT MISSION PHASE

DISCUSSION

OCCURS DUE TO HYDROGEN RECOMBINATION ON THE POSITIVE PLATE

DATA SHOW 50% LOSS IN CAPACITY OVER A 13 DAY STAND AT 68 F A TEMPERATURE DEPENDENT FUNCTION

BATTERY RECEIVES NO CHARGING POWER FROM T-2 DAYS UNTIL DEPLOYMENT - APPROXIMATELY 6 DAYS WORSE CASE

CONTINGENCY PLAN TO HANDLE WORSE CASE IS REQUIRED

HST BATTERY SUBCOMMITTEE REVIEW FINDINGS: Ni-H_2 WEAK POINTS

HIGH SELF DISCHARGE RATE

IMPACT:

WORSE CASE IS LOSS OF HST - LOSS OF CAPACITY FROM LAUNCH OR ORBITAL DELAYS COULD PREVENT SUCCESSFUL DEPLOYMENT

HST BATTERY SUBCOMMITTEE REVIEW

FINDINGS: Ni-H_2 WEAK POINTS

NO DIODE PROTECTION - The HST Ni-H_2 battery system has been designed without by-pass circuitry to protect against a failed open cell. All other use of nickel-hydrogen batteries has incorporated the use of bypass diodes. MSFC considers the cell reliability to be greater than that of the diodes. The battery redundancy also reduces the risk associated with the lack of diode protection. The loss of one cell would result in the loss of one battery. Loss of two batteries results in total loss of redundancy.

HST BATTERY SUBCOMMITTEE REVIEW FINDINGS: Ni-H_2 WEAK POINTS

NO DIODE PROTECTION

THE HST Ni-H2 BATTERY SYSTEM HAS BEEN DESIGNED WITHOUT BY-PASS CIRCUITRY TO PROTECT AGAINST A FAILED OPEN CELL

DISCUSSION:

OTHER PROGRAMS USE BYPASS DIODES

TOO LATE TO INCORPORATE FOR INITIAL LAUNCH

MSFC CONSIDERS CELL RELIABILITY GREATER THAN DIODES
REDUNDANCY IN THE 6 BATTERIES REDUCES THE RISK

HST BATTERY SUBCOMMITTEE REVIEW FINDINGS: NiH2 WEAK POINTS

NO DIODE PROTECTION (CON'T)

IMPACT:

LOSS OF ONE CELL CAUSES LOSS OF ONE BATTERY - IMPACT FOR TWO BATTERIES FAILING IS TOTAL LOSS OF REDUNDANCY

LOSS OF ADDITIONAL CELLS CAN RESULT IN LOSS OF MISSION IF LOSS OCCURS IN ANOTHER BATTERY

HST BATTERY SUBCOMMITTEE REVIEW

FINDINGS: Ni-H_2 WEAK POINTS

PRESSURE VESSEL INTEGRITY - SEALS - The cell design operates at 900 to 1200 psi and contains two penetrations for electrode terminals, 164 seals on the spacecraft. A failed seal results in an open circuit cell and since there is no diode protection, an open cell would lead to the loss of a battery. A fault in a pressure vessel could lead to a leak and have the same effect as a failed seal. To date no seal or pressure vessel problems have been experienced with INTELSAT V, G STAR, SPCC, ASC, or SATCOM K1 and K2, satellites flying nickel-hydrogen batteries, with accumulative 30 million cell hours of flight time.

HST BATTERY SUBCOMMITTEE REVIEW FINDINGS: Ni-H_2 WEAK POINTS

PRESSURE VESSEL INTEGRITY - SEALS

CELL DESIGN OPERATES AT 900 TO 1200 PSI AND CONTAINS 2 PENETRATIONS FOR ELECTRODE TERMINALS (2 PER CELL), 164 SEALS ON THE SPACECRAFT.

DISCUSSION

FAILED SEAL ==> RESULTS IN OPEN CIRCUIT ==> LOSS OF BATTERY (CELLS UNPROTECTED BY DIODES)

FAULT IN PRESSURE VESSEL

POTENTIAL SEAL LEAK - NONE OBSERVED TO DATE

HST BATTERY SUBCOMMITTEE REVIEW FINDINGS: Ni-H_2 WEAK POINTS

PRESSURE VESSEL INTEGRITY - SEALS (CON'T)

IMPACT:

LESS TOLERANT TO CELL FAILURE THAN Ni-CD - ONE OPEN CELL CAN RESULT IN LOSS OF A BATTERY.

HST BATTERY SUBCOMMITTEE REVIEW

FINDINGS: Ni-H_2 WEAK POINTS

BATTERY DESIGN - SHORTING POTENTIAL - The HST's Ni-H_2 battery design is particularly sensitive to shorts. There is a need for electrical insulation redundancy; the design incorporates only one layer of insulation between the cell case and ground - the thermal sleeve + 5 mil kapton. HST insulation is designed differently from commercial spacecraft. Shorts have been experienced when the insulation is not done properly. Proper design has redundant insulation. There is the possibility that particles can become wedged between the cell thermal sleeve and the battery case and cause a short. A short results in the loss of a battery and a potential fire.

HST BATTERY SUBCOMMITTEE REVIEW FINDINGS: NiH_2 WEAK POINTS

BATTERY DESIGN - SHORTING POTENTIAL

THE HST'S Ni-H2 BATTERY DESIGN IS PARTICULARLY SENSITIVE TO SHORTS.

DISCUSSION

NEED FOR ELECTRICAL INSULATION REDUNDANCY

ONLY ONE LAYER OF INSULATION BETWEEN CASE AND GROUND - THE THERMAL SLEEVE + 5 MIL KAPTON

CHOTHERM (15 MILS) ~ RTV TAPE (AROUND WELD) COMPRISE THE ELECTRICAL INSULATION FOR THE CASE

HST BATTERY SUBCOMMITTEE REVIEW FINDINGS: NiH_2 WEAK POINTS

BATTERY DESIGN - SHORTING POTENTIAL (CON'T)

DISCUSSION

POTENTIAL WIRING SHORT NOTED BY THE SUBCOMMITTEE MEMBER - CORRECTED BY EP

IMPACT

SHORT RESULTS IN BATTERY LOSS AND FIRE POTENTIAL - SYSTEM CAN ACCEPT 2 BATTERY FAILURES

HST BATTERY SUBCOMMITTEE REVIEW

FINDINGS: NiH_2 WEAK POINTS

NiH_2 CAPACITY MORE SENSITIVE TO TEMPERATURE - Nickel-hydrogen cell performance degrades with temperature. It is difficult to adequately charge the nickel-hydrogen cells if low temperatures cannot be maintained. Modifications to thermal system design are required to accommodate the Ni-H_2 batteries. Maintenance of adequate temperatures is required to efficiently charge on pad. If the batteries cannot be cooled adequately enough to maintain sufficient trickle charge levels the batteries will require removal from the spacecraft to achieve sufficient recharge. The logistics of operation with the Ni-H_2 system is more complicated.

HST BATTERY SUBCOMMITTEE REVIEW FINDINGS: NiH_2 WEAK POINTS

NiH_2 CAPACITY MORE SENSITIVE TO TEMPERATURE

CELL PERFORMANCE DEGRADES WITH TEMPERATURE

DISCUSSION

MODIFICATIONS TO THERMAL SYSTEM DESIGN REQUIRED TO ACCOMMODATE NiH_2

MAINTENANCE OF ADEQUATE TEMPERATURES REQUIRED TO EFFICIENTLY CHARGE ON PAD

IMPACT

LOGISTICS OF OPERATION WITH NiH_2 SYSTEM MORE COMPLICATED

HST BATTERY SUBCOMMITTEE REVIEW

CONSIDERATIONS FOR THE PROGRAM

Both designs, if kept fully active in the launch planning process and in the ground test program, provide the HST with a quick, emergency option using only a three week turnaround.

Testing is the best indicator of the design of choice. The more data obtained, the better the confidence level and the lower the risk. Deferring the final commitment as long as possible (up to T-3 weeks) minimizes the program impact in the event that any sudden change in plans are indicated. Continue testing after launch for flight support and analysis -- provides predictive capability and real time trouble shooting system.

A check of all battery modules for potential areas for shorts before launch would be of benefit to reduce the shorting risk. The subcommittee noted one such situation but was unable to inspect more than the nickel hydrogen FM-1 module since they were either sealed, not completed, or located elsewhere. Short concerns apply to both chemistries. With the Ni-Cd batteries, electrolyte leakage throught the vent relief valve is a concern. Particulate cleanliness is a concern which warrants a prelaunch inspection.

Properly perform DPA on cycled cells and evaluate cell degradation from storage.

Evaluate the Ni-H_2 hazard of cell shorts by the conduct of tests.

Make detailed close-out photos. These could be of value in case of trouble shooting and in any possible future investigations.

HST BATTERY SUBCOMMITTEE REVIEW CONSIDERATIONS FOR THE PROGRAM

MAINTAIN BOTH OPTIONS - CONTINUE TESTING ON BOTH OPTIONS

CHECK FOR ELECTRICAL SHORT HAZARDS

CERTIFY RSN 55-15 CELL FOR LIFE CYCLE PERFORMANCE AFTER STORAGE

PERFORM VIBRATION QUAL TESTING ON THE RSN 55-15 CELLS

EVALUATE THE Ni-H2 HAZARD OF CELL SHORTS BY THE CONDUCT OF TESTS.

MAKE DETAILED CLOSE-OUT PHOTOS

HST BATTERY SUBCOMMITTEE REVIEW

RELATIVE RISK SUMMARY - CATASTROPHE

The HST is less likely to experience a sudden, catastrophic loss of power using the nickel-cadmium batteries. A catastrophic loss, for the purposes of this review, is defined as a loss of capacity within one year. The use of the BPRC protects the nickel-cadmium system in the event of cell failures resulting from leakage and loss. The chance of a sudden loss of energy storage is not considered to be large, based upon experience to date regarding either chemistry.

HST BATTERY SUBCOMMITTEE REVIEW
RELATIVE RISK SUMMARY - CATASTROPHE

THE HST IS LESS LIKELY TO EXPERIENCE A SUDDEN, CATASTROPHIC LOSS OF POWER USING Ni-CD BATTERIES.

CATASTROPHIC CONDITIONS LEADING TO LOSS OF BATTERY POWER

	Ni-Cd	$Ni-H_2$
CELL FAILURES		
LEAK CONSEQUENCES	+	-
EXTERNAL SHORTS	+	-
INTERNAL SHORTS	-	+
ELECTROLYTE REDISTRIBUTION	+	-
SYSTEM FAILURES		
BPRC FAILURE	-	+
SHORTS	-	-

THE CHANCE OF A SUDDEN LOSS OF ENERGY STORAGE IS NOT CONSIDERED TO BE LARGE REGARDING EITHER CHEMISTRY BASED UPON EXPERIENCE TO DATE

1 CATASTROPHE = LOSS OF CAPACITY WITHIN ONE YEAR - THE ASSUMED M & R TIME
2 FAILURE OF THE BPRC TO PROTECT AGAINST CELL VOLTAGE DEGRADATION

HST BATTERY SUBCOMMITTEE REVIEW

RELATIVE RISK SUMMARY - MISSION LIFE

The HST is more likely to achieve the desired five year energy storage life cycle capability using the Ni-H_2 batteries. The testing on the nickel-cadmium batteries is much more extensive than that performed on the nickel-hydrogen batteries. However, the confidence gained from this level of testing is diminished by the fact that the cells have experienced five years of storage and the effects of the storage are unknown. The members of the subcommittee have more confidence in the nickel-hydrogen cell design, quality, and qual adequacy. In both cases the operation regime for the batteries is considered to be conservative. NASA has relatively little experience with Eagle Picher cells for flight programs. Eagle Picher experience with nickel-hydrogen batteries has been favorable. The nickel-hydrogen batteries provide an on-orbit capacity margin not available with the nickel-cadmium system which provides more capacity for contingency maneuvers. Given all of the above the subcommittee consensus was that either battery system should be able to provide the minimum life requirement of thirty months, however, nickel-hydrogen batteries are more likely to provide power for extended periods of time.

HST BATTERY SUBCOMMITTEE REVIEW
RELATIVE RISK SUMMARY - MISSION LIFE

THE HST IS MORE LIKELY TO ACHIEVE THE DESIRED 5 YEAR ENERGY STORAGE LIFE CYCLE CAPABILITY USING THE HST Ni-H2 BATTERIES.

INDICATORS WHICH PROVIDE CONFIDENCE IN THE ATTAINMENT OF THE REQUIRED POWER OUTPUT OVER A MISSION DUTY CYCLE

	Ni-Cd	Ni-H2
HST TESTING: CYCLE LIFE DATA	+[1]	-
CELL DESIGN	-	+
CELL QUALITY	-	+
QUAL ADEQUACY	-	+
CONSERVATIVE OPERATION	+	+[2]
FLIGHT EXPERIENCE WITH EPI CELLS	-	-
ON ORBIT MARGIN IN CAPACITY	-	+
AGE OF FLIGHT CELLS	-	+

1 THE POSITIVE POINT ASSUMES NEW CELLS

2 THERE IS EXTENSIVE EXPERIENCE WITH Ni-H2 CELLS IN GEO, NOT LEO. ONLY TWO OTHER NASA PROGRAMS USED EPI Ni-CD CELLS

HST BATTERY SUBCOMMITTEE REVIEW

SUMMARY OF MAJOR FINDINGS

NOTE:
THESE FINDINGS ADDRESS ONLY THE EPI NICKEL-CADMIUM AND NICKEL-HYDROGEN CELLS/BATTERIES AS READY FOR LAUNCH FOR THE HST PROGRAM IN CONSIDERATION OF THEIR ABILITY TO PERFORM 3 HST MISSION OPTIONS.

EPI Ni-H_2 CELLS ARE BETTER SUITED FOR HST CYCLE/CAPACITY REQUIREMENTS - The HST program, whether considering a mission duration of 30, 60, or 60^+ months, will more likely meet the program's energy storage requirements and contingency capacity requirements using the nickel-hydrogen batteries.

Ni-H_2 RISK: LACK OF QUALIFICATION DATA -There is risk associated with reliance upon the limited Ni-H_2 data base, particularly since this is the first major LEO mission application of this new technology and its operation in a new, more demanding operational regime than that currently experienced in GEO.
The degree of risk, however is reasonable but not without concerns. With the exceptions (lack of diode and redundant wiring protection) as noted in the findings, the Program has taken prudent measures to assure the success of the energy storage subsystem. Consequently, the risk identified is judged to be a reasonable one, based upon this subcommittee's analysis and battery experience.

PERFORMANCE OF NICKEL-CADMIUM FLIGHT CELLS FOLLOWING 5 YEAR STORAGE HAS NOT BEEN PROVEN - The nickel-cadmium battery testing has been performed on new cells. New flight cells have demonstrated life exceeding the thirty month minimum requirement. The actual nickel-cadmium flight batteries can be expected to perform for the duration of the 30 month mission only if the 5 year shelf life has not resulted in unacceptable cell degradation. Based upon the members electrochemical understandings, some cell degradation has occurred.

Ni-Cd CELLS: FLIGHT CELLS NOT LIKELY TO BE DEPENDABLE MUCH BEYOND 30 MONTHS - For a mission duration beyond 30 months, the subcommittee considers that there is a high program risk in relying upon these particular nickel-cadmium batteries.

HST BATTERY SUBCOMMITTEE REVIEW
SUMMARY OF MAJOR FINDINGS

NOTE:
THESE FINDINGS ADDRESS ONLY THE EPI NICKEL-CADMIUM AND NICKEL-HYDROGEN CELLS/BATTERIES AS READY FOR LAUNCH FOR THE HST PROGRAM IN CONSIDERATION OF THEIR ABILITY TO PERFORM 3 HST MISSION OPTIONS.

EPI Ni-H2 CELLS: BETTER SUITED FOR HST'S CYCLE/CAPACITY REQUIREMENTS

Ni-H2 RISK: LACKS HST LIFE CYCLE QUALIFICATION DATA AND DATA BASE FOR LEO APPLICATION.

DEGREE OF Ni-H2 RISK: REASONABLE BUT NOT WITHOUT CONCERN.

PERFORMANCE OF NICKEL-CADMIUM FLIGHT CELLS FOLLOWING 5 YEAR STORAGE HAS NOT BEEN PROVEN

Ni-CD CELLS: FLIGHT CELLS NOT LIKELY TO BE DEPENDABLE MUCH BEYOND 30 MONTHS.

NASA
George C. Marshall
Space Flight Center

Nickel-Hydrogen LEO Cycling at 20% - 50% DOD

John E. Lowery

National Aeronautics and Space Administration

George C. Marshall Space Flight Center

Information and Electronic Systems Laboratory

Marshall Space Flight Center, AL 35812

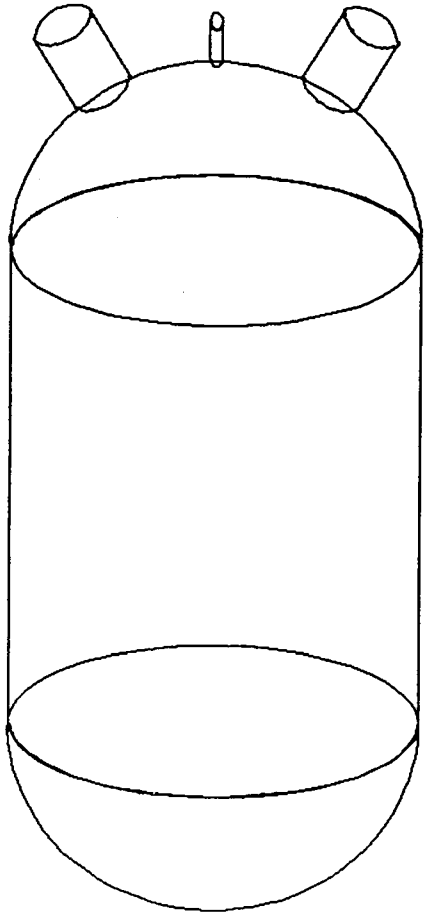

NASA

George C. Marshall
Space Flight Center

At the Marshall Space Flight Center 2 Ni-H2 2-cell pacs made up of engineering cells built according to the Hubble Space Telescope design are currently being LEO cycled at 20% - 50% depth of discharge. The cells were manufactured by Eagle-Picher Industries, Inc., activated with electrolyte (KOH) concentrations of 26% (pac #1) and 31% (pac #2), for use during evaluation of the HST cell design. This test was set up to study the behavior of Ni-H2 cells of HST design, having differing electrolyte concentrations, when operated at high depths of discharge (20% - 50%) in a Low Earth Orbit cycling program. The cells are being cycled 60 minutes charge and 36 minutes discharge with an end of charge cutoff voltage. End of charge cutoff voltages vary between 1.48 V and 1.56 V. The test was designed specifically to allow the cells to pick their own recharge ratio for varying depths of discharge and varying end of charge voltages. The test utilizes cells which were previously used in the HST cell testing program at Marshall to gather design and performance data for analysis in the development of Ni-H2 cell technology for use aboard the HST. The four test cells were cycled approximately 2500 LEO orbits in the HST test bed according to an HST profile with sixty-one minutes charge and thirty-five minutes discharge, to a depth of discharge of eight percent, before being replaced in the HST test bed by a four cell pac of HST "flight type" cells. The four test cells then sat open circuit at room temperature for eight months before being installed in the current test setup.

NASA

George C. Marshall
Space Flight Center

The test setup consists of four major elements: the programmable power supplies and load banks, the data acquisition and control system the control computer and the NiH2 specimen test cells. A simplified block diagram of the test setup is shown in Figure 1. The test setup provides complete battery isolation should a fault occur, and fusing as necessary to protect the battery cells and other equipment. Front panel switches provide for power supply configuration and battery isolation. Front panel meters provide continuous real-time visual monitoring of the voltage and current for each pac of cells. A strip chart recorder provides a hard copy of the voltage and current profiles for each of the pacs. The test operates continuously with minimal human interface, except during special tests.

The two power supplies are controlled by resistance programming. A bank of resistors and relays was built which can be switched by the control computer to provide control over the charge current to the batteries. The load banks are controlled by the 3497A. The 3497A is equipped with a 0 - 5 volt programmable power supply which is used to voltage program the load banks. A Hewlett-Packard Vectra 9000 running an HP Basic program is used as the control computer to remotely instruct the 3497A (Data acquisition and control) to scan the data channels and retrieve test data. The program then reads, calculates and stores the data. If an anomaly occurs, the program will disconnect the cells and shut down the test to avoid damage to the cells or equipment.

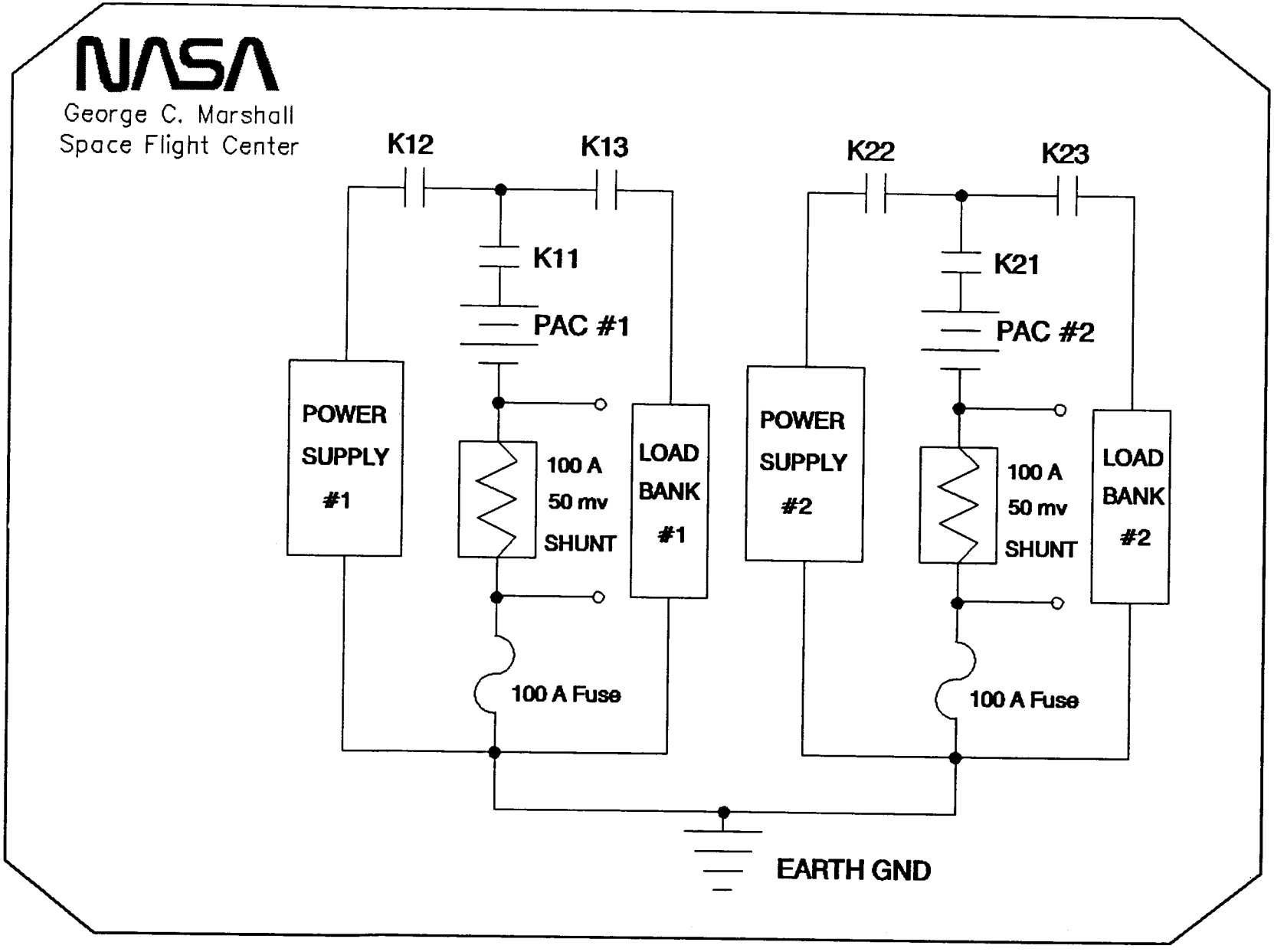
NASA
George C. Marshall
Space Flight Center
K12
K13
K22
K23
K11
K21
PAC #1
PAC #2
POWER SUPPLY #1
POWER SUPPLY #2
100 A 50 mv SHUNT
100 A 50 mv SHUNT
LOAD BANK #1
LOAD BANK #2
100 A Fuse
100 A Fuse
EARTH GND

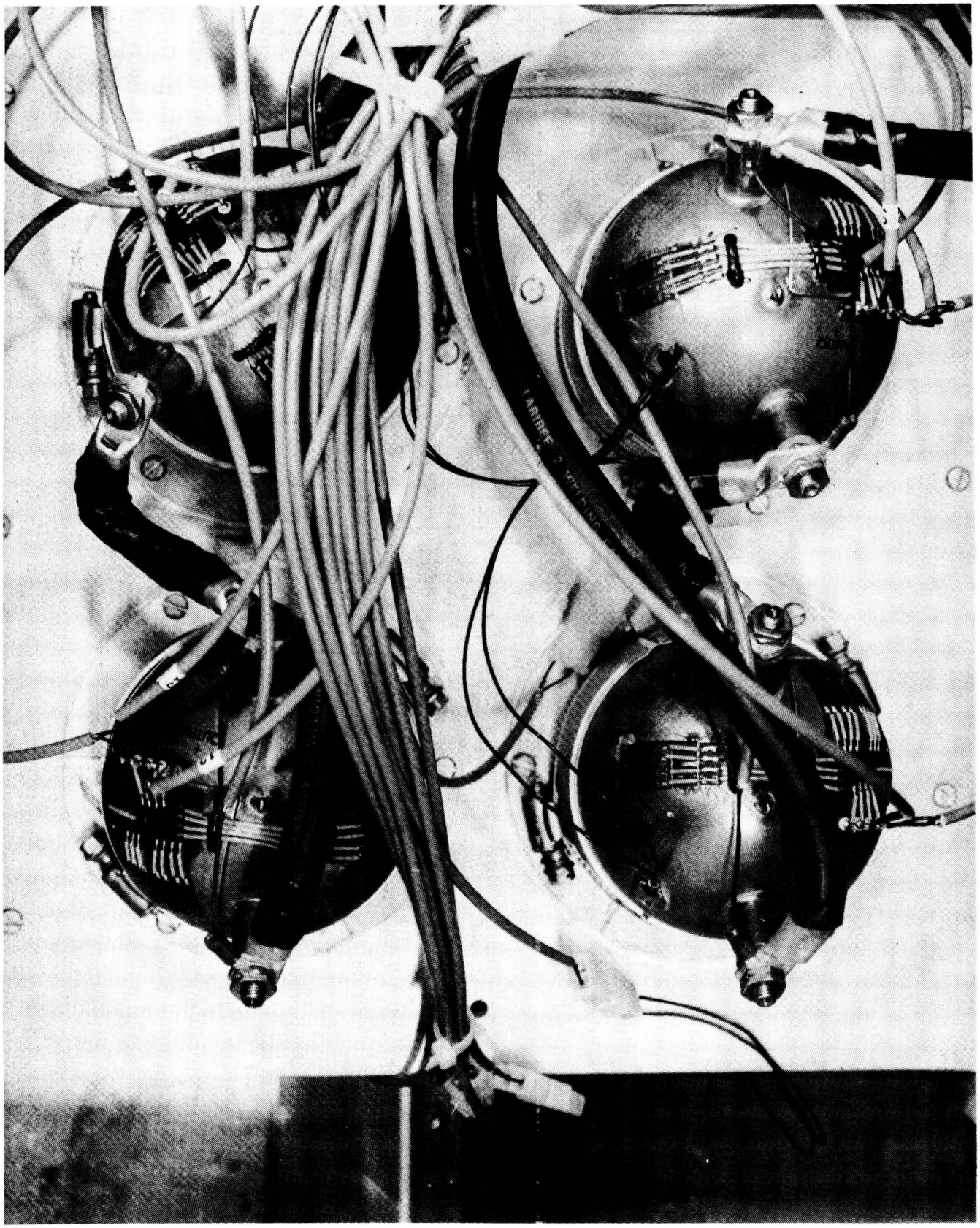

RNH 90-3 TEST CELLS

ORIGINAL PAGE
BLACK AND WHITE PHOTOGRAPH

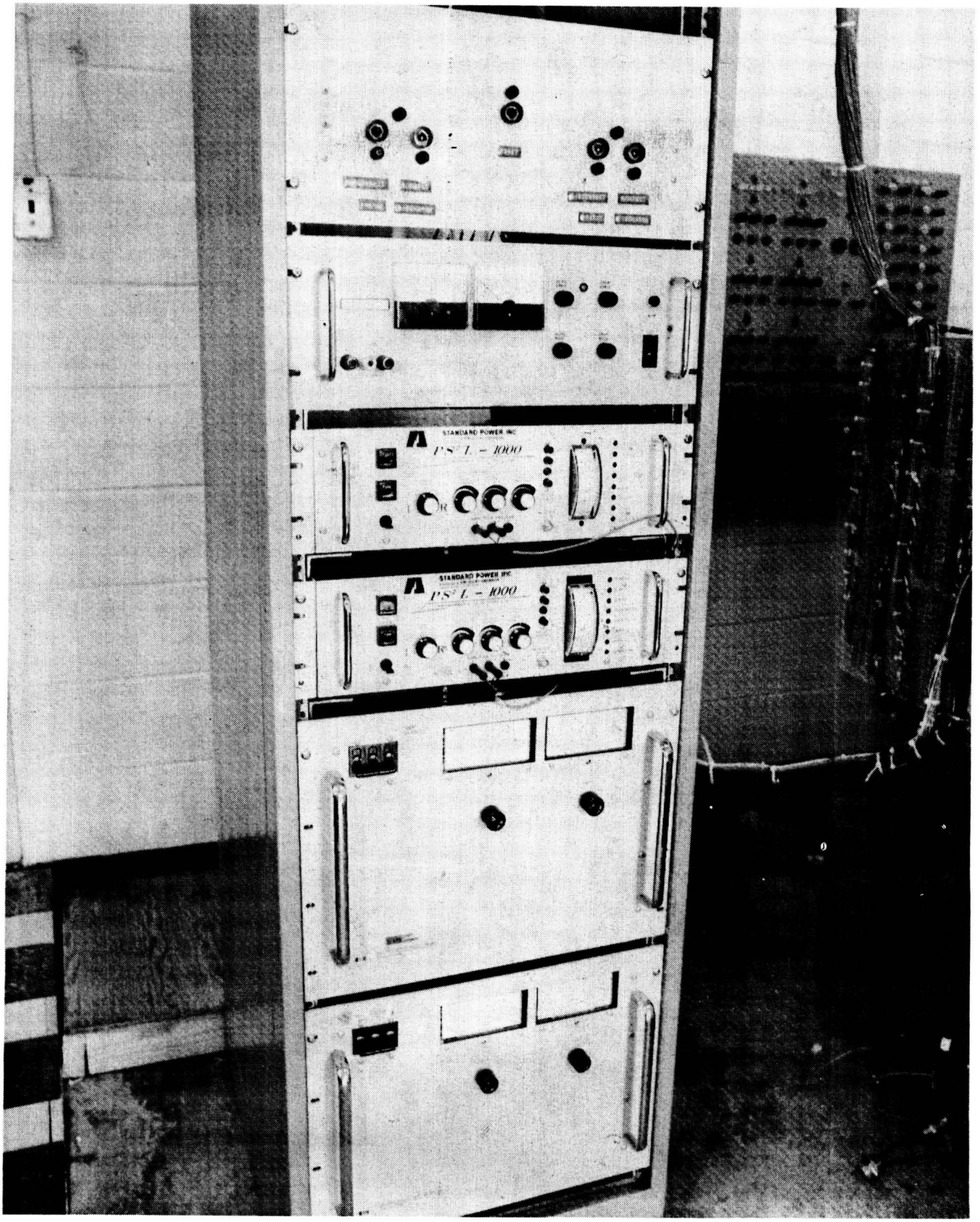

POWER SUPPLY, LOAD BANKS AND CONTROL PANEL

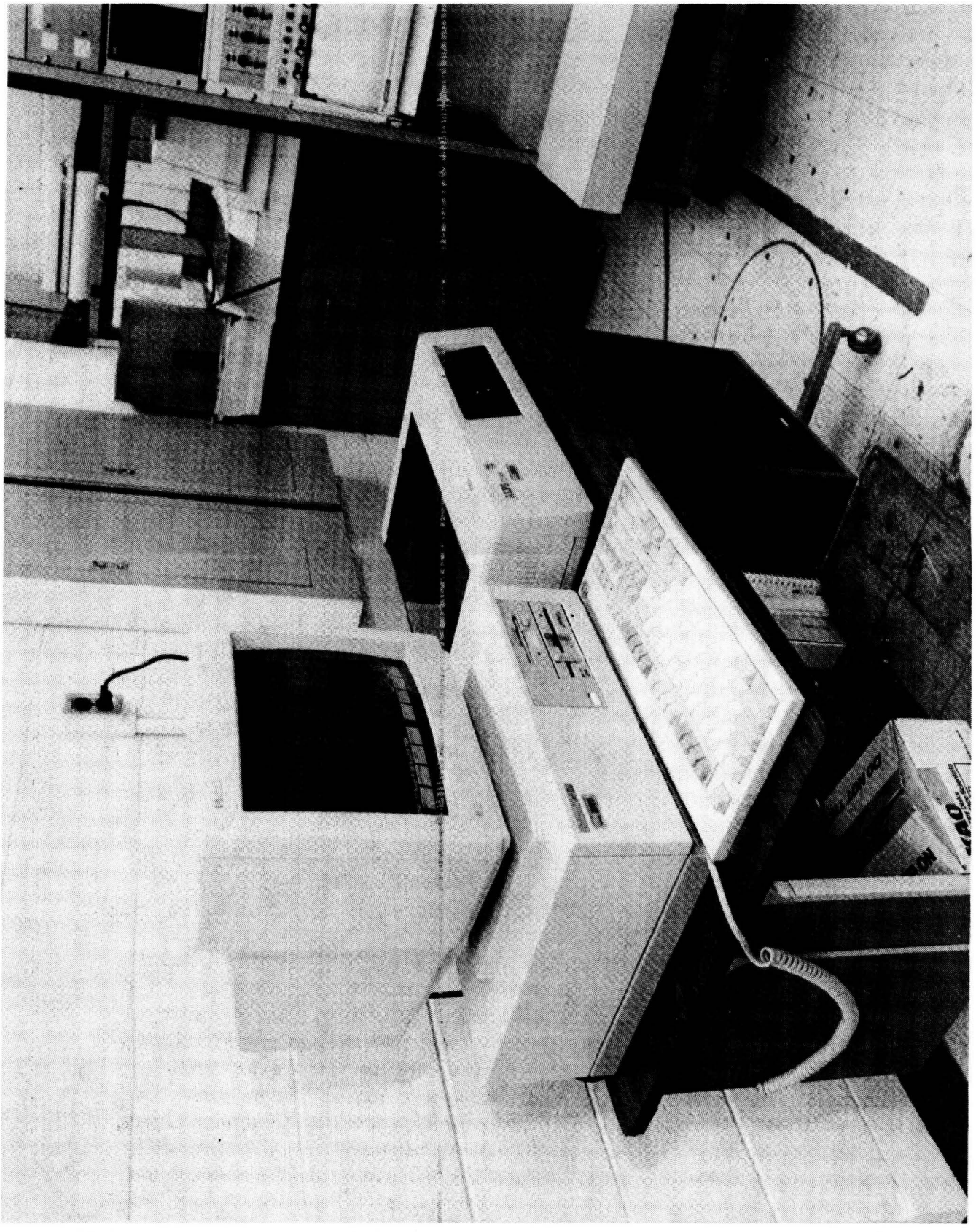

CONTROL COMPUTER AND DATA ACQUISITION SYSTEM

NASA

George C. Marshall
Space Flight Center

The test plan was written to gain experience with the characteristics of NiH2 cells operated in a LEO cycling program. The cells used in the test are of the

design flying onboard the Hubble Space Telescope. These cells were from the engineering lot of cells built to verify design parameters and cell operation and to determine the optimum electrolyte concentration. There are two cells with 26% Potassium Hydroxide (KOH) electrolyte and two cells with 31% KOH electrolyte. The test charges the cells to an end of charge voltage and then discharges them to a set depth of discharge; most tests of this type would pick

a depth of discharge and then charge the cells to a set recharge ratio. This test scheme characterizes the cells in terms of end of charge voltage and allows the cells to pick a recharge ratio if the end of charge voltage is high enough to allow operation at the depth of discharge.

The test begins with wake up cycling of the cells, production of initial capacity graphs and Pressure vs. State of Charge curves. After a prolonged open circuit stand of 8 months at room temperature, the cells are awakened by cycling 480 60/36 LEO orbits where charge equals 23.4 Amps for 60 minutes or until 1.56 V/cell is reached. If 1.56 V/cell is reached before the end of the 60 minute charge period, the pac will be open circuited for the remainder of the 60 minute period. The cells will then be discharged at 30 Amps for 36 minutes or until lower voltage limit of 1.0 V/cell is reached. If the lower voltage limit is reached before the end of the 36 minute discharge period, the cells will be open circuited for the remainder of the 36 minute discharge period. A Capacity check is then performed by charging at 23.4 Amps for 60 minutes or until 1.56 V/cell is reached. If 1.56 V/cell is reached before the end of the 60 minute charge period, the pac is open circuited for the remainder

of the 60 minute period. The pac is then discharged at 30 Amps to .3 V/cell.

An initial capacity is next measured for the cells by doing a baseline charge which consists of charging at 9.3 Amps, 0x C for 10 hours followed by 4 Amps for 14 hours and then allowing cells to sit open circuit for one hour and discharging at 15 Amps to .3 V/cell. Pressure vs. State of Charge curves for each of the cells are obtained by the following procedure: Charge at 8 Amps, 0x C to 1.54 V/cell and then immediately discharge at 12 Amps to .3 V/cell. The data gathered during this phase of the test is to be used to measure the condition of the cells at later points in the test.

NASA
George C. Marshall
Space Flight Center

2 Cell Engineering Pac Tests

RNH 90-3

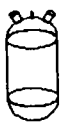

Wake Up Cycles

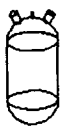

Initial Capacity Test

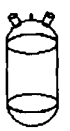

Pressure vs. State of Charge

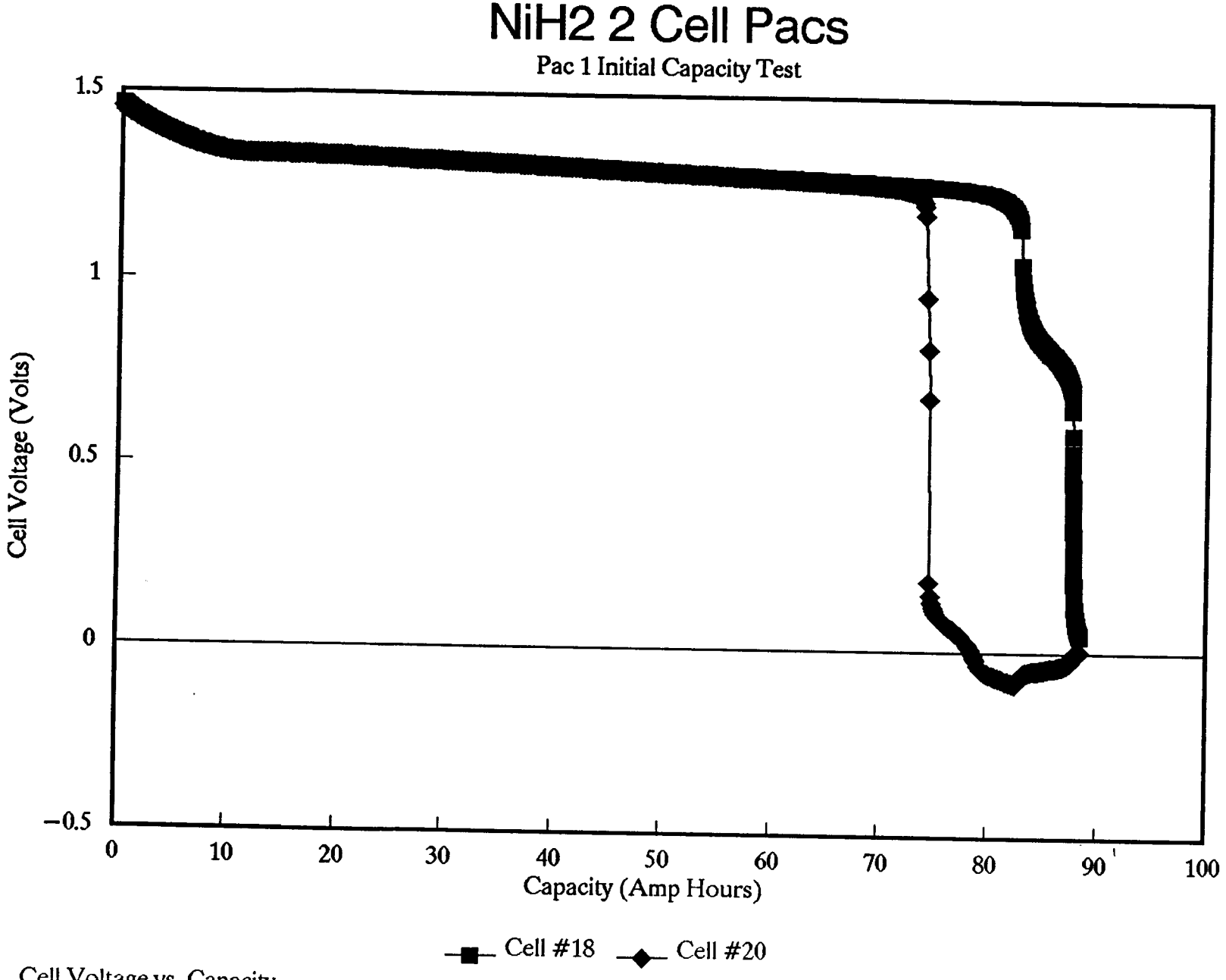

Cell Voltage vs. Capacity
4/3/90–4/5/90

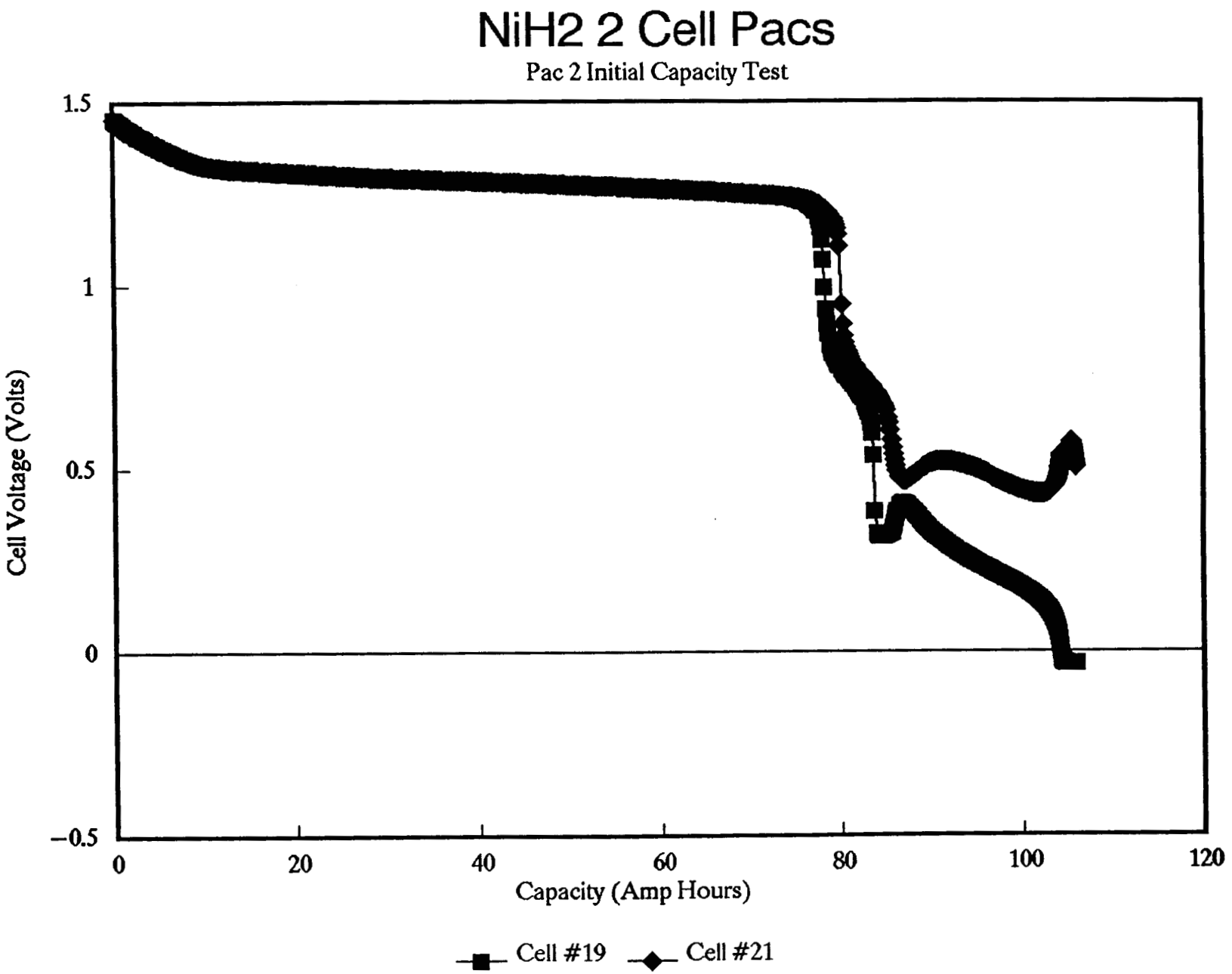

Cell Voltage vs. Capacity
4/3/90–4/5/90

NASA
George C. Marshall
Space Flight Center

2 Cell Engineering Pac Tests
RNH 90-3

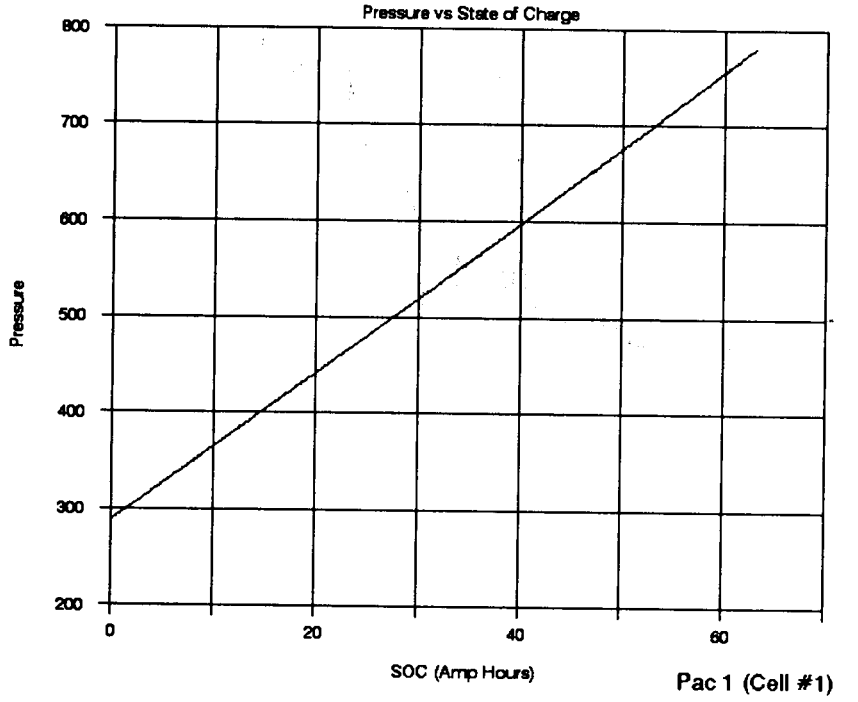

Pac 1 (Cell #1)

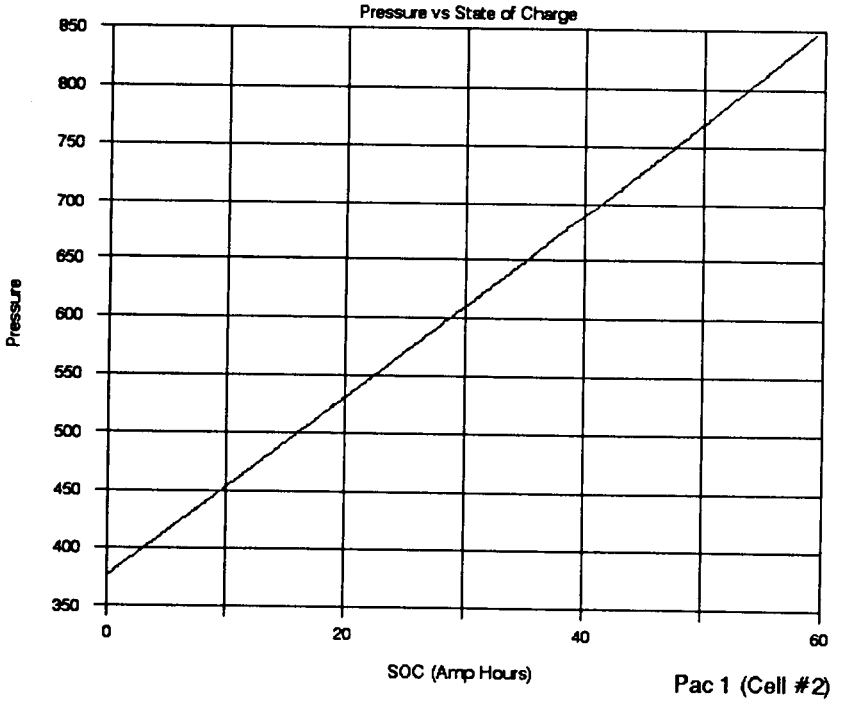

Pac 1 (Cell #2)

NASA

George C. Marshall
Space Flight Center

2 Cell Engineering Pac Tests

RNH 90-3

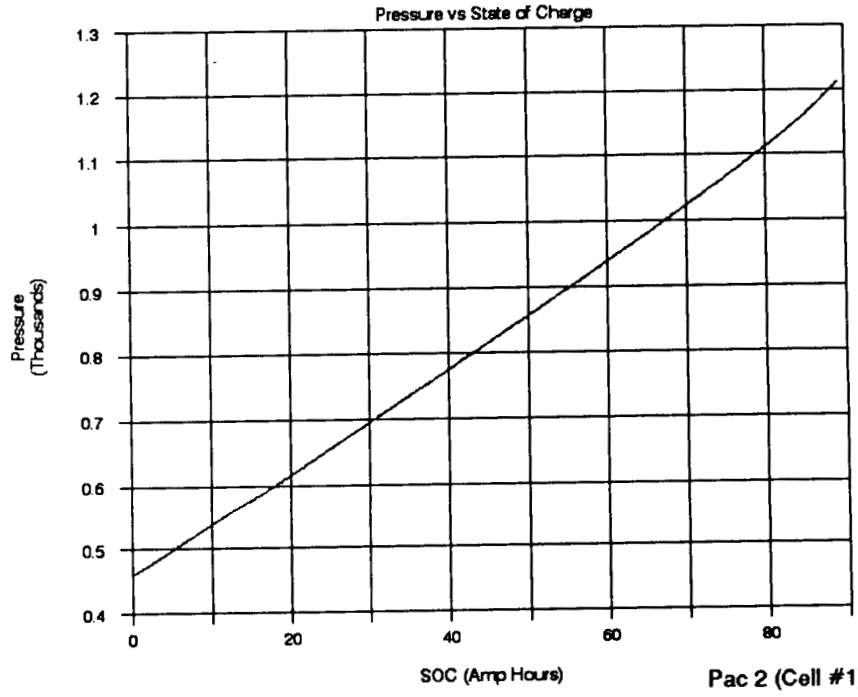

Pac 2 (Cell #1)

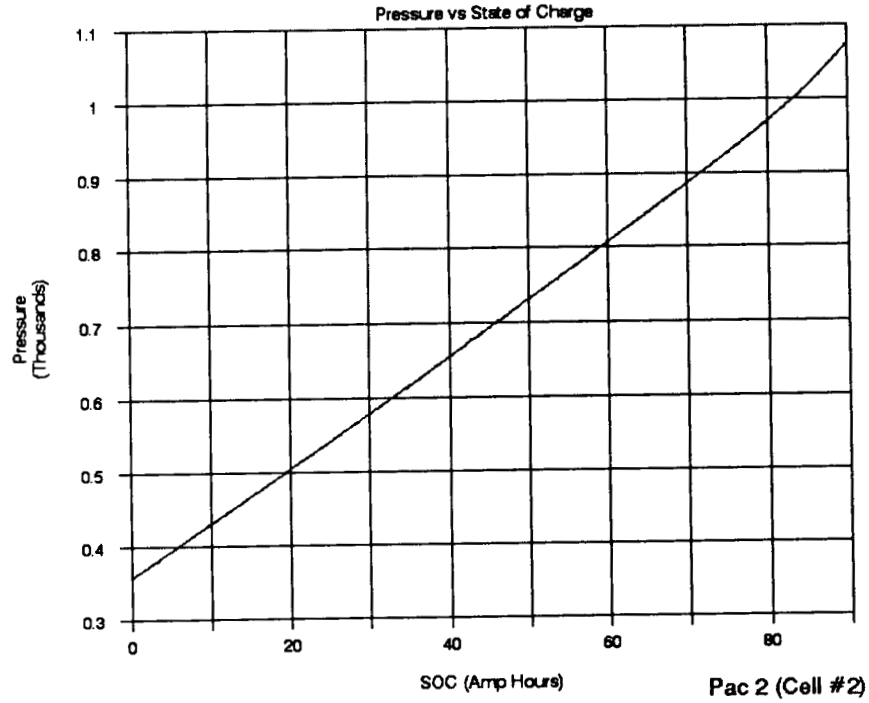

Pac 2 (Cell #2)

NASA
George C. Marshall
Space Flight Center

The cells are cycled according to the test matrix shown on the facing chart with varying depths of discharge for several end of charge voltages. This data will be used to help characterize the operation of the NiH2 cell at depths of discharge in the 20 - 50 percent range.

NASA

George C. Marshall
Space Flight Center

2 Cell Engineering Pac Tests

RNH 90-3

	EOC VOLTAGE	% DOD	DISCHARGE RATE AMPS	CHARGE RATE AMPS
1.	1.48	20	30	23.4
2.	1.48	30	45	35.1
3.	1.48	40	60	46.8
4.	1.48	50	75	58.5
5.	1.50	20	30	23.4
6.	1.50	30	45	35.1
7.	1.50	40	60	46.8
8.	1.50	50	75	58.5
9.	1.52	20	30	23.4
10.	1.52	30	45	35.1
11.	1.52	40	60	46.8
12.	1.52	50	75	58.5
13.	1.54	20	30	23.4
14.	1.54	30	45	35.1
15.	1.54	40	60	46.8
16.	1.54	50	75	58.5
17.	1.56	20	30	23.4
18.	1.56	30	45	35.1
19.	1.56	40	60	46.8
20.	1.56	50	75	58.5

NASA

George C. Marshall
Space Flight Center

Step #1 of the test plan at EOC voltage = 1.48, 20% DOD with no trickle charge showed an unexpected behavior. The cells with 26% KOH accepted charge at 23.4 amps and supported a 30 amp discharge for 125 - 130 LEO orbits and then began to accept less charge. The result was an inability to support the 30 amp discharge. This was not a case of gradual cell discharge because a capacity test and reconditioning had been done before beginning step #1. This occurrence is most puzzling when studied from a pressure perspective. The cell pressure continued to rise indicating an increase in capacity while capacity to .3 V (test bottom limit) at 15 amps was nonexistant. It seemed as if an internal resistance had built up which prevented charge acceptance before the 1.48 V EOC voltage. There was a noticeable difference in the two electrolyte concentrations. The cells with 31% electrolyte exhibited behavior analogous to the cells with 26% KOH supporting the orbital cycling for 190 - 200 cycles, approximately 65 additional cycles. The cells with 26% KOH showed a higher ability to accept charge while the cells with 31% KOH were better able to support high charge and discharge rates. A capacity test verified that the cells with 26% KOH had accepted more charge.

2 Cell Engineering Pac Tests
RNH 90-3

ORBIT vs. AMP HOURS OUT

1.48 V EOC, 20% DOD, 26% KOH

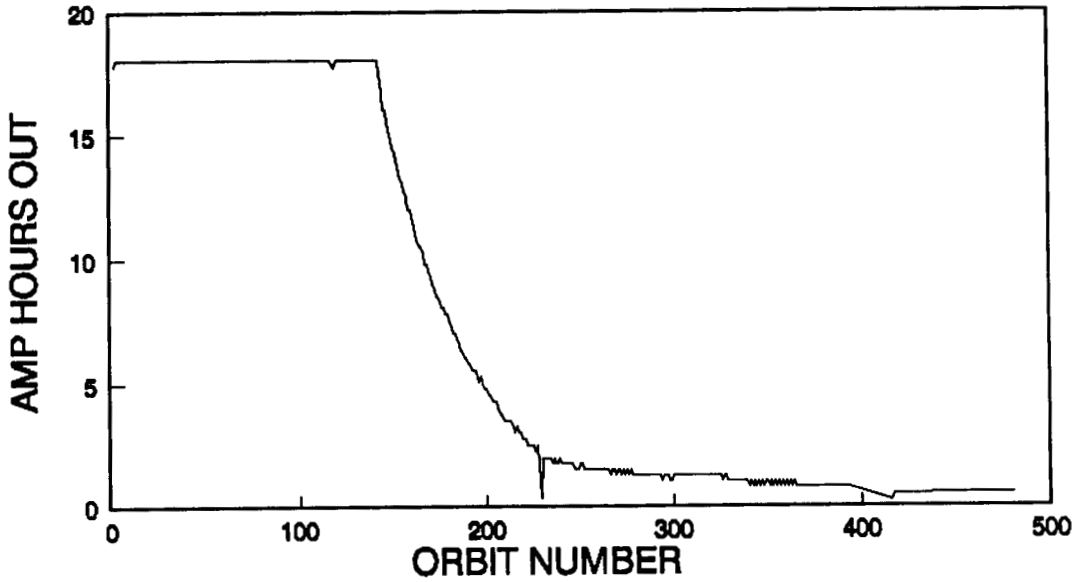

CHG = 23.4 Amps, DSCHG = 30 Amps
Aug 90

ORBIT vs. MINUTES CHARGE

1.48 V EOC, 20% DOD, 26% KOH

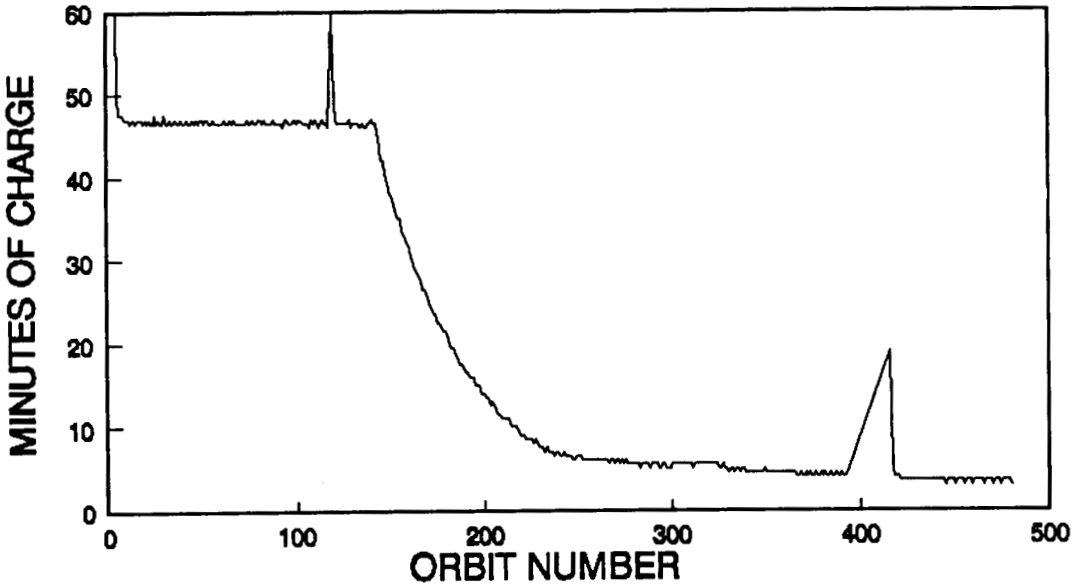

CHG = 23.4 Amps, DSCHG = 30 Amps
Aug 90

2 Cell Engineering Pac Tests
RNH 90-3

ORBIT vs. EFFICIENCY

1.48 V EOC, 20% DOD, 26% KOH

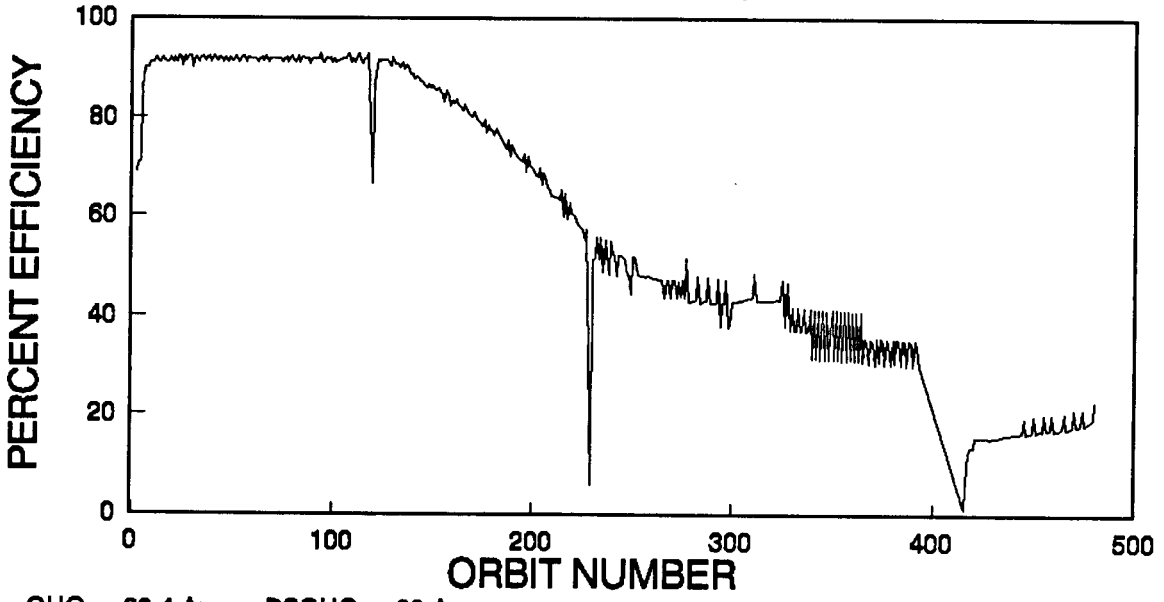

CHG = 23.4 Amps, DSCHG = 30 Amps
Aug 90

ORBIT vs. RECHARGE RATIO

1.48 V EOC, 20% DOD, 26% KOH

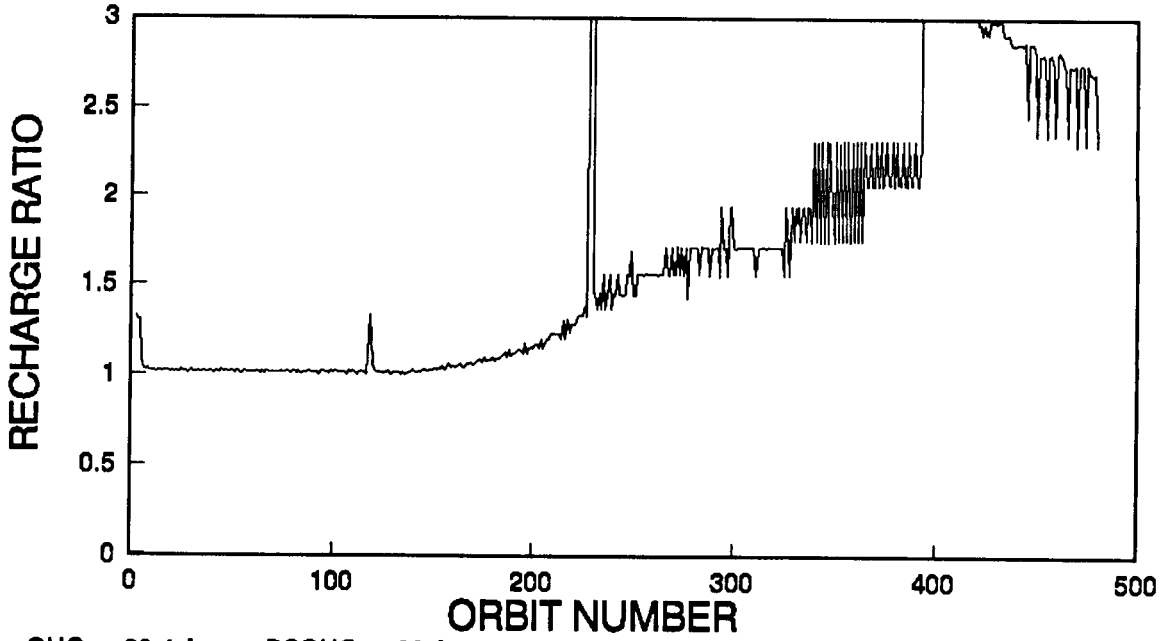

CHG = 23.4 Amps, DSCHG = 30 Amps
Aug 90

2 Cell Engineering Pac Tests
RNH 90-3

ORBIT vs. AMP HOURS OUT

1.48 V EOC, 20% DOD, 31% KOH

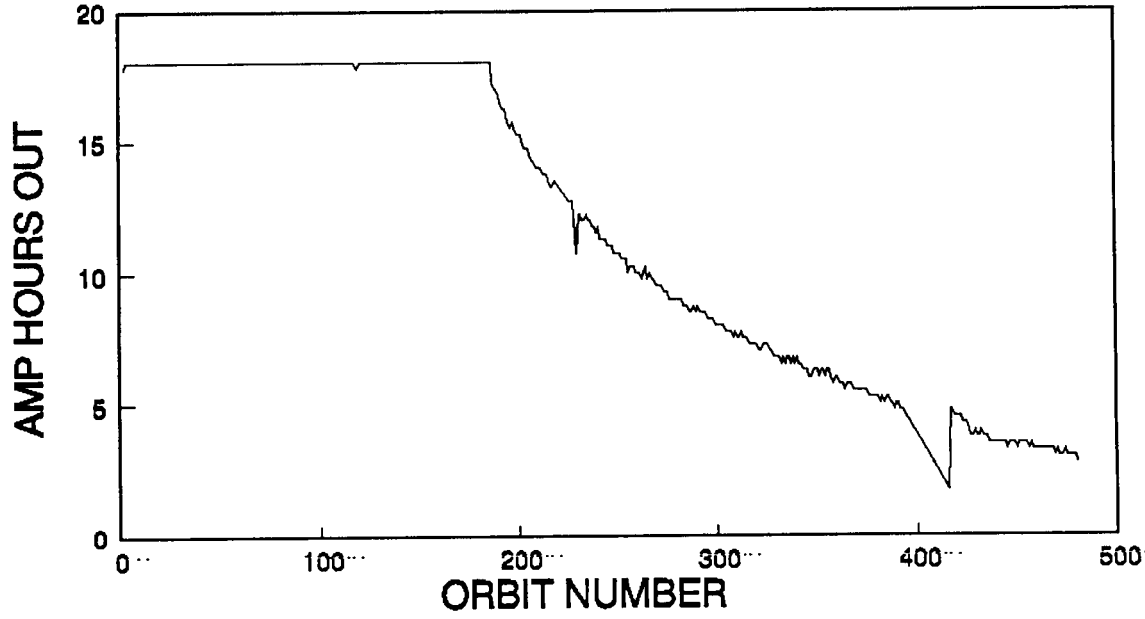

CHG = 23.4 Amps, DSCHG = 30 Amps
Aug 90

ORBIT vs. MINUTES CHARGE

1.48 V EOC, 20% DOD, 31% KOH

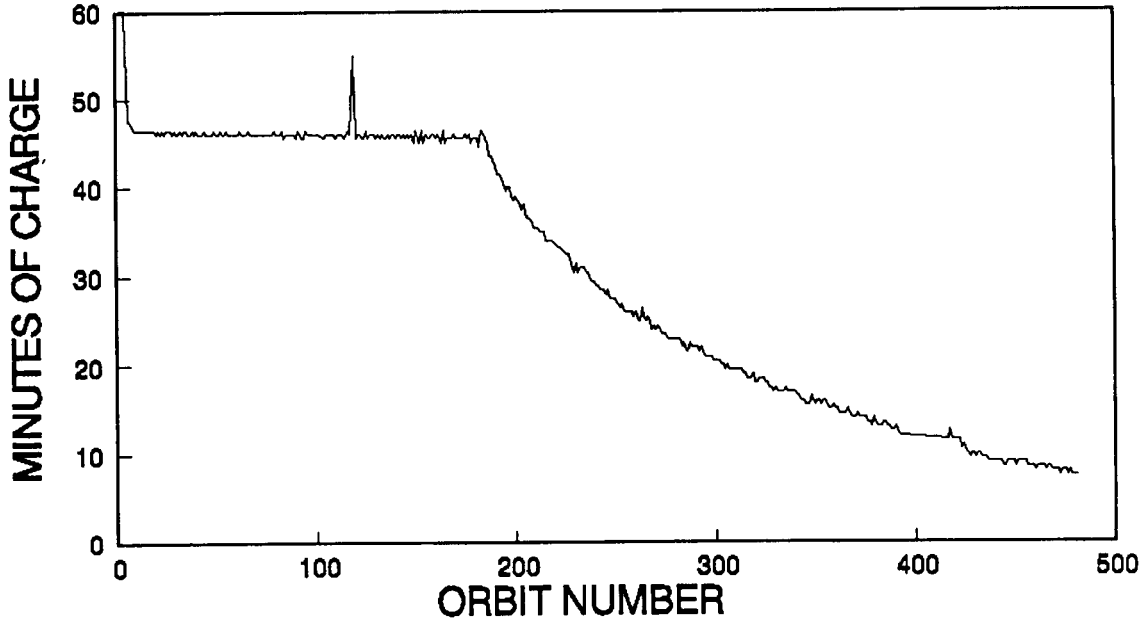

CHG = 23.4 Amps, DSCHG = 30 Amps
Aug 90

2 Cell Engineering Pac Tests
RNH 90-3

ORBIT vs. EFFICIENCY

1.48 V EOC, 20% DOD, 31% KOH

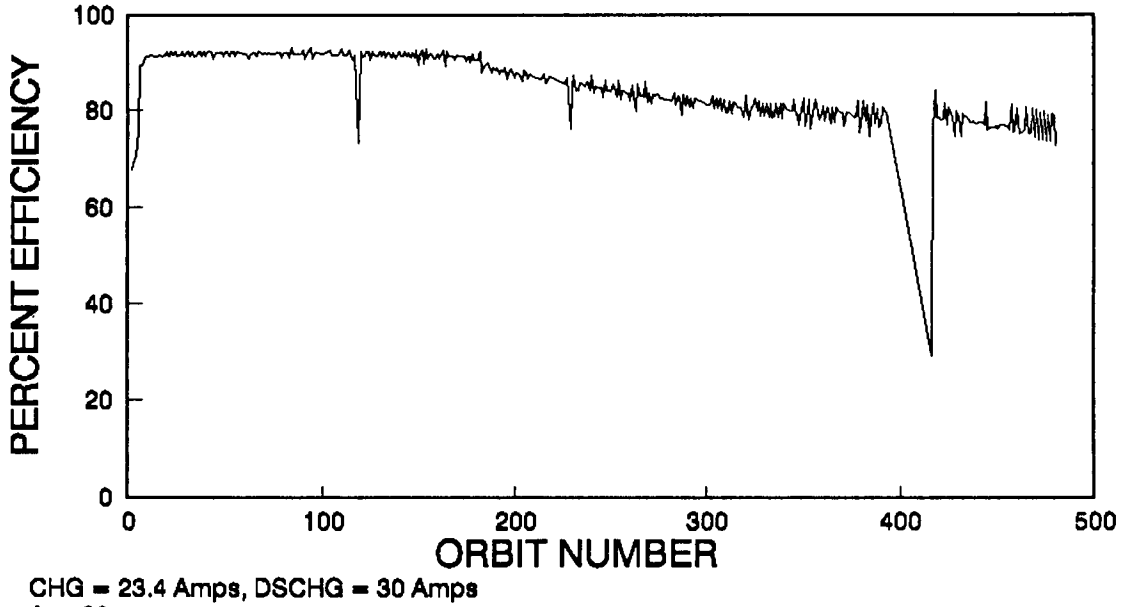

CHG = 23.4 Amps, DSCHG = 30 Amps
Aug 90

ORBIT vs. RECHARGE RATIO

1.48 V EOC, 20% DOD, 31% KOH

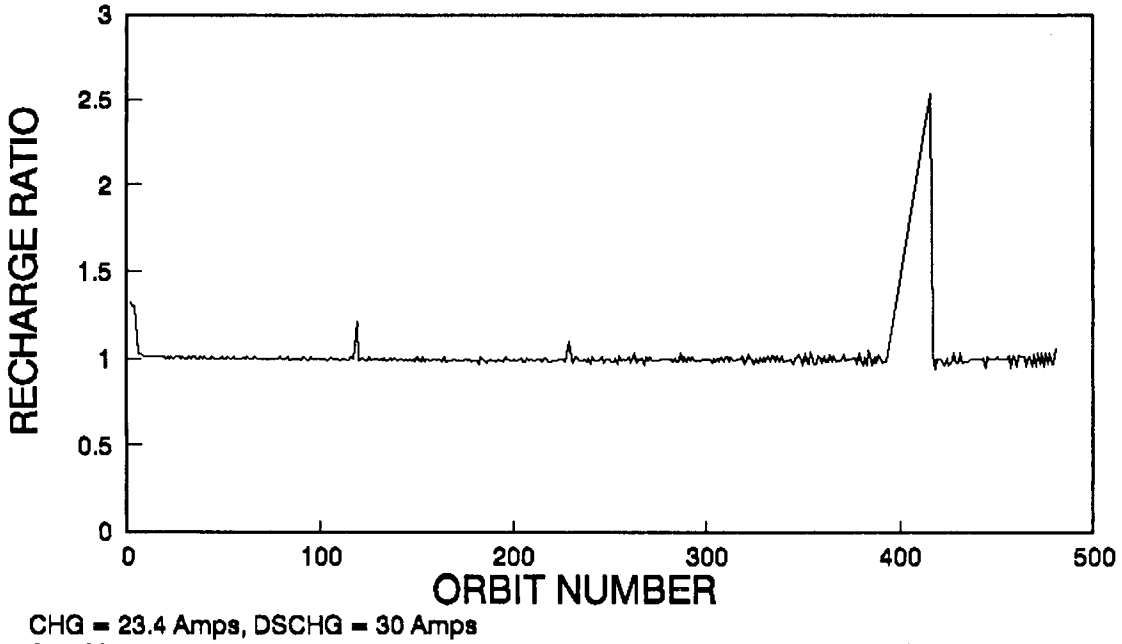

CHG = 23.4 Amps, DSCHG = 30 Amps
Aug 90

NASA

George C. Marshall
Space Flight Center

Step #5 was next in the test after skipping steps #2, 3 and 4. At EOCV = 1.50, 20% DOD the cells exhibited good performance. There was no inability to accept charge in either of the pacs and a 20% DOD (18 Amp Hours) was supported for 480 orbits. The cell pressure for this series reached a maximum at 110 orbits and began to steadily decrease (constant slope). The low voltage during discharge also began to move downward after 110 orbits with a constant slope; however, the cell pressures after 480 orbits were still 100 - 125 psi higher at EOCV = 1.50 that at EOCV = 1.48.

The capacity test after step #5 showed the increase in capacity expected from the increase in cell pressure and showed the cells operating with more unity. All cells except #20 showed an increase in capacity.

2 Cell Engineering Pac Tests
RNH 90-3

ORBIT vs. AMP HOURS OUT

1.50 V EOC, 20% DOD, 26% KOH

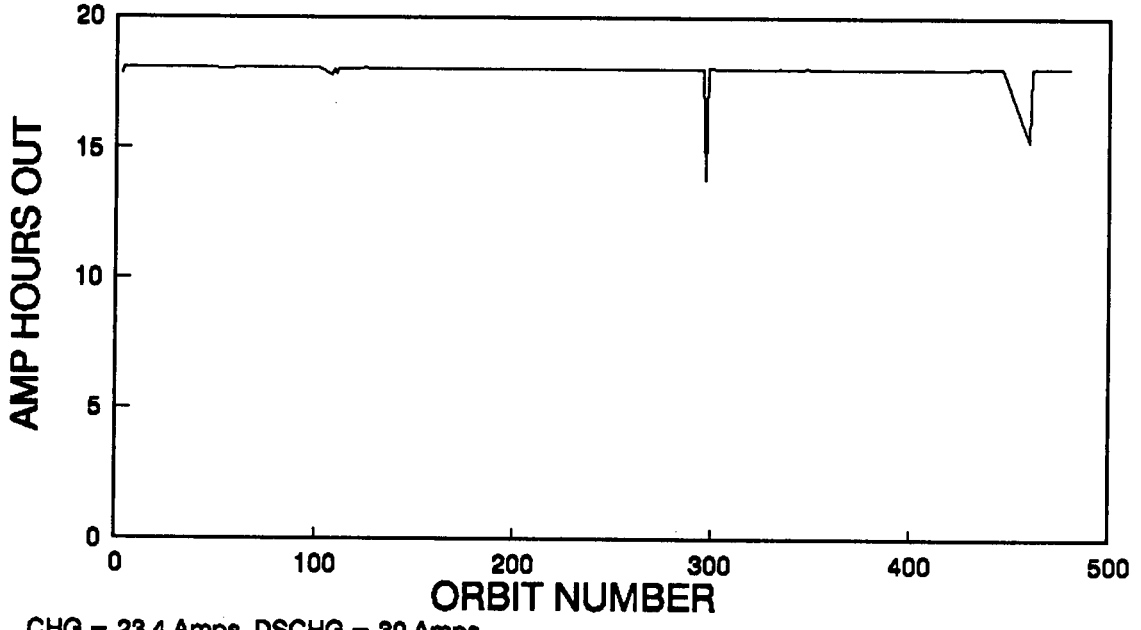

CHG = 23.4 Amps, DSCHG = 30 Amps
Sept 90

ORBIT vs. MINUTES CHARGE

1.50 V EOC, 20% DOD, 26% KOH

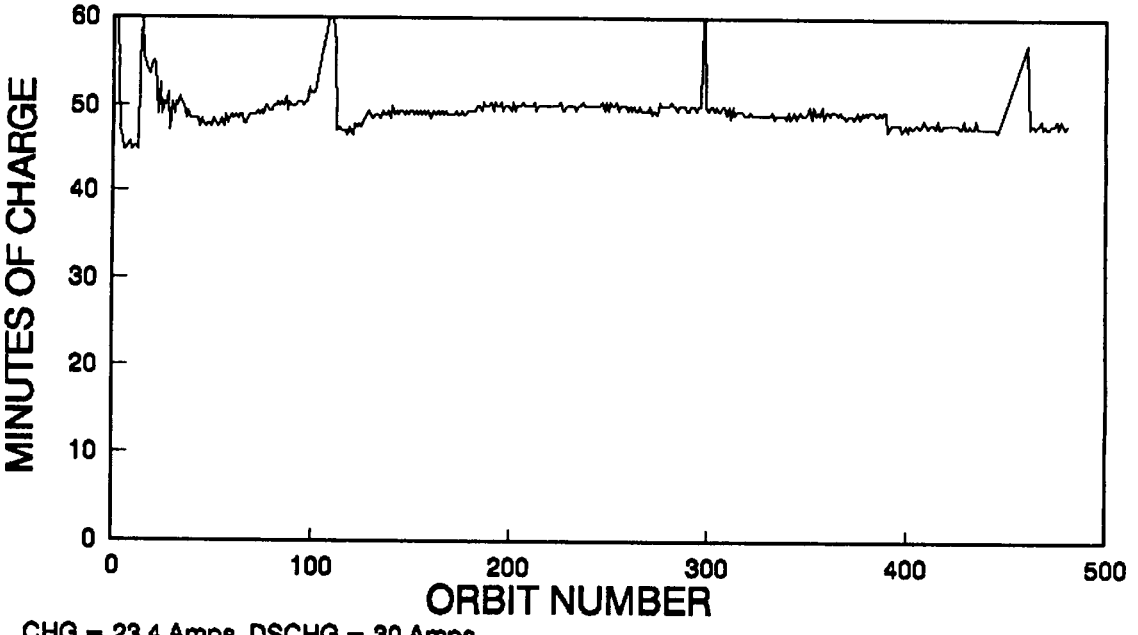

CHG = 23.4 Amps, DSCHG = 30 Amps
Sept 90

2 Cell Engineering Pac Tests
RNH 90-3

ORBIT vs. EFFICIENCY

1.50 V EOC, 20% DOD, 26% KOH

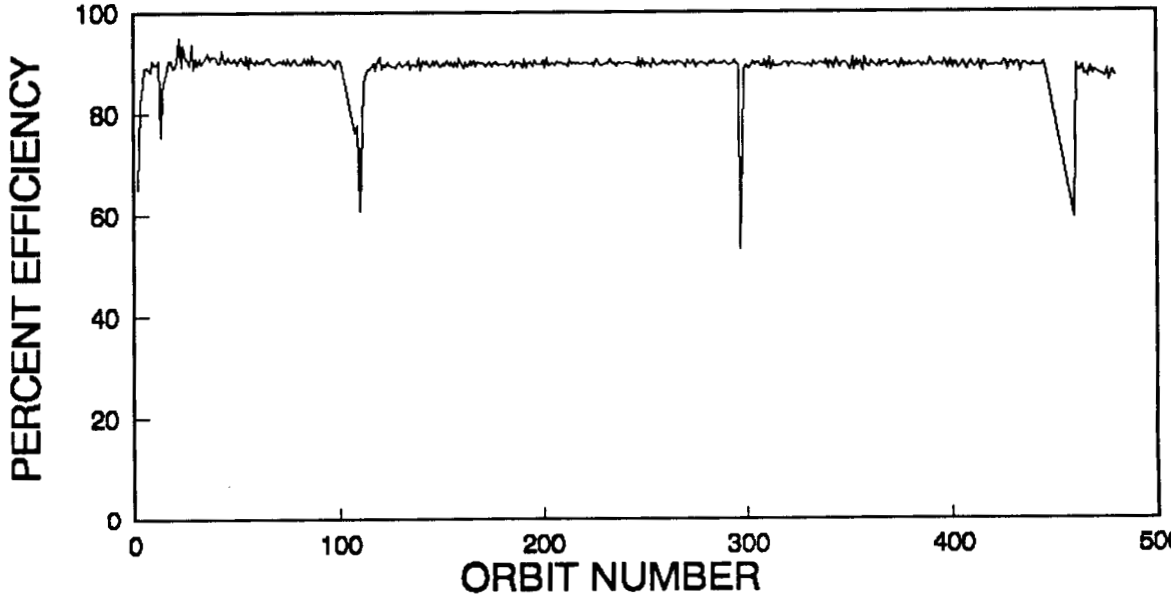

CHG = 23.4 Amps, DSCHG = 30 Amps
Sept 90

ORBIT vs. RECHARGE RATIO

1.50 V EOC, 20% DOD, 26% KOH

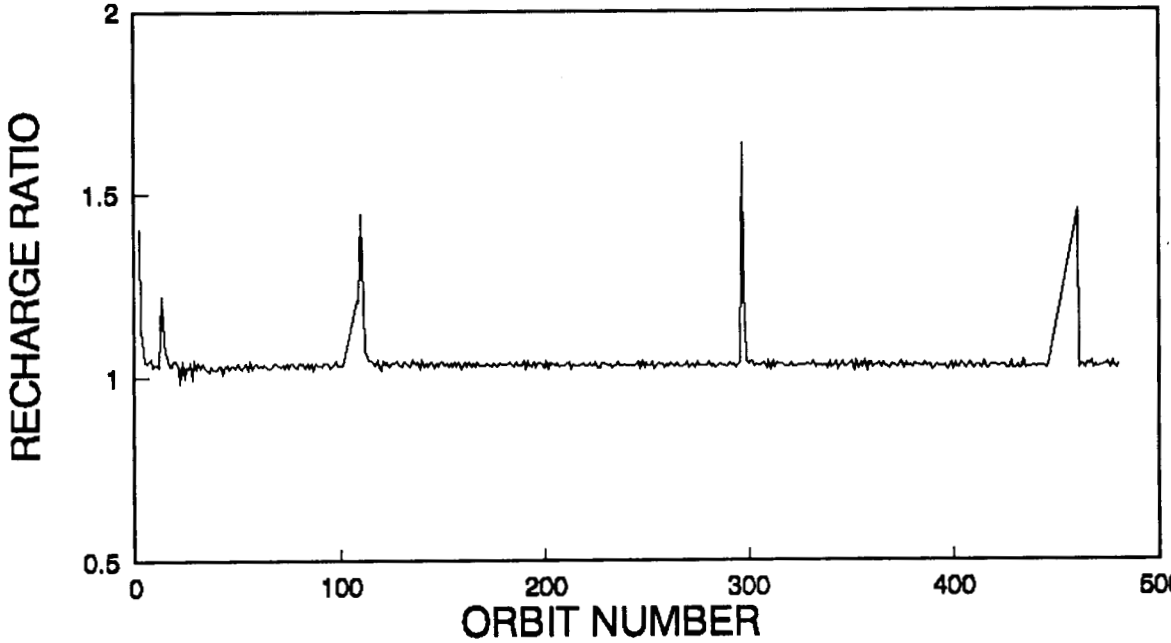

CHG = 23.4 Amps, DSCHG = 30 Amps
Sept 90

2 Cell Engineering Pac Tests
RNH 90-3

ORBIT vs. AMP HOURS OUT

1.50 V EOC, 20% DOD, 31% KOH

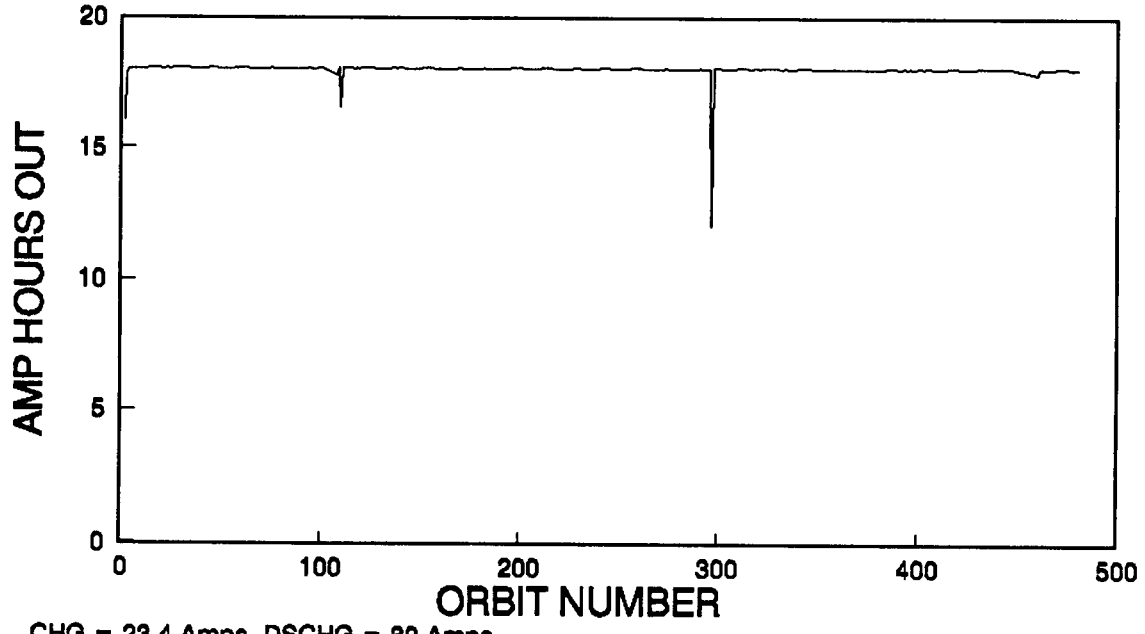

CHG = 23.4 Amps, DSCHG = 30 Amps
Sept 90

ORBIT vs. MINUTES CHARGE

1.50 V EOC, 20% DOD, 31% KOH

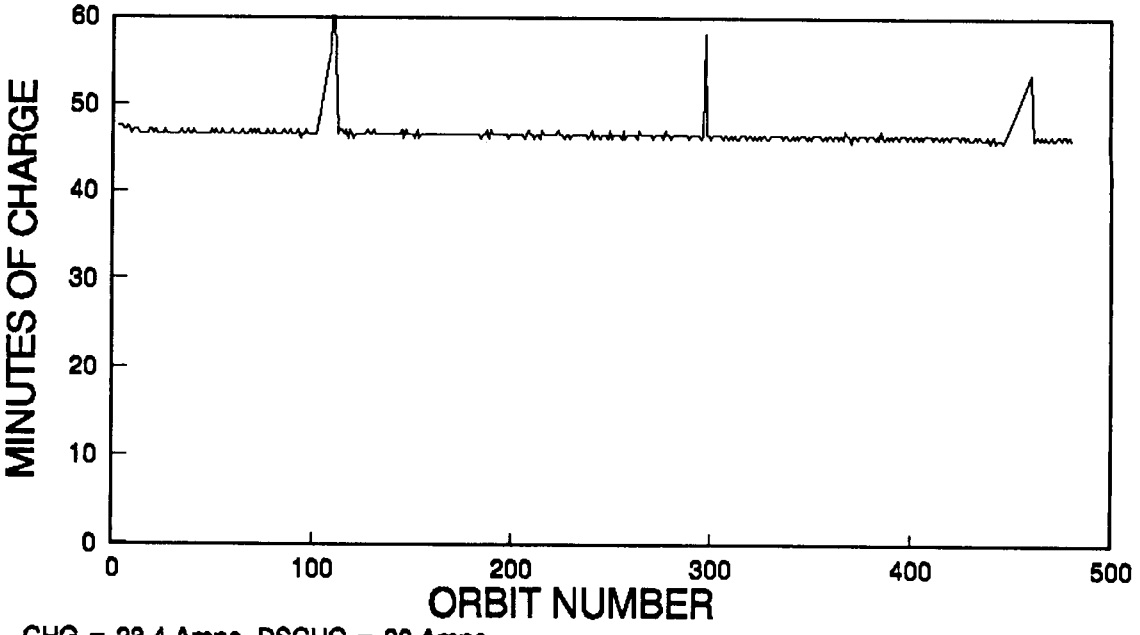

CHG = 23.4 Amps, DSCHG = 30 Amps
Sept 90

NASA
George C. Marshall
Space Flight Center

Step #6 of the plan at 1.50 EOCV, 30% DOD showed the same behavioral trends as the cycling at 1.48 EOCV, 20% DOD. The cells supported the discharge for a very short time (7 - 10 orbits pac #1 and 45 - 50 orbits pac #2) and then began accepting less charge; however, the charge acceptance leveled out and the amp hours out curve became relatively flat (12 -13 amp hours). The pressure curves also became flat indicating no increase in state of charge.

Step #9 of the plan was the next one performed because the cells would not support a 30% DOD at 1.50 EOCV. This level showed no unusual results. This portion of the test demonstrated the ability of these cells to operate at 20% DOD with no anomalies.

2 Cell Engineering Pac Tests
RNH 90-3

ORBIT vs. AMP HOURS OUT

1.50 V EOC, 30% DOD, 26% KOH

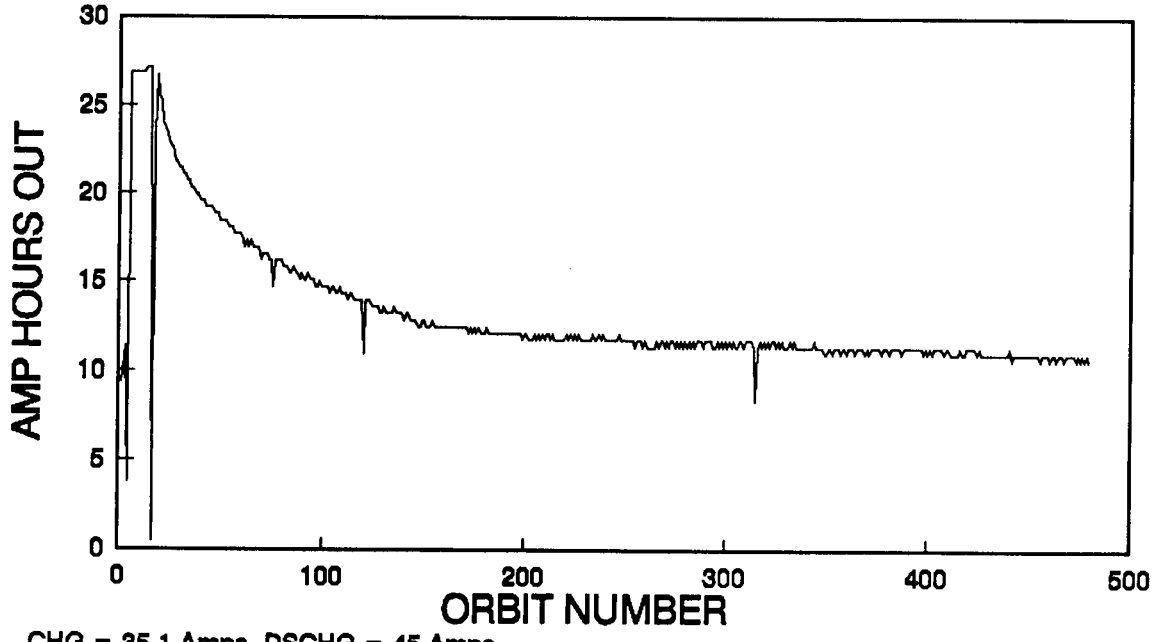

CHG = 35.1 Amps, DSCHG = 45 Amps
October 1990

ORBIT vs. AMP HOURS OUT

1.50 V EOC, 30% DOD, 31% KOH

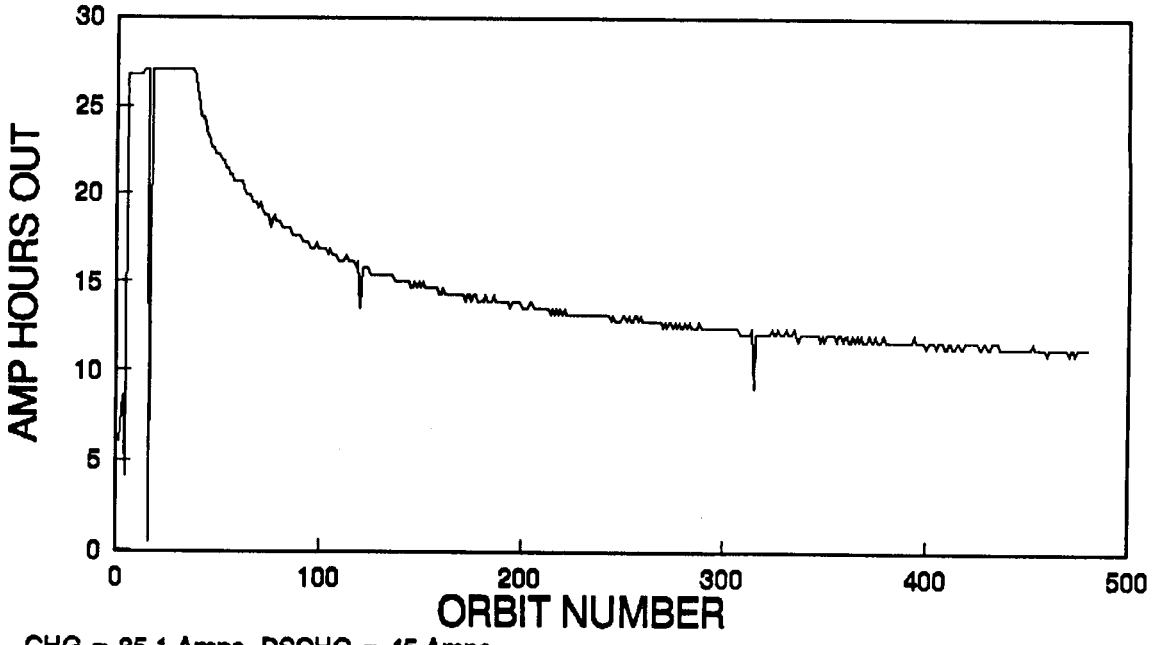

CHG = 35.1 Amps, DSCHG = 45 Amps
October 1990

2 Cell Engineering Pac Tests
RNH 90-3

ORBIT vs. EFFICIENCY

1.50 V EOC, 30% DOD, 26% KOH

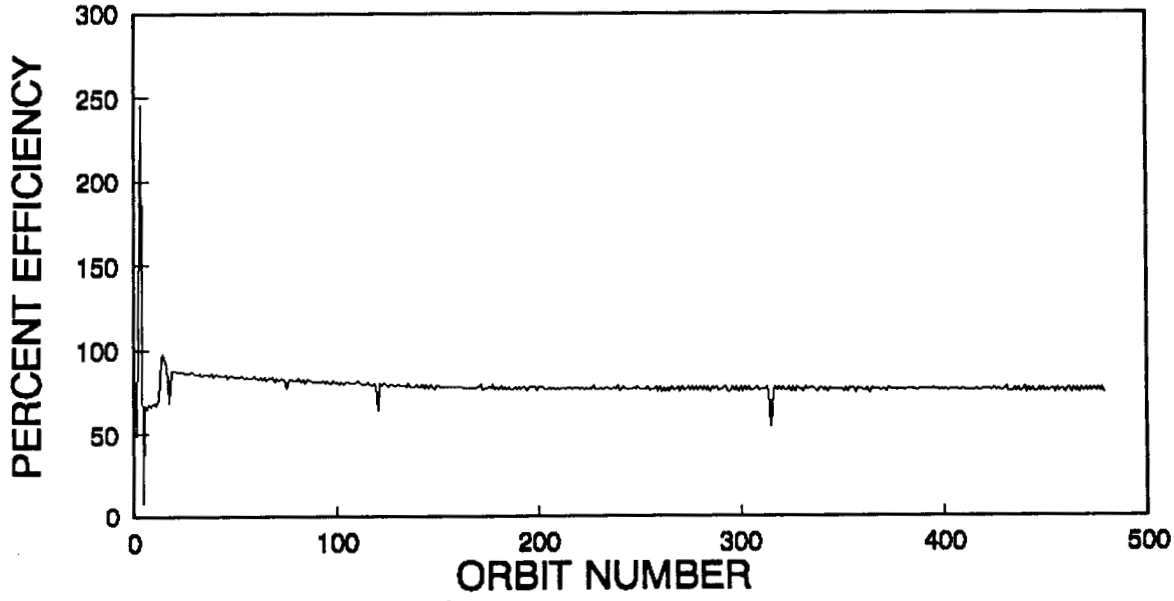

CHG = 35.1 Amps, DSCHG = 45 Amps
October 1990

ORBIT vs. RECHARGE RATIO

1.50 V EOC, 30% DOD, 26% KOH

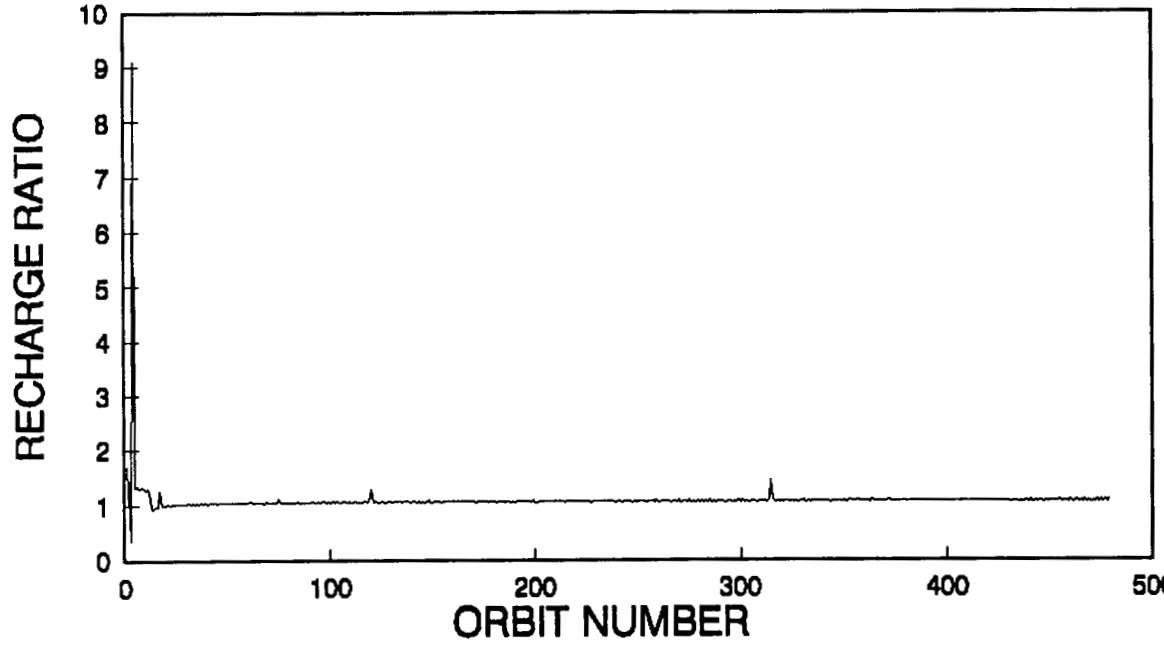

CHG = 35.1 Amps, DSCHG = 45 Amps
October 1990

2 Cell Engineering Pac Tests
RNH 90-3

ORBIT vs. EFFICIENCY

1.50 V EOC, 20% DOD, 31% KOH

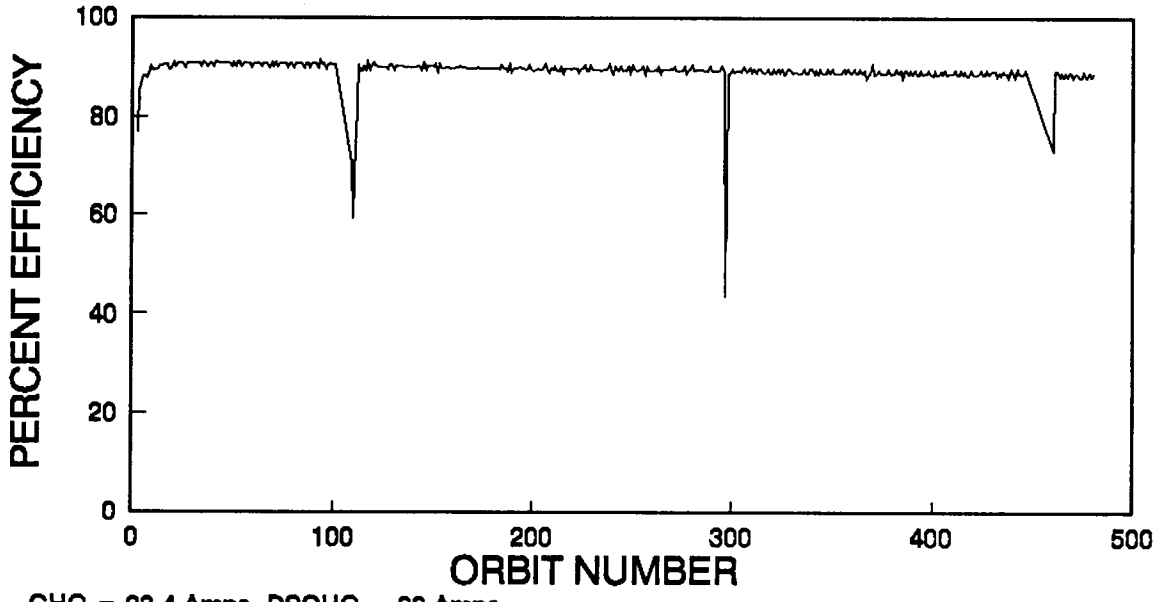

CHG = 23.4 Amps, DSCHG = 30 Amps
Sept 90

ORBIT vs. RECHARGE RATIO

1.50 V EOC, 20% DOD, 31% KOH

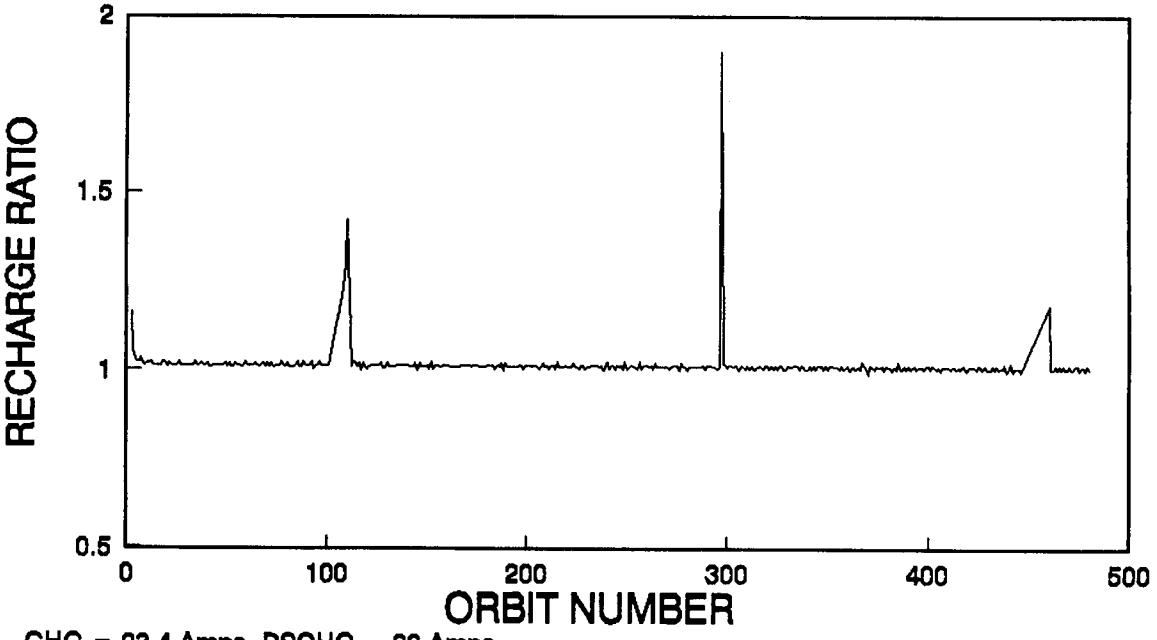

CHG = 23.4 Amps, DSCHG = 30 Amps
Sept 90

2 Cell Engineering Pac Tests
RNH 90-3

ORBIT vs. EFFICIENCY

1.50 V EOC, 30% DOD, 31% KOH

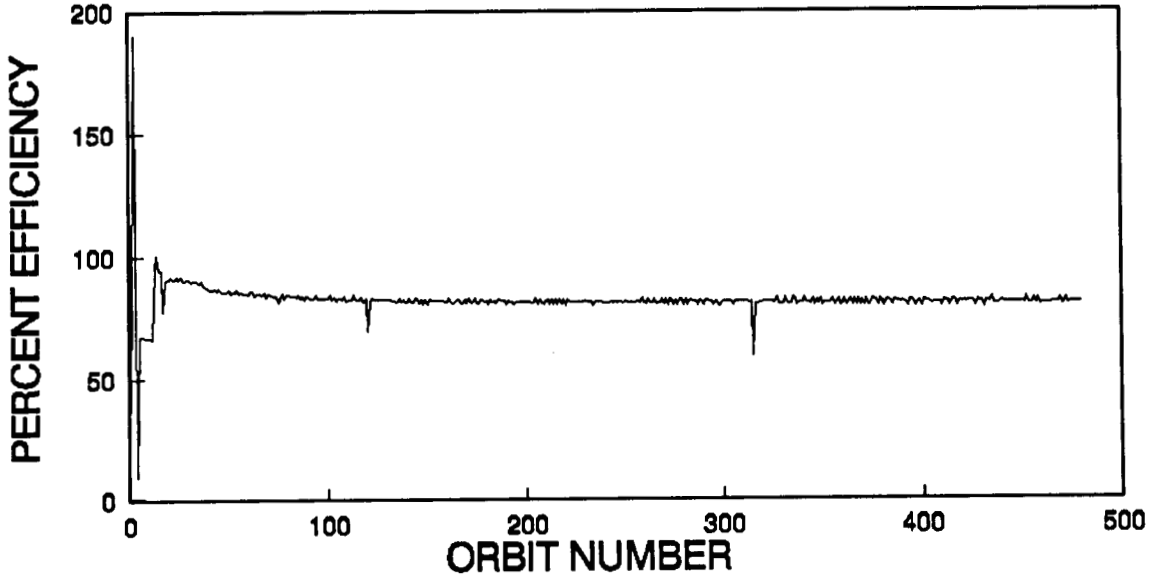

CHG = 35.1 Amps, DSCHG = 45 Amps
October 1990

ORBIT vs. RECHARGE RATIO

1.50 V EOC, 30% DOD, 31% KOH

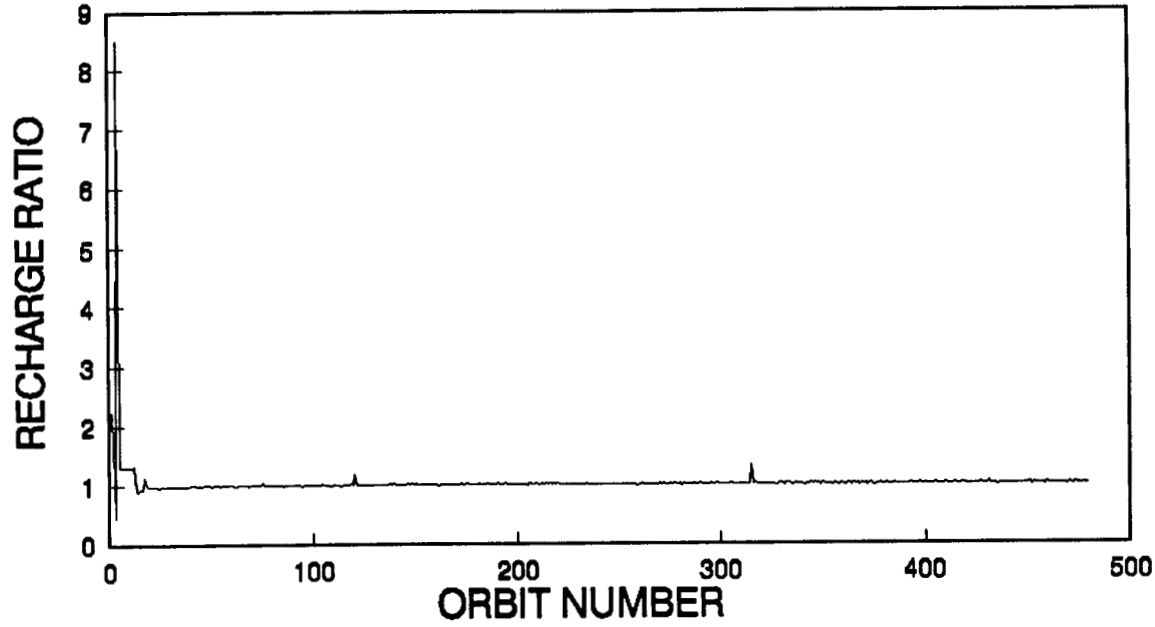

CHG = 35.1 Amps, DSCHG = 45 Amps
October 1990

2 Cell Engineering Pac Tests
RNH 90-3

ORBIT vs. AMP HOURS OUT

1.52 V EOC, 20% DOD, 26% KOH

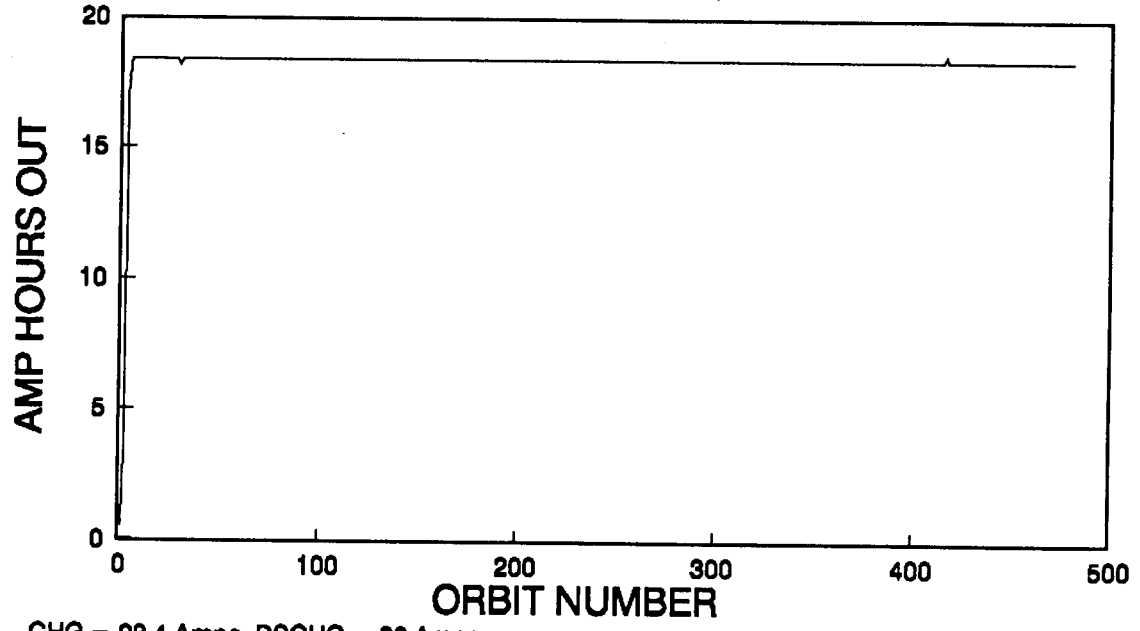

CHG = 23.4 Amps, DSCHG = 30 Amps
November 1990

ORBIT vs. MINUTES CHARGE

1.52 V EOC, 30% DOD, 26% KOH

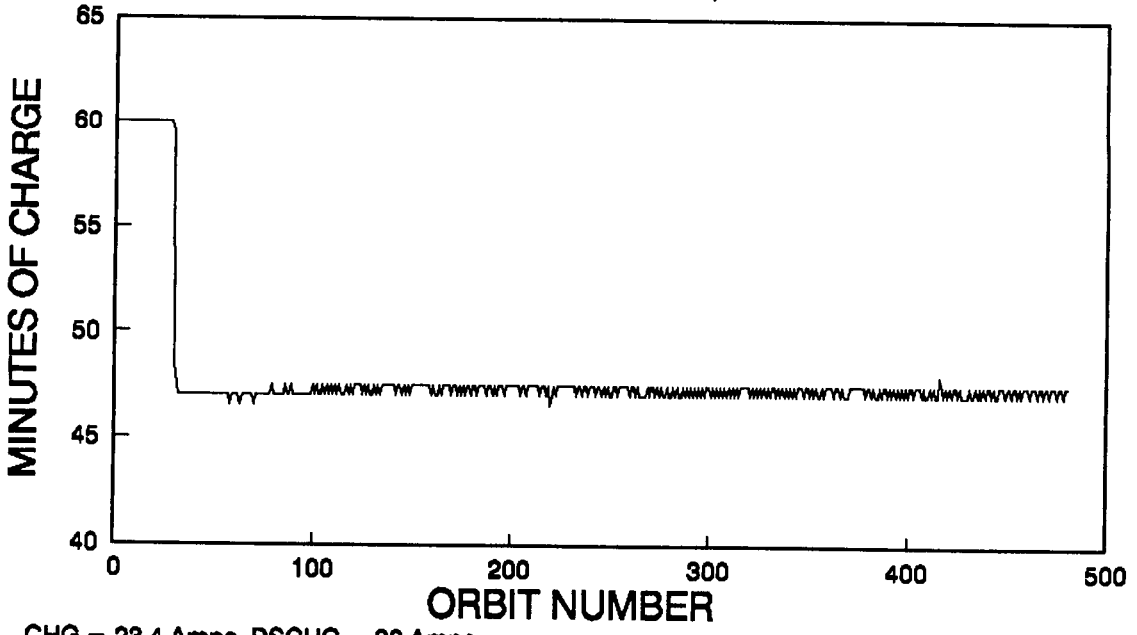

CHG = 23.4 Amps, DSCHG = 30 Amps
November 1990

2 Cell Engineering Pac Tests
RNH 90-3

ORBIT vs. EFFICIENCY

1.52 V EOC, 20% DOD, 26% KOH

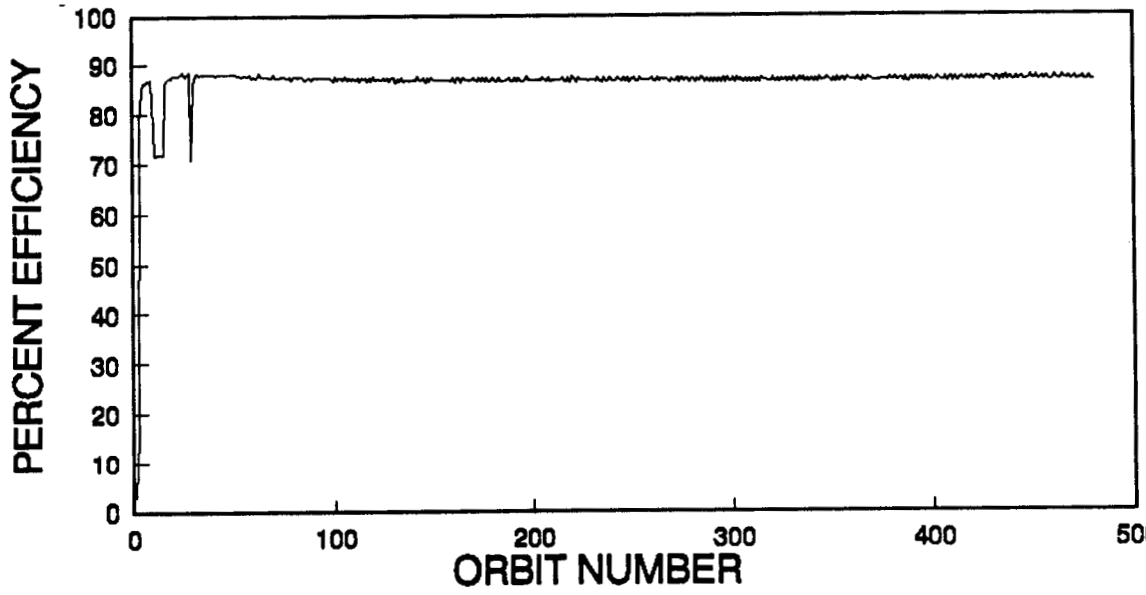

CHG = 23.4 Amps, DSCHG = 30 Amps
November 1990

ORBIT vs. RECHARGE RATIO

1.52 V EOC, 20% DOD, 26% KOH

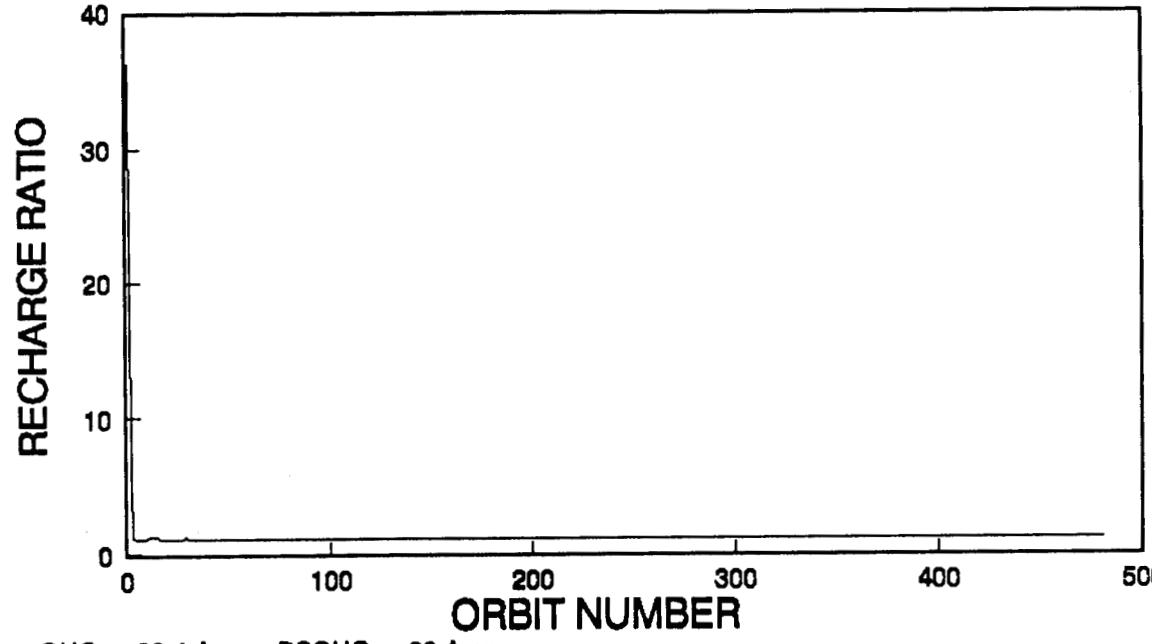

CHG = 23.4 Amps, DSCHG = 30 Amps
November 1990

2 Cell Engineering Pac Tests
RNH 90-3

ORBIT vs. AMP HOURS OUT

1.52 V EOC, 20% DOD, 31% KOH

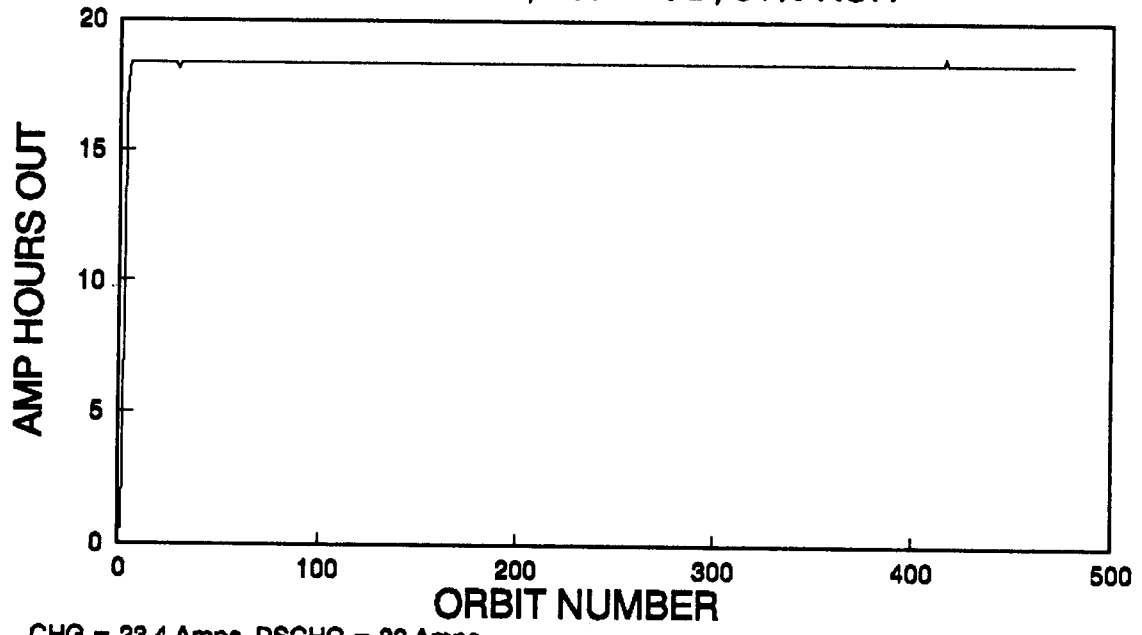

CHG = 23.4 Amps, DSCHG = 30 Amps
November 1990

ORBIT vs. MINUTES CHARGE

1.52 V EOC, 20% DOD, 31% KOH

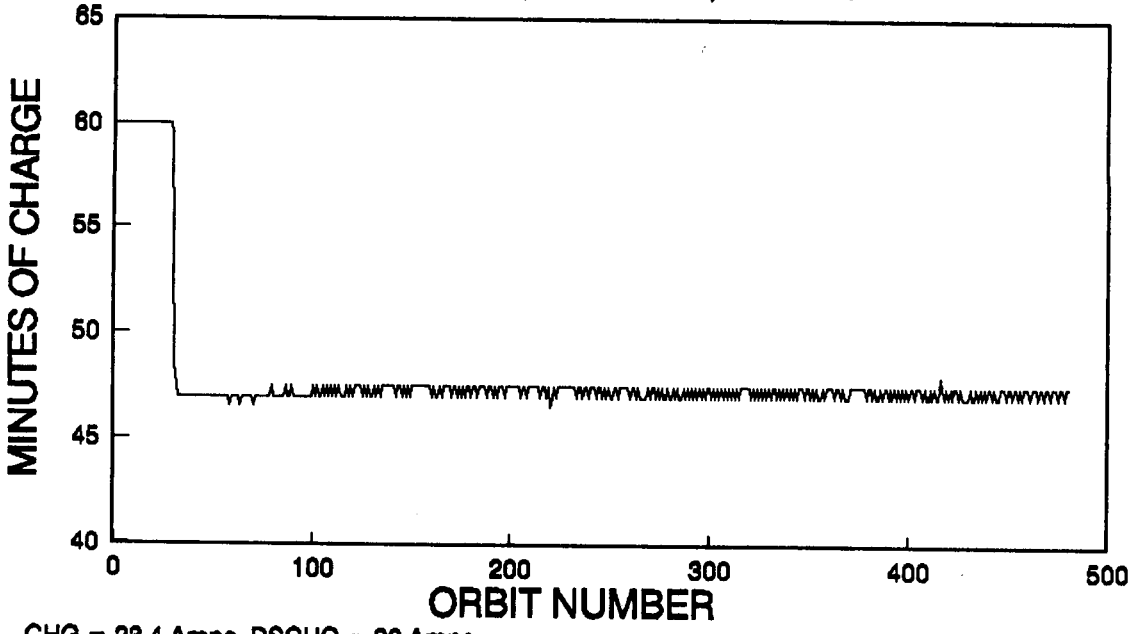

CHG = 23.4 Amps, DSCHG = 30 Amps
November 1990

2 Cell Engineering Pac Tests
RNH 90-3

ORBIT vs. EFFICIENCY

1.52 V EOC, 20% DOD, 31% KOH

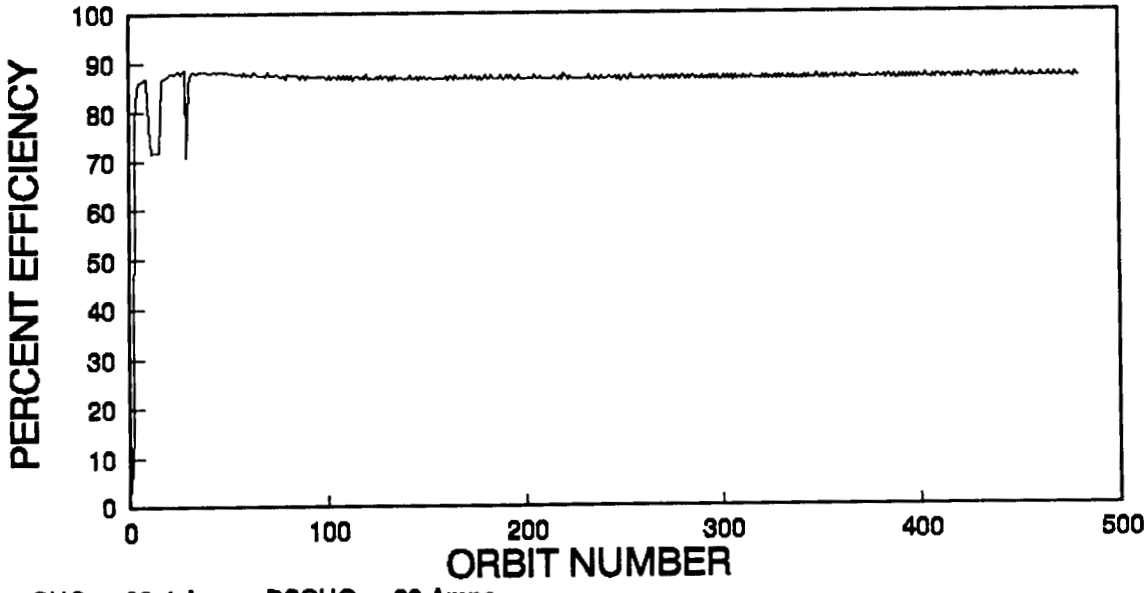

CHG = 23.4 Amps, DSCHG = 30 Amps
November 1990

ORBIT vs. RECHARGE RATIO

1.52 V EOC, 20% DOD, 31% KOH

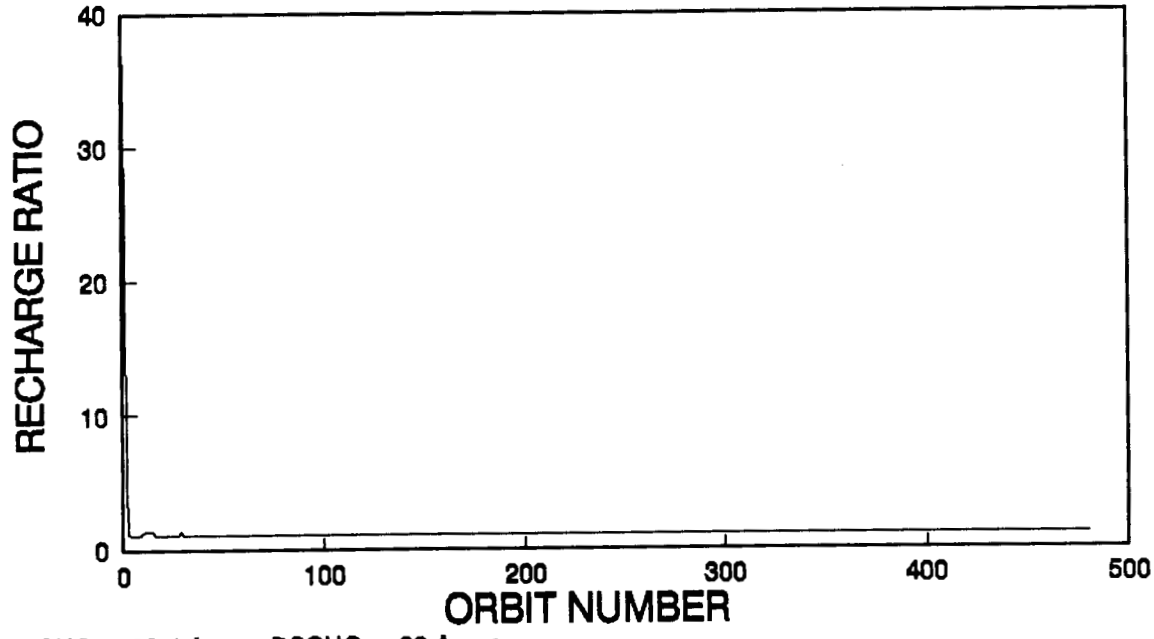

CHG = 23.4 Amps, DSCHG = 30 Amps
November 1990

NASA
George C. Marshall
Space Flight Center

2 Cell Engineering Pac Tests
RNH 90-3

Initial Capacity Test

	Capacity Cell #18 Amp Hrs	Capacity Cell #20 Amp Hrs	Capacity Cell #19 Amp Hrs	Capacity Cell #21 Amp Hrs
1.2 V/cell	82.21	73.82	77.41	76.66
1.0 V/cell	83.01	74.19	78.25	79.95
.5 V/cell	87.72	74.48	83.47	86.09

Capacity 1.48 EOCV

20% DOD

	Capacity Cell #18 Amp Hrs	Capacity Cell #20 Amp Hrs	Capacity Cell #19 Amp Hrs	Capacity Cell #21 Amp Hrs
1.2 V/cell	0.20	41.60	1.40	6.32
1.0 V/cell	0.78	41.99	3.74	8.26
.5 V/cell	2.60	48.10	5.75	12.49

Capacity 1.50 EOCV

20% DOD

	Capacity Cell #18 Amp Hrs	Capacity Cell #20 Amp Hrs	Capacity Cell #19 Amp Hrs	Capacity Cell #21 Amp Hrs
1.2 V/cell	16.25	35.36	18.96	21.67
1.0 V/cell	20.15	35.75	22.45	23.90
.5 V/cell	21.78	44.62	25.15	35.35

NASA
George C. Marshall
Space Flight Center

2 Cell Engineering Pac Tests
RNH 90-3

Capacity 1.50 EOCV

30% DOD

	Capacity Cell #18 Amp Hrs	Capacity Cell #20 Amp Hrs	Capacity Cell #19 Amp Hrs	Capacity Cell #21 Amp Hrs
1.2 V/cell	31.08	6.70	10.10	11.97
1.0 V/cell	31.80	11.26	13.83	16.10
.5 V/cell	35.00	14.40	15.82	29.00

Capacity 1.52 EOCV

20% DOD

	Capacity Cell #18 Amp Hrs	Capacity Cell #20 Amp Hrs	Capacity Cell #19 Amp Hrs	Capacity Cell #21 Amp Hrs
1.2 V/cell	60.97	59.41	61.05	61.05
1.0 V/cell	61.10	59.63	62.64	62.38
.5 V/cell	62.85	60.85	68.09	67.70

NASA

George C. Marshall
Space Flight Center

Discussion

This test has shown the lower end of the operational spectrum of the HST NiH2 cells. It has demonstrated their ability to operate at 20% DOD satisfactorily and will show their operation at 50% DOD.

APPENDIX

Distribution

A. Warren Adam
Sundstrand ATG
4747 Harrison Ave.
POB 7002
Rockford, IL 61125-7002
815-226-6419

Brian Alexander
USBI
POB 1900
Huntsville, AL 35816
205-721-2336

Douglas M. Allen
Wright Research & Development Center
WRDC/POOX
Wright-Patterson AFB, OH 45433
513-255-4450

Menahem Anderman
ACME Electric
528 W. 21st Street, #6
Tempe, AZ 85282
602-894-6864

John A. Andrasik
Lewis Research Center
MS 501-4
21000 Brookpark Rd.
Cleveland, OH 44135
216-433-2358

Isaac Angres
6 War Admiral Ct.
Gaithersburg, MD 20878
301-926-2742

Joseph Appelbaum
NASA Lewis Research Center
MS 302-1
21000 Brookpark Rd.
Cleveland, OH 44135
216-433-xxxx

Anthony Applewhite
Ford Aerospace Corporation
3825 Fabian Way
Paol Alto, CA 94303
415-852-5048

Jon D. Armantrout
Lockheed Missiles & Space Co.
O/62-12 B/551
1111 Lockheed Way
Sunnyvale, CA 94089-3504
408-742-1800

Raymond F. Askew
Auburn University
Space Power Institute
Al 36849-3501
205-826-5894

Daniel Augenstene
DOJ
8199 Backlick Rd.
Lorton, VA 22079
202-324-2800

David Baer
Hughes Aircraft Co.
MS A315 Bldg. S41
POB 92919
Los Angeles, CA 90009
213-416-xxxx

John Baker
Catalyst Research
38 Loveton Circle
Sparks, MD 21152
301-628-5416

James Barnes
NSWC Code R33
Silver Spring, MD 20903-5000
301-394-1312

Wilbert L. Barnes
Naval Research Lab, Code 8112
4555 Overlook Ave. SW
Washington, DC 20375
202-767-6517

Louis Barraza
Westinghouse Electric Corp
4960 Corporate Dr. Ste 125F
Huntsville, AL 35805
205-722-4738

Bobby Batten
NASA Langley Research Center
M/S 231
Hampton, VA 23665

Terry Bavaro
Aerospace Corporation
MS M4/988
POB 92957
Los Angeles, CA 90009-2957
213-336-xxxx

Carl Baxam
TRACOR Battery
3805 Mt. Vernon Ave.
Alexandria, VA 22305
703-769-6833

Mike Bayes
Naval Weapons Support Center - Crane
Code 305, Bldg. 2949
Crane, IN 47522-5030
812-854-1593

Jim Bell
Hughes Aircraft Company
Bldg. S41 M/S A315
POB 92919
Los Angeles, CA 90009

Dr. Klaus von Benda
Daimler-Benz FA/EE
POB 85
7300 Esslingen, Germany
01149-711-17-46018

James Bene
NASA Langley Research Center
SM-488
Hampton, VA 23665

Chuck Bennett
GE Astro Space Div.
MS 410-2-C19
POB 800
Princeton, NJ 08540-0800
609-490-6804

Gary L. Bennett
NASA HQ
Code RP
Washington, DC 20546
202-453-2843

Don Berrier
TRW R4/1136
One Space Park
Redondo Beach, CA 90278
213-813-4888

E.R. Berry
Aerospace Corporation
MS M4/988
POB 92957
Los Angeles, CA 90009-2957
213-336-1027

William J. Billerbeck
MRJ Inc.
10455 White Gramite Dr., Suite 200
Oakton, VA 22124
703-385-0742

John D. Bingley
GE ASTRO Space
POB 800
Princeton, NJ 08540
609-426-2462

Sam Birken
Aerospace Corporation
MS M4/986
POB 92957
Los Angeles, CA 90009-2957
2113-336-6080

Frank Bis
Advanced Power Sources
5513 Ridge Rd.
Mt. Airy, MD 21771
301-831-7469

Grant William Bishop
Lockheed Missiles & Space Co.
O/81-76 B/157
1111 Lockheed Way
Sunnyvale, CA 94089-3504
408-756-1886

Harlan F. Bittner
Aerospace Corporation
MS M2/275
POB 92957
Los Angeles, CA 90009-2957
213-336-1027

James B. Blackmon
McDonnell Douglas Astronautics Co.
5301 Bolsa Ave.
Huntington Beach, CA 92647
714-896-4007

Carole Bleser
Eagle-Picher Industries, Inc.
3820 South Hancock Expressway
Colorado Springs, CO 80911
719-392-4266

Sam Bogner
Hughes Aircraft Company
M/S 231/1915
POB 2999
Torrance, CA 90509

Richard Bolt
Code 302
Greenbelt, MD 20771
301-286-xxxx

Francis R. Boyce
RCA
13305 Finsbury Ct. #1
Laurel, MD 20708
301-763-7577

William Boyd
Acme/Aero
3675 So Crmg Circle
Salt Lake City, UT 84109
801-596-0075

Gerard Boyle
Yardney Technical Products
82 Mechanic Street
Pawcatuck, CT 06379
617-890-3040ex3711

Robert Bragg
Johnson Space Center
MS EP5
NASA Rd. 1
Houston, TX 77058
713-483-9060

Wayne Brem
Allied Signal
3799 Buckingham Dr.
Doylestown, PA 18901
215-348-5152

Jeffery C. Brewer
NASA MSFC EB12
Marshall Space Flight Ctr.
AL 35812
205-544-3345

Marc Brideau
Martin Marietta
10111 City View Dr.
Morrison, CO 80465
303-971-8286

Jack N. Brill
Eagle-Picher Industries, Inc.
POB 47
Joplin, MO 64802
417-623-8000

Doris L. Britton
Lewis Research Center
MS 309-1
21000 Brookpark Rd.
Cleveland, OH 44135
216-433-5246

Richard J. Broderick
GTE Spacenet
4398 Canterbury Ln.
Gainesville, VA 22065
703-848-0421

Mike Brookman
DME Corporation
111 S.W. 33rd Street
Ft. Lauderdale, Fl. 33315
305-463-5966

Jim Brooks
Eagle-Picher Industries, Inc.
3820 South Hancock Expressway
Colorado Springs, CO 80911
719-392-4266

Dung Q. Bul
FDA/CDRH
12720 Twinbrook Parkway
Rockville, MD 29857
301-443-2536

Kathie Burch
COMSAT Laboratories
22300 Comsat Dr.
Clarksburg, MD 20871
301-428-4503

Todd Burke
COMSAT Laboratories
22300 Comsat Dr.
Clarksburg, MD. 20871
301-428-4503

Brad Burris
Eagle-Picher Industries
C & Porter
Joplin, MO 64801
417-623-8000

Robert B. Byrnes
Dept. of the Army
27 Kelvin Dr.
Stafford, VA 22554
202-695-3516

Joe Bytella
Catalyst Research
38 Loveton Circle
Sparks, MD 21152
301-628-5440

Peter J. Cannon
American Cyanamid Co.
POB 34
Edgewater, MD 21037
202-471-9933

Joe Carcone
Sanyo Energy Corporation
1201 Sanyo Ave.
San Deigo, CA 92073

Uno Carlsson
Fairchild Space Co.
MS A-28
20301 Century Blvd.
Germantown, MD 20874
301-428-6022

Howard E. Carpenter
Gould Inc.
35129 Curtis Blvd.
Eastlake, OH 44094
216-953-5065

Boyd Carter
Aerospace Corporation
POB 92957
Los Angeles, CA 90009
213-336-5052

Alan Cash
Teldyne Brown Engineering
300 Sparkman Dr. NW
Huntsville, AL 35805-1994

Robert Cataldo
Lewis Research Center
MS 501-1
21000 Brookpark Rd.
Cleveland, OH 44135
216-433-5254

Rebecca Chang
Ford Aerospace
3825 Fabian Way
Palo Alto, CA 94303
415-852-4435

Lee Christensen
Freudenberg Nonwovens
20 Industrial Ave.
Chelmsford, MA 01824
617-256-6588

James J. Ciesla
DME Corporation
111 S.W. 33rd Street
Ft. Lauderdale, FL 33315
305-463-5066

William D.K. Clark
Wilson Greatbatch Ltd.
10000 Wehrle Dr.
Clarence, NY 14031
716-759-6901

Karla Clark
Jet Propulsion Laboratory
MS 277-212
4800 Oak Grove Drive
Pasadena, CA 91109
818-354-9033

William Clark
Wilson Greatbatch Ltd.
10000 Wehrle Dr.
Clarence, NY 14031
716-759-6901

Joe Le Clear
Newport News SB&DD Co.
Dept. E55
Newport News, VA 23607
804-380-2842

Dale Cochran
Martin Marietta Astronautics
POB 179, MS 8041
Denver, CO 80201
303-977-6987

C.L. Cody
Eveready Battery Co.
Technology Lab, Rm 225
25225 Detroit Rd.
Westlake, OH 44145

Betty Colhoun
On the Ivy Neck
POB 38
Harwood, MD 20776

Richard Congo
EH32
Marshall Space Flight Ctr.
Alabama 35812
205-544-2629

Robert Cool
COMSAT Laboratories
22300 Comsat Dr.
Clarksburg, MD 20871
301-428-4275

Dennis B. Cooper
INTELSAT Box 34
3400 International Dr. NW
Washington, DC 20008-3098
202-744-7349

J.C. Cope
4313 Marlowe Dr.
San Jose, CA 95124

Robert E. Corbett
Sanders Company
POB 2004, NCA 1-6703
Nashua, NH 03061

Timothy Counts
4102 E. 25th
Joplin, MO 64804
417-623-0258

Ed Cruz
Ford Aerospace Corporation
3825 Fabian Way
Palo Alto, CA 94303
415-852-6633

Edward F. Cuddihy
Jet Propulsion Laboratory
MS 300-314
4800 Oak Grove Dr.
Pasadena, CA 91109
818-354-3188

Harry Culver
Goddard Space Flight Center
Code 711.1
Greenbelt, MD 20771
301-286-6841

Don Curtis
Texas A&M University
Dept. of Chemistry/Eng.
C. Station, TX 77843
409-845-3307

Frank Cushing
3-E Labs
840 W. Main Street
Landsdale, PA 19446

George Dakermanji
Fairchild Space Company
MS A-14
20401 Century Blvd.
Germantown, MD 20874
301-428-6394

Penni Dalton
Lewis Research Center
MS 500-222
21000 Brookpark Rd.
Cleveland, OH 44135
216-433-xxxx

Ivan Danzig
6812 Wild Court
Springfield, VA 22152

Eric C. Darcy
Johnson Space Center
MS EP5
NASA Rd. 1
Houston, TX 77058
713-483-9055

Stuart Daughtridge
INTELSAT M/S 33A
3400 International Dr.
Washington, DC 20008-3098
202-944-7334

John Day
Goddard Space Flight Center
Code 711.2
Greenbelt, MD 20771
301-286-5752

Frank Deligiannis
Jet Propulsion Labaoratory
MS 277-104
4800 Oak Grove Dr.
Pasadena, CA 91109
818-354-0404

Dan Dell
Gates Aerospace Batteries
POB 2520
Gainesville, FL 32602
904-462-3098

T.P. Dirkse
Calvin College
3201 Burton, SE
Grand Rapids, MI 49506

Marlene Dix
EAC
2047 Unit E
Powers Ferry Rd.
Marietta, GA 30067
404-951-8935

Kurt Dobrenz
2541 Oak Valley Dr.
Vienna, VA. 22181
703-695-3520

George Dochat
Mechanical Technology Inc.
968 Albany Shaker Rd.
Latham, NY 12110
518-785-2211

Harrison S. Dodge
FDA
HFZ141
12720 Twinbrook Parkway
Rockville, MD 20850
301-443-2536

Gary Dodson
Eagle-Picher Industries, Inc.
POB 47
Joplin, MO 64802
417-623-8000

Loyd Doering
POB 1500
CSSD-SL-K
Huntsville, AL 35807-3801

Mike Domeniconi
Lockheed Missles & Space Co. Inc.
1111 Lockheed Way
O/62-12 B/551
Sunnyvale, CA 94088
408-743-7267

Michael Donnelly
Goddard Space Flight Center
Code 050.0
Greenbelt, MD 20771
301-286-2147

Rajiv Doreswamy
EB12
Marshall Space Flight Ctr.
Alabama 35812
205-544-3366

Loxie L. Doud
Roger E. Rickey & Assocs.
200 Yancy Rd.
Madison, AL 35758
205-837-3077

Joseph R. Driscoll
Lockheed Missles & Space Co. Inc.
O/62-12 B/551
POB 3504
Sunnyvale, CA 94088
408-743-2639

Rene J. Dubois
Whittaker-Yardney Power Systems
82 Mechanic St.
Pawcatuck, CT 02891
203-599-1100

G.J. Dudley
ESTEC / XPB
POB 299
2200AG Noordwijk
The Netherlands
31-1719-83834

James Dunlop
COMSAT Laboratories
22300 Comsat Dr.
Clarksburg, MD 20871
301-428-4503

Andrew F. Dunnet
INTELSAT
3400 International Dr.
Washington, DC 20008-3098
202-944-7245

Capt. Ross Durber
Dept. of Chemistry
USAF Academy
Colorado Springs, CO 80840-5000
719-472-3240

Martin Earl
COMSAT Laboratories
22300 Comsat Dr.
Clarksburg, MD 20871
301-428-4503

Tim Edgar
Eagle-Picher Industries, Inc.
3820 South Hancock Expressway
Colorado Springs, CO 80911
719-392-4266

Teddy M. Edge
EB13
Marshall Space Flight Ctr.
Alabama 35812
205-544-3381

Larry Edsinger
Ames Research Center
MS 213-2
Moffet Field, CA 94035
415-694-4079

Vickie Edwards
AT&T Bell Labs
Rm 1E207
600 Mountain Ave.
Murray Hill, NJ 07974
201-582-3286

Marlon Enciso
Goddard Space Flight Center
Code 711.1
Greenbelt, MD 20771
301-286-5070

Patricia H. Enns
Aerospace Corporation
2350 El Segundo Blvd.
El Segundo, CA 90245
213-336-5902

Rex Erisman
Eagle-Picher Industries, Inc.
POB 47
Joplin, MO 64801
417-623-8000

Richard Charles Ewell
MS 303-308
Jet Propulsion Laboratory
4800 Oak Grove Dr.
Pasadena, CA 91109
818-354-6794

Rolan Farmer
Eagle-Picher Industries, Inc.
3820 South Hancock Expressway
Colorado Springs, CO 80911
719-392-4266

David O. Feder
Electrochemical Energy
Storage Systems, Inc.
35 Ridgedale Ave.
Madison, NJ 07940
201-327-0163

Tony Felts
Naval Weapons Support Center - Crane
Code 30523
Crane, IN 47522
812-854-1593

John Finnearty
293 Stagecoach Rd.
Athens, OH 45701

Ed Fitzgerald
1026 Seina Vista Dr.
Madison, AL 35758
205-716-2865

Richard A. Flake
U.S. Air Force
AFWAL/POOS-2
Area B / Bldg.18
Wright-Patterson AFB, OH 45433
513-255-7770

Charles W. Fleischman
C&D Power Systems
3043 Walton Rd.
Plymouth Meeting, PA 19462

Nicanor Flordeliza
GE American Communications
4 Research Way
Princeton, NJ 08540
609-987-4453

R.F. Fogle
Rockwell International
POB 4192, GF42
3370 Miraloma Ave.
Anaheim, CA 92803

Robert W. Francis
Aerospace Corporation
2350 El Segundo Blvd.
El Segundo, CA 90245
213-336-6272

Allan Frandsen
NASA HQ
Code ES
Washington, DC 20546
202-453-1676

David H. Fritts
U.S. Air Force
AFWAL/POOS-2
Wright-Patterson AFB, OH 45433
513-255-2372

Kenneth H. Fuhr
Martin Marietta Astronautics
POB 179, MS S-8072
Denver, CO 80201
303-977-4495

Randall F. Gahn
Lewis Research Center
MS 301-3
21000 Brookpark Rd.
Cleveland, OH 44135
216-433-6158

Daniel T. Gallagher
Fairchild Space Co.
MS D-1
20301 Century Blvd.
Germantown, MD 20874
301-428-6848

M.G. Gandel
LMSC
B\152 O/62-55
POB 504
Sunnyvale, CA 94086

Chris Garner
Naval Research Laboratory
4555 Overlook Ave, SW
Washington, DC 20375-5000
202-767-9075

John Garske
U.S. Navy
580 Fox Hunt Circle
Highlands Ranch, CO 80126
303-978-8878

Stephen J. Gaston
G.E. Astrospace Div.
MS 410-2-C19
POB 800
Princeton, NJ 08540
609-426-2559

Dr. Wm. O. Gentry
Johnson Controls Inc.
POB 591
Milwaukee, WI 53201
414-228-2228

Pete George
1110 Pratt Ave. NE
Huntsville, AL 35801
205-544-3331

Richard M. Gerber
Aerospace Corporation
2350 El Segundo Blvd.
El Segundo, CA 90245
213-416-7033

Ann Gibney
14841 NW Todd ST.
Beaverton, OR 97066
503-646-4235

Al Gillis
Goddard Space Flight Center
Code 405
Greenbelt, MD 20771
301-286-6776

Richard D. Glover
NASA Ames - Dryden
POB 273
Edwards, CA 93523
805-258-3680

Elva Glover
Goddard Space Flight Center
Code 713.2
Greenbelt, MD 20771
301-286-6784

Peter Gluck
Jet Propulsion Laboratory
MS 303-300
4800 Oak Grove Drive
Pasadena, CA 91109
818-354-9425

Dee Gnacek
USBI
POB 1900
Huntsville, AL 35807
205-721-2954

Ray Goins
Rt. 2 Box 287-B
Toney, AL 35773
205-423-6902

Luara T. Goliaszewski
Johns Hopkins University/ APL
Rm 23-210
Johns Hopkins RD.
Laurel, MD 301-953-5000

Olga D. Gonzalez-Sanabria
Lewis Research Center
MS 301-3
21000 Brookpark Rd.
Cleveland, OH 44135
216-433-6158

Glen Gooch
USBI
POB 1900
Huntsville, AL 35807
205-721-2232

Vera Gor
TRW
One Space Park
Redondo Beach, CA 90278
213-297-5521

Lester A. Gordy
U.S. Army
8219 Running Creek Ct.
Springfield, VA 22153
202-965-3420

Jaques Goualard
SAFT Space Program
156 Avenue De Metz
93230 Romainville, France
33-1-49-42-3417

Joe Gowdy
NASA Langley Research Center
M/S 433
Hampton, VA 23665

Janet Grala
GE Astrospace Div.
MS 410-2-C19
POB 800
Princeton, NJ 08540
609-426-3349

John G. Gray
6200 East Mercer Way
Mercer Island, WA 98040
206-773-3655

Robert S. Green
GTE Spacenet
1700 Old Meadow Rd.
McLean, VA 22102
703-848-0452

Sid Gross
Boeing Aerospace MS 8W-08
POB 3999
Seattle, WA 98124
206-234-9847

Richard Gruenfelder
Grumman Aircraft Systems Div.
1111 Stewart Ave.
Bethpage, NY 11714-3582
516-346-9158

James A. Guckinski
Naval Weapons Support Center - Crane
Code 305, Bldg. 2949
Crane, IN 47522-5030
812-854-1593

Ronald D. Hahn
General Electric
M2450 VF100
POB 8555
Philadelphia, PA 19101
215-354-2737

Arnold Hall
Whittaker-Yardney Power Systems
82 Mechanic St.
Pawcatuck, CT 02891
203-599-1100

Charles I. Hall
NASA MSFC EB12
Marshall Space Flight Ctr.
AL 35812
205-544-3330

David K. Hall
EB12
Marshall Space Flight Ctr.
Alabama 35812
205-544-4215

Steve Hall
Naval Weapons Support Center - Crane
Code 30561, Bldg. 2949
Crane, IN 47522-5000
812-854-1593

Gerald Halpert
Jet Propulsion Laboratory
4800 Oak Grove Drive
Pasadena, CA 91109
818-354-5474

Phil Hamilton
GE American Communications
95 Edsall Dr.
Sussex, NJ 07461
201-827-7900

Ken Hanson
MS M9509
General Electric Co.
POB 8555
Philadelphia, PA 19101
215-354-4975

Zia Haq
Energetics
9210 Rt. 108
Columbia, MD 21045
301-992-4000

Dany Harel
GE American Communications
4 Research Way
Princeton, NJ 08540
609-987-4243

John H. Harlow
TA31
Marshall Space Flight Ctr.
Alabama 35812
205-544-0663

Abbey Harper
Goddard Space Flight Center
Code 303
Greenbelt, MD 20771
301-286-7954

Bill Harris
Westinghouse Corp.
4960 Corporate Dr.
Suite 125
Huntsville, AL 35805-6246

Mike Harrison
Gates Aerospace Batteries
POB 2520
Gainesville, FL 32602
904-462-4742

Gary L. Hartjen
Rockwell International
M/S LB-31
6633 Canoga Park, CA 91303
818-700-2202

JoAnn Hastings
SAFT America, Inc.
107 Beaver Ct.
Cockeysville, MD 21030
301-771-3200

Robert Hawkins
POB 1900
Huntsville, AL 35803
205-721-2373

Joseph H. Hayden
MS A314 Bldg S41
Hughes Aircraft Co.
POB 92919
Los Angeles, CA 90009
213-648-0977

Jeff Hayden
Eagel-Picher Industries
3820 S. Hancock Expy.
Colorado Springs, CO 80911
719-392-4266

Ken Hearn
Data Entry Systems
POB 2127
Huntsville, AL 35804
205-539-2483

Robert Hellen
Yardney Technical Products
82 Mechanic Street
Pawcatuck, CT 06379
203-599-1100

E.A. Hendee
Telesat Canada
333 River Road
Ottawa, Ontario
Canada KIL8B9

Tom Hennigan
T.J. Hennigan, Assoc's
900 Fairoak Ave.
W. Hyattsville, MD 20783
301-559-0613

Gregg A. Herbert
Johns Hopkins University/ APL
Rm 23-210
Johns Hopkins RD.
Laurel, MD 20707
301-953-5000

Terry L. Hershey
Aerospace Corporation
POB 92957
Los Angeles, CA 90009-2957
213-336-1032

Carole A. Hill
Aerospace Corporation
MS 2-275 Bldg. A-6
POB 92957
Los Angeles, CA 90009-2957
213-336-0175

Albert Himy
100 Cerasi Dr. Apt. 311
West Mifflin, PA 15122

Gerald L. Holleck
EIC Laboratories, Inc.
111 Downey St.
Norwood, MA 02062
617-769-9450

Lt. Hopun
Space Division/YDE
POB 92960
Worldway Postal Center
Los Angeles, CA 90009

Franklin L. Hornbuckle
Fairchild Space Co.
20301 Century Blvd.
Germantown, MD 20874
301-428-6221

Paul Howard
P.L. Howard Associates
POB 280
Greensboro, MD 21639
301-482-6088

Jim Hughes
Westinghouse Electric Corp
4960 Corporate Dr. Ste 125F
Huntsville, AL 35805
205-722-4744

Daniel L. Hutchins
Western Development
Laboratories Div.
3939 Fabian Way
Palo Alto, CA 94303
415-852-4715

Warren Hwang
Aerospace Corporation
2350 El Segundo Blvd.
El Segundo, CA 90245
213-336-6962

A. D. Little, Inc.
Acorn Park
Cambridge, MA 02140

Todd Iwamiya
Lockheed Missles & Space Co. Inc.
1272 Borregas Ave.
O/62-12 B/551
Sunnyvale, CA 94086
408-742-1934

Lorna G. Jackson
EB12
Marshall Space Flight Ctr.
Alabama 35812
205-544-3318

Robert A. Jamieson
Aerospace Corporation
2350 El Segundo Blvd.
El Segundo, CA 90245
213-336-5225

Anisa Jamil
Goddard Space Flight Center
Code 711.4
Greenbelt, MD 20771
301-286-8842

Jason E. Jenkins
Johns Hopkins University/ APL
Rm 23-214
Johns Hopkins RD.
Laurel, MD 20723
301-953-5106

Ian Jenkins
MBB Deutsche Aerospace
Hanger AM, CCAFS
Kennedy Space Center
FL 32899
407-853-9781

Calvin R. Johnson
Auburn University
Space Power Institute
Al 36849-3501
205-826-5894

Sheila Johnson
1961 Schrader Dr.
San Jose, CA 95124
408-743-7220

Joseph Jolson
Catalyst Research
3706 Crondall Lane
Owings Mills, MD 21117
301-356-2933

Dr. Wade H. Jordon
1 Mountain Top Rd.
Front Royal, VA 22630
703-635-9311

Orville O. Dunham, Jr.
National-Standard Comp.
Woven Products Div.
Industrial Blvd.
POB 1620
Corbin, KY 40701
606-528-2141

John R. Lanier, Jr.
EB12
Marshall Space Flight Ctr.
Alabama 35812
205-544-3301

John R. Lapinski, Jr.
MS 1063323
McDonnell Douglas Electronic Systems
POB 516
St. Louis, MO 63166-0516
314-233-2404

Herman A. Lewis, Jr.
McDonnell Douglas Astronautics Co.
5301 Bolsa Ave.
Huntington Beach, CA 92647
714-896-3137

Carlos D. Judkins
12623 88th PL ne
Kirkland, WA 98034
206-773-2456

David Jung
Goddard Space Flight Center
Code 711.2
Greenbelt, MD 20771
301-286-xxxx

Quentin L. Kampf
Freudenberg Nonwovens
221 Jackson St.
Lowell, MA 01852
508-454-0461

Ed Kantner
Exxon Research and Engineering
POB 45
Linden, NJ 07036

Vic Kardarper
General Dynamics SSD
POB 85990
MZ 24-8721
San Diego, CA 92138
619-547-4017

Alexander P. Karpinski
Whittaker-Yardney Power Systems
82 Mechanic St.
Pawcatuck, CT 02891
203-599-1100

P.R. Kchetty
Fairchild Space Company
M/S D8
20301 Century Blvd.
Germantown, MD 20874

D.E. Kennedy
Box 56
Amanda, OH 43102

John H. Kennedy
Whittaker-Yardney Power Systems
82 Mechanic St.
Pawcatuck, CT 02891
203-599-1100

Lew Kennedy
3529 Spann St. NW
Huntsville, AL 35810
205-544-3329

R. L. Kerr
AFWAL/GLXPP
Wright-Patterson AFB
OH 45433

Randy Kientz
Gates Aerospace Batteries
POB 2520
Gainesville, FL 32602
904-462-3557

Brian C. Kimsey
Aerospace Corporation
2350 El Segundo Blvd.
El Segundo, CA 90245
213-336-1665

David Kirkpatrick
Lockheed Missles & Space Co. Inc.
1111 Lockheed Way
O/62-12 B/551
Sunnyvale, CA 94088
408-756-6149

Glenn Klein
Gates Aerospace Batteries
POB 2520
Gainesville, FL 32602
904-462-3569

Martin Klein
Energy Research Corporation
3 Great Pasture Rd.
Danbury, CT 06810

John W. Klein
MS 303-300
Jet Propulsion Laboratory
4800 Oak Grove Dr.
Pasadena, CA 91109
818-354-2603

C.W. Koehler
Space Systems/ Loral
G 69
3825 Fabian Way
Palo Alto, CA 94539
415-852-5133

Albert A. Koenig
Chloride Silent Power, Ltd.
940 W. Valley Rd.
Suite 1804
Wayne, PA 19087
215-341-9207

S. Krause
Hughes Aircraft Company
Bldg. S12/V330
POB 92919
Los Angeles, CA 90009

Paul W. Krehl
Electochem Industries
10000 Wehrle Dr.
Clarence, NY 14031
716-759-2828

Jerry R. Kukulka
Spectrolab Inc.
12500 Gladstone Ave.
Sylmar, CA 91342
818-898-2837

John Lahzun
Goddard Space Flight Center
Code 480
Greenbelt, MD 20771
301-286-6129

Joe Lavelle
EES MS 213-2
Ames Research Center
Moffett Field, CA 94035

John Lear
Grumman Space Division
M/S T01-12
South Oyster Bay Rd.
Bethpage, NY 11714

Leo Lech
Martin Marietta Astronautics
POB 179, MS 8041
Denver, CO 80201
303-977-6964

Yen Lee
Goddard Space Flight Center
Code 313.2
Greenbelt, MD 20771
301-286-6685

Harold Leibecki
NASA Lewis Research Center
MS 301-3
21000 Brookpark Rd.
Cleveland, OH 44135
216-433-xxxx

Paul Leigh
Fairchild Space Co.
20301 Century Blvd.
Germantown, MD 20874
301-953-5000 ex 4034

Lt. K. Leili
HQ Space Division/YGJD
POB 92960
Worldway Postal Center
Los Angeles, CA 90009

Harlan L. Lewis
Naval Weapons Support Center - Crane
Crane, IN 47522
812-854-1431

Stacy Lewis
GE American Communications
4 Research Way
Princeton, NJ 08540
609-987-4350

Nick Liberto
Catalyst Research
38 Loveton Circle
Sparks, MD 21152
301-628-5423

Mark E. Liffring
Boeing Aerospace & Electronics
POB 3999
Seattle, WA 98124
206-773-0030

H.S. Lim
MS A315 Bldg S41
Hughes Aircraft Co.
POB 92919
Los Angeles, CA 90009
213-416-9432

David Linden
Duracell
78 Lovett Ave.
Little Silver, NJ 07739
201-741-2271

Stephen M. Lipka
American Cyanamid Co.
POB 60
1937 W. Main St.
Stamford, CT 06904
203-348-7331

John E. Lowery
NASA MSFC EB12
Marshall Space Flight Ctr.
AL 35812
205-544-0080

Mark [illegible]ker
ARINC Research
11770 E.Warner
Fountain Valley, CA 92708
714-979-8040

Chuck Lurie
TRW R4/1036
One Space Park
Redondo Beach, CA 90278
213-813-4888

Michael Mackowski
1621 Waterwood Ln.
St. Louis, MO 63146
314-233-2364

Dr. Tyler X. Mahy
U.S. Government
c/o OTS--2583 NHB
Washington, DC 20505
703-874-0739

Jenny Mai
EB12
Marshall Space Flight Ctr.
Alabama 35812
205-544-3312

Don Mains
Naval Weapons Support Center - Crane
Code 3056
Crane, IN 47522
812-854-1299

Paul A. Malachesky
Aerospace Corporation
MS M4/988
POB 92957
Los Angeles, CA 90009-2957
213-336-9572

Frank L. Manning
NASA Headquarters
Code QP
Washington, DC 20546
202-453-1876

Michelle Manzo
Lewis Research Center
MS 309-1
21000 Brookpark Rd.
Cleveland, OH 44135
216-433-5261

Sue Maras
Goddard Space Flight Center
Code 711.1
Greenbelt, MD 20771
301-286-7043

Lynn Marcoux
Marcoux Engineering, Inc
1631 Garland
Tustin, CA 92680
714-544-0495

N. Margalit
Tracor Battery Tech Center
4294 Mainsail Dr.
Burke, VA 22015
301-251-4881

Steven P. Marquis
U.S. Patent Trademark Office
2021 Jefferson Davis Highway
Arlington, VA 22202
703-557-6680

Tim Martin
1983-I McKelvey Hill Dr.
Maryland Heights, MO 63043
314-234-8436

James Masson
Martin Marietta Corp
S-0550
POB 179
Denver, CO 80201

J. Matsumoto
Aerospace Corporation
MS M2/275
POB 92957
Los Angeles, CA 90009-2957
213-336-1526

Richard H. Maurer
Johns Hopkins University/ APL
Johns Hopkins RD.
Laurel, MD 20707
301-953-5000ex 4009

Dean W. Maurer
AT&T
Princetown-Windsor Office Pk
379 Princeton-Hightstown Rd.
Cranbury, NJ 08512
609-448-0687

Stan Mavrogiannis
16 Twin Oaks
New Milford, CT 06776

Greg McDonald
MCI
POB 291
Clarksburg, MD 20871
301-540-5409

Dan McGuire
Martin Marietta Corp
S-4820
POB 179
Denver, CO 80201

William McHugh
GTE
520 Winter St.
Waltham, MA 02254
617-466-3609

Goerge G. McKhann
McDonnell Douglas Space Systems Co.
5301 Bolsa Ave.,MS 17-6
Huntington Beach, CA 92647
714-896-4669

Mitch Mendrek
EH24
Marshall Space Flight Ctr.
Alabama 35812
205-544-2619

Arthur A. Menichiello
Aerospace Corporation
MS M4/988
POB 92957
Los Angeles, CA 90009-2957
213-336-8269

George Methlie
2120 Natahoa Ct.
Falls Church, VA 22043
703-533-1449

John Meyer
Johns Hopkins University/ APL
Rm 23-209
Johns Hopkins RD.
Laurel, MD 20707
301-792-5000ex8604

Vernon Mielke
Goddard Space Flight Center
Code 711.1
Greenbelt, MD 20771
301-286-8477

M.J. Milden
Aerospace Corporation
MS M4/988
POB 92957
Los Angeles, CA 90009-2957
213-336-xxxx

Dave Miller
Eagle Picher Industries
C & Porter Streets
Joplin, MO 64804
417-623-8000ex376

Gene J. Miller
Johns Hopkins University/ APL
Rm 23-210
Johns Hopkins RD.
Laurel, MD 20707
301-953-5000

Jim Miller
NASA MSFC EB01
Marshall Space Flight Ctr.
AL 35812
205-544-3292

Lee Miller
Eagle-Picher Industries, Inc.
POB 47
Joplin, MO 64802
417-623-8000

Lee Miller
Eagle-Picher Industries, Inc.
POB 47
Joplin, MO 64801
417-623-8000

Robert T. Miller
Burgess Inc.
Foot of Exchange Street
Freeport, IL 61032

Tom Miller
Lewis Research Center
MS 500-222
21000 Brookpark Rd.
Cleveland, OH 44135
216-433-6300

John C. Moore
U.S. Air Force
HQ SD/CNDAST
2400 El Segundo Blvd.
El Segundo, CA 92960-2960
213-643-0524

George Morrow
Goddard Space Flight Center
Code 711.2
Greenbelt, MD 20771
301-286-6691

Kevin Moscatiello
GE American Communications
95 Edsall Dr. Sussex, NJ 07461
201-827-7900

H.C. Moses
Naval Research Laboratory
Code 7704
4555 Overlook Ave. SW
Washington, DC 20375

Michael Murphy
Martin Marietta, MS S1640
POB 179
Denver, CO 80201
303-977-9854

Dave Nawrocki
4935 Paseo Olivos
San Jose, CA 95130
408-743-0170

Chuong Nguyen
CS-PPD-32
Kennedy Space Center
FL 32899
FTS 823-3331

Ross Nordeen
CS-EED-22
Kennedy Space Center, FL 32899

Ed Norman
EL56
Marshall Space Flight Ctr.
Alabama 35812
205-544-9160

Al Norton
349 Scott Rd.
Toney, AL 35773
205-544-3362

Robert Nowak
Office of Naval Research
Code 113ES
800 N. Quincy St.
Arlington, VA 22217-5000
202-696-4409

Barry Trout /NSI
EP5
Johnson Space Center
NASA Road 1
Houston, TX 77058
713-483-xxxx

Scott A. Numbers
Lewis Research Center
MS 501-4
21000 Brookpark Rd.
Cleveland, OH 44135
216-433-2335

Pat O'Donnell
NASA Lewis Research Ctr.
MS 309-1
21000 Brookpark Rd.
Cleveland, OH 44135
216-433-5248

Masatomo Ohtaki
Mitsui & Co. Inc.
200 Park Ave.
New York, NY 10166-0130
212-878-4316

Dennis J. Okula
Missile Systems Div., Cs2-58
Raytheon Co.
Hartwell Rd.
Bedford, MA 01730
617-274-7200 x4068

Phil Olbert
Ball Aerospace
M9772
POB 1062
Boulder, CO 80306
303-939-4401

Jean R. Olivier
TA01
Marshall Space Flight Ctr.
Alabama 35812
205-544-0650

Major Steven Opel
HQ Space systems Div. SDEP
POB 92960
Los Angeles, CA 90029-2960

Burton Otzinger
857 E. Sierra Madre Ave.
Glendora, CA 91740
213-797-3724

George Pack
Lockheed Missles & Space Co.
1111 Lockheed Way
O/62-12 B/551
Sunnyvale, CA 94088
408-743-7248

Charles Palandati
4915 56th Ave.
Hyattville, MD 20781
301-277-8007

Paul E. Panneton
Johns Hopkins Univerwity/ APL
Rm 23-210
Johns Hopkins RD.
Laurel, MD 20707
301-953-5000

George B. Park
American Cyanamid Co.
POB 60
1937 W. Main St.
Stamford, CT 06904
203-348-7331

Robert E. Patterson
TRW R5/2241
One Space Park
Redondo Beach, CA 90278
213-813-0502

Gene Pearlman
GE Astro Space Div.
POB 800
Princeton, NJ 08816
609-490-3349

Daniel A. Pelhank
McDonnell Douglas Missile Systems Co.
POB 516
St. Louis, MO 63166-0516
314-233-1779

W.D. Perry
Dept. of Chemistry
Auburn University
Auburn, AL 36849
205-844-6956

David F. Pickett
Hughes Aircraft Co.
Electron Dynamics Div.
POB 2999 MS 231/1040
Torrance, CA 90509
213-517-7601

Anthony Pietsch
MS 1207-4R
Allied Signal Aerospace Co.
POB 22200
Tempe, AZ 85282
602-893-4490

Robert J. Pinkerton
Ford Aerospace Co.
1760 Business Center Drive
Reston, VA 22090
703-438-5438

Frank Pizzano
EL54
Marshall Space Flight Ctr.
Alabama 35812
205-544-7424

Michael Powell
AFAL/VSSP
Edwards AFB, CA 93534
805-275-5662

Allen R. Powers
Hughes Aircraft
MS 151B B/231
POB 2999
Torrance, CA 90509-2999
213-517-5435

Geoffrey Prentice
Johns Hopkins Unversity
Dept. of Chemical Eng.
Baltimore, MD 21218
301-338-7006

Kenneth W. Prince
E454/92/2W/F2
McDonnell Douglas Astronautics
POB 516
St. Louis, MO 63166-0516
314-925-7823

Vince Puglisi
Gates Aerospace Batteries
POB 114
Gainesville, FL 32602
904-462-4457

Olivier Puig
SAFT Space Program
156 Avenue De Metz
93230 Romainville, France
33-1-48-43-9361

Michael F. Pyszczek
Wilson Greatbatch Ltd.
10000 Wehrle Dr.
Clarence, NY 14031
716-759-6901

Guy Rampel
Gates Energy
POB 114
Gainsville, FL
904-462-3698

Joseph Randall
EB01
Marshall Space Flight Ctr.
Alabama 35812
205-544-3282

Gopal Rao
Code 711.2
Greenbelt, MD 20771
301-286-3051

Margaret A. Reid
Lewis Research Center
MS 309-1
21000 Brookpark Rd.
Cleveland, OH 44135
216-433-5253

Robert N. Richards
Martin Marietta Astronautics
POB 179, MS 8041
Denver, CO 80201
303-977-3828

Roger E. Rickey
Roger E. Rickey & Assocs.
1222 Kingsway Rd. SE
Huntsville, AL 35802
205-881-2785

Paul Ritterman
ACME-Advanced Power Systems
528 West 21st Street
Tempe, AZ 85282
602-894-6864

Howard H. Rogers
MS A315 Bldg. S41
Hughes Aircraft Co.
POB 92919
Los Angeles, CA 90009
213-416-9432

Teresa M. Romanofsky
Lewis Research Center
21000 Brookpark Rd.
Cleveland, OH 44135
216-433-5363

Max E. Rosenthal
TA61
Marshall Space Flight Ctr.
Alabama 35812
205-544-0682

Gilbert L. Roth
NASA HQ
Code Q-1
Washington, DC 20546
202-453-8971

Mike Sanders
Hughes Aircraft
MS 231/1524
3100 W. Lomita Blvd.
Torrance, CA 90505
213-517-5713

Frank J. Scalici
INTELSAT
3400 International Dr. Box 34
Washington, DC 20008-3098
202-944-7353

Stephen Schiffer
GE Astro Space Div.
MS 410-2-C19
POB 800
Princeton, NJ 08540-0800
609-490-3277

Lee Schmidlin
Hughes Aircraft
2970 Presidential Dr.
Suite 300
Fairborn, OH 45324-6270
513-429-5429

Dave Schmidt
Gates Aerospace Batteries
POB 2520
Gainesville, FL 32602
904-462-4752

Jack Schmidt
GE American Communications
95 Edsall Dr.
Sussex, NJ 07461
201-827-7900

Authur D. Schoenfeld
Hughes Aircraft Co.
MS A314 Bldg. S41
POB 92919
Los Angeles, CA 90009
213-615-8107

Norm Schulze
NASA HQ
Code QP
Washington, DC 20546
202-453-2763

Joe Sciabica
AL/XRX
Edwards AFB, CA 93523-5000
805-275-5344

Darren Scoles
Eagel-Picher Industries
3820 S. Hancock Expy.
Colorado Springs, CO 80911
719-392-4266

Eddie Seo
Gates Corp.
POB 5887
Denver, CO 80217
303-744-4614

Eddie T. Seo
Hughes Aircraft Company
M/S 231/1915
POB 2999
Torrance, CA 90509

Dick Shaw
Martin Marietta Astronautics
POB 179, MS 0533
Denver, CO 80201
303-977-3726

George H. Shipley
Honey Well, Inc.
13350 U.S. 19 South
Clearwater, FL 34624
813-539-5712

Robert Siegler
Electrochem Industries
10000 Wherle Dr.
Clarence, NY 14031
716-759-2828

D. Sieminski
Electrochem Industries
10000 Wherle Dr.
Clarence, NY 14031
716-759-6901

Lenard F. Silvester
Lockheed Missles & Space Co.
1272 Borregas Ave.
O/62-12 B/551
Sunnyvale, CA 94086
408-743-7267

Jack Sindorf
Johnson Controls
POB 591
Milwaukee, WI 53201
414-961-6494

A.B. Singh
MDAC 7375
Executive Place
Seabrook, MD 20706
301-464-7400

Nick Smilanich
Eveready Battery Co.
POB 45035
Westlake, OH 44145
216-835-7755

Marc A. Smith
GTE Spacenet
1700 Old Meadow Rd.
McLean, VA 22102
703-848-0414

David Smith
Altus Corp.
1610 Crane St.
San Jose, CA 95112
408-436-1300

Owen Smith
1241 W. Long Ct.
Littleton, CO 80120
303-971-1174

John J. Smithrick
Lewis Research Center
MS 302-1
21000 Brookpark Rd.
Cleveland, OH 44135
216-433-5255

Frank Snow
U.S. Navy - SPAWAR
Attn: PMW 142-52A
Washington, DC 20363-5100
202-692-7137

D.G. Soltis
NASA Lewis Research Center
MS 501-6
21000 Brookpark Rd.
Cleveland, OH 44135
216-433-2667

Thomas Spitzer
Goddard Space Flight Center
Code 711.1
Greenbelt, MD 20771
301-286-4383

Steven Stadnick
Hughes Aircraft Co.
MS A315 Bldg. S41
POB 92919
Los Angeles, CA 90009
213-648-9322

Dan Standlee
Eagle-Picher Industries, Inc.
POB 47
Joplin, MO 64801
417-623-8000

Robert Staniewicz
SAFT America
107 Beaver Ct.
Cockeysville, MD 21030
301-771-3200

Bob Stearns
GE Astro Space Division
M2508
POB 8555
Philadelphia, PA 19101

J.K. Stedman
International Fuel Cells
POB 739
South Windsor, CT 06074
203-727-2211

Sal Di Stefano
Jet Propulsion Laboratory
MS 189-100
4800 Oak Grove Drive
Pasadena, CA 91109
818-354-6320

Ken Stephens
EB11
Marshall Space Flight Ctr.
Alabama 35812
205-544-6616

James A. Stepro
National Standard Co.
2401 N. Home St.
Mishawaka, IN 46545
219-259-8505

Thoedore G. Stern
General Dynamics Space Systems Div.
MS 24-8730
POB 85990
San Diego, CA 92138
619-547-4519

Joseph Stockel
Office of Research & Development
Washington, DC 20505
703-351-2065

Martin Sulkes
USALABWM SLCET-PB
Ft. Monmouth, NJ 07703-5000
201-544-2458

Ralph M. Sullivan
JHU/ Applied Physics Lab
MS 23-214
Johns Hopkins Rd.
Laurel, MD 20723
301-953-5095

David Surd
Catalyst Research
3706 Crondall Lane
Owings Mills, MD 21117
201-356-2908

Daniel W. Swallom
Avco Research Labortatory Inc.
2385 Revere Beach Pkwy
Everett, MA 02149
617-381-4384

William A. Swartz
Johns Hopkins University/ APL
Rm 23-210
Johns Hopkins RD.
Laurel, MD 20707
301-953-5000

Larry Swette
Giner, Inc.
14 Spring Street
Waltham, MA 02254-9147
617-899-7270

Mike Takao
Sanyo Energy Corporation
200 Riser Rd.
Little Ferry, NJ 07643
201-641-2333ex416

Michael Tasevoli
Goddard Space Flight Center
Code 711.2
Greenbelt, MD 20771
301-286-xxxx

William E. Taylor
EJ31
Marshall Space Flight Ctr.
Alabama 35812
205-544-6614

Steve Tesney
EB12
Marshall Space Flight Ctr.
Alabama 35812
205-544-3400

Lawrence H. Thaller
The Aerospace Corp.
MS M2/275
POB 92957
Los Angeles, CA 90009
213-336-5180

Peter C. Theisinger
Jet Propulsion Laboratory
4800 Oak Grove Drive
Pasadena, CA 91109
818-354-6094

H.E. Thierfelder
GE Astrospace Div.
POB 8555
Philadelphia, PA 19101
215-354-2027

Daniel L. Thomas
Chemical Engineering Dept.
University of Alabama, H
Huntsville, AL 35899
205-895-6266

William Thompson
Goddard Space Flight Center
Code 711.1
Greenbelt, MD 20771
301-286-8014

Anne Van Thuyne
GE Astro
MS NP-2C
100 Nasa Park Blvd.
West Winsor, NJ 08543
609-951-7084

Jim Tidwell
Motorola, Inc.
8000 W. Sunrise Blvd.
Ft. Lauderdale, FL 33322

William H. Tiedeman
Johnson Controls, Inc.
M/S G3
5757 N. Greenbay Ave.
Milwaukee, WI 53201

Sid Tiller
Goddard Space Flight Center
Code 711.2
Greenbelt, MD 20771
301-286-6489

Paul Timmerman
927 E. Atchison
Pasadena, CA 91109
818-354-5388

Lawrence Tinker
Gates Aerospace Batteries
POB 2520
Gainesville, FL 32602
904-462-4715

Robert F. Tobias
TRW R4/1136
One Space Park
Redondo Beach, CA 90278
213-813-5961

Mark R. Toft
1405 Sun Lake Dr.
St. Charles, MO 63301-3006
314-233-8649

Hari Vaidyanathan
COMSAT
22300 Comsat Dr.
Clarksburg, MD 20871
301-428-4507

Kunigahalli L. Vasanth
Naval Suface Weapons Center
10901 New Hampshire Ave.
Silver Spring, MD 20903-5000
202-394-3549

Donald C. Verrier
TRW R4/1112
One Space Park
Redondo Beach, CA 90278
213-535-2354

Scott Verzwyvelt
Boeing Aerospace & Electronics
POB 3999 MS 85-84
Seattle, WA 98124-2499
206-773-3524

Micheal Viens
Goddard Space Flight Ctr.
Code 313
Greenbelt, MD 20771-0001
301-286-2049

Stephen P. Vukson
U.S. Air Force
AFWAL/POOS-2
Wright-Patterson AFB, OH 45433
513-255-5461

James R. Waggoner
Catalyst Research
3706 Crondall Lane
Owings Mills, MD 21117
301-356-2400

Harry Wajsgras
12205 Valerie Lane
Laurel, MD 20708
301-776-3101

Ray L. Walchle
FDA
HFZ 141 Rm 164
12720 Twinbrook Parkway
Rockville, MD 20850
301-443-2536

Richard Walraven
Naval Research Lab, Code 8112
4555 Overlook Ave. SW
Washington, DC 20375-5000
202-767-6517

Harry Wannemacher
Goddard Space Flight Center
Code 711.1
Greenbelt, MD 20771
301-286-5914

Don R. Warnock
AFWAL/POOC
Wright-Patterson AFB
OH 45433

Marvin Warshay
Lewis Research Center
MS 301-5
21000 Brookpark Rd.
Cleveland, OH 44135
216-433-5261

Don Webb
Martin Marietta Astronautics
MS S-4017 Dept. 4345
POB 179
Denver, CO 80201
303-977-3833

Capt. Alexander H. Webster
U.S. Air Force
AFAL/VSSP
Edwards AFB, CA 93523-5000
805-275-5928

Bob Weed
Nichols Research Corp.
4040 Memorial Pkwy. SW
Huntsville, AL 35801-5838

Howard Weiner
Aerospace Corporation
MS M4/988
POB 92957
Los Angeles, CA 90009-2957
213-336-xxxx

Irwin B. Weinstock
Catalyst Research
3706 Crondall Lane
Owings Mills, MD 21117
301-356-2400

Ralph White
Texas A&M University
Dept. of Chemisty/Eng.
C. Station, TX 77843
409-845-3307

Richard V. Whiteley
Pacific Unversity
Chemistry Dept.
2043 College Way
Forest Grove. OR 97116
503-357-6151

Thomas H. Whitt
EB12
Marshall Space Flight Ctr.
Alabama 35812
205-544-3313

Steven P. Wicelinski
Catalyst Research
3706 Crondall Lane
Owings Mills, MD 21117
301-356-2914

Robert L. Wiley
WJ Schafer Assoc.
1901 North Fort Myer Dr.
Arlington, VA 22209
703-558-7900

Wade W. Wilkerson
MS 1063323
McDonnell Douglas Elec Sys
POB 516
St. Louis, MO 63166-0516
314-233-2184

Lt. Col. Robert Winn
HWUSAFA/ DFAN
USAF Academy
Colorado Springs, CO 80840-5701
719-472-4010

James H. Wise
EJ31
Marshall Space Flight Ctr.
Alabama 35812
205-544-6620

Richard Wissoker
GTE Government Systems
520 Winter St.
Waltham, MA 02154
617-466-3216

Fred S. Wojtalik
TA01
Marshall Space Flight Ctr.
Alabama 35812
205-544-0647

Brenda Wolfe
Eagle-Picher Industries, Inc.
3820 South Hancock Expressway
Colorado Springs, CO 80911
719-392-4266

Clifford L. Wooten
Contel ASC
POB 370687
Decatur, GA 30037
404-244-2302

Robert Wright
1840 Shellbrook Dr.
Huntsville, AL 35806
205-895-9659

W. Wright
Box 461
Ardmore, TN 38449
615-468-2059

Richard A. Wynveen
Life Systems, Inc.
24755 Highpoint Rd.
Cleveland, OH 44122

Thomas Yi
Goddard Space Flight Center
Code 711.2
Greenbelt, MD 20771
301-286-3051

Leighton E. Young
EJ31
Marshall Space Flight Ctr.
Alabama 35812
205-544-0707

R.F. Youngblood
GE American Communications
95 Edsall Dr.
Sussex, NJ 07461
201-827-7900

Jeff Zagrodnik
Johnson Controls
MS K21
900 E. Keefe
Milwaukee, WI 53212
414-961-6494

Albert H. Zimmerman
Aerospace Corporation
MS M2/275
POB 92957
Los Angeles, CA 90009-2957
213-336-7415

NASA

Report Documentation Page

1. Report No.	2. Government Accession No.	3. Recipient's Catalog No.
NASA CP- 3119		

4. Title and Subtitle	5. Report Date
The 1990 NASA Aerospace Battery Workshop	May 1991
	6. Performing Organization Code
7. Author(s)	8. Performing Organization Report No.
Lewis M. Kennedy, Compiler	
	10. Work Unit No. M-661
9. Performing Organization Name and Address	11. Contract or Grant No.
George C. Marshall Space Flight Center Marshall Space Flight Center, Alabama 35812	
	13. Type of Report and Period Covered
12. Sponsoring Agency Name and Address	Conference Publication
National Aeronautics and Space Administration Washington, D.C. 20546	14. Sponsoring Agency Code

15. Supplementary Notes

Proceedings of a workshop sponsored by the NASA Aerospace Battery Steering Committee, hosted by the Marshall Space Flight Center, and held at the U. S. Space and Rocket Center, Huntsville, Alabama, on December 4-6, 1990.

16. Abstract

This document contains the proceedings of the 21st annual NASA Aerospace Battery Workshop, hosted by the Marshall Space Flight Center on December 4-6, 1990. The workshop was attended by scientists and engineers from various agencies of the U.S. Government, aerospace contractors, and battery manufacturers as well as participation in like kind from the European Space Agency member nations. The subjects covered included nickel-cadmium, nickel-hydrogen, silver-zinc, lithium based chemistries, and advanced technologies as they relate to high reliability operations in aerospace applications.

A Sampling of the workshop scope ranges over:

- o reports on current light operations including Hubble Space Telescope, COBE, Megellan, CRRES, Solar Max, and Eutelsat II.
- o histories of development and performance, and expected performance of current design developments.
- o problem analysis, testing, cell and cell test safety

17. Key Words (Suggested by Author(s))	18. Distribution Statement
Battery Electrode Hubble Space Telescope, Separator Nickel Cadmium, Nickel Hydrogen Lithium Thionyl Chloride Sodium Nickel Chloride	Unclassified-Unlimited Subject Category: 20

19. Security Classif. (of this report)	20. Security Classif. (of this page)	21. No. of pages	22. Price
Unclassified	Unclassified	946	A99

NASA FORM 1626 OCT 86

For sale by the National Technical Information Service, Springfield, VA 22161-2171